SMITHIAN (EARLY TRIASSIC) AMMONOID FAUNAS OF THE TETHYS: TAXONOMY, BIOCHRONOLOGY, DIVERSITY DYNAMICS AND PALEOENVIRONMENTS

Dissertation

zur

Erlangung der naturwissenschaftlichen Doktorwürde
(Dr. sc. nat.)

vorgelegt der

Mathematisch-naturwissenschaftlichen Fakultät

der

Universität Zürich

von

Thomas Brühwiler

aus

Fischingen TG

Promotionskomitee

Prof. Dr. Hugo Bucher
(Leiter der Dissertation, Vertreter der Universität Zürich)
Prof. Dr. Leopold Krystyn
Prof. Dr. Marcelo Sanchez
Prof. Dr. Jean Guex
Dr. Arnaud Brayard

Zürich, 2010

CONTENTS

ABSTRACT

The end-Permian mass extinction is the biggest known crisis in life history and wiped out more than 90% of all marine species. In its aftermath, the Early Triassic was a time of profound instabilities in the sedimentary, geochemical and climatic evolution. Full recovery of many marine, essentially benthic clades as well as pre-crisis level of marine ecosystem complexity was not reached until the Middle Triassic (e.g. reefal communities). On the contrary, at least some faunal groups such as ammonoids and conodonts recovered much faster than other marine clades. However, the evolution of Early Triassic ammonoids was not a smooth, nor a gradual process. It was characterized by the following main features: (i) a very low diversity in the Griesbachian (early Induan), (ii) a moderate diversity increase in the Dienerian (late Induan), (iii) an explosive radiation in the early Smithian (early Olenekian), (iv) a late Smithian extinction event followed by (v) a second explosive radiation in the early Spathian (late Olenekian).

In the first part of this thesis, the first report of reasonably well preserved Griesbachian and Dienerian ammonoids from South China is provided. Since localities yielding ammonoids of this time interval are rare in the low palaeolatitude record, our report is a significant contribution to the biostratigraphy and biogeography of the evolutionary recovery of ammonoids. However, the record of Griesbachian and Dienerian ammonoid still remains far from complete in the Tethyan realm.

Second, the Lower Triassic sedimentary record from the Tulong area in South Tibet is entirely documented for the first time. New age control is provided by ammonoid and conodont biostratigraphy. Comparison of the Tulong record with other Tethyan localities reveals striking similar facies in parts of the Lower Triassic record. Deciphering such large-scale patterns may provide new insights into the climatic control that regulated sedimentation and the Early Triassic biotic recovery, as well. High-resolution sampling leads to a new carbonate carbon isotope record for the Early Triassic in South Tibet, which provides additional evidence for the global character of the carbon cycle instabilities during the recovery interval, thus confirming the well-documented perturbations of the global carbon cycle in the aftermath of the Permian–Triassic mass extinction event.

The main part of this dissertation focuses on the taxonomic revision and biostratigraphy of Smithian ammonoid faunas from several basins of the Northern Indian Margin. We conducted extensive field studies in two classical regions for the Early Triassic, namely the Salt Range (Pakistan) and Spiti (Indian Himalayas). Additionally, we studied a section at Tulong (South Tibet) as well as extremely ammonoid-rich exotic blocks of Hallstatt Limestone in the Oman Mountains. Our abundant, bed-rock-controlled and well-preserved material enables us to revise many classical ammonoid taxa that were previously only poorly known. Each species is analyzed to account for its intraspecific variation and its ontogenetic changes. Moreover, a large number of new taxa was found, which enables us to define one new family, 23 new genera and 41 new species.

Finally, biochronological data for the three well-documented basins Salt Range, Spiti and Tulong are analysed by means of the Unitary Associations Method, resulting in a biochronological scheme of unprecedented high resolution for the Smithian of the Northern Indian Margin. Analysis of ammonoid diversity dynamics based on this new high-resolution time frame highlights (i) a marked diversification during the early Smithian, (ii) a severe extinction during the late Smithian, and (iii) an overall very high turnover throughout the Smithian. At rather low spatial and temporal resolutions, the evolutionary tempo of Early Triassic ammonoids appears surprisingly high, as highlighted by a recent study. We show here that at the finest possible scale, the Smithian recovery peak of ammonoids is characterized by extremely high turnover rates.

Key words: Early Triassic recovery, Ammonoids, Sedimentology, Carbon isotopes, Griesbachian, Dienerian, Smithian, South China, Salt Range, Spiti, South Tibet, Oman.

ZUSAMMENFASSUNG

Das endpermische Massenaussterben ist die grösste bekannte Krise in der Geschichte des Lebens und löschte mehr als 90% der marinen Arten aus. Die darauffolgende Frühe Trias war eine Zeit tief greifender Veränderungen in den sedimentären, geochemischen und klimatischen Abläufen. Die marinen Ökosysteme erreichten erst in der Mitteltrias ähnliche Komplexitätsgrade wie vor der Krise (z. B. Riff-Vergesellschaftungen), und auch die Erholungsphase vieler, im wesentlichen benthischer, mariner Organismengruppen dauerte ebenso lang. Im Gegensatz dazu erholten sich zumindest einige Tiergruppen wie die Ammonoideen und die Conodonten viel schneller als andere marine Gruppen. Allerdings war die Erholung der frühtriassischen Ammonoideen kein gleichmässiger, gradueller Prozess, sondern war durch die folgenden Eigenschaften charakterisiert: (i) eine sehr tiefe Diversität im Griesbachium (frühes Induum), (ii) eine moderate Diversitätszunahme im Dienerium (spätes Induum), (iii) eine explosive Radiation im frühen Smithium (frühes Olenekium), (iv) ein Aussterbeereignis im späten Smithium, gefolgt von (v) einer zweiten explosiven Radiation im frühen Spathium (spätes Olenekium).

Im ersten Teil dieser Dissertation wird die erste Beschreibung von vernünftig gut erhaltenen Ammonoideen des Griesbachiums und des Dieneriums von Südchina geliefert. Da Lokalitäten mit Ammonoideen dieses Zeitabschnittes in den tiefen Paläobreiten selten sind, ist unsere Arbeit ein wichtiger Beitrag zur Biostratigraphie und Biogeographie der evolutionären Erholung der Ammonoideen. Der Fossilbericht für Ammonoideen des Griesbachiums und Dieneriums im Bereich der Tethys bleibt jedoch immer noch lückenhaft.

Zweitens wird die frühtriassische Sedimentabfolge in der Gegend von Tulong im Südtibet zum ersten Mal in ihrer Gesamtheit beschrieben und mittels detaillierter Ammonoideen- und Conodonten-Biostratigraphie neu datiert. Der Vergleich der frühtriassischen Abfolge von Tulong mit anderen Lokalitäten in der Tethys zeigt starke Ähnlichkeiten in Teilen der Abfolge auf. Die Entschlüsselung solcher grossräumiger Muster kann neue Einblicke in die klimatischen Einflüsse ermöglichen, die die Sedimentation und auch die frühtriassische biotische Erholung regulierten. Hochauflösende Beprobung liefert eine neue Karbonat-Kohlenstoffisotopen-Kurve für die Frühe Trias im Südtibet, die zusätzliche Beweise für den globalen Charakter der Störungen des Kohlenstoffkreislaufs während der Erholungsphase nach dem endpermischen Aussterbeereignis liefert.

Der Hauptteil dieser Dissertation fokussiert auf die taxonomische Revision und die Biostratigraphie von Ammonoideen des Smithiums von mehreren Becken auf dem Nordindischen Rand. Dazu führten wir ausführliche Feldstudien in zwei klassischen Regionen der Frühen Trias, nämlich in der Salt Range (Pakistan) und in Spiti (indischer Himalaya). Ausserdem studierten wir ein Profil in Tulong (Südtibet) wie auch extrem fossilreiche exotische Blöcke in der Hallstatt-Fazies aus dem Oman-Gebirge. Unser umfangreiches und gut erhaltenes Material ermöglicht es uns, viele klassische Ammonoideen-taxa zu revidieren, die bis anhin nur unzulänglich bekannt waren. Jede Art wird hinsichtlich ihrer intraspezifischen Variation und ihrer ontogenetischen Veränderungen untersucht. Ausserdem fanden wir eine grosse Anzahl neuer Taxa, was uns ermöglicht, eine neue Familie, 23 neue Gattungen und 41 neue Arten zu definieren.

Schliesslich werden die biochronologischen Daten der drei gut dokumentierten Regionen Salt Range, Spiti und Tulong mittels der Unitary Associations Methode analysiert, was in einem biochronologischen Schema von nie dagewesener hoher Auflösung für das Smithium des Nordindischen Rands resultiert. Die Analyse der Diversitäts-Dynamik basierend auf diesem neuen Zeitrahmen hebt (i) eine deutliche Diversifizierung im frühen Smithium, (ii) ein starkes Aussterbeereignis im späten Smithium, und (iii) ein sehr hoher Umsatz (turnover) während des ganzen Smithiums hervor. Mit geringerer räumlicher und zeitlicher Auflösung hat eine vorhergehende Studie gezeigt, dass das evolutionäre Tempo der frühtriassischen Ammonoideen überraschend hoch ist. Wir zeigen hier, dass die explosive Erholung der Ammonoideen im Smithium auf der kleinstmöglichen Skala durch extrem hohe Turnover-Raten charakterisiert ist.

Schlüsselwörter: Frühe Trias, Erholungsphase, Ammonoideen, Sedimentologie, Kohlenstoffisotopen, Griesbachium, Dienerium, Smithium, Südchina, Salt Range, Spiti, Südtibet, Oman.

CHAPTER 1:

Introduction

INTRODUCTION

Permian/Triassic mass extinction

The end-Permian mass extinction is the biggest known crisis in life history and wiped out more than 90% of all marine species (e.g. Raup and Sepkoski, 1982). This event drastically affected the evolution of life with the replacement of typical Palaeozoic faunas by typical modern communities (Fig. 1; Sepkoski, 1984). Geochronological data from South China reveal that the main pulse of extinction occurred at an age of 252.6±0.2 Ma over a relatively short interval (Mundil et al., 2004).

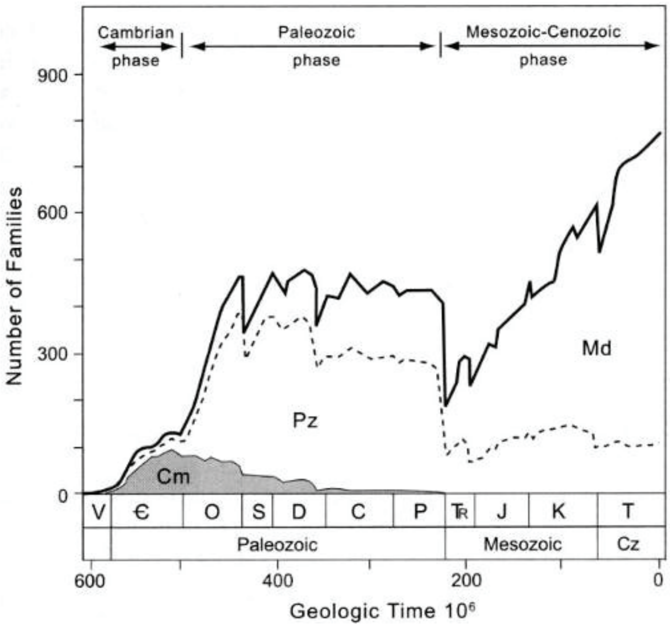

Figure 1. Marine diversity throughout the Phanerozoic. Cm: Cambrian fauna; Pz: Palaeozoic fauna; Md: Mesozoic-Cenozoic, or Modern, fauna. From Sepkoski (1984).

Various scenarios for this extinction have been proposed, including sea-level regression (Holser et al., 1989), voluminous volcanism (Renne et al., 1995; Payne and Kump, 2007), extraterrestrial impacts (Becker et al., 2004), widespread marine anoxia (Wignall and Twitchett, 1996; Isozaki, 1997; Kakuwa, 2008), hypercapnia (Knoll et al., 2007), euxinia (Grice et al., 2005; Meyer and Kump, 2008), methane release (Krull and Retallack, 2000), massive release of carbon dioxide via vaporization of coal deposits (Erwin, 2006), and contact metamorphism of the Siberian Traps with evaporites and organic-rich deposits inducing the venting of halocarbons and greenhouse gases causing ozone depletion and global warming (Svensen et al., 2009). It has also been argued that the end-Permian extinction event has been caused by a combination of multiple factors rather than a single cause (Berner, 2002; Erwin, 2006).

Early Triassic biotic recovery

The Early Triassic recovery of marine and terrestrial ecosystems is usually considered to have been delayed when compared with other mass extinctions and to have lasted until the end of the Early Triassic (e.g Erwin, 1998, 2006). Metazoan reef communities were completely absent in the Early Triassic (Pruss and Bottjer, 2005). Instead, unusual, microbially-mediated carbonate factories (e.g. microbialites) were common worldwide (e.g. Baud et al., 2007; Kershaw et al., 2007; Galfetti et al., 2008; Woods, 2009). Many marine clades such as corals (Stanley, 2003), foraminifers (Tong and Shi, 2000) or radiolarians (Racki, 1999) did not completely recover until the Spathian or the Anisian. Poorly diversified and small-sized benthonic shelly faunas were abundant during the Early Triassic (e.g. Fraiser and Bottjer, 2004; Fraiser et al., 2005).

However, new findings of large-sized gastropods have recently refuted the Lilliput hypothesis in this clade, at least for the last 75% of the Early Triassic, which is compatible with a more rapid recovery than previously assumed (Brayard et al., 2010). A very rapid Early Triassic recovery has been detected for two important marine clades, namely ammonoids and conodonts (Orchard, 2007; Brayard et al., 2009b; see appendix). Moreover, recent analysis of outer platform paleoenvironments from South China reveals that increasing rates of diversity and abundance of skeletal material occurred already during well-oxygenated carbonate episodes of early Smithian and Spathian age, respectively (Galfetti et al., 2008; see appendix).

This dissertation is part of a multidisciplinary study conducted under the leadership of Prof. H. Bucher at the Palaeontological Institute and Museum of the University of Zurich (PIMUZ), in which different aspects of the Early Triassic recovery and its climatic/oceanographic constraints are being investigated. The project initially started in South China, but also includes sections in Spitsbergen and Greenland, several localities on the Northern Indian Margin (NIM; i.e. Salt Range, Spiti, Tibet, Oman), in the western USA as well as in the Italian Alps (Fig. 2).

One major outcome of the project has been the calibration of the Early Triassic time scale by means of new U-Pb zircon ages obtained from Guangxi, South China (Ovtcharova et al., 2006; Galfetti et al., 2007b, see appendix). These results indicate that the four Early Triassic substages (Griesbachian, Dienerian, Smithian, Spathian) are of extremely uneven duration (Figure 3).

Combined with absolute age calibrations, acquisition of precise biochronological data is the cornerstone to which all other aspects of the research on the Early Triassic recovery are linked with. A firm basis for this purpose has been laid by the revision of ammonoid faunas from South China (Brayard and Bucher, 2008; Brühwiler et al., 2008 [Chapter 2 of this thesis]; Bucher et al., ongoing work). High resolution sampling and taxonomic revision of Early Triassic key ammonoid successions from the NIM and correlation of these sequences with South China, and other areas aim at the construction of a high-resolution Early Triassic ammonoid zonation (Chapters 4-9 of this thesis; Ware et al., ongoing work; Bucher et al., ongoing work).

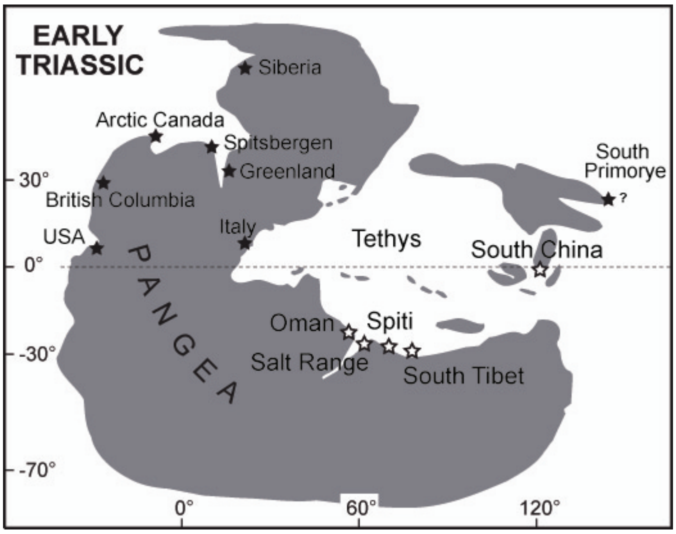

Figure 2. Simplified palaeogeographical map of the Early Triassic with the palaeoposition of the Salt Range (Pakistan), Spiti (Northern India), Tulong (South Tibet), Oman, South China and other localities mentioned in this thesis (modified after Brayard et al., 2006).

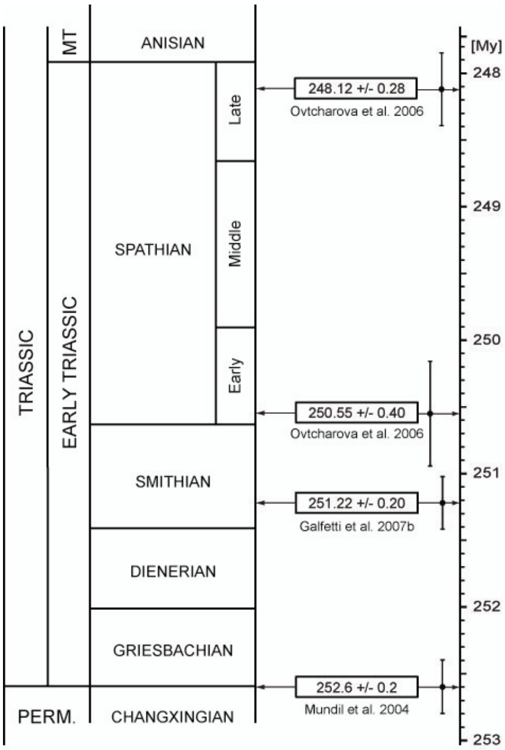

Figure 3. Early Triassic stage subdivision (Tozer, 1967) calibrated with recently published radiometric ages from South China (Mundil et al., 2004; Ovtcharova et al., 2006; Galfetti et al., 2007b).

In the aftermath of the end-Permian mass extinction, ammonoids were among the fastest clades to recover: the recent analysis of a global diversity data set of ammonoid genera from the Late Carboniferous to the Late Triassic shows that Triassic ammonoids actually reached levels of diversity higher than in the Permian less than 2 million years after the PTB (Brayard et al., 2009b; see appendix). The evolution of Early Triassic ammonoids was not a smooth, nor a gradual process. It is characterized by the following main features: (i) a very low diversity in the Griesbachian (early Induan), (ii) a moderate diversity increase in the Dienerian (late Induan), (iii) an explosive radiation in the early Smithian (early Olenekian), (iv) a late Smithian extinction event followed by (v) a second explosive radiation in the early Spathian (late Olenekian) (Fig. 4).

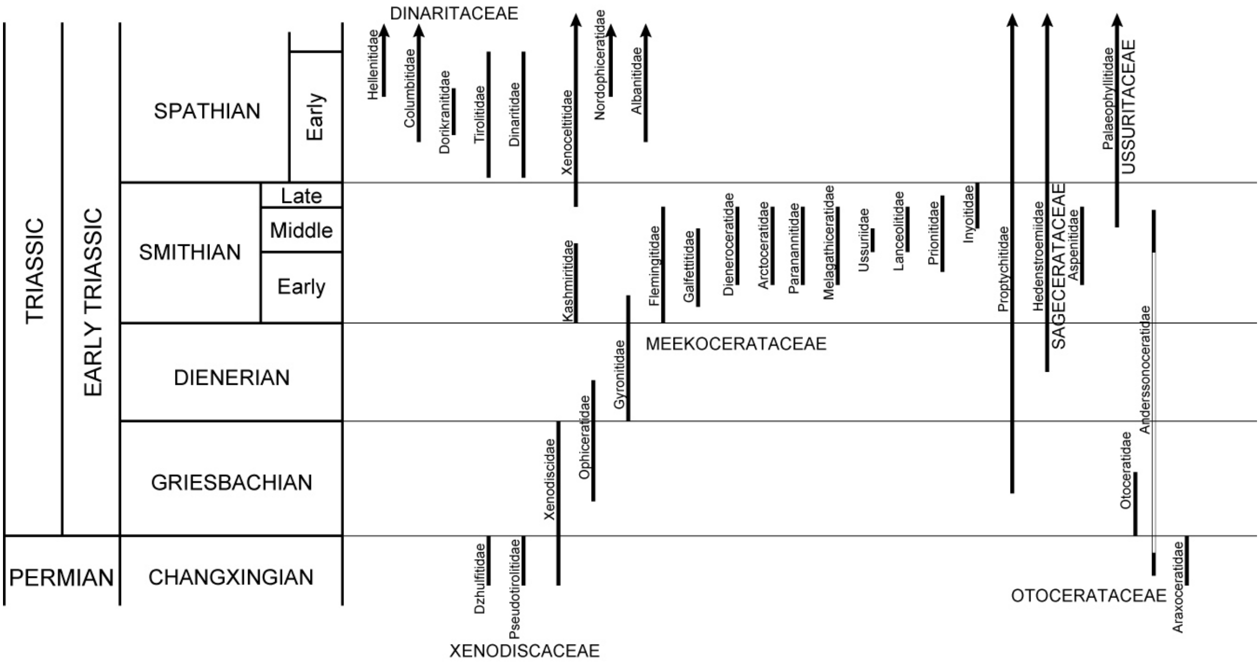

Figure 4. Temporal distribution of ammonoid families in the Early Triassic (based on Tozer, 1981; modified according to Brayard et al., 2007a; Brayard and Bucher, 2008; this thesis [chapters 2, 4-8]; and Bucher [unpublished]).

An important step in the understanding of spatial recovery patterns of ammonoids has been reached with the reconstruction of latitudinal diversity gradients at the genus level for each of the four Early Triassic substages (Brayard et al., 2006; Brayard et al., 2007b). These diversity gradients are largely controlled by sea-surface temperatures, thus bearing a clear climatic signature. Ammonoid biogeogeography strongly suggests that the Griesbachian was a time of warm and equal climate and that the stepwise edification of latitudinal climatic belts was completed during the Spathian. However, this trend was severely set back near the end of the Smithian, coinciding with a massive extinction of ammonoids and conodonts.

The Permian-Triassic transition and the Early Triassic were times of major perturbations of the carbon cycle. Following a major negative carbon isotope shift around the P/T boundary, several large and short-lived $\delta^{13}C$ fluctuations occurred during the Early Triassic, before the carbon cycle stabilized in the Middle Triassic (Holser et al., 1989; Baud et al., 1996; Atudorei and Baud, 1997; Atudorei, 1999; Payne et al., 2004; Richoz, 2004; Corsetti et al., 2005; Galfetti et al., 2007a-c; Horacek et al., 2007a, b; Richoz et al., 2009; and see chapter 3 of this thesis [Brühwiler et al., 2009]). It has been shown by Bucher's research group that the major positive δ13C excursion at the Smithian–Spathian boundary coincides with the most severe ammonoid and conodont intra-Triassic extinction event, associated with deposition of organic-rich sediments, changes in palynological assemblages indicating major climatic change, and possibly acidification of surface waters (Brayard et al., 2006; Galfetti et al., 2007a-c; Galfetti et al., 2008). CO_2 degassing via volcanism, possibly related to a late eruptive phases of the Siberian Traps, has been proposed as a trigger for these global disturbances (Payne et al., 2004; Ovtcharova et al., 2006). Such an explanation is favoured also by carbon cycle modelling which suggests that the Early Triassic carbon cycle perturbations result from recurring environmental disturbances rather than from lingering effects of a single disturbance at the Permian–Triassic boundary (Payne and Kump, 2007).

Current Early Triassic research of Bucher's group investigates the following aspects of the Early Triassic biotic recovery:

- Early Triassic conodonts from South China, the NIM and from the USA (N. Goudemand)
- Dienerian ammonoids from the Salt Range, Spiti and Nevada (D. Ware)
- Palynology and palaeoenvironments from the Salt Range and comparison with the boreal realm (E. Hermann, P.A. Hochuli)
- Early Triassic fishes from Spitsbergen, Nevada and Spiti; oxygen isotopic composition of biogenic phosphate from the Salt Range (C. Romano)
- Early Triassic benthic faunas (M. Hautmann, R. Hofmann)
- Griesbachian marine faunas from Greenland (H. Bucher, M. Hautmann)

Outline of the thesis

Chapters 2 to 9 of this thesis correspond to manuscripts, which are either published, accepted for publication or under review. The following main objectives are addressed:

(i) Description of Griesbachian-Dienerian ammonoids from South China

Recently conducted, extensive studies of ammonoid faunas from northwestern Guangxi have yielded excellent, well documented faunal successions for the Smithian (Brayard and Bucher, 2008) and for the Spathian (Bucher et al., ongoing work). On the contrary, earliest Triassic (i.e. Griesbachian and Dienerian) ammonoid faunas from this area have proved to be rare, and often less well preserved. Nevertheless, since very little is known about Griesbachian and especially Dienerian ammonoids, any new report of ammonoids of this time interval is crucial for a better understanding of the taxonomy, biostratigraphy, phylogeny, recovery and the palaeobiogeography of Early Triassic ammonoid faunas as well. Chapter 2 of this thesis represents an article published in *Palaeontology* (Brühwiler et al., 2008), and focuses on the taxonomy and biostratigraphical significance of newly collected ammonoid faunas from Guangxi and Guizhou. Note that a more comprehensive study of Dienerian ammonoids is currently in progress, based on newly collected material from the Salt Range, Spiti, South Tibet and Nevada (Ware et al. ongoing work).

(ii) Detailed documentation of the Lower Triassic sedimentary and carbon isotope records from South Tibet and their significance for Tethyan palaeoceanography

Various sections from South Tibet have long been known for their Lower Triassic sedimentary and palaeontological records (e.g. Garzanti et al., 1998). However, for the area of Tulong, previously published documentations of the Lower Triassic succession were incomplete and/or poorly or incorrectly dated. In Chapter 3, which is an article published in *Sedimentary Geology* (Brühwiler et al., 2009), we provide the first complete and detailed description of the Lower Triassic sedimentary and carbon isotope records from the Tulong area in South Tibet. Extensive sampling enabled us to precisely date the section by means of detailed ammonoid and conodont biostratigraphy. Comparison of the Tulong record with other Tethyan localities reveals striking similar facies in parts of the Lower Triassic record. Deciphering such large-scale patterns may provide new insights into the processes related to the Early Triassic biotic recovery (compare with Galfetti et al., 2007a). High-resolution sampling throughout the entire Tulong Formation yields a new ammonoid and conodont age-constrained, carbonate carbon isotope record for the Early Triassic in South Tibet. The comparison of this new C-isotope record with other Lower Triassic profiles described in the literature provides additional evidence for the global character of the carbon cycle instabilities during the Early Triassic recovery interval.

Smithian ammonoids from Tulong are described in detail in Chapter 4 of this thesis. Spathian ammonoids are the subject of ongoing work (Bucher et al.). Early Triassic conodonts from Tulong are studied by Goudemand et al. (ongoing work). Ostracods from Tulong have been studied by Forel and Crasquin (in press) and Forel et al. (submitted; see appendix).

(iii) Taxonomic revision and biostratigraphy of Smithian ammonoids from the Northern Indian Margin (NIM)

For more than a century, Smithian ammonoids have been known from various localities in the Tethyan realm, such as the Salt Range in Pakistan (Waagen, 1895; Noetling, 1905; Guex, 1978), Afghanistan (Kummel and Erben, 1968), Spiti in Northern India (Diener, 1897; Krafft and Diener, 1909; Krystyn et al., 2007a, b), Kashmir (Diener, 1913), Tibet (Wang and He, 1976), Madagascar (Collignon, 1933-1934), Guangxi in South China (Chao, 1959; Brayard and Bucher, 2008), Vietnam (Khuc, 1984) and Timor (Welter, 1922). Among these, the Salt Range and Spiti have played central roles in the development of the Early Triassic time scale (Mojsisovics et al., 1895). The NIM actually represents a key area for the study of Early Triassic ammonoids, due to its very abundant, diverse and well preserved faunas. However, the majority of Smithian ammonoids from the NIM areas were hitherto insufficiently known due to the small numbers of specimens and/or poor preservation, all of which bears on the definition of taxa and on their biostratigraphic distributions. Moreover, the exact stratigraphic occurrences of many taxa remained either approximate or unknown, and the number of studies based on bed by bed sampling from this region is very limited (Guex, 1978; Krystyn et al., 2007a, b). Therefore, additional high-resolution ammonoid successions from various localities are crucial for establishing a precise and laterally reproducible biochronological subdivision of the Smithian within the Tethys and within the Early Triassic tropics.

The main part of this thesis (Chapters 4-8) deals with the taxonomic revision and biostratigraphy of Smithian ammonoids based on intensive, high-resolution sampling in the following regions on the NIM: Tulong, South Tibet (Chapter 4); the Salt Range, Pakistan (Chapter 5); Spiti in Himachal Pradesh, Northern India (Chapters 6 and 7); and Oman (Chapter 8).

Our investigations in the Tulong area in South Tibet (compare Chapter 3) have yielded abundant, diverse and reasonably well preserved Smithian ammonoid faunas including several new taxa. In Chapter 4, which represents an article that has been accepted for publication in *Geobios* (Brühwiler et al., accepted), we focus on the description of these faunas. They add significantly to our knowledge of

Smithian ammonoid taxonomy and biostratigraphy and facilitate the construction of a highly-resolved middle and late Smithian ammonoid succession. Early Smithian ammonoid faunas are almost absent in Tulong because of a preservation bias (absence of carbonate rocks).

Waagen's contribution on Early Triassic ammonoids from the Salt Range (Pakistan) in the late 19th century (1895) was of immense importance for the study of Early Triassic ammonoids. In his master work entitled *Fossils from the Ceratite Formation*, he described a large number of new ammonoid taxa, thus making the Salt Range a classic Early Triassic locality. Our extensive investigations in the Salt Range have yielded abundant, well-preserved ammonoid faunas of earliest to latest Smithian age that are of prime importance for the revision of ammonoid taxonomy and their biostratigraphy. Our data allow the construction of a highly-resolved ammonoid succession spanning the entire Smithian times. These results are presented in a monographic treatment submitted to the *Special Papers in Palaeontology* (Brühwiler et al., submitted [d]), which represents Chapter 5 of this thesis.

Since the pioneer works of Diener (1897) and Krafft and Diener (1909), the Spiti area in Himachal Pradesh (Northern India) became another classic region for Early Triassic ammonoids. Recently, a section near Mud has been proposed as a GSSP for the Induan-Olenekian (Dienerian-Smithian) boundary (Krystyn et al., 2007a, b). However, ammonoid faunas from the beds just underlying the proposed GSSP level were hitherto known only insufficiently. We have thoroughly sampled these beds and discovered several new and well preserved ammonoid faunas. In Chapter 6, which is an article submitted to the *Journal of Asian Earth Sciences* (Brühwiler et al., submitted [e]), we focus on the stratigraphic distribution and the taxonomic description of these faunas. Our data shed a new light on the definitive choice for a GSSP level for the Induan/Olenekian boundary since several elements of typical Smithian (early Olenekian) affinity were found in a relatively low stratigraphical position compared to the previously proposed GSSP.

Chapter 7 represents an article submitted to *Palaeontology* (Brühwiler et al., submitted [c]). Herein, ammonoids of middle-late Smithian age from several localities in Spiti (Northern India) are described. These abundant and well preserved faunas allow us to establish a high-resolution ammonoid succession spanning the middle to latest Smithian time interval. Note that ammonoid faunas of the early Smithian *Flemingites* beds are currently under study (Krystyn, ongoing work).

The presence of Smithian ammonoids in exotic blocks of red pelagic limestone (Hallstatt facies) in Oman has been known since the works of Tozer and Calon (1990) and of Blendinger (1995). However, these faunas have never been studied in details. Chapter 8 is a monographic description of these ammonoids which has been submitted to *Palaeontographica* (Brühwiler et al., submitted [b]). The exotic blocks from Oman have yielded several well preserved and highly diversified Smithian (Early Triassic) ammonoid faunas. Most of the blocks contain only a single fauna each, which limits the biostratigraphic significance of these faunas. However, they add significantly to our knowledge of the Smithian ammonoid taxonomy and biogeography. Moreover, the excellent preservation of the ammonoids from Oman improves our knowledge of several taxa that have previously been known only from imperfect material (e.g. *Guodunites*; Brayard et al., 2009a; see appendix). Some exceptionally well preserved specimens of *Juvenites* from this locality have even preserved organic remains of so-called "false colour pattern" (Klug et al., 2007; see appendix). The comparison of the assemblages from Oman with data from other Tethyan basins such as the Salt Range, Spiti, Tibet and South China shows that nearly all known Smithian ammonoid faunal assemblages are present in the exotic blocks from Oman.

(iv) Construction of a high-resolution Smithian ammonoid zonation and analysis of diversity dynamics of Smithian ammonoids of the NIM

Chapter 9 represents an article submitted to *Palaeogeography, Palaeoclimatology, Palaeoecology* (Brühwiler et al., submitted [a]). In this work, biochronological data for the three well-documented basins Salt Range, Spiti and Tulong are analysed by means of the Unitary Associations Method (Guex, 1991) (the data from Oman is not included in this analysis due to its scattered nature). This results in a biochronological scheme of unprecedented high resolution for the Smithian of the NIM, which provides a firm basis for further palaeogeographical extension of Early Triassic biochronological correlations towards global correlations and the analysis of recovery patterns in a highly resolved time frame.

Based on this new zonation, we then analyze patterns of ammonoid diversity throughout the Smithian of the NIM with an unprecedented resolution. The following three main features for the Smithian ammonoids of the NIM are highlighted: i) a radiation during the early Smithian, (ii) a severe extinction in the late Smithian, (iii) an overall extremely high turnover throughout the Smithian. Results of this work focusing only on the Smithian substage thus confirm the very high evolutionary tempo of Early Triassic ammonoids, as previously shown in a study with lower spatial and temporal resolutions (Brayard et al., 2009b; see appendix). We show that at a smaller geographic scale and with the highest time resolution, Smithian ammonoids of the NIM reached their explosive diversity peak essentially through extremely high turnover rates rather than through a classic diversification process of high origination rates coupled with low extinction rates.

References

Atudorei, N.-V. 1999: Constraints on the upper Permian to upper Triassic marine carbon isotope curve. Case studies from the Tethys. PhD Thesis, Lausanne, 155 pp.

Atudorei, N.-V., Baud, A., 1997. Carbon isotope events during the Triassic. Albertiana 20, 45-49.

Baud, A., Atudorei, V., Sharp, Z., 1996. Late Permian and Early Triassic evolution of the Northern Indian margin: Carbon isotope and sequence stratigraphy. Geodinamica Acta 9, 57-77.

Baud, A., Richoz, S., Pruss, S., 2007. The lower Triassic anachronistic carbonate facies in space and time. Global and Planetary Change 55, 81-89.

Becker, L., Poreda, R.J., Basu, A.R., Pope, K.O., Harrison, T.M., Nicholson, C., Iasky, R., 2004. Bedout: a possible end-Permian impact crater offshore of northwestern Australia. Science 304, 1469-1476.

Berner, R.A., 2002. Examination of hypothesis for the Permo-Triassic boundary extinction by carbon cycle modeling. Proceedings of the National Academy of Sciences of the United States of America 99, 4172-4177.

Blendinger, W., 1995. Lower Triassic to Lower Jurassic cephalopod limestones of the Oman Mountains. Neues Jahrbuch fuer Geologie und Palaeontologie. Monatshefte 1995, 577-593.

Brayard, A., Brühwiler, T., Bucher, H., Jenks, J., 2009a. *Guodunites*, a low-palaeolatitude and trans-panthalassic Smithian (Early Triassic) ammonoid genus. Palaeontology 52, 471-481.

Brayard, A., Bucher, H., 2008. Smithian (Early Triassic) ammonoid faunas from northwestern Guangxi (South China): taxonomy and biochronology. Fossils and Strata 55, 1-179.

Brayard, A., Bucher, H., Bruhwiler, T., Galfetti, T., Goudemand, N., Guodun, K., Escarguel, G., Jenks, J., 2007a. *Proharpoceras* Chao: a new ammonoid lineage surviving the end-Permian mass extinction. Lethaia 40, 175-181.

Brayard, A., Bucher, H., Escarguel, G., Fluteau, F., Bourquin, S., Galfetti, T., 2006. The Early Triassic ammonoid recovery: Paleoclimatic significance of diversity gradients. Palaeogeography, Palaeoclimatology, Palaeoecology 239, 374-395.

Brayard, A., Escarguel, G., Bucher, H., 2007b. The biogeography of early Triassic ammonoid faunas: Clusters, gradients, and networks. Geobios 40, 749-765.

Brayard, A., Escarguel, G., Bucher, H., Monnet, C., Brühwiler, T., Goudemand, N., Galfetti, T., Guex, J., 2009b. Good Genes and Good Luck: Ammonoid Diversity and the End-Permian Mass Extinction. Science 325, 1118-1121.

Brayard, A., Nützel, A., Stephen, D.A., Bylund, K.G., Jenks, J., Bucher, H., 2010. Gastropod evidence against the Early Triassic Lilliput effect. Geology 38, 147-150.

Brühwiler, T., Brayard, A., Bucher, H., Guodun, K., 2008. Griesbachian and Dienerian (Early Triassic) ammonoid faunas from northwestern Guangxi and southern Guizhou (South China). Palaeontology 51, 1151-1180.

Brühwiler, T., Bucher, H., Brayard, A., Goudemand, N., submitted [a]. Smithian (Early Triassic) ammonoids of the Northern Indian Margin: high-resolution biochronology and diversity dynamics Palaeogeography, Palaeoclimatology, Palaeoecology.

Brühwiler, T., Bucher, H., Goudemand, N., accepted. Smithian (Early Triassic) ammonoids from Tulong, South Tibet. Geobios.

Brühwiler, T., Bucher, H., Goudemand, N., Galfetti, T., submitted [b]. Smithian (Early Triassic) ammonoid faunas from Exotic Blocks from Oman: taxonomy and biochronology. Palaeontographica.

Brühwiler, T., Bucher, H., Krystyn, L., submitted [c]. Middle and late Smithian (Early Triassic) ammonoids from Spiti (India). Palaeontology.

Brühwiler, T., Bucher, H., Ware, D., Roohi, G., Rehman, K., Yaseen, A., submitted [d]. Smithian (Early Triassic) ammonoids from the Salt Range, Pakistan. Special Papers in Palaeontology.

Brühwiler, T., Goudemand, N., Galfetti, T., Bucher, H., Baud, A., Ware, D., Hermann, E., Hochuli, P.A., Martini, R., 2009. The Lower Triassic sedimentary and carbon isotope records from Tulong (South Tibet) and their significance for Tethyan palaeoceanography. Sedimentary Geology 222, 314-332.

Brühwiler, T., Ware, D., Bucher, H., Krystyn, L., Goudemand, N., submitted [e]. New Early Triassic ammonoid faunas from the Dienerian/Smithian boundary beds at the Induan/Olenekian GSSP candidate at Mud (Spiti, Northern India). Journal of Asian Earth Sciences.

Chao, K., 1959. Lower Triassic ammonoids from Western Kwangsi, China. Palaeontologia Sinica. New Series B 9, 355 pp.

Collignon, M., 1933-1934. Paléontologie de Madagascar XX - Les céphalopodes du Trias inférieur. Annales de Paléontologie 12-13, 151-162 & 1-43.

Corsetti, F.A., Baud, A., Marenco, P.J., Richoz, S., 2005. Summary of Early Triassic carbon isotope records. Comptes Rendus Palevol 4, 473-486.

Diener, C., 1897. The Cephalopoda of the Lower Trias. Palaeontologia Indica, ser. 15, Himalayan Fossils 2, 1-181.

Diener, C., 1913. Triassic faunae of Kashmir. Palaeontologia Indica, n. ser. 5, 1-133.

Erwin, D.H., 1998. The end and the beginning: recoveries from mass extinctions. Trends in Ecology & Evolution 13, 344-349.

Erwin, D.H. 2006: Extinction: How Life on Earth Nearly Ended 250 Millions Years Ago. Princeton University Press, 296 pp.

Forel, M.-B., Crasquin, S., Brühwiler, T., Goudemand, N., Bucher, H., Baud, A., Randon, C., submitted. Ostracod recovery after Permian-Triassic boundary mass-extinction in South Tibet. Palaeogeography, Palaeoclimatology, Palaeoecology.

Forel, M.B., Crasquin, S., in press. In the aftermath of Permian-Triassic boundary mass-extinction: ostracod new species and genus from South Tibet. Geodiversitas.

Fraiser, M.L., Bottjer, D.J., 2004. The non-actualistic early triassic gastropod fauna: A case study of the lower triassic sinbad limestone member. Palaios 19, 259-275.

Fraiser, M.L., Twitchett, R.J., Bottjer, D.J., 2005. Unique microgastropod biofacies in the Early Triassic: Indicator of long-term biotic stress and the pattern of biotic recovery after the end-Permian mass extinction. Comptes Rendus Palevol 4, 543-552.

Galfetti, T., Bucher, H., Brayard, A., Hochuli, P.A., Weissert, H., Guodun, K., Atudorei, V., Guex, J., 2007a. Late Early Triassic climate change: Insights from carbonate carbon isotopes, sedimentary evolution and ammonoid paleobiogeography. Palaeogeography, Palaeoclimatology, Palaeoecology 243, 394-411.

Galfetti, T., Bucher, H., Martini, R., Hochuli, P.A., Weissert, H., Crasquin-Soleau, S., Brayard, A., Goudemand, N., Brühwiler, T., Guodun, K., 2008. Evolution of Early Triassic outer platform paleoenvironments in the Nanpanjiang Basin (South China) and their significance for the biotic recovery. Sedimentary Geology 204, 36-60.

Galfetti, T., Bucher, H., Ovtcharova, M., Schaltegger, U., Brayard, A., Brühwiler, T., Goudemand, N., Weissert, H., Hochuli, P.A., Cordey, F., Guodun, K.A., 2007b. Timing of the Early Triassic carbon cycle perturbations inferred from new U-Pb ages and ammonoid biochronozones. Earth and Planetary Science Letters 258, 593-604.

Galfetti, T., Hochuli, P.A., Brayard, A., Bucher, H., Weissert, H., Vigran, J.O., 2007c. Smithian-Spathian boundary event: Evidence for global climatic change in the wake of the end-Permian biotic crisis. Geology 35, 291-294.

Garzanti, E., Nicora, A., Rettori, R., 1998. Permo-Triassic boundary and lower to middle Triassic in South Tibet. Journal of Asian Earth Sciences 16, 143-157.

Grice, K., Cao, C.Q., Love, G.D., Bottcher, M.E., Twitchett, R.J., Grosjean, E., Summons, R.E., Turgeon, S.C., Dunning, W., Jin, Y.G., 2005. Photic zone euxinia during the Permian-Triassic superanoxic event. Science 307, 706-709.

Guex, J., 1978. Le Trias inférieur des Salt Ranges, Pakistan: problèmes biochronologiques. Eclogae Geologicae Helvetiae 71, 105-141.

Guex, J. 1991: Biochronological correlations. Springer-Verlag.

Holser, W.T., Schönlaub, H.-P., Attrep, M., Boeckelmann, K., Klein, P., Magaritz, M., Orth, C.J., Fenninger, A., Jenny, C., Kralik, M., Mauritsch, H., Pak, E., Schramm, J.-M., Stattegger, K., Schmöller, R., 1989. A unique geochemical record at the Permian/Triassic boundary. Nature 337, 39-44.

Horacek, M., Brandner, R., Abart, R., 2007a. Carbon isotope record of the P/T boundary and the Lower Triassic in the Southern Alps: Evidence for rapid changes in storage of organic carbon. Palaeogeography, Palaeoclimatology, Palaeoecology 252, 347-354.

Horacek, M., Richoz, S., Brandner, R., Krystyn, L., Spötl, C., 2007b. Evidence for recurrent changes in Lower Triassic oceanic circulation of the Tethys: The δ^{13}C record from marine sections in Iran. Palaeogeography, Palaeoclimatology, Palaeoecology 252, 355-369.

Isozaki, Y., 1997. Permo-Triassic boundary superanoxia and stratified superocean: record from lost deep sea. Science 276, 235-238.

Kakuwa, Y., 2008. Evaluation of palaeo-oxygenation of the ocean bottom across the Permian-Triassic boundary. Global and Planetary Change 63, 40-56.

Kershaw, S., Li, Y., Crasquin-Soleau, S., Feng, Q.L., Mu, X.N., Collin, P.Y., Reynolds, A., Guo, L., 2007. Earliest Triassic microbialites in the South China block and other areas: controls on their growth and distribution. Facies 53, 409-425.

Khuc, V. 1984: Triassic ammonoids in Vietnam. Geoinform and Geodata Institute, Hanoi, Vietnam, 134 pp.

Klug, C., Bruhwiler, T., Korn, D., Schweigert, G., Brayard, A., Tilsley, J., 2007. Ammonoid shell structures of primary organic composition. Palaeontology 50, 1463-1478.

Knoll, A.H., Bambach, R.K., Payne, J.L., Pruss, S., Fischer, W.W., 2007. Paleophysiology and end-Permian mass extinction. Earth and Planetary Science Letters 256, 295-313.

Krafft, A.v., Diener, C., 1909. Lower Triassic cephalopoda from Spiti, Malla Johar, and Byans. Palaeontologia Indica, ser. 15, 6, 1-186.

Krull, E.S., Retallack, G.J., 2000. δ^{13}C depth profiles from paleosols across the Permian-Triassic boundary: Evidence for methane release. Geological Society of America Bulletin 112, 1459-1472.

Krystyn, L., Bhargava, O.N., Richoz, S., 2007a. A candidate GSSP for the base of the Olenekian Stage: Mud at Pin Valley; district Lahul & Spiti, Himachal Pradesh (Western Himalaya), India. Albertiana 35, 5-29.

Krystyn, L., Richoz, S., Bhargava, O.N., 2007b. The Induan-Olenekian Boundary (IOB) in Mud – an update of the candidate GSSP section M04. Albertiana 36, 33-45.

Kummel, B., Erben, H.K., 1968. Lower and Middle Triassic cephalopods from Afghanistan. Palaeontographica, Abt. A 129, 95-148.

Meyer, K.M., Kump, L.R., 2008. Oceanic euxinia in Earth history: Causes and consequences. Annual Review of Earth and Planetary Sciences 36, 251-288.

Mojsisovics, E., Waagen, W., Diener, C., 1895. Entwurf einer Gliederung der pelagischen Sedimente des Trias-Systems. Sitzungsberichte der Akademie der Wissenschaften in Wien (I) 104, 1271-1302.

Mundil, R., Ludwig, K.R., Metcalfe, I., Renne, P.R., 2004. Age and timing of the Permian mass extinctions: U/Pb dating of closed-system zircons. Science 305, 1760-1763.

Noetling, F., 1905. Die asiatische Trias. In: F. Frech (Editor), Lethaea geognostica. Das Mesozoicum, 1. Band, Trias. Lethaia Mesozoica 1. Schweizerbart, Stuttgart, pp. 107-221.

Orchard, M.J., 2007. Conodont diversity and evolution through the latest Permian and Early Triassic upheavals. Palaeogeography, Palaeoclimatology, Palaeoecology 252, 93-117.

Ovtcharova, M., Bucher, H., Schaltegger, U., Galfetti, T., Brayard, A., Guex, J., 2006. New Early to Middle Triassic U-Pb ages from South China: Calibration with ammonoid biochronozones and implications for the timing of the Triassic biotic recovery. Earth and Planetary Science Letters 243, 463-475.

Payne, J.L., Kump, L.R., 2007. Evidence for recurrent Early Triassic massive volcanism from quantitative interpretation of carbon isotope fluctuations. Earth and Planetary Science Letters 256, 264-277.

Payne, J.L., Lehrmann, D.J., Wei, J.Y., Orchard, M.J., Schrag, D.P., Knoll, A.H., 2004. Large perturbations of the carbon cycle during recovery from the end-Permian extinction. Science 305, 506-509.

Pruss, S.B., Bottjer, D.J., 2005. The reorganization of reef communities following the end-Permian mass extinction. Comptes Rendus Palevol 4, 553-568.

Racki, G., 1999. Silica-secreting biota and mass extinctions: survival patterns and processes. Palaeogeography, Palaeoclimatology, Palaeoecology 154, 107-132.

Raup, D.M., Sepkoski, J.J., 1982. Mass Extinctions in the Marine Fossil Record. Science 215, 1501-1503.

Renne, P.R., Zhang, Z., Richardson, M.A., Black, M.T., Basu, A.R., 1995. Synchrony and causal relations between Permo-Triassic boundary crises and Siberian flood volcanism. Science 269, 1413-1416.

Richoz, S., 2004. Stratigraphie et variations isotopiques du carbone dans le Permian supérieur et le Trias inférieur de la Néotéthys (Turquie, Oman et Iran). PhD., University of Lausanne, Switzerland. 281p.

Richoz, S., Krystyn, L., Baud, A., Brandner, R., Horacek, M., Mohtat-Aghai, P., 2009. Permian-Triassic boundary interval in the Middle East (Iran and N. Oman): Progressive environmental change from detailed carbonate carbon isotope marine curve and sedimentary evolution. Journal of Asian Earth Sciences, doi:10.1016/j.jseaes.2009.12.014.

Sepkoski, J.J., 1984. A Kinetic-Model of Phanerozoic Taxonomic Diversity .3. Post-Paleozoic Families and Mass Extinctions. Paleobiology 10, 246-267.

Stanley, G.D., 2003. The evolution of modern corals and their early history. Earth-Science Reviews 60, 195-225.

Svensen, H., Planke, S., Polozov, A.G., Schmidbauer, N., Corfu, F., Podladchikov, Y.Y., Jamtveit, B., 2009. Siberian gas venting and the end-Permian environmental crisis. Earth and Planetary Science Letters 277, 490-500.

Tong, J., Shi, G.R., 2000. Evolution of the Permian and Triassic foraminifera in south China. In: H. Yin, Dickins, J.M., Shi, G.R., Tong, J. (Editor), Permian-Triassic Evolution of Tethys and

Western Circum-Pacific. Developments in Palaeontology and Stratigraphy. Elsevier, Amsterdam, pp. 291-307.

Tozer, E.T., 1967. A standard for Triassic time. Geologic Survey of Canada Bulletin 156, 141 pp.

Tozer, E.T., 1981. Triassic Ammonoidea; classification, evolution and relationship with Permian and Jurassic forms. In: M.R. House and J.R. Senior (Editors), The Ammonoidea; the evolution, classification, mode of life and geological usefulness of a major fossil group. Systematics Association Special Volume. Academic Press [for the] Systematics Association, London-New York, International, pp. 65-100.

Tozer, E.T., Calon, T.J., 1990. Triassic ammonoids from Jabal Safra and Wadi Alwa, Oman, and their significance. In: A.H.F. Robertson, M.P. Searle and A.C. Ries (Editors), The geology and tectonics of the Oman region. Geological Society Special Publications. Geological Society of London, London, United Kingdom, pp. 203-211.

Waagen, W., 1895. Salt-Range fossils. Vol 2: Fossils from the Ceratite Formation. Palaeontologia Indica 13, 1-323.

Wang, Y.G., He, G.X., 1976. Triassic ammonoids from the Mount Jolmo Lungma region, A report of scientific expedition in the Mount Jolmo Lungma region (1966-1968).

Welter, O.A., 1922. Die Ammoniten der unteren Trias von Timor. Palaeontologie von Timor 11, 83-154.

Wignall, P.B., Twitchett, R.J., 1996. Oceanic anoxia and the end Permian mass extinction. Science 272, 1155-1158.

Woods, A.D., 2009. Anatomy of an anachronistic carbonate platform: Lower Triassic carbonates of the southwestern United States. Australian Journal of Earth Sciences 56, 825-839.

CHAPTER 2:

Griesbachian and Dienerian (Early Triassic) ammonoid faunas from northwestern Guangxi and southern Guizhou (South China)

[Palaeontology, Vol. 51, Part 5, 2008, pp. 1151–1180]

GRIESBACHIAN AND DIENERIAN (EARLY TRIASSIC) AMMONOID FAUNAS FROM NORTHWESTERN GUANGXI AND SOUTHERN GUIZHOU (SOUTH CHINA)

by THOMAS BRÜHWILER*, ARNAUD BRAYARD†‡, HUGO BUCHER*§ *and* KUANG GUODUN¶

*Paläontologisches Institut und Museum, Universität Zürich, Karl Schmid-Strasse 4, CH-8006 Zürich, Switzerland; e-mails: bruehwiler@pim.uzh.ch; hugo.fr.bucher@pim.uzh.ch
†LMTG, UMR 5563 CNRS – Université Toulouse – IRD, Observatoire Midi-Pyrénées, 14 Avenue Edouard Belin, F-31400 Toulouse, France; e-mail: brayard@lmtg.obs-mip.fr
‡CNRS Biogéosciences, Université de Bourgogne, 6 Boulevard Gabriel, F-21000, Dijon, France
§Departement Erdwissenschaften, ETH Zürich, CH-8092 Zürich, Switzerland
¶Guangxi Bureau of Geology and Mineral Resources, Jiangzheng Road 1, 530023 Nanning, China; e-mail: kuangdm@gmail.com

Typescript received 22 October 2007; accepted in revised form 21 December 2007

Abstract: Intensive sampling of the Luolou (northwestern Guangxi) and the Daye (southern Guizhou) Formations in South China leads to the recognition of a regional Griesbachian and Dienerian ammonoid succession for this key palaeobiogeographical area. The new biostratigraphical sequence comprises the upper Griesbachian '*Ophiceras* beds' and the lower Dienerian '*Proptychites candidus* beds', which are separated from the uppermost Dienerian '*Clypites* beds' by an unfossiliferous interval. These faunas contain some taxa with wide geographic distribution (e.g. *Ambites*, *Pleurambites*, *Pleurogyronites*, *Proptychites candidus*), thus facilitating correlation with faunal successions from other regions (i.e. British Columbia, Canadian Arctic, Himalayas and South Primorye). Two new genera (*Jieshaniceras* and *Shangganites*) and three new species (*Anotoceras subtabulatus*, *Pleurambites radiatus* and *Shangganites shangganense*) are described.

Key words: Ammonoidea, Early Triassic, South China, Luolou Fm., Daye Fm., biostratigraphy.

In the aftermath of the end-Permian mass extinction, ammonoids were among the fastest clades of marine organisms to recover (Brayard *et al.* 2006), with at least two diversification phases occurring during the Early Triassic. Following extremely low values during the Griesbachian, diversity increased slowly during the Dienerian and first peaked in the Smithian. This recovery was followed by a severe near-extinction during the end-Smithian, after which an explosive evolutionary radiation took place during the Spathian. Despite the extensive history of research on the Permian/Triassic boundary, relatively little is known about Griesbachian and especially Dienerian ammonoids. Only a few areas such as Canada (Tozer 1994*a*), the Salt Range in Pakistan (Waagen 1895) and Spiti in Northern India (Diener 1897; Krafft and Diener 1909; Krystyn *et al.* 2007) yield well preserved Dienerian material. Therefore, any new report of well preserved Griesbachian and Dienerian ammonoids is crucial in order to better understand the taxonomy, biostratigraphy and phylogeny as well as the recovery and palaeobiogeography of Early Triassic ammonoid faunas.

Recently conducted, extensive studies of Smithian ammonoid faunas from northwestern Guangxi by Brayard *et al.* (2007*b*) and Brayard and Bucher (2008) have yielded an excellent, well documented faunal succession, which is laterally reproducible in other Tethyan basins (Brühwiler *et al.* 2007). Early Triassic ammonoids have long been known from South China (Tien 1933; Hsü 1937), but unfortunately, most reports regarding Griesbachian and Dienerian ammonoids from this area are based on poorly preserved material. In his pioneer contributions, Chao (1950, 1959) essentially described Smithian ammonoid faunas from northwestern Guangxi, but included very few descriptions of Dienerian and Spathian taxa. Since Chao, several authors have reported on the earliest Triassic ammonoids from South China (Wang 1984; Xu 1988; Lidong *et al.* 1992; Tong *et al.* 2004; Bu *et al.* 2006; Mu *et al.* 2007). However, due to the generally poor preservation of this material, very little taxonomic data and information concerning biostratigraphic successions are available for these faunas.

doi: 10.1111/j.1475-4983.2008.00796.x

Our investigations in northern Guangxi and southern Guizhou add significantly to the knowledge of Griesbachian and Dienerian ammonoid faunas. In this paper, we focus on the taxonomy and biostratigraphical significance of this newly collected material.

PALAEOGEOGRAPHICAL AND GEOLOGICAL SETTING

During Early Triassic time, the Pangean supercontinent was surrounded by two wide oceans, namely the Panthalassa and the Tethys (Text-fig. 1), and during this period, several microcontinents (e.g. Cimmerian and Cathaysian) crossed these two oceans (e.g. Tozer 1982; Ricou 1994; Ehiro *et al.* 2005). Most of these terranes are known only by their approximate palaeopositions during the Early Triassic (e.g. Shi 2006; Brayard *et al.* in press). Present-day China consists of several tectonic blocks of Gondwanian origin, which amalgamated and accreted to the southern Eurasian margin. During Early Triassic time, the two main blocks referred to as the South China Block and the North China Block were located at the eastern end of the Tethys. The area studied herein belongs to the South China Block, which was located at the equator at the interface between the Panthalassa and the Tethys (Text-fig. 1). Thus, South China occupied a key geographical area for biogeographical studies of Early Triassic faunas (Brayard *et al.* 2006).

Marine Triassic sediments are widespread in South China and are represented by carbonate platforms and basinal successions (Lehrmann *et al.* 2007). Triassic marine deposits, in northern Guangxi and southern Guizhou, belong to the so-called ‘Nanpanjiang Basin’ and consist of clastic and carbonate rocks formed in a deep-water basin with a few smaller, isolated carbonate platforms. In its present position, the basin is bordered on the north and west by the large Yangtze carbonate platform. The ammonoids described herein were collected from the Luolou (northwestern Guangxi) and Daye (southern Guizhou) Formations.

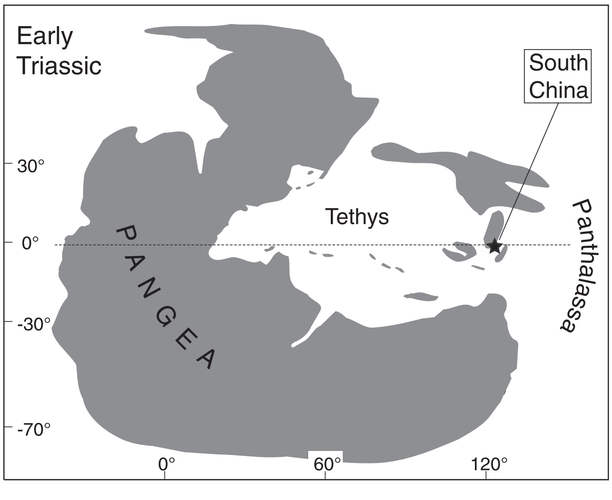

TEXT-FIG. 1. Palaeogeographical map of the Early Triassic with the palaeoposition of South China (modified after Brayard *et al.* 2006).

GRIESBACHIAN AND DIENERIAN AMMONOIDS FROM THE LUOLOU FORMATION

The Luolou Formation

The Luolou Fm. essentially consists of deep-marine, basinal deposits of the Nanpanjiang basin in southern Guizhou and northwestern Guangxi. A high-resolution carbonate isotope record (Galfetti *et al.* 2007*a*, *b*), as well as volcanic ash derived high-precision U–Pb ages (Ovtcharova *et al.* 2006; Galfetti *et al.* 2007*b*) have been obtained from the Luolou Fm. The lowermost part of the formation usually consists of a microbial limestone (Griesbachian), overlain by thin, micritic and partly laminated limestone beds alternating with dark shales (Dienerian; Text-fig. 3, and see Galfetti *et al.* 2008 for details). Overlying the Griesbachian and Dienerian beds is a conspicuous, c. 3 m thick, grey, thin-bedded limestone unit termed ‘*Flemingites rursiradiatus* beds’ of early Smithian age (Brayard and Bucher 2008). This unit represents an important lithological marker found in all sections. The middle and late Smithian succession consists of thin-bedded limestone alternating with dark shales, while the Spathian portion of the Luolou Fm. is composed of massive, grey, nodular limestone, whose facies and age are similar to those of the Himalayan Niti Limestone (Galfetti *et al.* 2007*a*). The Luolou Fm. is overlain by >1000 m of siliciclastic turbidites referred to as the Baifeng Fm. of Middle Triassic age.

Ammonoids are very abundant in the Smithian and Spathian parts of the Loulou Fm. (Brayard and Bucher 2008; Bucher *et al.* unpublished data), but are relatively rare in the lower part.

Sections and ammonoid content

The studied sections, located in northwestern Guangxi Province, South China (Text-fig. 2), were sampled bed-by-bed in order to obtain a precise and detailed ammonoid record. Only those ammonoid beds of pre-Smithian age are shown on the sections illustrated in Text-fig. 3. The ammonoid content of each sample is given in Table 1.

TEXT-FIG. 2. Location map of sampled sections in the Guangxi and Guizhou Provinces, South China. 1, Jinya; 2, Waili/Laren; 3, Shanggan; 4, Yuping; 5, Jieshan Lake.

In the Jinya section ammonoids are relatively rare in the lower part of the Luolou Fm. except for one horizon (sample Jin14), in which '*Koninckites*' cf. *timorense*, *Pleurambites radiatus* sp. nov. and *Vishnuites pralambha* co-occur with abundant *Claraia*, thus indicating a Dienerian age.

Similar to the Jinya section, ammonoids are rare within the lower part of the Luolou Fm. at the Waili and Laren sections, except for three horizons. Sample Wai22 yielded only very poorly preserved ammonoids, which are tentatively assigned to ?*Ophiceras*, possibly indicating a Griesbachian age. *Vishnuites pralambha* was found in sample Jin102. Sample FW9 yielded *Ambites* sp. indet., '*Koninckites*' cf. *timorense*, and a proptychitid gen. indet., thus indicating a Dienerian age.

At Shanggan, a few kilometres north of Leye, the Griesbachian and lower Dienerian part of the Luolou Fm. is well exposed and displays several highly fossiliferous horizons. Sample Sha3 yielded very abundant, small-sized specimens of *Ophiceras* sp. indet., thus indicating a late Griesbachian age. This sample, taken from a well-sorted coquina lense intercalated within the uppermost portion of the microbial limestone, also contains abundant bivalves, gastropods and brachiopods. *Anotoceras subtabulatus* sp. nov., '*Koninckites*' cf. *timorense* and a proptychitid gen. indet. were found in sample Sha7 higher up section, thus indicating a Dienerian age. Sample Sha5 contains abundant '*K.*' cf. *timorense*, and sample Sha4 is characterized by the association of *Gyronites frequens*, '*K.*' cf. *timorense*, *Pleurogyronites* sp. indet., *Prionolobus* cf. *atavus*, and *Shangganites shangganense* gen. nov. sp. nov. Only *S. shangganense* gen. nov. sp. nov. was found in sample Sha8. Unfortunately, the higher part of the Dienerian is cut off by a fault.

The Luolou Fm. is relatively well exposed north of Yuping. Within the lower part of this section, three horizons with ammonoids were sampled. Sample YR59 contains *Jieshaniceras guizhouensis* gen. nov., *Proptychites candidus* and *Xenodiscoides* sp. indet., while sample YR1 yielded only small specimens of *Proptychites* sp. indet. Sample YR30 yielded '*Koninckites*' cf. *timorense* and *Proptychites candidus*. All samples from Yuping indicate a Dienerian age.

DIENERIAN AMMONOIDS FROM THE DAYE FORMATION

The Daye Formation

The Daye Fm., interpreted as a slope equivalent of the Loulou Fm. by Lehrmann *et al.* (2007), is represented by several hundred metres of shales alternating with thin-bedded, partly laminated limestone. Thicker and coarser allodapic limestone beds are intercalated throughout the section. Macrofossils are generally rare in the formation.

Jieshan Lake section

North of Guiding, the Daye Fm. is exposed intermittently along the western flank of the Guiding syncline. Mu *et al.* (2007) reported cephalopods from this formation at Wenjiangsi, three kilometres northwest of Guiding. However, exposures of Permian and Early Triassic strata are relatively poor in this area. A better outcrop of the lower part of the Daye Fm. is located along Jieshan Lake, 8 km north of Guiding. The uppermost beds of the underlying Dalong Fm. contain the ammonoid *Pseudotirolites* of Changxingian (uppermost Permian) age (sample JL1), but the overlying, presumably lowermost Triassic strata, which consist mainly of dark shales, are poorly exposed. Several ammonoid-rich, thin limestone beds of Dienerian age occur c. 8 m above sample JL1. Sample JL2 contains *Hubeitoceras yanjiaensis*, '*Koninckites*' cf. *timorense* and *Vishnuites pralambha*. '*K.*' cf. *timorense* was also found with *Jieshaniceras guizhouensis* gen. nov. in sample JL3. Furthermore, the nautiloid *Xiaohenautilus* Xu, 1988, is also abundant in samples JL2 and JL3. Sample JL6 contains *Proptychites candidus*. Macrofossils were not found higher in the section.

BIOSTRATIGRAPHICAL DISCUSSION

General subdivisions of the Early Triassic

The Early Triassic is commonly divided into two, three or four stages as follows: two stages (Induan and Olenekian, Kiparisova and Popov 1956, with the Induan encompassing the Griesbachian and Dienerian, and the Olenekian encompassing the Smithian and the Spathian); three stages (Griesbachian, Nammalian and Spathian, Guex 1978); or four stages (Griesbachian, Dienerian, Smithian and Spathian, Tozer 1965, 1967; Silberling and Tozer 1968). In this paper, we use the four stage subdivision, whose boundaries are well defined in terms of ammonoids. Moreover, new radiometric ages from South China indicate that the Spathian (*c.* 3 Ma) accounts for *c.* half of the duration of the Early Triassic (Ovtcharova *et al.* 2006). Durations of 1.4 ± 0.4 myr for the Griesbachian-Dienerian interval and of 0.7 ± 0.6 myr for the Smithian have been estimated (Galfetti *et al.* 2007*b*).

At Meishan, the Permian/Triassic boundary has been defined on the basis of the FAD of the conodont species *Hindeodus parvus* (Yin *et al.* 2001). If we recognize this definition, parts of the lower Griesbachian '*Otoceras* beds' would fall within the Permian, a premise not accepted by all Triassic workers (e.g. Tozer 2003; Shevyrev 2006). The Griesbachian/Dienerian boundary is defined by the first occurrence of Meekoceratids, which is a bio-event that can be traced world-wide (e.g. Shevyrev 2001). Interest in the Dienerian/Smithian (e.g. Induan/Olenekian) boundary is relatively recent, and several sections from China and the Himalayas have been proposed as GSSP candidates (Tong *et al.* 2003; Kozur 2006; Krystyn *et al.* 2007).

Chinese subdivisions of the earliest Triassic

Tien (1933) first documented the '*Ophiceras* beds' (Griesbachian) and '*Meekoceras* beds' (Dienerian) from Guizhou, thus indicating the presence of earliest Triassic ammonoid faunas. Hsü (1937) also reported an '*Otoceras* fauna' with very few well preserved specimens from Nanjing, Jiangsu, possibly signifying a Griesbachian age. However, Wang (1984) restudied this ammonoid assemblage and referred to it as a '*Koninckites* fauna', thus indicating a Dienerian age. Chao (1950, 1959), focussing essentially on Smithian ammonoids, recognized the following biostratigraphical subdivisions: 'Gyronitan', 'Flemingitan', 'Owenitan' and 'Columbitan', based on the scheme previously established by Spath (1934). More recently, Wang and He (1980) gave the following general, but perfectible outline of Early Triassic ammonoid successions of China (in ascending order): *Otoceras latilobatum* Zone, *Ophiceras (Lytophiceras) sakuntala* Zone and *Gyronites psilogyrus* Zone (based on data from Tibet); and *Proptychites kwangsiensis* Zone, *Koninckites lingyuensis* Zone and *Owenites costatus* Zone (based on Chao's data from South China). Xu (1988) reported mostly very poorly preserved cephalopods from Lichuan (Western Hubei) distributed within a sequence of three beds in the lower part of the Daye Fm. He assigned them to an early Dienerian *Vishnuites-Gyronites* assemblage and a late Dienerian *Koninckites-Xenodiscoides* assemblage. More recently, Tong *et al.* (2004) recognized the following ammonoid succession in Chaohu: the *Ophiceras-Lytophiceras* Zone, the *Gyronites-Prionolobus* Zone, and the *Flemingites-Euflemingites* Zone. However, ammonoid preservation in this section is very poor, and consequently, their identifications are questionable. Ammonoids of the *Ophiceras-Lytophiceras* zone from the Dongpan section (Guangxi) reported by Bu *et al.* (2006) are also very poorly preserved and not useful for comparison. Mu *et al.* (2007) interpreted their poorly preserved cephalopod fauna from the Daye Fm. of Guizhou as being of late Griesbachian age. However, we propose that this fauna is of early Dienerian age (see systematic section).

Our new findings essentially confirm Tien's (1933) report of the existence of two Early Triassic pre-Smithian ammonoid zones in South China. Based on our well preserved material from bed-rock controlled collections, we are able to update the biostratigraphical succession. Among the taxa documented herein, several possess broad geographical distribution and are therefore important for biostratigraphical correlation. In consideration of the present, somewhat inadequate state of knowledge of pre-Smithian ammonoid faunas from South China, it would be premature to introduce formal zonal names. Such usage would imply a well-established lateral reproducibility of the faunal sequence. Hence, the informal term 'beds' is utilized in this work to describe the local faunal sequence (Text-fig. 4).

'Otoceras *beds*'. Thus far, a correlative of the lower Griesbachian '*Otoceras* beds' has not been reported from southern Guizhou or northern Guangxi. In general, the

TEXT-FIG. 3. Stratigraphical columns of the studied sections showing horizons from which ammonoid samples were taken. Ammonoid faunas: *Opb*, '*Ophiceras* beds'; *Pcb*, '*Proptychites candidus* beds'; *Cb*, '*Clypites* beds'; *Kb*, '*Kashmirites kapila* beds'; *Fb*, '*Flemingites rursiradiatus* beds'; *Owb*, '*Owenites koeneni* beds'; *Ab*, '*Anasibirites multiformis* beds'; *TAb*, 'Tirolitid n. gen. A. beds'; *T/*Cb, '*Tirolites/*Columbites beds'; *Pb*, '*Procolumbites* beds'. See Text-fig. 2 for location and Table 1 for faunal content. Radiometric ages from Ovtcharova *et al.* 2006 and Galfetti *et al.* 2007*b*.

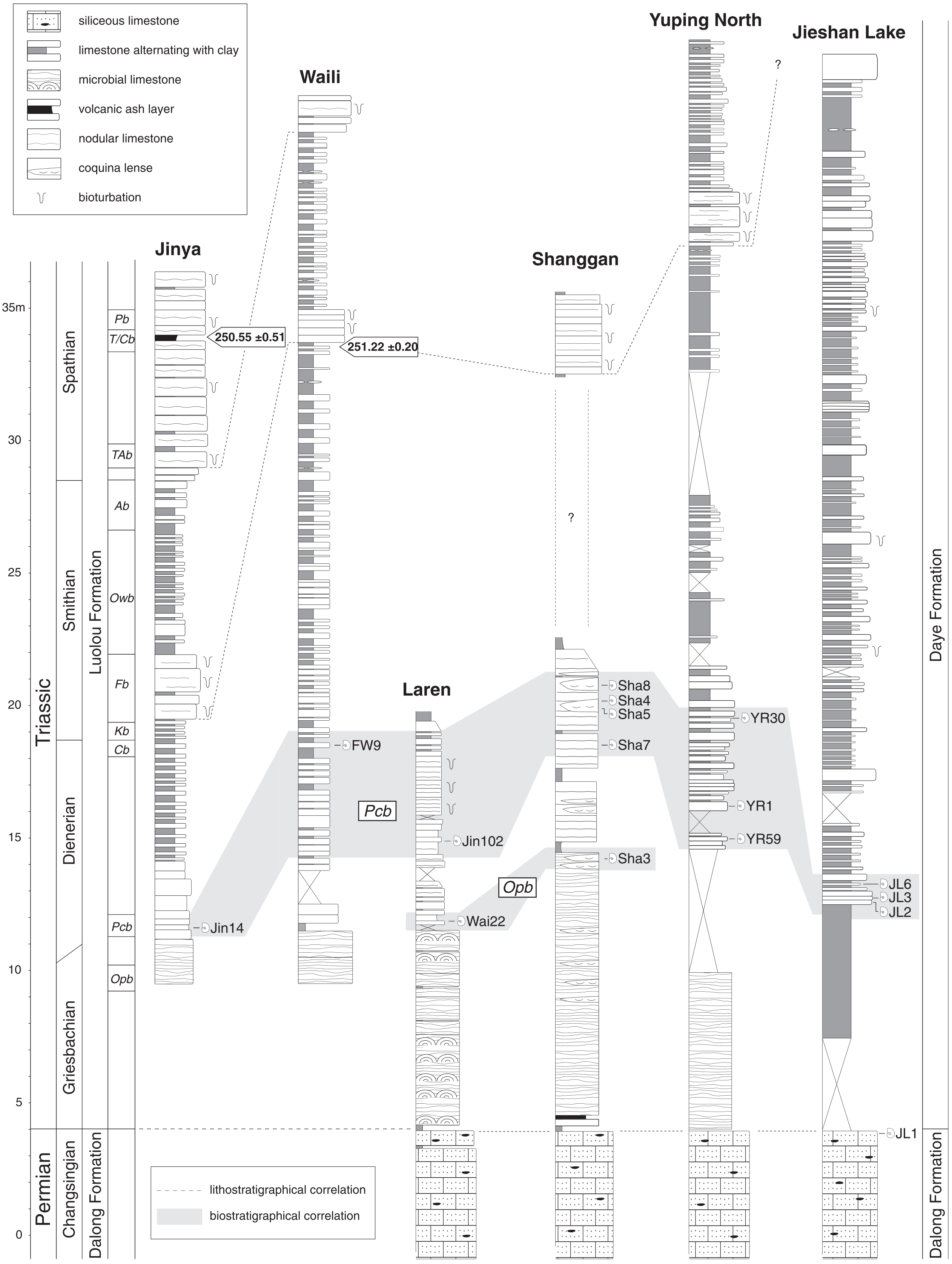
siliceous limestone
limestone alternating with clay
microbial limestone
volcanic ash layer
nodular limestone
coquina lense
bioturbation
Jinya
Waili
Laren
Shanggan
Yuping North
Jieshan Lake
35m
30
25
20
15
10
5
0
Triassic
Permian
Spathian
Smithian
Dienerian
Griesbachian
Changsingian
Luolou Formation
Dalong Formation
Daye Formation
Dalong Formation
Pb
T/Cb
TAb
Ab
Owb
Fb
Kb
Cb
Pcb
Opb
250.55 ±0.51
251.22 ±0.20
?
?
Jin14
FW9
Jin102
Wai22
Sha8
Sha4
Sha5
Sha7
Sha3
YR30
YR1
YR59
JL6
JL3
JL2
JL1
Pcb
Opb
lithostratigraphical correlation
biostratigraphical correlation

TABLE 1. Ammonoid occurrences in the studied sections.

Section	Sample	*Ophiceras* sp. indet.	*Xenodiscoides* sp. indet.	*Shangganites shangganense*	*Vishnuites pralambha*	*Proptychites candidus*	*Proptychites* sp. indet.	*Proptychitid* gen. indet.	*Hubeitoceras yanjiaensis*	*Anotoceras subtabulatus*	'*Koninckites*' cf. *timorense*	*Pleurambites radiatus*	*Prionolobus* cf. *atavus*	*Gyronites frequens*	*Pleurogyronites* sp. indet.	*Ambites* sp. indet.	*Jieshaniceras guizhouensis*
Jinya	Jin14				■						■	■					
Waili	FW9							■			■					■	
Laren	Jin102				■												
	Wai22	?															
Shanggan	Sha8			■													
	Sha4			■							■		■	■	■		
	Sha5										■						
	Sha7							■		■	■						
	Sha3	■															
Yuping	YR30					■					■						
	YR1						■										
	YR59		■			■											■
Jieshan Lake	JL6					■											
	JL3										■						■
	JL2				■				■		■						

'*Otoceras* beds' are less complete in the Tethyan realm than in the Boreal realm. For example, correlatives of the lowermost Griesbachian *Otoceras concavum* zone are still unknown within the Tethyan realm (Shevyrev 2006).

Wang (1984) reported a '*Hypophiceras* fauna', including ?*Otoceras* sp. from Meishan, but this fauna has been the subject of substantial controversy (Wang 1984; Yang *et al.* 1996). The questionable occurrence of ?*Otoceras* sp. is based on a single specimen, which is too poorly preserved for identification (e.g. Tozer 1994*b*; Shevyrev 2006). The '*Hypophiceras*' fauna, while probably Upper Permian in age, certainly shares no common elements with the Early Triassic '*Otoceras* beds' (Shevyrev 2006).

'Ophiceras *beds*'. These beds are hitherto characterized by the single occurrence of *Ophiceras* sp. indet. Thus, beds containing this ammonoid at Shanggan (sample Sha3) and probably also Waili (sample Wai22) are interpreted as being late Griesbachian in age.

Correlation of the 'Ophiceras beds' with other South Chinese sections remains uncertain since most other age-equivalent occurrences in China (including the Permian/Triassic GSSP at Meishan) yield only poorly preserved ammonoids. Most probably, the '*Ophiceras* beds' from Guangxi correspond to the *Ophiceras* beds from Guizhou described by Tien (1933), the *Ophiceras-Claraia* acme zone at Meishan (Yin *et al.* 1996), the *Ophiceras-Lytophiceras* zone from Chaohu (Tong *et al.* 2004), and the *Ophiceras-Lytophiceras* zone from Dongpan (Bu *et al.* 2006; Text-fig. 4).

Ophiceras is a cosmopolitan genus whose stratigraphical range is indicative of the upper Griesbachian (e.g. Shevyrev 2001). However, the Chinese species differs slightly from those of the Tethyan and the Arctic realm. Therefore, correlation with these realms must remain tentative since further substantiation is required.

'Proptychites candidus *beds*'. These well documented beds are characterized mainly by the *Proptychites candidus* – '*Koninckites*' cf. *timorense* association, but the following other taxa may co-occur: *Vishnuites pralambha*, *Hubeitoceras*, *Jieshaniceras guizhouensis* gen. nov., *Anotoceras subtabulatus* sp. nov., *Prionolobus*, *Gyronites*, *Pleurogyronites*, *Pleurambites radiatus* sp. nov., and *Shangganites shangganense* gen. nov. sp. nov. Due to the scattered occurrences of this fauna, no further reliable subdivision of these beds can be made. However, it appears that horizons with *Vishnuites* and *Hubeitoceras* are slightly older than those with *Shangganites shangganense* gen. nov. sp. nov., *Gyronites* and *Prionolobus*. All studied samples (except for Sha3 and Wai22) belong to the '*P. candidus* beds'.

The Chinese '*P. candidus* beds' are correlative with the *Candidus* Zone of British Columbia (Tozer 1994*a*), with which they share the following taxa: *P. candidus*, *Pleurogyronites*, *Prionolobus*, *Pleurambites*, and *Ambites*.

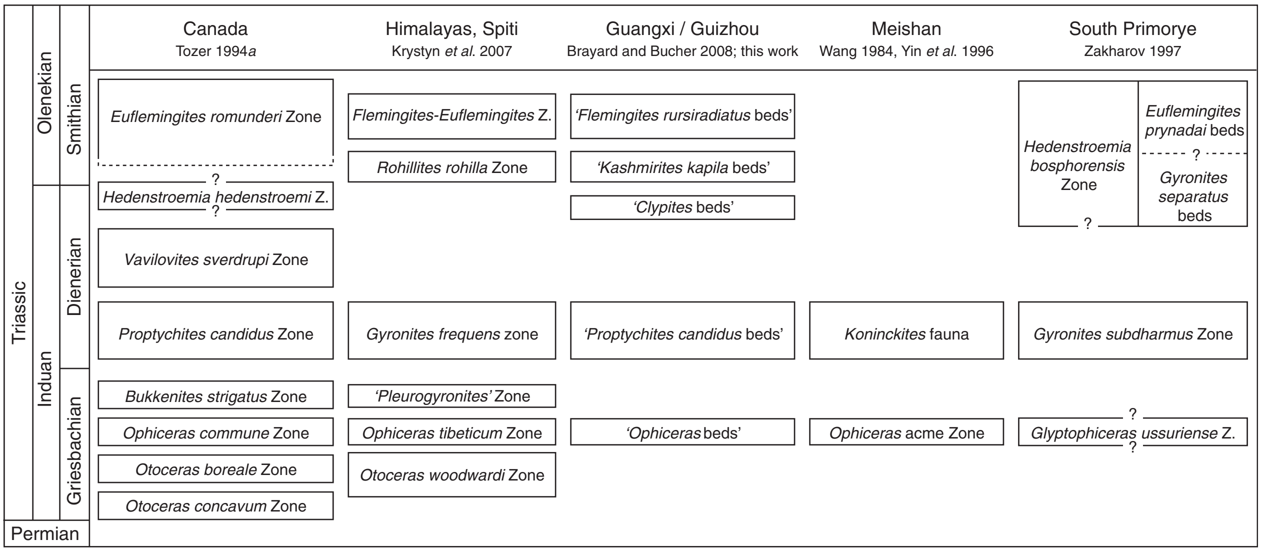

TEXT-FIG. 4. Biostratigraphical subdivisions of the Early Triassic of South China and correlation with zonations of other regions.

These beds are also correlative of the *Gyronites subdharmus* Zone of South Primorye (Kiparisova 1961; Zakharov 1968, 1997). Common taxa include '*Koninckites*' cf. *timorense*, and probably *P. candidus* (see systematic palaeontology). Furthermore, the Chinese '*P. candidus* beds' correlate well with the '*Gyronites* beds' of the Himalayas (Krystyn *et al.* 2007). In the Salt Range (Pakistan) *Gyronites frequens* and *Prionolobus atavus* are known from the Lower Ceratite Limestone (Waagen 1895; Guex 1978). Therefore, the '*P. candidus* beds' of South China correspond to this interval in the Salt Range section (*Gyronites frequens* Zone of Noetling [1905] and Guex [1978]). Correlation with the ammonoid succession from Nepal is hampered by the poor preservation of ammonoids from this area. Most probably the Chinese '*P. candidus* beds'correspond to the '*Gyronites frequens* Zone' of Waterhouse (1996*a*).

Unfossiliferous interval. Although ammonoids have not been found thus far in the interval between the '*P. candidus* beds' and the '*Clypites* sp. beds' (Brayard and Bucher 2008), ample room does exist for the upper Dienerian *Sverdrupi* zone of British Columbia (Tozer 1994*a*).

'Clypites *sp. beds*'. Brayard and Bucher (2008) have illustrated beds with the unique occurrence of a monospecific fauna, which probably corresponds to the latest Dienerian. Note than in Galfetti *et al.* (2007*a–c*) these beds were termed '*Hedenstroemia hedenstroemi* beds' and interpreted as correlatives of the early Smithian *Hedenstroemi hedenstroemi* Zone of the high-latitudes. Similarly, the subsequent earliest Smithian beds were first documented as '*Kashmirites densistriatus* beds' by Galfetti *et al.* (2007*a–c*) and renamed '*Kashmirites kapila* beds' by Brayard and Bucher (2008).

CONCLUSIONS

Intensive sampling of the Luolou Fm. in northwestern Guangxi and the Daye Fm. in southern Guizhou has resulted in the first report of reasonably well preserved Griesbachian and Dienerian ammonoids from these areas. The new local biostratigraphical sequence consists of the upper Griesbachian '*Ophiceras* beds', as well as the lower Dienerian '*Proptychites candidus* beds', which correlate with the *Candidus* Zone of British Columbia (Tozer 1994*a*). Since these faunas are remarkably similar to those from high palaeolatitude regions, they lend further support to the concept of weak and poorly contrasted latitudinal gradients of generic richness in the aftermath of the end-Permian mass extinction. Steep diversity gradients were not restored until Smithian time (Brayard *et al.* 2006, 2007*a*).

Since Griesbachian and Dienerian ammonoid localities are rare in the low palaeolatitude record, this report is a significant contribution to the biostratigraphy and biogeography of ammonoid evolutionary recovery. The Dienerian ammonoid record remains very incomplete, and thus far, data for the late Dienerian time interval are still far from adequate in the Tethyan realm.

Institutional abbreviations. PIMUZ, Paläontologisches Institut und Museum der Universität Zürich, Switzerland.

SYSTEMATIC PALAEONTOLOGY

Systematic descriptions follow the classification established by Tozer (1981, 1994*a*). The quantitative morphological range of each species is expressed utilizing the four classic geometrical parameters of the ammonoid shell: diameter (D), whorl height (H), whorl width (W) and umbilical diameter (U). The three parameters (H, W and U) are plotted in absolute values as well as in relation to diameter (H/D, W/D, and U/D) provided measurements were available for at least five specimens. All measurements are given in the Appendix. Sample numbers are reported on the measured profiles (Text-fig. 3).

Family XENOCELTITIDAE Spath, 1930

Genus XENODISCOIDES Spath, 1930

Type species. Xenodiscus perplicatus Frech, 1905, pl. 22, fig. 4.

Xenodiscoides sp. indet.

Plate 1, figure 22a–c

? 1959 *Xenodiscoides rotula* (Waagen); Chao, p. 212, pl. 5, fig. 9; pl. 7, figs 11–12.
? 1959 *Xenodiscoides serpentinus* Chao, p. 212, pl. 3, figs 3–5; pl. 4, figs 1–4; pl. 7, fig. 10.
? 1959 *Xenodiscoides* aff. *trapezoidalis* (Diener); Chao, p. 213, pl. 8, fig. 7.

Occurrence. A single small specimen from sample YR59.

Description. Very evolute, laterally compressed shell with a subtabulate venter and slightly convex flanks. Umbilicus wide and shallow with rounded shoulders. Ornamentation consists of rursiradiate ribs that are prominent on the inner flank, but disappear towards the outer part, not reaching the ventrolateral shoulders. Suture line not preserved.

Measurements. See Appendix.

Discussion. The type species, *Xenodiscoides perplicatus*, is more involute. Our specimen may be conspecific with specimens assigned to *X. rotula* Waagen by Chao (1959). However, Waagen's specimens differ by their falciform radial folds.

Family OPHICERATIDAE Arthaber, 1911

Genus OPHICERAS Griesbach, 1880

Type species. Ophiceras tibeticum Griesbach, 1880, p. 109, pl. 3, fig. 4.

Ophiceras sp. indet.

Plate 1, figures 1–12

? 1933 *Ophiceras sinense* Tien, p. 8, pl. 1, figs 1–3.
? 1933 *Ophiceras tingi* Tien, p. 9, pl. 1, fig. 4a–e.
? 1933 *Ophiceras* cf. *demissum* Tien, p. 10, pl. 1, fig. 5a, b.
? 1937 *Ophiceras* sp. Hsü, p.319, pl. 2, figs 3–5.
? 2004 *Lytophiceras* sp. Tong *et al.*, p. 43, pl. 1, fig. 6.
? 2006 *Lytophiceras* cf. *chamunda* (Diener); Bu *et al.*, fig. 3c.
? 2006 *Ophiceras tingi* Tien; Bu *et al.*, fig. 3h–i.
? 2006 *Ophiceras* sp. Bu *et al.*, fig. 3g, j, k.

Occurrence. Very common in sample Sha3, and possibly in sample Wai22.

Description. Small, evolute shell with a rounded venter and flat, subparallel flanks. Umbilicus relatively wide with vertical wall and marked, slightly rounded shoulders. Surface smooth or ornamented with fine prorsiradiate, slightly sinuous folds. Suture line ceratitic with a deep, weakly indented lateral lobe.

Measurements. Text-fig. 5; Appendix.

Discussion. Our specimens possibly represent juvenile individuals of *Ophiceras sinense*, which displays the same relative dimensions and shape. However, without adult specimens, no definitive assignment can be made. *O. tingi* and *O.* cf. *demissum* reported by Tien (1933) probably are synonyms of *O. sinense*. All other occurrences of

---

EXPLANATION OF PLATE 1

Figs 1–12. *Ophiceras* sp. indet. 1, PIMUZ 26725. 2a–c, PIMUZ 26726. 3a–e, PIMUZ 26727; 3e ×5. 4a–d, PIMUZ 26735. 5a–d, PIMUZ 26729. 6a–c, PIMUZ 26728. 7a–c, PIMUZ 26733. 8a–c, PIMUZ 26730. 9a–c, PIMUZ 26734; ×2. 10a, b, PIMUZ 26736; ×2. 11a–c, PIMUZ 26731; ×2. 12a–c, PIMUZ 26732. All from sample Sha3, Shanggan, Guangxi. Griesbachian.

Figs 13–17. *Shangganites shangganense* gen. nov. sp. nov. 13a, b, PIMUZ 26741; 13b ×2.5. 14a–d, holotype, PIMUZ 26737. 15a, b, PIMUZ 26739. 16a–c, PIMUZ 26740. 17a–c, PIMUZ 26738. All from sample Sha4, Shanggan, Guangxi. Dienerian.

Figs 18–21. *Vishnuites pralambha* Diener, 1897. 18a, b, PIMUZ 26744. 19a–c, PIMUZ 26742. 20a–c, PIMUZ 26743. 21, PIMUZ 26745; ×2. All from sample JL2, Jieshan Lake, Guizhou. Dienerian.

Fig. 22a–c. *Xenodiscoides* sp. indet. PIMUZ 26746; ×1.5. From sample YR59, Yuping North, Guangxi. Dienerian.

All natural size unless otherwise indicated. Asterisks indicate phragmocone end where known.

PLATE 1

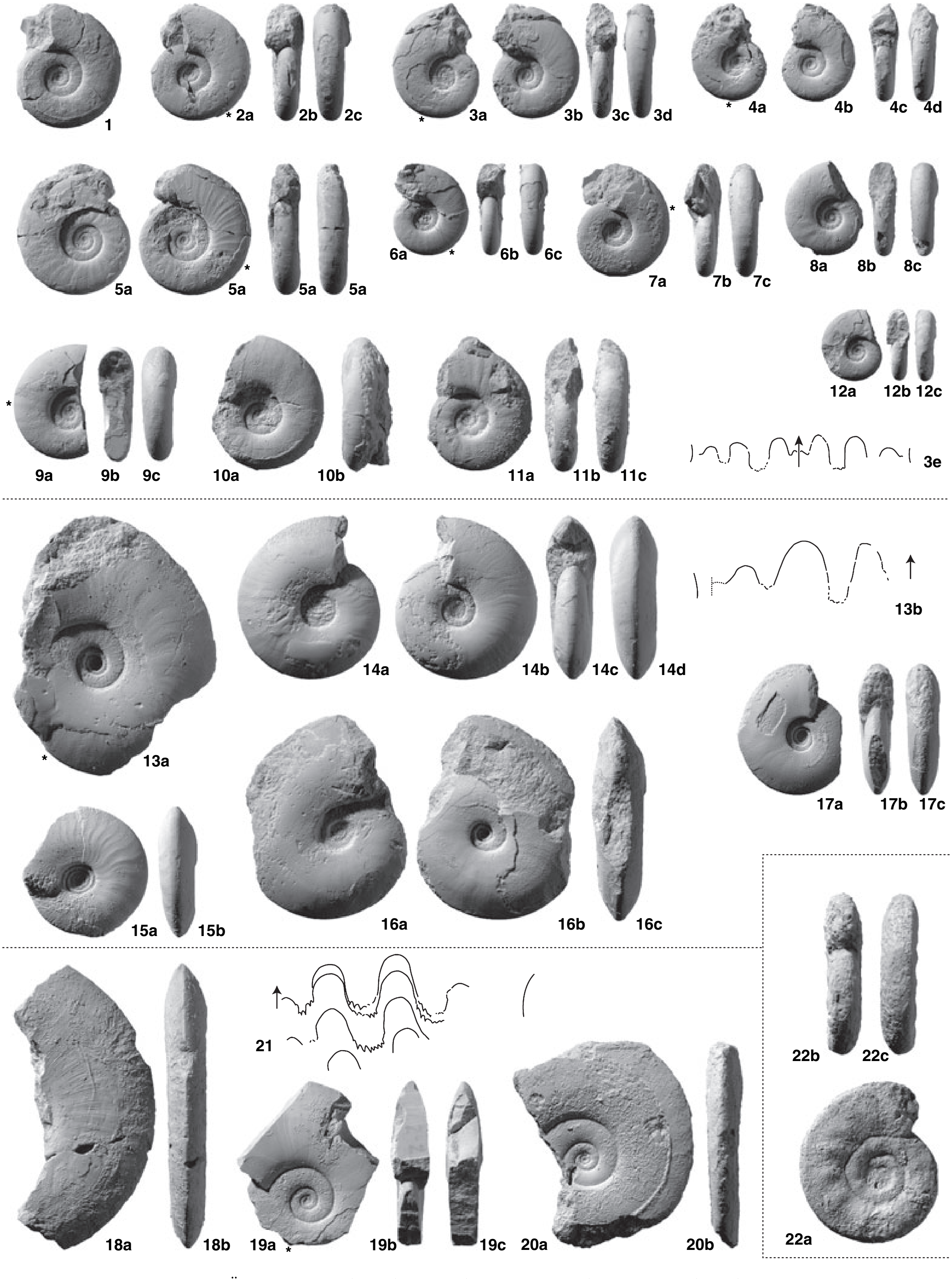

BRÜHWILER *et al.*, *Ophiceras, Shangganites, Vishnuites, Xenodiscoides*

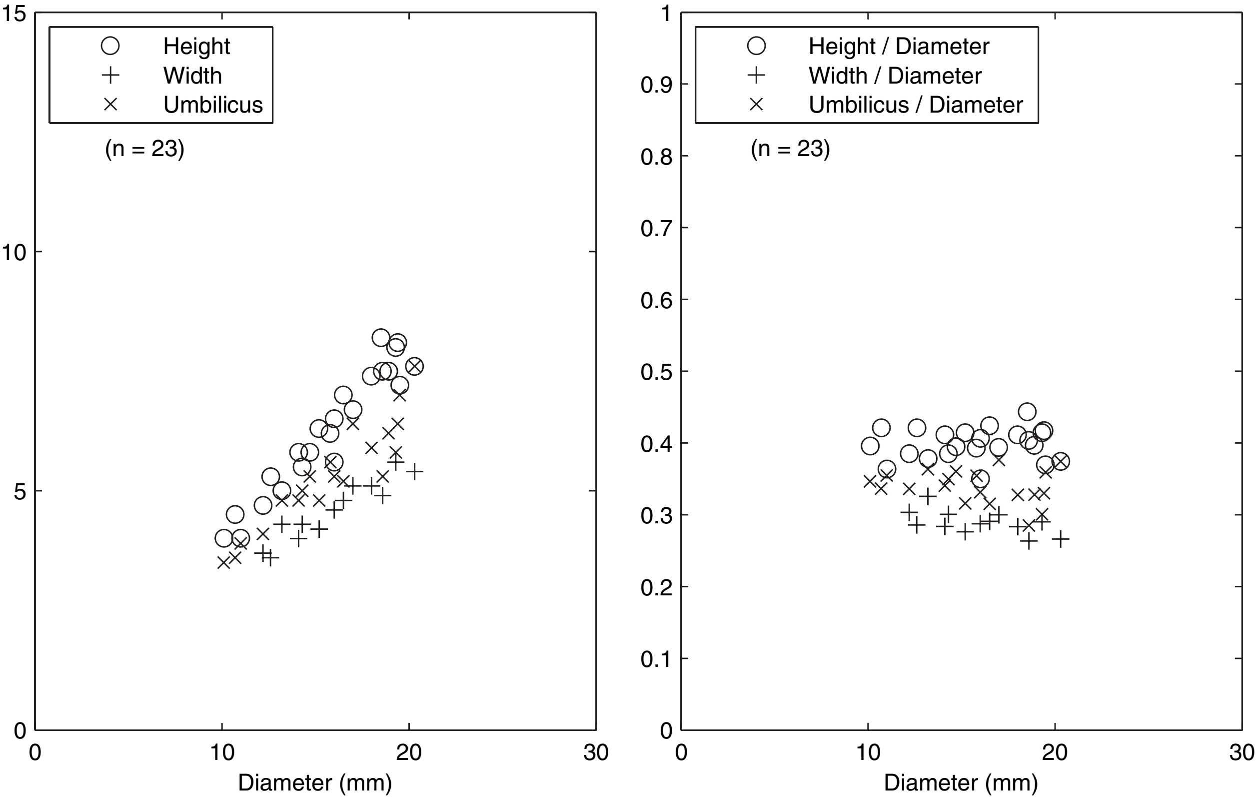

TEXT-FIG. 5. Scatter diagram of H, W, and U, and of H/D, W/D, and U/D for *Ophiceras* sp. indet.

Ophiceras and '*Lytophiceras*' reported from South China are based on very poorly preserved material and cannot be used for comparison.

Other species assigned to *Ophiceras* from the Himalayas (Griesbach 1880, Diener 1897), the Salt Range (Kummel 1970) and the Boreal realm (Spath 1935; Tozer 1994*a*) differ from *O.* aff. *sinense* by having convergent flanks and an oblique umbilical wall.

Genus SHANGGANITES gen. nov.

Derivation of name. Genus name refers to the type locality, Shanggan, Guangxi Province, South China.

Type species. Shangganites shangganense sp. nov.

Composition of the genus. Type species only.

Diagnosis. Smooth, discoidal and moderately involute ophiceratid with a narrowly rounded, subacute venter and angular umbilical shoulders.

Discussion. This genus is more involute and much thicker than *Vishnuites* Diener, 1897. It also resembles *Subvishnuites* Spath, 1930, of Smithian age. However, *Shangganites* is much more involute and displays a vertical umbilical wall. The assignment of *Shangganites* to Ophiceratidae is based mainly on its similarity with *Vishnuites*.

Shangganites shangganense gen. nov. sp. nov.
Plate 1, figures 13–17

Derivation of name. From the town of Shanggan, Guangxi Province, South China.

Holotype. Specimen PIMUZ 26737 (Pl. 1, fig. 14a–d).

Type locality and horizon. Loc. Sha4, Shanggan, Guangxi, South China (Text-fig. 2); Early Triassic, Dienerian.

Occurrence. Very common in samples Sha4 and Sha8.

Diagnosis. As for the genus.

Description. Discoidal, moderately involute shell with convex flanks converging to a narrowly rounded venter. Venter very slightly flattened on some specimens. Maximum whorl width located slightly below mid-flank. Umbilicus small with vertical wall and angular shoulders. Growth lines fine and biconcave. Ornamentation consists of fine biconcave folds and a very delicate strigation on the venter of some specimens. Suture line weakly ceratitic with broad second lateral saddle.

Measurements. Text-fig. 6; Appendix.

Genus VISHNUITES Diener, 1897

Type species. Xenaspis (Vishnuites) pralambha Diener, 1897, p. 88, pl. 7, figs 4–5.

Vishnuites pralambha Diener, 1897
Plate 1, figures 18–21

1897 *Xenaspis (Vishnuites) pralambha* Diener, p. 88, pl. 7, figs 4–5.
? 1913 *Vishnuites pralambha* Diener; Diener, p. 21, pl. 3, fig. 4a, b.
? 1959 *Vishnuites marginalis* Chao, p. 190, pl. 11. figs 17–18.
1961 *Vishnuites (Vishnuites)* sp. indet. Kiparisova, p. 44, pl. 9, fig. 1, text-fig. 12.
1961 *Vishnuites (Paravishnuites?)* sp. indet. Kiparisova, p. 45, pl. 8, figs 7–8, text- fig. 13.
1981 *Vishnuites* cf. *pralambha* Diener; Bando, p. 152, pl. 15, fig. 2.
? 1988 *Vishnuites huazhongensis* Xu, p. 441, pl. 1, fig. 8, text-fig. 6.
? 1988 *Vishnuites lichuanensis* Xu, p.441, pl. 1, fig. 3, pl. 2, fig. 10, text-fig. 7.
? 1988 *Vishnuites marginalis* Xu, p. 443, pl. 2, fig. 1, text-fig. 8.
? 1988 *Vishnuites orientalis* Xu, p. 443, pl. 2, fig. 6, text-fig. 9.
1988 *Vishnuites yangziensis* Xu, p. 444, pl. 1, fig. 9, pl. 2, fig. 3, text-fig. 10.
? 1994 *Vishnuites pralambha* Diener; Waterhouse, p. 61, pl. 4, figs 11–14.
2007 *Vishnuites wenjiangsiensis* Zakharov and Mu, figs 3.12–17, 5.1.
2007 *Vishnuites* cf. *yangziensis* Xu; Zakharov and Mu, p. 860, figs 5.2, 6.3, 6.4, 6.6, 6.8, 6.10, 6.12.
2007 *Pseudovishnuites guidingensis* Zakharov and Mu, p. 862, figs 5.3, 6.1, 6.2, 6.5.
v 2007*b* *Vishnuites*, Galfetti *et al.*, p. 594.

Occurrence. Common in sample JL2.

Description. Moderately evolute, very compressed shell with an acute venter and convex flanks. Maximum whorl width occurs at mid-flank. Umbilicus broad and shallow with low, rounded shoulders. Outer shell smooth, except for sinuous growth lines. Suture line ceratitic with small, numerous indentations of the lobes. One specimen exhibits septal crowding at H = 22 mm.

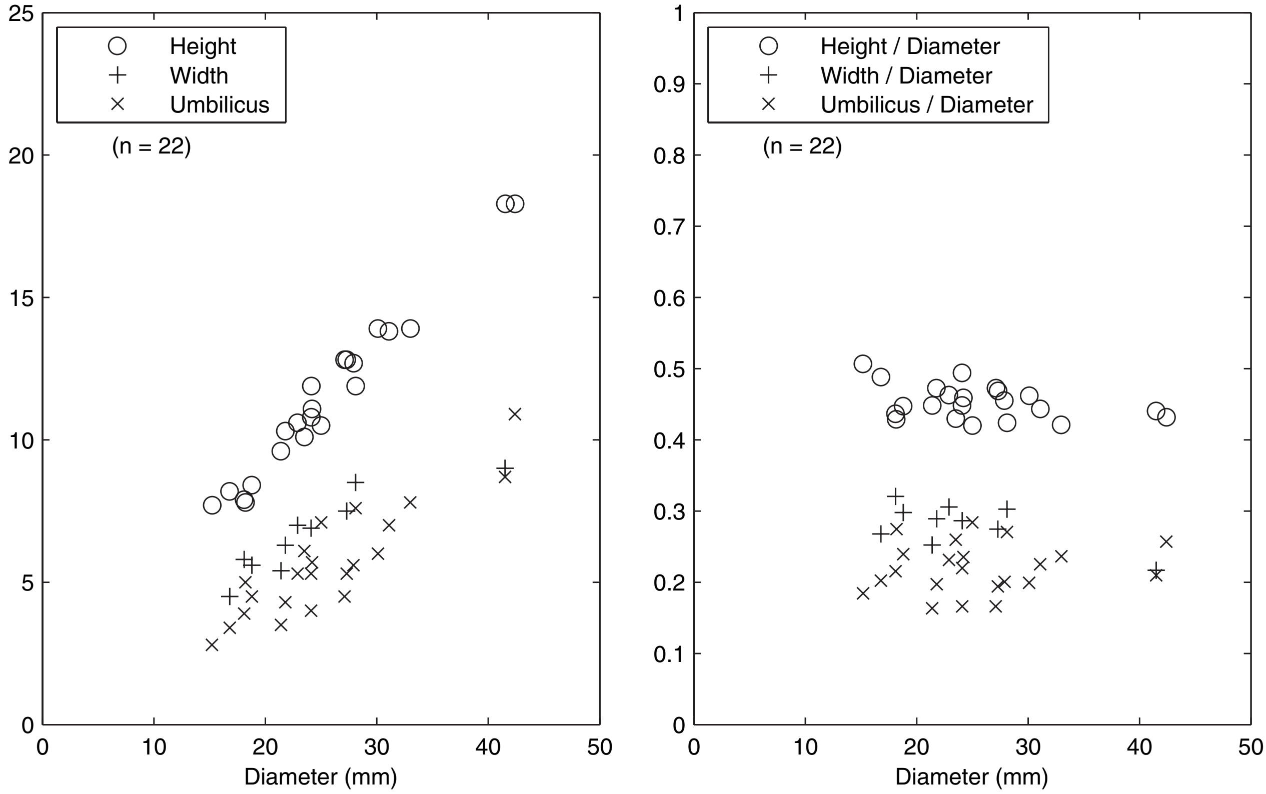

TEXT-FIG. 6. Scatter diagram of H, W, and U, and of H/D, W/D, and U/D for *Shangganites shangganense* gen. nov. sp. nov.

Measurements. See Appendix.

Discussion. The specimen from Kashmir assigned to *Vishnuites pralambha* by Diener (1913) is associated with *Glyptophiceras*, which is known to be of latest Smithian age (Brühwiler *et al.* 2007). Therefore, it is unlikely that Diener's specimen is assignable to *Vishnuites*. The numerous Chinese species of *Vishnuites* and the genus *Pseudovishnuites* erected by Xu (1988) and Zakharov and Mu (in Mu *et al.* 2007), respectively, exhibit no significant differences from *V. pralambha*, as near as can be seen from their illustrated specimens, which are poorly preserved. The single specimen of *Vishnuites marginalis* described by Chao (1959) is too small and too poorly preserved for comparison. *Vishnuites ('Paravishnuites') oxynotus* and *V. ('P.') striatus* from Greenland (Spath 1935) are more involute and have a slightly higher whorl section than the Tethyan species, *V. pralambha*. *'Paravishnuites' sterni* Trümpy, 1969, differs by having a low, but steep, umbilical wall, and *'P.' paradigma* Trümpy, 1969, by a high umbilical wall on the outer whorls. *'Vishnuites' wordiei* and *'V.' decipiens* Spath, 1930, from Greenland display broader whorl sections and much less acute venters than true *Vishnuites*, and were subsequently assigned to *Wordieoceras* by Tozer (1971, 1994*a*). *V. kummeli* Tozer, 1994*a*, from the Griesbachian *Otoceras boreale* Zone of Arctic Canada, is more involute and inflated and displays a less acute venter than *V. pralambha*. The Nepalese ammonoids assigned to *V. pralambha* by Waterhouse (1994) are too poorly preserved for proper identification.

Unfortunately, the precise stratigraphical distribution of *Vishnuites* remains unclear. According to Diener (1897), *Vishnuites* occurs within the '*Otoceras* beds' of the Himalayas, and this stratigraphical occurrence is similar to the Griesbachian boreal occurrences of this genus (Spath 1935; Tozer 1994*a*). However, Bando (1981) indicated that *Vishnuites* from Kashmir occurs well above the horizon with *Ophiceras tibeticum* within the *Paranorites-Vishnuites* Zone, possibly indicating a Dienerian age. This is at oddd with the stratigraphical position given by Diener (1897) and Tozer (1994*a*). Chao's (1959) *Vishnuites marginalis* originates from the 'Gyronitan', which may correspond to the Dienerian. In northwestern Guangxi and southern Guizhou (this work), *Vishnuites* is associated with *Hubeitoceras yangjiaensis*, '*Koninckites*' cf. *timorense* and *Pleurambites radiatus* sp. nov., thereby, indicating a true Dienerian age. Thus, in light of previous work and based on our new data, *Vishnuites* is now known to occur both in the Griesbachian and the lower Dienerian.

Family PROPYTCHITIDAE Waagen, 1895

Genus PROPTYCHITES Waagen, 1895

Type species. Ceratites lawrencianus de Koninck, 1863, p. 14, pl. 6, fig. 3.

Proptychites candidus Tozer, 1961

Plate 2, figures 1–2

? 1933 *Meekoceras kweichowense* Tien, p. 16, pl. 2, fig. 1a–e.
1961 *Proptychites candidus* Tozer, p. 57, pl. 11, fig. 1a–c.
1967 *Proptychites candidus* Tozer; Tozer, p. 18, 51, 52, pl. 4, fig. 1a, b.
? 1968 *Proptychites hiemalis* Diener; Zakharov, p. 93, pl. 17, figs 6–7.
? 1988 *Lytophiceras? vishnuoides* Spath; Xu, p. 441, pl. 1, figs 5, 10; pl. 2. fig. 5: pl. 4; text-fig. 5.
? 1988 *Paranorites elegans* Xu, p. 448, pl. 4, figs 4–5.
1994 *Proptychites candidus* Tozer; Tozer, p. 61, pl. 11, figs 4–5; pl. 12, figs 3–5, 13.
? 2007 *Proptychites* aff. *candidus* Tozer; Zakharov and Mu, p. 864, figs 10.17, 10.18, 11.1.

Occurrence. Samples YR59, YR30 and JL6.

Description. Moderately involute, thick platyconic shell with an arched venter, indistinct ventral shoulders and slightly convex flanks. High, vertical umbilical wall with rounded shoulders. Outer shell smooth, except for fine, radial, slightly sinuous growth lines. Occasionally, bundled growth lines may impart

---

EXPLANATION OF PLATE 2

Figs 1–2. *Proptychites candidus* Tozer, 1961. 1a–d, PIMUZ 26748; 1a–c ×0.5. From sample JL6, Jieshan Lake, Guizhou. Dienerian. 2a–c, PIMUZ 26747. From sample YR30, Yuping North, Guangxi. Dienerian.

Figs 3–5. *Proptychites* sp. indet. 3a–c, PIMUZ 26749. 4a–c, PIMUZ 26750. 5, PIMUZ 26751. All from sample YR1, Yuping North, Guangxi. Dienerian.

Figs 6–8. Proptychitid gen. et sp. indet. 6a–d, PIMUZ 26752; 6d ×1.5. From sample Sha 7, Shanggan, Guangxi. Dienerian. 7, PIMUZ 26753. From sample Sha 7, Shanggan, Guangxi. Dienerian. 8a–c, PIMUZ 26754; 8a ×2. From sample FW9, Waili, Guangxi. Dienerian.

All natural size unless otherwise indicated.

PLATE 2

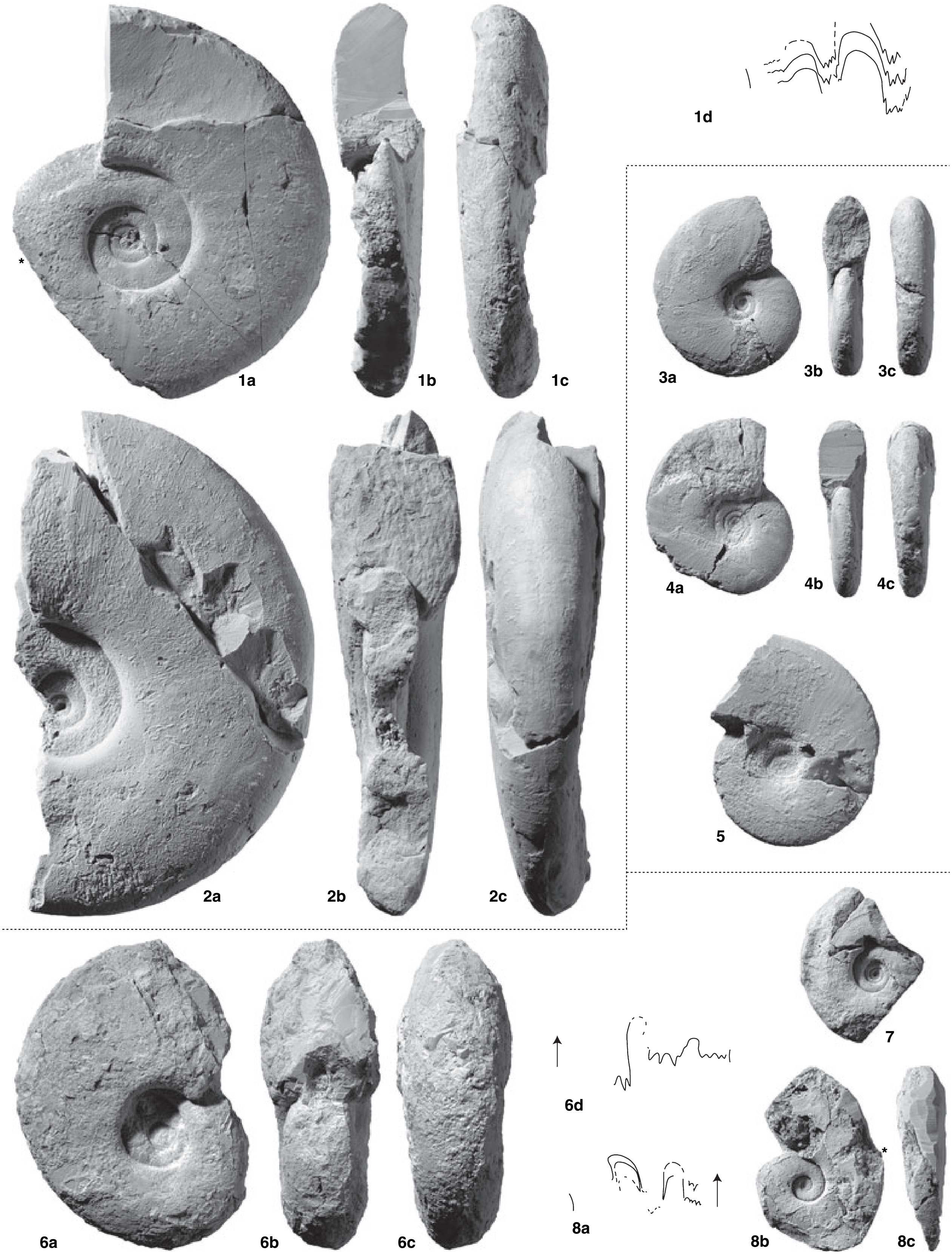

BRÜHWILER *et al.*, *Proptychites*, proptychitid gen. indet.

weak folds on flanks and venter. Suture line with rather deeply indented lobes and broad saddles. Second lateral saddle slightly asymmetrical, top of third lateral saddle flattened.

Measurements. See Appendix.

Discussion. Whorl sections of our specimens are thinner than most of the Canadian specimens illustrated by Tozer (1961, 1994*a*). However, as stated by Tozer (1961), this species displays a rather variable width. '*Meekoceras*' *kweichowense* Tien, 1933, is possibly a compressed variant of *Proptychites candidus*. *P. hiemalis* Diener, 1895, from eastern Siberia differs by its high, narrow saddles. However, the specimen from the same area assigned to *P. hiemalis* by Zakharov (1968) is very close to *P. candidus*. *P. candidus* is the index species of the lower Dienerian *Candidus* Zone of the Canadian Arctic (Tozer 1994*a*).

Proptychites sp. indet.
Plate 2, figures 3–5

Occurrence. Sample YR1.

Description. Moderately involute, thick platyconic shell with rounded venter and convex flanks. Maximum whorl width located slightly below mid-flank. Umbilicus with rounded shoulders and an oblique wall. Growth lines fine, projected and sinuous. Suture line not preserved on our material.

Measurements. Text-fig. 7; Appendix.

Discussion. *Proptychites* sp. indet. differs from *Proptychites candidus* by its oblique umbilical wall and projected growth lines.

Proptychitid gen. et sp. indet.
Plate 2, figures 6–8

? 1988 *Gyrophiceras orientale* Xu, p. 445, pl. 2, fig. 4a, b, text-fig. 13.
? 1988 *Gyrophiceras hubeiense* Xu, p. 445, pl. 2, fig. 12, text-fig. 12.

Occurrence. Only three relatively poorly preserved specimens from samples FW9 and Sha7.

Description. Evolute shell with a subquadrate whorl section characterized by rapidly increasing whorl height and nearly flat, parallel, but slightly convex flanks. Subtabulate venter with angular ventral shoulders on inner whorls, and rounded venter with rounded shoulders on outer whorls. Umbilicus deep with high,

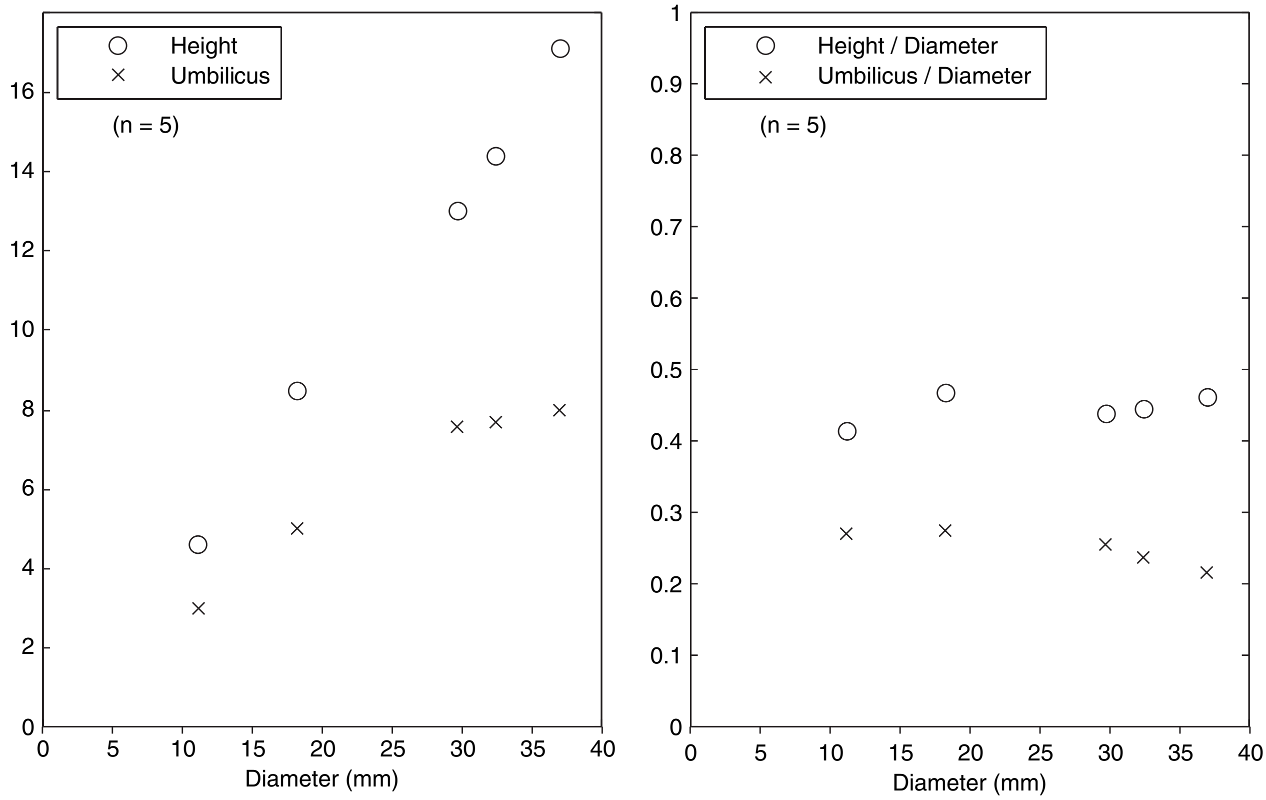

TEXT-FIG. 7. Scatter diagram of H, W, and U, and of H/D, W/D, and U/D for *Proptychites* sp. indet.

vertical wall and rounded shoulders. Surface smooth. Suture line incompletely known, but visible portion is ceratitic with high, narrow saddles.

Measurements. See Appendix.

Discussion. This species resembles *Proptychites scheibleri* Diener 1897. However, due to the relatively poor preservation of our specimens, it is not possible to make a generic or specific assignment with any degree of confidence.

Genus HUBEITOCERAS Waterhouse, 1994

Type species. Koninckites yanjiaensis Xu, 1988, p. 452, pl. 3, figs 12–13.

Hubeitoceras yanjiaensis (Xu, 1988)
Plate 4, figures 3–6

1988	*Koninckites yanjiaensis* Xu, p. 452, pl. 3, figs 12–13.
? 1988	*Koninckites hubeiensis* Xu, p. 450, pl. 3, figs 8, 15.
? 1988	*Koninckites kraffti* Spath; Xu, p. 451, pl. 3, figs 10, 14.
? 1988	*Koninckites lingyunensis* Chao; Xu, p. 451, pl. 3, fig. 5, pl. 4, fig. 1.
? 1988	*Koninckites xiaohensis* Xu, p. 452, pl. 1, fig. 4, pl. 2, figs 11, 13.

Occurrence. Common in sample JL2.

Description. Very involute, thick platyconic shell with a narrowly rounded venter and slightly convex flanks. Venter slightly flattened on inner whorls. Small umbilicus with a high, slightly oblique to vertical wall and rounded shoulders. Growth lines distinct, fine and falciform. Ornamentation consists of low falciform folds. Suture line ceratitic with broad third lateral saddle.

Measurements. Text-fig. 8; Appendix.

Discussion. Hubeitoceras yanjiaensis differs from '*Koninckites*' cf. *timorense* described below by its distinct ornamentation and its rounded venter.

Among our material, one specimen (Pl. 4, fig. 6) differs from the others by its greater involution, more compressed whorls and prorsiradiate folds. It is interpreted herein as being a compressed variant.

Genus KONINCKITES Waagen, 1895

Type species. Koninckites vetustus Waagen, 1895, p. 261, pl. 27, figs 4–5.

'*Koninckites*' cf. *timorense* (Wanner, 1911)
Plate 3, figures 1–4; Plate 4, figures 1–2

? 1895	*Koninckites davidsonianus* (*not* de Koninck); Waagen, p. 272, pl. 33, fig. 4a–d.
? 1911	*Meekoceras timorense* Wanner, p. 185, pl. 6, figs 2–3, text-fig. 2.
1961	*Koninckites timorensis* (Wanner); Kiparisova, p. 82, pl. 16, figs 2–4, 6, text-figs 39–42.
1968	*Koninckites timorensis* (Wanner); Zakharov, p. 89, pl. 17, figs 1–3, text-fig. 20a.
? 1988	*Koninckites kraffti* Spath; Xu, p. 451, pl. 3, figs 10, 14, text-fig. 23.
? 1988	*Prionolobus hubeiensis* Xu, p. 447, pl. 1, fig. 2, text-fig. 15.
? 2007	*Proptychites* cf. *markhami* Diener; Zakharov and Mu, p. 864, figs 7.4, 9.3–9.9, 10.1–10.9.
v 2007*b*	*Meekophiceras*, Galfetti *et al.*, p. 594.

Occurrence. Common in the samples JL2, JL3, Sha4, Sha5, Jin14, FW9 and YR30.

Description. Involute, platyconic shell with tabulate venter and somewhat abruptly rounded ventral shoulders. Venter becomes slightly rounded on outer whorls. Maximal thickness above the inner third of the height of the flanks. Narrow umbilicus with a high, vertical wall and marked, abruptly rounded shoulders. Growth lines fine and biconcave, most pronounced near the umbilicus. Low radial folds may be present on the outer part of the flanks. Venter ornamented with fine strigation. Suture line with narrow first lateral saddle, and numerous denticulations of the lobes, which tend to partly ascend the sides of the saddles.

Measurements. Text-fig. 9; Appendix.

Discussion. The specimens from Primorye assigned to *Koninckites timorensis* (Wanner 1911) by Kiparisova (1961) and Zakharov (1968) are without any doubt identical with our specimens. However, the type material of *Meekoceras timorense* Wanner 1911 from Timor is slightly more evolute than our species, and has a suture line with a slightly more complex auxiliary series. They may also be of younger, i.e. early Smithian age since they are associated with *Rohillites* but this may also be an effect of condensation. Thus, the specimens from Timor are not definitely conspecific with our specimens and the specimens from Primorye. The assignment of this species to *Koninckites* as proposed by Kiparisova (1961) and Zakharov (1968) is not fully convincing either since the type species (*K. vetustus* Waagen 1895) differs by having a shallow umbilicus with a rounded margin. However, no other known genus (e.g. *Fuchsites*, *Kingites*, *Kymatites*, *Meekophiceras*, or *Radioceras*) corresponds to our species any better but in view of the incomplete knowledge and the general similarity of these genera, it seems unwise to

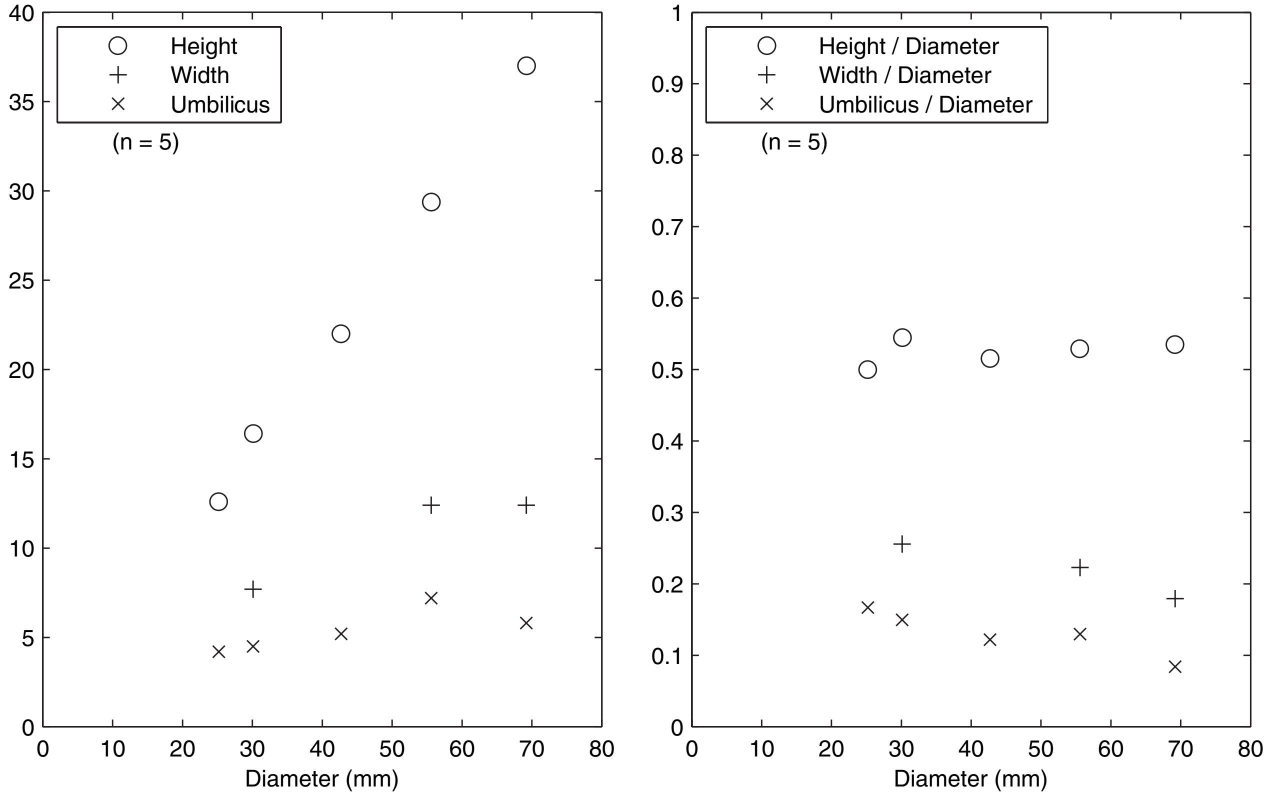

TEXT-FIG. 8. Scatter diagram of H, W, and U, and of H/D, W/D, and U/D for *Hubeitoceras yanjiaensis* (Xu, 1988).

erect a new genus before a profound revision of the Dienerian ammonoid systematics has been made. Therefore, we use the genus name as proposed by Kiparisova (1961) and Zakharov (1968) for the time being.

Genus PRIONOLOBUS Waagen, 1895

Type species. Prionolobus atavus Waagen, 1895, p. 309, pl. 34, fig. 4a, b; pl. 35, fig. 4a, b.

Prionolobus cf. *atavus* Waagen, 1895
Plate 5, figs 4–6

1895 *Prionolobus atavus* Waagen, p. 309, pl. 34, fig. 4a, b; pl. 35, fig. 4a, b.

Occurrence. Sha4.

Description. Moderately involute, compressed shell with distinctively tabulate venter and angular ventrolateral shoulders. Flanks convex, becoming flatter towards ventral shoulders. Maximum whorl width occurs at mid-flank. Umbilical wall low with rounded shoulders. Surface either smooth or ornamented with very faint radial folds at mid-flank region. Suture line incompletely known; preserved portion with broad, tapering saddles.

Measurements. See Appendix.

Discussion. The flanks of *Prionolobus atavus* from the Salt Range are more broadly rounded than our specimens. Waagen (1895) reported various species of *Prionolobus,* which essentially differ by being more or less involute. This phenomenon may simply reflect intraspecific variation.

EXPLANATION OF PLATE 3

Figs1–4. '*Koninckites*' cf. *timorense* (Wanner, 1911). 1a–c, PIMUZ 26763. From sample JL3, Jieshan Lake, Guizhou. Dienerian. 2a, b, PIMUZ 26762. From sample Sha5, Shanggan, Guangxi. Dienerian. 3a–c, PIMUZ 26765; 3c ×1.5. From sample JL3, Shanggan, Guangxi. Dienerian. 4a–c, PIMUZ 26764. From sample JL3, Jieshan Lake, Guizhou. Dienerian.

Fig. 5a–d. *Anotoceras subtabulatus* sp. nov. Holotype, PIMUZ 26755. From sample Sha7, Shanggan, Guangxi. Dienerian.

All natural size unless otherwise indicated.

PLATE 3

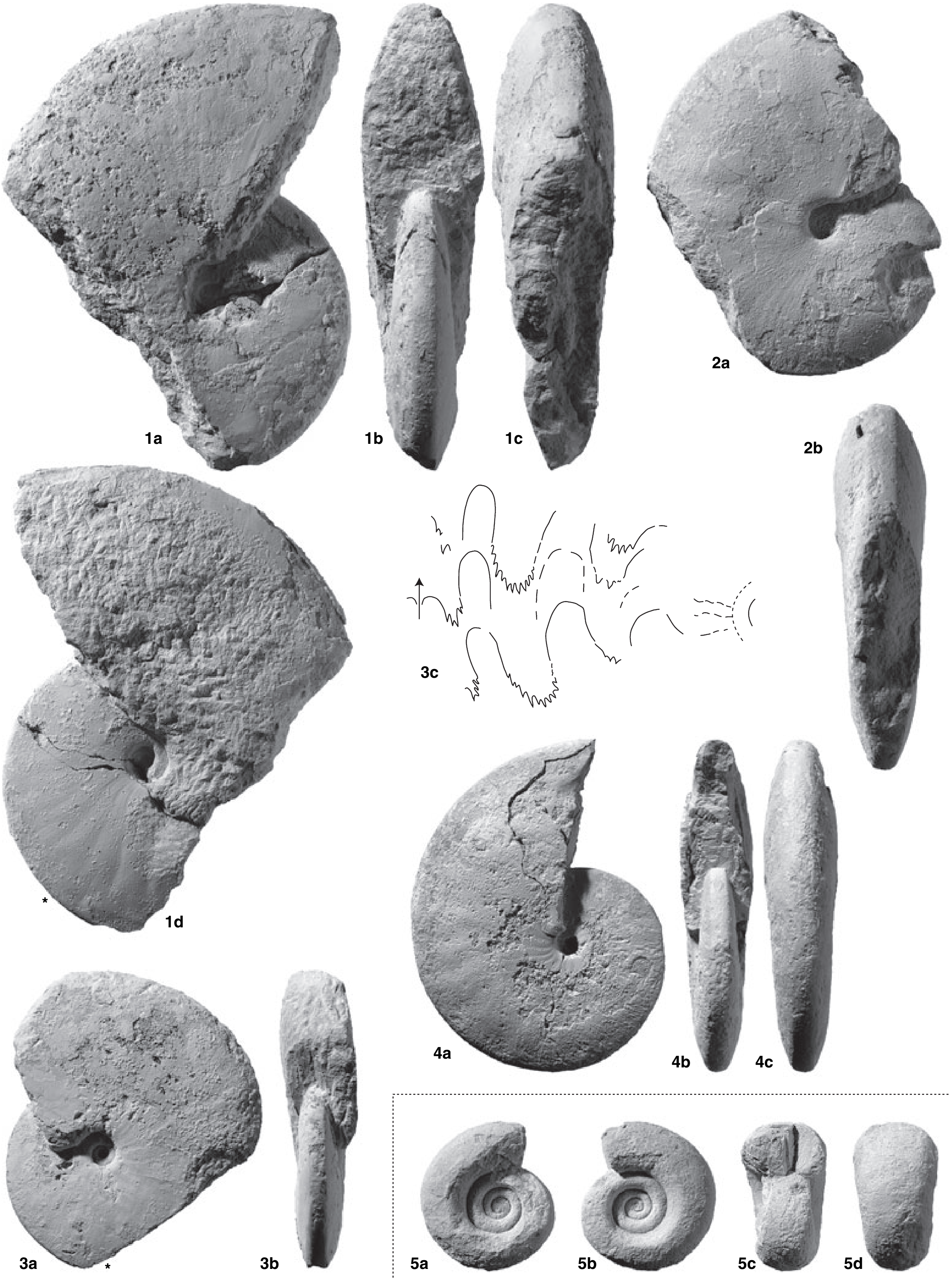

BRÜHWILER *et al.*, ‘*Koninckites*’ *Anotoceras*

Genus GYRONITES Waagen, 1895

Type species. Gyronites frequens Waagen, 1895, p. 292, pl. 37, figs 1–4; pl. 40, fig. 4.

Gyronites frequens Waagen, 1895
Plate 5, figs 7–8

1895 *Gyronites frequens* Waagen, p. 292, pl. 37, figs 1–4; pl. 40. fig. 4.
v 1978 *Gyronites frequens* Waagen; Guex, pl. 1, fig. 3.

Occurrence. Sha4.

Description. Evolute, compressed shell with distinctively tabulate venter and angular ventrolateral shoulders. Flanks convex, becoming flatter towards ventral shoulders. Maximum whorl width occurs just above umbilical shoulders. Umbilical wall low, with rounded shoulders. Outer shell smooth. Suture line with broad saddles and narrow lateral lobe. Indentations of the lobes not visible on our specimens.

Measurements. See Appendix.

Discussion. Whorls of our specimens are slightly wider than those measured by Waagen (1895). *Gyronites frequens* typically is more evolute than *Prionolobus* cf. *atavus. G. subdharmus* from South Primorye (Kiparisova 1961; Zakharov 1968) is very close, but differs by having low ribs.

Genus PLEURAMBITES Tozer 1994*a*

Type species. Pleurambites frechi Tozer, 1994*a*, p. 68, pl. 13, figs 1–3, 6, 14.

Pleurambites radiatus sp. nov.
Plate 5, figures 1–3

? 1937 *Ophiceras* sp. – Hsü, p. 319, pl. 2, fig. 3 only.

Derivation of name. Refers to the radial ribbing of this species.

Holotype. Specimen PIMUZ 26766 (Pl. 5, fig. 1a–d).

Type locality and horizon. Loc. Jin14, Jinya, Guangxi Province, South China (Text-fig. 2); Early Triassic, Dienerian, '*Proptychites candidus* beds'.

Occurrence. Jin14.

Diagnosis. Pleurambites with radial and very slightly sinuous ribs.

Description. Evolute, compressed shell with distinctively tabulate venter, angular ventrolateral shoulders and convex flanks. Umbilicus with vertical or slightly overhanging wall and rounded shoulders. Ornamentation consists of radial, very slightly sinuous ribs on the flanks. Ribs broad on inner whorls, becoming finer and denser on outer whorls. Suture line with rather high saddles and deep lobes. Indentations of first lateral lobe not totally preserved, second lateral lobe smooth on our specimens.

Measurements. See Appendix.

Discussion. The type species *Pleurambites frechi* is distinguished by its projected, more sinuous ribs. *Xenodiscoides* sp. indet. is more evolute and has broader, more distant ribs.

Genus PLEUROGYRONITES Tozer, 1994*a*

Type species. Pleurogyronites kraffti Tozer, 1994*a*, p. 66, pl. 10, fig. 5a, b; fig. 11a.

Pleurogyronites sp. indet.
Plate 5, figure 9a–d

? 1895 *Gyronites plicosus* Waagen, p. 298, pl. 38, fig. 11a, b.
? 1895 *Gyronites rotula* Waagen, p. 300, pl. 38, figs 3–5.
? 1895 *Gyronites radians* Waagen, p. 302, pl. 38, figs 6–8.

Occurrence. A single specimen from sample Sha4.

Description. Very evolute, platyconic shell with subtabulate venter and rounded ventrolateral shoulders. Umbilicus wide with vertical wall and rounded shoulders. Surface ornamented with slightly rursiradiate, distant, sinuous ribs. Ribs more

---

EXPLANATION OF PLATE 4

Figs 1–2. '*Koninckites*' cf. *timorense* (Wanner, 1911). 1a–c, PIMUZ 26760. Dienerian. 2a, b, PIMUZ 26761. All from sample Sha4, Shanggan, Guangxi.

Figs 3–6. *Hubeitoceras yanjiaensis* (Xu, 1988). 3a–e, PIMUZ 26757; 3e ×3. 4a–c, PIMUZ 26759. 5a–d, PIMUZ 26758. 6a–d, PIMUZ 26756. All from sample JL2, Jieshan Lake, Guizhou, Dienerian.

All natural size unless otherwise indicated.

PLATE 4

BRÜHWILER *et al.*, ‘*Koninckites*’ *Hubeitoceras*

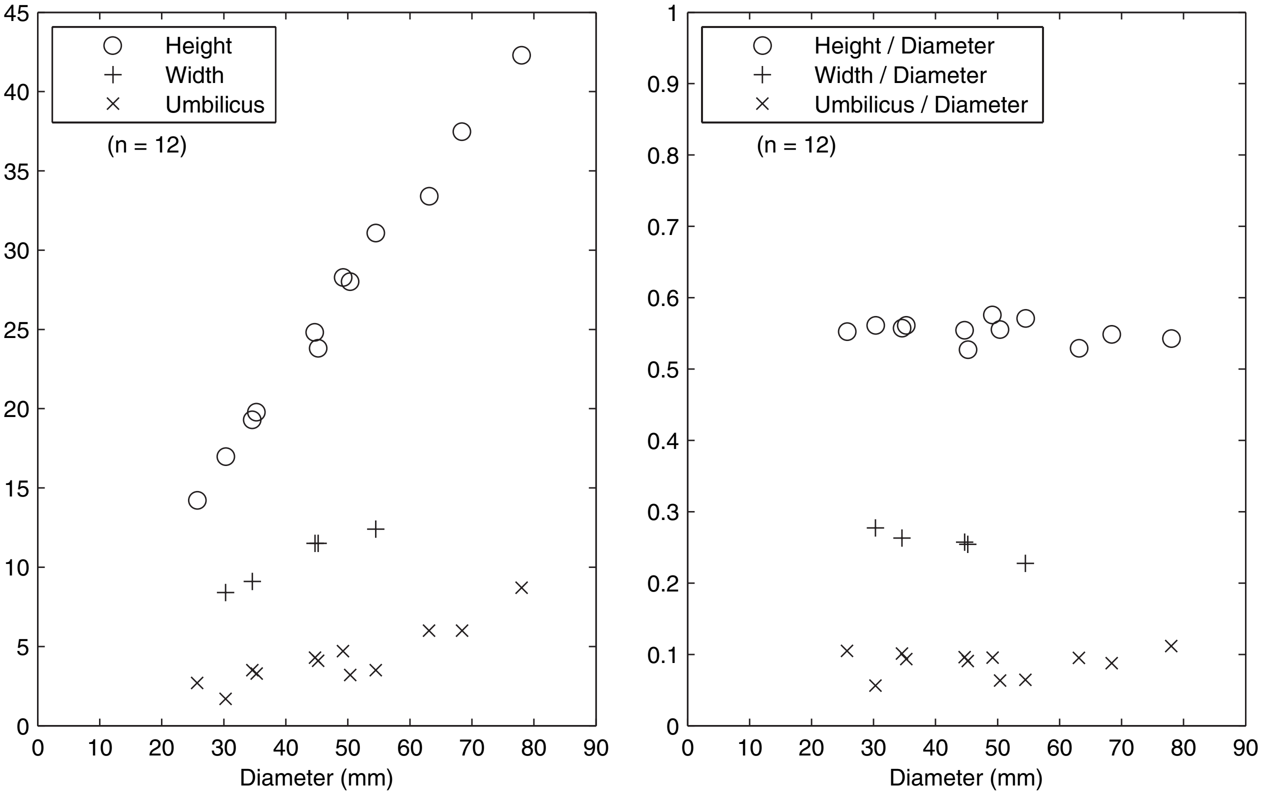

TEXT-FIG. 9. Scatter diagram of H, W, and U, and of H/D, W/D, and U/D for '*Koninckites*' cf. *timorense* (Wanner, 1911).

prominent near the umbilical shoulders, eventually fading away toward the venter. Suture line not preserved.

Measurements. See Appendix.

Discussion. Pleurogyronites kraffti is distinguished by its more tabulate venter, more angular umbilical shoulders and pronounced, stronger ribbing. A few specimens, described as *Gyronites* by Waagen (1895) and assigned to *Pleurogyronites* by Waterhouse (1996*a*), may be conspecific with our specimen, but the poor preservation of Waagen's specimen as well as ours prevents unambiguous identification.

Genus AMBITES Waagen 1895

Type species. Ambites discus Waagen, 1895, p. 152, pl. 21, figs 4–5.

EXPLANATION OF PLATE 5

Figs1–3. *Pleurambites radiatus* sp. nov. 1a–e, holotype, PIMUZ 26766; 1e ×6 . 2a–c, PIMUZ 26767; ×2. 3a–d, PIMUZ 26768; ×2. All from sample Jin14, Jinya, Guangxi. Dienerian.

Figs 4–6. *Prionolobus* cf. *atavus* Waagen, 1895. 4a–d, PIMUZ 26770; 4d ×3. 5a–d, PIMUZ 26769. 6, PIMUZ 26771. All from sample Sha4, Shanggan, Guangxi. Dienerian.

Figs 7–8. *Gyronites frequens* Waagen, 1895. 7a–e, PIMUZ 26773; 7e ×4. 8a–d, PIMUZ 26772. All from sample Sha4, Shanggan, Guangxi. Dienerian.

Fig. 9a–d. *Pleurogyronites* sp. indet. PIMUZ 26774. From sample Sha4, Shanggan, Guangxi. Dienerian.

Fig. 10a–d. ?*Ambites* sp. indet. PIMUZ 26775; 10d ×5. From sample JL3, Jieshan Lake, Guizhou. Dienerian.

Figs 11–14. *Ambites* sp. indet. 11a, b, PIMUZ 26777. 12a–c, PIMUZ 26779. 13a–c, PIMUZ 26776. 14a–d, PIMUZ 26778. All from sample FW9, Waili, Guangxi. Dienerian.

All natural size unless otherwise indicated.

PLATE 5

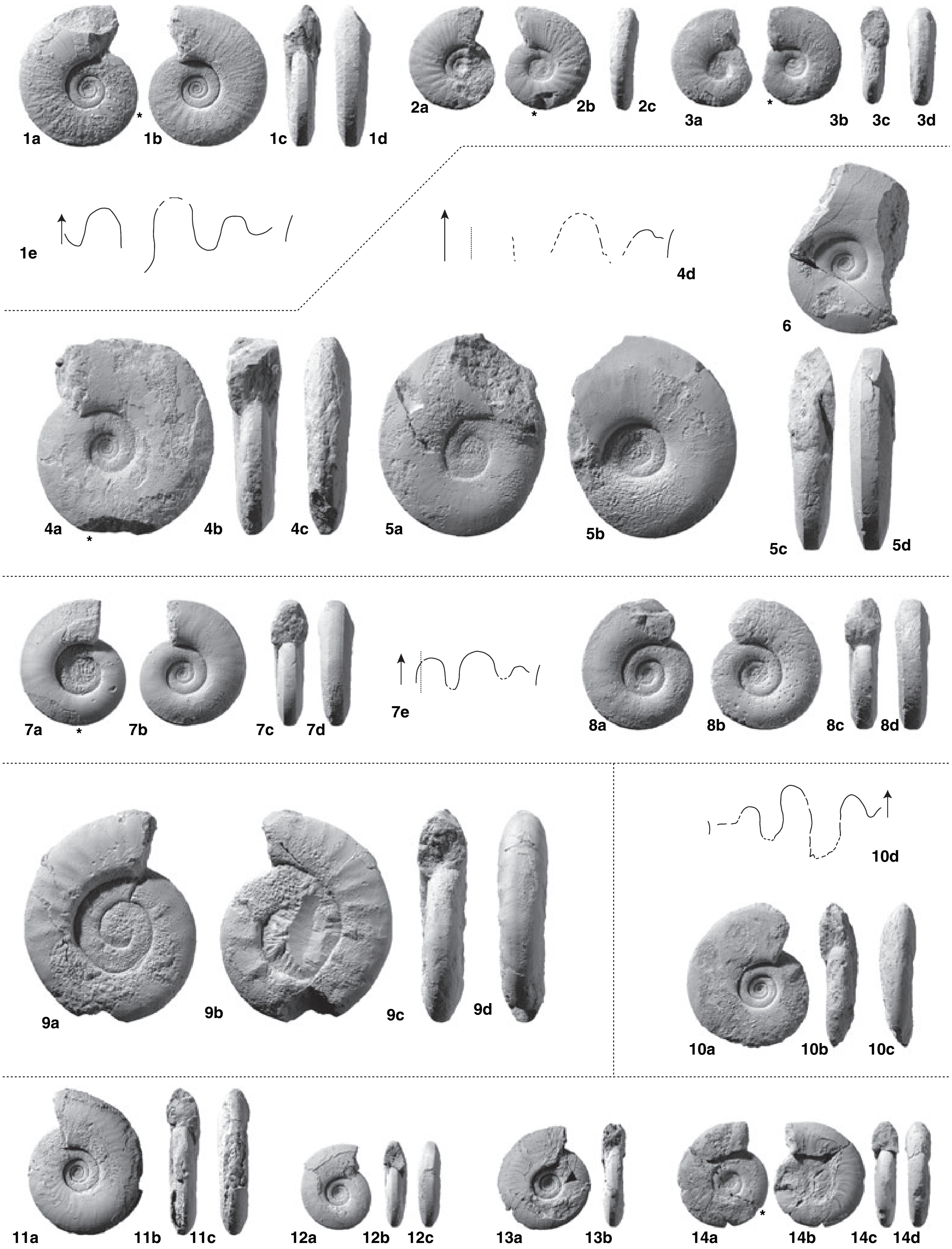

BRÜHWILER *et al.*, *Pleurambites, Prionolobus, Gyronites, Pleurogyronites, Ambites*

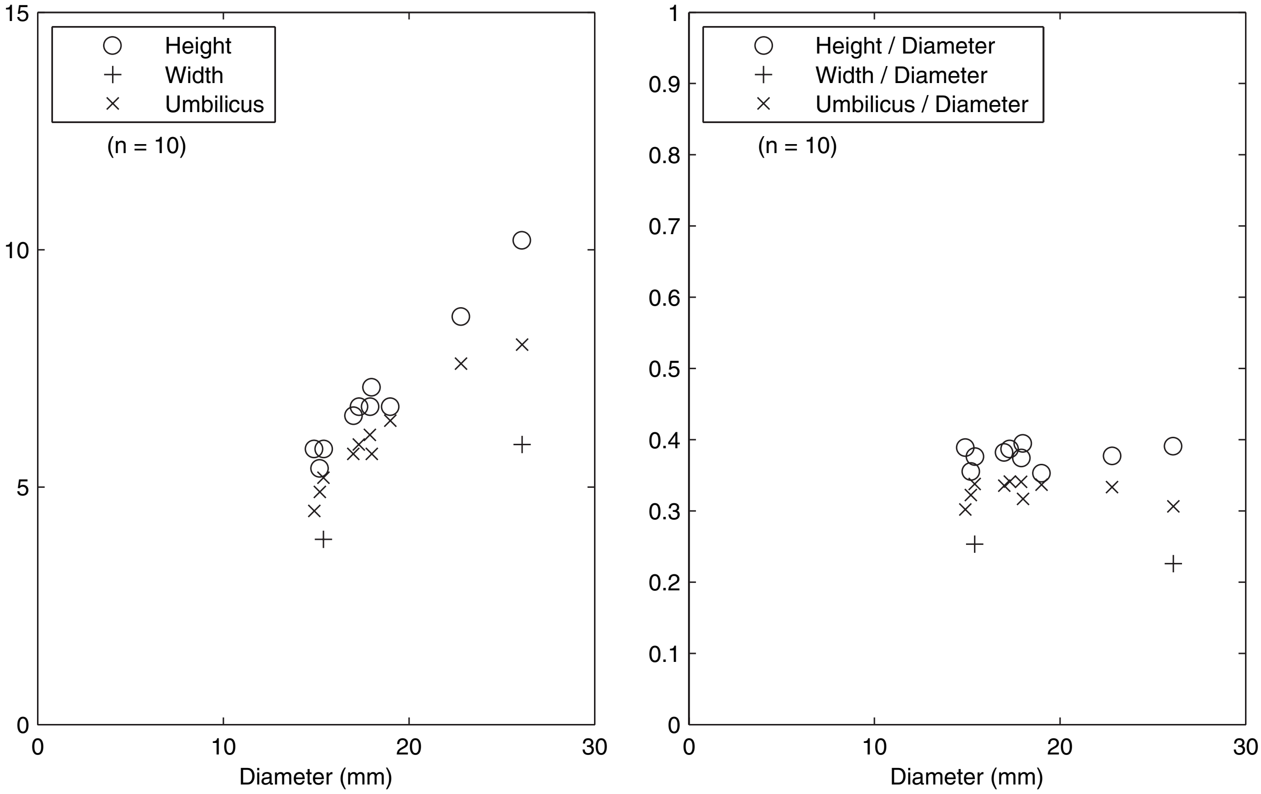

TEXT-FIG. 10. Scatter diagram of H, W, and U, and of H/D, W/D, and U/D for *Ambites* sp. indet.

Ambites sp. indet.
Plate 5, figures 11–14

v 2007*b* *Ambites*, Galfetti *et al.*, p. 594.

Occurrence. Common in sample FW9.

Description. Small, moderately involute, platyconic shell with a tabulate subtabulate venter, more or less angular ventrolateral shoulders, and convex flanks. Umbilicus with vertical to overhanging wall and angular shoulders. Flanks ornamented with sinuous folds. Growth lines distinct and sinuous. Suture line not preserved.

Measurements. Text-fig. 10; Appendix.

Discussion. *Ambites discus* Waagen, 1895, is slightly more involute and has a proportionally higher whorl section.

?*Ambites* sp. indet.
Plate 5, figure 10a–d

Occurrence. A single specimen from sample JL3.

Description. Similar to *Ambites* sp. indet. described above, but with a smooth outer shell. Suture line with deep lobes, second lateral saddle slender and curved slightly toward umbilicus. Indentations of the lobes poorly visible.

Measurements. See Appendix.

EXPLANATION OF PLATE 6

Figs1–4. *Jieshaniceras guizhouensis* (Mu et al. 2007) gen. nov. 1a–c, PIMUZ 26781. From sample JL3, Jieshan Lake, Guizhou. Dienerian. 2a, b, PIMUZ 26783. From sample YR59, Yuping North, Guangxi. Dienerian. 3a–d, PIMUZ 26782; 3d ×1.5. From sample JL3, Jieshan Lake, Guizhou. Dienerian. 4a–e, PIMUZ 26780; 4e ×1.5. From sample JL2, Jieshan Lake, Guizhou. Dienerian.

All ×0.75 unless otherwise indicated.

PLATE 6

BRÜHWILER *et al.*, *Jieshaniceras*

Discussion. Ambites discus Waagen, 1895, differs by its suture line, which has shorter, wider saddles, and its slightly more involute shell, which has a proportionally higher whorl section.

Family FLEMINGITIDAE Hyatt, 1900

Genus JIESHANICERAS gen. nov.

Derivation of name. Genus name refers to the locality Jieshan Lake where the type species of this genus is abundant.

Type species. Jieshaniceras guizhouensis (Zakharov and Mu 2007).

Composition of the genus. Type species only.

Diagnosis. Compressed flemingitid with rounded venter, without strigation and with low radial folds.

Occurrence. JL2, JL3, YR59.

Discussion. This genus differs from other representatives of Flemingitidae such as *Euflemingites* Spath, 1934, *Flemingites* Waagen, 1895, *Larenites* Brayard and Bucher, 2008, and *Rohillites* Waterhouse, 1996*b*, by the absence of strigation. It can also be distinguished from *Anaflemingites* Kummel and Steele, 1962, *Galfettites* Brayard and Bucher, 2008, *Pseudoflemingites* Spath, 1930, and *Rohillites* by its rounded venter. *Anaxenaspis* Diener, 1895, is more evolute and has rounded umbilical shoulders, and *Guangxiceras* Brayard and Bucher, 2008, differs by its inner whorls having a more circular whorl section. *Subflemingites* Spath, 1934, is more involute and has more rounded umbilical shoulders.

The assignment of *Jieshaniceras* to Flemingitidae is based on its similar morphology with other flemingitids and the presence of phylloid saddles on the immature stage. However, this assignment remains uncertain since the family is typically of Smithian age, and only one genus (*Larenites*) has thus far been reported from the upper Dienerian. Therefore, *Jieshaniceras*, of early Dienerian age, would be the oldest known representative of the Flemingitidae.

Jieshaniceras guizhouensis (Zakharov and Mu *in* Mu *et al.* 2007)

Plate 6, figures 1–4

? 1933 *Ophiceras aff. chamunda* Diener; Tien, p. 11, pl. 1, fig. 6a–e.
? 1933 *Meekoceras evolutum* Tien, p. 17, pl. 3, fig. 1a–d.
? 1988 *Dieneroceras ovale* Chao; Xu, p. 444, pl. 1, fig. 6a–c; pl. 2, fig. 9a–c.
2007 *Wordieoceras* aff. *wordiei* Spath; Zakharov and Mu, p. 862, figs 6.7, 6.9, 6.11, 7.1, 7.2, 8.
2007 *Wordieoceras guizhouensis* Zakharov and Mu, p. 862, figs 7.3, 9.1, 9.2.

Occurrence. Samples JL2, JL3 andYR59.

Description. Large, moderately evolute, compressed shell with a rounded venter, rounded ventrolateral shoulders and convex flanks. Umbilicus with a low vertical wall and rounded shoulders. Ornamentation consists of broad, low radial folds on the flanks, which are stronger on inner flanks, but fade away on outer flanks. Growth lines fine and very slightly sinuous. Suture line with high saddles and relatively deeply indented lobes. One immature specimen displays slightly phylloid saddles (pl. 6, fig. 4e).

Measurements. Text-fig. 11; Appendix.

Discussion. This species was assigned to the genus *Wordieoceras* Tozer, 1971 by Zakharov and Mu (2007). However, *Wordieoceras* is characterized by a gabled, acute venter with distinct ventral shoulders, and therefore, differs considerably from *Jieshaniceras*.

Family incertae sedis

Genus ANOTOCERAS Hyatt, 1900

Type species. Prosphingites nala Diener, 1897, p. 54, pl. 1, fig. 4a, b; pl. 7, fig. 13a–c.

Discussion. Following the classification of Spath (1934) *Anotoceras* was provisionally placed into Otoceratidae by Tozer (1981), which is not convincing due to the significant differences in suture line. However, the acute venter of *A. kama* (Diener 1897) favours this assignment whereas the rounded or subtabulate venter of *A. nala* (Diener 1897) and *A. subtabulatus* sp. nov., respectively, are clearly different from that of Otoceratidae. The slightly phylloid suture line of *Anotoceras* (as illustrated by Diener [1897] and Wang and He [1976]) suggests affinities with Proptychitidae but the step-like and crateriform umbilicus and the evolute coiling distinguish *Anotoceras* from representatives of this family. Waterhouse (1994) erected a distinct new family Anotoceratidae for *Anotoceras*. This is perhaps premature in the view of the rather incomplete knowledge of this genus. Cladistic analysis by McGowan and Smith (2007) places *Anotoceras* as a sister group of the Wuchiapingian genus *Araxoceras* and *Otoceras*. However, *Araxoceras* and other members of

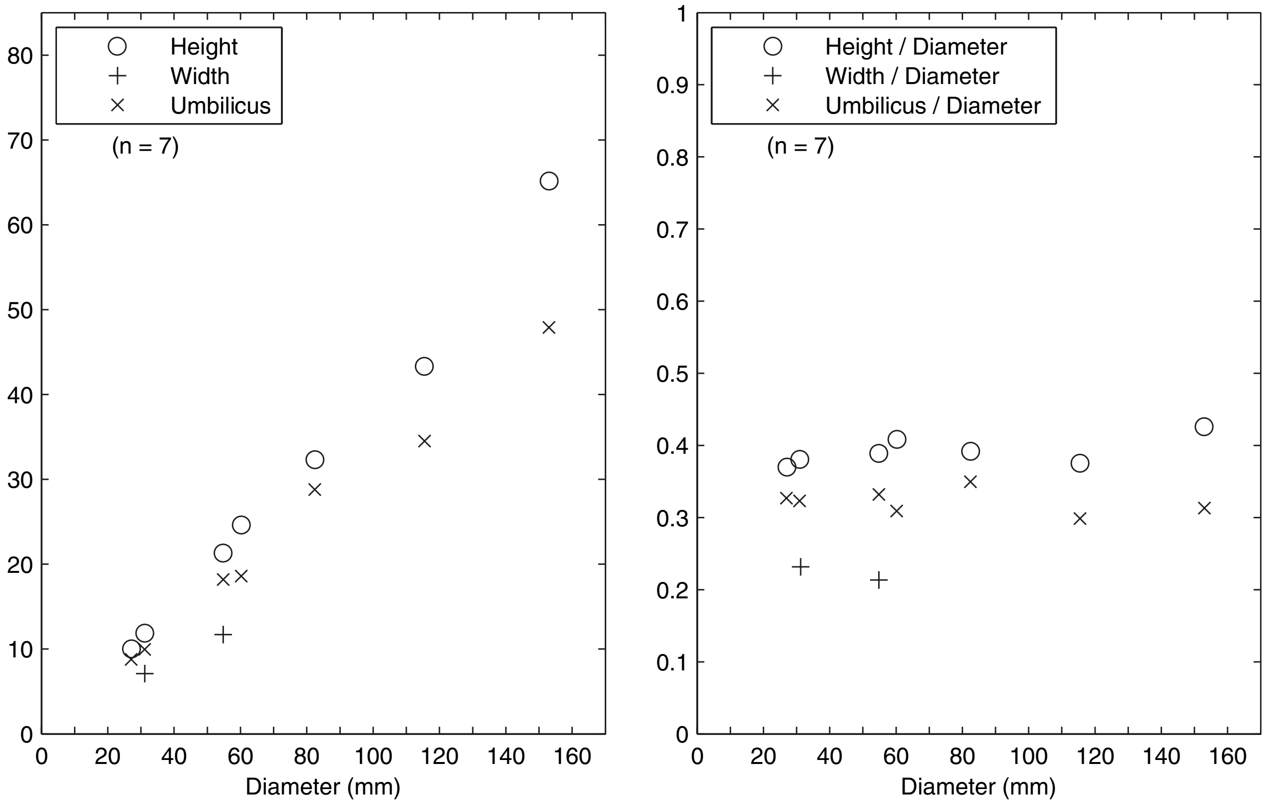

TEXT-FIG. 11. Scatter diagram of H, W, and U, and of H/D, W/D, and U/D for *Jieshaniceras guizhouensis* (Mu et al. 2007) gen. nov.

Araxoceratidae differ from *Anotoceras* by their tricarinate venter, concave flanks and suture lines with much broader saddles.

Thus, taking into consideration the particular morphology (i.e. poorly resolved morphological affinities) of *Anotoceras*, it seems best to leave open its systematic position for the time being.

Anotoceras subtabulatus sp. nov.

Plate 3, figure 5a–d

? 1976 *Anotoceras nala* Diener; Wang and He, p. 268, pl. 1, figs 1–3, text-fig. 5b.

Derivation of name. Refers to the subtabulate nature of its venter.

Holotype. Specimen PIMUZ 26755 (Pl. 3, fig. 5a–d).

Type locality and horizon. Loc. Sha7, Shanggan, Guangxi Province, South China (Text-fig. 2); Early Triassic, Dienerian, *Proptychites candidus* beds.

Occurrence. A single, well preserved specimen from Sha7.

Diagnosis. Anotoceras with a broad, subtabulate venter and an oblique umbilical wall.

Description. Evolute shell with broad, depressed whorl section and subtabulate venter with rounded ventral shoulders. Maximum whorl width occurs on the umbilical shoulders. Umbilicus wide and deep with an oblique, convexly rounded wall. Surface smooth. Suture line not preserved.

Measurements. See Appendix.

Discussion. Anotoceras subtabulatus sp. nov. differs from the Indian species *A. kama* and *A. nala* (Diener, 1897) by its broad subtabulate venter. In addition, it also differs from *A nala* by having a less steep umbilical wall and more rounded umbilical shoulders. *A nala,* reported from Tibet by Wang and He (1976), has a flatter venter than the Indian specimens and in fact, is closer to our new species.

The genus *Anotoceras* is known from the '*Otoceras* Beds' of Spiti (Diener 1897), the '*Ophiceras* beds' of South Tibet (Wang and He 1976) and the late Griesbachian of Oman (Krystyn *et al.* 2003). However, our new South Chinese species is accompanied by '*Koninckites*' cf.

timorense and consequently, is interpreted to be of Dienerian age.

Acknowledgements. Thomas Galfetti and Nicolas Goudemand (Zürich) are acknowledged for their support in the field. Jim Jenks (Salt Lake City) improved the English text of this work. Claude Monnet (Zürich) is thanked for providing his statistical analyses software. Technical support for photography and preparation was provided by Rosemarie Roth, Markus Hebeisen, Julia Huber and Leonie Pauli (Zürich). This paper is a contribution to the Swiss National Science Foundation project 200020-113554 (to HB).

REFERENCES

ARTHABER, G. 1911. Die Trias von Albanien. *Beiträge zur Paläontologie und Geologie Österreich-Ungarns und des Orients*, **24**, 169–288.

BANDO, Y. 1981. Lower Triassic ammonoids from Guryul Ravine and the Spur three kilometres north of Burus. 137–178. *In* NAKAZAWA, K. and KAPOOR, H. R. (eds.). *The Upper Permian and Lower Triassic faunas of Kashmir*. Palaeontologia Indica, New Series, Calcutta, **46**, 204 pp.

BRAYARD, A. and BUCHER, H. 2008. Smithian (Early Triassic) ammonoid faunas from northwestern Guangxi (South China): taxonomy and biochronology. *Fossils and Strata*, **55**, 1–179.

—— —— BRÜHWILER, T., GALFETTI, T., GOUDEMAND, N., GUODUN, K., ESCARGUEL, G. and JENKS, J. 2007*a*. *Proharpoceras* Chao: a new ammonoid lineage surviving the end-Permian mass extinction. *Lethaia*, **40**, 175–181.

—— —— ESCARGUEL, G., FLUTEAU, F., BOURQUIN, S. and GALFETTI, T. 2006. The Early Triassic ammonoid recovery: paleoclimatic significance of diversity gradients. *Palaeogeography, Palaeoclimatology, Palaeoecology*, **239**, 374–395.

—— ESCARGUEL, G. and BUCHER, H. 2007*b*. The biogeography of Early Triassic ammonoid faunas: clusters, gradients, and networks. *Geobios*, **40**, 749–765.

—— —— —— and BRÜHWILER, T. in press. Smithian and Spathian (Early Triassic) ammonoid assemblages: paleogeographic and paleoceanographic implications for terranes. *Journal of Asian Earth Sciences*.

BRÜHWILER, T., BUCHER, H., GOUDEMAND, N. and BRAYARD, A. 2007. Smithian (Early Triassic) ammonoid faunas of the Tethys: new preliminary results from Tibet, India, Pakistan and Oman. The global Triassic, Albuquerque, USA. *Bulletin of the New Mexico Museum of Natural History and Science*, **41**, 25–26.

BU, J., WU, S., ZHANG, H., MENG, Y., ZHANG, F. and ZHANG, L. 2006. Permian-Triassic cephalopods from Dongpan Section, Guangxi, and its geological significance. *Geological Science and Technology Information*, **25**, 47–51 [In Chinese, English summary].

CHAO, K. 1950. Some new ammonite genera of Lower Triassic from western Kwangsi. *Palaeontological Novitates*, **5**, 1–11.

—— 1959. Lower Triassic ammonoids from Western Kwangsi, China. *Palaeontologia Sinica New Series B*, **9**, 1–355, pls 1–45.

DIENER, C. 1895. Triadische Cephalopodenfaunen der ostsibirischen Küstenprovinz. *Mémoires du Comité Géologique St Petersburg*, **14**, 1–59, pls 1–5.

—— 1897. The Cephalopoda of the Lower Trias. *Palaeontologia Indica, Series 15*, **2**, 1–181, pls 1–23.

—— 1913. Triassic faunae of Kashmir. *Palaeontologia Indica*, **5**, 1–133, pls 1–13.

EHIRO, M., HASEGAWA, H. and MISAKI, A. 2005. Permian ammonoids *Prostacheoceras* and *Perrinites* from the southern Kitakami Massif, Northeast Japan. *Journal of Paleontology*, **79**, 1222–1228.

GALFETTI, T., BUCHER, H., BRAYARD, A., HOCHULI, P. A., WEISSERT, H., GUODUN, K., ATUDOREI, V. and GUEX, J. 2007*a*. Late Early Triassic climate change: insights from carbonate carbon isotopes, sedimentary evolution and ammonoid paleobiogeography. *Palaeogeography, Palaeoclimatology, Palaeoecology*, **243**, 394–411.

—— —— MARTINI, R., HOCHULI, P. A., WEISSERT, H., CRASQUIN-SOLEAU, S., BRAYARD, A., GOUDEMAND, N., BRÜHWILER, T. and GOUDUN, K. 2008. Evolution of Early Triassic outer platform paleoenvironments in the Nanpanjiang Basin (South China) and their significance for the biotic recovery. *Sedimentary Geology*, **204**, 36–60.

—— —— OVTCHAROVA, M., SCHALTEGGER, U., BRAYARD, A., BRÜHWILER, T., GOUDEMAND, N., WEISSERT, H., HOCHULI, P. A., CORDEY, F. and GUODUN, K. 2007*b*. Timing of the Early Triassic carbon cycle perturbations inferred from new U-Pb ages and ammonoid biochronozones. *Earth and Planetary Science Letters*, **258**, 593–604.

—— HOCHULI, P. A., BRAYARD, A., BUCHER, H., WEISSERT, H. and VIGRAN, J. O. 2007*c*. Smithian/Spathian boundary event: evidence for global climatic change in the wake of the end-Permian biotic crisis. *Geology*, **34**, 291–294.

GRIESBACH, C. L. 1880. Palaeontological notes on the Lower Trias of the Himalayas. *Records of the Geological Survey of India*, **13**, 94–113, pls 1–4.

GUEX, J. 1978. Le Trias inférieur des Salt Ranges, Pakistan: problèmes biochronologiques. *Eclogae Geologicae Helvetiae*, **71**, 105–141.

HSÜ, T. Y. 1937. Contribution to the marine Lower Triassic fauna of Southern China. *Bulletin of the Geological Society of China*, **16**, 303–347.

HYATT, A. 1900. Cephalopoda. 502–592. *In* ZITTEL, K. A. (ed.). *Textbook of Palaeontology*. Eastman, C. R., London.

KIPARISOVA, L. D. 1961. Palaeontological fundamentals for the stratigraphy of Triassic deposits of the Primorye region, I, Cephalopod Mollusca. *Transactions of the All Union Scientific Research Geological Institute (VSEGEI), New Series*, **48**, 278 pp. (in Russian).

—— and POPOV, Y. D. 1956. Subdivision of the lower series of the Triassic System into stages. *Doklady Akademija Nauk SSSR*, **109**, 842–845, (in Russian).

KONINCK, L. G. DE. 1863. Description of some fossils from India, discovered by Dr A. Fleming, of Edingburgh. *The Quarterly Journal of the Geological Society of London*, **19**, 1–19, pls 1–8.

KOZUR, H. W. 2006. Remarks to the base of Olenekian. *Albertiana*, **34**, 66–72.

KRAFFT, A. V. and DIENER, C. 1909. Lower Triassic cephalopoda from Spiti, Malla Johar, and Byans. *Palaeontologia Indica*, **6**, 1–186, pls 1–31.

KRYSTYN, L., RICHOZ, S., BAUD, A. and TWITCHETT, R. J. 2003. A unique Permian-Triassic boundary section from the Neotethyan Hawasina Basin, Central Oman Mountains. *Palaeogeography, Palaeoclimatology, Palaeoecology*, **191**, 329–344.

—— BHARGAVA, O. N. and RICHOZ, S. 2007. A candidate GSSP for the base of the Olenekian Stage: Mud at Pin Valley; district Lahul & Spiti, Himachal Pradesh (Western Himalaya), India. *Albertiana*, **35**, 5–29.

KUMMEL, B. 1970. Ammonoids from the Kathwai Member, Mianwali Formation, Salt Range, West Pakistan. 177–192. *In* KUMMEL, B. and TEICHERT, C. (eds). *Stratigraphic Boundary Problems: Permian and Triassic of West Pakistan*. Special Publication of the Department of Geology, University of Kansas, **4**, 474 pp.

—— and STEELE, G. 1962. Ammonites from the *Meekoceras gracilitatus* Zone at Crittenden Spring, Elko County, Nevada. *Journal of Paleontology*, **36**, 638–703.

LEHRMANN, D. J., DONGHONG, P., ENOS, P., MINZONI, M., ELLWOOD, B. B., ORCHARD, M. J., JIYAN, Z., JIAYONG, W., DILLETT, P., KOENIG, J., STEFFEN, K., DRUKE, D., DRUKE, J., KESSEL, B. and NEWKIRK, T. 2007. Impact of differential tectonic subsidence on isolated carbonate-platform evolution: Triassic of the Nanpanjiang Basin, South China. *AAPG Bulletin*, **91**, 287–320.

LIDONG, Z., MEIHUA, D. and HUAXIA, L. 1992. The discovery of ammonoid and bivalve faunas of the Lower Triassic and their stratigraphic significance in Shatian, Daye County, Hubei Province. *Earth Science – Journal of China University of Geoscience*, **17**, 337–344. pl. 5 (in Chinese, English Summary).

McGOWAN, A. J. and SMITH, A. 2007. Ammonoids across the Permian/Triassic boundary: a cladistic perspective. *Palaeontology*, **50**, 573–590.

MU, L., ZAKHAROV, Y. D., LI., W. and SHEN, S. 2007. Early Induan (Early Triassic) cephalopods from the Daye Formation at Guiding, Guizhou Province, South China. *Journal of Paleontology*, **81**, 858–872.

NOETLING, F. 1905. Die asiatische Trias. 107–221, pls 9–33. *In* FRECH, F. (ed.). *Lethaea Geognostica: Handbuch der Erdgeschichte mit Abbildungen der für die Formationen bezeichnendsten Versteinerungen*. Schweizerbart, Stuttgart.

OVTCHAROVA, M., BUCHER, H., SCHALTEGGER, U., GALFETTI, T., BRAYARD, A. and GUEX, J. 2006. New Early to Middle Triassic U–Pb ages from South China: calibration with ammonoid biochronozones and implications for the timing of the Triassic biotic recovery. *Earth and Planetary Science Letters*, **243**, 463–475.

RICOU, L. E. 1994. Tethys reconstructed: plates, continental fragments and their boundaries since 260 Ma from Central America to Southeastern Asia. *Geodinamica Acta*, **7**, 169–218.

SHEVYREV, A. A. 2001. Ammonite zonation and interregional correlation of the Induan stage. *Stratigraphy and Geological Correlation*, **9**, 473–482.

—— 2006. Triassic biochronology: state of the art and main problems. *Stratigraphy and Geological Correlation*, **14**, 629–641.

SHI, G. R. 2006. The marine Permian of East and Northeast Asia: an overview of biostratigraphy, palaeobiogeography and palaeogeographical implications. *Journal of Asian Earth Sciences*, **26**, 175–206.

SILBERLING, N. J. and TOZER, E. T. 1968. Biostratigraphic classification of the marine Triassic in North America. *Special Paper of the Geological Society of America*, **110**, 63 pp.

SPATH, L. F. 1930. The Eotriassic invertebrate fauna of East Greenland. *Meddelelser om Grønland*, **83**, 1–90. 12 pls.

—— 1934. *Catalogue of the Fossil Cephalopoda in the British Museum (Natural History). The ammonoidea of the Trias*. The Trustees of the British Museum, London, 521 pp., 18 pls.

—— 1935. Additions to the Eo-Triassic invertebrate fauna of East Greenland. *Meddelelser om Grønland*, **98**, 1–115. 23 pls.

TIEN, C. C. 1933. Lower Triassic cephalopods of South China. *Palaeontologia Sinica, Series B*, **15**, 1–53.

TONG, J. N., ZAKHAROV, Y. D., ORCHARD, M. J., YIN, H. and HANSEN, H. J. 2003. A candidate of the Induan-Olenekian boundary stratotype in the Tethyan region. *Science in China Series D-Earth Science*, **46**, 1182–1200.

—— —— and WU, S. B. 2004. Early Triassic ammonoid succession in Chaohu, Anhui Province. *Acta Palaeontologica Sinica*, **43**, 192–204.

TOZER, E. T. 1961. Triassic stratigraphy and faunas, Queen Elizabeth Islands, Arctic Archipelago. *Memoirs of the Geological Survey of Canada*, **316**, 116. pp.

—— 1965. Lower Triassic stages and ammonoid zones of Arctic Canada. *Paper of the Geological Survey of Canada*, **65-12**, 14 pp.

—— 1967. A standard for Triassic time. *Bulletin of the Geological Survey of Canada*, **156**, 141 pp.

—— 1971. Triassic time and ammonoids. *Canadian Journal of Earth Sciences*, **8**, 989–1031.

—— 1981. Triassic Ammonoidea; classification, evolution and relationship with Permian and Jurassic forms. 65–100. *In* HOUSE, M. R. and SENIOR, J. R. (eds). *The Ammonoidea*. The Systematics Association, Academic Press, London, Special Volume, **18**, 593 pp.

—— 1982. Marine Triassic Faunas of North-America – their significance for assessing plate and terrane movements. *Geologische Rundschau*, **71**, 1077–1104.

—— 1994*a*. Canadian Triassic ammonoid faunas. *Bulletin of the Geological Survey of Canada*, **467**, 663 pp.

—— 1994*b*. Age and correlation of the *Otoceras* beds at the Permian-Triassic boundary. *Albertiana*, **14**, 31–37.

—— 2003. Interpretation of the Boreal *Otoceras* Beds: Permian or Triassic? *Albertiana*, **28**, 90–91.

TRÜMPY, R. 1969. Lower Triassic ammonites from Jameson Land (East Greenland). *Meddelelser om Grønland*, **168**, 77–116, pls 1–2.

WAAGEN, W. 1895. Salt-Range fossils. Vol. 2: fossils from the ceratite formation. *Palaeontologia Indica*, **13**, 323, pp., 40 pls.

WANG, Y. G. 1984. Earliest Triassic ammonoid faunas from Jiangsu and Zhejiang and their bearing on the definition of Permo/Triassic boundary. *Acta Palaeontologica Sinica*, **23**, 257–269, pls 1–3 [In Chinese, English Summary].

—— and HE, G. X. 1976. *Triassic ammonoids from the Mount Jolmo Lungma region. A Report of Scientific Expedition in the Mount Jolmo Lungma Region 1966–1968, Palaeontology*. Science Press, Peking, 223–438, pls 1–48 (in Chinese).

—— —— 1980. Triassic ammonoid sequence of China. *Rivista Italiana di Paleontologia e Stratigrafia*, **85**, 1207–1220.

WANNER, J. 1911. Triascephalopoden von Timor und Rotti. *Neues Jahrbuch für Mineralogie, Geologie und Paläontologie, Beilageband*, **32**, 177–196, pls 6–7.

WATERHOUSE, J. B. 1994. The Early and Middle Triassic ammonoid succession of the Himalayas in western and central Nepal. Part 1, stratigraphy, classification and Early Scythian ammonoid systematics. *Palaeontographica, Abteilung A*, **232**, 1–83, pls 1–6.

—— 1996*a*. The Early and Middle Triassic ammonoid succession of the Himalayas in western and central Nepal. Part 2, systematic studies of the early Middle Scythian. *Palaeontographica Abteilung A*, **241**, 27–100, pls 1–12.

—— 1996*b*. The Early and Middle Triassic ammonoid succession of the Himalayas in western and central Nepal, Part 3, late Middle Scythian ammonoids. *Palaeontographica Abteilung A*, **241**, 101–167, pls 1–11.

XU, G. H. 1988. Early Triassic cephalopods from Lichuan, Western Hubei. *Acta Palaeontologica Sinica*, **27**, 437–456, pls 1–4 (in Chinese, English Summary).

YANG, Z., YANG, F. and WU, S. B. 1996. The ammonoid *Hypophiceras* fauna near the Permian/Triassic boundary at Meishan section and in South China: stratigraphic significance. 49–56. *In* YIN, H. F. (ed.). *The Palaeozoic*/Mesozoic Boundary Candidates of Global Stratotype Section and Point of the Permian/Triassic Boundary. China University of Geosciences Press, Wuhan, 137 pp., 3 pls.

YIN, H. F., WU, S. B., DING, M., ZHANG, K., TONG, J. N., YANG, F. and LAI, X. 1996. The Meishan section, candidate of the global section and point of Permian/Triassic boundary. 31–48. *In* YIN, H. F. (ed.). *The Palaeozoic*/Mesozoic Boundary Candidates of Global Stratotype Section and Point of the Permian/Triassic Boundary. China University of Geosciences Press, Wuhan, 137 pp., 3 pls.

—— ZHANG, K. X., TONG, J. N., YANG, Z. Y. and WU, S. B. 2001. The Global Stratotype Section and Point (GSSP) of the Permian/Triassic Boundary. *Episodes*, **24**, 102–114.

ZAKHAROV, Y. D. 1968. *Lower Triassic Biostratigraphy and Ammonoids of South Primorye*. Nauka, Moskva, 172 pp., 31 pls (in Russian).

—— 1997. Recent view on the Induan, Olenekian and Anisian ammonoid taxa and zonal assemblages of South Primorye. *Albertiana*, **19**, 25–35.

APPENDIX

Measurements of the classic geometrical parameters of the ammonoid shell

Species	Specimen	D (mm)	H (mm)	W (mm)	U (mm)	Sample
Ophiceras sp. indet.	PIMUZ 26725	19.5	7.2	–	7.0	Sha3
	PIMUZ 26726	19.3	8.0	5.6	5.8	Sha3
	PIMUZ 26727	16.5	7.0	4.8	5.2	Sha3
	PIMUZ 26728	16.0	5.6	4.6	5.3	Sha3
	PIMUZ 26729	20.3	7.6	5.4	7.6	Sha3
	PIMUZ 26730	15.8	6.2	–	5.6	Sha3
	PIMUZ 26731	10.1	4.0	–	3.5	Sha3
	PIMUZ 26732	12.2	4.7	3.7	4.1	Sha3
	PIMUZ 26733	18.0	7.4	5.1	5.9	Sha3
	PIMUZ 26734	14.3	5.5	4.3	5.0	Sha3
	PIMUZ 26735	13.2	5.0	4.3	4.8	Sha3
	PIMUZ 26736	11.0	4.0	–	3.9	Sha3
	PIMUZ 26784	15.2	6.3	4.2	4.8	Sha3
	PIMUZ 26785	18.6	7.5	4.9	5.3	Sha3
	PIMUZ 26786	19.4	8.1	–	6.4	Sha3
	PIMUZ 26787	16.0	6.5	–	–	Sha3
	PIMUZ 26788	10.7	4.5	–	3.6	Sha3
	PIMUZ 26789	17.0	6.7	5.1	6.4	Sha3
	PIMUZ 26790	12.6	5.3	3.6	–	Sha3

APPENDIX (Continued)

Species	Specimen	D (mm)	H (mm)	W (mm)	U (mm)	Sample
	PIMUZ 26791	14.7	5.8	–	5.3	Sha3
	PIMUZ 26792	14.1	5.8	4.0	4.8	Sha3
	PIMUZ 26793	18.5	8.2	–	–	Sha3
	PIMUZ 26794	18.9	7.5	–	6.2	Sha3
Shangganites shangganense gen. nov. sp. nov.	PIMUZ 26737, Holotype	28.1	11.9	8.5	7.6	Sha4
	PIMUZ 26738	18.8	8.4	5.6	4.5	Sha4
	PIMUZ 26739	22.9	10.6	7.0	5.3	Sha4
	PIMUZ 26740	27.3	12.8	7.5	5.3	Sha4
	PIMUZ 26741	42.4	18.3	–	10.9	Sha4
	PIMUZ 26795	41.5	18.3	9.0	8.7	Sha4
	PIMUZ 26796	23.5	10.1	–	6.1	Sha4
	PIMUZ 26797	24.2	11.1	–	5.7	Sha4
	PIMUZ 26798	30.1	13.9	–	6.0	Sha4
	PIMUZ 26799	27.1	12.8	–	4.5	Sha4
	PIMUZ 26800	16.8	8.2	4.5	3.4	Sha4
	PIMUZ 26801	25.0	10.5	–	7.1	Sha4
	PIMUZ 26802	31.1	13.8	–	7.0	Sha4
	PIMUZ 26803	27.9	12.7	–	5.6	Sha4
	PIMUZ 26804	24.1	10.8	–	5.3	Sha4
	PIMUZ 26805	21.8	10.3	6.3	4.3	Sha4
	PIMUZ 26806	18.1	7.9	5.8	3.9	Sha4
	PIMUZ 26807	15.2	7.7	–	2.8	Sha4
	PIMUZ 26808	21.4	9.6	5.4	3.5	Sha4
	PIMUZ 26809	24.1	11.9	6.9	4.0	Sha4
	PIMUZ 26810	18.2	7.8	–	5.0	Sha4
	PIMUZ 26811	33.0	13.9	–	7.8	Sha4
Vishnuites pralambha Diener, 1897	PIMUZ 26812	30.5	12.7	6.1	9.7	JL2
	PIMUZ 26813	31.0	13.4	5.3	8.9	JL2
	PIMUZ 27223	51.5	23.0	–	13.8	jin102
Xenodiscoides sp. indet.	PIMUZ 26746	19.3	6.4	–	8.3	YR59
Proptychites candidus Tozer, 1961	PIMUZ 26747	88.6	38.6	21.8	22.6	YR30
	PIMUZ 26748	110.2	45.2	–	34.2	JL6
Proptychites sp. indet.	PIMUZ 26749	32.4	14.4	–	7.7	YR1
	PIMUZ 26750	29.7	13.0	–	7.6	YR1
	PIMUZ 26751	37.0	17.1	–	8.0	YR1
	PIMUZ 26814	18.2	8.5	–	5.0	YR1
	PIMUZ 26815	11.1	4.6	–	3.0	YR1
'*Koninckites*' cf. *timorense* (Wanner, 1911)	PIMUZ 26760	68.4	37.5	–	6.0	Sha4
	PIMUZ 26762	63.1	33.4	–	6.0	Sha5
	PIMUZ 26763	78.0	42.3	–	8.7	JL3
	PIMUZ 26764	54.5	31.1	12.4	3.5	JL3
	PIMUZ 26765	49.2	28.3	–	4.7	JL3
	PIMUZ 26816	50.4	28.0	–	3.2	Sha5
	PIMUZ 26817	35.3	19.8	–	3.3	Sha5
	PIMUZ 26818	44.7	24.8	11.5	4.3	Sha5
	PIMUZ 26819	45.2	23.8	11.5	4.1	Sha5
	PIMUZ 26820	30.3	17.0	8.4	1.7	jin14
	PIMUZ 26821	25.7	14.2	–	2.7	JL2
	PIMUZ 26822	34.6	19.3	9.1	3.5	JL3
Hubeitoceras yanjiaensis (Xu, 1988)	PIMUZ 26757	55.6	29.4	12.4	7.2	JL2
	PIMUZ 26758	30.1	16.4	7.7	4.5	JL2
	PIMUZ 26759	25.2	12.6	–	4.2	JL2
	PIMUZ 26823	42.7	22.0	–	5.2	JL2

APPENDIX (Continued)

Species	Specimen	D (mm)	H (mm)	W (mm)	U (mm)	Sample
Hubeitoceras sp. indet.	PIMUZ 26756	69.2	37.0	12.4	5.8	JL2
Anotoceras subtabulatus sp. nov.	PIMUZ 26755, Holotype	25.0	8.2	14.4	10.5	Sha7
Proptychitid gen. indet.	PIMUZ 26752	54.2	25.9	–	13.6	Sha7
	PIMUZ 26754	23.2	10.4	–	6.3	FW9
Prionolobus cf. *atavus* Waagen, 1895	PIMUZ 26769	35.1	14.7	8.0	9.5	Sha4
	PIMUZ 26770	33.7	15.1	8.5	9.4	Sha4
	PIMUZ 26771	30.1	13.4	–	7.6	Sha4
Gyronites frequens Waagen, 1895	PIMUZ 26772	22.1	7.7	6.0	8.7	Sha4
	PIMUZ 26773	22.3	7.8	6.3	9.0	Sha4
Pleurambites radiatus sp. nov.	PIMUZ 26766, Holotype	23.4	9.7	6.3	8.0	jin14
	PIMUZ 26767	9.5	3.6	2.4	3.0	jin14
	PIMUZ 26768	8.6	3.5	2.5	2.8	jin14
Pleurogyronites sp. indet.	PIMUZ 26774	35.3	10.7	8.4	15.4	Sha4
?Ambites sp. indet.	PIMUZ 26775	24.2	10.2	–	7.6	JL3
Ambites sp. indet.	PIMUZ 26776	18.0	7.1	–	5.7	FW9
	PIMUZ 26777	26.1	10.2	5.9	8.0	FW9
	PIMUZ 26778	19.0	6.7	–	6.4	FW9
	PIMUZ 26779	15.4	5.8	3.9	5.2	FW9
	PIMUZ 26827	22.8	8.6	–	7.6	FW9
	PIMUZ 26828	17.3	6.7	–	5.9	FW9
	PIMUZ 26829	17	6.5	–	5.7	FW9
	PIMUZ 26830	14.9	5.8	–	4.5	FW9
	PIMUZ 26831	15.2	5.4	–	4.9	FW9
	PIMUZ 26832	17.9	6.7	–	6.1	FW9
Jieshaniceras guizhouensis (Zakharov and Mu, 2007)	PIMUZ 26780	54.8	21.3	11.7	18.2	JL2
	PIMUZ 26781	153.0	65.2	–	47.9	JL3
	PIMUZ 26782	115.5	43.3	–	34.5	JL3
	PIMUZ 26783	60.2	24.6	–	18.6	YR59
	PIMUZ 26824	82.4	32.3	–	28.8	JL3
	PIMUZ 26825	31.0	11.8	7.2	10.0	JL3
	PIMUZ 26826	27.0	10.0	–	8.8	YR59

Diameter (D), whorl height (H), whorl width (W) and umbilical diameter (U).

CHAPTER 3:

The Lower Triassic sedimentary and carbon isotope records from Tulong (South Tibet) and their significance for Tethyan palaeoceanography

Sedimentary Geology 222 (2009) 314–332

Contents lists available at ScienceDirect

Sedimentary Geology

journal homepage: www.elsevier.com/locate/sedgeo

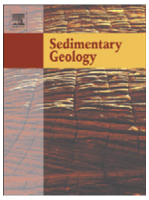

The Lower Triassic sedimentary and carbon isotope records from Tulong (South Tibet) and their significance for Tethyan palaeoceanography

Thomas Brühwiler [a,*], Nicolas Goudemand [a], Thomas Galfetti [b], Hugo Bucher [a,c], Aymon Baud [d], David Ware [a], Elke Hermann [a], Peter A. Hochuli [a,c], Rossanna Martini [e]

[a] *Paläontologisches Institut und Museum der Universität Zürich, Karl Schmid-Strasse 4, 8006 Zürich, Switzerland*
[b] *Holcim Group Support Ltd, Materials Technology, 5113 Holderbank, Switzerland*
[c] *Department of Earth Sciences, ETH, Universitätsstrasse 16, 8092 Zürich, Switzerland*
[d] *BGC, Parc de la Rouvraie 28, 1018 Lausanne, Switzerland*
[e] *Department of Geology and Paleontology, University of Geneva, Rue des Maraîchers 13, 1205 Geneva, Switzerland*

ARTICLE INFO

Article history:
Received 18 June 2009
Received in revised form 23 September 2009
Accepted 11 October 2009

Keywords:
Early Triassic
South Tibet
Microfacies
Palaeoenvironments
Carbon isotopes

ABSTRACT

The Lower Triassic sedimentary and carbonate/organic carbon isotope records from the Tulong area (South Tibet) are documented in their integrality for the first time. New age control is provided by ammonoid and conodont biostratigraphy. The basal Triassic series consists of Griesbachian dolomitic limestones, similar to the Kathwai Member in the Salt Range (Pakistan) and to the *Otoceras* Beds in Spiti (India). The overlying thin-bedded limestones of Dienerian age strongly resemble the Lower Ceratite Limestone of the Salt Range. They are followed by a thick series of dark green, silty shales of Dienerian–early Smithian age without fauna that strikingly resemble the Ceratite Marls of the Salt Range. This interval is overlain by thin-bedded, light grey fossil-rich limestones of middle to late Smithian age, resembling the Upper Ceratite Limestone of the Salt Range. These are followed by a shale interval of early Spathian age that has no direct counterpart in other Tethyan sections. Carbonate production resumes during the late early and middle Spathian with the deposition of red, bioclastic nodular limestone ("Ammonitico Rosso" type facies). Apart from its colour this facies is similar to the one of the Niti Limestone in Spiti and of the Spathian nodular limestone in Guangxi (South China). As in other Tethyan localities such as Spiti, the early–middle Anisian part of the Tulong section is strongly condensed and is characterized by grey, thin-bedded limestones with phosphatized ammonoids. As for many other Tethyan localities the carbon isotope record from Tulong is characterized by a late Griesbachian–Dienerian positive $\delta^{13}C_{carb}$ excursion (2‰), and a very prominent positive excursion (5‰) at the Smithian–Spathian boundary, thus confirming the well-documented perturbations of the global carbon cycle following the Permian–Triassic mass extinction event.

1. Introduction

The end-Permian mass extinction is the biggest known crisis in life history and wiped out more than 90% of all marine species (e.g. Raup and Sepkoski, 1982). The subsequent Early Triassic recovery of marine and terrestrial ecosystems is considered to have been delayed when compared with other mass extinctions and to have lasted until the end of the Early Triassic (e.g. Erwin, 1998). Many marine clades such as corals (Stanley, 2003), foraminifers (Tong and Shi, 2000) or radiolarians (Racki, 1999) did not completely recover until the Spathian or the Anisian, and poorly diversified and small-sized benthonic shelly faunas predominated during the Early Triassic (e.g. Fraiser and Bottjer, 2004; Fraiser et al., 2005). Metazoan reef communities were completely absent in the Early Triassic (Pruss and Bottjer, 2005). On the other hand, ammonoids and conodonts recovered very fast in comparison with other marine clades (Brayard et al., 2006, 2009; Orchard, 2007). Moreover, recent analysis of outer platform paleoenvironments from South China reveals that increasing rates of diversity and abundance of skeletal material occurred already during well-oxygenated carbonate episodes of early Smithian and Spathian age, respectively (Galfetti et al., 2008).

Stable carbon isotope studies have shown that the global carbon cycle was profoundly perturbed at the Permian–Triassic boundary and that several large and short-lived fluctuations occur in the Early Triassic, before the carbon cycle stabilizes in the Middle Triassic (Baud et al., 1996; Atudorei and Baud, 1997; Atudorei, 1999; Payne et al., 2004; Richoz, 2004; Corsetti et al., 2005; Galfetti et al., 2007a,b,c; Horacek et al., 2007a,b). The coincidence of carbon isotope cycle instabilities with the Early Triassic delayed recovery suggests a relationship between carbon cycling and biological rediversification in the aftermath of the extinction (Payne et al., 2004). Indeed, for instance, the major positive $\delta^{13}C$ excursion at the Smithian–Spathian

---

* Corresponding author. Tel.: +41 44 634 26 98; fax: +41 44 634 49 23.
E-mail address: bruehwiler@pim.uzh.ch (T. Brühwiler).

0037-0738/$ – see front matter © 2009 Elsevier B.V. All rights reserved.
doi:10.1016/j.sedgeo.2009.10.003

boundary coincides with the most severe ammonoid and conodont intra-Triassic extinction event (Brayard et al., 2006; Galfetti et al., 2007a,c; Orchard, 2007), associated with major climatic change (Brayard et al. 2006; Galfetti et al. 2007b). CO_2 degassing via volcanism, possibly related to a late eruptive phase of the Siberian Traps, has been proposed as a trigger for these global disturbances (Payne et al., 2004; Ovtcharova et al. 2006). Such an explanation is favoured also by carbon cycle modelling which suggests that the Early Triassic perturbations result from continuing environmental disturbances rather than from lingering effects from a single disturbance at the Permian–Triassic boundary (Payne and Kump, 2007).

Recent analysis of the late Early Triassic sedimentary facies evolution has revealed striking similarities between the South China Block and the widely distant Northern Indian Margin suggesting a common, at least Tethys-wide control on outer platform sedimentary environment evolution (Galfetti et al., 2007a). On the other hand, during the Early Triassic the Northern Indian Margin was characterized by extensional tectonics related to the opening of the Neothetys (e.g. Stampfli et al., 1991). Therefore, successions from closely spaced localities such as Selong and Tulong in South Tibet may show pronounced differences regarding facies and thickness (Garzanti et al., 1998; and Section 7.1. hereafter). Thus, additional detailed descriptions of well-dated successions from various paleogeographic settings are essential in order to differentiate between local patterns related to synsedimentary tectonics and large-scale patterns such as shown by Galfetti et al. (2007a). Deciphering such large-scale patterns may provide new insights into the processes related to the Early Triassic biotic recovery.

Various sections from South Tibet (Wang and He, 1976; Rao and Zhang, 1985; Wang et al., 1989; Liu and Einsele, 1994; Yugan et al., 1996; Garzanti et al., 1998; Shen et al., 2006) and adjacent North Nepal (Bassoullet and Colchen, 1976; Garzanti et al., 1994; von Rad et al., 1994; Baud et al., 1997) are known for their Lower Triassic sedimentary and palaeontological records. However, for the area of Tulong previously published documentations of the Lower Triassic succession were incomplete and/or poorly or incorrectly dated (see Section 7 below). Here we document for the first time the complete and well-dated Lower Triassic sedimentary record from this area and compare it with other Tethyan successions. We also present a new high-resolution carbonate carbon isotope record. The comparison of this new C-isotope record with other Lower Triassic profiles described in the literature (Baud et al., 1996; Payne et al., 2004; Galfetti et al., 2007a,b,c) provides additional evidence for the global character of the instabilities of the carbon cycle during the Early Triassic recovery interval.

2. Geologic background

2.1. Palaeogeography

During Early Triassic times the Tulong area was located in a distal position on the peri-Gondwanan margin, on the southern side of the Tethys Ocean (Ogg and von Rad, 1994) (Fig. 1). As shown by different authors (Marcoux and Baud, 1996; Ricou, 1996; Garzanti and Sciunnach, 1997) at least two rifting processes affected the North Indian plate. The first event is linked to the detachment of the Quiantang block from Gondwana during the Early Carboniferous. With a second rifting phase during the Early Permian the Lhasa block detached from the Gondwanan margin and the Neotethys developed. In this process the southern Neotethyan Indian margin was acting as upper plate inducing basalt flows (Panjal Traps) and volcanism (Stampfli et al., 1991; Baud et al., 1996; Garzanti et al., 1996). During the expansion of the Neotethys in the Early Triassic, the Indian margin underwent thermal subsidence and was characterized by large tilted blocks. This may explain the differences in lithological successions between presently closely spaced localities such as Tulong and Selong (35 km apart) in South Tibet (see Section 7.1.).

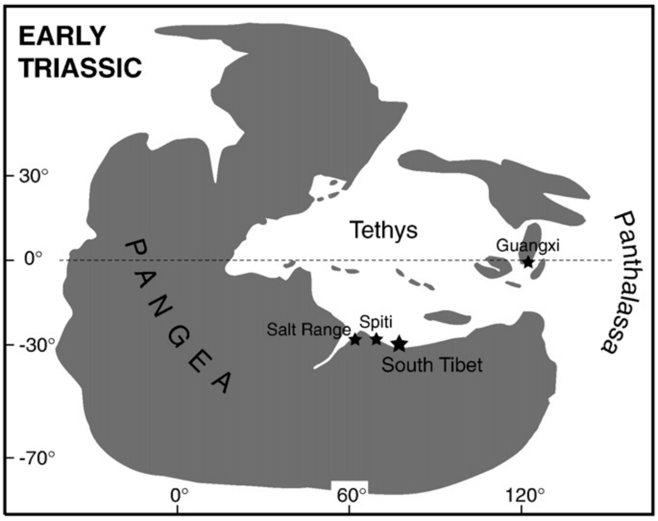

Fig. 1. Simplified Early Triassic palaeogeography (modified after Brayard et al., 2006) showing the location of South Tibet (Northern Indian Margin) and other localities cited in the text.

2.2. Thermal alteration

Based on conodont and palynomorph alteration indexes it appears that the Lower Triassic sediments of the studied area experienced some low-grade thermal metamorphism during the Himalayan orogeny. Conodonts recovered throughout the section are dark to very dark brown in colour, corresponding to a CAI (i.e. Conodont Alteration Index) of 3 to 4 (Epstein et al., 1977). This indicates an exposure to temperatures close to 200 °C (the temperature range of CAI 3/resp. 4 is 110–200/resp. 190–300 °C (Nowlan and Barnes, 1987). Palynological investigations from the studied area yield dark brown to almost opaque black palynomorphs, indicating a value of 6–7 on the thermal alteration scale (TAS) of Batten (1996). This value corresponds to exposure to temperatures of 170–200 °C confirming the values inferred from the CAI.

3. Lower Triassic sections

In addition to the classic section located near the village of Tulong (section Tu in this paper) (Garzanti et al., 1998; Shen et al., 2006), several new and more complete sections are reported here (Figs. 2 and 3). The stratigraphic successions obtained from several scattered outcrops can be correlated bed-by-bed, allowing establishment of an almost complete composite section spanning the Late Permian to Early Anisian time interval (Fig. 4). Only the total thickness of the Dienerian–early Smithian shale interval (Unit II; see Section 4.3.2. hereafter) remains uncertain. Biostratigraphic and facies description of each lithologic unit is provided below. Detailed descriptions of ammonoids, conodonts, palynomorphs and ostracods will be addressed in forthcoming papers.

4. Upper Permian to Lower Triassic litho-/biostratigraphic and microfacies description

4.1. Upper Permian

In the studied area the uppermost Permian consists of about 30 m of dark to black shales containing cm to dm-sized, black, phosphatic nodules. No macrofossils have been found within this interval, and our palynological samples from this interval proved to be barren.

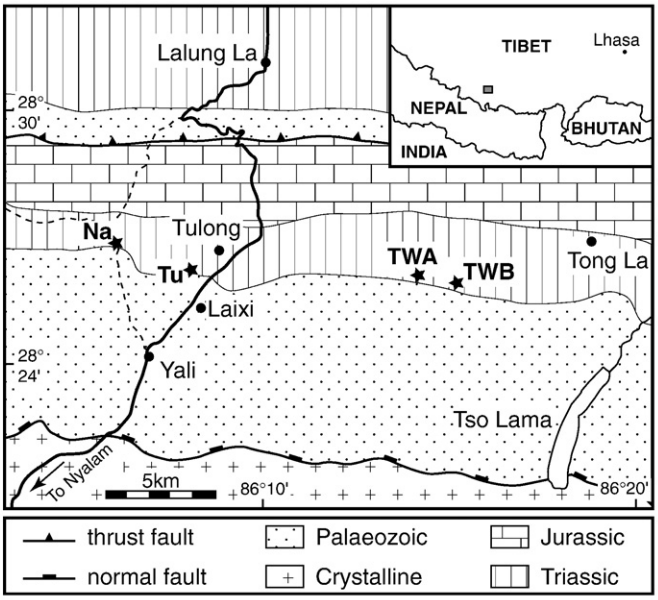

Fig. 2. Geologic sketch map of the study area (modified after Burg, 1983) and location of studied sections. Tu: classical section near the village of Tulong; Na: Nazapuo section; TWA: Tong La West A section; TWB: Tong La West B section.

These shales strikingly resemble the late Permian Kuling Shales of Spiti (Northern India) (Bucher et al., 1997).

4.2. Lower Triassic — Unit I

4.2.1. Description

In the studied area the basal Triassic deposits unconformably overlie the Kuling Shales. They consist of 3 m of carbonate rocks, which are here subdivided into two subunits (i.e. *Subunit Ia* and *Subunit Ib*).

Subunit Ia — 2 m of rusty, yellowish-reddish, thin-bedded dolomitic limestones intercalated with few, thin shale layers (Fig. 5a). The basal bed has an irregular base (Fig. 5b). The first 80 cm of the Subunit consists of thin-bedded dolomitic mudstone with thin shale interbeds showing the progressive appearance of thin-shelled bivalves, rare crinoid fragments and foraminifera (*Earlandia* sp., *Rectocornuspira* sp., microlagenids and other microforaminifera) (Fig. 5c). The upper part of *Subunit Ia* consists of essentially barren, thin-bedded dolomitic mudstone with thin shale interbeds.

In *Subunit Ia* ammonoids are very rare and too poorly preserved for identification. The occurrence of the conodont species *Hindeodus parvus* in the upper part of the first carbonate bed (sample TWB5) suggests a probable basal Early Triassic (Griesbachian) age. Besides the occurrence of *Hindeodus* spp. conodont assemblages of this subunit are mostly dominated by *Neogondolella* spp. including *Ng. planata*, *Ng. taylorae*, and *Ng. tulongensi*. This assemblage unambiguously indicates a Griesbachian age.

Subunit Ib — 1 m of light grey, thin-bedded limestone (Fig. 5d). Although partly recristallized and slightly dolomitized, this horizon yields juvenile ammonoids, rare ostracods and peculiar spherical bioclasts (i.e. "microspheres", possibly radiolaria; compare discussion in Galfetti et al., 2008, p. 42) (Fig. 5e). The upper part of *Subunit Ib* consists of shelly mudstones–wackestones with thin-shelled microbivalves (Fig. 5f) and contains abundant ammonoids. In the topmost bed abundant framboidal pyrite is preserved in ammonoid body chambers.

The horizon located 20 cm below the top of *Subunit Ib* (sample TWB32) yielded rather poorly preserved specimens of *Proptychites* sp., *Gyronites undatus* and *Gyronites* aff. *planissimus*. The uppermost bed (sample TWB35) contains an assemblage characterized by *Ambites* cf. *discus*, ?*Pleurambites* sp., *Gyronites* aff. *planissimus*, *Proptychites haydeni* and ?*Meekophiceras* sp., indicating a Dienerian age (Spath, 1934; Tozer, 1994; Brühwiler et al., 2008).

The presence of *Ng.*? *discreta* in the lower part (sample TWB25) of this subunit indicates a latest Griesbachian age (*discreta* conodont Zone/*Bukkenites strigatus* ammonoid Zone). Note that one reworked specimen of *Jinogondolella* of Guadalupian age has been observed in this sample. The occurrence of *Sweetospathodus kummeli* in the sample above (TWB29) confirms a succession already observed at Guling (Spiti, India) (Orchard and Krystyn, 1998) and at Chhidru (Salt Range, Pakistan; Goudemand et al., ongoing work). Although *Sw. kummeli* is commonly regarded as a Dienerian species, it may appear as early as in the Strigatus Zone from Otto Fjord as observed in the Canadian Arctic (Orchard, 2008). The beginning of the first major radiation of conodonts in the Early Triassic is well expressed within samples TWB32 and TWB35 with the noticeable appearance of *Neospathodus* species. Numerous P1 elements of the *Ns. dieneri* group, including *Ns. svalbardensis* confirm a Dienerian age for the uppermost part of this subunit.

4.2.2. Interpretation

The Permian–Triassic boundary in the study area is marked by an erosive boundary as shown by the irregular base of Unit I (Fig. 5a). No evidence for reworked Permian rocks (e.g. pebbles derived from the Kuling phosphate nodules) has been found. It is interesting to note the presence of foraminifera disaster taxa such as *Earlandia* sp. and *Rectocornuspira* sp. in *Subunit Ia*. This corresponds to the well-known bloom of these disaster taxa that occur in the extinction interval and continue well into the basal Triassic sediments as shown by Altiner et al. (1980), Baud et al. (1997, 2005) and Groves and Altiner (2005). With the appearance of abundant ammonoids and possibly radiolarians ("microspheres") the biomicrites in *Subunit Ib* indicate a probable drowning. The topmost bed of this subunit possibly suggests a low sedimentation rate, but without any indication of paleontological condensation.

4.3. Lower Triassic — Unit II

4.3.1. Description

The basal Triassic carbonates of Unit I are overlain by an interval of barren, dark green shales. Since no continuous outcrop has been found in these strongly faulted and folded shales, the thickness of Unit II can roughly be estimated to be greater than 50 m and probably less than 100 m (Fig. 3a). In the upper part the shales of Unit II contain very thin lenses of cross-bedded siltstone (Fig. 5g) showing dolomitization and fracturation in thin section (Fig. 5h).

So far, no ammonoids or conodonts have been found in this unit. Its age ranges from Dienerian to early Smithian. However, the precise position of the Dienerian–Smithian boundary remains unknown.

4.3.2. Interpretation

It is unclear whether or not the lenticular cross-bedded dolomitized siltstones in the upper part of this unit are part of distal turbidites or not. Cross-bed laminations found within these lenses suggest the presence of bottom currents. However, given the absence of hummocky cross stratification it is suggested that this unit was deposited below storm wave base.

4.4. Lower Triassic — Unit III

4.4.1. Description

The shale interval of Unit II is followed by about 9 m of mostly grey limestone beds alternating with thin shale intervals. They are here subdivided into four subunits.

Subunit IIIa — 1 m of red-weathering ferruginous, dolomitized coarse grained limestone containing silt- to sand-sized skeletal debris

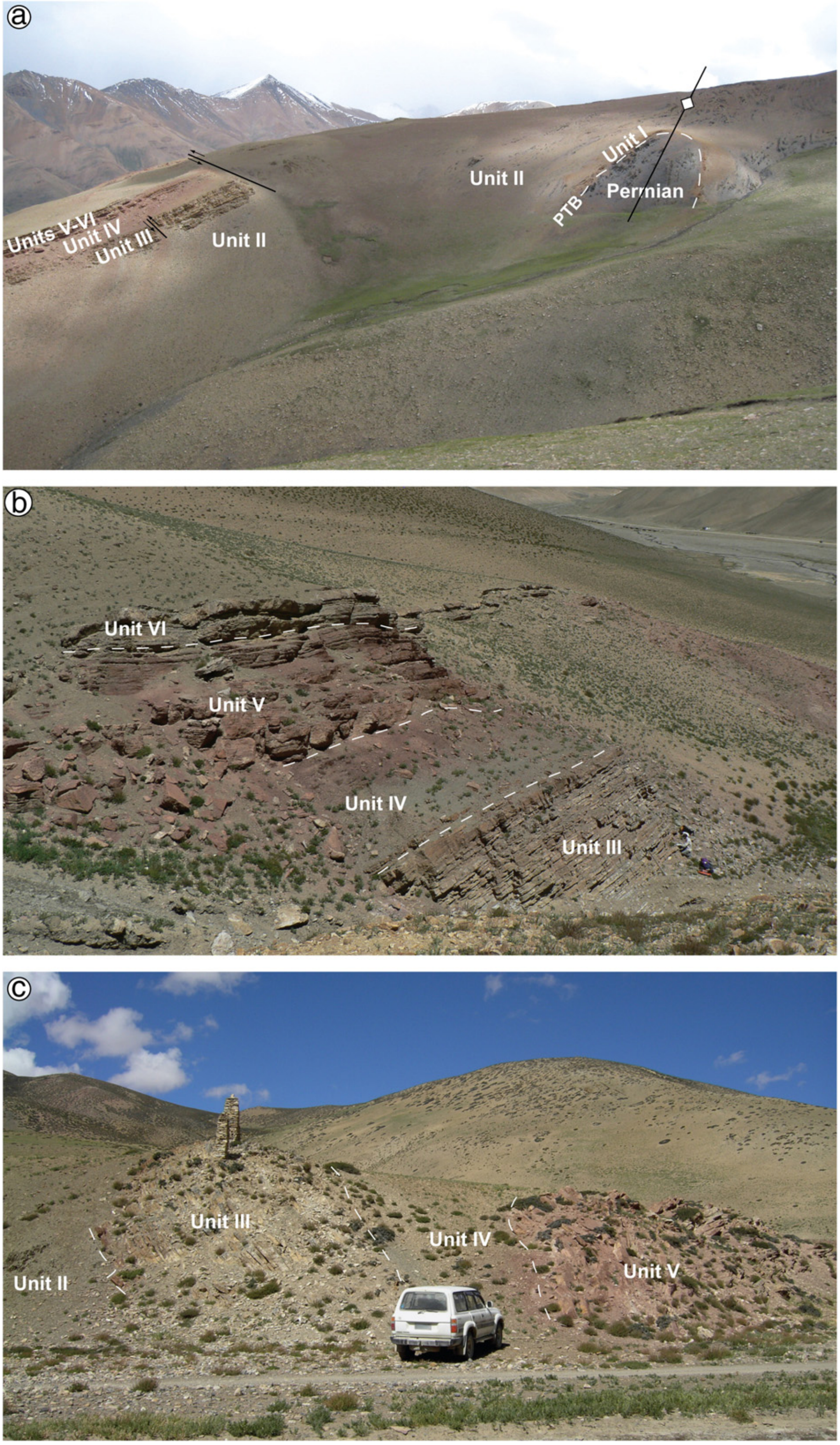

Fig. 3. Outcrop photographs with indicated Lower Triassic lithologic units. (a) Section TWB. Unit II is discontinuously exposed, folded and faulted. (b) Classical section (Tu) near the village of Tulong. (c) Nazapuo section (Na).

(thin-shelled microbivalves, echinoids, spicules) (Fig. 6a–b). This is followed by 60 cm of dm-scale-bedded grey lime packstones consisting of packed, partly oriented thin-shelled microbivalves.

Ammonoids are rare in *Subunit IIIa* and too poorly preserved for unambiguous identification. Conodonts are also relatively rare in this subunit but the occurrence of *Novispathodus waageni* in its lower part (sample Na3) indicates a Smithian age.

Subunit IIIb — 2 m of mostly thin-bedded, platy to nodular, grey or light red limestone alternating with shale interbeds (Fig. 6c). It starts with packstones with a microfacies similar to *Subunit IIIa*, containing

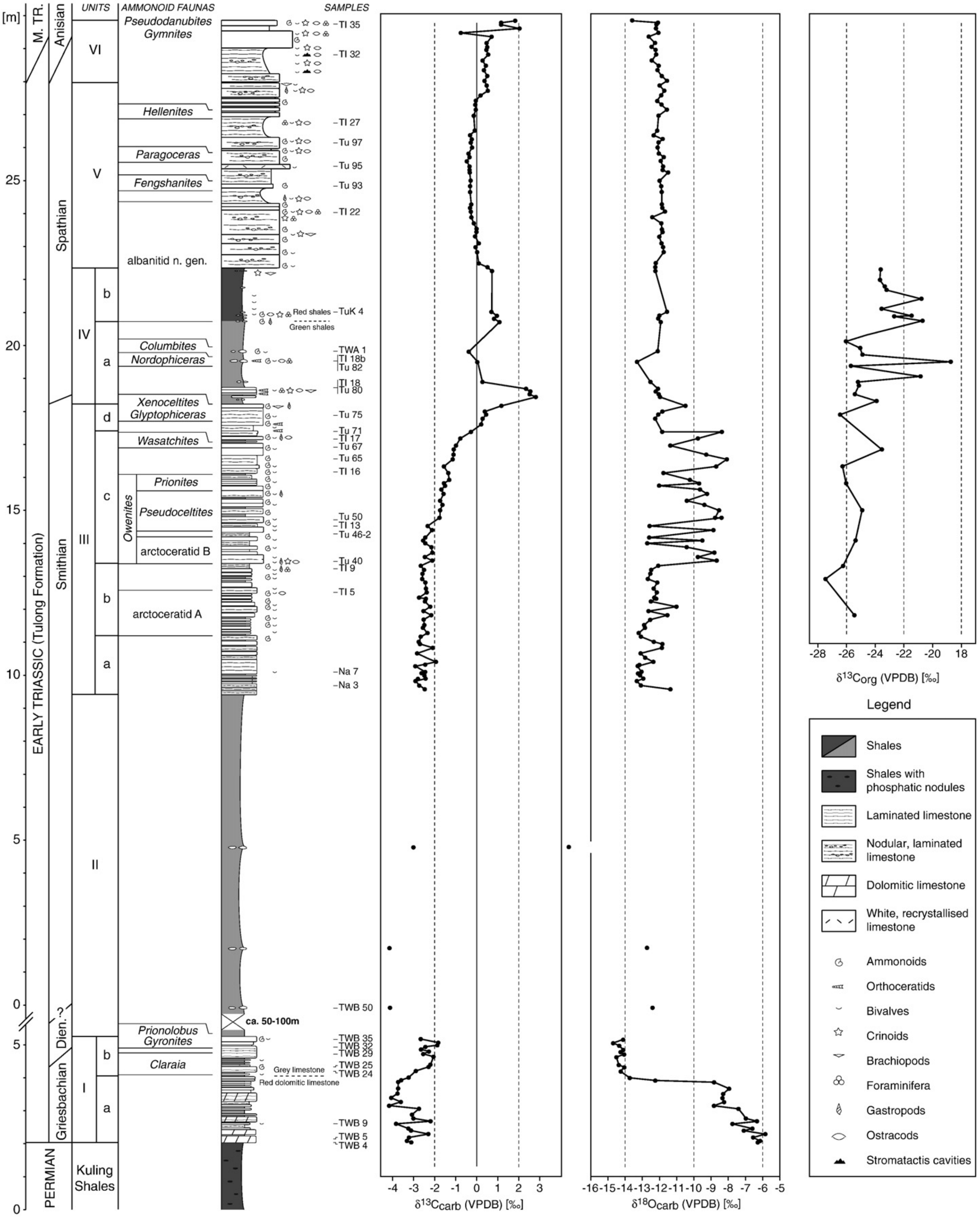

Fig. 4. Composite section of the Tulong Formation (Tulong area, South Tibet) showing lithology, microfossil content, distribution of ammonoid faunas, carbonate carbon/oxygen and organic carbon isotopes, as well as ammonoid, conodont and microfacies samples mentioned in the text. Note the large gap in the record of about 50–100 m in Unit II (see also Fig. 3a). Abbreviations: Dien.: Dienerian; M. TR.: Middle Triassic.

cemented thin-shelled microbivalves. This interval is followed by packstones with completely preserved bivalves (Fig. 6d). The upper part of *Subunit IIIb* is largely dominated by mudstones–wackestones containing microgastropods, juvenile ammonoids, echinoids and calcitic spheres (Fig. 6e).

Subunit IIIb yields a distinct ammonoid fauna including a new taxon here provisionally referred to as arctoceratid A, associated with *Jinyaceras hindostanus* and *Aspenites acutus*. This association has also been recently discovered in beds of middle Smithian age in the Salt Range (Pakistan) and in Northern India (provisionally termed “new prionitid A beds”, cf. Brühwiler et al., 2007). However, no correlative of these beds is known from Guangxi (South China) (Brayard and Bucher, 2008).

The occurrence of conodont species like *Wapitiodus robustus*, *Novispathodus spitiensis* or *Ns.* n. sp. S (Orchard, unpublished) confirms a middle Smithian age for this subunit.

Subunit IIIc — 4 m of medium-bedded grey limestone, alternating with shales or distinctly nodular, marly limestone (Fig. 6f). Limestone microfacies are represented by (i) sparitic packestones-grainstones, packed with crushed thin-shelled microbivalves with a few microgastropods and juvenile ammonoids (Fig. 6g); and (ii) wackestones with thin-shelled microbivalves and microgastropods in a nodular muddy matrix (Fig. 6h). The first occurrence of sparitic cement in the Lower Triassic series of the studied area is recorded in this subunit.

Occasionally *Subunit IIIc* contains beds or nodules that have been referred to as “pseudostromatolithic structures” by Garzanti et al. (1998) (Fig. 7a). However, no typical microbial structures are visible in thin section. These structures consist of thin, alternating laminae of lime mudstone and of lime wackestone/packstone containing thin-shelled microbivalves, ostracods and probably sponge spicules (Fig. 7b).

The lower and middle parts of *Subunit IIIc* are characterized by typical ammonoid faunas of middle Smithian age, i.e. the *Owenites* beds. These beds can be subdivided into three parts. The lower part contains a new genus here provisionally referred to as arctoceratid B, together with *Owenites simplex*, *Paranannites spathi*, and *Kashmirites* sp. In the middle part *Owenites koeneni*, *Pseudoceltites multiplicatus* and ?*Anaxenaspis* sp. indet. occur. The upper part contains the association of *Prionites* sp., “*Pseudoceltites*” *angustecostatus*, *Owenites koeneni*, *Owenites carpentieri*, ?*Subflemingites* n. sp., and *Stephanites superbus*. Differing from these middle Smithian faunas, one bed in the uppermost part of *Subunit IIIc* (sample Tu67) contains the ammonoid *Wasatchites distractum*, which indicates a late Smithian age (Tozer, 1994; Brühwiler et al., 2007).

Besides the rare specimens of the conodont genus *Discretella*, various forms of *Nv. waageni* and *Nv. pakistanensis* largely dominate the assemblages of *Subunit IIIc*. New, very short segminate platform elements (similar but shorter than *Ns. soleiformis*) may characterize its lower part (samples Tu40 to Tu50). Conodont faunas start to change strikingly from sample Tu65 on, where the *waageni/pakistanensis* group almost disappears and is replaced by coniform elements and ellisonids. Above (sample Tu67) we observe a fauna dominated by specimens of *Guangxidella? robustus*, also found in South China and which correlates well with the late Smithian *Wasatchites/Anasibirites* ammonoid beds. The next conodont sample (sample Tu71) contains again a distinct, characteristically late Smithian assemblage, including *Scythogondolella mosheri* and *Sc. milleri*.

Subunit IIId — 1 m of massive, nodular, marly orange to grey limestone (Fig. 7c). Distinct orange bands appear on weathered surfaces. Brachiopods are very abundant in these beds.

In *Subunit IIId* ammonoids are abundant but are usually poorly preserved. *Glyptophiceras sinuatus* and *Xenoceltites* sp. have been found, both genera indicate a latest Smithian age (Brühwiler et al., 2007; Brayard and Bucher, 2008). This subunit contains the conodonts *Nv. pingdingshanensis* as well as *Borinella* aff. *buurensis*, two species which occur worldwide (Goudemand et al., ongoing work) just below the Smithian–Spathian boundary as here defined by ammonoids. From the horizon Tu75 on, *Borinella* becomes the dominant conodont genus.

4.4.2. Interpretation

Abundant benthic and nectonic fossils throughout Unit III indicate well-oxygenated conditions. The highly fragmented shelly material in *Subunit IIIa* indicates a high-energy depositional environment. The changes in the paleoenvironment within *Subunit IIIb* indicate a marked decrease in water energy related to deepening. This modification is coincident with a diversification of the biotas as indicated by the appearance of microgastropods, calcispheres and abundant ammonoids. Water energy increases in the basal part of *Subunit IIIc* as indicated by crushed shells and a sudden shift from micritic matrix to sparry calcite cement. Alternatively, sparry calcite cement could indicate increasing carbonate saturation. Water energy is relatively low again in the remaining part of Unit III as indicated by many complete shells.

4.5. Lower Triassic — Unit IV

4.5.1. Description

This Unit consists of about 4 m of early Spathian shales with a few limestone beds and nodules (Fig. 7d). They can readily be subdivided into a lower green part (*Subunit IVa*) and an upper red part (*Subunit IVb*).

Subunit IVa — 2.5 m of dark green shales At its base it contains a few thin limestone beds made of wackestone with skeletal fragments, thin-shelled bivalves, ostracods, crinoid spines and plates and foraminifera of lagenid type as well as *Glomospirella* cf. *jefimowae* (Fig. 7e–f). In these beds orthoceratids and brachiopods are very abundant. In its middle part, *Subunit IVa* contains ammonoid-rich limestone nodules. One of these nodules consists of lime mudstone and contains thin skeletal fragments, rare ostracods and the benthic foraminifer *Meandrospira pusilla* (Fig. 7. g–h).

The lowermost beds of *Subunit IVa* yields only the ammonoid? *Pseudaspidites* sp., which is not of great age significance because *Peudaspidites* is a long-ranging genus. Two different ammonoid faunas of early Spathian age have been sampled in limestone nodules from about the same horizon in the middle part of the subunit at two different outcrops, i.e. a *Nordophiceras* fauna (sample Tu 82 from outcrop Tu) containing *Nordophiceras* sp., *Paranoritoides* n. sp., columbitid n. gen. and *Hedenstroemia augusta*; and a probably slightly younger *Columbites* fauna (sample TWA 1 from outcrop TWA) containing *Columbites* cf. *parisianus*, *Nordophiceratoides* n. sp., *Evenites* n. sp. and two new genera belonging to Xenoceltitidae. Note that the relative stratigraphic position of these two samples is not known.

The lowermost beds (Tu80) of *Subunit IVa* contain typical Spathian conodonts like *Borinella*? n. sp. C (Orchard, unpublished), transitional forms to *Gladigondolella*, as well as early forms of *Icriospathodus*. The nodules in the middle part of the subunit are almost barren. The presence of *Spathicuspus spathi* in sample Tu82 confirms a Spathian age.

Subunit IVb — 1.8 m of red shale containing abundant, but poorly preserved bivalves. At its base the subunit contains small limestone nodules with abundant but poorly preserved ammonoids. The reddish lime wackestone is slightly dolomitized and contains broken thin-shelled bivalves, crinoid plates, echinoids, microgastropods, ostracods and phantoms of foraminifera (Fig. 8a).

The nodules at the base of *Subunit IVb* contain the ammonoids *Evenites* n. sp. and a new early representative of Albanitidae, which is also known from NW Guangxi (Bucher et al, unpublished data). The occurrence of the conodont *Columbitella elongatus* in these nodules indicates an early Spathian age (*Columbites* beds).

4.5.2. Interpretation

The minor carbonate content in Unit IV may be explained by an increased input of siliciclastics, possibly related to tectonic instability

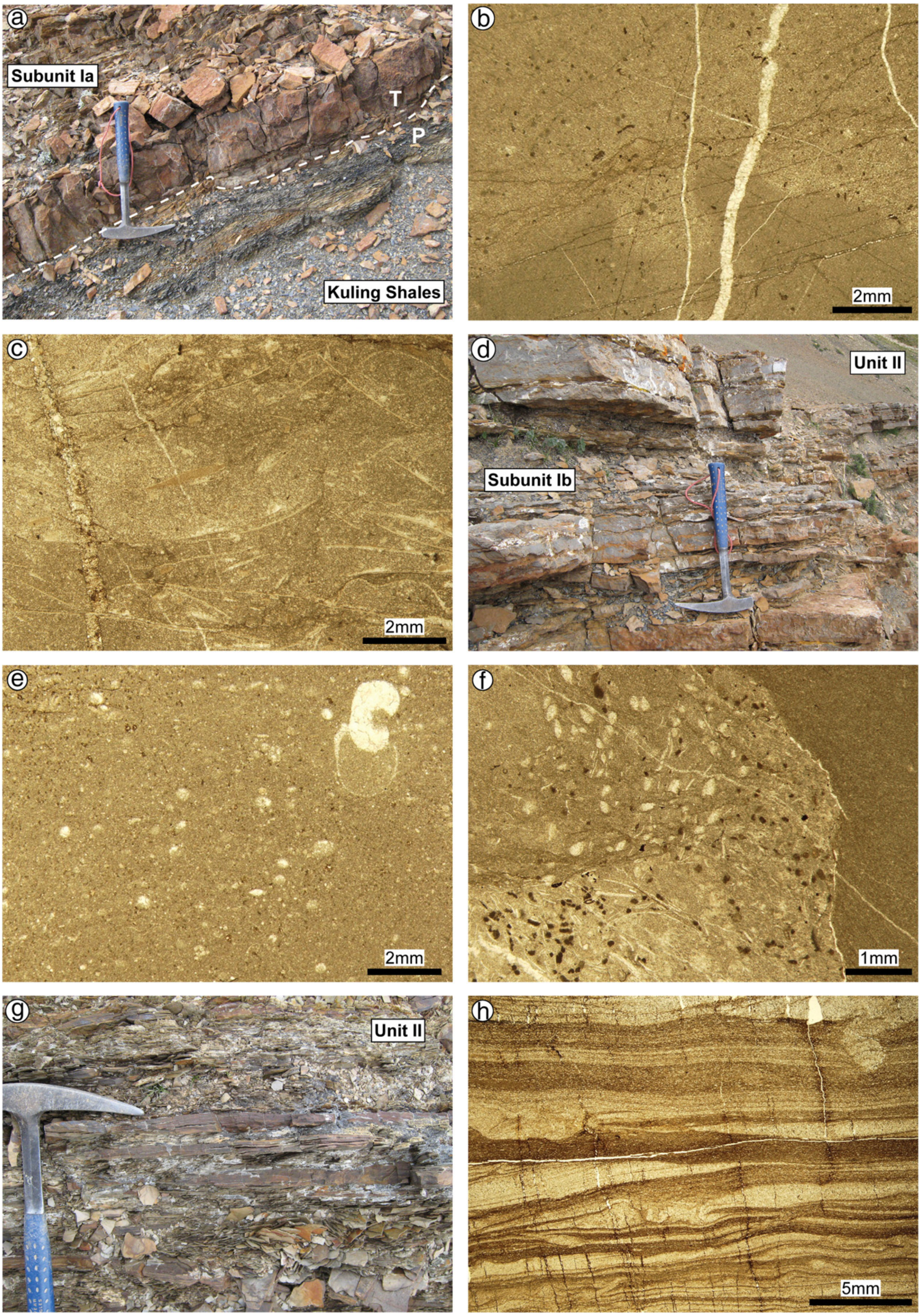
a
Subunit Ia
T
P
Kuling Shales
b
2mm
c
2mm
d
Unit II
Subunit Ib
e
2mm
f
1mm
g
Unit II
h
5mm

of the passive margin (e.g. tilting of blocks). The striking change from barren, dark green shales in *Subunit IVa* to red, bivalve-rich shales in *Subunit IVb* probably corresponds to a change in redox conditions caused by a change from a suboxic to a well-oxygenated sediment-water interface.

4.6. Lower Triassic — Unit V

4.6.1. Description

This red coloured, distinctive unit is about 6 m thick and consists of nodular, marly and bioturbated limestone resembling an “Ammonitico Rosso” facies (Fig. 8b; Garzanti et al., 1998). Due to its characteristic red colour it can very easily be recognized in the field. This unit consists of slightly to strongly bioturbated wackestones/packstones containing abundant thin-shelled bivalves, ostracods, crinoid spines and plates, microgastropods, lagenid and biseriammidid foraminifera, calcitic spheres (i.e. calcitized radiolarians) as well as rare brachiopods (Fig. 8c, e). Clay seams and stylolites are frequent and in some levels, microdolomite (neodolomite) occurs as spots. Discrete stromatactis cavities appear in the lower part of the unit, and become more frequent in the upper part.

The middle part of Unit V is marked by the presence of a peculiar white coquinoid limestone bed (sample Tu95; Fig. 8b). This 20 to 30 cm thick and distinct white bed consists of an accumulation of packed, cemented thin-shelled bivalves with some lenses rich in brachiopods at its top (Fig. 8d).

The same ammonoid fauna as in *Subunit IVb* was found in the lower part of Unit V. In a horizon just below the white coquinoid bed an association with *Fengshanites*, *Procarnites* and *Albanites* was found, indicating the early part of the *Hellenites* Beds of the middle Spathian (Guex et al., 2005a,b). The horizon just above the white bed yielded *Paragoceras*. The upper part of Unit V contains the ammonoids *Hellenites* and *Albanites*, indicating a middle Spathian age (Guex et al., 2005a,b).

The lower part of Unit V still contains the conodont *Columbitella elongatus*. The middle part (from Tu93) contains forms of the *Neogondolella regalis* group. A distinct fauna with *Triassospathodus* aff. *chionensis* appears in Tu97, indicating again a middle Spathian age. From this bed upward, the previously dominating elongate forms (neogondolellids) almost disappear, which may signal the return of shallower and/or warmer waters (Orchard, 2007). *Tr. homeri* dominates the upper part of the unit together with *Spathicuspus* spp.

4.6.2. Interpretation

The Ammonitico Rosso facies is well-known from the Jurassic of the Mediterranean (e.g. Jenkyns, 1974). In the Lower Triassic of the Tethys–Himalaya a similar facies was first described by von Rad et al. (1994) at Thini (Thakkhola area, Nepal), and later by Garzanti et al. (1998) at Tulong. This facies has been interpreted as having been deposited on a deep outer shelf plateau (upper bathyal pelagic carbonates), under well-oxygenated conditions (von Rad et al., 1994). It differs from the more distal, red Hallstatt Limestone facies (Lower to Upper Triassic, Tethyan realm; Tozer and Calon, 1990), by its high clay content and its nodular fabric. In the Himalayas, the Hallstatt facies is only known from exotic blocks (Heim and Gansser, 1939; Bassoulet et al., 1978). As reported from the Smithian ammonoid-rich Hallstatt limestones from Oman Exotics (Woods and Baud, 2008), the stromatactis cavities observed in Unit V at Tulong probably indicate microbial activity. Ammonoid and conodont biostratigraphy indicates that sedimentation rates were low, and the upper part of Unit V is condensed.

4.7. Middle Triassic — Unit VI

4.7.1. Description

The lower part of Unit VI consists of 1 m of yellowish, thin-bedded, nodular limestone (Fig. 8f). The microfacies is composed of biomicritic wacke/packstones showing remains of thin-shelled bivalves with some ostracods and crinoid spines (Fig. 8g). Microdolomite (neodolomite) occurs as spots. Some stromatactis cavities also occur. This interval is followed by a very prominent, ca. 50 cm thick grey limestone bed (Fig. 8f), overlain by two 15–20 cm thick ammonoid-rich, yellowish limestone beds showing phosphatic preservation of ammonoids. In this upper part of the unit the bioclastic content is identical to the one in the lower part (Fig. 8h). Small stromatactis cavities are present in all the microfacies of this unit. Unit VI is overlain by a thick series of dark to greenish turbiditic sandstones and shales of the Qudenggongba Formation (Liu and Einsele, 1994; Garzanti et al., 1998).

No ammonoids have been found in the lower part of Unit VI. The prominent thick limestone bed in the upper part yields representatives of *Gymnites* of Anisian age. From the two beds above this horizon Garzanti et al. (1998) mentioned the Early Anisian ammonoid *Japonites* sp. indet. In the upper of these two beds the ammonoids *Pseudodanubites* sp. and *Acrochordiceras hyatti* were found, an association diagnostic of the upper part of the early Middle Anisian Hyatti Zone (Bucher, 1992).

The lower part of Unit VI is still dominated by *Triassospathodus homeri* and *Cratognathus* spp. An Anisian fauna strongly dominated by *Chiosella timorensis* appears in the uppermost two beds.

4.7.2. Interpretation

As suggested by the phosphatic preservation of ammonoids and indicated by ammonoid and conodont biostratigraphy, Unit VI is highly condensed. No late Spathian ammonoid faunas have been documented from this unit.

5. Comparison with previous stratigraphic work

Our study, which includes several new sections and detailed biostratigraphical data, modifies and improves our knowledge of the Lower Triassic successions in the Tulong area. It reveals that previously published documentations of the Lower Triassic succession in this area were incomplete and/or poorly or incorrectly dated. The first report of Lower Triassic ammonoids from South Tibet was provided by Wang and He (1976) from the Mount Everest region. However, these authors did not publish any stratigraphical succession, which hampers the interpretation of their data. Moreover, preservation of their material is partly rather poor.

The stratigraphic profile of the Permian–Triassic boundary at Tulong provided by Rao and Zhang (1985) corresponds to our Units I and II. However, their ammonoid identifications seem dubious since they mention unusual associations of Dienerian and Smithian taxa, which are unknown from any other section in the world (e.g. Tozer, 1994; Brühwiler et al., 2007, 2008; Brayard and Bucher, 2008).

Fig. 5. (a) Outcrop photograph showing the Permian–Triassic boundary and *Subunit Ia* at section TWB. Hammer (33 cm) for scale. (b) Thin-section photomicrograph of sample TWB4 (lowest bed of *Subunit Ia*) from section TWB. Fractured and dolomitized micritic mudstone with possible phantoms of microfossils. (c) Photomicrograph of sample TWB9 (*Subunit Ia*) from section TWB. Dolomitized biomicritic mudstone, with abundant thin-shelled bivalves and broken echinoid plates. (d) Outcrop photograph showing *Subunit Ib* near section TWB. Hammer (33 cm) for scale. (e) Photomicrograph of sample TWB24 (*Subunit Ib*) from section TWB. Dolomitized biomicritic mudstone, containing ammonoids and spherical microfossils (“microspheres”; possibly radiolarians). (f) Photomicrograph of sample TWB35 (topmost bed of *Subunit Ib*) from section TWB. Recrystallized wackestone with abundant thin-shelled bivalves and ammonoids (not figured on the photo) on the left side, mudstone on the right side. Nodular texture, Stylolites and pyrite common. (g) Outcrop photograph showing thin cross-bedded dolomitic siltstone lenses in the upper part of Unit II from section TWB. Hammer (33 cm) for scale. (h) Photomicrograph of sample TWB50 (Unit II) from section TWB. Dolomitized, wavy laminated siltstone.

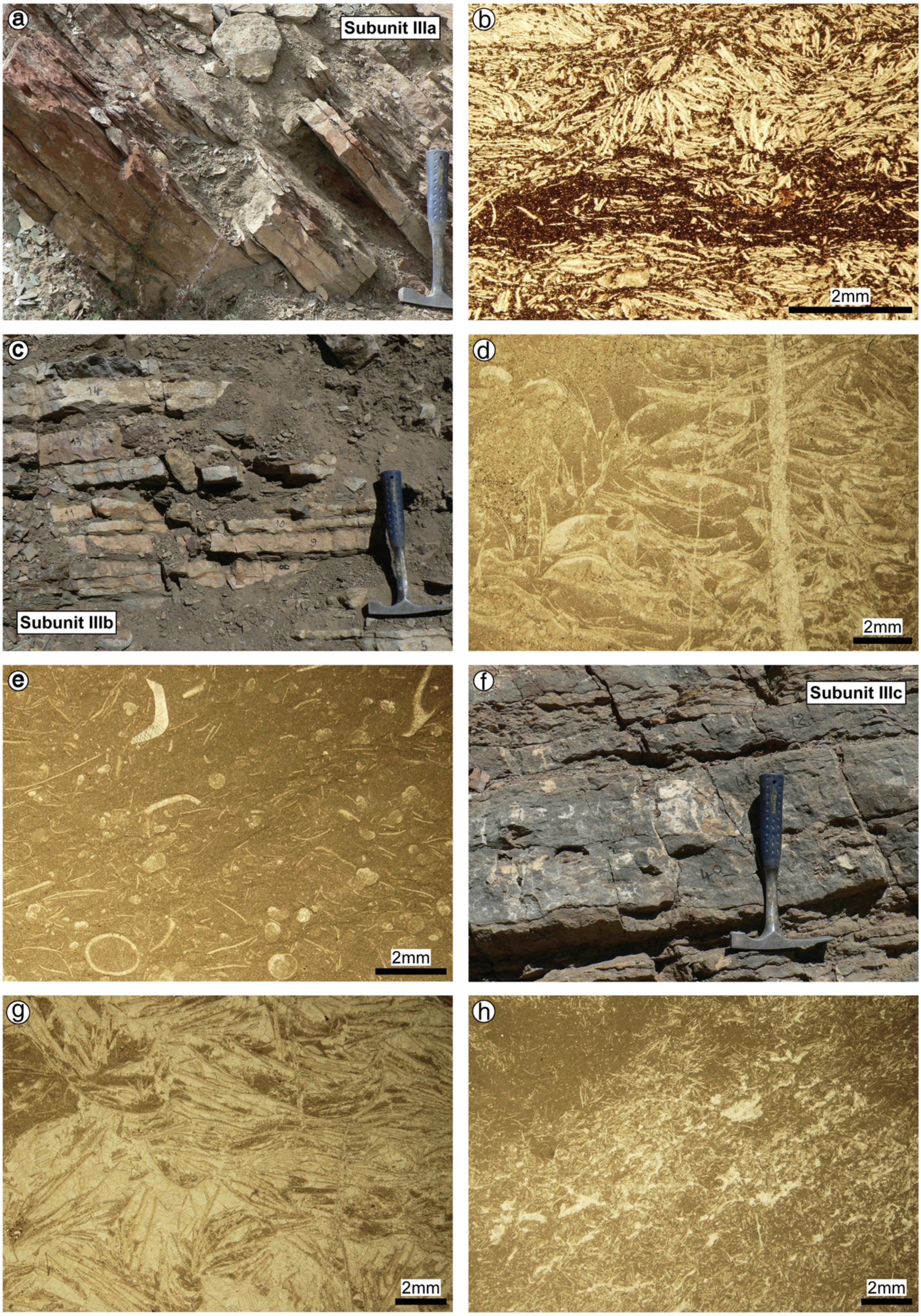
a
Subunit IIIa
b
2mm
c
Subunit IIIb
d
2mm
e
2mm
f
Subunit IIIc
g
2mm
h
2mm

Liu (1992) and Liu and Einsele (1994) provided a general overview on the Permian to Tertiary sedimentary history of South Tibet. They described the Lower Triassic Tulong Formation as 100–300 m thick, consisting in the lower part of dark, grey to purple shale, limestone and dolomite, and in the upper part of limestone and grey shale. They also mention the presence of the ammonoids *Otoceras*, *Owenites*, *Pseudosageceras* and *Procarnites* in this formation. However, it turns out to be difficult to compare their stratigraphic section with our observation of the sedimentary succession. Liu's (1992) Unit 3 probably corresponds to the Spathian red nodular limestone (i.e. our Unit V). In this case, his Lower–Middle Triassic boundary is placed some 100 m too high, and our Units I and II would be missing.

The classic Tulong section reported by Garzanti et al. (1998) shows no Permian–Triassic boundary since the Kuling shales and the entire Griesbachian and Dienerian parts of the section (Units I and II) are not exposed. Moreover, the conodont-based biostratigraphic interpretation of the section of these authors turns out to be erroneous: (i) the base of the outcrop is not Dienerian, but Smithian in age, and (ii) their Smithian–Spathian boundary is placed about 4 m too high, at the base of Unit V instead of the base of Unit IV.

The data on the Permian–Triassic boundary at Tulong reported by Shen et al. (2006) were based on Tian (1982) and Rao and Zhang (1985). However, this boundary as indicated on their photographs of the Tulong section (Shen et al., 2006, fig. 2E, p. 5) corresponds in fact more or less to the Lower–Middle Triassic boundary. Our extensive investigations did not reveal any exposed Permian–Triassic boundary on this hillside.

6. Carbonate carbon/oxygen and organic carbon isotope profiles

6.1. Samples and methods

High-resolution sampling (5–20 cm) was carried out throughout the entire Lower Triassic Tulong Formation. We analyzed the micritic matrix of 160 carbonate rock samples for the carbonate carbon and oxygen isotope ratios. Thirteen of these samples were also analyzed for the organic carbon isotope ratios. Additionally, 16 shale samples from Unit IV were analyzed for the organic carbon isotope ratios. Heterogeneous samples, containing visibly weathered parts, calcite veins or voids were carefully cleaned and cut into thin slabs. The visually least altered spots were selectively drilled with a diamond-tipped drill to produce a fine powder. All samples have been analyzed for their isotopic composition at the Institute of Mineralogy and Geochemistry of Lausanne University.

Stable carbonate carbon and oxygen isotope ratios were measured using a Thermo–Finnigan GasBench II equipped with a CTC Combi-Pal autosampler and linked to a Delta Plus XL mass spectrometer. Runs were calibrated with Carrara Marble as internal standard (+2.05‰ for C and −1.7‰ for O), which in turn has been calibrated against NBS-19 (see procedure described in Spötl and Vennemann, 2003). Reproducibility of replicate analyses was better than 0.1‰ for standards and 0.15‰ for whole rock sediment samples for both carbon and oxygen isotope ratios.

The organic carbon isotope ratio has been measured using a Carlo Erba EA-1500 connected to a Finnigan MAT Delta-S mass spectrometer. The samples were individually wrapped in tin foil cups and dropped into the reactor while a small dose of oxygen gas was mixed into the He stream. The samples have then been oxidized in the reactor held at about 1050 °C and filled with cobalt oxide as a catalyst for the oxidation. Excess oxygen from the He stream was adsorbed in another reactor column filled with metallic Cu held at 500 °C. The residual gases of CO_2, (N_2), and H_2O were then passed over a water trap of magnesium perchlorate [$Mg_4(ClO_4)_2$] and into a gas chromatograph filled with a molecular sieve (5 Å) to separate N_2 and CO_2. CO_2 was then transported by the He stream via a CONFLO III (open split) system into the mass spectrometer for isotopic analyses.

Reproducibility of the internal graphite standard used was better than ±0.12‰ and USGS-24 graphite (−16.0‰ VPDB) and NBS-22 oil (−29.6‰ VPDB) were used as calibration standards. All isotope results are reported using the conventional δ notation, defined as per mil (‰) deviation vs. VPDB (i.e. Vienna Pee Dee Belemnite).

6.2. Results

All analytical data ($\delta^{13}C_{carb}$–$\delta^{18}O_{carb}$–$\delta^{13}C_{org}$) are provided in the Supplementary Online Material (Table 1). The measured ratios are plotted against the composite profile, which combines the four sampled sections in the Tulong area (Fig. 4).

6.2.1. Carbonate carbon isotope record

Between the Permian–Triassic boundary and the Lower–Middle Triassic boundary the Lower Triassic carbonate carbon isotope record ($\delta^{13}C_{carb}$) of the Tulong Formation shows essentially 3 positive and 3 negative excursions. Its trend varies over a broad range comprised between −4.2‰ and +2.8‰ and displays a well-defined curve along the section.

Low and highly variable values ranging between −4.2‰ and −2.2‰ are obtained from the dolomitic limestones of the Griesbachian interval (*Subunit Ia*). Subsequently an increase in the C_{carb}-isotope values from −4.2‰ to −2.4‰ is observed from the Griesbachian–Dienerian boundary up to the limestone horizon at the top of *Subunit Ib* yielding the *Pleurambites* and *Proptychites* ammonoid fauna. This maximum is followed by a large gap which is due to the shales of Unit II lacking any limestone beds in the lower part. The few small dolomitic siltstone lenses in the upper part of Unit II yield C_{carb}-isotope values around −4‰. Nearly constant C_{carb}-isotope values around −2.5‰ characterize the lower part of the Smithian carbonates (*Subunits IIIa–b*). The most prominent positive C_{carb}-isotope excursion of the entire Lower Triassic Tulong Fm. starts around the horizon in *Subunit IIIc* yielding the first *Owenites* fauna, i.e. the Arctoceratid B fauna. This excursion is characterized by a gradual increase from −2.5‰ up to −1‰ (e.g. in the bed yielding *Wasatchites*), then rises abruptly and reaches peak values of up to 2.8‰ at the base of *Subunit IVa* (earliest Spathian). This well-defined, latest Smithian to earliest Spathian positive shift in C_{carb}-isotope values is then followed by a major drop ranging from −0.4‰ to 1‰, which coincides with the change to siliciclastics (Unit IV). Following this interval the C_{carb}-isotope values remain essentially stable between −0.2‰ and 0‰ during most of the Spathian limestone deposition (Unit V). A slightly positive excursion starts with the onset of the thin-bedded limestones in the uppermost part of Unit V yielding *Hellenites* and *Albanites* faunas and reaches maximum values around +2‰.

Fig. 6. (a) Outcrop photograph showing *Subunit IIIa* at section Na. Hammer (28 cm) for scale. (b) Thin-section photomicrograph of sample Na7 (*Subunit IIIa*) from section Na. Dolomitized, laminated biomicrosparitic packstone–grainstone containing densely packed, mostly broken, thin-shelled bivalves. Dolomitic matrix. (c) Outcrop photograph showing *Subunit IIIb* at section Tu. Hammer (28 cm) for scale. (d) Thin-section photomicrograph of sample Tl5 (*Subunit IIIb*) from section Tu. Packstone containing thin-shelled bivalves and probably ostracods. Note geopetal structures. (e) Thin-section photomicrograph of sample Tl9 (*Subunit IIIb*) from section Tu. Biomicritic mudstone–wackestone containing microspheres (probably microgastropods) and ammonitellas. (f) Outcrop photograph showing *Subunit IIIc* at section Tu. Hammer (28 cm) for scale. (g) Thin-section photomicrograph of sample Tl13 (*Subunit IIIc*) from section Tu. Biosparitic grainstone with packed, thin-shelled bivalves. (h) Thin-section photomicrograph of sample Tl16 (*Subunit IIIc*) from section Tu. Wackestone–packstone containing thin-shelled bivalves.

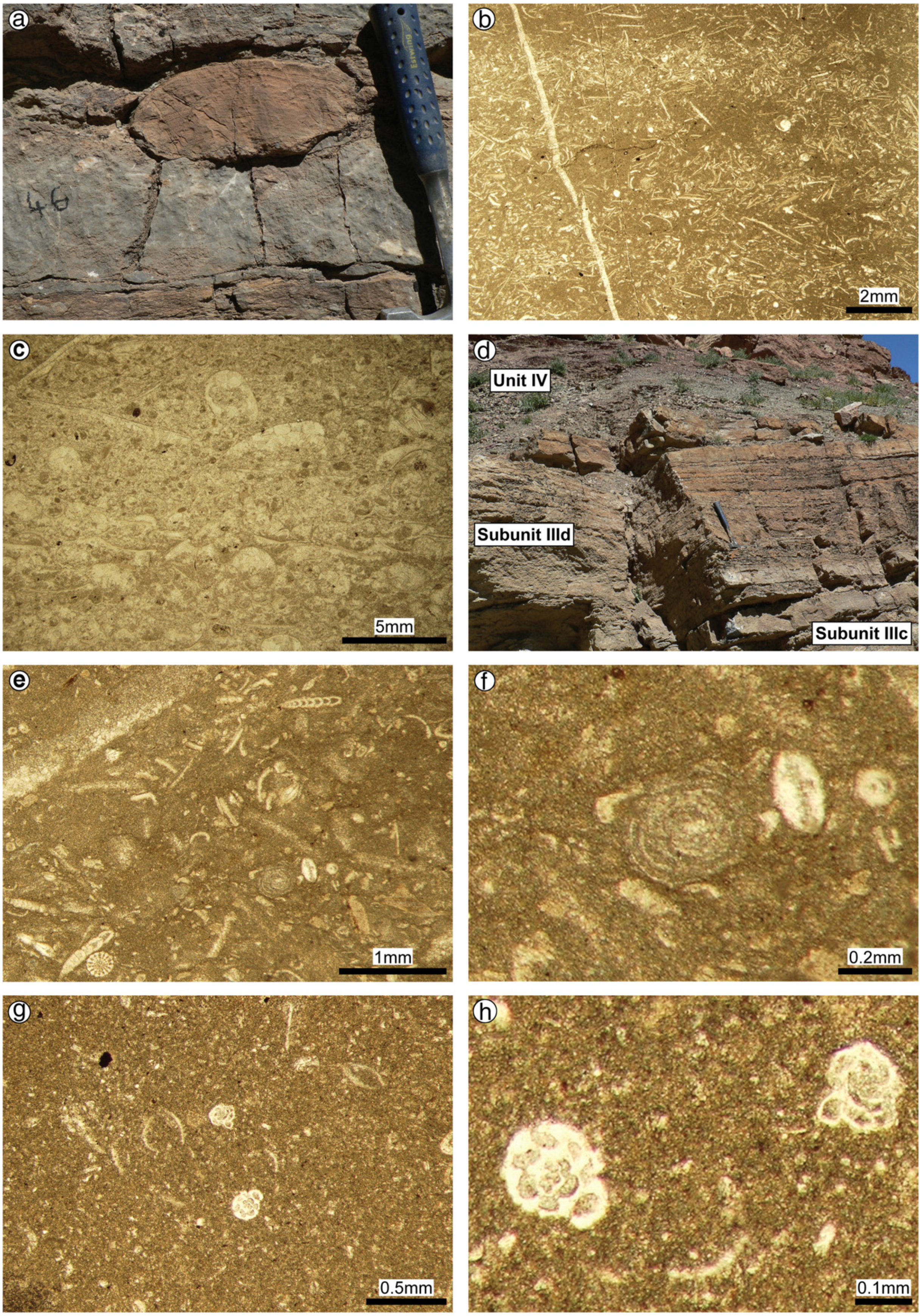
a
46
b
2mm
c
5mm
d
Unit IV
Subunit IIId
Subunit IIIc
e
1mm
f
0.2mm
g
0.5mm
h
0.1mm

6.2.2. Organic carbon isotope record

The organic carbon isotope record from the Lower Triassic Tulong Fm. has been obtained from the Smithian–early Spathian interval (*Subunit IIIb*–Unit IV). Its values vary over a wide range from −18.7‰ to −27.5‰. While the late Smithian record displays a slight increase in the $\delta^{13}C_{org}$ composition, the latest Smithian–earliest Spathian interval shows a highly fluctuating record. The $\delta^{13}C_{carb}$–$\delta^{13}C_{org}$ cross-plot for the carbonate samples, for which both $\delta^{13}C_{carb}$ and $\delta^{13}C_{org}$ have been analyzed, shows no covariance (Pearson's correlation coefficient $r = 0.386$, $p = 0.192$) (Fig. 9c). Due to the erratic nature of the signal, especially in Unit IV, the $\delta^{13}C_{carb}$ record appears as inconclusive. Therefore, any interpretation in terms of isotope excursions and correlations with the measured C_{carb} and O_{carb} isotope profiles would be rather speculative.

6.2.3. Carbonate oxygen isotope record

The $\delta^{18}O_{carb}$ values of the Lower Triassic Tulong Fm. are generally very low ranging from −5.8‰ to −14.2‰ for the Griesbachian–Dienerian and from −8‰ to −13.6‰ for the Smithian–Spathian time intervals. Extremely low values around −17‰ are detected within the carbonate lenses in the upper part of Unit II. Two major oxygen isotope anomalies are identified. The first one is a sharp, well-defined, negative excursion dropping from −5.8‰ to −14.2‰. It coincides with a lithologic change from dolomitic limestone to limestone around the Griesbachian/Dienerian boundary (*Subunits Ia–b*). The second one, less well-marked, is a change from relatively stable oxygen isotope values in *Subunits IIIa–b* to a strongly erratic signal in *Subunits IIIc–d*, coinciding with the onset of the major positive $\delta^{13}C_{carb}$-isotope shift within the middle-late Smithian time interval. Background values, ranging from −12‰ to −13.5‰, shift toward more positive values up to −8‰ during this interval. Following this perturbation constant oxygen isotope values around −12‰ are observed throughout the Spathian.

6.3. Diagenetic alteration of the isotope record

Since samples of the Lower Triassic Tulong Fm. display very low $\delta^{18}O_{carb}$ values (i.e. average: −12‰) and unusually low $\delta^{13}C_{carb}$ values (e.g. essentially during the Griesbachian–early/middle Smithian: average −2.5‰) one may question whether the primary marine signature has been preserved or if the measured isotope values represent diagenetic features. The comparison between the $\delta^{13}C_{carb}$ and $\delta^{18}O_{carb}$ profiles (see cross-plots in Fig. 9a–b) shows that $\delta^{18}O_{carb}$ covaries with $\delta^{13}C_{carb}$ values in some parts of the section (i.e. mostly the Griesbachian/Dienerian interval; the Smithian shows also a slight covariance [i.e. Unit III]). This suggests some influence of diagenesis on the isotope records (e.g. Glumac and Walker, 1998).

Oxygen isotope values are known to be more prone to alteration during diagenesis than carbon isotope values (Marshall, 1992). For instance, in other Tethys–Himalayan sections of Kashmir, Spiti and Nepal, very low $\delta^{18}O$ values (similar to those from Tulong) have been found and explained by a thermal metamorphism process of up to 300 °C (Baud et al., 1996; Atudorei, 1999). It is interesting to note that even in such conditions of low-grade metamorphism the relative changes in the carbon isotopic signal are preserved and correlate with other records for the same time span, although the changes in oxygen isotopes have been completely obliterated.

Another interesting case is the lithological change from dolomite to limestone at the *Subunit Ia/Ib* boundary, concomitant with a strong negative shift of the $\delta^{18}O$ values from −8 to −14.5‰ without affecting the $\delta^{13}C$ values. Similarly, an even more negative shift of the $\delta^{18}O$ values from −9 to −23‰ is recorded at exactly the same lithological change of Thini Chu section (Nepal), 300 km to the west with no influence on the $\delta^{13}C$ values (Baud et al., 1996).

Considering that rocks of the Tulong area experienced regional metamorphism with temperatures up to about 200 °C (see Section 2.2.) we suspect an overprint of the isotope signal by deep burial diagenesis, shifting both carbon and oxygen isotope ratios toward more negative values (e.g. Galfetti et al., 2007a). The oxygen isotope record of Tulong is very unlikely to preserve any primary signal. It is probably completely controlled by diagenetic processes. However, taking into consideration the striking similarity with other age-constrained, Lower Triassic sections from the Tethys (see Corsetti et al. (2005) and Galfetti et al. (2007a) for reviews; and discussion and correlations hereafter) it is assumed that all the relative fluctuations in the $\delta^{13}C_{carb}$ signal of the Lower Triassic Tulong Formation are reliable.

7. Discussion

7.1. Comparison with the Lower Triassic section of Selong, South Tibet

The described lithological Late Permian to Lower Triassic succession from Tulong shows distinct differences to the sections from the area of Selong which is located only 35 km to the NW (cf. Wang et al., 1989; Yugan et al., 1996; Garzanti et al., 1998; Wignall and Newton, 2003). At Selong the late Permian consists of fossil-rich limestones of Djulfian and Changhsingian age (Garzanti et al., 1998; Orchard et al., 1994), contrasting with the Kuling Shales at Tulong. The Griesbachian–Dienerian interval is similar to Tulong regarding facies and thickness. A shale interval similar to Unit II also exists in Selong, but is has an extremely reduced stratigraphic thickness (ca.1.5 m). The Smithian–Spathian interval of the Selong section is much less developed than in Tulong and is only about 4.5 m thick. At Selong the "Ammonitico Rosso" facies is missing.

Such facies and thickness changes appear to be compatible with large-scale tilted blocks that developed on the northern Gondwana passive, extensional margin (Stampfli et al., 1991). Tulong and Selong belong to two contiguous thrust sheets (Burg, 1983). Because of the unknown amount of N–S tectonic shortening between these two thrust sheets, it cannot be established whether the two areas were part of a single tilted block or belonged to two distinct blocks.

7.2. Comparison with other Lower Triassic Tethyan sections

Griesbachian — The dolomitic facies of *Subunit Ia* from Tulong seems not uncommon in the earliest Triassic. It is known from other Tethyan localities, such as in (i) the *Otoceras latilobatum* beds at Selong (Wignall and Newton, 2003); (ii) the Panjang unit of the Thakkhola area of N central Nepal, about 300 km to the West (Hatleberg, 1982; Baud et al., 1996); (iii) the brown, ferruginous, dolomitic limestone of the lower part of the Lower Limestone Member (*Otoceras* beds) in Spiti, Northern India (Bhargava et al., 2004; pers. observation); and in (iv) the dolomitic Kathwai Member of the Salt Range, Pakistan (Kummel, 1970; Guex, 1978; pers. observation).

For the Selong area Wignall and Newton (2003) suggested that the common formation of pyrite and dolomite in the Griesbachian *Otoceras latilobatum* beds may be caused by anoxic pore-waters during deposition of anoxic sediments in the Dienerian ("diagenetic anoxia

Fig. 7. (a) Outcrop photograph showing a nodule with so-called "pseudostromatolithic structures" (Garzanti et al., 1998) (*Subunit IIIc*, section Tu). Hammer (28 cm) for scale. (b) Photomicrograph of a thin-section through the same nodule (sample Tu46-2, section Tu). Note alternating domains of lime mudstone and of lime wackestone with thin-shelled microbivalves, ostracods and spicules. (c) Thin-section photomicrograph of sample Tl17 (*Subunit IIIc*) from section Tu. Recristallized packstone with juvenile ammonoids, thin-shelled bivalves, microgastropods, ostracods, peloids and geopetal structures. (d) Outcrop photograph showing *Subunit IIId* and Unit IV at section Tu. Hammer (28 cm) for scale. (e) Thin-section photomicrograph of sample Tl18 (*Subunit IVa*) from section Tu. Wackestone–packstone containing thin-shelled bivalves, ostracods, crinoid spines and plates together with Nodosariids foraminifera. (f) Detail of previous figure showing the foraminifer *Glomospirella* cf. *jefimowae*. (g) Thin-section photomicrograph of sample Tl18b (*Subunit IVa*) from section Tu. Mudstone containing small bioclasts and rare ostracods and foraminifera. (h) Detail of previous figure showing the foraminifer *Meandrospira pusilla*.

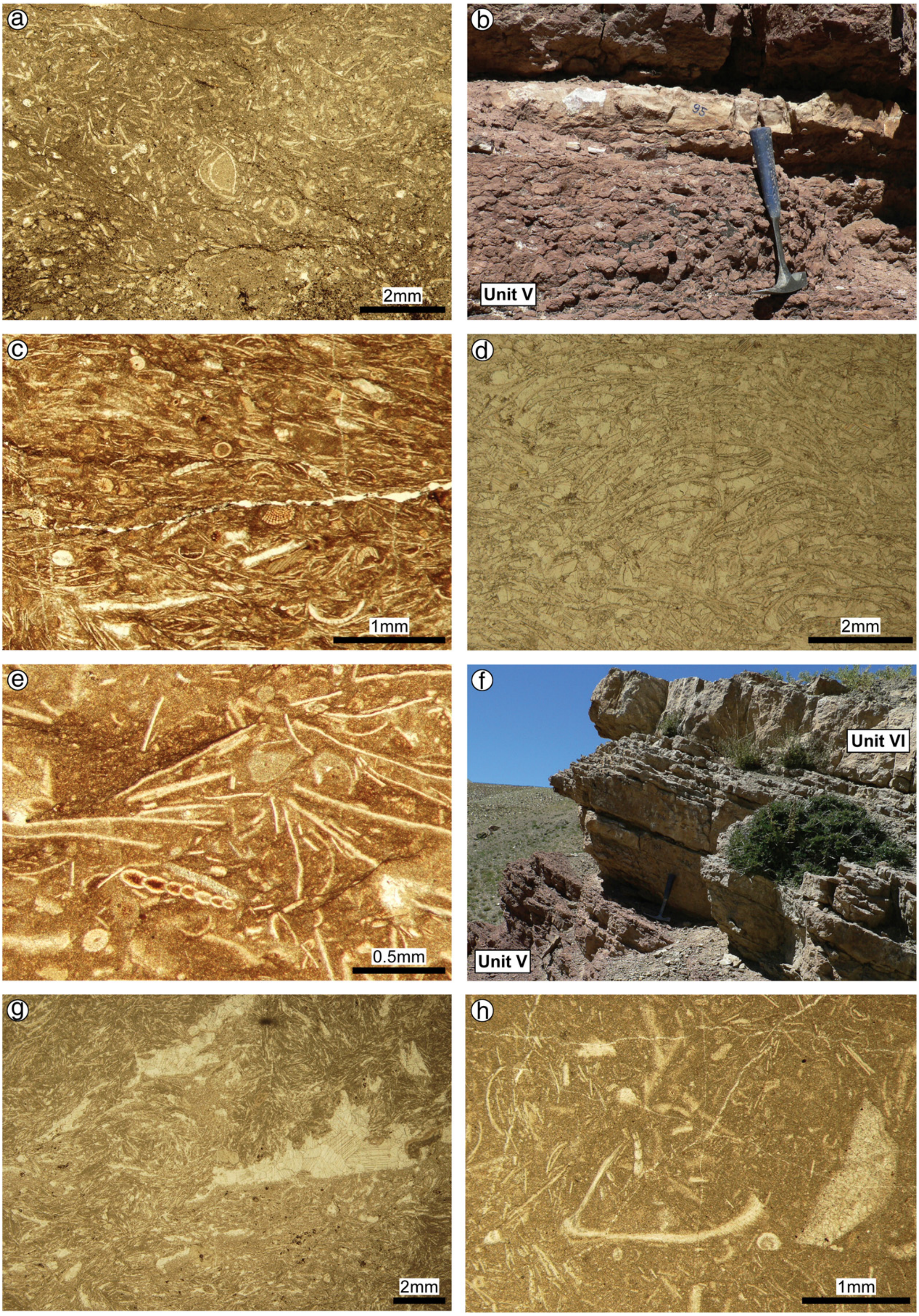
a
2mm
b
95
Unit V
c
1mm
d
2mm
e
0.5mm
f
Unit VI
Unit V
g
2mm
h
1mm

imposed upon a bed deposited in fully oxygenated conditions" (Wignall and Newton, 2003, p. 158)). However, this explanation is at variance with the widespread and synchronous distribution of dolomites in the Griesbachian in Tulong, Spiti and the Salt Range and the absence of evidence for anoxia in the overlying Dienerian carbonates in all of these areas (see below).

Microbial limestones, a common feature of the earliest Triassic as shown by Baud et al. (1997, 2002, 2005, 2007), Kershaw et al. (1999, 2002, 2007) and Galfetti et al. (2008) (e.g. South China, Japan, Iran, Turkey, Hungary, Armenia, Greenland and possibly Madagascar), are not present in the Tulong section. However, the synchroneity of widespread dolomite and microbial limestone deposition in the aftermath of the Permian/Triassic extinction may suggest a relationship between the two facies. In present-day hypersaline, anoxic environments microbial sulfate-reducing activity can induce an environment favouring the precipitation of dolomite (Vasconcelos and McKenzie, 1997). Burns et al. (2000) suggested that throughout the Phanerozoic the amount of dolomite formation is negatively correlated with the amount of atmospheric oxygen. Thus, they proposed that oxygen is the primary factor controlling widespread dolomite formation and suggested that sulfate-reducing microbial communities associated with seafloor hydrothermal systems may be an ultimate factor controlling massive dolomite formation on a global scale. Similarly, widespread and possibly sulfate-reducing microbial communities as exemplified by the global occurrence of microbial limestone (Baud et al., 2007) as well as deep oceanic anoxia (Isozaki, 1997; Kakuwa, 2008) might have favoured dolomite formation during the Griesbachian. However, further investigation is needed to test this hypothesis.

Dienerian — Regarding facies as well as thickness, the late Griesbachian to Dienerian ammonoid-rich, thin-bedded, grey carbonates of *Subunit Ib* strongly resemble the Lower Ceratite Limestone from the Salt Range (Waagen, 1895; Guex, 1978; pers. observation) and the age-equivalent carbonates of the upper Lower Limestone Member in Spiti (Bhargava et al., 2004; pers. observation). The overlying shales of Unit II (Dienerian and early Smithian) are strikingly similar to the Ceratite Marls of the Salt Range (Waagen, 1895; Guex, 1978; pers. observation). During the Dienerian clastic sedimentation also predominates in Guangxi (South China) and Spiti.

Smithian — As in many other Tethyan sections such as Guangxi, Spiti and in the Salt Range, the Smithian series in Tulong (Unit III) are dominated by carbonate rocks (Waagen, 1895; Guex, 1978; Galfetti et al., 2007a; pers. observation). However, detailed comparison reveals important differences between these areas. In Guangxi and in Spiti the early Smithian is marked by a conspicuous episode of carbonate deposition (i.e. the *Flemingites* beds; Galfetti et al., 2007a). However, in Tulong and in the Salt Range the early Smithian is still characterized by clastic deposition (Unit II; Ceratite Marls/Ceratite Sandstones), and massive carbonate sedimentation starts only in the middle Smithian (Unit III; Upper Ceratite Limestone). The middle and late Smithian parts of the Tulong and the Salt Range sections contain more carbonates than in Guangxi and Spiti, where the *Owenites* beds and the *Anasibirites* beds consist of dark, organic rich shales with interbedded limestones or limestone nodules. In the late Smithian (*Anasibirites* beds) these shales often show signs of anoxia or dysoxia (Galfetti et al., 2007a), a feature which is absent in Tulong and in the Salt Range (pers. observation).

Spathian — The early Spathian shales of Unit IV have no known direct counterpart in other Tethys–Himalaya sections. Time-equivalent rocks usually consist of nodular limestone similar to those of Unit V. This local absence of carbonates may be the result of an increased input of clastic sediments, possibly related to tectonic instability of the passive margin (e.g. tilting of blocks). The colour change from green to red in the shales in the Early Spathian Unit IV indicates a change in redox conditions.

The Middle Spathian red nodular limestone of Unit V ("Ammonitico Rosso" facies) has also been described from the Thakkhola (north of the Anapurna, Nepal) (von Rad et al., 1994). This facies also resembles the Lower to Upper Spathian Niti Limestone from the Indian Himalayas and the Lower to Upper Spathian nodular limestone from Guangxi (South China) (Galfetti et al., 2007a), differing only by its red colour. This colour is probably caused by fine Fe-rich terrigenous material (Liu, 1992) and an oxidizing water-sediment interface.

Anisian — In the studied area the interval ranging from the late Spathian to the middle Anisian is strongly condensed. Although less extreme, similar low sedimentation rates and/or hiatuses in this time interval are observed also in other Tethyan localities such as Spiti (India) (Bhargava et al., 2004).

7.3. Carbon isotope correlations

Fig. 10 shows the late Permian to late Spathian part of the carbonate carbon isotope record from northwestern Guangxi (South China), which has recently been calibrated by means of high-precision U–Pb ages and ammonoid biochronozones (Ovtcharova et al., 2006; Galfetti et al., 2007b). The correlation of the new carbon isotope record from Tulong with South China by means of ammonoid faunas results in a strong contraction of the Smithian part of the Tulong record and reveals striking similarities between the two records.

The observed positive shift around the Griesbachian/Dienerian boundary correlates well with coeval positive shift shown by Baud et al. (1996) from the Guryul Ravine section (lower Khunamuh Formation) and from the Thini Chu section (basal Tamba Kurkur Formation) and can be compared with the late Griesbachian positive shift observed in other localities such as South China (Fig. 10; Galfetti et al., 2007a).

The large positive excursion at the Dienerian–Smithian boundary, which has been documented in various areas such as South China, Spiti and Italy (Payne et al., 2004; Galfetti et al., 2007a; Horacek et al., 2007a; Krystyn et al., 2007; Richoz et al., 2007) is missing in our record (Fig. 10). Therefore, the corresponding time interval may lie within Unit II, and the excursion was not documented because of the lack of carbonates. Consequently, Unit III does not include the base of the Smithian and the Dienerian/Smithian boundary lies within Unit II.

Like in other sections the middle Smithian is characterized by low $\delta^{13}C_{carb}$ values (Galfetti et al., 2007a). The following well-defined positive $\delta^{13}C_{carb}$ excursion at the Smithian–Spathian boundary correlates well with that from other Tethyan and boreal profiles (Baud et al., 1996; Payne et al., 2004; Galfetti et al., 2007a,c; Horacek et al., 2007a,b). Differing from other profiles there is an unexpected and sudden $\delta^{13}C_{carb}$ drop following the Smithian–Spathian boundary excursion (*Subunit IVa*), which does not appear in other Tethyan

Fig. 8. (a) Thin-section photomicrograph of sample TuK4 (*Subunit IVb*) from section Tu. Nodular, dolomitized biomicritic wackestone–packstone, containing fragments of thin-shelled bivalves and echinoids and phantoms of foraminifera and ostracods. (b) Outcrop photograph showing Unit V with the peculiar white bed in its middle part (section Tu). Hammer (28 cm) for scale. (c) Thin-section photomicrograph of sample Tl22 (Unit V) from section Tu. Reddish packstone–grainstone, packed with thin-shelled bivalves, crinoids, ostracods and foraminifera. (d) Thin-section photomicrograph of the white bed (sample Tu95, Unit V) from section Tu. Biosparitic packstone containing bivalves. (e) Thin-section photomicrograph of sample Tl27 (Unit V) from section Tu. Reddish packstone with thin-shelled bivalves, ostracods, crinoid spines and plates as well Nodosariids foraminifera. (f) Outcrop photograph showing Unit VI at section Tu. Hammer (28 cm) for scale. (g) Thin-section photomicrograph of sample Tl32 (Unit VI) from section Tu. Packstone containing thin-shelled bivalves, rare ostracods and stromatactis cavities. (h) Thin-section photomicrograph of sample Tl35 (Unit VI) from section Tu. Grey mudstone–wackestone with thin-shelled bivalves, crinoid plates, ostracods and Nodosariids foraminifera.

Table 1
Analytical data for carbonate carbon/oxygen and organic carbon isotopes (relative to VPDB) from the Lower Triassic Tulong Formation, South Tibet.

Section	Sample	Unit	$\delta^{13}C_{carb}$ (‰)	$\delta^{18}O_{carb}$ (‰)	Section	Sample	Unit	$\delta^{13}C_{carb}$ (‰)	$\delta^{18}O_{carb}$ (‰)	$\delta^{13}C_{org}$ (‰)
TWB	4	Ia	−3.11	−6.26	Tu	7	IIIb	−2.36	−13.21	
TWB	5a	Ia	−3.32	−6.12	Tu	9	IIIb	−2.58	−12.85	
TWB	5b	Ia	−3.22	−6.53	Tu	11	IIIb	−2.51	−12.90	
TWB	7a	Ia	−2.31	−5.82	Tu	13	IIIb	−2.54	−12.52	
TWB	7b	Ia	−3.12	−7.08	Tu	14	IIIb	−2.18	−11.54	−25.44
TWB	8	Ia	−3.25	−6.57	Tu	16.1	IIIb	−2.55	−12.64	
TWB	9	Ia	−3.83	−7.74	Tu	16.2	IIIb	−2.23	−11.01	
TWB	10	Ia	−2.20	−6.27	Tu	18	IIIb	−2.48	−12.50	
TWB	11	Ia	−3.01	−6.95	Tu	22	IIIb	−2.44	−12.19	
TWB	12	Ia	−3.08	−7.11	Tu	26	IIIb	−2.76	−12.30	
TWB	14	Ia	−2.75	−7.39	Tu	29	IIIb	−2.40	−12.16	
TWB	15	Ia	−4.16	−8.82	Tu	30	IIIb	−2.43	−12.34	
TWB	16	Ia	−3.61	−8.23	Tu	33	IIIb	−2.46	−12.13	
TWB	17	Ia	−4.07	−8.32	Tu	35	IIIb	−2.59	−12.68	−27.46
TWB	18	Ia	−3.78	−8.28	Tu	37	IIIb	−2.60	−12.53	
TWB	20	Ia	−3.74	−7.94	Tu	38	IIIb	−2.53	−12.48	
TWB	21	Ia	−3.73	−8.82	Tu	39	IIIb	−2.68	−12.07	−26.24
TWB	22	Ia	−3.60	−12.25	Tu	40	IIIc	−2.14	−8.67	
TWB	23	Ia	−3.24	−13.75	Tu	41	IIIc	−2.49	−9.77	
TWB	24	Ib	−2.90	−14.29	Tu	42	IIIc	−2.13	−8.80	
TWB	25	Ib	−2.29	−14.06	Tu	44	IIIc	−2.17	−10.42	
TWB	26	Ib	−2.20	−14.39	Tu	45	IIIc	−2.46	−12.71	
TWB	28	Ib	−2.06	−14.52	Tu	46.1	IIIc	−2.55	−9.50	−25.37
TWB	29	Ib	−2.54	−14.07	Tu	46.2	IIIc	−2.45	−12.60	
TWB	30	Ib	−2.27	−14.28	Tu	47	IIIc	−2.14	−8.86	
TWB	31	Ib	−2.65	−14.13	Tu	48	IIIc	−2.35	−12.58	
TWB	32	Ib	−2.45	−14.27	Tu	50	IIIc	−1.79	−8.39	
TWB	33	Ib	−1.88	−14.36	Tu	52.1	IIIc	−1.77	−8.76	−24.91
TWB	34	Ib	−1.84	−14.72	Tu	52.2	IIIc	−1.76	−8.53	
TWB	35	Ib	−2.67	−14.13	Tu	53	IIIc	−1.65	−9.38	
TWB	50	II	−4.13	−12.41	Tu	54	IIIc	−1.76	−10.41	
TWB	51	II	−4.15	−12.73	Tu	55	IIIc	−1.60	−9.23	
TWB	52	II	−3.00	−17.35	Tu	56	IIIc	−1.70	−9.64	
TWB	54	IIIa	−2.79	−13.03	Tu	57	IIIc	−1.52	−12.02	
TWB	55	IIIa	−2.62	−13.26	Tu	58	IIIc	−1.56	−9.65	−26.02
TWB	56	IIIa	−2.44	−13.19	Tu	59	IIIc	−1.33	−10.23	
					Tu	61	IIIc	−1.37	−11.77	
Na	2	IIIa	−2.48	−11.36	Tu	63	IIIc	−1.58	−8.70	−26.28
Na	3	IIIa	−2.74	−13.08	Tu	64	IIIc	−1.16	−8.08	
Na	4	IIIa	−2.92	−13.32	Tu	66.1	IIIc	−1.12	−9.28	
Na	5	IIIa	−2.45	−12.94	Tu	66.2	IIIc	−1.11	−10.47	−23.54
Na	6	IIIa	−2.49	−13.14	Tu	67	IIIc	−1.01	−11.37	
Na	7	IIIa	−2.46	−13.05	Tu	69	IIIc	−0.80	−9.76	
Na	8	IIIa	−2.92	−13.27	Tu	71	IIIc	−0.29	−8.37	
					Tu	72	IIId	0.21	−11.84	
Tu	202	IIIa	−1.96	−12.36	Tu	73.1	IIId	0.26	−12.25	
Tu	201	IIIa	−2.41	−12.83	Tu	73.2	IIId	0.43	−12.07	−26.44
Tu	200	IIIa	−2.85	−13.10	Tu	74	IIId	0.37	−11.83	
Tu	1	IIIa	−2.09	−11.86	Tu	75	IIId	1.15	−10.49	
Tu	2.1	IIIa	−2.71	−11.83	Tu	P1	IVa			−23.91
Tu	2.2	IIIa	−2.76	−12.33	Tu	77	IVa	2.78	−11.97	
Tu	5	IIIb	−2.66	−13.08	Tu	78	IVa	2.49	−12.04	−25.42
Tu	91	V	−0.28	−11.86	Tu	79	IVa	2.52	−12.22	
Tu	92.2	V	−0.34	−11.87	Tu	80	IVa	2.32	−12.09	
Tu	93	V	−0.32	−11.90	Tu	P2	IVa			−25.14
Tu	94.1	V	−0.31	−12.00	Tu	81	IVa	0.25	−12.53	−25.20
Tu	94.2	V	−0.35	−11.50	Tu	P3	IVa			−20.84
Tu	94.3	V	−0.37	−11.81	Tu	P4	IVa			−25.67
Tu	95	V	−0.36	−11.79	Tu	82	IVa	0.03	−13.31	−18.74
Tu	96.1	V	−0.49	−11.93	Tu	P5	IVa			−24.89
Tu	96.2	V	−0.36	−11.75	TWA	1	IVa	−0.40	−12.08	
Tu	96.3	V	−0.41	−12.03	Tu	P6	IVa			−25.05
Tu	97.1	V	−0.24	−12.11	Tu	P7	IVa			−26.04
Tu	97.2	V	−0.30	−12.05	Tu	P8	IVa			−24.57
Tu	97.3	V	−0.25	−11.81	Tu	K1	IVb	1.06	−11.93	
Tu	98	V	−0.34	−12.34	Tu	P10	IVb			−20.70
Tu	99.1	V	−0.11	−12.13	Tu	K2	IVb	0.80	−12.07	
Tu	100	V	−0.16	−12.05	Tu	P11	IVb			−22.68
Tu	101	V	−0.07	−11.57	Tu	K3	IVb	0.94	−12.01	−21.47
Tu	102	V	−0.08	−11.89	Tu	K4	IVb	0.70	−11.57	
Tu	103	V	−0.07	−12.14	Tu	P12	IVb			−23.56
Tu	104.1	V	0.16	−11.91	Tu	P13	IVb			−20.78
Tu	104.2	V	0.50	−11.72	Tu	P14	IVb			−23.21
Tu	105	V	0.45	−11.99	Tu	P15	IVb			−23.34

Table 1 (*continued*)

Section	Sample	Unit	$\delta^{13}C_{carb}$ (‰)	$\delta^{18}O_{carb}$ (‰)	Section	Sample	Unit	$\delta^{13}C_{carb}$ (‰)	$\delta^{18}O_{carb}$ (‰)	$\delta^{13}C_{org}$ (‰)
Tu	106.1	VI	0.35	−11.56	Tu	P16	IVb			−23.67
Tu	106.2	VI	0.48	−11.88	Tu	86	IVb	0.71	−12.24	
Tu	107	VI	0.32	−12.12	Tu	P17	IVb			−23.62
Tu	108.1	VI	0.41	−12.05	Tu	87.1	V	0.49	−12.24	
Tu	108.2	VI	0.26	−12.44	Tu	87.2	V	0.08	−12.22	
Tu	108.3	VI	0.52	−12.19	Tu	87.3	V	−0.01	−11.76	
Tu	108.4	VI	0.44	−12.23	Tu	87.4	V	−0.08	−11.79	
Tu	109.1	VI	0.48	−12.46	Tu	87.5	V	0.08	−11.88	
Tu	109.2	VI	0.46	−12.26	Tu	87.6	V	−0.08	−12.01	
Tu	109.3	VI	0.68	−12.62	Tu	88.1	V	−0.02	−11.82	
Tu	109.4	VI	−0.78	−12.06	Tu	88.2	V	−0.03	−11.86	
Tu	110	VI	2.01	−12.20	Tu	88.3	V	−0.16	−11.90	
Tu	111.1	VI	1.14	−12.18	Tu	89.1	V	−0.27	−12.42	
Tu	111.2	VI	1.13	−12.09	Tu	89.2	V	−0.29	−11.68	
Tu	111.3	VI	1.82	−13.60	Tu	90	V	−0.34	−11.83	

profiles. This drop may represent a lithologic effect related to a conspicuous input of clastic material rather than a primary signature, i.e. decarbonation reactions in presence of siliciclastic components (Kaufman and Knoll, 1995).

Like in all known localities the Spathian interval is characterized by equilibrium $\delta^{13}C_{carb}$ values fluctuating only slightly around zero. The comparison of the new record from Tulong with the one from South China reveals strong similarities in these minor fluctuations during the Spathian, both in terms of variations and of absolute values (Fig. 10). At both localities the $\delta^{13}C$ values show a slight decrease in the early Spathian and reach a minimum in the middle Spathian. From there on values show a continuous increase. The few data points

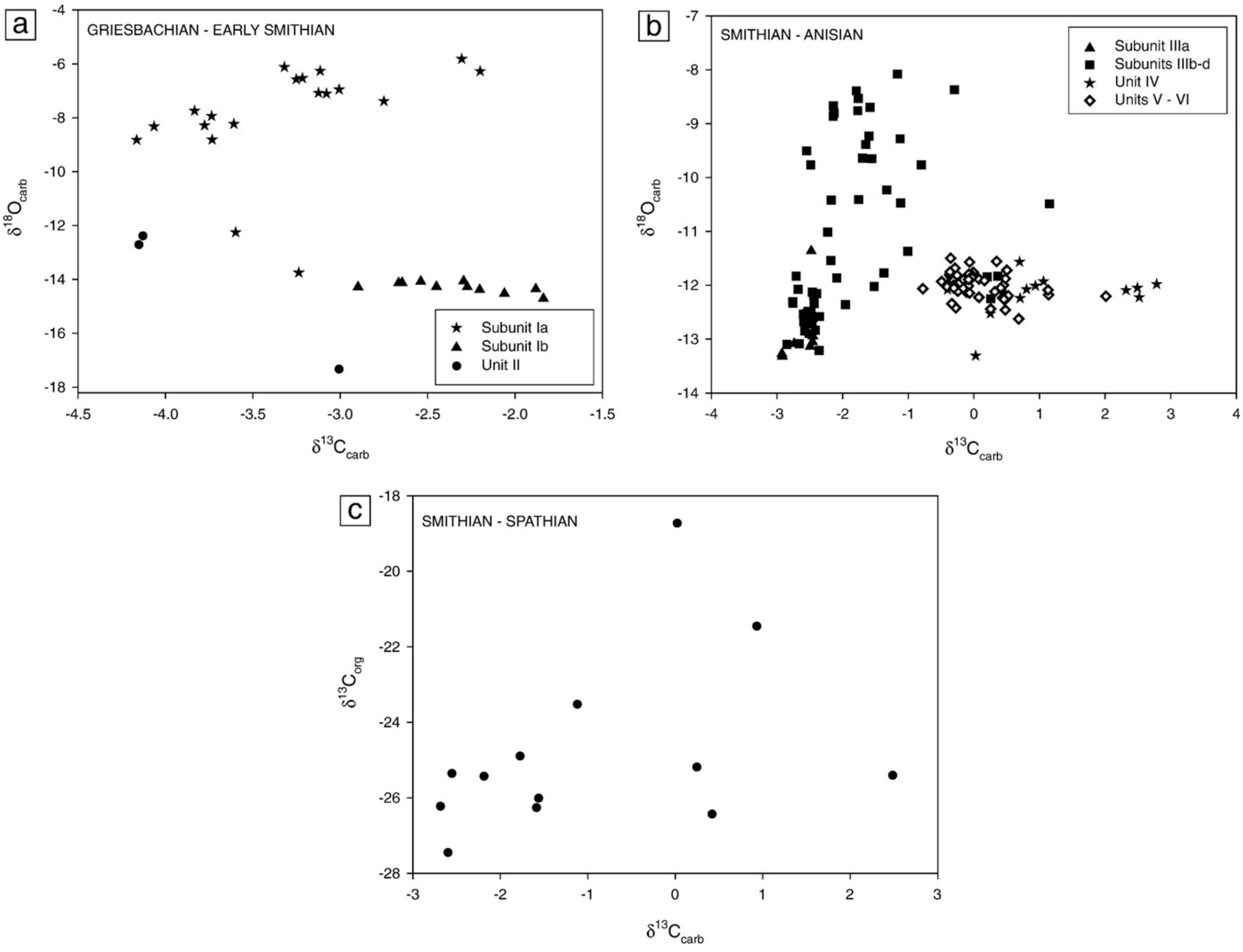

Fig. 9. Isotopic cross-plots of the Tulong Formation. All isotope values are expressed in ‰ deviation vs. VPDB. (a) $\delta^{13}C_{carb}$ versus $\delta^{18}O_{carb}$ for the Griesbachian–early Smithian. (b) $\delta^{13}C_{carb}$ versus $\delta^{18}O_{carb}$ for the Smithian–Anisian. (c) $\delta^{13}C_{carb}$ versus $\delta^{13}C_{org}$ values from carbonate samples.

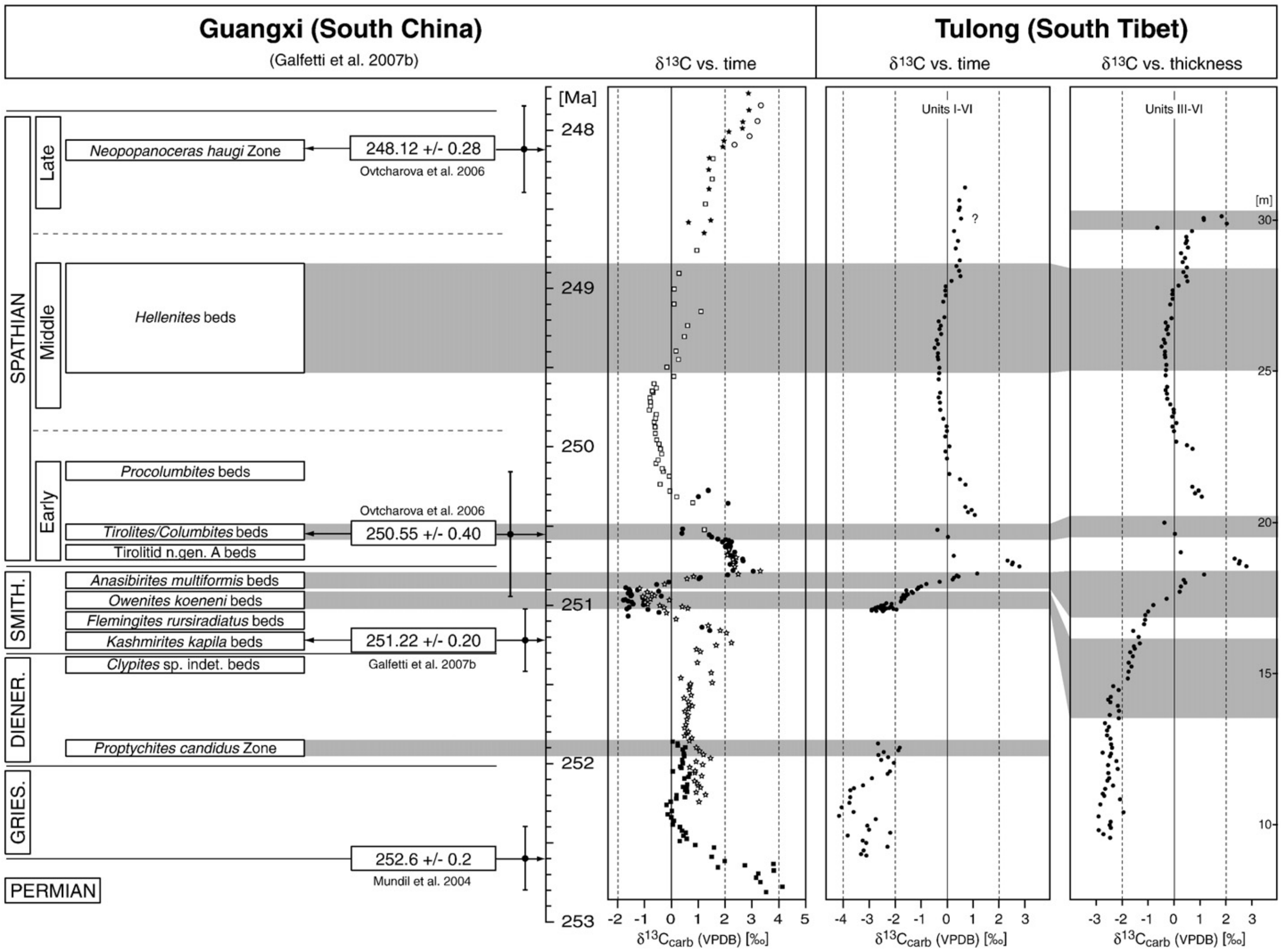

Fig. 10. δ^{13}C record from Tulong against stratigraphical thickness (Units III–VI only), and versus time (Units I–VI) by means of comparison with the record from northwestern Guangxi (South China), calibrated against U–Pb ages and ammonoid biochronozones (Galfetti et al., 2007b). The middle Smithian Arcoceratid A beds from Tulong (*Subunit IIIb*) have hitherto no direct counterpart in the South Chinese ammonoid succession; they probably correlate with a stratigraphic level between the Chinese *Flemingites rursiradiatus* beds and the *Owenites koeneni* beds (Brühwiler et al., 2007). Note the strong contraction of the Smithian part of the Tulong record resulting from calibration with time. Abbreviations: Gries.: Griesbachian; Diener.: Dienerian; Smith.: Smithian.

around the Spathian–Anisian boundary interval from Tulong indicate a positive $\delta^{13}C_{carb}$ shift as in other localities such as South China (Payne et al., 2004; Galfetti et al., 2007a), but due to condensation and possible hiatuses these data remain too spotty for a sound interpretation.

8. Conclusions

Our work provides a first precise and complete description of the Lower Triassic sedimentary record from the area of Tulong (South Tibet). Extensive bedrock-controlled sampling yields detailed ammonoid and conodont biostratigraphy that allows precise dating of the succession. The differences in the sedimentary evolution of the Lower Triassic section from Tulong with nearby sections such as Selong (i.e. prominent thickness and facies changes) reveal that sedimentation was influenced by large-scale block-faulting tectonics of the northern Gondwanian extensional margin. More importantly, comparison of the Tulong record with other Tethyan localities (Waagen, 1895; Guex, 1978; Bhargava et al., 2004; Galfetti et al., 2007a, 2008; pers. observation) reveals striking similar facies in parts of the Lower Triassic record. These similarities include (i) dolomites in the Griesbachian (Tulong, Spiti, Salt Range); (ii) thin-bedded, ammonoid-rich limestones in the early Dienerian (Tulong, Spiti, Salt Range); (iii) predominant clastic sedimentation in the late Dienerian (Tulong, Spiti, Salt Range, South China) which continues into the early Smithian in the Salt Range and in Tulong; (v) fossil-rich limestones in the middle Smithian (Tulong, Salt Range); and (vi) massive, fossil-rich nodular limestones in the Spathian (Tulong, Spiti, South China).

The striking similarities of the late Early Triassic sedimentary evolution from two widely distant localities in South China and Spiti were recently described by Galfetti et al. (2007a). Here, two distinct carbonate deposition episodes occur in the early Smithian (i.e. *Flemingites* beds) and in the Spathian, respectively. These are coeval with two major ammonoid and conodont diversification phases during the Early Triassic recovery (Brayard et al., 2006; Orchard, 2007). These carbonate episodes are characterized by increased levels of diversity and abundance of skeletal material, and therefore reflect an increasing recovery of the biosphere during favourable oceanographic conditions (Galfetti et al., 2008). In contrast with these well-oxygenated episodes, two Early Triassic dysoxic/anoxic episodes occur in South China in the late Dienerian and in the late Smithian, respectively, concomitant with large global positive carbon isotope excursions (Galfetti et al., 2007a, 2008). The late Smithian event was accompanied by a severe ammonoid and conodont extinction event (Brayard et al., 2006; Orchard 2007) and major climatic change (Brayard et al., 2006; Galfetti et al., 2007a,c). However, our new data indicate that well-oxygenated waters and carbonate production persisted in the middle and late Smithian in Tulong. Only the earliest Spathian green shales suggest some indications of possible oxygen-poor bottom waters.

High-resolution sampling throughout the entire Tulong Formation yields a new ammonoid and conodont age-constrained, carbonate carbon isotope record for the Early Triassic in South Tibet. It confirms the well-documented perturbations of the global carbon cycle following the Permian–Triassic mass extinction event (Baud et al., 1996; Atudorei and Baud, 1997; Atudorei, 1999; Payne et al., 2004; Richoz, 2004; Corsetti et al., 2005; Galfetti et al., 2007a,b,c; Horacek et al., 2007a,b), such as a late Griesbachian positive shift and a major positive carbon isotope excursion at the Smithian/Spathian boundary. However, the well-known positive carbon isotope excursion at the Dienerian/Smithian boundary could not be replicated because of the lack of carbonates in this time interval. In combination with previously published carbon isotope records and new ammonoid data from several other Tethyan sections such as the Salt Range (Pakistan), Spiti (Northern India), and NW Guangxi (South China) (Brühwiler et al., 2007, ongoing work; Brayard and Bucher, 2008), our new data from Tulong provide additional evidence for the synchronicity of the positive carbon isotope excursion at the Smithian/Spathian boundary. The Smithian/Spathian boundary C-isotope excursion therefore represents a global perturbation of the carbon cycle as well as a key chemostratigraphic marker. Finally, minor fluctuations of carbonate carbon isotopes during the Spathian (i.e. a slight decrease of δ^{13}C values until the middle Spathian and a subsequent continuous increase) represent an at least Tethys-wide signal.

Acknowledgments

W. Xiaoqiao (Beijing) and Li Guobiao (Lhasa) are thanked for facilitating the field work in Tibet. T. Vennemann (Lausanne) is thanked for measuring carbon and oxygen isotopes at the Institute of Mineralogy and Geochemistry of the University of Lausanne. We are grateful to the Geological Institute of the University of Lausanne for providing the thin sections. P. Moix and S. Crasquin (Paris) helped one of us (A.B.) in the field and in lab preparation of samples. T. Algeo (Cincinnati) and an anonymous referee are thanked for their useful reviews of the manuscript. R.M. wishes to thank the Swiss NSF (project 200021-113816). This work was supported by the Swiss NSF project no. 200020-113554 (to H.B.).

References

Altiner, D., Baud, A., Guex, J., Stampfli, G., 1980. La limite Permien–Trias dans quelques localités du Moyen–Orient: recherches stratigraphiques et micropaléontologiques. Rivista Italiana di Paleontologia e Stratigrafia 85, 683–714.

Atudorei, N.–V., 1999. Constraints on the upper Permian to upper Triassic marine carbon isotope curve. Case studies from the Tethys. PhD Thesis, Lausanne, 155 pp.

Atudorei, N.-V., Baud, A., 1997. Carbon isotope events during the Triassic. Albertiana 20, 45–49.

Bassoullet, J.P., Colchen, M., 1976. La limite Permien–Trias dans le domaine tibétain de l'Himalaya du Népal. In: Jest, C. (Ed.), Himalaya. Colloques internationaux du CNRS. CNRS, Sèvres-Paris, pp. 41–52.

Batten, D.J., 1996. Palynofacies and petroleum potential. In: Jansonius, J., McGregor, D.C. (Eds.), Palynology: Principles and Applications. American Association of Stratigraphic Palynologists Foundation, pp. 1065–1084.

Baud, A., Atudorei, V., Sharp, Z., 1996. Late Permian and Early Triassic evolution of the Northern Indian margin: carbon isotope and sequence stratigraphy. Geodinamica Acta 9, 57–77.

Baud, A., Cirilli, S., Marcoux, J., 1997. Biotic response to mass extinction: the lowermost Triassic microbialites. Facies 36, 238–242.

Baud, A., Richoz, S., Cirilli, S. and Marcoux, J., 2002. Basal Triassic carbonate of the Tethys: a microbialite world. In: IAS (Ed.), 16th International Sedimentological Congress. RAU University, Johannesburg, pp. 24–25.

Baud, A., Richoz, S., Marcoux, J., 2005. Calcimicrobial cap rocks from the basal Triassic units: western Taurus occurrences (SW Turkey). Comptes Rendus Palevol 4, 569–582.

Baud, A., Richoz, S., Pruss, S., 2007. The lower Triassic anachronistic carbonate facies in space and time. Global and Planetary Change 55, 81–89.

Bassoulet, J.-P., Colchen, M., Guex, J., Lys, M., Marcoux, J., Mascle, G., 1978. Permien terminal néritique, Scythien pélagique et volcanisme sousmarin, indices de processus tectono-sédimentaires distensifs à la limite Permien-Trias dans un bloc exotique de la suture de l'Indus (Himalaya du Ladakh). Comptes Rendues de l'Académie des Sciences 287, 675–678.

Bhargava, O.N., Krystyn, L., Balini, M., Lein, R., Nicora, A., 2004. Revised litho- and sequence stratigraphy of the Spiti Triassic. Albertiana 30, 21–39.

Brayard, A., Bucher, H., 2008. Smithian (Early Triassic) ammonoid faunas from northwestern Guangxi (South China): taxonomy and biochronology. Fossils and Strata 55, 1–179.

Brayard, A., Bucher, H., Escarguel, G., Fluteau, F., Bourquin, S., Galfetti, T., 2006. The Early Triassic ammonoid recovery: paleoclimatic significance of diversity gradients. Palaeogeography, Palaeoclimatology, Palaeoecology 239, 374–395.

Brayard, A., Escarguel, G., Bucher, H., Monnet, C., Brühwiler, T., Goudemand, N., Galfetti, T., Guex, J., 2009. Good Genes and Good Luck: Ammonoid Diversity and the End-Permian Mass Extinction. Science 325, 1118–1121.

Brühwiler, T., Brayard, A., Bucher, H., Guodun, K., 2008. Griesbachian and Dienerian (Early Triassic) ammonoid faunas from northwestern Guangxi and southern Guizhou (South China). Palaeontology 51, 1151–1180.

Brühwiler, T., Bucher, H., Goudemand, N., Brayard, A., 2007. Smithian (Early Triassic) ammonoid faunas of the Tethys: new preliminary results from Tibet, India, Pakistan and Oman. New Mexico Museum of Natural History and Science Bulletin 41, 25–26.

Bucher, H., 1992. Ammonoids of the Hyatti Zone (Middle Anisian, Middle Triassic) and the Anisian transgression in the Star Peak Group (northwestern Nevada). Palaeontographica Abt. A 223, 137–166.

Bucher, H., Nassichuk, W.W., Spinosa, C., 1997. A new occurrence of the upper Permian ammonoid *Stacheoceras trimurti* Diener from the Himalayas; Himachal Pradesh, India. Eclogae Geologicae Helvetiae 90, 599–604.

Burg, J.P., 1983. Carte géologique du sud du Tibet / Ministère de la Géologie – Pékin (République Populaire de Chine); Contours synth. par J.P. Burg. China. Ministry of Geology and Mineral Resources, Paris.

Burns, S.J., McKenzie, J.A., Vasconcelos, C., 2000. Dolomite formation and biogeochemical cycles in the Phanerozoic. Sedimentology 47, 49–61.

Corsetti, F.A., Baud, A., Marenco, P.J., Richoz, S., 2005. Summary of Early Triassic carbon isotope records. Comptes Rendus Palevol 4, 405–418.

Epstein, A.G., Epstein, J.B., Harris, L.D., 1977. Conodont color alteration — an index to organic metamorphism. U.S. Geological Survey Professional Paper 995, 1–27.

Erwin, D.H., 1998. The end and the beginning: recoveries from mass extinctions. Trends in Ecology & Evolution 13, 344–349.

Fraiser, M.L., Bottjer, D.J., 2004. The non-actualistic Early Triassic gastropod fauna: a case study of the Lower Triassic Sinbad Limestone Member. Palaios 19, 259–275.

Fraiser, M.L., Twitchett, R.J., Bottjer, D.J., 2005. Unique microgastropod biofacies in the Early Triassic: indicator of long-term biotic stress and the pattern of biotic recovery after the end-Permian mass extinction. Comptes Rendus Palevol 4, 543–552.

Galfetti, T., Bucher, H., Brayard, A., Hochuli, P.A., Weissert, H., Guodun, K., Atudorei, V., Guex, J., 2007a. Late Early Triassic climate change: insights from carbonate carbon isotopes, sedimentary evolution and ammonoid paleobiogeography. Palaeogeography, Palaeoclimatology, Palaeoecology 243, 394–411.

Galfetti, T., Bucher, H., Ovtcharova, M., Schaltegger, U., Brayard, A., Brühwiler, T., Goudemand, N., Weissert, H., Hochuli, P.A., Cordey, F., Guodun, K.A., 2007b. Timing of the Early Triassic carbon cycle perturbations inferred from new U–Pb ages and ammonoid biochronozones. Earth and Planetary Science Letters 258, 593–604.

Galfetti, T., Hochuli, P.A., Brayard, A., Bucher, H., Weissert, H., Vigran, J.O., 2007c. Smithian–Spathian boundary event: evidence for global climatic change in the wake of the end-Permian biotic crisis. Geology 35, 291–294.

Galfetti, T., Bucher, H., Martini, R., Hochuli, P.A., Weissert, H., Crasquin-Soleau, S., Brayard, A., Goudemand, N., Brühwiler, T., Guodun, K., 2008. Evolution of Early Triassic outer platform paleoenvironments in the Nanpanjiang Basin (South China) and their significance for the biotic recovery. Sedimentary Geology 204, 36–60.

Garzanti, E., Angiolini, L., Sciunnach, D., 1996. The Permian Kuling Group (Spiti, Lahaul and Zanskar; NW Himalaya): sedimentary evolution during rift/drift transition and initial opening of Neo-Tethys. Rivista Italiana di Paleontologia e Stratigrafia 102, 175–200.

Garzanti, E., Nicora, A., Rettori, R., 1998. Permo-Triassic boundary and lower to middle Triassic in South Tibet. Journal of Asian Earth Sciences 16, 143–157.

Garzanti, E., Nicora, A., Tintori, A., 1994. Triassic stratigraphy and sedimentary evolution of the Anapurna Tethys Himalaya (Manang area, central Nepal). Rivista Italiana di Paleontologia e Stratigrafia 100, 195–226.

Garzanti, E., Sciunnach, D., 1997. Early Carboniferous onset of Gondwanian glaciation and Neo-Tethyan rifting in Southern Tibet. Earth and Planetary Science Letters 148, 359–365.

Glumac, B., Walker, K.R., 1998. A Late Cambrian positive carbon-isotope excursion in the southern Appalachians: relation to biostratigraphy, sequence stratigraphy, environments of deposition, and diagenesis. Journal of Sedimentary Research 68, 1212–1222.

Groves, J.R., Altiner, D., 2005. Survival and recovery of calcareous foraminifera pursuant to the end-Permian mass extinction. Comptes Rendus Palevol 4, 419.

Guex, J., 1978. Le Trias inferieur des Salt Ranges, Pakistan; problemes biochronologiques. Eclogae Geologicae Helvetiae 71, 105–141.

Guex, J., Hungerbühler, A., Jenks, J., Taylor, D., Bucher, H., 2005a. Dix-huit nouveaux genres d'ammonites du Spathien (Trias inférieur) de l'Ouest américan (Idaho, Nevada, Californie): Note préliminaire. Bulletin de Géologie Lausanne 362.

Guex, J., Hungerbühler, A., Jenks, J., Taylor, D., Bucher, H., 2005b. Dix-neuf nouvelles espèces d'ammonites du Spathien (Trias inférieur) de l'Ouest américan (Idaho, Nevada, Californie): Note préliminaire. Bulletin de Géologie Lausanne 363.

Hatleberg, E.W., 1982. Conodont biostratigraphy of the lower Triassic at Van Keulenfjorden, Spitsbergen and Thakhola Valley, Nepal. Wisconsin University, Madison. 148 pp.

Heim, A., Gansser, A., 1939. Central Himalaya: geological observations of the Swiss expedition 1936. Denkschriften der Schweizerischen Naturforschenden Gesellschaft 73 (Abh. 1, 245 pp.).

Horacek, M., Brandner, R., Abart, R., 2007a. Carbon isotope record of the P/T boundary and the Lower Triassic in the Southern Alps: evidence for rapid changes in storage of organic carbon. Palaeogeography, Palaeoclimatology, Palaeoecology 252, 347–354.

Horacek, M., Richoz, S., Brandner, R., Krystyn, L., Spötl, C., 2007b. Evidence for recurrent changes in Lower Triassic oceanic circulation of the Tethys: the δ^{13}C record from marine sections in Iran. Palaeogeography, Palaeoclimatology, Palaeoecology 252, 355–369.

Isozaki, Y., 1997. Permo-Triassic boundary superanoxia and stratified superocean: record from lost deep sea. Science 276, 235–238.

Jenkyns, H.C., 1974. Origin of red nodular limestone (Ammonitico Rosso, Knollenkalke) in the Mediterranean Jurassic: a diagenetic model. Special Publication of the International Association of Sedimentologists 1, 249–271.

Kakuwa, Y., 2008. Evaluation of palaeo-oxygenation of the ocean bottom across the Permian–Triassic boundary. Global and Planetary Change 63, 40–56.

Kaufman, A.J., Knoll, A.H., 1995. Neoproterozoic variations in the C-isotopic composition of seawater: stratigraphic and biogeochemical implications. Precambrian Research 73, 27–49.

Kershaw, S., Guo, L., Swift, A., Fan, J.S., 2002. Microbialites in the Permian–Triassic boundary interval in Central China: structure, age and distribution. Facies 47, 83–89.

Kershaw, S., Li, Y., Crasquin-Soleau, S., Feng, Q.L., Mu, X.N., Collin, P.Y., Reynolds, A., Guo, L., 2007. Earliest Triassic microbialites in the South China block and other areas: controls on their growth and distribution. Facies 53, 409–425.

Kershaw, S., Zhang, T.S., Lan, G.Z., 1999. A ?microbialite carbonate crust at the Permian–Triassic boundary in South China, and its palaeoenvironmental significance. Palaeogeography, Palaeoclimatology, Palaeoecology 146, 1–18.

Krystyn, L., Richoz, S., Bhargava, O.N., 2007. The Induan–Olenekian boundary (IOB) in mud — an update of the candidate GSSP section M04. Albertiana 36, 33–45.

Kummel, B., 1970. Ammonoids from the Kathwai Member, Mianwali Formation, Salt Range, West Pakistan. In: B. Kummel and C. Teichert (Eds.), Stratigraphic Boundary Problems: Permian and Triassic of West Pakistan. Department of Geology, University of Kansas, Special Publication pp. 177–192.

Liu, G., 1992. Permian to Eocene sedimenst and Indian passive margin evolution in the Tibetan Himalayas. Tübinger Geowissenschaftliche Arbeiten. Reihe A 13, 1–268.

Liu, G., Einsele, G., 1994. Sedimentary history of the Tethyan basin in the Tibetan Himalayas. Geologische Rundschau 83, 32–61.

Marcoux, J., Baud, A., 1996. Late Permian to Late Triassic Tethyan paleoenvironments. Three snapshots: Late Murgabian, Late Anisian, Late Norian. In: Nairn, X., Ricou, L.E., Vrielynck, B., Dercourt, J. (Eds.), The Tethys Ocean. The Ocean Basins and Margins. Plenum Press, New York, pp. 153–190.

Marshall, J.D., 1992. Climatic and oceanographic isotopic signals from the carbonate rock record and their preservation. Geological Magazine 129, 143–160.

Nowlan, G.S., Barnes, C.R., 1987. Application of conodont colour alteration indices to regional and economic geology. In: Austin, R.L. (Ed.), Conodonts : Investigative Techniques and Applications. Bristish Micropalaeontological Society Series. Ellis Horwood Limited, Chichester, West Sussex, PO19 1EB, England, pp. 188–202.

Ogg, J.G., von Rad, U., 1994. The Triassic of the Thakkola (Nepal). II: Paleolatitudes and comparison with other Eastern Tethyan Margins of Gondwana. Geologische Rundschau 83, 107–129.

Orchard, M.J., 2007. Conodont diversity and evolution through the latest Permian and Early Triassic upheavals. Palaeogeography, Palaeoclimatology, Palaeoecology 252, 93–117.

Orchard, M.J., 2008. Lower Triassic conodonts from the Canadian Arctic, their intercalibration with ammonoid-based stages and a comparision with other North American Olenekian faunas. Polar Research 27, 393–412.

Orchard, M.J., Krystyn, L., 1998. Conodonts of the Lowermost Triassic of Spiti, and New Zonation Based on *Neogondolella* Successions. Rivista Italiana di Paleontologia e Stratigrafia 104, 341–368.

Orchard, M.J., Nassichuk, W.W., Rui, L., 1994. Conodonts from the Lower Griesbachian *Otoceras Latilobatum* bed of Selong, Tibet and the Position of the Permian – Triassic Boundary, Pangea: global environments and resources. Canadian Society of Petroleum Geologists, pp. 823–843.

Ovtcharova, M., Bucher, H., Schaltegger, U., Galfetti, T., Brayard, A., Guex, J., 2006. New Early to Middle Triassic U–Pb ages from South China: calibration with ammonoid biochronozones and implications for the timing of the Triassic biotic recovery. Earth and Planetary Science Letters 243, 463–475.

Payne, J.L., Kump, L.R., 2007. Evidence for recurrent Early Triassic massive volcanism from quantitative interpretation of carbon isotope fluctuations. Earth and Planetary Science Letters 256, 264–277.

Payne, J.L., Lehrmann, D.J., Wei, J.Y., Orchard, M.J., Schrag, D.P., Knoll, A.H., 2004. Large perturbations of the carbon cycle during recovery from the end-Permian extinction. Science 305, 506–509.

Pruss, S.B., Bottjer, D.J., 2005. The reorganization of reef communities following the end-Permian mass extinction. Comptes Rendus Palevol 4, 553–568.

Racki, G., 1999. Silica-secreting biota and mass extinctions: survival patterns and processes. Palaeogeography, Palaeoclimatology, Palaeoecology 154, 107–132.

Rao, R.B., Zhang, Z.G., 1985. A discovery of Permo–Triassic transitional fauna in the Qomolangma Feng area: its implications for the Permo–Triassic boundary. Xizang Geology 1, 19–31.

Raup, D.M., Sepkoski, J.J., 1982. Mass Extinctions in the Marine Fossil Record. Science 215, 1501–1503.

Richoz, S., 2004. Stratigraphie et variations isotopiques du carbone dans le Permian supérieur et le Trias inférieur de la Néotéthys (Turquie, Oman et Iran). PhD., University of Lausanne, Switzerland. 281pp.

Richoz, S., Krystyn, L., Horacek, M., Spötl, C., 2007. Carbon isotope record of the Induan–Olenekian candidate GSSP Mud and comparison with other sections. Albertiana 35, 35–40.

Ricou, L.E., 1996. The plate tectonic history of the past Tethys ocean. In: Nairn, X., Ricou, L.E., Vrielynck, B., Dercourt, J. (Eds.), The Tethys Ocean. The Ocean Basins and Margins. Plenum Press, New York, pp. 3–70.

Shen, S.Z., Cao, C.Q., Henderson, C.M., Wang, X.D., Shi, G.R., Wang, Y., Wang, W., 2006. End-Permian mass extinction pattern in the northern peri-Gondwanan region. Palaeoworld 15, 3–30.

Spath, L.F., 1934. Part 4: The ammonoidea of the Trias, catalogue of the fossil cephalopoda in the British Museum (Natural History). The Trustees of the British Museum, London. 521 pp.

Spötl, C., Vennemann, T.W., 2003. Continuous-flow isotope ratio mass spectrometric analysis of carbonate minerals. Rapid Communications in Mass Spectrometry 17, 1004–1006.

Stampfli, G., Marcoux, J., Baud, A., 1991. Tethyan margins in space and time. Palaeogeography, Palaeoclimatology, Palaeoecology 87, 373–409.

Stanley, G.D., 2003. The evolution of modern corals and their early history. Earth Science Reviews 60, 195–225.

Tian, C.R., 1982. Triassic conodonts in the Tulong section from Nyalam County, Xizang (Tibet), China. Contributions to Geology Qinghai-Xizang (Tibet) Plateau 8, 153–165.

Tong, J., Shi, G.R., 2000. Evolution of the Permian and Triassic foraminifera in south China. In: Yin, H., Dickins, J.M., Shi, G.R., Tong, J. (Eds.), Permian–Triassic Evolution of Tethys andWestern Circum-Pacific. Developments in Palaeontology and Stratigraphy. Elsevier, Amsterdam, pp. 291–307.

Tozer, E.T., 1994. Canadian Triassic ammonoid faunas. Bulletin — Geological Survey of CanadaGeological Survey of Canada, Ottawa, ON, Canada. 663 pp.

Tozer, E.T., Calon, T.J., 1990. Triassic ammonoids from Jabal Safra and Wadi Alwa, Oman, and their significance. In: Robertson, A.H.F., Searle, M.P., Ries, A.C. (Eds.), The geology and tectonics of the Oman region. Geological Society Special Publications. Geological Society of London, London, United Kingdom, pp. 203–211.

Vasconcelos, C., McKenzie, J.A., 1997. Microbial mediation of modern dolomite precipitation and diagenesis under anoxic conditions (Lagoa Vermelha, Rio de Janeiro, Brazil). Journal of Sedimentary Research 67, 378–390.

von Rad, U., Dürr, S.B., Ogg, J.G., Wiedmann, J., 1994. The Triassic of the Thakhola (Nepal). I: stratigraphy and paleoenvironment of a north-east Gondwana rifted margin. Geologische Rundschau 83, 76–106.

Waagen, W., 1895. Salt-range fossils. Vol 2: fossils from the Ceratite Formation. Palaeontologia Indica 13, 1–323.

Wang, Y.G., Chen, C., Rui, L., Wang, Z., Liao, Z., He, J., 1989. A potential global stratotype of Permian–Triassic boundary. In: Zengquan, L., Fa'er, J. (Eds.), Developments in geoscience: Contribution to 28th International Geological Congress, July 1989, Washington, D. C., USA. Science Press, Beijing, pp. 221–230.

Wang, Y.G., He, G.X, 1976. Triassic ammonoids from the Mount Jolmo Lungma region. A report of scientific expedition in the Mount Jolmo Lungma region (1966–1968).

Wignall, P.B., Newton, R., 2003. Contrasting deep-water records from the Upper Permian and Lower Triassic of South Tibet and British Columbia: evidence for a diachronous mass extinction. Palaios 18, 153–167.

Woods, A.D., Baud, A., 2008. Anachronistic facies from a drowned Lower Triassic carbonate platform: lower member of the Alwa Formation (Ba'id Exotic), Oman Mountains. Sedimentary Geology 209, 1–14.

Yugan, J., Shuzhong, S., Zili, Z., Silong, M., Wei, W., 1996. The Selong section, candidate of the Global Stratotype section and point of the Permian–Triassic boundary. In: Yin, H. (Ed.), The Palaeozoic–Mesozoic Boundary Candidates of Global Stratotype Section and Point of the Permian–Triassic Boundary. China University Press, Wuhan, pp. 127–137.

CHAPTER 4:

Smithian (Early Triassic) ammonoids from Tulong, South Tibet

Smithian (Early Triassic) ammonoids from Tulong, South Tibet

Ammonoïdes du Smithien (Trias inférieur) de Tulong, Tibet du Sud

Thomas Brühwiler [a, *], Hugo Bucher [a, b], Nicolas Goudemand [a]

[a] *Paläontologisches Institut und Museum der Universität Zürich, Karl Schmid-Strasse 4, CH-8006 Zürich, Switzerland*

[b] *Department of Earth Sciences, ETH, Universitätsstrasse 16, 8092 Zürich, Switzerland*

[*] Corresponding author.
E-mail address: bruehwiler@pim.uzh.ch
Phone: +41 44 634 26 98
Fax: +41 44 634 49 23

Accepted for publication in *Geobios*.

Abstract: Intensive sampling of the Tulong Formation in South Tibet has facilitated the construction of a highly-resolved middle and late Smithian ammonoid succession. The new biostratigraphical sequence comprises the middle Smithian *Brayardites compressus* beds, *Nammalites pilatoides* beds, and the *Nyalamites angustecostatus* beds followed by the late Smithian *Wasatchites distractus* beds and *Glyptophiceras sinuatum* beds. This faunal succession correlates very well with that of other Tethyan sequences such as the Salt Range (Pakistan), Spiti (India), Oman and South China. The Smithian faunal sequence from Tulong contains several taxa with broad geographic distribution (e.g. *Owenites*, *Paranannites spathi*, *Shigetaceras*, *Wasatchites*), thus enabling correlation with faunal successions from areas outside the Tethys (i.e. USA, British Columbia, Arctic Canada, South Primorye, Siberia). Early Smithian ammonoid faunas are almost absent in Tulong because of a preservation bias (absence of carbonate rocks).

Five new ammonoid genera (*Brayardites*, *Nammalites*, *Nyalamites*, *Shigetaceras*, *Tulongites*) and six new species (*Brayardites crassus*, *Brayardites compressus*, *Prionites involutus*, ?*Subflemingites compressus*, *Tulongites xiaoqiaoi*, *Urdyceras tulongensis*) are described.

Résumé

Un échantillonnage intensif de la Formation Tulong du sud-Tibet permet l'établissement d'une séquence très détaillée des faunes d'ammonites du Smithien moyen et supérieur. Cette nouvelle séquence comprend les faunes d'assemblage du Smithien moyen à *Brayardites compressus*, à *Nammalites pilatoides*, à *Nyalamites angustecostatus* suivies par les faunes du Smithien supérieur à *Wasatchites distractus* et à *Glyptophiceras sinuatum*. Cette succession faunique se corrèle très bien avec celles d'autres localités téthysiennes telles que les Salt Ranges (Pakistan), le Spiti (Inde), l'Oman et le sud de la Chine. Les faunes smithiennes de Tulong contiennent également plusieurs taxons ayant une large distribution biogéographique (e.g. *Owenites*, *Paranannites spathi*, *Shigetaceras*, *Wasatchites*) permettant ainsi des corrélations avec d'autres successions en dehors de la Téthys (p. ex. USA, Colombie britannique, Arctique canadien, sud du Primorye, Sibérie). Les faunes du Smithien inférieur sont par contre quasiment absente de Tulong en raison d'un biais de préservation (absence de roches carbonatées).

Cinq genres (*Brayardites*, *Nammalites*, *Nyalamites*, *Shigetaceras*, *Tulongites*) et six nouvelles espèces (*Brayardites crassus*, *Brayardites compressus*, *Prionites involutus*, ?*Subflemingites compressus*, *Tulongites xiaoqiaoi*, *Urdyceras tulongensis*) sont nouvellement introduits.

Key words: Ammonoidea, Early Triassic, South Tibet, Smithian, biostratigraphy.

Mots clés: Ammonoidea, Trias inférieur, sud-Tibet, Smithien, biostratigraphie.

1. Introduction

In the aftermath of the end-Permian mass extinction that wiped out more than 90 percent of all marine species (e.g. Raup and Sepkoski, 1982), ammonoids recovered very fast in comparison with other marine clades (Brayard et al., 2006, 2009c). Following low values in the Griesbachian, diversity increased slowly during the Dienerian and first peaked in the Smithian. This first major evolutionary radiation was followed by a severe extinction event in the end Smithian, after which a second major and explosive radiation took place during the Spathian.

For more than a century, Smithian ammonoids have been known from various localities in the Tethyan realm, such as the Salt Range in Pakistan (Waagen, 1895; Noetling, 1905; Guex, 1978), Afghanistan (Kummel and Erben, 1968), Spiti in Northern India (Diener, 1897; Krafft and Diener, 1909; Krystyn et al., 2007a, b), Kashmir (Diener, 1913), Madagascar (Collignon, 1933-1934), Guangxi in South China (Chao, 1959; Brayard and Bucher, 2008), Vietnam (Khuc, 1984) and Timor

(Welter, 1922). However, the number of studies based on bed by bed sampling is very limited (Guex, 1978; Krystyn et al., 2007a, b; Brayard and Bucher, 2008). Therefore, additional high-resolution ammonoid successions from various localities are crucial for establishing a precise and laterally reproducible biochronological subdivision of the Smithian within the Tethys and within the Early Triassic tropics.

Recently, we provided the first complete and detailed description of the Lower Triassic sedimentary and carbon isotope records from the Tulong area in South Tibet (Brühwiler et al., 2009). Extensive sampling enabled us to precisely date the section by means of detailed ammonoid and conodont biostratigraphy. Our investigations have yielded abundant, diverse and reasonably well preserved Smithian ammonoid faunas including several new taxa. Here, we focus on the description of these faunas. They add significantly to our knowledge of Smithian ammonoid taxonomy and biostratigraphy and provide valuable data for biogeographical, phylogenetic and chemostratigraphic studies.

2. General palaeogeographical and geological setting

During Early Triassic times, the Tulong area was located in a distal position of the northern Gondwanian margin, on the southern side of the Tethys Ocean (Ogg and von Rad, 1994) (Fig. 1). As shown by different authors (Marcoux and Baud, 1996; Ricou, 1996; Garzanti and Sciunnach, 1997) at least two rifting processes affected the North Indian plate. The first event is linked to the break-off of the Quiantang block from Gondwana during the Early Carboniferous. A second rifting phase during the Early Permian detached the Lhasa block from the Gondwanian margin, thus giving birth to the Neotethys. In this process the southern Neotethyan Indian margin was acting as the upper plate, thereby inducing basalt flows (Panjal Traps) and volcanism (Stampfli et al., 1991; Baud et al., 1996; Garzanti et al., 1996). During the expansion of the Neotethys in the Early Triassic, the Indian margin underwent thermal subsidence and was characterized by large tilted blocks. This may at least partly explain the differences in lithological successions between closely spaced localities such as Tulong and Selong (35 km apart) in South Tibet (Garzanti et al., 1998; Brühwiler et al., 2009).

3. The Tulong succession

For the Tulong area (Fig. 2), previously published reports of the Lower Triassic sedimentary succession (Liu, 1992; Liu and Einsele, 1994; Garzanti et al., 1998; Shen et al., 2006) are incomplete and/or poorly or incorrectly dated. Only recently has the complete Lower Triassic sedimentary record from this area been described and dated by means of detailed ammonoid and conodont biostratigraphy

(Brühwiler et al., 2009). In that work we subdivided the Lower Triassic succession of Tulong into six lithostratigraphic units as follows (Fig. 3).

The basal Triassic sequence consists of three meters of carbonates (Unit I) that are subdivided into two meters of Griesbachian yellow dolomite (Subunit Ia), and one meter of Dienerian light grey, thin-bedded limestone (Subunit Ib). These are followed by about 50-100 m of Dienerian-early Smithian aged, dark green, silty shales (Unit II) devoid of macrofossils. This interval is overlain by nine meters of thin-bedded, light grey fossil-rich limestone of middle to late Smithian age (Unit III; subdivided into four Subunits IIIa-d). These are followed by four meters of early Spathian shales containing a few limestone beds and nodules (Unit IV). The shales are typically green in the lower part (Subunit IVa) and red in the upper part (Subunit IVb). The late early and middle Spathian consists of six meters of red, bioclastic nodular limestone ("Ammonitico Rosso" type facies) (Unit V). The late Spathian-Anisian part of the succession is strongly condensed and is characterized by two meters of grey, thin-bedded limestone with phosphatized ammonoids (Unit VI).

In addition to the classic section located near the village of Tulong (Garzanti et al., 1998; Shen et al., 2006), several new and complementary sections were discovered both west and east of Tulong (Figs. 2-3). These new localities were essential for establishing the entire Lower Triassic succession since exposures in the classic Tulong section only include the middle Smithian-Anisian interval (Brühwiler et al., 2009). All outcrops of Lower Triassic rocks can be correlated on a bed-by-bed basis across a minimal distance of ca. 15 km along the W-E tectonic strike, thus revealing remarkable lateral depositional continuity within the same thrusted sheet.

The studied sections were sampled bed-by-bed in order to obtain a precise, detailed ammonoid record (Fig. 4). The dark green shales of Unit II are essentially barren and only one incomplete float specimen (*Kashmirites* sp. indet.) was found in the upper part of the unit. On the contrary ammonoids are very abundant in almost all beds of Unit III, except for Subunit IIIa, where they are rare and too poorly preserved for identification. Preservation is highly variable throughout Unit III, and in some levels an intensive sampling effort was necessary to obtain reasonably well preserved material.

4. Biostratigraphical discussion

4.1. General subdivisions of the Early Triassic

Subdivision of the Early Triassic into stages is still controversial. It is commonly subdivided into two (Induan and Olenkian, Kiparisova and Popov, 1956), three (Griesbachian, Nammalian and Spathian, Guex, 1978) or four stages (Griesbachian, Dienerian, Smithian and Spathian, Tozer, 1965; Tozer, 1967). In this paper we use the four-stage subdivision, whose boundaries are well defined in terms of ammonoid evolution. The Griesbachian/Dienerian boundary is defined by the first occurrence of Meekoceratidae, which is a bio-event that can be traced worldwide (e.g. Shevyrev, 2001). The early Smithian is characterized by the first major ammonoid diversification phase during the Early Triassic recovery. Therefore, the Dienerian/Smithian (or Induan/Olenekian) boundary is easily recognizable with the appearance of several new ammonoid families such as the Flemingitidae, the Paranannitidae and the Xenoceltitidae (e.g. Brayard and Bucher, 2008). Interest in this boundary is relatively recent, and a section near Mud in the Indian Himalayas has been chosen as GSSP (Krystyn et al., 2007a, b). The Smithian/Spathian boundary is marked by a profound faunal turnover and it is only crossed by very few ammonoid lineages such as the Xenoceltitidae, the Proptychitidae and the Hedenstroemiidae (Brayard et al., 2006). Several new families such as the Tirolitidae and the Columbitidae appear in the early Spathian. The main weakness of the two-stages scheme (Induan-Olenekian) is that it completely ignores the largest intra-Triassic extinction event (i.e. the end-Smithian extinction) that profoundly affected both ammonoids and conodonts (Brayard et al., 2006; Orchard et al., 2007).

4.2. The Smithian of South Tibet and correlation with other Tethyan localities

Until now, the only illustrations of Smithian ammonoids from South Tibet were provided by Wang and He (1976) from the Mount Everest region, but these authors did not publish a stratigraphical succession, which seriously hampers the interpretation of their data. Moreover, the preservation of their material is rather poor. Our study, based on bed-by-bed sampling, provides for the first time the distribution of Smithian ammonoids in the Tulong succession (Figs. 4, 5). A total of six well differentiated ammonoid faunas of middle to latest Smithian age occurs throughout Unit III. This Smithian ammonoid succession of South Tibet is entirely new except for a preliminary version presented in a conference abstract (Brühwiler et al., 2007). A description of the faunas as well as discussion of their correlation with ammonoid zonations from other areas is provided hereafter. No formal zone names are introduced here since we prefer to use the term "beds" for the time being to describe the local faunal sequence. Such usage would imply a well-established lateral reproducibility of the faunal sequence between various basins, which is still a subject of ongoing work.

Early Smithian. - Equivalent faunas of the early Smithian *Kashmirites kapila* beds and the *Flemingites rursiradiatus* beds of South China (Brayard and Bucher, 2008) have not been found in the Tulong area because of the lack of carbonate sediments for this time interval. The single specimen of *Kashmirites* sp. indet. found as float in the upper part of Unit II may possibly have been derived from one of these faunas. It is notable that in other localities on the Northern Indian Margin such as Spiti, the Salt Range and Oman, equivalents of the *Flemingites rursiradiatus* beds are present (Waagen, 1895; Bhargava et al., 2004; Brühwiler et al., 2007, ongoing work; Krystyn et al., 2007a, b).

Brayardites compressus beds. - These beds in Subunit IIIb are characterized by the association of *Aspenites acutus*, *Brayardites compressus* nov. gen. et sp., *B. crassus* nov. gen. et sp., *Jinyaceras hindostanum*, *Pseudaspidites* sp. indet., *Tulongites xiaoqiaoi* nov. gen. et sp., *Urdyceras tulongensis* nov. sp. and Genus indet. A. Recently, this association was also discovered in the Salt Range (Pakistan) and in Spiti (India) (Brühwiler et al., 2007, ongoing work; provisionally labeled "new prionitid A beds"), but a faunal equivalent is not known from South China. It probably correlates with an interval between the *Flemingites rursiratiatus* beds and the *Owenites koeneni* beds in the South China succession (Fig. 5).

Nammalites pilatoides beds. - These beds at the base of Subunit IIIc are characterized by the association of abundant *Nammalites pilatoides* nov. gen., *Owenites simplex*, *Paranannites spathi* and *Shigetaceras dunajensis* nov. gen. Rare specimens of ?*Leyeceras* sp. indet., Flemingitidae gen. indet. A and B, Prionitidae gen. indet. A and *"Anasibirites"* cf. *pluriformis* also co-occur. This association was also recently discovered in the Salt Range, in Spiti, and in an exotic block of Hallstatt facies from Oman (i.e."new prionitid B beds" in Brühwiler et al., 2007, ongoing work). Note that *"Anasibirites" pluriformis* Guex, 1978 is herein not regarded as a true *Anasibirites*, which is a genus of late Smithian age (see systematic section). The *Nammalites pilatoides* beds correlate with the lower part of the middle Smithian *Owenites koeneni* beds of South China (i.e. *Ussuria* and *Hanielites* horizons; Brayard and Bucher, 2008), with which they share the occurrences of *Owenites simplex* and *Paranannites spathi*.

Pseudoceltites multiplicatus beds. - These beds in Subunit IIIc are characterized by the association of *Anaxenaspis* sp. indet. A and B, *Owenites koeneni* and *Pseudoceltites multiplicaus*. This fauna occurs also in the Salt Range and in Spiti (Brühwiler et al., 2007, ongoing work; preliminarily termed Flemingitid A beds). An exact correlative is not known from South China.

Nyalamites angustecostatus beds. - These beds in Subunit IIIc contain a diverse fauna that is characterized by the association of *Nyalamites angustecostatus* nov. gen., *Owenites carpentieri*, *O. koeneni*, *Prionites involutus* nov. sp., *Stephanites superbus*, ?*Subflemingites compressus* nov. sp., *Subvishnuites* sp. indet., and Xenoceltitidae gen. indet. A. This fauna is also known from Spiti, the Salt Range and Oman (Brühwiler et al., 2007, ongoing work), and it correlates with the *Inyoites* horizon in the upper part of the *Owenites koeneni* beds of South China, with which it shares *Owenites carpentieri*.

Wasatchites distractus beds. - These beds at the top of Subunit IIIc include the occurrence of *Wasatchites distractus*, associated with Genus indet. B. Correlatives of this late Smithian fauna, which contain *Anasibirites* and/or *Wasatchites*, are known from many Tethyan localities such as Oman, Salt

Range, Spiti (Bhargava, 2004; Brühwiler et al., 2007, ongoing work) and South China (Brayard and Bucher, 2008) as well as worldwide localities (see below).

Glyptophiceras sinuatum beds. - These beds in Subunit IIId are characterized by the association of *Glyptophiceras sinuatum*, *Pseudosageceras augustum* and *Xenoceltites* cf. *variocostatus*. This latest Smithian fauna also occurs in Spiti and in the Salt Range (Brühwiler et al., 2007; ongoing work). In South China the *Xenoceltites variocostatus* fauna also occurs above the horizons with *Anasibirites*, but was included in the *Anasibirites multiformis* beds by Brayard and Bucher (2008). Note that the genus *Glyptophiceras* was originally considered to be of Griesbachian age, but is now known to be restricted to the latest Smithian (see systematic section for disscussion).

Early Spathian. - The lowermost limestone beds in the shales of Subunit IVa yielded only the ammonoid ?*Pseudaspidites* sp., which is not age diagnostic. However, conodonts *Borinella*? n. sp. C (Orchard, unpublished), transitional forms to *Gladigondolella*, as well as early forms of *Icriospathodus* from this level indicate an early Spathian age (Brühwiler et al., 2009). The limestone nodules in the middle part of Subunit IVa have yielded two different early Spathian ammonoid faunas, i.e. a *Nordophiceras* fauna and a *Columbites* fauna. The Spathian ammonoid faunas from the Tulong area will be discussed in more detail in a separate paper.

4.3. Biostratigraphical correlations with other regions

As shown above, Smithian ammonoid successions are very uniform on the Northern Indian Margin and they correlate well with the South China record. However, correlations with records from outside the Tethys are less precise. Since most early-middle Smithian ammonoids have latitudinally restricted geographic distributions (Brayard et al., 2007; Brayard et al., 2009a), correlations of early-middle Smithian successions across palaeolatitudes are difficult. In contrast, the extinction phase during the late Smithian is marked by a low latitudinal gradient of diversity and a high degree of cosmopolitanism (Brayard et al., 2006). A few genera such as *Anasibirites*, *Wasatchites* and *Xenoceltites* occur world-wide (e.g. Tozer, 1994; Brühwiler et al., 2007; Brayard and Bucher, 2008), thus facilitating the correlation of late Smithian ammonoid faunas across palaeolatitudes.

Western USA (low-palaeolatitudes). - The Smithian of the USA is subdivided into two ammonoid zones, i.e. the *Meekoceras gracilitatis* Zone and the *Anasibirites* beds (Silberling and Tozer 1968; Jenks 2007). Several genera such as *Guodunites*, *Inyoites*, *Lanceolites*, *Metussuria* and *Owenites* from the *Meekoceras gracilitatis* Zone are known also from the middle Smithian *Owenites* beds of the Tethys (Brühwiler et al., 2007, ongoing work; Brayard and Bucher, 2008; Brayard et al., 2009a). On the other hand, the *Meekoceras gracilitatis* Zone also contains early Smithian ammonoids such as *Euflemingites*. Thus, the *Meekoceras gracilitatis* Zone probably corresponds to the Tethyan early and middle Smithian , but a better resolved documentation of this interval in the USA is still needed for more precise correlations. Correlation of the late Smithian *Anasibirites* beds between the Tethys and the USA is straight-forward, but no equivalent of the latest Smithian *Glyptophiceras sinuatum* beds is known from USA.

South Primorye (Russia). - While a recent quantitative biogeographical analysis has emphasized the low-palaeolatitude affinities of Early Triassic ammonoids from South Primorye (Brayard et al., 2009b), monazite age patterns in the sandstones favor a middle palaeolatitude origin for this terrane (Yokoyama et al., 2009a, b). Early-middle Smithian ammonoid faunas from South Primorye have recently been described by Shigeta et al. (2009b), but according to these authors our knowledge of these faunas is still insufficient. The early Smithian *Clypeoceras timorense* Zone is followed by three successive beds containing three different faunas, i.e. the *Radioprionites abrekensis* bed, the *Balhaeceras balhaense* bed and the *Arctoceras subhydaspis* bed. An early Smithian age for the *Clypeoceras timorense* Zone is indicated by the occurrence of *Rohillites* in this zone (Krystyn et al., 2007a, b; Brayard and Bucher, 2008). The *Balhaeceras balhaense* bed contains *Shigetaceras* (termed *Hemiprionites* sp. in Shigeta et al., 2009b) and therefore, correlates with the *Nammalites pilatoides* beds from Tulong. The late Smithian in Primorye is characterized by the *Anasibirites nevolini* Zone (Markevich and Zakharov, 2004), which correlates with beds containing *Anasibirites* and/or *Wasatchites* in the Tethys.

British Columbia (mid-palaeolatitudes). – In this realm, the Smithian is subdivided into the *Euflemingites romunderi* Zone and the *Wasatchites tardus* Zone (Silberling and Tozer, 1968; Tozer, 1994). The former is more or less correlative with the *Meekoceras gracilitatis* Zone (Tozer, 1967) and thus, also with the *Owenites* beds of the Tethys. However, some taxa from the *Euflemingites romunderi* Zone such as *Euflemingites* are known also from the early Smithian in the Tethys (Krystyn et al., 2007a). Correlation of the late Smithian *Wasatchites tardus* Zone from British Columbia with the beds containing *Anasibirites* and/or *Wasatchites* in the Tethys is clear-cut. Moreover, in British Columbia beds with *Xenoceltites subevolutus* occur above the beds with *Wasatchites tardus* (Tozer, 1994), similar to the *Glyptophiceras sinuatum* beds in the Tethys.

Arctic Canada, Spitsbergen, Siberia (high-palaeolatitudes). - In the palaeoartic realm the Smithian is subdivided into three ammonoid zones: the *Hedenstroemia hedenstroemi* Zone, the *Euflemingites romunderi* Zone (equivalent to the *Lepiskites kolymensis* Zone in Siberia) and the *Wasatchites tardus* Zone (Silberling and Tozer, 1968; Dagys and Ermakova, 1990; Tozer, 1994; Ermakova, 2002). Correlation of the *Hedenstroemia hedenstroemi* Zone with the Tethys is difficult since this zone is characterized by very few taxa. Moreover, *Hedenstroemia* has proved to be a long-ranging genus and has been found in the late Smithian (Brayard and Bucher, 2008; this work). A few taxa from the next younger *Euflemingites romunderi* Zone such as *Anaxenaspis* and *Parananannites spathi* from Canada (Tozer, 1994) are known also from the Tethys, thus indicating that at least part of this zone correlates with the middle Smithian *Owenites* beds from the Tethys. However, as mentioned earlier some taxa from this zone such as *Euflemingites* are known also from the early Smithian in the Tethys (Krystyn et al., 2007a). Again, correlation of the late Smithian *Wasatchites tardus* Zone of the palaeoartic realm with beds containing *Anasibirites* and/or *Wasatchites* in the middle-/low-palaeolatitudes is beyond question. However, in Spitsbergen *Xenoceltites* co-occurs with *Anasibirites* and *Wasatchites* (Weitschat and Lehmann, 1978). Therefore, the subdivision of the late Smithian as observed in low- and middle-palaeolatitudes (i.e. *Anasibirites* beds followed by *Glyptophiceras/Xenoceltites* beds) cannot be extended to the high-palaeolatitudes.

5. Conclusions

Intensive bed-by-bed sampling of the Smithian series in the area around the village of Tulong in South Tibet has resulted in the first detailed description of Smithian ammonoids from this area. A total of six different middle to latest Smithian ammonoid associations have been found. In ascending order the new local biostratigraphical sequence comprises the *Brayardites compressus* beds, the *Nammalites pilatoides* beds, the *Pseudoceltites multiplicatus* beds, the *Nyalamites angustecostatus* beds, the *Wasatchites distractus* beds and the *Glyptophiceras sinuatum* beds. Early Smithian ammonoid faunas are almost lacking in the studied area because of the absence of carbonate sediments in this time interval. Comparison of the new faunal sequence from Tulong with Oman, the Salt Range and Spiti reveals that the Smithian ammonoid successions are very uniform on the Northern Indian Margin (Brühwiler et al., 2007, ongoing work). Moreover, a detailed correlation with the well-studied record from Guangxi, South China (Brayard and Bucher, 2008) is facilitated by many common taxa. However, detailed correlations with sections from outside the Tethys are hampered by the still somewhat inadequate knowledge of Smithian ammonoid faunas from these areas on the one hand, and by the latitudinally restricted distribution of most early-middle Smithian ammonoids on the other hand.

6. Taxonomy

Systematic descriptions mainly follow the classification established by Tozer (1981; 1994) and refined by Brayard and Bucher (2008). Provided that measurements were available for at least four specimens, the quantitative morphological range of each species is expressed utilizing the four classic geometrical parameters of the ammonoid shell: diameter (D), whorl height (H), whorl width (W) and umbilical diameter (U). The three parameters (H, W and U) are plotted in absolute values as well as in relation to diameter (H/D, W/D, and U/D). Occurrence of taxa described herein includes the number of specimens obtained from each sample. For example, Tu50 (2) means that two specimens were identified from sample Tu50. Sample numbers are reported in the composite section (Fig. 4). Photographs of ammonoids and corresponding plots of measurements are shown in Figs. 6-23.

Abbreviations: non = material not forming part of the current species; p. = pars (from Latin, means that only part of the material belongs to the current species); v. = *video* or *vidimus* (from Latin, means that the material was seen in person by the authors); ? = questionable; PIMUZ, Paläontologisches Institut und Museum der Universität Zürich, Switzerland.

Class CEPHALOPODA Cuvier, 1797
Subclass AMMONOIDEA Zittel, 1884
Order CERATITIDA Hyatt, 1884
Superfamily XENODISCACEAE Frech, 1902
Family XENOCELTITIDAE Spath, 1930

Genus ***Pseudoceltites*** Hyatt, 1900

Type species: *Celtites multiplicatus* Waagen, 1895.

Pseudoceltites multiplicatus (Waagen, 1895)
Fig. 6(1-7)
1895. *Celtites multiplicatus* nov. sp. - Waagen, p. 78, Pl. 7, Fig. 2a-c.
1895. *Celtites dimorphus* nov. sp. - Waagen, p. 80, Pl. 7, Fig. 5a-c.
1976. *Pseuodceltites multiplicatus* (Waagen) - Wang and He, p. 289, Pl. 6, Figs. 7-11.
? 1976. *Eukashmirites* cf. *blaschkei* (Diener) - Wang and He, p. 290, Pl. 6, Fig. 12.
? 1976. *Eukashmirites* cf. *subarmatus* (Diener) - Wang and He, p. 291, Pl. 6, Figs. 13-14.

Occurrence: Samples Tu47 (1), Tu48 (1?), Tu50 (2), TuB1 (30), Tu52 (6), Tu53 (1), Tu54 (1), Tu55 (1?) (*Pseudoceltites multiplicatus* beds).

Description: Evolute shell with a subrectangular whorl section. Flanks flattened, converging very weakly. Venter broad and subtabulate, arched, with rounded shoulders. Umbilicus with a high vertical wall and marked, slightly rounded shoulders. Ornamentation varies from strong, distant radial ribs to fine, dense and slightly sinuous ribs. Ribs usually fade out on ventral shoulders, but occasionally cross the venter as faint ridges. Suture line ceratitic with broad saddles.

Measurements: See Fig. 7.

Discussion: *Celtites dimorphus* Waagen, 1895 comes from the same horizon as *Celtites multiplicatus* and is here regarded as a synonym of this species; representing a variant with distant ribs on inner whorls. The older (early Smithian) species *Kashmirites armatus* (Waagen, 1985) from the

Ceratite Sandstone of the Salt Range differs from *P. multiplicatus* by a more depressed whorl section, a more rounded umbilical edge and a suture with slightly phylloid saddles (Waagen, 1895; Brühwiler et al., ongoing work). The specimens from Kashmir described as *Kashmirites blaschkei*, *K. subarmatus* and *K.* aff. *subarmatus* by Diener (1913) differ from *P. multiplicatus* by their flatter venter and more pronounced ribs on the venter. The specimens from South Tibet described as *Eukashmirites* cf. *blaschkei* and *E.* cf. *subarmatus* by Wang and He (1976) are similar in shape and ornamentation but too poorly preserved for a definitive assignment.

Genus ***Kashmirites*** Diener, 1913

Type species: *Celtites armatus* Waagen, 1895.

Kashmirites sp. indet.

Fig. 6(9a-d)

Occurrence: Near section Na, a single incomplete specimen was found as float in the upper part of the shales of Unit II, about ten meters below Unit III. The exact stratigraphic position cannot be inferred due to faulting.

Description: Evolute shell with flat, parallel flanks. Venter subtabulate, low arched with rounded shoulders. Umbilicus wide with a vertical wall and rounded but narrow shoulders. Ornamentation consists of fine, rursiradiate ribs fading out on the ventral shoulders. Suture line not preserved.

Discussion: The evolute coiling and the subrectangular whorl section of our specimen favour assignment to *Kashmirites*. However, the specimen differs from typical *Kashmirites* by its rursiradiate ribbing and is relatively large size. It may represent a new species, but its poor preservation prevents the erection of a new taxon.

Genus ***Glyptophiceras*** Spath, 1930

Type species: *Xenodiscus aequicostatus* Diener, 1913 (=*Dinarites sinuatus* Waagen, 1895).

Discussion: The genus *Glyptophiceras* was erected by Spath (1930) for the species *"Xenodiscus" aequicostatus* Diener, 1913, which is herein considered as a synonym of *"Dinarites" sinuatus* Waagen, 1895. As already suspected by Tozer (1969), *Glyptophiceras* is now known to be of latest Smithian age and not Griesbachian. The so-called "*Glyptophiceras*" from the Griesbachian of the high latitudes (Spath, 1930; Trümpy, 1969) belongs to the genus *Hypophiceras* Trümpy, 1969 (see also Guex, 1978). *Glyptophiceras* is close to *Xenoceltites*, with which it has been synonymzed (Guex, 1978). However, its very distinct stout ribbing clearly separates it from this genus.

Glyptophiceras sinuatum (Waagen, 1895)

Fig. 8(1-7)

1895. *Dinarites sinuatus* nov. sp. - Waagen, p. 33, Pl. 10, Fig. 4.

? 1913. *Xenodiscus* cf. *lissarensis* Diener - Diener, p. 5, Pl. 1, Fig. 11.

1913. *Xenodiscus aequicostatus* nov. sp. - Diener, p. 6, Pl. 2, Fig. 10.

1913. *Xenodiscus salomonii* nov. sp. - Diener, p. 7, Pl. 2, Fig. 5.

1913. *Xenodiscus althothae* nov. sp. - Diener, p. 8, Pl. 2, Figs. 6, 11.

1913. *Xenodiscus* cf. *ellipticus* Diener; Diener, p. 9, Pl. 3, Fig. 1.

1913. *Xenodiscus comptoni* - Diener, p. 10, Pl. 2, Fig. 7.

? 1913. *Xenodiscus* cf. *rotula* Waagen - Diener, p. 11, Pl. 3, Fig. 2.

1913. *Xenodiscus* cf. *ophioneus* Waagen - Diener, p. 12, Pl. 2, Figs. 8-9.

? 1913. *Xenodiscus* cf. *sitala* Diener - Diener, p. 14, Pl. 3, Fig. 3.

v. 1978. *Xenoceltites pulcher* nov. sp. - Guex, p. 112, Pl. 7, Fig. 8.

Occurrence: Samples Tu73a (1), Tu73b (6), TWA4 (13) (*Glyptophiceras sinuatum* beds).

Description: Evolute, platycone shell with convex and convergent flanks. Venter narrowly rounded with rounded shoulders. Umbilicus wide and shallow with low vertical wall and rounded shoulders. Ornamentation highly variable from low, dense and sinuous to very strong, distant and concave ribs. Ribs may occasionally cross the venter, depending on their overall strength. Suture line ceratitic with slightly tapered saddles, but poorly preserved.

Discussion: A comprehensive study of this species based on newly collected, abundant and well preserved material from the Salt Range (Pakistan) and from Spiti (India) is currently under progress by our group. That new material shows the same high intraspecific variation that can also be seen on Diener's (1913) numerous specimens from a single layer in Kashmir that he described as various species of *Xenodiscus*. Thus, *Glyptophiceras sinuatum* is here understood as a species exhibiting a high intraspecific variation. Although rather poorly preserved, our specimens from Tulong reported here clearly fall within this variation. The three specimens illustrated on Figs.8-5, 8-6 and 8-7 are rather poorly preserved and are only tentatively included within this species.

Genus ***Xenoceltites*** Spath, 1930

Type species: *Xenoceltites subevolutus* Spath, 1930.

Xenoceltites cf. *variocostatus* Brayard and Bucher, 2008

Fig. 9(1-2)

Occurrence: Samples TWA4 (2), Tu75 (1), TWA2 (3) (*Glyptophiceras sinuatum* beds).

Description: Moderately evolute, platycone shell with flat, only slightly convex flanks. Venter narrowly rounded with indistinct shoulders. Umbilicus shallow with rounded shoulders. Inner whorls ornamented with low, slightly prorsiradiate ribs, outer whorls smooth or with very faint ribs on mid-flanks. Suture line simple, but poorly preserved.

Discussion: This species resembles *Xenoceltites variocostatus* from South China, but the relatively poor preservation of our material precludes a definitive specific assignment.

Genus ***Nyalamites*** nov. gen.

Etymology: Named after the small town of Nyalam, south of Tulong.

Type species: *Xenodiscus angustecostatus* Welter, 1922.

Diagnosis: Small-sized, evolute Xenoceltitidae with ornamentation consisting of evenly distributed, sharp ribs that do not cross the venter.

Discussion: *Preflorianites* differs from *Nyalamites* by its rounded ribs. *Nyalamites* also differs from other Xenoceltitidae such as *Kashmirites*, *Pseudoceltites*, *Xenoceltites* and *Glyptophiceras* by its evenly distributed ribs. The type species was assigned to *Anakashmirites* (genotype: *K. nivalis* Diener, 1897) by Kummel and Steele (1962), which is herein considered as a synonym of *Kashmirites*. Guex (1978) assigned this species to *Eukashmirites* (genotype: *E. acutangularis* Welter, 1922) which differs however, by its distinct rectangular whorl section.

Nyalamites angustecostatus (Welter, 1922) nov. gen.

Fig. 9(3-5)

? 1895. *Celtites acuteplicatus* nov. sp. - Waagen, 1895, p. 82, Pl. 7a, Figs. 5, 5c, 6, 7.

1922. *Xenodiscus angustecostatus* nov. sp. - Welter, p. 110, Pl. 4, Figs. 14-17.

? 1922. *Xenodiscus oyensi* nov. sp. - Welter, p. 111, Pl. 5, Figs. 1, 2, 17

1968. *Anakashmirites angustecostatus* (Welter) - Kummel and Erben, p. 128, Pl. 19, Figs. 1-8.

1973. *Anakashmirites angustecostatus* (Welter) - Collignon, p. 144, Pl. 5, Figs. 7-8.

? 1973. *Anakashmirites oyensi* (Welter) - Collignon, p. 146, Pl. 5, Figs. 9-10.

1976. *Pseudoceltites angustecostatus* (Welter) - Wang and He, p. 289, Pl. 6, Figs. 3-6.

v. 1978 . *Eukashmirites angustecostatus* (Welter) - Guex, Pl. 7, Figs. 4, 9.

v. non. 2008. *Pseudoceltites? angustecostatus* (Welter) - Brayard and Bucher, p. 18; Pl. 3, Figs. 1-7; Fig. 19 (=*Preflorianites radians*).

Occurrence: Samples Tu56 (8), Tu59 (1), Tu60 (1) (*Nyalamites angustecostatus* beds).

Description: Small, very evolute shell with slightly convex, subparallel flanks. Venter subtabulate with rounded shoulders. Umbilicus shallow and wide with inclined wall and rounded shoulders. Ornamentation consists of regularly spaced, strong, radial, sharp ribs that fade out on ventral shoulders. Suture line ceratitic with broad saddles.

Discussion: This species is very common in the late middle Smithian of the Tethys. *"Celtites" acuteplicatus* Waagen, 1895 is probably conspecific but is too poorly preserved for definive identification. "*Xenodiscus" oyensi* Welter, 1922 is very similar too, but differs mainly by its larger size. "*Celtites" trapezoidalis* Waagen, 1895 from the Salt Range is older and differs by its divergent flanks.

Xenoceltitidae gen. indet. A

Fig. 8(8-9)

Occurrence: Sample Tu58 (2) (*Nyalamites angustecostatus* beds).

Description: Moderately involute shell with a subrectangular whorl section. Flanks slightly convex. Venter broad and subtabulate with rounded shoulders. Umbilicus with a high, steep wall and rounded shoulders. Ornamentation consists of slightly sinuous ribs. Most ribs fade out on ventral shoulders, but some may cross the venter as faint ridges. Suture line simple with rather broad first lateral saddle.

Discussion: This species is close to *Pseudoceltites multiplicatus*, but it is more involute.

Superfamily MEEKOCERATACEAE Waagen, 1895

Family PROPYTCHITIDAE Waagen, 1895

Genus ***Leyeceras*** Brayard and Bucher, 2008

Type species: *Leyeceras rothi* Brayard and Bucher, 2008.

?*Leyeceras* sp. indet.

Fig. 9(8a-b)

Occurrence: A single specimen from sample TuB3 (*Nammalites pilatoides* beds).

Description: Large, moderately evolute shell with convex flanks and an elliptical whorl section. Venter rounded with rounded shoulders. Umbilical wall moderately high, umbilical shoulders rounded. Surface with weak, distant plications near umbilicus. Suture line not preserved on our specimen.

Discussion: The elliptical whorl section and the amount of involution of our specimen is similar to that of *Leyeceras rothi* Brayard and Bucher, 2008, but its rather poor preservation precludes a definitive generic assignment. *Anaflemingites* is also similar in shape but is more evolute. *Arctoceras* and *Submeekoceras* differ by their subangular umbilical shoulders.

Genus ***Tulongites*** nov. gen.

Etymology: Named after the type locality of the type species near the village of Tulong, South Tibet.

Type species: *Tulongites xiaoqiaoi* nov. gen. et sp.

Composition of the genus: Type species only.

Diagnosis: Compressed Proptychitidae with weak, prorsiradiate and biconcave folds, umbilicus with steeply inclined wall and rounded shoulders.

Discussion: This genus differs from other Proptychitidae by its prorsiradiate folds. However, its shape and suture line favor assignment to this family. *Lingyunites* Chao, 1959 differs by its more involute coiling and its umbilicus with a vertical umbilical wall and narrowly rounded shoulders.

Tulongites xiaoqiaoi nov. gen. et sp.

Fig. 9(9-10)

Etymology: Named after Wan Xiaoqiao (China University of Geosciences, Beijing).

Holotype: Specimen PIMUZ 27621, Fig. 8(9a-e).

Type locality: Section TuB, Tulong, Nyalam County, South Tibet.

Type horizon: Sample TuB5; Early Triassic, Smithian, *Brayardites compressus* beds.

Diagnosis: As for the genus.

Occurrence: Sample TuB5 (2) (*Brayardites compressus* beds).

Description: Involute, platycone shell with slightly convex flanks. Maximum whorl width near mid flank. Venter narrow and rounded with rounded shoulders. Umbilicus small with steeply inclined wall and rounded shoulders. Shell ornamented with weak, biconcave and prorsiradiate folds. Suture line ceratitic; first and second lateral saddles tapered; second lateral saddle slightly asymmetrical; third lateral saddle small.

Genus ***Pseudaspidites*** Spath, 1934

Type species: *Aspidites muthianus* Krafft and Diener, 1909.

Pseudaspidites sp. indet.

Fig. 9(11a-e)

Occurrence: Samples Na23 (1), TuB5 (1) (*Brayardites compressus* beds).

Description: Involute, compressed shell with slightly convex, convergent flanks. Maximum whorl width near umbilicus. Venter subtabulate with rounded shoulders. Umbilicus small and deep with high, vertical wall and marked, slightly rounded shoulders. Surface smooth. Suture line ceratitic with deep lobes; first lateral saddle narrow, second lateral saddle slightly phylloid and slightly curved towards umbilicus; auxiliary series with a small fourth saddle.

Discussion: Typical *Pseudaspidites* differ from this species by a more complex suture line with phylloid and more distinctly curved saddles.

Family FLEMINGITIDAE Hyatt, 1900

Genus ***Subflemingites*** Spath, 1934

Type species: *Subflemingites involutus* Spath (=*Aspidites meridianus involutus* Welter, 1922).

?Subflemingites compressus sp. nov.

Fig. 10(1-6)

Etymology: Refers to the compressed whorl section of the species.

Holotype: Specimen PIMUZ 27625, Fig. 10(2a-d).

Type locality: Section Tu, Tulong, Nyalam County, South Tibet.

Type horizon: Sample Tu58; Early Triassic, Smithian, *Nyalamites angustecostatus* beds.

Diagnosis: *Subflemingites* with a compressed whorl section.

Occurrence: Samples Tu56 (2?), Tu58 (6), Tu63 (2), Tu64 (2), Tu65 (1?) (*Nyalamites angustecostatus* beds).

Description: Moderately involute, compressed shell with flat, slightly convex flanks. Venter rounded without distinct shoulder. Umbilicus with low, inclined wall and rounded shoulders. Surface smooth or with weak radial folds on inner flanks. Suture line ceratitic with slightly phylloid saddles.

Measurements: See Fig. 11.

Discussion: This species differs from the type species by its more compressed whorl section, but it is otherwise very similar. Unfortunately, the suture line of the type species has never been illustrated. Based on the descriptions by Welter (1922) and Spath (1934), it has possibly a longer auxiliary series than our species. Therefore, the generic assignment to *Subflemingites* of this new species is only tentative. *Flemingites* Waagen, 1895 differs by its strigation and radial ribs; *Galfettites* Brayard and Bucher, 2008 differs by its convergent flanks and its tabulate venter; *Anaflemingites* Kummel and Steele, 1962 is more evolute.

Genus ***Anaxenaspis*** Kiparisova, 1956

Type species: *Xenaspis orientale* Diener, 1895.

?Anaxenaspis sp. indet. A

Fig. 12(1a-c)

Occurrence: A single specimen from Sample TuB1 (*Pseudoceltites multiplicatus* beds).

Description: Compressed and moderately evolute shell with convex flanks. Venter rounded with rounded shoulders. Umbilicus with low rounded wall without distinct shoulders. Surface smooth except for weak folds on outer flanks. Suture line not preserved.

Discussion: Our single specimen is very similar to the type species *Anaxenaspis orientale*, but since the suture line is not preserved, no definitive specific assignment can be made.

?Anaxenaspis sp. indet. B

Fig. 12(3-7)

Occurrence: Sample TuB1 (11) (*Pseudoceltites multiplicatus* beds).

Description: Evolute, compressed shell with convex flanks. Maximum whorl width slightly below mid-flank. Venter narrowly rounded without distinct shoulders. Umbilicus wide and shallow with inclined wall and rounded shoulders. Ornamented with slightly rursiradiate folds that fade out above mid-flank. Suture line not preserved.

Discussion: This species is common in the *Pseudoceltites multiplicatus* beds. It is similar in shape with the type species *Anaxenaspis orientale*, which does not exhibit rursiradiate folds. Since the suture line is not preserved, the assignment to *Anaxenaspis* is only provisional. Our single specimen described below as Flemingitidae gen. indet. B from the *Nammalites pilatoides* beds (Fig. 12[2a-b]) differs by its thicker whorls.

Flemingitidae gen. indet. A

Fig. 10(7-8)

Occurrence: Sample TuB3 (1), Tu44 (1) (*Nammalites pilatoides* beds).

Description: Compressed and moderately involute shell with convex and convergent flanks. Venter rounded with rounded shoulders. Umbilicus with steeply inclined wall and rounded shoulders. Ornamentation consists of blunt radial ribs that disappear on the external third of the flank. Ribs are strong on the inner whorls and become weaker on the outer whorls. Suture line with rather deep lobes and slightly phylloid saddles.

Discussion: This species differs from *Anaxenaspis* sp. indet. described above by its more involute coiling and different umbilical wall and shoulders.

Flemingitidae gen. indet. B

Fig. 12(2a-b)

Occurrence: A single specimen from sample Tu44 (*Nammalites pilatoides* beds).

Description: Compressed and evolute shell with convex and convergent flanks. Venter rounded with indistinct shoulders. Umbilicus with steeply inclined wall and rounded shoulders. Ornamentation consists of blunt radial ribs that fade out on the external third of the flank. Strength of ribbing decreases throughout growth. Suture line not preserved.

Discussion: This species is close to Flemingitidae gen. indet. A described above, but differs by its more evolute coiling.

Genus ***Urdyceras*** Brayard and Bucher, 2008

Type species: *Urdyceras insolitus* Brayard and Bucher, 2008.

Discussion: This genus was originally assigned to Proptychitidae by Brayard and Bucher (2008). However, based on our new material from Tibet it is now clear that *Urdyceras,* with its relatively evolute coiling and tabulate venter with very angular shoulders, is not representative of Proptychitidae.

The genus is herein provisionally included in Flemingitidae since these traits are found in certain other members of this family (e.g. *Rohillites*, *Galfettites*).

Urdyceras tulongensis nov. sp.

Fig. 13(5-11)

Etymology: Named after the type locality near the village of Tulong.

Holotype: Specimen PIMUZ 27644, Fig.13(6a-e).

Type locality: Section TuB, Tulong, Nyalam County, South Tibet.

Type horizon: Sample TuB5; Early Triassic, Smithian, *Brayardites compressus* beds.

Diagnosis: *Urdyceras* with a relatively narrow venter and flanks that have a tendency to become concave near the venter.

Occurrence: Samples Na23 (1), TuB5 (8) (*Brayardites compressus* beds).

Description: Compressed and moderately evolute shell. Flanks convex and convergent, tending to become concave near the venter. Venter tabulate with very angular shoulders. Umbilicus with vertical wall and marked, but slightly rounded shoulders. Ornamentation on flanks consists of fine radial, slightly sinuous folds. One specimen (Fig. 13[8a-c]) displays rather strong folds on inner flanks. Suture line ceratitic with deep lobes and slightly phylloid saddles. First lateral saddle narrow; second lateral saddle slightly curved towards umbilicus.

Measurements: See Fig. 14.

Discussion: The slightly older type species *Urdyceras insolitus* from the *Flemingites rursiradiatus* beds of South China differs by its thicker whorls and broader venter. The inner whorls of *Urdyceras tulongensis* are similar to *Anaflemingites hochulii* Brayard and Bucher, 2008, which differs by its rounded ventral shoulders.

Family ARCTOCERATIDAE Arthaber, 1911

Genus ***Nammalites*** nov. gen.

Etymology: Named after the type locality of the type species, Nammal Gorge in the Salt Range, Pakistan.

Type species: *Kazakhstanites pilatoides* Guex, 1978.

Composition of the genus: Type species only.

Diagnosis: Moderately evolute Arctoceratidae with convergent flanks and ribs that tend to develop umbilical tubercles.

Discussion: When describing the type species, GUEX (1978) assigned it to the genus *Kazakhstanites* Shevyrev, 1968 of Spathian age (associated with *Columbites*), which indeed is very close in shape. However, *Kazakhstanites* clearly differs from *Nammalites* by having a simplified suture line with only two lateral saddles. The similarity of these two genera is herein interpreted as a case of convergence.

The assignment of *Nammalites* to the familiy Artoceratidae is based on its high vertical umbilical wall and the tendency of its ribs to form umbilical tubercles or bullae. Superficially, *Nammalites* resembles some members of the family Prionitidae, such as *Wasatchites*. However, all Prionitidae differ by their distinctly sloped umbilical wall, which forms a more or less funnel-shaped umbilicus, as well as by their suture line, which is characterized by low and broad saddles.

Nammalites pilatoides (Guex, 1978) nov. gen.

Fig. 21 (6-8)

1909. *Meekoceras* sp. ind. aff. *pilato* - Krafft and Diener, p. 42, Pl. 28, Fig. 2a-c.

1968a. *Wasatchites* sp. indet. - Kummel, p. 500, Pl. 3, Figs. 10-11.

1968. *Eoptychites* sp. indet. - Kummel and Erben, p. 120, Pl. 22, Figs. 10-11.

v. 1978. *Kazakhstanites pilatoides* nov. sp. - Guex, p. 109, Pl. 6, Fig. 5, 6, 16.

v. ? 1978. *Kazakhstanites pilatoides* nov. sp. - Guex, p. 109, Pl. 8, fig. 6.

v. p. 1978. *Anasibirites pluriformis* nov. sp. - Guex, Pl. 4, Fig. 3 only.

Occurrence: Samples TuB2 (1?), Tu40 (2?), TuB3 (3), Tu44 (11), TuB4 (2) (*Nammalites pilatoides* beds).

Description: Moderately involute, compressed shell with convex, convergent flanks. Maximum whorl width at umbilical border. Venter subtabulate with rounded shoulders. Umbilicus with vertical wall and rounded shoulders. Ornamentation consists of rursiradiate to radiate ribs that tend to develop tubercles or elongated bullae near the umbilicus and then fade out towards the venter. Suture line ceratitic with tapered second lateral saddle on one specimen.

Genus ***Brayardites*** nov. gen.

Etymology: Named after Arnaud Brayard (Dijon, France).

Type species: *Brayardites crassus* nov. gen. et sp.

Composition of the genus: *Brayardites crassus* nov. gen. et sp. and *B. compressus* nov. gen. et sp.

Diagnosis: Moderately involute, compressed to subglobose Arctoceratidae with convergent flanks and prorsiradiate ribs that form strong tubercles near umbilical margin.

Discussion: *Brayardites* is slightly older than *Nammalites* and differs essentially by its prorsiradiate ribbing and stronger tubercles.

Brayardites crassus nov. gen. et sp.

Fig. 15(1-4), 16(1-6)

Etymology: Refers to the thick whorls of this species.

Holotype: Specimen PIMUZ 27651, Fig.15(2a-d).

Type locality: Section TWB, Tulong, Nyalam County, South Tibet.

Type horizon: Sample TWB71; Early Triassic, Smithian, *Brayardites compressus* beds.

Diagnosis: Evolute *Brayardites* with thick whorls and strongly convex flanks.

Occurrence: Samples TuB5 (14), TWB71 (2), TWB72 (2), Na22 (1), Na23 (1), Na25 (1), Na28 (1), Na41 (1?) (*Brayardites compressus* beds).

Description: Moderately evolute, shell with thick whorls and strongly convex flanks. Maximum whorl width below mid-flank. Venter broadly rounded with rounded shoulders. Umbilicus with steeply inclined wall and rounded shoulders. Ornamentation consists of prorsiradiate ribs that develop strong tubercles near umbilicus and fade out towards mid-flank. Suture line ceratitic, with broad, slightly tapered saddles.

Measurements: See Fig. 17.

Discussion: *Brayardites compressus* nov. gen. et sp. described below differs by its more compressed whorl section and more involute coiling.

Brayardites compressus nov. gen. et sp.

18(1-6)

Etymology: Refers to the compressed shape of this species.

Holotype: Specimen PIMUZ 27660, Fig.18(1a-e).

Type locality: Section TWB, Tulong, Nyalam County, South Tibet.

Type horizon: Sample TWB71; Early Triassic, Smithian, *Brayardites compressus* beds.

Diagnosis: Involute *Brayardites* with compressed whorls and flat flanks.

Occurrence: Samples Tu16 (1), Tu18 (1), Tu33 (1), TuB5 (10), TuB6 (1), TWB72 (3), Na23 (2), (*Brayardites compressus* beds).

Description: Moderately involute, compressed shell with flat, converging flanks. Maximum whorl width near umbilical border. Venter subtabulate with rounded shoulders. Umbilicus with high vertical wall and rounded shoulders. Ornamentation consists of prorsiradiate ribs that develop strong tubercles near umbilicus and fade out towards mid-flank. Growth lines biconcave. Suture line ceratitic with deep lobes and slightly tapered saddles.

Measurements: See Fig. 17.

Discussion: *Ceratites sagitta* Waagen, 1895 from the lower part of the Upper Ceratite Limestone of the Salt Range has similar ornamentation. Apparently, it differs by a rounded umbilical margin, but the preservation of Waagen's single specimen is rather poor. *B. crassus* and *B. compressus* co-occur in the Tulong succession. Whether or not these two species represent end-member variants of a single, highly variable species cannot be demonstrated on the basis of the limited number of available specimens, but a disparity of intermediate values of whorl width apparently does exist (Fig. 16).

Family PRIONITIDAE Hyatt, 1900

Genus ***Prionites*** Waagen, 1895

Type species: *Prionites tuberculatus* Waagen, 1895

Prionites involutus nov. sp.

Fig. 19(1-6)

Etymology: Refers to the involute coiling of this species in comparison with other *Prionites*.

Holotype: Specimen PIMUZ 27671, Fig. 19(3a-b).

Type locality: Section Tu, Tulong, Nyalam County, South Tibet.

Type horizon: Sample Tu58; Early Triassic, Smithian, *Nyalamites angustecostatus* beds.

Diagnosis: Involute and smooth *Prionites* with a persisting compressed whorl section at maturity.

Occurrence: Samples Tu56 (1), Tu58 (9) (*Nyalamites angustecostatus* beds).

Description: Involute, compressed shell with slightly convex flanks. Maximum whorl width below mid-flank. Venter broad and tabulate with slightly angular shoulders. Umbilicus small, deep and funnel-shaped. Umbilical wall inclined with rounded shoulders. Surface smooth. Suture line ceratitic with broad saddles; third lateral saddle very low.

Measurements: See Fig. 20.

Discussion: The inner whorls of this species are similar to those of the type species and differ only by their more involute coiling (Waagen, 1895). The outer whorls of the type species differ by being more evolute and having a broader whorl section with broad swellings, whereas the new Tibetan species retains a compressed whorl section and involute coiling throughout ontogeny. *Hemiprionites klugi* Brayard and Bucher, 2008 is similar but differs by its smaller umbilicus with a steeper wall as well as by its suture line with charcteristically tapered saddles.

Genus ***Stephanites*** Waagen, 1895

Type species: *Stephanites superbus* Waagen, 1895.

Discussion: *Stephanites* differs from the younger *Wasatchites* by the dorso-ventral elongation of its tubercles (especially on the inner whorls). Additionally, *Wasatchites* has more compressed and smoother inner whorls. Otherwise, these two genera are very similar, and thus, *Stephanites* is herein assigned to Prionitidae.

Stephanites superbus Waagen, 1895

Fig. 19(7-12)

1895. *Stephanites suberbus* nov. sp. - Waagen, p. 101, Pl. 2, Fig. 2a-c.

1895. *Stephanites corona* nov. sp. - Waagen, p. 102, Pl. 3, Fig. 1a-b.

Occurrence: Samples Tu56 (1), Tu57 (1), Tu58 (3), Tu60 (2), Tu63 (4) (*Nyalamites angustecostatus* beds).

Description: Moderately involute shell with convex, convergent flanks. Maximum whorl width slightly below mid-flank. Venter broad and subtabulate with rounded shoulders. Umbilicus deep with well-rounded, inclined wall without distinct shoulders. Ornamentation consists of strong, distant tubercles on flanks, coinciding with maximum whorl width. Tubercles are elongated dorso-ventrally. Suture line with very broad first lateral saddle and very low third lateral saddle. Indentations of lobes not preserved.

Discussion: The minor differences between the type species and *Stephanites corona* Waagen, 1895 are here regarded as intraspecific variation.

Genus ***Wasatchites*** Mathews, 1929

Type species: *Wasatchites perrini* Mathews, 1929.

Wasatchites distractus (Waagen, 1895)

Fig. 21(1a-b)

1895. *Acrochordiceras distractum* nov. sp. - Waagen, p. 94, Pl. 3, Fig. 4a-c.

1895. *Acrochordiceras coronatum* nov. sp. - Waagen, p. 96, Pl. 3, Fig. 5a-c.

1895. *Acrochordiceras* cf. *damesi* Noetling - Waagen, p. 97, Pl. 4, Fig. 5a-b.

1895. *Acrochordiceras compressum* nov. sp. - Waagen, p. 98, Pl. 4, Fig. 4a-c.

v. ? 1978. *Stephanites corona* Waagen - Guex, pl. 5, fig. 2.

Occurrence: Samples Tu67 (1), TWA3 (1) (*Wasatchites distractus* beds).

Description: Moderately involute shell with convex flanks. Maximum whorl width at mid-flank. Venter broad and subtabulate with rounded shoulders. Umbilicus deep with well-rounded, inclined wall without shoulders. Ornamentation very distinct, consisting of distant spiny tubercles on mid-flank. Venter poorly preserved and apparently smooth, but at some points there are faint indications of distant broad ribs. Suture line not preserved.

Discussion: The minor differences between the four species described by Waagen (1895) are here regarded as intraspecific variation of a single species, *W. distractum*. Note that a more comprehensive study of this species based on abundant and well preserved material from the Salt Range (Pakistan) and Spiti (India) is under progress by our group. The specimen described as *Stephanites corona* by Guex (1978) is probably conspecific but too poorly preserved for a definitive assignment. The boreal *Wasatchites* (i.e. *W. perrini* Spath 1934) differs essentially by the lower position of spines on flanks.

Prionitidae gen. indet. A

Fig. 21(5a-c)

Occurrence: A single specimen from sample TuB3 (*Nammalites pilatoides* beds).

Description: Involute shell with convex flanks. Maximum whorl width below mid-flank. Venter broad and tabulate with rounded shoulders, but poorly preserved. Umbilicus deep with well-rounded, inclined wall and rounded shoulders. Ornamented with distant ribs that are most prominent near umbilicus and fade out towards venter. Suture line ceratitic with broad first lateral saddle and low third lateral saddle.

Discussion: This specimen differs from *Nammalites pilatoides* by its inclined umbilical wall, which is indicative of Prionitidae. The poor preservation of this single specimen hinders a generic assignment.

"Anasibirites" cf. *pluriformis* (Guex, 1978)

Fig. 6(8a-c)

Occurrence: A single specimen from sample Tu44 (*Nammalites pilatoides* beds).

Description: Moderately involute shell with flat, slightly converging flanks. Venter subtabulate, slightly arched, with rounded shoulders. Umbilicus with a high, vertical wall and marked, slightly rounded shoulders. Ornamentation consists of radial, slightly sinuous ribs with a faint thickening at ventral shoulders, not crossing the venter. Suture line not preserved.

Discussion: Our single specimen is very similar to weakly ornamented variants of *"Anasibirites" pluriformis*, but without additional material a definitive specific assignment would be speculative. This species was attributed to *Anasibirites* by Guex (1978). However, typical *Anasibirites* as well as all other Prionitidae differ greatly by having an umbilicus with an inclined wall and well-rounded shoulders. A revision of this species based on new material from the Salt Range is in progress by our group.

Family INYOITIDAE Spath, 1934

Genus ***Subvishnuites*** Spath, 1930

Type species: *Subvishnuites welteri* Spath, 1930 (= *Vishnuites* spec. Welter, 1922).

Subvishnuites sp. indet.

Fig. 22(9a-d)

Occurrence: A single specimen from sample Tu58 (*Nyalamites angustecostatus* beds).

Description: Compressed, moderately evolute shell. Flanks convex, subparallel on inner half and converging strongly towards venter on outer half. Venter subacute. Umbilicus moderately deep with a vertical wall and rounded shoulders. Surface entirely smooth. Suture line not preserved.

Discussion: This species differs from the type species by its more involute coiling and thicker whorls. It is also more involute than *Subvishnuites stokesi*. It may represent a new species of *Subvishnuites*, but because of our sparse material we prefer to use an open nomenclature.

Family MELAGATHICERATIDAE Tozer, 1971

Genus ***Jinyaceras*** Brayard and Bucher, 2008

Type species: *Jinyaceras bellum* Brayard and Bucher, 2008.

Jinyaceras hindostanum (Diener, 1897)

Fig. 22(4-6)

1897. *Nannites hindostanus* nov. sp. - Diener, p. 68, Pl. 7, Figs. 3, 11-12.

1897. *Nannites herberti* nov. sp. - Diener, p. 69, Pl. 7, Fig. 2.

Occurrence: Samples Na14 (3), Na23 (1), TuB5 (4), Tu16 (1) (*Brayardites compressus* beds).

Description: Small, moderately involute, laterally compressed shell with flat, subparallel flanks. Venter broadly arched, with rounded ventral shoulders. Umbilicus with vertical wall and subangular shoulders. Ornamentation consists of prorsiradiate constrictions that nearly disappear on venter. Suture line not preserved.

Discussion: This specis is very similar to *Jinyaceras bellum* and differs only by its more involute coiling. "*Nannites" herberti* Diener, 1897 is slightly more involute than *Jinyaceras hindostanum*, but this minor difference is here regarded as intraspecific variation. The specimens described as *Paranannites aspenensis* by Kummel and Erben (1968) are very similar and may be conspecific, but differ by their larger size.

Family PARANANNITIDAE Tozer, 1971

Genus ***Paranannites*** Hyatt and Smith, 1905

Type species: *Paranannites aspenensis* Hyatt and Smith, 1905.

Paranannites spathi (Frebold 1930)

Fig. 22(1-2)

1930. *Prosphingites spathi* nov. sp. - Frebold, p. 20, Pl. 4, Figs. 2-3, 3a.

1934. *Prosphingites spathi* Frebold - Spath, p. 195, Pl. 13, Figs. 1-2.

p. ? 1959. *Prosphingites kwangsianus* nov. sp. - Chao, p. 296, Pl. 28, Figs. 17-18

p. ? 1959. *Prosphingites sinensis* nov. sp. - Chao, p. 297, Pl. 27, Figs. 14-17, Fig. 40a

? 1961. *Prosphingites spathi* Frebold - Tozer, p. 58, Pl. 13, Figs. 1-2.

? 1982. *Prosphingites spathi* Frebold - Korchinskaya, Pl. 5, Fig. 2.

? 1994. *Paranannites spathi* Frebold - Tozer, p. 77, Pl. 36, Figs. 1-2.

v. 2008. *Paranannites spathi* Frebold - Brayard and Bucher, p. 63, Pl. 35, Figs. 10-19.

Occurrence: Samples TuB3 (2), Tu44 (6) (*Nammalites pilatoides* beds).

Description: Moderately involute, globose shell with outer whorls characterized by a subtrigonal whorl section. Flanks convex, converging strongly to the venter from the umbilical margin. Umbilicus deep, with vertical wall and rounded shoulders. Ornamentation consists of prorsiradiate constrictions that cross the venter. Suture line not preserved.

Discussion: *Paranannites spathi* is very widely distributed in the middle Smithian (Brühwiler et al., 2007; Brayard and Bucher, 2008). It differs from other representatives of the genus by its subtrigonal outer whorls as well as by its stair-like umbilicus.

Paranannites sp. indet.

Fig. 22(3a-d)

Occurrence: Sample Tu44 (3) (*Nammalites pilatoides* beds).

Description: Moderately involute, globose shell with a curved venter. Flanks flat, subparallel. Umbilicus deep with vertical wall and rounded shoulders. Ornamentation consists of faint prorsiradiate constrictions. Suture line with all three lateral saddles located on flanks. Indentations of lobes not preserved.

Discussion: This species differs from *Paranannites spathi* described above by its subparallel flanks and lower umbilical wall. Another perhaps more significant difference is that in the suture line of *P. spathi* the third lateral saddle is located on the umbilical wall (Brayard and Bucher, 2008), whereas for this species it is located on the flanks.

Genus ***Owenites*** Hyatt and Smith, 1905

Type species: *Owenites koeneni* Hyatt and Smith, 1905.

Owenites koeneni Hyatt and Smith, 1905

Fig. 21(9a-b)

1905. *Owenites koeneni* nov. sp. - Hyatt and Smith, p. 83, Pl. 10, Figs. 1-22.

v. 2008. *Owenites koeneni* Hyatt and Smith - Brayard and Bucher, p. 67, Pl. 36, Figs. 1-8.

Occurrence: Samples Tu50 (1), Tu55 (1), Tu59 (1) (*Pseudoceltites multiplicatus* beds, *Nyalamites angustecostatus* beds)

Description: Involute, somewhat compressed shell with an inflated, lenticular whorl section. Umbilical wall inclined with a cone-shaped umbilicus**,** whose umbilical seam is hardly discernible. Venter narrowly rounded to acute. Surface generally smooth, weak concave folds may be present. Suture line not preserved.

Discussion: See Brayard and Bucher (2008) for a recent comprehensive study and a complete synonymy list for this species.

Owenites carpenteri Smith 1932

Fig. 22(7-8)

1932. *Owenites carpenteri* nov. sp. - Smith, p. 100, Pl. 54, Figs. 31-34.

1966. *Owenites carpenteri* Smith - Hada, p. 112, Pl. 4, Figs. 1a-e.

1968. *Owenites carpenteri* Smith - Kummel and Erben, p. 122, Fig. 12P.

1973. *Owenites carpenteri* Smith - Collignon, p. 139, Pl. 4, Figs. 5-6.

v. 2008. *Owenites carpenteri* Smith - Brayard and Bucher, p. 70, Pl. 43, Figs. 15-16.

Occurrence: Samples Tu 56 (1?), Tu58 (4), Tu59 (1?), Tu63 (1) (*Nyalamites angustecostatus* beds).

Description: Small, extremely involute to occluded shell with a subtriangular whorl section. Venter narrow and subangular. Umbilicus occluded. Maximum whorl width at umbilicus. Shell surface smooth except for very strong constrictions visible on internal mould only. Suture line with four lateral saddles; indentations of lobes poorly preserved.

Discussion: As shown by new material from Spiti (Brühwiler et al., ongoing work) constrictions may become closely spaced on outer whorls. If the shell is not preserved, this feature gives the false impression that the conch is ornamented with "strong bundled radial ribs" as described on the holotype by Smith (1932).

Owenites simplex Welter 1922

Fig. 21(10-12)

1922. *Owenites simplex* nov. sp. - Welter, p. 153, Pl. 15, Figs. 1-8.

1934. *Parowenites simplex* Welter - Spath, p. 187, Fig. 58.

1959. *Owenites kwangsiensis* nov. sp. - Chao, p. 250, Pl. 22, Figs. 1-6, Fig. 26b.

1959. *Owenites plicatus* nov. sp. - Chao, p. 251, Pl. 22, Figs. 19-21, 24, 25, Fig. 26e.

1968b. *Owenites simplex* Welter - Kummel, p. 2, Pl. 1, Figs. 1-9.

1968. *Owenites simplex* Welter - Kummel and Erben, p. 122, Figs. 12k, n, o.

v. 2008. *Owenites simplex* Welter - Brayard and Bucher, p. 69, Pl. 35, Figs. 20-22; Fig. 59.

Occurrence: Samples TuB3 (1?), Tu44 (4) (*Nammalites pilatoides* beds).

Description: Small, moderately involute, compressed shell with subparallel flanks. Venter narrowly rounded. Umbilicus deep with perpendicular wall and angular shoulder. Ornamentation consists of prosiradiate, slighlty concave folds. Suture line not preserved.

Discussion: *Owenites simplex* is more evolute than *O. koeneni* and it has a more compressed shell.

Family INCERTAE SEDIS

Genus ***Shigetaceras*** nov. gen.

Etymology: Named after Yasunari Shigeta (National Museum of Nature and Science, Tokyo).

Type species: *Hemiprionites dunajensis* Zakharov, 1968.

Composition of the genus: Type species only.

Diagnosis: Compressed and involute Meekocerataceae. Venter broad and tabulate with angular shoulders. Umbilicus with vertical wall. Suture line with broad, tapered saddles.

Discussion: The type species was assigned to *Hemiprionites* by Zakharov (1968). However, true *Hemiprionites* as well as all other Prionitidae clearly differ from this species by having a funnel-shaped umbilicus with an inclined wall (Waagen, 1895; Brayard and Bucher, 2008). *Shigetaceras* is close to *Wailiceras* Brayard and Bucher, 2008 of earliest Smithian age (i.e. *Kashmirites kapila* beds), which differs by its narrower venter and a suture line with long, deep lobes and narrow saddles. Although more involute, the shape of *Shigetaceras* is also close to that of *Urdyceras tulongensis* described above, but its suture line is also notably different.

The familial affinity of *Shigetaceras* is unclear. Its shape and suture line are similar to Prionitidae, from which it differs by its umbilicus with a high, vertical wall and marked shoulders. Proptychitidae differ by having a rounded venter and a more complex suture line.

Shigetaceras dunajensis (Zakharov, 1968) nov. gen.

Fig. 13(1-4)

1968. *Hemiprionites dunajensis* nov. sp. - Zakharov, p. 125, Pl. 23, Figs. 6-8.

? 2009. *Hemiprionites* sp. indet. - Shigeta and Zakharov, p. 87, Fig. 74.

Occurrence: Samples TuB3 (1), Tu44 (3) (*Nammalites pilatoides* beds).

Description: Compressed and involute shell with convex and convergent flanks. Venter tabulate with angular shoulders. Umbilicus small and deep with vertical wall and narrow, slightly rounded shoulders. Surface smooth. Suture line with broad, tapered saddles. Indentations of lobes not preserved.

Measurements: See Fig. 23, which includes measurements of the type material from Primorye (Zakharov 1968) for comparison.

Discussion: This species has recently been found in age-equivalent beds in Spiti (Brühwiler et al., unpublished).

Genus indet. A

Fig. 9(6-7)

Occurrence: Sample Na28 (2) (*Brayardites compressus* beds).

Description: Evolute shell with convex flanks. Inner whorls with subquadratic whorl section, outer whorls becoming laterally compressed. Venter subtabulate with rounded shoulders. Umbilicus wide and shallow with rounded umbilical wall. Surface smooth except for very small nodes at umbilical shoulders. Suture line ceratitic with distinctly phylloid saddles and deeply indented lobes.

Genus indet. B

Fig. 21(2-4)

Occurrence: Samples Tu66 (1), TWA3 (2?), Tu67 (2) (*Wasatchites distractus* beds).

Description: Moderately evolute, compressed shell with slightly convex flanks. Maximum whorl width slightly below mid-flank. Venter narrow and rounded with rounded shoulders. Umbilicus with inclined wall and rounded shoulders. Ornamented with distant radial ribs that fade out near mid-flank. Suture line ceratitic with large first lateral saddle and low third lateral saddle.

Discussion: The evolute coiling and the rather peculiar ornamentation suggest that this ammonoid represents a new genus, but our poorly preserved material precludes the erection of a new taxon. The familial affinity of this ammonoid is unclear. Its general shape is similar to that of some Flemingitidae, but its ornamentation is rather uncharacteristic of this family. On the other hand, some Xenoceltitidae such as *Xenoceltites* are relatively similar.

Superfamily SAGECERATACEAE Hyatt 1884

Family HEDENSTROEMIIDAE Waagen 1895

Genus ***Pseudosageceras*** Diener 1895

Type species: *Pseudosageceras* sp. indet. - Diener 1895.

Pseudosageceras multilobatum Noetling, 1905

Fig. 22(14a-c)

1895. *Pseudosageceras* sp. indet. - Diener, p. 28, Pl. 1, Fig. 8.

1905. *Pseudosageceras multilobatum* nov. sp. - Noetling, Pl. 25, Figs. 1a, b; Pl. 26, Figs. 3a, b.

v. 2008. *Pseudosageceras multilobatum* Noetling - Brayard and Bucher, p. 70, Pl. 37, Figs. 1-5, Text-fig. 61.

2009. *Pseudosageceras multilobatum* Noetling - Shigeta and Zakharov, p. 140, Figs. 129-130.

Occurrence: A single specimen from sample Tu56.

Description: Oxycone, very involute shell (closed umbilicus) with narrow, bicarinate venter. Suture line complex with several adventitious lobes. Main lateral lobe trifid, others bifid.

Discussion: *Pseudosageceras multilobatum* is one of the most long-ranging and cosmopolitan ammonoid species of the Early Triassic. See Brayard and Bucher (2008) for a recent comprehensive study and a complete synonymy list for this species.

Pseudosageceras augustum (Brayard and Bucher, 2008)

Fig. 22(10-11)

v. 2008. *Hedenstroemia augusta* nov. sp. - Brayard and Bucher, p. 72, Pl. 39, Figs. 1-11, Text-fig. 63.

Occurrence: Samples Tu71 (2), TWA4 (1), (*Glyptophiceras sinuatum* beds), Tu82 (2) (*Procolumbites* beds [early Spathian]).

Description: Extremely involute, compressed oxyconic shell. Venter very narrow and weakly bicarinate. Umbilicus closed. Surface smooth. Suture line complex with several adventitious saddles and a long auxiliary series. Indentations of lobes poorly preserved.

Discussion: This species differs from true *Hedenstroemia* by its suture line with several adventitious saddles. Brayard and Bucher differentiated it from *Pseudosageceras multilobatum* on the basis of its apparently non-trifid main lateral lobe. However, an examination of the type material has revealed that the indentations of the lobes are rather poorly preserved and that the main lateral lobe could actually be trifid. Thus, this species is herein tentatively transferred to *Pseudosageceras*. The type species *P. multilobatum* differs by its different whorl section: its maximum width is located at the umbilicus, whereas on *P. augustus* it is located near mid-flanks. Moreover, juvenile specimens of *P. augustus* differ by their longitudinal line at mid-flank on, marking a very slight change in slope between umbilical and ventral portions of flanks (Brayard and Bucher, 2008). The Tulong section provides the first evidence that *P. augustus* crossed the Smithian-Spathian boundary.

Family ASPENITIDAE Spath, 1934

Type species: *Aspenites acutus* Hyatt and Smith 1905.

Aspenites acutus Hyatt and Smith 1905

Fig. 22(12-13)

1905. *Aspenites acutus* nov. sp. - Hyatt and Smith, 1905, p. 96, Pl. 2, Figs. 9-13; Pl. 3, Figs. 1-5.

v. 2008. *Aspenites acutus* Hyatt and Smith - Brayard and Bucher, p. 77, Pl. 42, Figs. 1-9.

Occurrence: Samples TuB5 (1), Tu16 (2) (*Brayardites compressus* beds).

Description: Extremely involute, very compressed shell with slightly convex flanks. Maximum whorl width at mid-flank. Venter lanceolate with an acute keel. Umbilicus probably occluded, but outer shell is not preserved. Umbilical region slightly depressed. Surface nearly smooth except for fine radial folds and falcoid growth lines. Suture line not preserved.

Discussion: *Aspenites acutus* is a relatively long-ranging species and is known from the early to the middle Smithian (Brayard and Bucher, 2008, Brühwiler et al., unpublished). See Brayard and Bucher (2008) for a recent comprehensive study and a complete synonymy list for this species.

Acknowledgements

W. Xiaoqiao (Beijing) and Li Guobiao (Lhasa) are thanked for facilitating field work in Tibet. Jim Jenks (Salt Lake City) is thanked for improving the English text. Technical support for preparation and photography was provided by Markus Hebeisen, Julia Huber, Leonie Pauli and Rosemarie Roth (Zürich). Claude Monnet (Zürich) is thanked for providing his statistical analyses software. Yasunari Shigeta (Tokyo) and Arnaud Brayard (Dijon) are thanked for their constructive reviews. This paper is a contribution to the Swiss National Science Foundation project 200020-113554 (to HB).

References

Arthaber, G., 1911. Die Trias von Albanien. Beiträge zur Paläontologie und Geologie Österreich-Ungarns und des Orients 24, 169-277.

Baud, A., Atudorei, V., Sharp, Z., 1996. Late Permian and Early Triassic evolution of the Northern Indian margin: Carbon isotope and sequence stratigraphy. Geodinamica Acta 9, 57-77.

Bhargava, O.N., Krystyn, L., Balini, M., Lein, R., Nicora, A., 2004. Revised litho- and sequence stratigraphy of the Spiti Triassic. Albertiana 30, 21-39.

Brayard, A., Brühwiler, T., Bucher, H., Jenks, J., 2009a. *Guodunites*, a low-palaeolatitude and trans-panthalassic Smithian (Early Triassic) ammonoid genus. Palaeontology 52, 471-481.

Brayard, A., Bucher, H., 2008. Smithian (Early Triassic) ammonoid faunas from northwestern Guangxi (South China): taxonomy and biochronology. Fossils and Strata 55, 1-179.

Brayard, A., Bucher, H., Escarguel, G., Fluteau, F., Bourquin, S., Galfetti, T., 2006. The Early Triassic ammonoid recovery: Paleoclimatic significance of diversity gradients. Palaeogeography, Palaeoclimatology, Palaeoecology 239, 374-395.

Brayard, A., Escarguel, G., Bucher, H., 2007. The biogeography of early Triassic ammonoid faunas: Clusters, gradients, and networks. Geobios 40, 749-765.

Brayard, A., Escarguel, G., Bucher, H., Brühwiler, T., 2009b. Smithian and Spathian (Early Triassic) ammonoid assemblages from terranes: Paleoceanographic and paleogeographic implications. Journal of Asian Earth Sciences 36, 420-433.

Brayard, A., Escarguel, G., Bucher, H., Monnet, C., Brühwiler, T., Goudemand, N., Galfetti, T., Guex, J., 2009c. Good Genes and Good Luck: Ammonoid Diversity and the End-Permian Mass Extinction. Science 325, 1118-1121.

Brühwiler, T., Bucher, H., Goudemand, N., Brayard, A., 2007. Smithian (Early Triassic) ammonoid faunas of the Tethys: new preliminary results from Tibet, India, Pakistan and Oman. New Mexico Museum of Natural History and Science Bulletin 41, 25-26.

Brühwiler, T., Goudemand, N., Galfetti, T., Bucher, H., Baud, A., Ware, D., Hermann, E., Hochuli, P.A., Martini, R., 2009. The Lower Triassic sedimentary and carbon isotope records from Tulong (South Tibet) and their significance for Tethyan palaeoceanography. Sedimentary Geology 222, 314-332.

Burg, J.P., 1983. Carte géologique du sud du Tibet / Ministère de la Géologie - Pékin (République Populaire de Chine); Contours synth. par J.P. Burg. China. Ministry of Geology and Mineral Resources, Paris.

Chao, K., 1959. Lower Triassic ammonoids from Western Kwangsi, China. Palaeontologia Sinica. New Series B 9, 355 pp.

Collignon, M., 1933-1934. Paléontologie de Madagascar XX - Les céphalopodes du Trias inférieur. Annales de Paléontologie 12-13, 151-162 & 1-43.

Collignon, M., 1973. Ammonites du Trias inférieur et moyen d'Afghanistan. Annales de Paléontologie (Invertebrés) 59, 127-163.

Cuvier, G., 1797. Tableau élémentaire de l'histoire naturelle des animaux. Baudouin, Paris.

Dagys, A.S., Ermakova, S.P., 1990. Early Olenekian Ammonoids of Siberia. Nauka, Moscow, 112 pp.

Diener, C., 1895. Triadische Cephalopodenfaunen der ostsibirischen Küstenprovinz. Mémoirs du Comité Géologique St. Petersburg 14, 1-59.

Diener, C., 1897. The Cephalopoda of the Lower Trias. Palaeontologia Indica, ser. 15, Himalayan Fossils 2, 1-181.

Diener, C., 1913. Triassic faunae of Kashmir. Palaeontologia Indica, n. ser. 5, 1-133.

Ermakova, S.P., 2002. Zonal standard of the Boreal Lower Triassic. Nauka, Moscow, 109 pp.

Frebold, H., 1930. Die Altersstellung des Fischhorizontes, des Grippianniveaus und des unteren Saurierhorizontes in Spitzbergen. Scrifter om Svalbard og Ishavet 28, 1-36.

Frech, F., 1902. Lethaea Geognostica, I. Lethaea Palaeozoica, v. 2 (4), Die Dyas (Schluss). 579-788.

Garzanti, E., Angiolini, L., Sciunnach, D., 1996. The Permian Kuling Group (Spiti, Lahaul and Zanskar; NW Himalaya): sedimentary evolution during rift/drift transition and initial opening of Neo-Tethys. Rivista Italiana di Paleontologia Stratigrafia 102, 175-200.

Garzanti, E., Nicora, A., Rettori, R., 1998. Permo-Triassic boundary and lower to middle Triassic in South Tibet. Journal of Asian Earth Sciences 16, 143-157.

Garzanti, E., Sciunnach, D., 1997. Early Carboniferous onset of Gondwanian glaciation and Neo-Tethyan rifting in Southern Tibet. Earth Planetary Science Letters 148, 359-365.

Guex, J., 1978. Le Trias inferieur des Salt Ranges, Pakistan; problemes biochronologiques. Eclogae Geologicae Helvetiae 71, 105-141.

Hada, S., 1966. Discovery of Early Triassic ammonoids from Gua Musang, Kelantan, Malaya. Journal of Geosciences, Osaka University 9, 111-121.

Hyatt, 1884. Genera of fossil cephalopods. Proceedings of the Boston Society of Natural History 22, 253-338.

Hyatt, A., 1900. Cephalopoda. In: K.A.v. Zittel (Editor), Textbook of palaeontology, vol. 1, 1st English ed. Eastman, C. R. London.

Hyatt, A., Smith, J.P., 1905. Triassic cephalopod genera of America. U. S. Geological Survey Professional Paper 40, 1-394.

Jenks, J., 2007. Smithian (Early Triassic) ammonoid biostratigraphy at Crittenden Springs, Elko County, Nevada and a new ammonoid from the *Meekoceras gracilitatis* zone. New Mexico Museum of Natural History and Science Bulletin 40, 81-90.

Khuc, V., 1984. Triassic ammonoids in Vietnam. Geoinform and Geodata Institute, Hanoi, Vietnam, 134 pp.

Kiparisova, L.D., Popov, Y.D., 1956. Subdivision of the lower series of the Triassic System into stages. Doklady Akad. Nauk SSSR 109, 842-845.

Korchinskaya, M.V., 1982. Explanatory note on the biostratigraphic scheme of the Mesozoic (Trias) of Spitsbergen. USSR Ministry of Geology, PGO Sevmorgeologia, 40-99.

Krafft, A.v., Diener, C., 1909. Lower Triassic cephalopoda from Spiti, Malla Johar, and Byans. Palaeontologia Indica, ser. 15, 6, 1-186.

Krystyn, L., Bhargava, O.N., Richoz, S., 2007a. A candidate GSSP for the base of the Olenekian Stage: Mud at Pin Valley; district Lahul & Spiti, Himachal Pradesh (Western Himalaya), India. Albertiana 35, 5-29.

Krystyn, L., Richoz, S., Bhargava, O.N., 2007b. The Induan-Olenekian Boundary (IOB) in Mud – an update of the candidate GSSP section M04. Albertiana 36, 33-45.

Kummel, B., 1968a. Additional Scythian Ammonoids from Afghanistan. Bulletin of the Museum of Comparative Zoology, Harvard University 136, 483-509.

Kummel, B., 1968b. Scythian ammonoids from Timor. Breviora 283, 1-21.

Kummel, B., Erben, H.K., 1968. Lower and Middle Triassic cephalopods from Afghanistan. Palaeontographica, Abt. A 129, 95-148.

Kummel, B., Steele, G., 1962. Ammonites from the *Meekoceras gracilitatus* Zone at Crittenden Spring, Elko County, Nevada. Journal of Paleontology 36, 638-703.

Liu, G., 1992. Permian to Eocene sediments and Indian passive margin evolution in the Tibetan Himalayas. Tübinger Geowissenschaftliche Arbeiten, Reihe A 13, 1-268.

Liu, G., Einsele, G., 1994. Sedimentary history of the Tethyan basin in the Tibetan Himalayas. Geologische Rundschau 83, 32-61.

Marcoux, J., Baud, A., 1996. Late Permian to Late Triassic Tethyan paleoenvironments. Three snapshots: Late Murgabian, Late Anisian, Late Norian. In: X. Nairn, L.E. Ricou, B. Vrielynck and J. Dercourt (Eds.), The Tethys Ocean. The Ocean Basins and Margins. Plenum Press, New York, pp. 153-190.

Markevich, P.V., Zakharov, Y., 2004. [Triassic and Jurassic of the Sikhote-Alin], 420 pp. Dalnauka, Vladivostok, Russia. (In Russian with English summary).

Mathews, A.A.L., 1929. The Lower Triassic cephalopod fauna of the Fort Douglas area, Utah. Walker Museum Memoirs 1, 1-46.

Noetling, F., 1905. Die asiatische Trias. In: F. Frech (Editor), Lethaea geognostica: Handbuch der Erdgeschichte mit Abbildungen der für die Formationen bezeichnendsten Versteinerungen. Schweizerbart, Stuttgart, pp. 107-221.

Ogg, J.G., von Rad, U., 1994. The Triassic of the Thakkola (Nepal). II: Paleolatitudes and Comparison with other Eastern Tethyan Margins of Gondwana. Geologische Rundschau 83, 107-129.

Orchard, M.J., 2007. Conodont diversity and evolution through the latest Permian and Early Triassic upheavals. Palaeogeography, Palaeoclimatology, Palaeoecology 252, 93-117.

Raup, D.M., Sepkoski, J.J., 1982. Mass Extinctions in the Marine Fossil Record. Science 215, 1501-1503.

Ricou, L.E., 1996. The plate tectonic history of the past Tethys ocean. In: X. Nairn, L.E. Ricou, B. Vrielynck and J. Dercourt (Eds.), The Tethys Ocean. The Ocean Basins and Margins. Plenum Press, New York, pp. 3-70.

Shen, S.Z., Cao, C.Q., Henderson, C.M., Wang, X.D., Shi, G.R., Wang, Y., Wang, W., 2006. End-Permian mass extinction pattern in the northern peri-Gondwanan region. Palaeoworld 15, 3-30.

Shevyrev, A.A., 1968. Triassic ammonoidea from the southern part of the USSR. Transactions of the Palaeontological Institute 119. Nauka, Moscow, 272 pp.

Shevyrev, A.A., 2001. Ammonite zonation and interregional correlation of the Induan stage. Stratigraphy and Geological Correlation 9, 473-482.

Shigeta, Y., Maeda., H., Yokoyama, K., Zakharov, Y., 2009a. Paleogeographical and geological setting. In: Y. Shigeta, Y. Zakharov, H. Maeda and A.M. Popov (Eds.), The Lower Triassic system in the Abrek Bay area, South Primorye, Russia. National Museum of Nature and Science Monographs 38, Tokyo, 3-4.

Shigeta, Y., Maeda., H., Zakharov, Y., 2009b. Biostratigraphy: ammonoid succession. In: Y. Shigeta, Y. Zakharov, H. Maeda and A.M. Popov (Eds.), The Lower Triassic system in the Abrek Bay area, South Primorye, Russia. National Museum of Nature and Science Monographs 38, Tokyo, 24-27.

Shigeta, Y., Zakharov, Y., 2009. Systematic paleontology: cephalopods. In: Y. Shigeta, Y. Zakharov, H. Maeda and A.M. Popov (Eds.), The Lower Triassic system in the Abrek Bay area, South Primorye, Russia. National Museum of Nature and Science Monographs 38, Tokyo, 44-140.

Silberling, N.J., Tozer, E.T., 1968. Biostratigraphic classification of the marine Triassic in North America. Special Paper - Geological Society of America, 110. Geological Society of America (GSA), Boulder, CO, United States, 63 pp.

Smith, J.P., 1932. Lower Triassic ammonoids of North America. U. S. Geological Survey Professional Paper 167, 1-199.

Spath, 1930. The Eotriassic invertebrate fauna of East Greenland. Meddelelser om Grønland 83.

Spath, L.F., 1934. Part 4: The ammonoidea of the Trias, Catalogue of the fossil cephalopoda in the British Museum (Natural History). The Trustees of the British Museum, London, 521 pp.

Stampfli, G., Marcoux, J., Baud, A., 1991. Tethyan Margins in Space and Time. Palaeogeography, Palaeoclimatology, Palaeoecology 87, 373-409.

Tozer, E.T., 1961. Triassic stratigraphy and faunas, Queen Elizabeth Islands, Arctic Archipelago. Geologic Survey of Canada, Memoir 316, 116 pp.

Tozer, E.T., 1965. Lower Triassic stages and ammonoid zones of Arctic Canada. Geologic Survey of Canada Paper 65-12, 14 pp.

Tozer, E.T., 1967. A standard for Triassic time. Geologic Survey of Canada Bulletin 156, 141 pp.

Tozer, E.T., 1969. Xenodiscaceaen ammonoids and their bearing on the discrimination of the Permo-Triassic boundary. Geological Magazine, 106, 348-361.

Tozer, E.T., 1971. Triassic time and ammonoids. Canadian Journal of Earth Sciences 8, 989-1031.

Tozer, E.T., 1981. Triassic Ammonoidea; classification, evolution and relationship with Permian and Jurassic forms. In: M.R. House and J.R. Senior (Eds.), The Ammonoidea; the evolution, classification, mode of life and geological usefulness of a major fossil group. Systematics Association Special Volume. Academic Press [for the] Systematics Association, London-New York, International, pp. 65-100.

Tozer, E.T., 1994. Canadian Triassic ammonoid faunas. Bulletin - Geological Survey of Canada. Geological Survey of Canada, Ottawa, ON, Canada, 663 pp.

Trümpy, R., 1969. Lower Triassic ammonites from Jameson Land (East Greenland). Meddelelser om Grønland 168.

Waagen, W., 1895. Salt-Range fossils. Vol 2: Fossils from the Ceratite Formation. Palaeontologia Indica 13, 1-323.

Wang, Y.G., He, G.X., 1976. Triassic ammonoids from the Mount Jolmo Lungma region, A report of scientific expedition in the Mount Jolmo Lungma region (1966-1968). Palaeontology, fasc. 3 (in Chinese).

Weitschat, W., Lehmann, U., 1978. Biostratigraphy of the uppermost part of the Smithian Stage (Lower Triassic) at the Botneheia, W-Spitsbergen. Mitteilungen aus dem Geologisch-Paläontologischen Institut der Universität Hamburg 54, 27-54.

Welter, O.A., 1922. Die Ammoniten der unteren Trias von Timor. Paläontologie von Timor 11, 83-154.

Yokoyama, K., Shigeta, Y., Tsutsumi, Y., 2009a. Age distribution of detrital monazites in the sandstone. In: Y. Shigeta, Y. Zakharov, H. Maeda and A.M. Popov (Eds.), The Lower Triassic system in the Abrek Bay area, South Primorye, Russia. National Museum of Nature and Science Monographs 38, Tokyo, 30-34.

Yokoyama, K., Shigeta, Y., Tsutsumi, Y., 2009b. Age data of monazites. In: Y. Shigeta, Y. Zakharov, H. Maeda and A.M. Popov (Eds.), The Lower Triassic system in the Abrek Bay area, South Primorye, Russia. National Museum of Nature and Science Monographs 38, Tokyo, 34-36.

Zakharov, Y.D., 1968. Biostratigraphiya i amonoidei nizhnego triasa Yuzhnogo Primorya [Lower

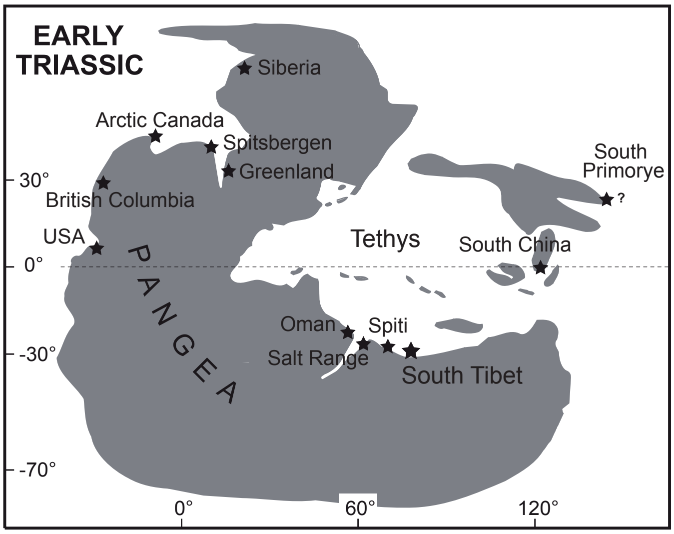

Fig. 1. Simplified Early Triassic palaeogeography (modified after Brayard et al., 2006, 2009b; Shigeta et al., 2009a) with the position of South Tibet and other localities mentioned in the text.

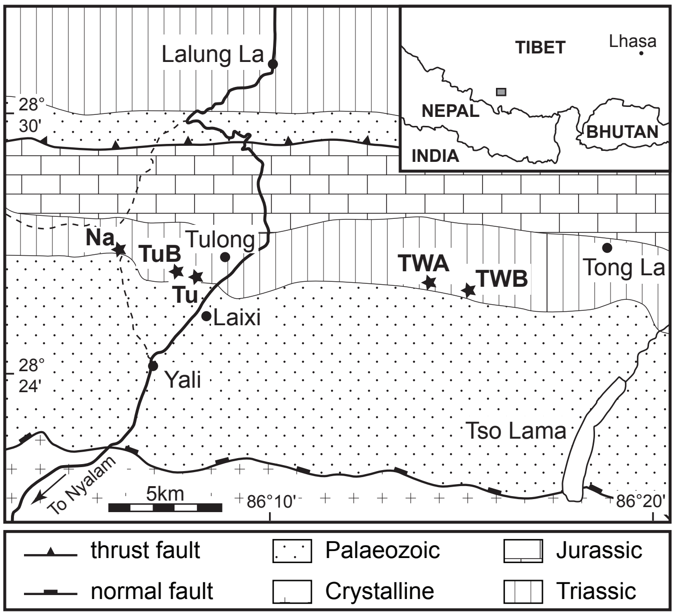

Fig. 2. Geological sketch map of the study area (modified after Burg, 1983) and location of studied sections.

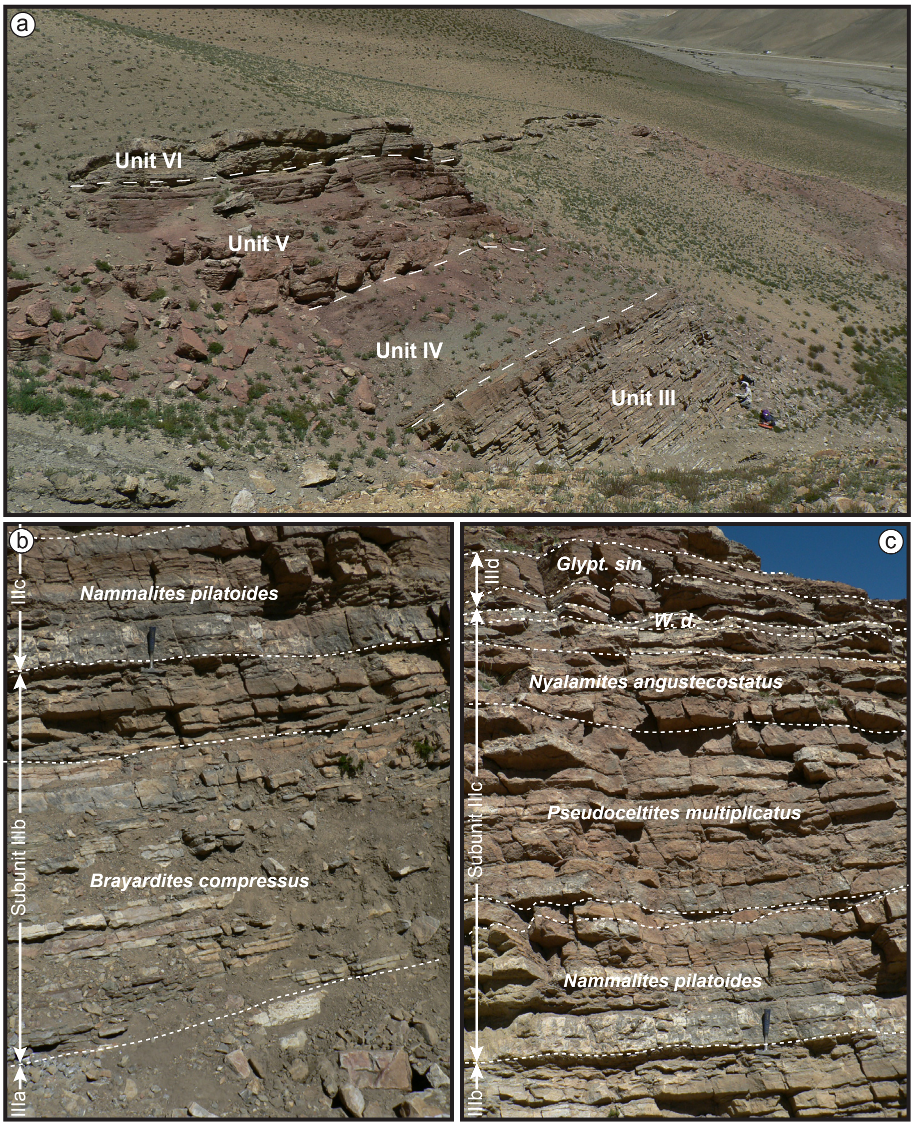

Fig. 3. (a) Classical section (Tu) near the village of Tulong, with lithologic units (Brühwiler et al., 2009). (b) Subunits IIIb and IIIc, with stratigraphic positions of ammonoid faunas. (c) Subunits IIIc and IIId, with stratigraphic positions of ammonoid faunas. Abbreviations: *W. d. Wasatchites distractus; Glypt. sin. Glyptophiceras sinuatum.* Hammer (28 cm in length) for scale.

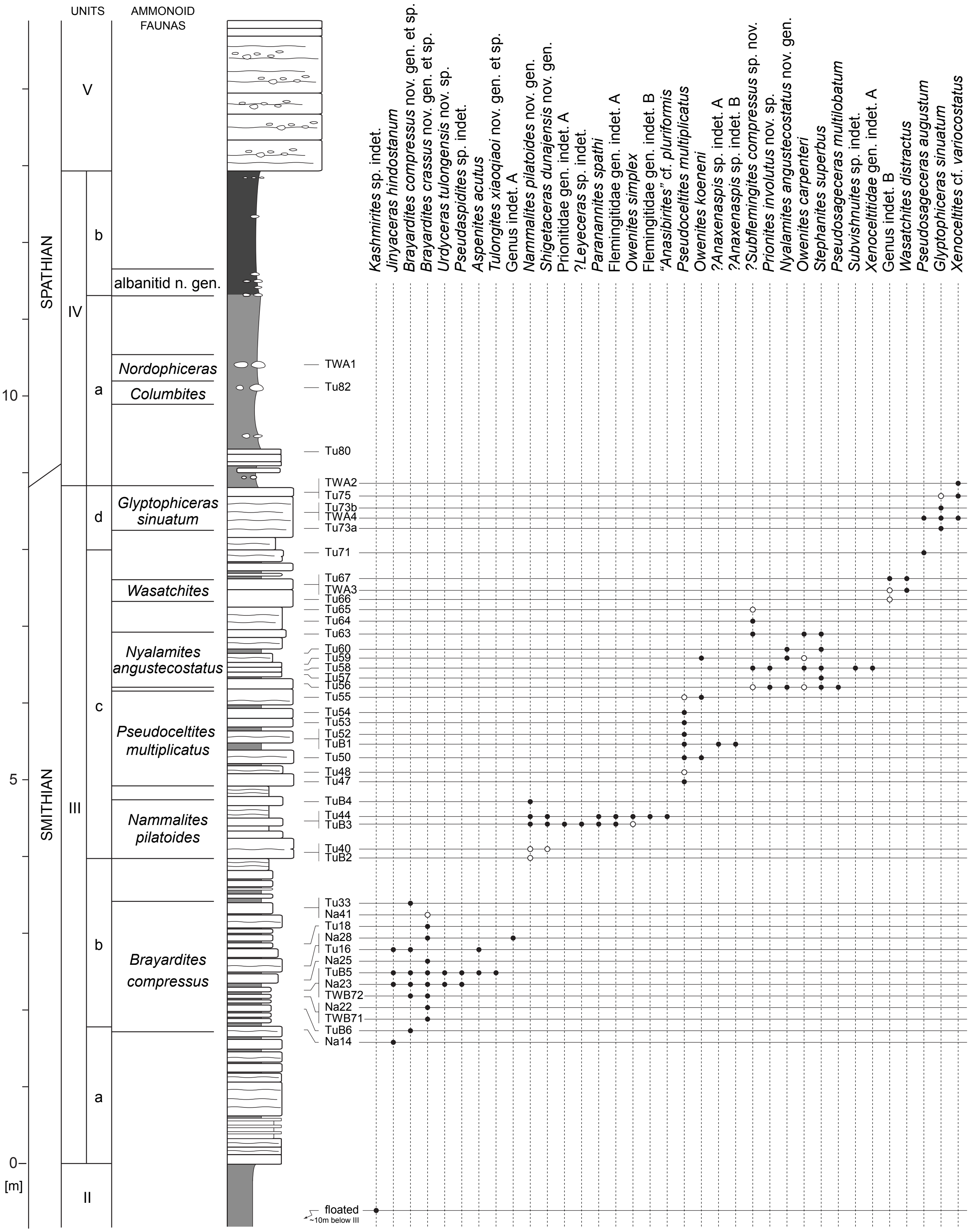
UNITS
AMMONOID FAUNAS
SPATHIAN
SMITHIAN
V
IV
III
II
a
b
c
d
10
5
0
[m]
albanitid n. gen.
Nordophiceras
Columbites
Glyptophiceras sinuatum
Wasatchites
Nyalamites angustecostatus
Pseudoceltites multiplicatus
Nammalites pilatoides
Brayardites compressus
TWA1
Tu82
Tu80
TWA2
Tu75
Tu73b
TWA4
Tu73a
Tu71
Tu67
TWA3
Tu66
Tu65
Tu64
Tu63
Tu60
Tu59
Tu58
Tu57
Tu56
Tu55
Tu54
Tu53
Tu52
TuB1
Tu50
Tu48
Tu47
TuB4
Tu44
TuB3
Tu40
TuB2
Tu33
Na41
Tu18
Na28
Tu16
Na25
TuB5
Na23
TWB72
Na22
TWB71
TuB6
Na14
floated
~10m below III
Kashmirites sp. indet.
Jinyaceras hindostanum
Brayardites compressus nov. gen. et sp.
Brayardites crassus nov. gen. et sp.
Urdyceras tulongensis nov. sp.
Pseudaspidites sp. indet.
Aspenites acutus
Tulongites xiaoqiaoi nov. gen. et sp.
Genus indet. A
Nammalites pilatoides nov. gen.
Shigetaceras dunajensis nov. gen.
Prionitidae gen. indet. A
?Leyeceras sp. indet.
Parannanites spathi
Flemingitidae gen. indet. A
Owenites simplex
Flemingitidae gen. indet. B
“Anasibirites” cf. pluriformis
Pseudoceltites multiplicatus
Owenites koeneni
?Anaxenaspis sp. indet. A
?Anaxenaspis sp. indet. B
?Subflemingites compressus sp. nov.
Prionites involutus nov. sp.
Nyalamites angustecostatus nov. gen.
Owenites carpenteri
Stephanites superbus
Pseudosageceras multilobatum
Subvishnuites sp. indet.
Xenoceltitidae gen. indet. A
Genus indet. B
Wasatchites distractus
Pseudosageceras augustum
Glyptophiceras sinuatum
Xenoceltites cf. variocostatus

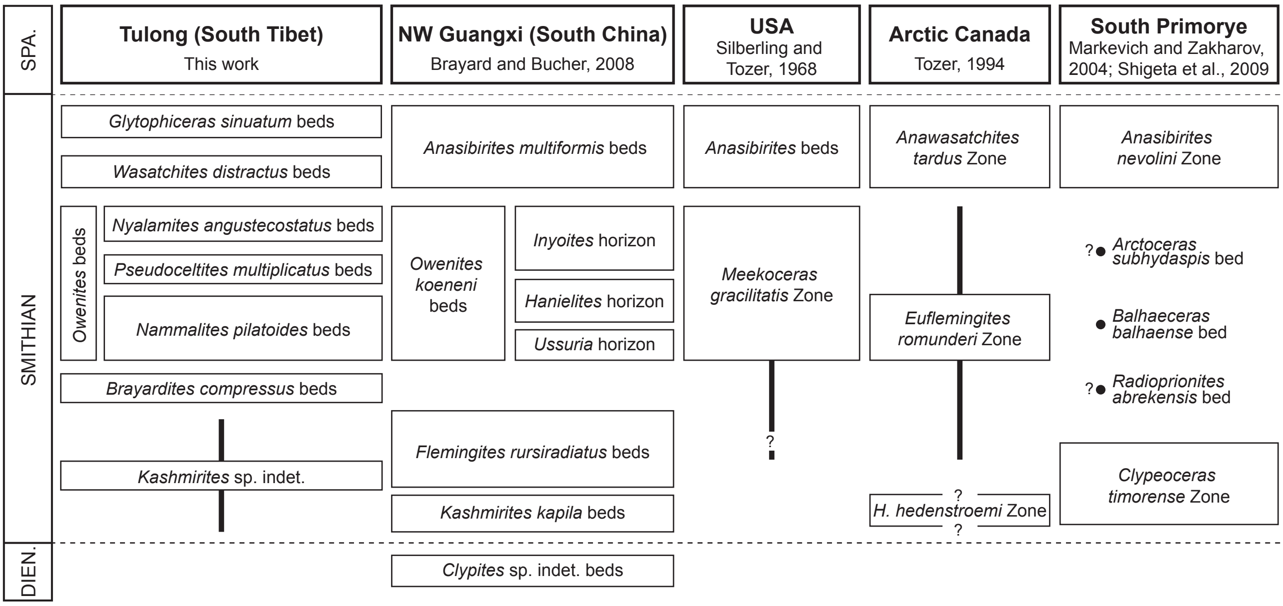

Fig. 5. Biostratigraphical subdivisions of the Smithian of South Tibet and correlation with zonations of other regions. See text for discussion. Three middle Smithian ammonoid faunas (*Nammalites pilatoides*, *Pseudoceltites multiplicatus* and *Nyalamites angustecostatus* beds) from Tulong are grouped together as equivalent of *Owenites* beds.

Fig. 4. Composite section of the Smithian to Early Spathian of the Tulong area showing distribution of ammonoid faunas. Lithostratigraphic subdivisions after Brühwiler et al. (2009).

Fig. 6. **1-7**. *Pseudoceltites multiplicatus* Waagen, 1895; **1a-c**, PIMUZ 27595, sample TuB1; **2a-b**, PIMUZ 27596, sample TuB1; **3a-c**, PIMUZ 27597, sample TuB1; **4a-c**, PIMUZ 27598, sample TuB1; **5a-e**, PIMUZ 27599, sample Tu50, 5e ×1.5; **6a-c**, PIMUZ 27600, sample TuB1; **7a-c**, PIMUZ 27601, sample TuB1. **8a-c**. *"Anasibirites"* cf. *pluriformis* Guex, 1978; PIMUZ 27602, sample Tu44. **9a-d**. *Kashmirites* sp. indet, PIMUZ 27603, found as float in Unit II. All natural size unless otherwise indicated.

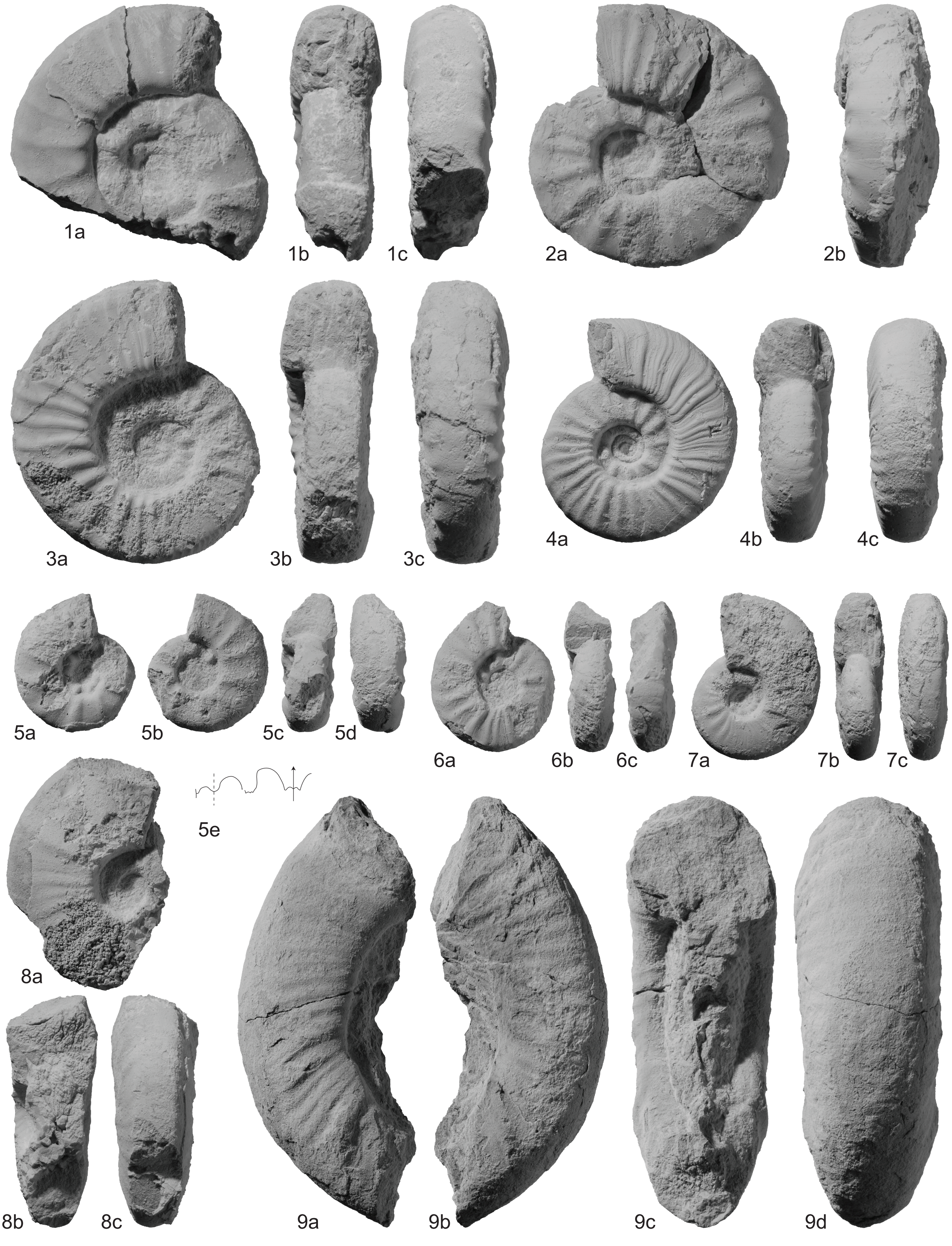
1a
1b
1c
2a
2b
3a
3b
3c
4a
4b
4c
5a
5b
5c
5d
6a
6b
6c
7a
7b
7c
5e
8a
8b
8c
9a
9b
9c
9d

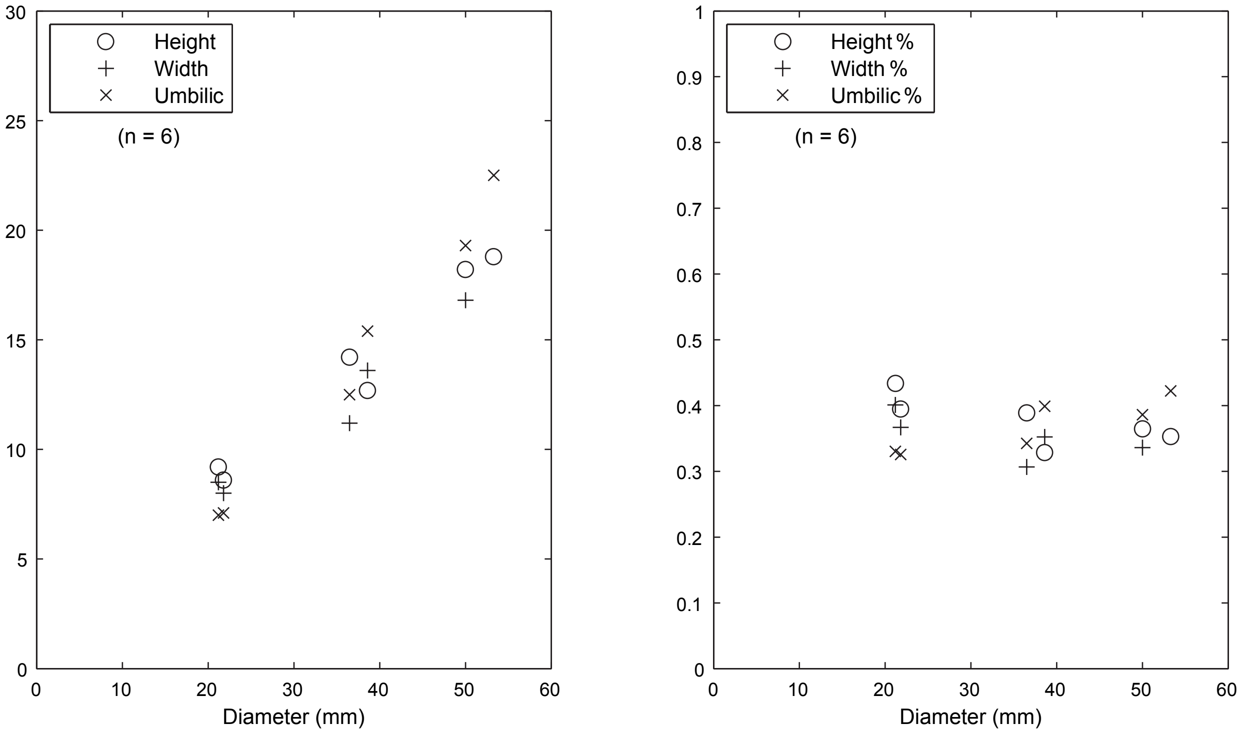

Fig. 7. Scatter diagram of H, W, and U, and of H/D, W/D, and U/D for *Pseudoceltites multiplicatus* Waagen, 1895.

Fig. 8. **1-7**. *Glyptophiceras sinuatum* (Waagen, 1895); **1a-e**, PIMUZ 27604, sample TWA4, 1e ×1.5; **2a-b**, PIMUZ 27605, sample Tu73a; **3a-d**, PIMUZ 27606, sample TWA4; **4a-c**, PIMUZ 27607, sample TWA4; **5a-d**, PIMUZ 27608, sample Tu75; **6a-c**, PIMUZ 27609, sample Tu73b; **7a-c**, PIMUZ 27610, sample TWA4. **8-9**. Xenoceltitidae gen. indet. A; **8a-d**, PIMUZ 27611, sample Tu58; **9a-e**, PIMUZ 27612, sample Tu58, 9e ×1.5. All natural size unless otherwise indicated.

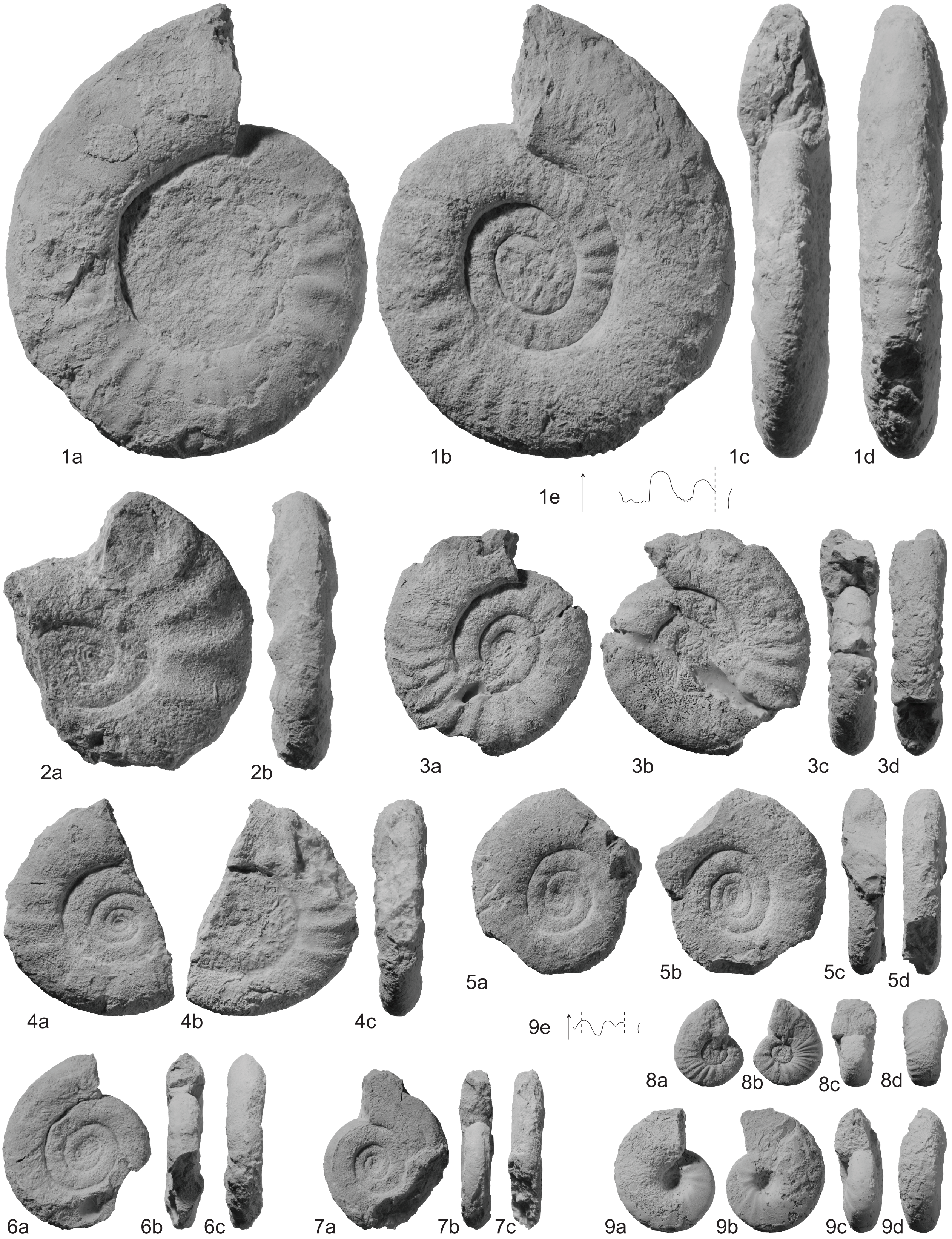
1a
1b
1c
1d
1e
2a
2b
3a
3b
3c
3d
4a
4b
4c
5a
5b
5c
5d
9e
8a
8b
8c
8d
6a
6b
6c
7a
7b
7c
9a
9b
9c
9d

Fig. 9. **1-2**. *Xenoceltites* cf. *variocostatus* Brayard and Bucher, 2008; **1a-e**, PIMUZ 27613, sample TWA4, 1e ×1.5; **2a-c**, PIMUZ 27614, sample Tu75. **3-5**. *Nyalamites angustecostatus* (Welter, 1922). **3a-e**, PIMUZ 27615, sample Tu56, 3e ×1.5; **4a-b**, PIMUZ 27616, sample Tu56; **5a-b**, PIMUZ 27617, sample Tu56. **6-7**. Genus indet. A; **6a-e**, PIMUZ 27618, sample Na28, 6e ×2; **7a-e**, PIMUZ 27619, sample Na28, 7e ×2. **8a-b**. ?*Leyeceras* sp. indet., PIMUZ 27620, sample TuB3, ×0.5. **9-10**. *Tulongites xiaoqiaoi* nov. gen. et sp.; **9a-e**, PIMUZ 27621, sample TuB5, 9e ×1.5. **10a-d**, PIMUZ 27622, sample TuB5. **11a-e**. *Pseudaspidites* sp. indet., PIMUZ 27623, sample TuB5. All natural size unless otherwise indicated.

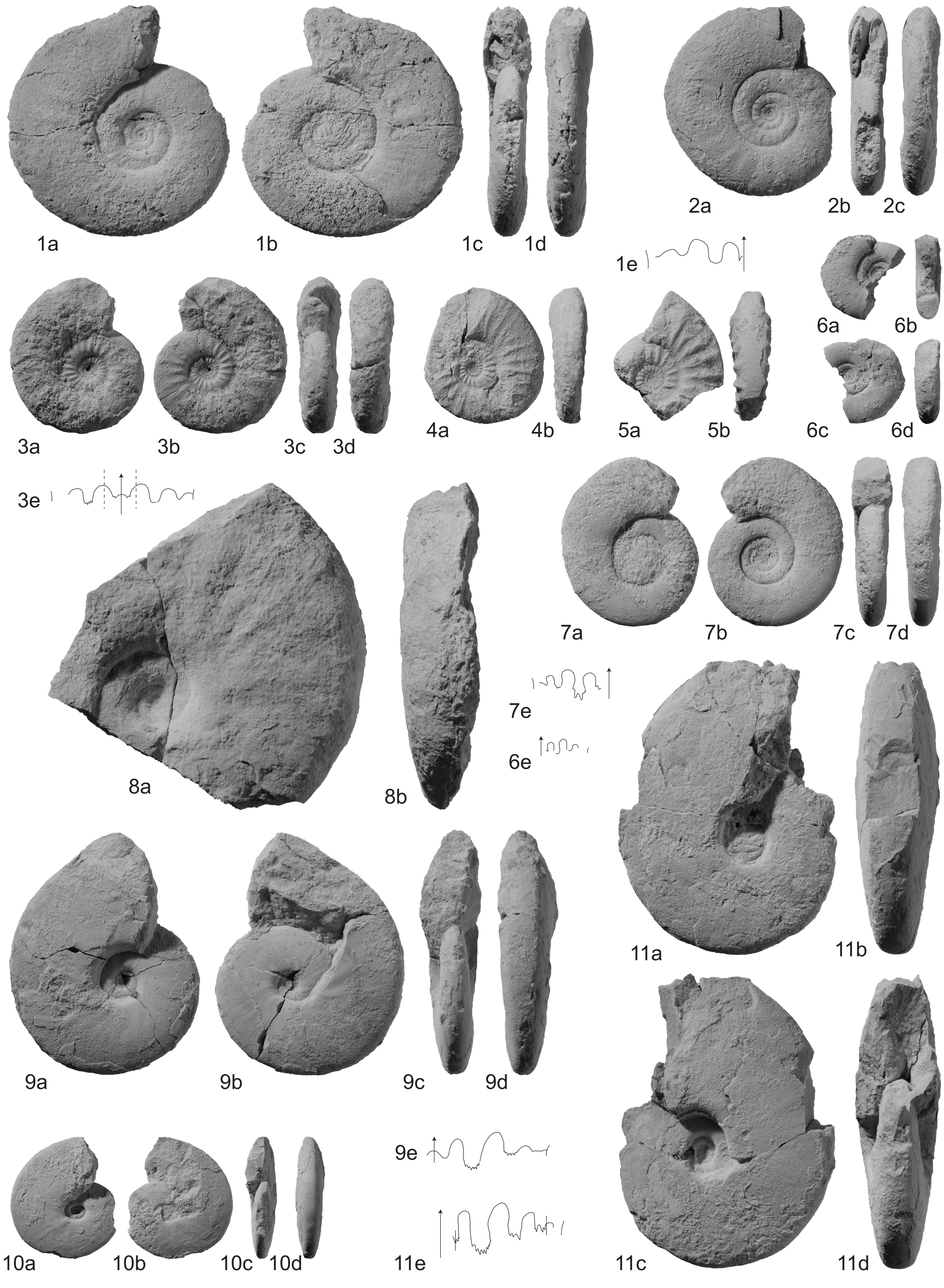
1a
1b
1c
1d
1e
2a
2b
2c
3a
3b
3c
3d
3e
4a
4b
5a
5b
6a
6b
6c
6d
6e
7a
7b
7c
7d
7e
8a
8b
9a
9b
9c
9d
9e
10a
10b
10c
10d
11a
11b
11c
11d
11e

Fig. 10. **1-6**. ?*Subflemingites compressus* nov. sp.; **1a-d**, PIMUZ 27624, sample Tu58, 1d ×1.5; **2a-d**, PIMUZ 27625, sample Tu58, 2d ×1.5; **3a-c**, PIMUZ 27628, sample Tu58; **4a-d**, PIMUZ 27627, sample Tu58; **5a-d**, PIMUZ 27626, sample Tu58; **6a-c**, PIMUZ 27629, sample Tu63. **7-8.** Flemingitidae gen. indet. A; **7a-c**, PIMUZ 27630, sample TuB3; **8a-d**, PIMUZ 27631, sample Tu44, 8d ×1.5. All natural size unless otherwise indicated.


1a 1b 1c

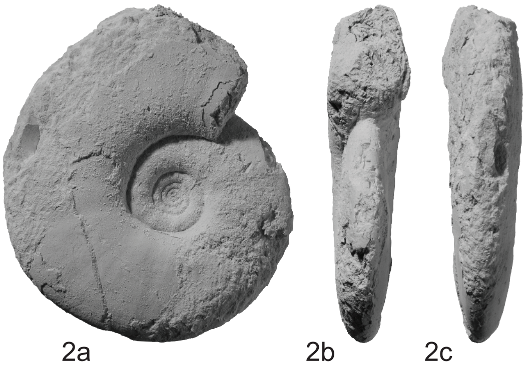
2a 2b 2c


1d


2d

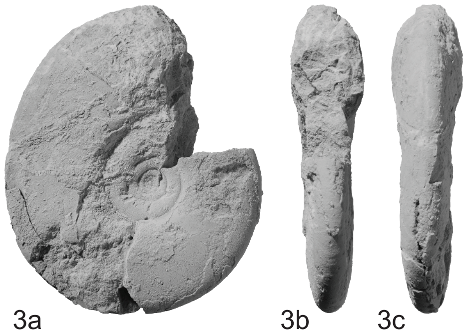
3a 3b 3c


4a 4b 4c 4d


5a 5b 5c 5d


6a 6b 6c


7a 7b 7c


8d

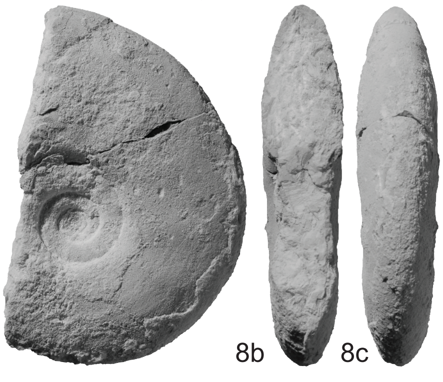
8a 8b 8c

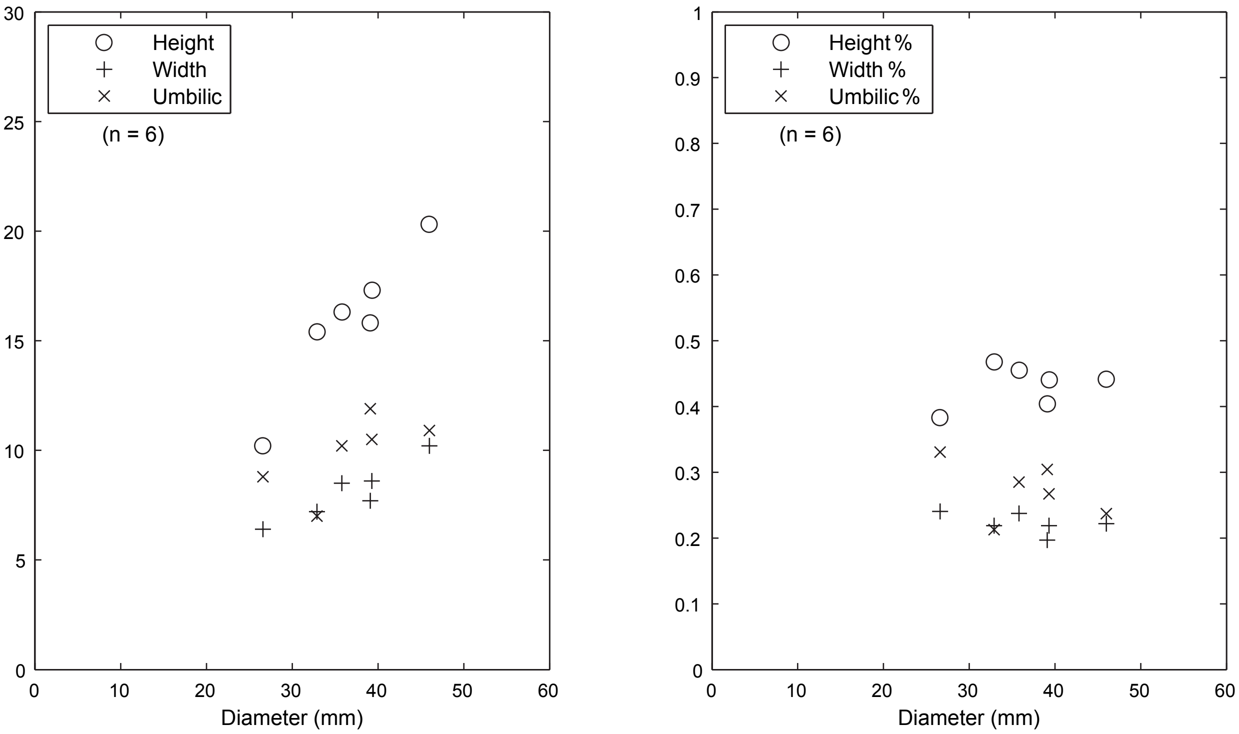

Fig. 11. Scatter diagram of H, W, and U, and of H/D, W/D, and U/D for ?*Subflemingites compressus* nov. sp.

Fig. 12. **1a-c**. *?Anaxenaspis* sp. indet. A, PIMUZ 27632, sample TuB1, ×0.85. **2a-c**. Flemingitidae gen. indet. B, PIMUZ 27633, sample Tu44. **3-7**. *?Anaxenaspis* sp. indet. B; **3**, PIMUZ 27634, sample TuB1; **4a-d**, PIMUZ 27635, sample TuB1; **5a-c**, PIMUZ 27636, sample TuB1; **6a-d**, PIMUZ 27637, sample TuB1; **7a-c**, PIMUZ 27638, sample TuB1. All natural size unless otherwise indicated.

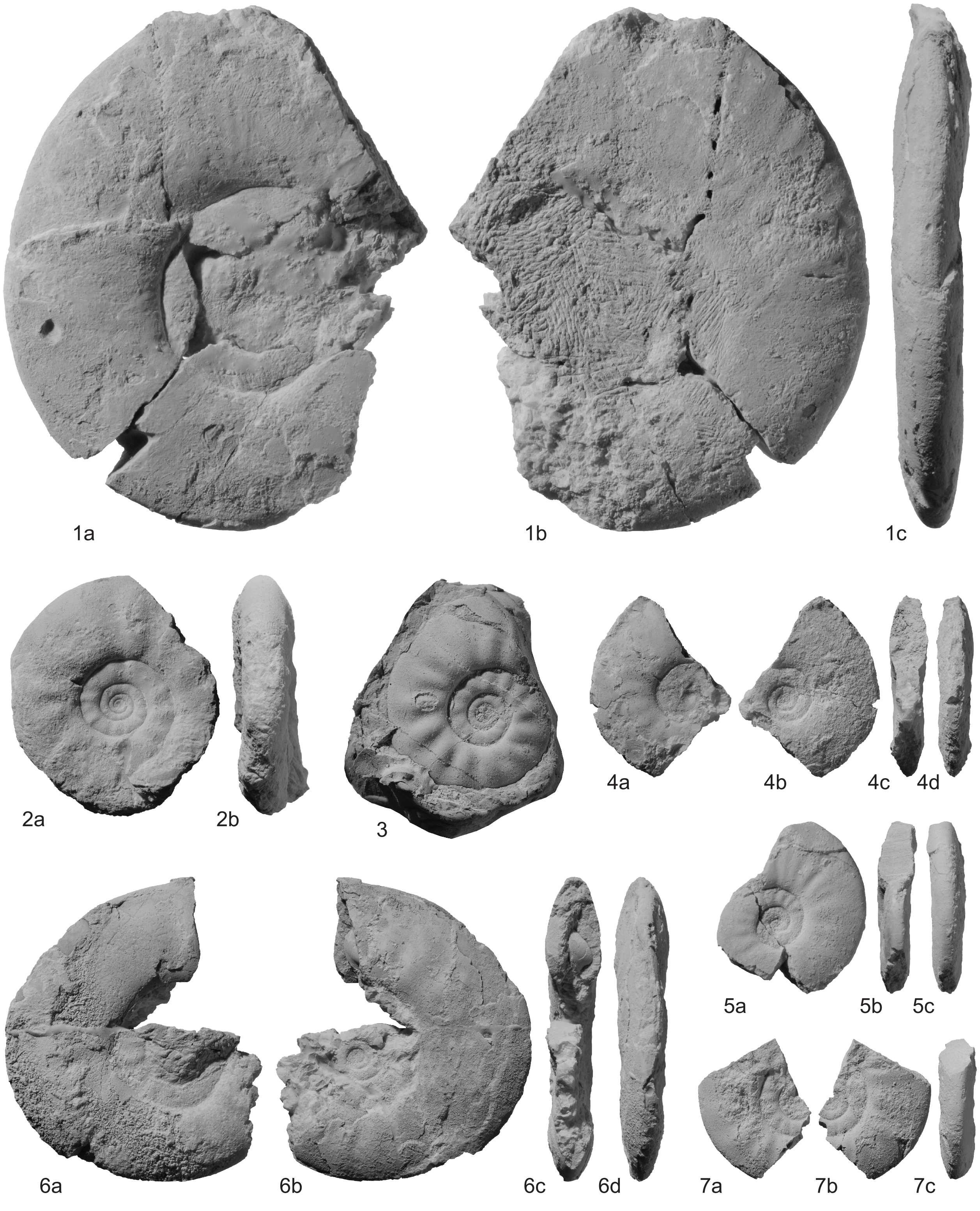
1a
1b
1c
2a
2b
3
4a
4b
4c
4d
5a
5b
5c
6a
6b
6c
6d
7a
7b
7c

Fig. 13. **1-4**. *Shigetaceras dunajensis* nov. gen.; **1a-d**, PIMUZ 27639, sample Tu44; **2a-c**, PIMUZ 27640, sample Tu44; **3a-d**, PIMUZ 27641, sample TuB3; **4a-b**, PIMUZ 27642, sample Tu44. **5-11**. *Urdyceras tulongensis* nov. sp.; **5a-b**, PIMUZ 27643, sample TuB5; **6a-e**, PIMUZ 27644, sample TuB5, 6e ×2; **7a-e**, PIMUZ 27645, sample TuB5, 7e ×2; **8a-c**, PIMUZ 27646, sample TuB5; **9a-e**, PIMUZ 27647, sample Na23, 9e ×2; **10a-d**, PIMUZ 27648, sample TuB5. **11a-e**, PIMUZ 27649, sample TuB5, 11e ×2. All natural size unless otherwise indicated.

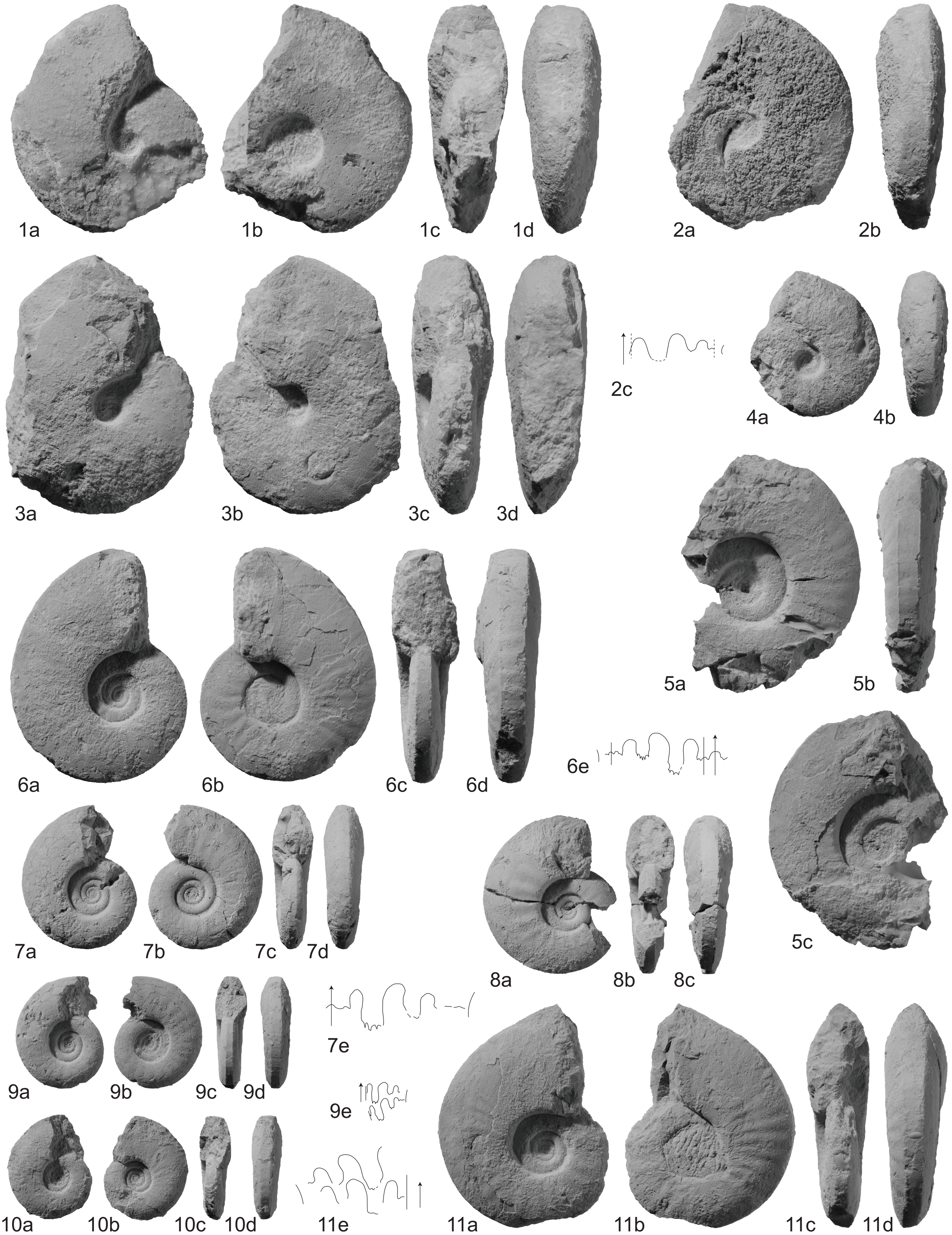
1a
1b
1c
1d
2a
2b
2c
3a
3b
3c
3d
4a
4b
5a
5b
5c
6a
6b
6c
6d
6e
7a
7b
7c
7d
7e
8a
8b
8c
9a
9b
9c
9d
9e
10a
10b
10c
10d
11e
11a
11b
11c
11d

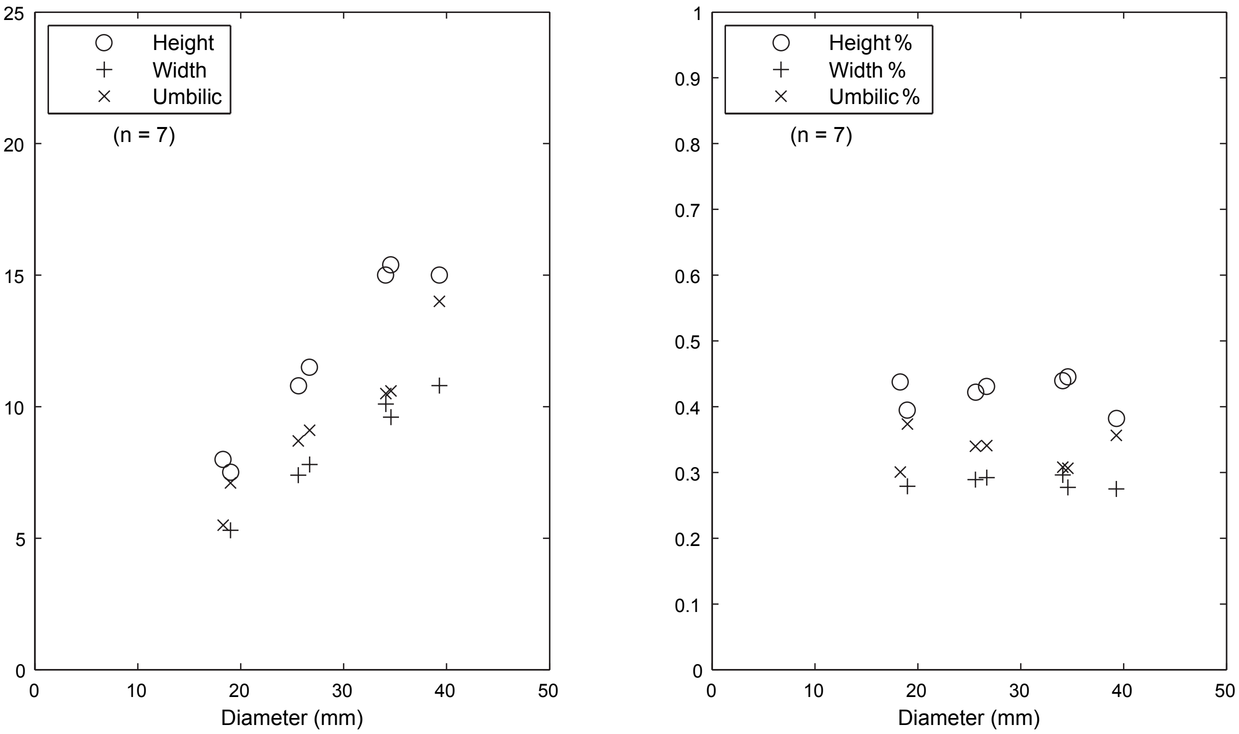

Fig. 14. Scatter diagram of H, W, and U, and of H/D, W/D, and U/D for *Urdyceras tulongensis* nov. sp.

Fig. 15. **1-4**. *Brayardites crassus* nov. gen. et sp.; **1a-d**, PIMUZ 27650, sample Na28; **2a-d**, PIMUZ 27651, sample TWB71; **3a-d**, PIMUZ 27652, sample TuB5; **4a-c**, PIMUZ 27653, sample TuB5. All natural size.

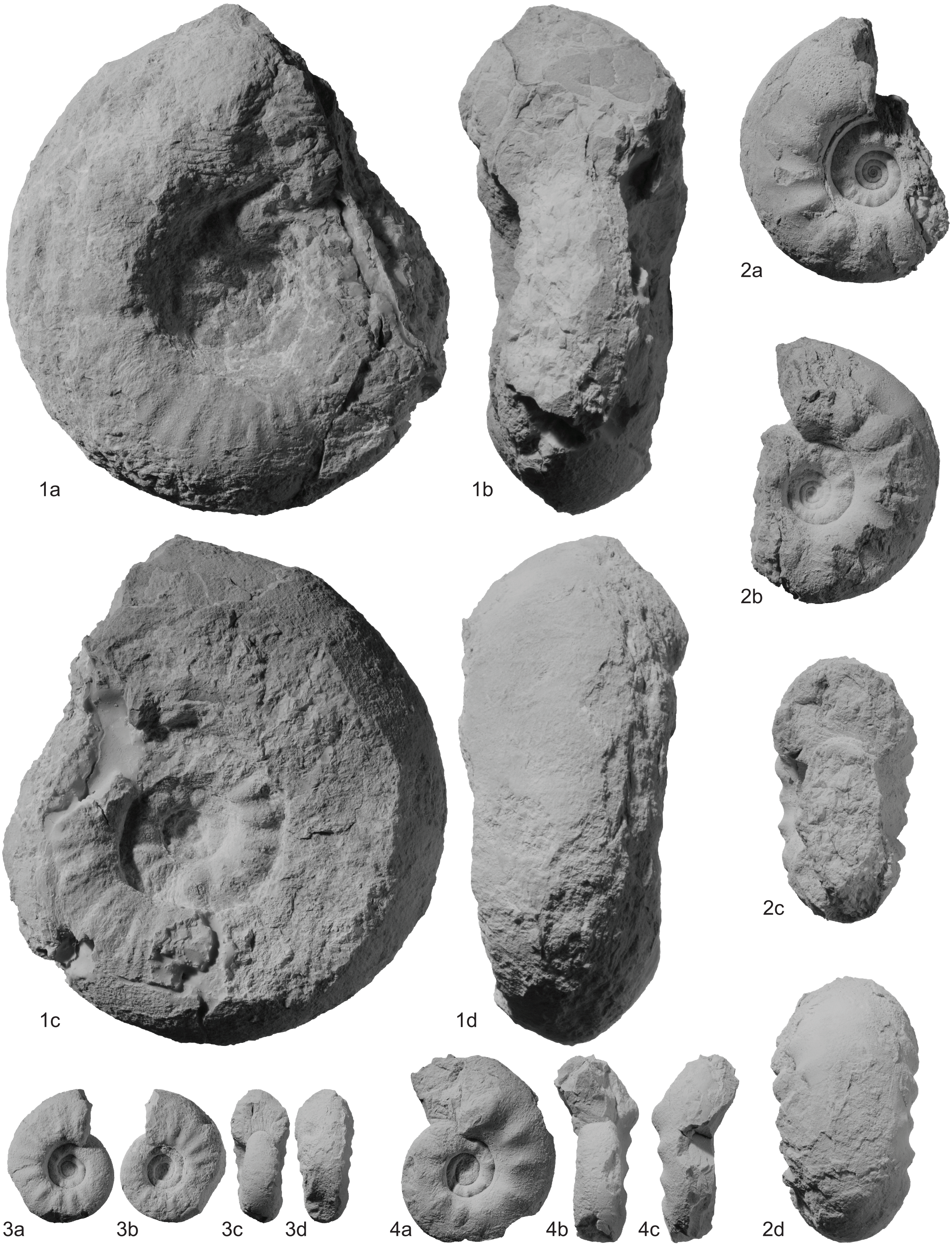
1a
1b
2a
2b
2c
1c
1d
3a
3b
3c
3d
4a
4b
4c
2d

Fig. 16. **1-6**. *Brayardites crassus* nov. gen. et sp.; **1a-d**, PIMUZ 27654, sample TuB5; **2a-e**, PIMUZ 27655, sample TuB5, 2e ×1.5; **3a-e**, PIMUZ 27656, sample Na23, 3e ×1.5; **4a-d**, PIMUZ 27657, sample TuB5; **5a-d**, PIMUZ 27658, sample TuB5; **6a-d**, PIMUZ 27659, sample TuB5. All natural size unless otherwise indicated.


1a


1b


2a


1c


1d


2b


3a


3b


3c


3d

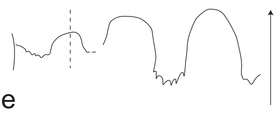
2e


3e


2c


2d


4a


4b


4c


4d


5a


5b


5c


5d


6a


6b


6c


6d

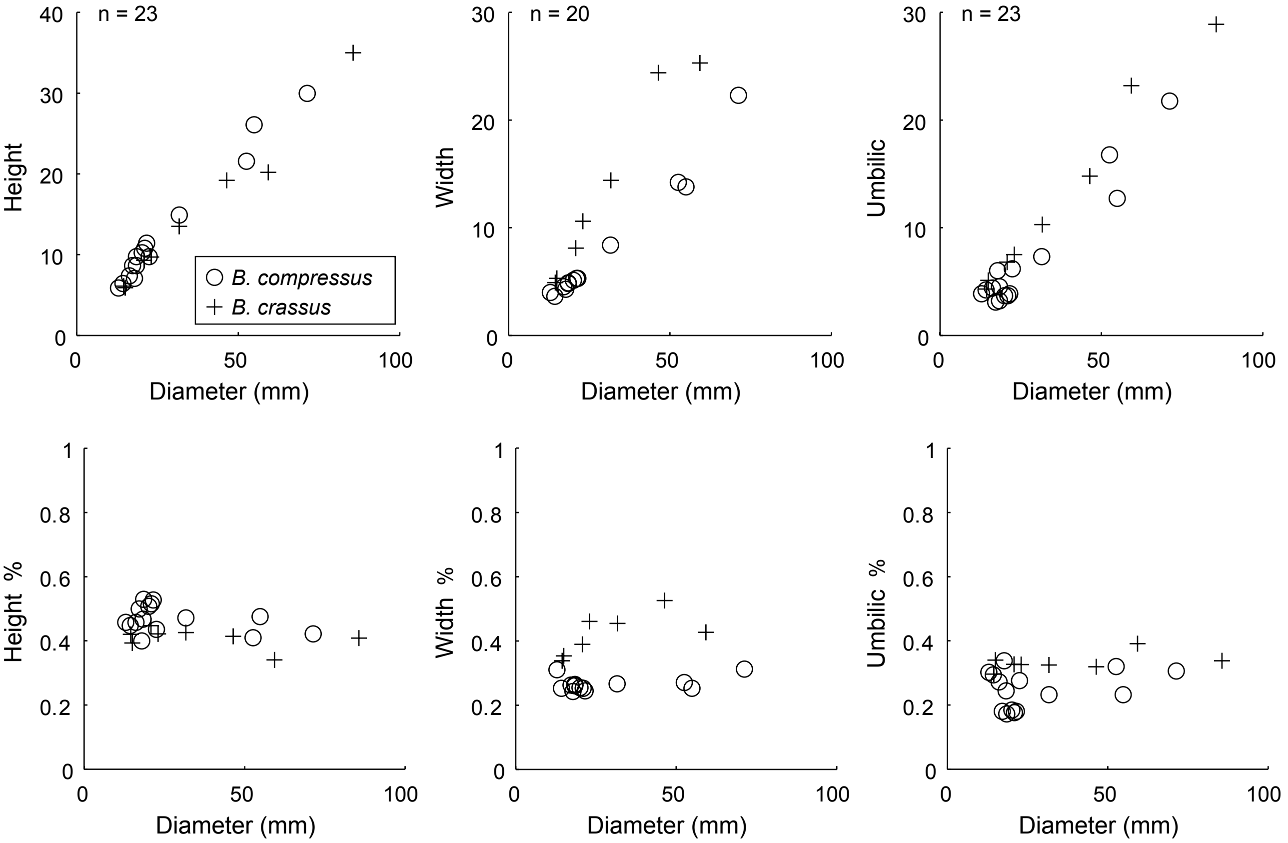

Fig. 17. Scatter diagram of H, W, and U, and of H/D, W/D, and U/D for *Brayardites crassus* nov. gen. et sp. and for *B. compressus* nov. gen. et sp.

Fig. 18. **1-6**. *Brayardites compressus* nov. gen. et sp.; **1a-e**, PIMUZ 27660, sample TuB5, 1e ×2; **2a-b**, PIMUZ 27661, sample TuB5; **3a-d**, PIMUZ 27662, sample Na23; **4a-e**, PIMUZ 27663, sample TuB5, 1e ×2; **5a-c**, PIMUZ 27664, sample TuB5. **6a-d**, PIMUZ 27667, sample Na23. All natural size unless otherwise indicated.

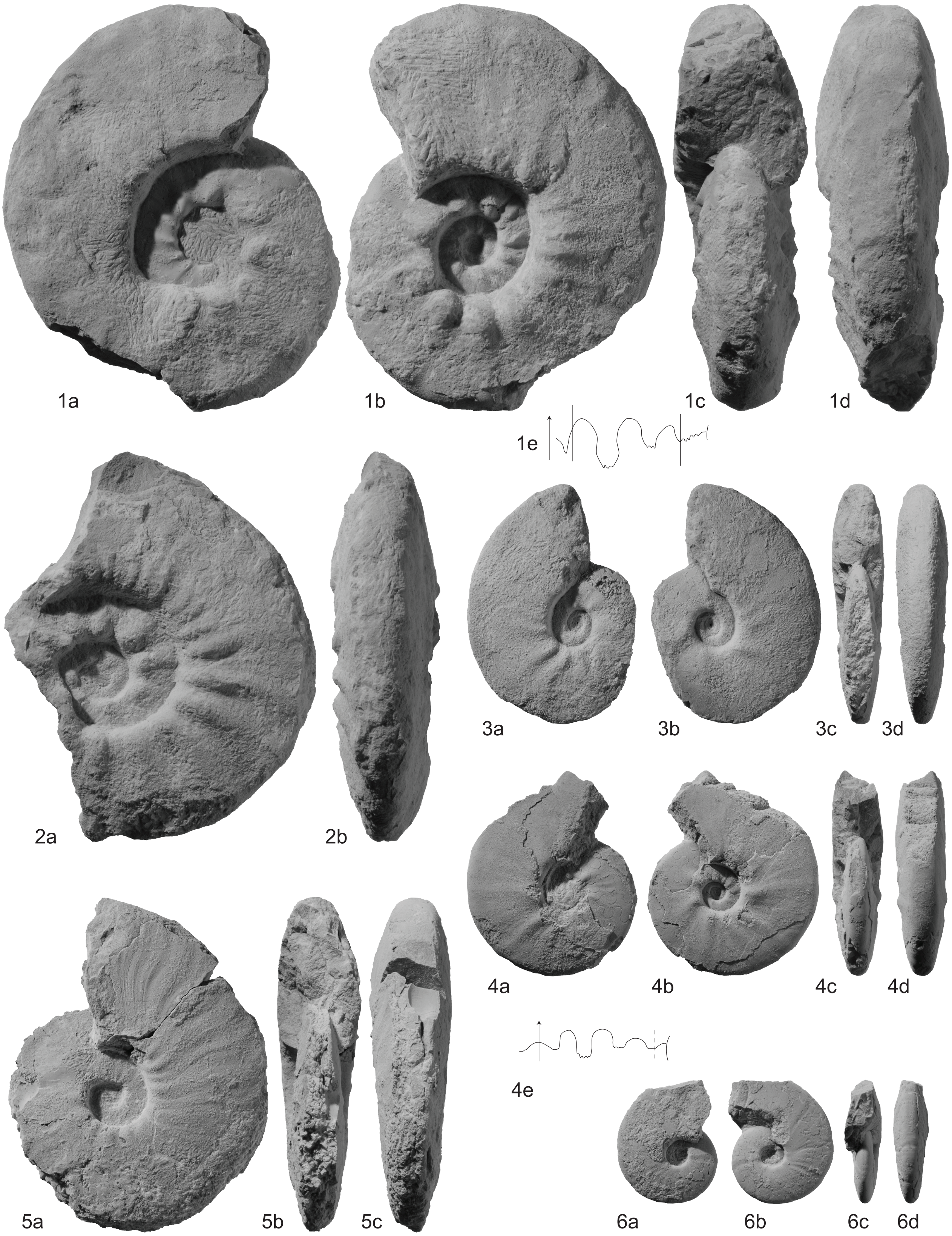
1a
1b
1c
1d
1e
2a
2b
3a
3b
3c
3d
4a
4b
4c
4d
4e
5a
5b
5c
6a
6b
6c
6d

Fig. 19. **1-6**. *Prionites involutus* nov. sp.; **1a-b**, PIMUZ 27669, sample Tu58; **2a-d**, PIMUZ 27670, sample Tu58; **3a-b**, PIMUZ 27671, sample Tu58; **4a-d**, PIMUZ 27672, sample Tu58; **5**, PIMUZ 27673, sample Tu58, ×2; **6a-d**, PIMUZ 27674, sample Tu58. **7-12**. *Stephanites superbus* Waagen, 1895; **7a-d**, PIMUZ 27675, sample Tu56; **8a-c**, PIMUZ 27676, sample Tu63; **9a-d**, PIMUZ 27677, sample Tu58; **10a-b**, PIMUZ 27678, sample Tu63, ×0.5; **11a-d**, PIMUZ 27679, sample Tu63; **12a-d**, PIMUZ 27680, sample Tu63. All natural size unless otherwise indicated.

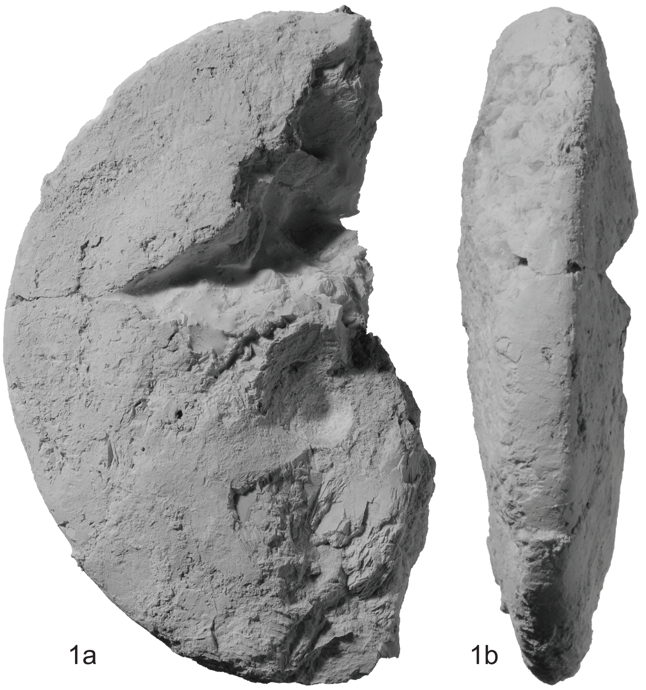
1a
1b


2a
2b
2c
2d

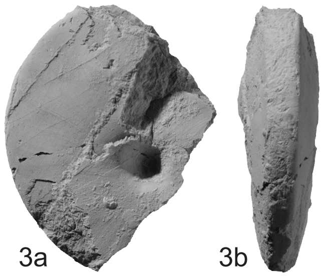
3a
3b

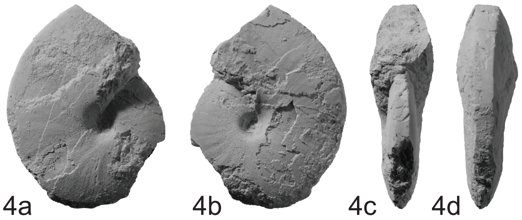
4a
4b
4c
4d

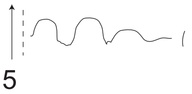
5


6a
6b
6c
6d

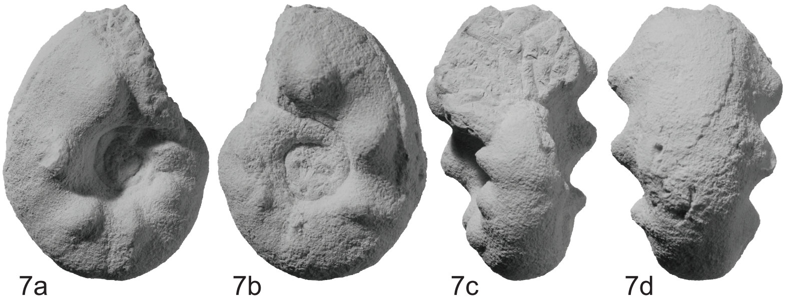
7a
7b
7c
7d

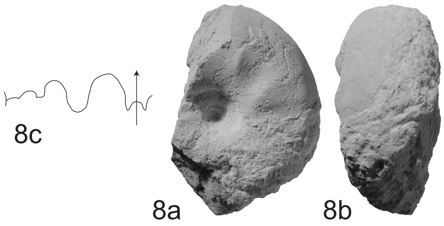
8c
8a
8b

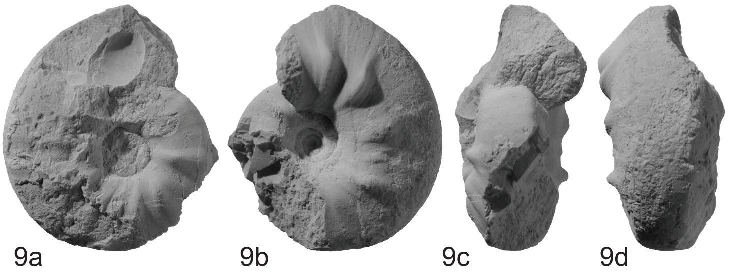
9a
9b
9c
9d

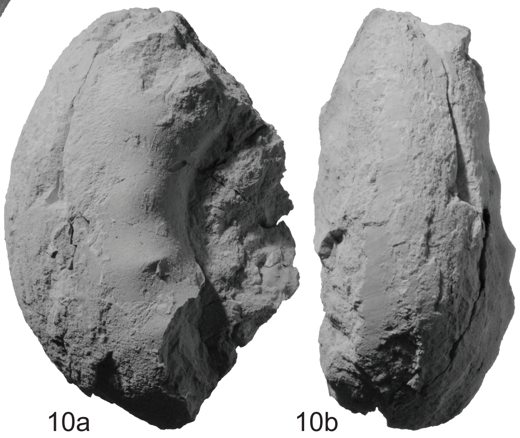
10a
10b


11a
11b
11c

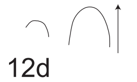
11d


12d

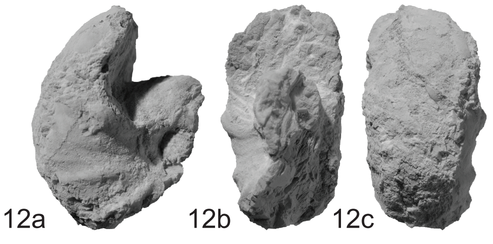
12a
12b
12c

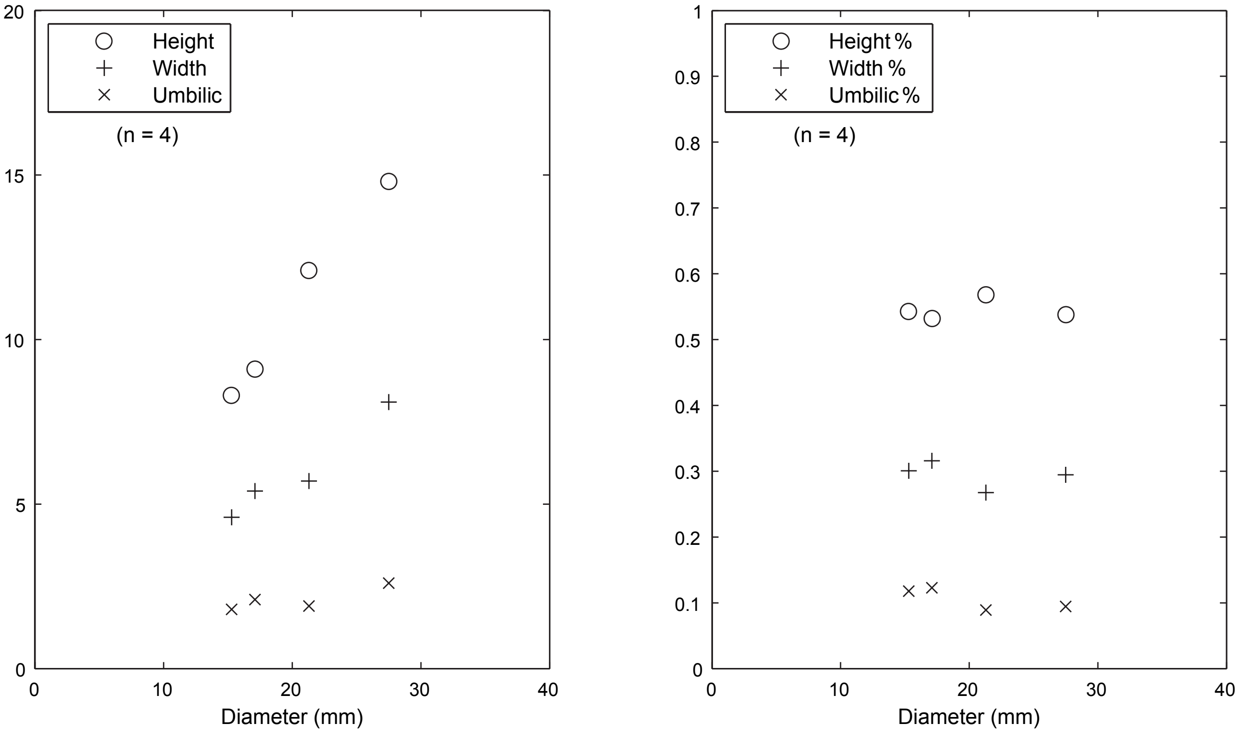

Fig. 20. Scatter diagram of H, W, and U, and of H/D, W/D, and U/D for *Prionites involutus* nov. sp.

Fig. 21. **1a-b**, *Wasatchites distractus* (Waagen, 1895), PIMUZ 27681, sample Tu67. **2-4.** Genus indet. B; **2a-e**, PIMUZ 27682, sample Tu67, 2e ×1.5; **3a-b**, PIMUZ 27683, sample Tu66; **4a-c**, PIMUZ 27684, sample Tu67. **5a-d**. Prionitidae gen. indet. A, PIMUZ 27685, sample TuB3, 5c ×1.5. **6-8**. *Nammalites pilatoides* (Guex, 1978) nov. gen.; **6a-c**, PIMUZ 27686, sample Tu44; **7a-c**, PIMUZ 27687, sample Tu44; **8a-d**, PIMUZ 27688, sample Tu44, 8d ×2. **9a-b**. *Owenites koeneni* Hyatt and Smith, 1905, PIMUZ 27689, sample Tu55. **10-12**. *Owenites simplex* Welter, 1922; **10a-d**, PIMUZ 27690, sample Tu44; **11**, PIMUZ 27691, sample Tu44, ×2; **12a-c**, PIMUZ 27692, sample Tu44. All natural size unless otherwise indicated.

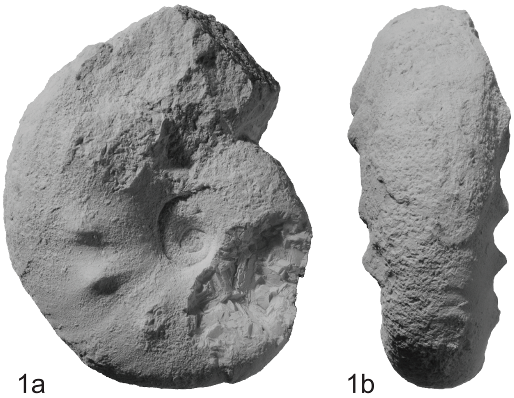
1a
1b


2a
2b
2c
2d


2e


4a
4b
4c

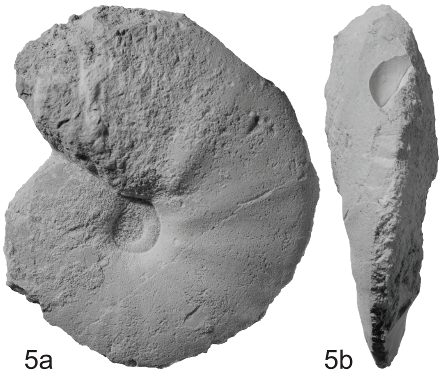
5a
5b

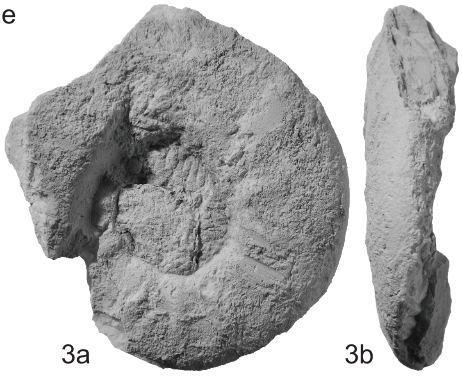
3a
3b


5c

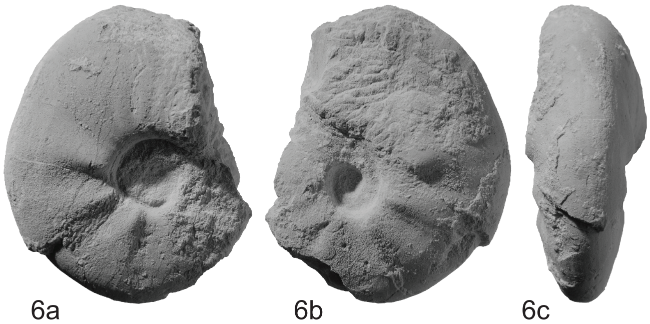
6a
6b
6c

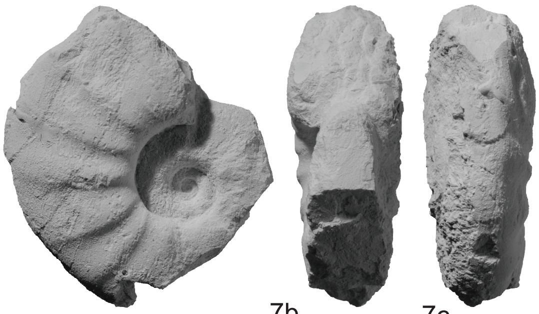
7a
7b
7c

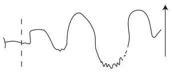
8d


8a
8b
8c

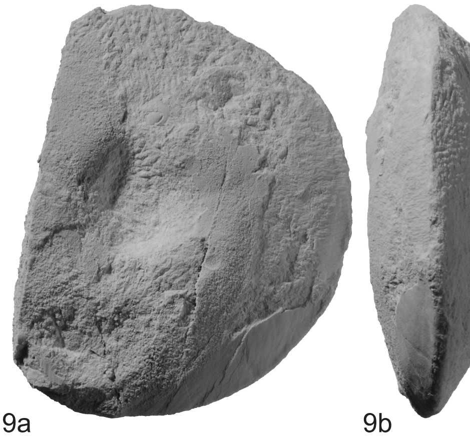
9a
9b

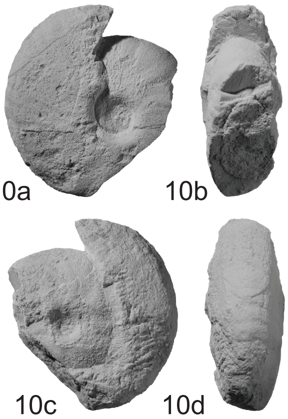
10a
10b
10c
10d


11


12a
12b
12c

Fig. 22. **1-2**. *Paranannites spathi* (Frebold, 1930); **1a-b**, PIMUZ 27693, sample TuB3; **2a-c**, PIMUZ 27694, sample Tu44. **3a-d**. *Paranannites* sp. indet., PIMUZ 27695, sample Tu44, ×1.5. **4-6**. *Jinyaceras hindostanum* (Diener, 1897); **4a-d**, PIMUZ 27700, sample TuB5; **5a-c**, PIMUZ 27698, sample TuB5; **6**, PIMUZ 27699, sample TuB5, ×2. **7-8**. *Owenites carpenteri* Smith, 1932; **7a-e**, PIMUZ 27696, sample Tu58, 7e ×2; **8a-c**, PIMUZ 27697, sample Tu58.

9a-d. *Subvishnuites* sp. indet, PIMUZ 27668, sample Tu58.**10-11**. *Pseudosageceras augustum* (Brayard and Bucher, 2008); **10a-c**, PIMUZ 27702, sample Tu71; **11a-e**, PIMUZ 27701, sample Tu71, 11e ×1.5. **12-13.** *Aspenites acutus* Hyatt and Smith, 1905; **12a-e**, PIMUZ 27703, sample TuB5; **13a-b**, PIMUZ 27704, sample Tu16, 12e ×1.5. **14a-c**. *Pseudosageceras multilobatum* Noetling, 1905, PIMUZ 27705, sample Tu56. All natural size unless otherwise indicated.

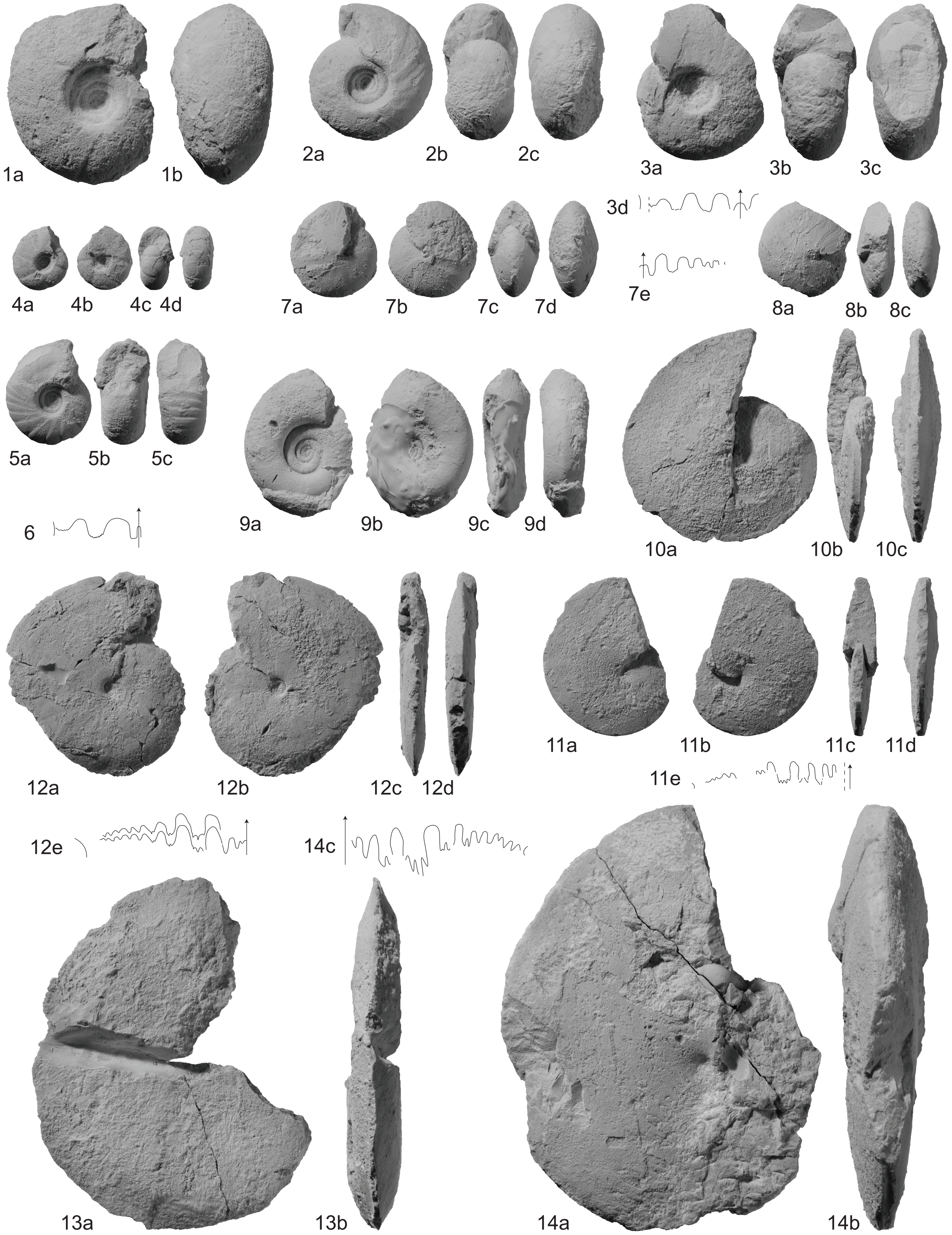
1a
1b
2a
2b
2c
3a
3b
3c
3d
4a
4b
4c
4d
7a
7b
7c
7d
7e
8a
8b
8c
5a
5b
5c
6
9a
9b
9c
9d
10a
10b
10c
12a
12b
12c
12d
11a
11b
11c
11d
11e
12e
14c
13a
13b
14a
14b

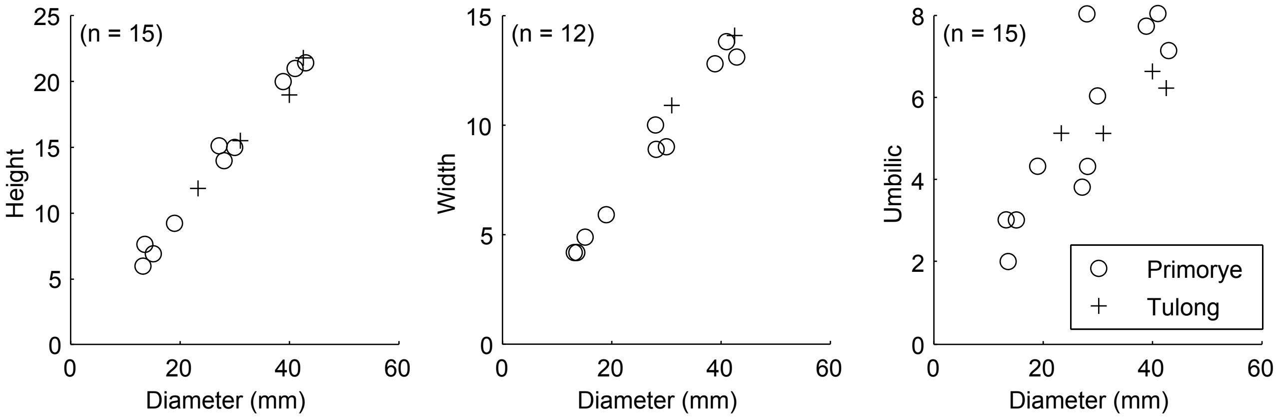

Fig. 23. Scatter diagram of H, W, and U, and of H/D, W/D, and U/D for *Shigetaceras dunajensis* nov. gen. including the type material from Primorye illustrated by Zakharov (1968).

CHAPTER 5:

Smithian (Early Triassic) ammonoids from the Salt Range, Pakistan

SMITHIAN (EARLY TRIASSIC) AMMONOIDS FROM THE SALT RANGE, PAKISTAN

by THOMAS BRÜHWILER*, HUGO BUCHER*, DAVID WARE*, ELKE HERMANN*, PETER A. HOCHULI*, GHAZALA ROOHI†, KHALIL REHMAN†, AAMIR YASEEN†

*Paläontologisches Institut und Museum der Universität Zürich, Karl Schmid-Strasse 4, CH-8006 Zürich, Switzerland; e-mails: bruehwiler@pim.uzh.ch; hugo.fr.bucher@pim.uzh.ch; david.ware@pim.uzh.ch; ehermann@pim.uzh.ch; peter.hochuli@erdw.ethz.ch
†Pakistan Museum of Natural History, Earth Science Division, Garden Avenue, Shakarparian, Islamabad 44000, Pakistan, e-mails: roohighazala@yahoo.com; reman_geol@yahoo.com; geologistgeologist@yahoo.com

Submitted to *Special Papers in Palaeontology*.

Abstract: Intensive sampling of the Early Triassic successions at the Chiddru, Nammal and Zaluch localities in the Salt Range (Pakistan) has yielded abundant and well-preserved Smithian (Early Triassic) ammonoid faunas that are of prime importance for ammonoid taxonomy and biostratigraphy. The Salt Range is the type area of many Smithian taxa, and it has played a central role in the Early Triassic ammonoid zonation since the pioneer works of Waagen and Mojsisovics *et al.* in the late 19th century. Our data allow the construction of a highly-resolved ammonoid succession spanning the entire Smithian times. Boundary faunas with the older Dienerian and the younger Spathian are also well documented. The new biostratigraphical sequence comprises the following twelve distinct ammonoid faunas (in ascending order): the *Flemingites bhargavai* beds, the *Shamaraites rursiradiatus* beds, the *Xenodiscoides perplicatus* beds, the *Flemingites nanus* beds, the *Radioceras evolvens* beds, the *Flemingites flemingianus* beds, the *Brayardites compressus* beds, the *Nammalites pilatoides* beds, the *Pseudoceltites multiplicatus* beds, the *Nyalamites angustecostatus* beds, the *Wasatchites distractus* beds, and the *Glyptophiceras sinuatum* beds. Biostratigraphic correlations between Nammal and Chiddru reveal diachronisms of the lithological boundaries between the Lower Ceratite Limestone and the Ceratites Marls on one hand, and between the Ceratite Marls and the Ceratite Sandstone on the other. The faunal succession from the Salt Range correlates well with that of other Tethyan sequences such as Tulong (South Tibet), Spiti (India) and South China.

Six new genera (*Koiloceras*, *Monneticeras*, *Truempyceras*, *Punjabites*, *Hochuliites*, *Mianwaliites*) and 13 new species (*Koiloceras romanoi*, *Monneticeras compressum*, *Punjabites* *punjabiensis*, *Hochuliites retrocostatus*, *Mianwaliites multiradiatus*, *Paraspidites obesus*, *Flemingites hautmanni*, *F. hofmanni*, *F. planatus*, *Rohillites pakistanensis*, *Prionites nammalensis*, *Shamaraites rursiradiatus*, *Subinyoites punjabiensis*) are described.

Key words: Ammonoidea, Early Triassic, Smithian, Salt Range, Pakistan, biostratigraphy.

THE end-Permian mass extinction event, which resulted in the most severe crisis in the history of life, wiped out more than 90 percent of all marine species (e.g. Raup and Sepkoski 1982). During the Early Triassic, ammonoids and conodonts recovered very fast in comparison with other marine clades (Brayard *et al.* 2006, 2009; Orchard 2007). Early Triassic ammonoid evolution during this recovery is characterized by the following main developments: (i) very low diversity in the Griesbachian, (ii) a moderate diversity increase in the Dienerian, (iii) an explosive radiation in the early Smithian, and (iv) a late Smithian extinction event followed by a second explosive radiation in the early Spathian (Tozer 1981*a*, *b*; Brayard *et al.* 2006, 2009). Recently published U-Pb ages from South China and their calibration with ammonoid faunas (Ovtcharova *et al.* 2006; Galfetti *et al.* 2007*b*) indicate a maximum duration of the Griesbachian-Dienerian interval of 1.4±0.4 my, 0.7±0.6 my for the Smithian and ca. 3 my for the Spathian (Text-fig. 1). Therefore, the first Early Triassic major ammonoid diversification phase in the early Smithian occurred no later than 2 my after the Permo/Triassic Boundary (PTB) and ended less than 1 my later with the extinction event in the late Smithian.

Although the first Early Triassic ammonoids from the Salt Range were described by de Koninck (1863), Waagen's contribution in the late 19th century (1895) was of immense importance for the study of Early Triassic ammonoids. In his master work entitled *Fossils from the Ceratite Formation*, he described a large number of new ammonoid taxa, thus making the Salt Range a classic Early Triassic locality. Moreover, Waagen established a detailed lithostratigraphic succession, and precisely recorded the occurrence of the taxa he described within this lithostratigraphic scheme. Therefore, the biostratigraphic subdivision of the Early Triassic for the Tethys given by Mojsisovics *et al.* (1895), which was based on Waagen's data, is basically correct in its main lines (see below). Subsequently, Frech (1905) and Spath (1934) carried out additional work on Early Triassic ammonoids from the Salt Range, but did not provid much new information. Griesbachian ammonoids in the Salt Range were first discovered by Schindewolf (1953), and then later duplicated by Kummel (1970). Kummel (1966) also described some rather poorly preserved ammonoids of Spathian age. Guex (1978) provided a well-documented distribution of Dienerian, Smithian and Spathian ammonoids from the Salt Range, but his work was based on a relatively small amount of material collected during a single field campaign. Later, a few additional Early Triassic ammonoids were found by the Pakistani-Japanese Research Group (1985).

Our extensive investigations in the Salt Range have yielded abundant, well-preserved ammonoid faunas of earliest to latest Smithian age. This new material enables us to revise the taxonomy of Smithian ammonoids, and to establish a high-resolution biostratigraphical sequence for the Smithian of the Salt Range. Such data are crucial for establishing a precise and laterally reproducible biochronological subdivision of the Smithian within the Tethys and within the Early Triassic tropics (Brayard and Bucher 2008; Brühwiler *et al.* accepted, ongoing work). Dienerian and Spathian ammonoid faunas from the Salt Range will be discussed in forthcoming papers (Ware *et al.* ongoing work; Bucher *et al.* ongoing work).

PALAEOGEOGRAPHICAL AND GEOLOGICAL SETTINGS

During the Early Triassic, the Pangean supercontinent was surrounded by two wide oceans, namely the Panthalassa and the Tethys, and several microcontinents (e.g. Cimmerian and Cathaysian) crossed these two oceans (e.g. Tozer 1982; Ricou 1994; Ehiro *et al.* 2005). During this period, the Salt Range area was located on the northern Gondwanan margin, about 30° south of the equator on the southern side of the Tethys Ocean (e.g. Smith *et al.* 1994; Stampfli and Borel 2002) (Text-fig. 2A). Typically, Lower Triassic successions on the Northern Indian Margin consist of mixed siliciclastic - carbonate series (Galfetti *et al.* 2007*a*; Brühwiler *et al.* 2009).

Waagen (1895) subdivided the Lower Triassic sediments of the Salt Range as follows (from bottom to top): Lower Ceratite Limestone (LCL), Ceratite Marls (CM), Ceratite Sandstone (CS), Upper Ceratite Limestone (UCL), Bivalve Beds (BB), Dolomitic Beds, and Topmost Limestone. These lithological subdivisions can easily be identified in all studied sections, and we utilize them in this paper (Text-fig. 3). A few minor modifications have been adapted from Kummel and Teichert (1970; Kathwai Member [KM]) and Guex (1978; "Niveaux Intermédiaires" [NI]). For a thorough description of the Lower Triassic sedimentary evolution of the Salt Range, see Hermann *et al.* (in prep.).

SAMPLED LOCALITIES

The Salt Range is located about 170 km southwest of Islamabad, and three localities (Chiddru, Nammal and Zaluch) in the western part of the range were studied (Text-fig. 2B, C).

The area near the village of Chiddru, 25 km ESE of Mianwali (Text-fig. 2C), is one of the main localities studied by Waagen (1895), and he described numerous ammonoid taxa from the LCL, the CS, the UCL and the BB from this locality. Later, Schindewolf (1953) and Kummel (1970) documented ammonoids of Griesbachian age in the KM at Chiddru, and in 1985 the Pakistani-

Japanese Research Group described some rather poorly preserved Dienerian and Smithian ammonoids from the same locality. In addition to the sections at the entry of the gorge examined by Kummel (1966), we also studied a site about 1km to the east, where sections of the entire succession from the LCL to the BB are well exposed (Text-fig. 4). Abundant and well-preserved Smithian ammonoid faunas were collected from the base of the CM, from throughout the CS, from the UCL and from the base of the BB. Ammonoids are particularly abundant in the CS, and several species reach remarkably large size of up to mor than 30cm in diameter (Text-fig. 5). All ammonoid occurrences from Chiddru are given in Text-figures 6-8.

The Nammal Gorge section, located 25 km ENE of Mianwali (Text-fig. 2C), was described by Kummel (1966), who reported the occurrence of a few Spathian ammonoids but it was Guex (1978) who first described Dienerian and Smithian ammonoids from this locality. Excellent exposures of the entire Lower Triassic succession occur in the Nammal Gorge section (Text-fig. 9). Our intensive sampling of this section has yielded abundant and well preserved Smithian ammonoids from the middle and upper third of the CM, from the uppermost part of the CS and from numerous horizons throughout the UCL. All ammonoid occurrences from Nammal are given in Text-figures 10-12.

As a complement to the extensively studied localities of Chiddru and Nammal, we also investigated a third locality near the village of Zaluch, 24 km NNE of Mianwali (Text-fig. 2C). The Zaluch section was first described by Kummel (1966), but again, it was Guex (1978) who first described its Smithian ammonoids. Our sampling at this locality has yielded ammonoids from the upper part of the CS and from the UCL. All ammonoid occurrences from Zaluch are given in Text-figure 13.

BIOSTRATIGRAPHICAL DISCUSSION

Based on our extensive, bed-rock controlled sampling, we recognize a total of twelve distinct ammonoid faunas of earliest to latest Smithian age in the studied area (Text-figs 14-15). The resulting informal zonation presented herein is entirely new. Only a preliminary version was previously presented in a conference abstract (Brühwiler *et al.* 2007). A description of the ammonoid faunas as well as a discussion of their correlation with ammonoid zonations from other areas is provided, and synthetic range charts for Smithian ammonoid species and genera from the Salt Range are given in Text-figs 16 and 17, respectively. No formal zone names are introduced since we prefer to use the term "beds" at the present time to describe the local faunal sequence. The usage of formal zones would imply a well-established lateral reproducibility of the faunal sequence between various basins, which is still a subject of ongoing work.

Latest Dienerian ammonoid faunas

***Prionolobus rotundatus* beds.** The Dienerian ammonoid faunas of the Salt Range are currently being revised by our group (Ware *et al.*, ongoing work). The latest Dienerian ammonoid fauna in the studied area is characterized by *Prionolobus rotundatus* and *Clypites typicus* and has been found at Chiddru and at Nammal (Text-figs 6, 10, 15). A correlative of this fauna has recently been found near Mud in Spiti, India (Brühwiler *et al.* submitted [b]).

Early Smithian ammonoid faunas

***Flemingites bhargavai* beds.** In the Nammal section, the oldest fauna of typical Smithian affinity occurs at the top of the lower third of the CM and is characterized by *Flemingites bhargavai*, *Flemingites hautmanni* and *Radioceras* cf. *kraffti*. *Kashmirites* sp. indet. and poorly preserved specimens possibly belonging to *Koiloceras romanoi* gen. et sp. nov. occur slightly higher in the section.

At Chiddru, a similar fauna occurs in the first limestone beds at the base of the CM and is characterized by the association of *Koiloceras romanoi*, *Radioceras* cf. *kraffti*, *Flemingites planatus* sp. nov. and ?*Kingites parkashi*. The beds containing the Chiddru fauna are termed the *Flemingites planatus* beds, and they probably correlate with the *Flemingites bhargavai* beds from Nammal. This biostratigraphic correlation is further supported by the directly underlying *Prionolobus rotundatus* assemblage both at Nammal and Chiddru. It reveals an important diachronism of the lithological boundaries between the LCL and the CM between these two areas (Text-fig. 15).

An equivalent fauna including *Flemingites bhargavai*, *Koiloceras romanoi* and ?*Kingites parkashi* has recently been found near Mud in Spiti, India (Brühwiler *et al.*, submitted [b]). This particular section had been proposed as a GSSP candidate for the Induan-Olenekian boundary (Krystyn *et al.* 2007*a*, *b*), but the discovery of the *Flemingites bhargavai* fauna below the horizon of the proposed GSSP has led us to suggest that the boundary level should be lowered by ca. 1m (Brühwiler *et al.* submitted [b]).

***Shamaraites rursiradiatus* beds.** This ammonoid fauna was found only in a single bed, i.e. in the second limestone bed within the base of the CM at Chiddru. It is characterized by the association of *Shamaraites rursiradiatus* sp. nov., *Monneticeras compressum* gen. et sp. nov., *Pseudoflemingites* cf. *timorensis* and *Radioceras* cf. *kraffti*.

The occurrence of *Shamaraites* in this association indicates that it correlates at least partly with the early Smithian "*Clypeoceras timorense*" Zone from Primorye (Shigeta *et al.* 2009). Note that

"*Clypeoceras timorense*" from Primorye as described by Shigeta and Zakharov (2009) is a not true *Clypeoceras*, but is here assigned to *Radioceras* (see systematic section).

***Xenodiscoides perplicatus* beds.** This subdivision has been found in the middle part of the CM at Nammal and in a single float block most likely derived from the base of the CS at Chiddru (sample Chi1). The fauna is characterized by the association of *Xenodiscoides perplicatus*, *X. involutus*, *X. falcatum*, *Vercherites vercherei*, *Paraspidites obesus* sp. nov., *Kashmirites* sp. indet., *Flemingites hofmanni* sp. nov. and *Rohillites pakistanensis* sp. nov. The latter two species were found only in the single float block from Chiddru.

***Flemingites nanus* beds.** These beds are well-documented from the lower part of the CS at Chiddru and from the upper part of the CM at Nammal. They are characterized by the association of *Flemingites nanus*, *Kashmirites armatus*, *Paranorites ambiensis*, *Paraspidites praecursor* and *Vercherites pulchrum*. The nautilid *Tainionautilus trachyceras*, a Permian holdover, is here documented from these beds. Biostratigraphic correlation based on this ammonoid assemblage reveals an important diachronism of the lithological boundaries between the CM and the CS between these two areas (Text-fig. 15).

The *Flemingites nanus* beds probably correlate with the lowest part of the *Flemingites* beds of Spiti (Bed 12 in Krystyn *et al.* 2007*a*, *b*; *Vercherites* cf. *pulchrum* beds in Brühwiler *et al.* submitted [b]), and with part of the *Flemingites rursiradiatus* beds from South China (Brayard and Bucher 2008).

***Radioceras evolvens* beds.** This subdivision occurs in the middle part of the CS at Chiddru, and its fauna is characterized by the occurrence of *Radioceras evolvens*, *Pseudaspidites* cf. *muthianus* and ?*Paranorites* sp. indet. A. Note that according to Waagen (1895), *R. radiosum*, which is herein considered as a synonym of *R. evolvens*, occurs in the lower part of the CS. Moreover, *Radioceras* appears to be a long-ranging genus, since it occurs as low as the *Flemingites bhargavai* beds. Thus, this subdivision may be only of local significance.

***Flemingites flemingianus* beds.** The uppermost part of the Ceratite Sandstone at Chiddru, Nammal and Zaluch contains a distinctive fauna dominated by large-sized ammonoid specimens, and it is mainly characterized by the association of *Flemingites flemingianus* and *Hedenstroemia evoluta*. At Zaluch, these beds also contain *Clypeoceras superbum*, *Kashmirites baidi*, Arctoceratidae gen. et sp. indet. and Gen. et sp. indet. A.

The occurrence of *Flemingites flemingianus* and *Clypeoceras superbum* at this level has already been described by Waagen (1895) from several other localities in the Salt Range. This fauna correlates with at least part of the *Flemingites* beds of Spiti (Krystyn, *et al.* 2007*a*, *b*) and the *Flemingites rursiradiatus* beds from South China (Brayard and Bucher 2008).

Middle Smithian ammonoid faunas

***Brayardites compressus* beds.** This subdivision occurs in the lower part of the Upper Ceratite Limestone at Nammal and Zaluch and is characterized by the association of *Brayardites compressus* and *Juvenites* sp. indet.

Brayardites compressus was recently described from the middle Smithian *Brayardites compressus* beds of Tulong (South Tibet) (Brühwiler *et al.* accepted), and it has also been found in Spiti, Northern India ("new prionitid A" in Brühwiler *et al.* 2007). In these two regions, *Brayardites* co-occurs with a distinctive faunal association that includes *Jinyaceras hindostanus*, *Tulongites xiaoqiaoi* and *Urdyceras tulongensis*. In the Salt Range, this fauna is apparently less diverse, but the occurrence of *Brayardites compressus* nevertheless allows correlation with Tulong and Spiti.

***Nammalites pilatoides* beds.** This subdivision occurs in the UCL at Chiddru, Nammal and Zaluch. It is characterized by the association of *Nammalites pilatoides*, *Meekoceras* cf. *gracilitatis*, *Truempyceras pluriformis*, *Juvenites* cf. *kraffti*, Ussuriidae gen. et sp. indet. and Proptychitidae gen. et sp. indet. B.

This association correlates with the middle Smithian *Nammalites pilatoides* beds recently described from Tulong (Brühwiler *et al.* accepted), with the fauna of an exotic block of Hallstatt facies from Oman (Brühwiler *et al.* submitted [a]) and with the "new prionitid B beds" in Spiti (Brühwiler *et al.*, 2007). As shown by Brühwiler *et al.* (accepted) the *Nammalites pilatoides* beds of South Tibet correlate with the lower part of the middle Smithian *Owenites koeneni* beds of South China (i.e. *Ussuria* and *Hanielites* horizons; Brayard and Bucher 2008) with which they share the common occurrence of *Owenites simplex* and *Parananannites spathi*. The occurrence of Ussuriidae gen. et sp. indet. in the *Nammalites pilatoides* beds from the Salt Range may also corroborate this correlation.

The occurrence of *Meekoceras* cf. *gracilitatis* in these beds indicates that a portion of the *Meekoceras gracilitatis* Zone of the USA (Silberling and Tozer 1968; Jenks 2007) correlates with the *Nammalites pilatoides* beds. However, the presence of several genera, such as *Guodunites*, *Inyoites* and *Lanceolites*, in the *Meekoceras gracilitatis* Zone indicates that this zone comprises the entire middle Smithian (Brühwiler *et al.* accepted).

***Pseudoceltites multiplicatus* beds**. Hitherto, this subdivision has been found only in the UCL at Nammal, and it is characterized by the association of *Pseudoceltites multiplicatus*, *Prionites nammalensis* sp. nov. and *Hochuliites retrocostatus* gen. et sp. nov. In addition, rare specimens of *Punjabites punjabiensis* gen. et sp. nov., Proptychitidae gen. et sp. indet. A, *Dieneroceras* sp. indet. A and *Dieneroceras* sp. indet. B have also been found in these beds.

This fauna also occurs at Tulong (Brühwiler *et al.*, accepted) and at Spiti ("Flemingitid A beds" in Brühwiler *et al.*, 2007). An exact correlative is not known from South China.

***Nyalamites angustecostatus* beds.** This subdivision, well known from Chiddru and Nammal, occurs in the uppermost beds of the massive limestones in the middle part of the UCL. Its fauna is characterized by the association of abundant *Anaxenaspis nammalensis*, *Nyalamites angustecostatus* and *Prionites tuberculatus*. *Stephanites superbus* also occurs, but is less abundant. Additionally, a single, very small specimen described as *Owenites* sp. indet. as well as a single specimen referred to as ?*Pseudoceltites* cf. *normalis* has been found in these beds.

This fauna is also known from Tulong (Brühwiler *et al.* accepted), Spiti (*Stephanites* beds in Brühwiler *et al.* 2007) and Oman (Brühwiler *et al.* submitted [a]). It correlates with the *Inyoites* horizon in the upper part of the *Owenites koeneni* beds of South China (Brayard and Bucher 2008).

Late Smithian ammonoid faunas

***Wasatchites distractus* beds.** This subdivision occurs in the upper part of the UCL and thus far, has been documented only from Nammal. The fauna contains very abundant *Wasatchites distractus*, *Anasibirites kingianus*, *Anasibirites angulosus* and *Hemiprionites typus*. *Hemiprionites klugi*, *Subinyoites punjabiensis* sp. nov. and *Mianwaliites multiradiatus* gen. et sp. nov. also occur, but are relatively rare.

Correlatives of this late Smithian fauna, which contain *Anasibirites* and/or *Wasatchites*, are known from many Tethyan localities such as Oman (Brühwiler *et al.*, submitted [a]), Tulong (Brühwiler *et al.*, accepted), Spiti (Bhargava *et al.* 2004; Brühwiler *et al.* 2007), Timor (Welter 1922) and South China (Brayard and Bucher 2008). The fauna is also known from other worldwide localities such as Primorye (Markevich and Zakharov 2004), the USA (Silberling and Tozer 1968) and Arctic Canada (Tozer 1994).

***Glyptophiceras sinuatum* beds.** This subdivision occurs in the uppermost part of the UCL at Nammal and in the lowest bed of the Bivalve Beds at Chiddru. Its fauna is characterized by *Glyptophiceras sinuatum* and *Xenoceltites* cf. *variocostatus*.

This latest Smithian fauna also occurs in Spiti (Brühwiler *et al.* 2007) and in Tulong (Brühwiler *et al.* accepted). In South China the *Xenoceltites variocostatus* fauna also occurs above the horizons with *Anasibirites*, but was included in the *Anasibirites multiformis* beds by Brayard and Bucher (2008). Note that the genus *Glyptophiceras* was originally considered to be of Griesbachian age, but is now known to be restricted to the latest Smithian (Brühwiler *et al.* accepted).

Comparison with previous work

Based on the data of Waagen (1895), Mojsisovics *et al.* (1895) provided the first biostratigraphic subdivision of the Early Triassic of the Salt Range. In comparison with our new data, their subdivisions are correct in a general sense, but further refinement and some corrections are required (Text-fig. 18). Their first two zones, i.e. the *Gyronites frequens* Zone (LCL) and the *Proptychites lawrencianus* Zone (lower part of CM) contain typical Dienerian ammonoid faunas, and the subsequent *Proptychites trilobatus* Zone (CM) appears to contain a mixture of Dienerian taxa (such as *Ambites*, *Clypites*) and Smithian taxa (such as *Vercherites vercherei* and *V. pulchrum*). However, our extensive bed-rock controlled sampling has not revealed such associations. The following *Ceratites normalis* Zone (lower part of CS) is also problematic, since we found a specimen that probably belongs to this index species in a much higher horizon (i.e. in the *Nyalamites angustecostatus* beds). Moreover, most other species reported by Waagen (1895) from this zone are based on rather poorly preserved material. The subsequent *Flemingites radiatus* Zone (middle part of CS) and the *Flemingites flemingianus* Zone (upper part of CS) correspond to our *Flemingites nanus* beds and *Flemingites flemingianus* beds, respectively. The *Stephanites superbus* Zone (UCL) includes the middle and late Smithian interval from our *Brayardites compressus* beds to the *Wasatchites distractus* beds.

Noetling's (1905) zonation of the Lower Triassic of the Salt Range was based on non-bedrock controlled material collected from Chiddru and Virgal. Consequently, due to possible lateral diachronism of lithological boundaries (compare Text-fig. 15), some of Noetling's zones appear to be mixtures of faunas that cannot be directly compared with our data. A tentative correlation of Noetling's zonation with our data is given in Text-fig. 18. Noetling's lowermost zone, the *Celtites radiosus* Zone, contains Kashmiritidae and is possibly of earliest Smithian age. The second zone, the *Prionolobus rotundatus* Zone, contains a mixture of Dienerian and earliest Smithian ammonoids. The *Celtites fallax* Zone contains *Xenodiscoides* and is equivalent to our *Xenodiscoides perplicatus* beds. Noetling's *Prionolobus volutus* Zone corresponds more or less to our *Flemingites nanus* beds. However, the *Flemingites flemingianus* Zone as defined by Noetling encompasses the entire CS, which spans the interval from our *F. nanus* beds to the *F. Flemingianus* beds. Noetling's *Stephanites superbus* Zone includes all faunas from the UCL.

Our new biostratigraphic data have revealed important diachronisms of the lithological boundaries between the LCL and the CM, and between the CM and the CS, whereas the boundaries between the CS and UCL and between the UCL and the BB are relatively synchronous in the studied area (Text-fig. 15). When establishing their early ammonoid zonations for the Salt Range, Mojsisovics *et al.* (1895) and Noetling's (1905) did not account for such lateral diachronisms of Waagen's (1895) lithological subdivisions, which may explain most of the weaknesses of their zonations.

Guex (1978) formally introduced the late Griesbachian *Ophiceras connectens* Zone (based on the data from Schindewolf [1953] and Kummel [1970]), the early Dienerian *Gyronites frequens* Zone and the "*Anasibirites*" *pluriformis* Zone, which he correlated with the late Smithian *Tardus* Zone (Tozer 1967; Silberling and Tozer 1968). However, as we show here, the index species (herein transferred to *Truempyceras* gen. nov.) of the "*Anasibirites*" *pluriformis* Zone is not of late Smithian age, but instead occurs in the middle Smithian *Nammalites pilatoides* beds. Therefore, the *Pluriformis* Zone as defined by Guex (1978) corresponds to the entire interval from our *Nammalites pilatoides* beds to the end of the Smithian (Text-fig. 18).

CONCLUSIONS

Detailed sampling of the Lower Triassic succession at the Chiddru, Nammal and Zaluch localities in the Salt Range (Pakistan) has yielded abundant and well preserved ammonoid faunas of earliest to latest Smithian age. These faunas enable us to revise the taxonomy of Smithian ammonoids and also to address the important aspects of intraspecific variation and ontogenetic changes. The majority of Smithian ammonoid species from the Salt Range was insufficiently known due to small numbers of individual and/or poor preservation.

Our data have enabled us to establish a high-resolution biostratigraphic sequence for the Smithian of the Salt Range, consisting of a total of twelve successive, well differentiated ammonoid assemblages. Thus, the Salt Range provide the most complete record of Smithian ammonoids presently known world-wide. Such detailed documentations of ammonoid successions are a prerequisite for the establishment of a precise, laterally reproducible and robust chronostratigraphic framework for the Smithian and subsequent diversity and phylogenetic analyses.

SYSTEMATIC PALAEONTOLOGY

by THOMAS BRÜHWILER and HUGO BUCHER

Systematic descriptions mainly follow the classification established by Tozer (1981*b*; 1994) and refined by Brayard and Bucher (2008), Brühwiler *et al*. (accepted) and Brühwiler and Bucher (submitted). Provided that measurements were available for at least four specimens, the quantitative morphological range of each species is expressed utilizing the four classic geometrical parameters of the ammonoid shell: diameter (D), whorl height (H), whorl width (W) and umbilical diameter (U). The three parameters (H, W and U) are plotted in absolute values as well as in relation to diameter (H/D, W/D, and U/D). Sample numbers are reported on the stratigraphic sections (Text-figs 6-8, 10-13).

Abbreviations: non = material not forming part of the current species; p. = pars (from Latin, means that only part of the material belongs to the current species); v. = *video* or *vidimus* (from Latin, means that the material was seen in person by the authors); ? = questionable; PIMUZ, Paläontologisches Institut und Museum der Universität Zürich, Switzerland.

Class CEPHALOPODA Cuvier, 1797

Subclass AMMONOIDEA Zittel, 1884

Order CERATITIDA Hyatt, 1884

Superfamily XENODISCACEAE Frech, 1902

Family KASHMIRITIDAE Spath, 1934

Discussion. The family Kashmiritidae was synonymized with Xenoceltitidae Spath, 1930 (Tozer 1981*b*, 1994). However, the genera we include within Xenoceltitidae (i.e. *Xenoceltites* and *Glyptophiceras*, see descriptions below) differ from Kashmiritidae by their elliptical whorl sections, their projected ornamentation and their constrictions on inner whorls. Moreover, Kashmiritidae are of early to middle Smithian age, whereas the Xenoceltitidae appear in the late Smithian. A direct phylogenetic relationship between the two groups cannot be excluded but seems improbable. Thus, Xenoceltitidae in the sense of Tozer are probably polyphyletic.

Genus KASHMIRITES Diener, 1913

Type species: *Celtites armatus* Waagen, 1895.

Kashmirites armatus (Waagen, 1895)

Plate 1, figures 1-3

1895 *Celtites armatus* Waagen, 75, pl. 7, figs 1, 7.

Occurrence. Sample Chi10; middle part of CS, *Flemingites nanus* beds, Chiddru.

Description. Very evolute shell with slightly flattened flanks and depressed whorls. Venter subtabulate, low arched with rounded shoulders. Umbilicus wide with an almost vertical wall and rounded shoulders. Ornamentation consists of straight ribs fading out on the ventral shoulders. Ribs become fine and dense on outer whorls of one specimen. Suture line with relatively strongly indented lobes and slightly phylloid saddles.

Measurements. See appendix.

Discussion. The type material of this species was found by Waagen (1895) in the topmost beds of the Ceratite Sandstones from Chiddru.

Kashmirites cf. *nivalis* (Diener 1897)

Plate 1, figures 8-10

Occurrence. Three specimens found as float in the lower part of the Ceratite Marls at Chiddru.

Description. Very evolute shell with slightly convex flanks. Venter low arched with rounded shoulders. Umbilicus wide with an almost vertical wall and rounded shoulders. Ornamentation consists of straight ribs fading out on the ventral shoulders. Suture line ceratitic and simple.

Discussion. The imperfect preservation of our specimens precludes a definitive specific assignment.

Kashmirites sp. indet.

Plate 1, figures 11-14

Occurrence. Extremely abundant but poorly preserved in a thin, marly limestone bed slightly below the middle of the CM at Nammal (samples Nam64, Nam531, Nam534 and Nam546). Similar but also poorly preserved specimens are present higher up-section in the *Xenodiscoides perplicatus* beds, CM (sample Nam65).

Description. Very evolute shell with slightly convex flanks. Venter low arched with rounded shoulders. Umbilicus wide with an almost vertical wall and rounded shoulders. Ornamentation varies from strong, straight and distant ribs to fine, biconcave and dense ribs. Suture line not preserved; phragmocone flattend on all specimens.

Discussion. These specimens may be conspecific with *Kashmirites* cf. *nivalis* described above, but their poor preservation precludes an assignment at the species level.

Kashmirites baidi Brühwiler and Bucher (submitted)

Plate 1, figures 4-7

Occurrence. Sample Zal50; *Flemingites flemingianus* Beds, upper part of CS, Zaluch.

Description. Evolute shell with flat, parallel flanks. Venter subtabulate, slightly arched with slightly rounded but marked shoulders. Umbilicus wide with a vertical wall and slightly rounded but marked shoulders. Ornamentation is very distinct, consisting of simple or paired strong, radial ribs. Ribs become faint on the ventral shoulders, but do cross the venter. Suture line ceratitic and simple with three lateral saddles.

Measurements. See Text-fig. 19.

Discussion. This species was recently found in Oman associated with *Flemingites rursiradiatus* Chao, 1959 (Brühwiler and Bucher submitted).

Genus PSEUDOCELTITES Hyatt, 1900

Type species. *Celtites multiplicatus* Waagen, 1895.

Discussion. This genus is similar to the older *Kashmirites*, from which it differs by its less depressed whorl section, its more angular umbilical edge and its simpler suture with broad, non-phylloid saddles.

Pseudoceltites multiplicatus (Waagen, 1895)

Plate 2, figures 1-8

1895 *Celtites multiplicatus* Waagen, p. 78, pl. 7, fig. 2a-c.

1895. *Celtites dimorphus* Waagen, p. 80, Pl. 7, Fig. 5a-c.

1976 *Psdeuodceltites multiplicatus* (Waagen); Wang and He, p. 289, pl. 6, figs 7-11.

? 1976 *Eukashmirites* cf. *blaschkei* (Diener); Wang and He, p. 290, pl. 6, fig. 12.

? 1976 *Eukashmirites* cf. *subarmatus* (Diener); Wang and He, p. 291, pl. 6, figs 13-14.

v acc. *Pseudoceltites multiplicatus* (Waagen, 1895); Brühwiler *et al.*, fig. 6(1-7).

Occurrence. Samples Nam9, Nam16; *Pseudoceltites multiplicatus* beds, UCL, Nammal.

Description. Evolute shell with a subrectangular, slightly compressed whorl section. Flanks flat, converging very weakly. Venter broad and subtabulate, slightly arched with slightly rounded shoulders. Umbilicus with a high vertical wall and marked, slightly rounded shoulders. Ornamentation varies from strong, distant radial ribs to fine, dense and slightly sinuous ribs. Ribs usually fade out on ventral shoulders, but occasionally cross the venter as faint ridges. Suture line ceratitic with broad saddles; first and second lateral saddle large, third saddle low.

Measurements. See Text-fig. 20.

?*Pseudoceltites* cf. *normalis* (Waagen 1895)

Plate 2, figure 9a-c

1895 *Ceratites normalis* Waagen, p. 38, pl. 6, fig. 2a-d.

Occurrence. A single fragmentary specimen from sample Nam8; *Nyalamites angustecostatus* beds, UCL.

Description. Evolute shell with rectangular whorl section and flat, parallel flanks. Venter subtabulate, slightly arched with marked but slightly rounded shoulders. Umbilicus with vertical wall and marked, subangular shoulders. Ornamentation consists of slightly biconcave ribs that thicken at ventral shoulders and form small tubercles. Suture line not preserved.

Discussion. Our single specimen is very similar to *"Ceratites" normalis* Waagen, 1895 and is possibly conspecific. However, Waagen indicates that the holotype came from the lower region of the Ceratite Sandstone at Nanga, which is a much older (Early Smithian) horizon than our specimen. This indicates that either this species may be long-ranging, or that Waagen's stratigraphical position is erroneous. ?*Pseudoceltites* cf. *normalis* differs from *Pseudoceltites multiplicatus* by its ventrolateral tubercles and parallel flanks. The assignment to *Pseudoceltites* is based on the rectangular whorl section, but is only provisional.

Genus NYALAMITES Brühwiler, Bucher and Goudemand (accepted)

Type species. *Xenodiscus angustecostatus* Welter, 1922.

Nyalamites angustecostatus (Welter, 1922)

Plate 2, figures 10-15

? 1895 *Celtites acuteplicatus* Waagen, 1895, p. 82, pl. 7a, figs 5, 5c, 6, 7.
1922 *Xenodiscus angustecostatus* Welter, p. 110, pl. 4, figs 14-17.
? 1922 *Xenodiscus oyensi* Welter, p. 111, pl. 5, figs 1, 2, 17
1968 *Anakashmirites angustecostatus* (Welter); Kummel and Erben, p. 128, pl. 19, figs 1-8.
1973 *Anakashmirites angustecostatus* (Welter); Collignon, p. 144, pl. 5, figs 7-8.
1973 *Anakashmirites oyensi* (Welter); Collignon, p. 146, pl. 5, figs 9-10.
1976 *Pseudoceltites angustecostatus* (Welter); Wang and He, p. 289, pl. 6, figs 3-6.
v 1978 *Eukashmirites angustecostatus* (Welter); Guex, pl. 7, figs 4, 9.
v non 2008 *Pseudoceltites? angustecostatus* (Welter); Brayard and Bucher, p. 18; pl. 3, figs 1-7; Fig. 19 (=*Preflorianites radians*).
v acc. *Nyalamites angustecostatus* (Welter); Brühwiler *et al.*, fig. 9(3-5).
v subm. *Nyalamites angustecostatus* (Welter); Brühwiler and Bucher (submitted).

Occurrence. Samples Chi101, Nam8, Nam68; *Nyalamites angustecostatus* beds, UCL.

Description. Small, very evolute shell with slightly convex, subparallel flanks. Venter subtabulate with rounded shoulders. Umbilicus shallow and wide with inclined wall and rounded shoulders. Ornamentation consists of regularly spaced, strong, radial, sharp ribs that fade out on ventral shoulders. Suture line ceratitic with two broad lateral saddles; third saddle reduced.

Measurements. See Text-fig. 21.

Discussion. This species is very common in the late middle Smithian of the Tethys.

Family XENOCELTITIDAE Spath, 1930

Genus XENOCELTITES Spath, 1930

Type species. *Xenoceltites subevolutus* Spath, 1930.

Xenoceltites cf. *variocostatus* Brayard and Bucher, 2008

Plate 3, figures 1-10

1913 *Ophiceras demissum* Oppel; Diener, p. 17, pl. 1, figs 8-9.

Occurrence. Very abundant in sample Nam713; one specimen from sample Nam42(SFB).

Description. Moderately evolute, platycone shell with nearly flat, only slightly convex flanks. Venter narrowly rounded with indistinct shoulders. Umbilicus shallow with moderately low, inclined wall and rounded shoulders. Inner whorls ornamented with prorsiradiate constrictions, outer whorls smooth. Growth lines prorsiradiate. Suture line ceratitic with weakly indented lobes and slightly tapered saddles.

Measurements. See Text-fig. 20, which also includes the measurements of *Xenoceltites variocostatus* from South China (from Brayard and Bucher, 2008).

Discussion. *Xenoceltites variocostatus* from South China differs by its slightly thicker whorls, but is otherwise very similar.

Genus GLYPTOPHICERAS Spath, 1930

Type species. *Xenodiscus aequicostatus* Diener, 1913 (=*Dinarites sinuatus* Waagen, 1895).

Glyptophiceras sinuatum (Waagen, 1895)

Plate 3, figures 11-12; plate 4, figures 1-6

1895 *Dinarites sinuatus* Waagen, p. 33, Pl. 10, Fig. 4.
? 1913 *Xenodiscus* cf. *lissarensis* Diener; Diener, p. 5, Pl. 1, Fig. 11.
1913 *Xenodiscus aequicostatus* Diener, p. 6, Pl. 2, Fig. 10.
1913 *Xenodiscus salomonii* Diener, p. 7, Pl. 2, Fig. 5.
1913 *Xenodiscus althothae* Diener, p. 8, Pl. 2, Figs 6, 11.
1913 *Xenodiscus* cf. *ellipticus* Diener; Diener, p. 9, Pl. 3, Fig. 1.

1913 *Xenodiscus comptoni* Diener, p. 10, Pl. 2, Fig. 7.
? 1913 *Xenodiscus* cf. *rotula* Waagen; Diener, p. 11, Pl. 3, Fig. 2.
1913 *Xenodiscus* cf. *ophioneus* Waagen; Diener, p. 12, Pl. 2, Figs 8-9.
? 1913 *Xenodiscus* cf. *sitala* Diener; Diener, p. 14, Pl. 3, Fig. 3.
1966 *Xenoceltites sinuatus* Waagen; Kummel, pl. 1, figs 1-2.
? 1966 *Xenoceltites sinuatus* Waagen; Kummel, pl. 1, figs 3-4.
v 1978 *Xenoceltites pulcher* Guex, p. 112, Pl. 7, Fig. 8.
v acc. *Glyptophiceras sinuatum* (Waagen, 1895); Brühwiler *et al.*, fig. 8(1-7).

Occurrence. Sample Chi11, base of Bivalve Beds; samples Nam32, Nam36, Nam37, Nam42(SFB), Nam104, topmost part of UCL, just below Bivalve Beds. *Glyptophiceras sinuatum* beds.

Description. Evolute, platycone shell with convex, convergent flanks. Venter narrowly rounded with rounded shoulders. Umbilicus wide and shallow with low vertical wall and rounded shoulders. Inner whorls with prorsiradiate constrictions. Outer whorls ornamented with extremely variable ribs that vary from low, dense and sinuous to very strong, distant and concave. Ribs may occasionally cross the venter depending on their overall strength. Suture line ceratitic with weakly indented lobes, second lateral saddle tapered and slightly asymmetrical.

Measurements. See Text-fig. 23.

Discussion. Extreme smooth variants of *Glyptophiceras sinuatum* are similar to *X.* cf. *variocostatus* described above.

Superfamily MEEKOCERATACEAE Waagen, 1895

Family GYRONITIDAE Waagen, 1895

Genus KOILOCERAS gen. nov.

Derivation of name. From the greek κοῖλος, meaning hollow.

Type species. *Koiloceras romanoi* gen. et sp. nov.

Composition of the genus. Type species only.

Diagnosis. Gyronitidae with eggressive coiling and a slight but distinct concavity near the umbilical margin.

Discussion. This genus is close to *Ambites* and *Prionolobus* Waagen, 1895, from which it differs by its concave upper flanks.

Koiloceras romanoi gen. et sp. nov.

Plate 5, figures 1-4

? 1934 *Meekoceras* aff. *falcatum* Waagen; Collignon, p. 6, pl. 7, fig. 2.
1905 *Prionolobus plicatus* Waagen; Frech, pl. 23, fig. 2.

Derivation of name. Named after Carlo Romano (Zürich).

Holotype. Specimen PIMUZ 27923 (Pl. 5, fig. 2a-d).

Type locality. Chiddru section, Salt Range, Pakistan.

Type horizon. Sample Chi52; Early Triassic, Smithian, *Flemingites planatus* beds.

Diagnosis. As for the genus.

Occurrence. Samples Chi52 and Chi104, *Flemingites planatus* beds, base of CM, Chiddru.

Description. Compressed shell with eggressive coiling. Inner whorls involute, outer whorls moderately evolute. Flanks convex except for a slight but distinct concavity near the umbilical margin. Maximum whorl width at mid-flank. Venter tabulate with slightly rounded shoulders on inner whorls; subtabulate on outer whorls. Umbilicus with oblique wall and rounded shoulders. Surface ornamented with low folds and bioconcave growth lines. Suture line ceratitic with moderately shallow lobes.

Measurements. See Text-fig. 24.

Discussion. This species was recently found in Spiti, associated with *Flemingites bhargavai* (Brühwiler *et al.* submitted [b]).

Genus MUDICERAS Brühwiler, Ware, Bucher, Krystyn and Goudemand (submitted [b])

Type species. *Gyronites planissimus* Spath, 1934.

Mudiceras planissimum (Spath, 1934)

Plate 5, figure 5a-e

	1934	*Gyronites planissimus* Spath, p. 92; pl. 8, fig. 4a-b.
v	subm.	*Mudiceras planissimum* (Spath) Brühwiler *et al*.

Occurrence. A single specimen from sample Chi53, *Shamaraites rursiradiatus* beds, base of CM, Chiddru.

Description. Moderately evolute, platyconic shell with convex, converging flanks and maximal thickness above mid-flanks. Venter tabulate; shoulders sharp-edged. Umbilicus broad, with low wall and rounded shoulders. Surface smooth except for weak projected constrictions. Suture line ceratitic with a rather narrow first lateral saddle and relatively deep lobes.

Measurements. See appendix.

Genus RADIOCERAS Waterhouse 1996*a*

Type species. *Meekoceras radiosum* Waagen, 1895.

Discussion. The type species is herein considered as a synonym of *"Aspidites" evolvens* Waagen, 1895.

Radioceras evolvens (Waagen, 1895)

Plate 16, figures 1-2; plate 17, figures 1-5

1895	*Aspidites evolvens* Waagen, p. 223, pl. 25, fig. 1.
1895	*Aspidites discus* Waagen, p. 228, pl. 25, fig. 2.
1895	*Meekoceras radiosum* Waagen, p. 257, pl. 36, fig. 2a-d.

Occurrence. Abundant in the middle part of the CS at Chiddru (samples Chi3, Chi6, Chi14, Chi-SFB2, Chi-SFB5), *Radioceras evolvens* beds.

Description. Involute, platyconic shell with convex, convergent flanks exhibiting strong eggressive coiling at maturity. Venter tabulate with subangular shoulders on inner whorls; shoulders become rounded on outer whorls. Umbilicus with high vertical wall and rounded shoulders. Surface smooth. Suture line with strongly indented, deep lobes; second lateral saddle slightly tapered asymmetrically; auxiliary series relatively long and well individualized.

Measurements. See Text-fig. 25.

Discussion.This species differs from the slightly older *Vercherites pulchrum* by its more involute inner whorls and its stronger eggressive opening of the umbilicus on mature whorls.

Radioceras cf. *kraffti* (Spath, 1934)

Plate 17, figure 6a-d; plate 18, figures 1-6; plate 19, figures 1-8

? 1909 *Meekoceras varaha* Krafft and Diener, p. 17; pl. 2, figs 2-6.
? 1930 *Koninckites kraffti* Spath, p. 28.
? 1934 *Koninckites kraffti* Spath; Spath, p. 155, fig. 43c.
? 2009 *Clypeoceras timorense* (Wanner); Shigeta and Zakharov, p. 126, figs 115-124.

Occurrence. Abundant in samples Chi52, Chi53, Chi104, base of CM, Chiddru; present in samples Nam540 and Nam718, CM, Nammal. *Flemingites bhargavai* beds, *Shamaraites rursiradiatus* beds.

Description. Involute, platyconic shell with convex, convergent flanks exhibiting eggressive coiling at maturity. Venter tabulate with subangular shoulders on inner whorls; shoulders become rounded on outer whorls. Umbilicus with high vertical wall and slightly rounded shoulders. Surface smooth, some specimens exhibit weak radial constrictions on inner whorls. Suture line with deep lobes; second lateral saddle slightly tapered asymmetrically, third saddle broad; auxiliary series relatively long.

Measurements. See Text-fig. 26.

Discussion. This species differs from *Radioceras evolvens* by its less individualized auxiliary series. A definitive assignment to *Radioceras kraffti* is not possible due to the imperfect preservation of the type material illustrated by Krafft and Diener (1909).

Genus KINGITES Waagen, 1895

Type species. *Kingites lens* Waagen, 1895.

?*Kingites parkashi* Brühwiler, Ware, Bucher, Krystyn and Goudemand (submitted [b])

Plate 8, figure 2a-e

v subm. ?*Kingites parkashi* Brühwiler *et al*., fig. 16.

Occurrence. A single specimen from sample Chi52, base of CM, Chiddru.

Description. Very involute, oxyconic shell with convex flanks. Venter rounded with rounded shoulders. Umbilicus extremely narrow and deep with high, perpendicular wall and rounded shoulders. Surface smooth. Suture line ceratitic with strongly indented, broad lobes; second lateral saddle slightly tapered asymmetrically; third saddle broad and low.

Measurements. See appendix.

Discussion. This species is similar in shape to *Clypeoceras largisellatum* Spath, 1934, from which it differs by its suture line with its short auxiliary series.

Family PROPTYCHITIDAE Waagen, 1895

Genus PSEUDASPIDITES Spath, 1934

Type species. *Aspidites muthianus* Krafft and Diener, 1909.

Pseudaspidites cf. *muthianus* (Krafft and Diener, 1909)

Plate 6, figure 1a-c

Occurrence. A single well preserved specimen from sample Chi-SFB2; *Radioceras evolvens* beds, CS.

Description. Large, moderately involute and compressed shell with convex flanks. Venter rounded with indistinct shoulders. Umbilicus with high, perpendicular wall and marked but slightly rounded shoulders. Surface smooth except for faint radial folds. Suture ceratitic with strongly indented lobes and phylloid saddles; second and third saddle curved towards umbilicus.

Discussion. Our single specimen is considerably more evolute than specimens of *Pseudaspidites muthianus* of comparable size from the Himalayas (Krafft and Diener 1909) and South China (Brayard and Bucher 2008). However, it otherwise is very similar in shape and suture line, and it may simply represent an evolute variant.

Proptychitidae gen. et sp. indet. A

Plate 6, figures 2-3

Occurrence. Samples Nam9 and Nam16, *Pseudoceltites multiplicatus* beds, UCL, Nammal.

Description. Moderately involute, platyconic shell with convex flanks. Venter subtabulate with rounded shoulders. Umbilicus with high, perpendicular wall and rounded shoulders. Surface smooth except for slightly biconcave growth lines and very fine folds. Suture line ceratitic with broad first lateral lobe; second lateral saddle broad and tapered; indentations of lobes poorly preserved.

Discussion. This species is similar to *Pseudaspidites*, but differs by its simpler suture line.

Proptychitidae gen. et sp. indet. B

Plate 6, figure 4a-c

Occurrence. A single specimen from sample Nam20, middle part of UCL, slightly above the *Nammalites pilatoides* beds, Nammal.

Description. Moderately involute, compressed shell with convex flanks. Venter rounded, but imperfectly preserved. Flanks curve towards umbilicus without forming a distinct wall or shoulders. Surface smooth, but poorly preserved. Suture line with deeply indented and deep lobes; first lateral saddle long and narrow, second saddle tapered; third saddle broad; auxiliary series with a fourth saddle at umbilical suture.

Discussion. This specimen is similar in shape to *Guodunites* Brayard and Bucher, 2008. However, this genus typically differs by its involute coiling and by its subammonitic suture line.

Genus MONNETICERAS gen. nov.

Derivation of name. Named after Claude Monnet (Zürich).

Type species. *Monneticeras compressum* gen. et sp. nov.

Composition of the genus. Type species only.

Diagnosis. Strongly compressed, moderately involute Proptychitidae with a narrowly rounded venter and a shallow umbilicus.

Discussion. This genus may represent an evolute relative of *Clypeoceras*. The suture line of *C. superbus* differs by a much longer auxiliary series, but that of ?*Clypeoceras* sp. indet. described below is rather similar.

Monneticeras compressum gen. et sp. nov.

Plate 7, figure 2a-e

Derivation of name. Refers to the compressed whorl section of the genus.

Holotype. Specimen PIMUZ 27932 (Plate 7, figure 2a-e).

Type locality. Nammal, Salt Range, Pakistan.

Type horizon. Sample Chi53, base of CM, *Shamaraites rursiradiatus* beds.

Diagnosis. As for the genus.

Occurrence. A single specimen from sample Chi53, base of CM, *Shamaraites rursiradiatus* beds.

Description. Strongly compressed, moderately involute shell with convex flanks. Maximum whorl width at mid-flank. Venter narrowly rounded with indistinct shoulders. Umbilicus shallow with low wall and rounded shoulders. Surface ornamented with low prorsiradiate folds. Suture line ceratitic; first lateral saddle slightly phylloid, second saddle slightly tapered, third saddle broad and low; auxiliary series relatively long.

Measurements. See appendix.

Genus *Clypeoceras* Smith, 1932

Type species. *Aspidites superbus* Waagen, 1895.

Discussion. The two species recently described as *Clypeoceras spitiense* and *C. timorense* by Shigeta and Zakharov (2009) from South Primorye differ from true *Clypeoceras* by their tabulate venters. They are herein considered as belonging to *Clypites* and *Radioceras*, respectively.

Clypeoceras superbum (Waagen, 1895)

Plate 7, figure 3a-c; plate 8, figure 1a-d

1895 *Aspidites superbus* Waagen, p. 218, pl. 23, fig. 1; pl. 24, fig. 1a-b.
1905 *Aspidites superbus* Waagen; Frech, pl. 27, fig. 3.
non ? 1985 *Aspidites* aff. *superbus* Waagen; Pakistani-Japanese Research Group, pl. 12, fig. 2a-b.

Occurrence. A well-preserved specimen from sample Zal50 (Zaluch); and a poorly preserved specimen from sample Nam132 (Nammal). Both from the upper part of CS, *Flemingites flemingianus* beds. An additional specimen was found as float in the CS at Nammal.

Description. Large, very involute, oxyconic shell with convex flanks. Venter rounded with rounded shoulders. Umbilicus extremely narrow and deep with high, perpendicular wall and rounded shoulders. Surface smooth. Suture line ceratitic with strongly indented, broad lobes; first lateral saddle slightly phylloid on one specimen, second lateral saddle slightly tapered asymmetrically; auxiliary series very long with a several indented saddles.

Measurements. See appendix.

Discussion. The specimen described as *Aspidites* aff. *superbus* by the Pakistani-Japanese Research Group (1985) differs from this species by its shorter umbilical series and its slightly tabulate venter.

Genus PARASPIDITES Spath, 1934

Type species. *Aspidites superbus* mut. *praecursor* Frech, 1905.

Discussion. *Paraspidites* was tentatively included in Proptychitidae by Tozer (1981*b*). This assignment is supported by the suture line and the shape of the umbilicus. However, *Paraspidites* differs from other members of that family by its acutely keeled venter. Aspenitidae are similar in shape, but differ by their more complex suture line with two adventitious lobes.

Paraspidites praecursor (Frech, 1905)

Plate 44, figure 8a-e

1905 *Aspidites superbus* mut. *praecursor* Frech, pl. 24, fig. 4a-b.

non 1934 *Paraspidites praecursor* (Frech); Spath, p. 162, pl. 3, fig. 2 (=*Paraspidites obesus* sp. nov.).

Occurrence. A single specimen from sample Chi10, lower part of CS, *Flemingites nanus* beds, Chiddru.

Description. Very involute, compressed oxyconic shell with an acutely keeled venter. Umbilicus small with overhanging wall and angular shoulders. Surface smooth. Suture line ceratitic with very slightly phylloid saddles; lobes with numerous indentations; auxiliary series long.

Measurements. See appendix.

Discussion. In shape, this species closely resembles *Aspenites acutus* Hyatt and Smith, 1905, which differs by its occluded umbilicus and its suture line with two adventitious lobes.

Paraspidites obesus sp. nov.

Plate 44, figures 5-7

1934 *Paraspidites praecursor* (Frech); Spath, p. 162, pl. 3, fig. 2

? 2009 *Vishnuites?* sp. indet. Shigeta and Zakharov, p.68, fig. 53(1-4).

Derivation of name. From the latin *obesus*, meaning thick.

Holotype. Specimen PIMUZ 28156 (Pl. 44, fig. 5a-d).

Type locality. Nammal, Salt Range, Pakistan.

Type horizon. Sample Nam532, middle part of CM, *Xenodiscoides perplicatus* beds.

Diagnosis. Relatively evolute *Paraspidites* with thick whorls and a high, overhanging umbilical wall.

Occurrence. Sample Chi1 (SFB), CM or CS, Chiddru; sample Nam532, middle part of CM, Nammal. *Xenodiscoides perplicatus* beds.

Description. Moderately involute, slightly compressed oxyconic shell with an acutely keeled venter. Umbilicus with high, strongly overhanging wall and angular shoulders. Surface smooth. Suture line ceratitic; first lateral saddle long, narrow and slightly phylloid, second saddle broad and slightly asymmetrical; auxiliary series with a well-individualized, small fourth saddle.

Measurements. See appendix.

Discussion. This species is considerably more evolute and has a shorter auxiliary series than *Paraspidites praecursor*, but otherwise it is very similar. *Vishnuites?* sp. indet. Shigeta and Zakharov (2009) is similar but more evolute.

Family GALFETTITIDAE Brühwiler and Bucher (submitted)

Genus GALFETTITES Brayard and Bucher, 2008

Type species. *Galfettites simplicitatis* Brayard and Bucher, 2008

Galfettites cf. *omani* Brühwiler and Bucher (submitted)
Plate 9, figure 5

Occurrence. A single fragmentary specimen from sample Nam14, UCL, *Nammalites pilatoides* beds, Nammal.

Description. Evolute, compressed shell with convex flanks. Venter tabulate with slightly rounded shoulders. Umbilicus extremely shallow with very low, vertical wall and rounded shoulders. Surface smooth. Suture line not preserved.

Discussion. The fragmentary preservation of our single specimen hinders a definitive assignment. Yet, the extremely shallow umbilicus is very similar to that of *Galfettites omani* from the *Nammalites pilatoides* beds of Oman (Brühwiler and Bucher submitted).

Genus VERCHERITES Brühwiler,Ware, Bucher, Krystyn and Goudemand (submitted [b])

Type species. *Koninckites vercherei* Waagen, 1895.

Discussion. *Vercherites* is close to *Paranorites* Waagen, 1895, which differs by its later umbilical egression, its distinctly trigonal cross-section, weakly ribbed inner whorls and its suture line, which differs in having a distinctly slim and phylloid first lateral saddle (Brühwiler *et al.* submitted [b]).

Vercherites vercherei (Waagen, 1895)

Plate 9, figures 1-4; plate 10, figures 1-4; plate 11, figure 4a-d

1895 *Koninckites vercherei* Waagen, p.268, pl. 30, fig. 1a-c.

Occurrence. Sample Chi1 (SFB), CM or CS, Chiddru; very abundant in samples Nam65 and Nam532, middle part of CM, Nammal. *Xenodiscoides perplicatus* beds.

Description. Very large, compressed shell with convex, convergent flanks. Inner whorls moderately involute, umbilicus opening throughout ontogeny, outer whorls moderately evolute. Venter tabulate with subangular shoulders on inner whorls, shoulders become rounded on outer whorls. Umbilicus with high vertical wall and marked, slightly rounded shoulders. Surface smooth except for very weak folds and biconcave growth lines. Suture line with strongly indented, deep lobes; first lateral saddle relatively narrow and very slightly phylloid; second lateral saddle broader and tapered asymmetrically; auxiliary series relatively long.

Measurements. See Text-fig. 27.

Discussion. This species is similar to *Vercherites pulchrum*, but differs by its more evolute coiling.

Vercherites pulchrum (Waagen, 1895)

Plate 11, figures 2-3; plate 12, figures 1-5

1895 *Meekoceras pulchrum* Waagen, p. 249, pl. 29, fig. 1a-c; pl. 27, figs 2-3.

? 1985 *Koninckites* cf. *volutus* Waagen; Pakistani-Japanese Research Group, pl. 13, fig. 3.

v 2007*a* *Meekophiceras? vercherei* (Waagen); Krystyn et al., pl. 1, fig. 2.

v 2007*b* *Meekophiceras? vercherei* (Waagen); Krystyn et al., pl. 1, fig. 1.

v subm. *Vercherites* cf. *pulchrum* (Waagen, 1895); Brühwiler *et al*., fig. 14.

Occurrence. Very abundant in sample Chi10, lower part of CS, Chiddru. Present also in sample Chi4, lowest bed of CS, Chiddru; and in sample Nam528, upper part of CM, Nammal. *Flemingites nanus* beds.

Description. Very large, compressed shell with convex, convergent flanks. Inner whorls very involute, umbilicus gradually opening throughout ontogeny, outer whorls moderately involute.Venter tabulate with angular shoulders on inner whorls, becoming subtabulate with rounded shoulders on outer whorls. Umbilicus with high vertical wall and marked, slightly rounded shoulders. Surface smooth. Suture line with strongly indented, deep lobes; first lateral saddle relatively narrow; second lateral saddle broader and tapered asymmetrically; auxiliary series relatively long with well individualized small saddles.

Measurements. See Text-fig. 28.

Genus PARANORITES Waagen, 1895

Type species. *Paranorites ambiensis* Waagen, 1895.

Paranorites ambiensis Waagen, 1895

Plate 11, figure 1; plate 13, figures 1-3; plate 14, figures 1-3; plate 15, figures 1-2

1895 *Paranorites ambiensis* Waagen, p. 158, pl. 32, fig. 1a-d.

? 1895 *Aspidites kingianus* Waagen, p. 225, pl. 32, fig. 1, pl. 33, fig. 1a-b.

p 1895 *Koninckites volutus* Waagen, p.268, pl. 28, figs 1 only.

non ? 1895 *Koninckites volutus* Waagen, p.268, pl. 28, fig. 2a-b.

non 1985 *Paranorites ambiensis* Waagen; Pakistani-Japanese Research Group, pl. 12, fig. 3.

Occurrence. Sample Chi10, lower part of CS, *Flemingites nanus* beds; a single specimen in sample Chi3, middle part of CD, *Radioceras evolvens* beds; Chiddru.

Description. Very large, moderately involute, compressed shell with convex, convergent flanks. Venter tabulate with subangular shoulders. Umbilicus with high vertical wall and marked, slightly rounded shoulders. Ornamentation consists of distant, low folds that are most prominent near the umbilicus and fade out towards the venter. Additionally, fine blunt spiral lines are visible on the flanks. Suture line with strongly indented, deep lobes; first lateral saddle distinctly phylloid; second lateral saddle slightly phylloid and tapered; third lateral saddle flattened; auxiliary series relatively long with well individualized small saddles.

Measurements. See Text-fig. 29.

Discussion. The specimen from the LCL of Chiddru described as *Paranorites ambiensis* by the Pakistani-Japanese Research Group (1985) differs from this species by its evolute coiling.

Paranorites sp. indet. A

Plate 14, figures 4-6

Occurrence. Several poorly preserved specimens from samples Nam529 and Nam530, upper part of CM, *Flemingites nanus* beds, Nammal.

Description. Large, moderately evolute, compressed shell with convex, convergent flanks. Venter subtabulate with rounded shoulders. Umbilicus with high vertical wall and marked, slightly rounded shoulders. Surface smooth. Suture line ceratitic with deep lobes and relatively narrow saddles; auxiliary series relatively long and well individualized.

Discussion. These specimens may belong to *Paranorites ambiensis*, but a definitive assignment is not possible because of their poor preservation.

?*Paranorites* sp. indet. B

Plate 5, figure 6a-b

Occurrence. A single, poorly preserved specimens found as float on top of the LCL, Chiddru. Stratigraphic position unknown.

Description. Large, moderately evolute, compressed shell with convex flanks strongly convergent toward venter. Venter subtabulate rounded shoulders. Umbilicus with high vertical wall and rounded shoulders. Surface smooth. Suture line poorly preserved.

Discussion. This specimens probably belongs to *Paranorites*, but a definitive assignment is not possible because of its poor preservation.

?*Paranorites* sp. indet. C

Plate 7, figure 4a-d

Occurrence. A single specimen from sample Chi3, middle part of CS, *Radioceras evolvens* beds, Chiddru.

Description. Large, involute, slightly compressed shell with strongly convergent flanks. Venter subtabulate with rounded shoulders. Umbilicus deep with inclined wall and rounded shoulders. Surface smooth. Suture line ceratitic; first and second lateral saddle slightly tapered; auxiliary series long and well indididualized.

Discussion. The convergent flanks and the suture line with its long auxiliary series suggest a relationship with *Clypeoceras* Smith, 1932 (see below), which differs however, by being much more involute and by its well-rounded venter. The whorl section of our specimen is also similar to that of *Fuchsites* (Waterhouse 1996*a*) and *Vavilovites* Tozer, 1971. Our specimen differs from these by its inclined umbilical wall.

Family FLEMINGITIDAE Hyatt, 1900

Genus FLEMINGITES Waagen, 1895

Type species. *Ceratites flemingianus* de Koninck, 1863

Flemingites flemingianus (de Koninck, 1863)

Plate 20, figures 1-5; plate 21, figures 1-2

1863 *Ceratites flemingianus* de Koninck, p. 10, pl. 7, fig. 1.

1895 *Flemingites flemingianus* Waagen, p. 199, pl. 12, fig. 1, pl. 13, fig. 1, pl. 14, fig. 1.

1895 *Flemingites compressus* Waagen, p. 202, pl. 15, fig. 1, pl. 16, fig. 1a-c.

1895 *Flemingites trilobatus* Waagen, p. 193, pl. 26, fig. 2a-b.

1933 *Flemingites compressus* Waagen; Collignon, p. 170, pl. 3, fig. 1, 1a.

1933 *Flemingites flemingi madagascariensis* Collignon, p. 173, pl. 5, fig. 1.

1933 *Flemingites griesbachi* Krafft and Diener; Collignon, p. 176, pl. 4, fig. 3, 3a; pl. 5, fig. 4; pl. 6, fig. 1-2.

v non 2007 *Flemingites flemingianus* Waagen; Brayard and Bucher, p. 43, pl. 17, figs 1-5; text-fig. 38.

Occurrence. Very common in a calcareous sandstone horizon in the upper part of the Ceratite Sandstone at all visited localities (samples Chi2, Chi7, Chi15, Chi56a, Nam2, Nam78, Zal50); *Flemingites flemingianus* beds. This horizon was termed *Flemingites* beds by Waagen (1895). Fragmented and possibly reworked specimens were found in sample Nam12 at the base of the UCL, Nammal.

Description. Large, evolute shell with elliptical whorl section. Venter rounded with indistinct shoulders. Umbilicus wide with rounded wall. Flanks ornamented with coarse strigation and radial or rursiradiate, slightly biconcave ribs. Ribs are strongest on inner whorls, but become finer and closely spaced on outer whorls. Suture line ceratitic with long, slightly phylloid saddles and strongly indented lobes.

Measurements. See Text-fig. 30.

Discussion. This species exhibits a large variation in whorl width. The specimens described as *Flemingites flemingianus* from South China by Brayard and Bucher (2008) differ by their more evolute coiling and their lower whorls. They may represent weakly ribbed variants of *F. rursiradiatus* Chao, 1959.

Flemingites nanus Waagen, 1895

Plate 22, figures 1-6

1895 *Flemingites nanus* Waagen, p. 191, pl. 7, fig. 8a-b.

? 1895 *Flemingites rotula* Waagen, p. 195, pl. 11, fig. 3a-b.

1895 *Flemingites radiatus* Waagen, p. 197, pl. 11, fig. 1a-c.

Occurrence. Lower part of CS at Chiddru (sample Chi10); upper part of CM at Nammal (samples Nam528 and Nam530). *Flemingites nanus* beds.

Description. Evolute, moderately compressed shell with convex flanks. Venter rounded, but slightly flattened with rounded shoulders. Umbilicus wide with vertical wall and rounded shoulders. Flanks ornamented with fine strigation and distant, strong folds on inner whorls that disappear on outer whorls. Suture line ceratitic; saddles well-rounded; first lateral lobe deep.

Measurements. See Text-fig. 31.

Discussion. The ornamentation of the inner whorls is similar to that of *Xenodiscoides perplicatus*, which differs by its tabulate venter with angular shoulders and by its lack of strigation.

Flemingites hautmanni sp. nov.

Plate 24, figures 1-9; plate 25, figures 6-7

Derivation of name. Named after Michael Hautmann (Zürich).

Holotype. Specimen PIMUZ 28000 (Pl. 24, fig. 1a-d).

Type locality. Nammal, Salt Range, Pakistan.

Type horizon. Sample Nam718, CM, *Flemingites bhargavai* beds.

Diagnosis. Relatively involute, moderately compressed *Flemingites* with subtabulate venter and weak radial ornamentation.

Occurrence. Very abundant in a thin nodular carbonate horizon at the lower third of the CM in Nammal (samples Nam718 and Nam543), *Flemingites bhargavai* beds.

Description. Moderately evolute, compressed shell with slightly convex flanks and maximum whorl width slightly below mid-flank. Venter tabulate with rounded shoulders. Umbilicus with low, vertical wall and rounded shoulders. Ornamentation consists of radial folds as well as strigation on flanks and venter that is most prominent at ventrolateral shoulders, but becomes finer towards umbilicus. Suture line ceratitic with slightly tapered saddles and relatively deep lobes.

Measurements. See Text-figs 32-33.

Discussion. This species is considerably more involute than *Flemingites bhargavai* described below.

Flemingites hofmanni sp. nov.

Plate 23, figures 1-4

Derivation of name. Named after Richard Hofmann (Zürich).

Holotype. Specimen PIMUZ 27999 (Pl. 23, fig. 4a-d).

Type locality. Chiddru, Salt Range, Pakistan.

Type horizon. Sample Chi1 (SFB), CM or CS, *Xenodiscoides perplicatus* beds.

Diagnosis. Relatively involute, compressed *Flemingites* with subtabulate venter.

Occurrence. Very abundant in sample Chi1 (SFB), CM or CS, Chiddru; *Xenodiscoides perplicatus* beds.

Description. Moderately evolute, compressed shell with slightly convex flanks and maximum whorl width slightly above mid-flank. Venter tabulate with rounded shoulders. Umbilicus with low, vertical wall and rounded shoulders. Ornamentation consists of radial folds as well as strigation on flanks and venter that is most prominent at ventrolateral shoulders, but becomes finer towards umbilicus. Suture line ceratitic with deep lobes; first and second lateral saddle slightly tapered asymmetrically.

Measurements. See Text-figs 33-34.

Discussion. This species is very similar to the slightly older *Flemingites hautmanni* described above, but differs by its more compressed whorls and its slightly stronger ribs.

Flemingites bhargavai Brühwiler, Ware, Bucher, Krystyn and Goudemand (submitted [b])

Plate 28, figure 1a-c

v subm. *Flemingites bhargavai* Brühwiler *et al.*

Occurrence. A single specimen from sample Nam543.

Description. Evolute, platyconic shell with convex flanks and maximum whorl width near mid-flank. Venter tabulate with subangular shoulders. Umbilicus wide and shallow with low, vertical wall and rounded shoulders. Flanks ornamented with distant, low ribs. Fine strigation on venter and flanks. Suture line not preserved.

Discussion. This species differs from other species of *Flemingites* by its evolute coiling and its tabulate venter. *Rohillites* differs by its narrower tabulate venter.

Flemingites planatus sp. nov.

Plate 26, figures 1-3

Derivation of name. Refers to the flat flanks of this species.

Holotype. Specimen PIMUZ 28016 (Pl. 26, fig. 1a-e).

Type locality. Chiddru, Salt Range, Pakistan.

Type horizon. Sample Chi52, base part of CM, *Flemingites planatus* beds.

Diagnosis. Evolute, compressed *Flemingites* with flat flanks and subtabulate venter.

Occurrence. Samples Chi52 and Chi63, base of CM, *Flemingites planatus* beds, Chiddru.

Description. Evolute, platyconic shell with flat, subparallel flanks and maximum whorl width near mid-flank. Outer third of flanks convergent. Venter tabulate with slightly rounded shoulders. Umbilicus wide and shallow with low, vertical wall and rounded shoulders. Flanks smooth except for very fine radial folds and fine strigation on outer flanks and venter. Suture line ceratitic with relatively long saddles; second lateral saddle slightly tapered.

Measurements. See appendix.

Discussion. This species is similar to *Flemingites bhargavai* but differs by its flat flanks.

Genus ROHILLITES Waterhouse, 1996*b*

Type species. *Flemingites rohilla* Diener, 1897.

Rohillites pakistanensis sp. nov.

Plate 25, figures 1-5

Derivation of name. Named after Pakistan.

Holotype. Specimen PIMUZ 28011 (Pl. 25, fig. 3a-e).

*Type locality***.** Chiddru, Salt Range, Pakistan.

Type horizon. Sample Chi1 (SFB), CM or CS, *Xenodiscoides perplicatus* beds.

Diagnosis. *Rohillites* with relatively strong radial ribbing and furrow on the flanks near the venter.

Occurrence. Abundant in sample Chi1 (SFB), CM or CS, *Xenodiscoides perplicatus* beds.

Description. Moderately involute, compressed shell with convex flanks and maximum whorl width slightly above mid-flank. On the flanks near the venter, a furrow is visible on the inner mould. Venter narrow and subtabulate with subangular shoulders. Umbilicus shallow with low vertical wall and slightly rounded shoulders. Ornamentation consists of radial folds and coarse strigation that becomes finer towards the umbilicus. Suture line ceratitic with relatively strongly indented lobes; saddles well-rounded with parallel sides.

Measurements. See Text-fig. 35.

Discussion. This species differs from *Rohillites rohilla* (Diener, 1897) by its stronger radial ribbing, its slightly thicker whorl section and its furrow on the flanks near the venter.

Genus SHAMARAITES Shigeta and Zakharov, 2009

Type species. *Anakashmirites shamarensis* Zakharov, 1968.

Shamaraites rursiradiatus sp. nov.

Plate 26, figure 4a-e

Derivation of name. Refers to the rursiradiate ornamentation of this species.

Holotype. Specimen PIMUZ 28019 (Pl. 26, fig. 4a-e).

Type locality. Chiddru, Salt Range, Pakistan.

Type horizon. Sample Chi53, base of CM, *Shamaraites rursiradiatus* beds.

Diagnosis. *Shamaraites* with rursiradiate ribbing.

Occurrence. A single specimen from the type horizon.

Description. Evolute, platyconic shell with slightly convex flanks. Venter broad and tabulate with marked, subangular shoulders. Umbilicus with vertical wall and marked but rounded shoulders. Ornamentation consists of distant rursiradiate ribs on inner whorls; outer whorls nearly smooth. Suture line ceratitic and simple with relatively deep lobes; first lateral saddles slightly tapered.

Measurements. See appendix.

Discussion. The type species *Shamaraites shamaraensis* from the early Smithian of South Primorye differs by its prorsiradiate ribbing.

?Flemingitidae gen. indet. A

Plate 26, figure 5a-b

Occurrence. Abundant but poorly preserved in a thin, marly limestone bed slightly below the middle of the CM at Nammal (samples Nam531, Nam534 and Nam546), associated with very abundant *Kashmirites* sp. indet.

Description. Moderately evolute, platyconic shell with convergent flanks. Venter narrow and tabulate. Umbilicus with low, vertical wall and rounded shoulders. Surface smooth. Suture line ceratitic but poorly preserved.

Discussion. The shape of this species is similar to that of *Rohillites*, but the poor preservation precludes a generic assignment.

?Flemingitidae gen. et sp. indet. B

Plate 26, figure 6a-d

Occurrence. A single specimen from sample Chi104, base of CM, *Flemingites planatus* beds, Chiddru.

Description. Moderately involute, compressed shell with convex flanks and maximum whorl width slightly above mid-flank. Venter subtabulate with slightly rounded shoulders. Umbilicus shallow with low, indistinct wall and rounded shoulders. Inner whorls ornamented with distant, broad folds; outer whorls with finer, biconcave folds. No strigation visible, but the surface is rather poorly preserved. Suture line ceratitic with weakly indented, narrow lobes.

Discussion. This specimen is similar to typical *Rohillites* such as *R. rohilla* (Diener, 1897) or *R. bruehwileri* Brayard and Bucher, 2008, but differs by its slightly rounded ventral shoulders and the apparent absence of strigation.

Genus ANAXENASPIS Kiparisova, 1956

Type species. *Xenaspis orientale* Diener, 1895.

Anaxenaspis nammalensis (Guex, 1978)

Plate 27, figures 1-6

v	1978	*Xenoceltites nammalensis* Guex, p. 112, pl. 6, figs 1-2.
v ?	2008	?*Anaxenaspis* sp. indet. Brayard and Bucher, p. 49, pl. 23, fig. 1a-b.

Occurrence. Samples Chi101, Chiddru; Nam8, Nam10, Nam68, Nammal; UCL, *Nyalamites angustecostatus* beds.

Description. Moderately evolute shell with an elliptical whorl section. Venter narrowly rounded with indistinct shoulders. Umbilicus with inclined wall and rounded shoulders. Inner whorls ornamented with radial folds that fade out towards the venter; outer whorls smooth. Growth lines slightly biconcave. Suture line ceratitic with slightly phylloid saddles and strongly indented lobes; third lateral saddle asymmetrical with denticulation ascending its dorsal side.

Measurements. See Text-fig. 36.

Discussion. Our material comes from the same horizon as the type material. Guex (1978) assigned this species to *Xenoceltites*, but that genus clearly differs by its simple suture line, its flattened flanks and its projected ornamentation. On the other hand, the type species of *Anaxenaspis* is very similar to our species and differs only by its smoother inner whorls. *Hochuliites retrocostatus* gen. et sp. nov. described below is very similar in shape, but differs by its much simpler suture line, whose saddles are low with parallel sides.

Genus PSEUDOFLEMINGITES Spath, 1930

Type species. *Pseudoflemingites timorensis* Spath, 1930 = *Ophiceras nopscanum* Welter, 1922, p. 104, pl. 4, figs 4-5 only.

Pseudoflemingites cf. *timorensis* Spath, 1930

Plate 28, figures 2-4; plate 29, figure 1a-b

? 1895 *Celtites laevigatus* Waagen, p. 86, pl. 7a, fig. 3.

Occurrence. Sample Chi53, base of CM, Chiddru, *Shamaraites rursiradiatus* beds.

Description. Moderately evolute shell with an elliptical whorl section. Venter narrowly rounded with indistinct shoulders. Umbilicus with low inclined wall and rounded shoulders. Ornamentation consists of low radial ribs. One specimen exhibits strong ribs on outer whorl resulting from an injury. Growth lines slightly biconcave. Suture line ceratitic with slightly tapered saddles.

Measurements. See appendix.

Discussion. The holotype of *Pseudoflemingites timorensis* from Timor is slightly more evolute than our specimens.

Genus XENODISCOIDES Spath, 1930

Type species. *Xenodiscus perplicatus* Frech, 1905.

Xenodiscoides perplicatus (Frech, 1905).

Plate 29, figures 2-7

1905 *Xenodiscus perplicatus* Frech, pl. 22, fig. 4.

Occurrence. Sample Chi1(SFB), CM or CS, Chiddru, samples Nam65and Nam532, middle part of CM, Nammal. *Xenodiscus perplicatus* beds.

Description. Moderately evolute, slightly compressed shell with convex flanks. Venter broad and tabulate with subangular shoulders. Umbilicus with vertical wall and marked but rounded shoulders. Ornamentation consists of distant, broad and strong ribs or bullae. Suture line ceratitic with long and slightly phylloid saddles; auxiliary series relatively short.

Measurements. See Text-figs 37-38.

Discussion. The possibility that *Xenodiscoides perplicatus*, *X. involutus* and *X. falcatum* (see below) represent variants of a single, highly variable species cannot be excluded. However, based on the measurements, *X. perplicatus* and *X. involutus* seem to form two distinct groups.

Xenodiscoides involutus (Frech, 1905)

Plate 30, figures 1-8

1905 *Xenodiscus perplicatus* var. nov. *involuta* Frech, pl. 22, fig. 3.

Occurrence. Sample Chi1(SFB), CM or CS, Chiddru; very abundant in sample Nam532, middle part of CM, Nammal. *Xenodiscus perplicatus* beds.

Description. Moderately involute, compressed shell with slightly convex flanks. Venter tabulate with subangular shoulders. Umbilicus with vertical wall and marked but rounded shoulders. Ornamentation consists of dense, fine, biconcave ribs. Suture line ceratitic with relatively short, non-phylloid saddles; auxiliary series longer than in *Xenodiscus perplicatus*.

Measurements. See Text-figs 37-38.

Xenodiscoides falcatum (Waagen, 1895)

Plate 29, figure 8a-e

1895 *Meekoceras falcatum* Waagen, p. 242, pl, 36, fig. 4a-c.
non? 1933 *Meekoceras* aff. *falcatum* Waagen; Collignon, p. 6, pl. 7, fig. 2.
? 1996*b* *Pseudoflemingites falcatus* (Waagen); Waterhouse, p. 157. pl. 10, fig. 3.

Occurrence. A single specimen from sample Chi1(SFB), CM or CS, *Xenodiscus perplicatus* beds, Chiddru.

Description. Moderately evolute, compressed shell with slightly convex flanks. Venter subtabulate with rounded shoulders. Umbilicus with vertical wall and marked but rounded shoulders. Ornamentation consists of biconcave ribs that fade out towards umbilicus and venter. Suture line ceratitic with relatively long saddles; auxiliary series relatively short.

Measurements. See Text-figs 37-38.

Discussion. Our single specimen exhibits a slight concavity along the umbilical margin, which may be due to compaction. With regard to ornamentation, this species is very similar to *Xenodiscoides involutus*, but it differs by its more evolute coiling.

The specimen from Madagascar described as *Meekoceras* aff. *falcatum* by Collignon (1933) probably belongs to *Koiloceras romanoi* gen. et sp. nov. (see above). The specimen from Nepal described as *Pseudoflemingites falcatus* by Waterhouse (1996*b*) is too poorly preserved for identification.

Family DIENEROCERATIDAE Kummel, 1952

Genus DIENEROCERAS Spath, 1934

Type species. *Ophiceras dieneri* Hyatt and Smith, 1905.

Dieneroceras sp. indet. A

Plate 28, figure 6a-e

Occurrence. A single small specimen from sample Nam19; middle part of UCL, *Pseudoceltites multiplicatus* beds, Nammal.

Description. Very evolute serpenticonic shell with rectangular whorl section. Venter broad and tabulate with subangular shoulders. Umbilicus wide and shallow with rounded umbilical wall. Surface smooth. Suture line imperfectly known; showing only two lateral saddles; apparently goniatitic.

Measurements. See appendix.

Discussion. The scarcity of our material precludes a specific assignment.

Dieneroceras sp. indet. B

Plate 28, figure 5a-d

Occurrence. A single small specimen from sample Nam16; middle part of UCL, *Pseudoceltites multiplicatus* beds, Nammal.

Description. Very evolute serpenticonic shell with convex flanks. Venter broad and tabulate with slightly rounded shoulders. Umbilicus wide and shallow with rounded umbilical wall. Surface smooth. Suture line imperfectly known; shows only two lateral saddles; apparently goniatitic.

Measurements. See appendix.

Discussion. The scarcity of our material precludes a specific assignment. *Dieneroceras* sp. indet. A described above differs by its more compressed whorl section and its flat flanks.

Family ARCTOCERATIDAE Arthaber, 1911

Genus BRAYARDITES Brühwiler, Bucher and Goudemand (accepted)

Type species. *Brayardites crassus* Brühwiler, Bucher and Goudemand (accepted)

Brayardites compressus Brühwiler, Bucher and Goudemand (accepted)

Plate 31, figures 1-8

v acc. *Brayardites compressus* Brühwiler *et al.* fig. 18(1-6).

Occurrence. Samples Nam15, Nam22, Nam39(?), Zal52; *Brayardites compressus* beds, UCL.

Description. Moderately evolute, compressed shell with flat, convergent flanks. Maximum whorl width at lowermost flanks near umbilical shoulder. Venter subtabulate with rounded shoulders. Umbilicus with high, steeply inclined wall and rounded shoulders. Ornamentation consists of prorsiradiate, biconcave ribs that develop strong tubercles near umbilicus and fade out towards mid-flank. Growth lines biconcave. Suture line ceratitic with relatively deep lobes and broad saddles.

Measurements. See Text-fig. 39.

Discussion. *Ceratites sagitta* Waagen, 1895 from the lower part of the Upper Ceratite Limestone has a similar ornamentation. Apparently, it differs by a rounded umbilical margin, but the preservation of Waagen's single specimen is insufficient for comparison. Two species of *Brayardites* (*B. crassus* and *B. compressus*) co-occur in South Tibet (Brühwiler *et al.*, accepted).

Genus NAMMALITES Brühwiler, Bucher and Goudemand (accepted)

Type species. *Kazakhstanites pilatoides* Guex, 1978.

Nammalites pilatoides (Guex, 1978)

Plate 32, figures 1-4

1909 *Meekoceras* sp. ind. aff. *pilato* Krafft and Diener, p. 42, pl. 28, fig. 2a-c.

1968 *Subvishnuites* cf. *enveris* (Arthaber); Kummel, p. 491, pl. 1, figs 8-9.
1968 *Wasatchites* sp. indet. Kummel, p. 500, pl. 3, figs 10-11.
1968 *Eoptychites* sp. indet. Kummel and Erben, p. 120, pl. 22, figs 10-11.
v 1978 *Kazakhstanites pilatoides* Guex, p. 109, pl. 6, fig. 5, 6, 16.
v ? 1978 *Kazakhstanites pilatoides* Guex, p. 109, pl. 8, fig. 6.
v p 1978 *Anasibirites pluriformis* Guex, pl. 4, fig. 3 only.
v acc. *Nammalites pilatoides* (Guex); Brühwiler *et al.* fig. 21 (6-8).
v subm. *Nammalites pilatoides* (Guex); Brühwiler and Bucher.

Occurrence. Samples Chi13, Nam5, Nam18, Nam21, Zal53; *Nammalites pilatoides* beds, UCL.

Description. Moderately involute, compressed shell with convex, convergent flanks. Maximum whorl width at umbilical border. Venter subtabulate with rounded shoulders. Umbilicus with vertical wall and rounded shoulders. Ornamentation consists of rursiradiate ribs that tend to develop tubercles or elongated bullae near the umbilicus and then fade out towards the venter. Suture line ceratitic with deep lobes and slightly tapered saddles.

Measurements. See appendix.

Genus TRUEMPYCERAS gen. nov.

Derivation of name. Named after Daniel Trümpy (Zürich).

Type species. *Anasibirites pluriformis* Guex 1978.

Composition of the genus. Type species only.

Diagnosis. Arctoceratidae with a subtabulate venter; ornamented with strong, slightly biconcave ribs that thicken at ventral shoulders.

Discussion. The type species was attributed to *Anasibirites* by Guex (1978). However, typical *Anasibirites* as well as all other Prionitidae differ strongly by having an umbilicus with an inclined wall and well-rounded shoulders. Moreover, *Anasibirites* is of late Smithian age (e.g. Tozer 1994; Brayard and Bucher 2008; Brühwiler *et al.* 2007), whereas *Truempyceras* is restricted to the middle Smithian. *Truempyceras* is here provisionally assigned to Arctoceratidae based on its overall similarity with *Brayardites* and its similar shell geometry with *Arctoceras* Hyatt, 1900.

Truempyceras pluriformis (Guex 1978)

Plate 32, figures 5-7; plate 33, figures 1-3

v, p 1978 *Anasibirites pluriformis* Guex, p. 107, pl. 3, figs 7-9; pl. 4, figs 1-2, 4, 7-8 only; pl. 5, figs 6-7.

1985 *Anasibirites* sp. Pakistani-Japanese Research Group, pl. 14, fig. 1a-b.

v acc. *"Anasibirites" pluriformis* Guex; Brühwiler *et al.* fig. 6(8a-c).

Occurrence. Samples Chi13, Chi102, Chi105, Nam18, Nam19, Nam23; *Nammalites pilatoides* beds, UCL.

Description. Moderately involute to moderately evolute shell with flat, slightly convergent flanks. Venter subtabulate to slightly arched with narrow, rounded shoulders. Umbilicus with a high, vertical wall and marked, slightly rounded shoulders. Ornamentation consists of radial, slightly biconcave ribs that strengthen and form a marginal tuberculation. Strongest ribs cross the venter. Suture line ceratitic with relatively deep lobes and tapered saddles.

Measurements. See Text-fig. 40.

?Arctoceratidae gen. et sp. indet.

Plate 7, figure 1a-d

Occurrence. Sample Zal50, upper part of CS, *Flemingites flemingianus* beds, Zaluch.

Description. Moderately involute, compressed shell with nearly flat, slightly convex flanks. Venter subtabulate with rounded shoulders. Umbilicus with high, vertical wall and slightly angular shoulders. Surface smooth. Suture line ceratitic; saddles well-rounded and very slightly tapered.

Measurements. See appendix.

Discussion. Shape and suture line of this species are similar to those of some Arctoceratidae such as *Arctoceras* or *Submeekoceras*. These two genera differ by their rounded venter. *Urdyceras* differs by its more angular ventral shoulders and its suture line with long saddles.

Familiy USSURIIDAE Spath, 1930

Ussuriidae gen. et sp. indet.

Plate 32, figure 8a-c

Occurrence. A single, poorly preserved specimen from sample Chi105, UCL, Chiddru, *Nammalites pilatoides* fauna.

Description. Very involute, compressed oxycone with slightly convex flanks. Maximum thickness near umbilicus. Whorls increasing rapidly in height. Venter not preserved. Surface poorly preserved. Suture line ammonitic, imperfectly preserved.

Discussion. The ammonitic suture line and the shape of our specimen favor assignment to *Metussuria* Spath, 1934 or *Parussuria* Spath, 1934. *Parussuria* differs from *Metussuria* by its strigation, but otherwise these two genera are very similar and may in fact be synonyms. The poor preservation of our single specimen precludes an identification at the species level.

Family PRIONITIDAE Hyatt, 1900

Genus PRIONITES Waagen, 1895

Type species. *Prionites tuberculatus* Waagen, 1895.

Prionites tuberculatus Waagen, 1895

Plate 34, figures 1-8; plate 35, figure 1-3

1895 *Prionites tuberculatus* Waagen, p. 58, pl. 5, fig. 2a-c.
1895 *Prionites undatus* Waagen, p. 59, pl. 5, fig. 1a-b.
1895 *Prionites lingnatus* Waagen, p. 61, pl. 6, fig. 3-5.
1922 *Prionites laevis* Welter, p. 134, pl. 12, figs 8-10.
1922 *Prionites armatus* Welter, p. 135, pl. 12, figs 11-13.
1922 *Prionites elegans* Welter, p. 136, pl. 12, figs 14-16.

Occurrence. Very abundant in samples Chi5, Chi101, Chiddru; and Nam8, Nam68, Nammal; UCL, *Nyalamites angustecostatus* beds.

Description. Involute shell with eggressive coiling at maturity. Maximum whorl width at upper third of flank. Venter tabulate with angular shoulders on inner whorls, subtabulate with rounded shoulders on outer whorls. Umbilicus deep and funnel-shaped with inclined wall and rounded shoulders. Inner whorls smooth, outer whorls with prorsiradiate, distant bullae on inner flank that develop into strong, broad tubercles on some specimens. Growth lines biconcave. Suture line ceratitic with broad saddles; third lateral saddle very low.

Measurements. See Text-figs 41-42.

Prionites nammalensis sp. nov.

Plate 35, figures 4-9

Derivation of name. Named after the type locality.

Holotype. Specimen PIMUZ 28081, Plate 35, figure 6a-c.

Type locality. Nammal, Salt Range, Pakistan.

Type horizon. Sample Nam16; UCL, *Pseudoceltites multiplicatus* beds.

Diagnosis. Relatively evolute and smooth *Prionites* whose compressed whorl section persists to maturity.

Occurrence. Very abundant in samples Nam9, Nam16, UCL, *Pseudoceltites multiplicatus* beds, Nammal.

Description. Moderately involute, compressed shell with eggressive coiling at maturity and convex, convergent flanks. Maximum whorl width at upper third of flank. Venter tabulate with angular shoulders. Umbilicus funnel-shaped with inclined wall and rounded shoulders. Inner whorls smooth, outer whorls with low, prorsiradiate, distant wavy folds on lower flanks. Growth lines biconcave. Suture line ceratitic with moderately long saddles; auxiliary series relatively long.

Measurements. See Text-figs 42-43.

Discussion. This species is slightly older than *Prionites tuberculatus* and differs by its more evolute coiling, its more compressed outer whorls and its suture line with deeper lobes. It is considerably more evolute than *Prionites involutus* Brühwiler *et al.*, accepted from the *Nyalamites angustecostatus* beds at Tulong (South Tibet).

Genus MEEKOCERAS Hyatt, 1879

Type species. *Meekoceras gracilitatis* White, 1879.

Discussion. The genus *Meekoceras* was previously included in the family Meekoceratidae Waagen, 1895 (e.g. Tozer, 1994). Apart from *Meekoceras* of middle Smithian age, this family contains only Dienerian genera (e.g. *Ambites*, *Gyronites*, *Meekophiceras*, *Pleurambites*, *Pleurogyronites* and *Prionolobus*). On the other hand, *Meekoceras* shares the following important characters with Prionitidae: a compressed whorl shape (e.g. like *Prionites nammalensis* sp. nov.), a suture line with low, broad saddles, and an umbilicus with an inclined wall. On the basis of these similarities, *Meekoceras* is herein assigned to Prionitidae, and the family Meekoceratidae is herein no longer regarded as a valid taxon. The Dienerian genera that have been included in Meekoceratidae are herein treated as members of the family Gyronitidae Waagen, 1895. Any possible phylogenetic relationship between the Dienerian Gyronitidae and the middle-late Smithian Prionitidae has yet to be established. Their superficial similarities are here interpreted as the result of convergence.

Meekoceras cf. *gracilitatis* White, 1879
Plate 36, figures 1-7

v, ? 1978 *Meekoceras gracilitatis* White; Guex, pl. 1, fig. 8.
v 1978 *Meekoceras* sp. A Guex, pl. 1, fig. 9.

Occurrence. Abundant in the *Nammalites pilatoides* beds (middle part of UCL) at Chiddru (sample Chi105), at Nammal (samples Nam5, Nam18, Nam21) and at Zaluch (sample Zal53).

Description. Moderately involute, compressed shell with slightly convex flanks. Venter is narrow and sulcate with angular shoulders. Umbilicus with inclined wall and rounded shoulders. Surface smooth. Suture line ceratitic with broad saddles; third lateral saddle broad and low.

Measurements. See appendix.

Discussion. *Meekoceras gracilitatis* from the USA (Hyatt and Smith 1905, Smith 1932, Kummel and Steele 1962) is slightly more involute than our species, but otherwise, it is very similar.

Genus STEPHANITES Waagen, 1895

Type species. *Stephanites superbus* Waagen, 1895.

Discussion. *Stephanites* differs from the younger *Wasatchites* by the dorso-ventral elongation of its tubercles (especially on inner whorls). Additionally, *Wasatchites* has more compressed and smoother inner whorls. Otherwise, these two genera are very similar; therefore, *Stephanites* is herein assigned to Prionitidae. The outer whorls of *Stephanites* are also similar to robust variants of *Prionites tuberculatus*, but the inner whorls of *Stephanites* are much thicker and more coarsely ornamented than those of *Prionites*.

Stephanites superbus Waagen, 1895

Plate 37, figures 1-3

1895 *Stephanites suberbus* Waagen, p. 101, pl. 2, fig. 2a-c.
1895 *Stephanites corona* Waagen, p. 102, pl. 3, fig. 1a-b.
1905 *Stephanites corona* Waagen; Frech, pl. 28, fig. 1.
v, non 1978 *Stephanites corona* Waagen; Guex, pl. 5, fig. 2 (= *Wasatchites distractus*).
v acc. *Stephanites superbus* Waagen, 1895; Brühwiler *et al.*, fig. 19(7-12).

Occurrence. Samples Chi101, Nam68; (*Nyalamites angustecostatus* beds).

Description. Moderately involute shell with convex, convergent flanks. Maximum whorl width slightly above mid-flank. Venter broad and subtabulate with rounded shoulders. Umbilicus deep with well-rounded, inclined wall without distinct shoulders. Ornamentation consists of strong, distant tubercles on flanks, coincinding with maximum whorl width. Tubercles are elongated dorso-ventrally. Suture line with very broad first lateral saddle and very low third lateral saddle. Indentations of lobes not preserved.

Measurements. See appendix.

Discussion. The specimen described as *Stephanites corona* by Guex (1978) from the upper part of the UCL at Zaluch probably belongs to *Wasatchites distractus* (Waagen, 1895) (see below).

Genus PUNJABITES gen. nov.

Derivation of name. Named after the Pakistani Punjab Province.

Type species. *Punjabites punjabiensis* gen. et sp. nov.

*Composition of the genus***.** Type species only.

Diagnosis. Prionitidae with prorsiradiate ribs that thicken near umbilicus and fade out towards lower flanks.

Discussion. The ornamentation of this new genus closely resembles that of *Nammalites* (see above), but its umbilicus and suture line clearly show that it belongs to Prionitidae. Its shell shape is close to that of inner whorls of Wasatchites, but without spines and ventral ribs.

Punjabites punjabiensis gen. et sp. nov.

Plate 37, figure 4a-d

Derivation of name. Named after the Pakistani Punjab Province.

Holotype. Specimen PIMUZ 28094 (Plate 37, figure 4a-d).

Type locality. Nammal, Salt Range, Pakistan.

Type horizon. Sample Nam9, UCL, *Pseudoceltites multiplicatus* beds.

Diagnosis. As for the genus.

Occurrence. A single specimen from sample Nam9, UCL, *Pseudoceltites multiplicatus* beds.

Description. Moderately involute shell with convex and convergent flanks. Maximal whorl width above mid-flank. Venter subtabulate with rounded shoulders. Umbilicus deep with well-rounded, inclined wall and indistinct shoulders. Ornamentation consists of prorsiradiate ribs that thicken slightly above mid-flank and fade out before reaching the venter. Venter smooth. Suture line weakly ceratitic and simple with low, slightly flattened saddles.

Measurements. See appendix.

Genus WASATCHITES Mathews, 1929

Type species. *Wasatchites perrini* Mathews, 1929.

Wasatchites distractus (Waagen, 1895)

Plate 37, figures 5-8; plate 38, figures 1-7

1895 *Acrochordiceras distractum* Waagen, p. 94, pl. 3, fig. 4a-c.

1895 *Acrochordiceras coronatum* Waagen, p. 96, pl. 3, fig. 5a-c.

1895 *Acrochordiceras* cf. *damesi* Noetling; Waagen, p. 97, pl. 4, fig. 5a-b.

1895 *Acrochordiceras compressum* Waagen, p. 98, pl. 4, fig. 4a-c.

? 1909 *Sibirites* sp. indet. aff. *inflato* Waagen; Krafft and Diener, p. 134, pl. 27, fig. 7.

p 1909 *Sibirites* sp. indet. Krafft and Diener, p. 138, pl. 28, fig. 4a-c.

v ? 1978 *Stephanites corona* Waagen; Guex, pl. 5, fig. 2.

v acc. *Wasatchites distractus* (Waagen); Brühwiler *et al.* fig. 21(1a-b).

Occurrence. Samples Nam6, Nam17, Nam25, Nam38 (*Wasatchites distractus* beds).

Description. Moderately involute shell with eggressive coiling at maturity. Flanks nearly flat, slightly convex and convergent on inner whorls; strongly convex on outer whorls. Maximum whorl width at mid-flank. Venter tabulate with rounded shoulders on inner whorls; broadly rounded with indistinct shoulders on outer whorls. Umbilicus deep with well-rounded, inclined wall and indistinct shoulders. Ornamentation consists of spiny tubercles at mid-flank as well as strong radial ribs that gain in strength as they cross the venter. Suture line ceratitic; first and second lateral saddles broad and tapered; third lateral saddle broad and low.

Measurements. See Text-fig. 44.

Discussion. The boreal *Wasatchites* (e.g. *W. perrini* Spath, 1934) essentially differs from *W. distractum* by the more umbilical position of its spines.

Genus ANASIBIRITES Mojsisovics, 1896

Type species. *Sibirites kingianus* Waagen, 1895, p. 108, pl. 8, figs 1a-c, 2a-c.

Discussion. Due to the extreme intraspecific variation of ornamentation, the differentiation of species belonging to *Anasibirites* is difficult, and consequently, the genus has been splitted into a large number of species (e.g. Waagen, 1895; Mathews, 1929). A comprehensive study led Brayard and Bucher (2008) to suggest the existence of four main species: (i) *A. kingianus* Waagen, 1895, mainly differentiated by its arched venter, (ii) *A. pluriformis* Guex, 1978, which is herein transferred to *Truempyceras* gen. nov. on account of its different umbilicus (see above), (iii) *A. multiformis*, distinguished by its tabulate venter and its dense, concave, forward projected growth lines and fine ribs on all growth stages, and (iv) *A. nevolini* (Burij and Zharnikova 1968), distinguished by its regular alternation of concave weak and strong ribs. Upon examination of our new material from the Salt Range, it has become apparent that yet another species can be separated: namely, *A. angulosus* Waagen, 1895, distinguished by its tabulate venter and its ornamentation, which consists of biconcave ribs of highly varying strength. On adult specimens, its ribs thicken at mid-flank, forming elongated tubercles.

Anasibirites kingianus (Waagen, 1895)

Plate 39, figures 1-5

1895 *Sibirites kingianus* Waagen, p. 108, pl. 8, figs 1-2.
1895 *Sibirites chidruensis* Waagen, p. 109, pl. 8, figs 3-4.
1895 *Sibirites inaequicostatus* Waagen, p. 113, pl. 8, figs 7-8.
? 1895 *Sibirites ceratitoides* Waagen, p. 115, pl. 8, fig. 10a-c.
1909 *Sibirites spiniger* Krafft and Diener, p. 131, pl. 31, figs 2, 7.
1909 *Sibirites robustus* Krafft and Diener, p. 132, pl. 31, fig. 1.
? 1909 *Sibirites* sp. ind. ex aff. *robusto* Krafft and Diener, p. 133, pl. 31, fig. 6.
? 1909 *Sibirites spitiensis* Krafft and Diener, p. 136, pl. 31, fig. 8.
p 1909 *Sibirites* sp. indet. Krafft and Diener, p. 138, pl. 31, figs 4-5.
1929 *Anasibirites kingianus* (Waagen); Mathews, p. 8, pl. 7, figs 14-22.

1968 *Anasibirites kingianus* Waagen; Kummel and Erben, p. 135, pl. 22, figs 12-17; pl. 23, figs 1-18.

v 1978 *Anasibirites kingianus* (Waagen); Guex, pl. 3, fig. 2, 9, pl. 4, fig. 6.

Occurrence. Samples Nam6 and Nam25, UCL, *Wasatchites distractus* beds, Nammal.

Description. Moderately involute shell with convex, slightly compressed flanks. Venter low, arched with rounded shoulders. Umbilicus with inclined wall and rounded shoulders. Ornamentation consists of biconcave, projected ribs of varying strength that cross the venter.
Suture line with tapered saddles, poorly preserved.

Measurements. See Text-fig. 45.

Anasibirites angulosus (Waagen 1895)

Plate 39, figures 6-7; plate 40, figures 1-7; plate 41, figures 1-5

1895 *Sibirites angulosus* Waagen, p. 117, pl. 8, figs 12-13.

1895 *Sibirites ibex* Waagen, p. 121, pl. 9, fig. 3a-c.

1895 *Sibirites hircinus* Waagen, p. 123, pl. 9, fig. a-b.

Occurrence. Samples Nam6, Nam17, Nam701, UCL, *Wasatchites distractus* beds, Nammal.

Description. Slightly compressed shell with convex, flanks. Amount of involution varies from involute to moderately evolute. Venter tabulate with angular shoulders, becoming slightly rounded on outer whorls. Umbilicus with inclined wall and rounded shoulders. Ornamentation consists of biconcave ribs of highly variable strength. Ornamentation is strong on inner whorls and becomes finer throughout ontogeny, but on evolute adult specimens, ribs thicken at mid-flank, forming elongated tubercles. Suture line ceratitic with tapered first and second lateral saddle; third lateral saddle low, broad and asymmetrical.

Measurements. See Text-fig. 46.

Discussion. Involute variants of *Anasibirites angulosus* exhibit very weak ornamentation, whereas ornamentation on evolute variants is much stronger. This type of covariation is well known as Buckman's first law of covariation (Westermann 1966; Hammer and Bucher 2005).

Genus HEMIPRIONITES Spath, 1929

Type species. *Goniodiscus typus* Waagen, 1895.

Hemiprionites typus (Waagen, 1895)

Plate 42, figures 1-10

1895 *Goniodiscus typus* Waagen, p. 128, pl. 9, figs 7-10.
1929 *Goniodiscus typus* Waagen; Mathews, p. 31, pl. 5, figs 12-21.
1929 *Goniodiscus americanus* Mathews, p. 32, pl. 5, figs 22-27.
1929 *Goniodiscus shumardi* Mathews, p. 33, pl. 6, figs 11-14.
1929 *Goniodiscus utahensis* Mathews, p. 33, pl. 6, figs 29-31.
1929 *Goniodiscus ornatus* Mathews, p. 34, pl. 6, figs 6-9.
1934 *Hemiprionites typus* (Waagen); Spath, p. 33, fig. 114a-c.

Occurrence. Abundant in samples Nam6, Nam17, Nam701, UCL, *Wasatchites distractus* beds, Nammal.

Description. Moderately involute, compressed shell. Flanks convex and slightly convergent except for a concavity near the venter. Venter subtabulate with angular or slightly rounded shoulders, and ornamented with indistinct spiral lines, which sometimes give the impression of faint keels. Umbilicus deep with well-rounded, inclined wall with rounded shoulders. Ornamentation consists of low radial folds on inner flanks. Growth lines biconcave and projected. Suture line ceratitic with strongly tapered first and second lateral saddles.

Measurements. See Text-fig. 47.

Hemiprionites klugi Brayard and Bucher, 2008

Plate 41, figures 6-9

v 2008 *Hemiprionites klugi* Brayard and Bucher, p. 59, pl. 30, figs 1-4, text-fig. 51.

Occurrence. Sample Nam701, UCL, *Wasatchites distractus* beds, Nammal.

Description. Very involute and platyconic shell with convergent flanks. Maximum whorl width near umbilicus. Venter narrow and tabulate with angular shoulders. Umbilicus small and deep with well-rounded, inclined wall with indistinct shoulders. Surface smooth. Suture line with tapered first and second lateral saddle; third lateral saddle low and broad; indentations of lobes not preserved.

Measurements. See Text-fig. 48.

?Hemiprionites sp. indet.

Plate 42, figure 11a-e

Occurrence. A single specimen from sample Nam17; UCL, Nammal, *Wasatchites distractus* beds.

Description. Involute, compressed shell with convex, convergent flanks. Maximum whorl width near umbilicus. Venter narrow and tabulate with angular shoulders. Umbilicus small and deep with well-rounded, inclined wall with indistinct shoulders. Surface smooth. Suture line ceratitic with tapered first and second lateral saddle; third lateral saddle low, broad and asymmetrical.

Measurements. See appendix.

Discussion. This specimen has a narrower venter than *Hemiprionites typus* and lacks the concavity on lowermost flanks.

Family MELAGATHICERATIDAE Tozer, 1971

Genus JUVENITES Smith, 1927

Type species. *Juvenites kraffti* Smith, 1927.

Juvenites cf. *kraffti* Smith, 1927

Plate 42, figure 17a-e

v 1978 *Juvenites* sp. ind. Guex, pl. 5, fig. 3.
v 2008 *Juvenites* cf. *kraffti* Smith; Brayard and Bucher, p. 32, pl. 9, figs 20-23.

Occurrence. Rare in sample Nam5, UCL, *Nammalites pilatoides* beds.

Description. Moderately evolute shell with strongly depressed whorl. Venter arched with indistinct shoulders. Umbilicus with steep wall and rounded shoulders. Ornamentation consists of distinct, slightly projected constrictions. Suture line slightly weathered; apparently goniatitic with only two lateral saddles; saddles tapered.

Measurements. See appendix.

Discussion. The scarcity of our material hinders a definitive specific assignment.

Juvenites sp. indet.

Plate 42, figures 12-15

Occurrence. Samples Nam15, Nam22, Zal52(?), lower part of UCL, *Brayardites compressus* beds.

Description. Globose, moderately involute conch with depressed whorls. Flanks slightly flattened, forming an obtuse angle with the venter, which is broadly rounded. Umbilicus deep with perpendicular wall and marked but slightly rounded umbilical shoulders. Ornamented with strong, prorsiradiate, concave constrictions that cross the venter. Suture line ceratitic with relatively broad, slightly tapered saddles; third lateral saddle very low.

Measurements. See Text-fig. 49.

Discussion. This species differs from other representatives of *Juvenites* by its flattened flanks. *Juvenites spathi* (Frebold, 1930) differs by its inclined umbilical wall and its triangular outer whorls. *Juvenites* cf. *kraffti* described above is more evolute and more compressed laterally.

Family PARANANNITIDAE Tozer, 1971

Genus OWENITES Hyatt and Smith, 1905

Type species. *Owenites koeneni* Hyatt and Smith, 1905.

Owenites sp. indet.

Plate 42, figure 16a-c

Occurrence. A single, very small specimen from sample Nam8, UCL, *Nyalamites angustecostatus* beds, Nammal.

Description. Very involute, subglobose shell. Suture line goniatitic with three lateral saddles; auxiliary series with a fourth saddle.

Discussion. The globose shape and the suture line with four saddles suggest an assignment to *Owenites*. However, the very small size of our specimen precludes an identification at the species level.

Family INYOITIDAE Spath, 1934

Genus HOCHULIITES gen. nov.

Derivation of name. Named after Peter A. Hochuli (Zürich).

Type species. *Hochuliites retrocostatus* gen. et sp. nov.

Composition of the genus. Type species only.

Diagnosis. Moderately evolute Meekocerataceae with elliptical whorl section and folds on upper flank. Suture line with narrow lobes; saddles low and broad with parallel sides.

Discussion. In shape this genus closely resembles some Flemingitidae such as *Anaxenaspis*. However, its suture line differs greatly from this group. Shell geometry and ornamentation of *Hochuliites* also resemble that of *Subvishnuites* and *Inyoites*, and thus this genus is provisionally assigned to Inyoitidae.

Hochuliites retrocostatus gen. et sp. nov.

Plate 44, figures 1-4

v acc. *?Anaxenaspis* sp. indet. B Brühwiler *et al*., fig. 12(3-7).

Derivation of name. Refers to the rursiradiate ornamentation.

Holotype. Specimen PIMUZ 28153, (Pl. 44, fig. 2a-d).

Type locality. Nammal, Salt Range, Pakistan.

Type horizon. Sample Nam9, UCL, *Pseudoceltites multiplicatus* beds.

Diagnosis. As for the genus.

Occurrence. Nam9, Nam16, UCL, *Pseudoceltites multiplicatus* beds, Nammal.

Description. Moderately evolute, compressed shell with an elliptical whorl section. Venter narrowly rounded with indistinct shoulders. Umbilicus with inclined wall and rounded shoulders. Ornamentation consists of rursiradiate folds on upper flanks that fade out below mid-flank. Growth lines biconcave. Suture line ceratitic with shallow, narrow lobes; saddles low and broad with parallel sides.

Measurements. See appendix.

Discussion. This species was recently described from the *Pseudoceltites multiplicatus* beds of Tulong (South Tibet) (Brühwiler *et al.*, accepted). However, since the suture lines are not preserved on the Tibetan material, the species was provisionally assigned to *Anaxenaspis*.

Genus SUBINYOITES Spath, 1930

Type species: *Inyoites kashmiricus* Diener, 1913.

Subinyoites punjabiensis sp. nov.

Plate 43, figures 6-7

Derivation of name. Named after the Pakistani Punjab Province.

Holotype. Specimen PIMUZ 28150 (Pl. 43, fig. 6a-d).

Type locality. Nammal, Salt Range, Pakistan.

Type horizon. Sample Nam25, UCL, *Wasatchites distractus* beds.

Diagnosis. *Subinyoites* with a very weak ornamentation and a slightly phylloid suture line.

Occurrence. Samples Nam25 and Nam38, UCL, *Wasatchites distractus* beds, Nammal.

Description. Moderately involute shell with an elliptical whorl section. Venter narrowly rounded with indistinct shoulders. Umbilicus with inclined wall and rounded shoulders. Surface smooth except for slightly biconcave growth lines and faint folds. Suture line ceratitic with broad lobes; first lateral saddle slightly phylloid, second saddle slightly tapered.

Discussion. *Subinyoites kashmiricus* (Diener, 1897) is similar in shape, but differs by its stronger ornamentation and its suture line, which has a broader, non-phylloid first lateral saddle. On account of these differences in suture lines, the assignment of our new species to *Subinyoites* is tentative only. The holotype of *S. kashmiricus* was found in a loose block that is probably derived from the "*Ophiceras* layer" in Kashmir (Diener 1913). The ammonoids from this layer described as *Ophiceras* by Diener most probably belong to *Xenoceltites*, and since the same layer also contains *Glyptophiceras*, *S. kashmiricus* therefore, is probably of late Smithian age as is our newly described species.

Family incertae sedis

Gen. et sp. indet "Acro "

Plate 43, figure 1a-d

Occurrence. A single fragmentary, but well preserved specimen from sample Zal50, upper part of CS, *Flemingites flemingianus* beds, Zaluch.

Description. Shell is probably moderately evolute with depressed, stongly convex flanks. Maximum whorl width above mid-flank. Venter broadly rounded with indistinct shoulders. Umbilicus with rounded shoulders. Venter ornamented with plicate ribs that fade out towards the umbilicus. Suture line not completely known; preserved portion is ceratitic with strongly indented lobes and phylloid first and second lateral saddles.

Discussion. Our specimen exhibits a remarkable resemblance to the late Spathian-Anisian Acrochordiceratidae with regard to ornamentation as well as suture line (Monnet *et al.* in press). The suture line of this specimen is similar to that of Flemingitidae and Proptychitidae, but its plicate ribbing clearlyexcludes all members of these families. Some Prionitidae of younger age such as *Wasatchites* are somewhat similar in ornamentation, but they have a completely different suture line. Because of the fragmentary preservation of our single specimen, we choose not to erect a new taxon.

Superfamily SAGECERATACEAE Hyatt, 1884

Family HEDENSTROEMIIDAE Waagen, 1895

Genus HEDENSTROEMIA Waagen, 1895

Type species. *Ceratites hedenstroemi* Keyserling, 1845.

Hedenstroemia evoluta (Spath 1934)

Plate 45, figures 1-5

1905 *Hedenstroemia mojsisovicsi* Diener; Frech, pl. 27, fig. 4.
1934 *Anahedenstroemia evoluta* Spath, p. 219, pl. 6, fig. 6.

Occurrence. Samples Chi2 and Chi56a, Chiddru; samples Nam78 and Nam132, Nammal; samples Zal50 and Zaluch. *Flemingites flemingianus* beds, upper part of CS. A large specimen was found as a float in the Ceratite Sandstone at Chiddru.

Description. Very involute shell with eggressive coiling on outer whorls. Flanks convergent. Venter narrow and weakly bicarinate on inner whorls, becomes rounded on outer whorls. Umbilicus small and deep with vertical wall and angular shoulders. Surface smooth. Suture line ceratitic and complex with one adventitious lobe and a long, well individualized auxiliary series.

Measurements. See appendix.

Discussion. As already described by Spath (1934), this species differs from *Hedenstroemia himalayica* (Diener 1897) by the eggressive coiling of its outer whorls.

Genus PSEUDOSAGECERAS Diener, 1895

Type species. *Pseudosageceras* sp. indet. Diener, 1895.

Pseudosageceras multilobatum Noetling, 1905

Plate 46, figures 1-4

1895 *Pseudosageceras* sp. indet. Diener, p. 28, pl. 1, fig. 8.

1905 *Pseudosageceras multilobatum* Noetling, pl. 23, figs 4-5; pl. 25, figs 1a, b; pl. 26, figs 3a, b.

1905 *Pseudosageceras intermontanum* Hyatt and Smith, p. 99, pl. 4, figs 1-3; pl. 5, figs 1-6; pl. 63, figs 1-2.

1909 *Pseudosageceras multilobatum* Noetling; Krafft and Diener, p. 145, pl. 21, fig. 5.

1911 *Pseudosageceras multilobatum* Noetling; Wanner, p. 181, pl. 7, fig. 4.

1911 *Pseudosageceras drinense* Arthaber, p. 201, pl. 17, figs 6, 7.

1913 *Pseudosageceras clavisellatum* Diener, p. 28, pl. 4, figs 5-6.

1922 *Pseudosageceras multilobatum* Noetling; Welter, p. 94, fig. 3.

1929 *Pseudosageceras intermontanum* Hyatt and Smith; Mathews, p. 3, pl. 1, figs 18-22.

1932 *Pseudosageceras multilobatum* Noetling; Smith, p. 87-89, pl. 4, figs 1-3; pl. 5, figs 1-6; pl. 25, figs 7-16; pl. 60, fig. 32; pl. 63, figs 1-6.

1933 *Pseudosageceras multilobatum* Noetling; Collignon, p. 56-58, pl. 11, fig. 2.

1934 *Pseudosageceras multilobatum* Noetling; Spath, p. 54, fig. 6a.

1947 *Pseudosageceras multilobatum* Noetling; Kiparisova, p. 127, Pl. 25, figs 3-4.

1947 *Pseudosageceras multilobatum* var. *giganteum* Kiparisova, p. 127, pl. 26, figs 2-5.

1948 *Pseudosageceras* cf. *P. clavisellatum* Diener; Renz and Renz, p. 90, pl. 16, fig. 3.

1948 *Pseudosageceras drinense* Arthaber; Renz and Renz, p. 92, pl. 16, fig. 6.

1948 *Pseudosageceras intermontanum* Hyatt and Smith; Renz and Renz, p. 90-92, pl. 16, figs 4, 7

1959 *Pseudosageceras multilobatum* Noetling; Chao, p. 183, pl. 1, figs 9, 12.

1959 *Pseudosageceras curvatum* Chao, p. 184, pl. 1, figs 13, 14, text-fig. 5a.

1959 *Pseudosageceras tsotengense* Chao, p. 184, pl. 1, Figs 7, 8, text-fig. 5b.

? 1959 *Pseudosageceras multilobatum* var. nov. Jeannet, p. 30, pl. 6, fig. 1.

1961 *Pseudosageceras schamarense* Kiparisova, p. 31, pl. 7, figs 3-4.(Kiparisova 1961)

1961 *Pseudosageceras multilobatum* var. *gigantea* Popov, p. 13, pl. 2, figs 1-2.

non 1962 *Pseudosageceras multilobatum* Noetling; Kummel and Steele, p. 701, pl. 102, figs 1-2.

1966 *Pseudosageceras multilobatum* Noetling; Kummel, pl. 1, figs 11-12.

? 1966 *Pseudosageceras multilobatum* Noetling; Hada, p. 112, pl. 4, fig. 6.

1968 *Pseudosageceras multilobatum* Noetling; Kummel and Erben, p. 112, pl. 19, fig. 9.

1968 *Pseudosageceras multilobatum* Noetling; Shevyrev, p. 791, pl. 1, figs 1-2.

? 1973 *Pseudosageceras multilobatum* Noetling; Collignon, p. 5, pl. 1, fig. 1.

1978 *Pseudosageceras multilobatum* Noetling; Weitschat and Lehmann, p. 95, pl. 10, figs 2a-b.

1984 *Pseudosageceras multilobatum* Noetling; Vu Khuc, p. 26, pl. 1, fig. 1.

1985 *Pseudosageceras multilobatum* Noetling; Pakistani-Japanese Research Group, pl. 12, figs 5-7.

1994 *Pseudosageceras multilobatum* Noetling; Tozer, p. 83, Pl. 18, figs 1a-b; p. 384, Fig. 17.

v 2008 *Pseudosageceras multilobatum* Noetling; Brayard and Bucher, p. 70, Pl. 37, figs 1-5, text-fig. 61.

v acc. *Pseudosageceras multilobatum* Noetling, 1905; Brühwiler *et al.*, fig. 22(14a-c).

Occurrence. Samples Chi1, Chi10, Chi53, Nam15, Nam532. This species also occurs in the Spathian at Nammal (Bucher *et al.* unpubl.).

Description. Extremely involute, oxyconic shell (closed umbilicus) with narrow, bicarinate venter. Suture line complex with several adventitious lobes. Main lateral lobe trifid, others bifid.

Discussion. *Pseudosageceras multilobatum* is one of the most long-ranging and palaeogeographically widespread ammonoid species of the Early Triassic.

Order PHYLLOCERATITIDA Zittel, 1884

Superfamily USSURITACEAE Hyatt, 1900

Family PALAEOPHYLLITIDAE Popov, in Luppov and Drushchits, 1958

Genus MIANWALIITES gen. nov.

Derivation of name. Named after the town of Mianwali (Punjab Province, Pakistan).

Type species. *Mianwaliites multiradiatus* gen. et sp. nov.

Composition of the genus. *Mianwaliites multiradiatus* gen. et sp. nov., *M. pauciradiatus* (Brayard and Bucher, 2008).

Diagnosis. Moderately evolute palaeophyllitid with ribbed inner whorls and smooth outer whorls; suture line with weakly phylloid first and second lateral saddles.

Discussion. The phylloid saddles justify the assignment of this genus to Palaeophyllitidae. It has recently been suggested that the oldest Palaeophyllitidae may occur as early as the middle Smithian (i.e. *Goudemandites*; Brayard and Bucher, 2008; Brühwiler and Bucher, submitted).

Mianwaliites multiradiatus gen. et sp. nov.

Plate 43, figures 2-5

v acc. Genus indet. B Brühwiler *et al.*, fig. 21(2-4).

Derivation of name. Refers to the strongly ribbed inner whorls.

Holotype. Specimen PIMUZ 28149 (Pl. 43, fig. 5a-e).

Type locality. Nammal, Salt Range, Pakistan.

Type horizon. Sample Nam38, UCL, *Wasatchites distractus* beds.

Diagnosis. *Mianwaliites* with strongly ribbed inner whorls.

Occurrence. Nam38, UCL, *Wasatchites distractus* beds, Nammal.

Description. Moderately evolute, compressed shell with slightly convex flanks. Maximum whorl width slightly below mid-flank. Venter narrow and rounded with indistinct shoulders. Umbilicus with inclined wall and rounded shoulders. Inner whorls ornamented with distant radial ribs that fade out near mid-flank. Suture line ceratitic with deep lobes; first and second lateral saddles relatively long and weakly phylloid.

Measurements. See appendix.

Discussion. Specimens that are younger and probably conspecific have recently been found within the Bivalve Beds at Nammal, associated with *Columbites* (Bucher *et al*., unpublished data). Thus, this taxon crosses the Smithian-Spathian boundary. Less well preserved specimens of this species have recently been found in the *Wasatchites distractus* Beds in Tulong (South Tibet) (Genus indet. B in Brühwiler *et al.* accepted). *Mianwaliites pauciradiatus* (Brayard and Bucher, 2008) from the latest Smithian of Guangxi (South China) has a very similar shell shape and differs only by its finer and more distant ribbing which is restricted to the innermost whorls .

Subclass NAUTILOIDEA Agassiz, 1847

Order NAUTILIDA Agassiz, 1847

Family TAINOCERATIDAE Hyatt, 1884

Genus TAINIONAUTILUS Mojsisovics, 1902

Type species. *Nautilus transitorius* Waagen, 1879.

Tainionautilus trachyceras Frech, 1905

Plate 47, figures 1-3

? 1897 *Pleuronautilus* sp. ind. Diener, p. 14, pl. 23, fig. 6.
1905 *Temnocheilos (Taenionautilus) trachyceras* Frech, pl. 26, fig. 2.
1953 *Tainionautilus trachyceras* Frech; Kummel, p. 27, pl. 19, fig. 3.

Occurrence. Sample Chi10, lower part of CS, Chiddru; sample Nam529, upper part of CM, Nammal. *Flemingites nanus* beds. One specimen found as float in the CS at Chiddru.

Description. Moderately evolute shell with a subquadratic to trapezoidal whorl section. Flanks flat and slightly convergent. Venter very broad and tabulate with rounded shoulders. Umbilicus with high, vertical wall and slightly rounded shoulders. Ornamented with rursiradiate ribs bearing up to five rows of nodes.

Discussion. The the type species of *Tainionautilus* was described from the Permian of the Salt Range (Waagen, 1879). Thus this genus crossed the Permian/Triassic boundary, but it is locally absent from strata of Griesbachian and Dienerian age.

Acknowledgements. Jim Jenks (Salt Lake City) improved the English text of this work. Claude Monnet (Zürich) is thanked for providing his statistical analyses software. Technical support for preparation and photography was provided by Markus Hebeisen, Julia Huber Leonie Pauli and Rosemarie Roth (Zürich). This paper is a contribution to the Swiss National Science Foundation project 200020-113554 (to HB).

REFERENCES

AGASSIZ, L. 1847. Lettre sur quelques points de'organisation des animaux rayonnés. *Comptes Rendus de l'Académie de Sciences*, **25**, 677-682.

ARTHABER, G. 1911. Die Trias von Albanien. *Beiträge zur Paläontologie und Geologie Oesterreich-Ungarns und des Orients*, **24**, 169-288.

BHARGAVA, O. N., KRYSTYN, L., BALINI, M., LEIN, R. and NICORA, A. 2004. Revised litho- and sequence stratigraphy of the Spiti Triassic. *Albertiana*, **30**, 21-39.

BRAYARD, A. and BUCHER, H. 2008. Smithian (Early Triassic) ammonoid faunas from northwestern Guangxi (South China): taxonomy and biochronology. *Fossils and Strata*, **55**, 1-179.

BRAYARD, A., BUCHER, H., ESCARGUEL, G., FLUTEAU, F., BOURQUIN, S. and GALFETTI, T. 2006. The Early Triassic ammonoid recovery: Paleoclimatic significance of diversity gradients. *Palaeogeography, Palaeoclimatology, Palaeoecology*, **239**, 374-395.

BRAYARD, A., ESCARGUEL, G., BUCHER, H., MONNET, C., BRÜHWILER, T., GOUDEMAND, N., GALFETTI, T. and GUEX, J. 2009. Good Genes and Good Luck: Ammonoid Diversity and the End-Permian Mass Extinction. *Science*, **325**, 1118-1121.

BRÜHWILER, T. and BUCHER, H. submitted. Systematic palaeontology. *In* BRÜHWILER, T., BUCHER, H. GOUDEMAND, N. and GALFETTI, T. (submitted [a]). Smithian (Early Triassic) ammonoid faunas from Exotic Blocks from Oman: taxonomy and biochronology. *Palaeontographica*.

--- --- and GOUDEMAND, N. accepted. Smithian (Early Triassic) ammonoids from Tulong, South Tibet. *Geobios*.

--- --- --- and BRAYARD, A. 2007. Smithian (Early Triassic) ammonoid faunas of the Tethys: new preliminary results from Tibet, India, Pakistan and Oman. *New Mexico Museum of Natural History and Science Bulletin*, **41**, 25-26.

--- --- --- and GALFETTI, T. (submitted [a]). Smithian (Early Triassic) ammonoid faunas from Exotic Blocks from Oman: taxonomy and biochronology. *Palaeontographica*.

--- GOUDEMAND, N., GALFETTI, T., BUCHER, H., BAUD, A., WARE, D., HERMANN, E., HOCHULI, P. A. and MARTINI, R. 2009. The Lower Triassic sedimentary and carbon isotope records from Tulong (South Tibet) and their significance for Tethyan palaeoceanography. *Sedimentary Geology*, **222**, 314-332.

--- WARE, D., BUCHER, H., KRYSTYN, L. and GOUDEMAND, N. (submitted [b]). New Early Triassic ammonoid faunas from the Dienerian/Smithian boundary beds at the Induan/Olenekian GSSP candidate at Mud (Spiti, Northern India). *Journal of Asian Earth Sciences*.

BURIJ, I. V. and ZHARNIKOVA, N. K. 1968. On findings of *Anasibirites* - fauna in South Primorye and its stratigraphic position. 79-81. *In* BURIJ, I. V., ZAKHAROV, Y. D., ZHARNIKOVA, N. K. and NEVOLIN, L. A. (eds). *Sedimentary and Volcanogenic - Sedimentary Formations (Ustinovskyi Y.B., ed.)*. DVFAN Nauka, Vladivostok.

CHAO, K. 1959. Lower Triassic ammonoids from Western Kwangsi, China. *Palaeontologia Sinica. New Series B*, **9**, 1-355.

COLLIGNON, M. 1933-1934. Paléontologie de Madagascar XX - Les céphalopodes du Trias inférieur. *Annales de Paléontologie*, **12-13**, 151-162 & 1-43.

--- 1973. Ammonites du Trias inférieur et moyen d'Afghanistan. *Annales de Paléontologie (Invertebrés)*, **59**, 127-163.

DE KONINCK, L. G. 1863. Description of some fossils from India, discovered by Dr. A. Fleming, of Edingburgh. *The quarterly Journal of the Geological Society of London*, **19**, 1-19.

DIENER, C. 1895. Triadische Cephalopodenfaunen der ostsibirischen Küstenprovinz. *Mémoirs du Comité Géologique St. Petersburg*, **14**, 1-59.

--- 1897. The Cephalopoda of the Lower Trias. *Palaeontologia Indica, ser. 15,* **2**, 1-181.

--- 1913. Triassic faunae of Kashmir. *Palaeontologia Indica, n. ser.*, **5**, 1-133.

EHIRO, M., HASEGAWA, H. and MISAKI, A. 2005. Permian ammonoids *Prostacheocers* and *Perrinites* from the Southern Kitakami Massif, Northeast Japan. *Journal of Paleontology*, **79**, 1222-1228.

FREBOLD, H. 1930. Die Altersstellung des Fischhorizontes, des Grippianniveaus und des unteren Saurierhorizontes in Spitzbergen. *Scrifter om Svalbard og Ishavet*, **28**, 1-36.

FRECH, F. 1902. Die Dyas. *Lethaea Geognostica, I. Lethaea Palaeozoica*, v. 2 (4). 579-788.

--- 1905. Das Mesozoicum. *Lethaea geognostica. II, Trias*. Stuttgart, 623 pp.

GALFETTI, T., BUCHER, H., BRAYARD, A., HOCHULI, P. A., WEISSERT, H., GUODUN, K., ATUDOREI, V. and GUEX, J. 2007*a*. Late Early Triassic climate change: Insights from carbonate carbon isotopes, sedimentary evolution and ammonoid paleobiogeography. *Palaeogeography, Palaeoclimatology, Palaeoecology*, **243**, 394-411.

GALFETTI, T., BUCHER, H., OVTCHAROVA, M., SCHALTEGGER, U., BRAYARD, A., BRÜHWILER, T., GOUDEMAND, N., WEISSERT, H., HOCHULI, P. A., CORDEY, F. and GUODUN, K. A. 2007*b*. Timing of the Early Triassic carbon cycle perturbations inferred from new U-Pb ages and ammonoid biochronozones. *Earth and Planetary Science Letters*, **258**, 593-604.

GUEX, J. 1978. Le Trias inférieur des Salt Ranges, Pakistan: problèmes biochronologiques. *Eclogae Geologicae Helvetiae*, **71**, 105-141.

HADA, S. 1966. Discovery of Early Triassic ammonoids from Gua Musang, Kelantan, Malaya. *Journal of Geosciences, Osaka University*, **9**, 111-121.

HAMMER, O. and BUCHER, H. 2005. Buckman's first law of covariation - a case of proportionality. *Lethaia*, **38**, 67-72.

HYATT, A. 1879. Genus *Meekoceras* Hyatt. *In:* WHITE, C. A. 1879. Paleontological papers no. 9: Fossils from the Jura-Trias of south-eastern Idaho. *U. S. Geological and Geographical Survey of the Territories Bulletin*, **5**, 105-117.

--- 1884. Genera of fossil cephalopods. *Proceedings of the Boston Society of Natural History*, **22**, 253-338.

--- 1900. Cephalopoda. *In* ZITTEL, K. A. V. (ed.) *Textbook of palaeontology, vol. 1, 1st English ed.* Eastman, C. R. London.

HYATT, A. and SMITH, J. P. 1905. Triassic cephalopod genera of America. *U. S. Geological Survey Professional Paper*, **40**, 1-394.

JEANNET, A. 1959. Ammonites Permiennes et faunes Triasiques de l'Himalaya Central (Expedition Suisse Arn. Heim et A., Gansser, 1936). *Palaeontologia Indica, n. ser.*, **34**, 1-189.

JENKS, J. 2007. Smithian (Early Triassic) ammonoid biostratigraphy at Crittenden Springs, Elko County, Nevada and a new ammonoid from the *Meekoceras gracilitatis* zone. *New Mexico Museum of Natural History and Science Bulletin*, **40**, 81-90.

KEYSERLING, A. 1845. Beschreibung einiger von Dr. A. Th. v. Middendorff mitgebrachten Ceratiten des arctischen Sibiriens. *Bulletin de l'Academie Imperiale des Sciences de St. Pétersbourg*, **5**, 161-174.

KIPARISOVA, L. D. 1947. *Atlas of the guide forms of the fossil faunas of the USSR 7, Triassic*. All Union Scientific Geological Research Institute (VSEGEI), Leningrad (now St. Petersburg), Russia [in Russian].

--- 1956. Materials on paleontology, new families and genera. *Transactions of the All Union Scientific Research Geological Institute (VSEGEI), n. ser.*, **12,** Paleontology, 76-79.

--- 1961. Palaeontological fundamentals for the stratigraphy of Triassic deposits of the Primor'ye region, I, Cephalopod Mollusca. *Transactions of the All Union Scientific Research Geological Institute (VSEGEI), n. ser.*, **48**, 1-278.

KRAFFT, A. V. and DIENER, C. 1909. Lower Triassic cephalopoda from Spiti, Malla Johar, and Byans. *Palaeontologia Indica, ser. 15,*, **6**, 1-186.

KRYSTYN, L., BHARGAVA, O. N. and RICHOZ, S. 2007*a*. A candidate GSSP for the base of the Olenekian Stage: Mud at Pin Valley; district Lahul & Spiti, Himachal Pradesh (Western Himalaya), India. *Albertiana*, **35**, 5-29.

KRYSTYN, L., RICHOZ, S. and BHARGAVA, O. N. 2007*b*. The Induan-Olenekian Boundary (IOB) in Mud – an update of the candidate GSSP section M04. *Albertiana*, **36**, 33-45.

KUMMEL, B. 1952. A classification of the Triassic ammonoids. *Journal of Paleontology*, **26**, 847-853.

KUMMEL, B. 1953. American Triassic coiled nautilioids. *Geological Survey Professional Paper*, **250**, 1-104.

--- 1966. The Lower Triassic formations of the Salt Range and Trans-Indus Ranges, West Pakistan. *Bulletin of the Museum of Comparative Zoology, Harvard University*, **134**, 361-429.

--- 1968. Additional Scythian Ammonoids from Afghanistan. *Bulletin of the Museum of Comparative Zoology, Harvard University*, **136**, 483-509.

--- 1970. Ammonoids from the Kathwai Member, Mianwali Formation, Salt Range, West Pakistan. 177-192. *In* KUMMEL, B. and TEICHERT, C. (eds). *Stratigraphic Boundary Problems: Permian and Triassic of West Pakistan*. Department of Geology, University of Kansas, Special Publication 110 pp.

KUMMEL, B. and ERBEN, H. K. 1968. Lower and Middle Triassic cephalopods from Afghanistan. *Palaeontographica, Abt. A*, **129**, 95-148.

KUMMEL, B. and STEELE, G. 1962. Ammonites from the *Meekoceras gracilitatus* Zone at Crittenden Spring, Elko County, Nevada. *Journal of Paleontology*, **36**, 638-703.

KUMMEL, B. and TEICHERT, C. 1966. Relations between the Permian and Triassic formations in the Salt Range and Trans-Indus ranges, West Pakistan. *Neues Jahrbuch für Geologie und Paläontologie. Abhandlungen*, **125**, 297-333.

--- --- 1970. Stratigraphy and Paleontology of the Permian-Triassic Boundary Beds, Salt Range and Trans-Indus Ranges, West Pakistan. 1-110. *In* KUMMEL, B. and TEICHERT, C. (eds). *Stratigraphic Boundary Problems: Permian and Triassic of West Pakistan*. Department of Geology, University of Kansas, Special Publication 110 pp.

LUPPOV, N.P. and DRUSHCHITS, V.V. 1958. *Fundamentals of Palaeontology, Mollusca - Cephalopoda II, Ammonoidea (Ceratites and Ammonites)*, Moscow, 359 pp. (in Russian).

MARKEVICH, P. V. and ZAKHAROV, Y. 2004. *Triassic and Jurassic of the Sikhote-Alin*. Dalnauka, Vladivostok, Russia. [In Russian with English summary]. 420 pp.

MATHEWS, A. A. L. 1929. The Lower Triassic cephalopod fauna of the Fort Douglas area, Utah. *Walker Museum Memoirs*, **1**, 1-46.

MOJSISOVICS, E. VON (1873, 1875, 1902): Das Gebirge um Hallstatt. 1. Abtheilung. Die Cephalopoden der Hallstätter Kalke. 1. Band. *Abhandlungen der geologischen Reichsanstalt*, 6/1, 1. Lief. (1873): 1–82, Taf. 1–32; 2. Lief. (1875): 83–174, Taf. 33–70; 3. Lief. (Supplement, 1902): 175–356, Taf. 1–23; Wien.

MOJSISOVICS, E. 1896. Beiträge zur Kenntnis der obertriadischen Cephalopoden-Faunen des Himalaya. *Denkschriften der Akademie der Wissenschaften in Wien*, **63**, 573-701.

MOJSISOVICS, E., WAAGEN, W. and DIENER, C. 1895. Entwurf einer Gliederung der pelagischen Sedimente des Trias-Systems. *Sitzungsberichte der Akademie der Wissenschaften in Wien (I)*, **104**, 1271-1302.

MONNET, C. and BUCHER, H. 2005. New Middle and Late Anisian (Middle Triassic) ammonoid faunas from northwestern Nevada (USA): taxonomy and biochronology. *Fossils and Strata*, **52**, 1-121.

MONNET, C., BUCHER, H., WASMER, M. and GUEX, J. in press. Revision of the genus *Acrochordiceras* Hyatt, 1887 (ammonoidea, middle Triassic): Morphology, biometry, biostratigraphy and intraspecific varaibilty. *Palaeontology*.

MUNDIL, R., LUDWIG, K. R., METCALFE, I. and RENNE, P. R. 2004. Age and timing of the Permian mass extinctions: U/Pb dating of closed-system zircons. *Science*, **305**, 1760-1763.

NOETLING, F. 1905. Die asiatische Trias. 107-221. *In* FRECH, F. (ed.) *Lethaea geognostica. Das Mesozoicum, 1. Band, Trias. Lethaia Mesozoica 1*. Schweizerbart, Stuttgart, 623 pp.

ORCHARD, M. J. 2007. Conodont diversity and evolution through the latest Permian and Early Triassic upheavals. *Palaeogeography, Palaeoclimatology, Palaeoecology*, **252**, 93-117.

OVTCHAROVA, M., BUCHER, H., SCHALTEGGER, U., GALFETTI, T., BRAYARD, A. and GUEX, J. 2006. New Early to Middle Triassic U-Pb ages from South China: Calibration with ammonoid biochronozones and implications for the timing of the Triassic biotic recovery. *Earth and Planetary Science Letters*, **243**, 463-475.

PAKISTANI-JAPANESE RESEARCH GROUP 1985. Permian and Triassic systems in the Salt Range and Surghar Range, Pakistan. 221-312. *In* NAKAZAWA, K. and DICKINS, J. M. (eds). *The Tethys: Her Paleogeography and Paleobiogeography from Paleozoic to Mesozoic*. Tokai University Press, Tokyo, 317 pp.

POPOV, Y. 1961. Triassic ammonoids of northeastern USSR. *Transactions, Scientific Research Institute for the Geology of the Arctic (NIIGA)*, **79**, 1-179.

RAUP, D. M. and SEPKOSKI, J. J. 1982. Mass Extinctions in the Marine Fossil Record. *Science*, **215**, 1501-1503.

RENZ, C. and RENZ, O. 1948. Eine untertiadische Ammonitenfauna von der griechischen Insel Chios. *Schweizerische Paläontologische Abhandlungen*, **66**, 1-98.

RICOU, L. E. 1994. Tethys reconstructed - plates, continental fragments and their boundaries since 260 Ma from Central-America to South-Eastern Asia. *Geodinamica Acta*, **7**, 169-218.

SCHINDEWOLF, O. 1953. Über die Faunenwende vom Paläozoikum zum Mesozoikum. *Zeitschrift der Deutschen Geologischen Gesellschaft*, **105**, 153-182.

SHEVYREV, A. A. 1968. *Triassic ammonoidea from the southern part of the USSR*. Transactions of the Palaeontological Institute 119. Nauka, Moscow, 272 pp.

SHIGETA, Y., MAEDA., H. and ZAKHAROV, Y. 2009. Biostratigraphy: ammonoid succession. 24-27. *In* SHIGETA, Y., ZAKHAROV, Y., MAEDA, H. and POPOV, A. M. (eds). *The Lower Triassic system in the Abrek Bay area, South Primorye, Russia.* National Museum of Nature and Science Monographs 38, Tokyo, 218 pp.

SHIGETA, Y. and ZAKHAROV, Y. 2009. Systematic paleontology: cephalopods. 44-140. *In* SHIGETA, Y., ZAKHAROV, Y., MAEDA, H. and POPOV, A. M. (eds). *The Lower Triassic system in the Abrek Bay area, South Primorye, Russia.* National Museum of Nature and Science Monographs 38, Tokyo, 218 pp.

SILBERLING, N. J. and TOZER, E. T. 1968. *Biostratigraphic classification of the marine Triassic in North America*. Special Paper - Geological Society of America (GSA), Boulder, CO, United States, 63 pp.

SMITH, A. G., SMITH, D. G. and FUNNELL, B. M. 1994. *Atlas of Mesozoic and Cenozoic Coastlines*. Cambridge University Press, Cambridge, 109 pp.

SMITH, J. P. 1927. Upper Triassic marine invertebrate faunas of North America. *U. S. Gelogical Survey, Professional paper*, **141**, 262 pp.

--- 1932. Lower Triassic ammonoids of North America. *U. S. Geological Survey Professional Paper*, **167**, 1-199.

SPATH 1930. The Eotriassic invertebrate fauna of East Greenland. *Meddelelser om Grønland*, **83**,

SPATH, L. F. 1929. Corrections of cephalopod nomenclature. *The Naturalist*, 269-271.

--- 1934. *Part 4: The ammonoidea of the Trias, Catalogue of the fossil cephalopoda in the British Museum (Natural History)*. The Trustees of the British Museum, London, 521 pp.

STAMPFLI, G. M. and BOREL, G. D. 2002. A plate tectonic model for the Paleozoic and Mesozoic constrained by dynamic plate boundaries and restored synthetic oceanic isochrons. *Earth and Planetary Science Letters*, **196**, 17-33.

TOZER, E. T. 1967. A standard for Triassic time. *Geologic Survey of Canada Bulletin*, **156**, 141 pp.

--- 1971. Triassic time and ammonoids. *Canadian Journal of Earth Sciences*, **8**, 989-1031.

--- 1981*a*. Triassic ammonoidea: geographic and stratigraphic distribution. 397–431. *In* HOUSE, M. R., SENIOR, J.R. (ed.) *The Ammonoidea*. The Systematics association, Academic Press, London, 593 pp.

--- 1981*b*. Triassic Ammonoidea; classification, evolution and relationship with Permian and Jurassic forms. 65-100. *In* HOUSE, M. R. and SENIOR, J. R. (eds). *The Ammonoidea*. The Systematics association, Academic Press, London, 593 pp.

--- 1982. Marine Triassic Faunas of North-America - Their Significance for Assessing Plate and Terrane Movements. *Geologische Rundschau*, **71**, 1077-1104.

--- 1994. *Canadian Triassic ammonoid faunas*. Geological Survey of Canada, Ottawa, ON, Canada, 663 pp.

VU KHUC 1984. *Triassic ammonoids in Vietnam*. Geoinform and Geodata Institute, Hanoi, Vietnam, 134 pp.

WAAGEN, W. 1879. Salt-Range fossils Vol 1: Productus limestone fossils. *Palaeontologia Indica*, **13**, 1-72.

WAAGEN, W. 1895. Salt-Range fossils. Vol 2: Fossils from the Ceratite Formation. *Palaeontologia Indica*, **13**, 1-323.

WANG, Y. G. and HE, G. X. 1976. Triassic ammonoids from the Mount Jolmo Lungma region. *A report of scientific expedition in the Mount Jolmo Lungma region (1966-1968)*, 223-502 [in Chinese].

WANNER, J. 1911. Triascephalopoden von Timor und Rotti. *Neues Jahrbuch für Geologie und Paläontologie. Beilageband*, **32**, 177-196.

WATERHOUSE, J. B. 1996*a*. The Early and Middle Triassic ammonoid succession of the Himalayas in western and central Nepal. Part 2, systematic studies of the early Middle Scythian. *Palaeontographica Abt. A*, **241**, 27-100.

--- 1996*b*. The Early and Middle Triassic ammonoid succession of the Himalayas in western and central Nepal: Part 3. Late middle Scythian ammonoids. *Palaeontographica Abt. A*, **241**, 101-167.

WEITSCHAT, W. and LEHMANN, U. 1978. Biostratigraphy of the uppermost part of the Smithian Stage (Lower Triassic) at the Botneheia, W-Spitsbergen. *Mitteilungen aus dem Geologisch-Paläontologischen Institut der Universität Hamburg*, **54**, 27-54.

WELTER, O. A. 1922. Die Ammoniten der unteren Trias von Timor. *Paläontologie von Timor*, **11**, 83-154.

WESTERMANN, G. E. G. 1966. Covariation and taxonomy of the Jurassic ammonite *Sonninia dicra* (Waagen). *Neues Jahrbuch für Geologie und Paläontologie. Abhandlungen*, **124**, 289-312.

WHITE, C. A. 1879. Paleontological papers no. 9: fossils from the Jura-Trias of south-eastern Idaho. *U. S. Geological and Geographical Survey of the Territories Bulletin*, **5**, 105-117.

ZAKHAROV, Y. D. 1968. *Biostratigraphiya i amonoidei nizhnego triasa Yuzhnogo Primorya (Lower Triassic biostratigraphy and ammonoids of South Primorye)*. Nauka, Moskva, 175 pp. [in Rusian].

ZITTEL 1884. *Handbuch der Paläontologie. Cephalopoda.* Munich, 239-522.

APPENDIX

Measurements of the classic geometrical parameters of the ammonoid shell. Diameter (D), whorl height (H), whorl width (W) and umbilical diameter (U).

Species	Specimen	D (mm)	H (mm)	W (mm)	U (mm)	Sample
Kashmirites armatus (Waagen, 1895)	PIMUZ 27875	33.4	11.3	13	14.3	Chi10
	PIMUZ 27876	36	11.3	13.8	16.9	Chi10
	PIMUZ 27877	17.3	5.4	7	7.6	Chi10
Mudiceras planissimum (Spath, 1934)	PIMUZ 28377	20.7	8.1	4.5	7.4	Chi53
Monneticeras compressum gen. et sp. nov.	PIMUZ 27932, Holotype	58.9	26.5	9.5	14.8	Chi53
Clypeoceras superbum Waagen, 1895	PIMUZ 27935	193.1	116.3	40.9	3.9	Zal50
?Kingites parkashi Brühwiler *et al.* subm.[b]	PIMUZ 27936	95	55.1	20	0	Chi52
Paraspidites praecursor (Frech, 1905)	PIMUZ 28159	35.8	20.5	6.4	2.1	Chi10
Paraspidites obesus sp. nov.	PIMUZ 28156, Holotype	39.3	19.4	10.5	8	Nam532
	PIMUZ 28158	30.1	14.7	8	6.5	Chi1
Shamaraites rursiradiatus sp. nov.	PIMUZ 28019, Holotype	38.7	12.4	10.7	17.2	Chi53
Flemingites planatus sp. nov.	PIMUZ 28016, Holotype	73.7	24.2	13.3	31.8	Chi52
	PIMUZ 28017	57.1	20.4	-	20.8	Chi63
	PIMUZ 28018	31.3	10.8	7.2	13.4	Chi52
Pseudoflemingites cf. *timorensis*	PIMUZ 28029	71.6	27.1	13.4	24	Chi53
	PIMUZ 28030	88.4	29.7	18.1	35.5	Chi53
	PIMUZ 28031	66	24.4	13.1	22.9	Chi53
Dieneroceras sp. indet. A	PIMUZ 28032	24.5	7.5	7.6	11.9	Nam16
Dieneroceras sp. indet. B	PIMUZ 28033	17.8	6.1	-	8.1	Nam19
Nammalites pilatoides (Guex, 1978)	PIMUZ 28058	26	12.1	8.4	6.7	Nam18
	PIMUZ 28059	26.3	12.8	7.4	6	Nam18
	PIMUZ 28060	32.3	14.8	-	7.4	Nam21
?Arctoceratidae gen. et sp. indet.	PIMUZ 27931	42.4	19.6	12.8	9.8	Zal50
Meekoceras cf. *gracilitatis*	PIMUZ 28088	29.6	15.4	6.6	4.3	Nam18
	PIMUZ 28089	14.4	6.8	3.8	2.9	Nam18
	PIMUZ 28091	22.2	11.7	5.7	4.6	Nam18
Stephanites superbus Waagen, 1895	PIMUZ 28093	30.3	14.7	16	6.9	Nam68
	PIMUZ 28094	42.7	20	19.5	9.8	Nam68
Punjabites punjabiensis gen. et sp. nov.	PIMUZ 28095, Holotype	42.4	18.7	-	8.6	Nam9
?Hemiprionites sp. indet.	PIMUZ 28138	43.4	21.3	11	6.9	Nam17
Juvenites cf. *kraffti* Smith, 1927	PIMUZ 28144	13.4	4.7	8	5.2	Nam532
Hochuliites retrocostatus gen. et sp. nov.	PIMUZ 28152	49.5	19.6	9.9	17.6	Nam16
	PIMUZ 28153, Holotype	50.6	19	9.5	20.3	Nam9
	PIMUZ 28155	34.3	11.6	8.3	15.5	Nam16
Hedenstroemia evoluta (Spath, 1934)	PIMUZ 28160	53.1	29.7	13.4	4.3	Zal50
	PIMUZ 28162	18.7	9.5	4.6	2.9	Zal50
	PIMUZ 28163	57.8	32.8	11.4	5.4	Chi56a
Mianwaliites multiradiatus gen. et sp. nov.	PIMUZ 28146	28.6	11.5	6.7	8.5	Nam38
	PIMUZ 28147	47.3	20	12	14.7	Nam38
	PIMUZ 28149, Holotype	46.9	21	12.5	13.1	Nam38

Appendix.

FIGURE CAPTIONS

TEXT-FIG. 1. Early Triassic stage subdivision (Tozer, 1967) calibrated with recently published radiometric ages (Mundil *et al.* 2004, Ovtcharova *et al.* 2006, Galfetti *et al.* 2007*b*).

TEXT-FIG. 2. A) Palaeogeographical map of the Early Triassic with the palaeoposition of the Salt Range (modified after Brayard *et al.* 2006). B) Map of Pakistan with indication of the studied area. C) Location map of sampled sections in the Salt Range.

TEXT-FIG. 3. Stratigraphic nomenclature of the Early Triassic sediments in the Salt Range according to different authors. In this work we use Waagen's (1895) subdivisions with some minor adaptations from Kummel and Teichert (1970; Kathwai Member) and Guex (1978; NI = Niveaux Intermédiaires ["Intermediate Horizons"]).

TEXT-FIG. 4. Section near the village of Chiddru; 1km ESE of the sections at the entry of the gorge described by Kummel and Teichert (1966, 1970) and Kummel (1966), seen from NW. CM Ceratite Marls; CS Ceratite Sandstones; UCL Upper Ceratite Limestone.

TEXT-FIG. 5. A block from the Ceratite Sandstones of Chiddru containing several very large specimens of *Paranorites ambiensis* (Waagen, 1895). From Sample Chi10, *Flemingites nanus* beds.

TEXT-FIG. 6. Distribution of ammonoids in the Ceratite Marls in the Chiddru section. Abbreviations as in Text-figure 15.

TEXT-FIG. 7. Distribution of ammonoids in the Ceratite Sandstones in the Chiddru section. Abbreviations as in Text-figure 15.

TEXT-FIG. 8. Distribution of ammonoids in the Upper Ceratite Limestone in the Chiddru section. Abbreviations as in Text-figure 15.

TEXT-FIG. 9. Northwestern slope of the Nammal Gorge. KM Kathwai Member; LCL Lower Ceratite Limestone; CM Ceratite Marls; CS Ceratite Sandstones; UCL Upper Ceratite Limestone; NI Niveaux Intermédiaires; TL Topmost Limestone. Note the presence of normal and low angle reverse faults (black lines).

TEXT-FIG. 10. Distribution of ammonoids in the Ceratite Marls in the Nammal Gorge section. Abbreviations as in Text-figure 15.

TEXT-FIG. 11. Distribution of ammonoids in the Ceratite Sandstones in the Nammal Gorge section. Abbreviations as in Text-figure 15.

TEXT-FIG. 12. Distribution of ammonoids in the Upper Ceratite Limestone in the Nammal Gorge section. Abbreviations as in Text-figure 15.

TEXT-FIG. 13. Distribution of ammonoids in the Ceratite Sandstones in the Zaluch section. Abbreviations as in Text-figure 15.

TEXT-FIG. 14. Biostratigraphical subdivisions of the Smithian of the Salt Range and correlation with zonations of other regions. Thick black bars indicate uncertainty intervals for correlations. See text for discussion.

TEXT-FIG. 15. Biostratigraphical correlation of Chiddru, Nammal and Zaluch sections. Note the diachronism of the LCL/CM and CM/CS lithological boundaries between Chiddru and Nammal.

TEXT-FIG. 16. Synthetic range chart showing the biostratigraphical distribution of Smithian ammonoid species in the Salt Range.

TEXT-FIG. 17. Synthetic range chart showing the biostratigraphical distribution of Smithian ammonoid genera (grouped by families) in the Salt Range.

TEXT-FIG. 18. Comparison of previous biostratigraphic subdivisions of the Early Triassic of the Salt Range. Thick black bars indicate the range of uncertainty of some correlations.

TEXT-FIG. 19. Scatter diagram of H, W, and U, and of H/D, W/D, and U/D for *Kashmirites baidi* Brühwiler and Bucher (submitted).

TEXT-FIG. 20. Scatter diagram of H, W, and U, and of H/D, W/D, and U/D for *Pseudoceltites multiplicatus* (Waagen, 1895).

TEXT-FIG. 21. Scatter diagram of H, W, and U, and of H/D, W/D, and U/D for *Nyalamites angustecostatus* (Welter, 1922).

TEXT-FIG. 22. Scatter diagram of H, W, and U, and of H/D, W/D, and U/D for *Xenoceltites* cf. *variocostatus* Brayard and Bucher, 2008 from the Salt Range and for *Xenoceltites variocostatus* from

Guangxi, South China (data from Brayard and Bucher 2008). Note the slightly greater whorl width of the Chinese specimens.

TEXT-FIG. 23. Scatter diagram of H, W, and U, and of H/D, W/D, and U/D for *Glyptophiceras sinuatum* (Waagen, 1895).

TEXT-FIG. 24. Scatter diagram of H, W, and U, and of H/D, W/D, and U/D for *Koiloceras romanoi* gen. et sp. nov.

TEXT-FIG. 25. Scatter diagram of H, W, and U, and of H/D, W/D, and U/D for *Radioceras evolvens* (Waagen, 1895).

TEXT-FIG. 26. Scatter diagram of H, W, and U, and of H/D, W/D, and U/D for *Radioceras* cf. *kraffti* (Spath, 1934).

TEXT-FIG. 27. Scatter diagram of H, W, and U, and of H/D, W/D, and U/D for *Vercherites vercherei* (Waagen, 1895).

TEXT-FIG. 28. Scatter diagram of H, W, and U, and of H/D, W/D, and U/D for *Vercherites pulchrum* (Waagen, 1895).

TEXT-FIG. 29. Scatter diagram of H, W, and U, and of H/D, W/D, and U/D for *Paranorites ambiensis* Waagen, 1895.

TEXT-FIG. 30. Scatter diagram of H, W, and U, and of H/D, W/D, and U/D for *Flemingites flemingianus* (de Koninck, 1863).

TEXT-FIG. 31. Scatter diagram of H, W, and U, and of H/D, W/D, and U/D for *Flemingites nanus* Waagen, 1895.

TEXT-FIG. 32. Scatter diagram of H, W, and U, and of H/D, W/D, and U/D for *Flemingites hautmanni* sp. nov.

TEXT-FIG. 33. Boxplots (Monnet and Bucher 2005) for *Flemingites hautmanni* sp. nov. and *Flemingites hofmanni* sp. nov. The box plot displays the 25th, 50th (median) and 75th percentiles of the range of measures covered by 99% of the specimens from a normal distribution. Outliers represent specimens not falling within the normal distribution.

TEXT-FIG. 34. Scatter diagram of H, W, and U, and of H/D, W/D, and U/D for *Flemingites hofmanni* sp. nov.

TEXT-FIG. 35. Scatter diagram of H, W, and U, and of H/D, W/D, and U/D for *Rohillites pakistanensis* sp. nov.

TEXT-FIG. 36. Scatter diagram of H, W, and U, and of H/D, W/D, and U/D for *Anaxenaspis nammalensis* (Guex, 1978).

TEXT-FIG. 37. Scatter diagram of H, W, and U, and of H/D, W/D, and U/D for *Xenodiscoides perplicatus* (Frech, 1905), *X. involutus* (Frech, 1905) and *X. falcatum* (Waagen, 1895).

TEXT-FIG. 38. Boxplots (Monnet and Bucher 2005) for *Xenodiscoides perplicatus* (Frech, 1905), *X. involutus* (Frech, 1905) and *X. falcatum* (Waagen, 1895). The box plots display the 25th, 50th (median) and 75th percentiles of the range of measures covered by 99% of the specimens from a normal distribution.

TEXT-FIG. 39. Scatter diagram of H, W, and U, and of H/D, W/D, and U/D for *Brayardites compressus* Brühwiler *et al.* (accepted).

TEXT-FIG. 40. Scatter diagram of H, W, and U, and of H/D, W/D, and U/D for *Truempyceras pluriformis* (Guex, 1978) gen. nov.

TEXT-FIG. 41. Scatter diagram of H, W, and U, and of H/D, W/D, and U/D for *Prionites tuberculatus* Waagen, 1895.

TEXT-FIG. 42. Boxplots (Monnet and Bucher 2005) for *Prionites tuberculatus* and *Prionites nammalensis* sp. nov. The box plots display the 25th, 50th (median) and 75th percentiles of the range of measures covered by 99% of the specimens from a normal distribution.

TEXT-FIG. 43. Scatter diagram of H, W, and U, and of H/D, W/D, and U/D for *Prionites nammalensis* sp. nov.

TEXT-FIG. 44. Scatter diagram of H, W, and U, and of H/D, W/D, and U/D for *Wasatchites distractus* (Waagen, 1895).

TEXT-FIG. 45. Scatter diagram of H, W, and U, and of H/D, W/D, and U/D for *Anasibirites kingianus* (Waagen, 1895).

TEXT-FIG. 46. Scatter diagram of H, W, and U, and of H/D, W/D, and U/D for *Anasibirites angulosus* (Waagen, 1895).

TEXT-FIG. 47. Scatter diagram of H, W, and U, and of H/D, W/D, and U/D for *Hemiprionites typus* (Waagen, 1895).

TEXT-FIG. 48. Scatter diagram of H, W, and U, and of H/D, W/D, and U/D for *Hemiprionites klugi* Brayard and Bucher, 2008.

TEXT-FIG. 49. Scatter diagram of H, W, and U, and of H/D, W/D, and U/D for *Juvenites* sp. indet.

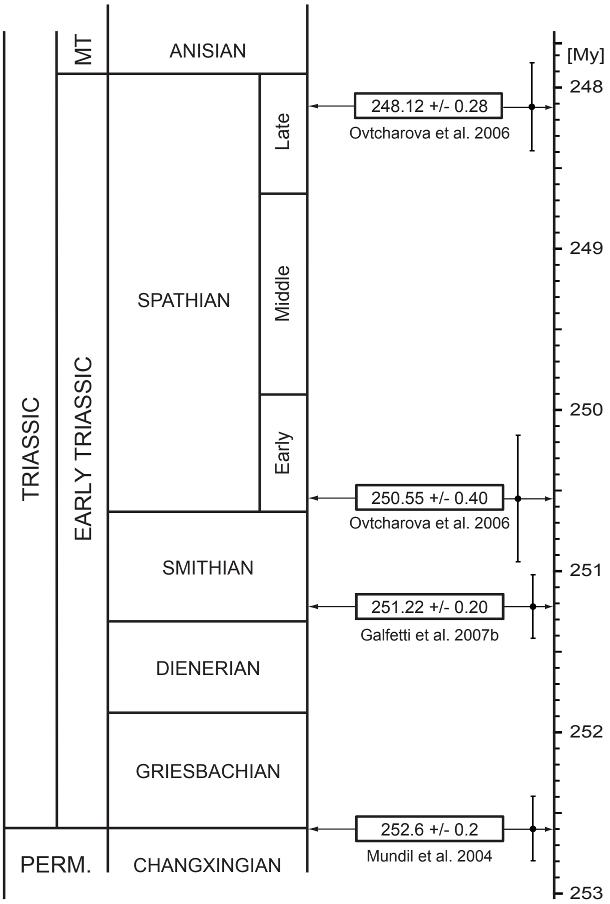

Text-fig. 1

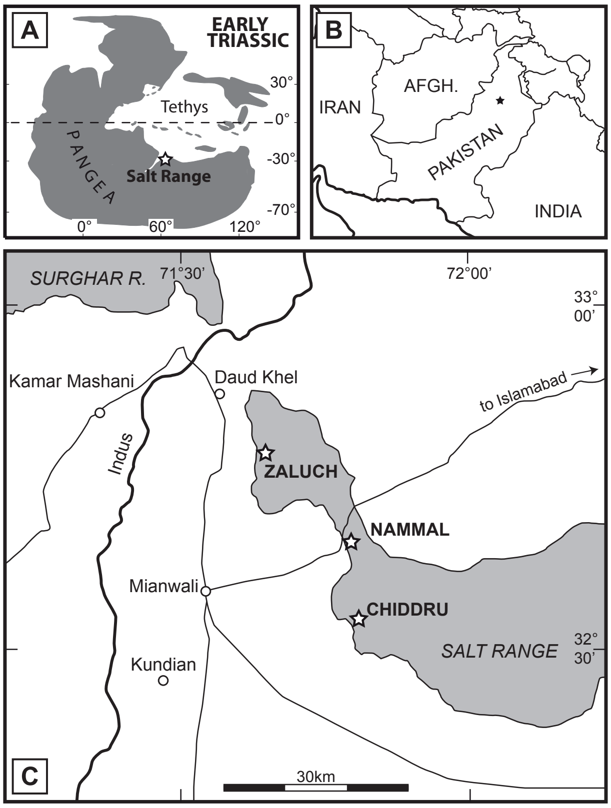

Text-fig. 2

Waagen, 1895			Kummel and Teichert, 1970		Guex, 1978	PJRG, 1985			This work	
Ceratite Formation	Dolomite Group	Topmost Limestone	Mianwali Formation	Narmia Member	TL	Mianwali Formation	Narmia Mb.		TL	TRIASSIC
		Dolomitic Beds			NI		Mittiwali Member	Unit 5	NI	
	Bivalve Limestone	Bivalve Beds			UCL			Unit 4	BB	
		Upper Ceratite Limestone		Mittiwali Member					UCL	
	Ceratite Beds	Ceratite Sandstone			CS			Unit 3	CS	
		Ceratite Marls			CM			Unit 2	CM	
		Lower Ceratite Limestone			LCL			Unit 1	LCL	
Upper Productus Limestone				Kathwai Member	KM		Kathwai Mb.		KM	
			Chhidru Formation			Chhidru Fm.				P.

Text-fig. 3

Text-fig. 4

Text-fig. 5

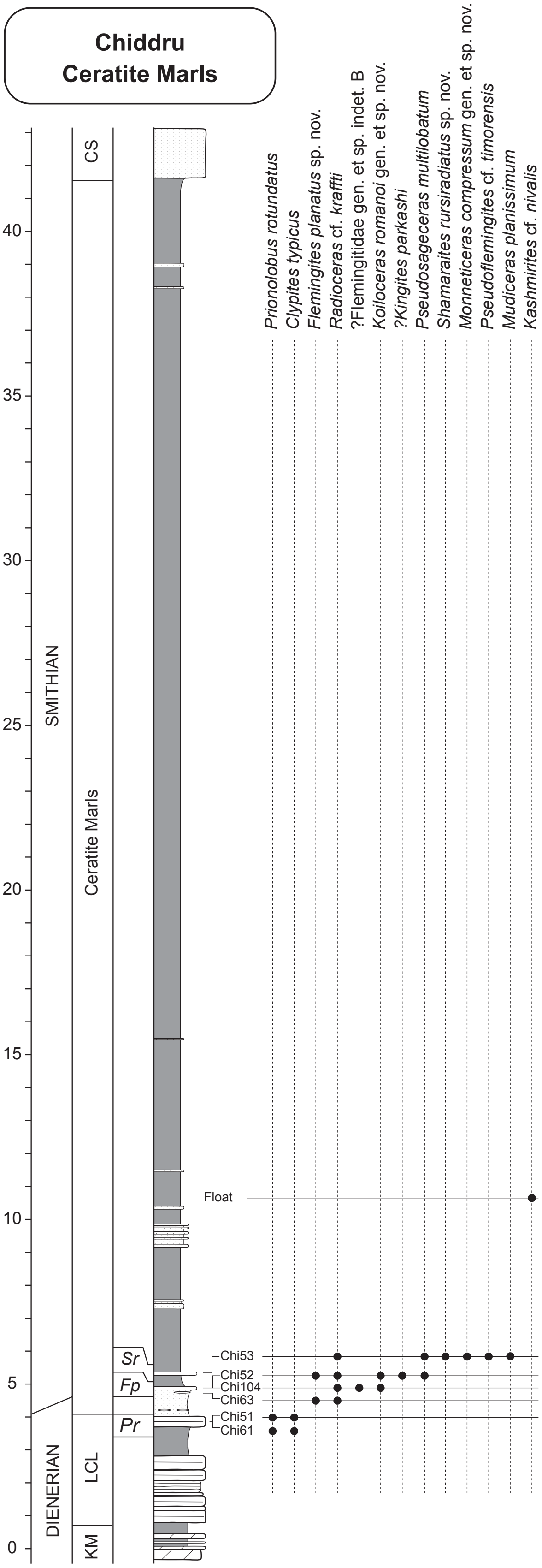
Chiddru
Ceratite Marls
CS
Ceratite Marls
SMITHIAN
DIENERIAN
LCL
KM
Sr
Fp
Pr
40
35
30
25
20
15
10
5
0
Prionolobus rotundatus
Clypites typicus
Flemingites planatus sp. nov.
Radioceras cf. kraffti
?Flemingitidae gen. et sp. indet. B
Koiloceras romanoi gen. et sp. nov.
?Kingites parkashi
Pseudosageceras multilobatum
Shamaraites rursiradiatus sp. nov.
Monneticeras compressum gen. et sp. nov.
Pseudoflemingites cf. timorensis
Mudiceras planissimum
Kashmirites cf. nivalis
Float
Chi53
Chi52
Chi104
Chi63
Chi51
Chi61

Text-fig. 6

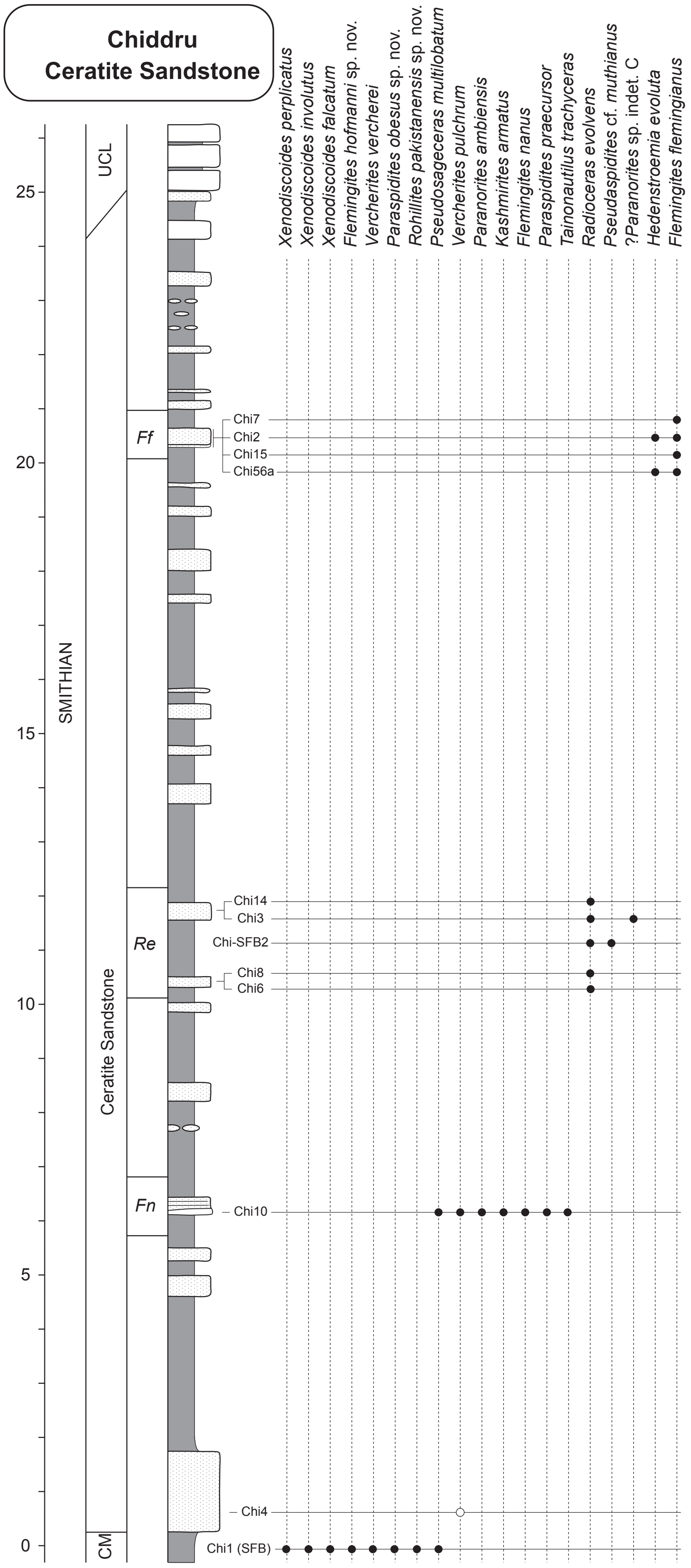
Chiddru
Ceratite Sandstone
Xenodiscoides perplicatus
Xenodiscoides involutus
Xenodiscoides falcatum
Flemingites hofmanni sp. nov.
Vercherites vercherei
Paraspidites obesus sp. nov.
Rohillites pakistanensis sp. nov.
Pseudosageceras multilobatum
Vercherites pulchrum
Paranorites ambiensis
Kashmirites armatus
Flemingites nanus
Paraspidites praecursor
Tainonautilus trachyceras
Radioceras evolvens
Pseudaspidites cf. muthianus
?Paranorites sp. indet. C
Hedenstroemia evoluta
Flemingites flemingianus
25
20
15
10
5
0
SMITHIAN
CM
Ceratite Sandstone
UCL
Ff
Re
Fn
Chi7
Chi2
Chi15
Chi56a
Chi14
Chi3
Chi-SFB2
Chi8
Chi6
Chi10
Chi4
Chi1 (SFB)

Text-fig. 7

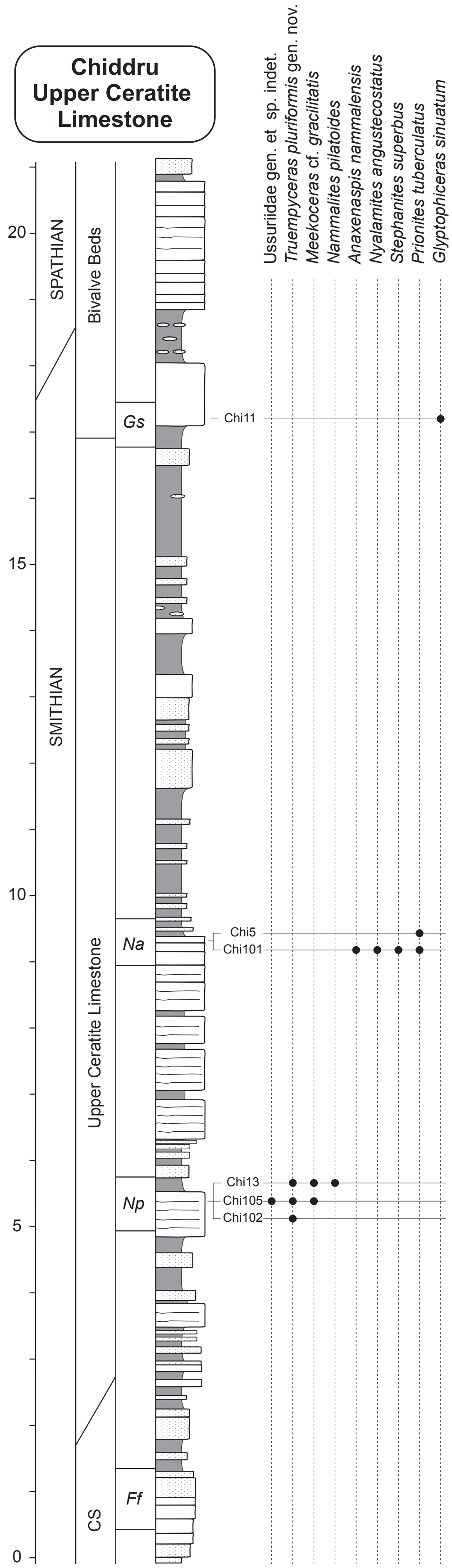
Chiddru
Upper Ceratite
Limestone
Ussuriidae gen. et sp. indet.
Truempyceras pluriformis gen. nov.
Meekoceras cf. gracilitatis
Nammalites pilatoides
Anaxenaspis nammalensis
Nyalamites angustecostatus
Stephanites superbus
Prionites tuberculatus
Glyptophiceras sinuatum
20
15
10
5
0
SPATHIAN
SMITHIAN
Bivalve Beds
Upper Ceratite Limestone
CS
Gs
Na
Np
Ff
Chi11
Chi5
Chi101
Chi13
Chi105
Chi102

Text-fig. 8

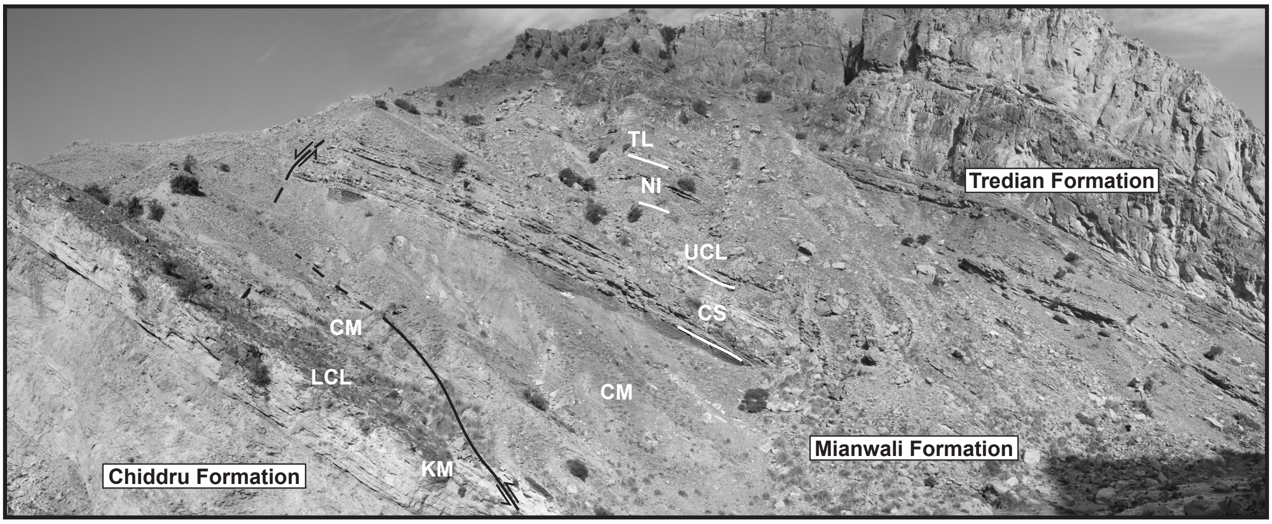
TL
NI
UCL
CS
CM
LCL
CM
KM
Tredian Formation
Mianwali Formation
Chiddru Formation

Text-fig. 9

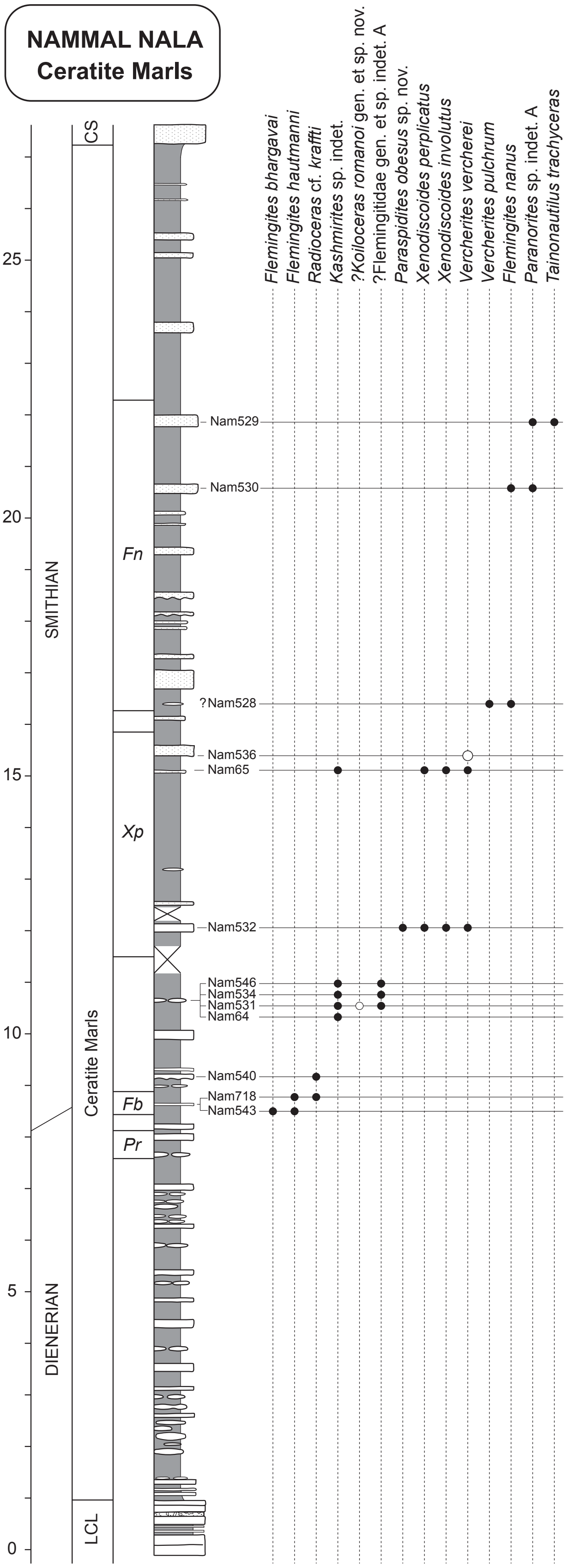
NAMMAL NALA
Ceratite Marls
Flemingites bhargavai
Flemingites hautmanni
Radioceras cf. kraffti
Kashmirites sp. indet.
?Koiloceras romanoi gen. et sp. nov.
?Flemingitidae gen. et sp. indet. A
Paraspidites obesus sp. nov.
Xenodiscoides perplicatus
Xenodiscoides involutus
Vercherites vercherei
Vercherites pulchrum
Flemingites nanus
Paranorites sp. indet. A
Tainonautilus trachyceras
CS
SMITHIAN
DIENERIAN
Ceratite Marls
LCL
Fn
Xp
Fb
Pr
25
20
15
10
5
0
Nam529
Nam530
?Nam528
Nam536
Nam65
Nam532
Nam546
Nam534
Nam531
Nam64
Nam540
Nam718
Nam543

Text-fig. 10

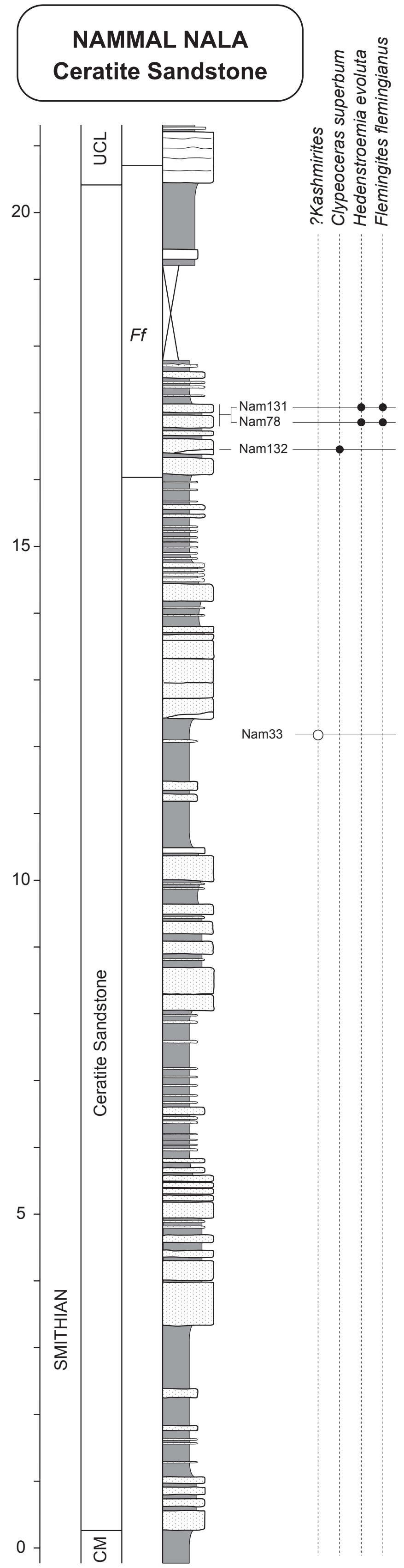
NAMMAL NALA
Ceratite Sandstone
?Kashmirites
Clypeoceras superbum
Hedenstroemia evoluta
Flemingites flemingianus
UCL
20
Ff
Nam131
Nam78
Nam132
15
Nam33
10
Ceratite Sandstone
5
SMITHIAN
0
CM

Text-fig. 11

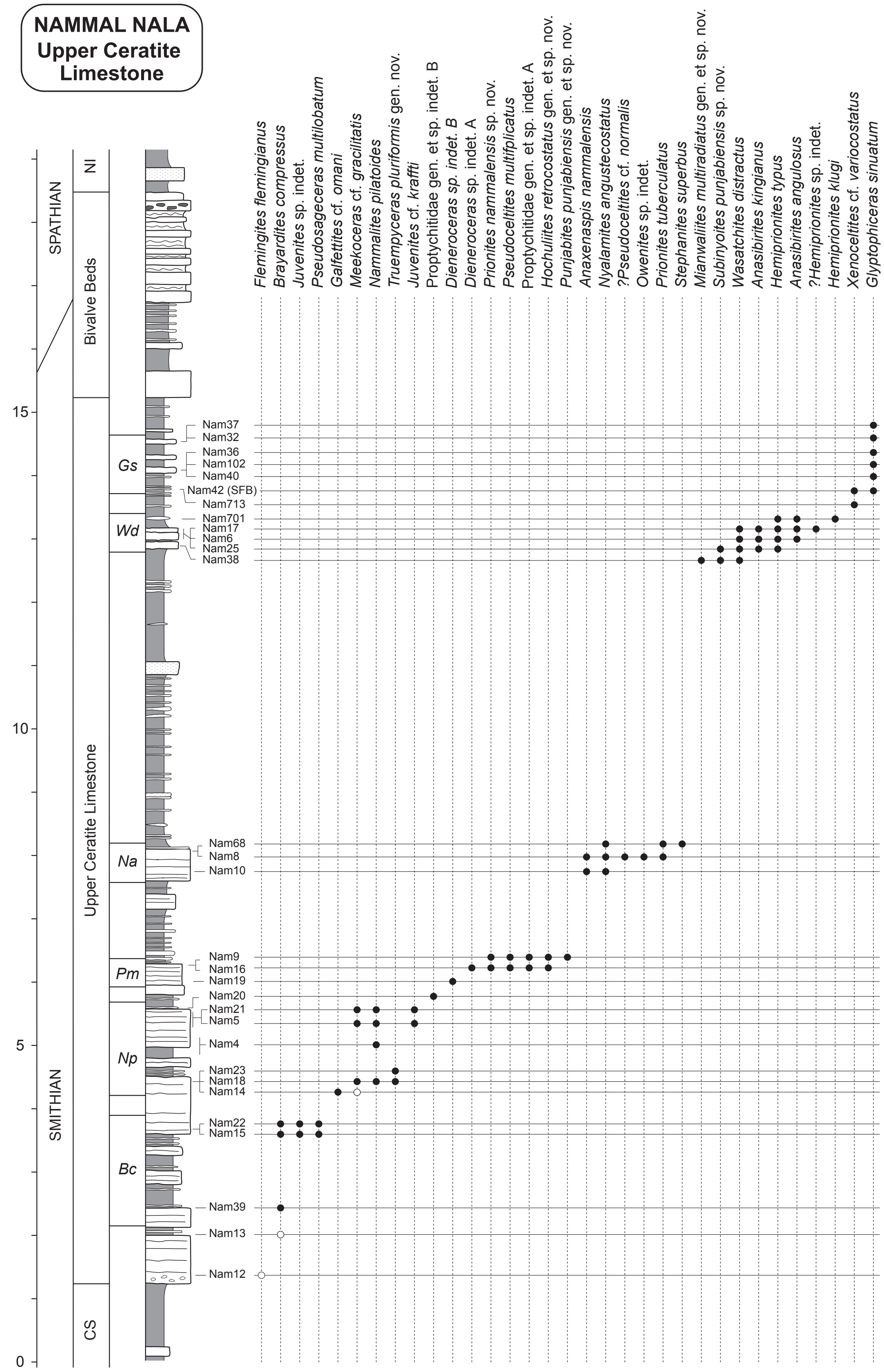
NAMMAL NALA
Upper Ceratite Limestone
SPATHIAN
SMITHIAN
Nl
Bivalve Beds
Upper Ceratite Limestone
CS
Gs
Wd
Na
Pm
Np
Bc
15
10
5
0
Nam37
Nam32
Nam36
Nam102
Nam40
Nam42 (SFB)
Nam713
Nam701
Nam17
Nam6
Nam25
Nam38
Nam68
Nam8
Nam10
Nam9
Nam16
Nam19
Nam20
Nam21
Nam5
Nam4
Nam23
Nam18
Nam14
Nam22
Nam15
Nam39
Nam13
Nam12
Flemingites flemingianus
Brayardites compressus
Juvenites sp. indet.
Pseudosageceras multilobatum
Galfettites cf. omani
Meekoceras cf. gracilitatis
Nammalites pilatoides
Truempyceras pluriformis gen. nov.
Juvenites cf. kraffti
Proptychitidae gen. et sp. indet. B
Dieneroceras sp. indet. B
Dieneroceras sp. indet. A
Prionites nammalensis sp. nov.
Pseudoceltites multiplicatus
Proptychitidae gen. et sp. indet. A
Hochulites retrocostatus gen. et sp. nov.
Punjabites punjabiensis gen. et sp. nov.
Anaxenaspis nammalensis
Nyalamites angustecostatus
?Pseudoceltites cf. normalis
Owenites sp. indet.
Prionites tuberculatus
Stephanites superbus
Mianwalites multiradiatus gen. et sp. nov.
Subinyoites punjabiensis sp. nov.
Wasatchites distractus
Anasibirites kingianus
Hemiprionites typus
Anasibirites angulosus
?Hemiprionites sp. indet.
Hemiprionites klugi
Xenoceltites cf. variocostatus
Glyptophiceras sinuatum

Text-fig. 12

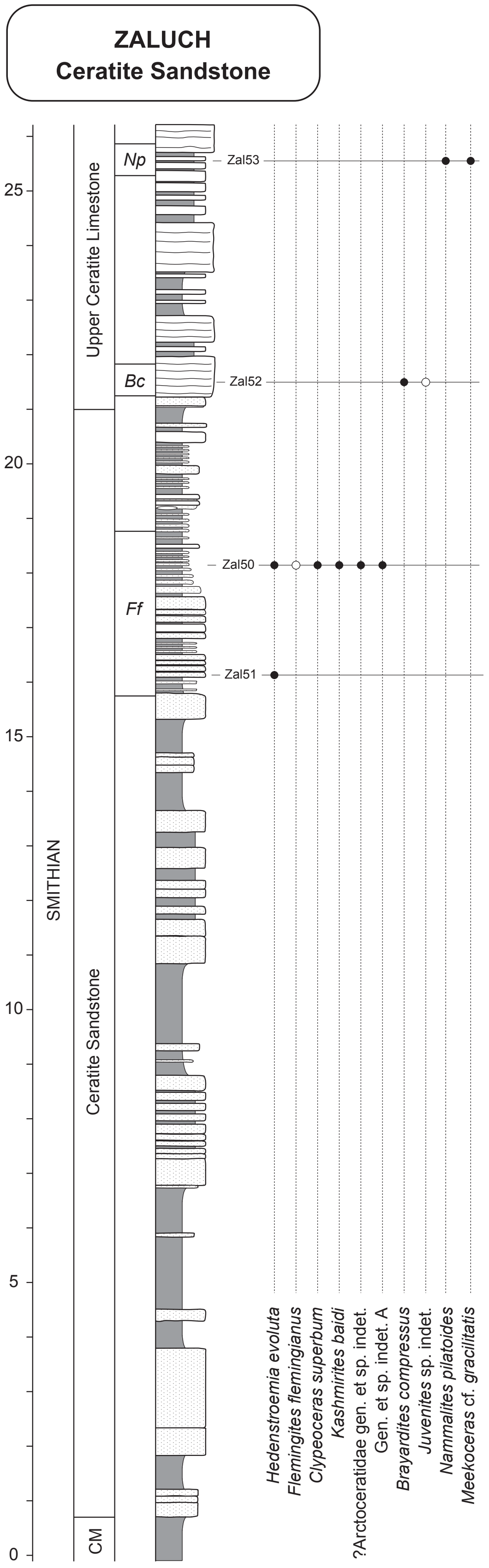
ZALUCH
Ceratite Sandstone
0
5
10
15
20
25
SMITHIAN
CM
Ceratite Sandstone
Upper Ceratite Limestone
Ff
Bc
Np
Zal53
Zal52
Zal50
Zal51
Hedenstroemia evoluta
Flemingites flemingianus
Clypeoceras superbum
Kashmirites baidi
?Arctoceratidae gen. et sp. indet.
Gen. et sp. indet. A
Brayardites compressus
Juvenites sp. indet.
Nammalites pilatoides
Meekoceras cf. gracilitatis

Text-fig. 13

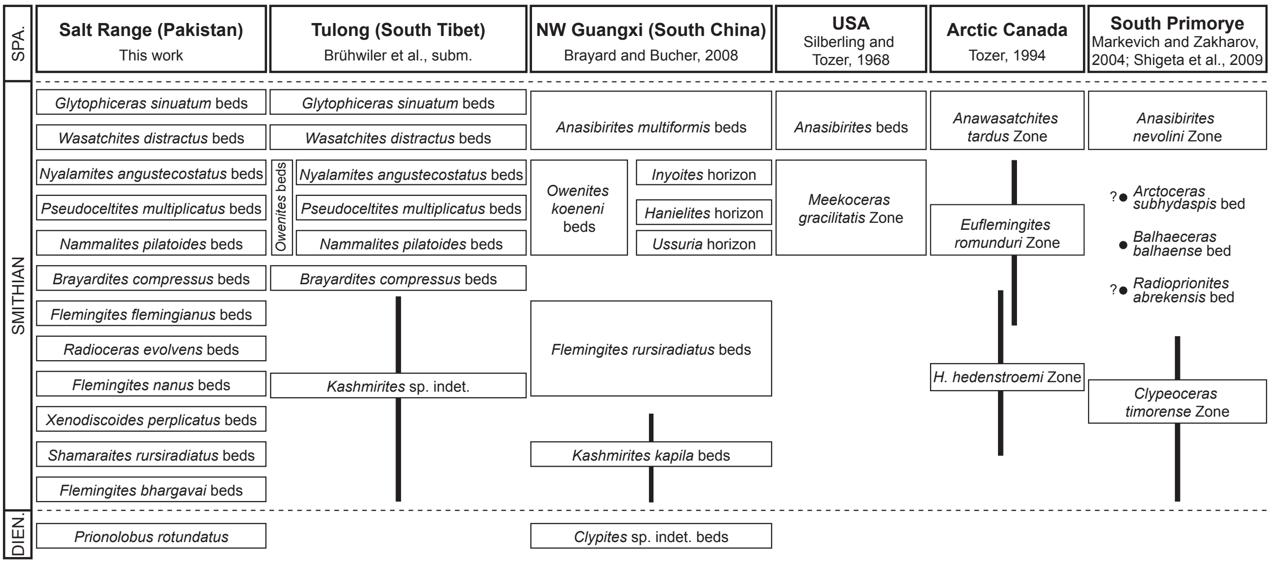
SPA.
SMITHIAN
DIEN.
Salt Range (Pakistan)
This work
Tulong (South Tibet)
Brühwiler et al., subm.
NW Guangxi (South China)
Brayard and Bucher, 2008
USA
Silberling and Tozer, 1968
Arctic Canada
Tozer, 1994
South Primorye
Markevich and Zakharov, 2004; Shigeta et al., 2009
Glytophiceras sinuatum beds
Wasatchites distractus beds
Nyalamites angustecostatus beds
Pseudoceltites multiplicatus beds
Nammalites pilatoides beds
Brayardites compressus beds
Flemingites flemingianus beds
Radioceras evolvens beds
Flemingites nanus beds
Xenodiscoides perplicatus beds
Shamaraites rursiradiatus beds
Flemingites bhargavai beds
Prionolobus rotundatus
Glytophiceras sinuatum beds
Wasatchites distractus beds
Owenites beds
Nyalamites angustecostatus beds
Pseudoceltites multiplicatus beds
Nammalites pilatoides beds
Brayardites compressus beds
Kashmirites sp. indet.
Anasibirites multiformis beds
Owenites koeneni beds
Inyoites horizon
Hanielites horizon
Ussuria horizon
Flemingites rursiradiatus beds
Kashmirites kapila beds
Clypites sp. indet. beds
Anasibirites beds
Meekoceras gracilitatis Zone
Anawasatchites tardus Zone
Euflemingites romunduri Zone
H. hedenstroemi Zone
Anasibirites nevolini Zone
?● Arctoceras subhydaspis bed
● Balhaeceras balhaense bed
?● Radioprionites abrekensis bed
Clypeoceras timorense Zone

Text-fig. 14

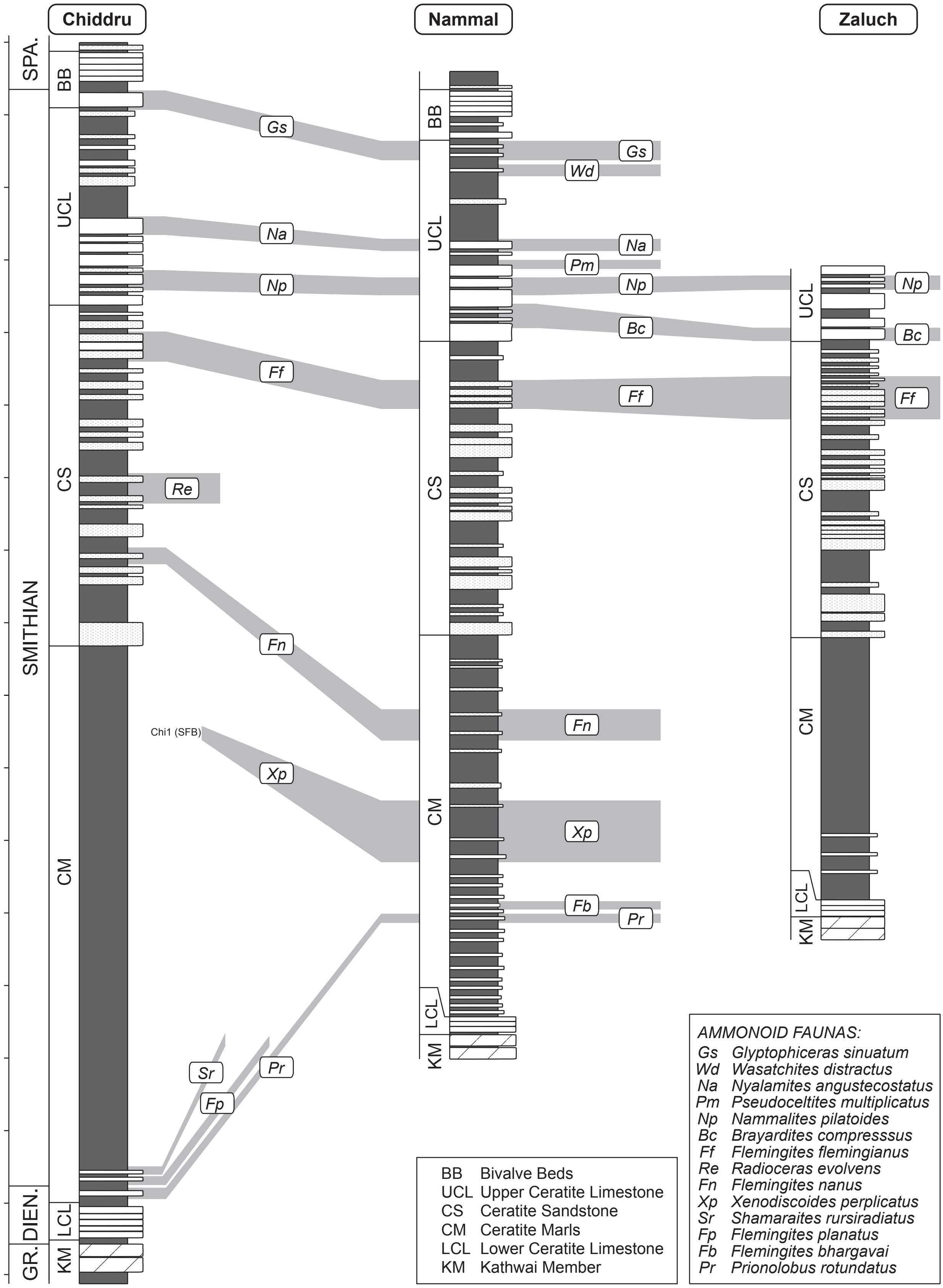
Chiddru
Nammal
Zaluch
SPA.
SMITHIAN
GR.
DIEN.
BB
UCL
CS
CM
LCL
KM
0
10
20
30
40
50
60
70
80
Gs
Wd
Na
Pm
Np
Bc
Ff
Re
Fn
Xp
Fb
Pr
Sr
Fp
Chi1 (SFB)
BB Bivalve Beds
UCL Upper Ceratite Limestone
CS Ceratite Sandstone
CM Ceratite Marls
LCL Lower Ceratite Limestone
KM Kathwai Member
AMMONOID FAUNAS:
Gs Glyptophiceras sinuatum
Wd Wasatchites distractus
Na Nyalamites angustecostatus
Pm Pseudoceltites multiplicatus
Np Nammalites pilatoides
Bc Brayardites compresssus
Ff Flemingites flemingianus
Re Radioceras evolvens
Fn Flemingites nanus
Xp Xenodiscoides perplicatus
Sr Shamaraites rursiradiatus
Fp Flemingites planatus
Fb Flemingites bhargavai
Pr Prionolobus rotundatus

Text-fig. 15

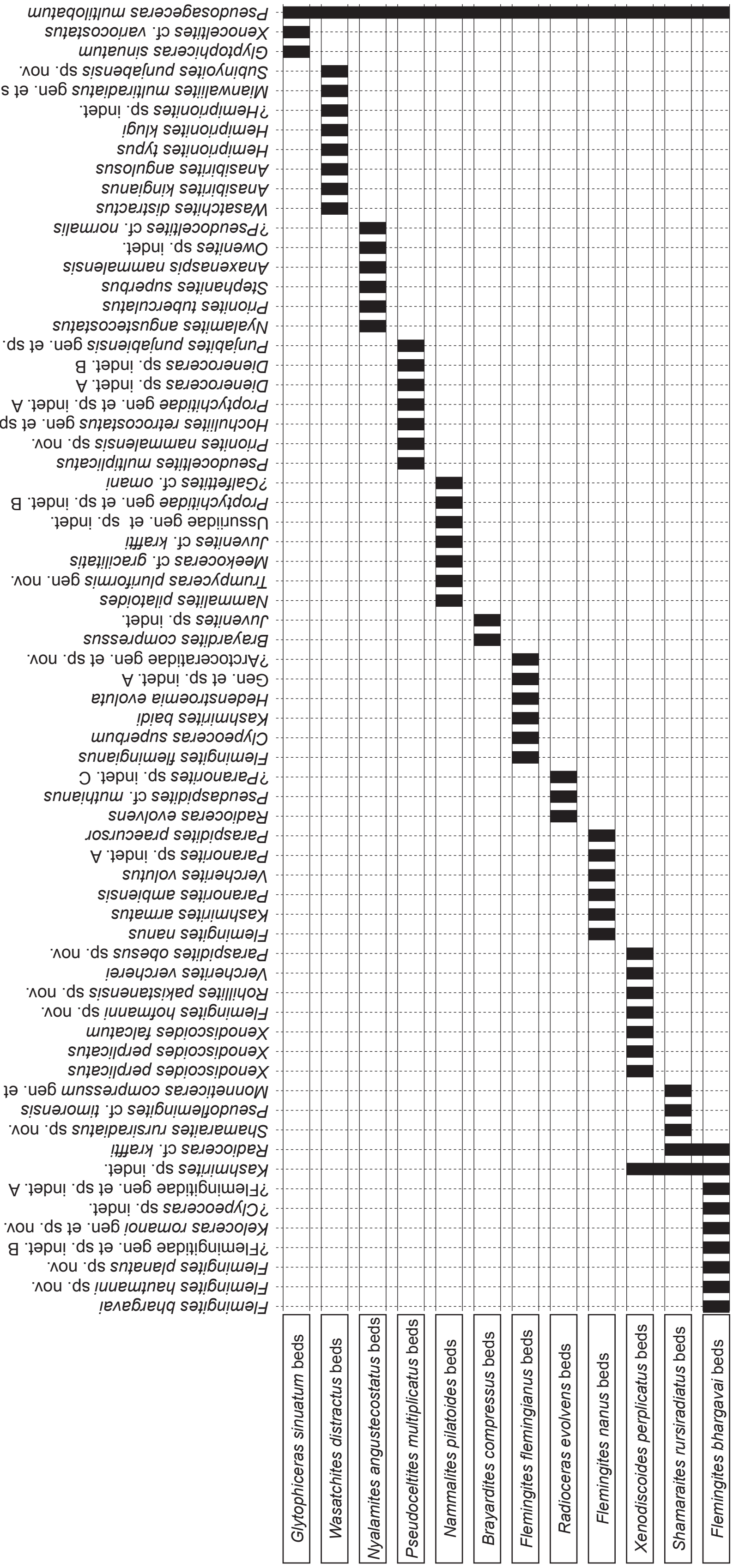
Pseudosageceras multilobatum
Xenoceltites cf. variocostatus
Glyptophiceras sinuatum
Subinyoites punjabensis sp. nov.
Mianwalites multiradiatus gen. et sp. nov.
?Hemiprionites sp. indet.
Hemiprionites klugi
Hemiprionites typus
Anasibirites angulosus
Anasibirites kingianus
Wasatchites distractus
?Pseudoceltites cf. normalis
Owenites sp. indet.
Anaxenaspis nammalensis
Stephanites superbus
Prionites tuberculatus
Nyalamites angustecostatus
Punjabites punjabiensis gen. et sp. nov.
Dieneroceras sp. indet. B
Dieneroceras sp. indet. A
Proptychitidae gen. et sp. indet. A
Hochuliites retrocostatus gen. et sp. nov.
Prionites nammalensis sp. nov.
Pseudoceltites multiplicatus
?Galfettites cf. omani
Proptychitidae gen. et sp. indet. B
Ussuriidae gen. et sp. indet.
Juvenites cf. kraffti
Meekoceras cf. gracilitatis
Trumpyceras pluriformis gen. nov.
Nammalites pilatoides
Juvenites sp. indet.
Brayardites compressus
?Arctoceratidae gen. et sp. nov.
Gen. et sp. indet. A
Hedenstroemia evoluta
Kashmirites baidi
Clypeoceras superbum
Flemingites flemingianus
?Paranorites sp. indet. C
Pseudaspidites cf. muthianus
Radioceras evolvens
Paraspidites praecursor
Paranorites sp. indet. A
Vercherites volutus
Paranorites ambiensis
Kashmirites armatus
Flemingites nanus
Paraspidites obesus sp. nov.
Vercherites vercherei
Rohillites pakistanensis sp. nov.
Flemingites hofmanni sp. nov.
Xenodiscoides falcatum
Xenodiscoides perplicatus
Xenodiscoides perplicatus
Mongoliceras compressum gen. et sp. nov.
Pseudoflemingites cf. timorensis
Shamaraites rursiradiatus sp. nov.
Radioceras cf. kraffti
Kashmirites sp. indet.
?Flemingitidae gen. et sp. indet. A
?Clypeoceras sp. indet.
Kelolceras romanoi gen. et sp. nov.
?Flemingitidae gen. et sp. indet. B
Flemingites planatus sp. nov.
Flemingites hautmanni sp. nov.
Flemingites bhargavai
Glytophiceras sinuatum beds
Wasatchites distractus beds
Nyalamites angustecostatus beds
Pseudoceltites multiplicatus beds
Nammalites pilatoides beds
Brayardites compressus beds
Flemingites flemingianus beds
Radioceras evolvens beds
Flemingites nanus beds
Xenodiscoides perplicatus beds
Shamaraites rursiradiatus beds
Flemingites bhargavai beds

Text-fig. 16

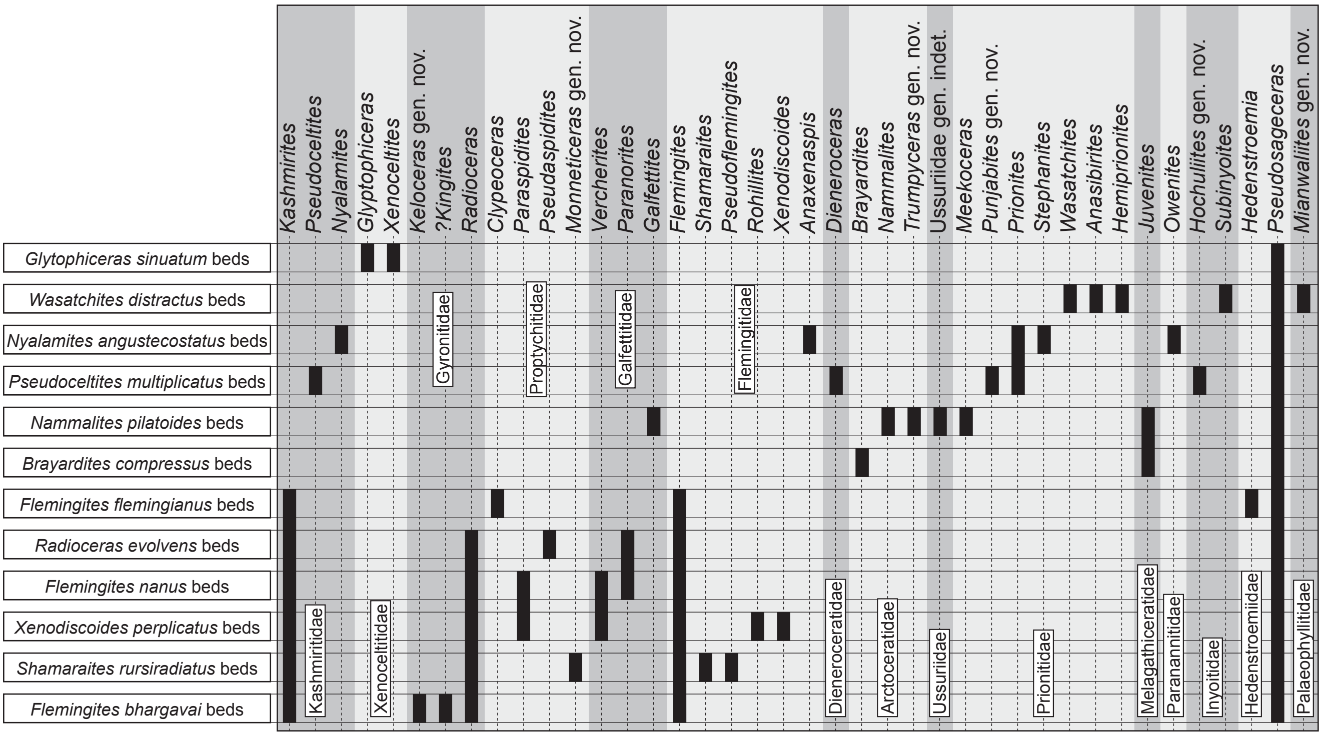
Kashmirites
Pseudoceltites
Nyalamites
Glyptophiceras
Xenoceltites
Keloceras gen. nov.
?Kingites
Radioceras
Clypeoceras
Paraspidites
Pseudaspidites
Monneticeras gen. nov.
Vercherites
Paranorites
Galfettites
Flemingites
Shamaraites
Pseudoflemingites
Rohillites
Xenodiscoides
Anaxenaspis
Dieneroceras
Brayardites
Nammalites
Trumpyceras gen. nov.
Ussuriidae gen. indet.
Meekoceras
Punjabites gen. nov.
Prionites
Stephanites
Wasatchites
Anasibirites
Hemiprionites
Juvenites
Owenites
Hochulites gen. nov.
Subinyoites
Hedenstroemia
Pseudosageceras
Mianwalites gen. nov.
Glytophiceras sinuatum beds
Wasatchites distractus beds
Nyalamites angustecostatus beds
Pseudoceltites multiplicatus beds
Nammalites pilatoides beds
Brayardites compressus beds
Flemingites flemingianus beds
Radioceras evolvens beds
Flemingites nanus beds
Xenodiscoides perplicatus beds
Shamaraites rursiradiatus beds
Flemingites bhargavai beds
Gyronitidae
Proptychitidae
Galfettitidae
Flemingitidae
Kashmiritidae
Xenoceltitidae
Dieneroceratidae
Arctoceratidae
Ussuriidae
Prionitidae
Melagathiceratidae
Paranannitidae
Inyoitidae
Hedenstroemiidae
Palaeophyllitidae

Text-fig. 17

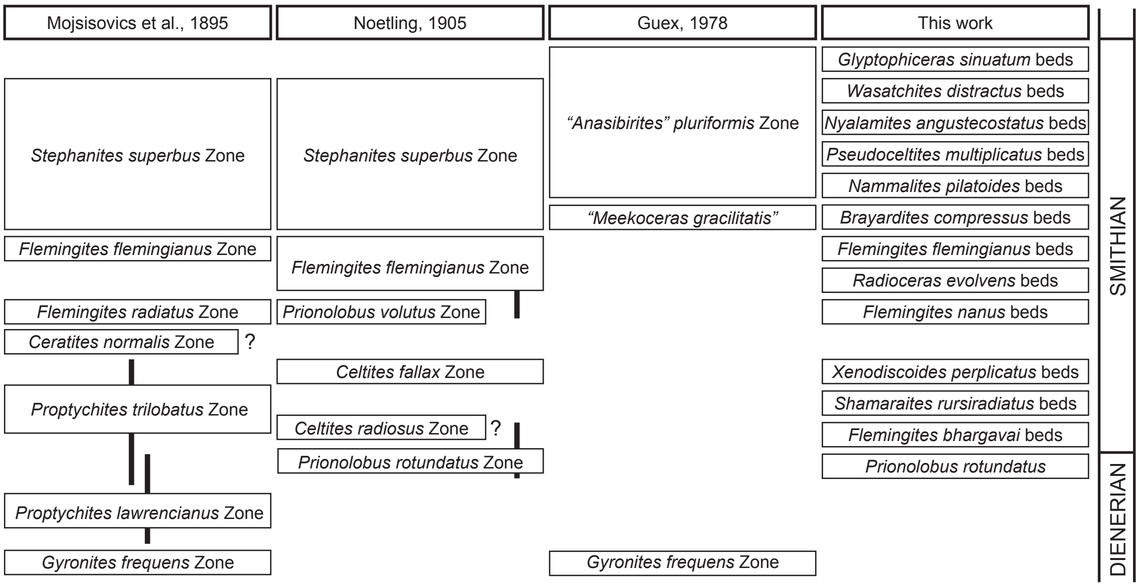

Text-fig. 18

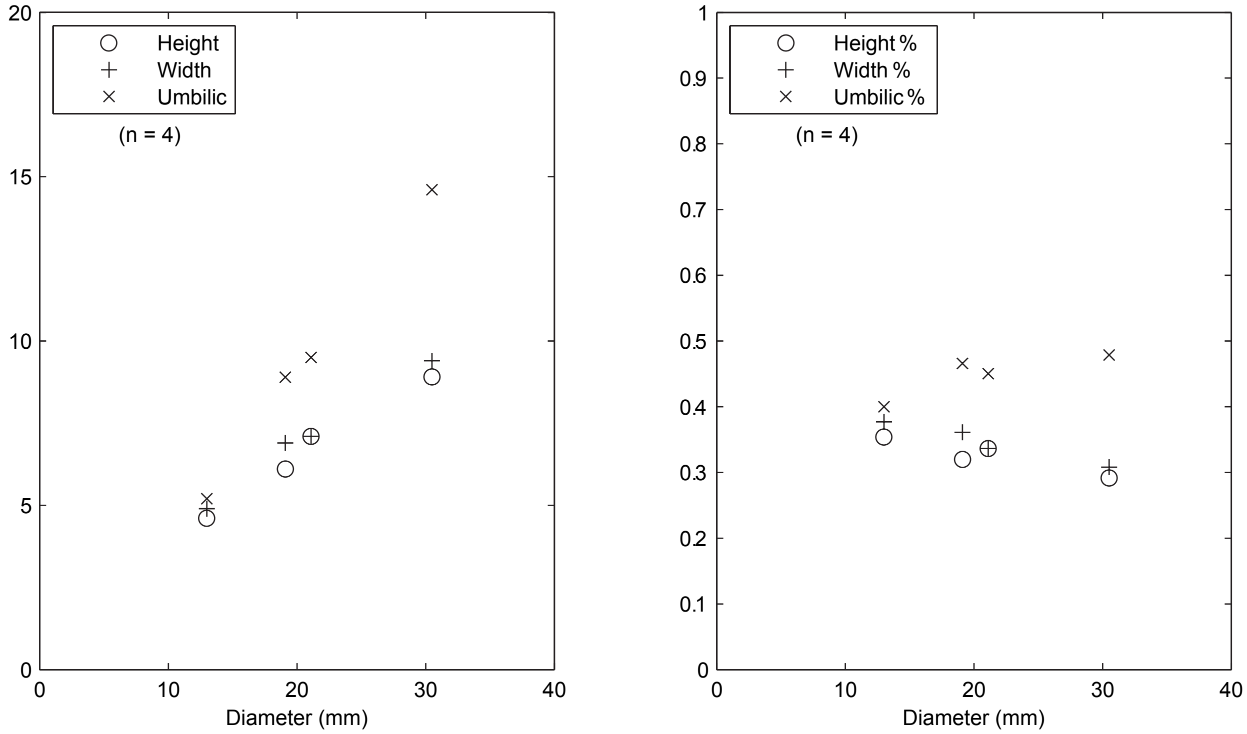

Text-fig. 19

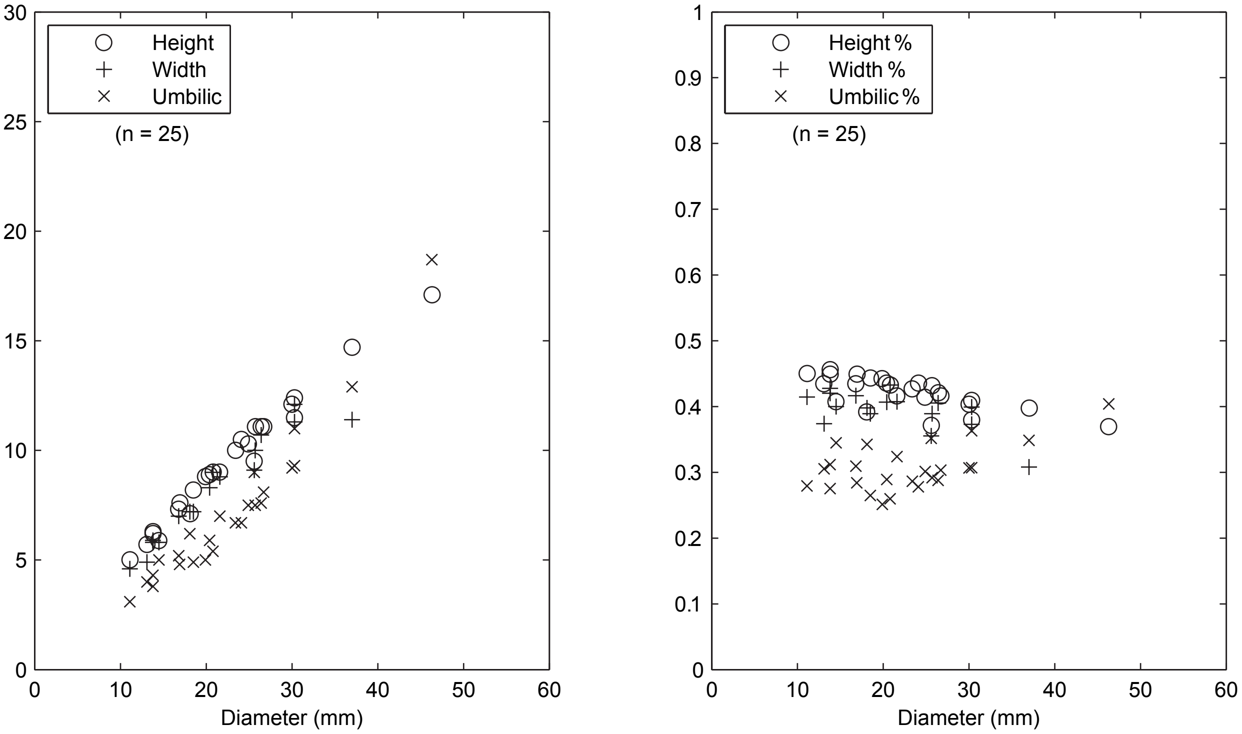

Text-fig. 20

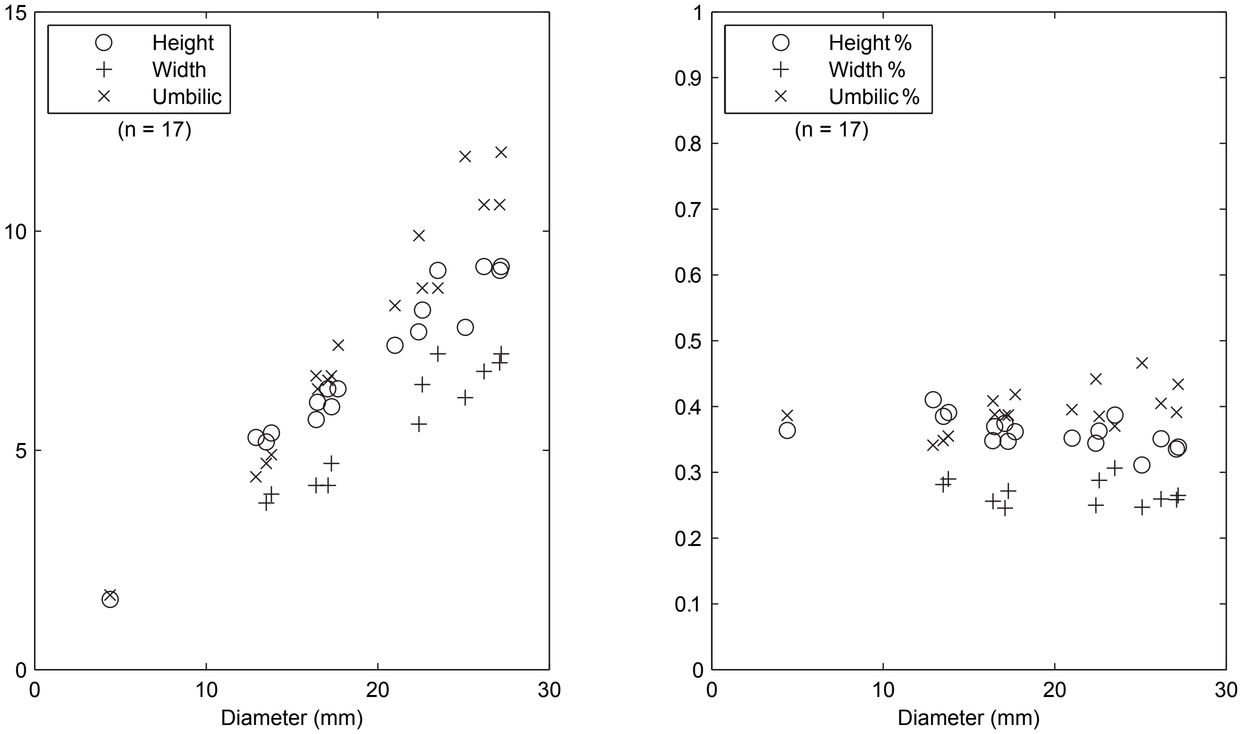

Text-fig. 21

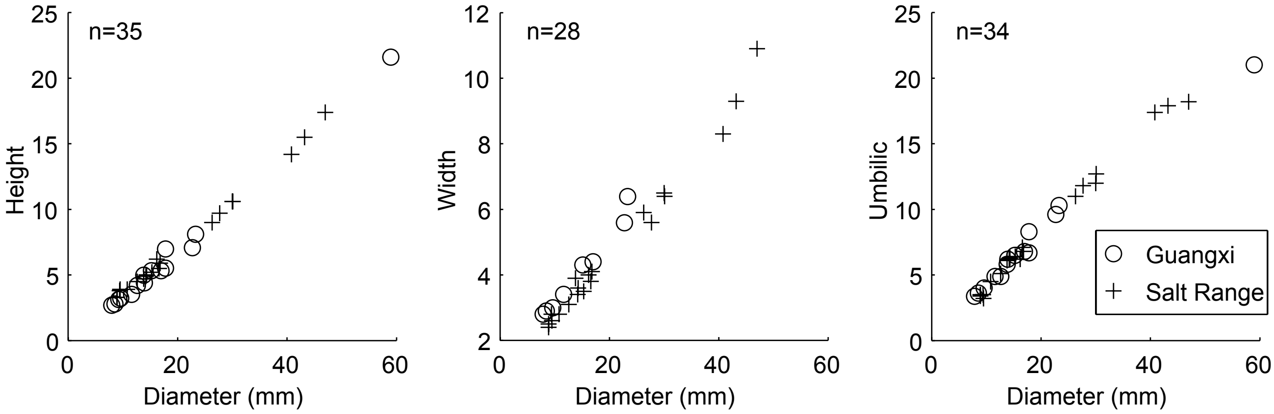

Text-fig. 22

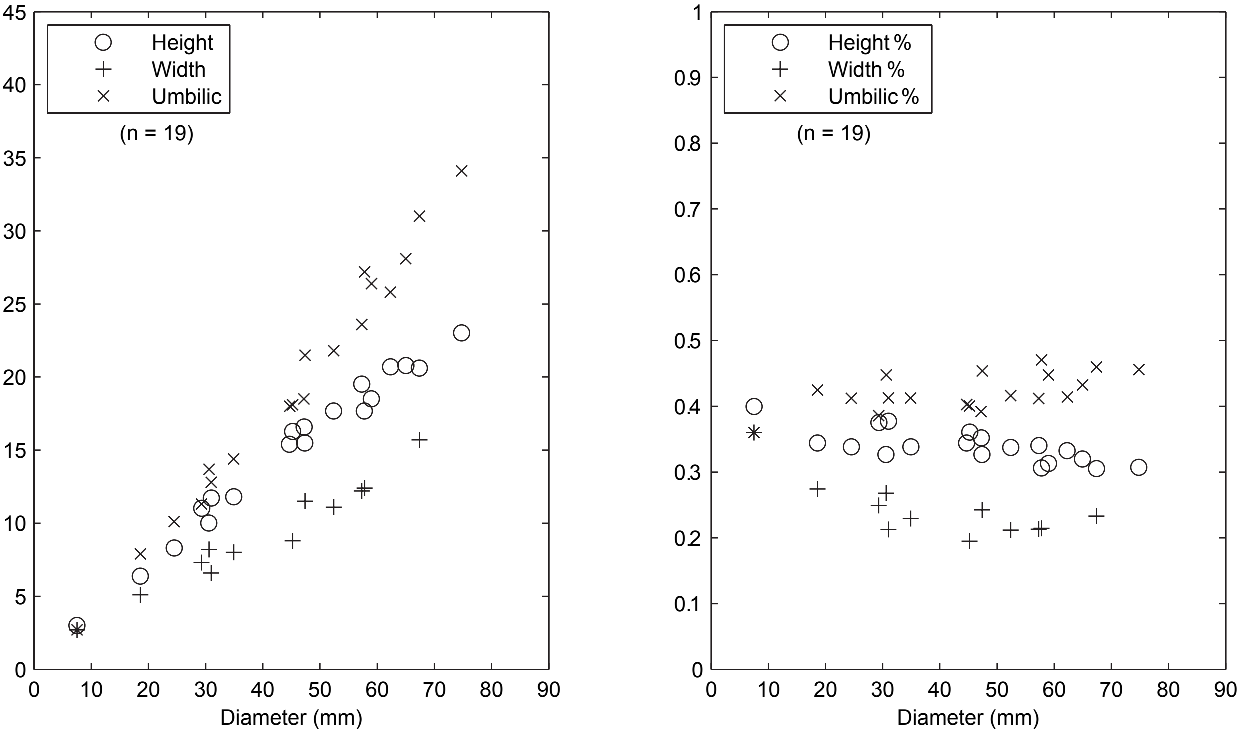

Text-fig. 23

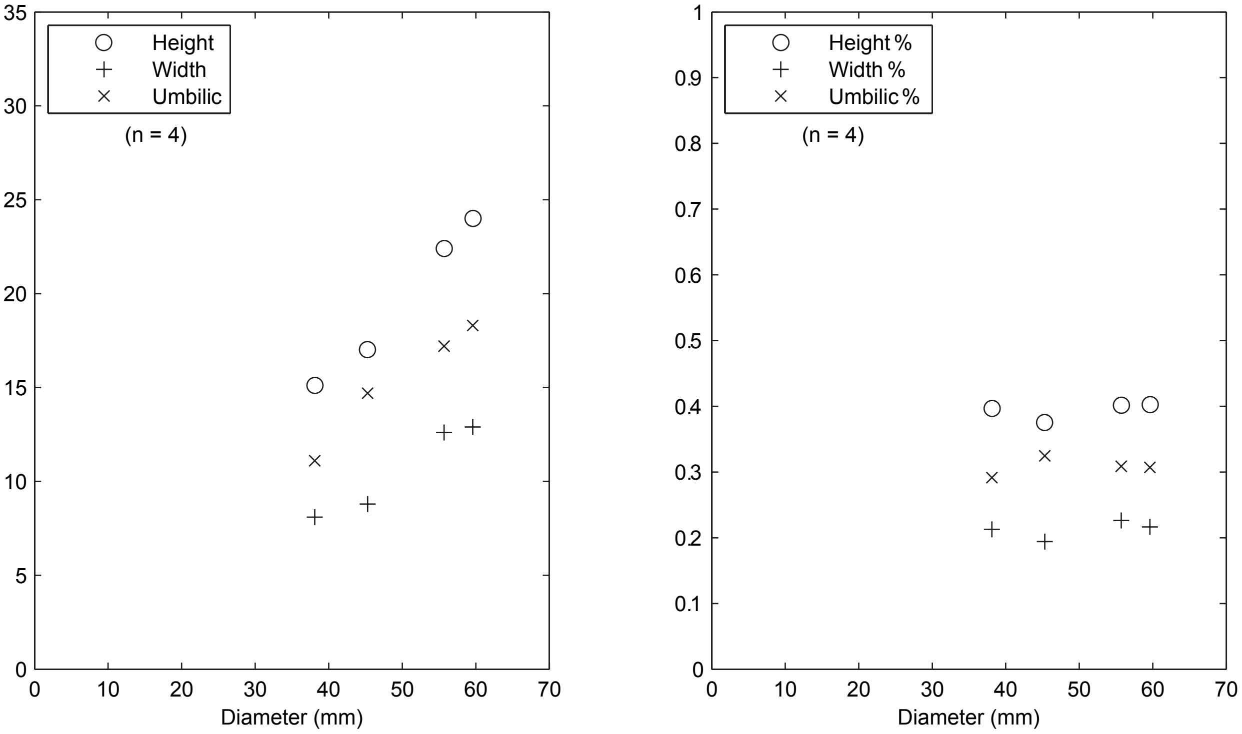

Text-fig. 24

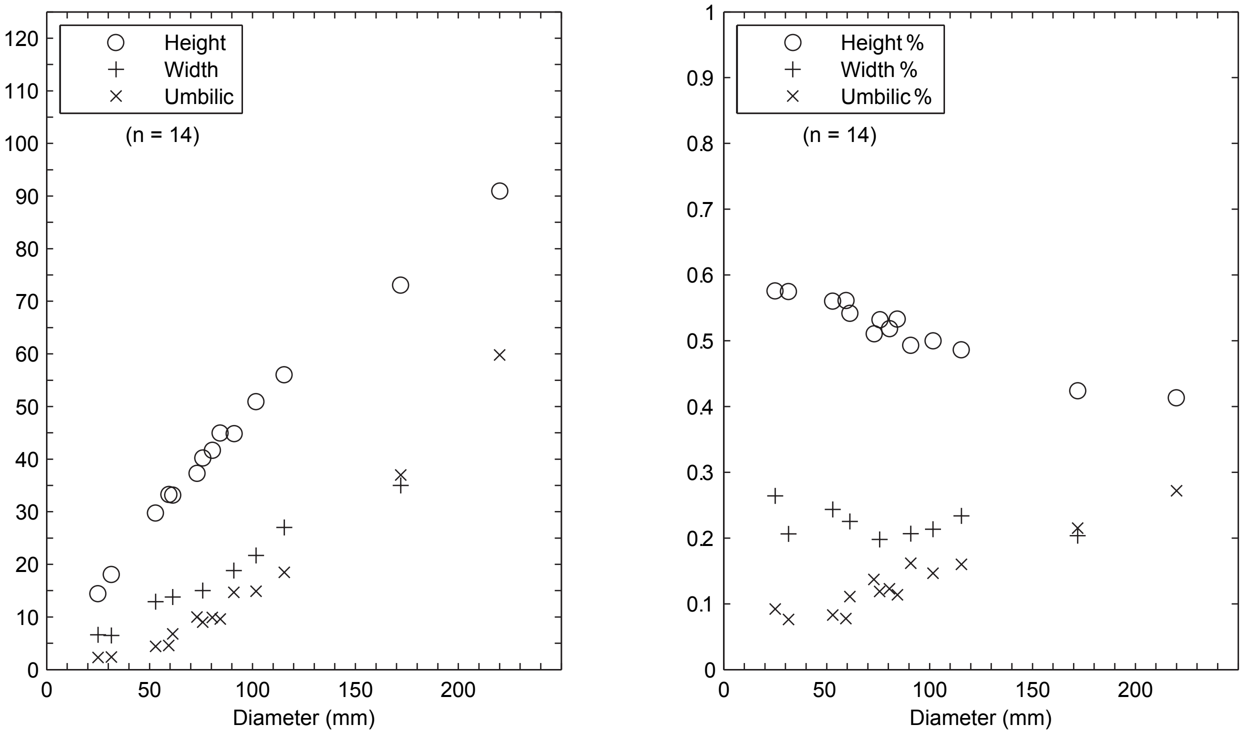

Text-fig. 25

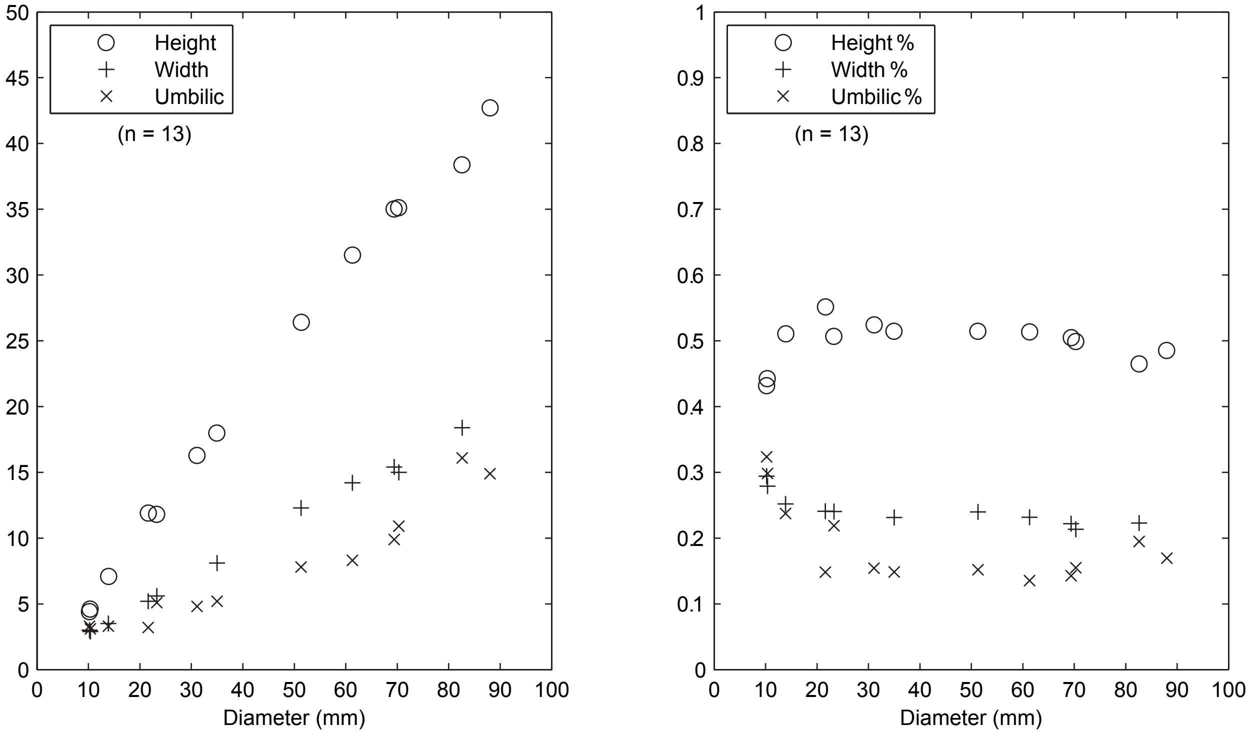

Text-fig. 26

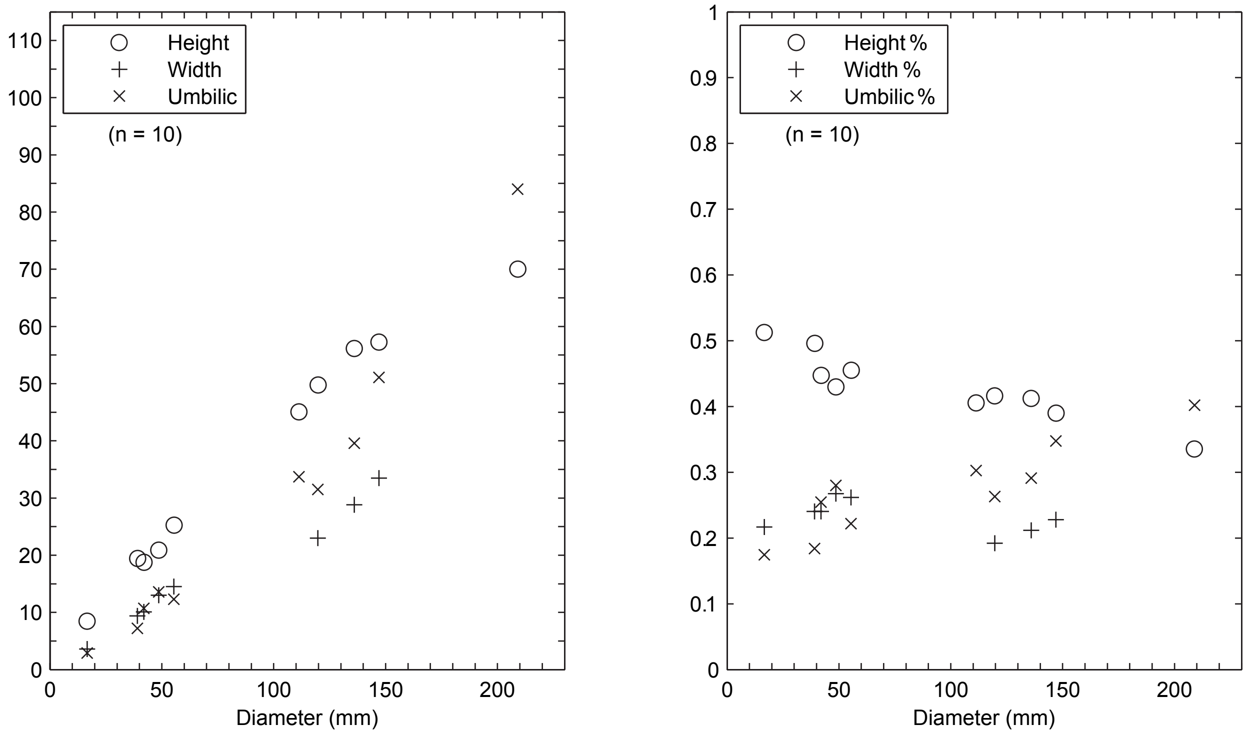

Text-fig. 27

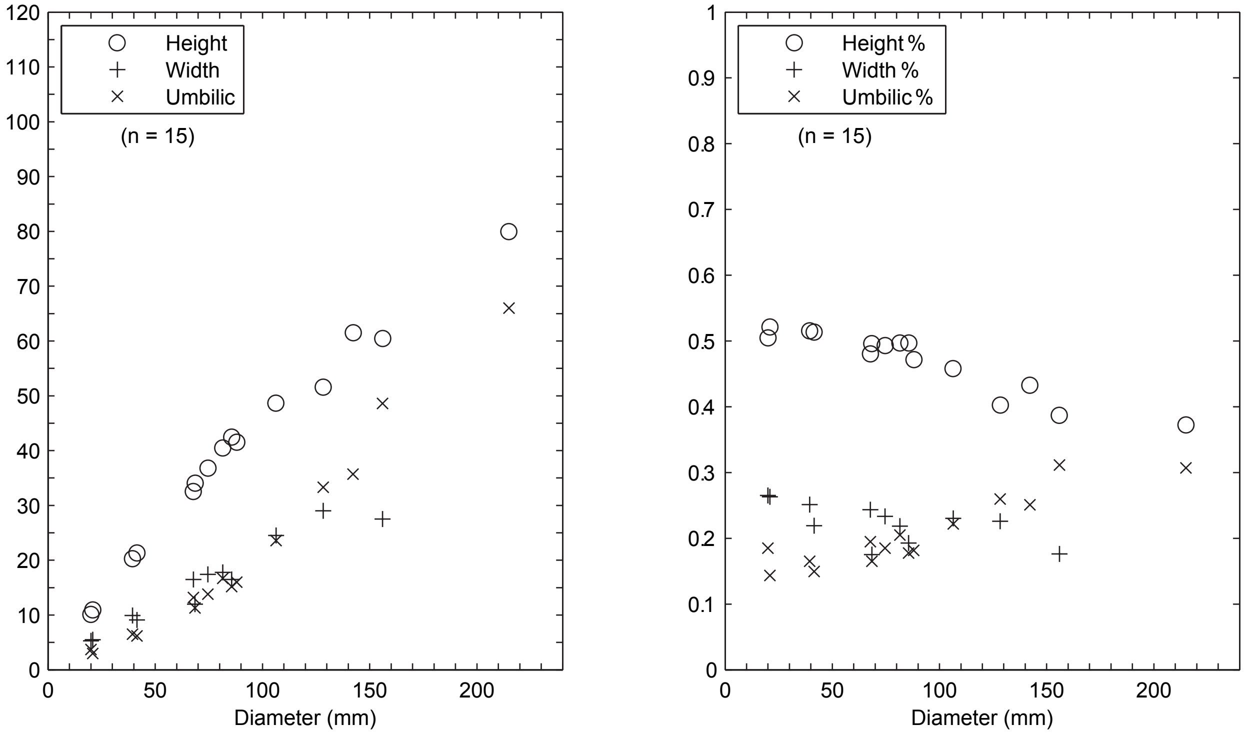

Text-fig. 28

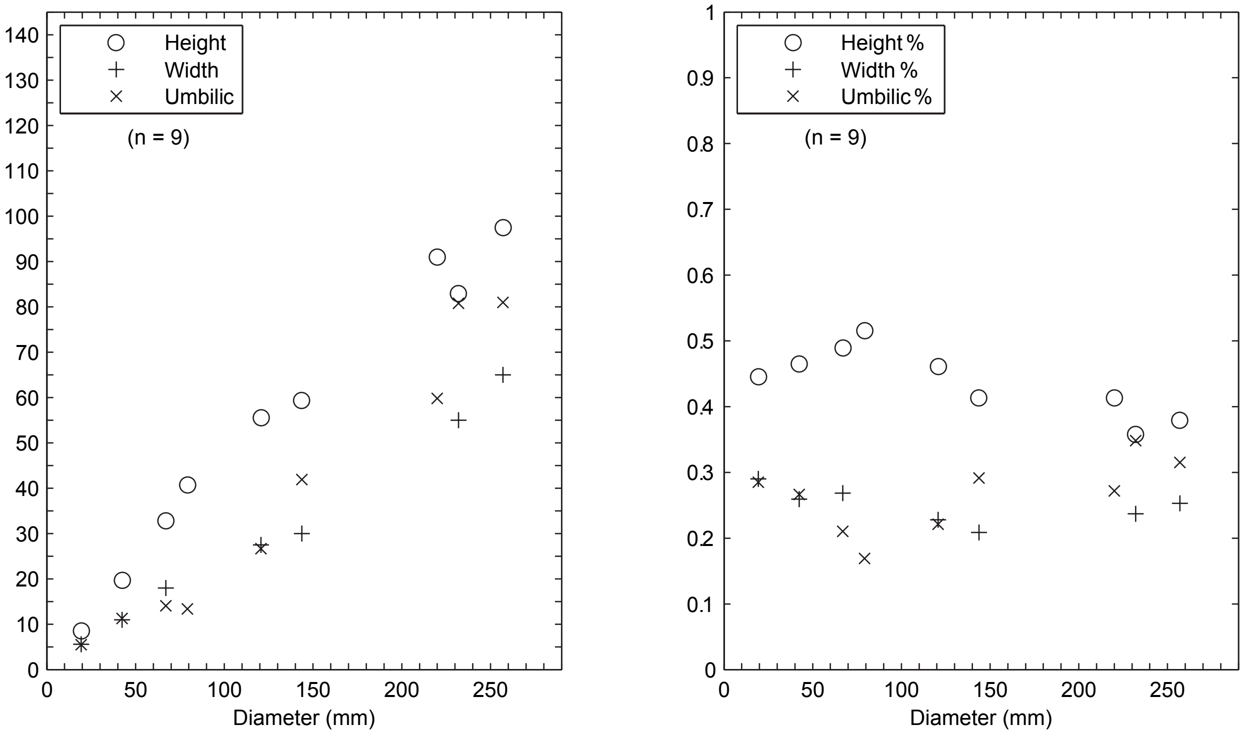

Text-fig. 29

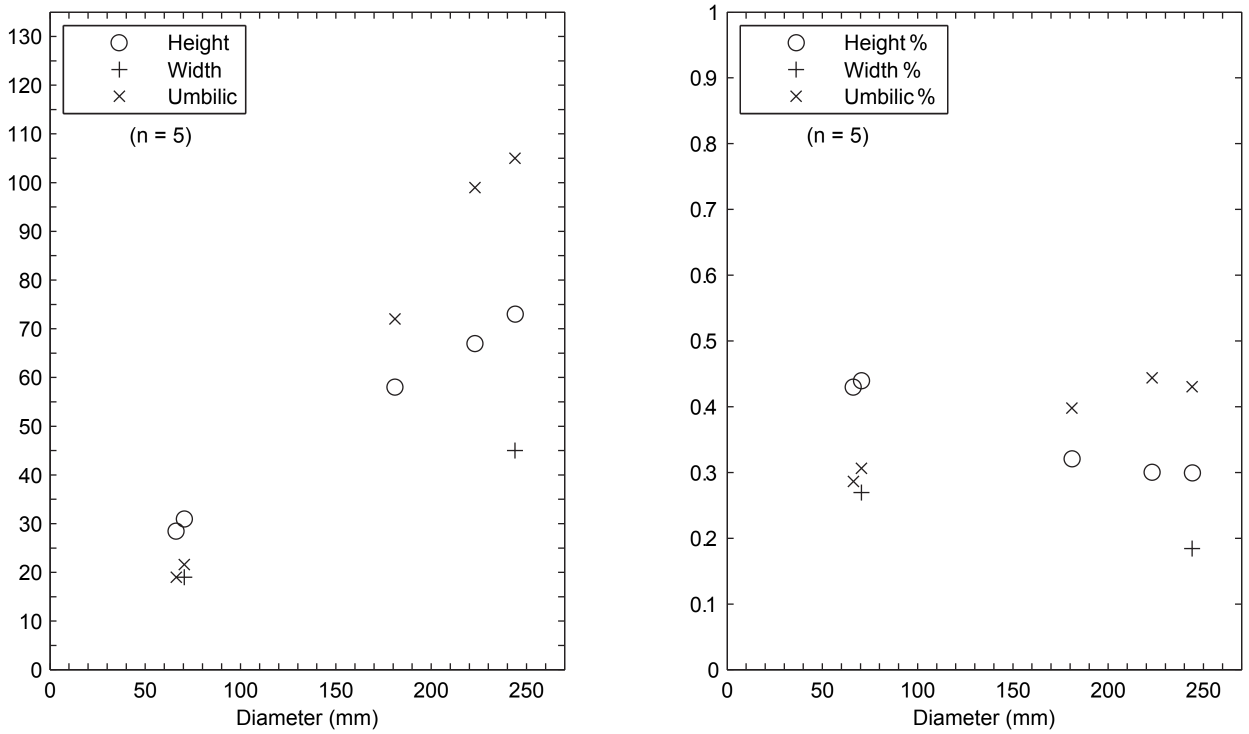

Text-fig. 30

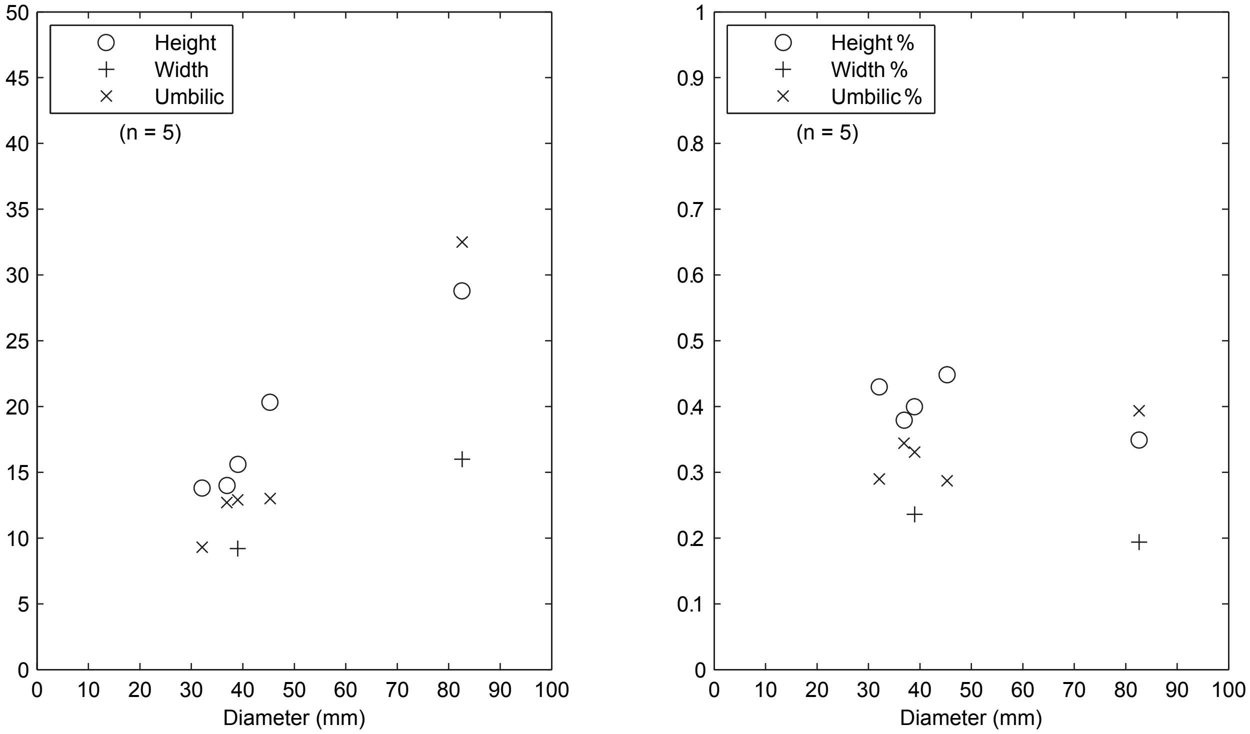

Text-fig. 31

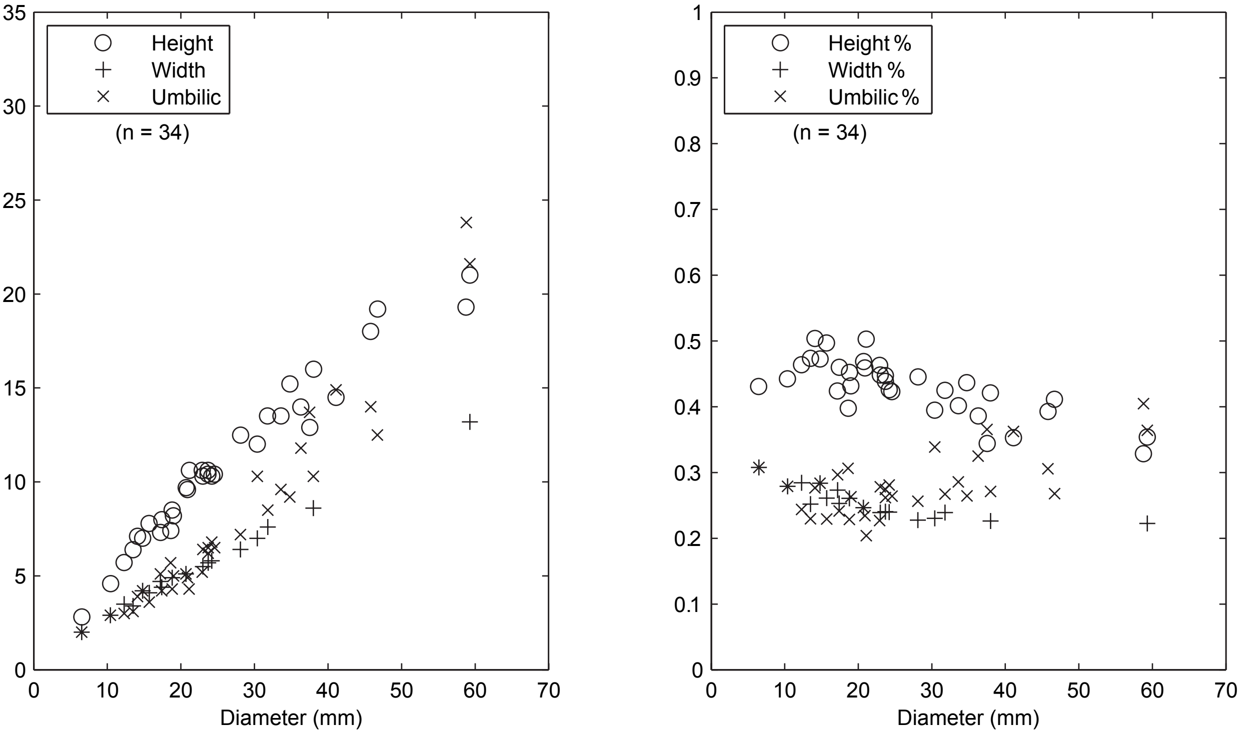

Text-fig. 32

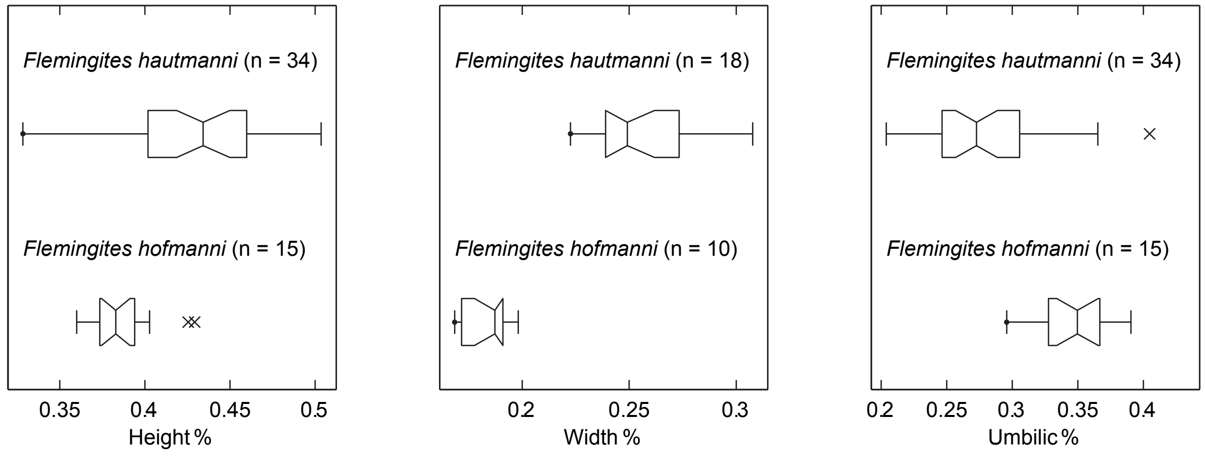

Text-fig. 33

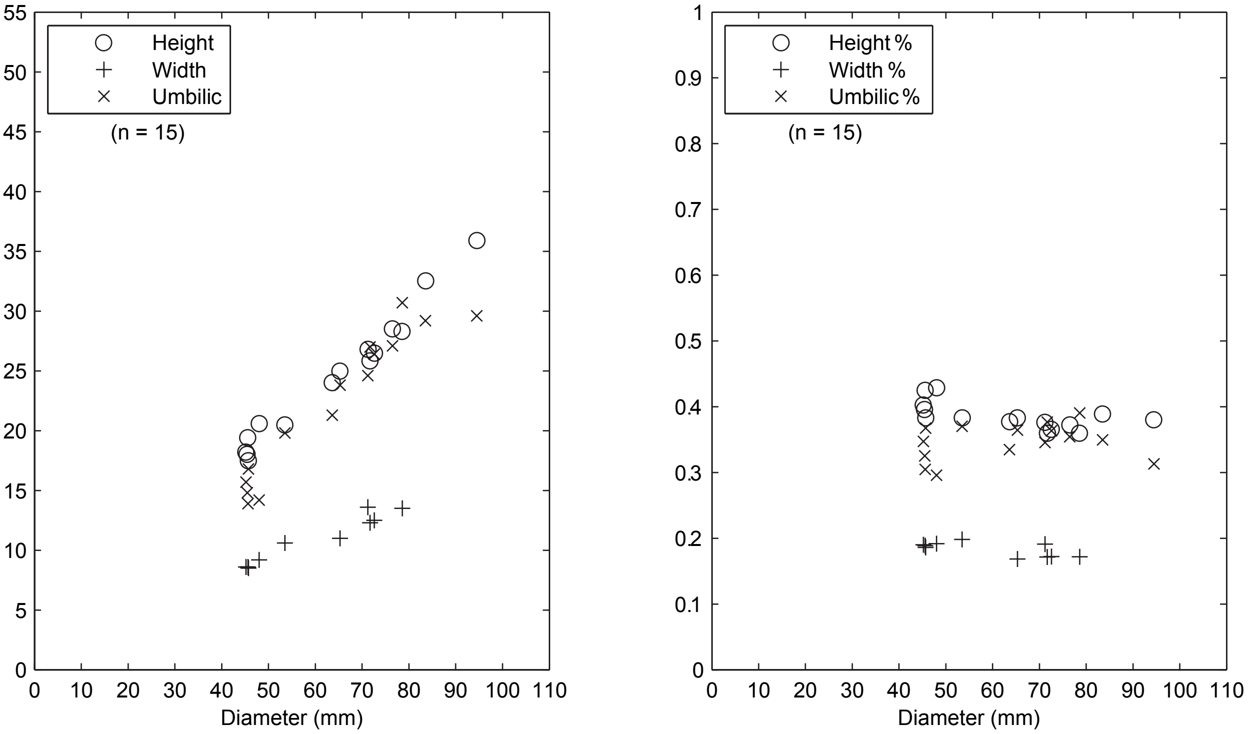

Text-fig. 34

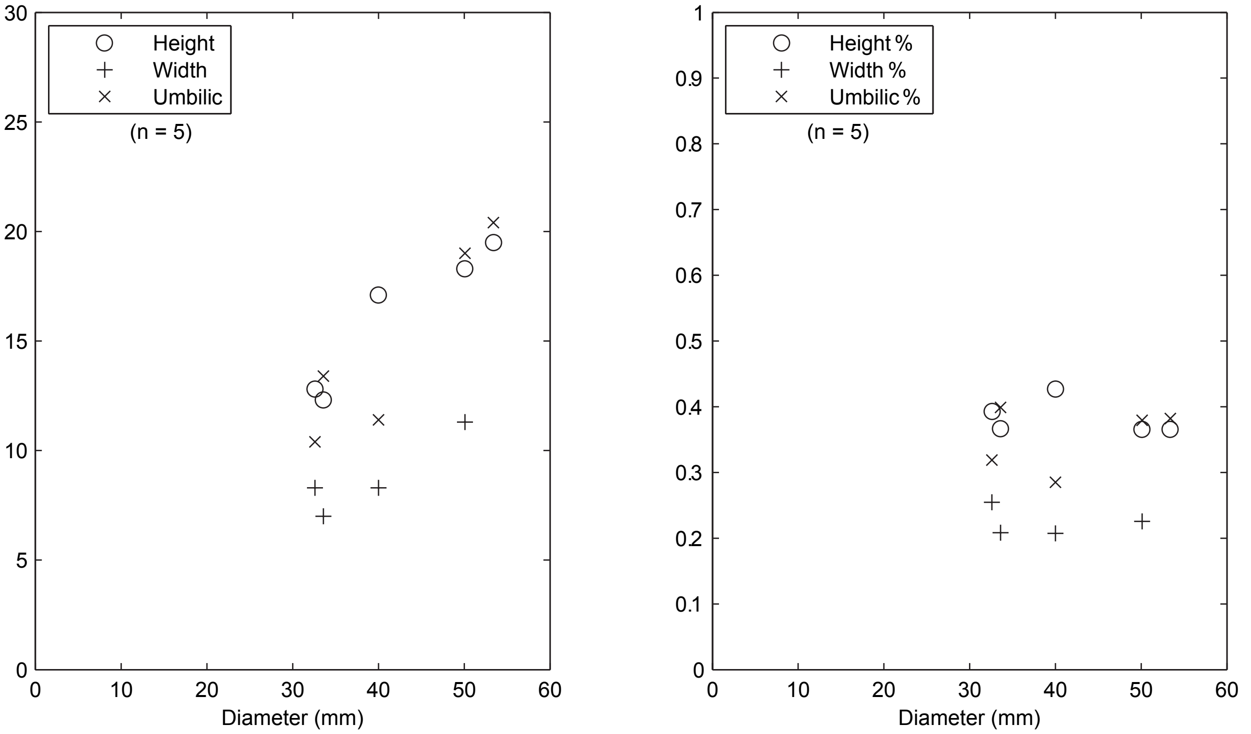

Text-fig. 35

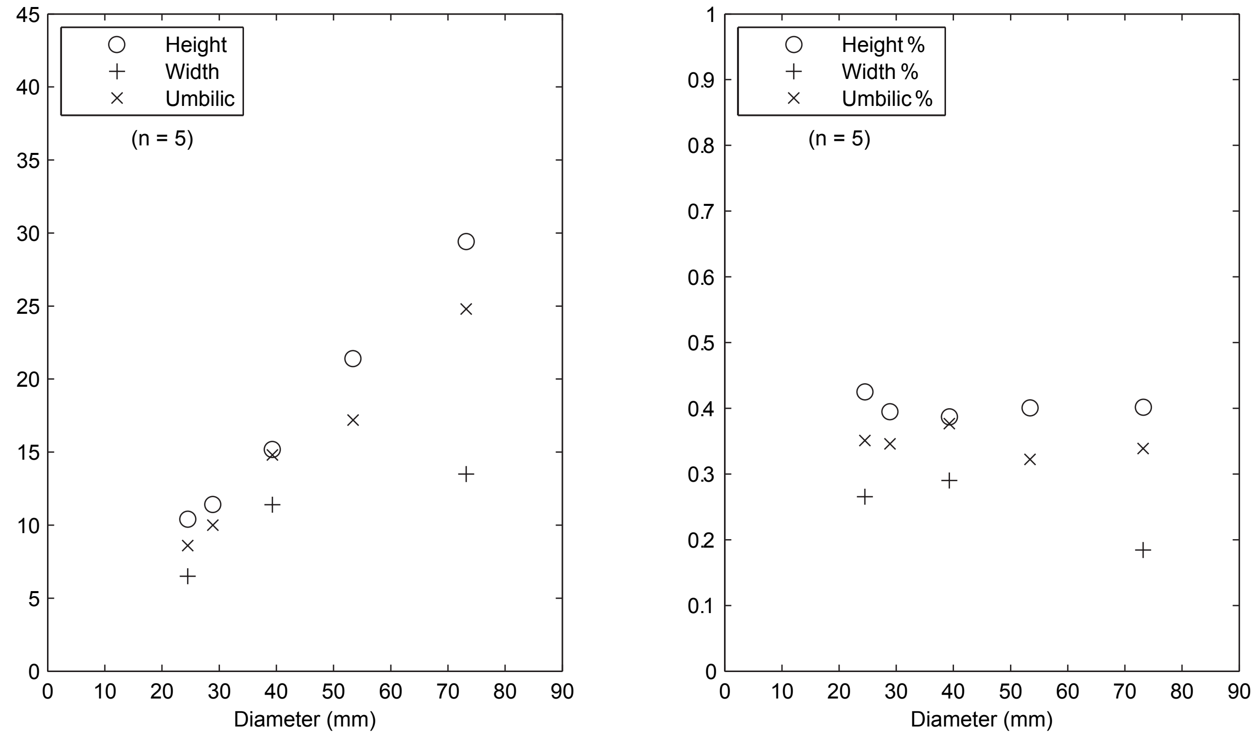

Text-fig. 36

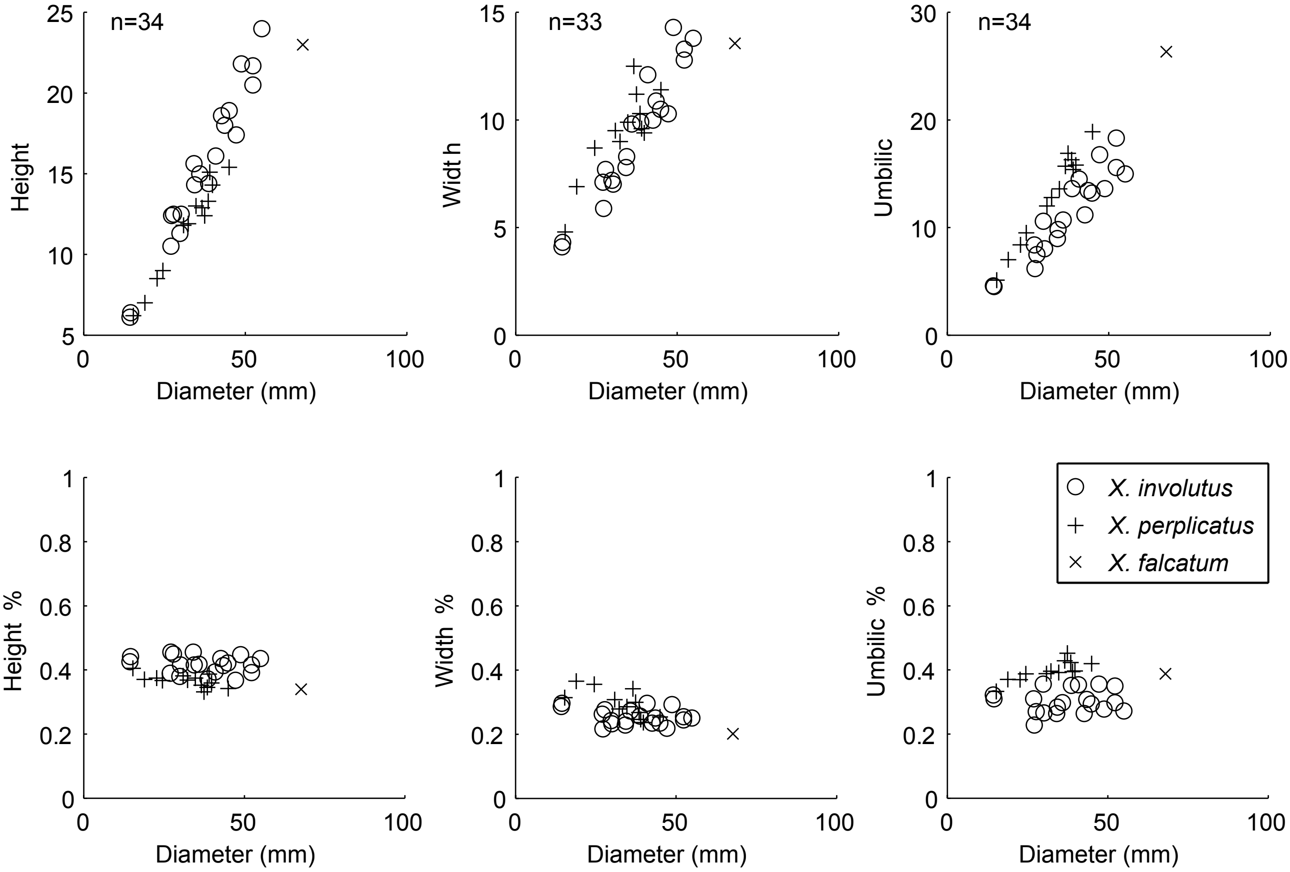

Text-fig. 37

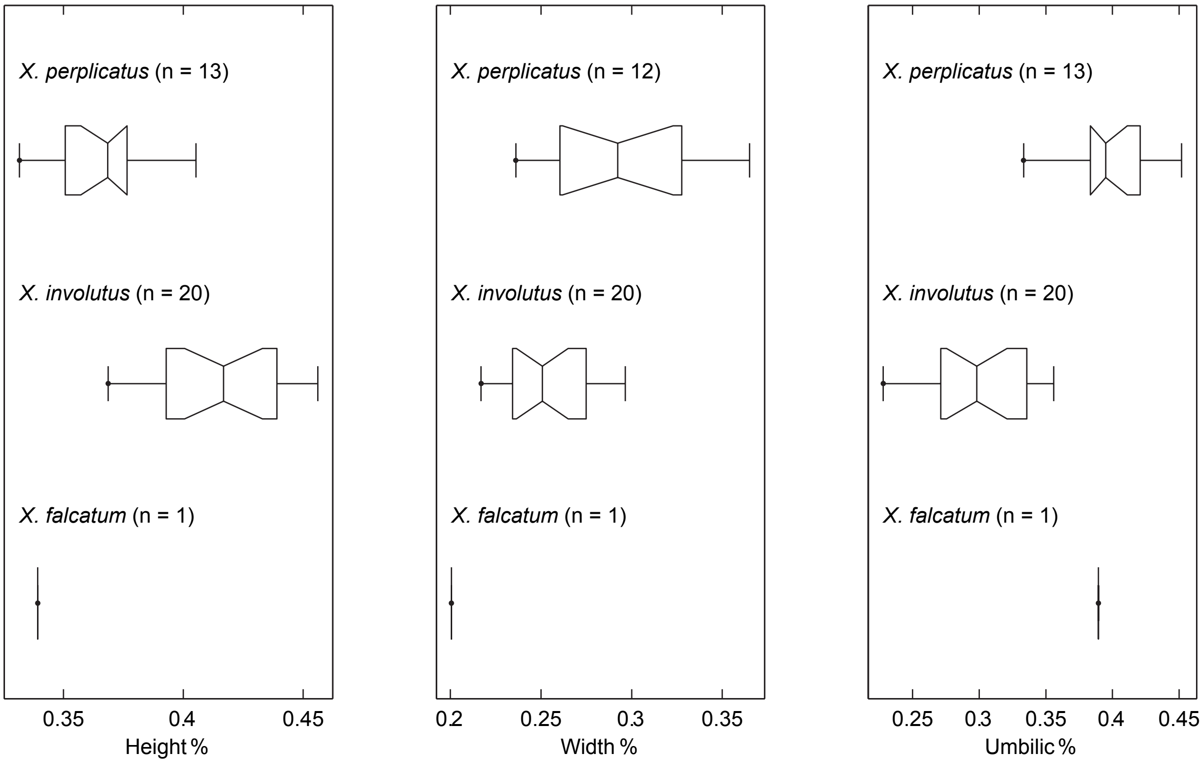

Text-fig. 38

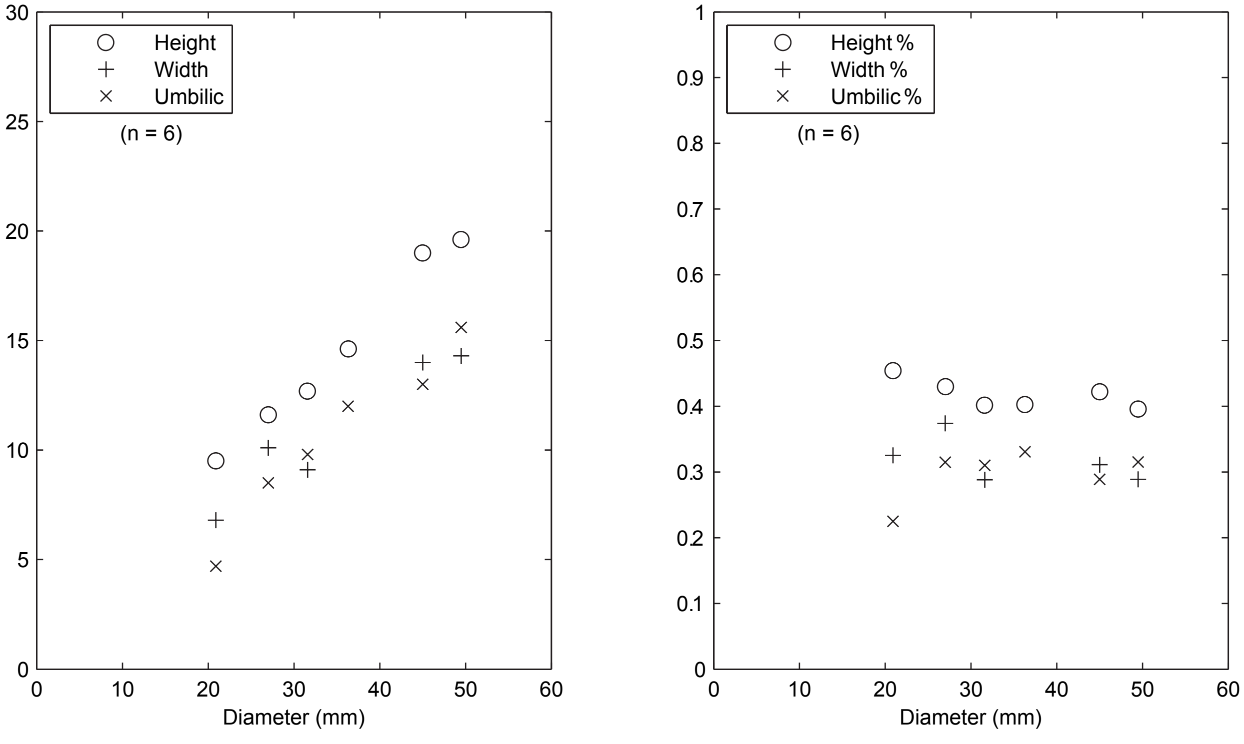

Text-fig. 39

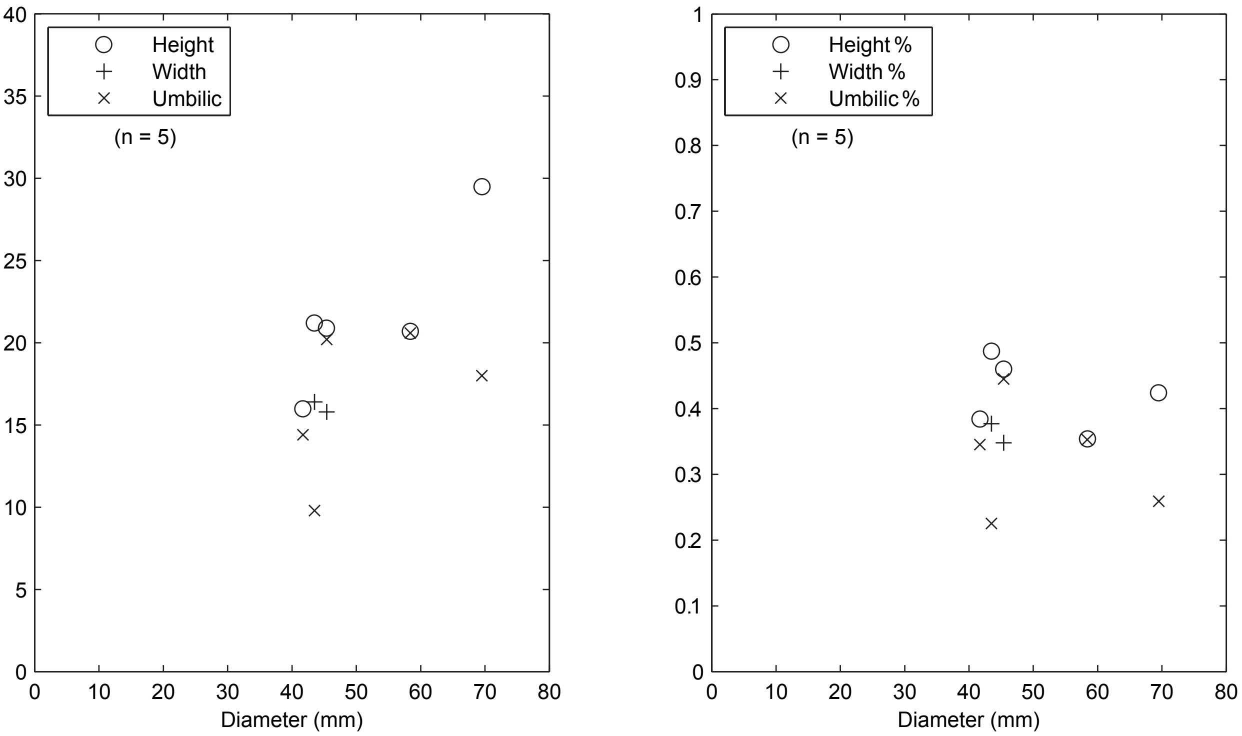

Text-fig. 40

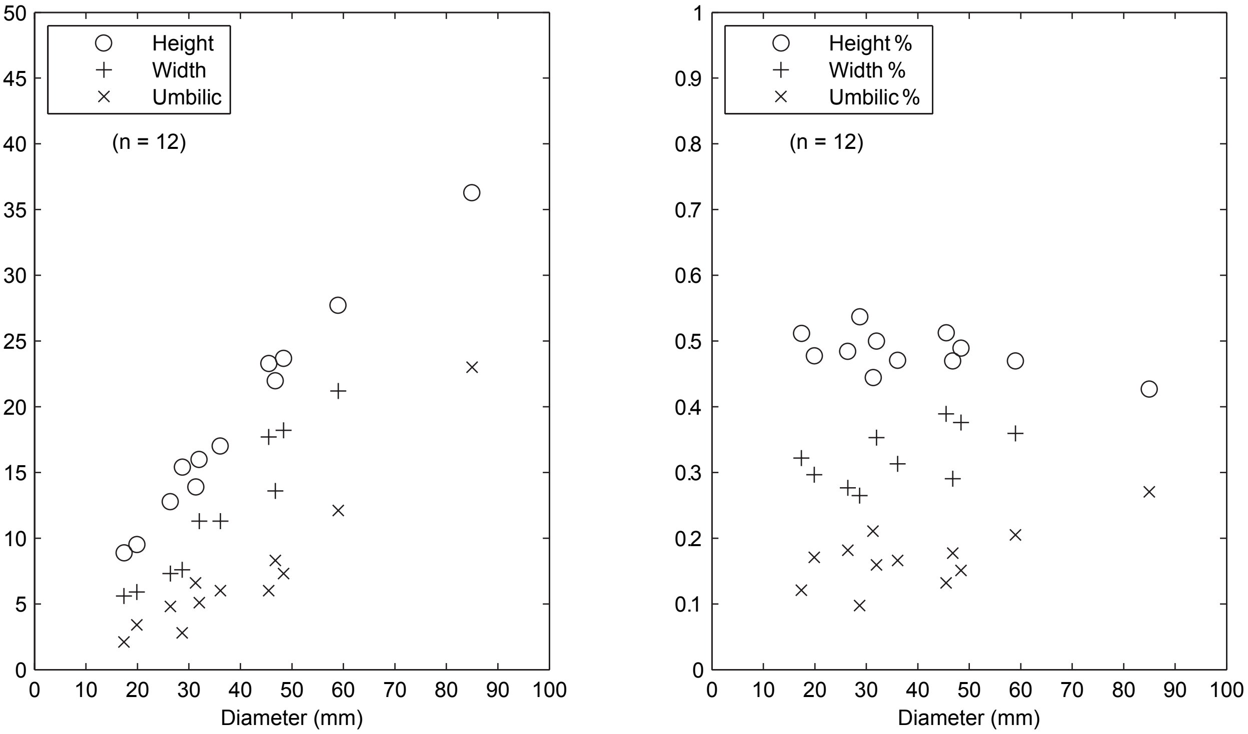

Text-fig. 41

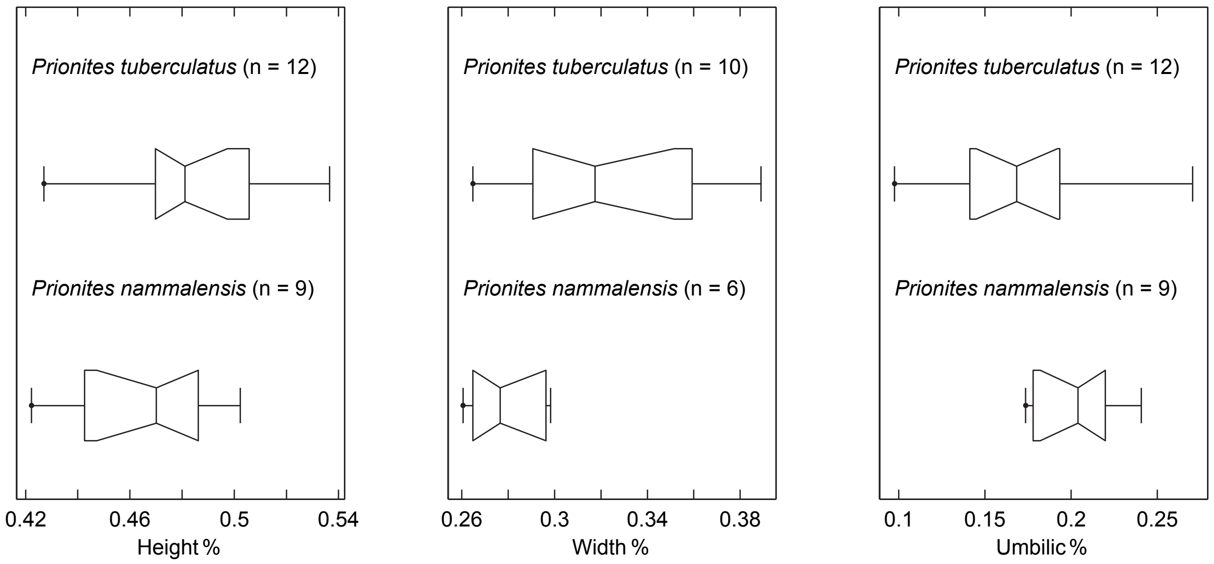

Text-fig. 42

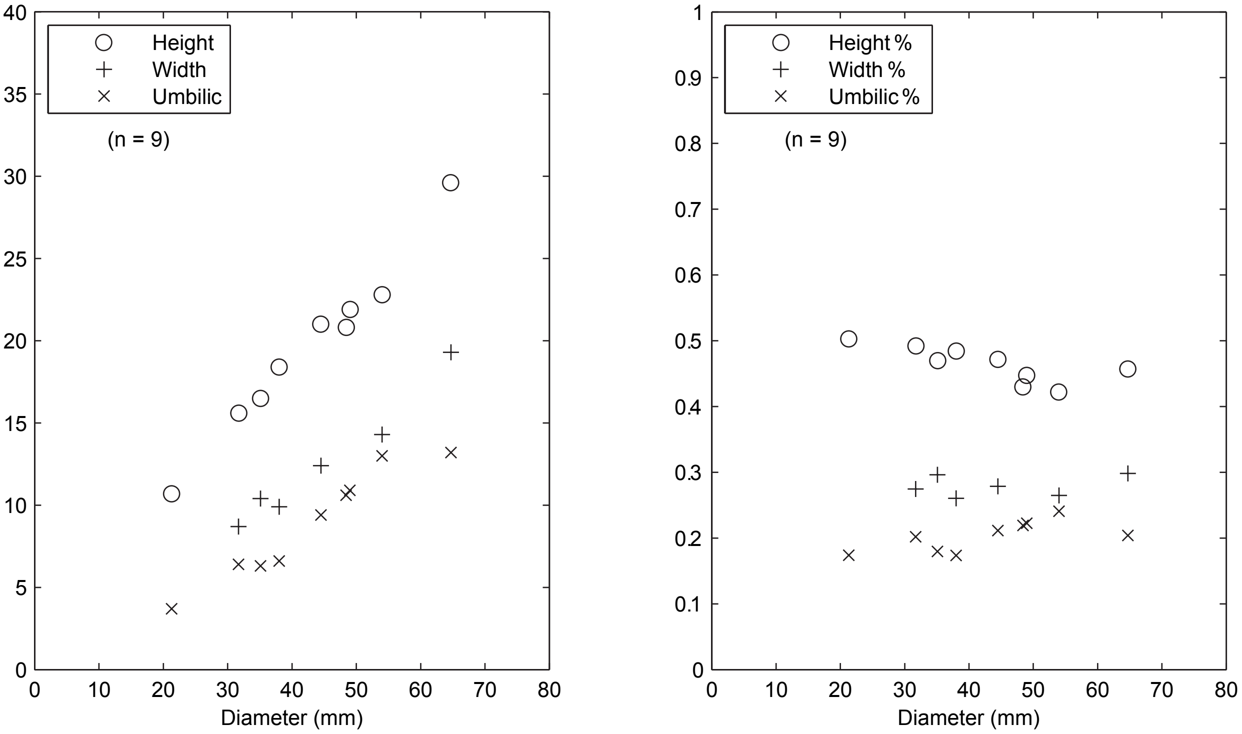

Text-fig. 43

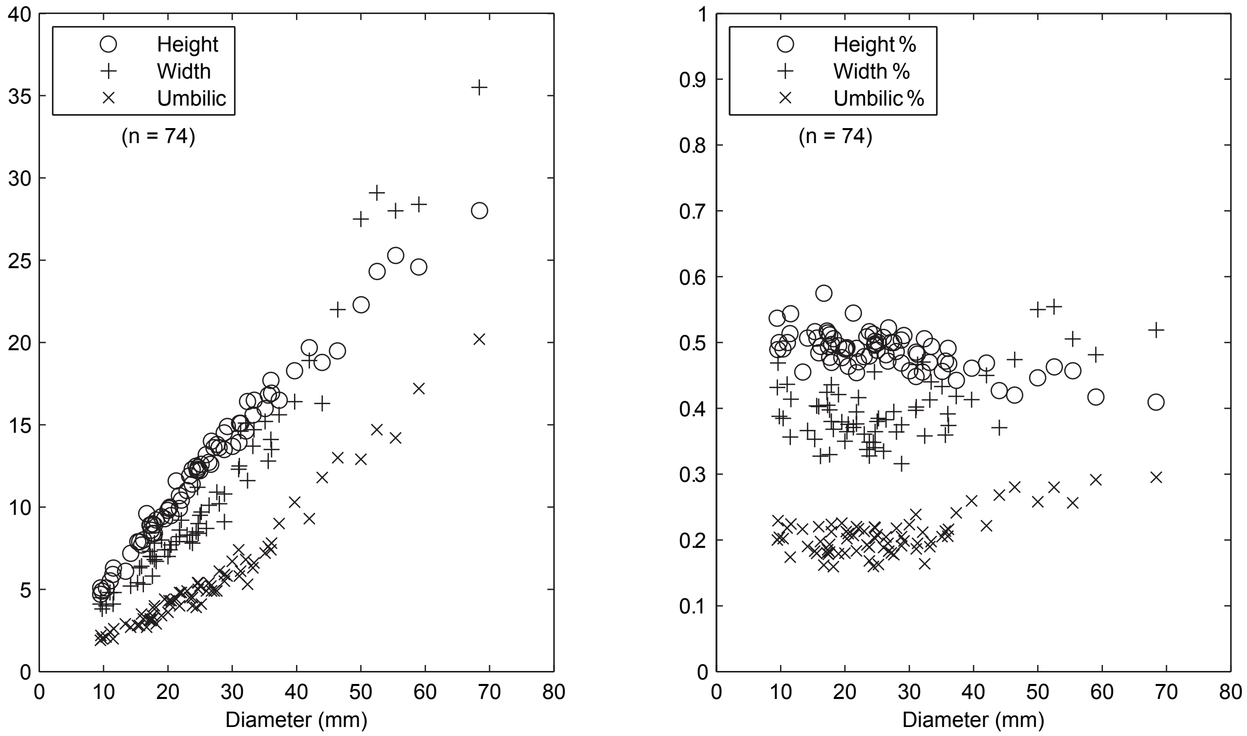

Text-fig. 44

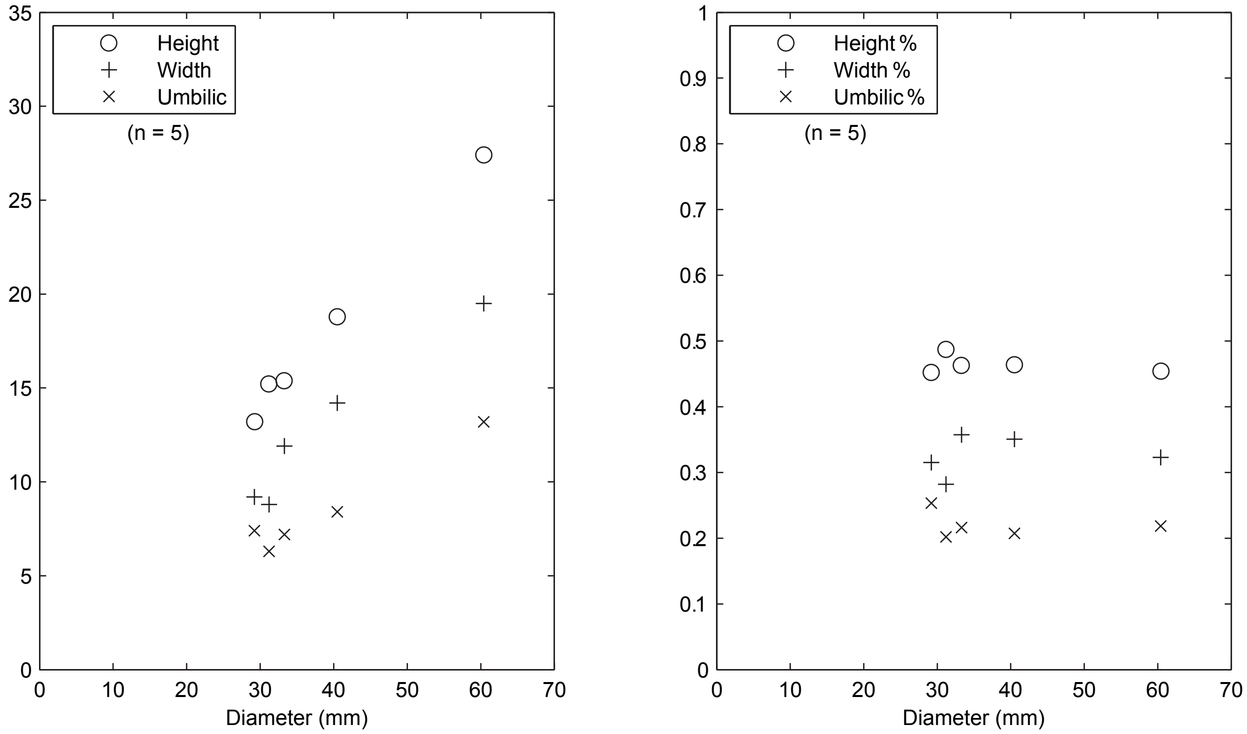

Text-fig. 45

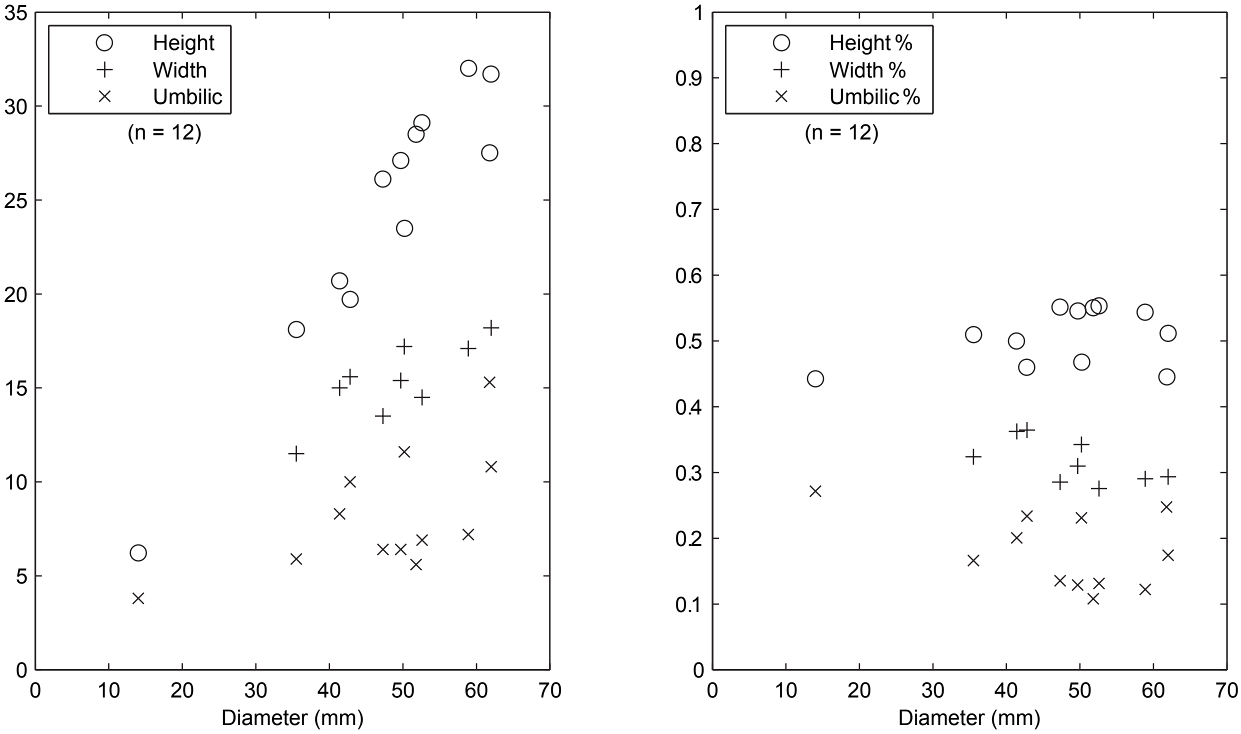

Text-fig. 46

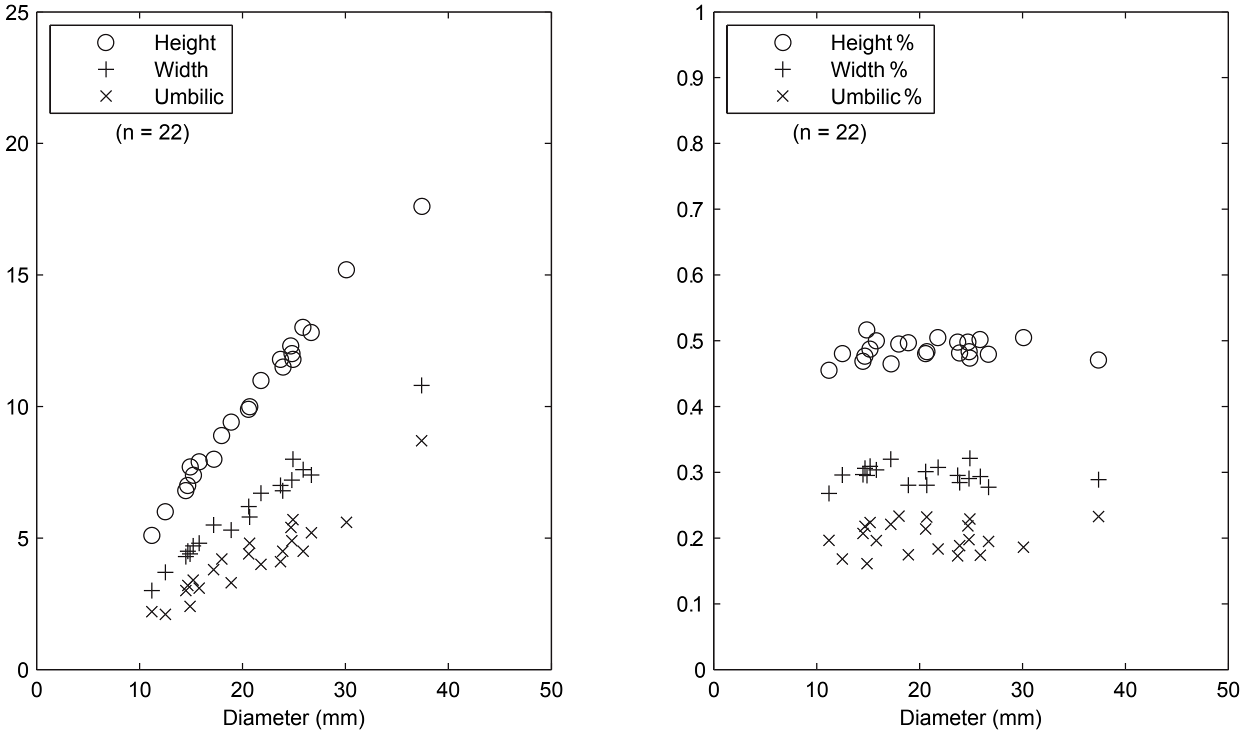

Text-fig. 47

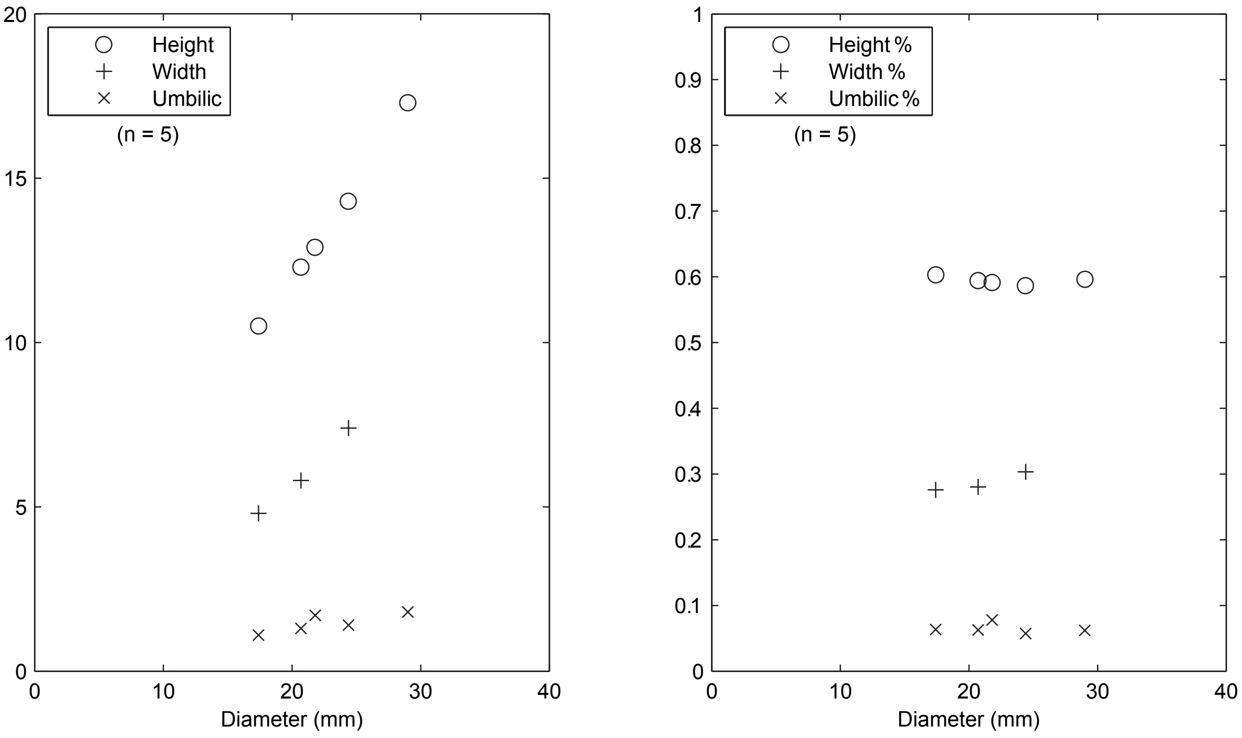

Text-fig. 48

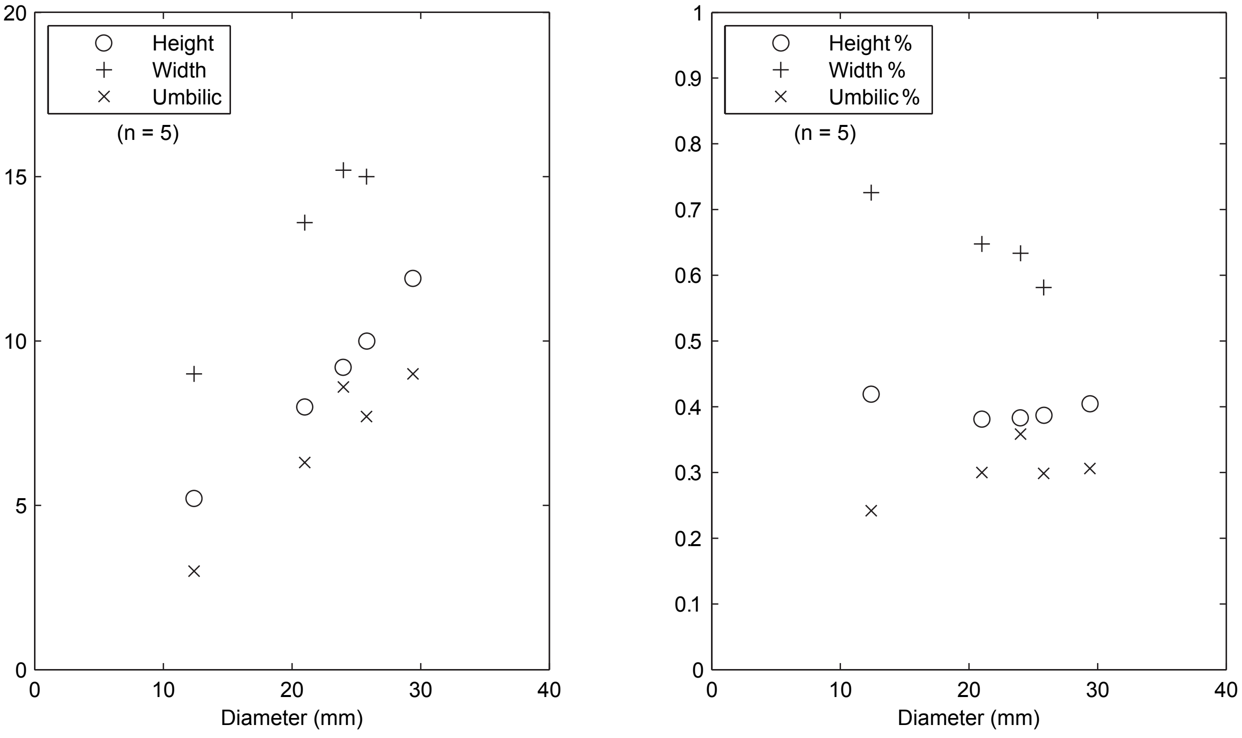

Text-fig. 49

EXPLANATION OF PLATE 1

Figs 1-3. *Kashmirites armatus* (Waagen, 1895). 1a-e, PIMUZ 27875; 1e ×2, at D=30.5mm, H=10.6mm. 2a-d, PIMUZ 27876. 3a-d, PIMUZ 27877; 3d ×2, at D=17.3mm, H=5.3mm. All from sample Chi10, *Flemingites nanus* beds, CS, Chiddru.

Figs 4-7. *Kashmirites baidi* Brühwiler and Bucher (submitted). 4a-b, PIMUZ 27878. 5a-c, PIMUZ 27879. 6a-d, PIMUZ 27880. 7a-d, PIMUZ 27881; 7d ×2, at D=23.3mm, H=7.2mm. All from sample Zal50, *Flemingites flemingianus* beds, CS, Zaluch.

Figs 8-10. *Kashmirites* cf. *nivalis* (Diener, 1897). 8a-e, PIMUZ 27882. 9a-c, PIMUZ 27883. 10, PIMUZ 27884; ×2, at H=11.6mm. All three specimens found as float in the lower part of the Ceratite Marls at Chiddru.

Figs 11-14. *Kashmirites* sp. indet. 11a-b, PIMUZ 27885. 12a-b, PIMUZ 27886. 13, PIMUZ 27887. 14a-b, PIMUZ 27888. All from Sample Nam534, CM, Nammal.

All natural size unless otherwise indicated.

Plate 1

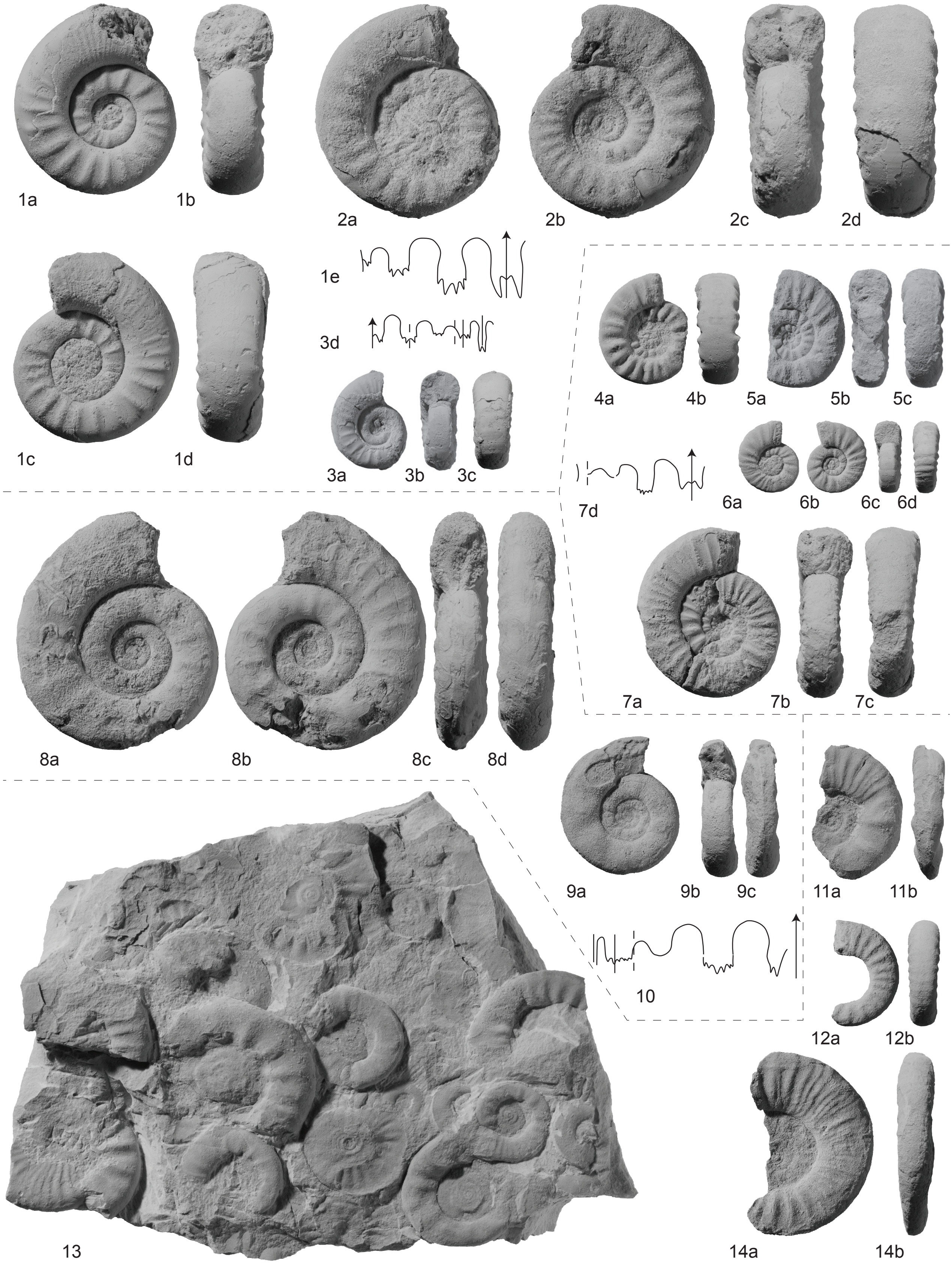
1a
1b
2a
2b
2c
2d
1e
3d
1c
1d
3a
3b
3c
4a
4b
5a
5b
5c
6a
6b
6c
6d
7d
7a
7b
7c
8a
8b
8c
8d
9a
9b
9c
10
11a
11b
12a
12b
13
14a
14b

EXPLANATION OF PLATE 2

Figs 1-8. *Pseudoceltites multiplicatus* (Waagen, 1895). 1a-d, PIMUZ 27889; 1d ×2, at H=13.2mm. From sample Nam16. 2a-b, PIMUZ 27890. From sample Nam9. 3a-d, PIMUZ 27891. From sample Nam16. 4a-c, PIMUZ 27892. From sample Nam16. 5a-e, PIMUZ 27893; 5e at D=17.4mm, H=7.3mm. From sample Nam16. 6a-c, PIMUZ 27894. From sample Nam9. 7a-d, PIMUZ 27895. From sample Nam9. 8a-d, PIMUZ 27896. From sample Nam16. All from the *Pseudoceltites multiplicatus* beds, UCL, Nammal.

Fig. 9a-c. ?*Pseudoceltites* cf. *normalis* (Waagen, 1895). PIMUZ 27897. From sample Nam8, *Nyalamites angustecostatus* beds, UCL.

Figs 10-15. *Nyalamites angustecostatus* (Welter, 1922). 10a-c, PIMUZ 27898. From sample Chi101. 11a-c, PIMUZ 27899. From sample Chi101. 12a-d, PIMUZ 27900. From sample Nam8. 13a-e, PIMUZ 27901; 13e ×2, at D=20.5mm, H=6.4mm. From sample Nam68. 14a-d, PIMUZ 27902. From sample Nam8. 15a-c, PIMUZ 27903. From sample Chi101. 10, 11 and 15 from Chiddru, others from Nammal. All from the *Nyalamites angustecostatus* beds, UCL.

All natural size unless otherwise indicated.

Plate 2

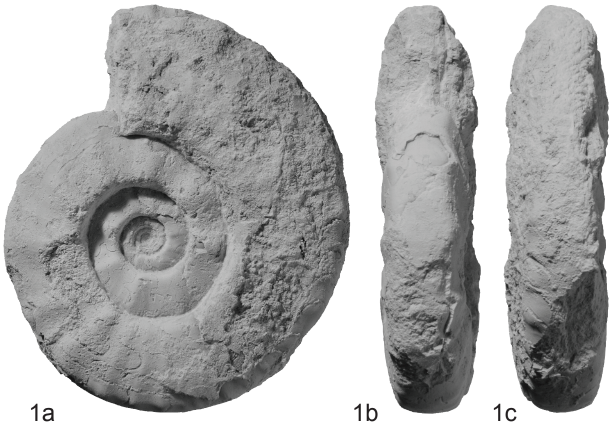

1a 1b 1c

2a 2b

3a 3b 3c 3d

5e

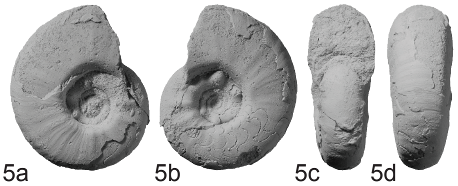

5a 5b 5c 5d

4a 4b 4c

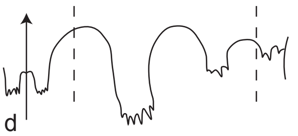

1d

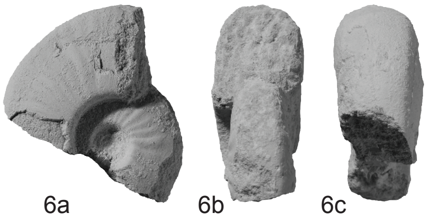

6a 6b 6c

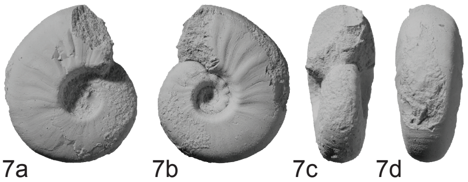

7a 7b 7c 7d

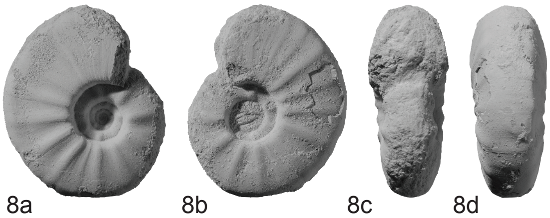

8a 8b 8c 8d

9a 9b 9c

10a 10b 10c

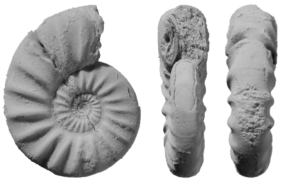

11a 11b 11c

12a 12b 12c 12d

13a 13b 13c 13d

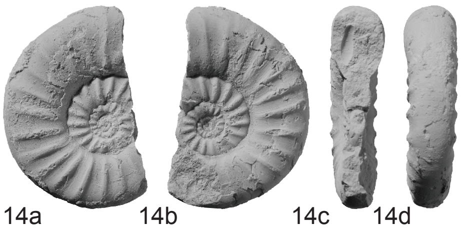

14a 14b 14c 14d

15a 15b 15c

13e

EXPLANATION OF PLATE 3

Figs 1-10. *Xenoceltites* cf. *variocostatus* (Brayard and Bucher, 2008). 1a-e, PIMUZ 27904; 1e ×2, at H=11.2mm. 2a-c, PIMUZ 27905. 3a-d, PIMUZ 27906. 4a-c, PIMUZ 27907. 5, PIMUZ 27908; ×2, at H=7.5mm. 6a-b, PIMUZ 27909. 7a-d, PIMUZ 27910. 8a-c, PIMUZ 27911. 9a-d, PIMUZ 27912. 10a-d, PIMUZ 27913. All from sample Nam713, *Glyptophiceras sinuatum* beds, UCL, Nammal.

Figs 11-12. *Glyptophiceras sinuatum* (Waagen, 1895). 10a-d, PIMUZ 27914. 11a-d, PIMUZ 27915. Both specimens from sample Nam32, *Glyptophiceras sinuatum* beds, UCL, Nammal..

All natural size unless otherwise indicated.

Plate 3

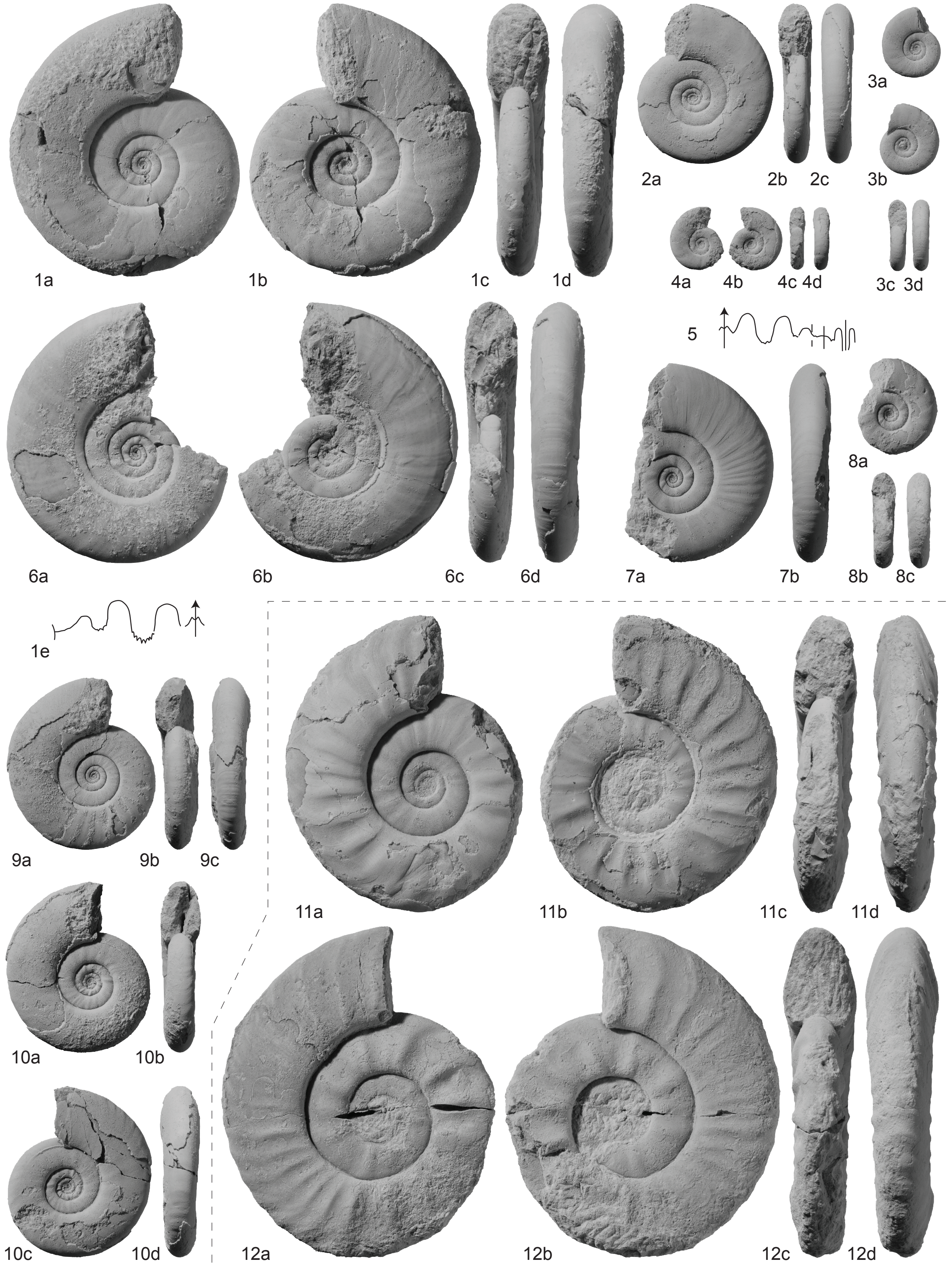
1a
1b
1c
1d
2a
2b
2c
3a
3b
4a
4b
4c
4d
3c
3d
5
6a
6b
6c
6d
7a
7b
8a
8b
8c
1e
9a
9b
9c
11a
11b
11c
11d
10a
10b
10c
10d
12a
12b
12c
12d

EXPLANATION OF PLATE 4

Figs 1-6. *Glyptophiceras sinuatum* (Waagen, 1895). 1a-d, PIMUZ 27916; 1d ×2, at H=18mm. From sample Nam32. 2a-c, PIMUZ 27917. From sample Nam42. 3, PIMUZ 27918, ×2, at D=34.8mm, H=12mm. From sample Nam32. 4a-h, PIMUZ 27919; 4e-h, inner whorls. From sample Nam32. 5a-b, PIMUZ 27920. From sample Nam32. 6a-b, PIMUZ 27921. From sample Nam42. All from the *Glyptophiceras sinuatum* beds, UCL, Nammal. All natural size unless otherwise indicated.

Plate 4


1a


1b


1c


2a


2b


2c

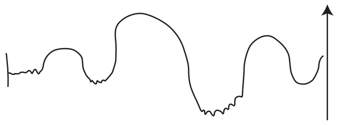
1d


3


4a


4b


4e


4f


4g


4h


5a


5b


4c


4d


6a


6b

EXPLANATION OF PLATE 5

Figs 1-4. *Koiloceras romanoi* gen. et sp. nov. 1a-e, PIMUZ 27922; 1e ×2, at H=15.2mm. From sample Chi104. 2a-d, holotype, PIMUZ 27923. From sample Chi52. 3a-d, PIMUZ 27924. From sample Chi52. 4a-c, PIMUZ 27925. From sample Chi52. All from the *Flemingites planatus* beds, base of CM, Chiddru.

Fig. 5a-e. *Mudiceras planissimum* (Spath, 1934). PIMUZ 28377, 5e ×2, at D=20.6mm, H=8.1mm. From sample Chi53, base of CM, Chiddru.

Fig. 6a-b. ?*Paranorites* sp. indet. B. PIMUZ 27926; ×0.5. Found as float on top of the LCL at Chiddru.

All natural size unless otherwise indicated.

Plate 5


1a


1b


1c


1d


2a


2b


3a


3b


4a


4b


4c

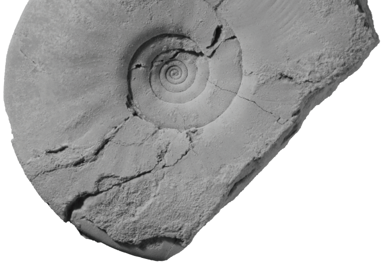
2c


2d


3c


3d


1e


5e


5a


5b


5c


5d


6a


6b

EXPLANATION OF PLATE 6

Fig. 1a-c. *Pseudaspidites* cf. *muthianus* (Krafft and Diener, 1909). PIMUZ 27927; ×0.8. 1c at H=36.6mm. From float block Chi-SFB2, probably derived from the horizon of sample Chi3.

Figs 2-3. Proptychitidae gen. et sp. indet. A. 2a-c, PIMUZ 27928. From sample Nam16. 3a-c, PIMUZ 27929; 3a ×2, at H=15.8mm. From sample Nam9. Both specimens from the *Pseudoceltites multiplicatus* beds, UCL, Nammal.

Fig. 4a-c. Proptychitidae gen. et sp. indet. B. PIMUZ 27930; ×0.8. 4c at D=114mm, H=50mm From sample Nam20, UCL, Nammal.

All natural size unless otherwise indicated.

Plate 6


1a


1b

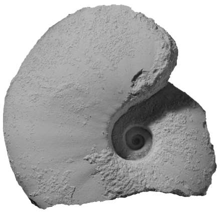
2a


2b


2c


3a

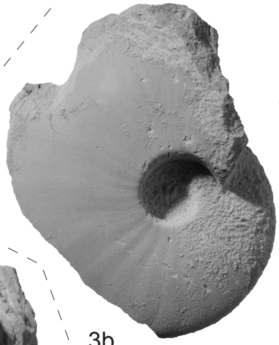
3b


3c


4a


4b


1c


4c

EXPLANATION OF PLATE 7

Fig. 1a-d. ?Arctoceratidae gen. et sp. indet. Zal50, PIMUZ 27931; 8d ×2, at H=14.5mm. From sample Zal50, *Flemingites flemingianus* beds, CS, Zaluch.

Fig. 2a-e. *Monneticeras compressum* gen. et sp. nov. Holotype, PIMUZ 27932; 2e ×2, at H=23.1mm. From sample Chi53, *Shamaraites rursiradiatus* beds, base of CM, Chiddru.

Fig. 3a-c. *Clypeoceras superbum* (Waagen, 1895). PIMUZ 27933; ×0.5. Found as float in the CS at Nammal.

Fig. 4a-d. ?*Paranorites* sp. indet. C. PIMUZ 27934; ×0.5, 4d at H=76mm. From sample Chi3, *Radioceras evolvens* beds, CS, Chiddru.

All natural size unless otherwise indicated.

Plate 7

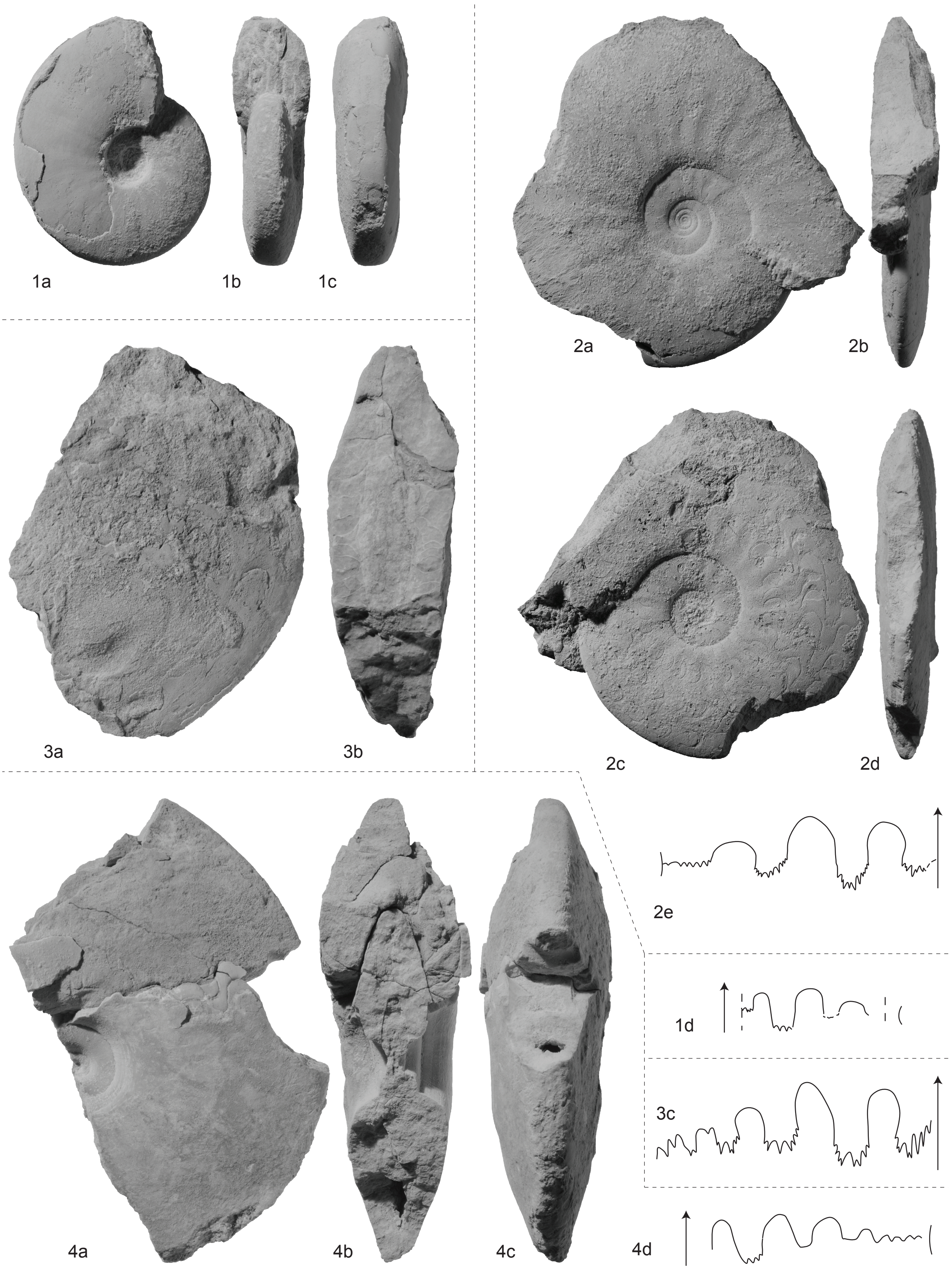

EXPLANATION OF PLATE 8

Fig. 1a-d. *Clypeoceras superbum* (Waagen, 1895). PIMUZ 27935; ×0.5, 1c at D=200mm, H=120mm From sample Zal50, *Flemingites flemingianus* beds, CS, Zaluch.

Fig. 2a-e. ?*Kingites parkashi* PIMUZ 27936; 2a-d ×0.8, 2e ×2, at H=27mm. From sample Chi52, *Flemingites planatus* beds, base of CM, Chiddru.

Plate 8


1a


1b


1c


1d


2e


2a


2b


2c


2d

EXPLANATION OF PLATE 9

Figs 1-4. *Vercherites vercherei* (Waagen, 1895). 1a-e, PIMUZ 27959; 1e at D=49.5mm, H=21mm. From sample Nam532, *Xenodiscoides perplicatus* beds, CM, Nammal. 2a-c, PIMUZ 27960. From sample Nam65, *Xenodiscoides perplicatus* beds, CM, Nammal. 3, PIMUZ 27955 (see also Pl. 14, fig. 1a-d); at H=41mm. From sample Nam532. 4a-c. PIMUZ 27961. From sample Chi1 (SFB), Chiddru.

Fig. 5. *Galfettites* cf. *omani* Brühwiler and Bucher (submitted). PIMUZ 27962; ×2. From sample Nam14, *Nammalites pilatoides* beds, UCL, Nammal.

All natural size unless otherwise indicated.

Plate 9

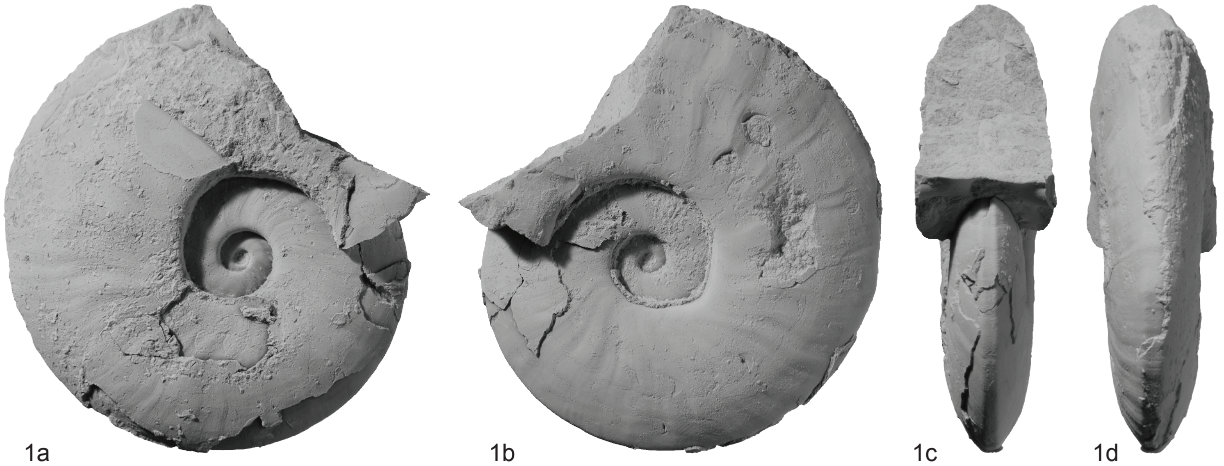

1a 1b 1c 1d

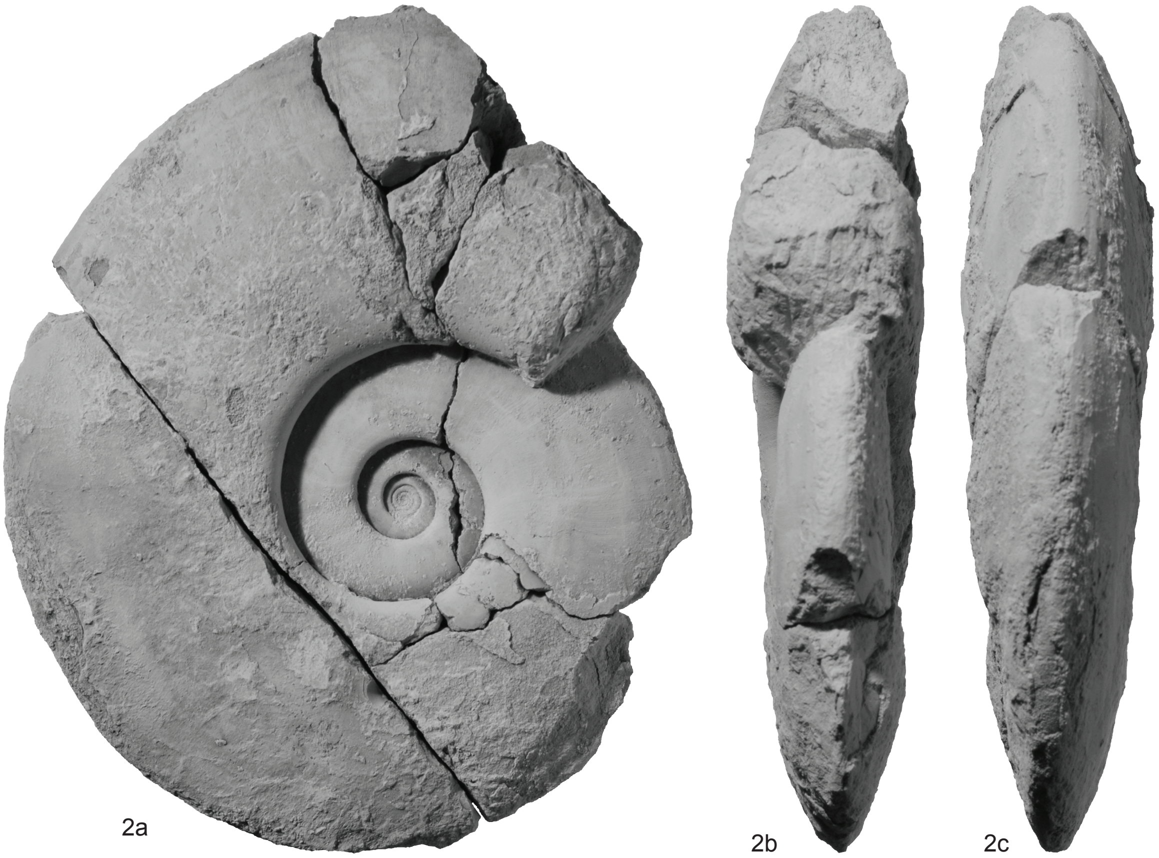

2a 2b 2c

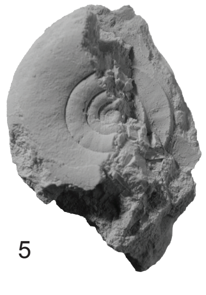

5

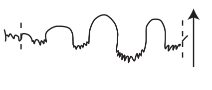

1e

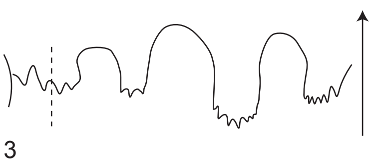

3

4a 4b 4c

EXPLANATION OF PLATE 10

Figs 1-4. *Vercherites vercherei* (Waagen, 1895). 1a-d, PIMUZ 27955; ×0.5. 2a-c, PIMUZ 27956; ×0.5. 3a-c, PIMUZ 27957. 4a-d. PIMUZ 27958. 1 from sample Nam532, *Xenodiscoides perplicatus* beds, CM, Nammal; 2-4 from sample Chi1 (SFB), CM or CS, Chiddru. All natural size unless otherwise indicated.

Plate 10

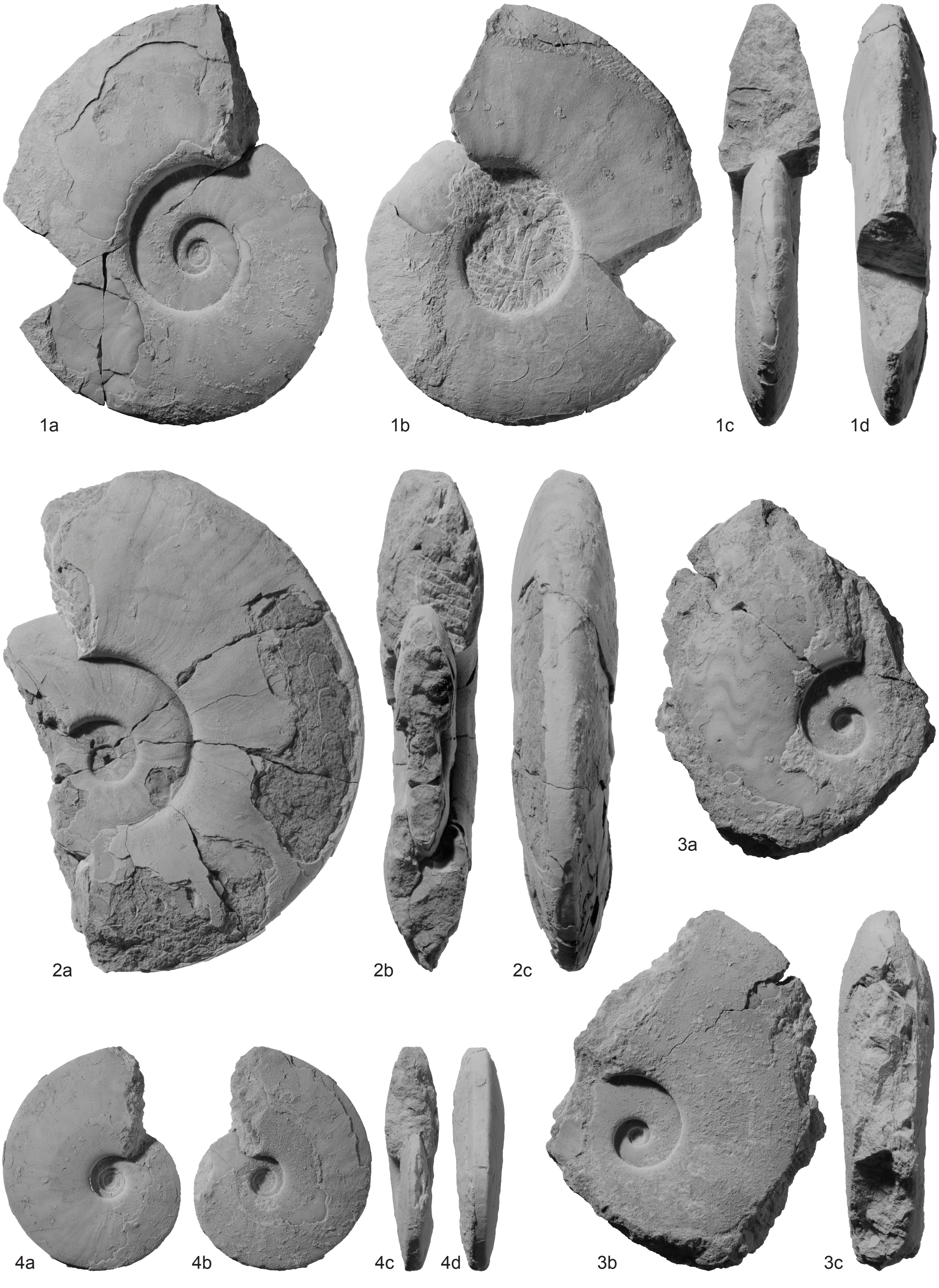

EXPLANATION OF PLATE 11

Fig. 1. *Paranorites ambiensis* (Waagen, 1895). PIMUZ 27950 (see also Pl. 15, fig. 1a-c); ×0.5, at D=247mm, H=92mm.

Figs 2-3. *Vercherites pulchrum* (Waagen, 1895). 2a-d, PIMUZ 27952; 1a-c ×0.5; 1d at H=45.5mm. 3a-c, PIMUZ 27953; ×0.5. All from sample Chi10, *Flemingites nanus* beds, CS, Chiddru.

Fig. 4a-d. *Vercherites vercherei* (Waagen, 1895). PIMUZ 27954; 4a-c ×0.5; 4d at D=175mm, H=59mm. From sample Nam65, CM, Nammal.

All natural size unless otherwise indicated.

Plate 11


2a


2b


2c


1

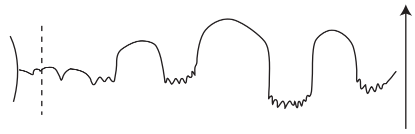
2d


4d


3a


3b


3c


4a


4b


4c

EXPLANATION OF PLATE 12

Figs 1-5. *Vercherites pulchrum* (Waagen, 1895). 1a-c, PIMUZ 27945. 2a-d, PIMUZ 27946. 3a-c, PIMUZ 27947. 4a-d, PIMUZ 27948; 4d at H=34mm. 5a-d, PIMUZ 27949. Specimen in 2 from sample Nam528; all others from sample Chi10, *Flemingites nanus* beds, CS, Chiddru. All natural size unless otherwise indicated.

Plate 12

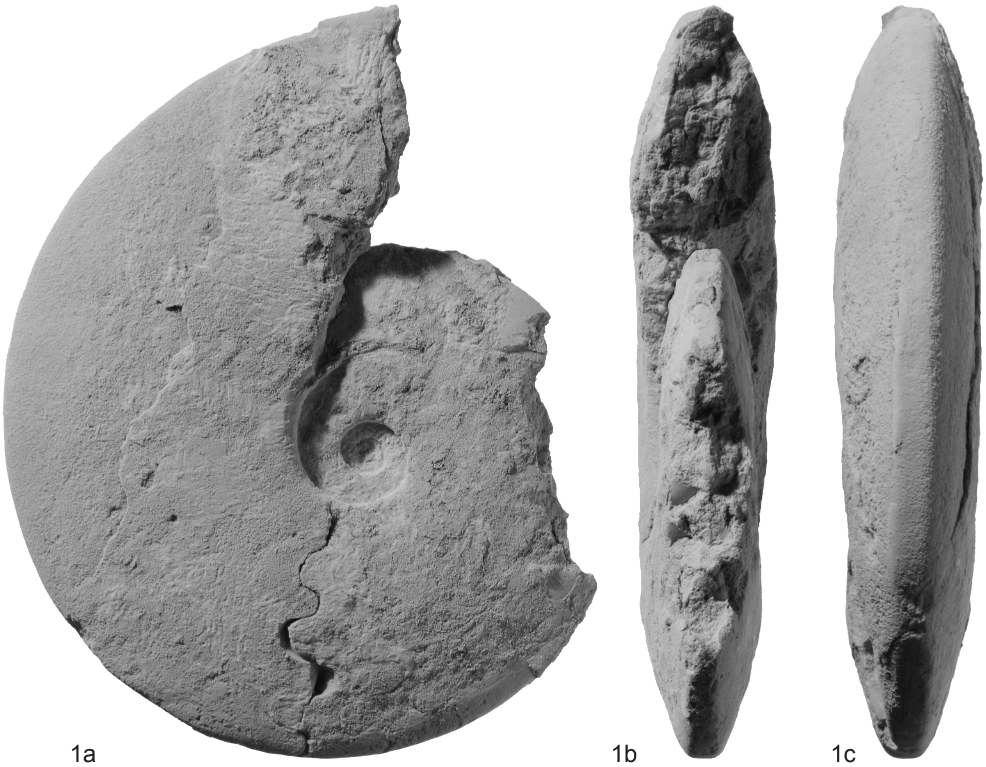
1a 1b 1c


2a 2b 2c 2d

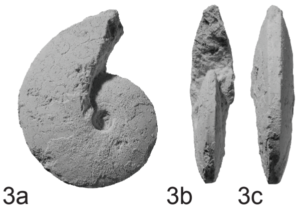
3a 3b 3c

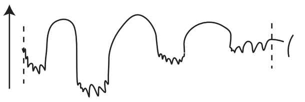
4d

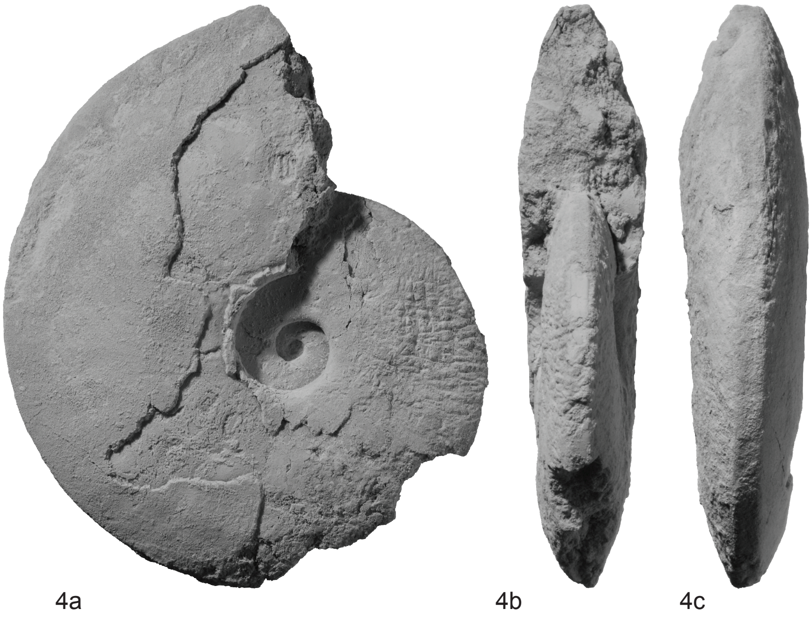
4a 4b 4c

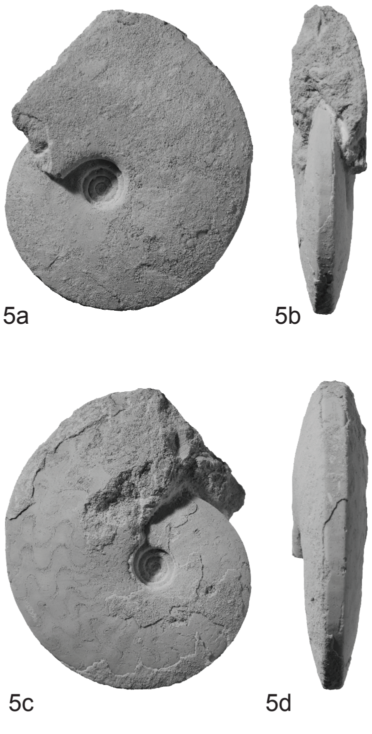
5a 5b 5c 5d

EXPLANATION OF PLATE 13

Figs 1-3. *Paranorites ambiensis* Waagen, 1895. 1a-c, PIMUZ 27937. 2a-c, PIMUZ 27938. 3a-c, PIMUZ 27939. All from sample Chi10, *Flemingites nanus* beds, CS, Chiddru. All natural size.

Plate 13

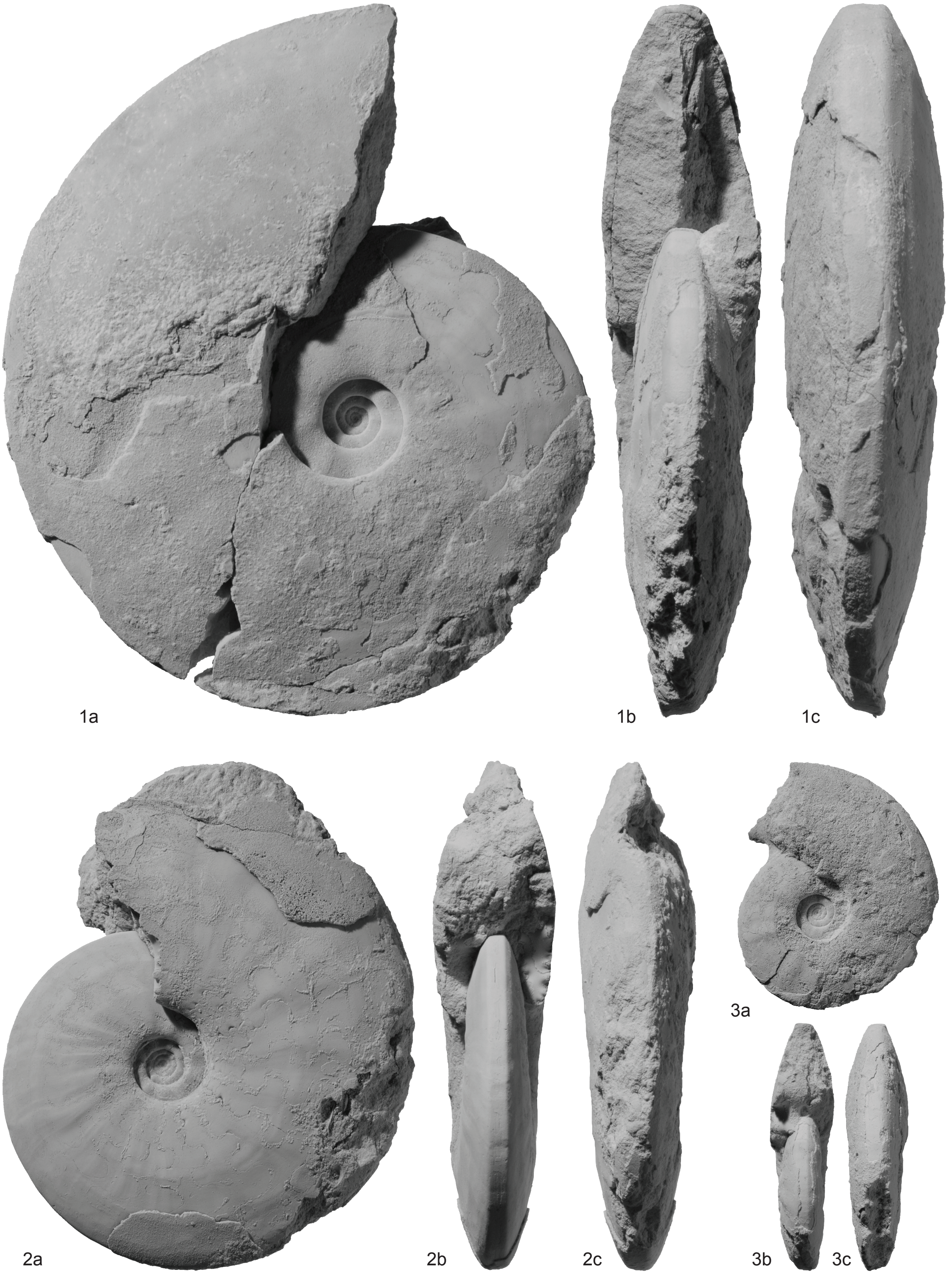

EXPLANATION OF PLATE 14

Figs 1-3. *Paranorites ambiensis* Waagen, 1895. 1a-d, PIMUZ 27940. 2a-b, PIMUZ 27938 (see also Pl. 9, fig. 2a-c); 2a at D=78mm, H=40.2mm; 2b at H=21.2mm. 3a-b, PIMUZ 27941. All from sample Chi10, *Flemingites nanus* beds, CS, Chiddru. All natural size.

Figs 4-6. *Paranorites* sp. indet. A. 4a-c, PIMUZ 27942; 4c at H=61mm. From sample Nam529. 5a-b, PIMUZ 27943. From sample Nam530. 6a-b, PIMUZ 27944. Found as float, most likely derived from the horizon of sample Nam529. All from the upper part of the CM, Nammal. All ×0.5.

Plate 14

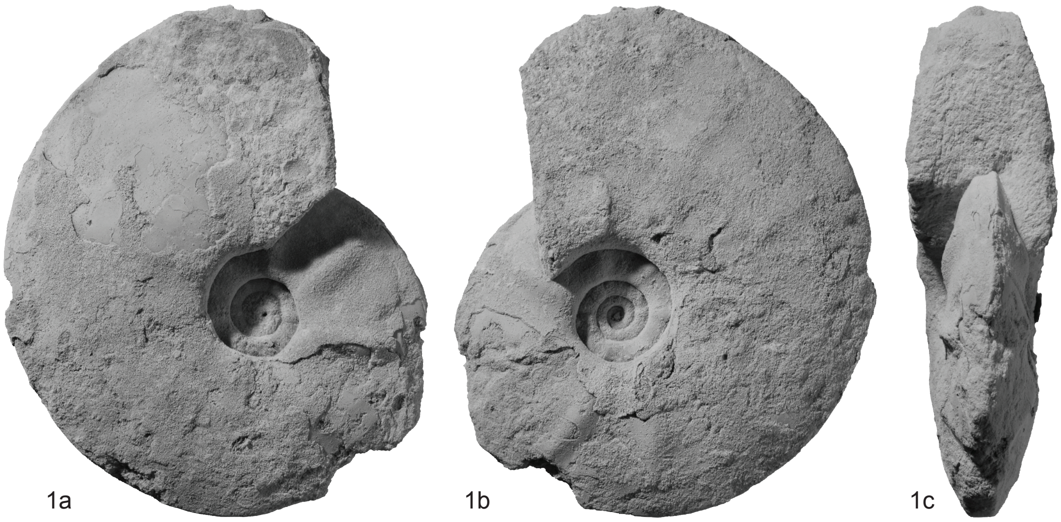

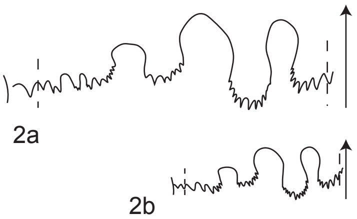

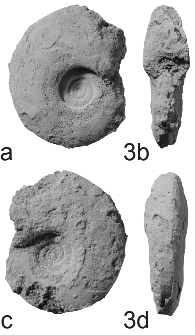

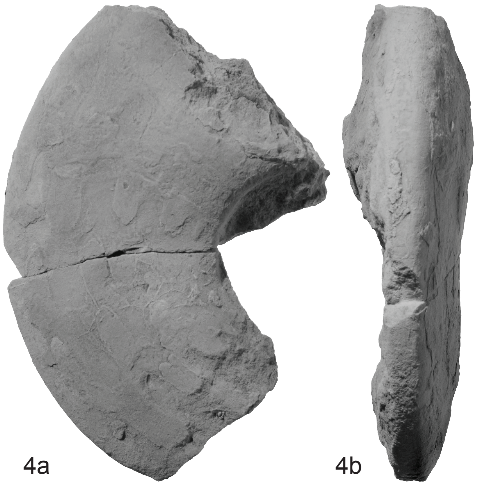

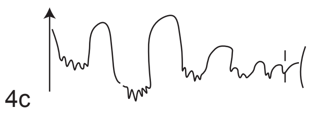

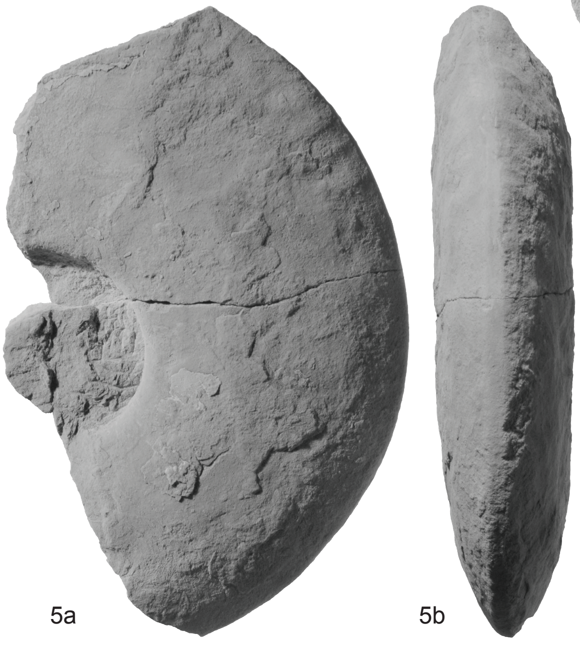

EXPLANATION OF PLATE 15

Figs 1-2. *Paranorites ambiensis* (Waagen, 1895). 1a-c, PIMUZ 27950. 2a-d, PIMUZ 27951. Both specimens from sample Chi10, *Flemingites nanus* beds, CS, Chiddru. All ×0.4.

Plate 15


1a


1b


1c


2a


2b


2c

EXPLANATION OF PLATE 16

Figs 1-2. *Radioceras evolvens* (Waagen, 1895). 1a-c, PIMUZ 27963. From sample Chi6. 2a-c, PIMUZ 27964. From sample Chi3. Both specimens from the *Radioceras evolvens* beds, CS, Chiddru. All ×0.8.

Plate 16


1a


1b


1c


2a


2b


2c


2d

EXPLANATION OF PLATE 17

Figs 1-5. *Radioceras evolvens* (Waagen, 1895). 1a-e, PIMUZ 27965; 1e at D=53.5mm, H=28mm. From sample Chi-SFB2. 2a-d, PIMUZ 27966. From sample Chi-SFB5. 3a-c, PIMUZ 27967. From sample Chi-SFB5. 4, PIMUZ 27963 (see also Pl. 16, fig. 1a-c); at H=60mm. From sample Chi6. 5a-c, PIMUZ 27968. From sample Chi3. All from the *Radioceras evolvens* beds, CS, Chiddru.

Fig. 6a-d. *Radioceras* cf. *kraffti* (Spath, 1934). PIMUZ 27969. From sample Nam540, CM, Nammal.

All natural size.

Plate 17


1a


1b


2a


2b


2c


2d


3a


3b


3c


1c


1d


1e

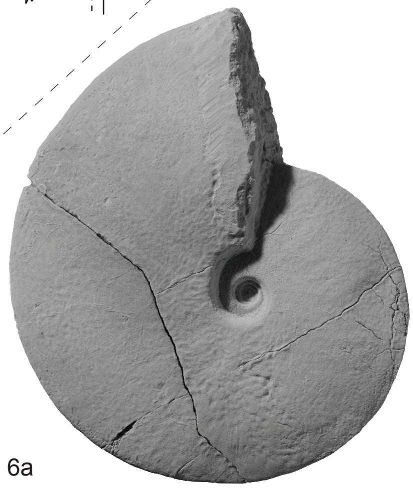
6a


6b

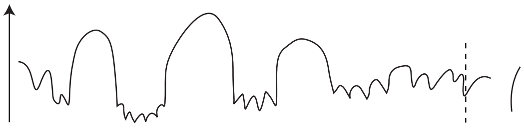
4


5a


5b


5c


6c


6d

EXPLANATION OF PLATE 18

Figs 1-6. *Radioceras* cf. *kraffti* (Spath, 1934). 1a-c, PIMUZ 27970. From sample Chi52. 2a-d, PIMUZ 27971. From sample Chi104. 3a-c, PIMUZ 27972. From sample Chi52. 4a-c, PIMUZ 27973. From sample Chi104. 5a-d, PIMUZ 27974. From sample Chi53, *Shamaraites rursiradiatus* beds. 6a-d, PIMUZ 27975. From sample Chi104. All except for 5 from the *Flemingites planatus* beds. All from the base of CM, Chiddru. All natural size unless otherwise indicated.

Plate 18

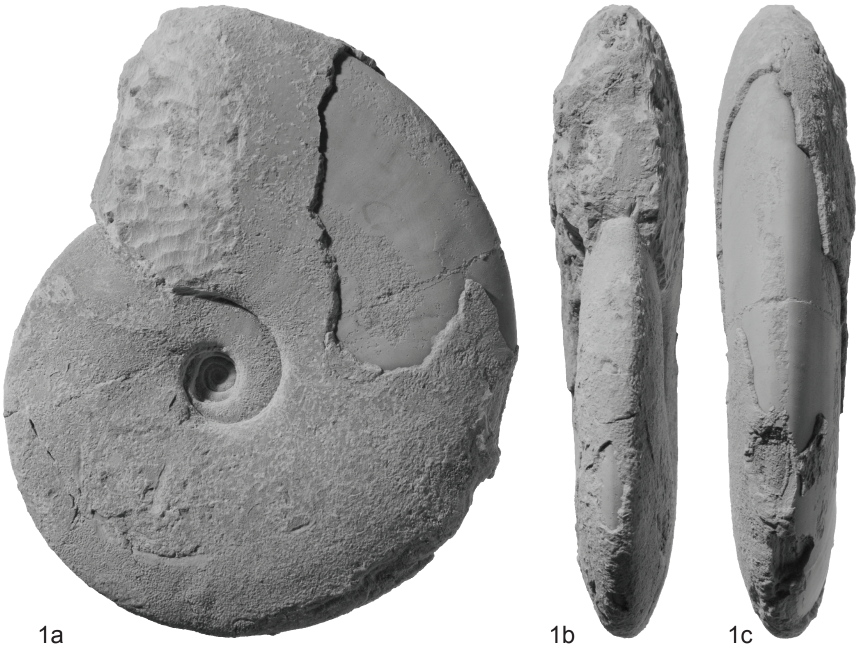

1a 1b 1c

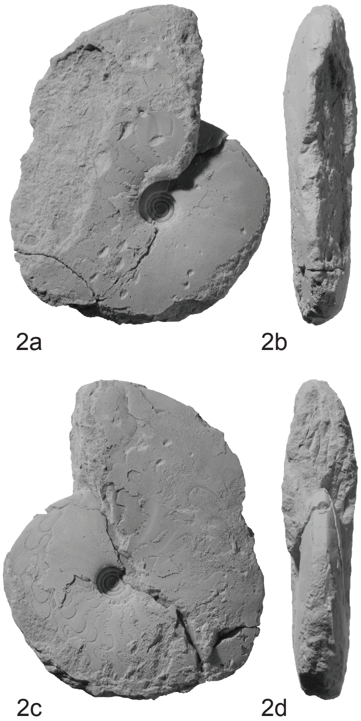

2a 2b 2c 2d

3a 3b 3c

4a 4b 4c

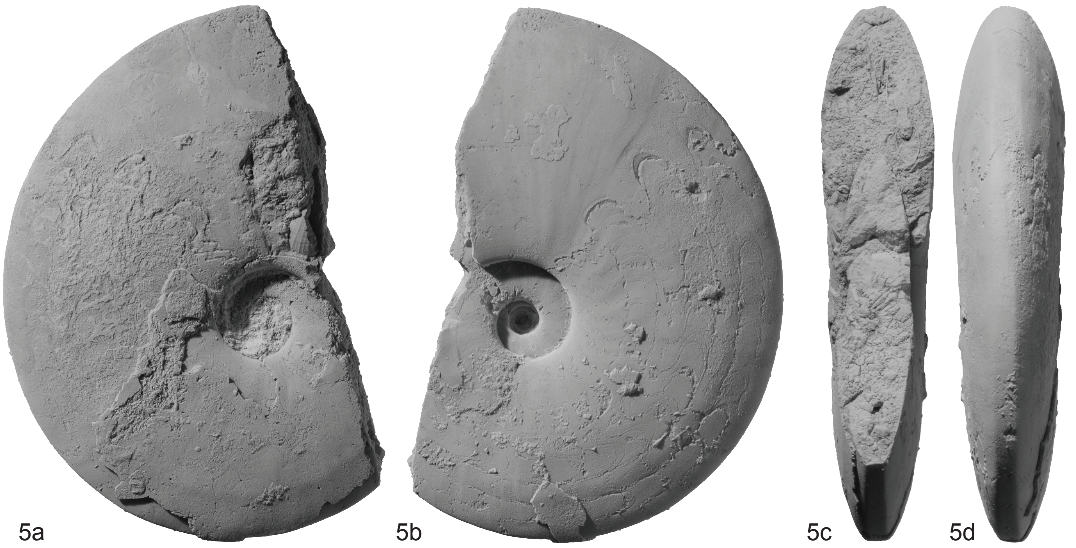

5a 5b 5c 5d

6a 6b 6c 6d

EXPLANATION OF PLATE 19

Figs 1-8. *Radioceras* cf. *kraffti* (Spath, 1934). 1a-d, PIMUZ 27976; 1d at H=30.3mm. From sample Chi104. 2a-d, PIMUZ 27977. From sample Chi104. 3a-c, PIMUZ 27978. From sample Chi104. 4a-d, PIMUZ 27979. From sample Chi52. 5a-b, PIMUZ 27980. From sample Chi104. 6, PIMUZ 27974 (see also Pl. 18, fig. 5a-d); at H=29mm. From sample Chi53, *Shamaraites rursiradiatus* beds. 7a-d, PIMUZ 27981. From sample Chi104. 8a-d, PIMUZ 27982. From sample Chi52. All except for 6 from the *Flemingites planatus* beds. All from the base of CM, Chiddru. All natural size.

Plate 19

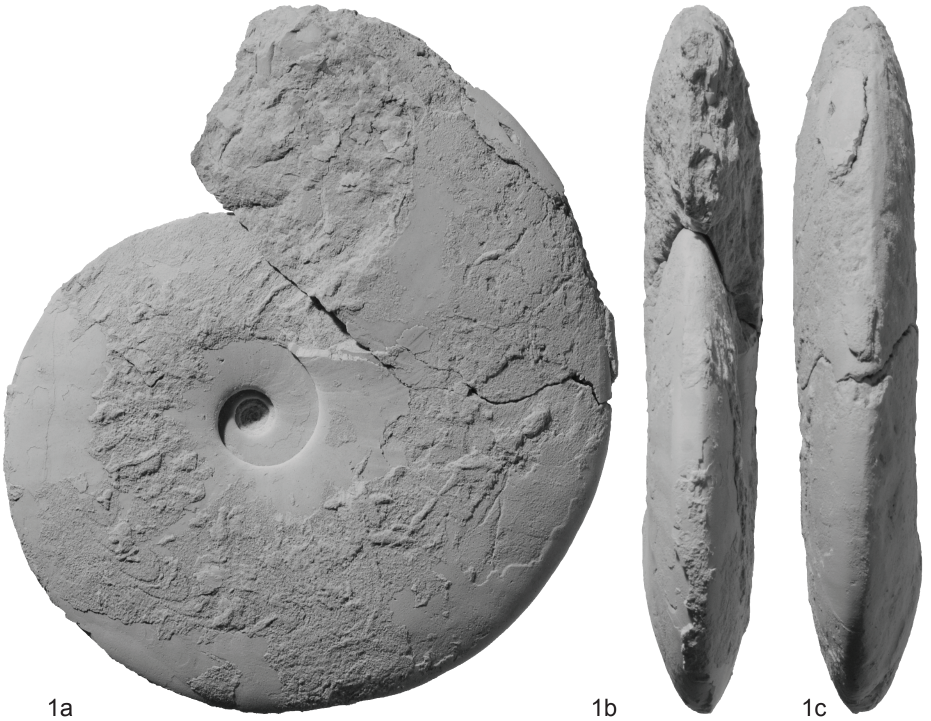
1a
1b
1c

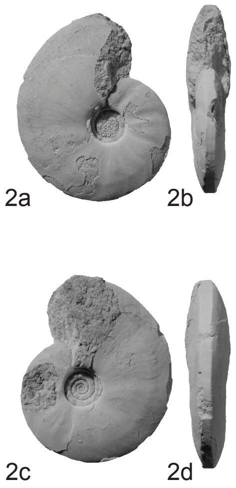
2a
2b
2c
2d


3a
3b
3c

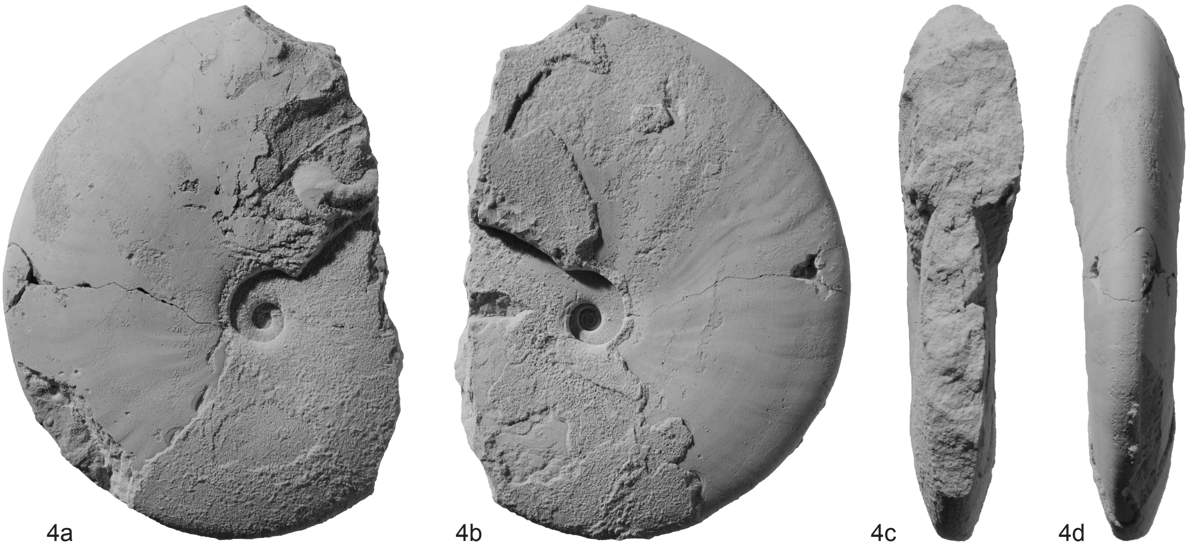
4a
4b
4c
4d

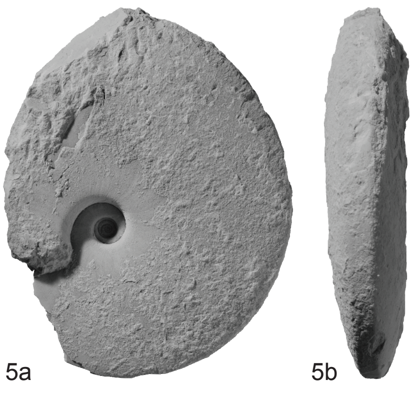
5a
5b

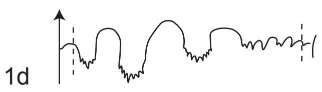
1d

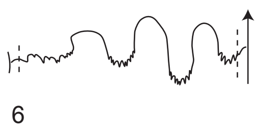
6

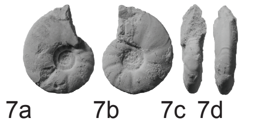
7a
7b
7c
7d

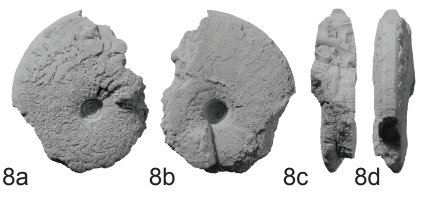
8a
8b
8c
8d

EXPLANATION OF PLATE 20

Figs 1-5. *Flemingites flemingianus* (de Koninck, 1863). 1a-b, PIMUZ 27983. From sample Nam78, Nammal. 2a-c, PIMUZ 27984; 2c ×1, at H=48mm. From sample Chi56a, Chiddru. 3a-b, PIMUZ 27985. From sample Nam78, Nammal. 4a-b, PIMUZ 27986. From sample Chi2, Chiddru. 5a-b, PIMUZ 27987. Found as float in the upper part of the CS, Nammal. All ×0.5 unless otherwise indicated.

Plate 20


1a


1b


2a


2b


2c


3a


3b


4a


4b


5a


5b

EXPLANATION OF PLATE 21

Figs 1-2. *Flemingites flemingianus* (de Koninck, 1863). 1a-e, PIMUZ 27988; 1a-d ×0.4; 1e natural size, at H=54mm. From sample Nam131. 2a-b, PIMUZ 27989; ×0.5. From sample Nam78. Both specimens from the *Flemingites flemingianus* beds, CS, Nammal.

Plate 21

EXPLANATION OF PLATE 22

Figs 1-6. *Flemingites nanus* Waagen, 1895. 1a-c, PIMUZ 27990. From sample Chi10. 2a-d, PIMUZ 27991; 2d ×2, at H=13.3mm. From sample Chi10. 3a-d, PIMUZ 27992. From sample Chi10. 4a-c, PIMUZ 27993. From sample Nam528. 5a-b, PIMUZ 27994. From sample Nam530. 6a-e, PIMUZ 27995; 6e ×2, at H=12mm. From sample Nam528. 1-3 from the *Flemingites nanus* beds, CS, Chiddru. 4-5 from the *Flemingites nanus* beds, CM, Nammal. All natural size unless otherwise indicated.

Plate 22


1a


1b


1c


2a


2b


2c

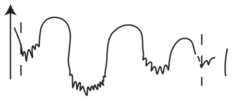
2d


3a


3b


3c


3d


4a


4b


4c


5a


5b


6e


6a


6b


6c


6d

EXPLANATION OF PLATE 23

Figs 1-4. *Flemingites hofmanni* sp. nov. 1a-d, PIMUZ 27996. 2a-d, PIMUZ 27997; 2a-c ×0.9, 2d ×2, at D=65.5mm, H=24.5mm. 3a-c, PIMUZ 27998. 4a-d, holotype, PIMUZ 27999; ×0.8. All from sample Chi1 (SFB), *Xenodiscoides perplicatus* beds, CM or CS, Chiddru. All natural size unless otherwise indicated.

Plate 23

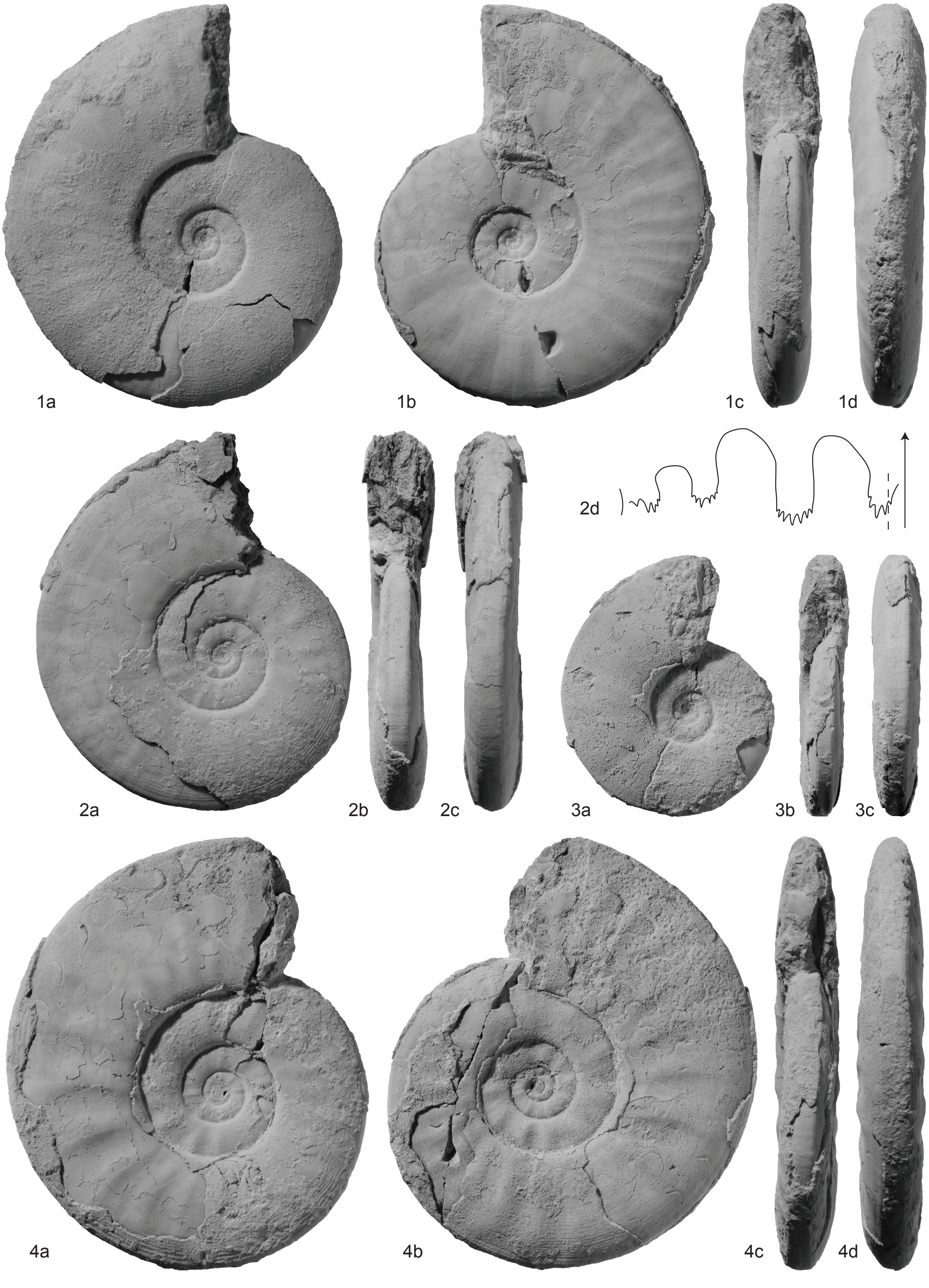

EXPLANATION OF PLATE 24

Figs 1-9. *Flemingites hautmanni* sp. nov. 1a-d, holotype, PIMUZ 28000. 2a-d, PIMUZ 28001. From sample Nam543. 3a-b, PIMUZ 28002. 4, PIMUZ 28003, ×2, at H=12mm. 5a-d, PIMUZ 28004. 6a-b, PIMUZ 28005. From sample Nam543. 7a-b, PIMUZ 28006. 8a-c, PIMUZ 28007. 9, PIMUZ 28008. All except for 2 and 6 from sample Nam718. All from the *Flemingites bhargavai* beds, CM, Nammal. All natural size unless otherwise indicated.

Plate 24

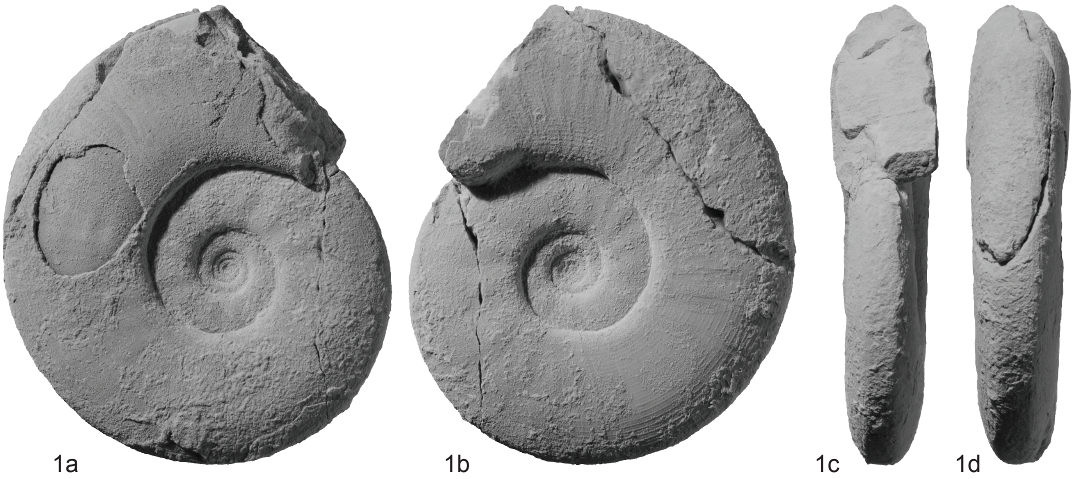

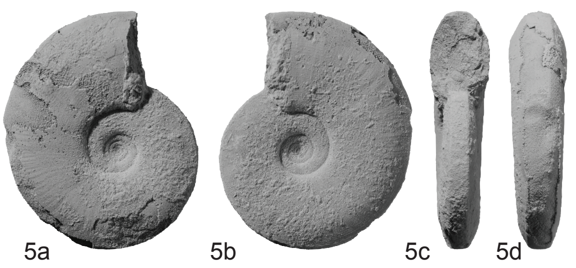

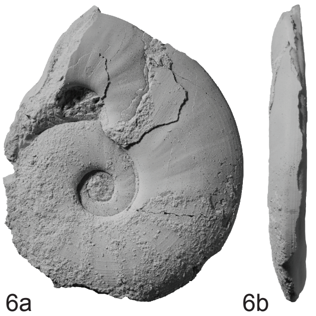

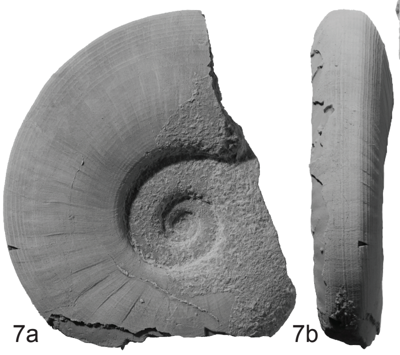

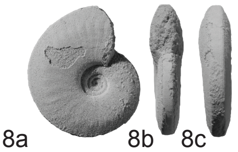

EXPLANATION OF PLATE 25

Figs 1-5. *Rohillites pakistanensis* sp. nov. 1a-d, PIMUZ 28009. 2a-d, PIMUZ 28010. 3a-e, holotype, PIMUZ 28011; 3e ×2, at D=37.4mm, H=13.7mm. 4a-d, PIMUZ 28012. 5a-d, PIMUZ 28013. All from sample Chi1 (SFB), *Xenodiscoides perplicatus* beds, CM or CS, Chiddru.

Figs 6-7. *Flemingites hautmanni* sp. nov. 6a-c, PIMUZ 28014. 7a-d, PIMUZ 28015. All from from sample Nam718, *Flemingites bhargavai* beds, CM, Nammal.

All natural size unless otherwise indicated.

Plate 25

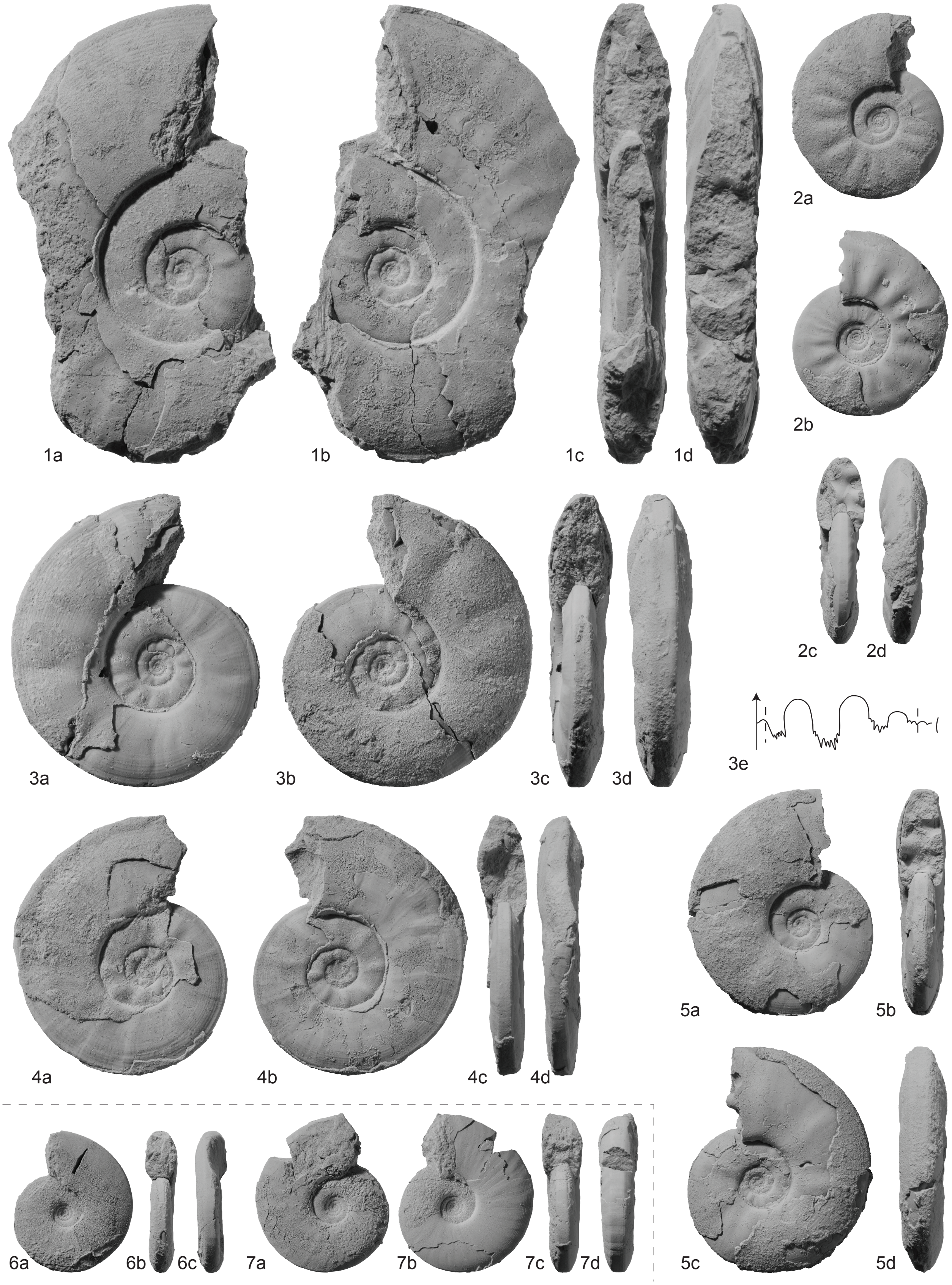
1a
1b
1c
1d
2a
2b
2c
2d
3a
3b
3c
3d
3e
4a
4b
4c
4d
5a
5b
5c
5d
6a
6b
6c
7a
7b
7c
7d

EXPLANATION OF PLATE 26

Figs 1-3. *Flemingites planatus* sp. nov. 1a-e, holotype, PIMUZ 28016; 1e ×2, at H=15.2mm. From sample Chi52. 2a-b, PIMUZ 28017. From sample Chi63. 3a-d, PIMUZ 28018. From sample Chi52. All from the *Flemingites planatus* beds, base of CM, Chiddru.

Fig 4a-e. *Shamaraites rursiradiatus* sp. nov. 4a-e, holotype, PIMUZ 28019; 4e ×2, at H=9.2mm. From sample Chi53, *Shamaraites rursiradiatus* beds, base of CM, Chiddru.

Fig. 5a-b. ?Flemingitidae gen. et sp. indet. A. PIMUZ 28020. From sample Nam546, *Flemingites bhargavai* beds, CM, Nammal.

Fig. 6a-d. ?Flemingitidae gen. et sp. indet. B. PIMUZ 28021; 6d ×2. From sample Chi104, *Flemingites planatus* beds, base of CM, Chiddru.

All natural size unless otherwise indicated.

Plate 26


1a 1b 1c 1d

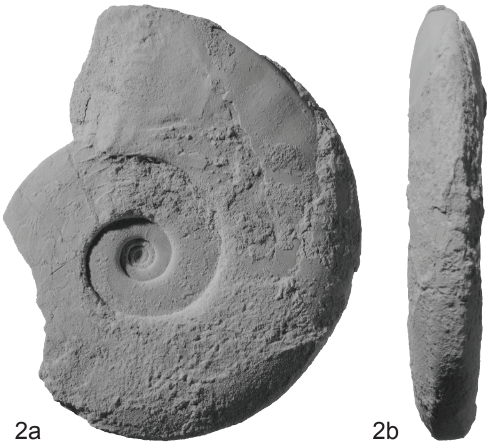
2a 2b


3a 3b 3c 3d


4a 4b 4c 4d

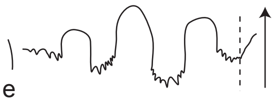
1e


4e


5a 5b

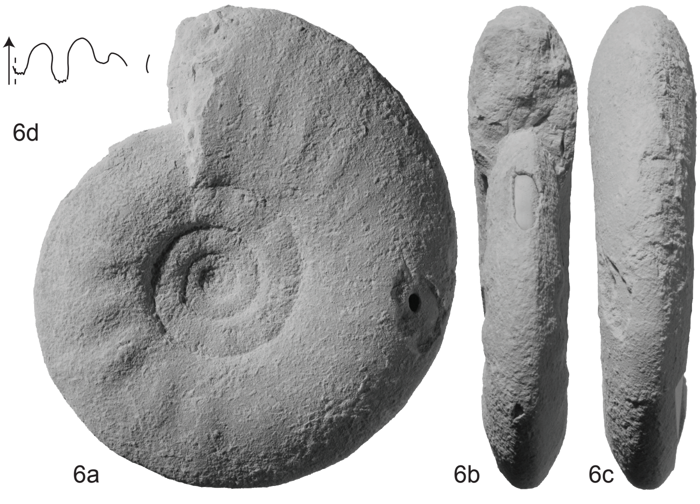
6a 6b 6c 6d

EXPLANATION OF PLATE 27

Figs 1-6. *Anaxenaspis nammalensis* (Guex, 1978). 1a-e, PIMUZ 28022; 1e×1.5, at H=17.3mm. From sample Nam10, Nammal. 2a-c, PIMUZ 28023. From sample Nam8, Nammal. 3a-d, PIMUZ 28024. From sample Nam8, Nammal. 4a-c, PIMUZ 28025. From sample Chi101, Chiddru. 5a-d, PIMUZ 28026. From sample Nam68, Nammal. 6a-c, PIMUZ 28027. From sample Chi101, Chiddru. All from the *Nylamites angustecostatus* beds, UCL.All natural size unless otherwise indicated.

Plate 27

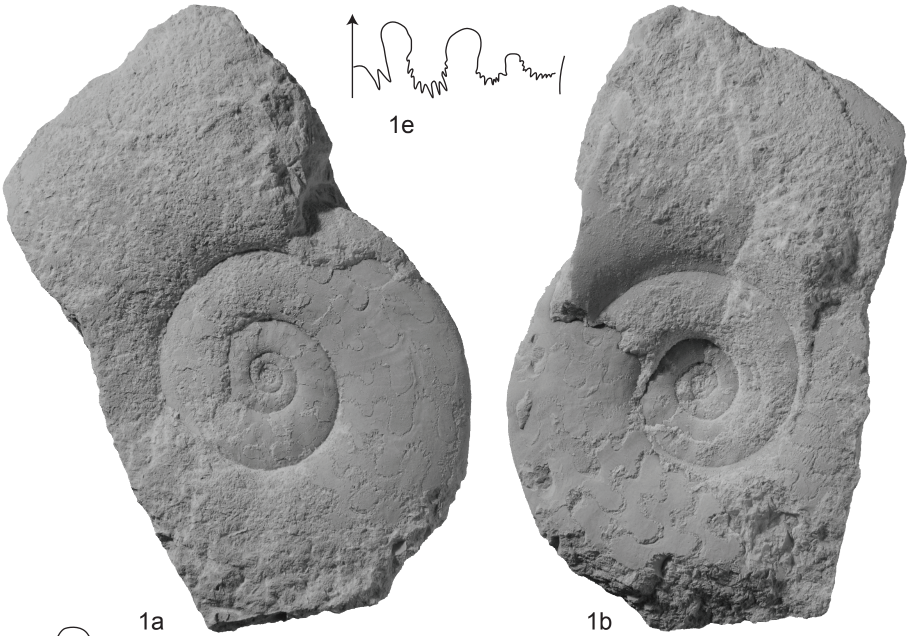
1e

1a

1b


1c


1d

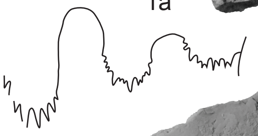
2c


2a


2b


3a


3b


3c


3d


4a


4b


4c


5a


5b


5c


5d


6a


6b


6c

EXPLANATION OF PLATE 28

Fig. 1a-c. *Flemingites bhargavai* Brühwiler *et al.* (submitted [b]). PIMUZ 28028. From sample Nam543, *Flemingites bhargavai* beds, CM, Nammal.

Figs 2-4. *Pseudoflemingites* cf. *timorensis* Spath, 1930. 2, PIMUZ 28029. 3a-e, PIMUZ 28030; 3e ×1.5, at H=23mm. 4a-b, PIMUZ 28031. All from sample Chi53, *Shamaraites rursiradiatus* beds, base of CM, Chiddru.

Fig. 5a-d. *Dieneroceras* sp. indet. B. PIMUZ 28032; 5d ×2, at D=24.3mm, H=6.5mm. From sample Nam16, *Pseudoceltites multiplicatus* beds, UCL, Nammal.

Fig. 6a-c. *Dieneroceras* sp. indet. A. PIMUZ 28033; 6e ×2, at D=17.3mm, H=5.7mm. From sample Nam19, *Pseudoceltites multiplicatus* beds, UCL, Nammal.

All natural size unless otherwise indicated.

Plate 28


1a


1b


1c

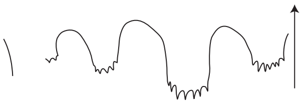
3e

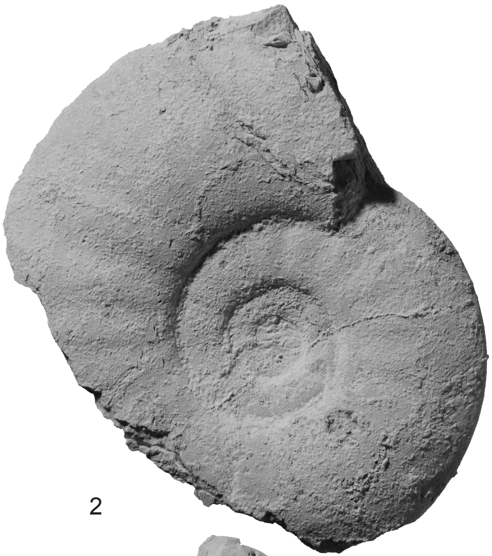
2


3a


3b


4a


3c


3d


4b


5a


5b


5c

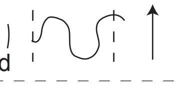
5d

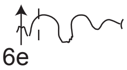
6e


6a


6b


6c


6d

EXPLANATION OF PLATE 29

Fig. 1a-b. *Pseudoflemingites* cf. *timorensis* Spath, 1930. PIMUZ 28029 (see Pl. 28, fig. 2 for lateral view of this specimen).

Figs 2-7. *Xenodiscoides perplicatus* (Frech, 1905). 2a-c, PIMUZ 28034. From sample Nam65, CM, Nammal. 3a-c, PIMUZ 28035. From sample Nam532, CM, Nammal. 4a-c, PIMUZ 28036. From sample Nam532, CM, Nammal. 5a-d, PIMUZ 28037. From sample Chi1 (SFB), CM or CS, Chiddru. 6a-c, PIMUZ 28038. From sample Nam532, CM, Nammal. 7a-e, PIMUZ 28039; 7e ×2, at D=30.6mm, H=10.3mm. From sample Nam532, CM, Nammal. All from the *Xenodiscoides perplicatus* beds.

Fig. 8a-e. *Xenodiscoides falcatum* (Waagen, 1895). PIMUZ 28040; 8e ×2, at H=14.2mm. From sample Chi1 (SFB), CM or CS, Chiddru. *Xenodiscoides perplicatus* beds.

All natural size unless otherwise indicated.

Plate 29


1a
1b

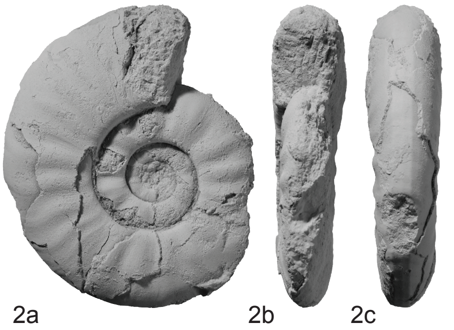
2a
2b
2c

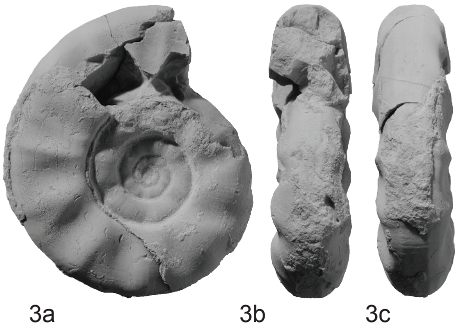
3a
3b
3c

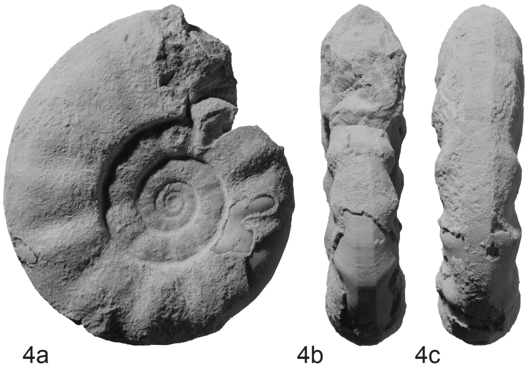
4a
4b
4c

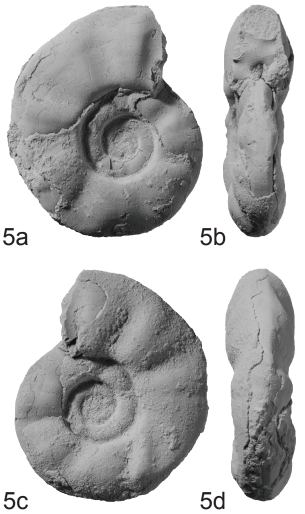
5a
5b
5c
5d

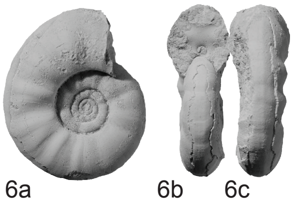
6a
6b
6c

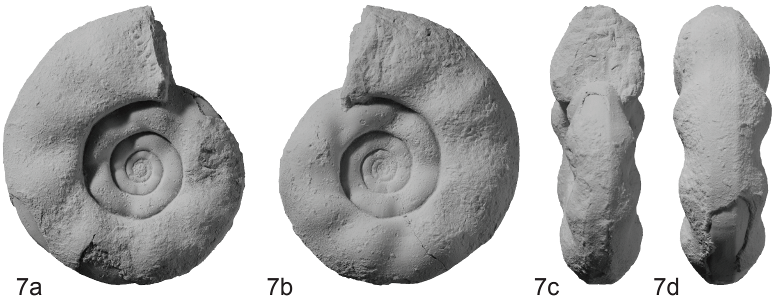
7a
7b
7c
7d


7e


8e

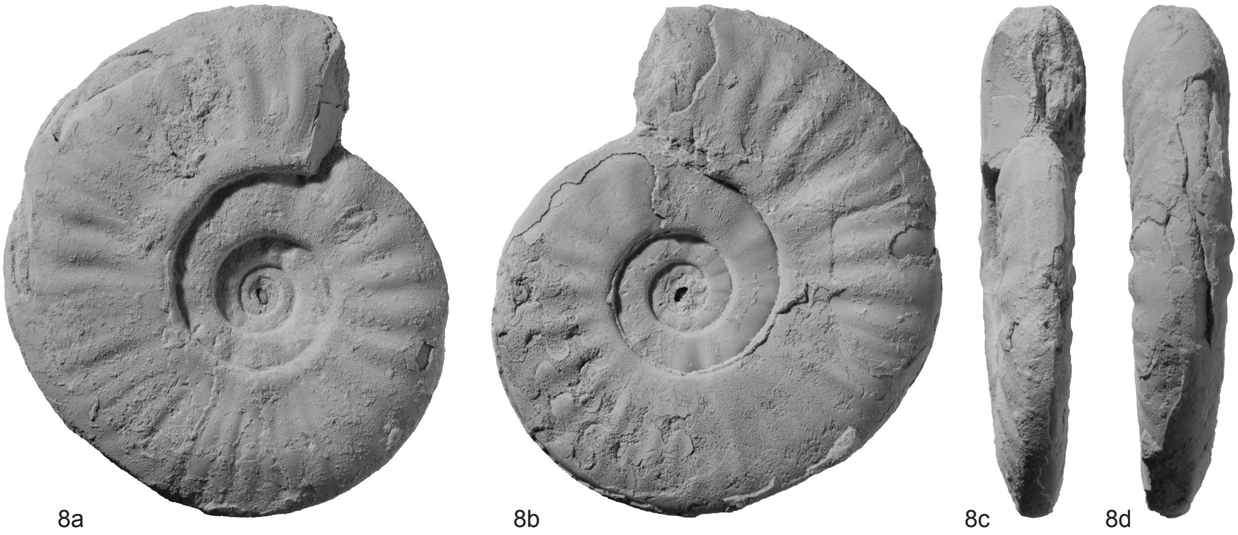
8a
8b
8c
8d

EXPLANATION OF PLATE 30

Figs 1-8. *Xenodiscoides involutus* (Frech, 1905). 1a-c, PIMUZ 28041. From sample Nam65. 2a-c, PIMUZ 28042. 3a-e, PIMUZ 28043; 3e×2, at H=15.9mm. 4a-c, PIMUZ 28044. 5a-c, PIMUZ 28045. 6a-d, PIMUZ 28046. 7a-c, PIMUZ 28047. 8a-e, PIMUZ 28048; 8e×2, at H=12.8mm. All except 1 from sample Nam532. All from the *Xenodiscoides perplicatus* beds, CM, Nammal.

All natural size unless otherwise indicated.

Plate 30

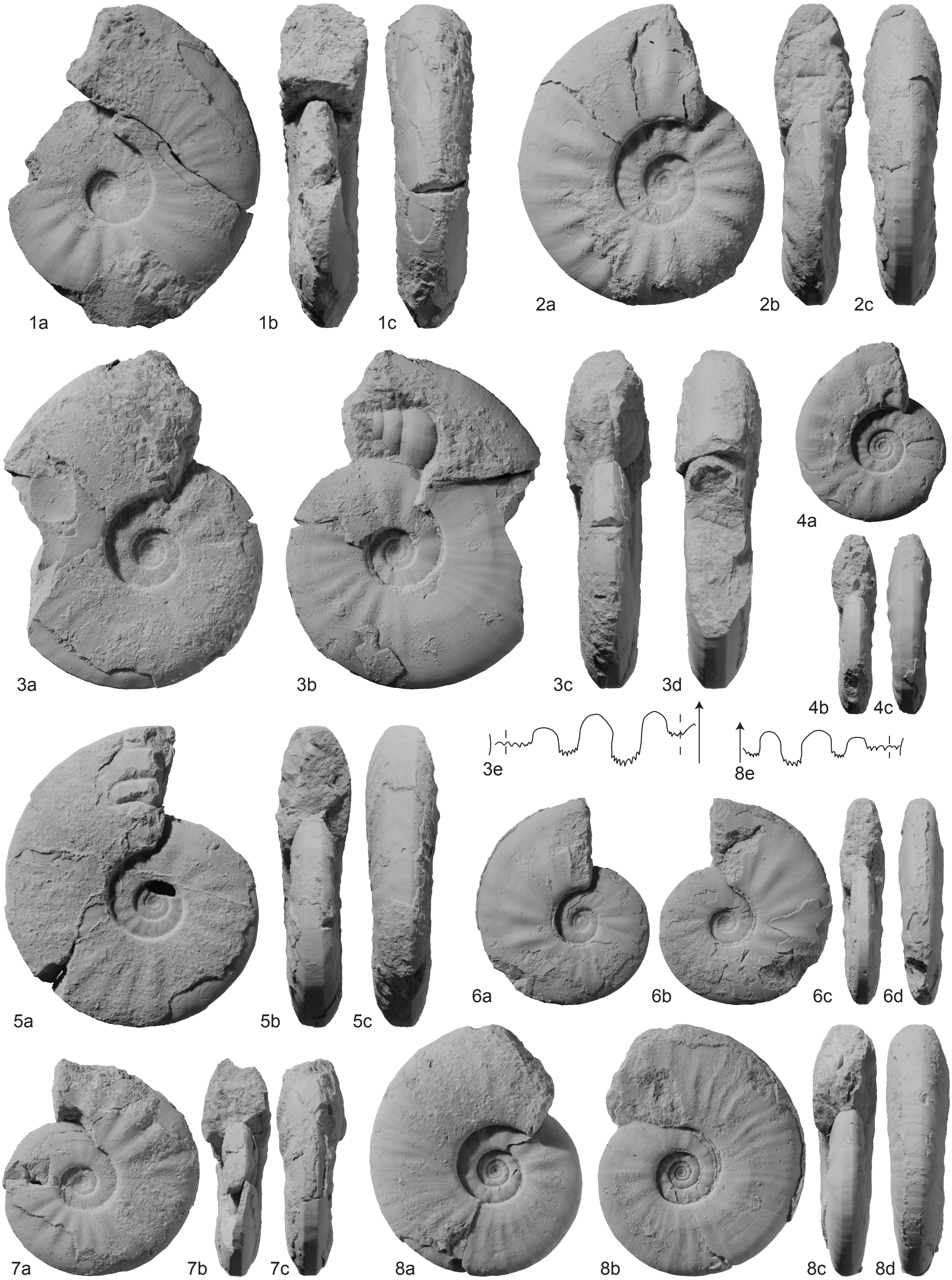
1a
1b
1c
2a
2b
2c
3a
3b
3c
3d
4a
4b
4c
3e
8e
5a
5b
5c
6a
6b
6c
6d
7a
7b
7c
8a
8b
8c
8d

EXPLANATION OF PLATE 31

Figs 1-8. *Brayardites compressus* Brühwiler *et al.* (accepted). 1a-c, PIMUZ 28049; 1c×1.5, at H=18.4mm. 2a-d, PIMUZ 28050. 3a-d, PIMUZ 28051; 3d×1.5, at H=16mm. 4a-c, PIMUZ 28052. 5a-d, PIMUZ 28053. From sample Nam22. 6a-d, PIMUZ 28054. 7a-c, PIMUZ 28055. 8a-d, PIMUZ 28056. All except Fig. 5 from sample Nam15. All from the *Brayardites compressus* beds, UCL, Nammal.

Fig. 9a-c. ?*Brayardites compressus* Brühwiler *et al.* (accepted). PIMUZ 28057. From sample Nam15.

All natural size unless otherwise indicated.

Plate 31


1a
1b


2a
2b
2c
2d


3a
3b
3c

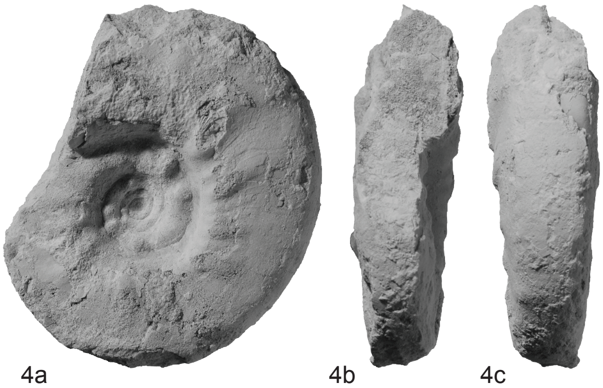
4a
4b
4c


5a
5b
5c
5d


3d


6a
6b
6c
6d

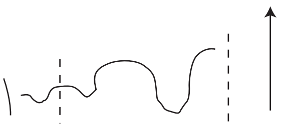
1c

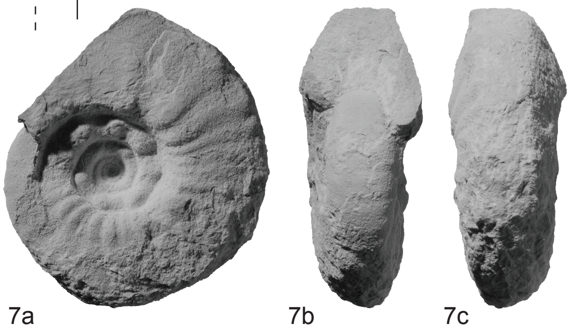
7a
7b
7c

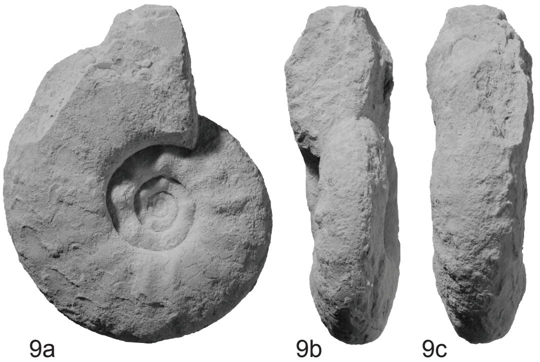
9a
9b
9c

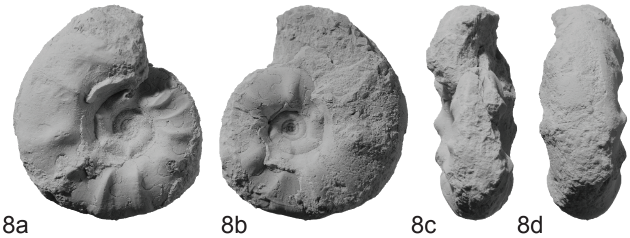
8a
8b
8c
8d

EXPLANATION OF PLATE 32

Figs 1-4. *Nammalites pilatoides* (Guex, 1978). 1a-d, PIMUZ 28058. From sample Nam18, Nammal. 2a-d, PIMUZ 28059. From sample Nam18, Nammal. 3a-c, PIMUZ 28060. From sample Chi13, Chiddru. 4a-d, PIMUZ 28061; 4d ×2, at D=24.8mm, H=11.5mm. From sample Nam21. All from the *Nammalites pilatoides* beds, UCL.

Figs 5-7. *Truempyceras pluriformis* (Guex, 1978) gen. nov. 5a-c, PIMUZ 28062. From sample Nam18. 6, PIMUZ 28063. From sample Nam18. 7a-b, PIMUZ 28064. From sample Chi13. All from the *Nammalites pilatoides* beds, UCL.

Fig. 8a-c. Ussuriidae gen. et sp. indet. PIMUZ 28065; 8c ×1.5, at H≈48mm. From sample Chi105, *Nammalites pilatoides* beds, UCL, Chiddru.

All natural size unless otherwise indicated.

Plate 32

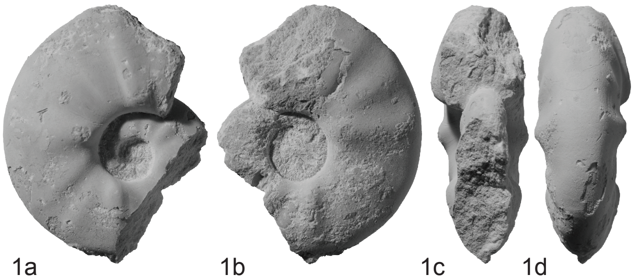

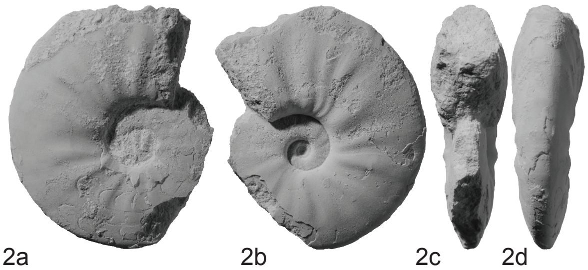

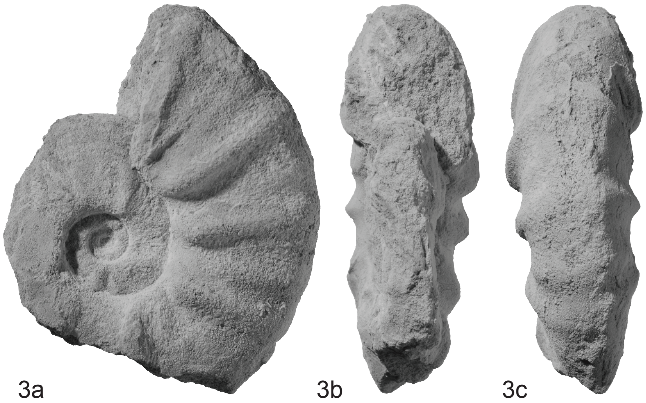

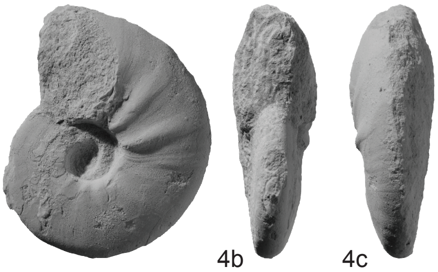

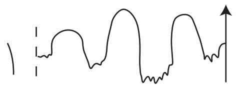
4d


6

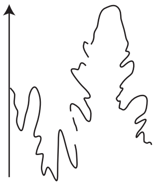
8c

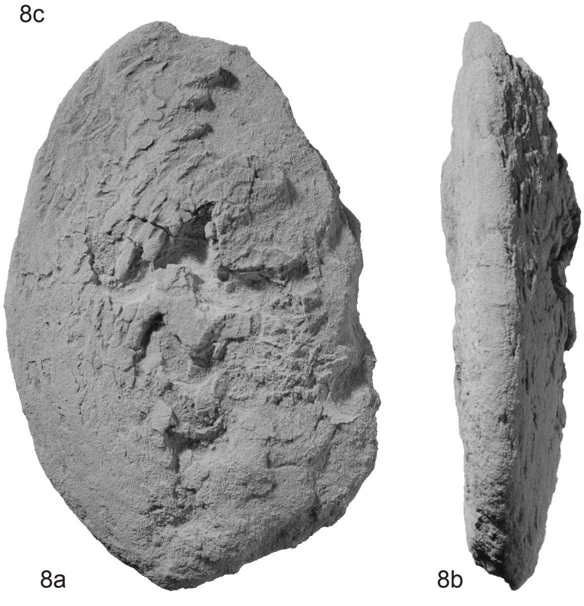

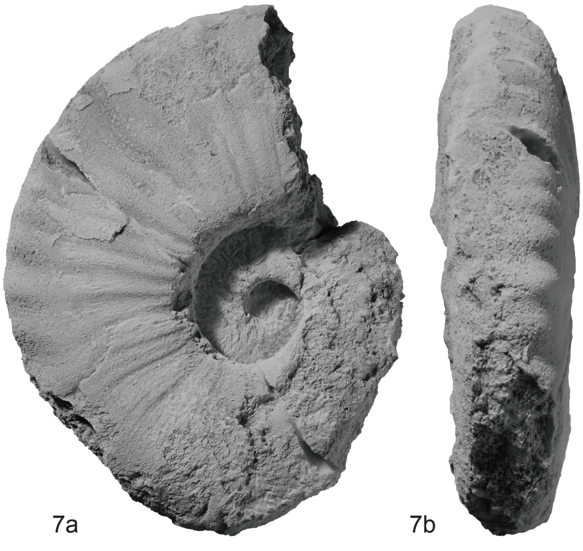

EXPLANATION OF PLATE 33

Figs 1-3. *Truempyceras pluriformis* (Guex, 1978) gen. nov. 1a-e, PIMUZ 28066; 1e ×2, at H=16.1mm. 2a-d, PIMUZ 28067. 3a-e, PIMUZ 28068; 3e×2, at H=17.3mm. All from sample Nam18, *Nammalites pilatoides* beds, UCL, Nammal. All natural size unless otherwise indicated.

Plate 33

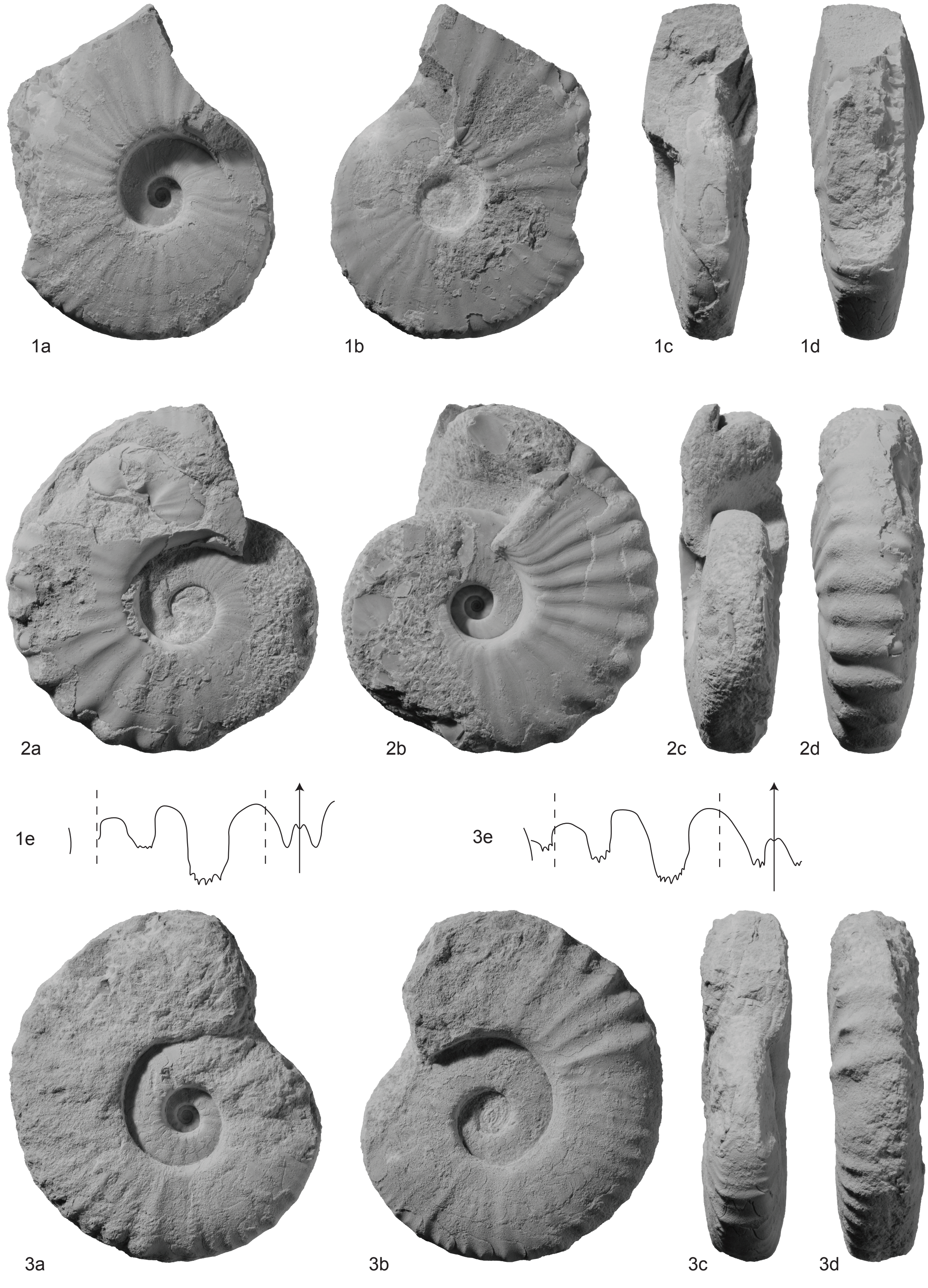

EXPLANATION OF PLATE 34

Figs 1-8. *Prionites tuberculatus* Waagen, 1895. 1a-b, PIMUZ 28069. 2a-c, PIMUZ 28070. 3a-b, PIMUZ 28071. 4a-c, PIMUZ 28072. 5a-c, PIMUZ 28073. 6a-d, PIMUZ 28074. 7a-c, PIMUZ 28075. 8a-b, PIMUZ 28076. All from sample Nam68, *Nyalamites angustecostatus* beds, UCL, Nammal. All natural size.

Plate 34


1a


1b


2a


2b


2c


3a


3b


4a


4b


4c


5a


5b


5c


6a


6b


6c


6d


7a


7b


7c

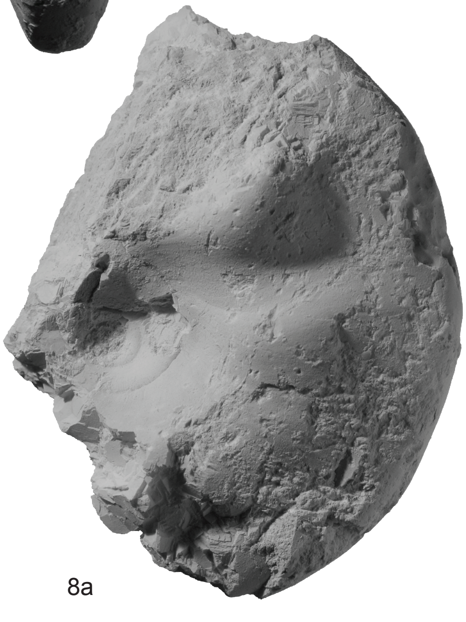
8a


8b

EXPLANATION OF PLATE 35

Figs 1-3. *Prionites tuberculatus* Waagen, 1895. 1a-c, PIMUZ 28077. 2, PIMUZ 28078; ×2, at H=16.5mm. 3, PIMUZ 28072 (see also Pl. 34, fig. 4a-c); ×2, at D=17.2mm, H=9mm. All from sample Nam68, *Nyalamites angustecostatus* beds, UCL, Nammal.

Figs 4-9. *Prionites nammalensis* sp. nov. 4a-c, PIMUZ 28079. 5a-c, PIMUZ 28080; 5c ×2, at D=53.6mm, H=22.1mm. 6a-c, holotype, PIMUZ 28081. 7a-b, PIMUZ 28082. 8a-e, PIMUZ 28083; 8e ×2, at D=37.7mm, H=18mm. From sample Nam9. 9a-c, PIMUZ 28084. All except 8 from sample Nam16. All from the *Pseudoceltites multiplicatus* beds, UCL, Nammal.

All natural size unless otherwise indicated.

Plate 35

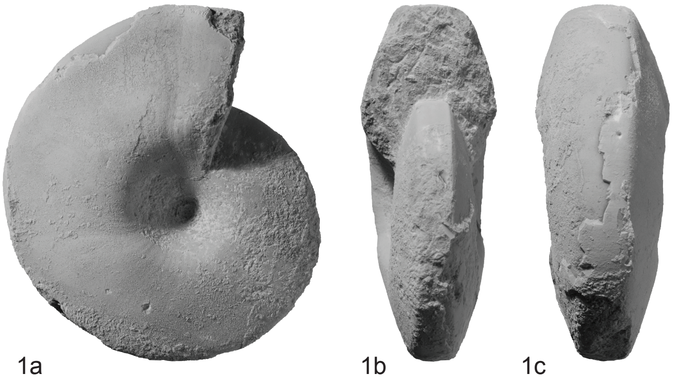
1a 1b 1c


2


3

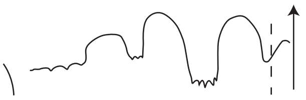
8e


5c

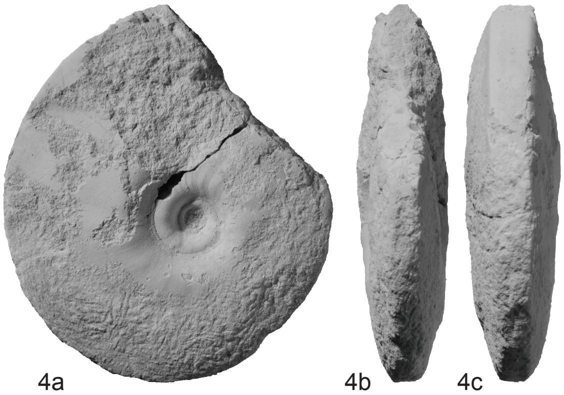
4a 4b 4c

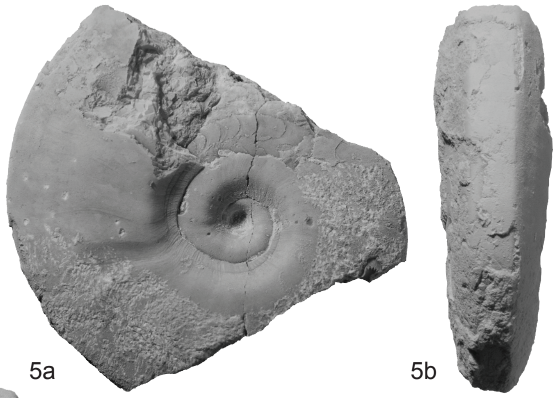
5a 5b

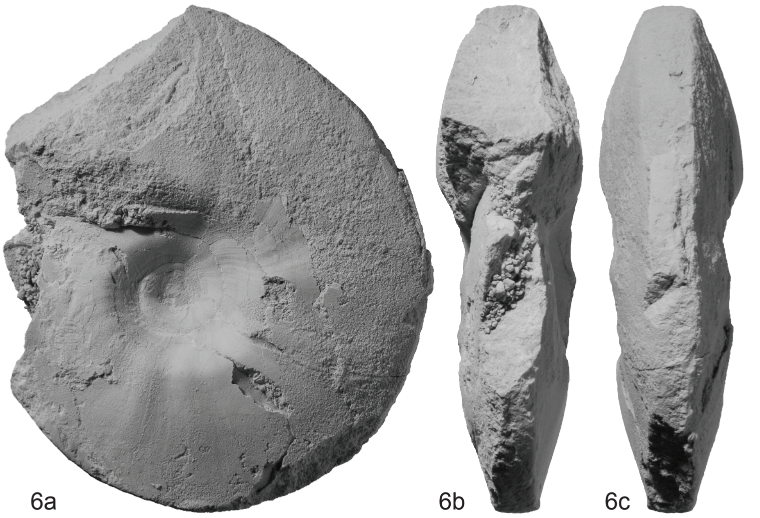
6a 6b 6c

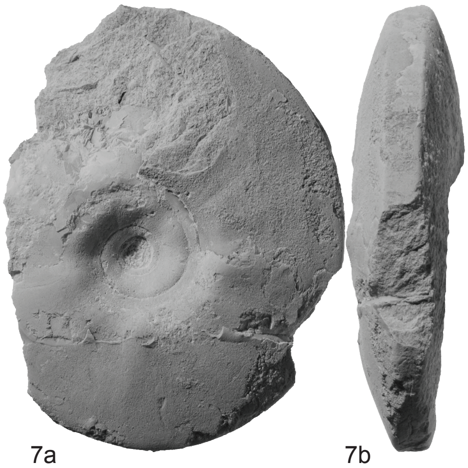
7a 7b


8a 8b 8c 8d

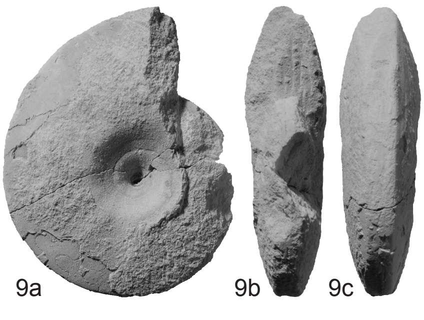
9a 9b 9c

EXPLANATION OF PLATE 36

Figs 1-7. *Meekoceras* cf. *gracilitatis* White, 1879. 1a-b, PIMUZ 28085; ×0.9. From sample Chi105, Chiddru. 2a-d, PIMUZ 28086; ×0.9. 3a-b, PIMUZ 28087; ×0.9. 4a-d, PIMUZ 28088. 5a-c, PIMUZ 28089. 6a-c, PIMUZ 28090; 6b-c ×2. 7a-e, PIMUZ 28091; 7e ×2, at D=19mm, H=9.3mm. All except 1 from sample Nam18, Nammal. All from the *Nammalites pilatoides* beds, UCL. All natural size unless otherwise indicated.

Plate 36

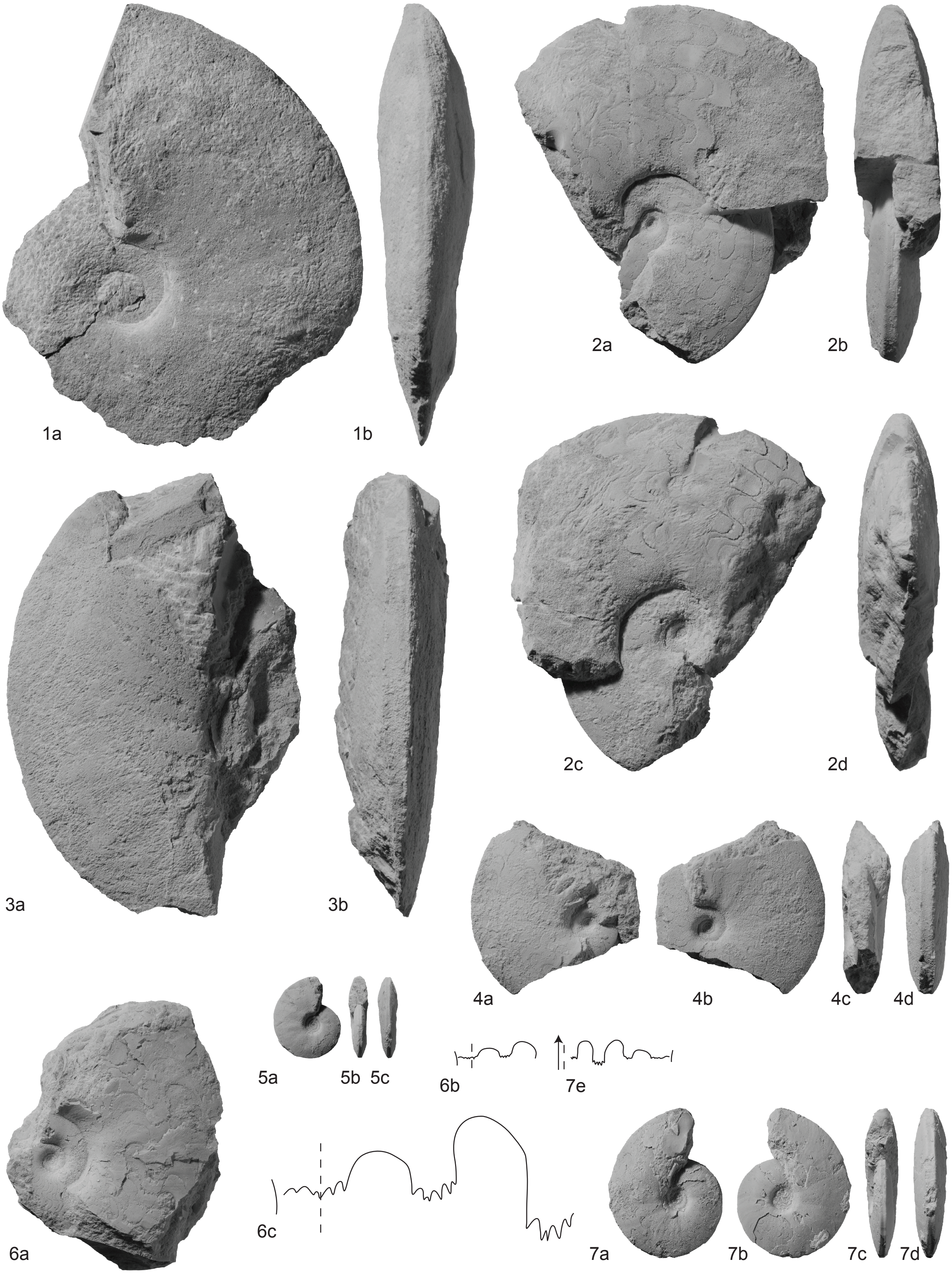

EXPLANATION OF PLATE 37

Figs 1-3. *Stephanites superbus* Waagen, 1895. 1a-b, PIMUZ 28092. From sample Chi101, Chiddru. 2a-c, PIMUZ 28093; 2c ×2, at H=10.7mm. From sample Nam68, Nammal. 3a-c, PIMUZ 28093. From sample Nam68, Nammal. All from the *Nyalamites angustecostatus* beds, UCL.

Fig. 4a-d. *Punjabites punjabiensis* gen. et sp. nov. Holotype. PIMUZ 28094; 4d ×2, at H=18.2mm. From sample Nam9, *Pseudoceltites multiplicatus* beds, Nammal.

Figs 5-8. *Wasatchites distractus* (Waagen, 1895). 5a-d, PIMUZ 28095. From sample Nam17. 6, PIMUZ 28096; ×2, at D=10.5mm, H=5.1mm. From sample Nam17. 7a-c, PIMUZ 28097. From sample Nam25. 8, PIMUZ 28098; ×2. From sample Nam17. 8, PIMUZ 28099; at D=54.6mm, H=22mm. From sample Nam17. All from the *Wasatchites distractus* beds, UCL, Nammal.

All natural size unless otherwise indicated.

Plate 37

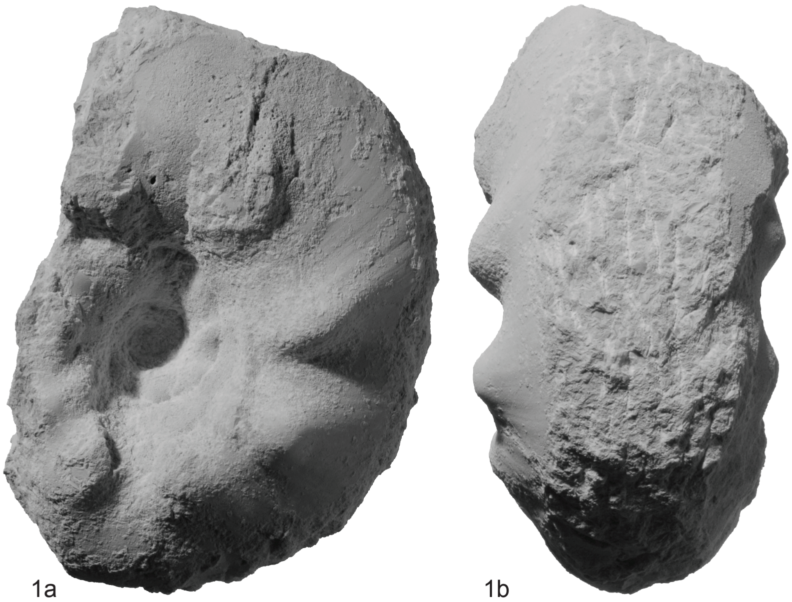
1a 1b

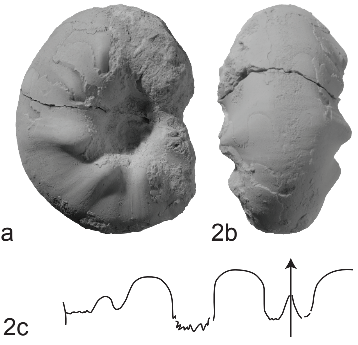
2a 2b 2c

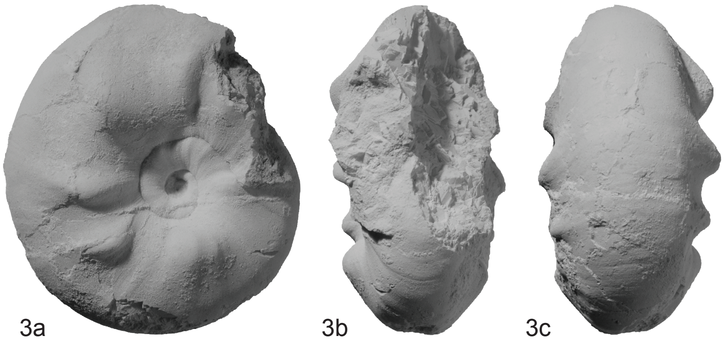
3a 3b 3c

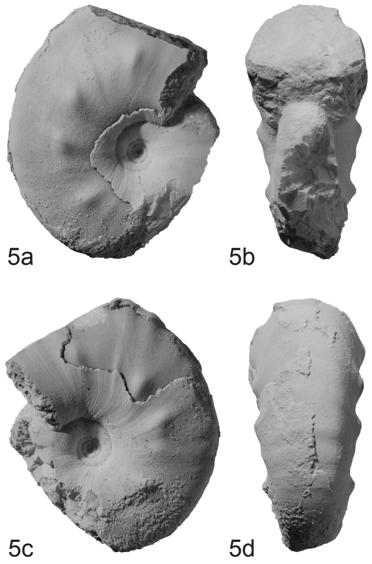
5a 5b 5c 5d

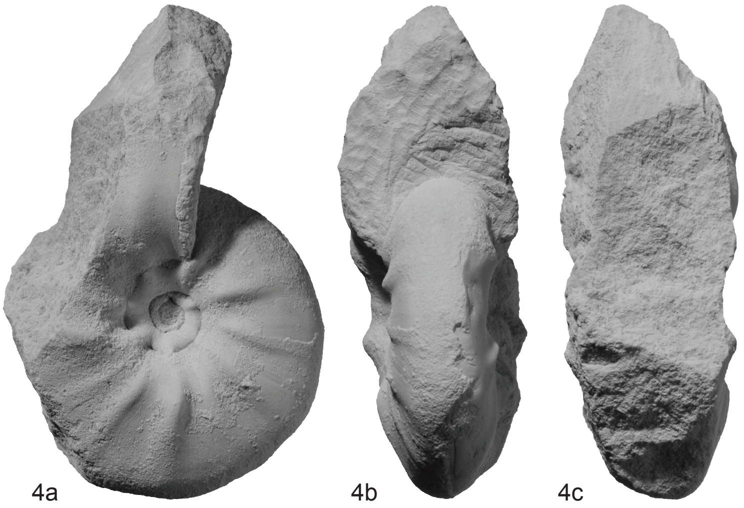
4a 4b 4c


6


7a

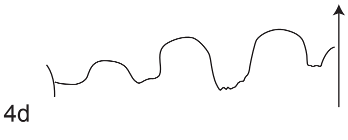
4d

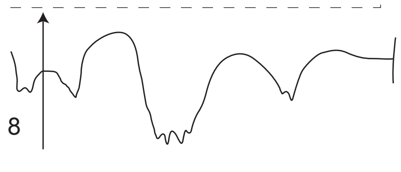
8

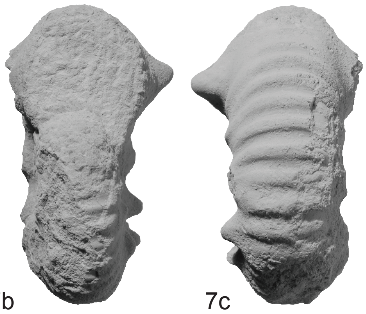
7b 7c

EXPLANATION OF PLATE 38

Figs 1-7. *Wasatchites distractus* (Waagen, 1895). 1a-d, PIMUZ 28100. From sample Nam17. 2a-d, PIMUZ 28101. From sample Nam17. 3a-d, PIMUZ 28102. From sample Nam6. 4a-d. PIMUZ 28096 (see also Pl. 37, fig. 6). From sample Nam17. 5a-c, PIMUZ 28103. From sample Nam17. 6a-c, PIMUZ 28104. From sample Nam25. 7a-b, PIMUZ 28105. From sample Nam17. All from the *Wasatchites distractus* beds, UCL, Nammal. All natural size.

Plate 38

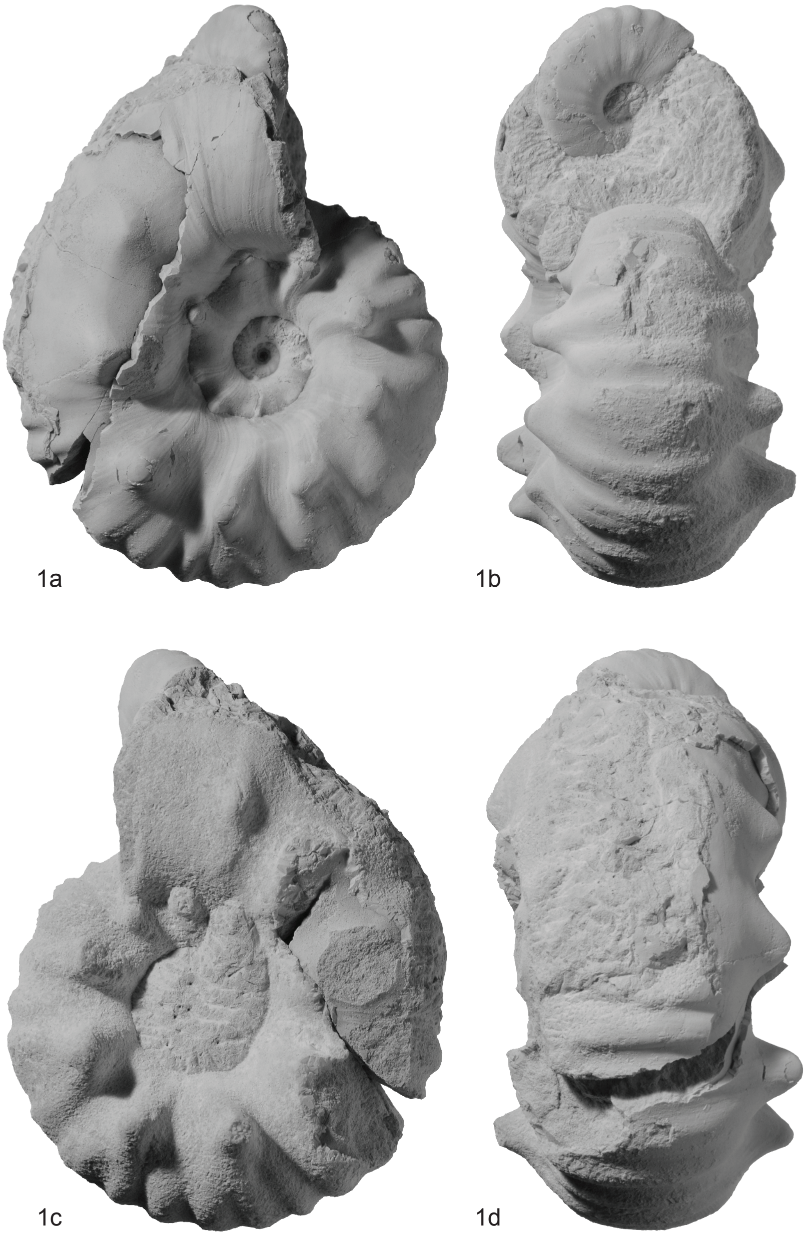
1a 1b 1c 1d

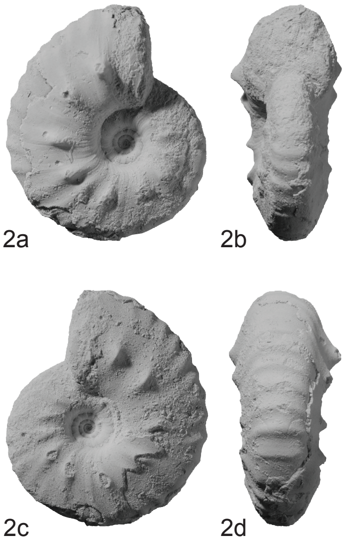
2a 2b 2c 2d


3a 3b 3c 3d

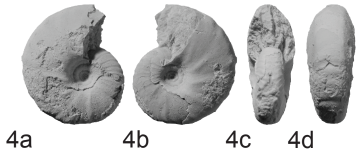
4a 4b 4c 4d


5a 5b 5c

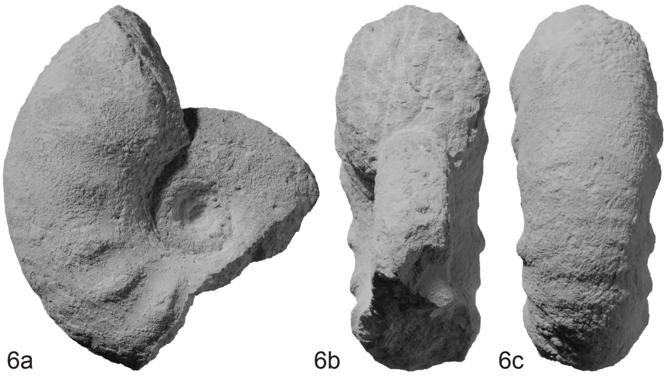
6a 6b 6c

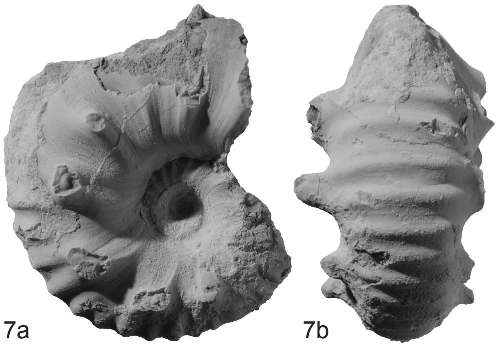
7a 7b

EXPLANATION OF PLATE 39

Figs 1-5. *Anasibirites kingianus* (Waagen, 1895). 1a-e, PIMUZ 28106; 1e at H=20.3mm. From sample Nam25. 2a-d, PIMUZ 28107. From sample Nam6. 3a-d, PIMUZ 28108. From sample Nam25. 4a-d. PIMUZ 28109. From sample Nam6. 5a-d, PIMUZ 28110. From sample Nam17. All from the *Wasatchites distractus* beds, UCL, Nammal.

Figs 6-7. *Anasibirites angulosus* (Waagen, 1895). 6a-b, PIMUZ 28111. From sample Nam6. 7a-d, PIMUZ 28112. From sample Nam17. *Wasatchites distractus* beds, UCL, Nammal.

All natural size.

Plate 39


1a
1b
1c
1d

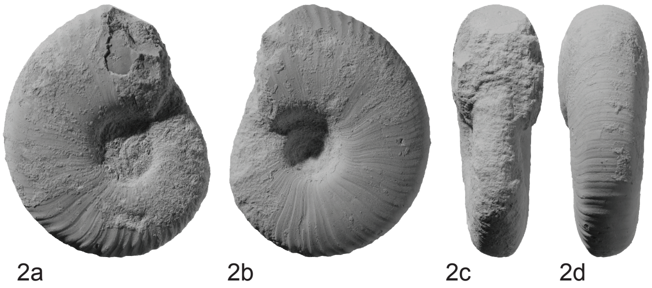
2a
2b
2c
2d

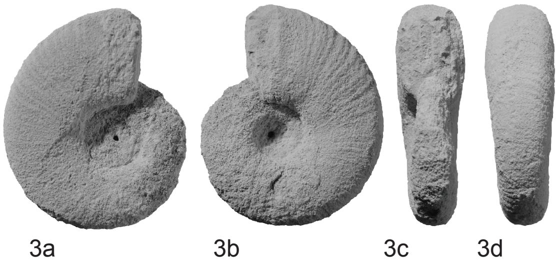
3a
3b
3c
3d

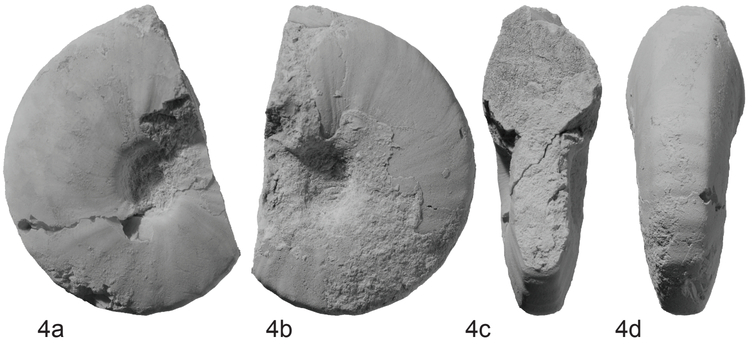
4a
4b
4c
4d

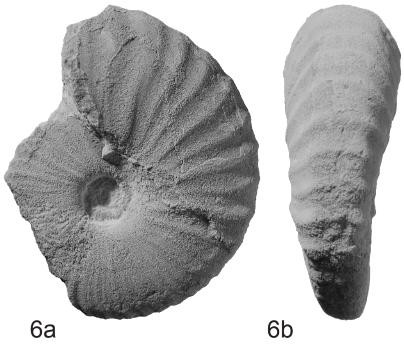
6a
6b

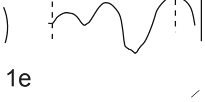
1e

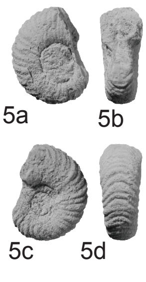
5a
5b
5c
5d

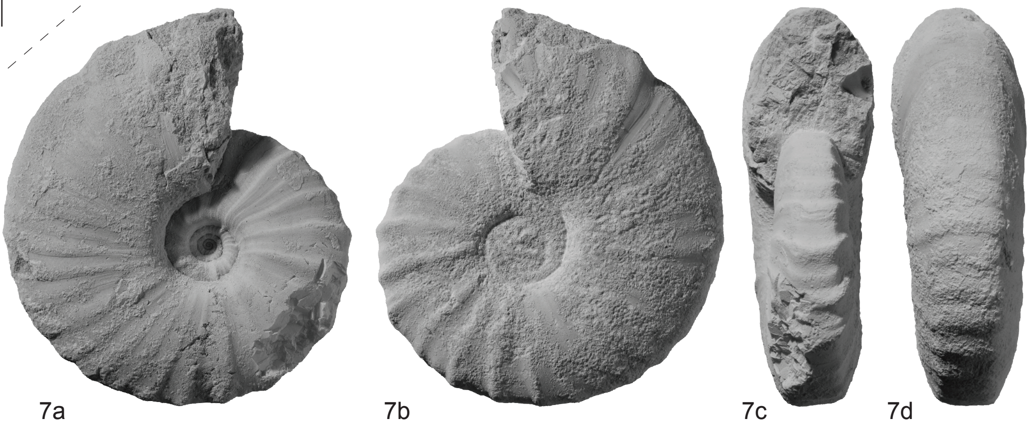
7a
7b
7c
7d

EXPLANATION OF PLATE 40

Figs 1-7. *Anasibirites angulosus* (Waagen, 1895). 1a-c, PIMUZ 28113. 2a-d, PIMUZ 28114. 3a-c, PIMUZ 28115. From sample Nam6. 4a-c. PIMUZ 28116. 5a-c, PIMUZ 28117; 5c ×2, at D=35.5mm, H=18mm. 6a-d, PIMUZ 28118. 7, PIMUZ 28119; ×2, at H=19.5mm. All except 3 from sample Nam701. All from the *Wasatchites distractus* beds, UCL, Nammal.

All natural size unless otherwise indicated.

Plate 40


1a


1b


1c


2a


2b


2c


2d


4a


4b


4c


3a


3b


3c

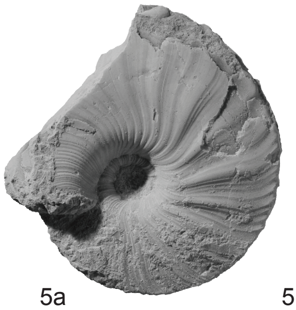
5a


5b


6a


6b


6c


6d

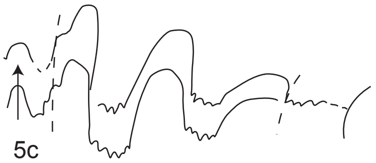
5c

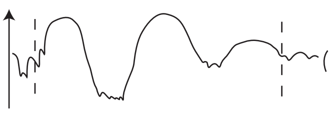
7

EXPLANATION OF PLATE 41

Figs 1-5. *Anasibirites angulosus* (Waagen, 1895). 1a-d, PIMUZ 28120. 2a-c, PIMUZ 28121. 3a-c, PIMUZ 28119 (see also Pl. 40, fig. 7). 4a-c. PIMUZ 28122. 5a-c, PIMUZ 28123. All from sample Nam701, *Wasatchites distractus* beds, UCL, Nammal.

Figs 6-9. *Hemiprionites klugi* Brayard and Bucher, 2008. 6a-d, PIMUZ 28124; 6d ×2, at H=16mm. 7a-c, PIMUZ 28125. 8a-b, PIMUZ 28126. 9a-c, PIMUZ 28127. All from sample Nam701, *Wasatchites distractus* beds, UCL, Nammal.

All natural size unless otherwise indicated.

Plate 41

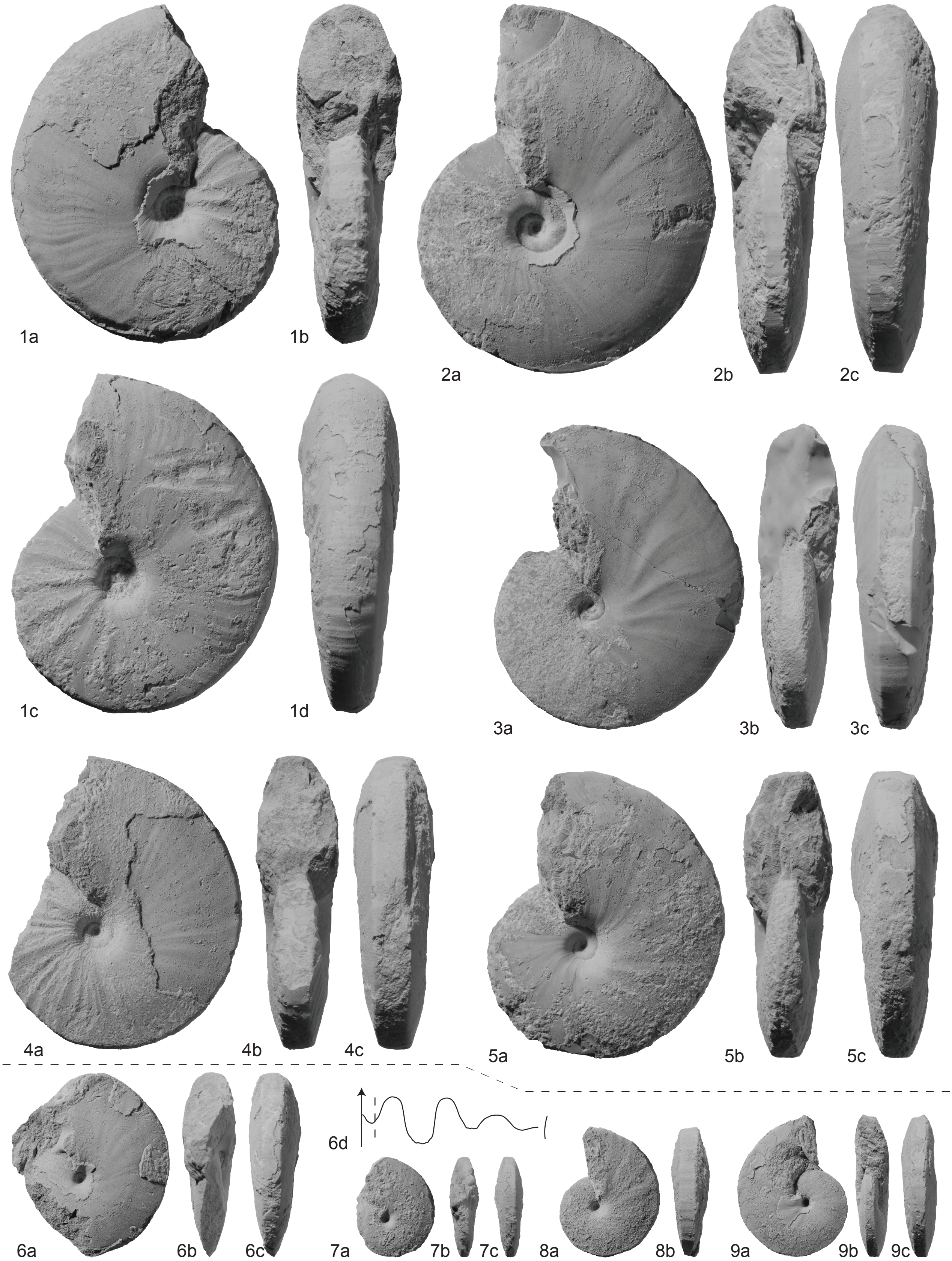
1a
1b
2a
2b
2c
1c
1d
3a
3b
3c
4a
4b
4c
5a
5b
5c
6d
6a
6b
6c
7a
7b
7c
8a
8b
9a
9b
9c

EXPLANATION OF PLATE 42

Figs 1-10. *Hemiprionites typus* (Waagen, 1895). 1a-b, PIMUZ 28128. From sample Nam25. 2a-c, PIMUZ 28129. 3a-d, PIMUZ 28130. From sample Nam17. 4a-c. PIMUZ 28131. 5a-c, PIMUZ 28132. 6a-e, PIMUZ 28133; 6e ×2, at D=36.7mm, H=16.6mm. 7a-d, PIMUZ 28134. 8a-c, PIMUZ 28135. 9a-c, PIMUZ 28136. 10a-d, PIMUZ 28137. All except 1 and 3 from sample Nam701. All from the *Wasatchites distractus* beds, UCL, Nammal.

Fig. 11a-e. ?*Hemiprionites* sp. indet. PIMUZ 28138; 11e ×2, at D=38.7mm, H=19.4mm. From sample Nam17, *Wasatchites distractus* beds, UCL, Nammal.

Figs 12-15. *Juvenites* sp. indet. 12a-d, PIMUZ 28139. 13a-c, PIMUZ 28140. 14a-c, PIMUZ 28141. 15, PIMUZ 28142; ×2, at D=21mm, H=9mm. All from sample Nam15, *Brayardites compressus* beds, UCL, Nammal.

Fig. 16a-c. *Owenites* sp. indet. PIMUZ 28143; 16a-b×2, 16c ×10, at D=3.9mm, H=2.2mm. From sample Nam8, *Nyalamits angustecostatus* beds, UCL, Nammal.

Fig. 17a-e. *Juvenites* cf. *kraffti* Smith, 1927. PIMUZ 28144; 17e ×3, at D=12.6mm, H=3.7mm. From sample Nam5, *Nammalites pilatoides* beds, UCL, Nammal.

All natural size unless otherwise indicated.

Plate 42

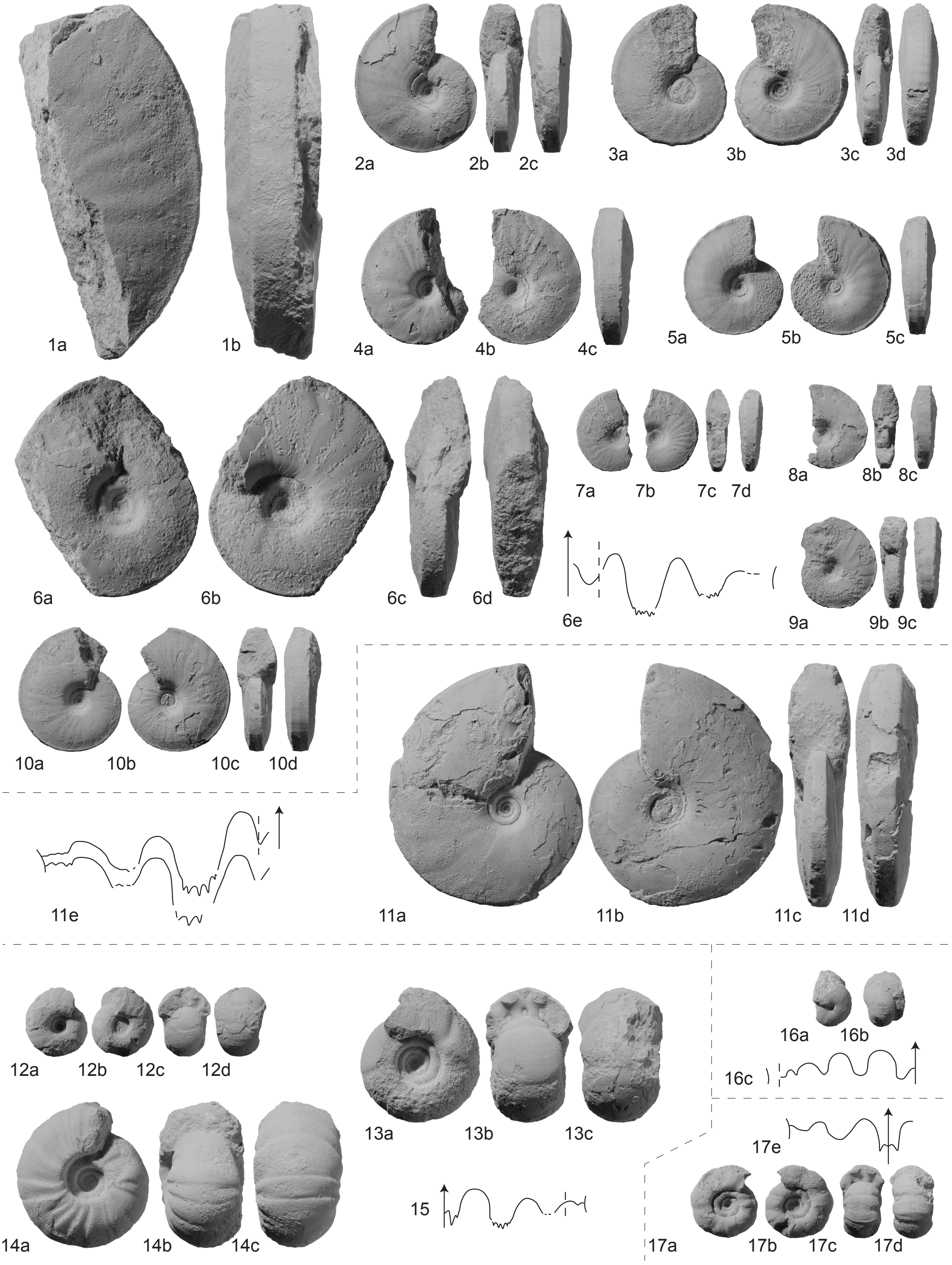
1a
1b
2a
2b
2c
3a
3b
3c
3d
4a
4b
4c
5a
5b
5c
6a
6b
6c
6d
6e
7a
7b
7c
7d
8a
8b
8c
9a
9b
9c
10a
10b
10c
10d
11a
11b
11c
11d
11e
12a
12b
12c
12d
13a
13b
13c
14a
14b
14c
15
16a
16b
16c
17a
17b
17c
17d
17e

EXPLANATION OF PLATE 43

Fig. 1a-d. Gen. et sp. indet. A. PIMUZ 28145; 1d at H≈35mm. From sample Zal50, *Flemingites flemingianus* beds, CS, Zaluch.

Figs 2-5. *Mianwaliites multiradiatus* gen. et sp. nov. 2a-c, PIMUZ 28146. 3a-c, PIMUZ 28147. 4a-c. PIMUZ 28148; 4c ×2, at H=16mm. 5-e, holotype, PIMUZ 28149; 5e ×2, at H=15mm. All from sample Nam38, *Wasatchites distractus* beds, UCL, Nammal.

Figs 6-7. *Subinyoites punjabiensis* sp. nov. 6a-d, holotype, PIMUZ 28150; 6d ×1.5, at H=18.5mm. From sample Nam25. 7a-e, PIMUZ 28151; 7e ×1.5, at H=15.8mm. From sample Nam37. Both specimens from the *Wasatchites distractus* beds, UCL, Nammal.

All natural size unless otherwise indicated.

Plate 43

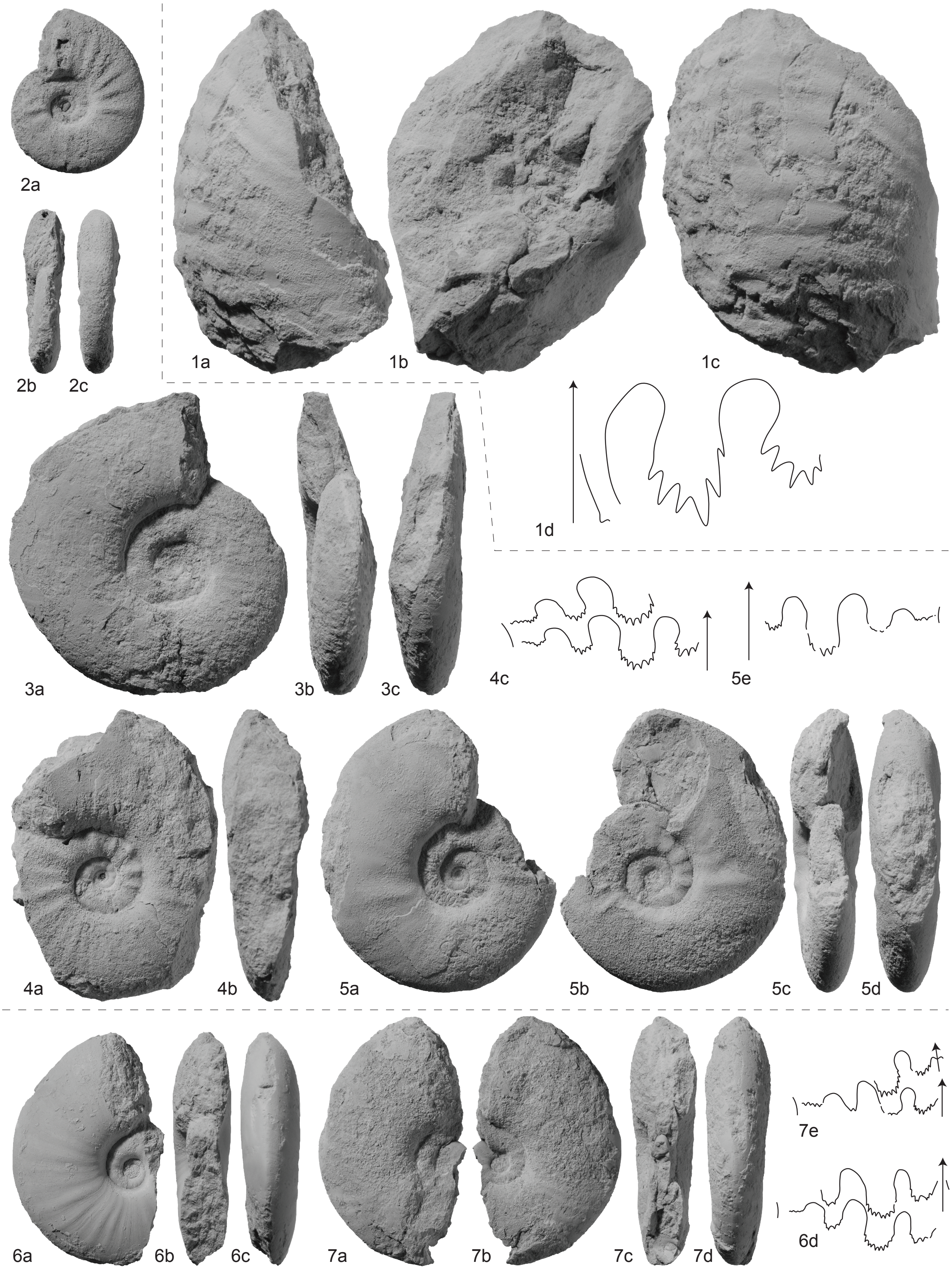
2a
2b
2c
1a
1b
1c
1d
3a
3b
3c
4c
5e
4a
4b
5a
5b
5c
5d
6a
6b
6c
7a
7b
7c
7d
7e
6d

EXPLANATION OF PLATE 44

Figs 1-4. *Hochuliites retrocostatus* gen. et sp. nov. 1a-c, PIMUZ 28152. From sample Nam16. 2a-d, holotype, PIMUZ 28153; 2d ×2, at H=18mm. From sample Nam9. 3a-c, PIMUZ 28154; from sample Nam16. 4a-b, PIMUZ 28155. From sample Nam16. All from the *Pseudoceltites multiplicatus* beds, UCL, Nammal.

Figs 5-7. *Paraspidites obesus* sp. nov. 5a-d, holotype, PIMUZ 28156. From sample Nam532, CM, Nammal. 6a-b, PIMUZ 28157. From sample Nam532, CM, Nammal. 7a-e, PIMUZ 28158; 7e ×1.5, at H=23.5mm. From sample Chi1 (SFB), CM or CS, Chiddru. All from the *Xenodiscoides perplicatus* beds.

Fig. 8a-e. *Paraspidites praecursor* (Frech, 1905). PIMUZ 28159; 8e ×2, at H=17.2mm. From sample Chi10, *Flemingites nanus* beds, CS, Chiddru.

All natural size unless otherwise indicated.

Plate 44


1a 1b 1c


2a 2b 2c


3a 3b 3c

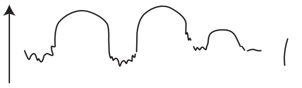
2d


4a 4b

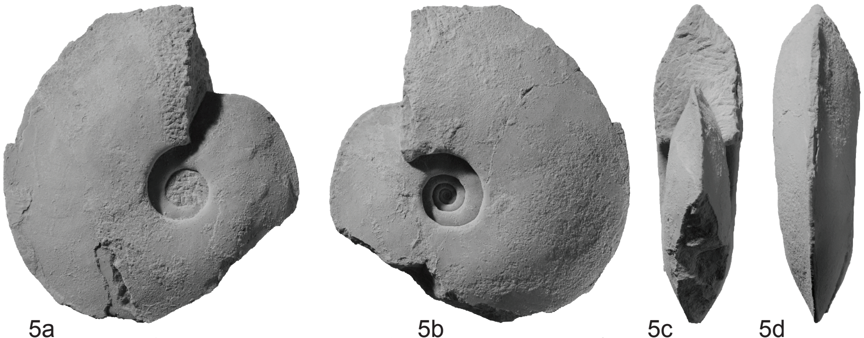
5a 5b 5c 5d

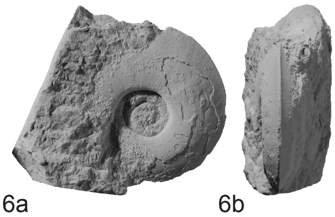
6a 6b


7e

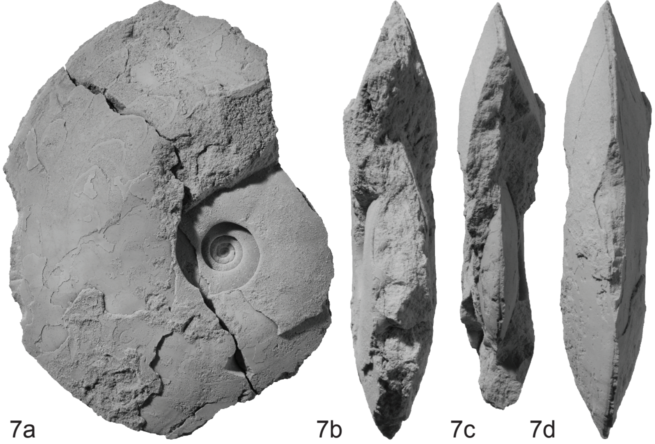
7a 7b 7c 7d


8e

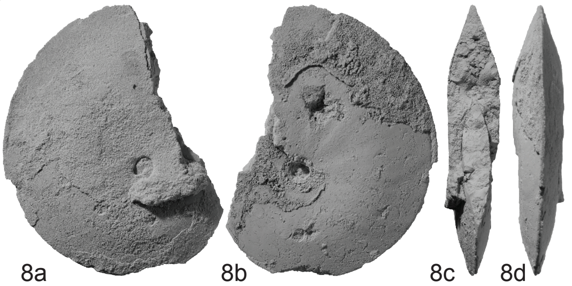
8a 8b 8c 8d

EXPLANATION OF PLATE 45

Figs 1-5. *Hedenstroemia evoluta* (Spath 1934). 1a-e. PIMUZ 28160; 1e at D=54mm, H=32.2mm. From sample Zal50, Zaluch. 2a-d, PIMUZ 28161; ×0.75; 2d at D=86mm, H=49mm. From sample Chi2, Chiddru. 3a-b, PIMUZ 28162. From sample Zal50, Zaluch. 4a-c, PIMUZ 28163; ×0.5. Found as float in the Ceratite Sandstone, Chiddru. 5a-c, PIMUZ 28164. From sample Chi56a, Chiddru. 1-3 and 5 from the *Flemingites flemingianus* beds, CS. All natural size unless otherwise indicated.

Plate 45

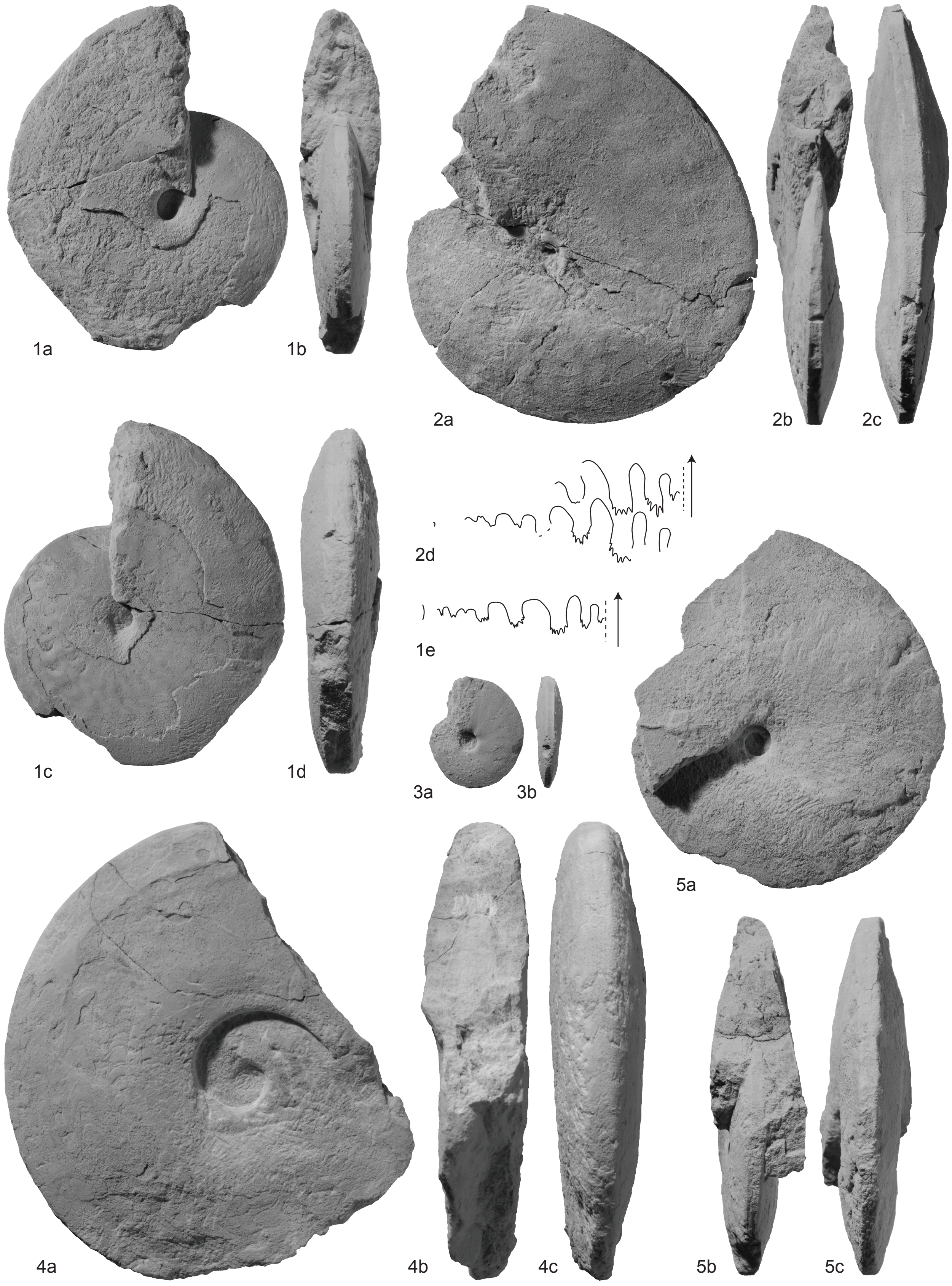

EXPLANATION OF PLATE 46

Figs 1-4. *Pseudosageceras multilobatum* Frech, 1905. 1a-c. PIMUZ 28165; 1c at H=66mm. From sample Chi10, *Flemingites nanus* beds, CS, Chiddru. 2a-d, PIMUZ 28166; 2d ×2, at H=16.6mm. From sample Chi10, *Flemingites nanus* beds, CS, Chiddru. 3a-d, PIMUZ 28167. From sample Chi52, *Flemingites planatus* beds, base of CM, Chiddru. 4a-c, PIMUZ 28168. From sample Nam532, *Xenodiscoides perplicatus* beds, CM, Nammal. All natural size unless otherwise indicated.

Plate 46


1a


1b


2a


2b


2c


4a


3a


3b


3c


3d


4b


4c


1c


2d

EXPLANATION OF PLATE 47

Figs 1-3. *Tainionautilus trachyceras* Frech, 1905. 1a-d. PIMUZ 28169. 2a-d, PIMUZ 28170. 3a-c, PIMUZ 28171. All from sample Chi10, *Flemingites nanus* beds, CS, Chiddru. All natural size.

Plate 47


1a


1b


2a


1c


1d


2b


2c


2d


3a


3b


3c

CHAPTER 6:

New Early Triassic ammonoid faunas from the Dienerian/Smithian boundary beds at the Induan/Olenekian GSSP candidate at Mud (Spiti, Northern India)

New Early Triassic ammonoid faunas from the Dienerian/Smithian boundary beds at the Induan/Olenekian GSSP candidate at Mud (Spiti, Northern India)

T. Brühwiler[1*], D. Ware[1], H. Bucher[1, 2], L. Krystyn[3] and N. Goudemand[1]

[1]Paläontologisches Institut und Museum, Universität Zürich, Karl Schmid-Strasse 4, 8006 Zürich, Switzerland.

[2] Department of Earth Sciences, ETH, Universitätsstrasse 16, 8092 Zürich, Switzerland.

[3]Institut für Paläontologie, Universität Wien, Althanstrasse 14, 1090 Wien, Austria.

[*]Corresponding author.

Key words: Early Triassic, Dienerian/Smithian boundary, Induan/Olenekian boundary, GSSP, ammonoids.

Submitted to *Journal of Asian Earth Sciences*.

Abstract: New collections at the Induan/Olenekian boundary GSSP candidate at Mud (Himachal Pradesh, Northern India) lead to the recognition of several well preserved ammonoid faunas that significantly improve the biostratigraphic resolution in the beds underyling the proposed GSSP level. In ascending order, the new biostratigraphical sequence comprises: the *Ambites lilangense* beds, the *Fuchsites markhami* beds, the *Kingites lens* beds, the *Prionolobus rotundatus* beds, the *Flemingites bhargavai* beds, the Kashmiritidae gen. nov. A beds and the *Vercherites* cf. *pulchrum* beds. The faunas from Bed 10, located about 1 m below the proposed GSSP level, contain certain ammonoids with typical early Smithian affinity (Flemingitidae, Kashmiritidae) and thus reflect the beginning of the early Smithian evolutionary radiation. Seen from an evolutionary point of view, the Dienerian/Smithian boundary can therefore be placed just below Bed 10. Ideally, the stage boundary should also be intercalibrated with other biological, chemical or physical proxies as additional tools for world-wide correlations.

Four new species (*Flemingites bhargavai*, *Kingites korni*, ?*Kingites parkashi* and *Xenodiscoides variocostatus*) and two new genera (*Mudiceras*, *Vercherites*) are described.

1. Introduction

Despite the extensive history of research on the Permian-Triassic mass extinction and its biotic recovery, stage subdivisions of the Early Triassic remains controversial. It is commonly divided into two, three or four stages as follows: two stages (Induan and Olenekian - Kiparisova and Popov, 1956), with the Induan encompassing the Griesbachian and Dienerian, and the Olenekian encompassing the Smithian and the Spathian; three stages (Griesbachian, Nammalian and Spathian - Guex, 1978); or four stages (Griesbachian, Dienerian, Smithian and Spathian - Tozer, 1965; Tozer, 1967; Silberling and Tozer, 1968).

The two-stage scheme has been authorized as the standard stage subdivision by the Triassic Subcommission of the International Stratigraphic Commission in Lausanne (Vischer, 1992). Originally, successions of the Salt Range and the Indian Himalayas were referred to as stratotype of the Induan, whereas the stratotype of the Olenekian is located in Siberia (Kiparisova and Popov, 1956). Only recently, a section near the village of Mud in the Himalayas (Himachal Pradesh, Northern India) has been selected as the best GSSP candidate for the Induan/Olenekian boundary (Krystyn et al., 2007a, b). Ammonoids from this classical Early Triassic locality have first been reported for more than a century (Diener, 1897; Krafft and Diener, 1909), and conodonts are abundant and well preserved (Krystyn et al., 2007a, b; Orchard, 2007b; Orchard and Krystyn, 2007). It has been proposed to define the Induan/Olenekian boundary at Mud with the FAD of the conodont species *Neospathodus waageni* at the base of the subbed 13A3, within the lower part of the *Flemingites* beds.

However, ammonoid faunas from the beds just underlying the proposed GSSP level were only insufficiently known. During a field trip in 2008 we thoroughly sampled these beds and discovered several new and well preserved ammonoid faunas. Here, we focus on the stratigraphic distribution and the taxonomic description of these faunas. Our data shed a new light on the definitive choice for a GSSP level for the Induan/Olenekian boundary since several elements of typical Smithian (early Olenekian) affinity were found in a relatively low stratigraphical position compared to the previously proposed GSSP. In order to analyse the detailed recovery patterns of Early Triassic marine fauna in time and space, a global biostratigraphic scheme of organisms with the highest recovery rates (i.e. ammonoids and conodonts; Brayard et al., 2006, 2009; Orchard et al., 2007a) is a prerequisite. Conodonts associated with the new ammonoid faunas are discussed in a separate paper (Goudemand et al., in prep.).

2. Geological setting

During Early Triassic times the Spiti area was located on the peri-Gondwanan margin, on the southern side of the Tethys Ocean (e.g. Smith et al., 1994) (Figure 1). The Lower Triassic sediments of the study area are represented by the Mikin Formation, which disconformably overlies the Kuling Shales of Late Permian age (Bucher et al., 1997). The Mikin Formation is subdivided into: (i) the Lower Limestone Member (LLM); (ii) the Limestone and Shale Member (LSM); and (iii) the Niti Limestone Member (Bhargava et al., 2004; Krystyn et al., 2007a) (Figure 2). The LLM is further subdivided into a lower part of Griesbachian age that consists of brown, ferruginous limestone containing *Otoceras*; and an upper part of Dienerian age that consists of grey thin-bedded limestone yielding "*Pleurogyronites*". The LSM is further subdivided into three parts: the Dienerian *Ambites* Beds (equivalent to the *Meekoceras* Beds of Krafft and Diener, 1909 and the *Gyronites* Beds of Bhargava et al., 2004) consisting of dark shales with intercalated limestone beds and nodules; the early Smithian *Flemingites* Beds, consisting of grey, slightly nodular limestone; and the middle-late Smithian *Parahedenstroemia* Beds, consisting of alternating shales and limestone beds.

3. New ammonoid data

The limestone beds and nodules underlying the proposed GSSP level were intensely sampled in order to obtain a precise and detailed ammonoid record. The detailed ammonoid stratigraphic distributions within this critical interval of rocks is given in Figure 3.

The beds 8 and 9 of Krystyn et al. (2007a, b) within the *Ambites* Beds, are in part discontinuous with large limestone nodules and lenses. Bed 8 contains the ammonoids *Ambites lilangense*, *Proptychites haydeni* and *Pleurambites* sp. indet. (sample Mud27). Bed 9 contains *Proptychites* sp. indet, *Ambites* aff. *discus*, *Fuchsites markhami*, *Clypites* sp. indet., *"Aspidites" spitiensis* and *Pseudosageceras* sp. indet. (samples Mud28 and Mud29). Small limestone nodules occurring ca. 60cm higher up section contain *Kingites lens*, *Proptychites* cf. *khoorensis* and *Pseudosageceras* sp. indet. (sample Mud30). The subsequent thin, lenticular limestone horizon contains *Prionolobus rotundatus*, *Clypites typicus*, *Kingites korni* sp. nov. and ?*Radioceras* cf. *kraffti* (samples Mud17 and Mud31).

Bed 10 of Krystyn et al. (2007a, b) at the top of the *Ambites* beds consists of pyrite-rich, yellowish-weathering grey limestone and is composed of three individual grey subbeds separated by two unfossiliferous, thin, reddish ferruginous layers. The lower subbed (samples Mud9, Mud32 and M05-10/1) contains *Flemingites bhargavai* sp. nov., *Mudiceras planissimum* gen. nov., ?*Radioceras* cf. *kraffti*, ?*Kingites parkashi* sp. nov. and Gyronitidae gen. indet. A and B. The middle subbed (samples Mud10 and Mud33) contains ?*Radioceras* cf. *kraffti*, Kashmiritidae gen. nov. A, *Xenodiscoides* sp. indet. A, *Xenodiscoides* cf. *variocostatus*, Gyronitidae gen. indet. B and *Pseudosageceras* sp. The upper subbed (samples Mud11 and Mud34) contains ?*Radioceras* cf. *kraffti*, *Xenodiscoides variocostatus, Xenodiscoides* cf. *variocostatus, Mudiceras planissimum* and *Pseudosageceras* sp.

Bed 11 of Krystyn et al. (2007b) contains very rare, poorly preserved ammonoids possibly belonging to *Vercherites*. Bed 12B contains relatively poorly preserved specimens of *Vercherites* cf. *pulchrum* and *Kashmirites nivalis*.

4. Discussion

4.1. Biostratigraphy

Based on our new sampling, the following local maximal horizons (Guex 1991) are recognized in the studied interval at Mud, in ascending order (Figure 3): (1) *Ambites lilangense*, *Pleurambites* sp. indet. and *Proptychites haydeni*; (2) *Ambites* aff. *discus* , *Proptychites* sp. indet., *Fuchsites markhami, "Aspidites" spitiensis* and *Clypites* sp. indet.; (3) *Kingites lens and Proptychites* cf. *khoorensis*; (4) *Prionolobus rotundatus*, *Clypites typicus* and *Kingites korni* sp. nov.; (5) *Flemingites bhargavai*, ?*Kingites parkashi* and Gyronitidae gen. indet. A; (6) Kashmiritidae gen. nov. A; (7) *Vercherites* cf. *pulchrum*. Horizons 1-6 are all within the "*Gyronites frequens* zone" of Krystyn et al. (2007a,b). The differentiation of these six horizons thus significantly improves the biostratigraphic resolution of this interval. Horizon 7 corresponds to the "*Meekophiceras? vercherei* Bed" of Krystyn et al. (2007a,b). Higher up section, taxa of the *Rohillites rohilla* zone appear in Bed 13A, including *Rohillites* sp. nov. 1and 2, *Rohillites rohilla*, *Kashmirites kapila*, *Vercherites* sp. nov.*, Pseudaspidites muthianus, Parakymatites discoides* and *Anahedenstroemia himalayica* (Krystyn et al. 2007a, b).

The ammonoid genera *Ambites*, *Clypites*, *Kingites*, *Prionolobus*, *Proptychites* and *Fuchsites* from the samples below Bed 10 (local maximal horizons 1-3) clearly indicate a Dienerian age (Waagen, 1895; Tozer, 1994; Brayard and Bucher, 2008; Brühwiler et al., 2008). Presently, more detailed correlations of the described faunal succession from Mud with other localities are not possible since the Dienerian ammonoid faunas of the Tethyan realm are still only imperfectly known (Brühwiler et al., 2008). The ammonoid associations from Bed 10 (local maximal horizons 4 and 5) to Bed 12 have no known exact correlatives in other published sections. However, new sampling in the Salt Range by our group have resulted in the discovery of faunas similar to those from Mud as reported here (Brühwiler et al., ongoing work; Ware et al., ongoing work). Preliminary results thus indicate that the revised ammonoid succession of Mud correlates with that of the Salt Range.

4.2. The early Smithian evolutionary radiation

The evolution of Early Triassic ammonoids is characterized by the following main features: (i) a very low diversity in the Griesbachian (early Induan), (ii) a moderate diversity increase in the Dienerian (late Induan), (iii) an explosive radiation in the early Smithian (early Olenekian), (iv) a late Smithian extinction event followed by a second explosive radiation in the early Spathian (late Olenekian) (Tozer, 1981a, b; Brayard et al., 2006, 2009). Thus, subdivision of the Early Triassic into four (sub)stages (Tozer, 1965) appears to be the most appropriate in terms of ammonoid evolution. The main weakness of the two-stages scheme (Induan-Olenekian) is that it ignores the largest intra-Triassic extinction event (i.e. the end-Smithian extinction) that profoundly affected both ammonoids and conodonts (Brayard et al., 2006; Galfetti et al., 2007b; Orchard, 2007a).

The evolutionary radiation in the early Smithian (early Olenekian) is characterized by the appearance of several new ammonoid families such as the Arctoceratidae, the Aspenitidae, the Flemingitidae, the Melagathiceratidae, the Paranannitidae or the Kashmiritidae (e.g. Brayard and Bucher, 2008). Moreover, existing Dienerian families such as the Hedenstroemiidae and the Proptychitidae exhibit a significant increase in the number of their genera. In the Mud succession, certain ammonoids with a typical Smithian affinity appear in Bed 10 (Figure 4). Among these are early representatives of Flemingitidae (*Flemingites bhargavai*) and Kashmiritidae (Kashmiritidae gen. nov. A). At the same time, several typical Dienerian taxa that are abundant below are no longer present in Bed 10 (genera *Fuchsites, Ambites*, *Clypites* and *Prionolobus*). This indicates that the early Smithian evolutionary radiation began during deposition of Bed 10 though part of its faunal composition is still of Dienerian character (?*Kingites,* Gyronitidae A-C). A fauna composed exclusively of Smithian genera appears as high as Bed 13 (genera *Rohillites, Anahedenstroemia, Pseudaspidites, Parakymatites*) but the meagre ammonoid documentation in Bed 11 and 12 (including the new genus *Vercherites*) can mask an earlier occurrence of these Smithian taxa and thus may not allow a definite decision on their first local appearance.

5. Conclusions

Based on new bedrock-controlled collections several well preserved additional ammonoid faunas have been found at the Induan-Olenekian GSSP candidate near the village of Mud (Himachal Pradesh, Himalaya, India). These new faunas greatly improve the biostratigraphic resolution of the beds underlying the previously proposed GSSP level in Bed 13. The faunas from Bed 10 of Krystyn et al. (2007a,b) contain the first ammonoids with typical early Smithian affinity and reflect the beginning of the early Smithian evolutionary radiation. Thus, as seen from an evolutionary point of view, the Dienerian/Smithian (or Induan/Olenekian) boundary could be placed above the limestone nodules (samples Mud17 and Mud31) and below Bed 10, i.e. in a 10 cm-thick interval (Figure 3). Ideally, the stage boundary should also be intercalibrated with other potential marker events such as a conodont bioevent (Zhao et al., 2007; Goudemand et al., unpublished data) or a carbon isotope excursion (Payne et al., 2004; Galfetti et al., 2007a) as additional proxies for long-distance or global correlation.

6. Systematic palaeontology

The systematic descriptions mainly follow the classification established by Tozer (1981b; 1994) and refined by Brayard and Bucher (2008). The systematics of Dienerian ammonoids is relatively poorly known and is currently being investigated by our research group. Measurements of the classical geometrical parameters of the ammonoid shell are given in the appendix. Sample numbers are reported on the measured profile (Figure 3). All illustrated material is housed at the Palaeontological Institute and Museum of the University of Zürich (PIMUZ).

Class CEPHALOPODA Cuvier, 1797
Order AMMONOIDEA Agassiz, 1847
Suborder CERATITINA Hyatt, 1884
Superfamily XENODISCACEAE Frech, 1902
Family KASHMIRITIDAE Spath, 1934
Genus *Kashmirites* Diener, 1913
Type species. - *Celtites armatus* Waagen, 1895.

Kashmiritidae gen. nov. A
(Fig. 5)

Occurrence. - Two poorly preserved specimens in Mud10.

Description. - Evolute, serpenticonic shell with slightly convex, subparallel flanks. Venter broadly rounded with rounded shoulders. Umbilicus wide with a moderately high, vertical wall and rounded shoulders. Surface more or less smooth except for low, distant ribs that fade out towards the external flanks. Suture line not preserved.

Measurements. - See appendix.

Discussion. - This ammonoid differs from *Kashmirites* by its weak ornamentation and its relatively large size. It most probably represents a new genus and a new species among Kashmiritidae. However, the poor preservation of our specimens precludes any new formal designation at the species and genus levels.

Superfamily MEEKOCERATACEAE Waagen, 1895
Family GYRONITIDAE Waagen, 1895

Genus *Prionolobus* Waagen, 1895
Type species. - *Prionolobus atavus* Waagen, 1895.

Prionolobus rotundatus Waagen, 1895

(Figs. 6-7)

1895 *Prionolobus rotundatus* Waagen, 1895, p. 310, pl. 34, figs. 1-3.

Occurrence. - Mud17, Mud31.

Description. - Moderately involute, platyconic shell with convex, converging flanks and maximal thickness below mid-flanks. Venter tabulate with angular shoulders for small specimens, shoulders becoming slightly rounded with increasing size. Umbilicus moderately deep and funnel-shaped with oblique wall and rounded shoulders. Flanks smooth or ornamented with low, distant folds, especially on small specimens. Growth lines fine, biconcave and projected. Suture line ceratitic, with rounded first and second saddle, a wide and flattened third saddle and a short auxiliary series.

Measurements. - See Figure 7; appendix.

Discussion. - Our specimens differ slightly from Waagen's type specimens by their short but quite pronounced umbilical wall and edge. However, newly collected material from the Salt Range shows that this trait can vary as a function of size, involution rate and with the state of preservation (specimen with the shell preserved or not). There is therefore no reason to consider our specimens as belonging to a different species than those of Waagen. This species differs from the type species *Prionolobus atavus* by its more involute coiling. However, the most evolute specimens are quite close to the type species, and the two species could possibly be synonyms. A detailed study of material from the type locality, the Salt Range, is in progress and should answer to this open question.

Genus *Radioceras* Waterhouse, 1996

Type species. - *Meekoceras radiosum* Waagen, 1895.

?Radioceras cf. *kraffti* (Spath, 1930)

(Figs. 8-9)

? 1909 *Meekoceras varaha* Krafft and Diener, p. 17; pl. 2, figs. 2-6.

? 1930 *Koninckites kraffti* Spath, p. 28.

? 1934 *Koninckites kraffti* Spath - Spath, p. 155, fig. 43c.

Occurrence. - Mud31-34.

Description. - Involute, platyconic shell with convex, converging flanks. Venter tabulate with angular shoulders on inner whorls, becoming slightly rounded on outer whorls. Umbilicus with a moderately high, steep and oblique wall and distinct, slightly angular shoulders. Growth lines fine, biconcave. Surface smooth. Venter ornamented with very fine strigation. Suture line ceratitic with narrow first lateral saddle, slightly tapered second saddle, broad third saddle and a long auxiliary series.

Measurements. - See Figure 9; appendix.

Discussion. - The type species *Radioceras radiosum* from the Ceratite Sandstones of the Salt Range is very similar in shape. It differs, however, by its persisting tabulate venter on outer whorls and a suture line with a slightly more individualized auxiliary series (Brühwiler et al., ongoing work). *Meekophiceras* from the early Dienerian Candidus Zone of the Arctic (Tozer, 1994) is similar but differs by its more rounded venter and its pronouced adult umbilical egression.

Gyronitidae gen. et sp. indet. A

(Fig. 10)

? 1934 *Meekoceras* aff. *falcatum* Waagen - Collignon, p. 6, pl. 7, fig. 2.

Occurrence. - Two specimens from the lower part of Bed 10 (samples Mud9, Mud32).

Description. - Platyconic shell with egressive coiling. Inner whorls involute, outer whorls moderately evolute. Flanks convex except for a slight concavity near the umbilical marging. Maximum whorl width at mid-flank. Venter tabulate with slightly rounded shoulders. Umbilicus with oblique wall and slightly rounded shoulders. Surface ornamented with low folds; growth lines slightly biconcave. Suture line ceratitic, second lateral saddle slightly tapered, auxiliary series well individualized.

Discussion. - In ornamentation, shape and suture line, this species resembles *Ambites discus* Waagen, 1895. However, it clearly differs by its distinct concavity on lower flanks and its less tabulate venter. A more comprehensive study of this taxon based on newly collected and much better preserved material from the Salt Range is under progress (Brühwiler et al., ongoing work).

Gyronitidae gen. et sp. indet. B

(Fig. 11)

Occurrence. - Two specimens from the lower and middle part of Bed 10 (samples M05-10/1, Mud10).

Description. - Platyconic shell with egressive coiling. Inner whorls involute, outer whorls moderately evolute. Flanks convex. Maximum whorl width at mid-flank. Venter tabulate with slightly rounded shoulders. Umbilicus with oblique wall and slightly rounded shoulders. Surface ornamented with low folds; growth lines slightly biconcave. Suture line ceratitic, second lateral saddle slightly tapered, auxiliary series well individualized.

Discussion. - This species is very similar to Gyronitidae gen. et sp. indet. A described above, but does not exhibit the characteristic concavity near the umbilical margin.

Gyronitidae gen. et sp. indet. C

(Fig. 12).

Occurrence. - A single specimen from Bed 10 (exact position within this bed unknown).

Description. - Small, evolute, platyconic shell with maximal thickness at mid-flanks. Flanks convex except for a weak but distinct concavity near the venter. Venter tabulate with angular shoulders. Umbilicus wide and shallow with indistinct wall and rounded shoulders. Surface smooth. Suture line simple and ceratitic with weakly indented lobes.

Discussion. - This species differs from Gyronitidae A and B by its broad, tabulate venter with angular shoulders and its more evolute coiling. In its shape this species resembles the genus *Gyronites*, which differs by its narrower venter and its deeper umbilicus with a distinct wall.

Genus *Mudiceras* gen. nov.

Derivation of name. - Genus name refers to the studied sections above Mud village.

Type species. - *Gyronites planissimus* Spath, 1934.

Composition of the genus. - Type species only.

Diagnosis. - Moderately evolute, strongly compressed Gyronitidae with tabulate venter and a wide and shallow umbilicus with low wall and rounded shoulders.

Discussion. - The type species was found in the Lower Ceratite Limestone at Chiddru (Spath, 1934). It was originally assigned to *Gyronites*, but it differs from this genus by its slender cross-section, its shallower umbilicus, its narrower venter and its suture line with less slender lobes. *Mudiceras* differs from the slightly younger *Vercherites* gen. nov. described below by its shallower umbilicus and its more compressed whorl section.

Mudiceras planissimum (Spath, 1934) gen. nov.

(Fig. 13).

1934 *Gyronites planissimus* Spath, p. 92; pl. 8, fig. 4a-b.

Occurrence. - Lower to upper part of Bed 10 (samples M05-10/1, Mud11).

Description. - Large, moderately evolute, platyconic shell with convex, converging flanks and maximal thickness below mid-flanks. Venter tabulate; shoulders sharp-edged. Umbilicus broad, with low wall and rounded shoulders. Surface probably smooth but poorly preserved. Suture line ceratitic with a rather narrow first lateral saddle and relatively deep lobes.

Measurements. - See appendix.

Genus *Vercherites* gen. nov.

Derivation of name. - Genus name derived from the name of the type species.

Type species. - *Koninckites vercherei* Waagen, 1895.

Composition of the genus. - *Vercherites vercherei* (Waagen, 1895), *V. pulchrum* (Waagen, 1895).

Diagnosis. - Large, compressed and smooth shell. Innermost whorls involute, becoming egressive much earlier than the adult stage. Venter tabulate with angular shoulders on inner whorls; shoulders become rounded on outer whorls. Umbilicus with vertical wall and shortly rounded shoulder. Suture line ceratitic with three broadly rounded saddles of which the first is the narrowest one.

Discussion. - *Vercherites* is close to *Paranorites* Waagen, 1895, which differs by its later umbilical egression, its distinctly trigonal cross-section, weakly ribbed inner whorls and its suture line, which differs in having a distinctly slim and phylloid first lateral saddle. The genus *Meekophiceras* is much more involute and shows only a late, adult umbilical opening. *Vercherites* is here provisionally included in Gyronitidae.

Vercherites cf. *pulchrum* (Waagen, 1895)

(Fig. 14)

1895 *Meekoceras pulchrum* Waagen, p. 249, pl. 27, figs. 2-3; pl. 29, fig. 1.

2007a *Meekophiceras? vercherei* (Waagen) - Krystyn et al., pl. 1, fig. 2.

2007b *Meekophiceras? vercherei* (Waagen) - Krystyn et al., pl. 1, fig. 1.

Occurrence. - Several relatively poorly preserved specimens from Bed 12B.

Description. - Large, moderately involute, platyconic shell with convex, strongly converging flanks and maximal thickness below mid-flanks. Venter tabulate with angular shoulders, becoming slightly rounded on outer whorls. Umbilicus with high vertical wall and rounded shoulders, initially narrow but opening on outer whorls. Surface smooth. Suture line ceratitic with narrow first lateral saddle and very slightly asymmetrical second saddle.

Discussion. - The relatively poor preservation of our specimens hinders a definitive specific assignment. *Vercherites pulchrum* differs from the type species by its later umbilical egression, but is otherwise very similar.

Genus *Kingites* Waagen, 1895

Type species. - *Kingites lens* Waagen, 1895.

Discussion. - This genus has been included within Proptychitidae (Tozer, 1981b, 1994), with which it shares a convergent shell shape, in particular with a rounded venter. However, *Kingites* is here assigned to Gyronitidae on the basis of its suture line, which exhibits a low and broad third lateral saddle, a diagnostic trait of this family.

Kingites korni sp. nov.

(Fig. 15)

Derivation of name. - Species named after Dr. Dieter Korn (Museum für Naturkunde, Berlin).

Holotype. - Specimen PIMUZ 27863 (Fig. 10).

Type locality and horizon. - Loc. Mud31, Spiti, Northern India; Early Triassic, Dienerian.

Occurrence. - Mud31.

Diagnosis. - *Kingites* with occluded umbilicus.

Description. - Very involute, discoconic shell with convex flanks and maximal thickness near mid-flanks. Venter rounded without distinct shoulders. Umbilicus occluded. Surface smooth except for some low folds at mid-flanks. A shallow constriction occurs at the beginning of the body chamber. The peristome is preceded by another, deeper constriction, which is more pronounced on the internal side of the outer shell. Growth lines distinct and biconcave. Suture line ceratitic, close to that of *Prionolobus rotundatus*, but with more rounded saddles and a longer auxiliary series.

Measurements. - See appendix.

Discussion. - This species is conspicuously more involute than the type species *Kingites lens*, but is very similar in all other characters.

?*Kingites parkashi* sp. nov.

(Fig. 16)

Derivation of name. - Named after Beli Parkash (Manali, India).

Holotype. - Specimen PIMUZ 27857 (Fig. 11-1).

Type locality and horizon. - Loc. Mud32, Spiti, Northern India; Early Triassic.

Occurrence. - Lower part of Bed 10 (sample Mud32).

Diagnosis. - Very involute ?*Kingites* with a narrowly rounded venter.

Description. - Very involute, oxyconic shell with convex, converging flanks and maximal thickness below mid-flanks. Venter narrowly rounded without any shoulders. Umbilicus occluded. Surface smooth, growth lines fine and biconcave. Suture line ceratitic with broad, deeply indented lobes. First lateral saddle~~s~~ rather narrow, second saddle long, slightly tapered and slightly turned towards umbilicus, third lateral saddle broad and low. Auxiliary series short.

Measurements. - See appendix.

Discussion. - This species differs from the type species of *Kingites* and from *K. korni* sp. nov. described above by its narrower venter. In shape, this species converges with the considerably younger *Clypeoceras superbum* (Waagen, 1895) from the Ceratite Sandstone of the Salt Range, the latter being distinguished by a much longer, well individualized auxiliary series of the suture line.

Genus *Xenodiscoides* Spath, 1930

Type species. - *Xenodiscus perplicatus* Noetling, 1905.

Discussion. - *Xenodiscoides* is here provisionally included in Gyronitidae. However, it shows also affinities with Flemingitidae. It could therefore represent a transitive form between these two families.

Xenodiscoides variocostatus sp. nov.

(Fig. 17)

Derivation of name. - Refers to the variocostate ribbing.

Holotype. - Specimen PIMUZ 27867 (Fig. 16-1).

Type locality and horizon. - Loc. Mud11, Spiti, Northern India; Early Triassic.

Occurrence. - Upper part of Bed 10 (samples Mud11, Mud34).

Diagnosis. - *Xenodiscoides* with relatively high whorls and variocostate ribbing.

Description. - Moderately evolute, platyconic shell with convex, converging flanks and maximal thickness below mid-flanks. Venter tabulate with slightly rounded shoulders. Umbilicus with moderately high, vertical wall and rounded shoulders. Ornamentation consists of strong, distant ribs on inner whorls, becoming weaker on outer whorls. No indication of strigation preserved. Growth lines slightly biconcave. Suture line simple, poorly preserved.

Measurements. - See appendix.

Discussion. - This species differs from the type species by its higher whorls, its variocostate ribbing and larger size. *X. calnani* Tozer, 1994 differs by its rounded ventral shoulders.

Xenodiscoides cf. *variocostatus*

(Fig. 18)

Occurrence. - Mud10.

Description. - Evolute, platyconic shell with convex, converging flanks and maximal thickness below mid-flanks. Venter tabulate with only slightly rounded shoulders on inner whorls, getting well rounded on outer whorls. Umbilicus wide with high vertical wall and rounded shoulders. Surface smooth except for few faint and distant spiral lines on flanks. Growth lines not preserved. Suture line ceratitic, poorly preserved.

Discussion. - These specimens are very similar to *Xenodiscoides variocostatus* sp. nov., from which they differ only by their smoother flanks. Due to the small amount of material in our collection, it can not be decided whether they represent smooth variants of a single species. On the other hand, *X.* cf. *variocostatus* is similar to *Vercherites* and *Paranorites* and may represent an ancestor of these genera.

Xenodiscoides sp. indet. A

(Fig. 19)

Occurrence. - Middle part of Bed 10 (sample Mud33).

Description. - Moderately involute, platyconic shell with convex, converging flanks and maximal thickness below mid-flanks. Venter tabulate with angular shoulders. Umbilicus with moderately high, vertical wall and subangular shoulders. Ornamentation consists of radial folds on inner flanks, fading towards venter. Suture line ceratitic and simple.

Measurements. - See appendix.

Discussion. - Our single specimen closely ressembles *Xenodiscoides perplicatus* var. *involuta* (Noetling, 1905), but its rather poor preservation precludes any determination at the species level.

Family FLEMINGITIDAE Hyatt, 1900

Genus *Flemingites* Waagen, 1895

Type species. - *Flemingites flemingianus* Waagen, 1895

Flemingites bhargavai sp. nov.

(Fig. 20)

Derivation of name. - Named for O. N. Bhargava (Haryana, India).

Holotype. - Specimen PIMUZ 27865 (Fig. 14).

Type locality and horizon. - Loc. Mud32, Spiti, Northern India; Early Triassic.

Occurrence. - Lower part of Bed 10 (sample Mud32).

Diagnosis. – Small evolute *Flemingites* with parallel flanks, a relatively broad, subtabulate venter, widely spaced ribs and fine strigation.

Description. - Evolute, platyconic shell with convex flanks and maximal thickness near mid-flanks. Venter tabulate with subangular shoulders. Umbilicus wide and shallow, with low, vertical wall and rounded shoulders. Flanks ornamented with distant, broad and low ribs. Fine strigation and reticulation on venter and flanks of shell and internal mold. Suture line ceratitic with relatively deep first lateral lobe.

Measurements. - See appendix.

Discussion. - *Flemingites bhargavai* differs from other species of *Flemingites* by its small size, its more evolute coiling and subtabulate venter. It represents the oldest known representative of this genus. The more typical, large *Flemingites* of the *flemingianus* group appear in Bed 14 in Mud. *Rohillites rohilla* (Diener, 1897) differs by its more involute coiling, its convergent flanks and its narrowly tabulate venter.

Superfamily SAGECERATACEAE Hyatt, 1884

Family HEDENSTROEMIIDAE Hyatt, 1884

Genus *Clypites* Waagen, 1895

Type species. - *Clypites typicus* Waagen, 1895

Clypites typicus Waagen, 1895

(Fig. 21)

1895 *Clypites typicus* Waagen, 1895, p. 143, pl. 21, fig. 7a-b.

Occurrence. - A single specimen from sample Mud17.

Description. - Very involute, oxyconic shell with convex, convergent flanks and maximum whorl width above mid-flanks. Venter very narrow and sulcate with angular shoulders. Umbilicus occluded, possibly opening on the body chamber. Surface smooth except for fine biconcave growth lines. Suture line characteristic, complex and slightly bent adapically, with a small, rounded adventive saddle, a bifid first lateral lobe followed by a larger, strongly denticulated lobe and an arched series of lobes which become smaller and less indented toward the umbilicus. The three first saddles are long and rounded, the second one is slightly bent toward the umbilicus, the fourth one is flattened and followed by a series of at least four small, narrow and rounded saddles, the second one of these divided by a small denticule.

Measurements. - See appendix.

Discussion. - Waagen (1895) recognised three different species within this genus, but it cannot be excluded that they are all variants of a single species. Our specimen has a suture line which is slightly different from those of Waagen, but as we have a single specimen only, we cannot evaluate the intraspecific variability of this character and thus prefer to assign it to the type species.

ACKNOWLEDGEMENTS

O. N. Bhargava (Haryana, India) and T. Galfetti (Zürich) are acknowledged for their help in the field. Photographs of ammonoids were taken by R. Roth (Zürich). This study was supported by the Swiss National Foundation (project n° 200020-113554; to H.B.). Earlier field work of LK was sponsored by the Austrian Academy of Sciences, National Committee for IGCP, within project 467 (Triassic Time).

REFERENCES

Bhargava, O.N., Krystyn, L., Balini, M., Lein, R., Nicora, A., 2004. Revised litho- and sequence stratigraphy of the Spiti Triassic. Albertiana 30, 21-39.

Brayard, A., Bucher, H., 2008. Smithian (Early Triassic) ammonoid faunas from northwestern Guangxi (South China): taxonomy and biochronology. Fossils and Strata 55, 1-179.

Brayard, A., Bucher, H., Escarguel, G., Fluteau, F., Bourquin, S., Galfetti, T., 2006. The Early Triassic ammonoid recovery: Paleoclimatic significance of diversity gradients. Palaeogeography, Palaeoclimatology, Palaeoecology 239, 374-395.

Brayard, A., Escarguel, G., Bucher, H., Monnet, C., Brühwiler, T., Goudemand, N., Galfetti, T., Guex, J., 2009. Good Genes and Good Luck: Ammonoid Diversity and the End-Permian Mass Extinction. Science 325, 1118-1121.

Brühwiler, T., Brayard, A., Bucher, H., Guodun, K., 2008. Griesbachian and Dienerian (Early Triassic) ammonoid faunas from northwestern Guangxi and southern Guizhou (South China). Palaeontology 51, 1151-1180.

Bucher, H., Nassichuk, W.W., Spinosa, C., 1997. A new occurrence of the upper Permian ammonoid *Stacheoceras trimurti* Diener from the Himalayas; Himachal Pradesh, India. Eclogae Geologicae Helvetiae 90, 599-604.

Collignon, M., 1934. Paléontologie de Madagascar XX - Les céphalopodes du Trias inférieur. Annales de Paléontologie 12-13, 151-162 & 1-43.

Diener, C., 1897. The Cephalopoda of the Lower Trias. Palaeontologia Indica, ser. 15, Himalayan Fossils 2, 1-181.

Diener, C., 1913. Triassic faunae of Kashmir. Palaeontologia Indica, n. ser. 5, 1-133.

Frech, F., 1902. Lethaea Geognostica, I. Lethaea Palaeozoica, v. 2 (4), Die Dyas (Schluss). 579-788.

Galfetti, T., Bucher, H., Ovtcharova, M., Schaltegger, U., Brayard, A., Brühwiler, T., Goudemand, N., Weissert, H., Hochuli, P.A., Cordey, F., Guodun, K.A., 2007a. Timing of the Early Triassic carbon cycle perturbations inferred from new U-Pb ages and ammonoid biochronozones. Earth and Planetary Science Letters 258, 593-604.

Galfetti, T., Hochuli, P.A., Brayard, A., Bucher, H., Weissert, H., Vigran, J.O., 2007b. Smithian-Spathian boundary event: Evidence for global climatic change in the wake of the end-Permian biotic crisis. Geology 35, 291-294.

Guex, J., 1978. Le Trias inférieur des Salt Ranges, Pakistan: problèmes biochronologiques. Eclogae Geologicae Helvetiae 71, 105-141.

Guex, J. 1991. Biochronological Correlations. Springer Verlag, Berlin.

Hyatt, 1884. Genera of fossil cephalopods. Proceedings of the Boston Society of Natural History 22, 253-338.

Hyatt, A., 1900. Cephalopoda. In: K.A.v. Zittel (Editor), Textbook of palaeontology, vol. 1, 1st English ed. Eastman, C. R. London.

Kiparisova, L.D., Popov, Y.D., 1956. Subdivision of the lower series of the Triassic System into stages. Doklady Akad. Nauk SSSR 109, 842-845.

Krafft, A.v., Diener, C., 1909. Lower Triassic cephalopoda from Spiti, Malla Johar, and Byans. Palaeontologia Indica, ser. 15, 6, 1-186.

Krystyn, L., Bhargava, O.N., Richoz, S., 2007a. A candidate GSSP for the base of the Olenekian Stage: Mud at Pin Valley; district Lahul and Spiti, Himachal Pradesh (Western Himalaya), India. Albertiana 35, 5-29.

Krystyn, L., Richoz, S., Bhargava, O.N., 2007b. The Induan-Olenekian Boundary (IOB) in Mud – an update of the candidate GSSP section M04. Albertiana 36, 33-45.

Noetling, F., 1905. Die asiatische Trias. In: F. Frech (Editor), Lethaea geognostica: Handbuch der Erdgeschichte mit Abbildungen der für die Formationen bezeichnendsten Versteinerungen. Schweizerbart, Stuttgart, pp. 107-221.

Orchard, M.J., 2007a. Conodont diversity and evolution through the latest Permian and Early Triassic upheavals. Palaeogeography, Palaeoclimatology, Palaeoecology 252, 93-117.

Orchard, M.J., 2007b. Report on 2007 conodont collections from Mud, Spiti. Albertiana 36, 46-49.

Orchard, M.J., Krystyn, L., 2007. Conodonts from the Induan-Olenekian boundary interval at Mud, Spiti. Albertiana 35, 30-34.

Payne, J.L., Lehrmann, D.J., Wei, J., Orchard, M.J., Schrag, D.P., Knoll, A.H., 2004. Large Perturbations of the Carbon Cycle During Recovery from the End-Permian Extinction. Science 305, 506-509.

Silberling, N.J., Tozer, E.T. 1968: Biostratigraphic classification of the marine Triassic in North America. Special Paper - Geological Society of America, 110. Geological Society of America (GSA), Boulder, CO, United States, 63 pp.

Smith, A.G., Smith, D.G., Funnell, B.M. 1994: Atlas of Mesozoic and Cenozoic Coastlines. Cambridge University Press, Cambridge.

Smith, J.P., 1913. Ammonoidea. In: K.A. Zittel (Editor), Textbook of palaeontology, 2nd English edition. Eastman, London, pp. 617-677.

Spath, 1930. The Eotriassic invertebrate fauna of East Greenland. Meddelelser om Gronland 83.

Spath, L.F. 1934: Part 4: The ammonoidea of the Trias, Catalogue of the fossil cephalopoda in the British Museum (Natural History). The Trustees of the British Museum, London, 521 pp.

Tozer, E.T., 1965. Lower Triassic stages and ammonoid zones of Arctic Canada. Geologic Survey of Canada Paper 65-12, 14 pp.

Tozer, E.T., 1967. A standard for Triassic time. Geologic Survey of Canada Bulletin 156, 141 pp.

Tozer, E.T., 1981a. Triassic ammonoidea: geographic and stratigraphic distribution. In: M.R. House, Senior, J.R. (Editor), The Ammonoidea. The Systematics association, London, pp. 397–431.

Tozer, E.T., 1981b. Triassic Ammonoidea; classification, evolution and relationship with Permian and Jurassic forms. In: M.R. House and J.R. Senior (Editors), The Ammonoidea; the evolution, classification, mode of life and geological usefulness of a major fossil group. Systematics Association Special Volume. Academic Press [for the] Systematics Association, London-New York, International, pp. 65-100.

Tozer, E.T. 1994: Canadian Triassic ammonoid faunas. Bulletin - Geological Survey of Canada. Geological Survey of Canada, Ottawa, ON, Canada, 663 pp.

Visscher, H., 1992. The new STS Triassic stage nomenclature. Albertiana 10, 1.

Waagen, W., 1895. Salt-Range fossils. Vol 2: Fossils from the Ceratite Formation. Palaeontologia Indica 13, 1-323.

Waterhouse, J.B., 1996. The Early and Middle Triassic ammonoid succession of the Himalayas in western and central Nepal. Part 2, systematic studies of the early Middle Scythian. Palaeontographica Abt. A 241, 27-100.

Zhao, L., Orchard, M.J., Tong, J., Sun, Z., Zuo, J., Zhang, S., Yun, A., 2007. Lower Triassic conodont sequence in Chaohu, Anhui Province, China and its global correlation. Palaeogeography, Palaeoclimatology, Palaeoecology 252, 24-38.

APPENDIX

Measurements of the classic geometrical parameters of the ammonoid shell

Diameter (D), whorl height (H), whorl width (W) and umbilical diameter (U).

Species	Specimen	D [mm]	H [mm]	W [mm]	U [mm]	Sample
Kashmiritidae gen. nov. A	PIMUZ 27800	74.3	24.4	-	32.5	Mud10
Kashmiritidae gen. nov. A	PIMUZ 27801	89.2	27.6	21	43.5	Mud10
Prionolobus rotundatus Waagen, 1895	PIMUZ 27802	44.3	21.5	10.5	9.8	Mud17
Prionolobus rotundatus Waagen, 1895	PIMUZ 27803	38.4	18.4	10	7.4	Mud17
Prionolobus rotundatus Waagen, 1895	PIMUZ 27804	62.7	29.8	14.7	14.3	Mud31
Prionolobus rotundatus Waagen, 1895	PIMUZ 27805	54.5	26.6	12.6	9.1	Mud31
Prionolobus rotundatus Waagen, 1895	PIMUZ 27806	36.9	16	9.2	9.6	Mud31
Prionolobus rotundatus Waagen, 1895	PIMUZ 27807	26.3	11.4	6.7	7.4	Mud31
Prionolobus rotundatus Waagen, 1895	PIMUZ 27808	52.4	23.3	12.8	11.1	Mud31
Prionolobus rotundatus Waagen, 1895	PIMUZ 27809	41.8	21	14.2	8.1	Mud31
Prionolobus rotundatus Waagen, 1895	PIMUZ 27810	39.4	17.4	9.3	8.1	Mud31
Prionolobus rotundatus Waagen, 1895	PIMUZ 27811	34	14.3	8.8	9.7	Mud31
Prionolobus rotundatus Waagen, 1895	PIMUZ 27812	25.2	10.2	6	7.4	Mud31
?*Radioceras* cf. *kraffti* Spath, 1930	PIMUZ 27813	57	29.2	12.8	7	Mud33
?*Radioceras* cf. *kraffti* Spath, 1930	PIMUZ 27814	29.3	15.7	7.2	3.7	Mud33
?*Radioceras* cf. *kraffti* Spath, 1930	PIMUZ 27815	30.7	17.5	7.8	3.1	Mud33
?*Radioceras* cf. *kraffti* Spath, 1930	PIMUZ 27816	37.4	18.6	9	6.9	Mud33
?*Radioceras* cf. *kraffti* Spath, 1930	PIMUZ 27817	38.6	20.3	-	5.7	Mud33
?*Radioceras* cf. *kraffti* Spath, 1930	PIMUZ 27818	43.9	22.3	12	8.3	Mud33
?*Radioceras* cf. *kraffti* Spath, 1930	PIMUZ 27819	30.5	17	7.5	3.3	Mud33
?*Radioceras* cf. *kraffti* Spath, 1930	PIMUZ 27820	33.8	19.2	7.8	3.3	Mud33
?*Radioceras* cf. *kraffti* Spath, 1930	PIMUZ 27821	44.5	24.3	-	4.5	Mud33
?*Radioceras* cf. *kraffti* Spath, 1930	PIMUZ 27822	60.6	29.2	12.8	11.6	Mud33
?*Radioceras* cf. *kraffti* Spath, 1930	PIMUZ 27823	71.7	38.5	-	7.7	Mud33
?*Radioceras* cf. *kraffti* Spath, 1930	PIMUZ 27824	9.7	5.2	2.8	1.6	Mud33
?*Radioceras* cf. *kraffti* Spath, 1930	PIMUZ 27825	72.7	38	-	10.5	Mud32
?*Radioceras* cf. *kraffti* Spath, 1930	PIMUZ 27826	35.7	17.2	-	6.1	Mud32
?*Radioceras* cf. *kraffti* Spath, 1930	PIMUZ 27827	33.4	18	7.5	3.9	Mud32
?*Radioceras* cf. *kraffti* Spath, 1930	PIMUZ 27828	33.8	18.3	8	4	Mud32
?*Radioceras* cf. *kraffti* Spath, 1930	PIMUZ 27829	66.3	34.2	-	9.6	Mud32
?*Radioceras* cf. *kraffti* Spath, 1930	PIMUZ 27830	62.5	33.2	14.5	9	Mud32
?*Radioceras* cf. *kraffti* Spath, 1930	PIMUZ 27831	59.4	33.8	14	5.8	Mud32
?*Radioceras* cf. *kraffti* Spath, 1930	PIMUZ 27832	63.4	35.5	-	6.5	Mud32
?*Radioceras* cf. *kraffti* Spath, 1930	PIMUZ 27833	57.9	26.4	-	9.8	Mud32
?*Radioceras* cf. *kraffti* Spath, 1930	PIMUZ 27834	64.3	33.9	14.4	9.3	Mud32
?*Radioceras* cf. *kraffti* Spath, 1930	PIMUZ 27835	50.9	26.4	11.2	7.3	Mud32
?*Radioceras* cf. *kraffti* Spath, 1930	PIMUZ 27836	61.3	33.1	14.4	7.8	Mud32
?*Radioceras* cf. *kraffti* Spath, 1930	PIMUZ 27837	62.4	32.9	-	9.2	Mud32
?*Radioceras* cf. *kraffti* Spath, 1930	PIMUZ 27838	59.6	33.3	15.1	5.9	Mud32
?*Radioceras* cf. *kraffti* Spath, 1930	PIMUZ 27839	75.8	40.5	-	10.2	Mud32
?*Radioceras* cf. *kraffti* Spath, 1930	PIMUZ 27840	69.4	35.5	-	10.2	Mud32
?*Radioceras* cf. *kraffti* Spath, 1930	PIMUZ 27841	45.3	23.5	11.4	6.9	Mud32
?*Radioceras* cf. *kraffti* Spath, 1930	PIMUZ 27842	50.7	25.2	-	7.9	Mud32
?*Radioceras* cf. *kraffti* Spath, 1930	PIMUZ 27843	41.5	21.3	10	6.5	Mud32
?*Radioceras* cf. *kraffti* Spath, 1930	PIMUZ 27844	42.4	22	-	5.5	Mud32
?*Radioceras* cf. *kraffti* Spath, 1930	PIMUZ 27845	41.6	23.3	9.6	2.9	Mud32
?*Radioceras* cf. *kraffti* Spath, 1930	PIMUZ 27846	33.3	18.6	7.7	3.8	Mud32
?*Radioceras* cf. *kraffti* Spath, 1930	PIMUZ 27847	41.3	21.7	9.5	5.3	Mud32
?*Radioceras* cf. *kraffti* Spath, 1930	PIMUZ 27848	37.5	18.6	7.5	6.6	Mud32
?*Radioceras* cf. *kraffti* Spath, 1930	PIMUZ 27849	37.8	20.6	-	4.4	Mud32
?*Radioceras* cf. *kraffti* Spath, 1930	PIMUZ 27850	31.7	17.1	7.1	4.2	Mud32
?*Radioceras* cf. *kraffti* Spath, 1930	PIMUZ 27851	23.8	13.2	-	3.4	Mud32
?*Radioceras* cf. *kraffti* Spath, 1930	PIMUZ 27852	32.5	17.8	7.9	3.8	Mud32
?*Radioceras* cf. *kraffti* Spath, 1930	PIMUZ 27853	30.7	16.1	-	4.1	Mud32
?*Radioceras* cf. *kraffti* Spath, 1930	PIMUZ 27854	15	8.1	3.9	3.2	Mud32
?*Radioceras* cf. *kraffti* Spath, 1930	PIMUZ 27855	8.9	4.3	3	1.9	Mud32
?*Kingites parkashi* sp. nov.	PIMUZ 27856	45.8	28.4	11	0	Mud32
?*Kingites parkashi* sp. nov.	PIMUZ 27857	88	53.2	28.6	0	Mud32
?*Kingites parkashi* sp. nov.	PIMUZ 27858	25.7	17.1	6.6	0	Mud32
Xenodiscoides cf. *variocostatus*	PIMUZ 27859	78.4	28.8	14.9	29.5	Mud10
Xenodiscoides cf. *variocostatus*	PIMUZ 27860	83.2	30.3	15.9	32.3	Mud34
Xenodiscoides cf. *variocostatus*	PIMUZ 27861	18.1	7.1	3.9	6.4	Mud33
Xenodiscoides cf. *variocostatus*	PIMUZ 27862	27.6	11.2	5.5	8.6	Mud10
Kingites korni sp. nov.	PIMUZ 27863	58.3	35.1	15.3	0	Mud31
Kingites korni sp. nov.	PIMUZ 27864	32.9	20.6	7.7	0	Mud31
Flemingites bhargavai sp. nov.	PIMUZ 27865	40	14	-	16.8	Mud32
Xenodiscoides variocostatus sp. nov.	PIMUZ 27866	69.6	27.3	15.2	24.6	Mud34
Xenodiscoides variocostatus sp. nov.	PIMUZ 27867	88.8	32.8	-	32.5	Mud11
Xenodiscoides variocostatus sp. nov.	PIMUZ 27868	63.7	24.4	-	23.1	Mud11
Xenodiscoides sp. indet. A	PIMUZ 27869	23.5	11.2	-	5.8	Mud33
Clypites typicus Waagen, 1895	PIMUZ 27870	51.2	29.5	12.1	0	Mud17
Gyronitidae gen. et sp. indet. A	PIMUZ 27871	34.1	13.6	7	10.1	Mud9

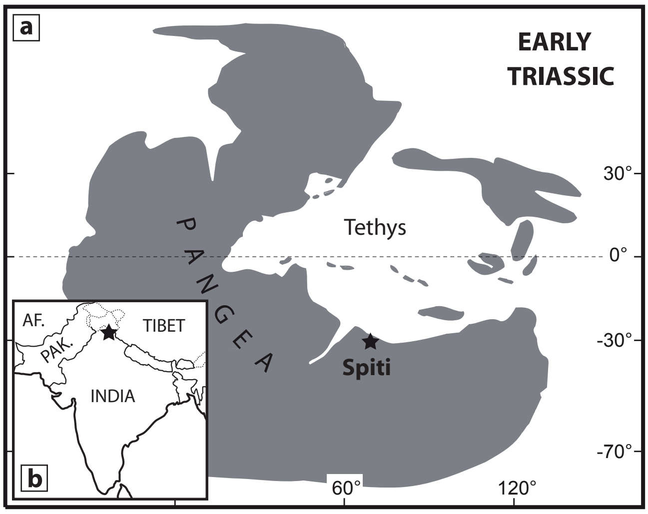

Fig. 1. (a) Simplified Early Triassic palaeogeography (modified after Brayard et al., 2006) and position of the Northern Indian Margin (NIM). (b) Present-day location of the Induan/Olenekian GSSP candidate Mud, in Himachal Pradesh, Northern India (see Krystyn et al. 2007a for a detailed description).

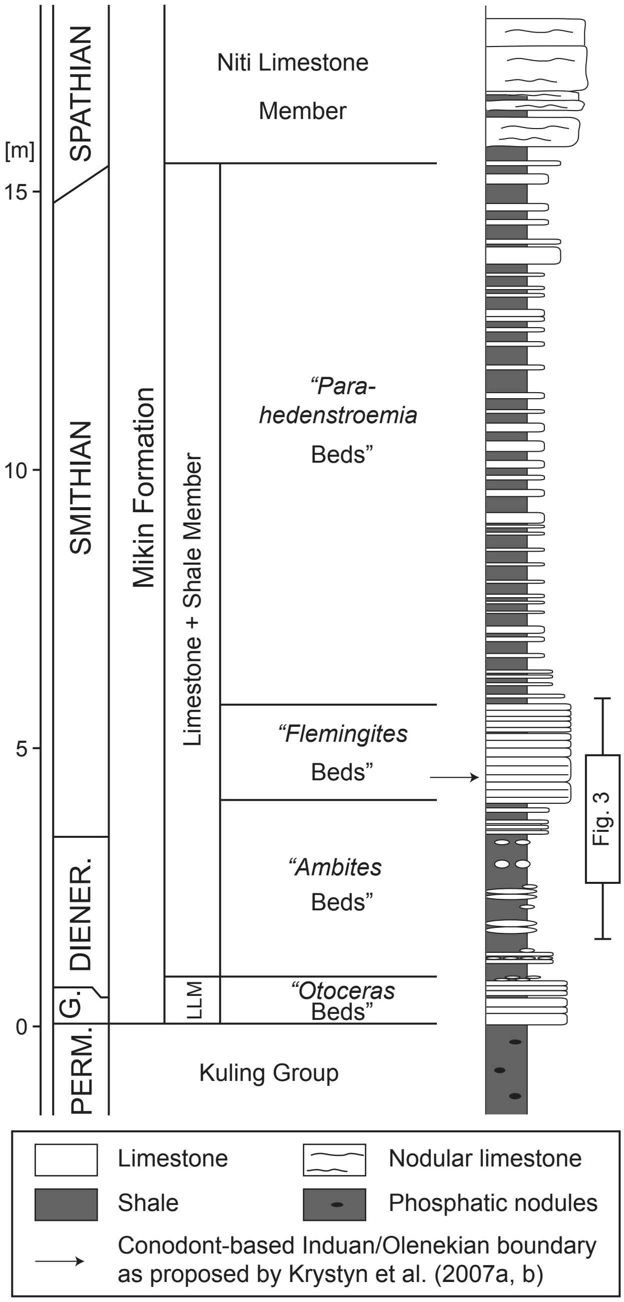

Fig. 2. Stratigraphic section of the Lower Triassic at Mud with indication of the detailed section in Fig. 3 (modified after Bhargava et al., 2004). PERM.= Permian; G.= Griesbachian; DIENER.= Dienerian; L.L.M.= Lower Limestone Member. The "*Ambites* beds" correspond to the "*Gyronites* beds" of Krystyn et al. (2007a, b) and to the "*Meekoceras* beds" of Krafft and Diener (1909); these beds need to be renamed here because they do not yield *Gyronites* nor *Meekoceras* but do contain abundant representatives of *Ambites*.

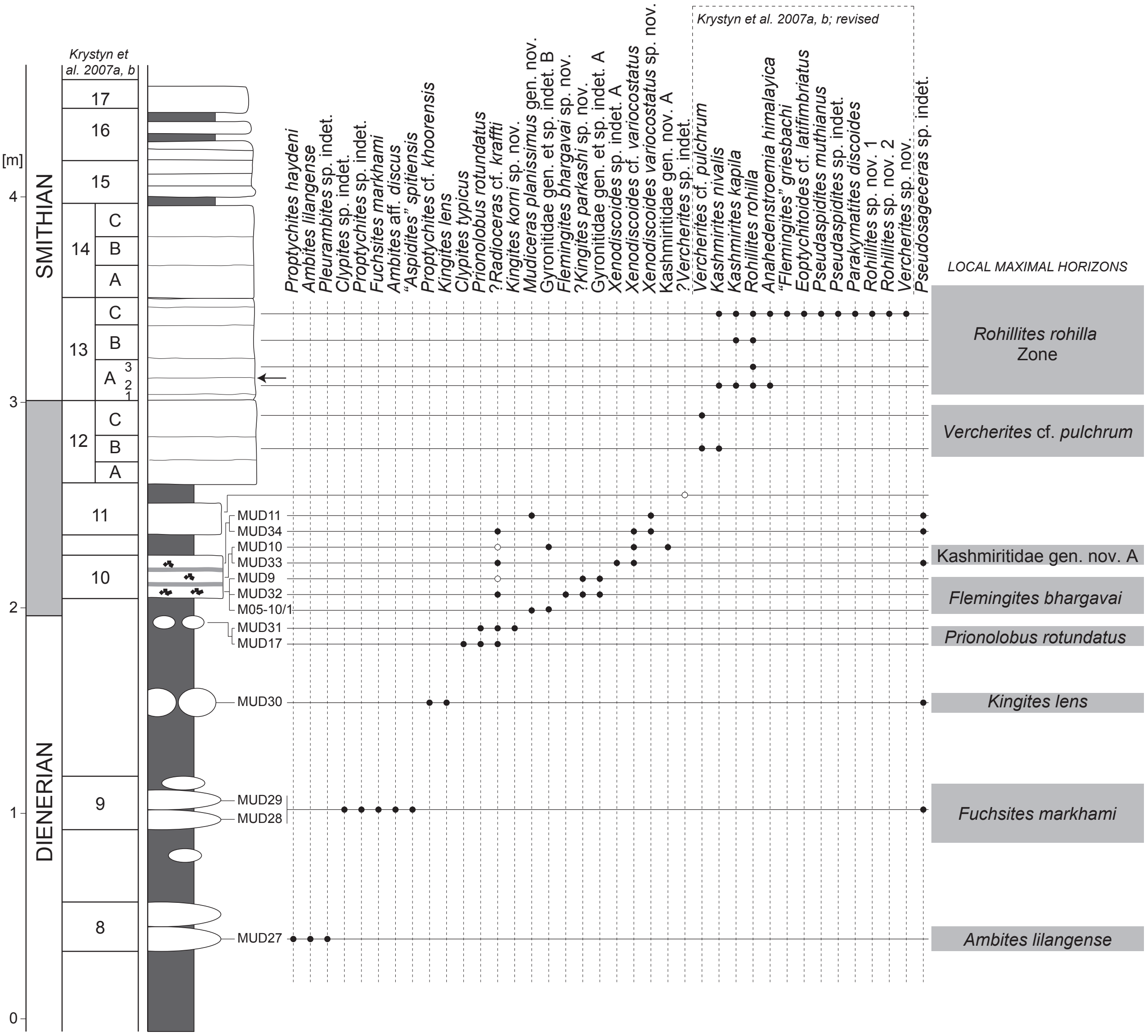

Fig. 3. Detailed stratigraphic section of the Dienerian/Smithian boundary at Mud with the distribution of ammonoid taxa and indicated local maximal horizons. Open circles indicate occurrences based on fragmentary or poorly preserved material. The arrow indicates the position of the Induan/Olenekian boundary GSSP as proposed by Krystyn et al. (2007a,b).

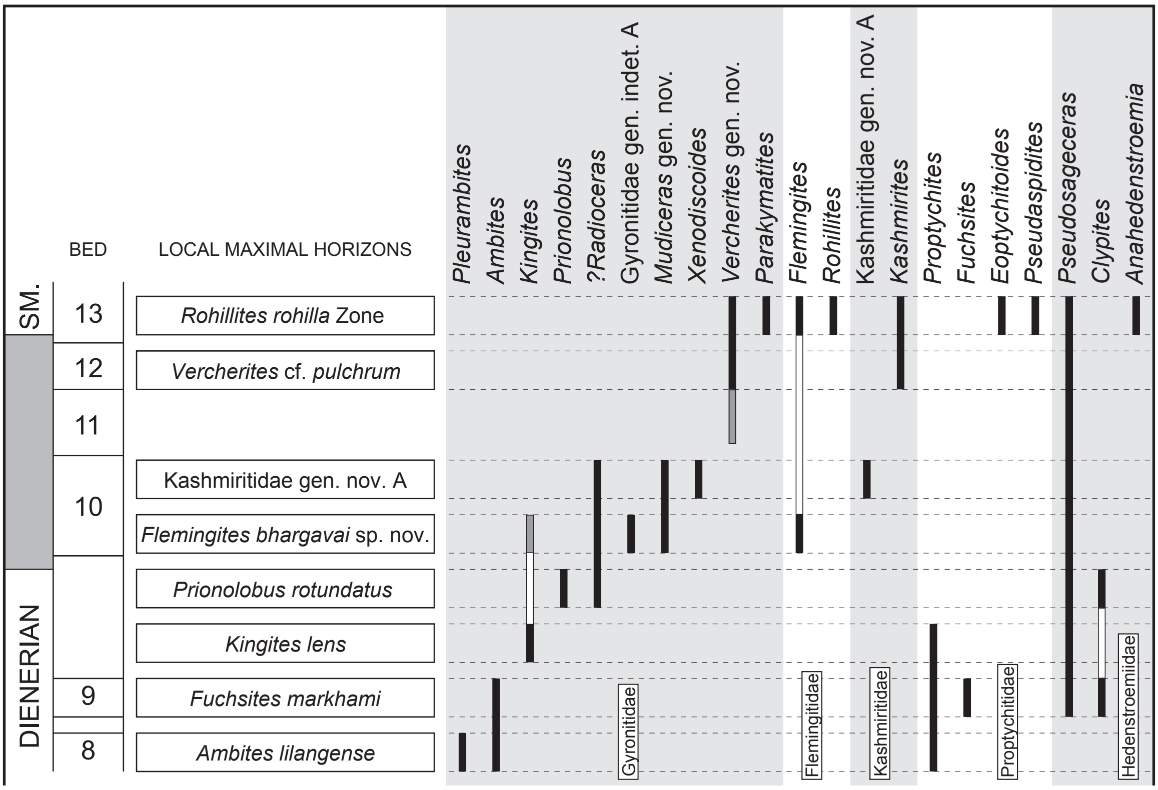

Fig. 4. Late Dienerian to early Smithian ranges of ammonoid genera in Mud with ammonoid-based boundary interval in grey. Observed occurrences in black, questionable occurrences in grey, virtual occurrences in white. Note poor faunal record in Beds 11 and 12. New ammonoid occurrences question the previous position of the proposed base of the Smithian in Bed 13A. The earlier evolutionary radiation of Flemingitidae and Kashmiritidae, which are diagnostic families of the Smithian, promote the lowering down of the base of the Smithian between the *F. bhargavai* sp. nov. and the *Priomolobus rotondatus* maximal horizons.

Fig. 5. Kashmiritidae gen. nov. A. (1) PIMUZ 27801, Loc. Mud10. (2) PIMUZ 27800, Loc. Mud10. Scale bar: 1cm.

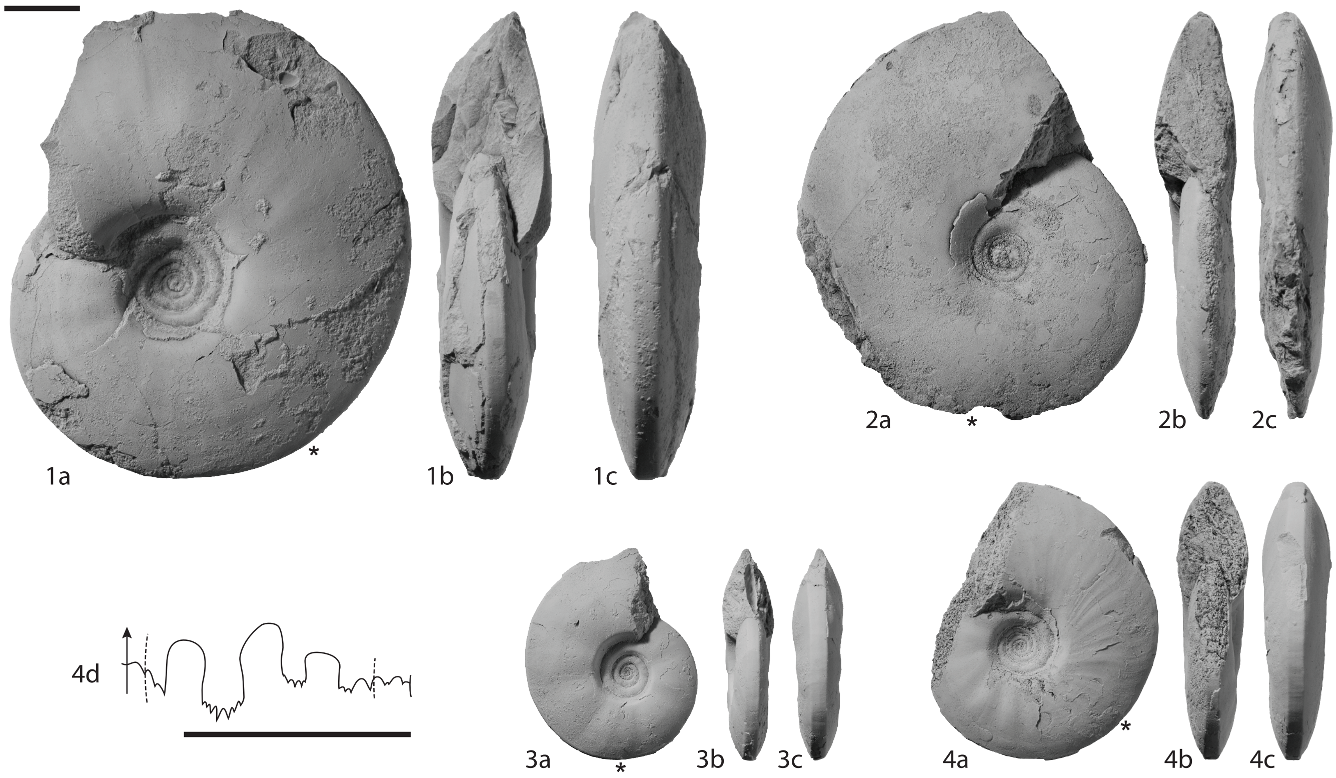

Fig. 6. *Prionolobus rotundatus* Waagen, 1895. (1) PIMUZ 27804, Loc. Mud31. (2) PIMUZ 27805, Loc. Mud31. (3) PIMUZ 27807, Loc. Mud31. (4) PIMUZ 27806; 4d at H = 12.5mm, D = 27.5mm, Loc. Mud31. Scale bars: 1cm. Asterisks indicate phragmocone end where known.

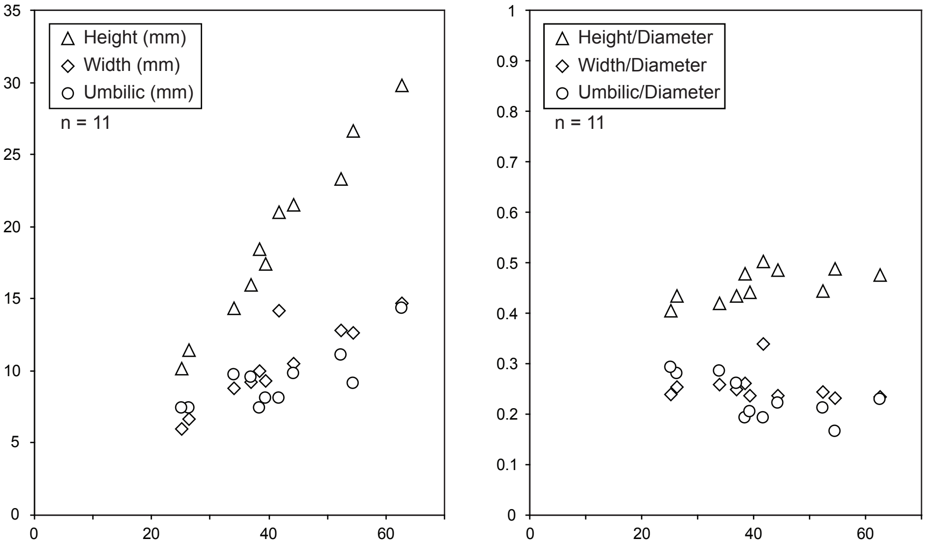

Fig. 7. Scatter diagrams of H, W, and U (left), and of H/D, W/D, and U/D (right) for *Prionolobus rotundatus* Waagen, 1895 from samples Mud17 and Mud31. Abbreviations: D, diameter; H, whorl height; U, umbilical diameter; W, whorl width.

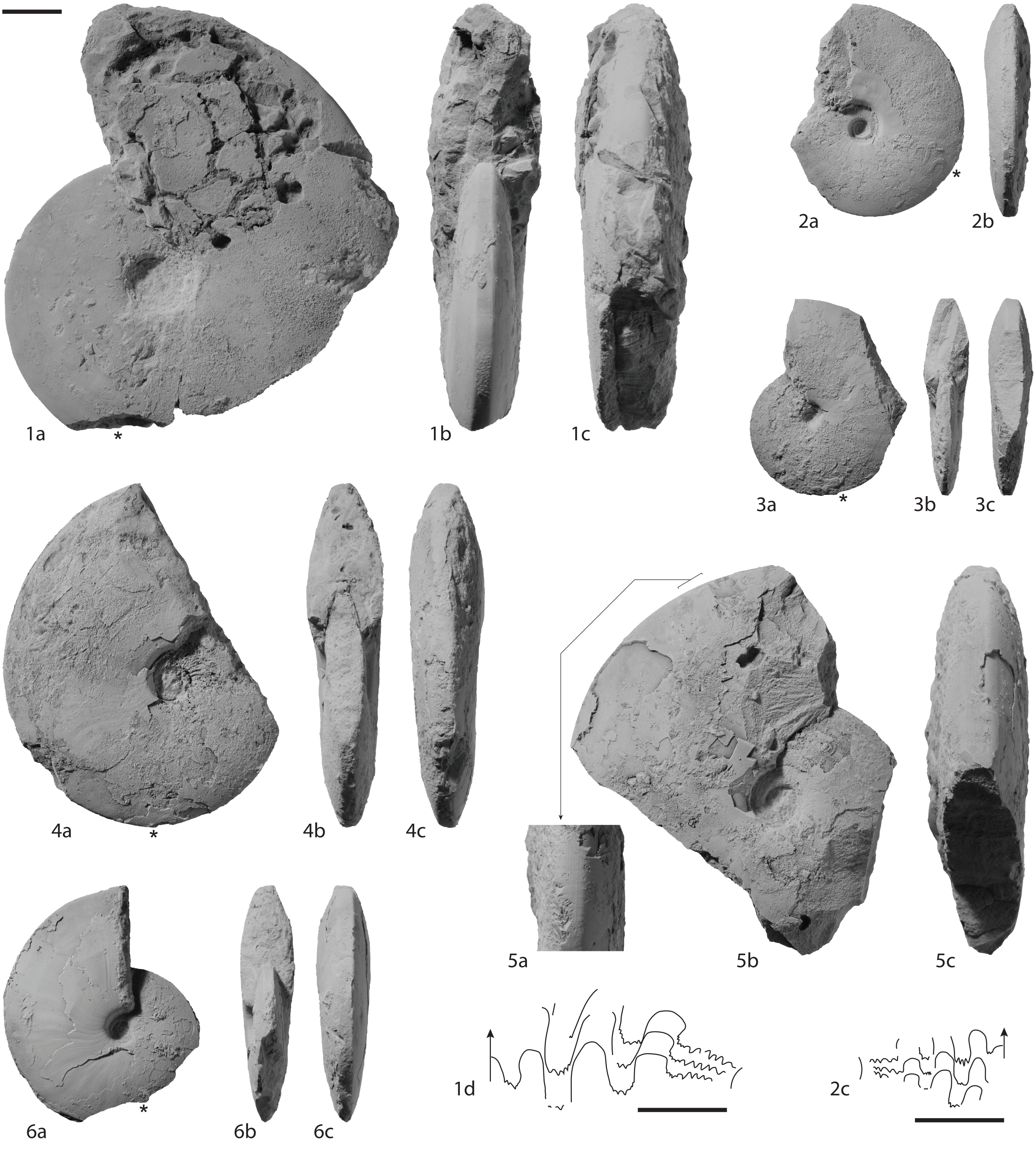

Fig. 8. ?*Radioceras* cf. *kraffti* (Spath, 1930). (1) PIMUZ 27825; 1d at H = 24mm, Loc. Mud32. (2) PIMUZ 27826; 2c at H = 14.5mm, Loc. Mud32. (3) PIMUZ 27827, Loc. Mud32. (4) PIMUZ 27813, Loc. Mud33. (5) PIMUZ 27829, Loc. Mud32. (6) PIMUZ 27828, Loc. Mud32. Scale bars: 1cm.

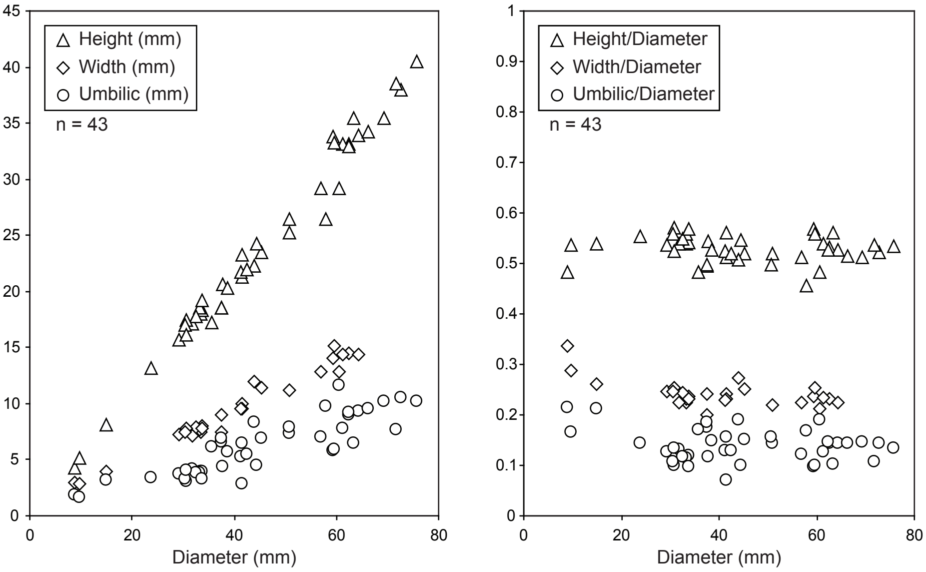

Fig. 9. Scatter diagrams of H, W, and U (left), and of H/D, W/D, and U/D (right) for *Radioceras* cf. *kraffti* (Spath, 1930) from Bed 10. Abbreviations: D, diameter; H, whorl height; U, umbilical diameter; W, whorl width.

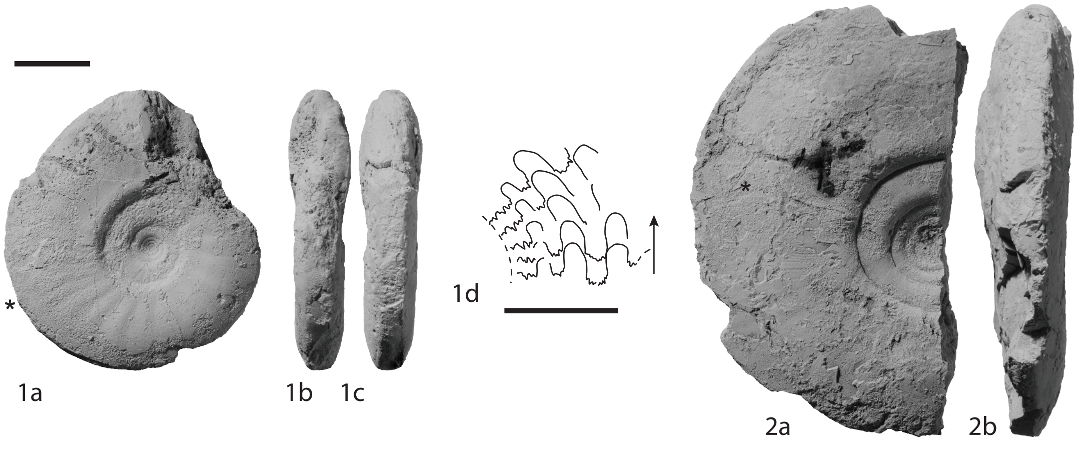

Fig. 10. Gyronitidae gen. et sp. indet. A. (1) PIMUZ 27871; 2d at H = 12.5mm, Loc. Mud9. (2) PIMUZ 27872, Loc. Mud32. Scale bars: 1cm.

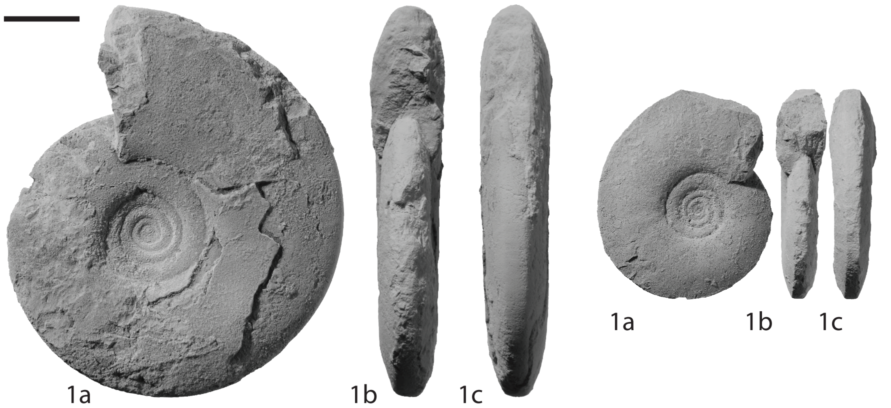

Fig. 11. Gyronitidae gen. et sp. indet. B. (1) PIMUZ 28172, Loc. M05-10/1. (3) PIMUZ 27860, Loc. Mud10.

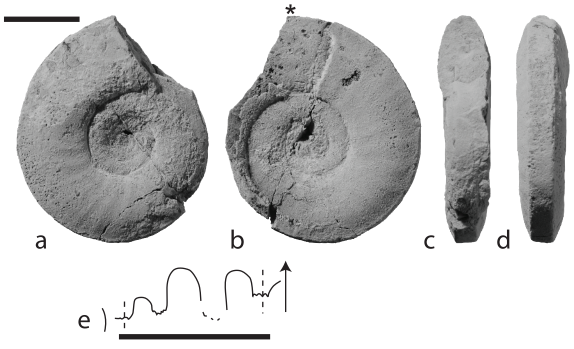

Fig. 12. Gyronitidae gen. indet. C, PIMUZ 28174, e at H = 10mm, D = 29mm, from Bed 10 of Krystyn et al. (2007a, b). Scale bars: 1cm.

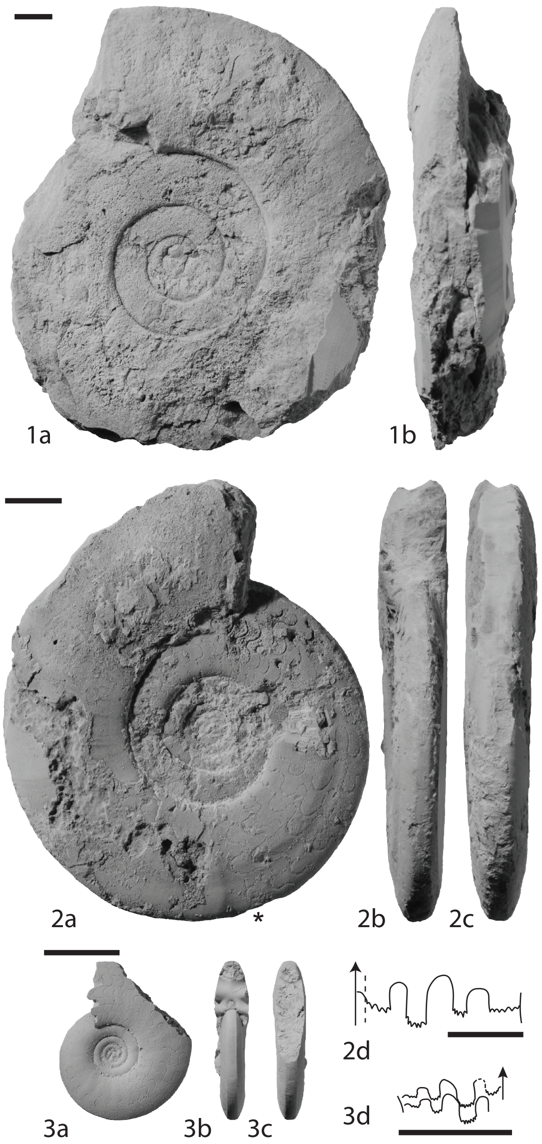

Fig. 13. *Mudiceras planissimum* (Spath, 1934) gen. nov. (1) PIMUZ 27874, Loc. Mud11. (2) PIMUZ 27173; 2d at H = 19mm, Loc. M05-10/1. (3) PIMUZ 27859; 3d at H = 8.5mm, D = 21.5mm, Loc. Mud11. Scale bars: 1cm.

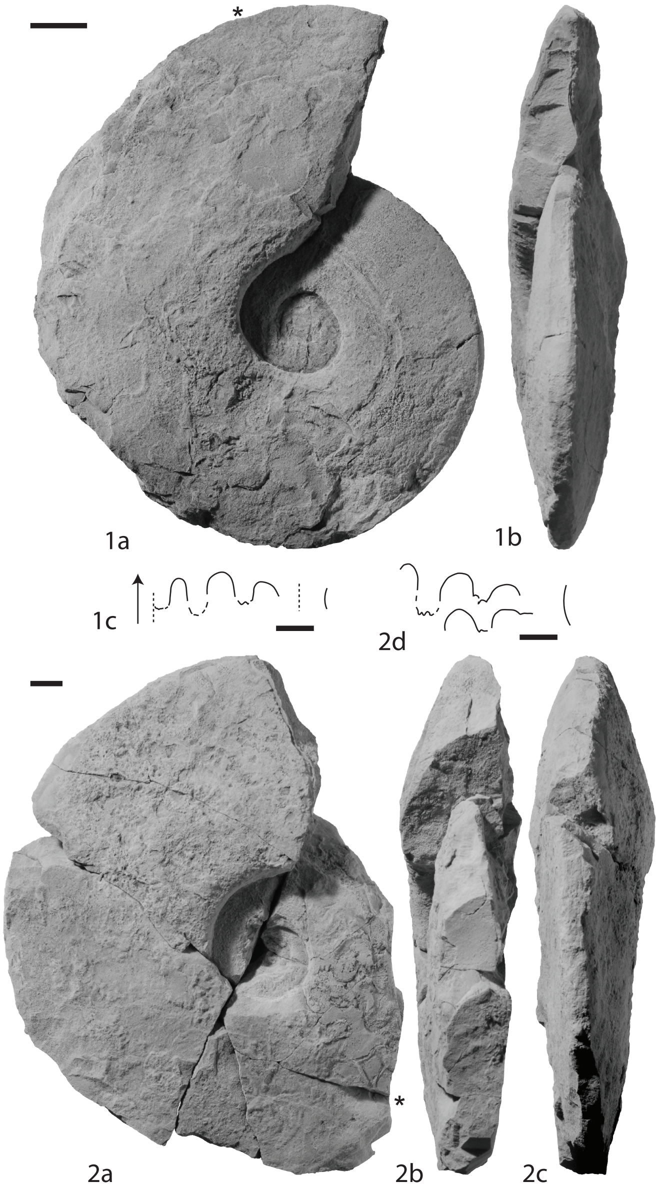

Fig. 14 . *Vercherites* cf. *pulchrum* (Waagen, 1895). (1) PIMUZ 28175; 1c at H = 43mm, D = 95mm, from Bed 12B of Krystyn et al. (2007a,b). (2) PIMUZ 27873, from Bed 12C. Scale bars: 1cm.

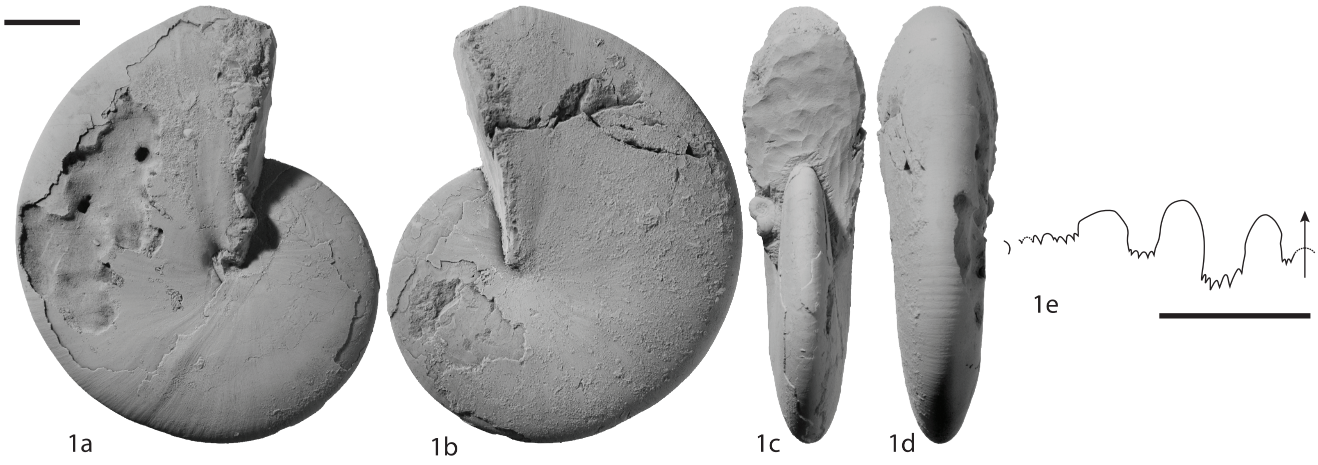

Fig. 15. *Kingites korni* sp. nov., PIMUZ 27863, holotype; 1e at H = 21mm, Loc. Mud31. Scale bars: 1cm.

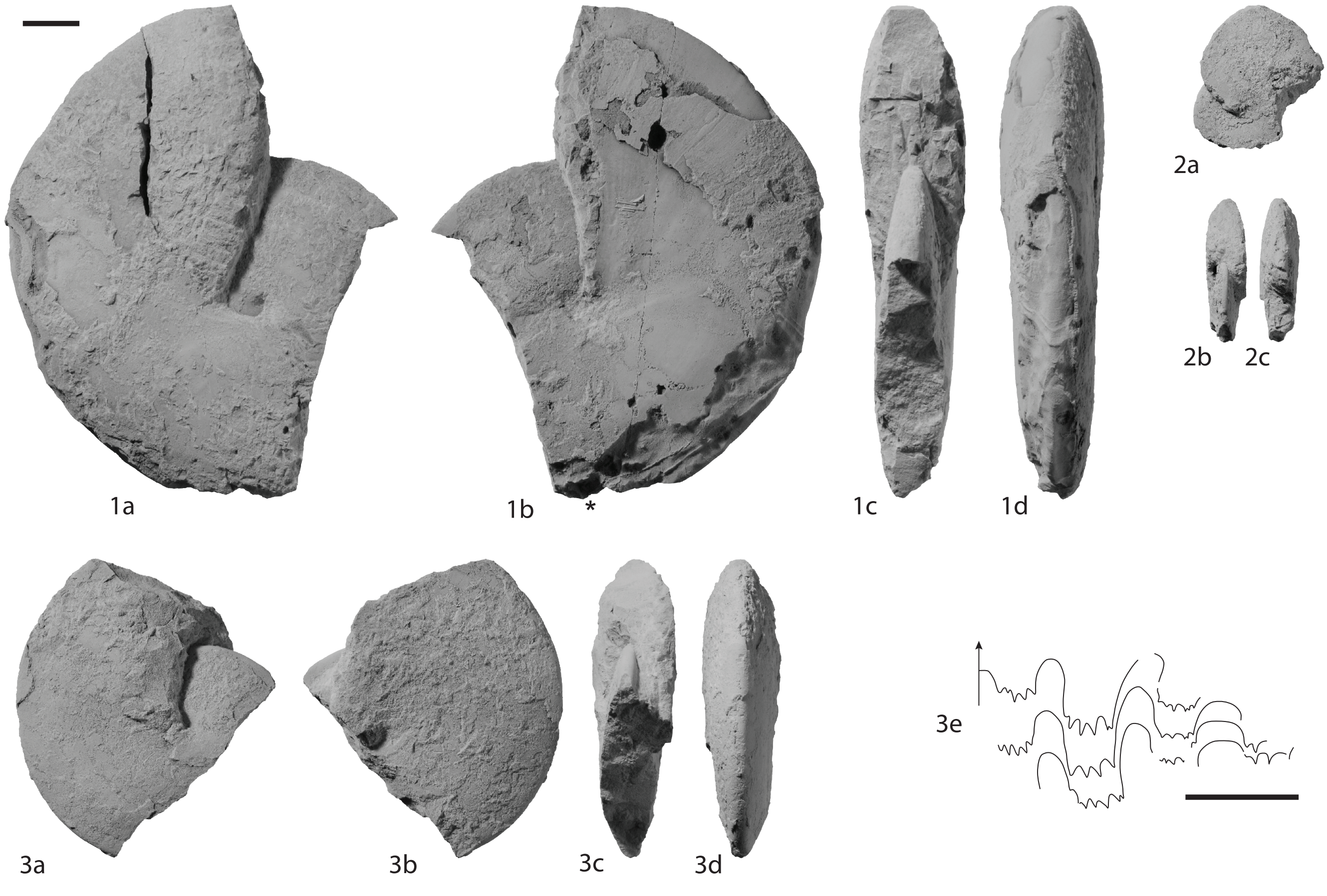

Fig. 16. ?*Kingites parkashi* sp. nov. (1) PIMUZ 27857, holotype, Loc. Mud32. (2) PIMUZ 27858, Loc. Mud32. (3) PIMUZ 27856; 3e at H = 27.5mm, Loc. Mud32. Scale bars: 1cm.

Fig. 17. *Xenodiscoides variocostatus* sp. nov. (1) PIMUZ 27867, holotype; 1d at H = 23mm, Loc. Mud11. (2) PIMUZ 27868, Loc. Mud11. (3) PIMUZ 27866, Loc. Mud34. Scale bars: 1cm.

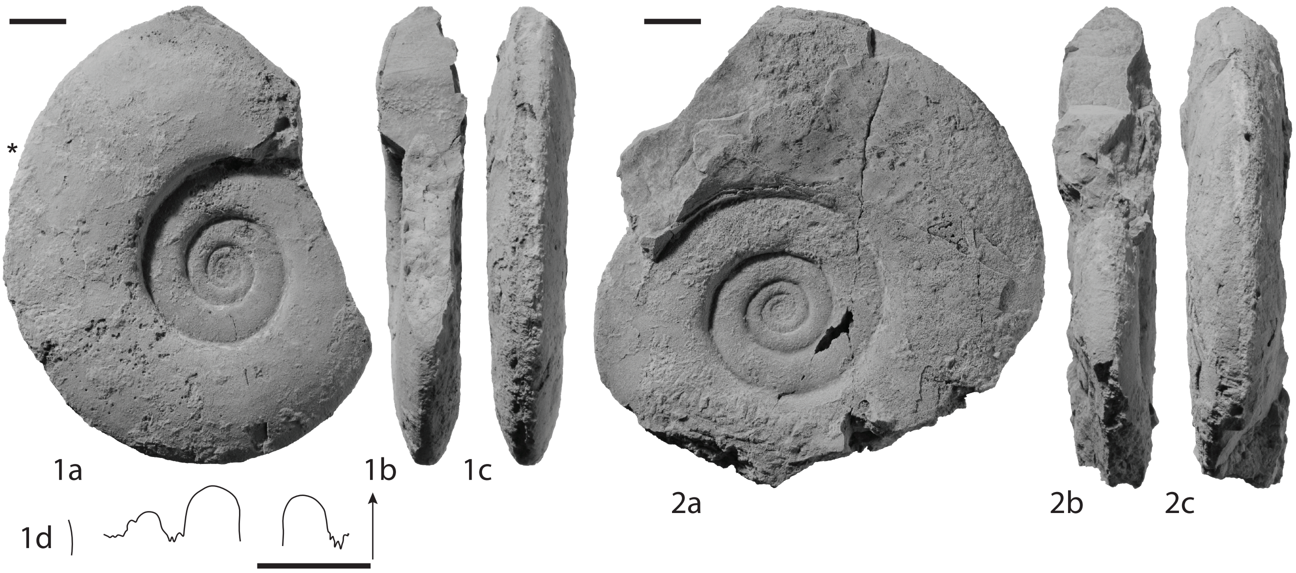

Fig. 18. *Xenodiscoides* cf. *variocostatus* sp. nov. (1), PIMUZ 27862; 1d at H = 25mm, Loc. Mud10, (2), PIMUZ 27861, Loc. Mud34. Scale bars: 1cm.

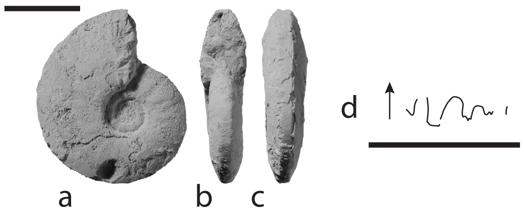

Fig. 19. *Xenodiscoides* sp. indet., A. PIMUZ 27869; d at H = 6.5mm, Loc. Mud33. Scale bars: 1cm.

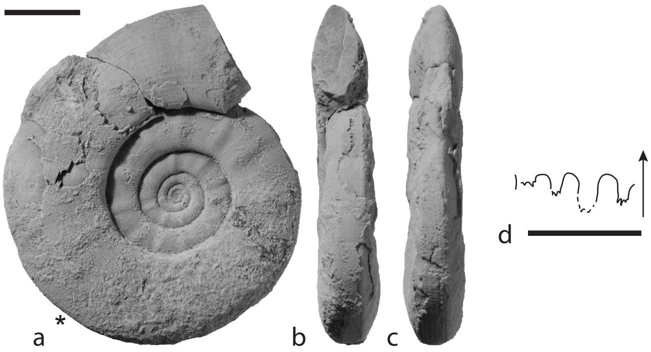

Fig. 20. *Flemingites bhargavai* sp. nov., PIMUZ 27865, holotype; 1d at H = 10.5mm, Loc. Mud32. Scale bars: 1cm.

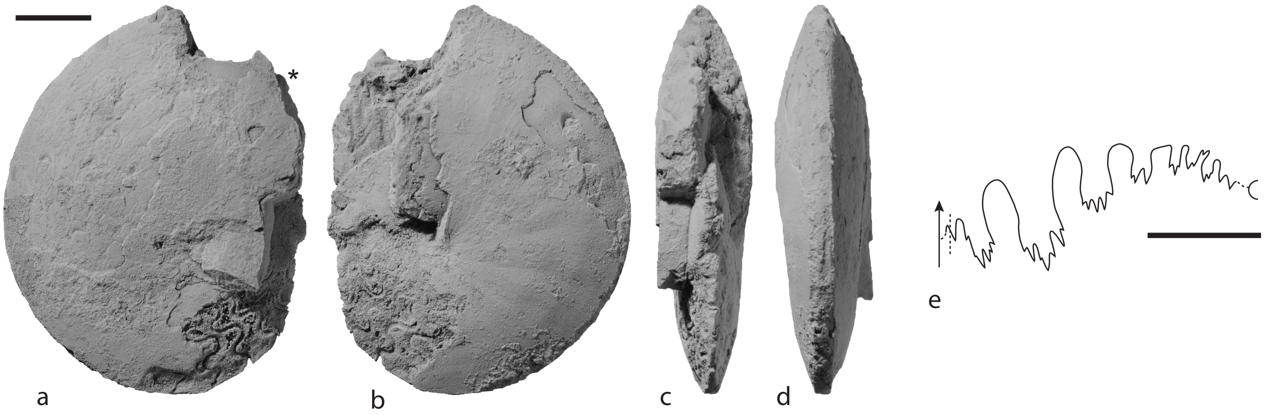

Fig. 21. *Clypites typicus* Waagen, 1895, PIMUZ 27870; e at H = 28mm, D = 59mm, Loc. Mud31. Scale bars: 1cm.

CHAPTER 7:

Middle and late Smithian (Early Triassic) ammonoids from Spiti (India)

MIDDLE AND LATE SMITHIAN (EARLY TRIASSIC) AMMONOIDS FROM SPITI (INDIA)

by THOMAS BRÜHWILER*, HUGO BUCHER* *and* LEOPOLD KRYSTYN†

*Paläontologisches Institut und Museum der Universität Zürich, Karl Schmid-Strasse 4, CH-8006 Zürich, Switzerland; e-mails: bruehwiler@pim.uzh.ch; hugo.fr.bucher@pim.uzh.ch
†Institut für Paläontologie, Althanstraße 14, 1090 Wien, Austria; e-mail: leopold.krystyn@univie.ac.at

Submitted to *Palaeontology.*

Abstract: Intensive sampling of the *"Parahedenstroemia"* Beds in the Mikin Formation at the Mud, Guling, Lalung and Losar localities in the Spiti area (Himachal Pradesh, Northern India) has yielded abundant and well-preserved Smithian (Early Triassic) ammonoid faunas. Our data allow the construction of a highly-resolved ammonoid succession spanning the middle to latest Smithian time interval. The new biostratigraphical sequence comprises the following eight distinct ammonoid faunas (in ascending order): the *Brayardites compressus* beds; the *Nammalites pilatoides* beds, subdivided into the *Escarguelites spitiensis* horizon and the *Truempyceras compressum* horizon; the *Pseudoceltites multiplicatus* beds; the *Nyalamites angustecostatus* beds; the *Wasatchites distractus* beds; the *Subvishnuites posterus* beds and the *Glyptophiceras sinuatum* beds. This faunal succession correlates well with that of other Tethyan sequences such as the Salt Range (Pakistan), Tulong (South Tibet) and Guangxi (South China).

Five new genera (*Escarguelites*, *Hermannites*, *Kraffticeras*, *Nuetzelia*, *Steckites*) and six new species (*Escarguelites spitiensis*, *Hermannites rursiradiatus*, *Nuetzelia himalayica*, *Steckites brevus*, *Subvishnuites posterus*, *Truempyceras compressum*) are described.

Key words: Ammonoidea, Early Triassic, Northern India, Mikin Formation, biostratigraphy.

IN the aftermath of the end-Permian mass extinction that wiped out more than 90 percent of all marine species (e.g. Raup and Sepkoski 1982), ammonoids recovered very fast in comparison with other marine clades (Brayard *et al.* 2006; Brayard *et al.* 2009). Following extremely low values in the Griesbachian, diversity increased slowly during the Dienerian and first peaked in the Smithian. This first major evolutionary radiation was followed by a severe extinction event in the end-Smithian, after which a second major and explosive radiation took place during the Spathian. Our knownledge on

Smithian ammonoids has significantly increased lately thanks to a number of recent studies from various basins in Guangxi, South China (Brayard and Bucher 2008), South Primorye, Russia (Shigeta *et al.* 2009; Shigeta and Zakharov 2009), Tulong, South Tibet (Brühwiler *et al.* accepted), the Salt Range, Pakistan (Brühwiler *et al.* submitted [b]) and Oman (Brühwiler *et al.* submitted [a]).

Since the pioneer works of Diener (1897) and Krafft and Diener (1909), the Spiti area in Himachal Pradesh (Northern India) became one of the classic regions for Early Triassic ammonoids. However, these authors did not include precise information on the stratigraphic position of their material, and there is a need for a revision of these faunas based on bed-rock controlled material. Recently, a section near Mud in Spiti has been proposed as GSSP candidate for the Induan/Olenekian (Dienerian/Smithian) boundary (Krystyn *et al.* 2007*a*, *b*; Brühwiler *et al.* submitted [c]). While these works concentrated on this boundary, our extensive investigations in Spiti during several field seasons have also yielded abundant, well-preserved ammonoid faunas of middle to late Smithian age. This new material enables us to revise the taxonomy of these faunas, and to establish a high-resolution biostratigraphical sequence for the Smithian of Spiti. Such data are crucial for establishing a precise and laterally reproducible biochronological subdivision of the Smithian within the Tethys and within the Early Triassic tropics.

PALAEOGEOGRAPHICAL AND GEOLOGICAL SETTING

During Early Triassic times the Spiti area was located on the peri-Gondwanan margin, on the southern side of the Tethys Ocean (e.g. Smith *et al.* 1994) (Text-fig. 1A). The Griesbachian to Ansisian mixed carbonate siliciclastic rocks of the study area are represented by the Mikin Formation, which disconformably overlies the Kuling Shales of Late Permian age (Bucher *et al.* 1997), and is overlain by the Upper Ladinian Kaga Formation (Bhargava *et al.* 2004). The Mikin Formation is subdivided into the following four members (from bottom to top) (Text-figs 2-3):

- Lower Limestone Member. This member is further subdivided into a lower part of Griesbachian age that consists of brown, ferruginous limestone containing *Otoceras*; and an upper part of Dienerian age that consists of grey thin-bedded limestone yielding "*Pleurogyronites*". This member also contains abundant specimens of the bivalve *Claraia*.

- Limestone and Shale Member. This member is further subdivided into three parts: the Dienerian *Ambites* Beds (equivalent to the *Meekoceras* Beds of Krafft and Diener 1909 and the *Gyronites* Beds of Bhargava *et al.* 2004; see also Brühwiler *et al.* submitted [c]), consisting of dark shales with intercalated limestone beds and early diagenetic nodules; the early Smithian *Flemingites* Beds, consisting of grey, slightly nodular limestone; and the middle-late Smithian "*Parahedenstroemia*" Beds (equivalent to the *Hedenstroemia* Beds of Krafft and Diener 1909), consisting of an alternance of shales and limestone beds.

- Niti Limestone Member. This member consists of light grey, nodular limestone of Spathian age.

- Himalayan Muschelkalk Member. This member consists of thin limestone bands, argillaceous limestones and minor shales of Anisian age. Iron oxides and phosphatic preservation of fossils indicate condensed sedimentary conditions. Comparison of the biostratigraphic data with the well-developped Anisian series of Nevada (Monnet and Bucher 2005) indicates that the Himalayan Muschelkalk is pervaded with gaps.

The Lower Triassic mixed siliciclastic-carbonate succession of the Spiti area shows striking similarities with the palaeogeographically distant basinal successions of the Luolou Formation in Guangxi (South China), thus suggesting a common, at least Tethys-wide control of climatic and eustatic origin on outer platform sedimentary evolution (Galfetti *et al.* 2007*a*). On the other hand, during the Early Triassic the Northern Indian Margin was characterized by extensional tectonics related to the opening of the Neothetys (e.g. Stampfli *et al.* 1991). Therefore, successions from closely spaced localities in South Tibet (e.g. Tulong and Selong) show pronounced differences regarding facies and thickness (Garzanti *et al.* 1998; Brühwiler *et al.* 2009).

SAMPLED LOCALITIES

The Spiti area is located east of the town of Manali in Himachal Pradesh, Northern India (Text-fig. 1B). Four localities (Mud, Guling, Lalung and Losar) were studied (Text-fig. 1C). All sections were sampled bed-by-bed in order to obtain a precise, detailed ammonoid record (Text-figs 4-7).

The area near the village of Mud in Pin Valley is one of the main localities studied by Diener (1897) and Krafft and Diener (1909). The Induan/Olenekian (Dienerian/Smithian) boundary interval at Mud has been thoroughly studied by Krystyn *et al.* (2007*a*, *b*) and Brühwiler *et al.* (submitted [c]). In this area, the Lower Triassic sediments are perfectly exposed (Text-fig. 2). We extensively studied several sections at elevations ranging from 3900m to 4800m. All sections can be correlated on a bed-by-bed basis. In the lower part of the *"Parahedenstroemia"* Beds, ammonoids are abundant and well preserved, but fossiliferous horizons are relatively rare in their middle and upper parts. All middle to late Smithian ammonoid occurrences from Mud are given in Text-fig. 4.

In the Guling area, two sections were studied; one near the village in the bottom of the Pin Valley (3550m), and one at an altitude of 3850m, above the village. Both sections can be correlated bed-by-bed. Fossiliferous horizons are relatively rare in the *"Parahedenstroemia"* Beds, but preservation of ammonoids is sometimes excellent. All middle to late Smithian ammonoid occurrences from Guling are given in Text-fig. 5.

Krafft and Diener (1909) described a large number of Dienerian ammonoids from the area near the village of Lalung (old spelling Lilang) in Lingti Valley. Our sampling at this locality has yielded well preserved ammonoids from the middle part of the *"Parahedenstroemia"* Beds. All middle Smithian ammonoid occurrences from Lalung are given in Text-fig. 6.

Excellent exposures of the Mikin Formation also occur high above the village of Losar in Spiti Valley (Garzanti *et al.* 1995; Galfetti *et al.* 2007b). Ammonoids are abundant but mostly poorly preserved in the *Flemingites* beds. Abundant and well preserved material was found in the lower and middle part of the *"Parahedenstroemia"* Beds. All Smithian ammonoid occurrences from Losar are given in Text-fig. 7.

BIOSTRATIGRAPHY

Based on our extensive, bed-rock controlled sampling, we recognize a total of eight distinct ammonoid faunas of middle to latest Smithian age in the studied area (Text-figs 4-10). The resulting informal zonation presented herein significantly improves the preliminary versions presented earlier (Krystyn *et al.* 2007*a*; Brühwiler *et al.* 2007). A description of the ammonoid faunas as well as a discussion of their correlation with ammonoid zonations from other areas is provided, and synthetic range charts for Smithian ammonoid species and genera from Spiti are given (Text-figs 8-10). No formal zone names are introduced since we prefer to use the term "beds" at the present time to describe the local faunal sequence. The usage of formal zones would imply a well-established lateral reproducibility of the faunal sequence between various basins, which is still a subject of ongoing work.

Dienerian/Smithian boundary ammonoid faunas

Ammonoid faunas from the Dienerian/Smithian boundary beds at Mud have recently been documented by Brühwiler *et al.* (submitted [c]). The latest Dienerian *Prionolobus rotundatus* beds are followed by faunas containing certain ammonoids with typical early Smithian affinity (Flemingitidae, Kashmiritidae) and thus reflecting the beginning of the early Smithian evolutionary radiation. These faunas include the *Flemingites bhargavai* beds, the Kashmiritidae gen. nov. A beds and the *Vercherites* cf. *pulchrum* beds.

Early Smithian ammonoid faunas

***Flemingites* beds**. In the Losar section, an association including *Kashmirites nivalis*, *Kashmirites* sp. indet., *Flemingites* sp. indet., *Dieneroceras* cf. *tientungense* and *Kraffticeras pseudoplanulatum* gen. nov. was found within the *Flemingites* beds, clearly indicating an early Smithian age. However, our limited sampling does not allow to significantly improve the biostratigraphy of this interval. A more comprehensive study of the ammonoid fauna of the *Flemingites* beds based on abundant and well preserved material from this interval is under progress (Krystyn *et al.* 2007*a*, *b*, ongoing work).

Middle Smithian ammonoid faunas

***Brayardites compressus* beds**. This subdivision was provisionally labeled "new prionitid A beds" by Brühwiler *et al.* (2007) and was found at Mud, Guling and Losar. It is characterized by the association of *Aspenites acutus*, *Brayardites compressus*, *B. crassus*, *Jinyaceras hindostanum*, *Pseudaspenites* cf. *layeriformis*, *Tulongites xiaoqiaoi* and *Urdyceras tulongensis*. *Hermannites rursiradiatus* gen. et sp. nov. and *Xiaoqiaoceras involutus* also co-occur in this fauna.

Recently, this association was also discovered at Tulong, South Tibet (Brühwiler *et al.* accepted) and in the Salt Range (Pakistan) (Brühwiler *et al.* submitted [b]), but a faunal equivalent is not known from South China. It probably correlates with an interval between the *Flemingites rursiratiatus* beds and the *Owenites koeneni* beds in the South China succession (Brayard and Bucher 2008).

***Nammalites pilatoides* beds**. This subdivision was provisionally labeled "new prionitid B beds" by Brühwiler *et al.* (2007) and comprises two different successive faunas in the Spiti area. *Nammalites pilatoides* and *Galfettites omani* are common to each of these. The succession consists of the following two horizons in ascending order:

- *Escarguelites spitiensis* horizon; found at Mud and Losar. Characterized by the co-occurrence of *Escarguelites spitiensis* gen. et sp. nov., *Hanielites elegans* and *Nuetzelia himalayica* gen. et sp. nov.
- *Truempyceras compressum* horizon; found at all studied localities. Characterized by the co-occurrence of *Truempyceras compressum* sp. nov., *Owenites* cf. *simplex*, *Paranannites* sp. indet., *Preflorianites radians*, *Shigetaceras dunajensis* and *Steckites brevus* gen. et sp. nov.

Equivalent faunas of the the upper part of the *Nammalites pilatoides* beds, i.e. the *Truempyceras compressum* horizon, were also recently discovered in the Salt Range (Brühwiler *et al.* submitted [b]), at Tulong (Brühwiler *et al.* accepted) and in an exotic block of Hallstatt facies from Oman (Brühwiler *et al.* submitted [a]). The *Nammalites pilatoides* beds correlate with the lower part of the middle Smithian *Owenites koeneni* beds of South China (i.e. *Ussuria* and *Hanielites* horizons; Brayard and Bucher, 2008).

***Pseudoceltites multiplicatus* beds**. This subdivision was preliminarily termed Flemingitid A beds by Brühwiler *et al.* (2007), and was found at Mud only. It is mainly characterized by the occurrence of very abundant *Pseudoceltites multiplicatus*. *Anaxenaspis* sp. indet. and *Juvenites procurvus* also co-occur.

This fauna occurs also in the Salt Range (Brühwiler *et al.* submitted [b]) and at Tulong (Brühwiler *et al.* accepted). An exact correlative is not known from South China.

***Nyalamites angustecostatus* beds**. This subdivision contains a diverse fauna and was found at Mud, Guling and Losar. It is characterized by the association of *Nyalamites angustecostatus*, *Owenites carpenteri* , *O. koeneni*, *Prionites* sp. indet., *Stephanites superbus* and ?*Subflemingites compressus* sp. nov. Rare specimens of *Anaxenaspis* sp. indet. and ?*Urdyceras* sp. indet. were also found in these beds.

This fauna is also known from Tulong (Brühwiler *et al.* accepted), the Salt Range (Brühwiler *et al.* submitted [b]) and Oman (Brühwiler *et al.* submitted [a]), and it correlates with the *Inyoites* horizon in the upper part of the *Owenites koeneni* beds of South China, with which it shares *Owenites carpenteri.*

Late Smithian ammonoid faunas

***Wasatchites distractus* beds**. This subdivision was found at Mud and Guling. It is characterized by the association of very abundant *Wasatchites distractus* and *Anasibirites kingianus*. Correlatives of this late Smithian fauna are known from many other Tethyan localities such as Oman, Salt Range, Tulong (Brühwiler *et al.* accepted; Brühwiler *et al.* submitted [a]; Brühwiler *et al.* submitted [b]), Timor (Welter 1922) and South China (Brayard and Bucher, 2008), as well as many other localities outside the Tethys (e.g. Markevich and Zakharov 2004; Silberling and Tozer 1968; Tozer 1994; Weitschat and Lehmann 1978).

***Subvishnuites posterus* beds**. This subdivision was found at Mud only. It is characterized by the association of *Subvishnuites posterus* sp. nov., *Pseudosageceras augustum* and *Xenocelties* cf. *variocostatus*.

An exact correlative of this fauna is not known from other localities. Note that both *Pseudosageceras augustum* and *Xenoceltites* are relatively long-ranging: *P. augustum* is known to cross the Smithian/Spathian boundary (Brühwiler *et al.* accepted), and *Xenoceltites* co-occurs with *Anasibirites* in South China (Brayard and Bucher 2008) and with *Glyptophiceras* in Tulong and in the Salt Range (Brühwiler *et al.* accepted, submitted [b]).

***Glyptophiceras sinuatum* beds**. These subdivision was found at Mud and Guling. It is characterized by the occurrence of *Glyptophiceras sinuatum*. This latest Smithian fauna also occurs in Tulong (Brühwiler *et al.* accepted) and in the Salt Range (Brühwiler *et al.* submitted [b]).

CONCLUSIONS

Detailed sampling of the Smithian series at Mud, Guling, Lalung and Losar in Spiti (Northern India) has yielded abundant and well preserved ammonoid faunas of middle to late Smithian age. Our work is the first detailed description of Smithian ammonoids from this area based on bed-rock controlled material. A total of eight distinct middle to latest Smithian ammonoid associations have been found within the *"Parahedenstroemia"* Beds. In ascending order the new local biostratigraphical sequence comprises the *Brayardites compressus* beds, the *Nammalites pilatoides* beds (subdivided into the *Escarguelites spitiensis* horizon and the *Truempyceras compressum* horizon), the *Pseudoceltites multiplicatus* beds, the *Nyalamites angustecostatus* beds, the *Wasatchites distractus* beds, the *Subvishnuites posterus* beds and the *Glyptophiceras sinnatus* beds. These biostratigraphic subdivisions of the Smithian can well be correlated with other areas on the Northern Indian Margin such as Tulong, South Tibet (Brühwiler *et al.* accepted), the Salt Range (Brühwiler *et al.* submitted [b]), Pakistan and Oman (Brühwiler *et al.* submitted [a]). Moreover, a detailed correlation with the well-studied record from Guangxi, South China (Brayard and Bucher, 2008) is facilitated by many common taxa.

SYSTEMATIC PALAEONTOLOGY

Systematic descriptions mainly follow the classification established by Tozer (Tozer 1981, 1994) and refined by Brayard and Bucher (2008), Brühwiler *et al.* (accepted) and Brühwiler and Bucher (submitted [a, b]). Provided that measurements were available for at least four specimens, the quantitative morphological range of each species is expressed utilizing the four classic geometrical parameters of the ammonoid shell: diameter (D), whorl height (H), whorl width (W) and umbilical diameter (U). The three parameters (H, W and U) are plotted in absolute values as well as in relation to diameter (H/D, W/D, and U/D). Sample numbers are reported on the stratigraphic sections (Text-figs 4-7).

Abbreviations: non = material not forming part of the current species; p. = pars (from Latin, means that only part of the material belongs to the current species); v. = *video* or *vidimus* (from Latin, means that the material was seen in person by the authors); ? = questionable; PIMUZ, Paläontologisches Institut und Museum der Universität Zürich, Switzerland.

Class CEPHALOPODA Cuvier, 1797

Subclass AMMONOIDEA Zittel, 1884

Order CERATITIDA Hyatt, 1884

Superfamily XENODISCACEAE Frech, 1902

Family KASHMIRITIDAE Spath, 1934

Genus PSEUDOCELTITES Hyatt, 1900

Type species. *Celtites multiplicatus* Waagen, 1895.

Pseudoceltites multiplicatus (Waagen, 1895)

Plate 1, figures 1-7

1895 *Celtites multiplicatus* Waagen, p. 78, pl. 7, fig. 2a-c.
1895. *Celtites dimorphus* Waagen, p. 80, Pl. 7, Fig. 5a-c.
1976 *Psdeuodceltites multiplicatus* (Waagen); Wang and He, p. 289, pl. 6, figs 7-11.
? 1976 *Eukashmirites* cf. *blaschkei* (Diener); Wang and He, p. 290, pl. 6, fig. 12.
? 1976 *Eukashmirites* cf. *subarmatus* (Diener); Wang and He, p. 291, pl. 6, figs 13-14.
v acc. *Pseudoceltites multiplicatus* (Waagen, 1895); Brühwiler *et al.*, fig. 6(1-7).
v subm. *Pseudoceltites multiplicatus* (Waagen); Brühwiler *et al.*, submitted [b].

Occurrence. Samples M05-46, M05-48, M08-48, Ma31a, E24; *Pseudoceltites multiplicatus* beds.

Description. Evolute shell with a subrectangular whorl section. Flanks flat, converging very weakly. Venter broad and subtabulate, slightly arched with slightly rounded shoulders. Umbilicus with a high vertical wall and marked, slightly rounded shoulders. Ornamentation varies from strong, distant radial ribs to fine, dense and slightly sinuous ribs. Ribs usually fade out on ventral shoulders, but occasionally cross the venter as faint ridges. Suture line ceratitic with broad saddles; first and second lateral saddle tapered and large, third saddle low.

Measurements. See Text-fig. 11.

?*Pseudoceltites* sp. indet.

Plate 1, figure 8a-e.

Occurrence. A single specimen from sample Ma26.

Description. Moderately evolute shell with a subrectangular whorl section. Flanks nearly flat, slightly convex. Venter broad and subtabulate, slightly arched with slightly rounded shoulders. Umbilicus with a high vertical wall and marked, slightly rounded shoulders. Ornamentation consists of weak, slightly sinuous ribs. Suture line ceratitic with relatively deep lobes.

Measurements. See appendix.

Discussion. This specimen is more involute than *Pseudoceltites multiplicatus*. It also differs by its weaker ornamentation.

Genus KASHMIRITES Diener, 1913

Type species. *Celtites armatus* Waagen, 1895.

Kashmirites nivalis (Diener, 1897)

Plate 2, figures 4-6

1897	*Danubites nivalis* Diener, p. 51, pl. 15, figs 17-18.
1909	*Xenodiscus nivalis* Diener, Krafft and Diener, p. 102. pl. 24, figs 1-3, 5; pl. 25, fig. 5.
1934	*Anakashmirites nivalis* Diener; Spath, p. 237, pl. 12, fig. 4a-e.

Occurrence. Samples HB1010, HB1019, HB1016, HB1022; *Flemingites* beds, Losar.

Description. Evolute, slightly compressed shell with convex flanks. Venter arched with rounded shoulders. Umbilicus with rounded shoulders. Ornamentation consists of strong, distant folds. Suture line not preserved.

Measurements. See appendix.

Kashmirites sp. indet.

Plate 2, figure 3a-c

Occurrence. Samples HB1009, HB1023; *Flemingites* beds, Losar.

Description. Evolute shell with flat, subparallel flanks. Venter subtabulate, low arched with rounded shoulders. Umbilicus wide with a steeply inclinded wall and slightly rounded shoulders. Ornamentation consists of strong, sharp ribs. Suture line not preserved.

Discussion. The evolute coiling, the ornamentation and the subrectangular whorl section of this species favour assignment to *Kashmirites*, but the poor preservation of our material precludes an assignment at the species level.

Genus PREFLORIANITES Spath, 1930

Type species. *Danubites strongi* Hyatt and Smith, 1905.

Preflorianites radians Chao, 1959

Plate 2, figures 1-2

? 1922 *Xenodiscus bittneri* Welter, p. 106, pl. 4, figs 8-9.

1959 *Preflorianites radians* Chao, p. 196, pl. 3, figs 6-8.

v 2008 *Pseudoceltites? angustecostatus* Welter; Brayard and Bucher, p. 18; pl. 3, figs 1-7; text-fig. 19.

Occurrence. Samples M06-39, M08-40; *Truempyceras compressum* horizon, Mud.

Description. Evolute shell with convex flanks. Venter rounded without any distinct shoulders. Umbilicus wide and shallow with vertical wall and rounded shoulders. Ornamentation of flanks consists of regularly spaced, strong, radial or rursiradiate rounded ribs that fade out towards lower flanks. Suture line not preserved.

Genus NYALAMITES Brühwiler, Bucher and Goudemand (accepted)

Type species. *Xenodiscus angustecostatus* Welter, 1922.

Nyalamites angustecostatus (Welter, 1922)
Plate 2, figures 7-9

? 1895 *Celtites acuteplicatus* Waagen, 1895, p. 82, pl. 7a, figs 5, 5c, 6, 7.
1922 *Xenodiscus angustecostatus* Welter, p. 110, pl. 4, figs 14-17.
? 1922 *Xenodiscus oyensi* Welter, p. 111, pl. 5, figs 1, 2, 17
1968 *Anakashmirites angustecostatus* (Welter); Kummel and Erben, p. 128, pl. 19, figs 1-8.
1973 *Anakashmirites angustecostatus* (Welter); Collignon, p. 144, pl. 5, figs 7-8.
1973 *Anakashmirites oyensi* (Welter); Collignon, p. 146, pl. 5, figs 9-10.
1976 *Pseudoceltites angustecostatus* (Welter); Wang and He, p. 289, pl. 6, figs 3-6.
v 1978 *Eukashmirites angustecostatus* (Welter); Guex, pl. 7, figs 4, 9.
v non 2008 *Pseudoceltites? angustecostatus* (Welter); Brayard and Bucher, p. 18; pl. 3, figs 1-7; fig. 19 (=*Preflorianites radians*).
v acc. *Nyalamites angustecostatus* (Welter); Brühwiler *et al.* fig. 9(3-5).
v subm. *Nyalamites angustecostatus* (Welter); Brühwiler and Bucher, submitted [a].
v subm. *Nyalamites angustecostatus* (Welter); Brühwiler and Bucher, submitted [b]

Occurrence. Samples Ma46, M03-57, M03-58, Mud; HB1900, Losar; *Nyalamites angustecostatus* beds.

Description. Small, very evolute shell with slightly convex, subparallel flanks. Venter subtabulate with narrowly rounded shoulders. Umbilicus shallow and wide with inclined wall and rounded shoulders. Ornamentation consists of regularly spaced, strong, sharp, radial ribs that fade out on ventral shoulders. Suture line ceratitic with two broad lateral saddles; third saddle reduced.

Measurements. See appendix.

Discussion. This species is very common in the late middle Smithian of the Tethys.

Genus HANIELITES Welter, 1922

Type species. *Hanielites elegans* Welter, 1922.

Hanielites elegans Welter, 1922

Plate 3, fig. 4a-c

1922 *Hanielites elegans* Welter, p. 145, pl. 14, figs 7-11.
1934 *Hanielites elegans* Welter; Spath, p. 243, fig. 82a-d.
1959 *Hanielites elegans* Welter; Chao, p. 280, pl. 37, figs 8-12, text-fig. 36b.
1959 *Hanielites elegans* var. *involutus* Chao, p. 281, pl. 37, figs 4-6, text-fig. 36a.
1959 *Hanielites rotulus* Chao, p. 281, pl. 37, figs 12-15.
1959 *Owenites kwangiensis* Chao, p. 250, pl. 22, figs 1-2, 5-6.
v 2008 *Hanielites elegans* Welter; Brayard and Bucher, p. 19, pl. 4, figs 1-5, text-fig. 20.

Occurrence. A single fragmentary specimen from sample M08-29; *Escarguelites spitiensis* beds, Mud.

Description. Small, moderately evolute and compressed shell with flat, parallel flanks. Venter subangular. Umbilicus with low, vertical wall. Ornamentation consists of biconcave plications. Suture line not preserved.

Family XENOCELTITIDAE Spath, 1930

Genus XENOCELTITES Spath, 1930

Type species. *Xenoceltites subevolutus* Spath, 1930.

Xenoceltites cf. *variocostatus* Brayard and Bucher, 2008

Plate 3, figures 1-2

1913 *Ophiceras demissum* Oppel; Diener, p. 17, pl. 1, figs 8-9.
v subm. *Xenoceltites* cf. *variocostatus* Brayard and Bucher; Brühwiler and Bucher submitted [b].

Occurrence. Samples M08-70, E30; *Subvishnuites posterus* beds, Mud.

Description. Moderately evolute, platycone shell with nearly flat, barely convex flanks. Venter narrowly rounded with indistinct shoulders. Umbilicus shallow with moderately low, inclined wall and rounded shoulders. Inner whorls occasionally ribbed, outer whorls smooth. Growth lines prorsiradiate and biconcave. Suture line simple; fine indentations of lobes not preserved.

Measurements. See appendix.

Discussion. *Xenoceltites variocostatus* from South China differs by its slightly thicker whorls, but is otherwise very similar. The specimens from the Salt Range described as *Xenoceltites* cf. *variocostatus* (Brühwiler *et al.*, submitted [b]) are identical with our specimens from Spiti.

Genus GLYPTOPHICERAS Spath, 1930

Type species. *Xenodiscus aequicostatus* Diener, 1913 (=*Dinarites sinuatus* Waagen, 1895).

Glyptophiceras sinuatum (Waagen, 1895)

Plate 2, figures 11-13

1895 *Dinarites sinuatus* Waagen, p. 33, pl. 10, fig. 4.
? 1913 *Xenodiscus* cf. *lissarensis* Diener; Diener, p. 5, pl. 1, fig. 11.
1913 *Xenodiscus aequicostatus* Diener, p. 6, pl. 2, fig. 10.
1913 *Xenodiscus salomonii* Diener, p. 7, pl. 2, fig. 5.
1913 *Xenodiscus althothae* Diener, p. 8, pl. 2, figs 6, 11.
1913 *Xenodiscus* cf. *ellipticus* Diener; Diener, p. 9, pl. 3, fig. 1.
1913 *Xenodiscus comptoni* Diener, p. 10, pl. 2, fig. 7.
? 1913 *Xenodiscus* cf. *rotula* Waagen; Diener, p. 11, pl. 3, fig. 2.
1913 *Xenodiscus* cf. *ophioneus* Waagen; Diener, p. 12, pl. 2, figs 8-9.
? 1913 *Xenodiscus* cf. *sitala* Diener; Diener, p. 14, pl. 3, fig. 3.
1966 *Xenoceltites sinuatus* Waagen; Kummel, pl. 1, figs 1-2.
? 1966 *Xenoceltites sinuatus* Waagen; Kummel, pl. 1, figs 3-4.
v 1978 *Xenoceltites pulcher* Guex, p. 112, pl. 7, fig. 8.
v acc. *Glyptophiceras sinuatum* (Waagen, 1895); Brühwiler *et al.* fig. 8(1-7).
v subm. *Glyptophiceras sinuatum* (Waagen, 1895); Brühwiler and Bucher submitted [b].

Occurrence. Sample Ma96, Mud; samples Gu110 and GD95, Guling; *Glyptophiceras sinuatum* beds.

Description. Evolute, platycone shell with convex, convergent flanks. Venter rounded with rounded shoulders. Umbilicus wide and shallow with low vertical wall and rounded shoulders. Ornamtentaion varies from low, dense and sinuous ribs to very strong, distant and concave ribs. Suture line ceratitic with weakly indented lobes, poorly preserved.

Measurements. See appendix.

Family PROPTYCHITIDAE Waagen, 1895

Genus PSEUDASPIDITES Spath, 1934

Type species. *Aspidites muthianus* Krafft and Diener, 1909.

Pseudaspidites muthianus (Krafft and Diener, 1909)

Plate 3, figures 5-6

1909 *Aspidites muthianus* Krafft and Diener, p. 59, pl. 6, fig. 5; pl. 15, figs 1-2.
1932 *Clypeoceras muthianum* (Krafft and Diener, 1909); Smith, p. 64, pl. 27, figs 1-7.
p 1932 *Ussuria waageni* Smith, pl. 21, figs 34-36 only.
1934 *Pseudaspidites muthianus* (Krafft and Diener, 1909); Spath, p. 164.
1959 *Pseudaspidites lolouensis* Chao, p. 229, pl. 13, figs 17-21, text-figs. 20a, 21a.
1959 *Pseudaspidites kwangsianus* Chao, p. 230, pl. 12, figs 6-8, text-fig. 21d.
1959 *Pseudaspidites simplex* Chao, p. 231, pl. 13, figs 6-13; pl. 45, figs 5-7, text-fig. 20b, 21b.
1959 *Pseudaspidites stenosellatus* Chao, p. 231, pl. 13, figs 4-5; pl.45, fig.8, text-fig. 21c.
1959 *Pseudaspidites aberrans* Chao, p. 232, pl. 13, figs 14-15, text-fig. 20d.
1959 *Pseudaspidites longisellatus* Chao, p. 232, pl. 13, figs 1-3, text-fig. 20c.
1959 *Proptychites pakungensis* Chao, p. 236, pl. 18, figs 1-2.
1959 *Proptychites hemialis* var. *involutus* Chao, p. 237, pl. 15, figs 13-16, text-fig. 24d.
? 1959 *Proptychites markhami* Chao, p. 239, pl. 15, figs 3-5, text-fig. 23c.
1959 *Proptychites angusellatus* Chao, p. 240, pl. 15, figs 1-2.
1959 *Proptychites sinensis* Chao, p. 240, pl. 16, figs 5-6; pl. 17, figs 14-16, text-fig. 22c.
1959 *Proptychites latilobatus* Chao, p. 243, pl. 16, figs 1-2; pl. 19, figs 4-5.

1959 *Proptychites abnormalis* Chao, p. 243, pl. 16, figs 3-4.

1959 *Clypeoceras lenticulare* Chao, p. 225, pl. 12, figs 3-5, text-fig. 19b.

1959 *Clypeoceras tsotengense* Chao, p. 225, pl. 12, figs 1-2.

? 1959 *Clypeoceras kwangiense* Chao, p. 226, pl. 17, figs 1-2, text-fig. 19a.

1959 *Ussuriceras* sp. indet. Chao, p. 247, pl. 19, fig. 1.

1959 *Pseudohedenstroemia magna* Chao, p. 265, pl. 41, figs 13-16; pl. 45, figs 1-2, text-fig. 32b.

? 1962 *Pseudaspidites wheeleri* Kummel and Steele, p. 673, pl. 101, fig. 1; text-fig. 7c-e.

v 2008 *Pseudaspidites muthianus* (Krafft and Diener, 1909); Brayard and Bucher, p. 33, pl. 10, figs 1-10; pl. 11, figs 1-4; text-fig. 31.

Occurrence. Sample M05-18, *Brayardites compressus* beds, Mud; sample G06-31, level equivalent of the *Escarguelites spitiensis* horizon, Guling. Sample HB1004, *Escarguelites spitiensis* horizon, Losar.

Description. Involute and compressed shell with flat, slightly convex flanks. Venter rounded with indistinct shoulders. Umbilicus with high, perpendicular wall and narrow but slightly rounded shoulders. Surface smooth. Suture ceratitic with strongly indented lobes and phylloid saddles; second and third saddle curved towards umbilicus.

Pseudaspidites sp. indet.

Plate 3, fig. 3a-b

Occurrence. A single specimen from sample M08-21, *Brayardites compressus* beds, Mud.

Description. Moderately involute, compressed shell with slightly convex, convergent flanks. Maximum whorl width near umbilicus. Venter subtabulate with rounded shoulders. Umbilicus small and deep with high, vertical wall and marked, slightly rounded shoulders. Surface smooth. Suture line not preserved.

Discussion. This species differs from *Pseudaspidites muthianus* by its subtabulate venter. It is probably conspecific with *Pseudaspidites* sp. indet. that has recently been found in the *Brayardites compressus* beds at Tulong, South Tibet (Brühwiler *et al.*, accepted), and which differs from typical *Pseudaspidites* by its less complex suture line. However, since the suture line is not preserved on our specimen from Spiti, no definitive assignment can be made.

Genus XIAOQIAOCERAS Brayard and Bucher, 2008

Type species. *Xiaoqiaoceras involutus* Brayard and Bucher, 2008.

Xiaoqiaoceras involutus Brayard and Bucher, 2008

pl. 3, figs 7-8

v 2008 *Xiaoqiaoceras involutus* Brayard and Bucher, p. 36, pl. 12, figs 12-16; text-fig. 32.

Occurrence. Sample HB1005; *Brayardites compressus* beds, Losar.

Description. Very involute shell with convex flanks and rapidly increasing whorl height and whorl width. Venter broadly arched with indistinct shoulders. Umbilicus occluded or very small and deep. Surface smooth except for sparse and weak radial folds. Suture line very distinct with narrow saddles and deeply indented lobes; first lateral lobe broad and trifid.

Measurements. See appendix.

Discussion. The type material of this species comes from a slightly older horizon (i.e. the *Flemingites rursiradiatus* beds) of Guangxi, South China (Brayard and Bucher, 2008) and is indistinguishable from our specimens.

Genus TULONGITES Brühwiler, Bucher and Goudemand (accepted)

Type species. *Tulongites xiaoqiaoi* Brühwiler *et al.*, accepted.

Tulongites xiaoqiaoi Brühwiler *et al.*, accepted

Plate 4, figs 1-11

v acc. *Tulongites xiaoqiaoi* Brühwiler *et al.*, fig. 9(9-10).

Occurrence. Samples M08-21, M05-25, Mud; HB1033, HB1005, Losar; *Brayardites compressus* beds.

Measurements. See Text-fig. 12.

Description. Involute, platycone shell with slightly convex flanks. Maximum whorl width near mid flank. Venter narrow and rounded with rounded shoulders. Umbilicus small with steeply inclined wall and rounded shoulders. Shell ornamented with weak, biconcave and prorsiradiate folds. Suture line ceratitic; first and second lateral saddles tapered; third lateral saddle small.

Discussion. This species has recently been described from the *Brayardites compressus* beds of Tulong, South Tibet (Brühwiler *et al.*, accepted). The inner whorls of this species are superficially similar to those of *Brayardites compressus* (see below), which differs by its higher, vertical umbilical wall.

Family GALFETTITIDAE Brühwiler and Bucher, submitted [a]

Genus *Galfettites* Brayard and Bucher, 2008

Type species. *Galfettites simplicitatis* Brayard and Bucher, 2008.

Galfettites omani Brühwiler and Bucher, submitted [a]

Plate 5, figures 1-8

v subm. *Galfettites omani* Brühwiler and Bucher, pl. 14, figs 6-8.

Occurrence. Samples M04-44, Ma24c, Mud; LoA-SFB, HB1004, Losar; *Nammalites pilatoides* beds.

Description. Moderately evolute, very compressed shell with slightly convex and converging flanks. Venter narrow and tabulate with angular shoulders. Umbilicus wide and very shallow with very low wall and rounded shoulders. Surface smooth or ornamented with weak radial folds. Suture line ceratitic with slightly phylloid saddles.

Measurements. See Text-fig. 13.

Discussion. This species has recently been found in an exotic block of Hallstatt limestone in Oman, associated with *Nammalites pilatoides* (Brühwiler *et al.*, submitted [a]).

?*Galfettites* sp. indet.

Plate 4, figures 12-17

Occurrence. Samples HB1005, HB1033, Losar; sample M08-21, Mud; *Brayardites compressus* beds.

Description. Moderately evolute, platycone shell with slightly convex flanks. Venter narrow and tabulate with slightly rounded shoulders. Umbilicus with low vertical wall and rounded shoulders. Surface smooth. Suture line ceratitic, simple.

Measurements. See appendix.

Discussion. This species is somewhat similar to *Galfettites omani* described above, but differs by its deeper umbilicus.

Genus PARANORITES Waagen, 1895

Type species. *Paranorites ambiensis* Waagen, 1895.

?*Paranorites* sp. indet.

Plate 3, figure 9a-c

Occurrence. A single specimen, found as float in the *"Parahedenstroemia"* Beds at Mud, probably from the level of sample M04-44 or higher.

Description. Large, moderately involute, slightly compressed shell with convex, convergent flanks. Venter subtabulate with rounded shoulders. Umbilicus with high vertical wall and rounded shoulders. Surface smooth. Suture line ceratitic, second lateral saddle tapered, third lateral saddle broad and low.

Measurements. See appendix.

Discussion. The trigonal whorl section of this species is similar to that of *Paranorites*. However, the type species *Paranorites ambiensis* differs by by its more complex suture line with a slender and phylloid first lateral saddle and a higher and narrower third lateral saddle. Thus, this specimen may actually represent a new genus. However, due to our scarce material and the unknown exact stratigraphic position, we prefer not to erect a new taxon.

Genus URDYCERAS Brayard and Bucher, 2008

Type species. *Urdyceras insolitus* Brayard and Bucher, 2008.

Urdyceras tulongensis Brühwiler, Bucher and Goudemand (accepted)

Plate 5, figs 10-17

v acc. *Urdyceras tulongensis* Brühwiler *et al.*, fig. 1(5-11).

Occurrence. Samples E17, M03-21, M05-23, Mud; HB1005, HB1033, Losar; G06-20, Gu21, Guling; *Brayardites compressus* beds.

Description. Compressed and moderately evolute shell. Flanks convex and convergent. Venter tabulate with very angular shoulders. Umbilicus with vertical wall and marked, but slightly rounded shoulders. Ornamentation on flanks consists of fine radial, slightly sinuous folds. One specimen (Plate 5, fig. 17) displays rather strong folds on upper flanks. Suture line ceratitic with deep lateral lobe and slightly phylloid saddles. First lateral saddle narrow; second lateral saddle slightly curved towards umbilicus.

Measurements. See Text-fig. 14.

Discussion. This species has recently been described from the *Brayardites compressus* beds of Tulong, South Tibet (Brühwiler *et al.*, accepted).

?*Urdyceras* sp. indet.

Plate 5, figs 10-17

Occurrence. A single specimen from sample Ma49; *Nyalamites angustecostatus* beds, Mud.

Description. Compressed and moderately involute shell. Flanks convex and convergent. Venter broad and tabulate with very angular shoulders. Umbilicus with vertical wall and angular shoulders. Surface smooth. Suture line not preserved.

Measurements. See appendix.

Discussion. This species is more involute and has broader whorls than *Urdyceras tulongensis*. Due to the small size of our specimen and the unknown suture line, no definitive assignment can be made.

Family DIENEROCERATIDAE Kummel, 1952

Genus DIENEROCERAS Spath, 1934

Type species. *Ophiceras dieneri* Hyatt and Smith 1905.

Dieneroceras cf. *tientungense* Chao, 1959

Plate 5, figures 18-21

Occurrence. Samples HB1013, HB1020; *Flemingites* beds, Losar.

Description. Serpenticone, very evolute shell with convex flanks. Venter subtabulate with rounded shoulders. Umbilicus wide and shallow with rounded umbilical wall. Surface smooth. Suture line and simple with relatively deep lobes; indentations of lobes not preserved.

Measurements. See Text-figure 15.

Discussion. *Dieneroceras tientungense* Chao, 1959 from South China differs slightly by its more rounded venter and its slightly more depressed whorls. However, it exhibits significant variation in whorl section (Brayard and Bucher 2008), and our specimens from Spiti may fall within the range of its intraspecific variation.

Family FLEMINGITIDAE Hyatt, 1900

Genus HERMANNITES gen. nov.

Derivation of name. Named after Elke Hermann (Zürich).

Type species. *Hermannites rursiradiatus* gen. et sp. nov.

Composition of the genus. Type species only.

Diagnosis. Subtabulate and evolute Flemingitidae with inclined umbilical. Surface without strigation, ornamentated with rursiradiate ribs that tend to thicken near the umbilical margin.

Discussion. The evolute coiling and the suture line with phylloid saddles justify the assignment of *Hermannites* to Flemingitidae. This genus differs from other Flemingitidae by its ornamentation. In its shape it is somewhat similar to *Baidites* Brühwiler and Bucher (submitted [a]) from Oman, which differs by its suture line with a very narrow ventral lobe, its more pronounced umbilical margin and its weaker ornamentation. In its suture line, *Hermannites* is similar to *Anaxenaspis*, which differs by its elliptical whorl shape with a well rounded venter.

Hermannites rursiradiatus gen. et sp. nov.

Plate 6, figures 1-3

Derivation of name. Refers to the rursiradate ribs.

Holotype. Specimen PIMUZ 28261, Plate 6, figure 1a-e.

Type locality. Mud, Spiti, India.

Type horizon. Sample M03-20; *Brayardites compressus* beds.

Diagnosis. As for the genus.

Occurrence. Samples M03-20, M03-24, M05-26A, Gu21, HB1005, HB1033, Lo-SFB1; *Brayardites compressus* beds.

Description. Large, evolute and compressed shell. Upper flanks subparall, lower flanks convergent. Venter subtabulate with rounded shoulders. Umbilicus wide with inclined wall and rounded shoulders. Ornamentated with rursiradiate ribs that tend to thicken at the umbilical margin. Ribs attenuated on outer whorls. Growth lines biconcave. Suture line ceratitic with moderately long saddles; auxiliary series relatively long.

Measurements. See appendix.

Genus FLEMINGITES Waagen, 1895

Type species. *Ceratites flemingianus* de Koninck, 1863.

Flemingites sp. indet.

Plate 7, figures 6a-b

Occurrence. Samples HB1013, HB1024; *Flemingites* beds, Losar.

Description. Large, evolute shell with elliptical whorl section. Venter subtabulate with rounded shoulders, but poorly preserved. Umbilicus wide with rounded wall. Flanks ornamented with coarse strigation and radial or rursiradiate, wavy ribs. Suture line not preserved.

Discussion. The poor preservation of our material precludes an identification at the species level.

Genus ANAXENASPIS Kiparisova, 1956

Type species. *Xenaspis orientale* Diener, 1895.

?*Anaxenaspis* sp. indet.

Plate 7, figures 1-4; plate 8 figure 1a-c

Occurrence. Samples M08-48, M05-48, Ma49; *Pseudoceltites multiplicatus* beds, *Nyalamites angustecostatus* beds, Mud.

Description. Moderately evolute shell with an elliptical whorl section. Venter narrowly rounded with indistinct shoulders. Umbilicus with inclined wall and rounded shoulders. Inner whorls ornamented with dense radial folds that fade out towards the venter; outer whorls smooth. Growth lines slightly biconcave. Suture line ceratitic with slightly phylloid saddles, poorly preserved.

Measurements. See Text-fig. 16.

Discussion. The assignment of this species to *Anaxenaspis* is only provisional, since typical members of this genus differ slightly by their suture line with more elongated saddles. This species is very similar to *Hochuliites retrocostatus* Brühwiler and Bucher submitted [b] from the Salt Range, which differs by its simpler suture line with short and non-phylloid saddles.

Genus *Subflemingites* Spath, 1934

Type species. *Subflemingites involutus* Spath (=*Aspidites meridianus involutus* Welter, 1922).

?*Subflemingites compressus* Brühwiler, Bucher and Goudemand (accepted)

Plate 8, figures 2-3

v acc. ?*Subflemingites compressus* Brühwiler *et al.*, fig. 10(1-5).

Occurrence. Samples Ma46, Ma49; *Nyalamites angustecostatus* beds, Mud.

Description. Moderately involute, compressed shell with flat, slightly convex flanks. Venter rounded without distinct shoulder. Umbilicus with low, inclined wall and rounded shoulders. Surface smooth or with weak radial folds on upper flanks. Suture line not preserved.

Measurements. See appendix.

Discussion. This species has recently been described from the *Nyalamites angustecostatus* beds of Tulong, South Tibet (Brühwiler *et al.*, accepted).

Family ARCTOCERATIDAE Arthaber, 1911

Genus BRAYARDITES Brühwiler, Bucher and Goudemand (accepted)

Type species. *Brayardites crassus* Brühwiler Brühwiler, Bucher and Goudemand (accepted).

Brayardites crassus Brühwiler, Bucher and Goudemand (accepted)

Plate 8, figures 4-5

v acc. *Brayardites crassus* Brühwiler *et al.*, fig. 15(1-4), 16(1-6).

Occurrence. Samples M05-20, M03-21; *Brayardites compressus* beds, Mud.

Description. Moderately evolute, shell with thick whorls and strongly convex flanks. Maximum whorl width above mid-flank. Venter broadly arched with rounded shoulders. Umbilicus with steeply inclined wall and rounded shoulders. Ornamentation consists of prorsiradiate ribs that develop elongated tubercles near umbilicus which fade out towards mid-flank. Ornamentation strongly attenuated on adult whorls: ribs become finer and denser, tuberculation disappear. Suture line not preseved.

Measurements. See appendix.

Discussion. This species has recently been described from the *Brayardites compressus* beds of Tulong, South Tibet (Brühwiler *et al.*, accepted).

Brayardites compressus Brühwiler, Bucher and Goudemand (accepted)

Plate 9, figures 1-5; plate 10, figure 1

v acc. *Brayardites compressus* Brühwiler *et al.*, fig. 18(1-6).

Occurrence. Samples M03-19, M08-21, M08-21, M08-22, M05-23, M03-24, M06-24, Mud; Gu-21, Guling; HB1005, Losar; *Brayardites compressus* beds.

Description. Moderately evolute, compressed shell with flat, convergent flanks. Maximum whorl width near umbilical border. Venter subtabulate with rounded shoulders. Umbilicus with high, vertical wall and rounded shoulders. Ornamentation consists of prorsiradiate, biconcave ribs that develop strong tubercles near umbilicus and fade out towards mid-flank. Ribs and tubercles become finer and denser on adult whorls. Growth lines biconcave. Suture line ceratitic with relatively deep lobes.

Measurements. See appendix.

Discussion. This species has recently been described from the *Brayardites compressus* beds of Tulong, South Tibet (Brühwiler *et al.*, accepted) and of the Salt Range (Brühwiler *et al.*, submitted [b]).

Genus NAMMALITES Brühwiler, Bucher and Goudemand (accepted)

Type species. *Kazakhstanites pilatoides* Guex, 1978.

Nammalites pilatoides (Guex, 1978)

Plate 10, figures 2-10; plate 11, figure 1a-d

	1909	*Meekoceras* sp. ind. aff. *pilato* Krafft and Diener, p. 42, pl. 28, fig. 2a-c.
	1968	*Subvishnuites* cf. *enveris* (Arthaber); Kummel, p. 491, pl. 1, figs 8-9.
	1968	*Wasatchites* sp. indet. Kummel, p. 500, pl. 3, figs 10-11.
	1968	*Eoptychites* sp. indet. Kummel and Erben, p. 120, pl. 22, figs 10-11.
v	1978	*Kazakhstanites pilatoides* Guex, p. 109, pl. 6, fig. 5, 6, 16.
v ?	1978	*Kazakhstanites pilatoides* Guex, p. 109, pl. 8, fig. 6.
v p	1978	*Anasibirites pluriformis* Guex, pl. 4, fig. 3 only.
v	acc.	*Nammalites pilatoides* (Guex); Brühwiler *et al.* fig. 21(6-8).
v	subm.	*Nammalites pilatoides* (Guex); Brühwiler and Bucher, submitted [a].
v	subm.	*Nammalites pilatoides* (Guex); Brühwiler and Bucher, submitted [b].

Occurrence. Samples M08-29, Ma28b, E22/23, M06-39, M05-40, Mud; sample LTB1, Lalung; sample G06-43, Guling; samples HB1029, HB1030, HB1004, HB1032 (?), Losar; *Nammalites pilatoides* beds.

Description. Moderately involute, slightly compressed shell with convex, convergent flanks. Maximum whorl width at umbilical border. Venter broadly rounded to subtabulate with rounded shoulders. Umbilicus with vertical wall and rounded shoulders. Ornamentation consists of distant, rursiradiate ribs that tend to develop tubercles or elongated bullae near the umbilicus and then fade out towards the venter. A fine strigation is observed on the venter of well preserved specimens. Suture line ceratitic with deep lobes.

Measurements. See Text-fig. 17.

Discussion. This species has recently been described from the *Nammalites pilatoides* beds of Tulong, South Tibet (Brühwiler *et al.*, accepted), of the Salt Range (Brühwiler *et al.* submitted [b]) and of Oman (Brühwiler *et al.* submitted [a]).

Genus ESCARGUELITES gen. nov.

Type species. *Escarguelites spitiensis* gen. et sp. nov.

Derivation of name. Named after Gilles Escarguel (Lyon).

Type species. *Escarguelites spitiensis* gen. et sp. nov.

Composition of the genus. Type species only.

Diagnosis. Evolute member of Arctoceratidae with strong, sharp and rursiradiate ribs.

Discussion. The assignment of *Escarguelites* to Arctoceratidae is based on its similarity with *Nammalites*. Especially the ornamentation of the inner whorls of *Escarguelites* is very similar to that of *Nammalites*.

Escarguelites spitiensis gen. et sp. nov.

Plate 11, figures 2-4

Derivation of name. Named derived from the Spiti region.

Holotype. Specimen PIMUZ 28294, Plate 11, figure 2a-e

Type locality. Mud, Spiti, India.

Type horizon. Sample M08-29; *Escarguelites spitiensis* horizon.

Diagnosis. As for the genus.

Occurrence. Sample M08-29, Mud; sample HB1004, Losar; *Escarguelites spitiensis* horizon.

Description. Moderately evolute shell with convex flanks. Venter broad and subtabulate with rounded shoulders. Umbilicus with vertical wall and rounded shoulders. Ornamentation consists of strong, sharp and rursiradiate ribs. On inner whorls, ribs are strongest near umbilicus. Ribs cross the venter. Suture line ceratitic; first lateral lobe deep, second lateral saddle very broad, third lateral saddle very small.

Measurements. See appendix.

Genus NUETZELIA gen. nov.

Type species. *Nuetzelia himalayica* gen. et sp. nov.

Derivation of name. Named after Alex Nützel (Munich).

Type species. *Nuetzelia himalayica* gen. et sp. nov.

Composition of the genus. Type species only.

Diagnosis. Strongly compressed, involute Arctoceratidae with a narrow, tabulate venter.

Discussion. The assignment to Arctoceratidae is mainly based on the overall similarity with *Arctoceras*, which differs, however, by its rounded venter and less compressed whorls. *Nuetzelia* differs from other arctoceratids by its involute coiling and its overhanging umbilical wall. Proptychitidae generally differ by a more complex suture line.

Nuetzelia himalayica gen. et sp. nov.

Plate 10, figures 11-13

Derivation of name. Named derived from the Himalayas.

Holotype. Specimen PIMUZ 28291, Plate 10, figure 12a-b.

Type locality. Losar, Spiti, India.

Type horizon. Sample HB1004; *Escarguelites spitiensis* horizon.

Diagnosis. As for the genus.

Occurrence. Samples HB1004; *Escarguelites spitiensis* horizon, Losar.

Description. Small, involute and strongly compressed shell with convergent flanks. Venter narrow and tabulate with angular shoulders. Umbilicus small and deep with an overhanging wall and angular shoulders. Surface smooth except for biconcave growth lines. Suture line ceratitic; first and second lateral saddle long and very narrow, lobes broad.

Measurements. See appendix.

Genus TRUEMPYCERAS Brühwiler and Bucher, submitted [b]

Type species. *Anasibirites pluriformis* Guex 1978.

Truempyceras compressum sp. nov.

Plate 12, figures 1-8

Derivation of name. Refers to the more compressed whorls with respect to the type species.

Holotype. Specimen PIMUZ 28304, Plate 12, figure 8a-e.

Type locality. Lalung, Spiti, India.

Type horizon. Sample LTB3; *Truempyceras compressum* horizon.

Diagnosis. Relatively compressed *Truempyceras* with weak ornamentation.

Occurrence. Samples M05-43, M05-44, E22, Mud; sample LTB3, Lalung; sample HB1029, Losar; *Truempyceras compressum* horizon.

Description. Moderately involute, compressed shell with flat, slightly convergent flanks. Venter subtabulate with angular to slightly rounded shoulders. Umbilicus with a high, vertical wall and marked, slightly rounded shoulders. Ornamentation consists of weak, slightly biconcave ribs that strengthen and form indistinct nodes on ventral and umbilical shoulders. Strongest ribs may cross the venter. Suture line ceratitic with relatively deep lobes.

Measurements. See Text-fig. 18.

Discussion. This species is very similar to the type species from the *Nammalites pilatoides* beds of the Salt Range (Brühwiler and Bucher submitted [b]) but differs by its more compressed whorl section and its weaker ornamentation.

Familiy USSURIIDAE Spath 1930

Ussuriidae gen. et sp. indet.

Plate 6, figure 4; plate 7, figure 5a-b

Occurrence. A single, incomplete specimen found as a float in the *"Parahedenstroemia"* Beds, probably from the horizon of sample M03-40 or higher.

Description. Very involute, compressed oxycone with slightly convex flanks. Maximum thickness near umbilicus. Venter narrowly rounded. Surface poorly preserved. Suture line ammonitic.

Discussion. The ammonitic suture line and the shape of our specimen favor assignment to *Metussuria* Spath, 1934 or *Parussuria* Spath, 1934. *Parussuria* differs from *Metussuria* by its strigation, but otherwise these two genera are very similar and may in fact be synonyms. The poor preservation of our single specimen precludes a identification at the species level.

Family PRIONITIDAE Hyatt, 1900

Genus PRIONITES Waagen, 1895

Type species. *Prionites tuberculatus* Waagen, 1895.

Prionites sp. indet.

Plate 13, figures 1-3

Occurrence. Sample Ma49; *Nyalamites angustecostatus* beds, Mud.
Description. Very involute, compressed shell with convergent flanks. Maximum whorl width at upper third of flanks. Venter tabulate with angular shoulders on inner whorls, subtabulate with rounded shoulders on outer whorls. Umbilicus deep and funnel-shaped with steeply inclined wall and rounded shoulders. Inner whorls smooth, outer whorls with prorsiradiate, distant swellings on upper flanks. Growth lines biconcave and slightly prorsiradiate. Suture line ceratitic with broad saddles and narrow lobes.

Measurements. See appendix.

Discussion. This species is somewhat intermediate between *Prionites tuberculatus* Waagen, 1895 from the Salt Range and *P. involutus* Brühwiler *et al.*, accepted from South Tibet. The former differs by its less steep umbilical wall, and the latter by its steeper umbilical wall. *P. laevis*, *P. armatus* and *P. elegans* Welter, 1922 from Timor are here considered as synonyms of *P. tuberculatus* (see Brühwiler *et al.*, submitted [b]).

Genus STEPHANITES Waagen, 1895

Type species. *Stephanites superbus* Waagen, 1895.

Stephanites superbus Waagen, 1895

Plate 13, figure 6a-d

1895 *Stephanites suberbus* Waagen, p. 101, pl. 2, fig. 2a-c.
1895 *Stephanites corona* Waagen, p. 102, pl. 3, fig. 1a-b.
1905 *Stephanites corona* Waagen; Frech, pl. 28, fig. 1.
v, non 1978 *Stephanites corona* Waagen; Guex, pl. 5, fig. 2 (= *Wastatchites distractum*).
v acc. *Stephanites superbus* Waagen; Brühwiler *et al.* fig. 19(7-12).

Occurrence. Samples M05-57, M06-57; *Nyalamites angustecostatus* beds, Mud.

Description. Large, moderately evolute shell with strongly convex flanks. Maximum whorl width near mid-flank. Venter broad and subtabulate with rounded shoulders. Umbilicus deep with well-rounded, inclined wall without distinct shoulders. Ornamentation consists of strong, distant tubercles on flanks, coincinding with maximum whorl width. Suture line ceratitic with very broad first lateral saddle and very low third lateral saddle.

Measurements. See appendix.

Genus WASATCHITES Mathews, 1929

Type species. *Wasatchites perrini* Mathews, 1929.

Wasatchites distractus (Waagen, 1895)

Plate 14, figures 1-8

1895 *Acrochordiceras distractum* Waagen, p. 94, pl. 3, fig. 4a-c.
1895 *Acrochordiceras coronatum* Waagen, p. 96, pl. 3, fig. 5a-c.
1895 *Acrochordiceras* cf. *damesi* Noetling; Waagen, p. 97, pl. 4, fig. 5a-b.
1895 *Acrochordiceras compressum* Waagen, p. 98, pl. 4, fig. 4a-c.
? 1909 *Sibirites* sp. indet. aff. *inflato* Waagen; Krafft and Diener, p. 134, pl. 27, fig. 7.
p 1909 *Sibirites* sp. indet. Krafft and Diener, p. 138, pl. 28, fig. 4a-c.
v ? 1978 *Stephanites corona* Waagen; Guex, pl. 5, fig. 2.
v acc. *Wasatchites distractus* (Waagen); Brühwiler *et al.* fig. 21(1a-b).

Occurrence. Samples Ma92, E29/30, Mud; samples Gu-69A, Gu106, GD92, Guling; *Wasatchites distractus* beds.

Description. Moderately involute shell with eggressive coiling at maturity. Flanks nearly flat, slightly convex and convergent on inner whorls; strongly convex on outer whorls. Maximum whorl width at mid-flank. Venter tabulate with slightly angular shoulders on inner whorls; broadly rounded with indistinct shoulders on outer whorls. Umbilicus deep with well-rounded, inclined wall and indistinct shoulders. Ornamentation consists of spiny tubercles at mid-flank as well as strong radial ribs whose strength increases when crossing the venter. Transition to maturity shows attenuation of ribbing but persistance of lateral spines. Suture line poorly preserved; first and second lateral saddles broad and tapered.

Measurements. See Text-fig. 19.

Discussion. Boreal representatives of *Wasatchites* (e.g. *W. perrini* Spath, 1934) essentially differ from *W. distractum* by the more umbilical position of their spines.

Genus ANASIBIRITES Mojsisovics, 1896

Type species. *Sibirites kingianus* Waagen, 1895, p. 108, pl. 8, figs 1a-c, 2a-c.

Anasibirites kingianus (Waagen, 1895)

Plate 13, figures 5; plate 14, figures 9-16

1895 *Sibirites kingianus* Waagen, p. 108, pl. 8, figs 1-2.
1895 *Sibirites chidruensis* Waagen, p. 109, pl. 8, figs 3-4.
1895 *Sibirites inaequicostatus* Waagen, p. 113, pl. 8, figs 7-8.
? 1895 *Sibirites ceratitoides* Waagen, p. 115, pl. 8, fig. 10a-c.
1909 *Sibirites spiniger* Krafft and Diener, p. 131, pl. 31, figs 2, 7.
1909 *Sibirites robustus* Krafft, p. 132, pl. 31, fig. 1.
? 1909 *Sibirites* sp. ind. ex aff. *robusto* Krafft; Krafft, p. 133, pl. 31, fig. 6.
? 1909 *Sibirites spitiensis* Krafft, p. 136, pl. 31, fig. 8.
p 1909 *Sibirites* sp. indet. Krafft, p. 138, pl. 31, figs 4-5.
1929 *Anasibirites kingianus* (Waagen); Mathews, p. 8, pl. 7, figs 14-22.
1968 *Anasibirites kingianus* Waagen; Kummel and Erben, p. 135, pl. 22, figs 12-17; pl. 23, figs 1-18.
v 1978 *Anasibirites kingianus* (Waagen); Guex, pl. 3, fig. 2, 9, pl. 4, fig. 6.

Occurrence. Sample Ma92, Mud; samples Gu106, GD92, Guling; *Wasatchites distractus* beds.

Description. Moderately involute shell with convex, slightly compressed flanks. Venter arched with rounded shoulders. Umbilicus with inclined wall and rounded shoulders. Ornamentation consists of straight to sinuous, projected ribs of varying strength that cross the venter.
Suture line simple with tapered saddles, poorly preserved.

Measurements. See Text-fig. 20.

Discussion. For recent discussions on the genus *Anasibirites*, see Brayard and Bucher (2008) and Brühwiler and Bucher (submitted [b]).

Family PARANANNITIDAE Tozer, 1971

Genus PARANANNITES Hyatt and Smith, 1905

Type species. *Paranannites aspenensis* Hyatt and Smith, 1905.

Paranannites sp. indet.

Plate 15, figures 1-7

Occurrence. Samples M06-39, M05-40, Ma28b, Mud; sample G06-43, Guling; sample HB1006, HB1032, Losar; *Truempyceras compressum* horizon.

Description. Moderately involute, globose shell with convex, slightly compressed flanks. Venter arched with indistinct shoulders. Umbilicus deep with high, vertical wall and subangular, slightly rounded shoulders. Ornamentation consists of fine, radial and concave folds. Suture line ceratitic with tapered first lateral saddle, incompletely preserved.

Measurements. See Text-fig. 21.

Discussion. This species is similar to the type species but differs by its thicker whorls and its slightly more evolute coiling.

Genus OWENITES Hyatt and Smith, 1905

Type species. *Owenites koeneni* Hyatt and Smith, 1905.

Owenites koeneni Hyatt and Smith, 1905.

Plate 15, figure 11a-c

1905 *Owenites koeneni* Hyatt and Smith, p. 83, pl. 10, figs 1-22.
1932 *Owenites koeneni* Hyatt and Smith; Smith, pl. 10, figs 1-22.
1932 *Owenites egrediens* Welter; Smith, p. 100, pl. 52, figs 6-8.
1932 *Owenites zitteli* Smith, p. 101, pl. 52, figs 1-5.
1934 *Owenites koeneni* Hyatt and Smith; Spath, p. 185, figs 57a-c.

1947 *Owenites* aff. *egrediens* Welter; Kiparisova, p. 139, pl. 32, figs 1-3.
1955 *Kingites shimizui* Sakagami, p. 138, pl. 2, fig. 2.
1957 *Owenites koeneni* Hyatt and Smith; Kummel, pl. 138, fig. 171: 8a-b.
1959 *Owenites costatus* Chao, p. 249, pl. 22, figs 7-18, 22, 23, fig. 26c.
1959 *Owenites pakungensis* Chao, p. 248, pl. 21, figs 6-8.
1959 *Owenites pakungensis* var. *compressus* Chao, p. 248, pl. 21, figs 4,5, fig. 26a.
1959 *Pseudowenites oxynotus* Chao, p. 252, pl. 23, figs 1-16, figs 27a-d.
? 1959 *Owenites* cf. *koeneni* Hyatt and Smith; Kummel, p. 441, figs 2-4.
1959 *Owenites shimizui* Sakagami; Kummel, p. 430.
1960 *Owenites shimizui* Sakagami; Kummel and Sakagami, p. 6, pl. 5, figs 5-6.
1962 *Owenites koeneni* Hyatt and Smith; Kummel and Steele, p. 674, pl. 101, figs 3-7.
1962 *Owenites koeneni* Hyatt and Smith; Popov, p. 44, pl. 6, fig. 6.
1965 *Owenites koeneni* Hyatt and Smith; Kuenzi, p. 374, pl. 53, figs 1-6, figs 3d,6.
1966 *Owenites koeneni* Hyatt and Smith; Hada, p. 112, pl. 4, figs 2-4.
1968 *Owenites koeneni* Hyatt and Smith; Kummel and Erben, p. 121, fig. 12, pl. 19, figs 10-15.
1968 *Owenites carinatus* Shevyrev, p. 189, pl. 16, fig. 1.
1968 *Owenites koeneni* Hyatt and Smith; Zakharov, p. 94, pl. 18, figs 1-3.
1973 *Owenites koeneni* Hyatt and Smith; Collignon, p. 139, pl. 4, figs 2-3.
1979 *Owenites koeneni* Hyatt and Smith; Nichols and Silberling, pl. 1, figs 17, 18.
1981 *Owenites koeneni* Hyatt and Smith; Bando, p. 158, pl. 17, fig. 7.
1984 *Owenites carinatus* Shevyrev; Vu Khuc, p. 81, pl. 6, figs 1-4.
1984 *Pseudowenites oxynotus* Chao; Vu Khuc, p. 82, pl. 7, figs 3, 4.
1990 *Owenites koeneni* Hyatt and Smith; Shevyrev, p. 118, pl. 1, fig. 5.
1995 *Owenites koeneni* Hyatt and Smith; Shevyrev, p. 51, pl. 5, figs 1-3.
2004 *Owenites pakungensis* Chao; Tong *et al.*, p. 199, pl. 2, figs 9-10, fig. 7.
v 2008 *Owenites koeneni* Hyatt and Smith; Brayard and Bucher, p. 67, pl. 36, figs 1-8.
v acc. *Owenites koeneni* Hyatt and Smith; Brühwiler *et al.* fig. 21(9a-b).

Occurrence. Sample M03-57, Mud; *Nyalamites angustecostatus* beds.

Description. Involute, somewhat compressed shell with an inflated, lenticular whorl section. Umbilical wall inclined, imparting a conical shape to the umbilicus. Venter narrowly rounded to acute. Surface smooth. Suture line not preserved.

Measurements. See appendix.

Owenites cf. *simplex* Welter, 1922

Plate 15, figures 8-9

Occurrence. Samples M06-39, Ma28b, Mud; sample G06-43, Guling; *Truempyceras compressum* horizon.

Description. Moderately involute, slightly compressed shell with convex flanks. Venter subangular with indistinct shoulders. Umbilicus deep with inclined wall and rounded shoulders. Ornamentation consists of fine, radial folds. Suture line not preserved.

Measurements. See appendix.

Discussion. The shape of this species is somewhat intermediate between that of *Paranannites* and *Owenites*. Typical *Paranannites* have a rounded venter; typical *Owenites* have a more acute venter. *Paranannites subangulosus* Brayard and Bucher, 2008 from South China differs by its thicker whorls.

Owenites carpenteri Smith 1932

Plate 15, figures 12-14

	1932	*Owenites carpenteri* Smith, p. 100, pl. 54, figs 31-34.
	1966	*Owenites carpenteri* Smith; Hada, p. 112, pl. 4, figs 1a-e.
	1968	*Owenites costatus* Chao; Kummel and Erben, p. 122, fig. 12l.
	1973	*Owenites carpenteri* Smith; Collignon, p. 139, pl. 4, figs 5-6.
v	2008	*Owenites carpenteri* Smith; Brayard and Bucher, p. 70, pl. 43, figs 15-16.
v	acc.	*Owenites carpenteri* Smith; Brühwiler *et al.* fig. 22(7-8).

Occurrence. Sample Ma49, Mud; sample Gu72, Guling; *Nyalamites angustecostatus* beds.

Description. Small, extremely involute shell with a subtriangular whorl section. Venter narrow and subangular. Umbilicus occluded. Maximum whorl width at umbilicus. Shell surface smooth except for deep constrictions visible on internal mould only. Suture line ceratitic with five lateral saddles; lobes weakly indented.

Measurements. See appendix.

Owenites sp. indet.

Plate 15, figure 10a-d

Occurrence. A single, very small specimen from sample Gu44, Guling; *Truempyceras compressum* horizon.

Description. Very small, involute shell. Venter narrow and subangular. Umbilicus small with inclined wall. Maximum whorl width at umbilical edge. Ornamentation consists of prorsiradiate, sinuous and weak plications. Suture line ceratitic with four lateral saddles; lobes weakly indented.

Discussion. Identification at the species level is not possible due to the small size of our specimen.

STECKITES gen. nov.

Derivation of name. Named after Albrecht Steck (Lausanne).

Type species. *Steckites brevus* gen. et sp. nov.

Composition of the genus. Type species only.

Diagnosis. Paranannitidae with an oxyconic shape similar to that of *Owenites*, but with a suture line with a very short auxiliary series.

Discussion. This genus is very similar to *Owenites*. However, *Owenites* displays a suture line with several well individualized auxiliary saddles.

Steckites brevus gen. et sp. nov.

Derivation of name. Refers to the short auxiliary series of the suture line.

Holotype. Specimen PIMUZ 28335, Plate 15, figure 15a-d

Type locality. Mud, Spiti, India.

Type horizon. Sample Ma26; *Truempyceras compressum* horizon.

Diagnosis. As for the genus.

Occurrence. Samples Ma26, Mud-E21/22, M06-39, M06-40; *Truempyceras compressum* horizon, Mud.

Description. Moderately involute, slightly compressed shell with convex flanks. Venter subangular with indistinct shoulders. Umbilicus with inclined wall and rounded shoulders. Surface smooth except for prorsiradiate, sinuous and weak plications that cross the venter. Suture line ceratitic, with three lateral saddles and a very short auxiliary series.

Measurements. See appendix.

Family MELAGATHICERATIDAE Tozer, 1971

Genus JUVENITES Smith, 1927

Type species. *Juvenites kraffti* Smith, 1927.

Juvenites cf. *spathi* (Frebold 1930)

Plate 16, figures 1-5

Occurrence. Sample M05-23, *Brayardites compressus* beds, Mud. A single specimen from sample LoA-SFB, *Nammalites pilatoides* beds (?), Losar.

Description. Moderately involute, globose shell with outer whorls. Flanks convex, converging to the venter from the umbilical margin. Umbilicus deep, with vertical wall and rounded shoulders. Ornamentation consists of prorsiradiate constrictions that cross the venter. Suture line not preserved.

Measurements. See Text-fig. 22.

Discussion. Typical representatives of *Juvenites spathi* display a subtrigonal whorl section, especially on outer whorls (e.g. Brayard and Bucher 2008), which is not observed on our specimens. Therefore, the assignment to *Juvenites spathi* is only tentative.

Genus JINYACERAS Brayard and Bucher, 2008

Type species. *Jinyaceras bellum* Brayard and Bucher, 2008.

Jinyaceras hindostanum (Diener, 1897)

Plate 16, figures 6-12

1897 *Nannites hindostanus* Diener, p. 68, pl. 7, figs 3, 11-12.
1897 *Nannites herberti* Diener, p. 69, pl. 7, fig. 2.
v acc. *Jinyaceras hindostanum* (Diener); Brühwiler *et al.*, fig. 22(4-6).

Occurrence. Samples Ma24c, M03-19, M03-20, M03-21, M08-21, M06-24, Mud; sample Gu-23, Guling; samples HB1005, HB1025, HB1033, Losar; *Brayardites compressus* beds.

Description. Small, moderately involute to moderately evolute, laterally compressed shell with flat, subparallel flanks. Venter broadly arched, with rounded ventral shoulders. Umbilicus with vertical wall and subangular shoulders. Ornamentation consists of prorsiradiate constrictions that nearly disappear on venter. Constrictions are deepest on evolute variants. Suture line simple with only two lateral saddles, lobes apparently not indented.

Measurements. See Text-fig. 23.

Genus JUVENITES Smith, 1927

Type species. *Jinyaceras kraffti* Smith, 1927.

Juvenites procurvus Brayard and Bucher, 2008

Plate 16, figures 13-14

v 2008 *Juvenites procurvus* Brayard and Bucher, p. 32, pl. 22, figs 6-12, text-fig. 30.

Occurrence. Sample M08-48; *Pseudoceltites multiplicatus* beds, Mud.

Description. Small, subglobose and moderately involute shell with rounded venter and convex flanks. Umbilicus with vertical wall and rounded shoulders. Ornamentation consists of numerous, deep and projected constrictions. Suture line simple with only two lateral saddles, and lobes apparently smooth.

Measurements. See appendix.

Genus SUBVISHNUITES Spath, 1930

Type species. *Subvishnuites welteri* Spath, 1930 (= *Vishnuites* spec. Welter, 1922).

Subvishnuites posterus sp. nov.

Plate 16, figures 15-20

v subm. *Subvishnuites* sp. indet. Brühwiler and Bucher, submitted [a]).

Derivation of name. Refers to the younger age of this species with respect to the type species.

Holotype. Specimen PIMUZ 28360, Plate 16, figure 20a-d.

Type locality. Mud, Spiti, India.

Type horizon. Sample M08-70; *Subvishnuites posterus* beds.

Diagnosis. Relatively involute *Subvishnuites* with flattened flanks and a relatively deep umbilicus.

Occurrence. Sample M08-70; *Subvishnuites posterus* beds, Mud.

Description. Moderately evolute, compressed shell. Flanks convex; subparallel on the upper half and strongly converging on the lower half. Venter narrowly rounded. Umbilicus with vertical wall and rounded shoulders. Surface smooth or ornamented with weak ribs that cross the venter. Suture line ceratitic with long, slightly phylloid saddles and deep lobes.

Measurements. Text-figure 24.

Discussion. The type species *Subvishnuites welteri* Spath, 1930 and *S. stokesi* Kummel and Steele, 1962 have a middle Smithian age and thus are slightly older than this species (see also Brayard and Bucher 2008). *S. posterus* differs from these species by being more involute. Additionally, *S. welteri* has a shallower umbilicus. *S. posterus* has recently been found in an exotic block of hallstatt facies from Oman, associated with *Anasibirites multiformis* (*Subvishnuites* sp. indet. in Brühwiler *et al.*, submitted [a]).

Family ASPENITIDAE Spath, 1934

Type species. *Aspenites acutus* Hyatt and Smith, 1905.

Aspenites acutus Hyatt and Smith, 1905

Plate 17, figures 1-4

1905 *Aspenites acutus* Hyatt and Smith, 1905, p. 96, pl. 2, figs 9-13; pl. 3, figs 1-5.
? 1909 *Hedenstroemia acuta* Krafft and Diener, p. 157, pl. 9, fig. 2.
1922 *Aspenites acutus* Hyatt and Smith; Welter, p. 98, fig. 7.
1922 *Aspenites laevis* Welter, p. 99, pl. 1, figs 4-5.
1932 *Aspenites acutus* Hyatt and Smith; Smith, p. 86, pl. 2, figs 9-13, pl. 3, figs 1-5, pl. 30, figs 1-26, pl. 60, figs 4-6.
1932 *Aspenites laevis* Welter; Smith, p. 86, pl. 28, figs 28-33.
1932 *Aspenites obtusus* Smith, p. 86, pl. 31, figs 8-10.
1934 *Aspenites acutus* Hyatt and Smith; Spath, p. 229, fig. 76.
? 1934 *Parahedenstroemia acuta* Krafft and Diener; Spath, p. 221, fig. 70.
1957 *Aspenites acutus* Hyatt and Smith; Kummel, p. L142, fig. 173a-c.
1959 *Aspenites acutus* Hyatt and Smith; Chao, p. 269, pl. 35, figs 12-18, 23, fig. 34a.
1959 *Aspenites laevis* Welter; Chao, p. 270, pl. 35, figs 9-11, fig. 34b.
1962 *Aspenites acutus* Hyatt and Smith; Kummel and Steele, p. 692, pl. 99, figs 16-17.
1962 *Hemiaspenites obtusus* Smith; Kummel and Steele, p. 666, pl. 99, fig. 18.
1979 *Aspenites* cf. *acutus* Hyatt and Smith; Nichols and Silberling, pl. 1, figs 10-11.
1979 *Aspenites acutus* Hyatt and Smith; Nichols and Silberling, pl. 1, figs 12-14.
v. 2008 *Aspenites acutus* Hyatt and Smith; Brayard and Bucher, p. 77, pl. 42, figs 1-9.
v acc. *Aspenites acutus* Hyatt and Smith; Brühwiler *et al.*, fig. 22(12-13).

Occurrence. Samples M03-19, M08-21, M05-23, M03-24(?), E18, Mud; samples G06-20, Gu-21, Guling; samples HB1005, HB1024, LoSFB1, Losar; *Brayardites compressus* beds.

Description. Extremely involute, very compressed shell with slightly convex flanks. Maximum whorl width at mid-flank. Whorl section lanceolate, with an acute keel. Umbilicus occluded. Umbilical region slightly depressed. Surface nearly smooth except for fine radial folds and falcoid growth lines. Suture line ceratitic with two adventitious saddles and a long auxiliay series.

Measurements. See appendix.

Discussion. *Aspenites acutus* is a relatively long-ranging species and is known from the early to the middle Smithian (Brayard and Bucher, 2008, Brühwiler *et al.*, submitted [a]).

Genus PSEUDASPENITES Spath, 1934

Type species. *Aspenites layeriformis* Welter, 1922.

Pseudaspenites cf. *layeriformis* (Welter, 1922)

Plate 17, figures 5-7

Occurrence. Samples M08-21, M03-24, Mud; sample HB1005, Losar; *Brayardites compressus* beds.

Description. Involute, very compressed oxycone similar to *Aspenites,* but with an egressive umbilicus. Venter acutely keeled and slightly convex flanks. Umbilicus with rounded shoulders. Surface smooth except for biconcave growth lines and very weak biconcave folds. Suture line ceratitic with an adventitious lobe and a well individualized auxiliary series.

Measurements. See appendix.

Discussion. The type species from Timor differs slightly by its folds but is otherwise very similar. The specimens from South China described as *Pseudaspenites layeriformis* by Brayard and Bucher (2008) are slightly more evolute than our specimens.

Family HEDENSTROEMIIDAE Waagen, 1895

Genus PSEUDOSAGECERAS Diener, 1895

Type species. *Pseudosageceras* sp. indet. Diener, 1895.

Pseudosageceras augustum (Brayard and Bucher, 2008)

Plate 17, figures 8-10

v 2008 *Hedenstroemia augusta* Brayard and Bucher, p. 72, pl. 39, figs 1-11, text-fig. 63.

v subm. *Pseudosageceras augustum* (Brayard and Bucher); Brühwiler *et al.*, fig. 21(10-11).

Occurrence. Sample M08-70; *Subvishnuites posterus* beds, Mud.

Description. Extremely involute, compressed oxyconic shell. Flanks with weak, but distinct longitudinal line at about mid-flank, marking a very slight change in slope between the lower and upper portions of flanks. Venter very narrow and weakly bicarinate. Umbilicus closed. Surface smooth except for strongly biconcave growth lines. Suture line ceratitic with several adventitious lobes and long auxiliary series.

Measurements. See appendix.

Discussion. This species was originally assigned to *Hedenstroemia*, but it has been transferred to *Pseudosageceras* on the basis of its suture line, which exhibits several adventitious lobes and not only a single one like true *Hedenstroemia* (Brühwiler *et al.*, accepted).

Family incertae sedis

Genus SHIGETACERAS Brühwiler, Bucher and Goudemand (accepted)

Type species. *Hemiprionites dunajensis* Zakharov, 1968.

Shigetaceras dunajensis (Zakharov, 1968)

Plate 17, figure 11a-d

1968 *Hemiprionites dunajensis* Zakharov, p. 125, pl. 23, figs 6-8.

? 2009 *Hemiprionites* sp. indet. Shigeta and Zakharov, p. 87, fig. 74.

v acc. *Shigetaceras dunajensis* (Zakharov, 1968); Brühwiler *et al.*, fig. 13(1-4).

Occurrence. A single specimen from sample M03-40; *Truempyceras compressum* horizon, Mud.

Description. Compressed and involute shell with slightly convex and convergent flanks. Venter tabulate with angular shoulders. Umbilicus small and deep with vertical wall and narrow, slightly rounded shoulders. Surface smooth. Suture line not preserved.

Measurements. See appendix.

Discussion. This species has recently been found in the *Nammalites pilatoides* beds at Tulong, South Tibet (Brühwiler *et al.* accepted).

Genus KRAFFTICERAS gen. nov.

Derivation of name. Named after A.v. Krafft.

Type species. *Meekoceras pseudoplanulatum* Krafft and Diener, 1909.

Composition of the genus. Type species only.

Diagnosis. Platyconic and moderately involute Meekocerataceae with a bicarinate venter and a deep umbilicus with a vertical wall.

Discussion. The bicarinate venter of *Kraffticeras* is similar to that of *Meekoceras*, which differs by its funnel-shaped umbilicus. The umbilicus and the ornamentation of *Kraffticeras* may indicate affinities with Arctoceratidae.

Kraffticeras pseudoplanulatum (Krafft and Diener, 1909) gen. nov.

Plate 16, figures 21-24

1909 *Meekoceras pseudoplanulatum* Krafft and Diener, p. 30, pl. 6, fig. 3a-c.

Occurrence. Samples HB1013, HB1026; *Flemingites* beds, Losar.

Description. Moderately involute, compressed shell. Flanks nearly flat, only slighlty convex. Venter bicarinate. Umbilicus deep with vertical wall and subangular shoulders. Surface smooth or ornamented with weak plications that are most prominent near umbilical margin. Suture line ceratitic with long saddles and deep lobes.

Measurements. See Text-fig. 25.

Gen. et sp. indet. A

Plate 13, figure 4a-d

Occurrence. A single specimen from sample HB1004; *Escarguelites spitiensis* horizon, Losar.

Description. Moderately involute, platycone shell with slightly convex flanks. Venter narrow and tabulate with angular shoulders. Umbilicus with inclined wall and rounded shoulders. Surface smooth except for distinctly biconcave growth lines. Suture line ceratitic with broad lobes.

Measurements. See appendix.

Discussion. The overall shape of this specimen is similar to that of *Meekoceras*, which differs by its bicarinate venter and its narrower umbilicus.

Acknowledgements. O. N. Bhargava (Haryana, India), D. Ware and T. Galfetti (both Zürich) are acknowleded for their help in the field. Technical support for preparation was provided by Markus Hebeisen, Julia Huber and Leonie Pauli. Photographs of ammonoids were taken by R. Roth. Claude Monnet is thanked for providing his statistical analyses software. This study was supported by the Swiss National Foundation (project n° 200020-127716; to H.B.). Earlier field work of L.K. was sponsored by the Austrian Academy of Sciences, National Committee for IGCP, within project 467 (Triassic Time).

REFERENCES

ARTHABER, G. 1911. Die Trias von Albanien. *Beiträge zur Paläontologie und Geologie Österreich-Ungarns und des Orients*, **24**, 169-288.

BANDO, Y. 1981. Lower Triassic ammonoids from Guryul Ravine and the spur three kilometers north of Barus. *Palaeontologia Indica n. ser.*, **46**, 135-178.

BHARGAVA, O. N., KRYSTYN, L., BALINI, M., LEIN, R. and NICORA, A. 2004. Revised litho- and sequence stratigraphy of the Spiti Triassic. *Albertiana*, **30**, 21-39.

BRAYARD, A. and BUCHER, H. 2008. Smithian (Early Triassic) ammonoid faunas from northwestern Guangxi (South China): taxonomy and biochronology. *Fossils and Strata*, **55**, 1-179.

--- --- ESCARGUEL, G., FLUTEAU, F., BOURQUIN, S. and GALFETTI, T. 2006. The Early Triassic ammonoid recovery: Paleoclimatic significance of diversity gradients. *Palaeogeography, Palaeoclimatology, Palaeoecology*, **239**, 374-395.

--- ESCARGUEL, G., BUCHER, H., MONNET, C., BRÜHWILER, T., GOUDEMAND, N., GALFETTI, T. and GUEX, J. 2009. Good Genes and Good Luck: Ammonoid Diversity and the End-Permian Mass Extinction. *Science*, **325**, 1118-1121.

BRÜHWILER, T. and BUCHER, H. submitted [a]. Systematic palaeontology. *In* BRÜHWILER, T., BUCHER, H. GOUDEMAND, N. and GALFETTI, T. (submitted [a]). Smithian (Early Triassic) ammonoid faunas from Exotic Blocks from Oman: taxonomy and biochronology. *Palaeontographica*.

--- --- submitted [b]. Systematic palaeontology. *In* BRÜHWILER, BUCHER, H., WARE, D., ROOHI, G., HERMANN, E., HOCHULI, P.A., ROOHI, G., REHMAN, K. and YASEEN, A. (submitted [b]). Smithian (Early Triassic) ammonoids from the Salt Range, Pakistan. *Special Papers in Palaeontology*.

--- --- and GOUDEMAND, N. accepted. Smithian (Early Triassic) ammonoids from Tulong, South Tibet. *Geobios*.

--- --- --- and BRAYARD, A. 2007. Smithian (Early Triassic) ammonoid faunas of the Tethys: new preliminary results from Tibet, India, Pakistan and Oman. *New Mexico Museum of Natural History and Science Bulletin*, **41**, 25-26.

--- --- --- and GALFETTI, T. (submitted [a]). Smithian (Early Triassic) ammonoid faunas from Exotic Blocks from Oman: taxonomy and biochronology. *Palaeontographica*.

--- --- WARE, D., ROOHI, G., HERMANN, E., HOCHULI, P.A., ROOHI, G., REHMAN, K. and YASEEN, A. (submitted [b]). Smithian (Early Triassic) ammonoids from the Salt Range, Pakistan. *Special Papers in Palaeontology*.

--- GOUDEMAND, N., GALFETTI, T., BUCHER, H., BAUD, A., WARE, D., HERMANN, E., HOCHULI, P. A. and MARTINI, R. 2009. The Lower Triassic sedimentary and carbon isotope records from Tulong (South Tibet) and their significance for Tethyan palaeoceanography. *Sedimentary Geology*, **222**, 314-332.

--- WARE, D., BUCHER, H., KRYSTYN, L. and GOUDEMAND, N. (submitted [c]). New Early Triassic ammonoid faunas from the Dienerian/Smithian boundary beds at the Induan/Olenekian GSSP candidate at Mud (Spiti, Northern India). *Journal of Asian Earth Sciences*.

BUCHER, H., NASSICHUK, W. W. and SPINOSA, C. 1997. A new occurrence of the upper Permian ammonoid *Stacheoceras trimurti* Diener from the Himalayas; Himachal Pradesh, India. *Eclogae Geologicae Helvetiae*, **90**, 599-604.

CHAO, K. 1959. Lower Triassic ammonoids from Western Kwangsi, China. *Palaeontologia Sinica. New Series B*, **9**, 355 pp.

COLLIGNON, M. 1973. Ammonites du Trias inférieur et moyen d'Afghanistan. *Annales de Paléontologie (Invertebrés)*, **59**, 127-163.

DE KONINCK, L. G. 1863. Description of some fossils from India, discovered by Dr. A. Fleming, of Edingburgh. *The quarterly Journal of the Geological Society of London*, **19**, 1-19.

DIENER, C. 1895. Triadische Cephalopodenfaunen der ostsibirischen Küstenprovinz. *Mémoirs du Comité Géologique St. Petersburg*, **14**, 1-59.

--- 1897. The Cephalopoda of the Lower Trias. *Palaeontologia Indica, ser. 15, Himalayan Fossils*, **2**, 1-181.

--- 1913. Triassic faunae of Kashmir. *Palaeontologia Indica, n. ser.*, **5**, 1-133.

FREBOLD, H. 1930. Die Altersstellung des Fischhorizontes, des Grippianniveaus und des unteren Saurierhorizontes in Spitzbergen. *Scrifter om Svalbard og Ishavet*, **28**, 1-36.

FRECH, F. 1905. *Lethaea geognostica. Das Mesozoicum. I, Trias*. Stuttgart, 623 pp.

GALFETTI, T., BUCHER, H., BRAYARD, A., HOCHULI, P. A., WEISSERT, H., GUODUN, K., ATUDOREI, V. and GUEX, J. 2007*a*. Late Early Triassic climate change: Insights from carbonate carbon isotopes, sedimentary evolution and ammonoid paleobiogeography. *Palaeogeography, Palaeoclimatology, Palaeoecology*, **243**, 394-411.

--- HOCHULI, P. A., BRAYARD, A., BUCHER, H., WEISSERT, H. and VIGRAN, J. O. 2007*b*. Smithian-Spathian boundary event: Evidence for global climatic change in the wake of the end-Permian biotic crisis. *Geology*, **35**, 291-294.

GARZANTI, E., JADOUL, F., NICORA, A. and BERRA, F. 1995. Triassic of Spiti (Tethys Himalaya, India). *Rivista Italiana di Paleontologia e Stratigrafia*, **101**, 267-300.

--- NICORA, A. and RETTORI, R. 1998. Permo-Triassic boundary and lower to middle Triassic in South Tibet. *Journal of Asian Earth Sciences*, **16**, 143-157.

GUEX, J. 1978. Le Trias inférieur des Salt Ranges, Pakistan: problèmes biochronologiques. *Eclogae Geologicae Helvetiae*, **71**, 105-141.

HADA, S. 1966. Discovery of Early Triassic ammonoids from Gua Musang, Kelantan, Malaya. *Journal of Geosciences, Osaka University*, **9**, 111-121.

HYATT, A. 1900. Cephalopoda. *In* ZITTEL, K. A. V. (ed.): *Textbook of palaeontology*. Eastman, C. R. London, 502-604.

--- and SMITH, J. P. 1905. Triassic cephalopod genera of America. *U. S. Geological Survey Professional Paper*, **40**, 1-394.

KEYSERLING, A. 1845. Beschreibung einiger von Dr. A. Th. v. Middendorff mitgebrachten Ceratiten des arctischen Sibiriens. *Bulletin de l'Academie Imperiale des Sciences de St. Pétersbourg*, **5**, 161-174.

KIPARISOVA, L. D. 1947. *Atlas of the guide forms of the fossil faunas of the USSR 7, Triassic*. All Union Scientific Geological Research Institute (VSEGEI), Leningrad (now St. Petersburg), Russia [in Russian].

--- 1956. Materials on paleontology, new families and genera. *Transactions of the All Union Scientific Research Geological Institute (VSEGEI), n. ser.*, 12, Paleontology, 76-79.

KRAFFT, A. V. and DIENER, C. 1909. Lower Triassic cephalopoda from Spiti, Malla Johar, and Byans. *Palaeontologia Indica, ser. 15,*, **6**, 1-186.

KRYSTYN, L., BHARGAVA, O. N. and RICHOZ, S. 2007*a*. A candidate GSSP for the base of the Olenekian Stage: Mud at Pin Valley; district Lahul & Spiti, Himachal Pradesh (Western Himalaya), India. *Albertiana*, **35**, 5-29.

--- RICHOZ, S. and BHARGAVA, O. N. 2007*b*. The Induan-Olenekian Boundary (IOB) in Mud – an update of the candidate GSSP section M04. *Albertiana*, **36**, 33-45.

KUENZI, W. D. 1965. Early Triassic (Scythian) ammonoids from northeastern Washington. *Journal of Paleontology*, **39**, 365-378.

KUMMEL, B. 1952. A classification of the Triassic ammonoids. *Journal of Paleontology*, **26**, 847-853.

--- 1957. Systematic descriptions, L138-L139, L142-L143. *In* Arkell, W.J., Kummel, B., Miller, A.K., Moore, R.C., Schindewolf, O., Sylvester-Bradley, P.C., and Wright, C.W. (eds): *Cephalopoda Ammonoidea. Treatise on Invertebrate Paleontology* (Moore, R.C. ed.): Part L, Mollusca 4. 490 pp. Geological Society of America, Boulder, Colorado, and University of Kansas Press, Lawrence, Kansas.

--- 1959. Lower Triassic ammonoids from Western Southland, New Zealand. *New Zealand Journal of Geology and Geophysics*, **2**, 429-47.

--- 1966. The Lower Triassic formations of the Salt Range and Trans-Indus Ranges, West Pakistan. *Bulletin of the Museum of Comparative Zoology, Harvard University*, **134**, 361-429.

--- 1968. Additional Scythian Ammonoids from Afghanistan. *Bulletin of the Museum of Comparative Zoology, Harvard University*, **136**, 483-509.

--- and ERBEN, H. K. 1968. Lower and Middle Triassic cephalopods from Afghanistan. *Palaeontographica, Abt. A*, **129**, 95-148.

KUMMEL, B. and SAKAGAMI, S. 1960. Mid-Scythian ammonites from Iwai Formation, Japan. *Breviora*, **126**, 1-11.

--- and STEELE, G. 1962. Ammonites from the *Meekoceras gracilitatus* Zone at Crittenden Spring, Elko County, Nevada. *Journal of Paleontology*, **36**, 638-703.

MARKEVICH, P. V. and ZAKHAROV, Y. 2004. Triassic and Jurassic of the Sikhote-Alin, 420 pp. Dalnauka, Vladivostok, Russia [in Russian with English summary].

MATHEWS, A. A. L. 1929. The Lower Triassic cephalopod fauna of the Fort Douglas area, Utah. *Walker Museum Memoirs*, **1**, 1-46.

MOJSISOVICS, E. 1896. Beiträge zur Kenntnis der obertriadischen Cephalopoden-Faunen des Himalaya. *Denkschriften der Akademie der Wissenschaften in Wien*, **63**, 573-701.

NICHOLS, K. M. and SILBERLING, N. J. 1979. Early Triassic (Smithian) ammonites of Paleoequatorial affinity from the Chulitna terrane, south central Alaska. *U. S. Gelogical Survey, Professional Paper*, **1121**, 1-5.

POPOV, Y. 1962. Some Early Triassic ammonoids of northern Caucasia. *Transactions of the Academy of Sciences of the USSR*, **127**, 176-184.

RAUP, D. M. and SEPKOSKI, J. J. 1982. Mass Extinctions in the Marine Fossil Record. *Science*, **215**, 1501-1503.

SAKAGAMI, S. 1955. Lower Triassic ammonites from Iwai, Orguno-Mura, Nishitamagun, Kwanto massif, Japan. *Science Reports Tokyo Kyoiku Diagaku, series C*, **30**, 131-40.

SHEVYREV, A. A. 1968. *Transactions of the Palaeontological Institute 119. Triassic ammonoidea from the southern part of the USSR*. Nauka, Moscow, 272 pp.

--- 1990. Ammonoids and chronostratigraphy of the Triassic. *Akad. Nauk SSSR, Palaeontol. Inst., Trudy*, **241**, 1-179.

--- 1995. Triassic ammonites of northwestern Caucasus. *Akad. Nauk SSSR, Palaeontol. Inst., Trudy*, **264**, 1-174.

SHIGETA, Y., MAEDA., H. and ZAKHAROV, Y. 2009. Biostratigraphy: ammonoid succession. 24-27. *In* SHIGETA, Y., ZAKHAROV, Y., MAEDA, H. and POPOV, A. M. (eds): *The Lower Triassic system in the Abrek Bay area, South Primorye, Russia.* National Museum of Nature and Science Monographs 38, Tokyo, 218 pp.

--- and ZAKHAROV, Y. 2009. Systematic paleontology: cephalopods. 44-140. *In* SHIGETA, Y., ZAKHAROV, Y., MAEDA, H. and POPOV, A. M. (eds): *The Lower Triassic system in the Abrek Bay area, South Primorye, Russia.* National Museum of Nature and Science Monographs 38, Tokyo, 218 pp.

SILBERLING, N. J. and TOZER, E. T. 1968. *Special Paper - Geological Society of America. Biostratigraphic classification of the marine Triassic in North America*. Geological Society of America (GSA), Boulder, CO, United States, 63 pp.

SMITH, A. G., SMITH, D. G. and FUNNELL, B. M. 1994. Atlas of Mesozoic and Cenozoic Coastlines. Cambridge University Press, Cambridge, 109 pp.

SMITH, J. P. 1927. Upper Triassic marine invertebrate faunas of North America. *U. S. Gelogical Survey, Professional Paper*, **141**, 262 pp.

--- 1932. Lower Triassic ammonoids of North America. *U. S. Geological Survey Professional Paper*, **167**, 1-199.

SPATH, L. F.1930. The Eotriassic invertebrate fauna of East Greenland. *Meddelelser om Grønland*, **83**, 1-90.

--- 1934. *Part 4: The ammonoidea of the Trias. Catalogue of the fossil cephalopoda in the British Museum (Natural History)*. The Trustees of the British Museum, London, 521 pp.

STAMPFLI, G., MARCOUX, J. and BAUD, A. 1991. Tethyan Margins in Space and Time. *Palaeogeography, Palaeoclimatology, Palaeoecology*, **87**, 373-409.

TONG, J. N., ZAKHAROV, Y. D. and WU, S. B. 2004. Early Triassic ammonoid succession in Chaohu, Anhui Province. *Acta Palaeontologica Sinica*, **43**, 192-204.

TOZER, E. T. 1971. Triassic time and ammonoids. *Canadian Journal of Earth Sciences*, **8**, 989-1031.

--- 1981. Triassic Ammonoidea; classification, evolution and relationship with Permian and Jurassic forms. 65-100. *In* HOUSE, M. R. and SENIOR, J. R. (eds): *The Ammonoidea.* Academic Press [for the] Systematics Association, London-New York, International.

--- 1994. Canadian Triassic ammonoid faunas. Geological Survey of Canada, Ottawa, ON, Canada, 663 pp.

VU KHUC 1984. *Triassic ammonoids in Vietnam*. Geoinform and Geodata Institute, Hanoi, Vietnam, 134 pp.

WAAGEN, W. 1895. Salt-Range fossils. Vol 2: Fossils from the Ceratite Formation. *Palaeontologia Indica*, **13**, 1-323.

WANG, Y. G. and HE, G. X. 1976. Triassic ammonoids from the Mount Jolmo Lungma region. *A report of scientific expedition in the Mount Jolmo Lungma region (1966-1968)*.

WEITSCHAT, W. and LEHMANN, U. 1978. Biostratigraphy of the uppermost part of the Smithian Stage (Lower Triassic) at the Botneheia, W-Spitsbergen. *Mitteilungen aus dem Geologisch-Paläontologischen Institut der Universität Hamburg*, **54**, 27-54.

WELTER, O. A. 1922. Die Ammoniten der unteren Trias von Timor. *Paläontologie von Timor*, **11**, 83-154.

ZAKHAROV, Y. D. 1968. Biostratigraphiya i amonoidei nizhnego triasa Yuzhnogo Primorya (Lower Triassic biostratigraphy and ammonoids of South Primorye). Nauka, Moskva, 175 pp. [in Russian].

APPENDIX

Measurements of the classic geometrical parameters of the ammonoid shell. Diameter (D), whorl height (H), whorl width (W) and umbilical diameter (U).

Species	Specimen	D (mm)	H (mm)	W (mm)	U (mm)	Sample
?*Pseudoceltites* sp. indet.	PIMUZ 28200	36.4	15.2	13	11.2	Ma26
Kashmirites nivalis (Diener, 1897)	PIMUZ 28205	23.4	7.9	-	10.2	HB1010
	PIMUZ 28204	27.2	9.7	-	11.8	HB1010
Nyalamites angustecostatus (Welter, 1922)	PIMUZ 28209	11.1	4.1	3.8	4.5	HB1900
	PIMUZ 28208	22.7	7.9	6	9.8	M03-58
Xenoceltites cf. *variocostatus* Brayard and Bucher, 2008	PIMUZ 28214	39.5	14.4	9.1	15	M08-70
Glyptophiceras sinuatum (Waagen, 1895)	PIMUZ 28212	65.2	20.3	14.2	28.5	Ma96
	PIMUZ 28211	18.9	7.3	5.2	6.7	Ma96
Xiaoqiaoceras involutus Brayard and Bucher, 2008	PIMUZ 28220	16.1	9.4	8.1	1.8	HB1005
	PIMUZ 28221	15.7	10	9	1.4	HB1005
?*Paranorites* sp. indet.	PIMUZ 28222	161	72	41	35	float
?*Urdyceras* sp. indet.	PIMUZ 28248	12.7	6.1	4.8	5	Ma49
Hermannites rursiradiatus gen. et sp. nov.	PIMUZ 28261	76.6	27	17.8	29.9	M03-20
?*Subflemingites compressus* Brühwiler *et al*., accepted	PIMUZ 28271	24.5	11.1	-	6.8	Ma49
	PIMUZ 28272	15.2	6.2	4.3	5	Ma46
Brayardites compressus Brühwiler *et al*., accepted	PIMUZ 28277	21.8	11.2	6.4	3.6	HB1005
	PIMUZ 28279	37	17.5	11.7	8.4	M08-21b
Brayardites crassus Brühwiler *et al*., accepted	PIMUZ 28273	35.1	14.5	20	10.6	M03-21
	PIMUZ 28274	109	42	-	42.8	M05-20
Nuetzelia himalayica gen. et sp. nov.	PIMUZ 28292	15.1	7.8	4.1	2.7	HB1004
	PIMUZ 28290	19.8	11.4	-	2.7	HB1004
	PIMUZ 28291	20.8	10.7	5.3	3.8	HB1004
Prionites sp. indet.	PIMUZ 28307	35.2	18.3	10	4.1	Ma49
	PIMUZ 28305	43.2	22.1	-	4.6	Ma49
Owenites cf. *simplex*	PIMUZ 28460	21.8	11	10.3	3.2	M06-39
Steckites brevus gen. et sp. nov.	PIMUZ 28337	29.3	13.5	-	5.5	Ma26
	PIMUZ 28378	22.1	10.1	8.4	3.5	E21-22
Owenites koeneni Hyatt and Smith, 1905	PIMUZ 28461	54.8	23.9	-	12	M03-57
	PIMUZ 28335	40	19	-	6	M03-57
Owenites carpenteri Smith, 1932	PIMUZ 28339	27.5	16	11.2	0	Gu72
	PIMUZ 28340	23.6	14.7	10	0	Gu72
Juvenites procurvus Brayard and Bucher, 2008	PIMUZ 28353	24.6	8.3	13.2	9.5	float
	PIMUZ 28354	21.5	7.9	12.7	8.2	M08-48
Aspenites acutus Hyatt and Smith, 1905	PIMUZ 28365	30.5	18.5	6.8	0	LoSFB1
	PIMUZ 28366	42.5	23.5	7.1	1.2	HB1005
Pseudaspenites cf. *layeriformis* (Welter, 1922)	PIMUZ 28369	49.1	24.5	6.5	5.5	M08-21b
Pseudosageceras augustum (Brayard and Bucher, 2008)	PIMUZ 28373	30.2	28.3	5.8	0	M08-70
	PIMUZ 28374	45.5	27.6	-	0	M08-70
Shigetaceras dunajensis (Zakhrov, 1968)	PIMUZ 28375	28.5	14.8	10.3	4.9	M03-40
?*Galfettites* sp. indet.	PIMUZ 28239	24.2	10	5.9	8	HB1005
	PIMUZ 28234	11.5	5.7	2.2	3	HB1005
	PIMUZ 28238	18.2	7.8	4.5	5.4	HB1033
Gen. et sp. indet. A	PIMUZ 28308	44.5	21.6	10.5	9.3	HB1004

FIGURE CAPTIONS

TEXT-FIG. 1. A, Palaeogeographical map of the Early Triassic with the palaeoposition of Spiti (modified after Brayard *et al.* 2006). B, Geographical map indicating the Spiti area in norwestern India. C, Location map of sampled sections.

TEXT-FIG. 2. Excellent exposures of the the Late Permian - Middle Triassic succession above the village of Mud in Pin Valley. Stratigraphic units after Bhargava *et al.* (2004). OB+AB: *Otoceras* beds + *Ambites* Beds.

TEXT-FIG. 3. Simplified stratigraphic log of the lower part of the Mikin Formation at Mud (modified after Bhargava *et al.* 2004). The lithostratigraphic units are well recognized in the other studied localities. "*Parahedenstroemia*" Beds are written with quotation marks because *Parahedenstroemia* is here regarded as a synonym of *Aspenites*.

TEXT-FIG. 4. Distribution of ammonoid taxa in the Mud section. Open dots indicate occurrences based on only fragmentary or poorly preserved material. Ammonoid faunas: *Bc=Brayardites compressus* beds; *Es=Escarguelites spitiensis* horizon; *Tc=Truempyceras compressum* horizon; *Pm=Pseudoceltites multiplicatus* beds; *Na=Nyalamites angustecostatus* beds; *Wd=Wasatchites distractus* beds; *Sp=Subvishnuites posterus* beds; *Gs=Glyptophiceras sinuatum* beds. See text-fig. 2 for location. Bed numbers of the lowermost part (i.e. *Flemingites* beds) after Krystyn *et al.* 2007*a*, *b*.

TEXT-FIG. 5. Distribution of ammonoid taxa in the Guling section. Open dots indicate occurrences based on only fragmentary or poorly preserved material. Abbreviations of ammonoid faunas as in Text-fig. 4.

TEXT-FIG. 6. Distribution of ammonoid taxa in the Lalung section. Abbreviations of ammonoid faunas as in Text-fig. 4.

TEXT-FIG. 7. Distribution of ammonoid taxa in the Losar section. Open dots indicate occurrences based on only fragmentary or poorly preserved material. Abbreviations of ammonoid faunas as in Text-fig. 4.

TEXT-FIG. 8. Synthetic range chart showing the biostratigraphical distribution of Smithian ammonoid species in Spiti.

TEXT-FIG. 9. Synthetic range chart showing the biostratigraphical distribution of Smithian ammonoid genera (grouped by families) in Spiti.

TEXT-FIG. 10. Biostratigraphical subdivisions of the Smithian of Spiti and correlation with other zonations. For discussion of the biostratigraphical correlations of the Tethyan successions with those from basins outside the Tethys see Brayard and Bucher (2008) and Brühwiler *et al.* (accepted). Note that the position of the Dienerian/Smithian (or Induan/Olenekian) boundary has not yet been formally defined (e.g. Krystyn *et al.* 2007*a*, *b*). Here, we use the ammonoid-based boundary definition as suggested earlier (Brühwiler *et al.* submitted [c]).

TEXT-FIG. 11. Scatter diagram of H, W, and U, and of H/D, W/C, and U/D for *Pseudoceltites multiplicatus* (Waagen, 1895).

TEXT-FIG. 12. Scatter diagram of H, W, and U, and of H/D, W/C, and U/D for *Tulongites xiaoqiaoi* (Brühwiler *et al.*, accepted).

TEXT-FIG. 13. Scatter diagram of H, W, and U, and of H/D, W/C, and U/D for *Galfettites omani* (Brühwiler *et al.*, PALAEONTOGRAPHICA).

TEXT-FIG. 14. Scatter diagram of H, W, and U, and of H/D, W/C, and U/D for *Urdyceras tulongensis* (Brühwiler *et al.*, accepted).

TEXT-FIG. 15. Scatter diagram of H, W, and U, and of H/D, W/C, and U/D for *Dieneroceras* cf. *tientungense* Chao, 1959.

TEXT-FIG. 16. Scatter diagram of H, W, and U, and of H/D, W/C, and U/D for *Anaxenaspis* sp. indet.

TEXT-FIG. 17. Scatter diagram of H, W, and U, and of H/D, W/C, and U/D for *Nammalites pilatoides* (Guex, 1978).

TEXT-FIG. 18. Scatter diagram of H, W, and U, and of H/D, W/C, and U/D for *Truempyceras compressum* sp. nov.

TEXT-FIG. 19. Scatter diagram of H, W, and U, and of H/D, W/C, and U/D for *Wasatchites distractus* (Waagen, 1895).

TEXT-FIG. 20. Scatter diagram of H, W, and U, and of H/D, W/C, and U/D for *Anasibirites kingianus* (Waagen, 1895).

TEXT-FIG. 21. Scatter diagram of H, W, and U, and of H/D, W/C, and U/D for *Paranannites* sp. indet.

TEXT-FIG. 22. Scatter diagram of H, W, and U, and of H/D, W/C, and U/D for *Juvenites* cf. *kraffti* (Frebold, 1930).

TEXT-FIG. 23. Scatter diagram of H, W, and U, and of H/D, W/C, and U/D for *Jinyaceras hindostanum* (Diener, 1897).

TEXT-FIG. 24. Scatter diagram of H, W, and U, and of H/D, W/C, and U/D for *Subvishnuites posterus* sp. nov.

TEXT-FIG. 25. Scatter diagram of H, W, and U, and of H/D, W/C, and U/D for *"Kraffticeras" pseudoplanulatum* (Krafft and Diener, 1909).

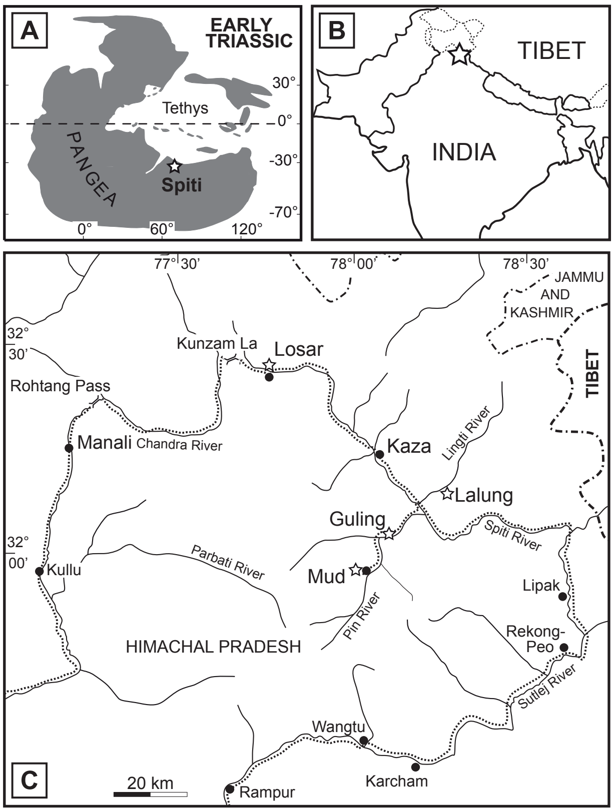

Text-fig. 1

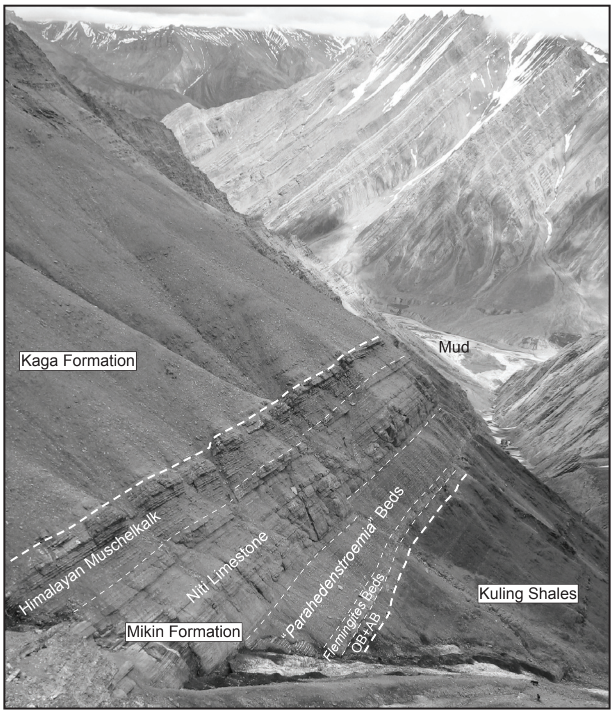

Text-fig. 2

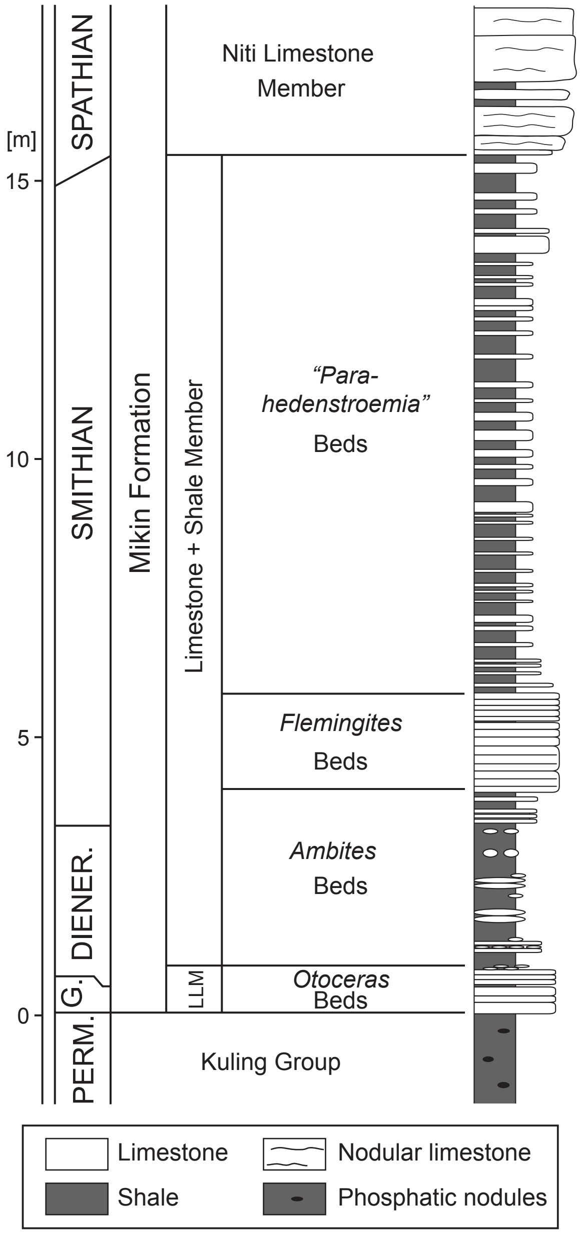
[m]
15
10
5
0
SPATHIAN
SMITHIAN
DIENER.
G.
PERM.
Mikin Formation
Limestone + Shale Member
LLM
Niti Limestone Member
"Para-hedenstroemia" Beds
Flemingites Beds
Ambites Beds
Otoceras Beds
Kuling Group
Limestone
Nodular limestone
Shale
Phosphatic nodules

Text-fig. 3

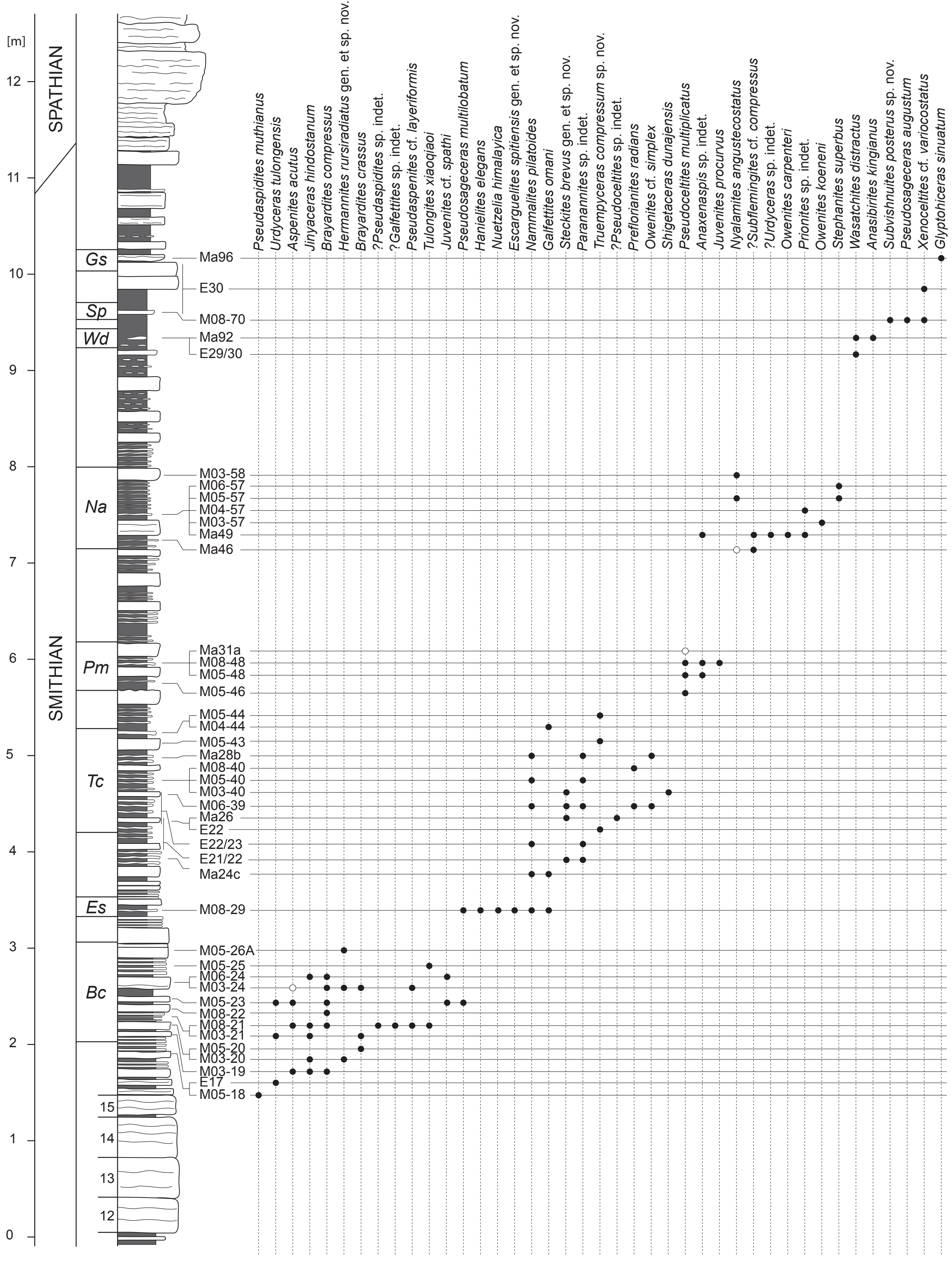
[m]
0
1
2
3
4
5
6
7
8
9
10
11
12
SPATHIAN
SMITHIAN
Gs
Sp
Wd
Na
Pm
Tc
Es
Bc
15
14
13
12
Ma96
E30
M08-70
Ma92
E29/30
M03-58
M06-57
M05-57
M04-57
M03-57
Ma49
Ma46
Ma31a
M08-48
M05-48
M05-46
M05-44
M04-44
M05-43
Ma28b
M08-40
M05-40
M03-40
M06-39
Ma26
E22
E22/23
E21/22
Ma24c
M08-29
M05-26A
M05-25
M06-24
M03-24
M05-23
M08-22
M08-21
M03-21
M05-20
M03-20
M03-19
E17
M05-18
Pseudaspidites muthianus
Urdyceras tulongensis
Aspenites acutus
Jinyaceras hindostanum
Brayardites compressus
Hermannites rursiradiatus gen. et sp. nov.
Brayardites crassus
?Pseudaspidites sp. indet.
?Galfettites sp. indet.
Pseudaspenites cf. layeriformis
Tulongites xiaoqiaoi
Juvenites cf. spathi
Pseudosageceras multilobatum
Hanielites elegans
Nuetzelia himalayica
Escarguelites spitiensis gen. et sp. nov.
Nammalites pilatoides
Galfettites omani
Steckites brevus gen. et sp. nov.
Parannanites sp. indet.
Truempyceras compressum sp. nov.
?Pseudoceltites sp. indet.
Preflorianites radians
Owenites cf. simplex
Shigetaceras dunajensis
Pseudoceltites multiplicatus
Anaxenaspis sp. indet.
Juvenites procurvus
Nyalamites angustecostatus
?Subflemingites cf. compressus
?Urdyceras sp. indet.
Owenites carpenteri
Prionites sp. indet.
Owenites koeneni
Stephanites superbus
Wasatchites distractus
Anasibirites kingianus
Subvishnuites posterus sp. nov.
Pseudosageceras augustum
Xenoceltites cf. variocostatus
Glyptohiceras sinuatum

Text-fig. 4

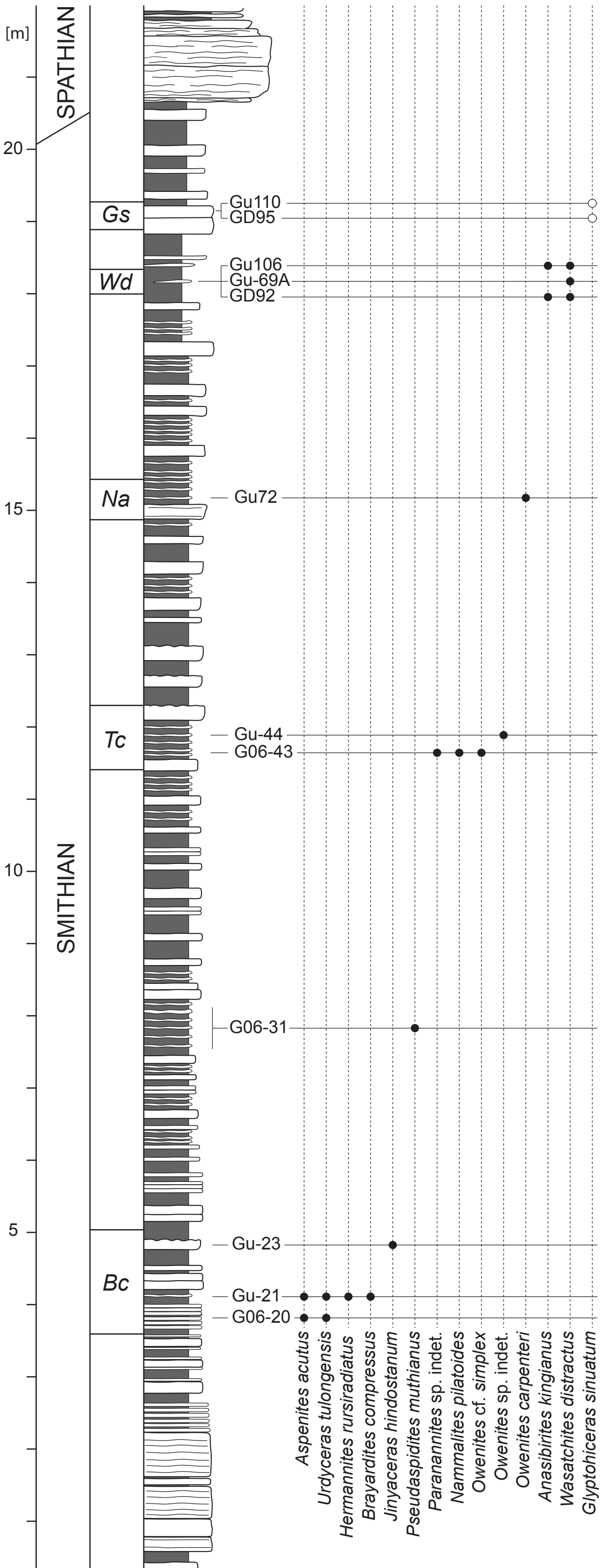
[m]
SPATHIAN
SMITHIAN
20
15
10
5
0
Gs
Wd
Na
Tc
Bc
Gu110
GD95
Gu106
Gu-69A
GD92
Gu72
Gu-44
G06-43
G06-31
Gu-23
Gu-21
G06-20
Aspenites acutus
Urdyceras tulongensis
Hermannites rursiradiatus
Brayardites compressus
Jinyaceras hindostanum
Pseudaspidites muthianus
Paranannites sp. indet.
Nammalites pilatoides
Owenites cf. simplex
Owenites sp. indet.
Owenites carpenteri
Anasibirites kingianus
Wasatchites distractus
Glyptohiceras sinuatum

Text-fig. 5

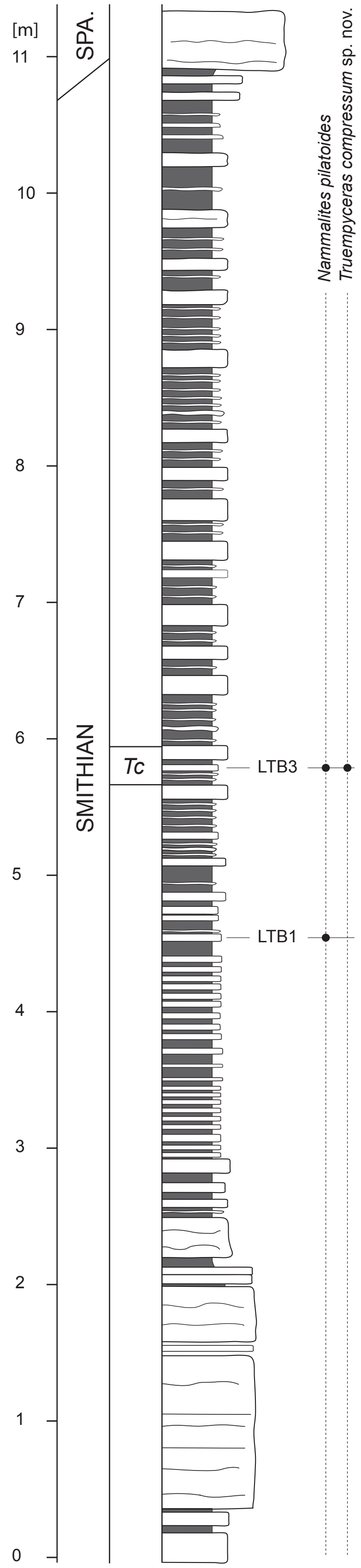
[m]
11
10
9
8
7
6
5
4
3
2
1
0
SPA.
SMITHIAN
Tc
LTB3
LTB1
Nammalites pilatoides
Truempyceras compressum sp. nov.

Text-fig. 6

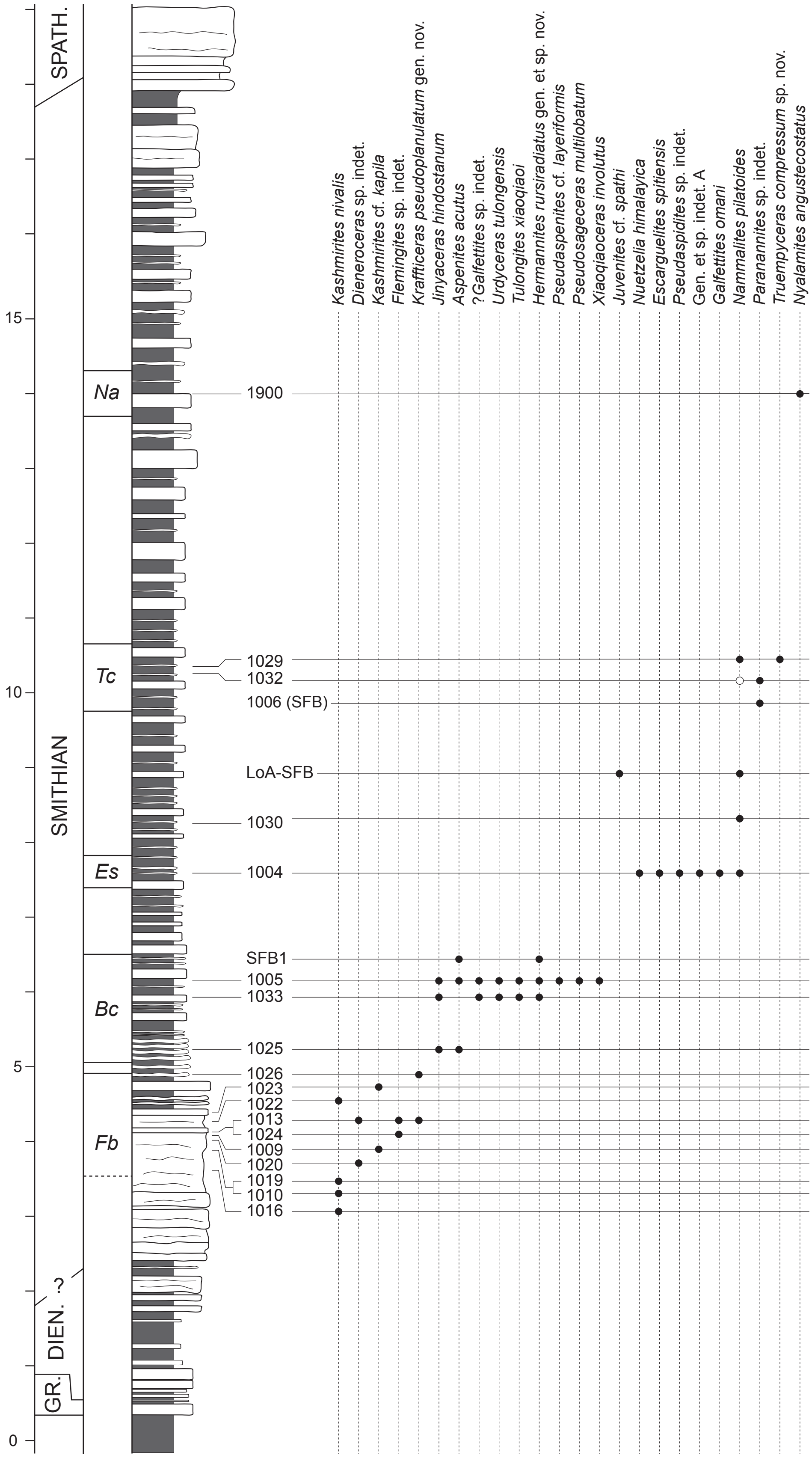
SPATH.
SMITHIAN
DIEN.
?
GR.
0
5
10
15
Na
Tc
Es
Bc
Fb
1900
1029
1032
1006 (SFB)
LoA-SFB
1030
1004
SFB1
1005
1033
1025
1026
1023
1022
1013
1024
1009
1020
1019
1010
1016
Kashmirites nivalis
Dieneroceras sp. indet.
Kashmirites cf. kapila
Flemingites sp. indet.
Kraffticeras pseudoplanulatum gen. nov.
Jinyaceras hindostanum
Aspenites acutus
?Galfettites sp. indet.
Urdyceras tulongensis
Tulongites xiaoqiaoi
Hermannites rursiradiatus gen. et sp. nov.
Pseudaspenites cf. layeriformis
Pseudosageceras multilobatum
Xiaoqiaoceras involutus
Juvenites cf. spathi
Nuetzelia himalayica
Escarguelites spitiensis
Pseudaspidites sp. indet.
Gen. et sp. indet. A
Galfettites omani
Nammalites pilatoides
Parannanites sp. indet.
Truempyceras compressum sp. nov.
Nyalamites angustecostatus

Text-fig. 7

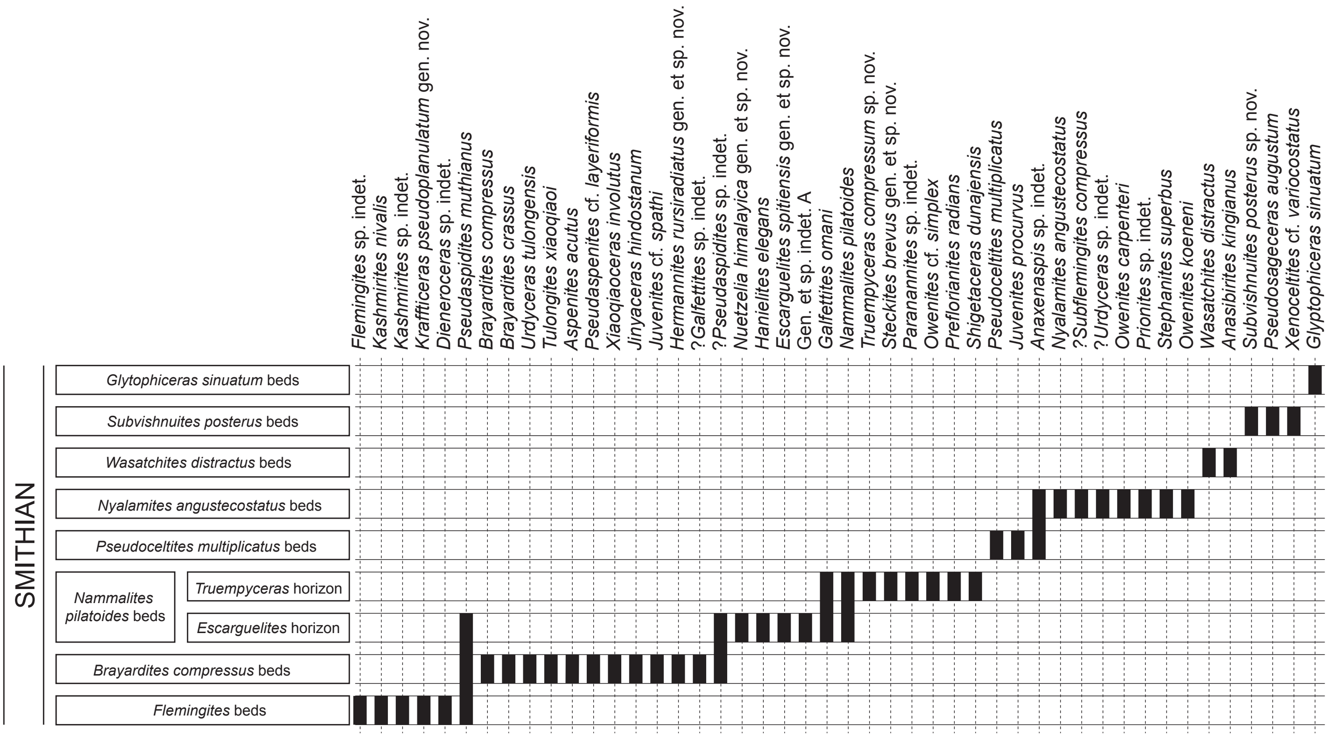

Text-fig. 8

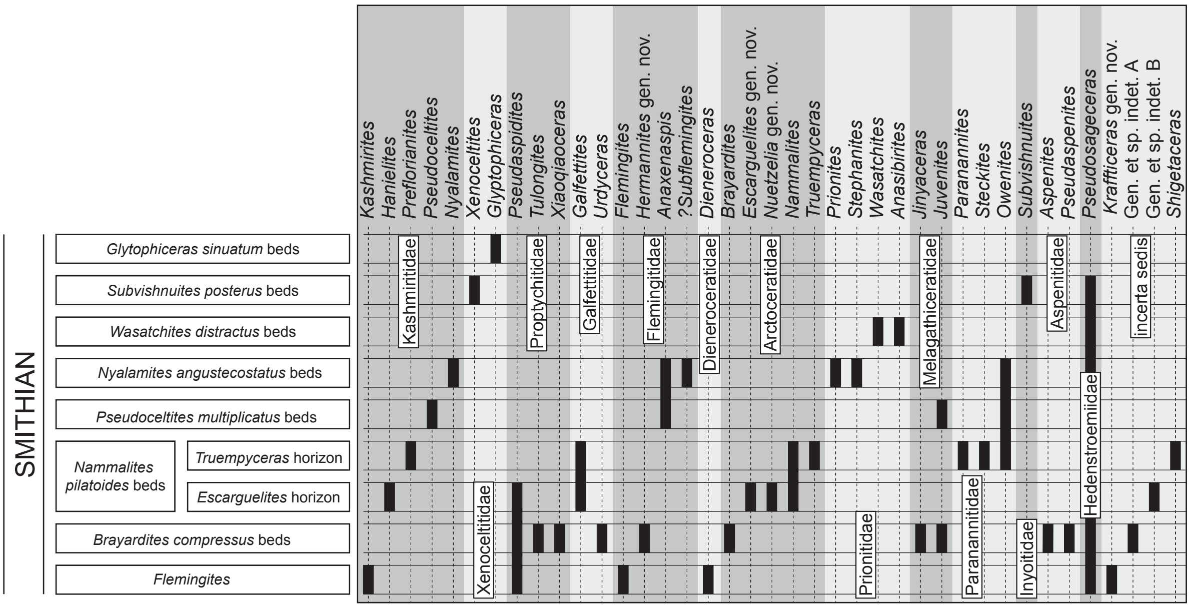

Text-fig. 9

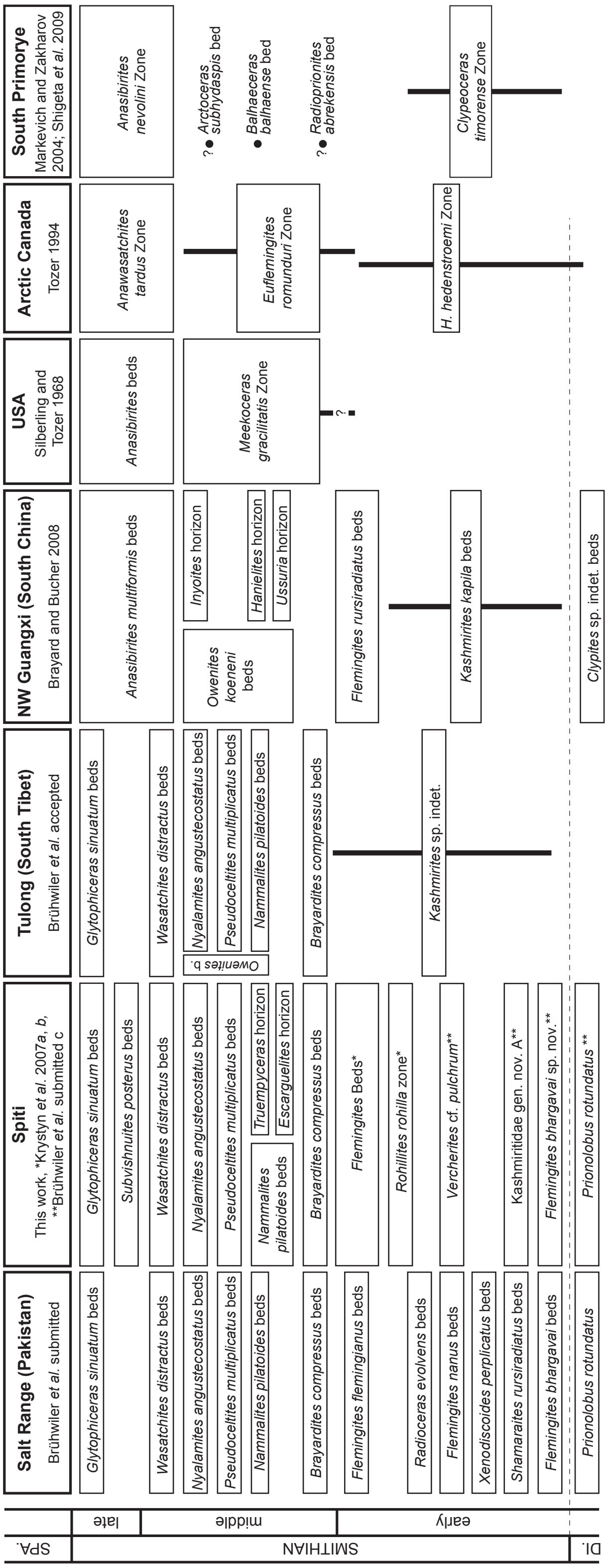
SPA.
SMITHIAN
DI.
late
middle
early
Salt Range (Pakistan)
Brühwiler et al. submitted
Glytophiceras sinuatum beds
Wasatchites distractus beds
Nyalamites angustecostatus beds
Pseudoceltites multiplicatus beds
Nammalites pilatoides beds
Brayardites compressus beds
Flemingites flemingianus beds
Radioceras evolvens beds
Flemingites nanus beds
Xenodiscoides perplicatus beds
Shamaraites rursiradiatus beds
Flemingites bhargavai beds
Prionolobus rotundatus
Spiti
This work, *Krystyn et al. 2007a, b, **Brühwiler et al. submitted c
Glytophiceras sinuatum beds
Subvishnuites posterus beds
Wasatchites distractus beds
Nyalamites angustecostatus beds
Pseudoceltites multiplicatus beds
Nammalites pilatoides beds
Truempyceras horizon
Escarguelites horizon
Brayardites compressus beds
Flemingites Beds*
Rohillites rohilla zone*
Vercherites cf. pulchrum**
Kashmiritidae gen. nov. A**
Flemingites bhargavai sp. nov.**
Prionolobus rotundatus **
Tulong (South Tibet)
Brühwiler et al. accepted
Glytophiceras sinuatum beds
Wasatchites distractus beds
Owenites b.
Nyalamites angustecostatus beds
Pseudoceltites multiplicatus beds
Nammalites pilatoides beds
Brayardites compressus beds
Kashmirites sp. indet.
NW Guangxi (South China)
Brayard and Bucher 2008
Anasibirites multiformis beds
Inyoites horizon
Owenites koeneni beds
Hanielites horizon
Ussuria horizon
Flemingites rursiradiatus beds
Kashmirites kapila beds
Clypites sp. indet. beds
USA
Silberling and Tozer 1968
Anasibirites beds
Meekoceras gracilitatis Zone
?
Arctic Canada
Tozer 1994
Anawasatchites tardus Zone
Euflemingites romunduri Zone
H. hedenstroemi Zone
South Primorye
Markevich and Zakharov 2004; Shigeta et al. 2009
Anasibirites nevolini Zone
? ● Arctoceras subhydaspis bed
● Balhaeceras balhaense bed
? ● Radioprionites abrekensis bed
Clypeoceras timorense Zone

Text-fig. 10

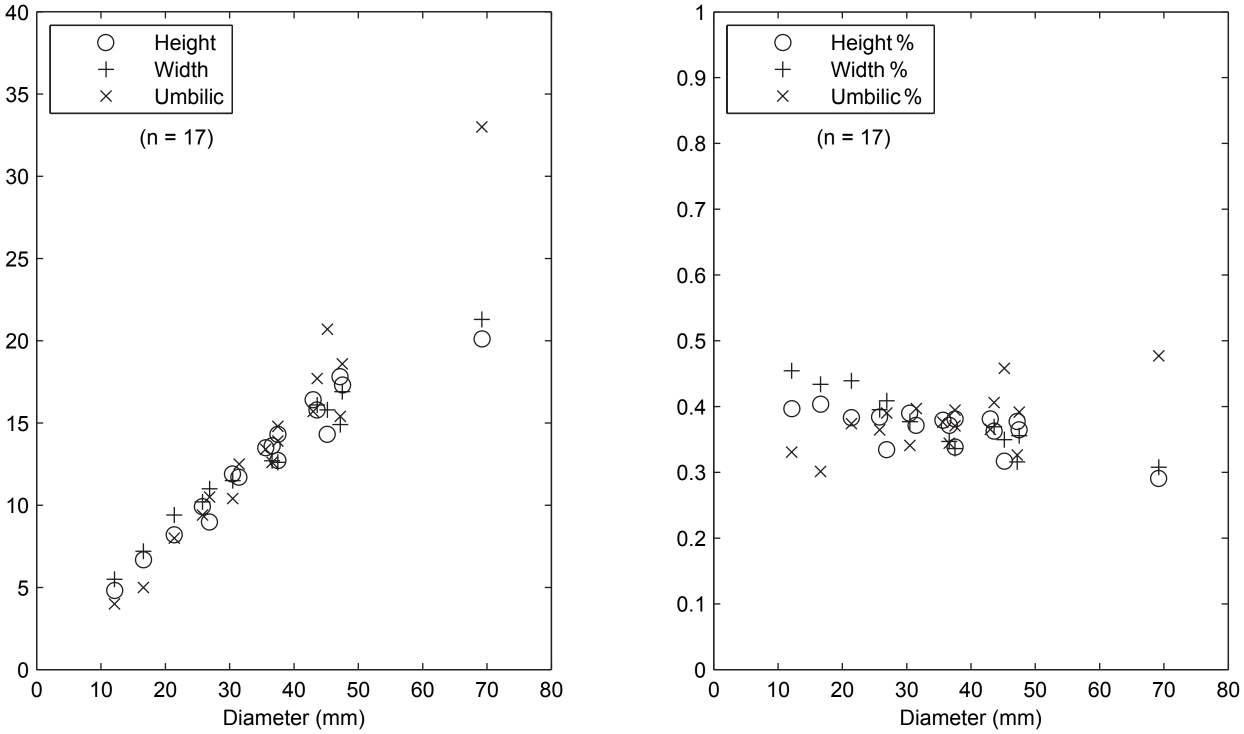

Text-fig. 11

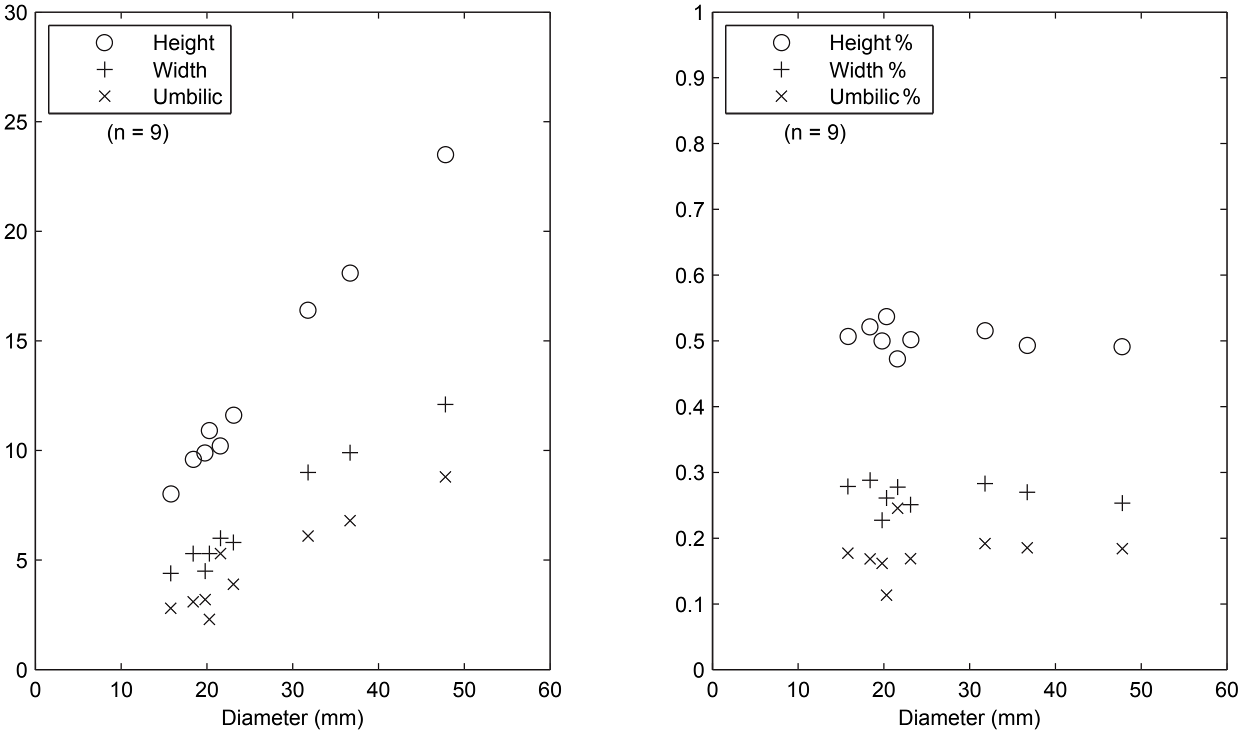

Text-fig. 12

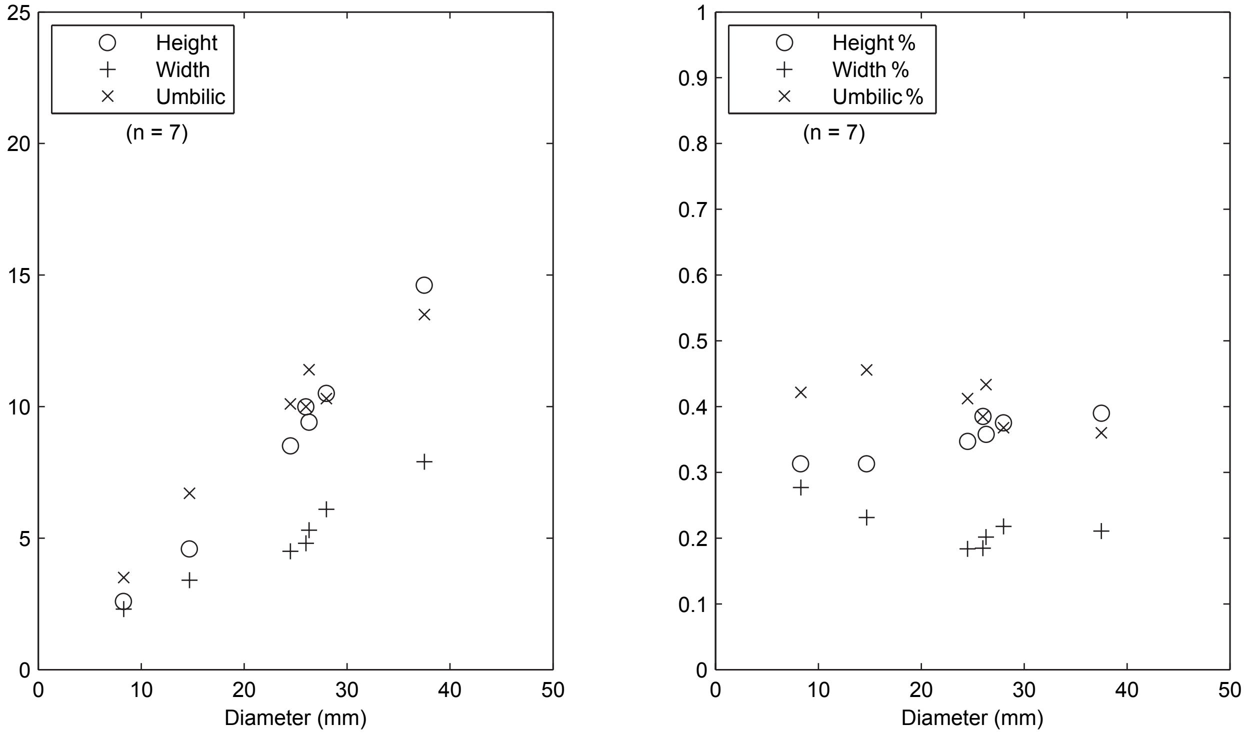

Text-fig. 13

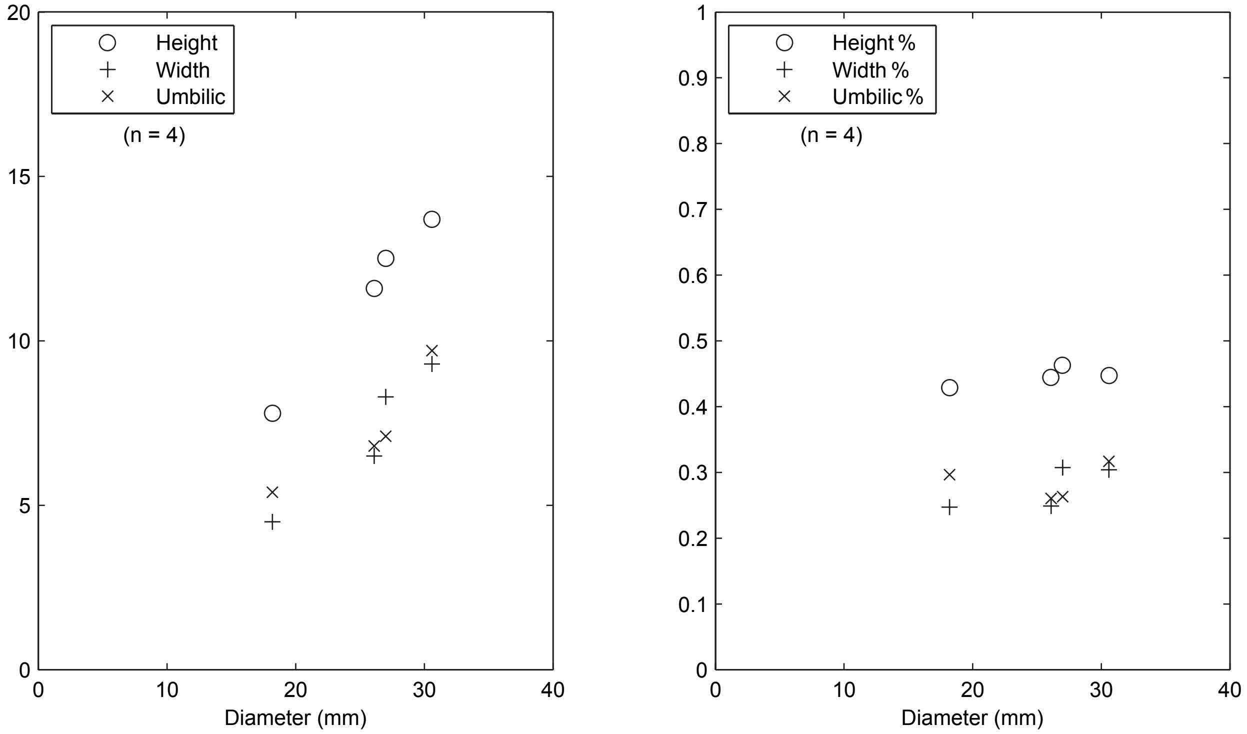

Text-fig. 14

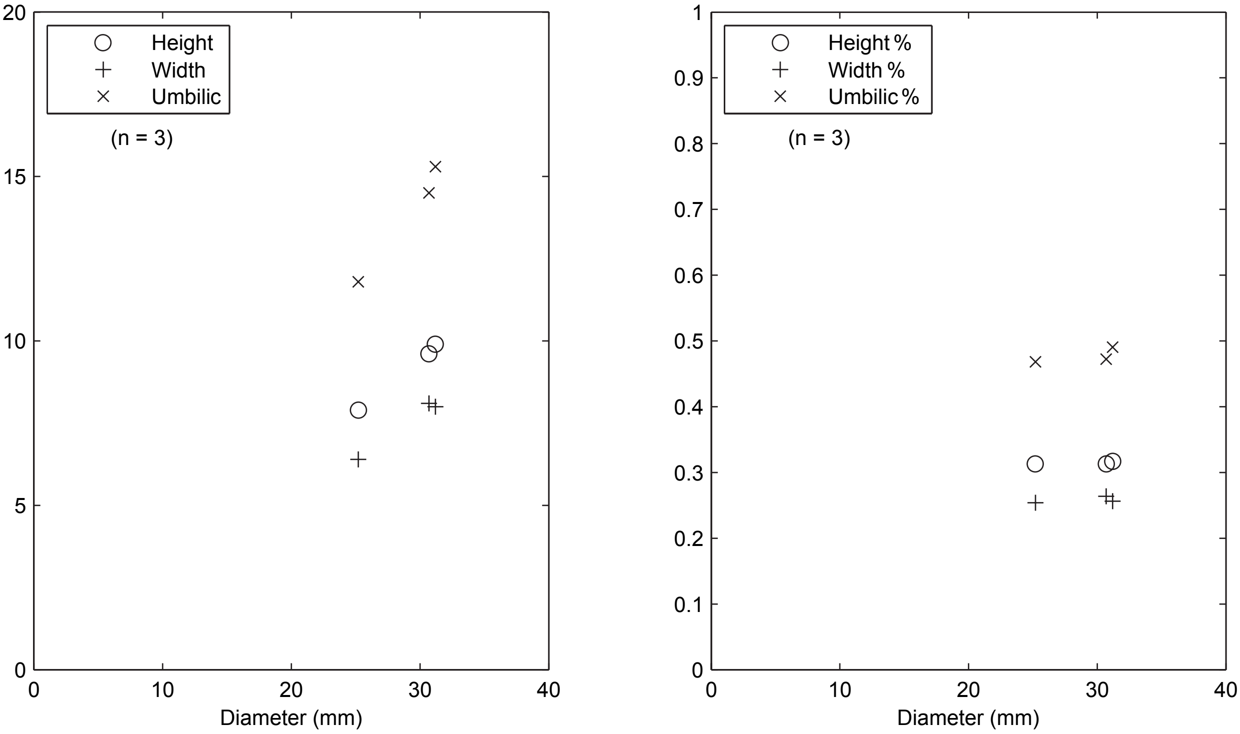

Text-fig. 15

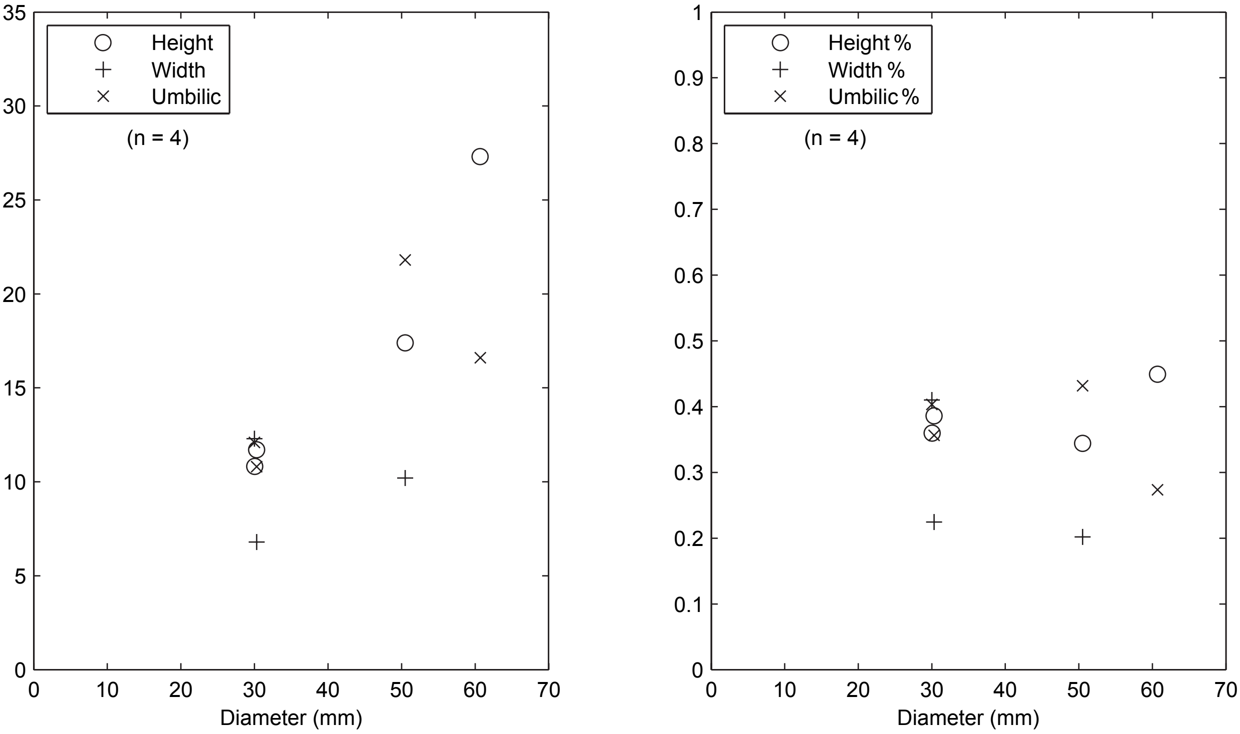

Text-fig. 16

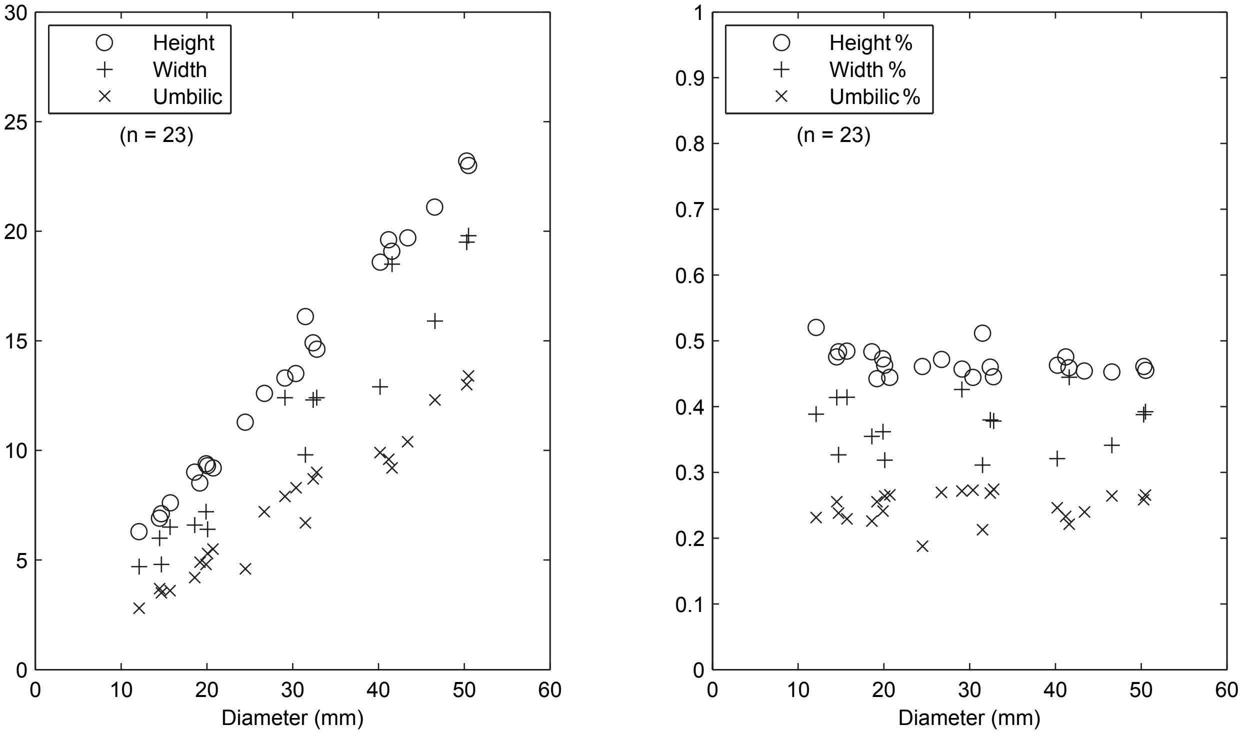

Text-fig. 17

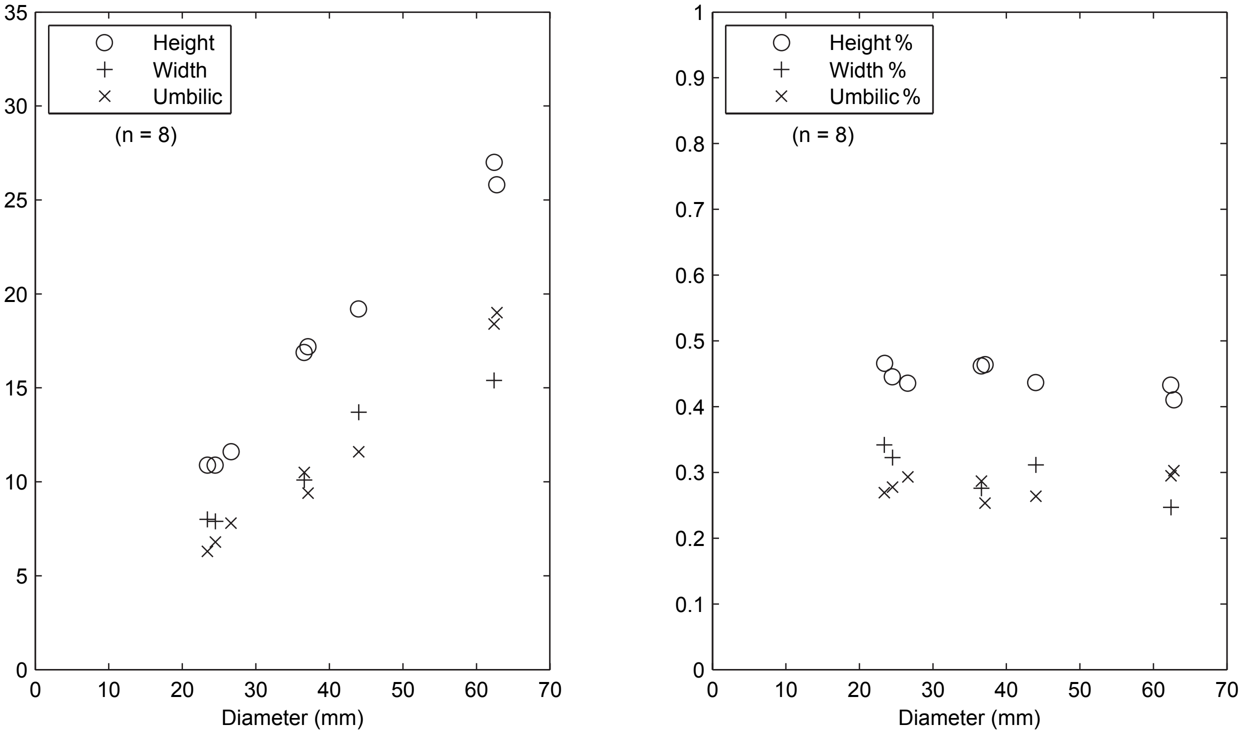

Text-fig. 18

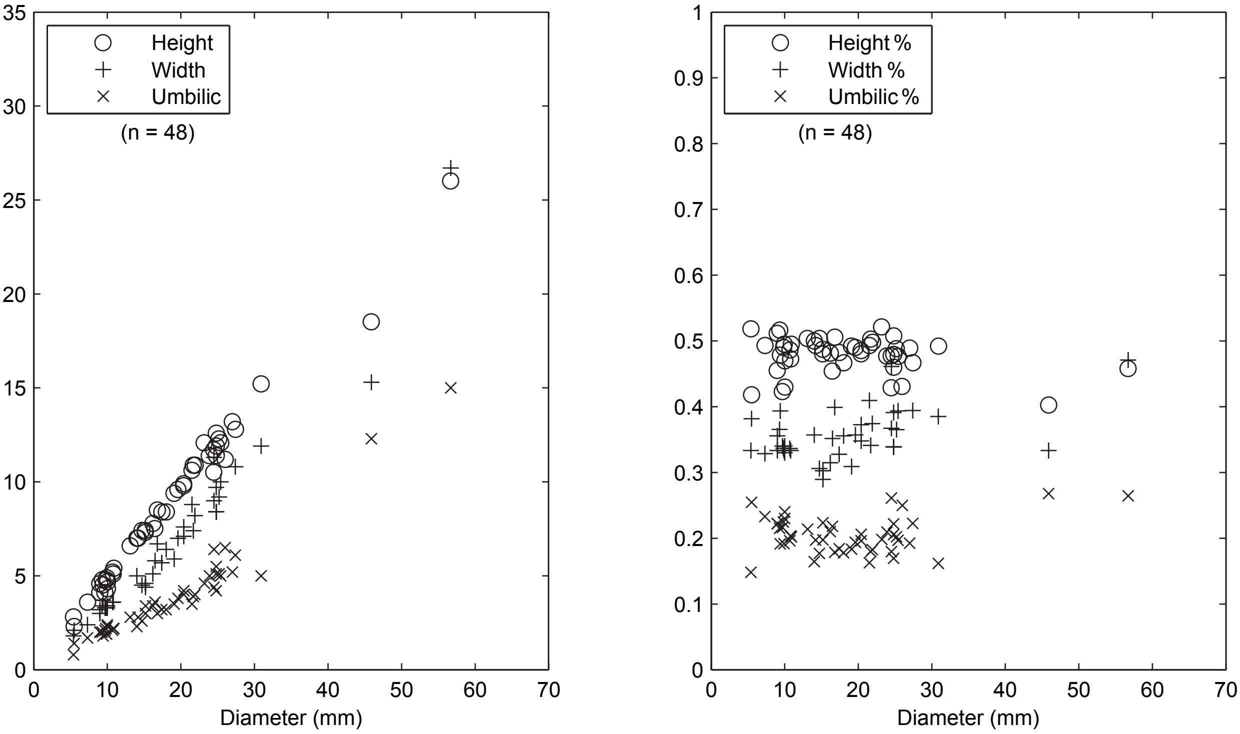

Text-fig. 19

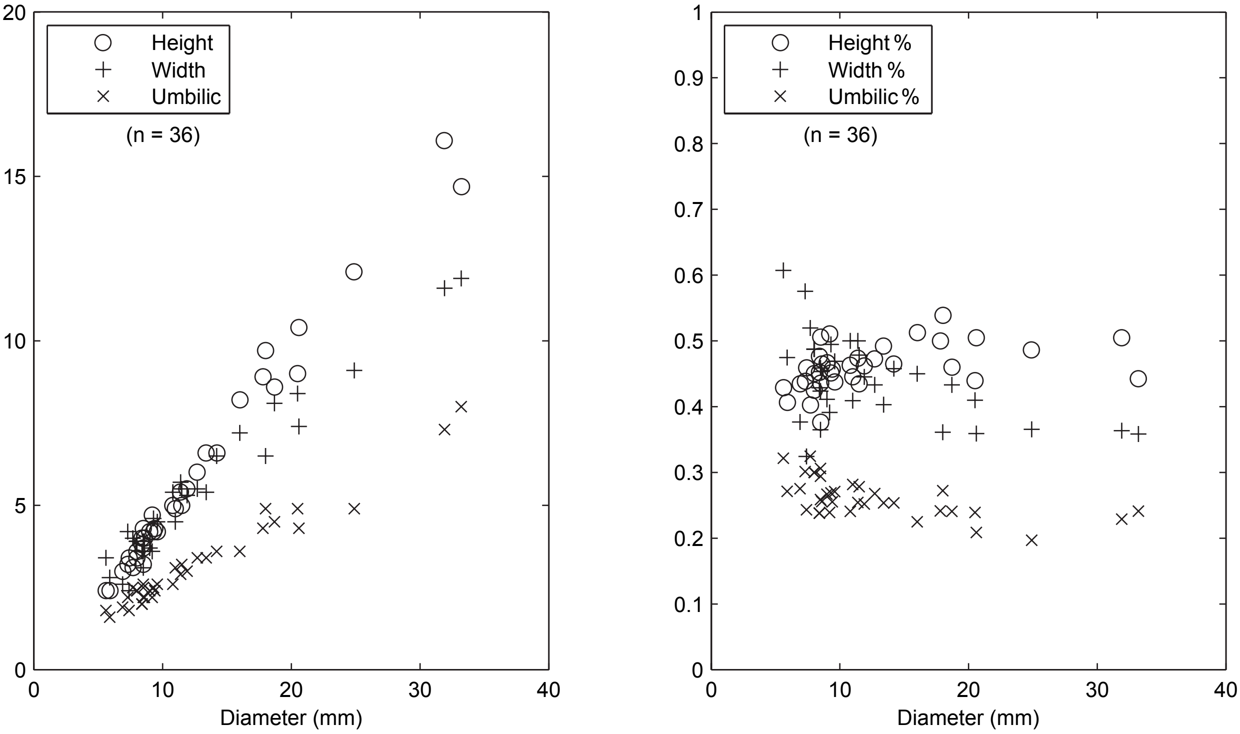

Text-fig. 20

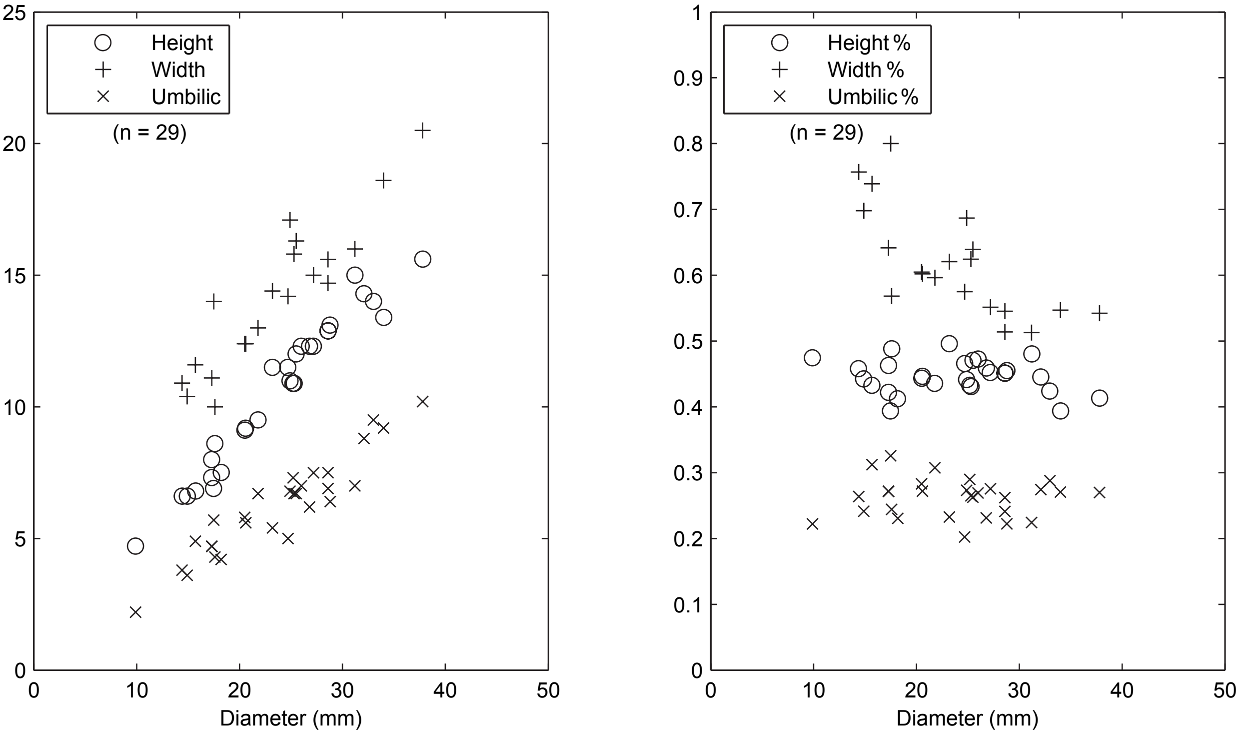

Text-fig. 21

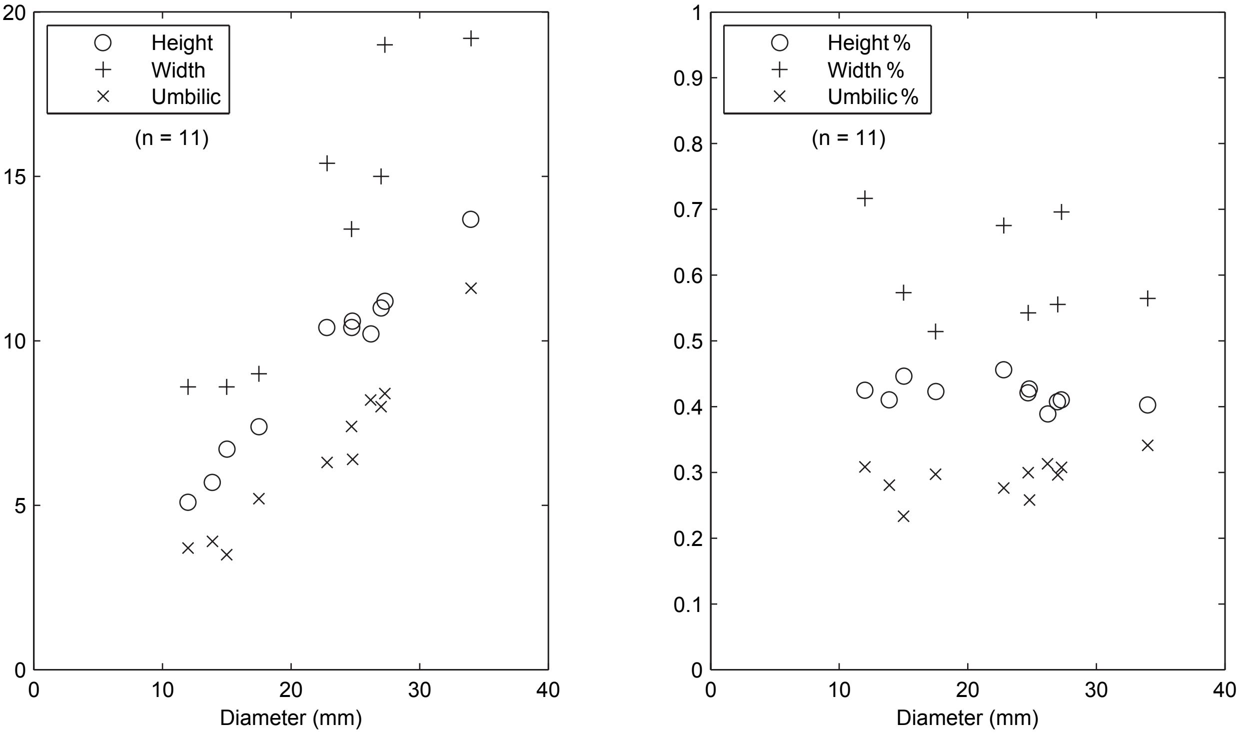

Text-fig. 22

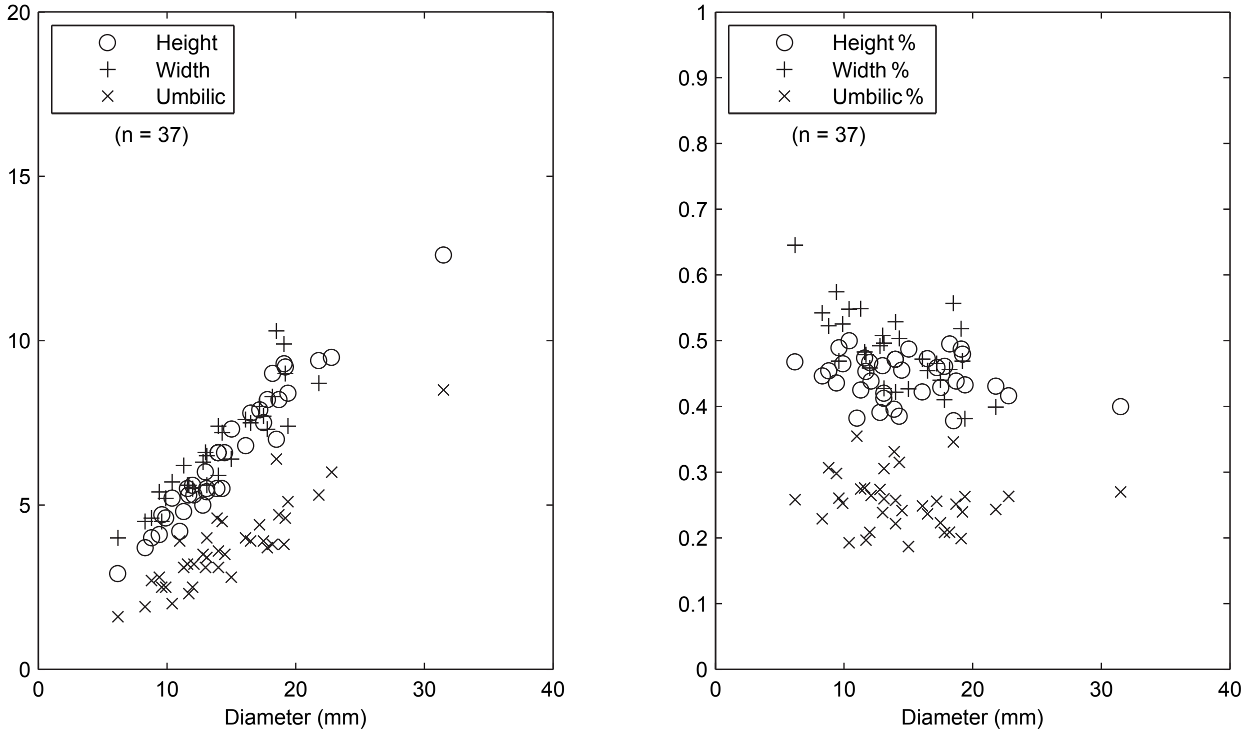

Text-fig. 23

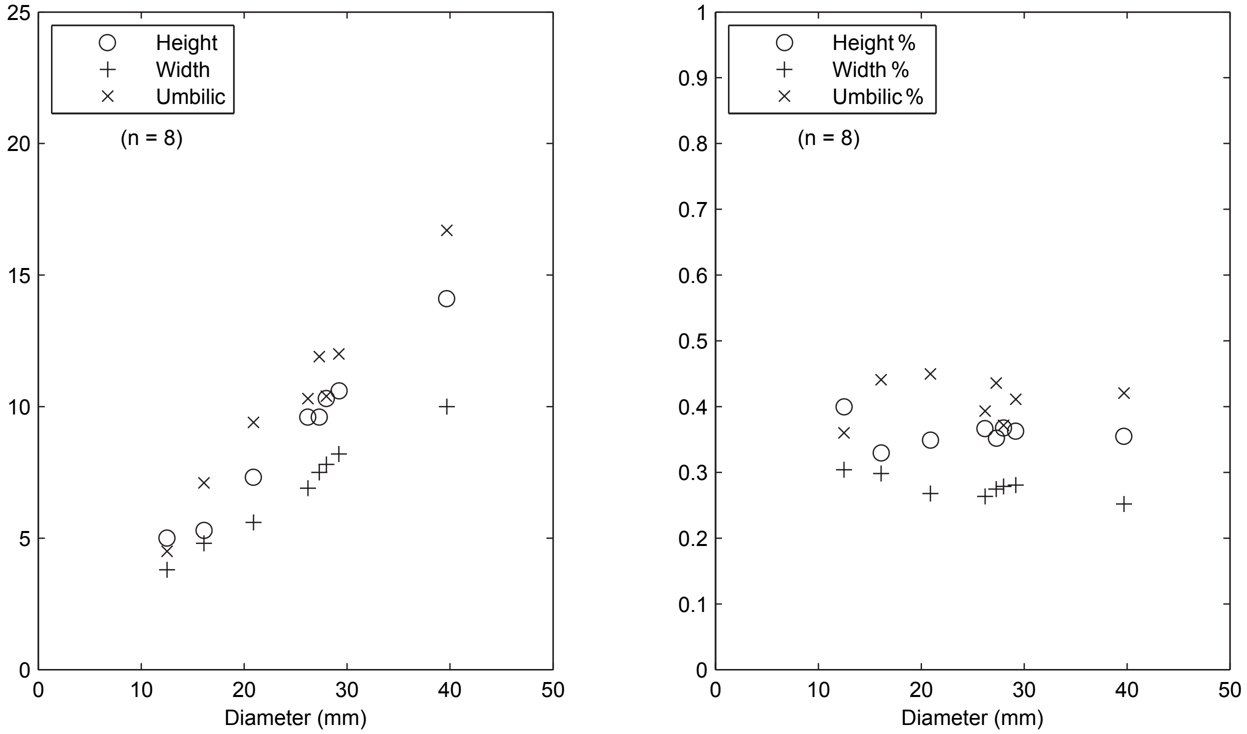

Text-fig. 24

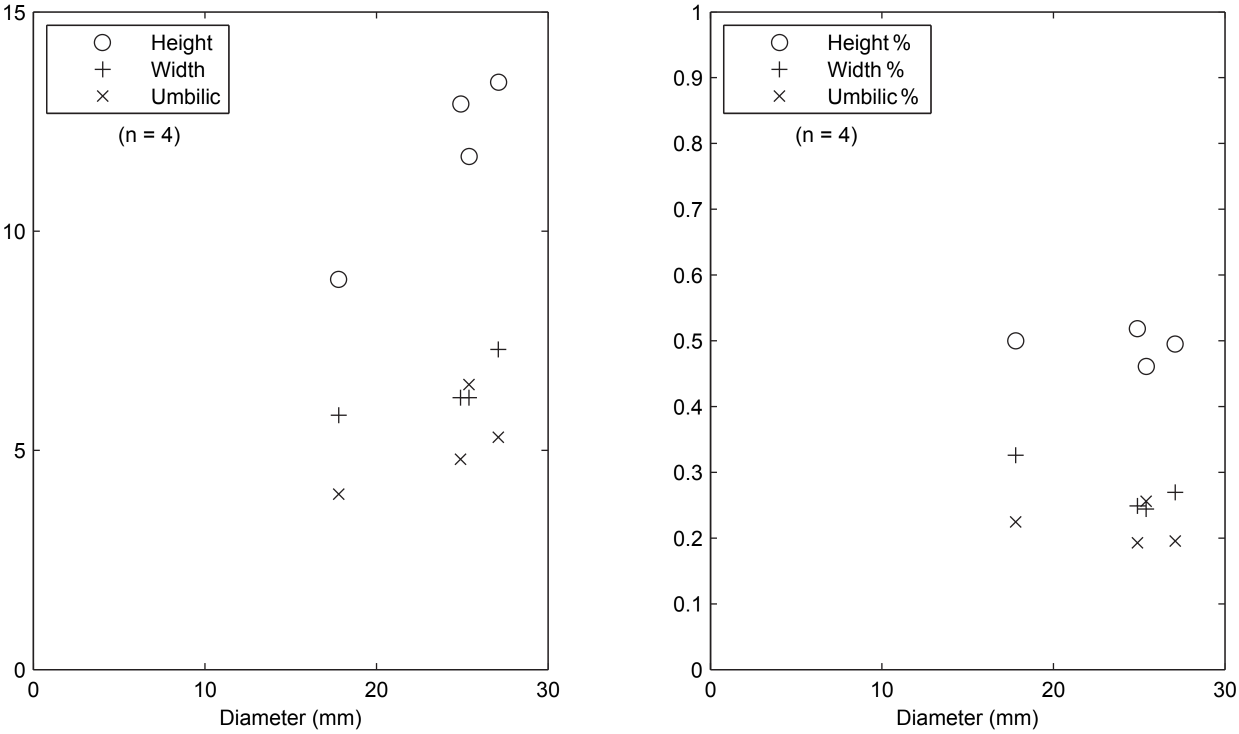
15
10
5
0
0
10
20
30
Diameter (mm)
○ Height
+ Width
× Umbilic
(n = 4)
1
0.9
0.8
0.7
0.6
0.5
0.4
0.3
0.2
0.1
0
0
10
20
30
Diameter (mm)
○ Height %
+ Width %
× Umbilic %
(n = 4)

Text-fig. 25

EXPLANATION OF PLATE 1

Figs 1-7. *Pseudoceltites multiplicatus* (Waagen, 1895). 1a-d, PIMUZ 28193. Found as float in the *Paraedenstroemia* Beds. 2a-d, PIMUZ 28194. From sample M08-48. 3a-c, PIMUZ 28195. From sample M05-48, Mud. 4a-d, PIMUZ 28196; 4d ×2, at H = 10.8 mm. From sample M08-48. 5a-c, PIMUZ 28197, found as float. 6a-c, PIMUZ 28198. From sample M08-48. 7a-d, PIMUZ 28199. From sample Ma31a. All from the *Pseudoceltites multiplicatus* beds, Mud.

Fig. 8a-e. ?*Pseudoceltites* sp. indet. PIMUZ 28200; 8e ×2, at H = 11 mm. From sample Ma26, *Truempyceras compressum* horizon, Mud.

All natural size unless otherwise indicated. Asterisks indicate phragmocone end where known.

Plate 1

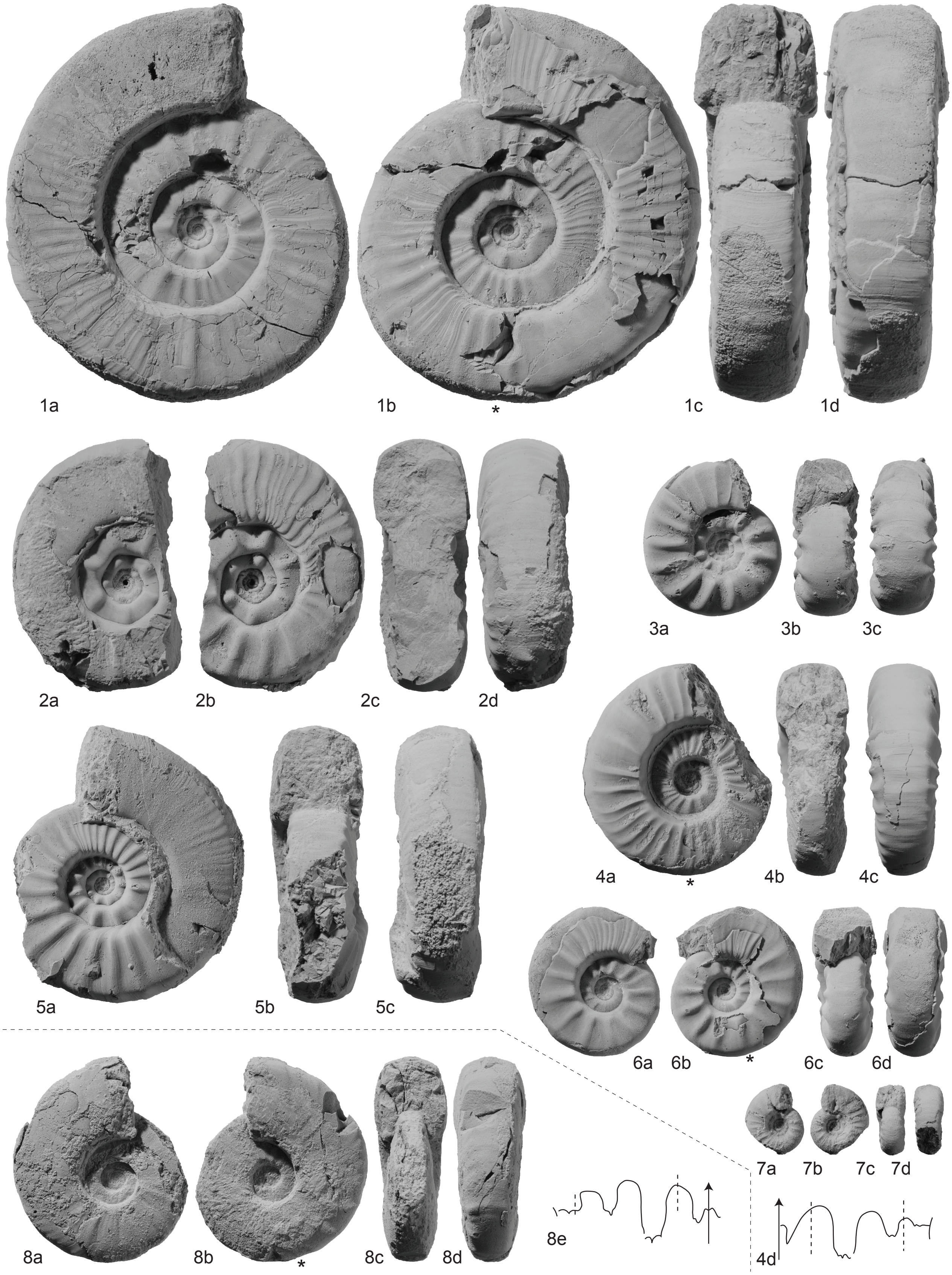
1a
1b
*
1c
1d
2a
2b
2c
2d
3a
3b
3c
4a
*
4b
4c
5a
5b
5c
6a
6b
*
6c
6d
7a
7b
7c
7d
8a
8b
*
8c
8d
8e
4d

EXPLANATION OF PLATE 2

Figs 1-2. *Preflorianites radians* Chao, 1959. 1a-c, PIMUZ 28201. From sample M06-39. 2a-b, PIMUZ 28202. From sample M08-40. Both specimens from the *Truempyceras compressum* horizon, Mud.

Fig. 3a-c. ?*Kashmirites* sp. indet. PIMUZ 28203. From sample HB1006, *Flemingites* beds, Losar.

Figs 4-6. *Kashmirites nivalis* (Diener, 1897). 4a-c, PIMUZ 28204. From sample HB1010. 5a-c, PIMUZ 28205. From sample HB1010. 6a-d, PIMUZ 28206. From sample HB1019. All from the *Flemingites* beds, Losar.

Figs 7-9. *Nyalamites angustecostatus* (Welter, 1922). 7a-b, PIMUZ 28207, ×2. From sample Ma46, Mud. 8a-c, PIMUZ 28208; 8d×2, at H = 5.9 mm. From sample M03-58, Mud. 9a-c, PIMUZ 28209. From sample HB1900, *Nyalamites angustecostatus* beds, Losar.

Figs 10-13. *Glyptophiceras sinuatum* (Waagen, 1895). 10, PIMUZ 28210, ×2, at H = 10.6 mm. 11a-d, PIMUZ 28211. 12a-c, PIMUZ 28212. 13a-b, PIMUZ 28213. All from sample Ma96, *Glyptophiceras sinuatum* beds, Mud.

All natural size unless otherwise indicated.

Plate 2

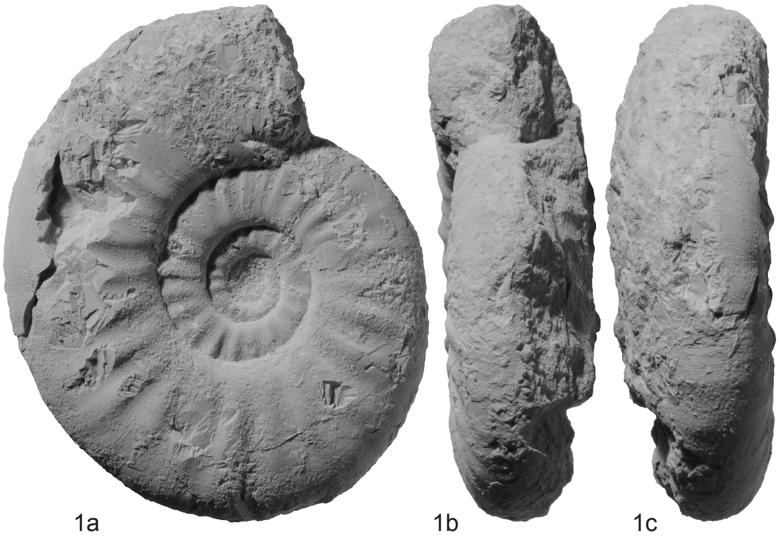
1a 1b 1c


3a 3b 3c

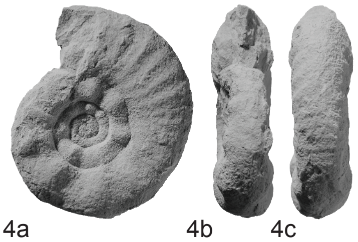
4a 4b 4c


2a 2b


5a 5b 5c

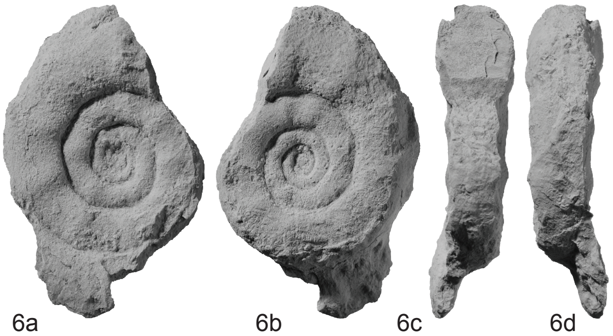
6a 6b 6c 6d


7a 7b

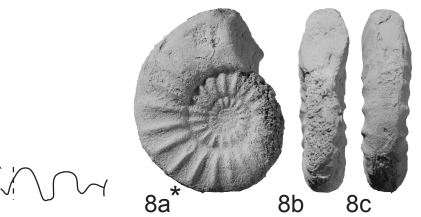
8d 8a* 8b 8c


9a 9b 9c

10



11a 11b 11c 11d

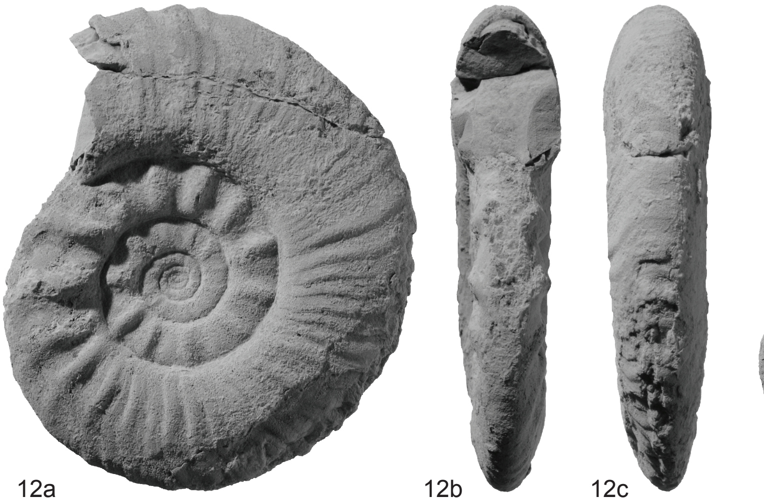
12a 12b 12c

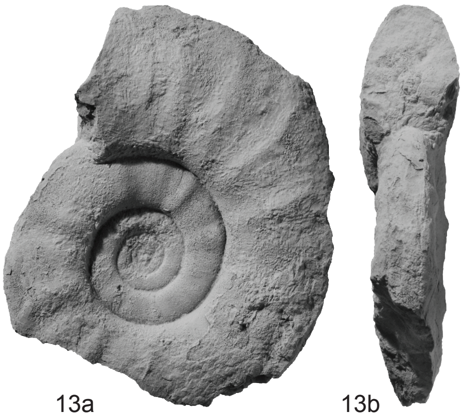
13a 13b

EXPLANATION OF PLATE 3

Figs 1-2. *Xenoceltites* cf. *variocostatus* Brayard and Bucher, 2008. 1a-e, PIMUZ 28214; 1e ×2, at H = 8.5 mm. From sample M08-70. 2a-b, PIMUZ 28215. From sample E30. Both specimens from the *Subvishnuites posterus* beds, Mud.

Figs 3a-b. *Pseudaspidites* sp. indet. PIMUZ 28218. From sample M08-21, *Brayardites compressus* beds, Mud.

Fig. 4a-c. *Hanielites* cf. *elegans* (Welter, 1922). PIMUZ 28217. From sample M08-29, *Escarguelites spitiensis* horizon, Mud.

Fig. 5-6. *Pseudaspidites muthianus* (Krafft and Diener, 1909). 5a-c. PIMUZ 28216; 3c at H = 21.7 mm. From sample M05-18, just below the *Brayardites compressus* beds, Mud. 6a-c. PIMUZ 28219. From sample HB1004, *Escarguelites spitiensis* horizon, Losar.

Figs 7-8. *Xiaoqiaoceras involutus* Brayard and Bucher, 2008. 7a-e, PIMUZ 28220, 7e at H = 8.5 mm, D = 13.5. 8a-d, PIMUZ 28221. Both specimens from sample HB1005, *Brayardites compressus* beds, Losar. All ×2.

Fig. 9a-d. ?*Paranorites* sp. indet. PIMUZ 28222. Found as float in the *"Parahedenstroemia"* Beds, Mud. All ×0.5.

All natural size unless otherwise indicated.

Plate 3

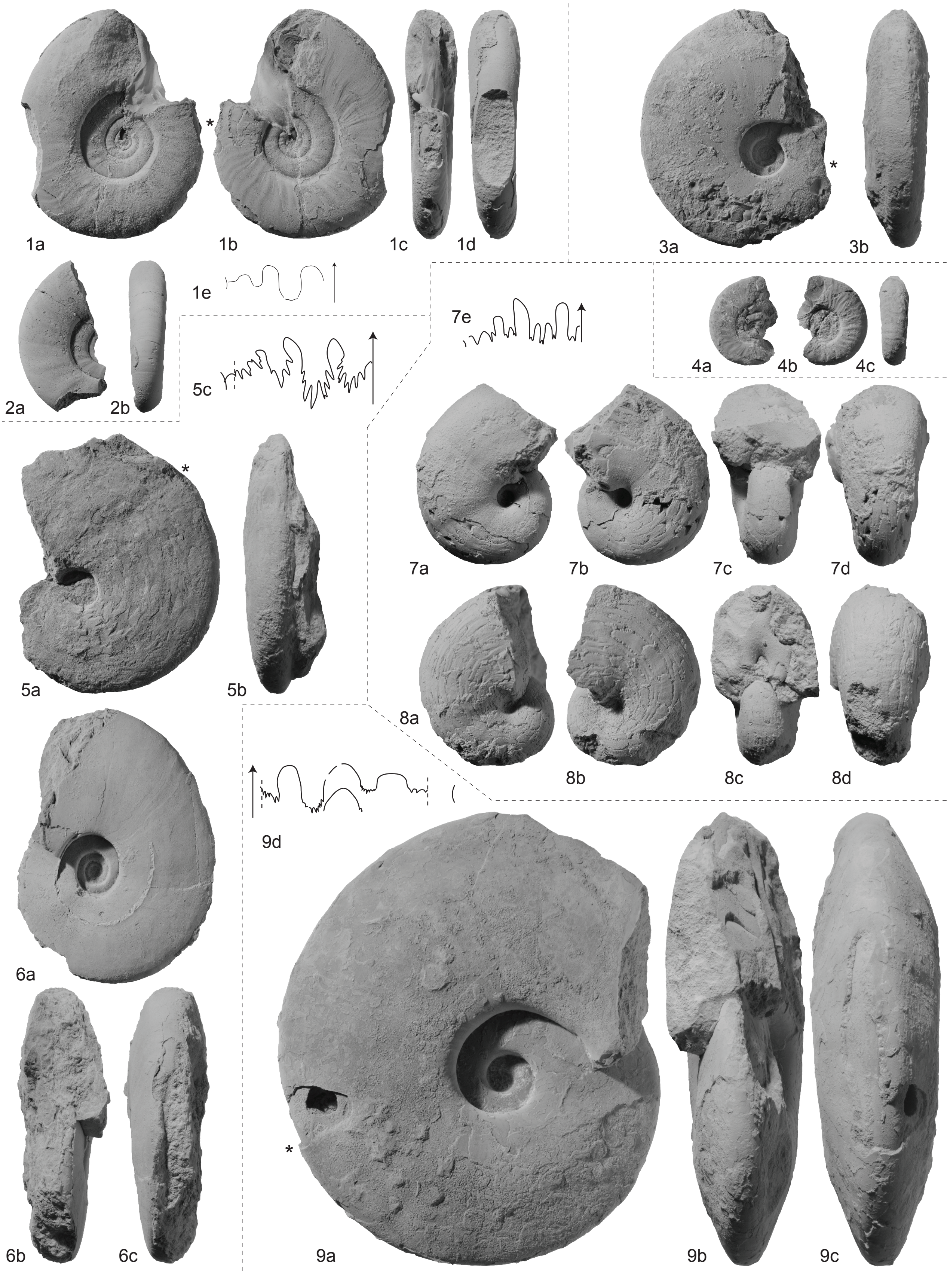
1a
1b
1c
1d
1e
2a
2b
3a
3b
4a
4b
4c
5a
5b
5c
6a
6b
6c
7a
7b
7c
7d
7e
8a
8b
8c
8d
9a
9b
9c
9d
*

EXPLANATION OF PLATE 4

Figs 1-11. *Tulongites xiaoqiaoi* Brühwiler *et al.*, accepted. 1a-d, PIMUZ 28223; 1d ×1.5, at H = 15.8 mm. From sample M08-21, Mud. 2a-d, PIMUZ 28224. From sample HB1033, Losar. 3a-d, PIMUZ 28225. From sample HB1005, Losar. 4a-d, PIMUZ 28226. From sample HB1033, Losar. 5a-d, PIMUZ 28227. From sample HB1005, Losar. 6a-d, PIMUZ 28228. From sample HB1033, Losar. 7a-b, PIMUZ 28229. From sample M08-21, Mud. 8a-d, PIMUZ 28230. From sample HB1033, Losar. 9a-d, PIMUZ 28231. From sample HB1005, Losar. 10a-c, PIMUZ 28232. From sample M08-21, Mud. 11a-c, PIMUZ 28233. From sample HB1005, Losar. All from the *Brayardites compressus* beds.

Figs 12-17. ?*Galfettites* sp. indet. 12a-c, PIMUZ 28234. 13a-c, PIMUZ 28235. 14a-d, PIMUZ 28236. 15 a-b, PIMUZ 28237. 16a-e, PIMUZ 28238; 16e ×3, at H = 5 mm. From sample HB1033. 17a-c, PIMUZ 28239. All from sample HB1005 except for Fig. 16. All from the *Brayardites compressus* beds, Losar.

All natural size unless otherwise indicated.

Plate 4

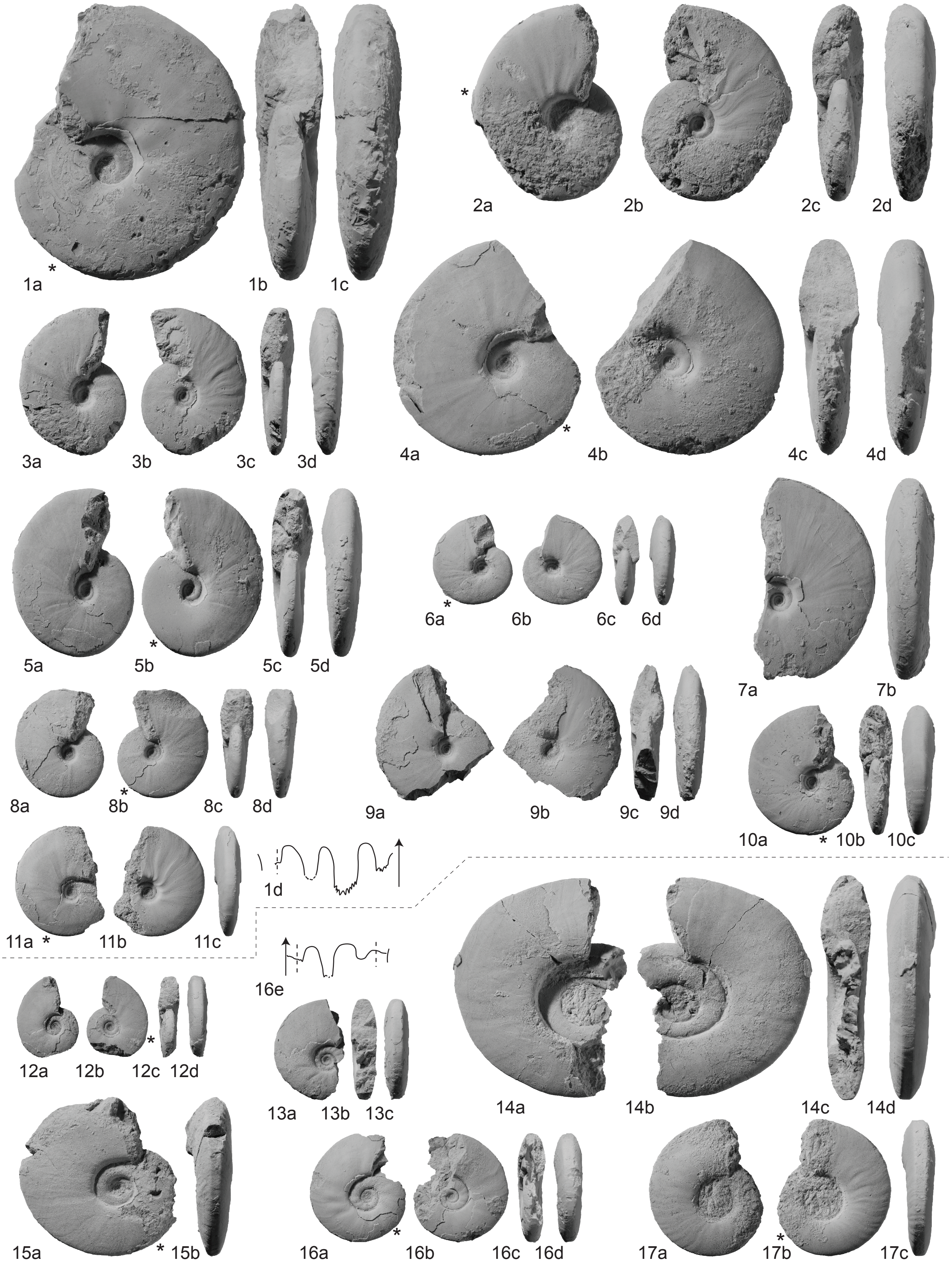
1a
*
1b
1c
2a
*
2b
2c
2d
3a
3b
3c
3d
4a
*
4b
4c
4d
5a
5b
*
5c
5d
6a
*
6b
6c
6d
7a
7b
8a
8b
*
8c
8d
9a
9b
9c
9d
10a
*
10b
10c
11a
*
11b
11c
1d
16e
12a
12b
*
12c
12d
13a
13b
13c
14a
14b
14c
14d
15a
*
15b
16a
*
16b
16c
16d
17a
17b
*
17c

EXPLANATION OF PLATE 5

Figs 1-8. *Galfettites omani* Brühwiler and Bucher, submitted [a]. 1a-c, PIMUZ 28240. From sample M04-44. 2a-d, PIMUZ 28241. From sample LoA-SFB. 3a-d, PIMUZ 28242. From sample LoA-SFB. 4a-d, PIMUZ 28243. From sample HB1004. 5a-d, PIMUZ 28244; 5d ×2, at H = 7.2 mm. From sample Ma24c. 6a-e, PIMUZ 28245; 6e ×2, at H = 5.7 mm. From sample LoA-SFB. 7a-d, PIMUZ 28246. From sample LoA-SFB. 8a-b, PIMUZ 28247. From sample HB1004. All from the *Nammalites pilatoides* beds.

Fig. 9a-c. ?*Urdyceras* sp. indet. PIMUZ 28248. From sample Ma49, *Nyalamites angustecostaus* beds, Mud.

Figs 10-17. *Urdyceras tulongensis* Brühwiler *et al.* accepted. 10a-d, PIMUZ 28249. From sample E17, Mud. 11a-c, PIMUZ 28250. From sampleHB1005. 12a-c, PIMUZ 28251. From sample HB1005. 13a-c, PIMUZ 28252; 13c ×2, at H = 7.3 mm. From sample HB1005. 14a-c, PIMUZ 28253. From sample HB1033. 15a-c, PIMUZ 28254. From sample HB1005. 16a-d, PIMUZ 28255. From sample HB1005. 17a-b, PIMUZ 28256. From sample HB1033. All from Losar except for Fig. 10. All from the *Brayardites compressus* beds.

Figs 18-21. *Dieneroceras* cf. *tientungense* Chao, 1959. 18a-d, PIMUZ 28257. From sample HB 1013. 19a-e, PIMUZ 28258. From sample HB1013; 20e ×3, at H = 5.8 mm. 20a-c, PIMUZ 28259. From sample HB1013. 21a-d, PIMUZ 28260. From sample HB1020. All from the *Flemingites* beds, Losar.

All natural size unless otherwise indicated.

Plate 5

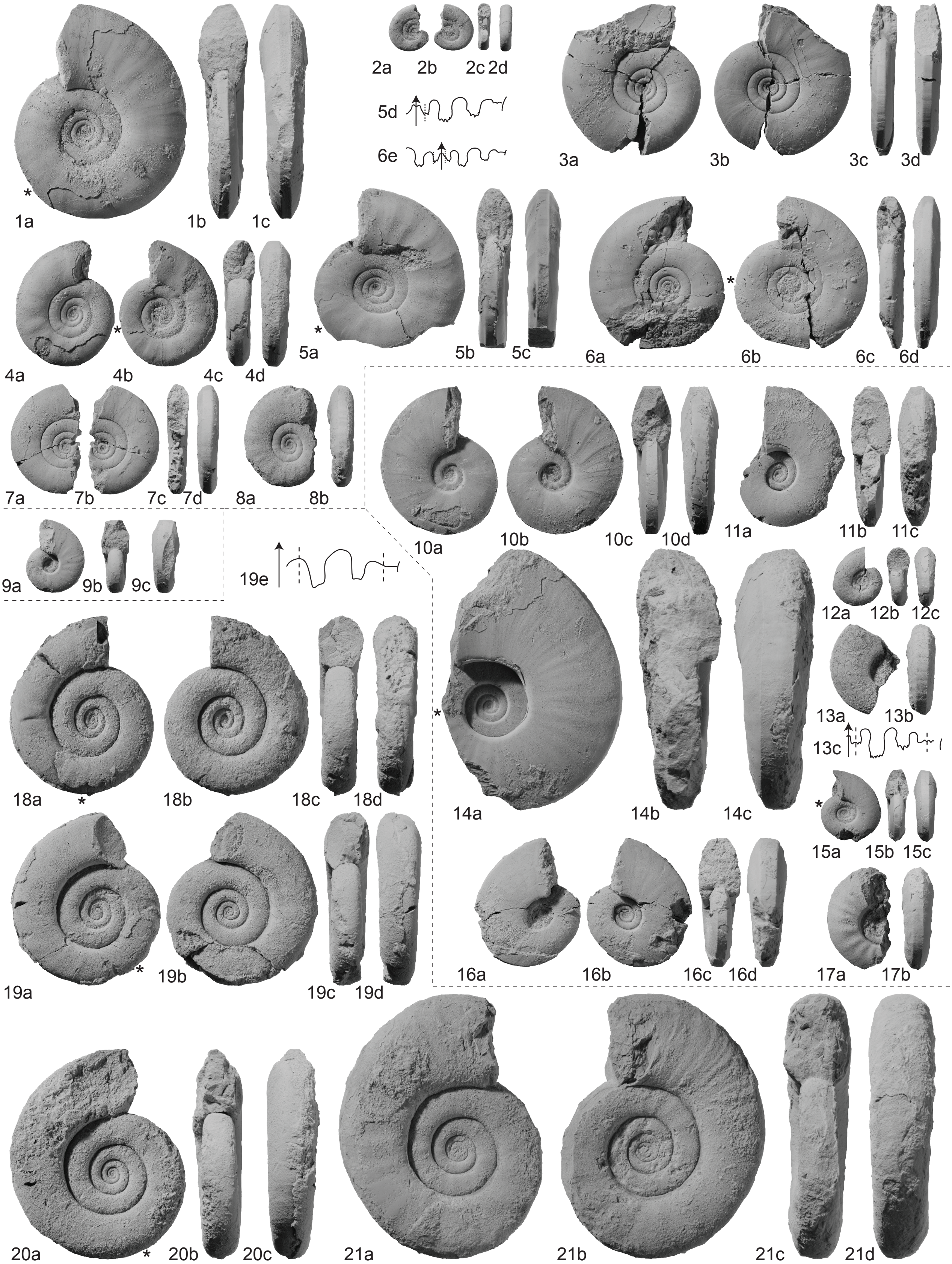
1a
1b
1c
2a
2b
2c
2d
5d
6e
3a
3b
3c
3d
4a
4b
4c
4d
5a
5b
5c
6a
6b
6c
6d
7a
7b
7c
7d
8a
8b
10a
10b
10c
10d
11a
11b
11c
9a
9b
9c
19e
12a
12b
12c
13a
13b
13c
14a
14b
14c
18a
18b
18c
18d
15a
15b
15c
19a
19b
19c
19d
16a
16b
16c
16d
17a
17b
20a
20b
20c
21a
21b
21c
21d

EXPLANATION OF PLATE 6

Figs 1-3.*Hermannites rursiradiatus* gen. et sp. nov. 1a-e, PIMUZ 28261; 1e ×1.5, at H = 26.5 mm, D = 76.6 mm. From sample M03-20, Mud. 2a-b, PIMUZ 28262. From sample LoSFB1, Losar. 3a-c, PIMUZ 28263. From sample HB1005, Losar. All from the *Brayardites compressus* beds.

Fig. 4. Ussuriidae gen. et sp. indet. PIMUZ 28376. Found as a float in the *Parahedenstroemia* Beds at Mud. See also Pl. 7, fig. 5a-b.

All natural size unless otherwise indicated.

Plate 6

EXPLANATION OF PLATE 7

Figs 1-4. *Anaxenaspis* sp. indet. 3a-c, PIMUZ 28266. From sample M08-48. 4a-d, PIMUZ 28267; 4d ×2, at H = 12.5 mm. From sample M05-48. 5a-c, PIMUZ 28268. From sample Ma49. 6a-c, PIMUZ 28269. From sample M08-48. All from Mud. 5 from the *Nyalamites angustecostatus* beds; all others from the *Pseudoceltites multiplicatus* beds.

Fig. 5a-b. Ussuriidae gen. et sp. indet. PIMUZ 28376. Found as a float in the *"Parahedenstroemia"* Beds at Mud. See also Pl. 6, fig. 4.

Figs 6a-b. *Flemingites* sp. indet. 1a-b, PIMUZ 28264. From sample HB1013. 2a-d, PIMUZ 28265. From sample HB1024. Both specimens from the *Flemingites* beds of Losar.

All natural size unless otherwise indicated.

Plate 7

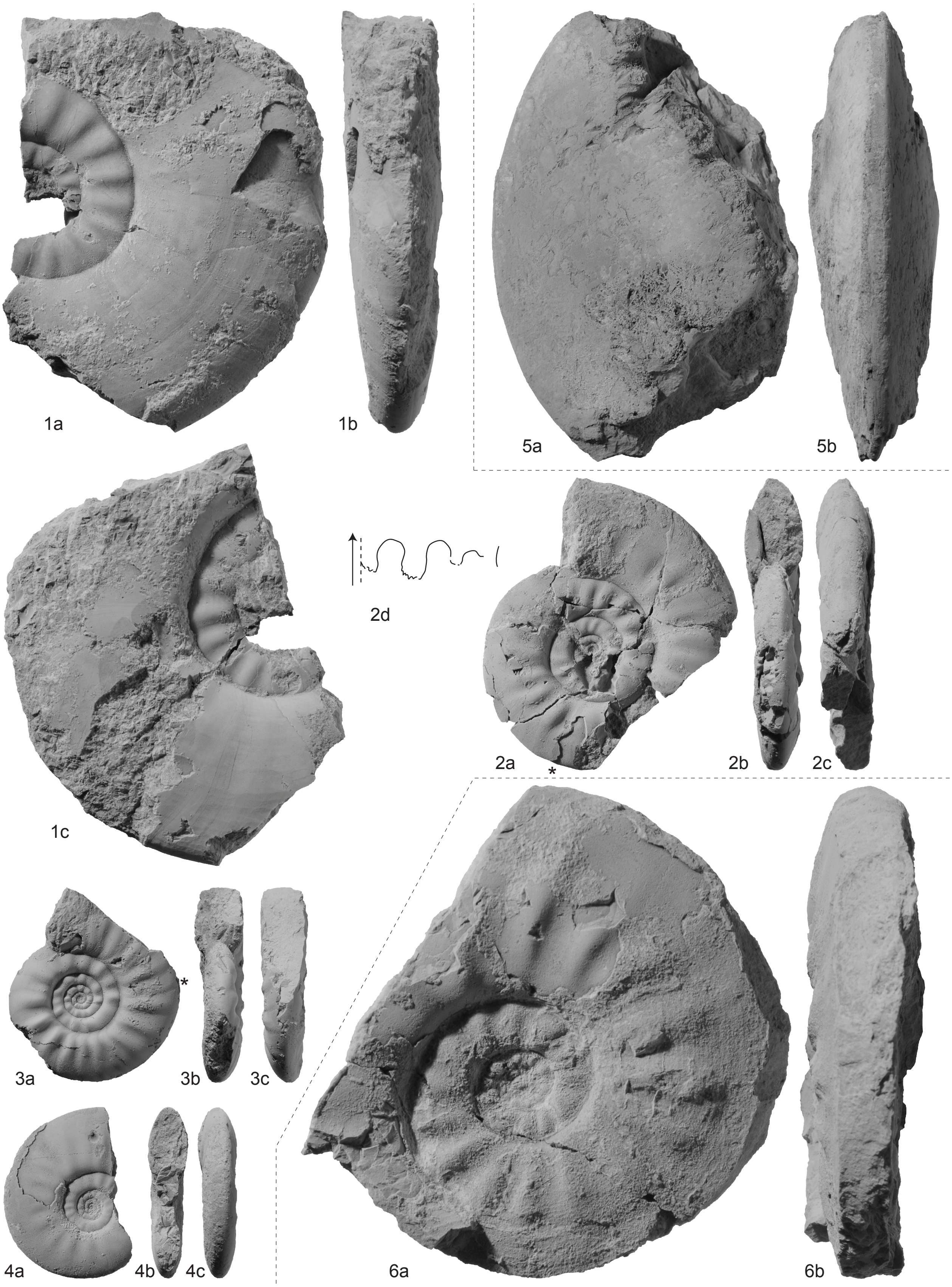

EXPLANATION OF PLATE 8

Fig. 1a-c. *Anaxenaspis* sp. indet. PIMUZ 28270. From sample M08-48, *Pseudoceltites multiplicatus* beds, Mud.

Figs 2-3. ?*Subflemingites compressus* Brühwiler *et al.*, accepted. 2a-d, PIMUZ 28271. From sample Ma49. 3a-c, PIMUZ 28272. From sample Ma46. Both specimens from the *Nylamites angustecostatus* beds, Mud.

Figs 4-5. *Brayardites crassus* Brühwiler *et al.*, accepted. 4a-d, PIMUZ 28273. From sample M03-21. 5a-c, PIMUZ 28274. From sample M05-20. Both specimens from the *Brayardites compressus* beds, Mud.

All natural size unless otherwise indicated.

Plate 8

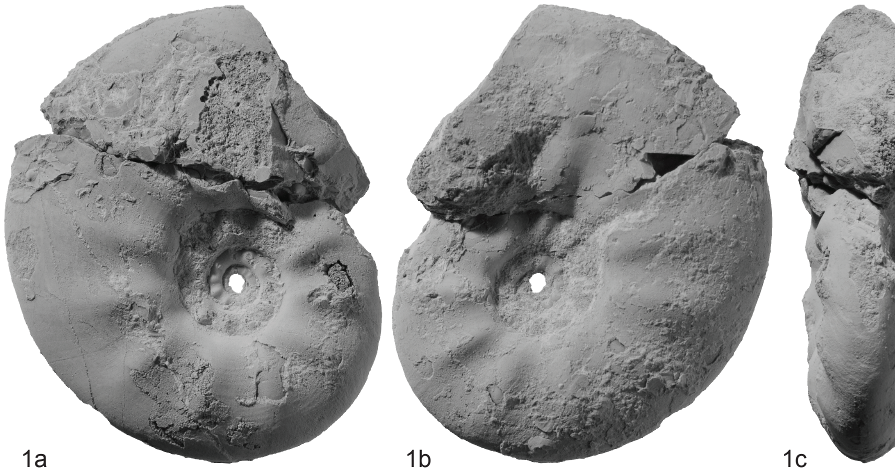

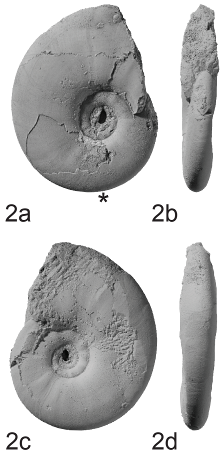

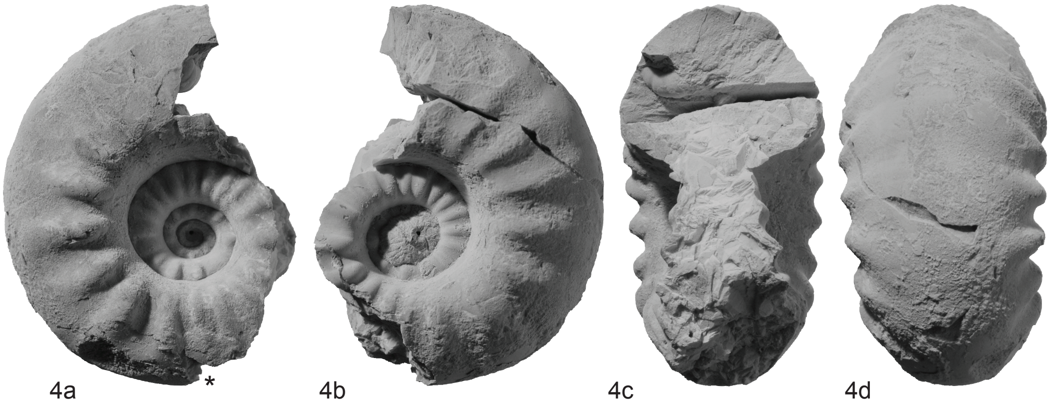

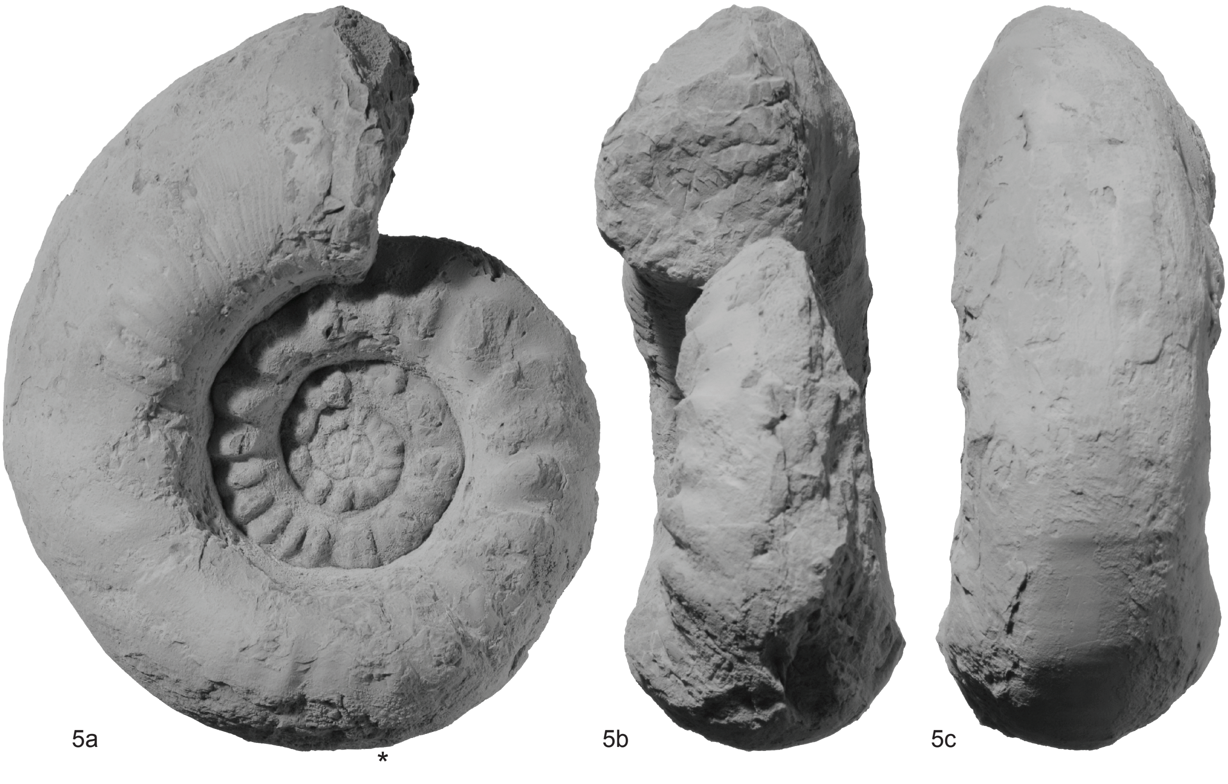

EXPLANATION OF PLATE 9

Figs 1-5. *Brayardites compressus* Brühwiler *et al.*, accepted. 1a-b, PIMUZ 28275. From sample M03-24, Mud. 2a-d, PIMUZ 28276; 2d ×2, at H = 18 mm. From sample HB1005, Losar. 3a-d, PIMUZ 28277. From sample HB1005, Losar. 4a-b, PIMUZ 28278. From sample M08-21, Mud. 5a-c, PIMUZ 28279. From sample M08-21, Mud. All from the *Brayardites compressus* beds. All natural size unless otherwise indicated.

Plate 9

1a

1b

2a

3a

3b

3c

3d

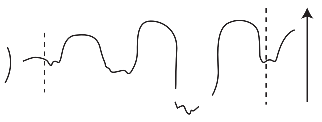

2d

2b

2c

4a

4b

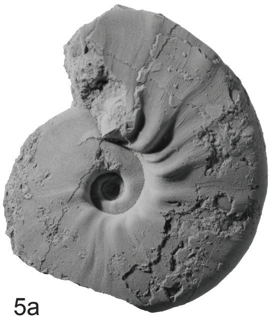

5a

5b

5c

EXPLANATION OF PLATE 10

Fig. 1. *Brayardites compressus* Brühwiler *et al.*, accepted. PIMUZ 28280. From sample M05-23, *Brayardites compressus* beds, Mud.

Figs 2-10. *Nammalites pilatoides* (Guex, 1978). 2a-c, PIMUZ 28281. From sample Ma28b, Mud. 3a-c, PIMUZ 28282. From sample HB1004, Losar. 4a-b, PIMUZ 28283. From sample HB1004, Losar. 5a-c, PIMUZ 28284. From sample Ma28b. 6a-c, PIMUZ 28285. From sample E22/23, Mud. 7, PIMUZ 28286; at H = 17.7 mm. From sample HB1004, Losar. 8a-b, PIMUZ 28287. From sample Ma28b, Mud. 9a-d, PIMUZ 28288. From sample HB1029, Losar. 10a-c, PIMUZ 28289. From sample Ma28b, Mud. All from the *Nammalites pilatoides* beds.

Figs 11-13. *Nuetzelia himalayica* gen. et sp. nov. 11a-c, PIMUZ 28290. 12a-c, PIMUZ 28291. 13a-e, PIMUZ 28292; 13e ×3, at H = 7.4 mm. All from sample HB 1004, *Escarguelites spitiensis* horizon, Losar.

All natural size unless otherwise indicated.

Plate 10

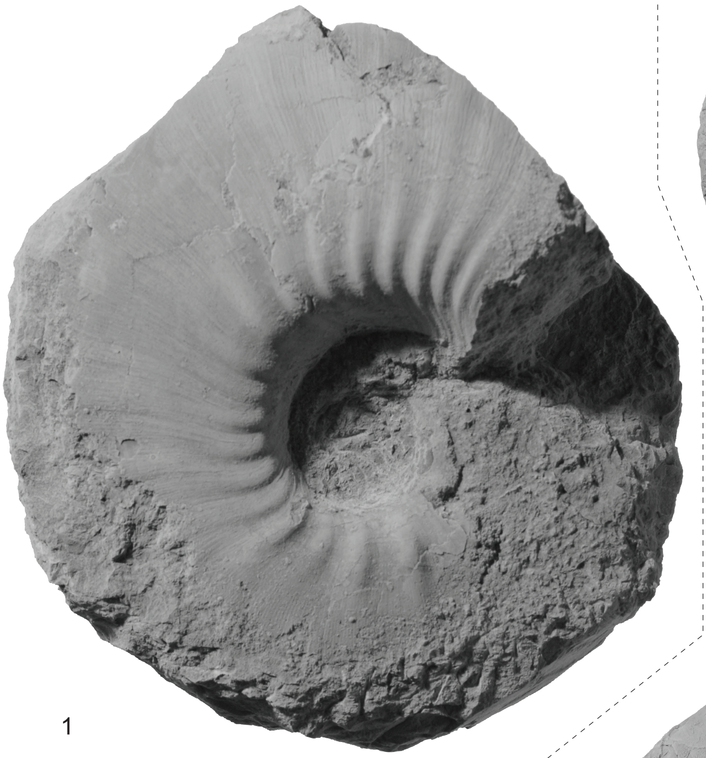
1

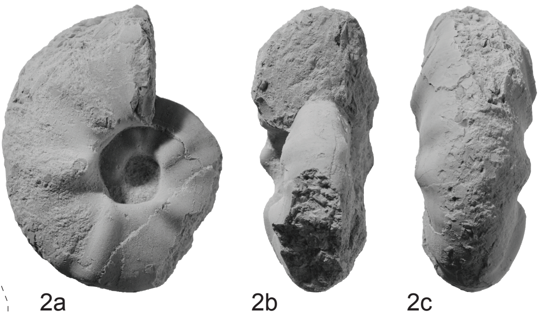
2a 2b 2c

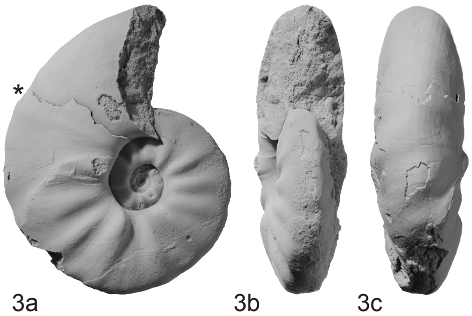
3a 3b 3c

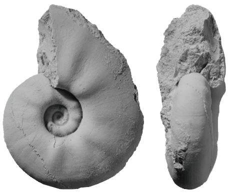
4a 4b


5a 5b 5c

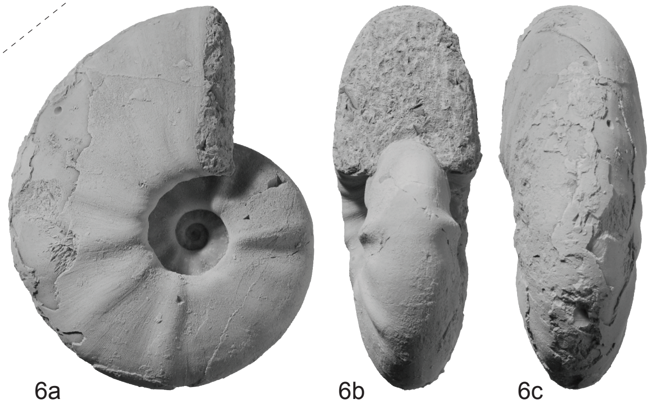
6a 6b 6c


7

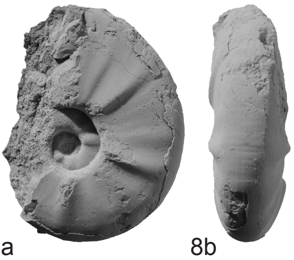
8a 8b


9a 9b 9c 9d


10a 10b 10c

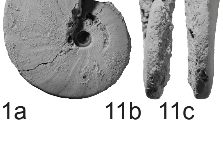
11a 11b 11c

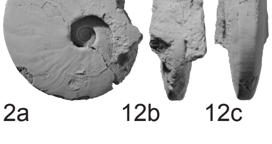
12a 12b 12c

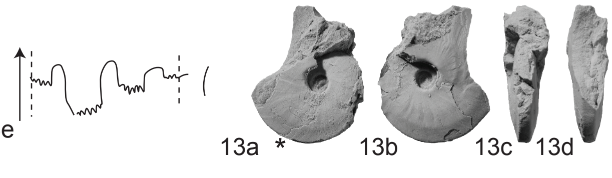
13a 13b 13c 13d 13e

EXPLANATION OF PLATE 11

Fig. 1a-d. *Nammalites pilatoides* (Guex, 1978). PIMUZ 28293. From sample M06-39, *Nammalites pilatoides* beds, Mud.

Figs 2-4. *Escarguelites spitiensis* gen. et sp. nov. 2a-e, PIMUZ 28294; 2e ×2, at H = 12.5 mm. From sample M08-29, Mud. 3a-c, PIMUZ 28295. From sample HB1004, Losar. 4a-c, PIMUZ 28296. From sample M08-29, Mud. All from the *Escarguelites spitiensis* horizon.

All natural size unless otherwise indicated.

Plate 11

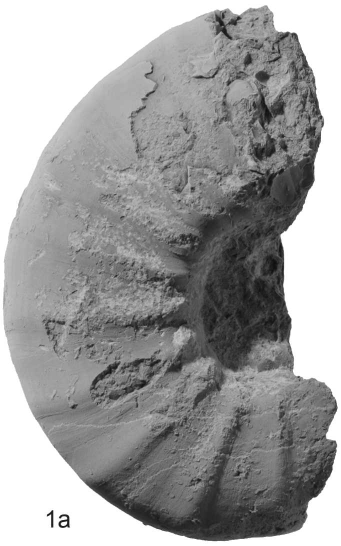
1a


1b

2a


2b


1c


1d


2c


2d

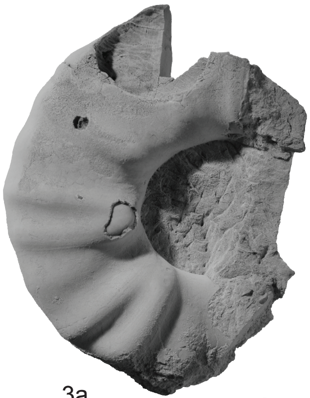
3a


3b

2e
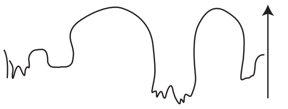

4a


4b


4c


3c

EXPLANATION OF PLATE 12

Figs 1-8. *Truempyceras compressum* sp. nov. 1a-d, PIMUZ 28297. From sample LTB3, Lalung. 2a-c, PIMUZ 28298. From sample LTB3, Lalung. 3a-c, PIMUZ 28299. From sample M05-43, Mud. 4a-d, PIMUZ 28300. From sample E22, Mud. 5a-b, PIMUZ 28301. From sample LTB3, Lalung. 6a-c, PIMUZ 28302. From sample HB1029, Losar. 7a-b, PIMUZ 28303. From sample LTB3, Lalung. 8a-f, PIMUZ 28304; 8f at H = 17.5 mm. From sample LTB3, Lalung. All from the *Truempyceras compressum* horizon. All natural size.

Plate 12

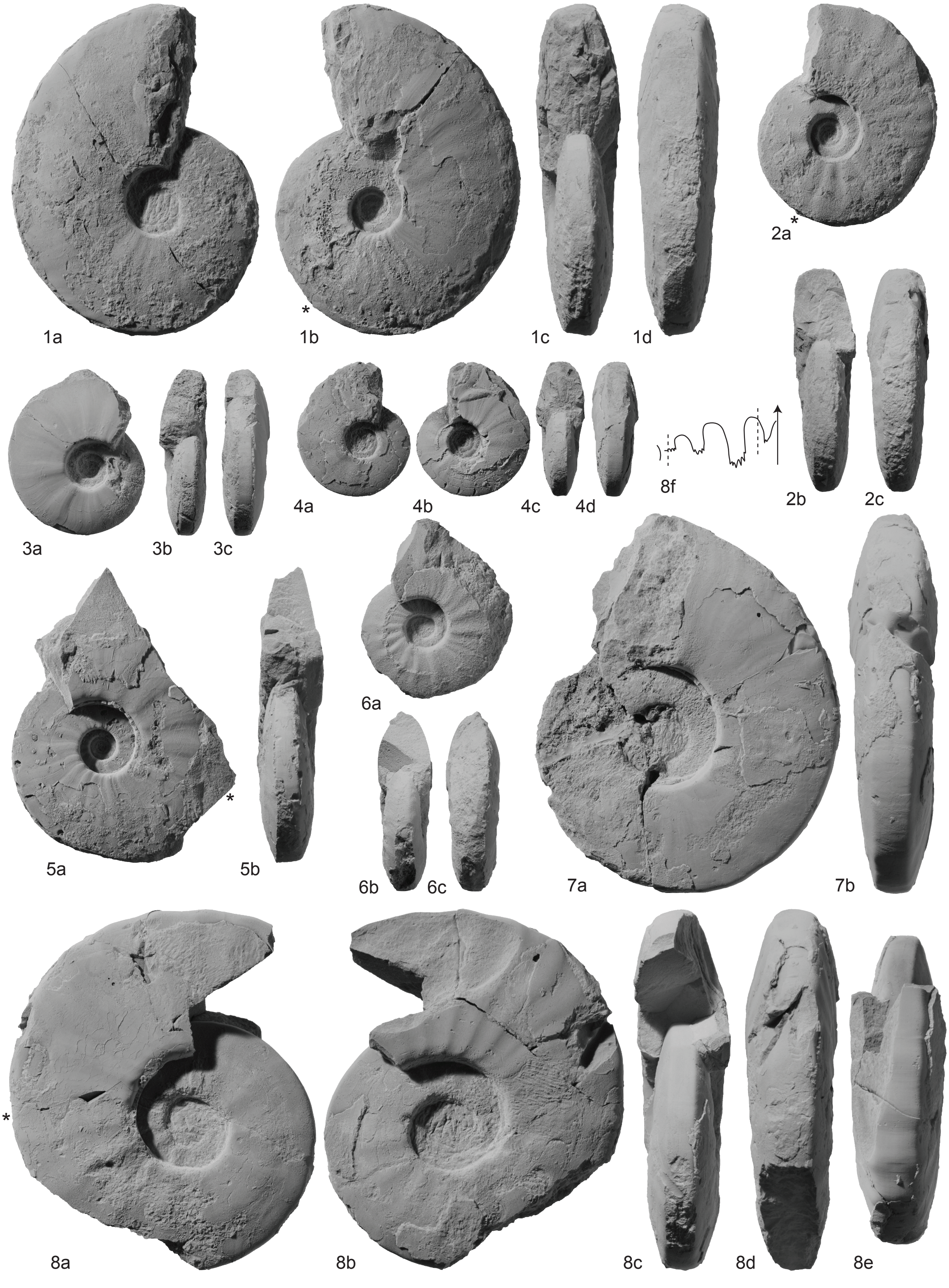
1a
1b
1c
1d
2a
2b
2c
3a
3b
3c
4a
4b
4c
4d
8f
5a
5b
6a
6b
6c
7a
7b
8a
8b
8c
8d
8e

EXPLANATION OF PLATE 13

Figs 1-3. *Prionites* sp. indet. 1a-b, PIMUZ 28305. 2a-c, PIMUZ 28306. 3a-d, PIMUZ 28307; 3e ×2, at H = 13.2 mm. All from sample Ma49, *Nyalamites angustecostatus* beds, Mud.

Fig. 4a-d. Gen. et sp. indet. A. PIMUZ 28308; 4d ×2, at H = 12.6 mm. From sample HB1004, *Escarguelites spitiensis* horizon, Losar.

Fig. 5. *Anasibirites kingianus* (Waagen, 1895). PIMUZ 28309, ×3, at H = 4.5 mm (see also Pl. 14, fig. 13a-d). From sample Gu106, *Wasatchites distractus* beds, Guling.

Fig. 6a-d. *Stephanites superbus* Waagen, 1895. PIMUZ 28310; 6d at H = 25 mm. From sample M05-57, *Nyalamites angustecostatus* beds, Mud.

All natural size unless otherwise indicated.

Plate 13

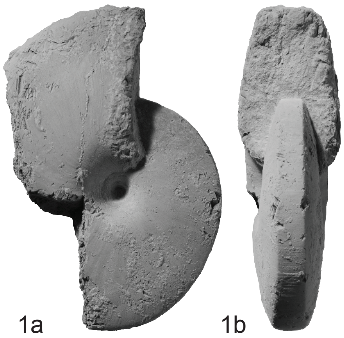

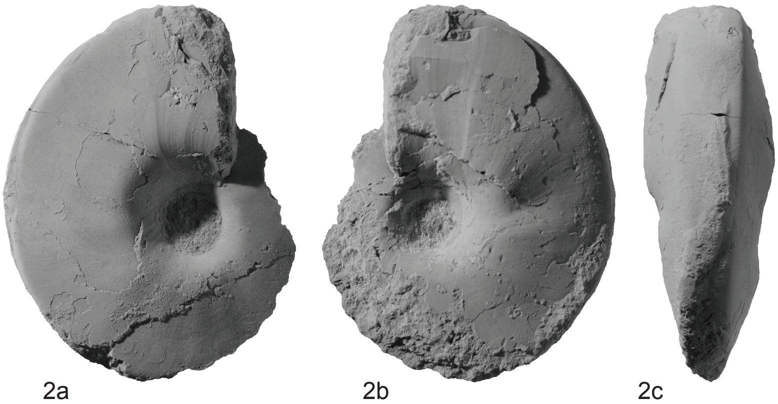

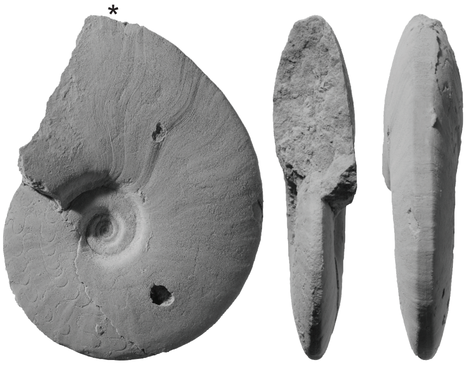

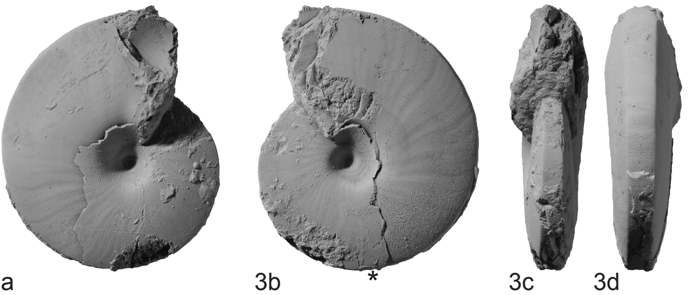

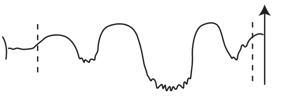

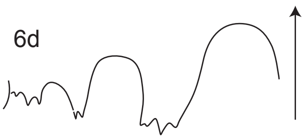

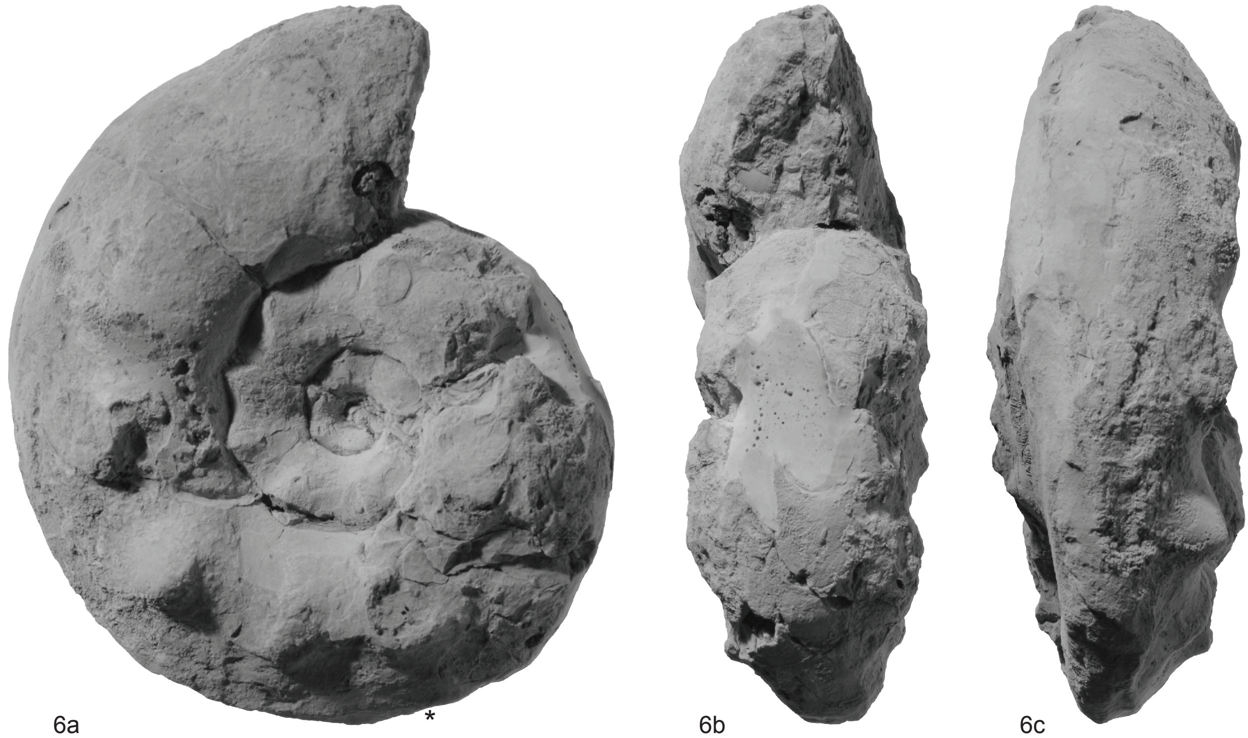

EXPLANATION OF PLATE 14

Figs 1-8. *Wasatchites distractus* (Waagen, 1895). 1a-c, PIMUZ 28311. From sample Ma92, Mud. 2a-d, PIMUZ 28312. From sample Gu106, Guling. 3a-d, PIMUZ 28313. From sample Gu106, Guling. 4a-d, PIMUZ 28314. From sample Gu106, Guling. 5a-d, PIMUZ 28315. From sample E29/30, Mud. 6a-c, PIMUZ 28316. From sample Gu106, Guling. 7, PIMUZ 28317; ×2, at H = 8.9 mm. From sample Gu106, Guling. 8a-c, PIMUZ 28318. From sample Gu106, Guling. All from the *Wasatchites distractus* beds.

Figs 9-16. *Anasibirites kingianus* (Waagen, 1895). 9a-d, PIMUZ 28319. 10a-c, PIMUZ 28320. 11a-d, PIMUZ 28321. 12a-c, PIMUZ 28322. 13a-d, PIMUZ 28309. 14a-d, PIMUZ 28323. 15a-d, PIMUZ 28324. From sample Ma92, Mud. 16a-d, PIMUZ 28325. All from sample Gu106, Guling, except for Fig. 15. All from the *Wasatchites distractus* beds.

All natural size unless otherwise indicated.

Plate 14

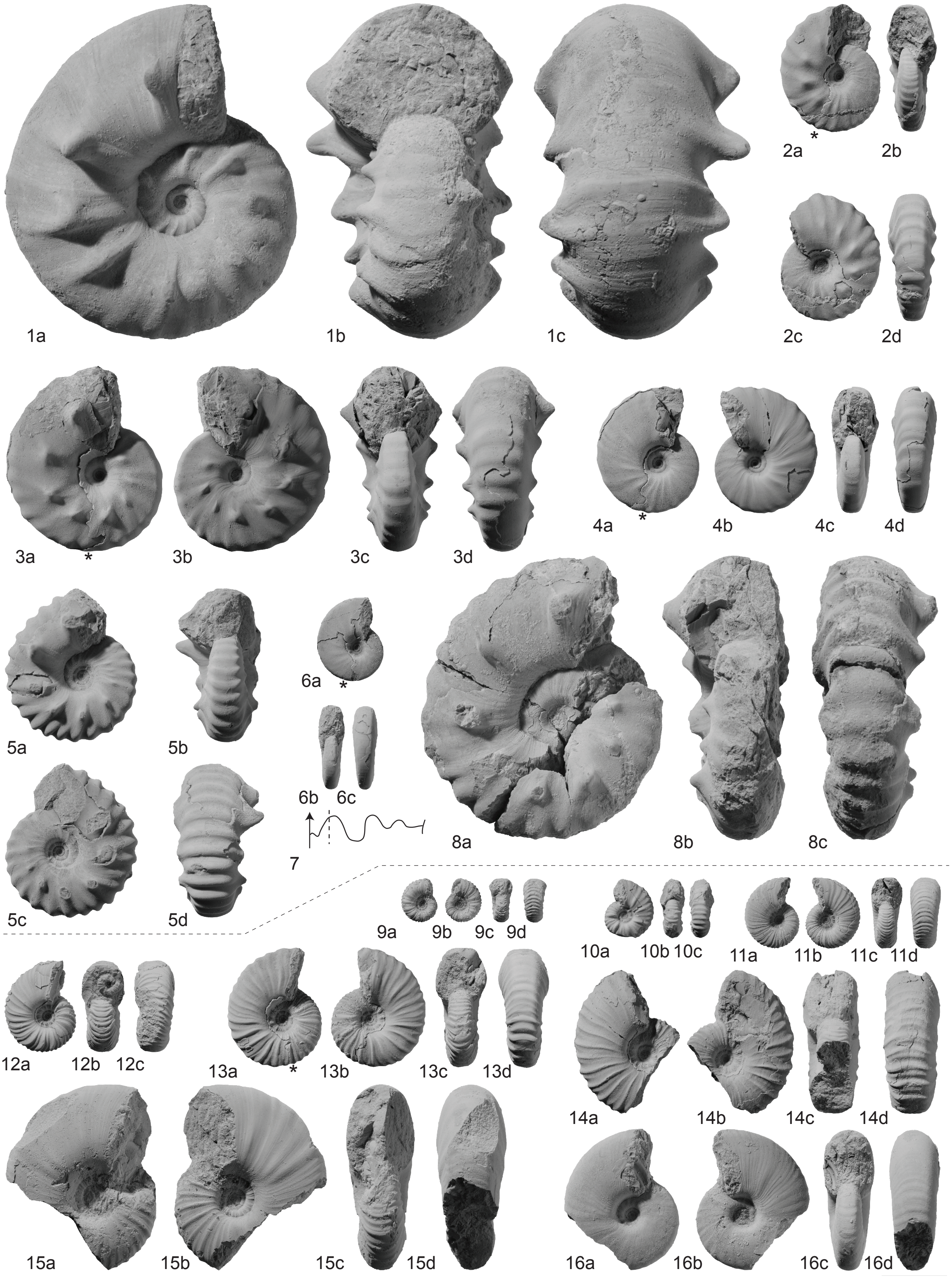
1a
1b
1c
2a
*
2b
2c
2d
3a
*
3b
3c
3d
4a
*
4b
4c
4d
5a
5b
5c
5d
6a
*
6b
6c
7
8a
8b
8c
9a
9b
9c
9d
10a
10b
10c
11a
11b
11c
11d
12a
12b
12c
13a
*
13b
13c
13d
14a
14b
14c
14d
15a
15b
15c
15d
16a
16b
16c
16d

EXPLANATION OF PLATE 15

Figs 1-7. *Paranannites* sp. indet. 1a-d, PIMUZ 28326. From sample M06-39. 2a-c, PIMUZ 28327. From sample M06-39. 3a-c, PIMUZ 28328. From sample M06-39. 4a-c, PIMUZ 28329. From sample HB1006, Losar. 5a-c, PIMUZ 28330. From sample Ma28b. 6a-d, PIMUZ 28331. From sample M06-39. 7a-c, PIMUZ 28332; 7d ×2. From sample Ma28b. All from Mud, except for Fig. 4. All from the *Truempyceras compressum* horizon.

Figs 8-9. *Owenites* cf. *simplex* Welter, 1922. 8a-c, PIMUZ 28333. 9a-b, PIMUZ 28334. Both specimens from sample Ma28b, *Truempyceras compressum* horizon.

Fig. 10a-d. *Owenites* sp. indet. PIMUZ 28336; 10d ×5, at H = 4mm. From sample Gu44, *Truempyceras compressum* horizon, Guling.

Fig. 11a-c. *Owenites koeneni* Hyatt and Smith, 1905. PIMUZ 28335. From sample M03-57, *Nyalamites angustecostatus* beds, Mud.

Figs 12-14. *Owenites carpenteri* Smith, 1932. 12a-c, PIMUZ 28338; 13c ×2, at H = 8.5 mm. From sample Ma49, Mud. 13a-d, PIMUZ 28340. From sample Gu72, Guling. 14a-d, PIMUZ 28339. From sample Gu72, Guling. All from the *Nyalamites angustecostatus* beds.

Figs 15-16. *Steckites brevus* gen. et sp. nov. 15a-c, PIMUZ 28337; 12d ×2, at H = 8.1 mm. From sample Ma26. 16a-d, PIMUZ 28378. From sample Mud-E21-22. *Truempyceras compressum* horizon, Mud.

All natural size unless otherwise indicated.

Plate 15

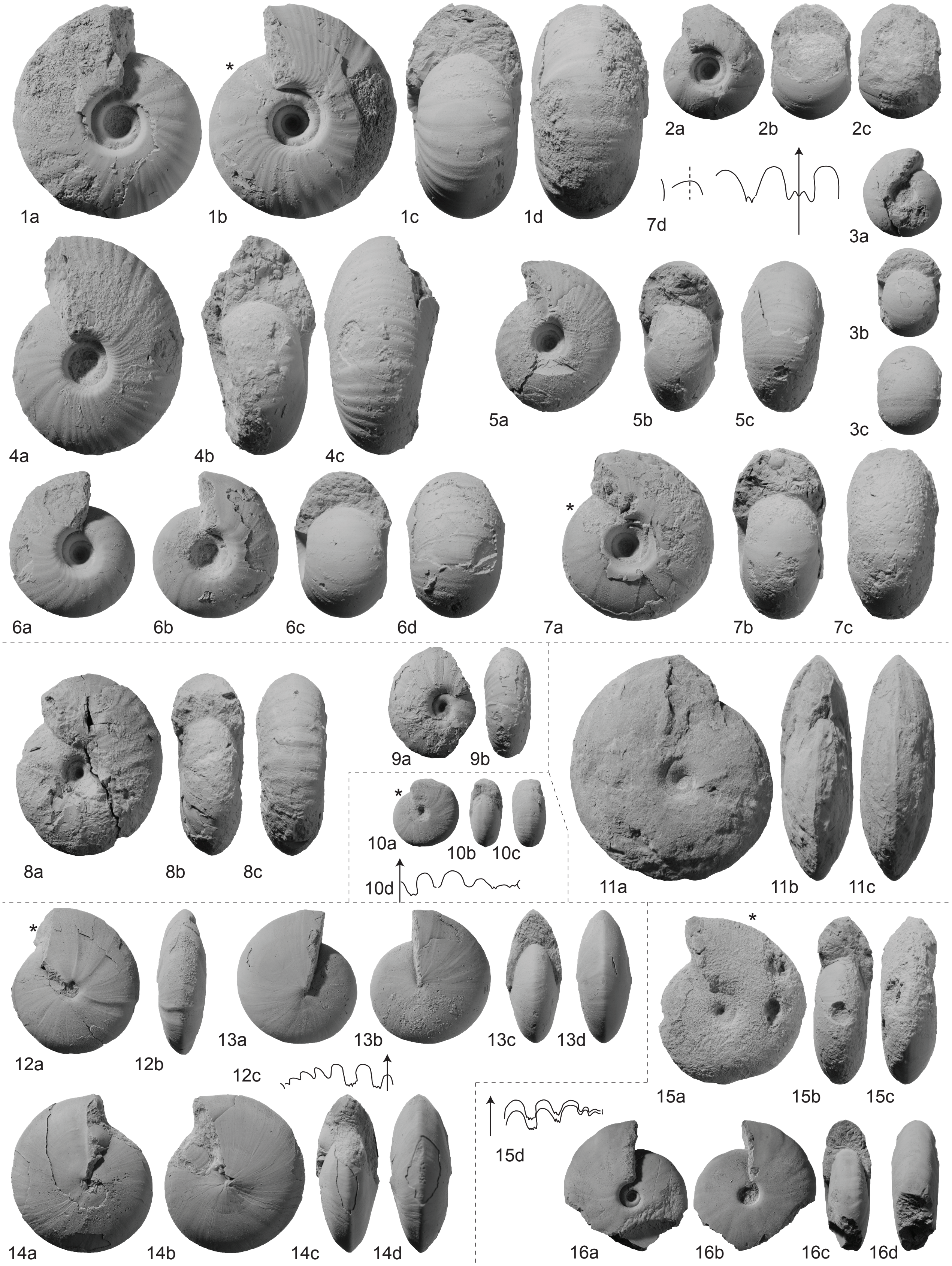
1a
*
1b
1c
1d
2a
2b
2c
7d
3a
4a
4b
4c
5a
5b
5c
3b
3c
6a
6b
6c
6d
*
7a
7b
7c
8a
8b
8c
9a
9b
*
10a
10b
10c
10d
11a
11b
11c
*
12a
12b
12c
13a
13b
13c
13d
*
15a
15b
15c
15d
14a
14b
14c
14d
16a
16b
16c
16d

EXPLANATION OF PLATE 16

Figs 1-5. *Juvenites* cf. *spathi* (Frebold, 1930). 1a-c, PIMUZ 28341. 2a-c, PIMUZ 28344. 3a-b, PIMUZ 28343. 4a-d, PIMUZ 28352. From sample LoA-SFB, *Nammalites pilatoides* beds (?), Losar. 5a-c, PIMUZ 28342. All from sample M05-23, *Brayardites compressus* beds, Mud, except for Fig. 4.

Figs 6-12. *Jiyaceras hindostanus* (Diener, 1897). 6a-d, PIMUZ 28351. From sample HB1005, Losar. 7a-c, PIMUZ 28349. From sample HB1005, Losar. 8a-c, PIMUZ 28348. From sample HB1005, Losar. 9a-c, PIMUZ 28346. From sample HB1005, Losar. 10a-c, PIMUZ 28345. From sample M06-24, Mud. 11a-d, PIMUZ 28347. From sample HB1005, Losar. 12, PIMUZ 28350; ×2, at H = 6.8 mm. From sample M08-21, Mud. All from the *Brayardites compressus* beds.

Figs 13-14. *Juvenites procurvus* Brayard and Bucher, 2008. 13a-c, PIMUZ 28353; 13c at H = 6.9 mm. Found as float in the *"Parahedenstroemia"* Beds. 14a-c, PIMUZ 28354. From sample M08-48, *Pseudoceltites multiplicatus* beds. Both specimens from Mud.

Figs 15-20. *Subvishnuites posterus* sp. nov. 15a-c, PIMUZ 28355. 16a-c, PIMUZ 28356. 17a-c, PIMUZ 28357. 18a-e, PIMUZ 28358; 18e ×2, at H = 6.1 mm. 19a-c, PIMUZ 28359. 20a-d, holotype, PIMUZ 28360. All from sample M08-70, *Subvishnuites posterus* beds, Mud.

Figs 21-24. *Kraffticeras pseudoplanulatum* (Krafft and Diener, 1909) gen. nov. 21a-c, PIMUZ 28361. From sample HB1013. 22a-e, PIMUZ 28362; 22e ×2, at H = 6.9 mm. From sample HB26. 23a-d, PIMUZ 28363. From sample HB1013. 24a-d. PIMUZ 28364. From sample HB1026. All from the *Flemingites* beds, Losar.

All natural size unless otherwise indicated.

Plate 16

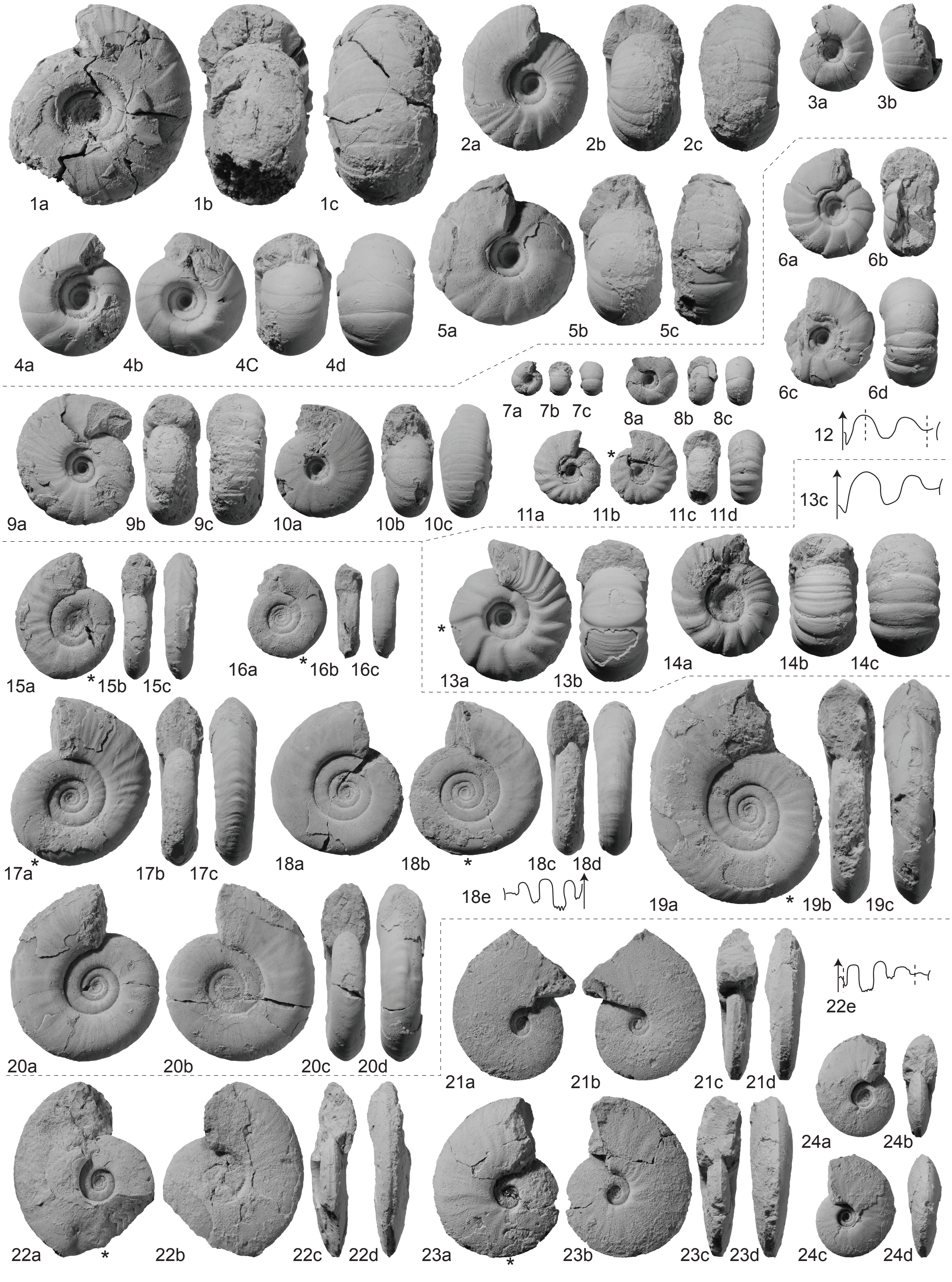
1a
1b
1c
2a
2b
2c
3a
3b
4a
4b
4C
4d
5a
5b
5c
6a
6b
6c
6d
7a
7b
7c
8a
8b
8c
12
9a
9b
9c
10a
10b
10c
11a
11b
11c
11d
13c
15a
15b
15c
16a
16b
16c
13a
13b
14a
14b
14c
17a
17b
17c
18a
18b
18c
18d
18e
19a
19b
19c
20a
20b
20c
20d
21a
21b
21c
21d
22e
22a
22b
22c
22d
23a
23b
23c
23d
24a
24b
24c
24d

EXPLANATION OF PLATE 17

Figs 1-4. *Aspenites acutus* Hyatt and Smith, 1905. 1a-d, PIMUZ 28365. From sample LoSFB1, Losar. 2a-d, PIMUZ 28366. From sample HB1005, Losar. 3a-c, PIMUZ 28367; 3c ×3, at H = 11.3 mm. From sample M08-21, Mud. 4a-b, PIMUZ 28368. From sample M03-19, Mud. All from the *Brayardites compressus* beds.

Figs 5-7. *Pseudaspenites* cf. *layeriformis* (Welter, 1922). 5a-d, PIMUZ 28369. From sample M08-21, Mud. 6a-d, PIMUZ 28370. From sample HB1005, Losar. 7a-d, PIMUZ 28371; 7d ×3, at H = 10 mm. From sample M03-24, Mud. All from the *Brayardites compressus* beds.

Figs 8-10. *Pseudosageceras augustum* Brayard and Bucher, 2008. 8a-c, PIMUZ 28372. 9a-c, PIMUZ 28373. 10a-d, PIMUZ 28374; 10d ×2, at H = 18.2 mm. All from sample M08-70, *Subvishnuites posterus* beds, Mud.

Fig. 11a-d. *Shigetaceras dunajensis* (Zakharov, 1968). PIMUZ 28375. From sample M03-40, *Truempyceras compressum* horizon, Mud.

All natural size unless otherwise indicated.

Plate 17

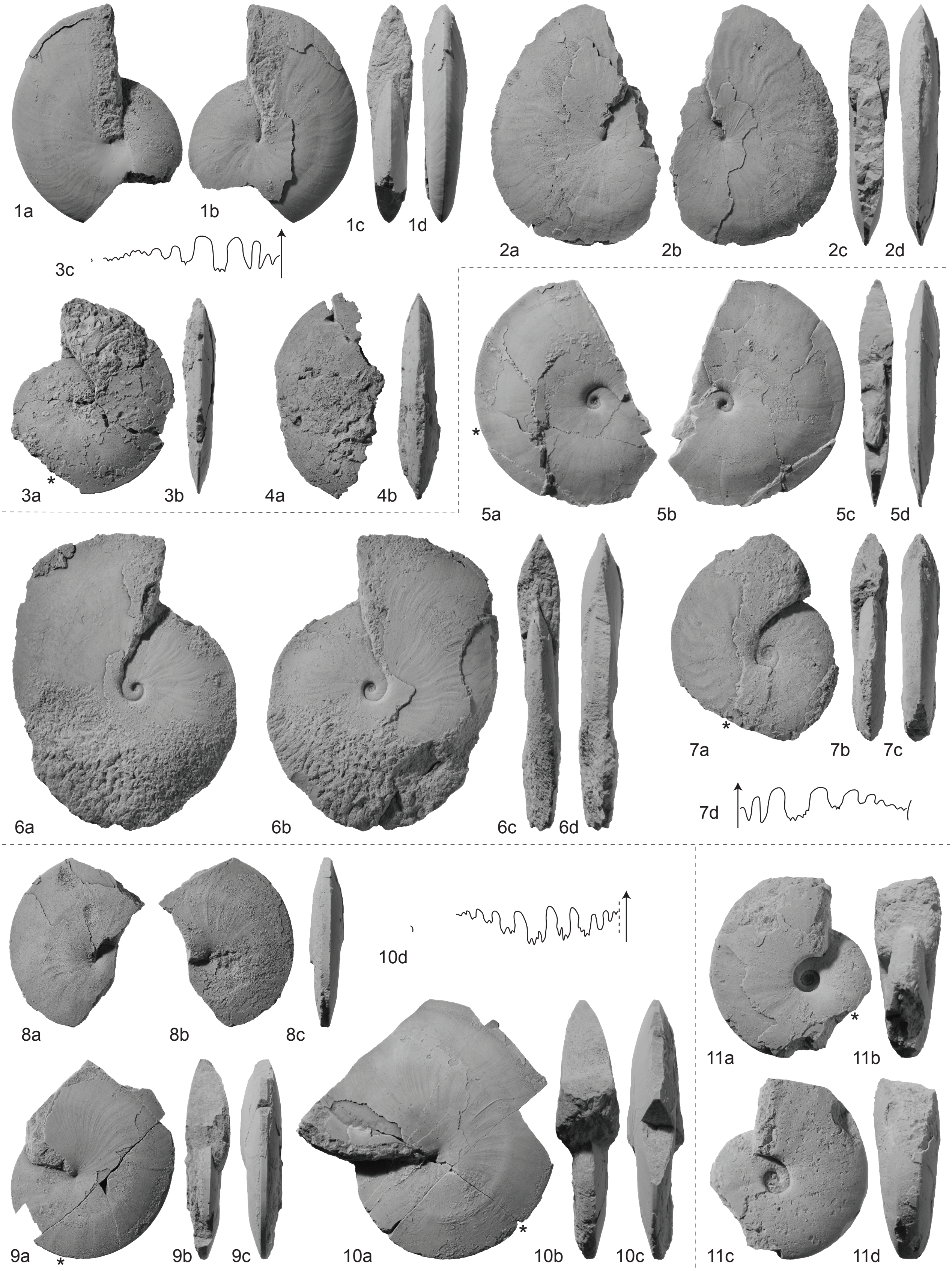
1a
1b
1c
1d
2a
2b
2c
2d
3c
3a
*
3b
4a
4b
*
5a
5b
5c
5d
6a
6b
6c
6d
*
7a
7b
7c
7d
8a
8b
8c
10d
11a
*
11b
9a
*
9b
9c
10a
*
10b
10c
11c
11d

CHAPTER 8:

Smithian (Early Triassic) ammonoid faunas from Exotic Blocks from Oman: taxonomy and biochronology

Smithian (Early Triassic) ammonoid faunas from Exotic Blocks from Oman: taxonomy and biochronology

by

THOMAS BRÜHWILER, HUGO BUCHER, NICOLAS GOUDEMAND and THOMAS GALFETTI

With 26 plates and 42 text-figures

Address of the authors: Paläontologisches Institut und Museum der Universität Zürich, Karl Schmid-Strasse 4, CH-8006 Zürich, Switzerland; e-mails: bruehwiler@pim.uzh.ch; hugo.fr.bucher@pim.uzh.ch, goudemand@pim.uzh.ch, thomasgalfetti@gmail.com

This work is dedicated to the memory of our friend and colleague Jean Philippe Marcoux (1940-2008), who was one of the few experts at the geology of Oman and who guided our first steps in this extraordinary slice of the lithosphere.

Submitted to *Palaeontographica*.

Summary

Ammonoid-rich exotic bocks of Hallstatt facies in Jebel Safra, in Wadi Musjah and at Baid (Oman Mountains) have yielded several well preserved and highly diversified Smithian (Early Triassic) ammonoid faunas (*Baidites hermanni* fauna, *Rohillites omanensis* fauna, *Flemingites rursiradiatus* fauna, *Nammalites pilatoides* fauna, *Owenites koeneni* fauna and *Anasibirites multiformis* fauna). The comparison of these assemblages with data from other Tethyan basins such as the Salt Range, Spiti, Tibet and South China shows that nearly all known Smithian ammonoid faunal assemblages are present in the exotic blocks from Oman. The new Oman data strengthens the remarkably uniform biogeographic distribution of the Smithian ammonoid faunas within the Tethys.

One new ammonoid family (Galfettitidae), five new genera (*Baidites*, *Goudemandites*, *Lucasites*, *Omanites*, *Safraites*), and twelve new species (*Baidites hermanni*, *Galfettites kyrae*, *G. omani*, *Goudemandites sinensis*, *Kashmirites baidi*, *Lucasites involutus, L. evolutus, Omanites musjahensis*, *Paranannites baudi*, *Pseudaspidites planus*, *Rohillites omanensis*, *Safraites simplex*) are described. Additionally, a new early Spathian (late Early Triassic) species (*Procolumbites safraensis*) is described.

Key words: Ammonoidea – Smithian – Early Triassic – Oman – exotic blocks – Hallstatt limestone.

Zusammenfassung

Ammonoideen-reiche exotische Blöcke aus Hallstätter Kalk vom Jebel Safra, aus dem Wadi Musjah und von Baid im Oman haben mehrere gut erhaltene und hoch diversifizierte Ammonoideenfaunen des Smithian (Frühe Trias) geliefert (*Baidites hermanni* Fauna, *Rohillites omanensis* Fauna, *Flemingites rursiradiatus* Fauna, *Nammalites pilatoides* Fauna, *Owenites koeneni* Fauna und *Anasibirites multiformis* Fauna). Der Vergleich dieser Faunen mit Daten von anderen Lokalitäten der Tethys zeigt, dass fast alle bekannten Ammonoideen-Vergesellschaftungen des Smithian in den exotischen Blöcken von Oman vertreten sind. Die neuen Daten von Oman bestätigen die aussergewöhnlich einheitliche biogeographische Verteilung der Ammonoideen des Smithian innerhalb der Tethys.

Eine neue Familie (Galfettitidae), fünf neue Gattungen (*Baidites*, *Goudemandites*, *Lucasites*, *Omanites*, *Safraites*) und zwölf neue Arten (*Baidites hermanni*, *Galfettites kyrae*, *G. omani*, *Goudemandites sinensis*, *Kashmirites baidi*, *Lucasites involutus, L. evolutus, Omanites musjahensis*, *Parananites baudi*, *Pseudaspidites planus*, *Rohillites omanensis*, *Safraites simplex*) werden beschrieben. Ausserdem wird eine neue Art aus dem frühen Spathian (späte Unter-Trias) beschrieben (*Procolumbites safraensis*).

Schlüsselwörter: Ammonoidea – Frühe Trias – Oman – Exotische Blöcke - Hallstätter Kalk.

Introduction

In the aftermath of the end-Permian mass extinction that wiped out more than 90% of all marine species (e.g. RAUP & SEPKOSKI 1982), ammonoids recovered very fast in comparison with other marine clades. Recent diversity and biogeographical studies (BRAYARD et al. 2006, 2007b, 2008, in press) have shown that the Early Triassic ammonoid recovery from Griesbachian to Spathian times was characterized by: (i) at least two major diversification phases in the Smithian and in the Spathian, respectively, (ii) an increase of the steepness of the latitudinal diversity gradient they formed, and (iii) an increasing number of latitudinally restricted, trans-Panthalassic genera. However, their recovery was almost completely interrupted at least once in the late Smithian when a severe extinction event set back the ammonoid diversity and biogeography to a Griesbachian-like configuration with a very low diversity and a high degree of cosmopolitanism. Recently published U-Pb ages from South China and their calibration with ammonoid faunas (OVTCHAROVA et al. 2006; GALFETTI et al. 2007b) indicate a maximal duration of the Griesbachian-Dienerian interval of 1.4±0.4 my, a duration of 0.7±0.6 my for the Smithian and of ca. 3 my for the Spathian (Text-fig. 1). Therefore, the first Early Triassic major ammonoid diversification phase in the early Smithian occurred no later than 2 my after the Permo/Triassic Boundary (PTB) and ended less than 1 my later with the extinction event in the late Smithian. The late Smithian was also associated with major perturbations of the global carbon cycle (PAYNE et al. 2004; GALFETTI et al. 2007a) and profound changes in palynological assemblages (GALFETTI et al. 2007c; HERMANN et al. 2008). CO_2 degassing via volcanism of a hypothetical late eruptive phases of the Siberian Traps has been proposed as a trigger for this global climatic and oceanographic event (OVTCHAROVA et al. 2006; GALFETTI et al. 2007c).

Oceanic basins documenting this first diversity peak in the Early Triassic ammonoid recovery during the Smithian with abundant and well preserved faunas are relatively rare. The most important among them are the Salt Range in Pakistan (WAAGEN 1895, GUEX 1978, BRÜHWILER et al. 2007), Spiti in Northern India (Diener 1897, KRAFFT & DIENER 1909, BRÜHWILER et al. 2007), South Tibet (WANG & HE 1976, BRÜHWILER et al. 2007, submitted), Madagascar (COLLIGNON 1933-34), Guangxi in South China (CHAO 1959, BRAYARD & BUCHER 2008), Japan (BANDO 1964), Timor (WELTER 1922), Siberia (ERMAKOVA 2002), South Primorye in eastern Russia (DIENER 1895, KIPARISOVA 1961, ZAKHAROV 1968, 1997, SHIGETA et al. 2009, SHIGETA & ZAKHAROV 2009), the western USA (HYATT & SMITH 1905, SMITH 1932, KUMMEL & STEELE 1962), the Canadian Arctic and British Columbia (TOZER 1994), and Spitsbergen (FREBOLD 1930, KUMMEL 1961, WEITSCHAT & LEHMANN 1978).

The presence of Smithian ammonoids in Oman has been known since the work of TOZER & CALON (1990) and BLENDINGER (1995). However, these faunas have never been studied in details. They occur in exotic blocks of red pelagic limestone (Hallstatt facies). Various cephalopod faunas from exotic blocks from Oman have also been reported from other time periods such as the Wordian (Middle Permian; BLENDINGER et al. 1992), the Griesbachian (KRYSTYN et al. 2003), the Spathian (TOZER & CALON 1990, BLENDINGER 1995), the Ladinian or Carnian (SHUJI et al. 1996), and the Norian (BLENDINGER 1991).

Our investigations in the Oman Mountains have led to the discovery of abundant, diverse and unusually well preserved Smithian ammonoid faunas. Very few ammonoid-bearing exotic blocks contain successions of different faunas. Most of the blocks contain only a single fauna each, which somehow limits the biostratigraphic significance of these faunas. However, they add significantly to our knowledge of the Smithian ammonoid taxonomy since on one hand they help to assess intraspecific variation, which is generally still poorly known for many species, and on the other hand, several new taxa have been found. Moreover, the good preservation of the ammonoids from Oman improves our knowledge of several taxa that have previously been known only from imperfect material (e.g. *Guodunites*, see BRAYARD et al. 2009). Additionally, these new faunas provide valuable data for biogeographical and phylogenetic studies.

Geological settings

During Early Triassic times, Oman was located on the Northern Gondwanan margin at about 20°S (SMITH et al. 1994) with the Neothethys ocean to the North (PILLEVUIT et al. 1997). The present-day Oman Mountains consist of five main structural units (GLENNIE et al. 1974): (i) the Autochthonous A and B (Arabian platform), (ii) the Parautochthonous (Sumeini Group; slope deposits); (iii) the Allochthonous (Hawasina Complex; basinal sediments), (iv) the Semail Ophiolite, and (v) the Mesoautochthonous (post-obduction sediments) (Text-fig. 2). The Hawasina complex is subdivided into six groups (from a proximal to a more distal depositional environment): the Ramaq Group, the Al Buda'ah Group, the Hamrat Duru Group, the Al Aridh Group, the Kawr Group, and the Umar Group (PILLEVUIT et al. 1997). Among these are the three different exotic groups in the Oman mountains recognised by PILLEVUIT et al. (1997): (i) the Ramaq Group which is characterised by an Ordovician to Carboniferous basement overlain by Permian to Triassic platform carbonates; (ii) the Al Buda'ah Group, comprising upper Permian platform limestones overlain by a Triassic to Jurassic pelagic series; and (iii) the Kawr Group which is composed of a thick middle Triassic volcanic series overlain by upper Triassic platform carbonates and by Jurassic to Cretaceous pelagic sediments. The Ramaq Group and the Al Buda'ah Group have been interpreted as tilted blocks related to Oman continental passive margin whereas the Kawr Group has been interpreted as an atoll-type seamount. Occasionally, olistoliths of these exotic units have been reworked into deeper units of the Hawasina basin such as the Hamrat Duru Group.

Ammonoid-bearing Triassic exotics of Hallstatt limestone are known from three localities in Oman (TOZER & CALON 1990, BLENDINGER 1995, KLUG et al. 2007): (i) in the famous Wadi Alwa mega-block in the Baid area (the Alwa Formation of the Al Buda'ah Group; PILLEVUIT et al. 1997), (ii) at Wadi Musjah, 26km SWS of Baid (large olistoliths in the Hawasina Unit), and (iii) in the Jebel Safra, 80km SW of Baid (smaller olistoliths in the Jurassic Guwayza Formation). The source of these olistoliths from Jebel Safra is unknown. Since Hallstatt limestones are not known from the Arabian margin, the source must have been isolated oceanic build-ups (seamounts; TOZER & CALON 1990). However, some olistoliths occur in channelized oolithic gravity flows suggesting a slope environment. These seamounts were probably located relatively close to the Arabian platform (BLENDINGER 1995).

Triassic limestones of the Hallstatt type occur throughout the Tethys from Austria, Greece, Albania, Oman over Tibet to Indonesia, and many of these localities have yielded abundant and well preserved ammonoid faunas (e.g. ARTHABER 1911, WELTER 1922, RENZ & RENZ 1948, BASSOULET et al. 1978). The Hallstatt facies is generally interpreted as a pelagic deposit without any input of terrigenous sediments. Sedimentation rate is generally low, and often such deposits show signs of condensation and submarine subsolution (e.g. neptunian dykes). Nevertheless, when comparing our new Smithian ammonoid faunas from Oman with faunal successions from well expanded sections such as Guangxi (South China; BRAYARD & BUCHER 2008), Tulong (South Tibet; BRÜHWILER et al. submitted) or the Salt Range (Pakistan; WAAGEN 1895, GUEX 1978, BRÜHWILER et al. ongoing work) no mixing of faunas due to condensation can be detected.

Sampled localities and ammonoids

In the Jebel Safra, located 125km SW of Muscat, olistoliths of Permian reefal limestone and Early Triassic Hallstatt limestone occur within the Middle Jurassic Oolithic Member of the Guwayza Formation (Text-fig. 3b, d; BECHENNEC 1988, TOZER & CALON 1990, BLENDINGER 1995, BLECHSCHMIDT et al. 2004). A total of 17 Hallstatt blocks ranging in stratigraphic thickness from 15cm to 5m was found in the western part of Jebel Safra. While some of these blocks are packed with ammonoids, others are barren. Those blocks yielding Smithian ammonoids and their detailed faunal contents are illustrated in Text-fig. 4. In some blocks, ammonoids are silicified (Text-fig. 3e). One block (sample SA4) yielded a fauna of late Early or mid Spathian age.

At Wadi Musjah a large Early Triassic exotic block (Text-fig. 2b) occurs, spanning from the middle Smithian into the Spathian (BAUD et al. 2001). The Smithian part of the main block and two smaller blocks have yielded abundant and very well preserved ammonoids. Some specimens of *Juvenites* from this locality have even preserved remains of so-called "false colour pattern" (KLUG et al. 2007). The detailed faunal content of the samples from Wadi Musjah is given is Text-fig. 5.

In the Wadi Alwa mega-block in the Baid area, a single isolated sample yielding abundant ammonoids was found on the Wadi Alwa Summit (sample HB911; Tex-fig. 3a). Additionally, a section in the southern part of the mega-block was studied, corresponding to section 4 of PILLEVUIT et al. (1997) and the section studied by WOODS & BAUD (2008). Within this area, the cephalopod limestones are highly fractured and strongly faulted including low-angle faults and in-situ breccias (BLENDINGER 1995). Stratigraphical positions of samples should therefore be handled with care and the samples are thus considered as isolated. The detailed faunal content of all samples from the Baid area is given in Text-fig. 6.

Biostratigraphical discussion and conclusions

General subdivisions of the Early Triassic

The Early Triassic is commonly divided into two, three or four stages as follows: two stages (Induan and Olenekian, KIPARISOVA & POPOV 1956; the Induan encompassing the Griesbachian and Dienerian, and the Olenekian encompassing the Smithian and the Spathian); three stages (Griesbachian, Nammalian and Spathian, GUEX 1978); or four stages (Griesbachian, Dienerian, Smithian and Spathian, TOZER 1967). In this paper, we use the four stage subdivision, whose boundaries are well defined in terms of ammonoid evolution. The Griesbachian/Dienerian boundary is defined by the first occurrence of Meekoceratidae which is a bio-event that can be traced worldwide (e.g. SHEVYREV 2001). The interest for the Dienerian/Smithian (or Induan/Olenekian) boundary is very recent, and a section near Mud in the Indian Himalayas has been selected as the best GSSP candidate (KRYSTYN et al. 2007a, b). This boundary is easily recognizable with the appearance of several new ammonoid families such as the Flemingitidae, the Paranannitidae or the Xenoceltitidae. The Smithian/Spathian boundary is marked by a profound faunal turnover and is only crossed by very few ammonoid lineages such as the Xenoceltitidae and the Proptychitidae (BRAYARD et al. 2006). Several new families such as the Tirolitidae and the Columbitidae appear in the Early Spathian.

Subdivisions of the Smithian of Oman

The biostratigraphical significance of the ammonoid occurrences in the Exotic Blocks from Oman is inherently limited since little or no information about the relative order of the different faunas is available. Nevertheless, in comparison with new biostratigraphical data from other Tethyan basins such as South China (BRAYARD & BUCHER 2008), Pakistan, India and Tibet (BRÜHWILER et al. 2007, submitted, ongoing work), the new assemblages from Oman can be indirectly replaced in chronological order (Text-fig. 7). This comparison also shows that nearly all presently known Smithian ammonoid associations occur in the exotic blocks from Oman. However, in consideration of the nature of the data no formal zonal names are introduced hereafter.

***Baidites hermanni* n. gen. n. sp. fauna:** This fauna has only been found in sample HB911 from Baid. It is dominated by *Baidites hermanni* and contains also *Paranorites jenksi*, *Jinyaceras* cf. *bellum* and *Pseudaspidites* cf. *muthianus*. In South China *Paranorites jenksi* occurs in the earliest Smithian '*Kashmirites kapila* beds' (BRAYARD & BUCHER 2008). On the contrary, *Jinyaceras bellum* and *Pseudaspidites muthianus* occur in the slightly younger '*F. rursiradiatus* beds'. Hence, the exact age of this fauna remains uncertain. Conodonts from this sample confirm an early Smithian age but do not allow more precision.

***Flemingites rursiradiatus* fauna:** This fauna has only been found in sample Baid-A. It is characterized by the association of *Flemingites rursiradiatus*, *Kashmirites baidi* n. sp. and *Pseudaspidites* cf. *muthianus*. This fauna correlates with the '*Flemingites rursiradiatus* beds' of Guangxi, South China (BRAYARD & BUCHER 2008). The co-occurrence of the conodonts *Conservatella conservativa* and *Smithodus* cf. *longiusculus* in this sample further suggests that this fauna correlates with the upper part of the '*Flemingites rursiradiatus* beds' of South China (GOUDEMAND et al., in prep.).

***Rohillites omanensis* n. sp. fauna:** This fauna has been found in the Jebel Safra in the blocks JS6, JS11 and SA3. It is characterized by the co-occurrence of *Rohillites omanensis* n. sp., *Paranannites baudi* n. sp., *Lucasites involutus* n. gen. et sp., *L. evolutus* n. gen. et sp. and *Aspenites acutus*. This fauna correlates more or less with the '*Flemingites rursiradiatus* beds' of Guangxi, South China (BRAYARD & BUCHER 2008). Its relative position with the above mentioned *Baidites hermanni* and *Flemingites rursiradiatus* faunas from Oman is uncertain. The co-occurrence of the conodonts *Neospathodus* n. sp. V (ORCHARD 2007) and *Novispathodus* n. sp. 1 (see below) suggests that this fauna is slightly younger than the *Flemingites rursiradiatus* fauna from Oman (GOUDEMAND et al., in prep.).

***Nammalites pilatoides* fauna:** This diverse fauna has been found in the block JS13 from Jebel Safra. It is characterized by the occurrence of *Aspenites acutus*, *Galfettites omani* n. sp., *Juvenites spathi*, *Nammalites pilatoides*, *Owenites simplex*, *Parussuria compressa*, *Safraites simplex* n. gen. et sp., *Subflemingites involutus*, and *?Meekoceras* sp. indet. This association has recently also been found in the Salt Range (Pakistan), in Spiti (India) and in Southern Tibet and was provisionally termed 'new prionitid B beds' by BRÜHWILER et al. (2007). It correlates with the *Ussuria* and *Hanielites* horizons in the lower part of the '*Owenites koeneni* beds' from South China (BRAYARD & BUCHER 2008). Note that in Oman *Owenites koeneni* has not been found within this association.

The fauna found in block SA1 is characterized by the association of *Aspenites acutus*, *Juvenites spathi*, *Pseudaspenites layeriformis* and *Proharpoceras carinatitabulatum*. *J. spathi* in this sample may indicate a similar age, but the occurrence of *Pseudaspenites* indicates that it is slightly older than the *Nammalites pilatoides* fauna since this genus is restricted to the early Smithian (BRAYARD & BUCHER 2008).

Only a small piece of matrix of JS13 was processed for conodonts and only a few platform elements could be retrieved, which does not allow to precise its relative position. SA1 sample however is rich in conodonts and the presence of *Wapitiodus robustus* may again indicate that this sample is slightly older. In South China this species is found in the lowermost part of the '*Owenites koeneni'* beds (GOUDEMAND et al., in prep.) and in Tibet it is found within the 'new arctoceratid A beds'

(Brühwiler et al., submitted [b]). In SA1 it co-occurs with *Novispathodus* n. sp. 1 (previsously included in the *waageni* group), a species that is also observed to co-exist with *Proharpoceras* in South China but whose range might extend down to the upper part of the '*Flemingites rursiradiatus* beds'.

***Owenites koeneni* fauna:** This fauna is the most abundant and diverse and has been found in the blocks HB912, JS2, JS4, JS8, JS12 from Jebel Safra, in all samples from Wadi Musjah except for sample HB901 (see below), and in sample Baid-B at Baid. The most common species are: *Preflorianites radians, Nyalamites angustecostatus*, *Inyoites oweni*, *Inyoites krystyni*, *Omanites musjahensis*, *Owenites koeneni*, *Owenites carpenteri*, *Prionites* sp. indet., *Juvenites spathi*, *Juvenites* cf. *thermarum*, *Parussuria compressa*, *Guodunites monneti*, *Dieneroceras* cf. *dieneri*, *Galfettites simplicitatis*, *Galfettites kyrae* n. sp., *Leyeceras* cf. *rothi*, *Pseudaspidites planus* n. sp., *Anaxenaspis* cf. *lidacensis*, *Lanceolites compactus*, *Lanceolites bicarinatus*, *Pseudoflemingites goudemandi, Subvishnuites welteri, Aspenites acutus*, *Goudemandites sinensis* n. gen. et n. sp.

Actually, not all of these species have been found associated with each other (Text-figs. 4-6), and it appears that e.g. samples with *Galfettites simplicitatis*, *Juvenites spathi*, and *Leyeceras* cf. *rothi* are slightly older than samples containing *Inyoites oweni*, *Omanites musjahensis*, *Owenites carpenteri, Nyalamites angustecostatus*, *Juvenites* cf. *thermarum*, and *Guodunites monneti*. However, on account of the isolated occurrence of samples, no further subdivision of the *Owenites koeneni* fauna can be made with any degree of confidence. This fauna correlates with the '*Inyoites* horizon' in the upper part of the '*Owenites koeneni* beds' from South China (BRAYARD & BUCHER 2008). This correlation is confirmed by the conodonts, namely by the occurrence of *Guangxidella* species (*bransoni*, *robustus*) associated with dominating ellisonids.

***Anasibirites multiformis* fauna:** This low-diversity fauna has only been found in sample HB901 from Wadi Musjah. It is characterized by the association of *Anasibirites multiformis*, *Hemiprionites* cf. *butleri* and *Subvishnuites* sp. indet. This fauna correlates with the late Smithian '*Anasibirites multiformis* beds' from South China (BRAYARD & BUCHER 2008). Equivalents of this fauna are known worldwide (BRÜHWILER et al. 2007; *Wasatchites tardus* zone of the Arctic realm, TOZER 1994). The presence of the conodonts *Scythogondolella mosheri* and *Sc. milleri* confirms this observation.

An equivalent of the latest Smithian fauna containing *Xenoceltites* and/or *Glyptophiceras* that has recently been found in the Salt Range, Spiti and South Tibet (BRÜHWILER et al. 2007, submitted) has not been found in Oman. Note that in South China this fauna occurs but was included in the '*Anasibirites multiformis* beds' by BRAYARD & BUCHER (2008).

Systematic palaeontology

by

THOMAS BRÜHWILER and HUGO BUCHER

The systematic descriptions principally follow the classification of Triassic ammonoids established by TOZER (1981, 1994) and refined by BRAYARD & BUCHER (2008). One new family (Galfettitidae) is introduced. The quantitative morphological range of each species is expressed utilizing the four classic geometrical parameters of the ammonoid shell: diameter (D), whorl height (H), whorl width (W) and umbilical diameter (U). The three parameters (H, W and U) are plotted in absolute values as well as in relation to diameter (H/D, W/D, and U/D) provided that measurements were available for at least four specimens. Measurements of other species are given in the appendix. Some species are also quantitatively compared by means of box plots (MONNET & BUCHER 2005). Repository of figured and measured specimens is abbreviated PIMUZ (Paläontologisches Institut und Museum der Universität Zürich). Sample numbers are reported in Text-figures 4-6.

Class Cephalopoda CUVIER 1797
Subclass Ammonoidea ZITTEL 1884
Order Ceratitida HYATT 1884
Superfamily Otocerataceae HYATT 1900

Family Anderssonoceratidae RUZHENCEV 1959

Genus *Proharpoceras* CHAO 1950

Type species: *Proharpoceras carinatitabulatum* CHAO 1950.

Proharpoceras carinatitabulatum CHAO 1950
Plate 1, figure 1a-c

1950 *Proharpoceras carinatitabulatus* CHAO, p. 8, pl. 1, figs. 8a, b
1950 *Tuyangites marginalis* CHAO, p. 9, pl. 1, fig. 9
1959 *Proharpoceras carinatitabulatum* – Chao, p. 324, pl. 43, figs. 1-7
1959 *Tuyangites marginalis* CHAO, p. 327, pl. 43, figs. 17, 18
1968 *Proharpoceras carinatitabulatum* – ZAKHAROV, p. 147, pl. 29, fig. 6

v 2007a *Proharpoceras carinatitabulatum* – BRAYARD et al., p.178, fig. 3a-s, v-z.

v 2008 *Proharpoceras carinatitabulatum* – BRAYARD & BUCHER, p. 80, pl. 38, figs. 5-9.

Occurrence: A single specimen from sample SA1; ?*Nammalites pilatoides* fauna.

Description: Moderately evolute shell with a quadratic whorl section and parallel, flat flanks. Venter tabulate with a raised median keel and angular shoulders. Umbilicus wide with oblique wall and rounded shoulders. Suture line not preserved.

Measurements: See appendix.

Discussion: Our specimen has previously been illustrated by BRAYARD et al. (2007a). Well preserved specimens from South China show that the venter of *P. carinatitabulatum* is actually tricarinate (BRAYARD & BUCHER 2008). *Proharpoceras* is probably a member of a Permian ammonoid lineage (Anderssonoceratidae) surviving the end-Permian mass extinction that dwindled away for some 2 myr before going extinct (BRAYARD et al. 2007a).

Superfamily Xenodiscaceae FRECH 1902

Family Xenoceltidae SPATH 1930

Genus *Nyalamites* BRÜHWILER et al., submitted

Nyalamites angustecostatus (WELTER 1922)

Plate 1, figures 3-6

? 1895 *Celtites acuteplicatus* WAAGEN, 1895, p. 82, pl. 7a, figs. 5, 5c, 6, 7.

1922 *Xenodiscus angustecostatus* WELTER, p. 110, pl. 4, figs. 14-17.

? 1922 *Xenodiscus oyensi* WELTER, p. 111, pl. 5, figs. 1, 2, 17

1968 *Anakashmirites angustecostatus* – KUMMEL & ERBEN, p. 128, pl. 19, figs. 1-8.

1973 *Anakashmirites angustecostatus* – COLLIGNON, p. 144, pl. 5, figs. 7-8.

1973 *Anakashmirites oyensi* – COLLIGNON, p. 146, pl. 5, figs. 9-10.

1976 *Pseudoceltites angustecostatus* – WANG & HE, p. 289, pl. 6, figs. 3-6.

v 1978 *Eukashmirites angustecostatus* – GUEX, pl. 7, figs. 4, 9.

v, non 2008 *Pseudoceltites? angustecostatus* – BRAYARD & BUCHER, p. 18; pl. 3, figs. 1-7; text-fig. 19 (=*Preflorianites radians*).

v submitted [a] *Nyalamites angustecostatus* – BRÜHWILER et al.

Occurrence: Samples WM7, WM8, HB904, HB905; *Owenites koeneni* fauna.

Description: Small, very evolute shell with slightly convex, subparallel flanks. Venter low rounded to subtabulate, with rounded shoulders. Umbilicus shallow and wide with vertical wall and rounded shoulders. Ornamentation of flanks consists of regularly spaced, strong, radial, sharp ribs that fade out on ventral shoulders. On our specimens from Oman, the suture line is simple, apparently goniatitic, but imperfectly preserved. Better preserved material from the Salt Range shows that it is in fact ceratitic.

Measurements: Text-figure 8.

Discussion: This species is common in the upper part of the *Owenites koeneni* beds of the Tethys (Oman, Pakistan, India, South Tibet [BRÜHWILER et al. 2007, submitted]), Afghanistan (KUMMEL & ERBEN 1968) and Timor (WELTER 1922).

Genus *Preflorianites* SPATH 1930

Type species: *Danubites strongi* HYATT & SMITH 1905.

Preflorianites radians CHAO 1959

Plate 1, figures 8-9; plate 2, figures 1-7

? 1922 *Xenodiscus bittneri* – WELTER, p. 106, pl. 4, figs. 8-9.
1959 *Preflorianites radians* CHAO, p. 196, pl. 3, figs. 6-8.
v 2008 *Pseudoceltites? angustecostatus* – BRAYARD & BUCHER, p. 18; pl. 3, figs. 1-7; text-fig. 19.

Occurrence: Samples HB912, JS2, JS12, Baid-B; *Owenites koeneni* fauna.

Description: Evolute shell with convex flanks. Venter rounded without any shoulders. Umbilicus wide and shallow with vertical wall and rounded shoulders. Ornamentation of flanks consists of regularly spaced, strong, radial or rursiradiate rounded ribs that fade out towards the external part of the flanks. Strength of ornamentation highly variable; outer whorls of some specimens almost smooth. Suture line simple and ceratitic with rather low saddles; poorly preserved.

Measurements: Text-figure 9.

Discussion: The type species of *Preflorianites* differs from this species by its highly arched, subangular venter on outer whorls. The specimens from South China reported as *Pseudoceltites? angustecostatus* by BRAYARD & BUCHER (2008) belong to *Preflorianites radians*. *Pseudoceltites* differs by a tabulate venter, a slightly trapezoidal whorl section and irregular ribbing. The species described as *Preflorianites* cf. *radians* by BRAYARD & BUCHER (2008) is slightly older (*Flemingites rursiradiatus* Beds) and differs by its weaker ornamentation and thicker whorls.

Genus *Kashmirites* DIENER 1913

Type species: *Celtites armatus* WAAGEN 1895.

Kashmirites baidi n. sp.

Plate 1, fig. 2a-d

Etymology: Named after the type locality Baid.

Holotype: PIMUZ 27304 (Plate 1, figure 2).

Type locality and horizon: Baid, Sample Baid-A, *Flemingites rursiradiatus* fauna.

Occurrence: Two specimens from sample Baid-A; *Flemingites rursiradiatus* fauna.

Diagnosis: *Kashmirites* with ornamentation consisting of simple, paired or triple strong, radial ribs.

Description: Evolute shell with flat, parallel flanks. Venter subtabulate, slightly arched, with slightly rounded but marked shoulders. Umbilicus wide, with a vertical wall and slightly rounded but marked shoulders. Ornamentation very distinct, consisting of simple, paired or triple strong, radial ribs. Ribs become faint on the ventral shoulders but do cross the venter. Suture line not preserved.

Measurements: See appendix.

Discussion: Other species of *Kashmirites* such as the type species, *K. nivalis* (DIENER 1897), *K. kapila* (DIENER 1897) or *K. evolutus* WELTER 1922 differ from this species by an ornamentation consisting of simple ribs. *K. baidi* has also been recently found associated with *Flemingites flemingianus* in the Ceratite Sandstone of the Salt Range, Pakistan (BRÜHWILER et al., ongoing work).

?Xenoceltitidae gen. indet.

Plate 1, figure 7a-d

Occurrence: A single specimen from sample JS2; *Owenites koeneni* fauna.

Description: Moderately evolute, slightly compressed shell with subparallel, slightly convex flanks. Venter broad and subtabulate with rounded shoulders. Umbilicus with vertical wall and rounded shoulders. Ornamentation distinct, consisting of strong, broad and slightly sinuous radial ribs. Suture line ceratitic with deep lobes and slightly phylloid second lateral saddle, incompletely known.

Measurements: See appendix.

Discussion: The unusual ornamentation of our specimen suggests that it may represent a new genus, but the scarcity and imperfect preservation of our material hinders any definitive assignment at generic level, and the assignment to Xenoceltitidae is only tentative.

Superfamily Meekocerataceae WAAGEN 1895

Familiy Proptychitidae WAAGEN 1895

Genus *Pseudaspidites* SPATH 1934

Type species: *Aspidites muthianus* KRAFFT & DIENER 1909.

Pseudaspidites cf. *muthianus* (KRAFFT & DIENER 1909)

Plate 3, figures 3-5

?	1909	*Aspidites muthianus* KRAFFT & DIENER, p. 59, pl. 6, fig. 5, pl. 15, figs. 1-2.
v, ?	2008	*Pseudaspidites muthianus* – BRAYARD & BUCHER, p. 33, pl. 10, figs. 1-10, pl. 11, figs. 1-4, text-fig. 31.

Occurrence: Samples Baid-A, Baid-G, HB911; *Baidites hermanni* fauna, *Flemingites rursiradiatus* fauna.

Description: Large, involute, compressed shell with slightly convex, strongly convergent flanks. Maximal thickness near umbilicus. Venter subtabulate with rounded shoulders. Umbilicus narrow and deep with high, vertical wall and marked, slightly rounded shoulders. Surface smooth. Suture line subammonitic and very typical for *Pseudaspidites*; with distinctly phylloid saddles and strongly indented lobes; second and third lateral saddles markedly curved towards the venter.

Measurements: Text-figure 10.

Discussion: Our specimens from Oman differ from *Pseudaspidites muthianus* from Spiti and South China by their more convergent and less convex flanks. In addition they are more involute than *P. muthianus* from South China (BRAYARD & BUCHER 2008).

Pseudaspidites planus n. sp.

Plate 4, figures 1-5

v, ?	2008	*Pseudaspidites* sp. indet. – BRAYARD & BUCHER, p. 35, pl. 11, fig. 6.

Etymology: Refers to the flattened shape of the flanks.

Holotype: PIMUZ 27326 (Pl. 4, fig. 1a-d).

Type locality and horizon: Exotic block HB912, Jebel Safra, Oman; Early Triassic, Smithian, *Owenites koeneni* fauna.

Occurrence: Samples JS11, JS12, HB912, Baid-B; *Rohillites omanense* fauna, *Owenites koeneni* fauna.

Diagnosis: Relatively evolute *Pseudaspidites* with flat, subparallel flanks.

Description: Involute, compressed shell with flat, subparallel flanks. Venter rounded with indistinct shoulders. Umbilicus with high and perpendicular wall, and marked but slightly rounded shoulders. Surface smooth, very faint radial folds present on some specimens. A distinct strigation is visible on the flanks of very well preserved specimens, only. Suture with slightly phylloid saddles and deeply indented lobes.

Measurements: Text-figures 10, 11.

Discussion: This species differs from *Pseudaspidites muthianus* by its flat, subparallel flanks and is slightly, but conspicuously more evolute. The suture of *Pseudaspidites planus* differs from that of *P. muthianus* by its straighter saddles and its less individualized auxiliaries. The single and rather poorly preserved specimen reported as *Pseudaspidites* sp. indet. from South China (BRAYARD & BUCHER 2008, p. 35, pl. 11, fig. 6) is probably conspecific with *Pseudaspidites planus*.

Pseudaspidites sp. indet. A

Plate 3, figure 2

Occurrence: A single small specimens from sample Baid-B; *Owenites koeneni* fauna.

Description: Moderately evolute, slightly compressed shell with convex flanks. Venter rounded with rounded shoulders. Umbilicus with perpendicular wall and rounded shoulders. Surface smooth. Suture with phylloid saddles and deeply indented lobes.

Measurements: Text-figure 10.

Discussion: This specimen differs from typical *Pseudaspidites* by its evolute coiling and the rounded umbilical shoulders. However, its suture line is very typical for this genus. *Pseudaspidites planus* differs also by its flat flanks.

Genus *Leyeceras* BRAYARD & BUCHER 2008

Type species: *Leyeceras rothi* BRAYARD & BUCHER 2008.

Leyeceras cf. *rothi* BRAYARD & BUCHER 2008

Plate 5, figures 1-5; plate 6, figures 1-3

v, ? 2008 *Leyeceras rothi* BRAYARD & BUCHER, p. 39, pl. 14, figs. 1-3.

v submitted [a] [a] *Leyeceras* cf. *rothi* BRÜHWILER et al.

Occurrence: Samples JS4, HB 912, Baid-B; *Owenites koeneni* fauna.

Description: Moderately evolute shell with convex flanks and thick, elliptical whorl section. Venter rounded, grading into flanks with indistinct shoulders. Umbilicus with moderately high wall and rounded shoulders. Shell smooth, except for weak and distant plications near umbilicus. Radial lirae visible on very well preserved specimens. Suture line with slender first lateral saddle and broad, deeply indented first lateral lobe.

Measurements: Text-figure 12.

Discussion: Flanks of *Leyeceras rothi* from South China are slightly flatter than on our specimens from Oman, and its suture line is slightly different with a narrower first lateral lobe.

Genus *Guodunites* BRAYARD & BUCHER 2008

Type species: *Guodunites monneti* BRAYARD & BUCHER 2008.

Guodunites monneti BRAYARD & BUCHER 2008

Plate 7, figures 1-5

? 1968 *Owenites slavini* KUMMEL & ERBEN, p. 124, pl. 21, figs. 3, 4.
v 2008 *Guodunites monneti* BRAYARD & BUCHER, p. 83, pl. 44, figs. 1-2.
v 2009 *Guodunites monneti* – BRAYARD et al., p. 473, pl. 1, figs. 1–14; text-fig. 3A–C.

Occurrence: Samples HB900, HB606, HB608, HB910, WM7; *Owenites koeneni* fauna.

Description: Moderately involute, compressed shell with convex flanks. Venter rounded without any distinct shoulders. Umbilical wall inclined without umbilical shoulder forming a shallow, crateriform umbilicus on inner whorls; umbilical suture markedly egressive in later growth stages. Ornamentation consists of a distinct, fine strigation on the flanks but not on the venter, and smooth folds that are more prominent near the umbilicus. Growth lines strongly projected towards the aperture on the external part of the flanks. Suture line subammonitic with strong indentions of lobes almost reaching to the top of the saddles.

Measurements: See appendix.

Discussion: On relatively poorly preserved specimens from South China, no strigation is preserved (BRAYARD & BUCHER 2008). The suture line of the South Chinese specimens shows some differences with an asymmetrical crenulation of the saddles, but this may also be linked to poor preservation. *Guodunites* has recently been shown to be a trans-panthalassic, low-palaeolatitude middle Smithian ammonoid genus (BRAYARD et al. 2009). Whether the specimen from Afghanistan described as *Owenites slavini* by KUMMEL & ERBEN (1968) really belongs to *Owenites* or rather to *Guodunites* cannot be decided since its suture line is unknown.

Family Meekoceratidae WAAGEN 1895

Genus *Meekoceras* HYATT 1879

Type species: *Meekoceras gracilitatis* WHITE 1879.

?Meekoceras sp. indet.

Plate 8, figure 12a-b

Occurrence: A single specimen from sample JS13, *Nammalites pilatoides* fauna.

Description: Moderately involute, compressed shell with slightly convex flanks. Venter narrow and slighlty sulcate with angular ventral shoulders, but poorly preserved. Umbilicus small on innermost whorls, strongly eggressive from 2nd-3rd whorls on. Umbilical wall gently inclined with subangular shoulders. Ornamentation consists of fine, biconcave, prorsiradiate folds that are most prominent near the umbilicus and fade out towards the venter. On outer whorls, folds become very faint. Suture line not preserved.

Discussion: The overall shape and the sulcate venter favor an assignment of this specimen to *Meekoceras*. However, without the suture line no definitive determination can be made. The type species, *M. gracilitatis* is more involute than our specimen.

Family Dieneroceratidae KUMMEL 1952

Genus *Dieneroceras* SPATH 1934

Type species: *Ophiceras dieneri* HYATT & SMITH 1905.

Dieneroceras cf. *dieneri* (HYATT & SMITH 1905)

Plate 8, figures 1-4; plate 9, figures 1-7; plate 10, figures 1-3

1905 *Ophiceras dieneri* HYATT & SMITH, p. 118, pl. 8, figs. 16-29

? 1905 *Lecanites knechti* HYATT & SMITH, p. 138, pl. 9, figs. 11-16.

1932 *Ophiceras dieneri* – SMITH, p. 48, pl. 8, figs. 16-29.
? 1955 *Ophiceras iwaiense* SAKAGAMI, p. 135, pl. 1, figs. 1-9.
? 1960 *Dieneroceras iwaiense* – KUMMEL & SAKAGAMI, p. 4, pl. 1, figs. 3-5.
? 1961 *Dieneroceras dieneri* – KIPARISOVA, p. 47, pl. 9, figs. 2.
? 1961 *Dieneroceras chaoi* KIPARISOVA, p. 48, pl. 9, figs. 3-6.
? 1962 *Dieneroceras knechti* – KUMMEL & STEELE, p. 662, pl. 99, figs.14-15.
? 1965 *Dieneroceras* cf. *dieneri* – KUENZI, p. 369, pl. 53, fig. 13-18, text-figs. 3A-C, 4.
? 1968 *Dieneroceras knechti* – KUMMEL & ERBEN, p. 116, pl. 22, fig. 1-3.
1968 *Dieneroceras dieneri* – NAKAZAWA & BANDO, p. 93, pl. 4, fig. 1-6, text-fig. 5.
1968 *Dieneroceras* aff. *chaoi* – NAKAZAWA & BANDO, p. 95, pl. 4, figs. 7-8, pl. 5, fig. 1.

Occurrence: Samples HB900, HB905, HB912, Baid-B ?Baid-G, JS2, JS12, ?JS8; *Owenites koeneni* fauna.

Description: Serpenticone, very evolute shell with convex flanks. Inner whorls with subquadratic whorl section, outer whorls becoming laterally compressed. Venter subtabulate with subangular shoulders on inner whorls, becoming less tabulate with rounded shoulders on outer whorls. Umbilicus wide and shallow with rounded umbilical wall. Surface smooth or ornamented with weak radial folds on some specimens. Suture line ceratitic and simple with relatively deep lobes.

Measurements: Text-figures 13, 14.

Discussion: This species closely resembles *Dieneroceras dieneri,* which differs in having a strigation that is only seldom preserved (HYATT & SMITH 1905). On our numerous and well preserved material from Oman, no strigation is present and therefore the assignment to this species is not definite. *D. tientungense* CHAO, 1959 from the *Flemingites rursiradiatus* beds of South China differs by its strigation, its perpendicular umbilical wall, its more evolute coiling and the lower whorls (Text-fig. 14; BRAYARD & BUCHER 2008). The specimens from Oman are relatively large-sized representatives of the genus *Dieneroceras*.

Family Flemingitidae HYATT 1900

Genus *Flemingites* WAAGEN 1895

Type species: *Ceratites flemingianus* DE KONINCK 1863.

Flemingites rursiradiatus CHAO 1959

Plate 12, figures 1-5

1959 *Flemingites rursiradiatus* CHAO, p. 205, pl. 6, figs. 1-5, 8-10, text-figs. 13a-b.
?, non 1984 *Flemingites* cf. *rursiradiatus* – VU KHUC, p. 34, pl. 1, figs. 4-5.
v 2008 *Flemingites rursiradiatus* – BRAYARD & BUCHER, p. 44, pl. 18, figs. 1-7; pl. 19, figs. 1-3.

Occurrence: Sample Baid-A; *Flemingites rursiradiatus* fauna.

Description: Large and evolute, serpenticone shell with convex flanks. Venter rounded with rounded ventral shoulders. Umbilicus wide with high wall and rounded shoulders. Flanks ornamented with coarse strigation and distant, strong, rursiradiate ribs. These ribs become finer, concave and closely spaced on adult whorls. Suture line ceratitic with long, slightly phylloid saddles and strongly indented lobes.

Measurements: Text-figure 15.

Flemingites sp. indet.

Plate 12, figure 6a-c

Occurrence: A single, well preserved specimen from sample SA3; *Rohillites omanensis* fauna.

Description: Evolute, serpenticonic shell with convex flanks. Venter slightly flattened with rounded ventral shoulders. Umbilicus wide with high wall and rounded shoulders. Flanks ornamented with distant, rursiradiate ribs. Suture line not preserved.

Discussion: This specimen differs from *Flemingites rursiradiatus* described above only by the absence of strigation and could perhaps be conspecific.

Genus *Anaxenaspis* KIPARISOVA 1956

Type species: *Xenaspis orientale* DIENER 1895.

Anaxenaspis cf. *lidacensis* (WELTER 1922)

Plate 13, figures 9-11; plate 14, figures 1-3

1922 *Flemingites lidacensis* WELTER, p. 115, pl. 7, fig. 1-4.
? 1959 *Flemingites* cf. *lidacensis* – KUMMEL
? 1968 *Flemingites* cf. *lidacensis* – KUMMEL & ERBEN, p. 115, pl. 24, fig. 2.

? 1973 *Flemingites lidacensis* – COLLINGON, p. 9, pl. 2, figs. 1-3.

Occurrence: Samples Baid-B, HB904, WM8; *Owenites koeneni* fauna.

Description: Large, compressed and moderately evolute shell with convex flanks. Venter rounded with rounded shoulders. Umbilicus with inclined wall and rounded shoulders. Ornamentation consists of blunt radial ribs that disappear on the external third of the flanks. Ribs are well developped on the inner whorls and gradually become weaker on the outer whorls. Distance between ribs increases considerably through ontogeny. Strongly projected fine growth lines are visible on the venter of one specimen. Length of body chamber probably about one whorl. Suture line with strongly indented lobes and elongated, slightly phylloid saddles.

Measurements: Text-figure 16.

Discussion: Specimens described here under *Anaxenaspis* cf. *lidacensis* differ from one another in the amount of involution which we regard as intraspecific variation. However, due to the limited number of specimens available no definitive determination is possible, and it is also possible that there might be more than one species among these specimens.

"Flemingites" lidacensis (WELTER 1922) is ornamented with a delicate strigation, which is usually not preserved. On our specimens from Oman, no strigation is observed, but this may be due to the relatively poor preservation. The species *lidacensis* is here assigned to *Anaxenaspis* because it shows no significant differences with the type species *Anaxenaspis orientale,* except for its delicate strigation. KUMMEL & STEELE (1962, p. 667) suggested that this species should probably be placed into *Anaflemingites,* which however exhibits no ribbing at all. In Timor *Anaxenaspis lidacensis* (WELTER 1922) occurs together with *Owenites* and is therefore of the same age as our specimens.

Genus *Subflemingites* SPATH 1934

Tpye species: *Aspidites meridianus involutus* WELTER 1922.

Subflemingites involutus (WELTER 1922)

Plate 13, figures 1-3

1922 *Aspidites meridianus* WELTER, p. 132, pl. 12, fig. 1-3.

1922 *Aspidites meridianus involutus* WELTER, p. 133, pl. 12, fig. 4-5.

1934 *Subflemingites involutus* – SPATH, p. 118, pl. fig. 32.

Occurrence: Sample JS13, *Nammalites pilatoides* fauna.

Description: Moderately evolute, compressed shell with convex flanks. Venter rounded without any shoulder. Umbilicus wide, with low, inclined wall and rounded shoulders. Surface smooth except for fine, biconcave growth lines and very weak folds. Suture line not preserved.

Measurements: See appendix.

Genus *Rohillites* WATERHOUSE 1996b

Type species: *Flemingites rohilla* DIENER 1897.

Rohillites omanensis n. sp.

Plate 13, figures 4-8

Etymology: Named after the Sultanate of Oman.

Holotype: PIMUZ 27371 (Pl. 13, fig. 5a-c).

Type locality and horizon: Exotic block SA3, Jebel Safra, Oman; Early Triassic, Smithian, *Rohillites omanensis* fauna.

Occurrence: Samples SA3, JS11; *Rohillites omanensis* fauna.

Diagnosis: Weakly ornamented *Rohillites* with strigation restricted to external flanks, and a relatively broad venter.

Description: Moderately evolute, compressed shell with convex flanks. Venter tabulate with subangular shoulders. Umbilicus with steep wall and rounded umbilical shoulders. Ornamentation consists of very weak radial folds and a fine strigation restricted to the external part of the flanks. Suture line not preserved.

Measurements: Text-figure 17.

Discussion: *Rohillites rohilla* (DIENER 1897) is more evolute and has a narrower venter. *R. bruehwileri* and *R. sobolevi* BRAYARD & BUCHER 2008 differ by their narrower venter and stronger ribbing.

Genus *Pseudoflemingites* SPATH 1930

Type species: *Pseudoflemingites timorensis* SPATH 1930 (= *Ophiceras nopscanum* WELTER 1922, *partim*, p. 104; pl. 4, figs. 4-5 only).

Pseudoflemingites goudemandi BRAYARD & BUCHER 2008

Plate 14, figures 4-5

v 2008 *Pseudoflemingites goudemandi* BRAYARD & BUCHER, p. 49, pl. 22, figs. 1-5, text-figure 44.

Occurrence: Sample JS12, *Owenites koeneni* fauna.

Description: Evolute, compressed shell with convex flanks. Venter subtabulate with slightly rounded shoulders. Umbilicus wide and shallow with low, nearly perpendicular wall and rounded shoulders. Surface almost smooth except for barely perceptible sinuous growth lines and folds. Suture line not preserved.

Measurements: See appendix.

Genus *Baidites* n. gen.

Etymology: Named after the type locality of the type species.

Type species: *Baidites hermanni* n. gen. et sp.

Composition of the genus: *Baidites hermanni* n. gen. et sp., *B. crassecostatum* (WELTER 1922), *B. tenue* (WELTER 1922).

Diagnosis: Evolute and tabulate to subtabulate Flemingitidae with inclined umbilical wall which is well separated from the flanks. Ornamentation consists of straight, slightly rursiradiate, blunt ribs.

Discussion: This genus differs from all other Flemingitidae by its distinct umbilicus with an inclined wall. Moreover, many other Flemingitidae such as *Anaflemingites*, *Flemingites*, *Pseudoflemingites*, *Subflemingites* or *Anaxenaspis* also differ by their rounded venter.

Baidites hermanni n. gen. et sp.

Plate 10, figures 4-5; plate 11, figures 1-4

Etymology: Named after Elke Hermann (Zürich).

Holotype: PIMUZ 27358 (pl. 11, fig. 1a-e).

Type locality and horizon: HB911, Baid, *Baidites hermanni* fauna.

Occurrence: Sample Baid HB911; *Baidites hermanni* fauna.

Diagnosis: *Baidites* with serpenticonic inner whorls; outer whorls tabulate with flat flanks, external part of flanks markedly convergent.

Description: Large and evolute shell displaying important ontogenetic changes (plate 10, figure 3). Inner whorls serpenticone with subquadratic whorl section and rounded venter. Outer whorls laterally compressed; venter tabulate with narrowly rounded shoulders. On outer whorls the inner two thirds of the flanks are converging only slightly, the outer third is converging towards the venter. Umbilicus wide and shallow. Umbilical wall steep on inner whorls becoming more inclined on outer whorls, umbilical shoulder marked but rounded. Ornamentation of the flanks consists of straight, slightly rursiradiate blunt ribs that do not cross the venter. Suture line ceratitic with rather narrow lobes, saddles with varying width; auxiliary series relatively long.

Measurements: Text-figure 18.

Discussion: *Baidites crassecostatum* (WELTER 1922) from Timor differs from *B. hermanni* by its flatter flanks converging towards the venter from the umbilical margin. *B. tenue* (WELTER 1922) is probably a synonym of *B. crassecostatum*.

Family Galfettitidae n. fam.

Etymology: Named after the type genus.

Type genus: *Galfettites* BRAYARD & BUCHER 2008.

Composition of the family: *Galfettites* BRAYARD & BUCHER 2008, *Lepiskites* DAGYS & ERMAKOVA 1990, *Paranorites* WAAGEN 1895, *Radioceras* WATERHOUSE 1996a, *Safraites* n. gen., *Shigetaceras* BRÜHWILER ET AL. submitted, *Urdyceras* BRAYARD & BUCHER 2008, possibly also *Lingyunites* BRAYARD & BUCHER 2008.

Diagnosis: Compressed Ceratitidae with tabulate to subtabulate venter. Suture line with tapered and/or asymmetrical second lateral saddle.

Discussion: When erecting the genus *Galfettites*, BRAYARD & BUCHER (2008) provisionally assigned it to Flemingitidae based on its overall similar shape with some members of that family such as *Rohillites*. However, the new material from Oman together with new collections from Pakistan (BRÜHWILER et al. 2007, ongoing work) clearly indicates that *Galfettites* represents a derived form of a distinct group distinguished here as Galfettitidae.

Genera we assign to the Galfettitidae have in common the following characters: (i) a laterally compressed shell with more or less converging flanks, (ii) a tabulate to subtabulate venter, mostly with slightly rounded shoulders, (iii) a vertical umbilical wall, (iv) a suture line with a characteristically tapered and/or asymmetrical second lateral saddle and a relatively long auxiliary series, (v) a weak ornamentation. The amount of involution varies from moderately evolute (e.g. *Galfettites*) to involute (e.g. *Radioceras*).

Flemingitidae mostly differ from Galfettitidae by (i) the presence of a strigation, (ii) a strong radial ornamentation, (iii) a suture line with well rounded saddles, and (iv) a rounded venter on most but not all members.

Genus *Galfettites* BRAYARD & BUCHER 2008

Type species: *Galfettites simplicitatis* BRAYARD & BUCHER 2008.

Galfettites simplicitatis BRAYARD & BUCHER 2008

Plate 15, figures 1-4; plate 16, figure 1a-d

v 2008 *Galfettites simplicitatis* BRAYARD & BUCHER, p. 48, pl. 21, figs. 1-2, text-fig. 43.

Occurrence: Samples HB912, JS2, JS4, Baid-B; *Owenites koeneni* fauna.

Description: Moderately evolute, compressed shell with convex flanks. Maximal thickness slightly below mid-flanks, from where the flanks converge to the venter. Venter narrow and tabulate with angular shoulders. Umbilicus shallow and wide with vertical wall and rounded shoulders. Ornamentation of surface consists of dense, delicate, concave folds. Suture line very distinct, the second lateral saddle having a distinctly trigonal tip and the third saddle being slightly curved towards the umbilicus. Lobes deeply indented, auxiliary series well individualized.

Measurements: Text-figures 19, 20.

Discussion: BRAYARD & BUCHER (2008) described the venter of this species as narrowly curved to subtabulate, but on their specimens from South China the ventral part is poorly preserved and probably also tabulate as in the specimens from Oman.

"Meekoceras" wanneri WELTER, 1922, from the "Meekoceraskalke" of Timor is very similar shape but unfortunately its suture line is unknown. In South China *G. simplicitatis* occurs within the "*Ussuria* horizon", in the lower part of the *Owenites* Beds.

Galfettites kyrae n. sp.

Plate 16, figures 3-5

Etymology: Named after Kyra Fanghänel-Galfetti (Zürich).

Holotype: Specimen PIMUZ 27391 (plate 16, fig. 5a-d).

Type locality and horizon: Baid-B; *Owenites koeneni* fauna.

Occurrence: Samples Baid-B, HB900, HB902; *Owenites koeneni* fauna.

Diagnosis: *Galfettites* with flat flanks on inner whorls, broad venter and folds on upper flanks.

Description: Moderately evolute, compressed shell. Flanks flat on inner whorls, only slightly convex and converging on outer whorls. Venter subtabulate on inner whorls; broad and tabulate with angular ventrolateral shoulders on outer whorls. Umbilicus with high vertical umbilical wall and subangular umbilical shoulders. Ornamentation of surface consists of radial folds on the upper half of the flanks. Suture line very similar to that of *Galfettites simplicitatis*.

Measurements: Text-figures 20, 21.

Discussion: This species differs from *G. simplicitatis* by the flat flanks, the broader venter, the folds on lower flanks and the angular umbilical shoulders.

Galfettites omani n. sp.

Plate 14, figures 6-8

Etymology: Named after the Sultanate of Oman.

Holotype: Specimen PIMUZ 27383 (plate 14, fig. 7a-b).

Type locality and horizon: Exotic block JS13, Jebel Safra; *Nammalites pilatoides* fauna.

Occurrence: Sample JS13; *Nammalites pilatoides* fauna.

Diagnosis: *Galfettites* with very shallow umbilicus and folds on outer whorls.

Description: Moderately evolute, very compressed shell with slightly convex and converging flanks. Venter narrow and tabulate with angular shoulders. Umbilicus wide and very shallow with very low wall and rounded shoulders. Inner whorls smooth, outer whorls ornamented with distant radial folds on the inner half of the flanks. Suture line ceratitic with slightly phylloid saddles, but poorly preserved.

Measurements: Text-figures 20, 22.

Discussion: This species has recently been found also in age-equivalent beds in Spiti (India) (BRÜHWILER et al. ongoing work). It is very similar to *Rohillites laevis* SHIGETA & ZAKHAROV 2009 from the early Smithian of Primorye but differs by its folds on outer whorls and the absence of strigation.

Genus *Safraites* n. gen.

Etymology: Named after the type locality Jebel Safra.

Type species: *Safraites simplex* n. gen. et sp.

Composition of the genus: Type species only.

Diagnosis: Small and involute Galfettitidae with slightly convex flanks and maximal thickness slightly above mid-flanks.

Discussion: This genus is more involute than *Galfettites* and has more angular umbilical shoulders. *Safraites* differs from Protpychitidae by its tabulate venter.

Safraites simplex n. gen. et sp.

Plate 8, figures 5-10

Etymology: Refers to the simple morphology of the species.

Holotype: Specimen PIMUZ 27395 (plate 8, figure 5a-c).

Type locality and horizon: Jebel Safra, exotic block JS13, *Nammalites pilatoides* fauna.

Occurrence: Sample JS13; *Nammalites pilatoides* fauna.

Diagnosis: As for the genus.

Description: Small, involute and compressed shell with slightly convex flanks. Maximal thickness slightly above mid-flanks. Venter tabulate with angular ventral shoulders. Umbilicus with low, vertical wall and angular shoulders. Shell exhibits egressive coiling. Suture line simple, indentions of lobes not visible, poorly preserved.

Measurements: Text-figure 23.

Galfettitidae gen. indet.

Plate 16, figure 2a-d

Occurrence: A single specimen from sample Baid-B; *Owenites koeneni* fauna.

Description: Involute and compressed shell with subparallel, slightly convex flanks. Venter tabulate with angular ventral shoulders. Umbilicus with high, vertical wall and angular shoulders. Suture line ceratitic with slightly asymmetrical second lateral saddle.

Measurements: See appendix.

Discussion: This specimen is more involute than all known species of *Galfettites*.

Genus *Paranorites* WAAGEN 1895

Type species: *Paranorites ambiensis* WAAGEN 1895.

Paranorites jenksi BRAYARD & BUCHER 2008

Plate 3, fig. 1a-c

?	1959	*Paranorites ellipticus* CHAO, p. 217, pl. 10, figs. 9-10, text-fig. 16a.
v	2008	*Paranorites jenksi* BRAYARD & BUCHER, p. 33, pl. 9, figs. 24-26.

Occurrence: A single specimen from sample HB911; *Baidites hermanni* fauna.

Description: Moderately evolute, compressed shell with subparallel, slightly convex flanks. Venter subtabulate, with rounded ventrolateral shoulder. Umbilicus with high, perpendicular wall and rounded umbilical shoulders. Suture line ceratitic with slightly phylloid first and third lateral saddles and tapered second lateral saddle.

Measurements: See appendix.

Discussion: In South China this species occurs in the earliest Smithian *Kashmirites kapila* beds (BRAYARD & BUCHER 2008). The type species *Paranorites ambiensis* differs by its more convergent flanks.

Family Arctoceratidae ARTHABER 1911

Genus *Submeekoceras* Spath 1934

Type species: *Meekoceras mushbachanum* WHITE 1879.

Submeekoceras mushbachanum (White 1879)

Plate 17, figures 1-3

1879 *Meekoceras mushbachanum* WHITE, p. 113.

1880 *Meekoceras mushbachanum* – WHITE, p. 114, pl. 32, figs. 1a-d.

1902 *Prionolobus mushbachanum* – FRECH, p. 631, fig. c

1904 *Meekoceras mushbachanum* – SMITH, p. 376, pl. 41, figs. 1-3; pl. 43, figs. 1-2.

1905 *Meekoceras* (*Konickites*) *mushbachanum* – HYATT & SMITH, p. 149, pl. 15, figs. 1-9; pl. 16, figs. 1-3; pl. 18, figs. 1-7; pl. 70, figs. 8-10.

1914 *Submeekoceras mushbachanum* – SMITH, p. 77, pl. 72, figs. 1-2; pl. 73, figs. 1-6; pl. 74, figs. 1-23.

? 1922 *Meekoceras mushbachanum* – WELTER, p. 126.

1932 *Meekoceras (Koninckites) mushbachanum* – SMITH, p. 61, pl. 15, figs. 1-9; pl. 16, figs. 1-3; pl. 18, figs. 1-7; pl. 38, fig. 1; pl. 59, figs. 17-21; pl. 70, figs. 8-10; pl. 74, figs. 1-23; pl. 75, figs. 1-6; pl. 76, figs. 1-3

1932 *Meekoceras (Koninckites) mushbachanum* var. *corrugatum* - SMITH, p. 61, pl. 38, fig. 1.

1932 *Meekoceras (Koninckites) evansi* SMITH, p. 60, pl. 35, figs. 1-3; pl. 36, figs. 1-18.

1934 *Submeekoceras mushbachanum* – SPATH, p. 255, fig. 87.

1959 *Paranorites ovalis* CHAO, p. 217, pl. 9, figs. 16-19, text-fig. 16b.

? 1959 *Prionolobus ophionus* var. *involutus* CHAO, p. 201, pl. 9, figs. 11-15, text-fig. 11b.

1959 *Prionolobus hsuyuchieni* CHAO, p. 202, pl. 9, figs. 9-10, text-fig. 11c.

? 1959 *Meekoceras (Submeekoceras) tientungense* CHAO, p. 317, pl. 14, figs. 6-7, text-fig. 45b.

1959 *Meekoceras (Submeekoceras) subquadratum* CHAO, p. 317, pl. 14, figs. 1-5; pl. 39, figs. 8-9, text-fig. 45c.

1959 *Meekoceras densistriatum* CHAO, p. 310, pl. 38, figs. 1-3, 19, text-fig. 43b.

1959 *Meekoceras yukiangense* CHAO, p. 311, pl. 39, figs. 1-7, text-fig. 44a.

1959 *Meekoceras kaohwaiense* CHAO, p. 311, pl. 40, figs. 16-18, text-fig. 44b.

1959 *Meekocerass pulchriforme* CHAO, p. 313, pl. 40, figs. 14-15, text-fig. 44c.

? 1959 *Meekoceras jolinkense* – CHAO, p. 314, pl. 14, figs. 12-15.

1959 *Meekoceras lativentrosum* CHAO, p. 309, pl. 38, figs. 15-18, text-fig. 43a.

1959 *Proptychites latumbilicutus* CHAO, p. 234, pl. 19, figs. 2-3, text-fig. 22a.

? 1959 *Proptychites kaoyunlingensis* CHAO, p. 234, pl. 16, figs. 7-8, text-fig. 22b.

p 1968 *Arctoceras mushbachanum* – KUMMEL & ERBEN, p. 131, pl. 21, fig. 1 only.

v 2008 *Submeekoceras mushbachanum* – BRAYARD & BUCHER, p. 52, pl. 16, fig. 4; pl. 26, figs. 1-9; text-fig. 46.

Occurrence: Samples Baid-A, JS4, JS12; *Flemingites rursiradiatus* fauna, *Owenites koeneni* fauna.

Description: Moderately evolute, somewhat compressed shell with rather flat, slightly convex flanks. Venter rounded with rounded ventrolateral shoulders. Umbilicus deep with vertical wall and abruptly rounded shoulders. Surface with faint, slightly biconcave folds and growth lines. Suture with deeply indented lobes, saddles with parallel sides.

Measurements: Text-figure 24.

Genus *Nammalites* BRÜHWILER et al., submitted

Type species: *Kazakhstanites pilatoides* GUEX 1978.

Nammalites pilatoides (GUEX 1978)

Plate 18, 1-7

1909 *Meekoceras* sp. ind. aff. *pilato* – KRAFFT & DIENER, p. 42, pl. 28, fig. 2a-c.

1968a *Wasatchites* sp. indet. – KUMMEL, p. 500, pl. 3, figs. 10-11.

1968 *Eoptychites* sp. indet. – KUMMEL & ERBEN, p. 120, pl. 22, figs. 10-11.

v 1978 *Kazakhstanites pilatoides* GUEX, p. 109, pl. 6, fig. 5, 6, 16, pl. 8, fig. 6.
v, p 1978 *Anasibirites pluriformis* GUEX, pl. 4, fig. 3 only.

Occurrence: Sample JS13; *Nammalites pilatoides* fauna.

Description: Moderately evolute, compressed shell with flat, slightly convergent flanks. Maximal thickness at umbilical border. Venter rounded, slightly flattened with rounded shoulders. Umbilicus with steep, almost vertical wall and rounded shoulders. Ornamentation consists of rursiradiate to prorsiradiate ribs that tend to develop tubercles near the umbilicus and mostly fade out towards the venter, but some do cross the venter. Suture line not preserved.

Measurements: Text-figure 25.

?Arctoceratidae gen. indet.

Plate 20, figure 2a-d

Occurrence: A single specimen from sample SA1; ?*Nammalites pilatoides* fauna.

Description: Moderately evolute, shell with flat, subparallel flanks. Venter subtabulate with rounded shoulders. Umbilicus with vertical wall and rounded shoulders. Ornamentation consists of prorsiradiate folds on inner flanks. Suture line with weakly indented lobes, first and second lateral saddles with parallel sides.

Measurements: See appendix.

Familiy Ussuriidae SPATH 1930

Genus *Parussuria* SPATH 1934

Type species: *Ussuria compressa* HYATT & SMITH 1905.

Parussuria compressa (HYATT & SMITH 1905)

Plate 18, figures 8-14

1905 *Ussuria compressa* HYATT & SMITH, p. 89, pl. 3, figs. 6-11.
1932 *Sturia compressa* – SMITH, p. 93, pl. 3, figs. 6-11.
1934 *Parussuria compressa* – SPATH, p. 213, figs. 66c, d.
1962 *Parussuria compressa* – KUMMEL & STEELE, p. 690, pl. 99, fig. 23; pl. 102, fig. 11.
? 1968 *Parussuria semenovi* ZAKHAROV, p. 59, pl. 5, fig. 4.

1995 *Parussuria compressa* – SHEVYREV, p. 37, pl. 4, fig. 6, text-fig. 16.
v 2008 *Parussuria compressa* – BRAYARD & BUCHER, p. 56, pl. 12, fig. 17.

Occurrence: Samples HB903, HB904, JS12, JS13, SA3; *Nammalites pilatoides* fauna, *Owenites koeneni* fauna.

Description: Extremely involute, compressed oxycone with slightly convex flanks. Maximal thickness near umbilicus. Whorls increasing rapidly in height. Umbilicus very small and deep on inner whorls, occluded on outer whorls. Venter narrowly rounded on outer whorls, broadly rounded on inner whorls. Ornamentation of the surface consists of delicate strigation, and weak radial folds on some specimens. Suture line ammonitic.

Measurements: Text-figure 26.

Family Prionitidae HYATT 1900

Genus *Prionites* WAAGEN 1895

Type species: *Prionites tuberculatus* WAAGEN 1895.

Prionites sp. indet.

Plate 20, figure 1a-d

Occurrence: A single specimen from HB912; *Owenites koeneni* fauna.

Description: Moderately involute, compressed shell with convex flanks. Venter broad and tabulate with slightly angular ventral shoulders. Umbilicus small, deep and funnel-shaped on inner whorls, with eggression on outer whorls. Umbilical wall inclined with slightly rounded shoulders. Surface smooth. Suture line ceratitic with rather deep lobes.

Measurements: See appendix.

Discussion: This species differs from *Prionites tuberculatus* by the flat flanks without tubercles and the more compressed whorls. Additionally, the suture line is slightly different with more elongated saddles. *P. laevis*, *P. armatus* and *P. elegans* from Timor (WELTER 1922) are here considered as synonyms of the type species. *P. tabulatus* WATERHOUSE 1996b is based on material illustrated by KRAFFT & DIENER (1909) which is too poorly preserved for identification.

Genus *Anasibirites* MOJSISOVICS 1896

Type species: *Sibirites kingianus* - WAAGEN, 1895, p. 108, pl. 8, figs. 1a-c, 2a-c

Anasibirites multiformis WELTER, 1922

Plate 19, figures 1-6

?p 1895 *Sibirites tenuistriatus* WAAGEN, p. 138, pl. 9, figs. 2a-b.
p 1922 *Anasibirites multiformis* WELTER, p. 138, pl. 15, figs. 12-13, 23-24; pl. 16, figs. 6-19 only.
? 1929 *Anasibirites welleri* MATHEWS, p. 14, pl. 2, figs. 17-19
? 1929 *Anasibirites emmonsi* MATHEWS, p. 14, pl. 2, figs. 20-26
v 2008 *Anasibirites multiformis* – BRAYARD & BUCHER, p. 56, pl. 28, figs. 1-6, text-figs. 48-49.

Occurrence: Sample HB 901; *Anasibirites multiformis* fauna.

Description: Moderately involute platycone with slighlty convex flanks. Venter subtabulate to tabulate with angular to subangular shoulders. Umbilicus moderately deep with oblique wall and rounded shoulders. Ornamentation consists of dense, concave, thick and projected striae crossing the venter. Suture line ceratitic with slightly tapered saddles.

Measurements: See appendix.

Discussion: As already noted by BRAYARD & BUCHER (2008) this species may be conspecific with *A. tenuistriatus* (WAAGEN 1895). It differs from the type species by its tabulate to subtabulate venter and the identical ornamentation on all growth stages.

Genus ***Hemiprionites*** SPATH 1929

Type species: *Goniodiscus typus* WAAGEN 1895.

Hemiprionites* cf. *butleri MATHEWS 1929

Plate 19, figures 9-10

1929 *Goniodiscus butleri* MATHEWS, p. 35, pl. 6, figs. 18-21.
v 2008 *Hemiprionites* cf. *butleri* – BRAYARD & BUCHER, p. 58, pl. 29, figs. 1-7; text-fig. 50.

Occurrence: Samples HB901, HB902; *Owenites koeneni* fauna, *Anasibirites multiformis* fauna.

Description: Involute platycone with slightly convex flanks. Venter slightly sulcate with angular shoulders. Umbilicus funnel-shaped and deep with inclined wall and rounded shoulders. Surface smooth. Suture line ceratitic with broad lobes and narrow saddles.

Measurements: See appendix.

Discussion: The type species of *Hemiprionites* (*Goniodiscus typus* WAAGEN 1895) has no sulcate venter. Other species described by MATHEWS in 1929 (except *H. walcotti*) can be joined together as variant of the type species (BRAYARD & BUCHER 2008). Specimen PIMUZ 27426 (plate 19, fig. 9) has an asymmetric ventral side and is considered to be a pathologic specimen.

Lucasites n. gen.

Etymology: Named after Spencer Lucas (Albuquerque).

Type species: *Lucasites involutus* n. gen. et sp.

Composition of the genus: *Lucasites involutus* n. gen. et sp., *Lucasites evolutus* n. gen. et sp.

Diagnosis: Compressed, relatively evolute Prionitidae with a broad, tabulate venter with angular shoulders.

Discussion: This genus is assigned to Prionitidae on account of the typical shape of the umbilicus, and the overall compressed shape similar to that of the inner whorls of *Prionites tuberculatus* (BRÜHWILER et al., unpublished material from the Salt Range). However, without the suture line this assignment can not be definitive. This genus would represent the oldest known member of the family Prionitidae.

Shamaraites from the early Smithian of South Primorye (SHIGETA & ZAKHAROV 2009) is similar in shape, but differs by its vertical umbilical wall and a stronger ornamentation.

Lucasites involutus n. gen. et sp.

Plate 6, figure 4a-c

Etymology: Referring to the involute coiling.

Holotype: Specimen PIMUZ 27339 (plate 6, fig. 4a-c).

Type locality and horizon: Jebel Safra, exotic block JS11, *Rohillites omanensis* fauna.

Occurrence: A single specimen from sample JS11; *Rohillites omanensis* fauna.

Diagnosis: Moderately involute *Lucasites*.

Description: Moderately involute platycone shell with convex flanks that become slightly concave near venter. Venter broad and tabulate with angular shoulders. Umbilicus with inclined umbilical wall and rounded shoulders. Ornamentation of the flanks consists of faint sinuous folds and growth lines. Suture line not preserved.

Measurements: See appendix.

Discussion: More involute than *Lucasites evolutus* described below. *L. involutus* and *L. evolutus* actually may be variants of a single species, but material demonstrating a gradation between these two poles is lacking.

Lucasites evolutus n. gen. et sp.

Plate 8, figure 11a-b

Etymology: Referring to the evolute coiling.

Holotype: Specimen PIMUZ 27340 (plate 8, fig. 11a-b).

Type locality and horizon: Jebel Safra, exotic block JS11, *Rohillites omanensis* fauna.

Occurrence: A single specimen from sample JS11; *Rohillites omanensis* fauna.

Diagnosis: Evolute *Lucasites*.

Description: Evolute platycone shell with convex flanks that become slightly concave near venter. Venter broad and tabulate with angular shoulders. Umbilicus with inclined umbilical wall and rounded shoulders. Ornamentation of the flanks consists of faint sinuous folds and growth lines. Suture line not preserved.

Measurements: See appendix.

Prionitidae gen. indet.

Plate 20, figure 3a-b

Occurrence: A single poorly preserved specimen from sample HB901; *Anasibirites multiformis* fauna.

Description: Moderately involute, compressed shell with convex flanks. Venter tabulate with subangular shoulders. Umbilicus with inclined wall and rounded shoulders. Ornamentation consists of prorsiradiate, slightly sinuous undulations on the flanks and ribs on the venter. Suture line not preserved.

Discussion: This specimen differs from *Anasibirites* by the absence of the typical ornamentation and the by the undulating flanks. However, its poor preservation prevents any definitive determination.

Family Inyoitidae SPATH 1934

Genus *Inyoites* HYATT & SMITH 1905

Type species: *Inyoites oweni* HYATT & SMITH 1905

Inyoites oweni HYATT & SMITH 1905

Plate 21, figures 1-6

1905 *Inyoites oweni* HYATT & SMITH, p. 134, pl. 6, figs. 1-16, pl. 69, figs. 1-9, pl. 78, figs. 1-8.
1932 *Inyoites oweni* – SMITH, p. 80, pl. 6, figs. 1-16, pl. 40, figs. 1-8, pl. 69, figs. 1-9.
1934 *Inyoites oweni* – SPATH, p. 138, fig. 37.
1968 *Inyoites spicini* ZAKHAROV, p. 151, pl. 30, fig. 2.
1973 *Inyoites oweni* – COLLIGNON, p. 12, pl. 1, fig. 9.

Occurrence: Samples HB900, HB902, HB906, HB910, WM8; *Owenites koeneni* fauna.

Description: Moderately involute, compressed shell with convex flanks. Venter with a high keel and rounded shoulders. Umbilicus shallow with rounded shoulders. Ornamentation highly variable but very conspicuous consisting of radiate or rursiradiate ribs on the upper half of the flanks that pass into growth lines on lower flanks. A faint strigation is present on some specimens. Suture line ceratitic with rather deep and narrow lobes.

Measurements: Text-figures 27, 28.

Inyoites krystyni BRAYARD & BUCHER 2008

Plate 21, figure 7a-b

? 1959 *Subvishnuites tientungensis* CHAO, p. 210, pl. 7, figs. 17-18.
? 1959 *Subvishnuites* sp. undet. – CHAO, p. 210, pl. 44, figs. 9-10.
v 2008 *Inyoites krystyni* BRAYARD & BUCHER, p. 60, pl. 31, figs. 1-4; pl. 32, figs. 1-2; text-fig. 52.

Occurrence: A single specimen from sample JS12; *Owenites koeneni* fauna.

Description: Evolute, compressed shell with convex flanks. Venter with a high keel and rounded shoulders. Umbilicus shallow with rounded shoulders. Surface smooth except for very weak folds and a faint strigation.

Measurements: Text-figure 28.

Discussion: This species is considerably more evolute than *Inyoites oweni*. It also differs by its very weak ornamentation. In South China this species occurs in the upper part of the *Owenites koeneni* beds (BRAYARD & BUCHER 2008).

Inyoites sp. indet.

Plate 21, figure 8a-c

Occurrence: A single specimen from sample HB902; *Owenites koeneni* fauna.

Description: Like *Inyoites krystyni*, but ornamented with distinctly rursiradiate ribs.

Measurements: Text-figure 28.

Discussion: This specimen differs from other *Inyoites* by its distinctly rursiradiate ribs and may represent a new species. However, in the absence of sufficient material an open nomenclature is preferred here.

Genus *Subvishnuites* SPATH 1930

Type species: *Subvishnuites welteri*, SPATH 1930 (= *Vishnuites* spec. WELTER 1922).

Subvishnuites welteri SPATH 1930

Plate 21, figures 9-13

1922 *Vishnuites* sp. – WELTER, p. 137, pl. 167, fig. 3-5.
1930 *Subvishnuites welteri* SPATH, p. 30, p. 90.
1934 *Subvishnuites welteri* – SPATH, p. 117, fig. 31.
1959 *Subvishnuites welteri* – KUMMEL, p. 443, fig. 7.

Occurrence: HB904, HB905; *Owenites koeneni* fauna.

Description: Compressed, evolute shell. The convex flanks are subparallel on the inner half and converge strongly towards the venter on the external half. Venter narrowly rounded, almost acute. Umbilicus wide and shallow with a low, steep wall and rounded shoulders. Surface smooth or with weak folds.

Measurements: Text-figures 29, 30.

Discussion: *Subvishnuites stokesi* (KUMMEL & STEELE 1962) is similar but differs in being ribbed and by its deeper umbilicus. *S. welteri* from Timor occurs together with *Owenites egrediens*.

Subvishnuites sp. indet.

Plate 21, figure 14a-c

Occurrence: A single specimen from sample HB901; *Anasibirites multiformis* fauna.

Description: Moderately involute, compressed shell. Flanks convex; subparallel on the inner half and strongly converging on the external half. Venter narrowly rounded. Umbilicus with a vertical wall and rounded shoulders. The surface is ornamented with very weak ribs that cross the venter.

Measurements: Text-figure 30.

Discussion: *Subvishnuites welteri* and *S. stokesi* are slightly more evolute. Additionally, *S. welteri* has a shallower umbilicus. Our specimen may therefore represent a new species, but our material is too poor to erect a new species. More abundant and better preserved material of this species has recently been found also in the *Anasibirites* beds in Spiti (BRÜHWILER et al. ongoing work).

Family Lanceolitidae SPATH 1934

Genus *Lanceolites* HYATT & SMITH 1905

Type species: *Lanceolites compactus*, HYATT & SMITH 1905.

Lanceolites compactus HYATT & SMITH 1905

Plate 20, figures 4-6

1905 *Lanceolites compactus* HYATT & SMITH, p. 113, pl. 4: 4-10 ; pl. 5: 7-9; pl. 78: 9-11.
1932 *Lanceolites compactus* – SMITH, p. 90, pl. 4, figs. 4-10; pl. 5, figs. 7-9; pl. 21, figs. 21-23; pl. 28, figs. 17-20; pl. 40, figs. 9-11; pl. 60, fig. 10.
1962 *Lanceolites compactus* – KUMMEL & STEELE, p. 692, pl. 102: 6-9.
? 1979 *Lanceolites compactus* – NICHOLS & SILBERLING, pl. 2: 39-43
1995 *Lanceolites compactus* – SHEVYREV, p. 39, pl. 2, figs. 1-2
2008 *Lanceolites compactus* – BRAYARD & BUCHER, p. 61, pl. 30, fig. 5, text-fig. 53.

Occurrence: Samples JS4, JS12; *Owenites koeneni* fauna.

Description: Extremely involute (occluded umbilicus) platycone with slightly convex flanks. Venter tabulate or sulcate with angular shoulders. Surface smooth or ornamented with low folds. Suture line subammonitic with deeply indented, very broad lobes. Third lateral saddle divided, hardly perciptible; auxiliary series long.

Measurements: See appendix.

Lanceolites bicarinatus SMITH 1932

Plate 20, figure 7

1932 *Lanceolites bicarinatus* SMITH, p. 90, pl. 55: 1-13.
1959 *Lanceolites orientalis* CHAO, p. 263, pl. 41, figs. 5-9.
1984 *Lanceolites bicarinatus* – VU KHUC, p. 85, pl. 7: 2a-b, text-fig. H18.
1995 *Lanceolites bicarinatus* – SHEVYREV, p. 40, pl. 4, fig. 3.
2008 *Lanceolites bicarinatus* – BRAYARD & BUCHER, p. 62, pl. 30, fig. 6, text-fig. 53.

Occurrence: A single fragmentary specimen from sample HB900; *Owenites koeneni* fauna.

Description: Extremely involute (occluded umbilicus) platycone with slightly convex flanks. Venter narrow and bicarinate with angular shoulders. Surface smooth. Suture line as in *Lanceolites compactus*.

Discussion: This species differs from the type species by its narrower venter.

Family Melagathiceratidae TOZER 1971

Genus *Jinyaceras* BRAYARD & BUCHER 2008

Type species: *Jinyaceras bellum* BRAYARD & BUCHER 2008.

Jinyaceras cf. *bellum* BRAYARD & BUCHER 2008

Plate 2, figures 8-10

v, ? 2008 *Jinyaceras bellum* BRAYARD & BUCHER, p. 31, pl. 9, figs. 1-19.

Occurrence: Sample HB911; *Baidites hermanni* fauna.

Description: Small, moderately evolute, laterally compressed shell with flat, subparallel flanks. Venter broadly arched, subtabulate with rounded ventral shoulders. Umbilicus with vertical wall and subangular shoulders. Ornamentation consists of prorsiradiate constrictions that nearly disappear on venter. Suture line not preserved.

Measurements: Text-figure 31.

Discussion: Our specimens are very similar to *Jinyaceras bellum* from South China, but the scarcity of our material prevents any definitive specific assignment.

Genus *Juvenites* SMITH 1927

Type species: *Juvenites kraffti* SMITH 1927.

Juvenites spathi (FREBOLD 1930)

Plate 22, figures 12-17

1930 *Prosphingites spathi* FREBOLD, p. 20, pl. 4, figs. 2-3, 3a.
1934 *Prosphingites spathi* – SPATH, p. 195, pl. 13, figs. 1-2.
p, ? 1959 *Prosphingites kwangsianus* CHAO, p. 296, pl. 28, figs. 17-18
p, ? 1959 *Prosphingites sinensis* CHAO, p. 297, pl. 27, figs. 14-17, text-fig. 40a
? 1961 *Prosphingites spathi* TOZER, p. 58, pl. 13, figs. 1-2.
? 1982 *Prosphingites spathi* – KORCHINSKAYA, pl. 5, fig. 2.
? 1994 *Paranannites spathi* – TOZER, p. 77, pl. 36, figs. 1-2
v 2008 *Paranannites spathi* – BRAYARD & BUCHER, p. 63, pl. 35, figs. 10-19.
v submitted [a] *Paranannites spathi* – BRÜHWILER et al.

Occurrence: Samples SA1, JS13, Baid-B, HB912; *Nammalites pilatoides* fauna, *Owenites koeneni* fauna.

Description: Moderately involute, globose shell, with a curved venter forming a subtrigonal whorl section on adult specimens. The flanks are convex and strongly converge to the venter from the umbilical margin. The umbilicus is deep, the umbilical wall perpendicular, the shoulder rounded. Ornamentation consists of prorsiradiate constrictions and growth lines that cross the venter. Suture line with rather broad saddles. Indentations of lobes not preserved.

Measurements: Text-figures 32, 33.

Discussion: This species was assigned to *Paranannites* by TOZER (1994). However, typical *Paranannites* differ by being more involute, more compressed laterally and having smoother whorls. *Juvenites spathi* differs from other species of the genus by its triangular venter.

Juvenites cf. *thermarum* (SMITH 1927)

Plate 22, figures 1-9

	1927	*Thermalites thermarum* SMITH, p. 24, pl. 21, figs. 11-20.
	1932	*Prenkites depressus* SMITH, p. 110, pl. 31, figs. 16-18.
	1932	*Thermalites thermarum* – SMITH, p. 111, pl. 21, figs. 11-20.
	1962	*Juvenites thermarum* – KUMMEL & STEELE, p. 689, pl. 100, figs. 12-13.
?	1973	*Arnautoceltites thermarum* – COLLIGNON, p.17, pl. 4, fig. 10.
v	2007	*Paranannites* sp. indet. – KLUG et al., p. 1467, text-fig. 4A-E.

Occurrence: Samples HB900, HB902, HB904, WM7; *Owenites koeneni* fauna.

Description: Globose, involute conch, with broadly rounded venter and radial constrictions. Umbilical wall perpendicular, umbilical shoulder rounded. Body chamber one whorl in length. Ornamentation consists of prorsiradiate constrictions that cross the venter.

Measurements: Text-figures 33, 34.

Discussion: On some extremely well preserved specimens from Wadi Musjah organic remains of so-called "false color pattern" has been preserved (KLUG et al. 2007). *Juvenites spathi* differs from this species by its triangular venter and a higher, more angular ventral shoulder. However, small specimens are not distinguishable.

Juvenites procurvus BRAYARD & BUCHER 2008

Plate 22, figures 10-11

v	2008	*Juvenites procurvus* BRAYARD & BUCHER, p. 32, pl. 22, figs. 6-12, text-fig. 30.

Occurrence: Two specimens from samples JS2 and JS12; *Owenites koeneni* fauna.

Description: Small, subglobose and moderately involute shell with rounded venter and convex flanks. Umbilicus with vertical wall and rounded shoulders. Ornamentation consists of numerous, strong and projected constrictions. Suture line not preserved.

Measurements: Text-figure 33.

Discussion: This species is similar to *Juvenites* cf. *thermarum* but differs by its much stronger and more closely spaced constrictions.

Familiy Paranannitidae SPATH 1930

Genus *Paranannites* HYATT & SMITH 1905

Type species: *Paranannites aspenensis* HYATT & SMITH 1905.

Paranannites baudi n. sp.

Plate 23, figures 1-10

Etymology: Named after Aymon Baud (Lausanne).

Holotype: PIMUZ 27462 (plate 23, figure 1a-c).

Type locality and horizon: Exotic block SA3, Jebel Safra, *Rohillites omanensis* fauna.

Occurrence: Samples SA3, JS6, JS11; *Rohillites omanensis* fauna.

Diagnosis: Very involute *Paranannites* without constrictions both on outer shell and inner mold.

Description: Relatively large, very involute shell with rounded venter. Subglobose on inner whorls, becoming slightly compressed on outer whorls. Flanks convex and converging; maximal thickness at umbilical margin. Umbilicus small and very deep with an overhanging wall and marked, only slightly rounded shoulders. Ornamentation consists of very fine prorsiradiate plications that cross the venter. Suture line not preserved.

Measurements: Text-figures 33, 35.

Discussion: This species is very similar to *Paranannites ovum* BRAYARD & BUCHER 2008, which is more evolute at all growth stages and displays egressive coiling at maturity. The type species *P. aspenensis* is more compressed laterally.

Genus *Omanites* n. gen.

Etymology: Named after the Sultanate of Oman.

Type species: *Omanites musjahensis* n. gen. et sp.

Composition: Type species only.

Diagnosis: Evolute, smooth Paranannitidae with rounded venter.

Discussion: This genus is similar to *Paranannites*, from which it differs essentially its by greater evolution.

Omanites musjahensis n. gen. et sp.

Plate 23, figure 11a-d; plate 24, figures 1-4

Etymology: Named after the type locality Wadi Musjah.

Holotype: PIMUZ 27475 (plate 24, figure 3a-d).

Type locality and horizon: Wadi Musjah, Sample HB910, *Owenites koeneni* fauna.

Occurrence: Samples HB910, WM8; *Owenites koeneni* fauna.

Diagnosis: As for the genus.

Description: Relatively large, evolute shell with a subglobose shape. Venter rounded without shoulders. Umbilicus deep with slightly overhanging wall and marked but rounded shoulder. Surface smooth except for fine radial lirae. Suture ceratitic and simple with a broad first lateral saddle.

Measurements: Text-figures 33, 36.

Discussion: This species is similar to *Paranannites ovum* BRAYARD & BUCHER 2008 and *Paranannites baudi* n. sp., but differs by being much more evolute. It differs from *Juvenites* cf. *thermarum* by larger size, thinner whorls, more evolute coiling and the absence of constrictions. Conch shape shows some convergence with the late Spathian procarnitid *Neopopanoceras haugi*.

Genus *Owenites* HYATT & SMITH 1905

Type species: *Owenites koeneni* HYATT & SMITH 1905, p. 83, pl. 10, figs. 1-22

Owenites koeneni HYATT & SMITH 1905

Plate 25, figures 1-6

1905 *Owenites koeneni* HYATT & SMITH, p. 83, pl. 10, figs. 1-22.
1932 *Owenites koeneni* – SMITH, pl. 10, figs. 1-22.
1932 *Owenites egrediens* – SMITH, p. 100, pl. 52, figs. 6-8.
1932 *Owenites zitteli* SMITH, p. 101, pl. 52, figs. 1-5.
1934 *Owenites koeneni* – SPATH, p. 185, figs. 57a-c.
1947 *Owenites* aff. *egrediens* – KIPARISOVA, p. 139, pl. 32, figs. 1-3.
1955 *Kingites shimizuii* SAKAGAMI, p. 138, pl. 2, fig. 2.
1957 *Owenites koeneni* – KUMMEL, pL138, figs. 171-8a-b.
1959 *Owenites costatus* CHAO, p. 249, pl. 22, figs. 7-18, 22, 23, text-fig. 26c.
1959 *Owenites pakungensis* CHAO, p. 248, pl. 21, figs. 6-8.
1959 *Owenites pakungensis* var. *compressus* CHAO, p. 248, pl. 21, figs. 4,5, text-fig. 26a.
1959 *Pseudowenites oxynotus* CHAO, p. 252, pl. 23, figs. 1-16, text-figs. 27a-d.
? 1959 *Owenites* cf. *koeneni* – KUMMEL, p. 441, figs. 2-4.
1959 *Owenites shimizui* – KUMMEL, p. 430.
1960 *Owenites shimizui* – KUMMEL & SAKAGAMI, p. 6, pl. 5, figs. 5-6.
1962 *Owenites koeneni* – KUMMEL & STEELE, p. 674, pl. 101, figs. 3-7.
1962 *Owenites koeneni* – POPOV, p. 44, pl. 6, fig. 6.
1965 *Owenites koeneni* – KUENZI, p. 374, pl. 53, figs. 1-6, text-figs. 3d,6.
1966 *Owenites koeneni* – HADA, p. 112, pl. 4, figs. 2-4.

1968 *Owenites koeneni* – KUMMEL & ERBEN, p. 121, fig. 12, pl. 19, figs. 10-15.
1968 *Owenites carinatus* SHEVYREV, p. 189, pl. 16, fig. 1.
1968 *Owenites koeneni* – ZAKHAROV, p. 94, pl. 18, figs. 1-3.
1973 *Owenites koeneni* – COLLIGNON, p. 139, pl. 4, figs. 2-3.
1979 *Owenites koeneni* – NICHOLS & SILBERLING, pl. 1, figs. 17, 18.
1981 *Owenites koeneni* – BANDO, p. 158, pl. 17, fig. 7.
1984 *Owenites carinatus* – VU KHUC, p. 81, pl. 6, figs. 1-4.
1984 *Pseudowenites oxynotus* – VU KHUC, p. 82, pl. 7, figs. 3, 4.
1990 *Owenites koeneni* – SHEVYREV, p. 118, pl. 1, fig. 5.
1995 *Owenites koeneni* – SHEVYREV, p. 51, pl. 5, figs. 1-3.
2004 *Owenites pakungensis* – TONG et al., p. 199, pl. 2, figs. 9-10, text-fig. 7.
v 2008 *Owenites koeneni* – BRAYARD& BUCHER, p. 67, pl. 36, figs. 1-8.
v submitted [a] *Owenites koenen* – BRÜHWILER et al.

Occurrence: Samples HB 904, HB 912, Baid B, JS4, JS 8; *Owenites koeneni* fauna.

Description: Involute, somewhat compressed shell with an inflated, lenticular whorl section. Umbilical inclined wall so that the umbilical seam is hardly perceptible and the umbilicus becomes cone-shaped. Coiling strongly egressive. Venter narrowly rounded to acute. Surface generally smooth, weak concave folds may be present. Suture line ceratitic with several divided umbilical lobes.

Measurements: Text-figures 37, 38.

Owenites carpenteri SMITH 1932

Plate 25, figures 7-8

1932 *Owenites carpenteri* SMITH, p. 100, pl. 54, figs. 31-34.
1966 *Owenites carpenteri* – HADA, p. 112, pl. 4, figs. 1a-e
1968 *Owenites costatus* KUMMEL & ERBEN, p. 122, fig. 121
1973 *Owenites carpenteri* – COLLIGNON, p. 139, pl. 4, figs. 5-6.
v 2008 *Owenites carpenteri* – BRAYARD & BUCHER, p. 70, pl. 43, figs. 15-16.
v in prep *Owenites carpenteri* – BRÜHWILER et al.

Occurrence: Sample HB904; *Owenites koeneni* fauna.

Description: Small, extremely involute, oxyconic shell. Venter subangular. Umbilicus occluded, umbilical region inflated. Shell surface smooth. Distant and deep constrictions on internal mould. Suture line not preserved.

Measurements: Text-figures 38, 39.

Discussion: As shown by new material from Spiti (BRÜHWILER et al., ongoing work) constrictions may become closely spaced on outer whorls. If the shell is not preserved this gives the impression of an ornamentation consisting of "strong bundled radial ribs" as described on the holotype by SMITH (1932). Since the holotype is preserved as an internal mould it is not observable if it exhibits the same inflation of the umbilical region as our specimens. It seems, however, to have a less angular venter.

Owenites simplex WELTER 1922

Plate 24, figures 10-14

1922 *Owenites simplex* WELTER, p. 153, pl. 15, figs. 1-8.
1934 *Parowenites simplex* – SPATH, p. 187, fig. 58.
1959 *Owenites kwangsiensis* CHAO, p. 250, pl. 22, figs. 1-6, text-fig. 26b.
1959 *Owenites plicatus* CHAO, p. 251, pl. 22, figs. 19-21, 24, 25, text-fig. 26e.
1968b *Owenites simplex* – KUMMEL, p. 2, pl. 1, figs. 1-9.
1968 *Owenites simplex* – KUMMEL & ERBEN, p. 122, figs. 12k, n, o.
v 2008 *Owenites simplex* – BRAYARD & BUCHER, p. 69, pl. 35, figs. 20-22; text-fig. 59.
v submitted [a] *Owenites simplex* – BRÜHWILER et al.

Occurrence: Sample JS13; *Nammalites pilatoides* fauna.

Description: Small, moderately involute, compressed shell with subparallel flanks. Venter narrowly rounded. Umbilicus deep with perpendicular wall and angular shoulder. Ornamentation consists of prosiradiate, slighlty concave folds. Suture line not preserved.

Measurements: Text-figures 38, 40.

Owenites sp. indet.

Plate 24, figures 5-9

Occurrence: Sample JS13; *Nammalites pilatoides* fauna.

Description: Involute, compressed shell with subparallel flanks and eggressive coiling. Venter narrowly rounded. The umbilicus is moderately deep, with a perpendicular wall and a marked shoulder. The ornamentation consists of marked prosiradiate ribs. Suture line apparently goniatitic with several divided umilical lobes.

Measurements: Text-figures 38, 41.

Discussion: *Owenites* sp. indet. differs from *Owenites simplex* by its more involute and eggressive coiling and slightly higher whorls.

Superfamily Sageceratacea HYATT 1884

Family Hedenstroemiidae WAAGEN 1895

Pseudosageceras DIENER 1895

Type species: *Pseudosageceras* sp. indet. - DIENER 1895

Pseudosageceras multilobatum NOETLING 1905.

Plate 26, figure 4

1905 *Pseudosageceras multilobatum* NOETLING, pl. 25, fig. 1, pl. 26, fig. 3.
1905 *Pseudosageceras intermontanum* - HYATT & SMITH, p. 99, pl. 4, figs. 1-3; pl. 5, figs. 1-6; pl. 63, figs. 1-2.
1909 *Pseudosageceras multilobatum* - KRAFFT & DIENER, p. 145, pl. 21, fig. 5.
1911 *Pseudosageceras multilobatum* - WANNER, p. 181, pl. 7, fig. 4
1911 *Pseudosageceras drinense* - ARTHABER, p. 201, pl. 17, figs. 6, 7
1922 *Pseudosageceras multilobatum* - WELTER, p. 94, fig. 3
1929 *Pseudosageceras intermontanum* - MATTHEWS, p. 3, pl. 1, figs. 18-22
1932 *Pseudosageceras multilobatum* - SMITH, p. 87-89, pl. 4, figs. 1-3; pl. 5, figs. 1-6; pl. 25, figs. 7-16; pl. 60, fig. 32; pl. 63, figs. 1-6
1933-34 *Pseudosageceras multilobatum* - COLLIGNON, p. 56-58, pl. 11, fig. 2
1934 *Pseudosageceras multilobatum* - SPATH, p. 54, fig. 6a.
1947 *Pseudosageceras multilobatum* - KIPARISOVA, p. 127, pl. 25, figs. 3-4
1947 *Pseudosageceras multilobatum* var. *giganteum* - KIPARISOVA, p. 127, pl. 26, figs. 2-5
1948 *Pseudosageceras* cf. *clavisellatum* - RENZ & RENZ, p. 90, pl. 16, fig. 3
1948 *Pseudosageceras drinense* - RENZ & RENZ, p. 92, pl. 16, fig. 6
1948 *Pseudosageceras intermontanum* - RENZ & RENZ, p. 90, pl. 16, figs. 4, 7
1959 *Pseudosageceras multilobatum* - CHAO, p. 183, pl. 1, figs. 9, 12
1959 *Pseudosageceras tsotengense* - CHAO, p. 184, pl. 1, figs. 7, 8, text-fig. 5b
1959 *Pseudosageceras curvatum* - CHAO, p. 185, pl. 1, figs. 13, 14, text-fig. 5a
? 1959 *Pseudosageceras multilobatum* var. nov. - JEANNET, p. 30, pl. 6, fig. 1
1961 *Pseudosageceras schamarense* - KIPARISOVA, p. 31, pl. 7, fig. 3.
1961 *Pseudosageceras multilobatum* var. *gigantea* - POPOV, p. 13, pl. 2, figs. 1-2

non 1962 *Pseudosageceras multilobatum* - KUMMEL & STEELE, p. 701, pl. 102, figs. 1-2
? 1966 *Pseudosageceras multilobatum* - HADA, p. 112, pl. 4, fig. 6
? 1968 *Pseudosageceras multilobatum* - KUMMEL & ERBEN, p. 112, pl. 19, fig. 9
1968 *Pseudosageceras multilobatum* - SHEVYREV, p. 791, pl. 1, figs. 1-2
? 1973 *Pseudosageceras multilobatum* - COLLIGNON, p. 5, pl. 1, fig. 1
? 1978 *Pseudosageceras multilobatum* - WEITSCHAT & LEHMANN, p. 95, pl. 10, figs. 2a-b
1984 *Pseudosageceras multilobatum* - VU KHUC, p. 26, pl. 1, fig. 1
1994 *Pseudosageceras multilobatum* - TOZER, p. 83, pl. 18, figs. 1a-b; p. 384, fig. 17
2008 *Pseudosageceras multilobatum* – BRAYARD & BUCHER, p. 70, pl. 37, figs. 1-5.
v submitted [a] *Pseudosageceras multilobatum* – BRÜHWILER et al.

Occurrence: Samples SA1, SA3, Baid-B; *Rohillites omanensis* fauna, ?*Nammalites pilatoides* fauna, *Owenites koeneni* fauna.

Description: Oxycone, very involute shell (occluded umbilicus) with extremely narrow, bicarinate venter. Suture line complex with several adventitious lobes. Main lateral lobe trifid, others bifid.

Measurements: See appendix.

Family Aspenitidae SPATH, 1934

Aspenites HYATT & SMITH 1905

Type species: *Aspenites acutus* HYATT & SMITH 1905.

Aspenites acutus HYATT & SMITH 1905

Plate 26, figures 1-2

1905 *Aspenites acutus* HYATT & SMITH, 1905, p. 96, pl. 2, figs. 9-13; pl. 3, figs. 1-5.
? 1909 *Hedenstroemia acuta* KRAFFT & DIENER, p. 157, pl. 9, fig. 2.
1922 *Aspenites acutus* WELTER, p. 98, fig. 7.
1922 *Aspenites laevis* WELTER, p. 99, pl. 1, figs. 4-5.
1932 *Aspenites acutus* – SMITH, p. 86, pl. 2, figs. 9-13, pl. 3, figs. 1-5, pl. 30, figs. 1-26, pl. 60, figs. 4-6.
1932 *Aspenites laevis* – SMITH, p. 86, pl. 28, figs. 28-33.
1932 *Aspenites obtusus* SMITH, p. 86, pl. 31, figs. 8-10.
1934 *Aspenites acutus* – SPATH, p. 229, fig. 76.

? 1934 *Parahedenstroemia acuta* – SPATH, p. 221, fig. 70.

1957 *Aspenites acutus* – KUMMEL, p. L142, fig. 173a-c.

1959 *Aspenites acutus* – CHAO, p. 269, pl. 35, figs. 12-18, 23, text-fig. 34a.

1959 *Aspenites laevis* – CHAO, p. 270, pl. 35, figs. 9-11, text-fig. 34b.

1962 *Aspenites acutus* – KUMMEL & STEELE, p. 692, pl. 99, figs. 16-17.

1962 *Hemiaspenites obtusus* – KUMMEL & STEELE, p. 666, pl. 99, fig. 18.

1979 *Aspenites* cf. *acutus* – NICHOLS & SILBERLING, pl. 1, figs. 10-11.

1979 *Aspenites acutus* – NICHOLS & SILBERLING, pl. 1, figs. 12-14.

v 2008 *Aspenites acutus* – BRAYARD & BUCHER, p. 77, pl. 42, figs. 1-9.

v in prep *Aspenites acutus* – BRÜHWILER et al.

Occurrence: Samples SA1, SA3, JS11, JS13, Baid-B; *Rohillites omanensis* fauna, *Nammalites pilatoides* fauna, *Owenites koeneni* fauna.

Description: Extremely involute, very compressed shell with slightly convex flanks. Maximum thickness at mid-flank. Venter with an acute keel. Umbilicus occluded, umbilical region slightly depressed. Surface nearly smooth except for fine radial folds and falcoid growth lines. Suture line not preserved.

Measurements: Text-figure 42.

Discussion: Specimens from Oman seem to be slightly more slender than the type material, have a higher keel and a more pronounced ventrolateral shoulder.

Genus *Pseudaspenites* SPATH, 1934

Type species: *Aspenites layeriformis* Welter, 1922, p. 97, pl. 1, figs. 6-8

Pseudaspenites layeriformis (WELTER 1922)

Plate 26, figure 3a-b

p 1922 *Aspenites layeriformis* WELTER, p. 97, pl. 1, figs. 6-7 only (fig. 8 = ? *Aspenites acutus*).

1934 *Pseudaspenites layeriformis* – SPATH, p. 230, fig. 77.

1959 *Inyoites striatus* CHAO, p. 197, pl. 2, figs.22-26.

1959 *Inyoites obliqueplicatus* CHAO, p. 198, pl. 2, figs.7, 17-21, 27.

v 2008 *Pseudaspenites layeriformis* – BRAYARD & BUCHER, p. 79, pl. 43, figs. 1-6.

Occurrence: Samples JS11, SA1; *Rohillites omanensis* fauna, ?*Nammalites pilatoides* fauna.

Description: Involute, very compressed oxycone similar to *Aspenites,* but with an open umbilicus. Venter acutely keeled and slightly convex flanks. Umbilicus with slightly angular shoulders. Ornamentation consists of fine, forward projecting folds that are more pronounced near the umbilicus. Suture line not preserved.

Discussion: Timor: with *Owenites*; China: *Flemingites* Beds, Spiti: lowermost "*Parahedenstroemia*" (=*Owenites*) Beds (?).

Superfamily Dinaritaceae MOJSISOVICS 1882

Family Columbitidae SPATH 1934

Genus *Procolumbites* ASTACHOVA 1960

Type species: *Procolumbites karataucikus* ASTACHOVA 1960.

Procolumbites safraensis n. sp.

Plate 19, figures 7-8

Etymology: Named after the type locality Jebel Safra.

Holotype: Specimen PIMUZ 27424 (plate 19, fig. 7a-c).

Type locality and horizon: Exotic block SA4, Jebel Safra.

Occurrence: Two specimens from sample SA4-D, associated with conodonts of late early or mid Spathian age (presence of genera *Cratognathus*, *Gladigondolella*, *Flatella*, *Spathicuspus*, and *Triassospathodus*; in particular the presence of *Triassospathodus homeri* indicates that this horizon correlates with the *Procolumbites* beds in South China or with younger strata).

Diagnosis: Strongly ornamented *Procolumbites*.

Description: Moderately evolute shell with convex flanks. Venter broadly rounded with rounded shoulders. Umbilicus deep with vertical wall and rounded shoulders. Ornamentation very conspicuous consisting of strong ribs on inner flanks fading out near mid-flanks. Some ribs at more or less periodical intervals are stronger with a tendency to form umbilical nodes. Venter apparently smooth, with exception of projected constrictions. Suture line simple and ceratitic; incompletely preserved.

Measurements: See appendix.

Discussion: More densely and heavily ribbed than any other representative of *Procolumbites*.

Order Phylloceratida ZITTEL 1884

Superfamily Ussuritaceae HYATT 1900

Family Palaeophyllitidae POPOV, in LUPPOV & DRUSHCHITS 1958

Genus *Goudemandites* n. gen.

Etymology: Named after Nicolas Goudemand (Zürich).

Type species: *Goudemandites sinensis* n. gen. et sp.

Composition of the genus: Type species only.

Diagnosis: Moderately evolute Palaeophyllitidae with circular venter, ornamented with radial plications and lirae.

Discussion: This new genus is erected based on a specimen that has been described from the middle Smithian *Owenites koeneni* beds from South China as ?Palaeophyllitidae gen. indet. by BRAYARD & BUCHER (2008). Our finding of a single conspecific specimen from an age-equivalent fauna from Wadi Musjah leads us to establish a new genus. As already stated by BRAYARD & BUCHER (2008) the morphology and uncommon ornamentation of *Goudemandites* is similar to some Spathian Palaeophyllitidae. The assignment to this family remains, however, tentative.

Goudemandites sinensis n. sp.

Plate 26, figure 5a-c

v 2008 ?Palaeophyllitidae gen. indet. – BRAYARD & BUCHER, p. 85, pl. 7, fig. 7a-d.

Etymology: Named after China, where this species was first described from.

Holotype: PIMUZ 25867 (BRAYARD & BUCHER 2008, p. 85, pl. 7, fig. 7a-d).

Type locality and horizon: Loc. Jin47, Jinya, Guangxi, South China; *Owenites koeneni* beds.

Occurrence: A single specimen from sample HB904; *Owenites koeneni* fauna.

Diagnosis: As for the genus.

Description: Moderately evolute, slightly compressed shell with convex, convergent flanks. Venter circular with rounded shoulders. Umbilicus relatively deep with vertical wall and rounded shoulders. Ornamentation very conspicuous, consisting of rursiradiate, slightly biconcave plications and lirae that do not cross the venter. Suture line not preserved on the specimen from Oman; ceratitic with slightly phylloid saddles and broad lobes on the Chinese specimen.

Discussion: This new specimen suggests again that the oldest palaeophyllitids may occur as early as the middle Smithian, provided that it does not represent a remarkable convergence with the classic palaeophyllitids of middle Spathian age.

Acknowledgements

Technical support for preparation was provided by Markus Hebeisen, Julia Huber and Leonie Pauli (all Zürich). Photographs were taken by Rosemarie Roth (Zürich). Claude Monnet (Zürich) is thanked for providing his statistical analysis software. This work is a contribution to the Swiss National Science Foundation project 200020-113554 (to HB).

References

ARTHABER, G. (1911): Die Trias von Albanien. - Beiträge zur Paläontologie und Geologie Österreich-Ungarns und des Orients, **24**: 169-288.

ASTACHOVA, T.V. (1960): Novye vidy drevnikh rastenii i bespozvonochnykh SSR. Chast' 2. Novye Rannetriasovye tseratity Mangyshlaka. Vsesoiuznyi Nauchno-issledovatel'skii Geologichiskii Institut (VSEGEI). (New species of fossil plants and invertebrates of the USSR pt. 2, New Lower Triassic ammonites of Mangyshlak.) All Union Scientific Geological Research Institute, 139-159.

BANDO, Y. (1964): The Triassic Stratigraphy and Ammonite Fauna of Japan. - The Scientific Reports of the Tohoku University, Sendai, Japan - Second Series (Geology), **36**: 1-137.

BANDO, Y. (1981): Lower Triassic ammonoids from Guryul Ravine and the spur three kilometers north of Barus. In: Nakazawa, K & Kapoor, H.M. (Editors): The Upper Permian and Lower Triassic fossils of Kashmir. - Palaeontologia Indica n. ser., **46**: 135-178.

BASSOULET, J.-P., COLCHEN, M., GUEX, J.L., M., MARCOUX, J. & MASCLE, G. (1978): Permien terminal néritique, Scythien pélagique et volcanisme sousmarine, indices de processus tectono-sédimentaires distensifs à la limite Permien-Trias dans un bloc exotique de la suture de l'Indus (Himalaya du Ladakh). - Comptes Rendus de l'Académie des Sciences Paris, **287**: 675-678.

BAUD, A., BÉCHENNEC, F., CORDEY, F., KRYSTYN, L., LE MÉTOUR, J., MARCOUX, J., MAURY, R., AND RICHOZ, S. (2001): Permo-Triassic Deposits: from the Platform to the Basin and Seamounts, Conference on the Geology of Oman, Field guidebook, Volume Excursion A01: Muscat, Oman, 54 pp.

BECHENNEC, F. (1988): Geologie des Nappes Hawasina dans les parties orientale et centrale des montagnes d'Oman. Documents - B.R.G.M., 127. Bureau de Recherches Geologiques et Minieres, (BRGM), Paris, France, 474 pp.

BLECHSCHMIDT, I., DUMITRICA, P., MATTER, A., KRYSTYN, L. & PETERS, T. (2004): Stratigraphic architecture of the northern Oman continental margin; Mesozoic Hamrat Duru Group, Hawasina Complex, Oman. - GeoArabia (Manama), **9**: 81-132.

BLENDINGER, W. (1991): Upper Triassic (Norian) Cephalopod Limestones of the Hallstatt-Type, Oman. - Sedimentology, **38**: 223-242.

BLENDINGER, W. (1995): Lower Triassic to Lower Jurassic cephalopod limestones of the Oman Mountains. - Neues Jahrbuch für Geologie und Palaeontologie. Monatshefte, 1995 (10): 577-593.

BLENDINGER, W., FURNISH, W.M. & GLENISTER, B.F. (1992): Permian cephalopod limestones, Oman Mountains; evidence for a Permian seaway along the northern margin of Gondwana. - Palaeogeography, Palaeoclimatology, Palaeoecology, **93**: 13-20.

BRAYARD, A., BRÜHWILER, T., BUCHER, H. & JENKS, J. (2009): *Guodunites* - a low-palaeolatitude and trans-panthalassic Smithian (Early Triassic) ammonoid genus. - Palaeontology, **52**: 471-481.

BRAYARD, A. & BUCHER, H. (2008): Smithian (Early Triassic) ammonoid faunas from northwestern Guangxi (South China): taxonomy and biochronology. - Fossils and Strata, **55**: 1-179.

BRAYARD, A., BUCHER, H., BRÜHWILER, T., GALFETTI, T., GOUDEMAND, N., GUODUN, K., ESCARGUEL, G. & JENKS, J. (2007a): *Proharpoceras* Chao: a new ammonoid lineage surviving the end-Permian mass extinction. - Lethaia, **40**: 175-181.

BRAYARD, A., BUCHER, H., ESCARGUEL, G., FLUTEAU, F., BOURQUIN, S. & GALFETTI, T. (2006): The Early Triassic ammonoid recovery: Paleoclimatic significance of diversity gradients. - Palaeogeography, Palaeoclimatology, Palaeoecology, **239**: 374-395.

BRAYARD, A., ESCARGUEL, G. & BUCHER, H. (2007b): The biogeography of early Triassic ammonoid faunas: Clusters, gradients, and networks. - Geobios, **40**: 749-765.

BRAYARD, A., ESCARGUEL, G., BUCHER, H. & BRÜHWILER, T. (in press): Smithian and Spathian (Early Triassic) ammonoid assemblages from terranes: Paleoceanographic and paleogeographic implications. - Journal of Asian Earth Sciences.

BRAYARD, A., ESCARGUEL, G., BUCHER, H., BRÜHWILER, H. & GOUDEMAND, N. (2008): Integrated Regional Diversity Analysis of the Early Triassic Ammonoid Recovery. - Geological Society of America, Houston. Paper No. 267-8.

BRÜHWILER, T., BUCHER, H. & GOUDEMAND, N. (submitted [a]): Smithian (Early Triassic) ammonoids from Tulong, South Tibet. - Geobios.

BRÜHWILER, T., BUCHER, H., GOUDEMAND, N. & BRAYARD, A. (2007): Smithian (Early Triassic) ammonoid faunas of the Tethys: new preliminary results from Tibet, India, Pakistan and Oman. - New Mexico Museum of Natural History and Science Bulletin, **41**: 25-26.

BRÜHWILER, T., GOUDEMAND, N., GALFETTI, T., BUCHER, H., BAUD, A., WARE, D., HERMANN, E., HOCHULI, P.A. & MARTINI, R. (submitted [b]): First complete and detailed documentation of the Early Triassic sedimentary and carbon isotope records from Tulong (South Tibet) and their significance for Tethyan palaeoceanography. - Sedimentary Geology.

CHAO, K. (1950): Some new ammonite genera of Lower Triassic from western Kwangsi. - Palaeontological Novitates, **5**: 1-11.

CHAO, K. (1959): Lower Triassic ammonoids from Western Kwangsi, China. - Palaeontologia Sinica. New Series B, **9**: 355 pp.

COLLIGNON, M. (1933-1934): Paléontologie de Madagascar XX - Les céphalopodes du Trias inférieur. - Annales de Paléontologie **12-13**: 151-162 & 1-43.

COLLIGNON, M. (1973): Ammonites du Trias inférieur et moyen d'Afghanistan. - Annales de Paléontologie (Invertebrés), **59**: 127-163.

DAGYS, A.S. & ERMAKOVA, S.P. (1990): Early Olenekian Ammonoids of Siberia. - Nauka, Moscow, 112 pp.

DE KONINCK, L.G. (1863): Description of some fossils from India, discovered by Dr. A. Fleming, of Edingburgh. - The quarterly Journal of the Geological Society of London, **19**: 1-19.

DIENER, C. (1895): Triadische Cephalopodenfaunen der ostsibirischen Küstenprovinz. - Mémoirs du Comité Géologique St. Petersburg, **14**: 1-59.

DIENER, C. (1897): The Cephalopoda of the Lower Trias. - Palaeontologia Indica, ser. 15, Himalayan Fossils, **2**: 1-181.

DIENER, C. (1913): Triassic faunae of Kashmir. - Palaeontologia Indica, n. ser., **5**: 1-133.

ERMAKOVA, S.P. (2002): Zonal standard of the Boreal Lower Triassic. Nauka, Moscow, 109 pp.

FREBOLD, H. (1930): Die Altersstellung des Fischhorizontes, des Grippianniveaus und des unteren Saurierhorizontes in Spitzbergen. - Scrifter om Svalbard og Ishavet, **28**: 1-36.

FRECH, F. (1902): Die Dyas: Lethaea Geognostica, Theil I. - Lethaea Palaeozoica, **2**: 579-788.

GALFETTI, T., BUCHER, H., BRAYARD, A., HOCHULI, P.A., WEISSERT, H., GUODUN, K., ATUDOREI, V. & GUEX, J. (2007a): Late Early Triassic climate change: Insights from carbonate carbon isotopes, sedimentary evolution and ammonoid paleobiogeography. - Palaeogeography, Palaeoclimatology, Palaeoecology, **243**: 394-411.

GALFETTI, T., BUCHER, H., OVTCHAROVA, M., SCHALTEGGER, U., BRAYARD, A., BRÜHWILER, T., GOUDEMAND, N., WEISSERT, H., HOCHULI, P.A., CORDEY, F. & GUODUN, K.A. (2007b): Timing of the Early Triassic carbon cycle perturbations inferred from new U-Pb ages and ammonoid biochronozones. - Earth and Planetary Science Letters, **258**: 593-604.

GALFETTI, T., HOCHULI, P.A., BRAYARD, A., BUCHER, H., WEISSERT, H. & VIGRAN, J.O. (2007c): Smithian-Spathian boundary event: Evidence for global climatic change in the wake of the end-Permian biotic crisis. - Geology, **35**: 291-294.

GLENNIE, K.W., BOEUF, M.G.A., HUGHES CLARKE, M.W., MOODY STUART, M., PILAAR, W.H.F. & REINHARDT, B.M. (1974): Geology of the Oman Mountains. - Verh. koninkl. Nederlands geol. mijnbouwk. Genootschap, **31**: 1-423.

GUEX, J. (1978): Le Trias inferieur des Salt Ranges, Pakistan; problemes biochronologiques. - Eclogae Geologicae Helvetiae, **71**: 105-141.

HADA, S. (1966): Discovery of Early Triassic ammonoids from Gua Musang, Kelantan, Malaya. - Journal of Geosciences, Osaka University, **9**: 111-121.

HERMANN, E., HOCHULI, P.A., BUCHER, H., BRÜHWILER, T., GOUDEMAND, N. & ROGHI, G. (2008): Major Climatic Change at the Smithian/Spathian Boundary - Evidence from Low Palaeolatitudinal Records. - Geological Society of America, Houston. Paper No. 318-1.

HYATT (1884): Genera of fossil cephalopods. - Proceedings of the Boston Society of Natural History, **22**: 253-338.

HYATT, A. (1879): In: WHITE, C.A. (1879): Paleontological papers no. 9: fossils from the Jura-Trias of south-eastern Idaho. - U. S. Geological and Geographical Survey of the Territories Bulletin, **5**: 105-117.

HYATT, A., 1900. Cephalopoda. In: ZITTEL K.A.v. (Editor): Textbook of palaeontology, vol. 1, 1st English ed. - Eastman, C. R. London.

HYATT, A. & SMITH, J.P. (1905): Triassic cephalopod genera of America. - U. S. Geological Survey Professional Paper, **40**: 1-394.

JEANNET, A. (1959): Ammonites Permiennes et faunes Triasiques de l'Himalaya Central (Expedition Suisse A. Heim et A. Gansser, 1936). - Palaeontologia Indica, n. ser., **34**.

KIPARISOVA, L.D. (1947): Atlas of the guide forms of the fossil faunas of the USSR 7, Triassic. - All Union Scientific Geological Research Institute (VSEGEI), Leningrad.

KIPARISOVA, L.D. (1956): Materials on paleontology, new families and genera. - Transactions of the All Union Scientific Research Geological Institute (VSEGEI), n. ser., **12,** Paleontology: 76-79.

KIPARISOVA, L.D. (1961): Palaeontological fundamentals for the stratigraphy of Triassic deposits of the Primor'ye region, I, Cephalopod Mollusca. - Transactions of the All Union Scientific Research Geological Institute (VSEGEI), n. ser., **48**.

KIPARISOVA, L.D. & POPOV, Y.D. (1956): Subdivision of the lower series of the Triassic System into stages. - Doklady Akad. Nauk SSSR, **109**: 842-845.

KLUG, C., BRÜHWILER, T., KORN, D., SCHWEIGERT, G., BRAYARD, A. & TILSLEY, J. (2007): Ammonoid shell structures of primary organic composition. - Palaeontology, **50**: 1463-1478.

KORCHINSKAYA, M.V. (1982): Explanatory note on the biostratigraphic scheme of the Mesozoic (Trias) of Spitsbergen. - USSR Ministry of Geology, PGO Sevmorgeologia: 40-99.

KRAFFT, A.V. & DIENER, C. (1909): Lower Triassic cephalopoda from Spiti, Malla Johar, and Byans. - Palaeontologia Indica, ser. 15, **6**: 1-186.

KRYSTYN, L., BHARGAVA, O.N. & RICHOZ, S., (2007a): A candidate GSSP for the base of the Olenekian Stage: Mud at Pin Valley; district Lahul & Spiti, Himachal Pradesh (Western Himalaya), India. - Albertiana, **35**, 5-29.

KRYSTYN, L., RICHOZ, S., BAUD, A. & TWITCHETT, R.J. (2003): A unique Permian-Triassic boundary section from the Neotethyan Hawasina Basin, Central Oman Mountains. - Palaeogeography Palaeoclimatology Palaeoecology, **191**: 329-344.

KRYSTYN, L., RICHOZ, S. & BHARGAVA, O.N. (2007b): The Induan-Olenekian Boundary (IOB) in Mud - an update of the candidate GSSP section M04. - Albertiana, **36**: 33-45.

KUENZI, W.D. (1965): Early Triassic (Scythian) ammonoids from northeastern Washington. - Journal of Paleontology, **39**: 365-378.

KUMMEL, B. (1952): A classification of the Triassic ammonoids. - Journal of Paleontology, **26**: 847-853.

KUMMEL, B. (1957): Systematic descriptions, L138-L139, L142-L143. - In Arkell, W. J., Furnish, W.M., Kummel, B., Miller, A.K., Moore, R.C., Schindewolf, O., Sylvester-Bradley, P.C. & Wright, C.W. (Editors): Cephalopoda Ammonoidea. Treatise on Invertebrate Paleontology (Moore, R.C. ed.): Part L, Mollusca 4. 490 pp. - Geological Society of America, Boulder, Colorado, and University of Kansas Press, Lawrence, Kansas.

KUMMEL, B. (1959): Lower Triassic ammonoids from Western Southland, New Zealand. - New Zealand Journal of Geology and Geophysics **2**: 429-47.

KUMMEL, B. (1961): The Spitsbergen arctoceratids. - Bulletin of the Museum of Comparative Zoology. Harvard University, **123**: 497-532.

KUMMEL, B. (1968a): Additional Scythian ammonoids from Afghanistan. - Bulletin of the Museum of Comparative Zoology, Harvard University **136**: 483-509.

KUMMEL, B. (1968b): Scythian ammonoids from Timor. - Breviora **283**: 1-21.

KUMMEL, B. & ERBEN, H.K. (1968): Lower and Middle Triassic cephalopods from Afghanistan. - Palaeontographica **129**: 95-148.

KUMMEL, B. & SAKAGAMI, S. (1960): Mid-Scythian ammonites from Iwai Formation, Japan. - Breviora, **126**: 1-11.

KUMMEL, B. & STEELE, G. (1962): Ammonites from the *Meekoceras gracilitatus* Zone at Crittenden Spring, Elko County, Nevada. - Journal of Paleontology, **36**: 638-703.

LUPPOV, N.P. & DRUSHCHITS, V.V. (1958): Fundamentals of Palaeontology, Mollusca - Cephalopoda II, Ammonoidea (Ceratites and Ammonites), Moscow, 359 pp. (in Russian).

MATHEWS, A.A.L. (1929): The Lower Triassic cephalopod fauna of the Fort Douglas area, Utah. - Walker Museum Memoirs, **1**: 1-46.

MOJSISOVICS, E. (1882): Die Cephalopoden der mediterranen Triasprovinz. - Abhandlungen der geologischen Reichsanstalt Wien, **10**.

MOJSISOVICS, E. (1896): Beiträge zur Kenntnis der obertriadischen Cephalopoden-Faunen des Himalaya. - Denkschriften der Akademie der Wissenschaften in Wien, **63**: 573-701.

MONNET, C. & BUCHER, H. (2005): New Middle and Late Anisian (Middle Triassic) ammonoid faunas from northwestern Nevada (USA): taxonomy and biochronology. - Fossils and Strata, **52**: 1-121.

MUNDIL, R., LUDWIG, K.R., METCALFE, I. & RENNE, P.R. (2004): Age and timing of the Permian mass extinctions: U/Pb dating of closed-system zircons. - Science, **305**: 1760-1763.

NAKAZAWA, K. & BANDO, Y. (1968): Lower and Middle Triassic Ammonites from Portuguese Timor (Palaeontological Study of Portuguese Timor, 4). - Memoirs of the Faculty of Science, Kyoto University, Series of Geology and Mineralogy, **34**: 83-114.

NICHOLS, K.M. & SILBERLING, N.J. (1979): Early Triassic (Smithian) ammonites of Paleoequatorial affinity from the Chulitna terrane, south central Alaska. - U. S. Gelogical Survey, Professional paper, **1121**: 1-5.

NOETLING, F., 1905. Die asiatische Trias. In: F. Frech (Editor): Lethaea geognostica: Handbuch der Erdgeschichte mit Abbildungen der für die Formationen bezeichnendsten Versteinerungen. - Schweizerbart, Stuttgart, 107-221.

OVTCHAROVA, M., BUCHER, H., SCHALTEGGER, U., GALFETTI, T., BRAYARD, A. & GUEX, J. (2006): New Early to Middle Triassic U-Pb ages from South China: Calibration with ammonoid biochronozones and implications for the timing of the Triassic biotic recovery. - Earth and Planetary Science Letters, **243**: 463-475.

ORCHARD, M.J. (2007): Conodont diversity and evolution through the latest Permian and Early Triassic upheavals. - Palaeogeography, Palaeoclimatology, Palaeoecology, 252: 93-117.

PAYNE, J.L., LEHRMANN, D.J., WEI, J.Y., ORCHARD, M.J., SCHRAG, D.P. & KNOLL, A.H. (2004): Large perturbations of the carbon cycle during recovery from the end-Permian extinction. - Science, **305**: 506-509.

PILLEVUIT, A., MARCOUX, J., STAMPFLI, G. & BAUD, A. (1997): The Oman exotics: a key to the understanding of the Neotethyan geodynamic evolution. - Geodinamica Acta, **10**: 209-238.

POPOV, Y. (1961): Triassic ammonoids of northeastern USSR. - Transactions, Scientific Research Institute for the Geology of the Arctic (NIIGA), **79**: 1-179.

POPOV, Y. (1962): Some Early Triassic ammonoids of northern Caucasia. - Transactions of the Academy of Sciences of the USSR, **127**: 176-184.

RAUP, D.M. & SEPKOSKI, J.J. (1982): Mass Extinctions in the Marine Fossil Record. - Science, **215**: 1501-1503.

RENZ, C. & RENZ, O. (1948): Eine untertriadische Ammonitenfauna von der griechischen Insel Chios. - Schweizerische Paläontologische Abhandlungen, **66**: 1-98.

RUZHENCEV, V.E. (1959): Classification of the superfamily Otocerataceae. - Paleontological Journal, **2**: 56–67.

SAKAGAMI, S. (1955): Lower Triassic ammonites from Iwai, Orguno-Mura, Nishitamagun, Kwanto massif, Japan. - Science Reports Tokyo Kyoiku Diagaku, series C, **30**: 131-40.

SHEVYREV, A.A. (1968): Triassic ammonoidea from the southern part of the USSR. Transactions of the Palaeontological Institute 119. - Nauka, Moscow, 272 pp.

SHEVYREV, A.A. (1990): Ammonoids and chronostratigraphy of the Triassic. - Trudy Paleontologiceskogo Instituta (Akademija Nauk SSR), **241**: 1-179.

SHEVYREV, A.A. (1995): Triassic ammonites of northwestern Caucasus. - Trudy Paleontologiceskogo Instituta (Akademija Nauk SSR), **264**: 1-174.

SHEVYREV, A.A. (2001): Ammonite zonation and interregional correlation of the Induan stage. - Stratigraphy and Geological Correlation, **9**: 473-482.

SHIGETA, Y., MAEDA., H. & ZAKHAROV, Y. (2009): Biostratigraphy: ammonoid succession. In: Shigeta, Y., Zakharov, Y., Maeda, H. & Popov, A.M. (Editors): The Lower Triassic system in the Abrek Bay area, South Primorye, Russia. National Museum of Nature and Science Monographs **38**, Tokyo, 24-27.

SHIGETA, Y. & ZAKHAROV, Y. (2009): Systematic paleontology: cephalopods. In: Shigeta, Y., Zakharov, Y., Maeda, H. & Popov, A.M. (Editors): The Lower Triassic system in the Abrek Bay area, South Primorye, Russia. National Museum of Nature and Science Monographs **38**, Tokyo, 44-140.

SHUJI, N., PILLEVUIT, A. & NISHIDA, T. (1996): Triassic aulacocerid (Mollusca: Cephalopoda) from the central Oman Mountains. - Transactions and Proceedings of the Palaeontological Society of Japan. New Series, **183**: 544-546.

SMITH, A.G., SMITH, D.G. & FUNNELL, B.M. (1994): Atlas of Mesozoic and Cenozoic Coastlines. - Cambridge University Press, Cambridge, 109 pp.

SMITH, J.P. (1904): The comparative stratigraphy of the marine Trias of Western America. - Proceedings of the California Academy of Sciences, series 3: 323-430.

SMITH, J.P. (1914): Middle Triassic marine invertebrate faunas of North America. - USGS Professional Paper, **83**: 1-254.

SMITH, J.P. (1927): Upper Triassic marine invertebrate faunas of North America. - U. S. Gelogical Survey, Professional paper, **141**: 262 pp.

SMITH, J.P. (1932): Lower Triassic ammonoids of North America. - USGS Professional Paper, **167**: 1-199.

SPATH, L.F. (1929): Corrections of cephalopod nomenclature. - The Naturalist: 269-271.

SPATH (1930): The Eotriassic invertebrate fauna of East Greenland. - Meddelelser om Grønland, **83**: 1-90.

SPATH, L.F. (1934): Part 4: The ammonoidea of the Trias, Catalogue of the fossil cephalopoda in the British Museum (Natural History). - The Trustees of the British Museum, London, 521 pp.

TONG, J.N., ZAKHAROV, Y. D. & WU, S. B. (2004): Early Triassic ammonoid succession in Chaohu, Anhui Province. - Acta Palaeontologica Sinica, **43**: 192-204.

TOZER, E.T. (1961): Triassic stratigraphy and faunas, Queen Elizabeth Islands, arctic archipelago. - Geologic Survey of Canada Memoir, **316**: 1-116.

TOZER, E.T. (1967): A standard for Triassic time. - Geologic Survey of Canada Bulletin, **156**: 1-141.

TOZER, E.T. (1971): Triassic time and ammonoids. - Canadian Journal of Earth Sciences, **8**: 989-1031.

TOZER, E.T. (1981): Triassic Ammonoidea; classification, evolution and relationship with Permian and Jurassic forms. In: HOUSE, M.R. & SENIOR, J.R. (Editors): The Ammonoidea. - Academic Press, The Systematics Association, London, 65-100.

TOZER, E.T. (1994): Canadian Triassic ammonoid faunas. - Geological Survey of Canada Bulletin, 663 pp.

TOZER, E.T. & CALON, T.J. (1990): Triassic ammonoids from Jabal Safra and Wadi Alwa, Oman, and their significance. In: ROBERTSON, A.H.F., SEARLE, M.P. & RIES, A.C. (Editors): The geology and tectonics of the Oman region. - Geological Society of London Special Publications, London, 203-211.

VU KHUC (1984): Triassic ammonoids in Vietnam. - Geoinform and Geodata Institute, Hanoi, 134 pp.

WAAGEN, W. (1895): Salt-Range fossils. Vol 2: Fossils from the Ceratite Formation. - Palaeontologia Indica, **13**: 1-323.

WANG, Y.G. & HE, G.X. (1976): Triassic ammonoids from the Mount Jolmo Lungma region. A report of scientific expedition in the Mount Jolmo Lungma region (1966-1968), Palaeontology. - Science Press, Peking, 223-438.

WANNER, J. (1911): Triascephalopoden von Timor und Rotti. - Neues Jahrbuch für Geologie und Paläontologie. Beilageband, **32**: 177-196.

WATERHOUSE, J.B. (1996a): The Early and Middle Triassic ammonoid succession of the Himalayas in western and central Nepal: Systematic studies of the early middle Scythian. - Palaeontographica, **241**: 27-100.

WATERHOUSE, J.B. (1996b): The Early and Middle Triassic ammonoid succession of the Himalayas in western and central Nepal: Part 3. Late middle Scythian ammonoids. - Palaeontographica, **241**: 101-167.

WEITSCHAT, W. & LEHMANN, U. (1978): Biostratigraphy of the uppermost part of the Smithian Stage (Lower Triassic) at the Botneheia, W-Spitsbergen. - Mitteilungen aus dem Geologisch-Palaeontologischen Institut der Universität Hamburg, **54**: 27-54.

WELTER, O.A. (1922): Die Ammoniten der unteren Trias von Timor. - Paläontologie von Timor, **11**: 83-154.

WHITE, C.A. (1879): Paleontological papers no. 9: fossils from the Jura-Trias of south-eastern Idaho. - U. S. Geological and Geographical Survey of the Territories Bulletin, **5**: 105-117.

WHITE, C.A. (1880): Contributions to invertebrate paleontology, no. 5: Triassic fossils of south-eastern Idaho. - U. S. Geological Survey of the Territories, 12th Annual Report, part 1: 105-118.

WOODS, A.D. & BAUD, A. (2008): Anachronistic facies from a drowned Lower Triassic carbonate platform: Lower member of the Alwa Formation (Ba'id Exotic), Oman Mountains. - Sedimentary Geology, **209**: 1-14.

ZAKHAROV, Y.D. (1968): Biostratigraphiya i amonoidei nizhnego triasa Yuzhnogo Primorya (Lower Triassic biostratigraphy and ammonoids of South Primorye). - Nauka, Moskva, 175 pp.

ZAKHAROV, Y. (1997): Recent view on the Induan, Olenekian and Anisian ammonoid taxa and zonal assemblages of south Primorye. - Albertiana, **19**: 25-35.

ZITTEL (1884): Handbuch der Palaeontologie. Cephalopoda. - Munich, 239-522.

Appendix

Measurements of the classic geometrical parameters of the ammonoid shell. Diameter (D), whorl height (H), whorl width (W) and umbilical diameter (U).

Species	**Specimen**	**D (mm)**	**H (mm)**	**W (mm)**	**U (mm)**	**Sample**
Proharpoceras carinatitabulatum Chao 1950	PIMUZ 26206	35	13	11.6	12.3	SA1
Kashmirites baidi n. sp.	PIMUZ 27304	32	9.5	9.9	15.3	Baid-A
	PIMUZ 27792	23.4	8.5	10.3	9.6	Baid-A
?Xenoceltitidae gen. indet.	PIMUZ 27303	50.3	20.1	14.4	17.5	JS2a
Guodunites monneti Brayard & Bucher 2008	PIMUZ 27249	66.7	31.7	-	13.4	HB900
	PIMUZ 27794	44.9	19.7	-	10	HB900
Pseudoflemingites goudemandi Brayard & Bucher 2008	PIMUZ 27382	39	13.1	-	16.3	JS12
	PIMUZ 27381	35	10.7	-	17.2	JS12
Subflemingites involutus (Welter 1922)	PIMUZ 27367	71.1	27	14.1	25.1	JS13e
	PIMUZ 27368	31.5	13	8.4	9.5	JS13f
	PIMUZ 27795	34.3	15	-	11	JS13f
Galfettitidae gen. et sp. indet.	PIMUZ 27394	41	20.5	-	8	Baid-B
Paranorites jenksi Brayard & Bucher 2008	PIMUZ 27321	64.6	27.8	15.4	15.2	HB911
Prionites sp. indet.	PIMUZ 27428	104	50.2	26.6	18.6	HB912
Anasibirites multiformis Welter 1922	PIMUZ 27421	20.2	9.4	-	4.6	HB901
Hemiprionites cf. *butleri* (Mathews 1929)	PIMUZ 27426	23.1	12.3	7.4	3	HB902
Lucasites involutus n. gen. et sp.	PIMUZ 27339	60	25	-	14	JS11a
?Prionitidae gen. indet.	PIMUZ 27430	57	28	18	11.5	HB901
?Arctoceratidae gen. indet.	PIMUZ 27429	44.9	19.4	14.5	12.5	SA1
Lanceolites compactus Hyatt & Smith 1905	PIMUZ 27432	12.1	7	-	0	HB900
	PIMUZ 27431	24	14.5	-	0	JS4b
Pseudosageceras multilobatum Noetling 1905	PIMUZ 27498	86.3	53	18.2	0	Baid-B
Subcolumbites safraensis n. sp.	PIMUZ 27424	34	11.4	-	13.1	SA4-D

Figure captions

Text-fig. 1. Early Triassic stage subdivision (TOZER, 1967) with indication of recently published radiometric ages (OVTCHAROVA et al. 2006, GALFETTI et al., 2007b).

Text-fig. 2. Simplified geological map of the Oman Mountains with indication of studied localities (modified from PILLEVUIT et al. 1997 after GLENNIE et al. 1974).

Text-fig. 3. (a) The Wadi Alwa megablock in the Baid area seen from SE, with indication of the studied sites. (b) Western part of Jebel Safra, view towards E. The arrow indicates the horizon in the Guwayza Formation with abundant Permian and Early Triassic exotic blocks. (c) Part of the main exotic block at Wadi Musjah, with indication of studied samples. Stratigraphic polarity inversed as inferred from geopetal structures. (d) An example of an exotic block of Hallstatt facies from Jebel Safra. (e) Residual of sample HB912 from Jebel Safra after treatment with acetic acid for conodont preparation. Note the strongly silicified ammonoid shells in this sample. Natural size.

Text-fig. 4. Distribution of ammonoid taxa in Smithian Exotic blocks of red or greenish Hallstatt facies from Jebel Safra. The blocks JS11, SA3 and JS6 contain the *Rohillites omanensis* fauna; the block JS13 holds the *Nammalites pilatoides* fauna, which possibly also the block SA1 belongs to; the blocks HB912, JS2, JS4, JS8 and JS12 belong to the *Owenites koeneni* fauna. Open dots indicate occurrences based only on fragmentary or poorly preserved material. Arrows indicate polarity inferred from geopetal structures.

Text-fig. 5. Distribution of ammonoid taxa in Exotic blocks from Wadi Musjah. Sample HB901 belongs to the *Anasibirites multiformis* fauna, all other samples form part of the *Owenites koeneni* fauna. Note that the top 4.5m of the main block yielding no ammonoids are not illustrated in this figure. Open dots indicate occurrences based only on fragmentary or poorly preserved material. Arrow indicates polarity inferred from geopetal structures.

Text-fig. 6. Distribution of ammonoid taxa in the samples from Baid. Sample HB911 contains the *Baidites hermanni* fauna; sample Baid-A belongs to the *Flemingites rursiradiatus* fauna; and Samples Baid-B and Baid-G belong to the *Owenites koeneni* fauna. The Hallstatt limestone is highly fractured and faulted, the samples Baid-A, Baid-B, and Baid-G should therefore be considered as isolated samples. Sample HB911 is an isolated sample from the Alwa summit. Open dots indicate occurrences based only on fragmentary or poorly preserved material.

Text-fig. 7. Correlation of the various ammonoid faunas from exotic blocks from Oman with the well-known ammonoid zonations for the Smithian from northwestern Guangxi, South China (BRAYARD & BUCHER 2008) and from Tulong, South Tibet (Brühwiler et al., submitted [a, b]). Black lines indicate uncertainty intervals. Dien.: Dienerian; Spa.: Spathian.

Text-fig. 8. Scatter diagrams of H, W and U, and of H/D, W/D and U/D for *Nyalamites angustecostatus* from Oman (Wadi Musjah, *Owenites koeneni* fauna) and from Afghanistan (data from KUMMEL & ERBEN 1968).

Text-fig. 9. Scatter diagrams of H, W and U, and of H/D, W/D and U/D for *Preflorianites radians* (Jebel Safra, Baid, *Owenites koeneni* fauna).

Text-fig. 10. Box plots of H/D, W/D and U/D for different species of *Pseudaspidites* found in Oman.

Text-fig. 11. Scatter diagrams of H, W and U, and of H/D, W/D and U/D for *Pseudaspidites planus* n. sp. (Jebel Safra, Baid, *Owenites koeneni* fauna, *Rohillites omanensis* fauna).

Text-fig. 12. Scatter diagrams of H, W and U, and of H/D, W/D and U/D for *Leyeceras* cf. *rothi* (Jebel Safra, Baid, *Owenites koeneni* fauna).

Text-fig. 13. Scatter diagrams of H, W and U, and of H/D, W/D and U/D for *Dieneroceras* cf. *dieneri* (Jebel Safra, Baid, Wadi Musjah, *Owenites koeneni* fauna).

Text-fig. 14. Box plots of H/D, W/D and U/D for *Dieneroceras* cf. *dieneri* from Oman and for *Dieneroceras tientungense* from South China (BRAYARD & BUCHER 2008).

Text-fig. 15. Scatter diagrams of H, W and U, and of H/D, W/D and U/D for *Flemingites rursiradiatus* (Baid, *Flemingites rursiradiatus* fauna).

Text-fig. 16. Scatter diagrams of H, W and U, and of H/D, W/D and U/D for *Anaxenaspis* cf. *lidacensis* (Wadi Musjah, Baid, *Owenites koeneni* fauna).

Text-fig. 17. Scatter diagrams of H, W and U, and of H/D, W/D and U/D for *Rohillites omanensis* n. sp. (Jebel Safra, *Rohillites omanensis* fauna).

Text-fig. 18. Scatter diagrams of H, W and U, and of H/D, W/D and U/D for *Baidites hermanni* n. gen. et. sp. (Baid, *Baidites hermanni* fauna).

Text-fig. 19. Scatter diagrams of H, W and U, and of H/D, W/D and U/D for *Galfettites simplicitatis* (Jebel Safra, Baid, *Owenites koeneni* fauna).

Text-fig. 20. Box plots of H/D, W/D and U/D for different species of *Galfettites* found in Oman.

Text-fig. 21. Scatter diagrams of H, W and U, and of H/D, W/D and U/D for *Galfettites kyrae* n. sp. (Wadi Musjah, Baid, *Owenites koeneni* fauna).

Text-fig. 22. Scatter diagrams of H, W and U, and of H/D, W/D and U/D for *Galfettites omani* n. sp. (Jebel Safra, *Nammalites pilatoides* fauna).

Text-fig. 23. Scatter diagrams of H, W and U, and of H/D, W/D and U/D for *Safraites simplex* n. gen. et sp. (Jebel Safra, *Nammalites pilatoides* fauna).

Text-fig. 24. Scatter diagrams of H, W and U, and of H/D, W/D and U/D for *Submeekoceras mushbachanum* (Jebel Safra, Baid, *Flemingites rursiradiatus* fauna, *Owenites koeneni* fauna).

Text-fig. 25. Scatter diagrams of H, W and U, and of H/D, W/D and U/D for *Nammalites pilatoides* n. gen. (Jebel Safra, *Nammalites pilatoides* fauna).

Text-fig. 26. Scatter diagrams of H, W and U, and of H/D, W/D and U/D for *Parussuria compressa* (Jebel Safra, Wadi Musjah, Baid, *Nammalites pilatoides* fauna, *Owenites koeneni* fauna).

Text-fig. 27. Scatter diagrams of H, W and U, and of H/D, W/D and U/D for *Inyoites oweni* (Wadi Musjah, Jebel Safra, *Owenites koeneni* fauna).

Text-fig. 28. Box plots of H/D, W/D and U/D for different species of *Inyoites* found in Oman.

Text-fig. 29. Scatter diagrams of H, W and U, and of H/D, W/D and U/D for *Subvishnuites welteri* (Jebel Safra, *Nammalites pilatoides* fauna).

Text-fig. 30. Box plots of H/D, W/D and U/D for different species of *Subvishnuites* found in Oman.

Text-fig. 31. Scatter diagrams of H, W and U, and of H/D, W/D and U/D for *Jinyaceras* cf. *bellum* (Baid, *Baidites hermanni* fauna).

Text-fig. 32. Scatter diagrams of H, W and U, and of H/D, W/D and U/D for *Juvenites spathi* (Jebel Safra, Baid, *Nammalites pilatoides* fauna, *Owenites koeneni* fauna).

Text-fig. 33. Box plots of H/D, W/D and U/D for different species of *Juvenites*, *Paranannites* and *Omanites* found in Oman.

Text-fig. 34. Scatter diagrams of H, W and U, and of H/D, W/D and U/D for *Juvenites* cf. *thermarum* (Wadi Musjah, *Owenites koeneni* fauna).

Text-fig. 35. Scatter diagrams of H, W and U, and of H/D, W/D and U/D for *Paranannites baudi* n. sp. (Jebel Safra, *Rohillites omanensis* fauna).

Text-fig. 36. Scatter diagrams of H, W and U, and of H/D, W/D and U/D for *Omanites musjahensis* n. gen. et sp. (Wadi Musjah, *Owenites koeneni* fauna).

Text-fig. 37. Scatter diagrams of H, W and U, and of H/D, W/D and U/D for *Owenites koeneni* (Jebel Safra, Wadi Musjah, Baid, *Owenites koeneni* fauna).

Text-fig. 38. Box plots of H/D, W/D and U/D for different species of *Owenites* found in Oman.

Text-fig. 39. Scatter diagrams of H, W and U, and of H/D, W/D and U/D for *Owenites carpenteri* (Wadi Musjah, *Owenites koeneni* fauna).

Text-fig. 40. Scatter diagrams of H, W and U, and of H/D, W/D and U/D for *Owenites simplex* (Jebel Safra, *Nammalites pilatoides* fauna).

Text-fig. 41. Scatter diagrams of H, W and U, and of H/D, W/D and U/D for *Owenites* sp. indet. (Jebel Safra, *Nammalites pilatoides* fauna).

Text-fig. 42. Scatter diagrams of H, W and U, and of H/D, W/D and U/D for *Aspenites acutus* (Jebel Safra, Wadi Musjah, *Rohillites omanensis* fauna, *Nammalites pilatoides* fauna, *Owenites koeneni* fauna).

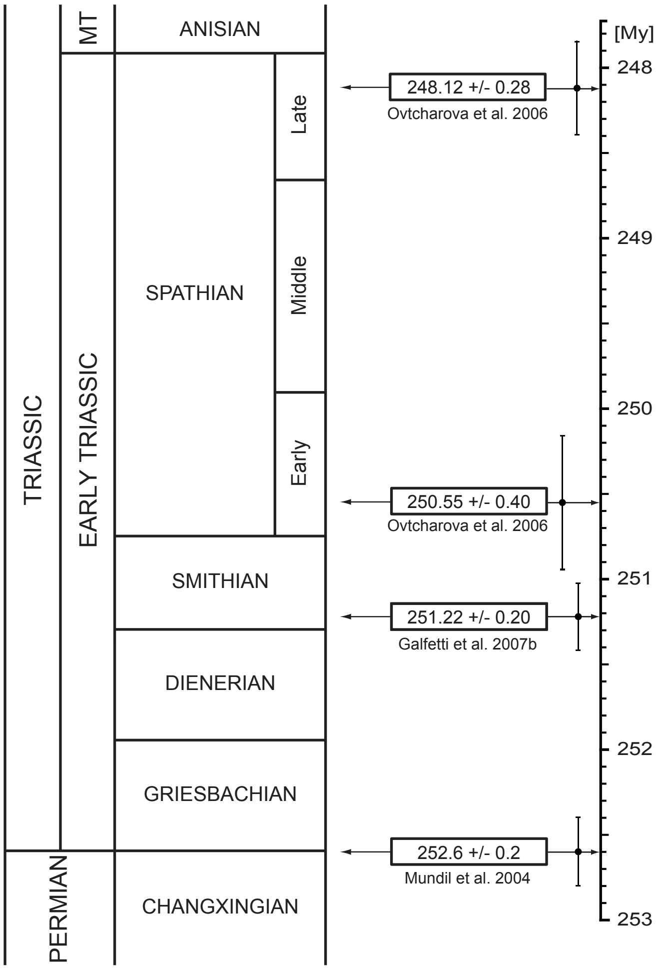

Text-figure 1

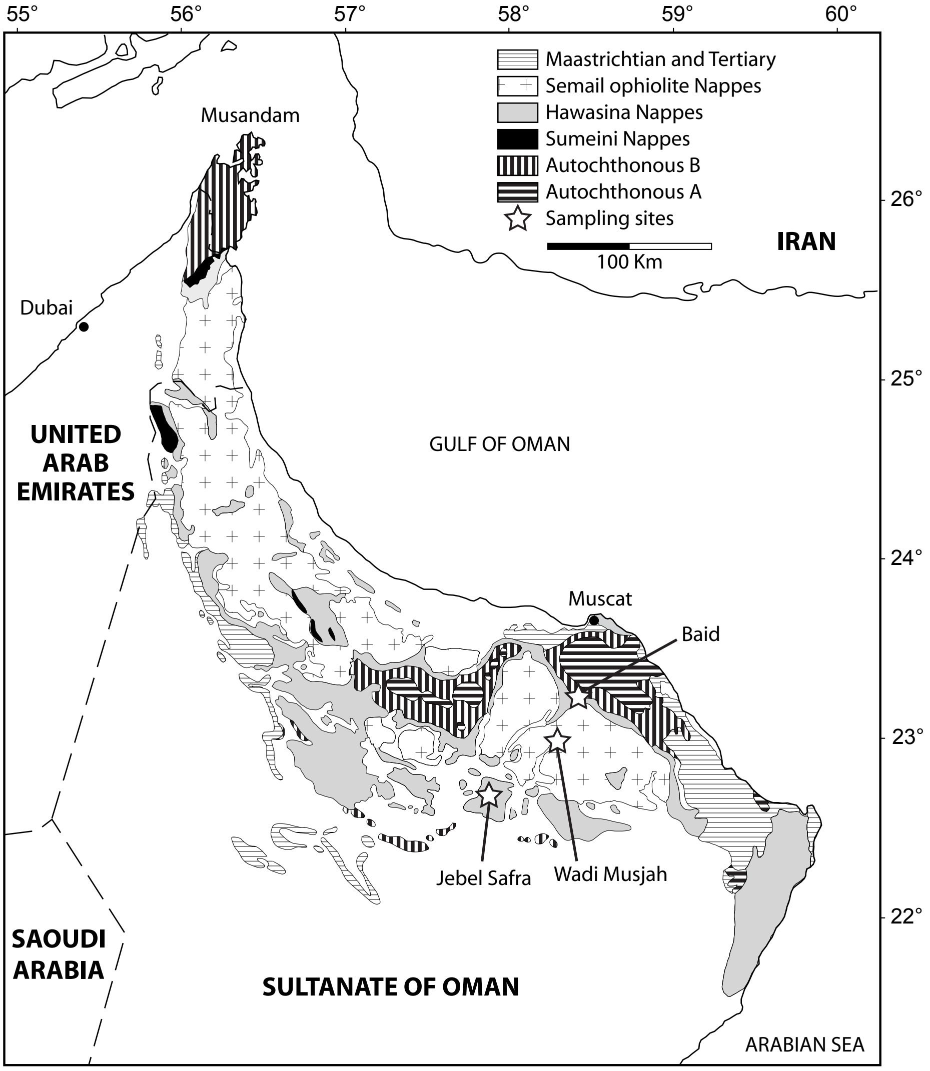

Text-figure 2

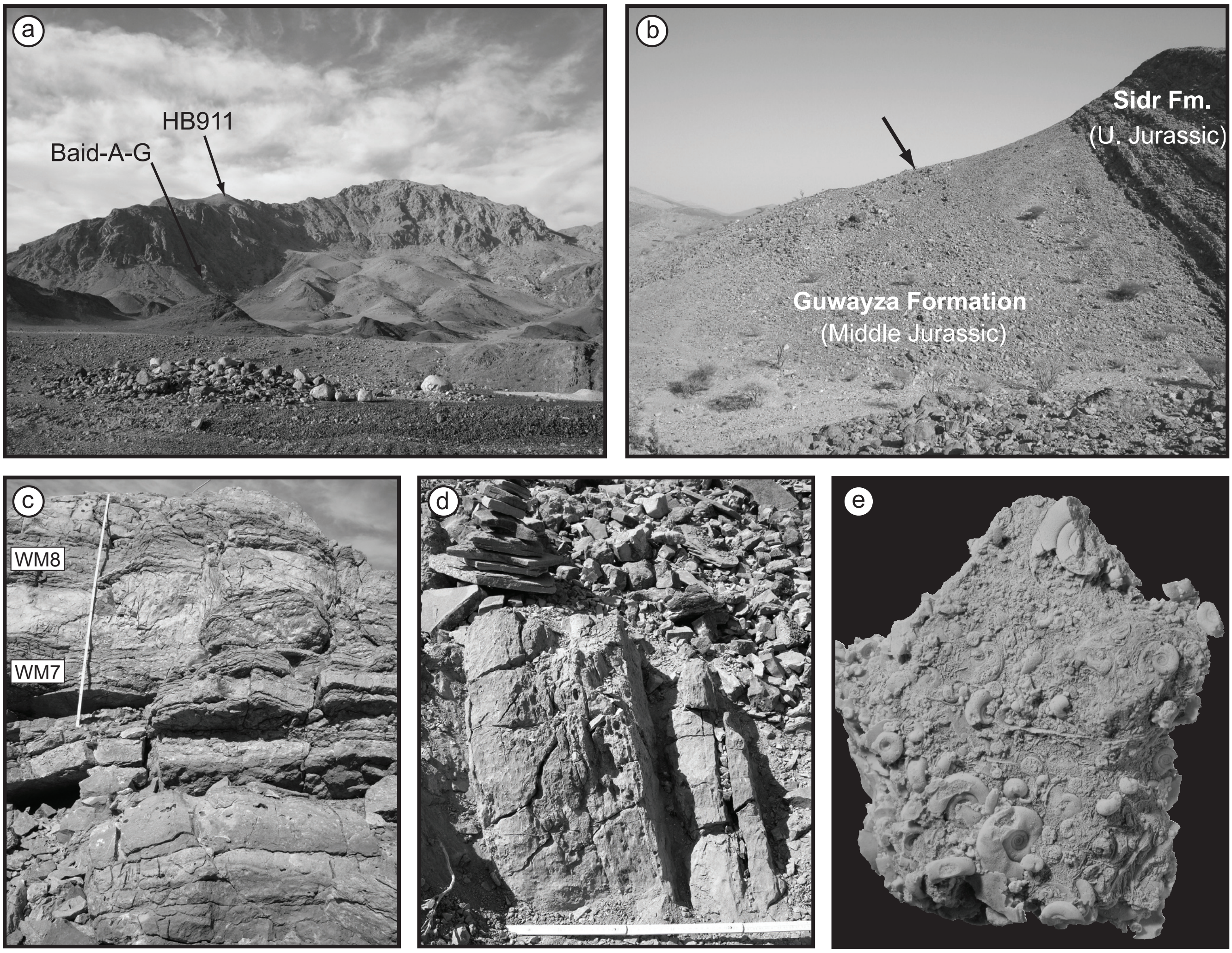

Text-figure 3

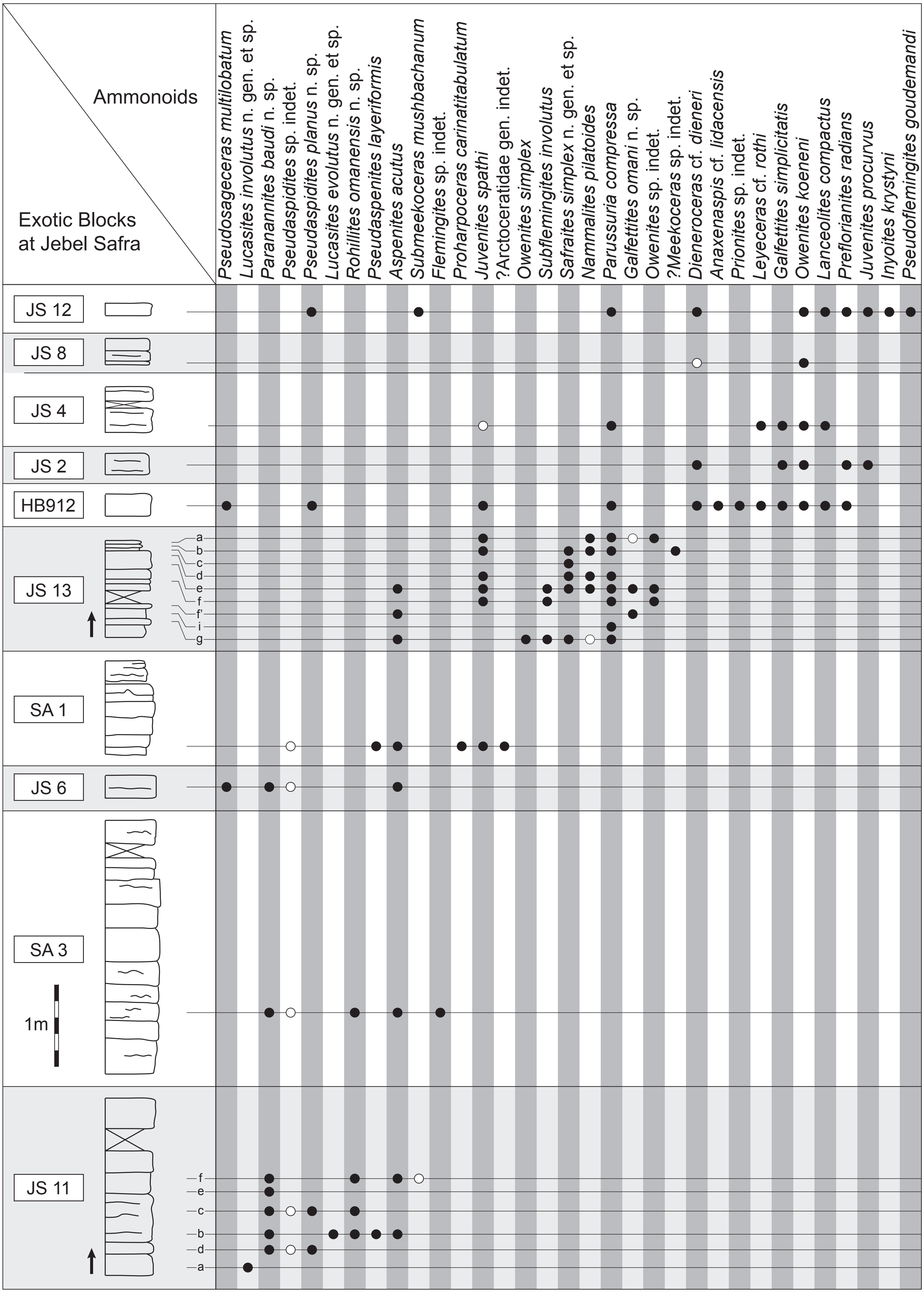

Text-figure 4

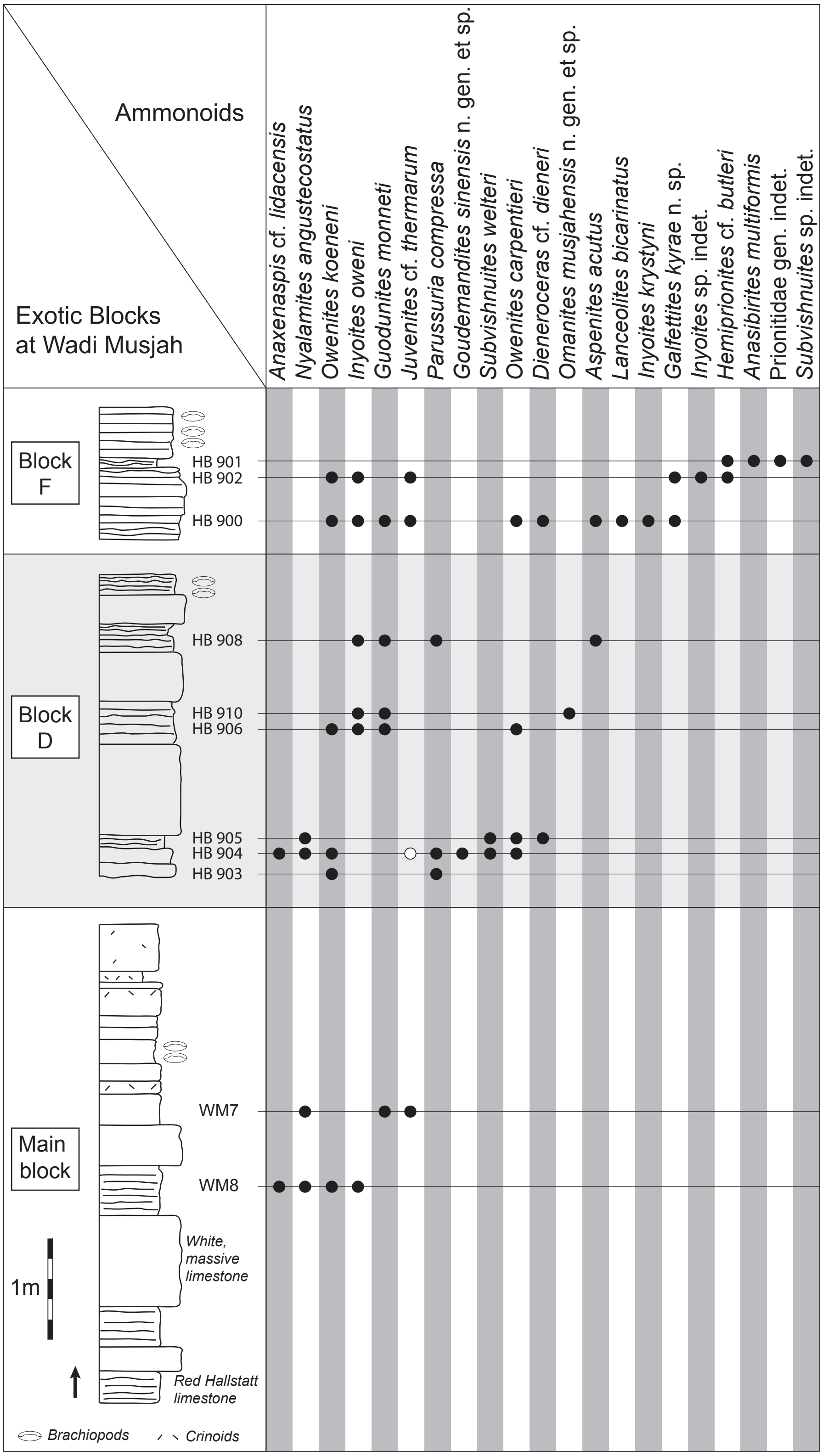

Text-figure 5

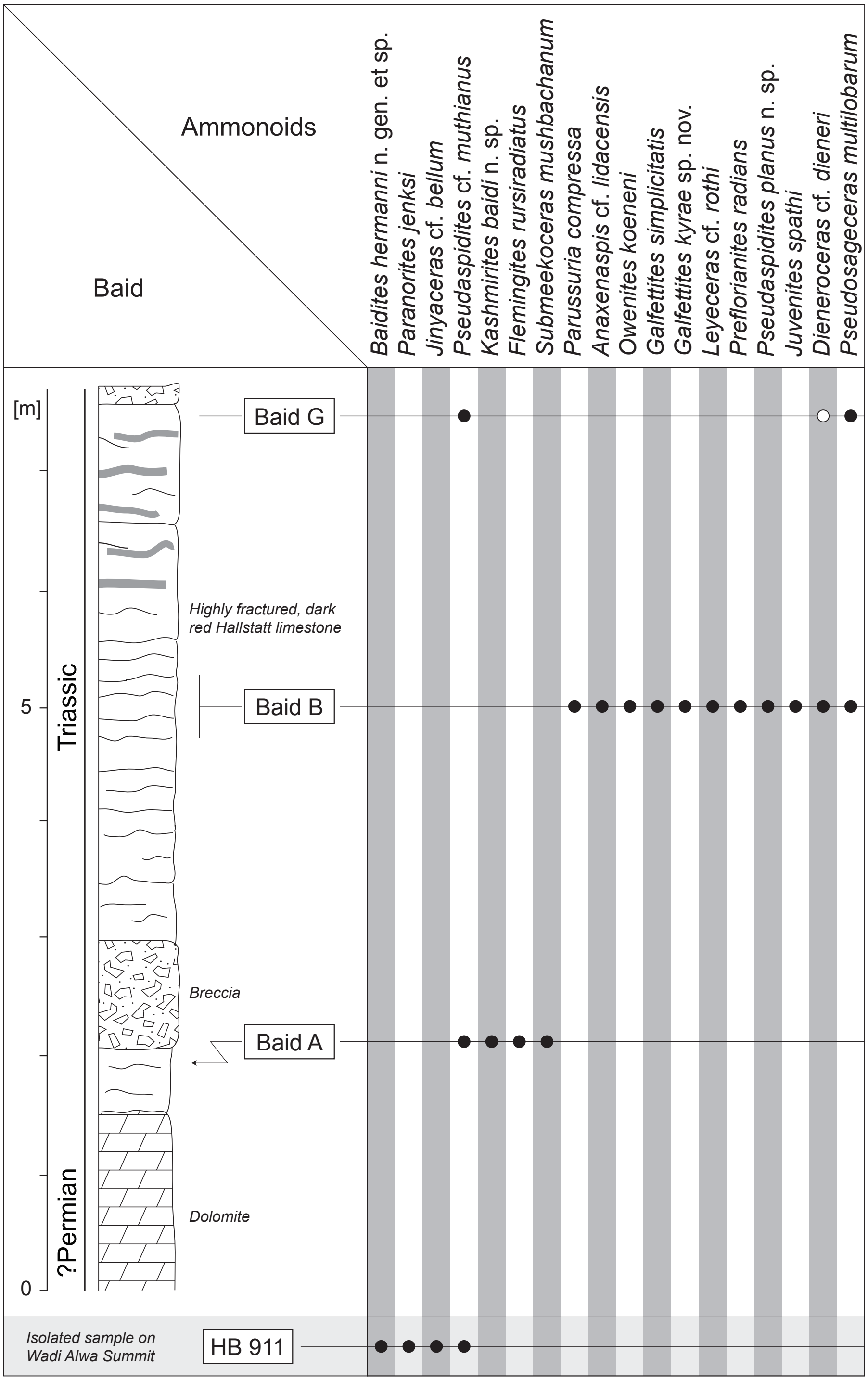

Text-figure 6

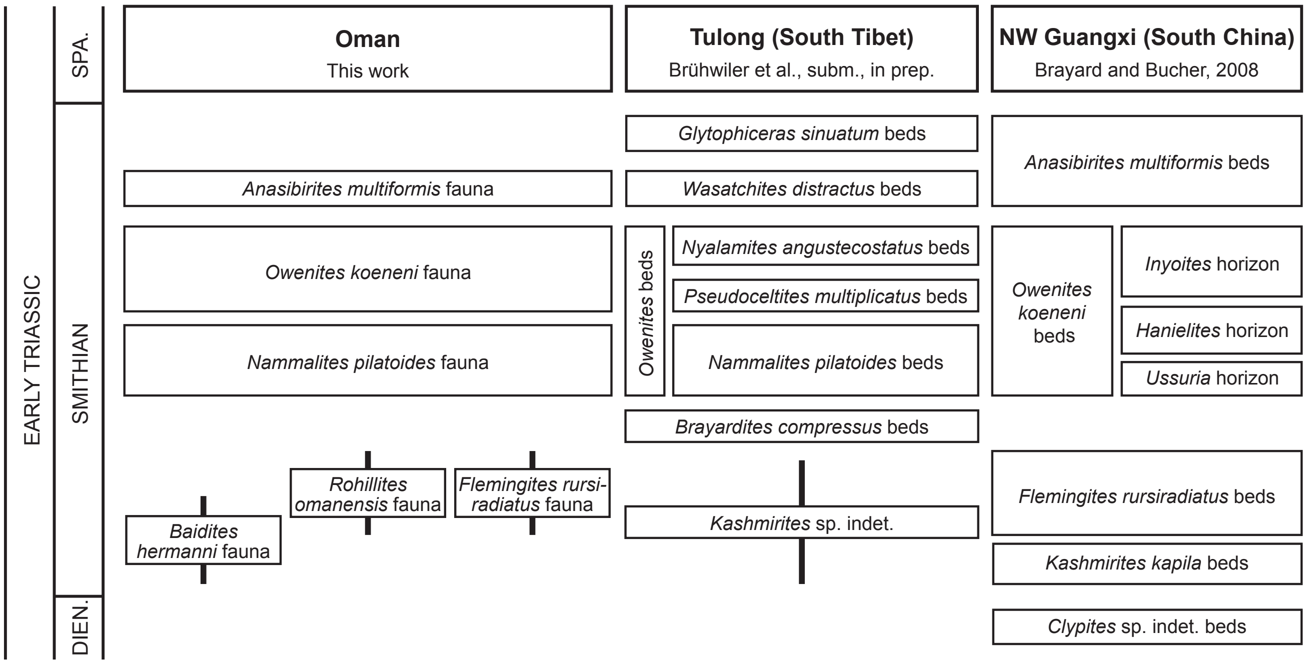

Text-figure 7

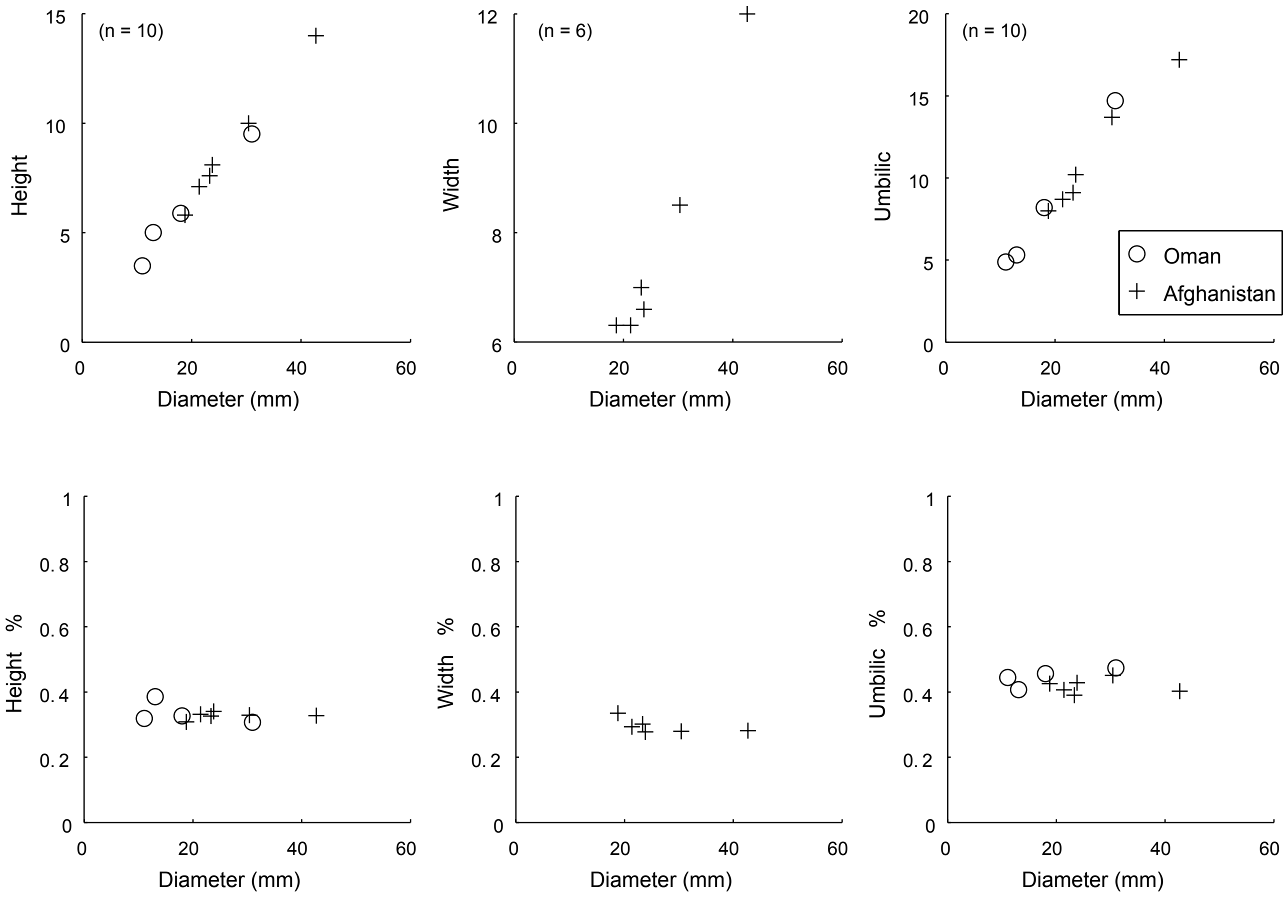

Text-figure 8

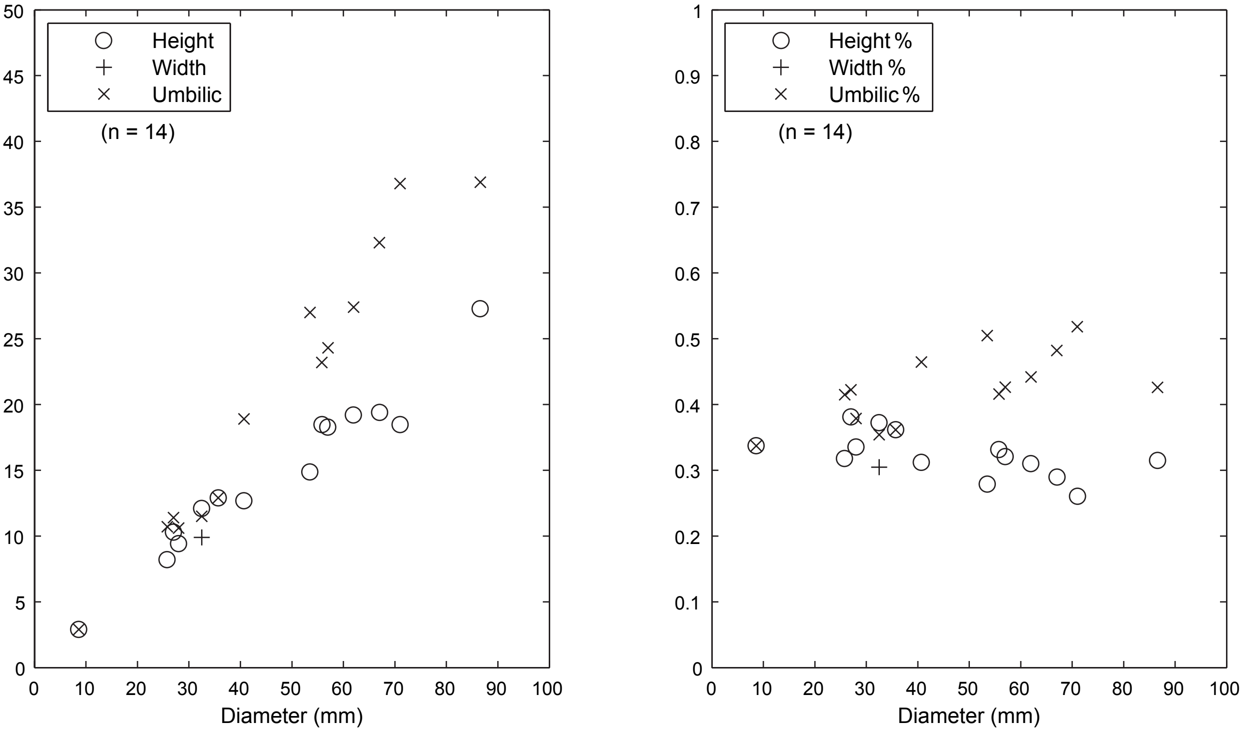

Text-figure 9

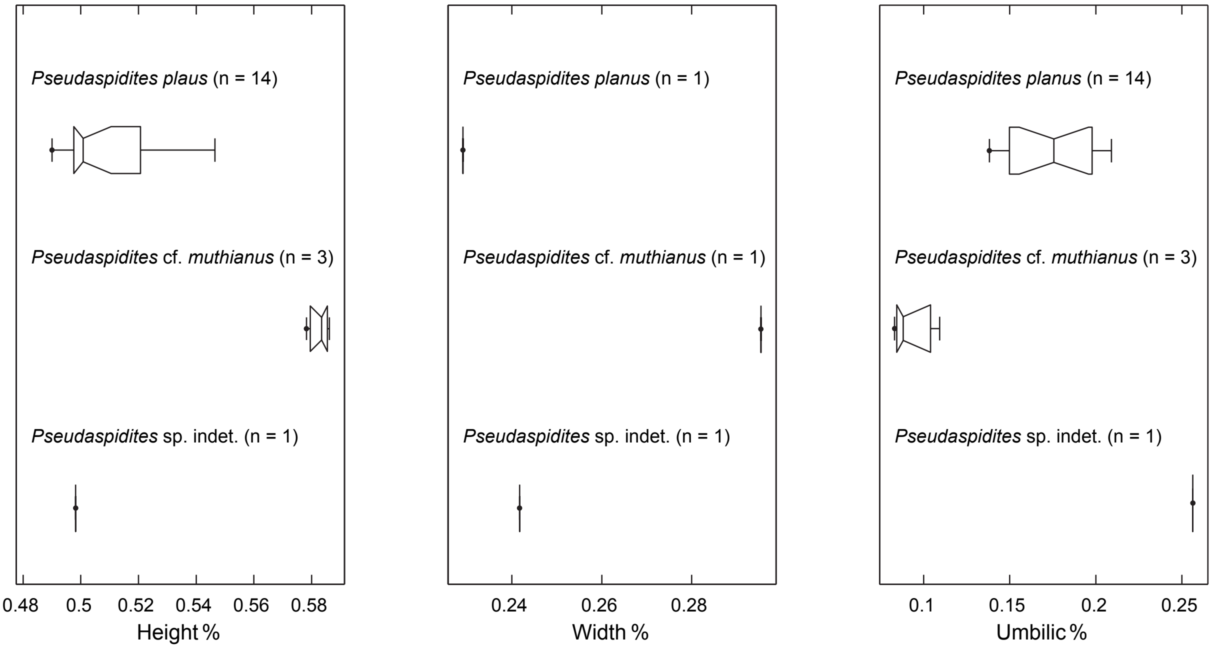

Text-figure 10

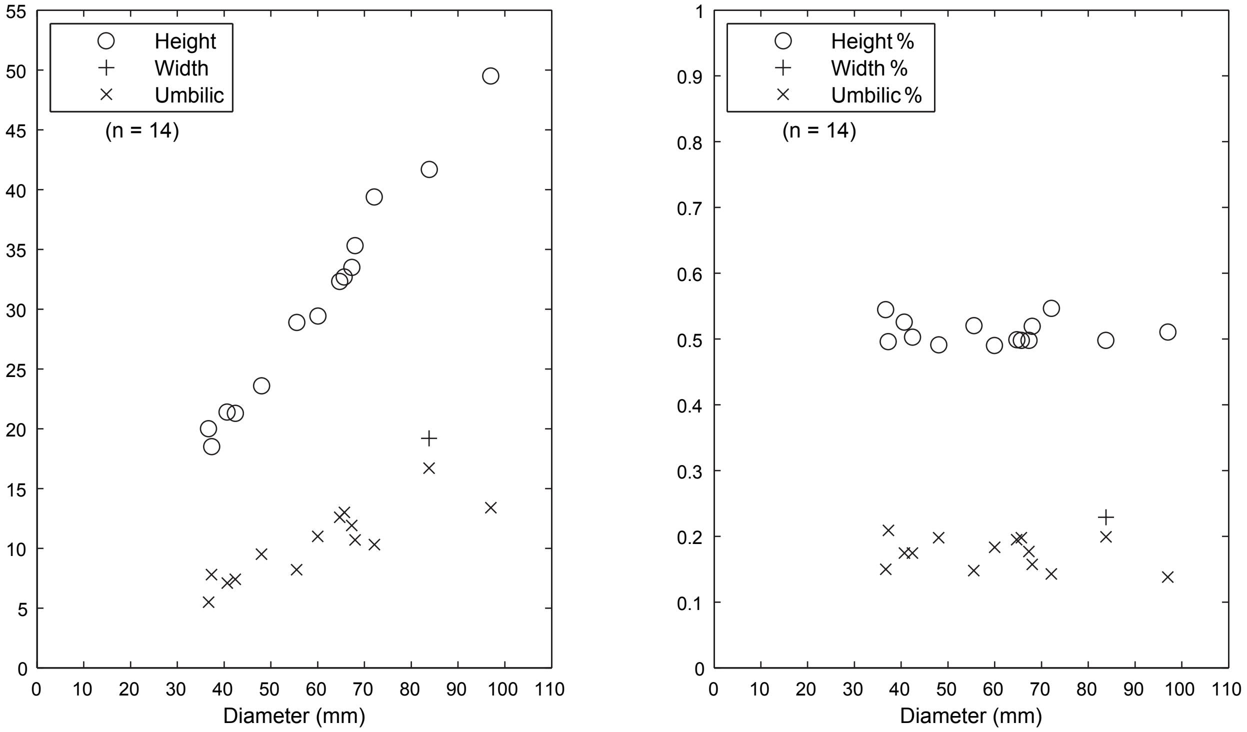

Text-figure 11

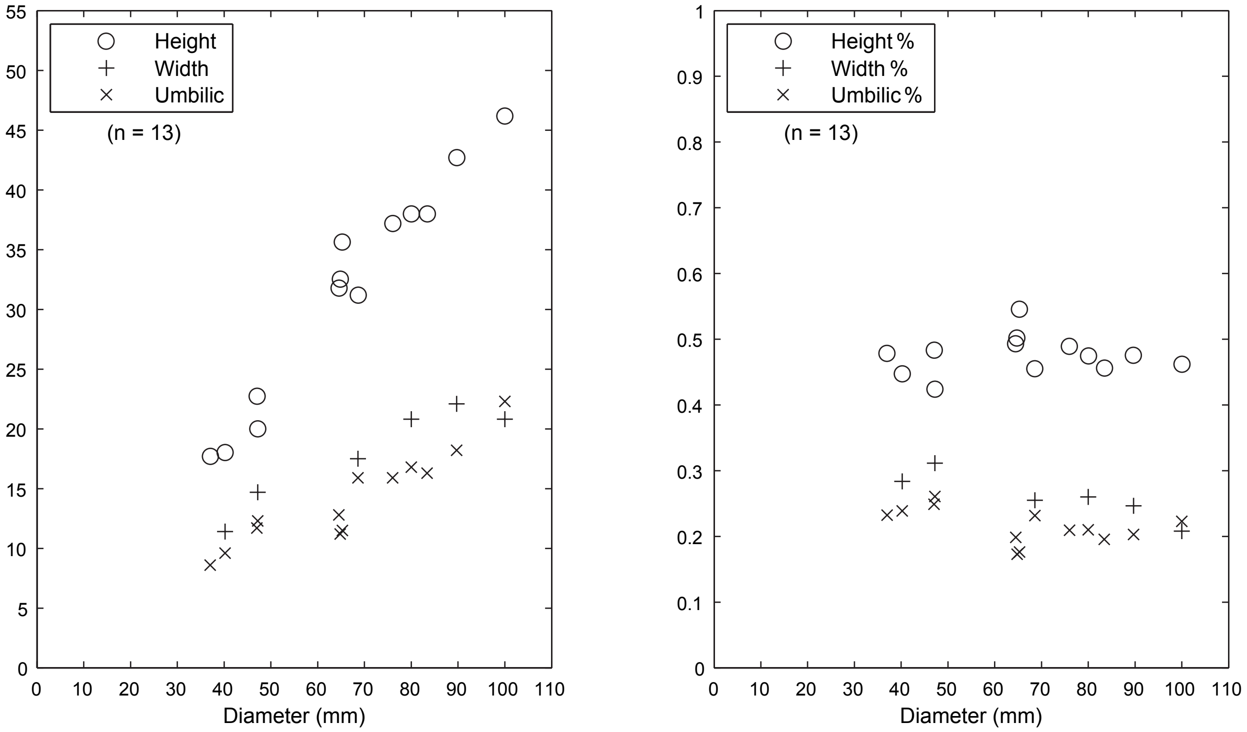

Text-figure 12

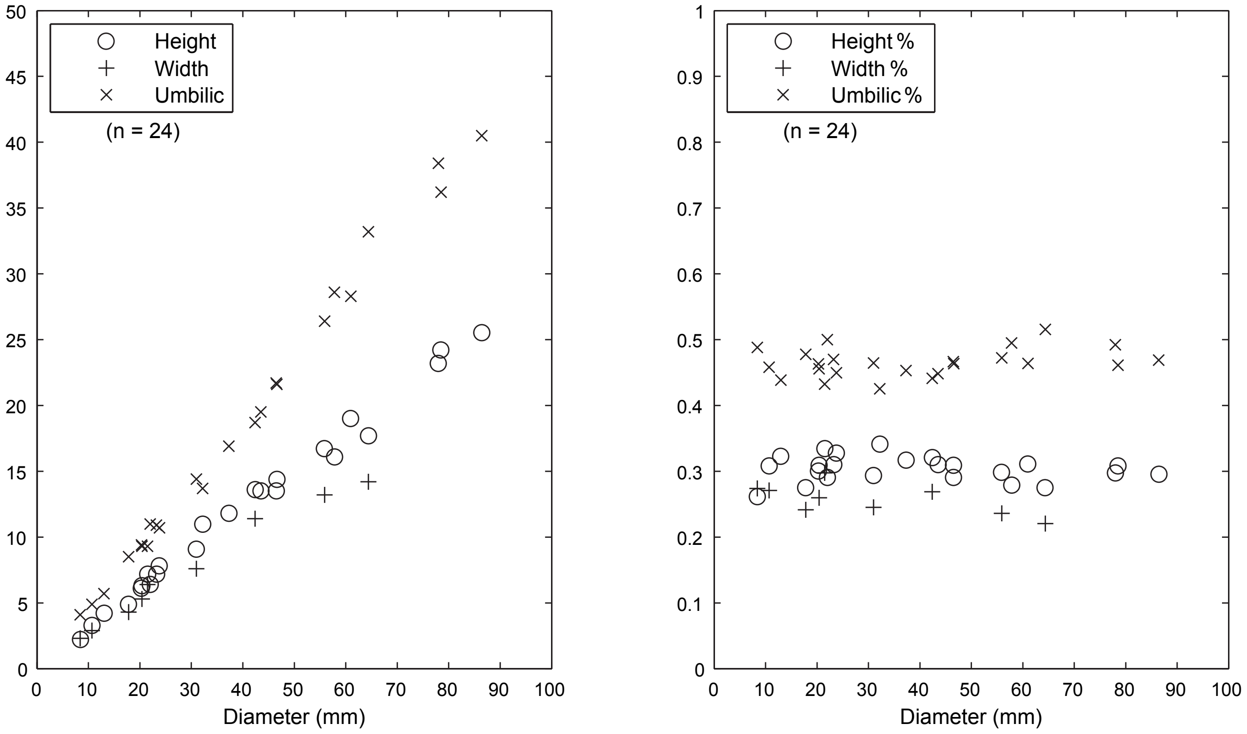

Text-figure 13

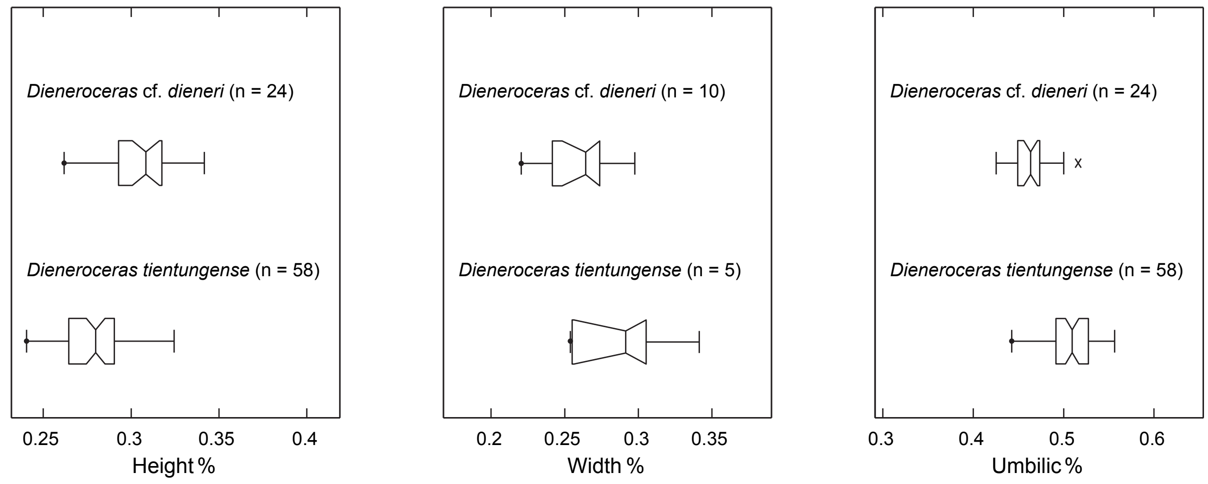

Text-figure 14

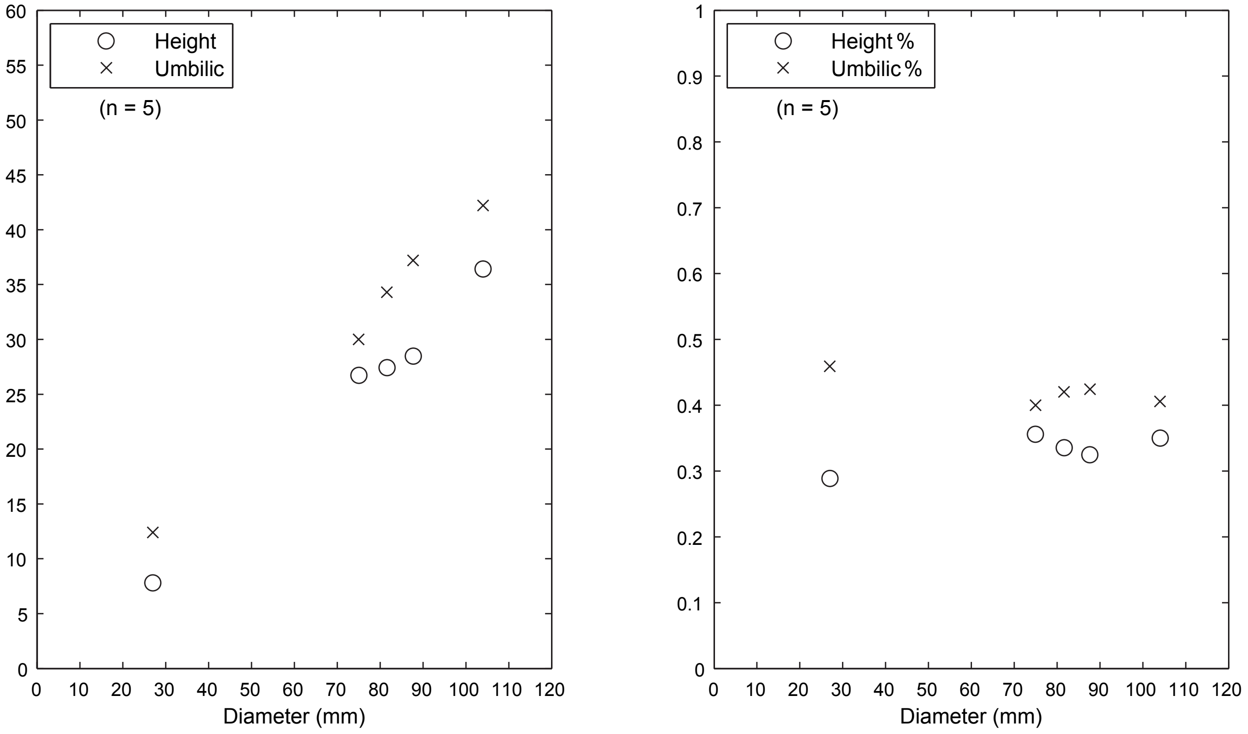

Text-figure 15

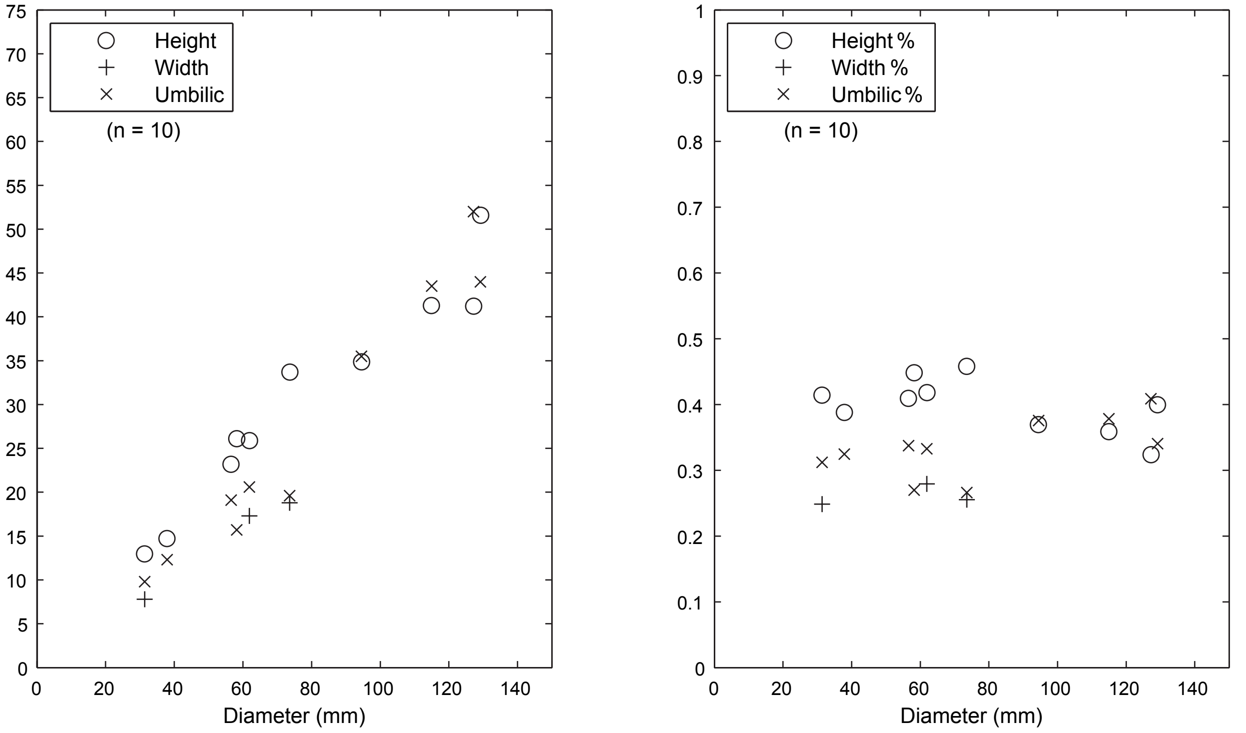

Text-figure 16

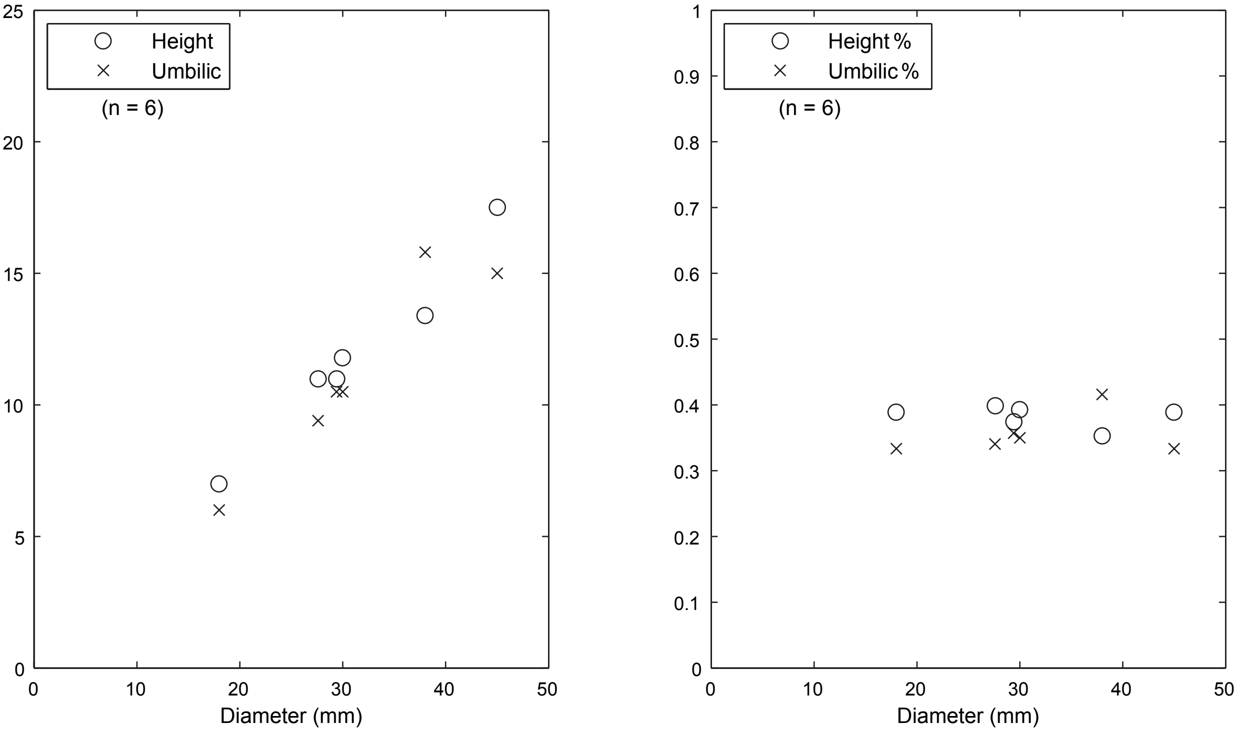

Text-figure 17

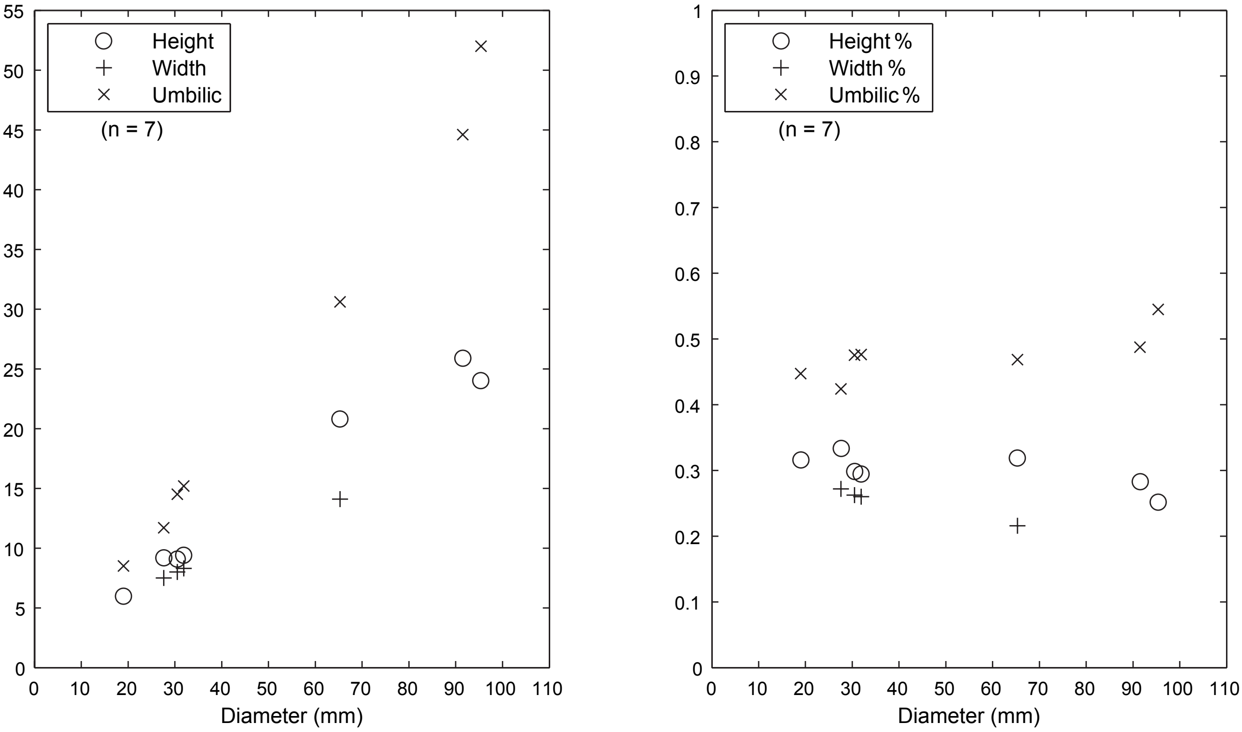

Text-figure 18

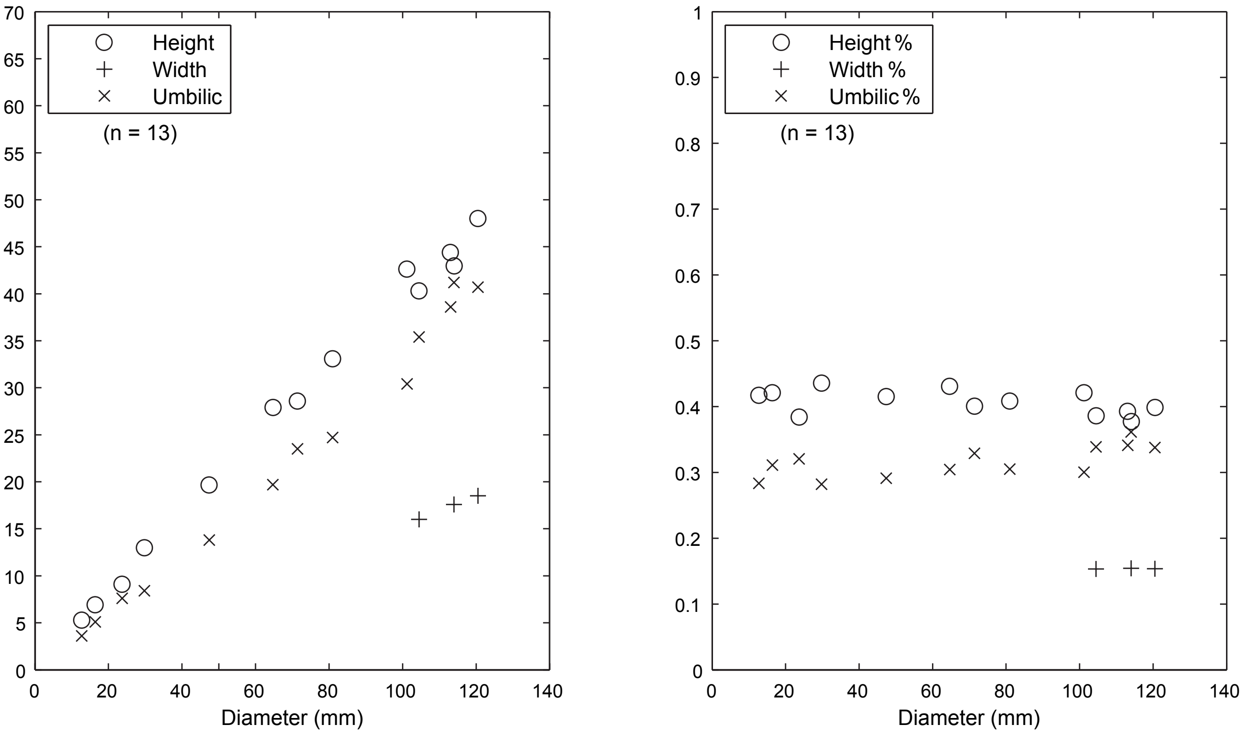

Text-figure 19

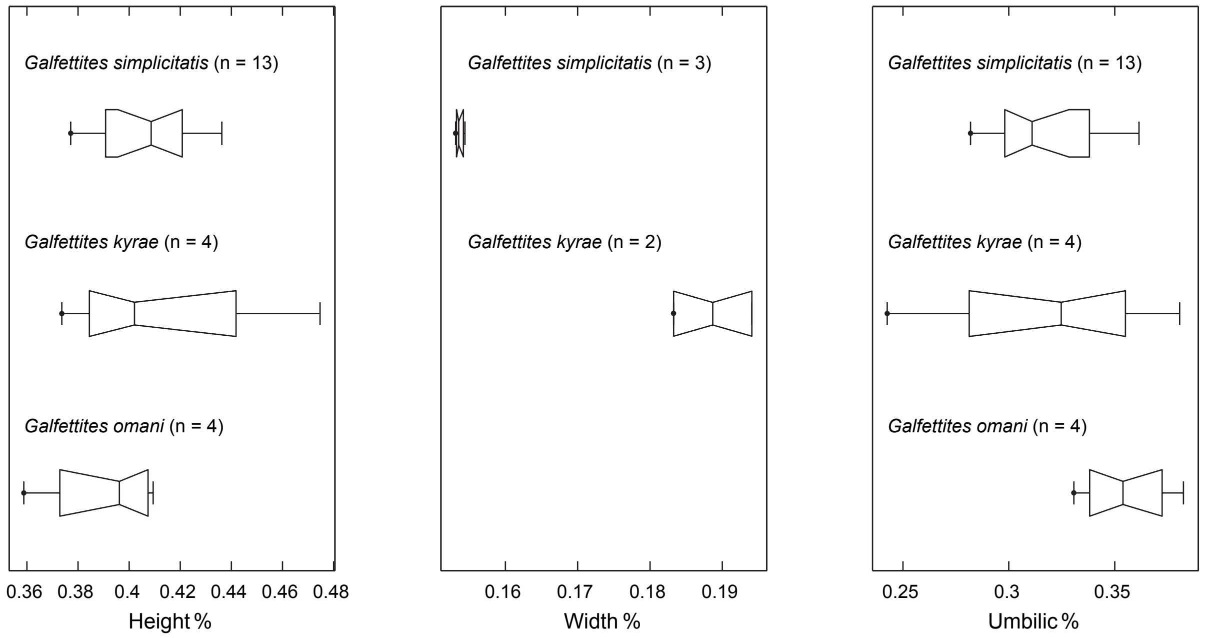

Text-figure 20

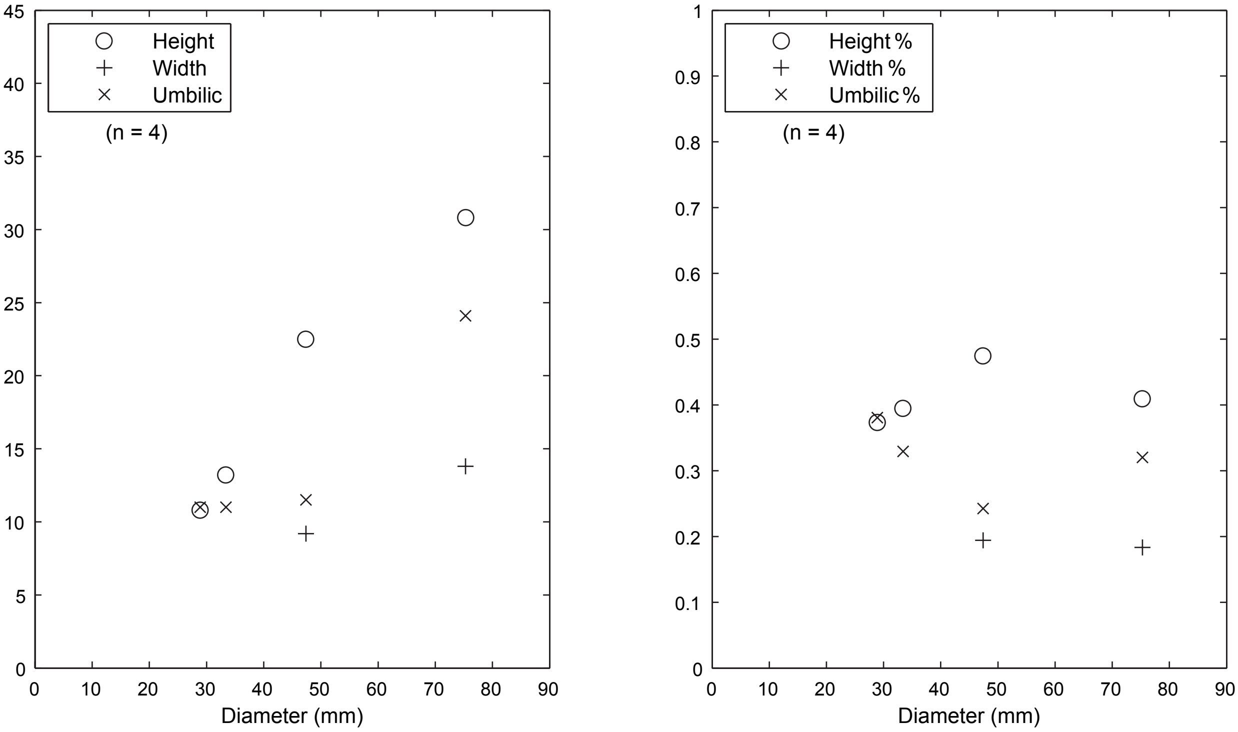

Text-figure 21

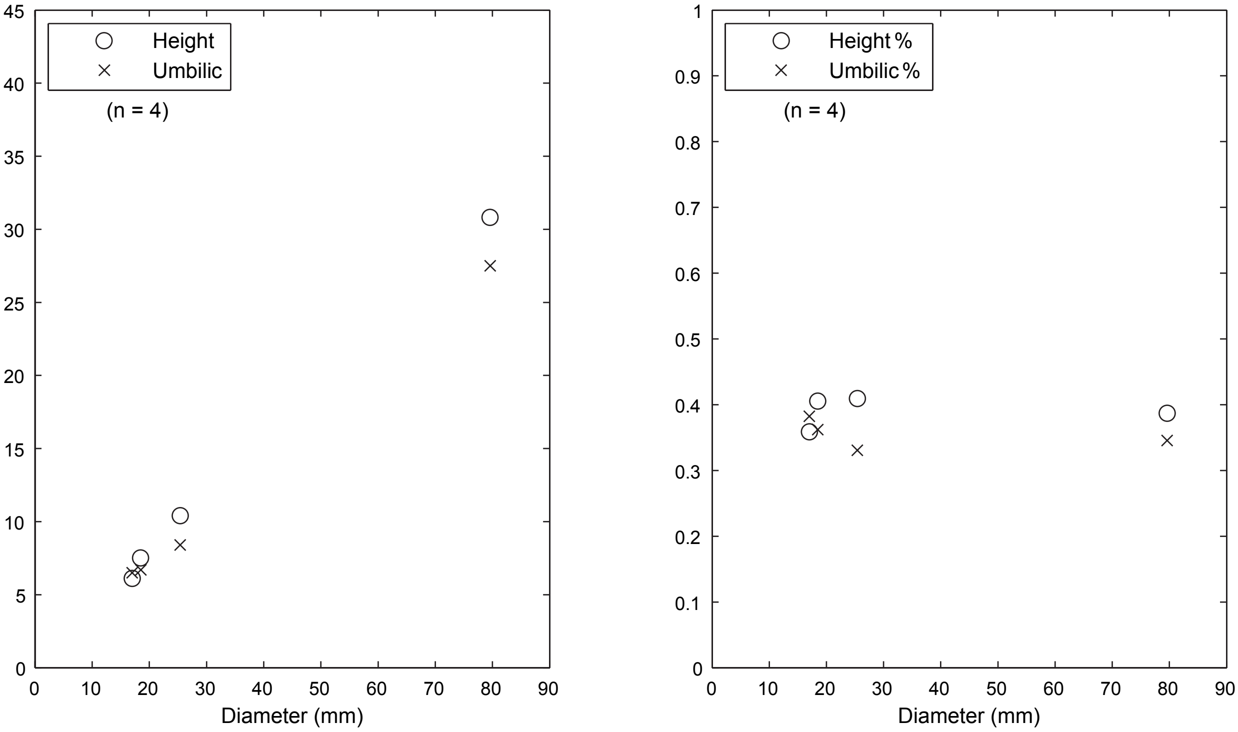

Text-figure 22

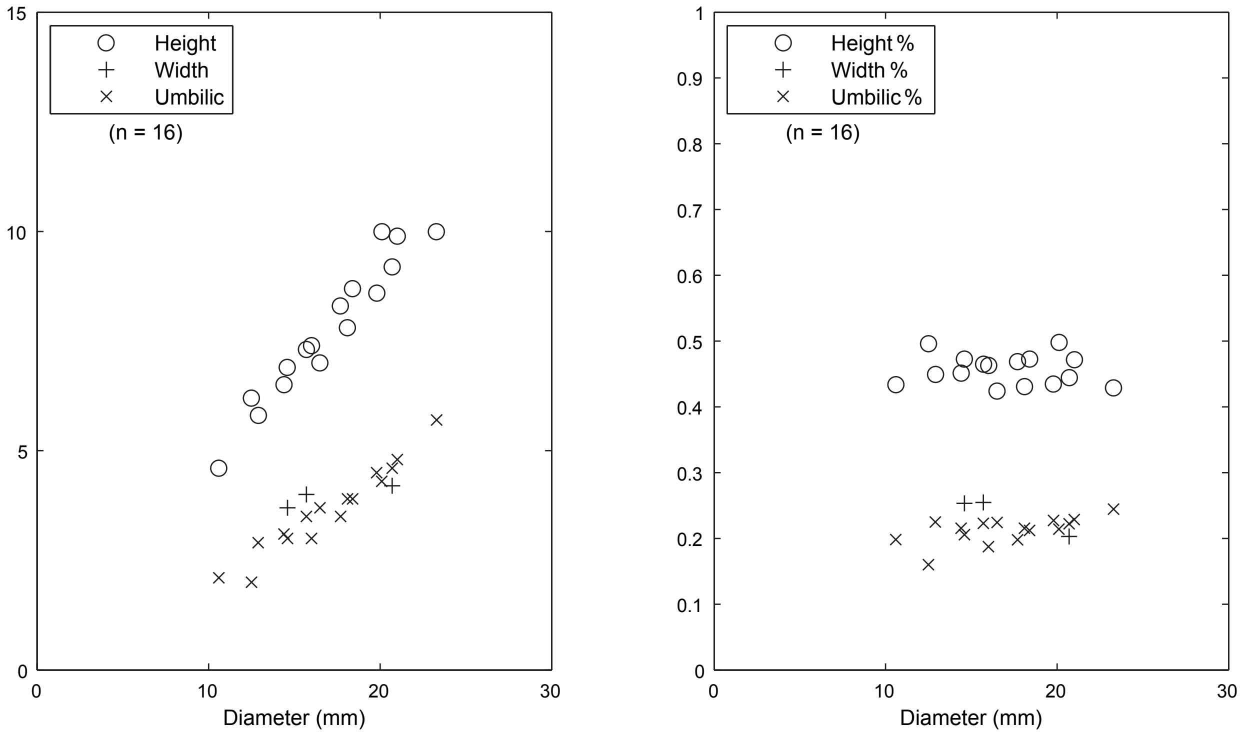

Text-figure 23

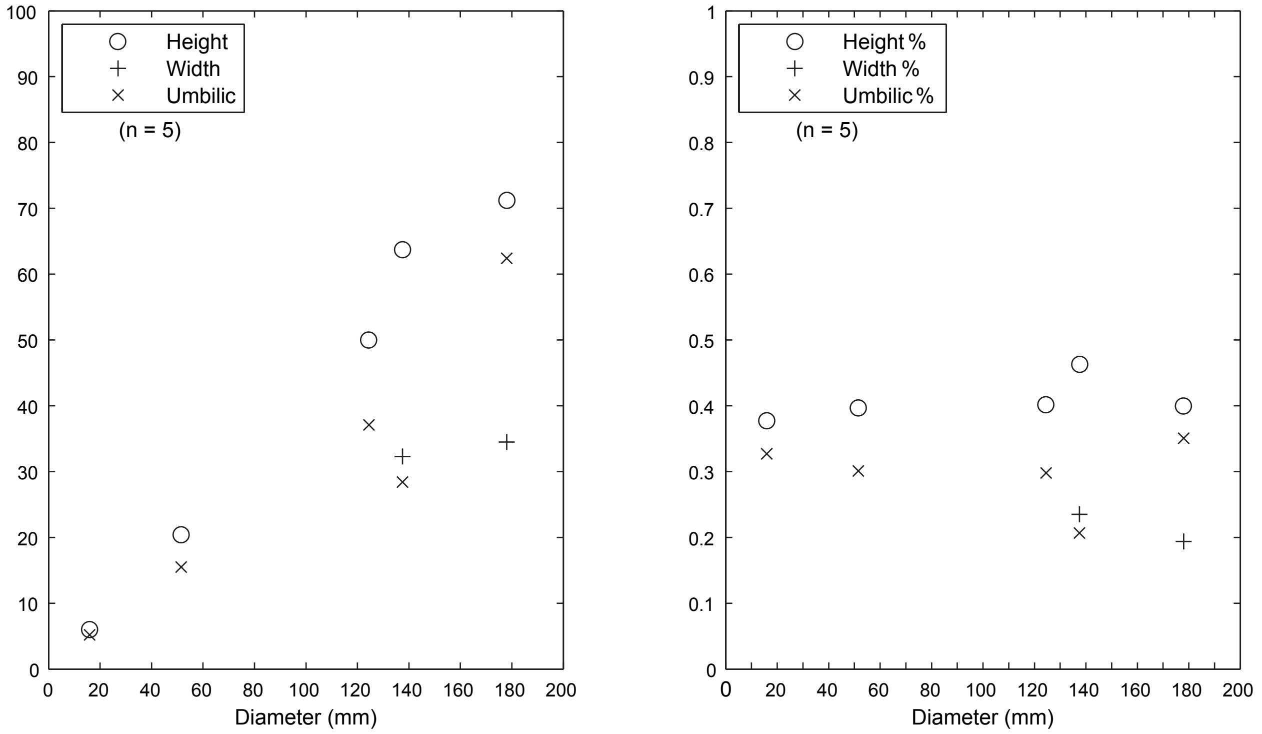

Text-figure 24

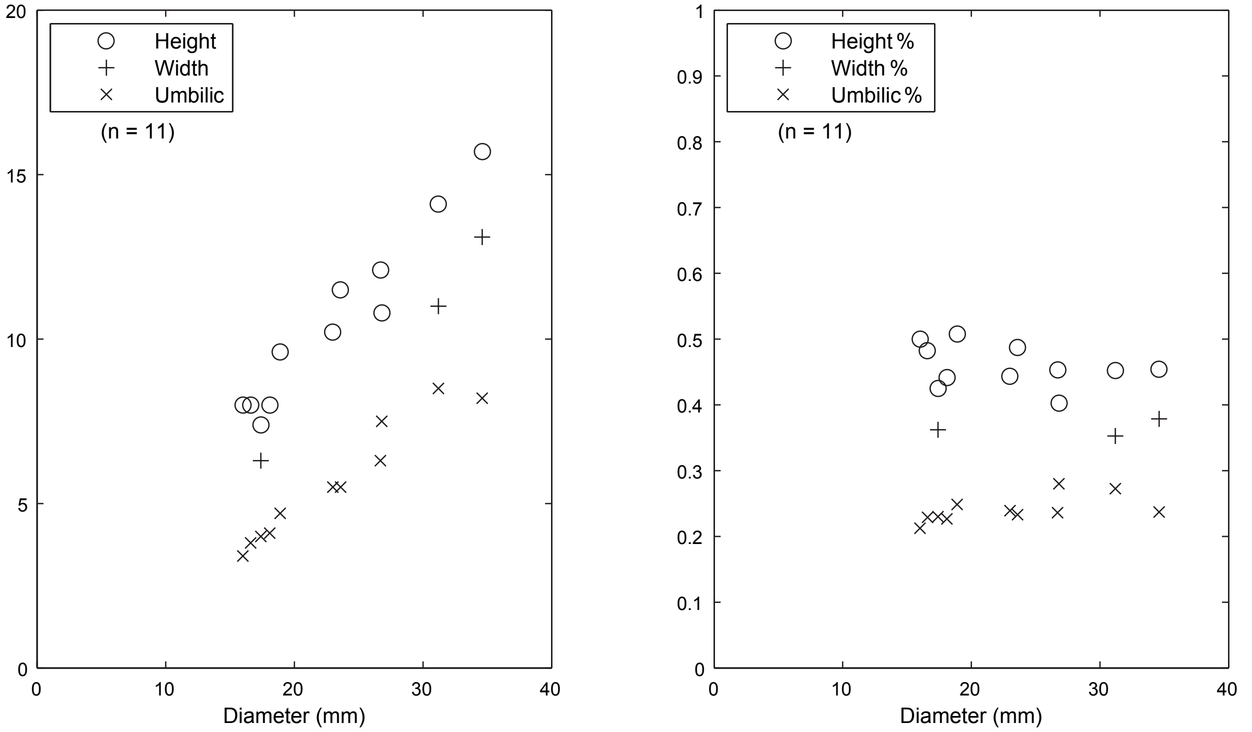

Text-figure 25

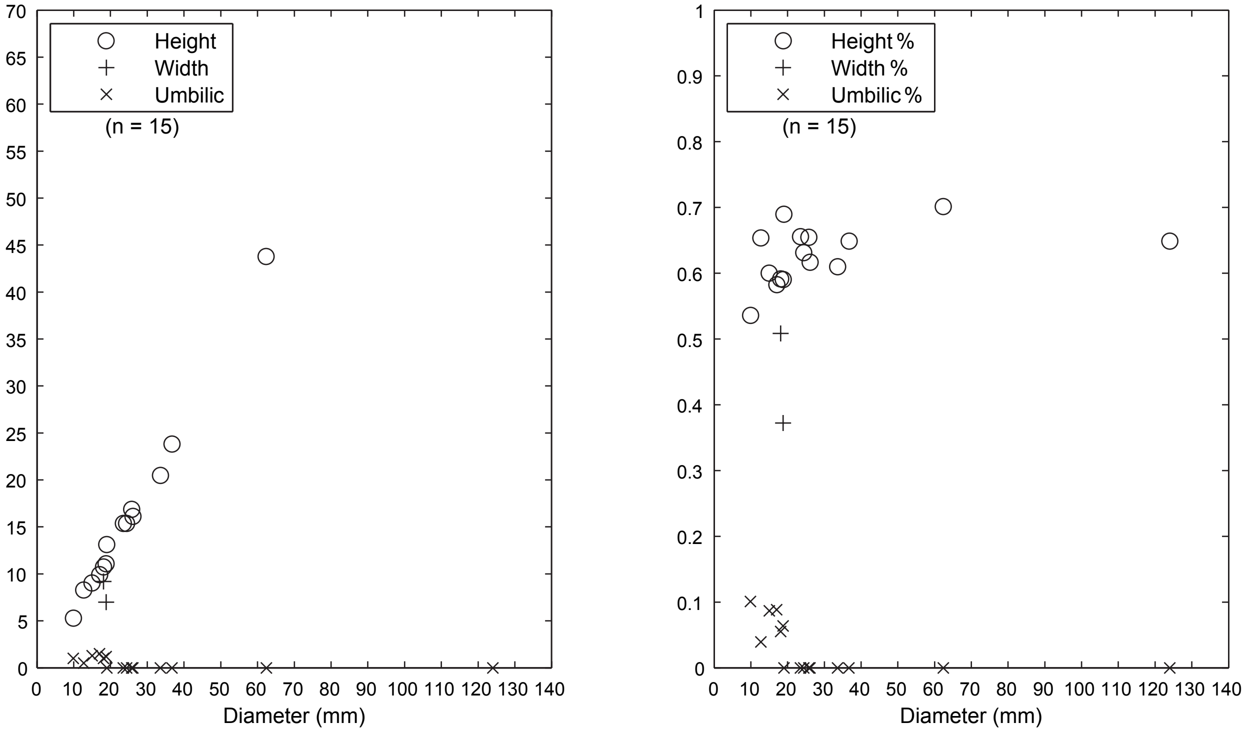

Text-figure 26

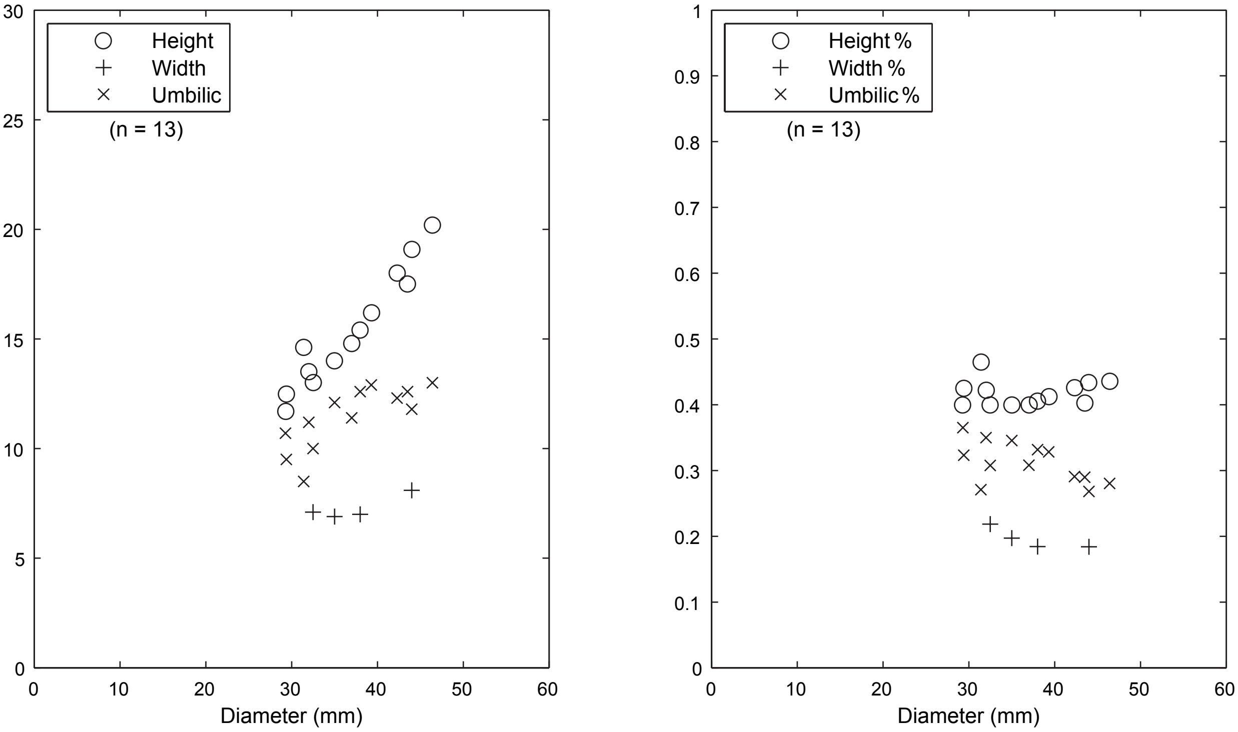

Text-figure 27

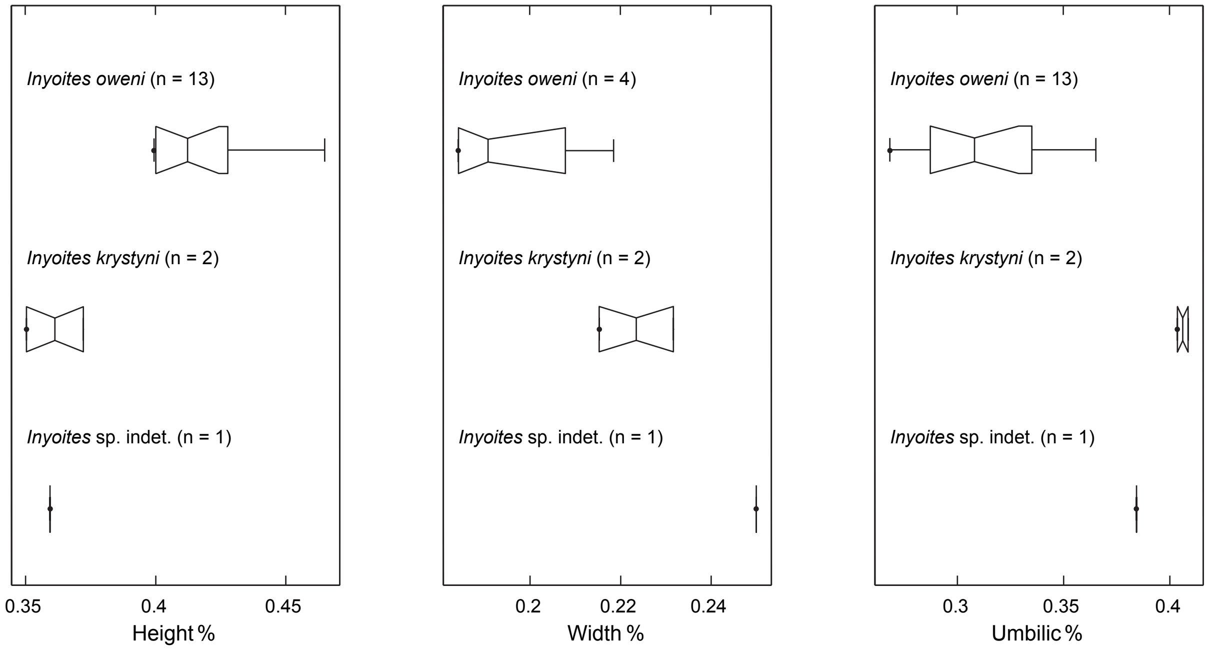

Text-figure 28

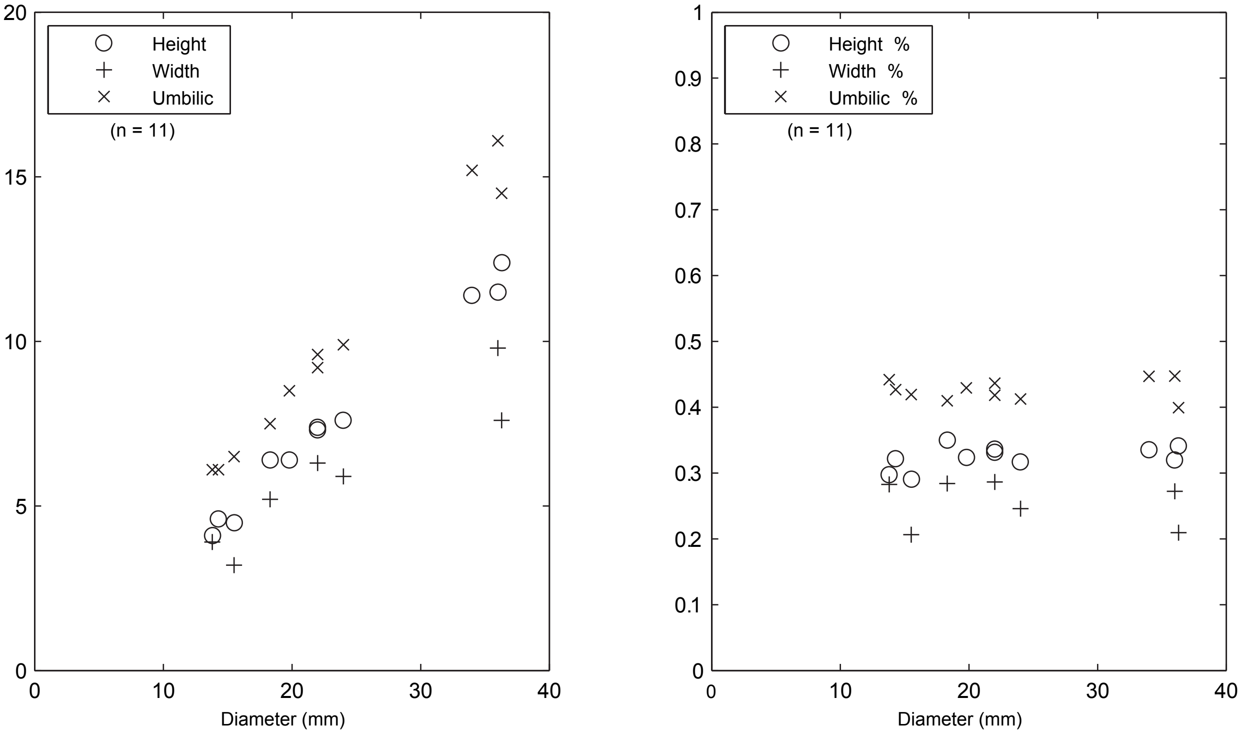

Text-figure 29

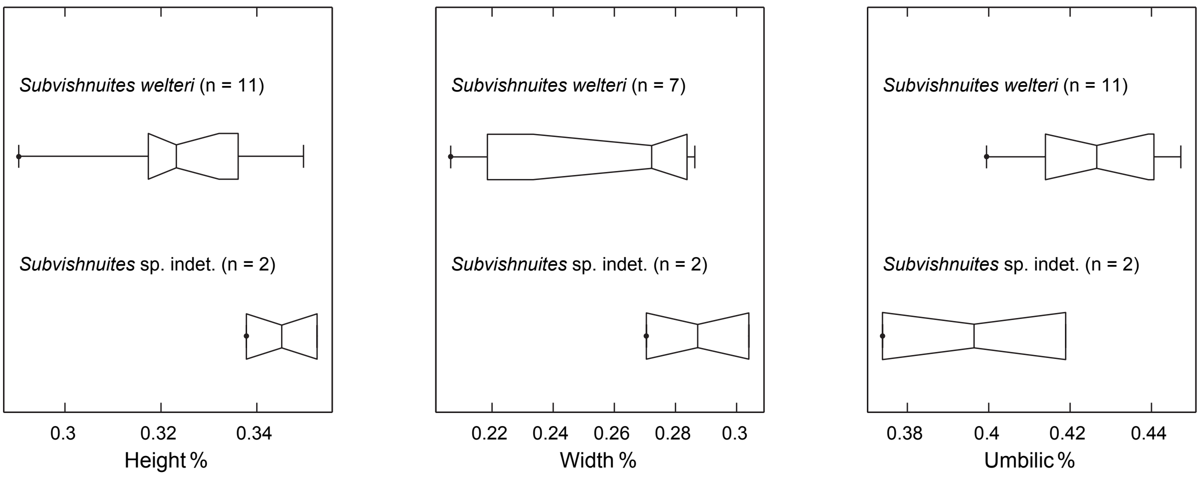

Text-figure 30

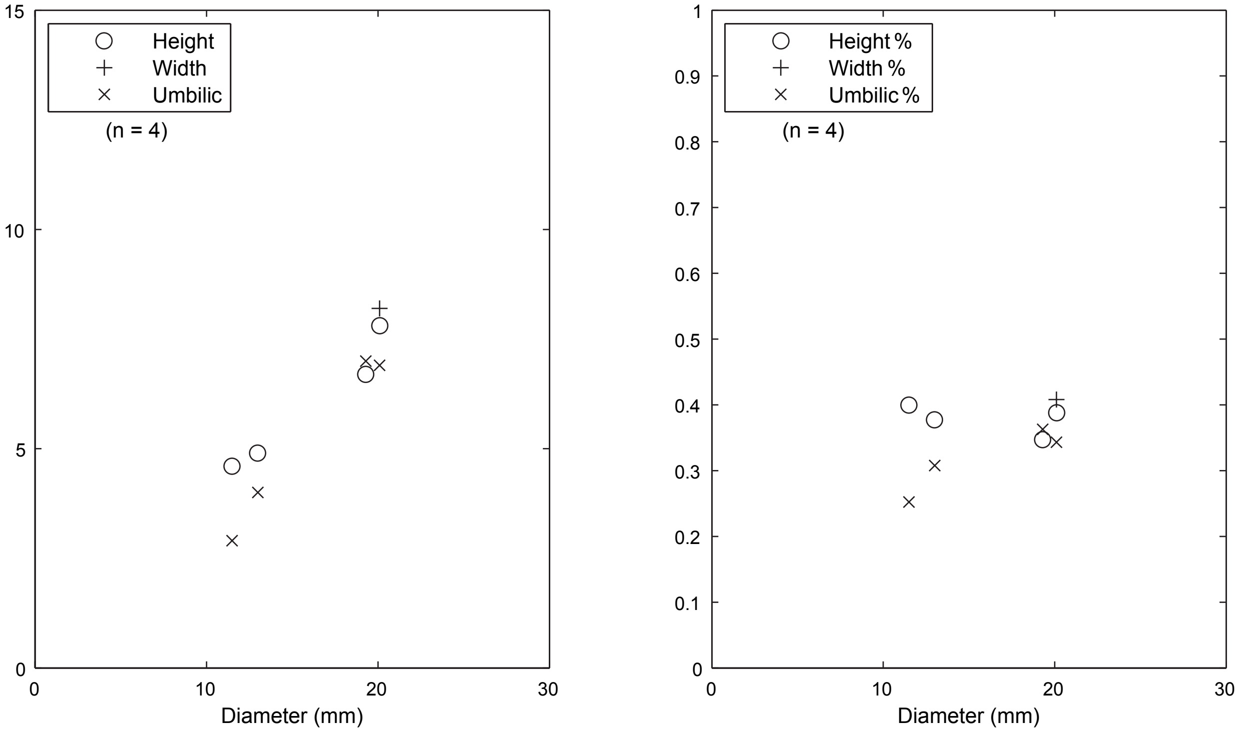

Text-figure 31

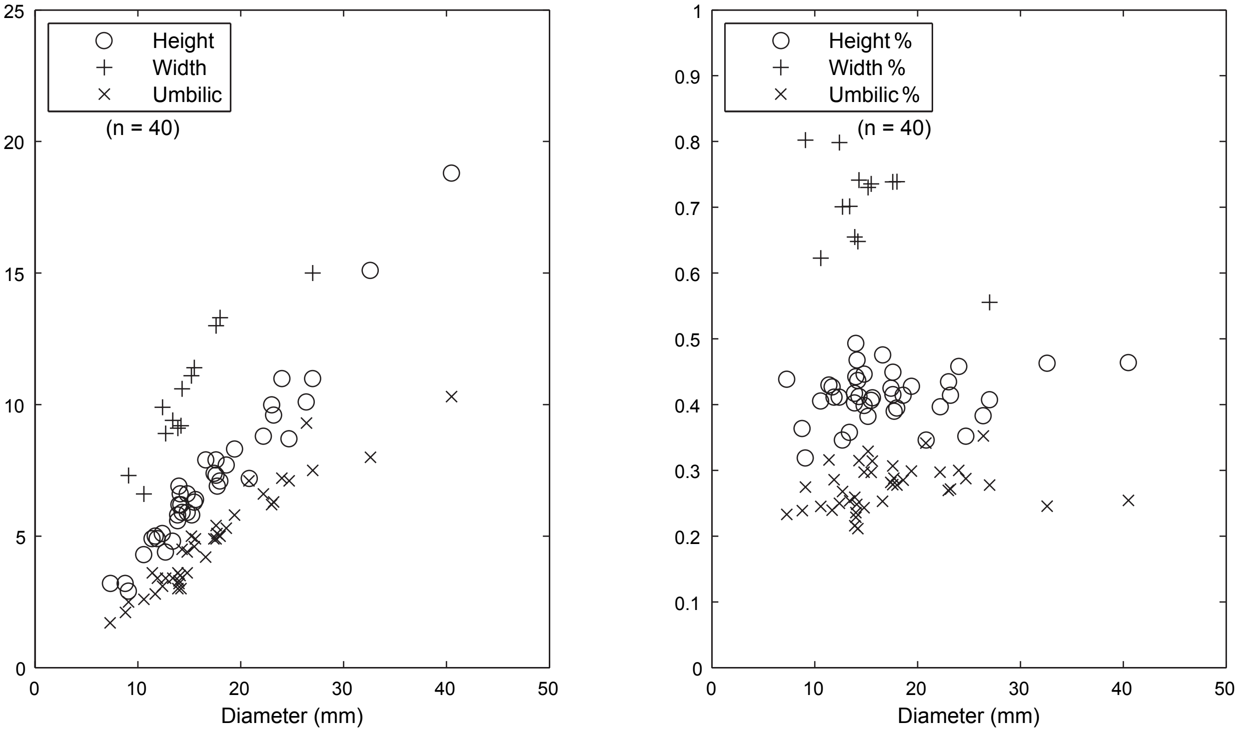

Text-figure 32

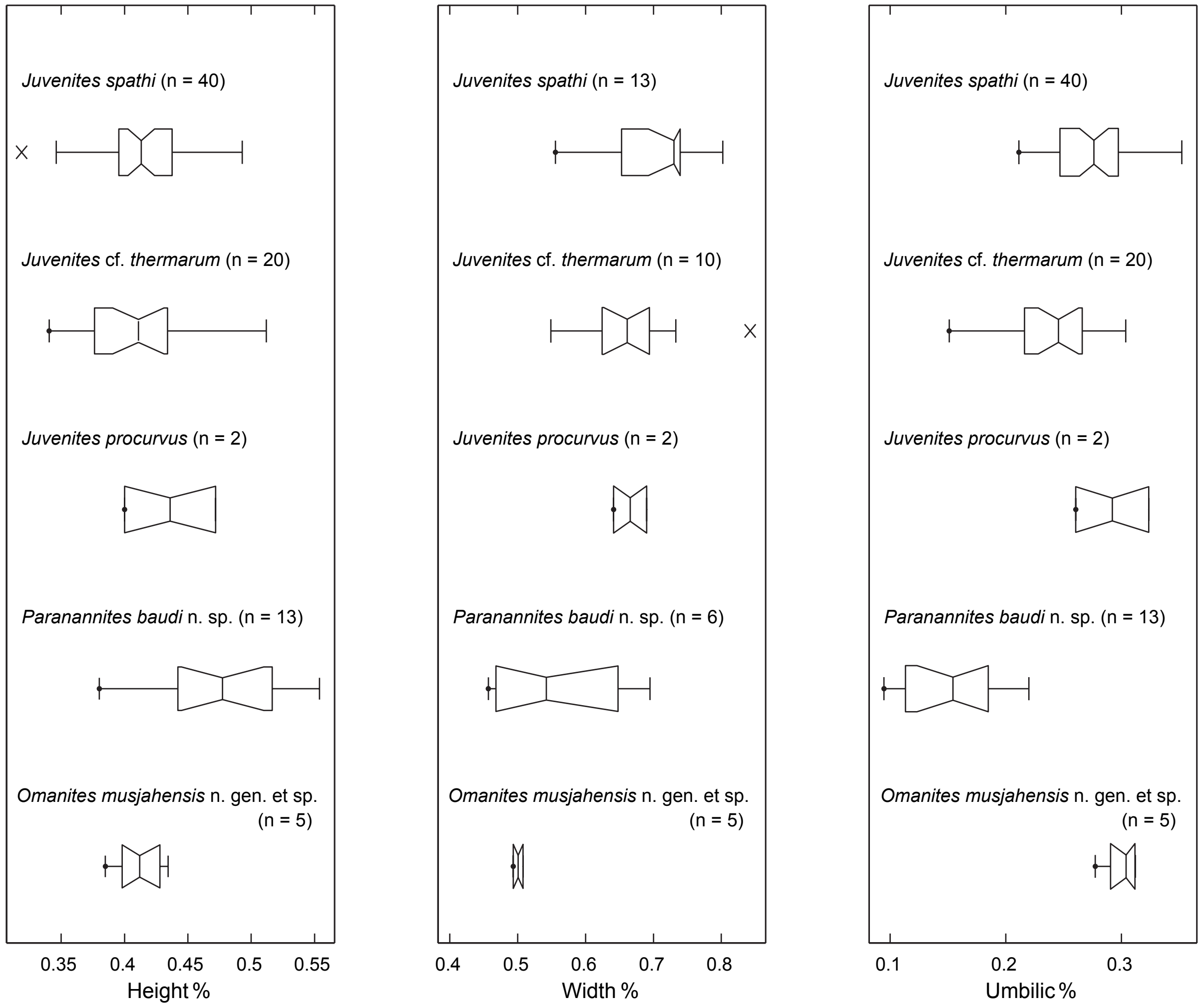

Text-figure 33

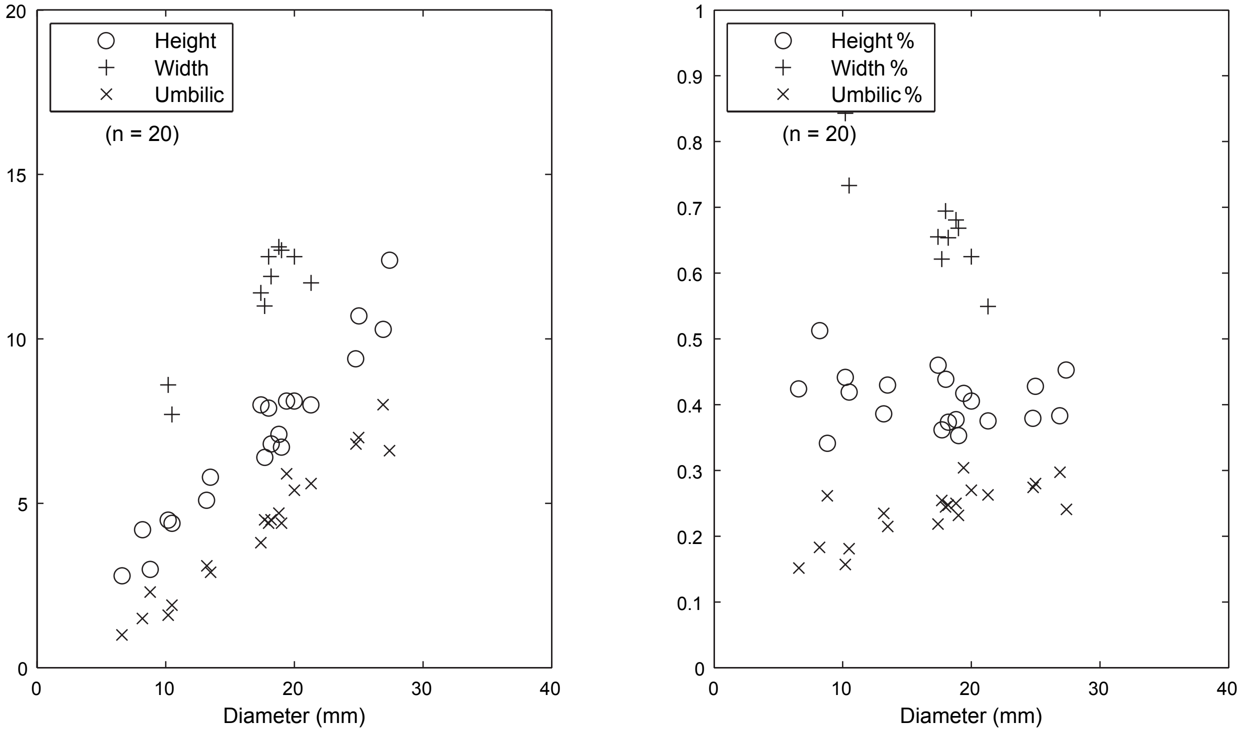

Text-figure 34

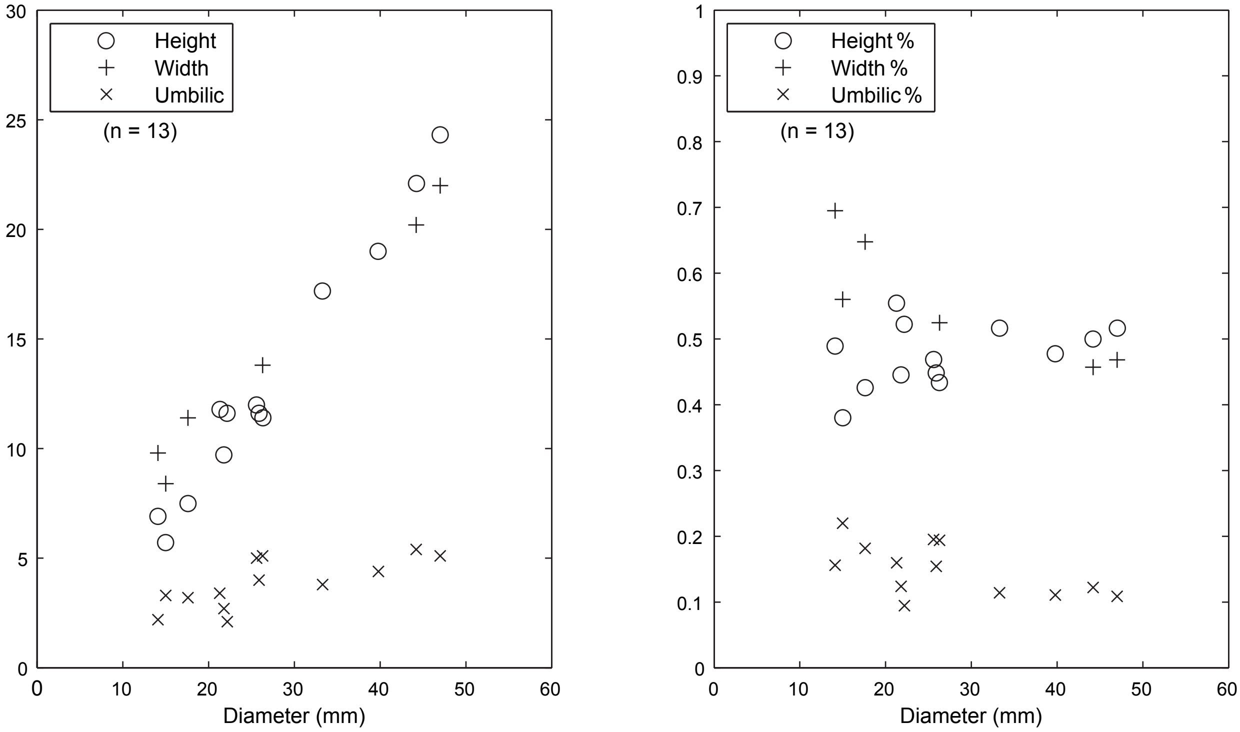

Text-figure 35

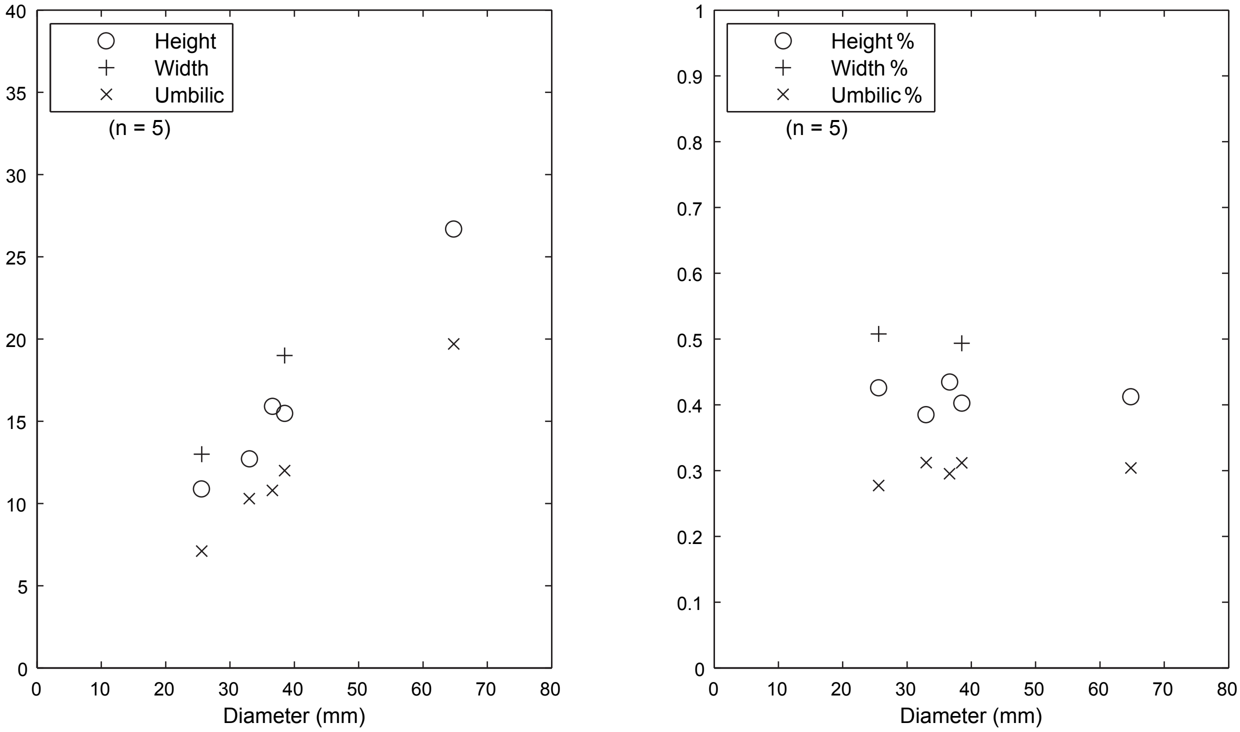

Text-figure 36

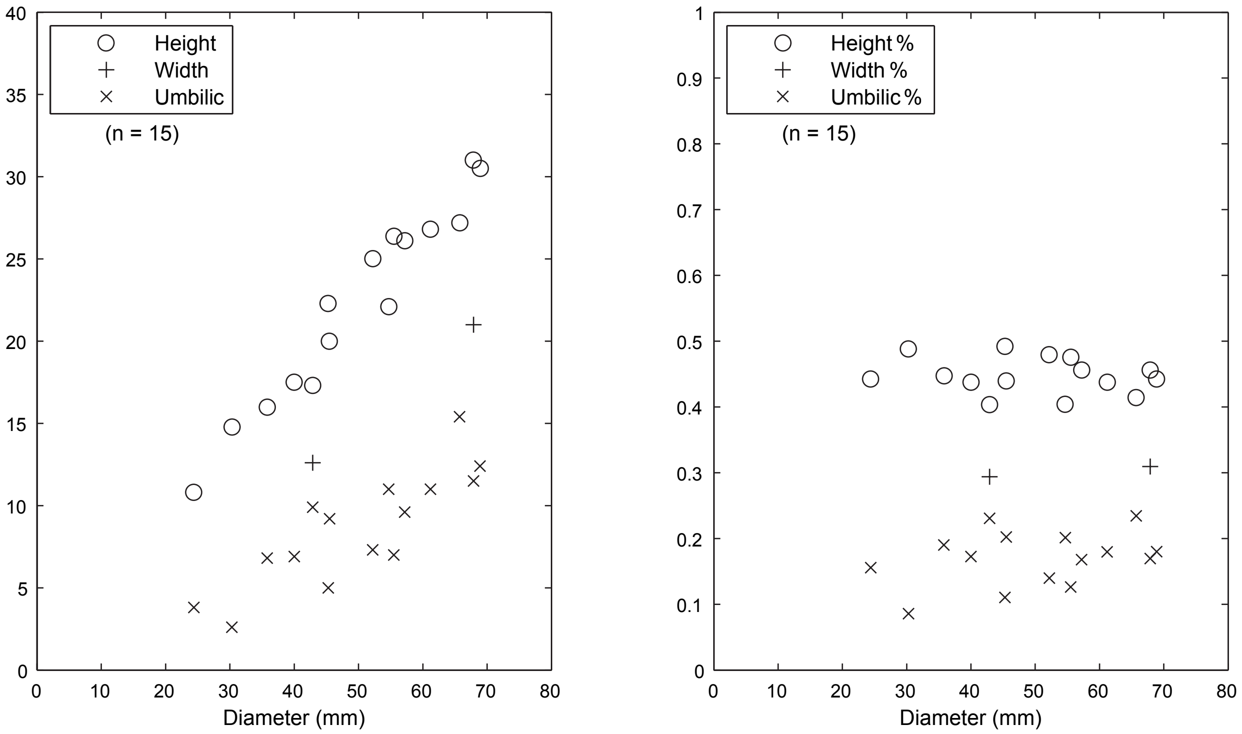

Text-figure 37

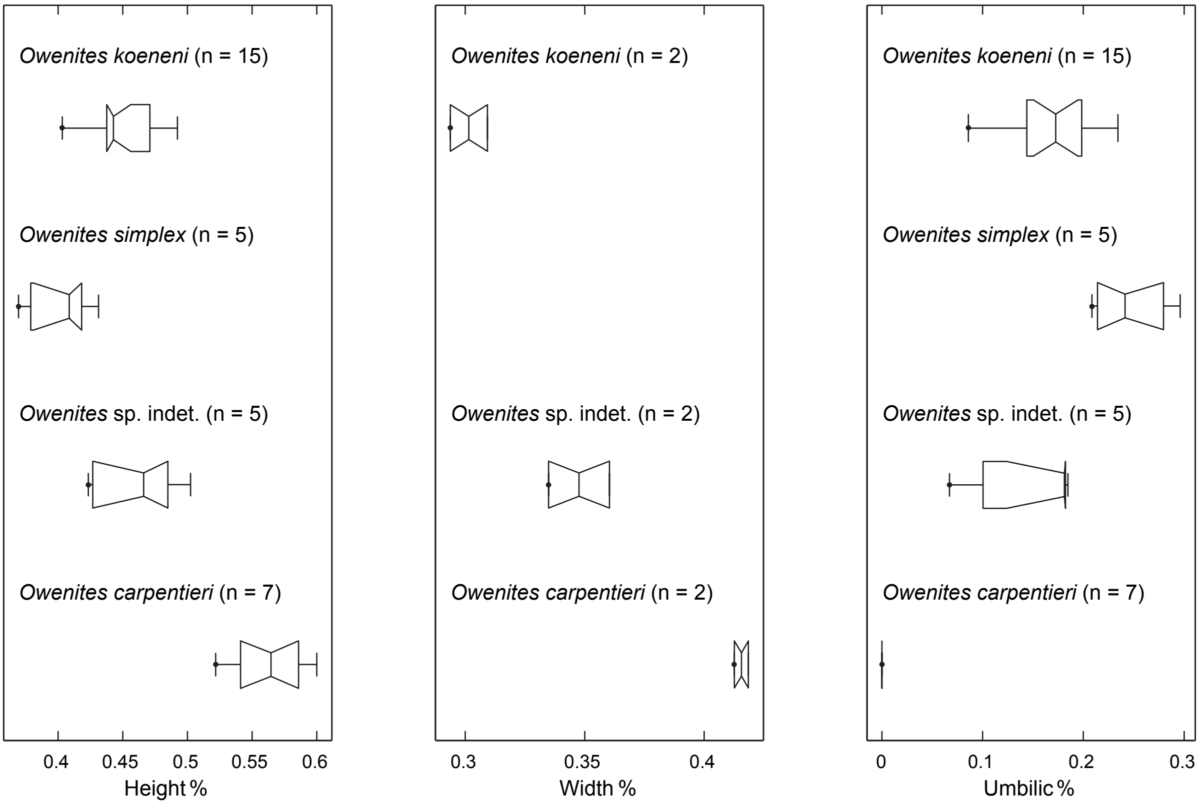

Text-figure 38

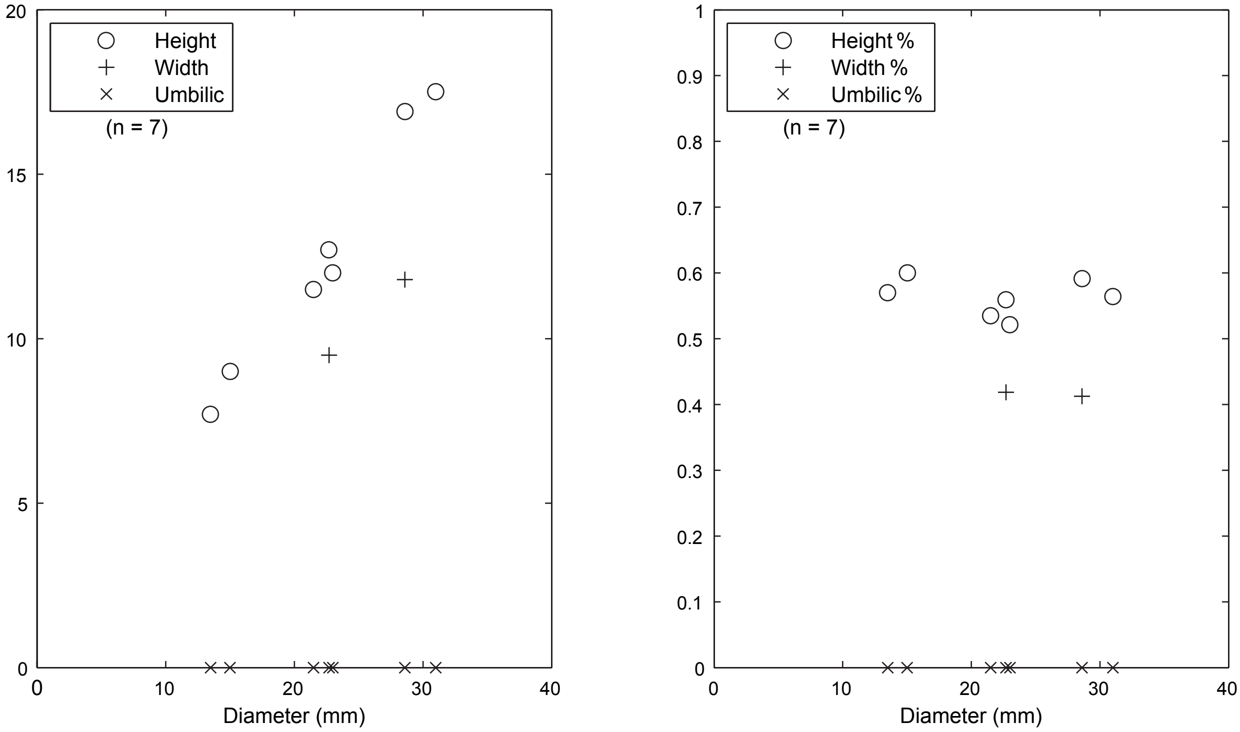

Text-figure 39

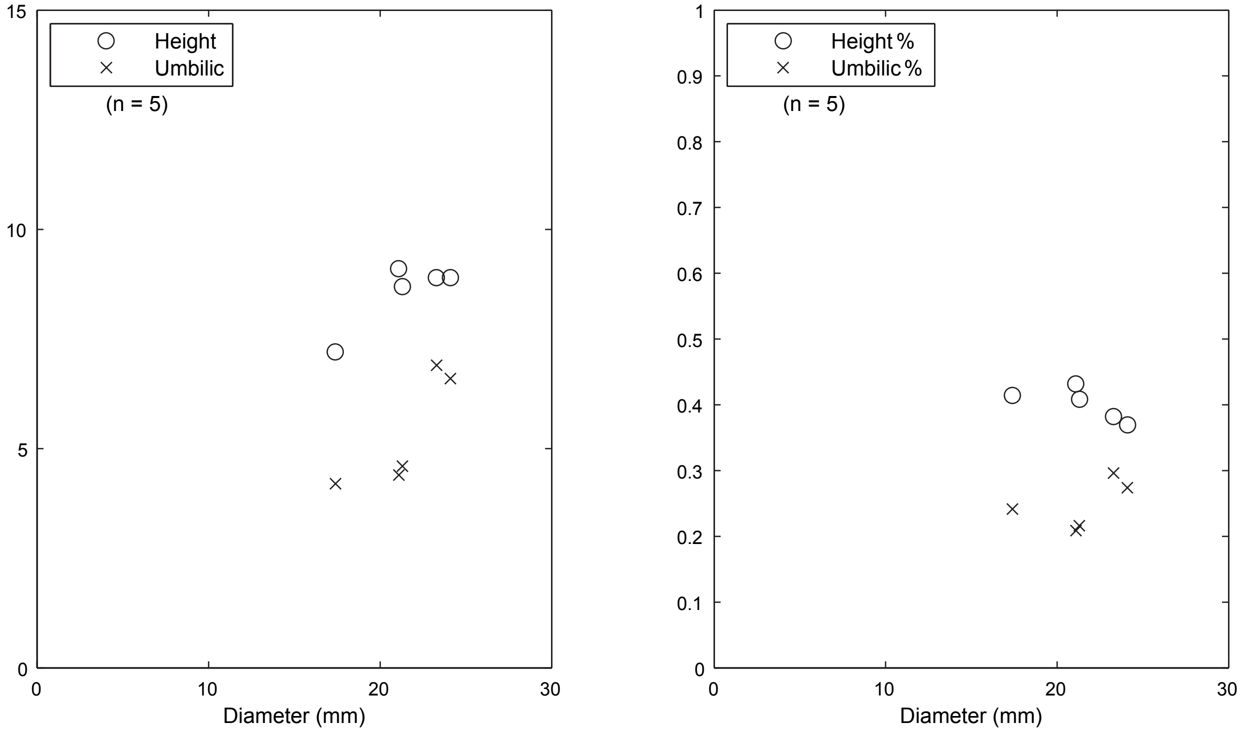

Text-figure 40

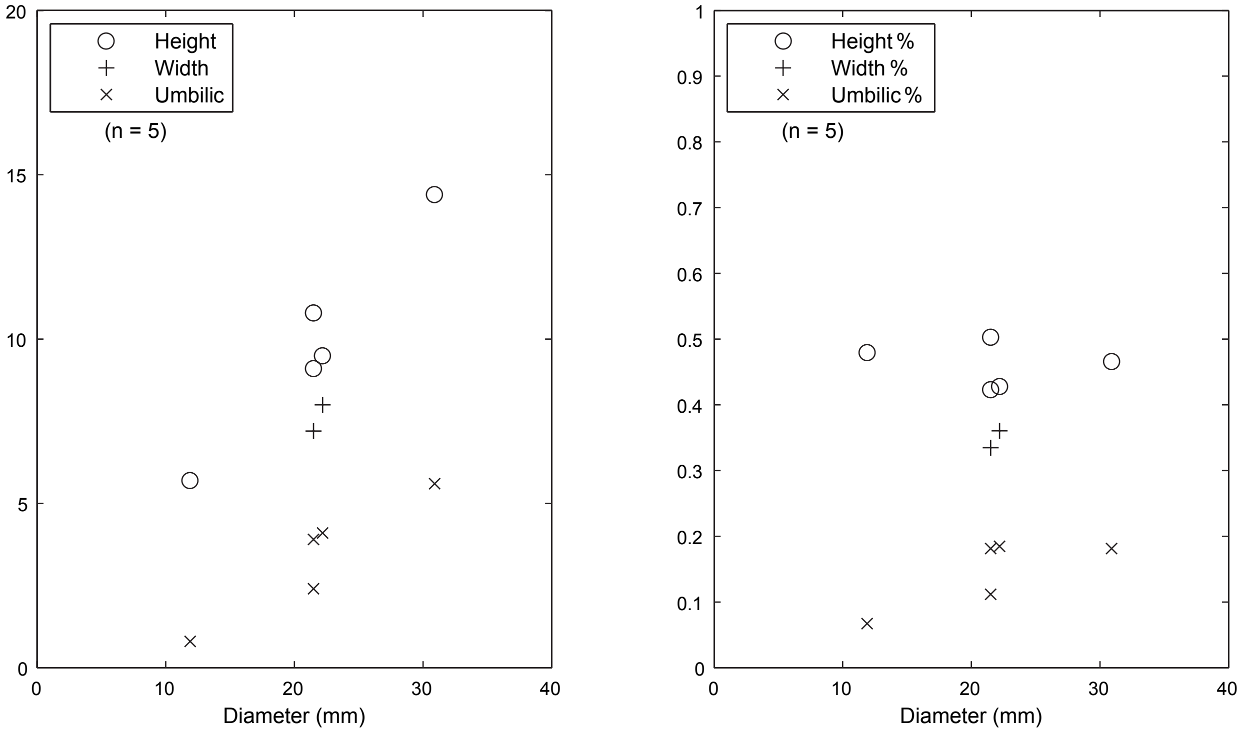

Text-figure 41

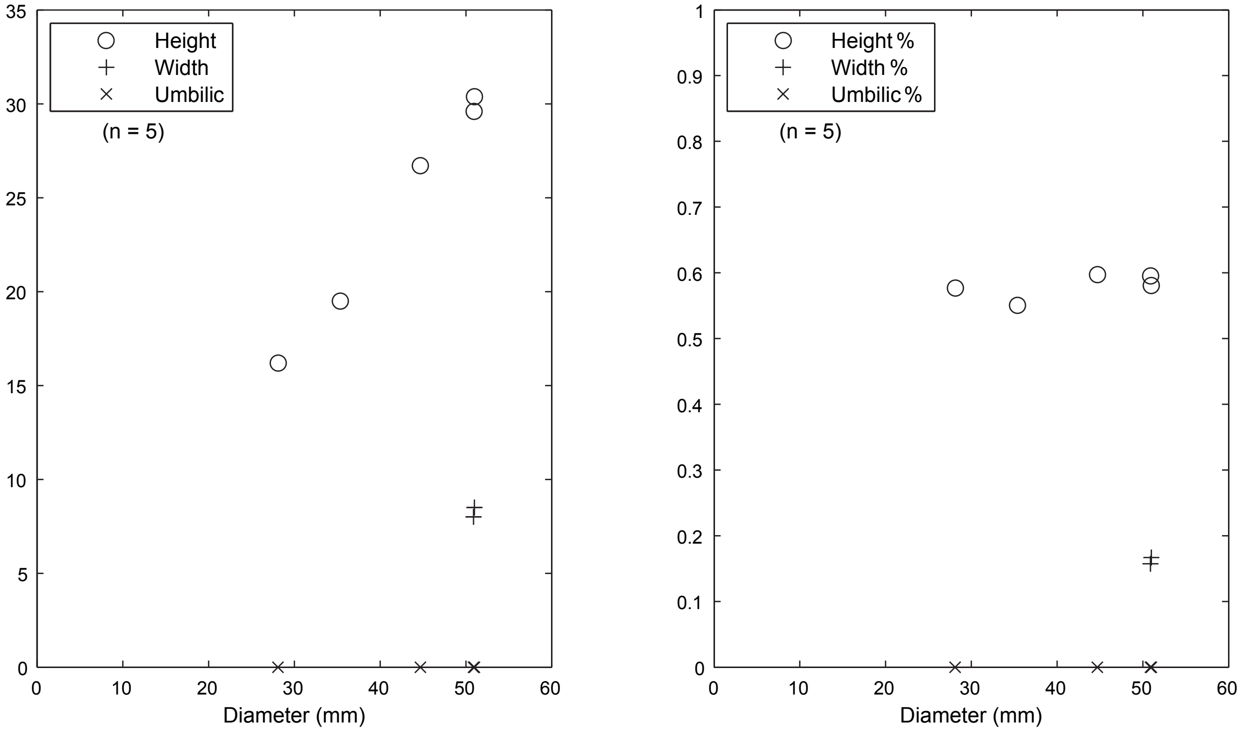

Text-figure 42

PLATE 1

Fig. 1a-c: *Proharpoceras carinatitabulatum* CHAO 1950. PIMUZ 26206. Loc. SA1, Jebel Safra. ?*Nammalites pilatoides* fauna, Smithian.

Fig. 2a-d: *Kashmirites baidi* n. sp. PIMUZ 27304. Loc. Baid-A. *Flemingites rursiradiatus* fauna, Smithian.

Fig. 3a-c: *Nyalamites angustecostatus* (WELTER 1922). PIMUZ 27305. Loc. HB905, Wadi Musjah. *Owenites koeneni* fauna, Smithian.

Fig. 4: *Nyalamites angustecostatus* (WELTER 1922). PIMUZ 27307. Loc. HB904, Wadi Musjah. *Owenites koeneni* fauna, Smithian.

Fig. 5a-b: *Nyalamites angustecostatus* (WELTER 1922). PIMUZ 27306. Loc. HB905, Wadi Musjah. *Owenites koeneni* fauna, Smithian.

Fig. 6: *Nyalamites angustecostatus* (WELTER 1922). PIMUZ 27308. Loc. HB905, Wadi Musjah. *Owenites koeneni* fauna, Smithian. ×3.

Fig. 7a-d: ?Xenoceltitidae gen. indet. PIMUZ 27303. Loc. JS2, Jebel Safra. *Owenites koeneni* fauna, Smithian. 7d ×2.

Fig. 8a-b: *Preflorianites radians* CHAO 1959. PIMUZ 27309. Loc. Baid-B. *Owenites koeneni* fauna, Smithian.

Fig. 9a-d: *Preflorianites radians* CHAO 1959. PIMUZ 27310. Loc. HB912, Jebel Safra. *Owenites koeneni* fauna, Smithian.

All natural size unless otherwise indicated.

Plate 1

1a 1b 1c

2a 2b 2c 2d

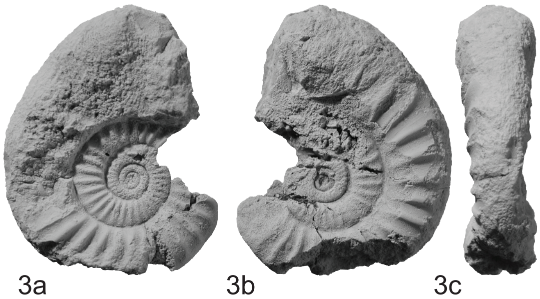

3a 3b 3c

4

5a 5b

6

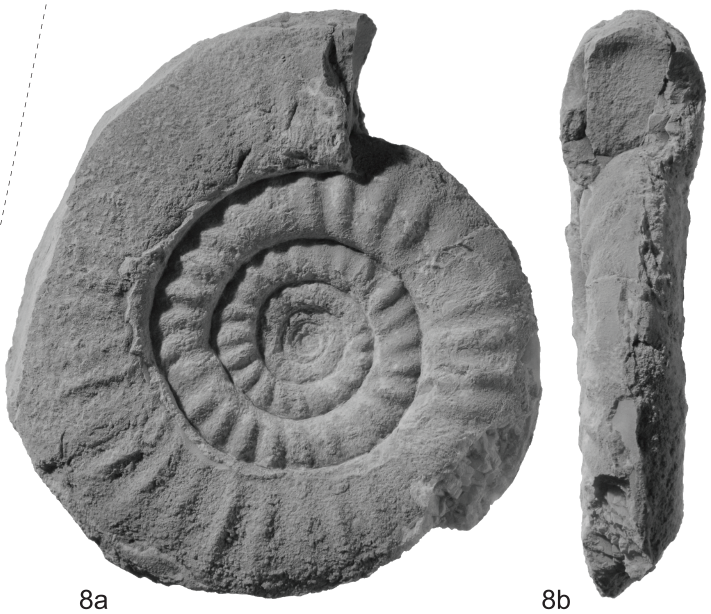

8a 8b

7a

7d

9d

7b 7c

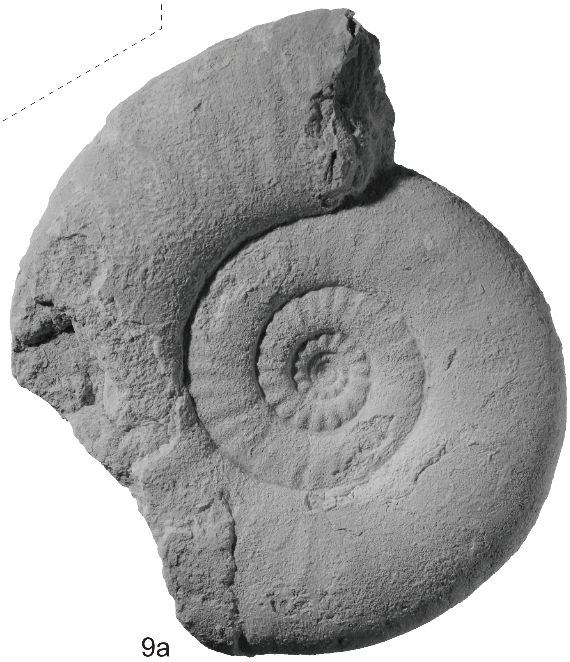

9a

9b 9c

PLATE 2

Fig. 1a-c: *Preflorianites radians* CHAO 1959. PIMUZ 27311. Loc. Baid-B. *Owenites koeneni* fauna, Smithian.

Fig. 2a-c: *Preflorianites radians* CHAO 1959. PIMUZ 27312. Loc. Baid-B. *Owenites koeneni* fauna, Smithian.

Fig. 3a-c: *Preflorianites radians* CHAO 1959. PIMUZ 27313. Loc. Baid-B. *Owenites koeneni* fauna a, Smithian.

Fig. 4a-b: *Preflorianites radians* CHAO 1959. PIMUZ 27317. Loc. Baid-B. *Owenites koeneni* fauna, Smithian.

Fig. 5a-b: *Preflorianites radians* CHAO 1959. PIMUZ 27314. Loc. Baid-B. *Owenites koeneni* fauna, Smithian.

Fig. 6a-c: *Preflorianites radians* CHAO 1959. PIMUZ 27315. Loc. HB912, Jebel Safra. *Owenites koeneni* fauna, Smithian.

Fig. 7a-c: *Preflorianites radians* CHAO 1959. PIMUZ 27316. Loc. HB912, Jebel Safra. *Owenites koeneni* fauna, Smithian.

Fig. 8a-d: *Jinyaceras* cf. *bellum* BRAYARD & BUCHER 2008. PIMUZ 27318. Loc. HB 911. *Baidites hermanni* fauna, Smithian.

Fig. 9a-c: *Jinyaceras* cf. *bellum* BRAYARD & BUCHER 2008. PIMUZ 27319. Loc. HB 911. *Baidites hermanni* fauna, Smithian.

Fig. 10a-b: *Jinyaceras* cf. *bellum* BRAYARD & BUCHER 2008. PIMUZ 27320. Loc. HB 911. *Baidites hermanni* fauna, Smithian.

All natural size unless otherwise indicated.

Plate 2


1a 1b 1c


2a 2b 2c


3a 3b 3c


4a 4b


5a 5b


6a 6b 6c

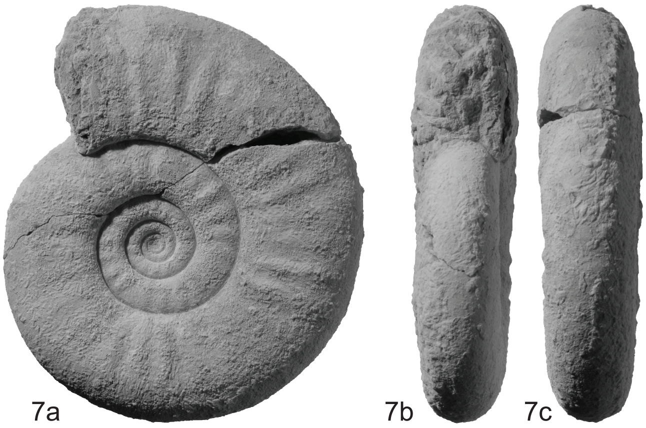
7a 7b 7c


8a 8b 8c 8d


9a 9b 9c


10a 10b

PLATE 3

Fig. 1a-c: *Paranorites jenksi* BRAYARD & BUCHER 2008. PIMUZ 27321. Loc. HB911. *Baidites hermanni* fauna, Smithian.

Fig. 2a-d: *Pseudaspidites* sp. indet. PIMUZ 27325. Loc. Baid-B. *Owenites koeneni* fauna, Smithian. 2d ×2.

Fig. 3a-c: *Pseudaspidites* cf. *muthianus* (KRAFFT & DIENER 1909). PIMUZ 27324. Loc. Baid-G. Smithian. ×0.5.

Fig. 4a-d: *Pseudaspidites* cf. *muthianus* (KRAFFT & DIENER 1909). PIMUZ 27322. Loc. Baid-A. *Flemingites rursiradiatus* fauna, Smithian. 4d ×2.

Fig. 5a-b: *Pseudaspidites* cf. *muthianus* (KRAFFT & DIENER 1909). PIMUZ 27323. Loc. Baid-A. *Flemingites rursiradiatus* fauna, Smithian.

All natural size unless otherwise indicated.

Plate 3

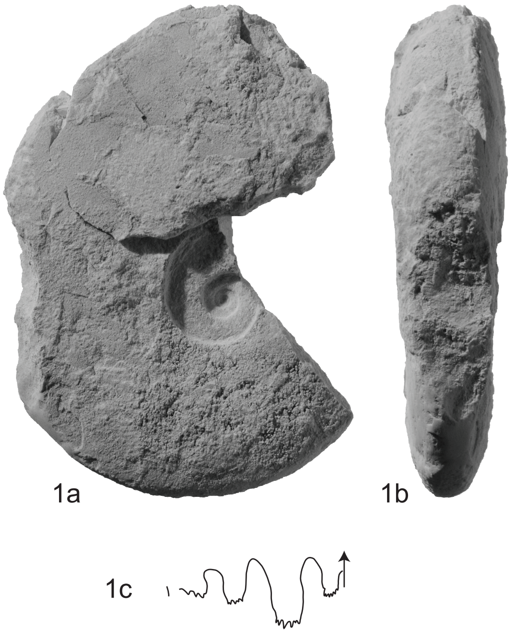

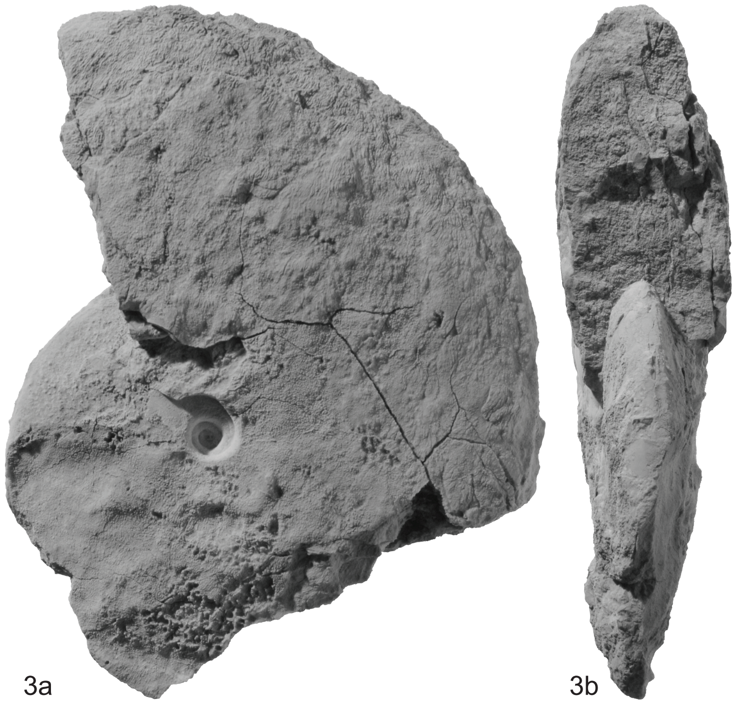

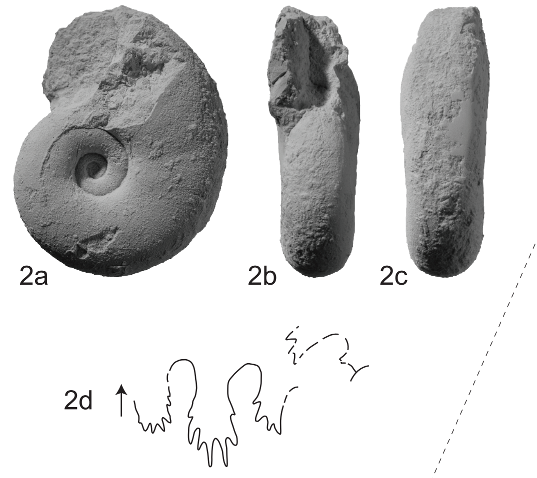

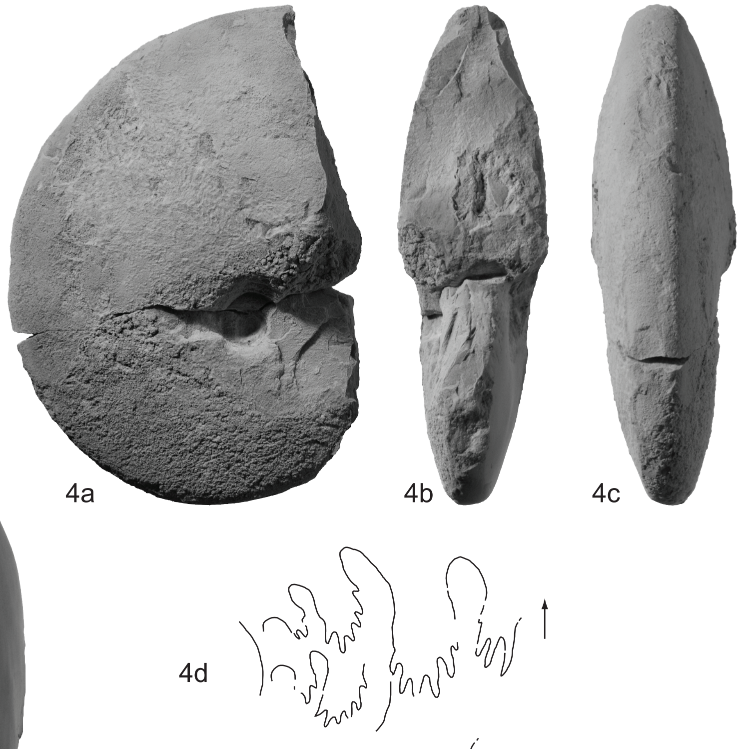

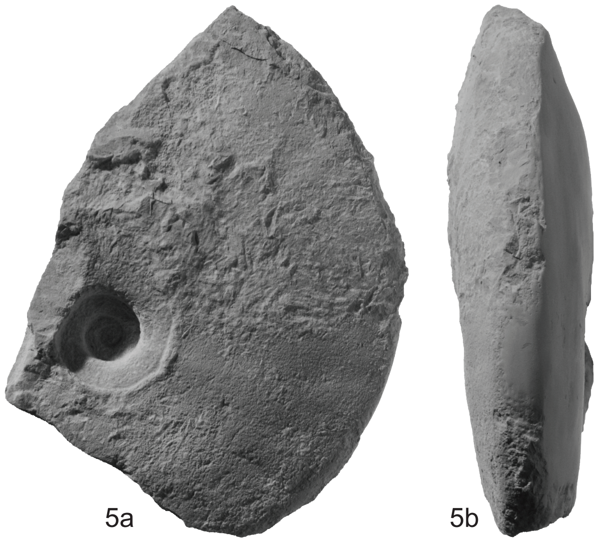

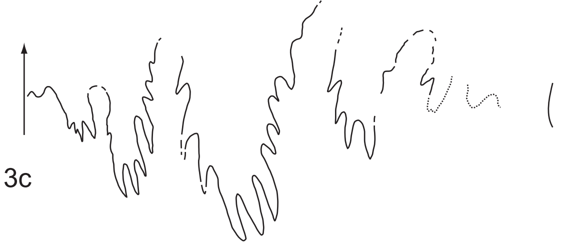

PLATE 4

Fig. 1a-d: *Pseudaspidites planus* n. sp. PIMUZ 27326, holotype. Loc. HB912. *Owenites koeneni* fauna, Smithian.

Fig. 2a-c: *Pseudaspidites planus* n. sp. PIMUZ 27327. Loc. HB912. *Owenites koeneni* fauna, Smithian.

Fig. 3a-c: *Pseudaspidites planus* n. sp. PIMUZ 27328. Loc. HB912. *Owenites koeneni* fauna, Smithian.

Fig. 4a-d: *Pseudaspidites planus* n. sp. PIMUZ 27329. Loc. HB912. *Owenites koeneni* fauna, Smithian.

Fig. 5a-c: *Pseudaspidites planus* n. sp. PIMUZ 27330. Loc. HB912. *Owenites koeneni* fauna, Smithian.

All natural size unless otherwise indicated.

Plate 4

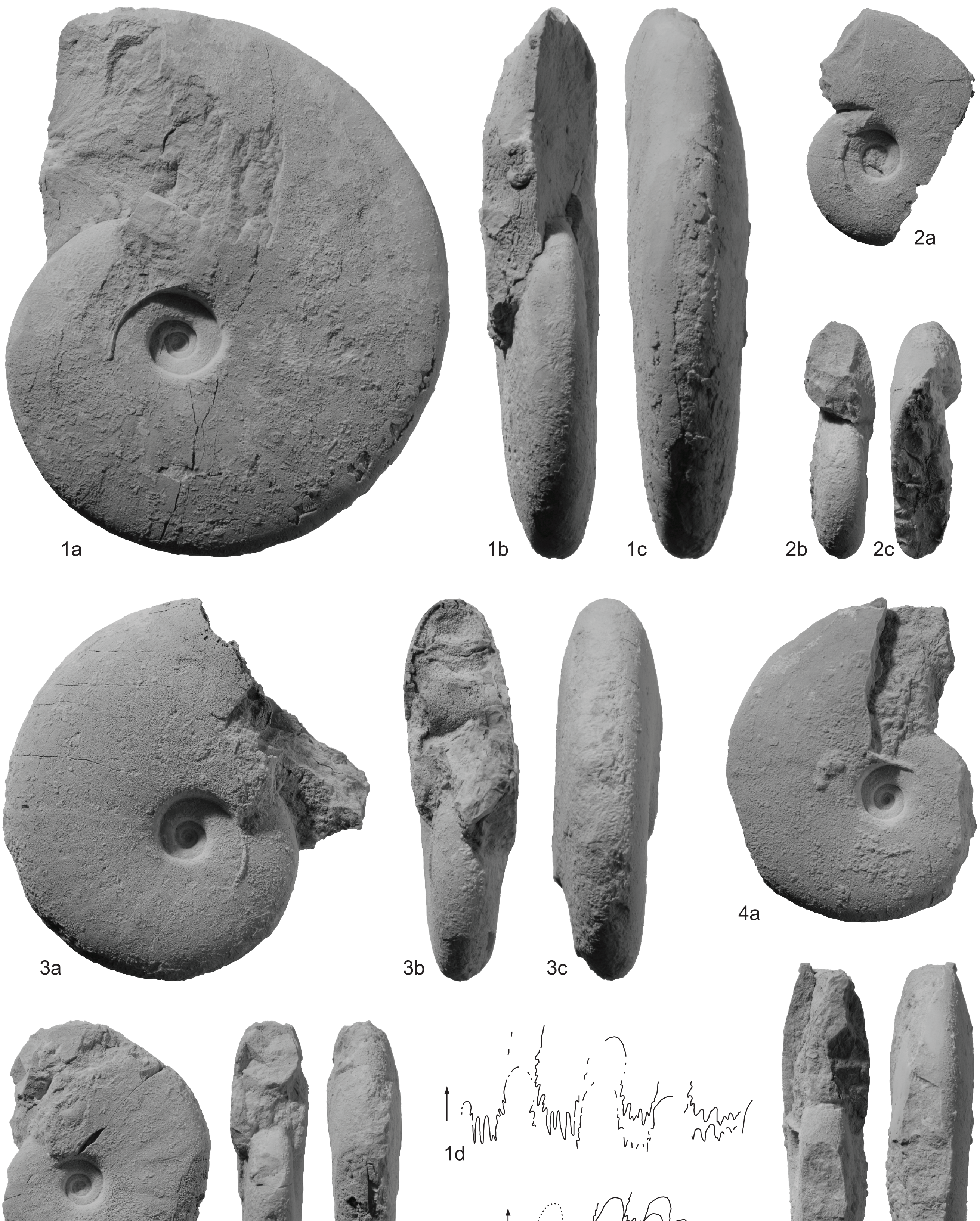

PLATE 5

Fig. 1a-d: *Leyeceras* cf. *rothi* BRAYARD & BUCHER 2008. PIMUZ 27331. Loc. JS4, Jebel Safra. *Owenites koeneni* fauna, Smithian.

Fig. 2a-b: *Leyeceras* cf. *rothi* BRAYARD & BUCHER 2008. PIMUZ 27332. Loc. Baid-B. *Owenites koeneni* fauna, Smithian.

Fig. 3a-c: *Leyeceras* cf. *rothi* BRAYARD & BUCHER 2008. PIMUZ 27333. Loc. HB912, Jebel Safra. *Owenites koeneni* fauna, Smithian.

Fig. 4a-d: *Leyeceras* cf. *rothi* BRAYARD & BUCHER 2008. PIMUZ 27334. Loc. HB912, Jebel Safra. *Owenites koeneni* fauna, Smithian.

Fig. 5a-c: *Leyeceras* cf. *rothi* BRAYARD & BUCHER 2008. PIMUZ 27335. Loc. Baid-B. *Owenites koeneni* fauna, Smithian.

All natural size unless otherwise indicated.

Plate 5


1a


1b


1c


2a


2b


3a


3b


3c

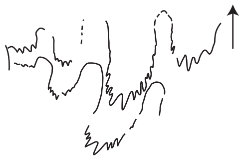
1d


4a


4b


4c


4d


5a


5b


5c

PLATE 6

Fig. 1a-c: *Leyeceras* cf. *rothi* BRAYARD & BUCHER 2008. PIMUZ 27336. Loc. HB912. *Owenites koeneni* fauna, Smithian.

Fig. 2a-c: *Leyeceras* cf. *rothi* BRAYARD & BUCHER 2008. PIMUZ 27337. Loc. Baid-B. *Owenites koeneni* fauna, Smithian.

Fig. 3a-c: *Leyeceras* cf. *rothi* BRAYARD & BUCHER 2008. PIMUZ 27338. Loc. Baid-B. *Owenites koeneni* fauna, Smithian.

Fig. 4a-c: *Lucasites involutus* n. gen. et sp. PIMUZ 27339, holotype. Loc. JS11a, Jebel Safra. *Rohillites omanensis* fauna, Smithian.

All natural size unless otherwise indicated.

Plate 6


1a


1b


1c


2a


2b


2c


3a


3b

3c

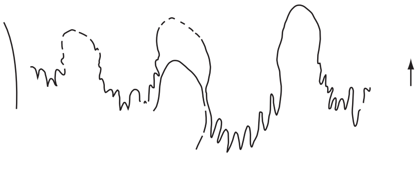


4a


4b


4c

PLATE 7

Fig. 1a-c: *Guodunites monneti* BRAYARD & BUCHER 2008. PIMUZ 27250. Loc. HB900, Wadi Musjah. *Owenites koeneni* fauna, Smithian.

Fig. 2: *Guodunites monneti* BRAYARD & BUCHER 2008. PIMUZ 27251. Loc. HB908, Wadi Musjah. *Owenites koeneni* fauna, Smithian.

Fig. 3a-c: *Guodunites monneti* BRAYARD & BUCHER 2008. PIMUZ 27249. Loc. HB900, Wadi Musjah. *Owenites koeneni* fauna, Smithian.

Fig. 4a-b: *Guodunites monneti* BRAYARD & BUCHER 2008. PIMUZ 27252. Loc. WM7, Wadi Musjah. *Owenites koeneni* fauna, Smithian.

Fig. 5: *Guodunites monneti* BRAYARD & BUCHER 2008. PIMUZ 27248. Loc. HB900, Wadi Musjah. *Owenites koeneni* fauna, Smithian.

All natural size unless otherwise indicated.

Plate 7

PLATE 8

Fig. 1a-c: *Dieneroceras* cf. *dieneri* HYATT & SMITH 1905. PIMUZ 27344. Loc. HB912, Jebel Safra. *Owenites koeneni* fauna, Smithian.

Fig. 2a-c: *Dieneroceras* cf. *dieneri* HYATT & SMITH 1905. PIMUZ 27345. Loc. Baid-B, Baid. *Owenites koeneni* fauna, Smithian.

Fig. 3a-b: *Dieneroceras* cf. *dieneri* HYATT & SMITH 1905. PIMUZ 27343. Loc. HB912, Jebel Safra. *Owenites koeneni* fauna, Smithian.

Fig. 4a-d: *Dieneroceras* cf. *dieneri* HYATT & SMITH 1905. PIMUZ 27342. Loc. HB900, Wadi Musjah. *Owenites koeneni* fauna, Smithian.

Fig. 5a-c: *Safraites simplex* n. gen. et sp. PIMUZ 27395, holotype. Loc. JS13, Jebel Safra. *Nammalites pilatoides* fauna, Smithian.

Fig. 6a-b: *Safraites simplex* n. gen. et sp. PIMUZ 27396. Loc. JS13, Jebel Safra. *Nammalites pilatoides* fauna, Smithian.

Fig. 7a-c: *Safraites simplex* n. gen. et sp. PIMUZ 27397. Loc. JS13, Jebel Safra. *Nammalites pilatoides* fauna, Smithian. 6d ×2.

Fig. 8a-c: *Safraites simplex* n. gen. et sp. PIMUZ 27398. Loc. JS13, Jebel Safra. *Nammalites pilatoides* fauna, Smithian.

Fig. 9: *Safraites simplex* n. gen. et sp. PIMUZ 27400. Loc. JS13, Jebel Safra. *Nammalites pilatoides* fauna, Smithian. ×2.

Fig. 10: *Safraites simplex* n. gen. et sp. PIMUZ 27399. Loc. JS13, Jebel Safra. *Nammalites pilatoides* fauna, Smithian. ×2.

Fig. 11a-b: *Lucasites evolutus* n. gen. et sp. PIMUZ 27340, holotype. Loc. JS11b, Jebel Safra. *Rohillites omanensis* fauna, Smithian.

Fig. 12: *?Meekoceras* sp. indet. PIMUZ 27341. Loc. JS13, Jebel Safra. *Nammalites pilatoides* fauna, Smithian.

All natural size unless otherwise indicated.

Plate 8

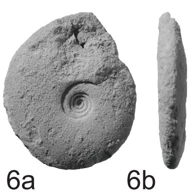

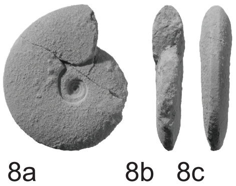

7c 

9 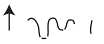

10 

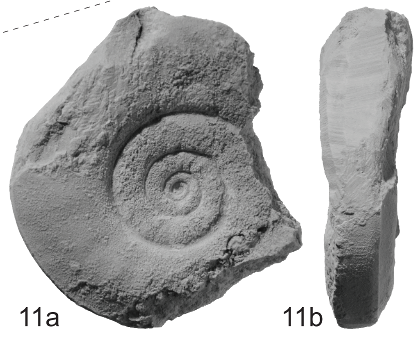

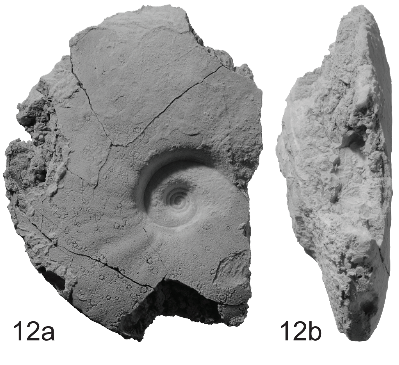

PLATE 9

Fig. 1a-c: *Dieneroceras* cf. *dieneri* HYATT & SMITH 1905. PIMUZ 27346. Loc. HB912, Jebel Safra. *Owenites koeneni* fauna, Smithian.

Fig. 2a-c: *Dieneroceras* cf. *dieneri* HYATT & SMITH 1905. PIMUZ 27347. Loc. HB912, Jebel Safra. *Owenites koeneni* fauna, Smithian.

Fig. 3: *Dieneroceras* cf. *dieneri* HYATT & SMITH 1905. PIMUZ 27348. Loc. HB912, Jebel Safra. *Owenites koeneni* fauna, Smithian.

Fig. 4a-b: *Dieneroceras* cf. *dieneri* HYATT & SMITH 1905. PIMUZ 27349. Loc. HB912, Jebel Safra. *Owenites koeneni* fauna, Smithian.

Fig. 5a-c: *Dieneroceras* cf. *dieneri* HYATT & SMITH 1905. PIMUZ 27350. Loc. HB912, Jebel Safra. *Owenites koeneni* fauna, Smithian.

Fig. 6a-b: *Dieneroceras* cf. *dieneri* HYATT & SMITH 1905. PIMUZ 27351. Loc. HB912, Jebel Safra. *Owenites koeneni* fauna, Smithian.

Fig. 7a-b: *Dieneroceras* cf. *dieneri* HYATT & SMITH 1905. PIMUZ 27352. Loc. HB912, Jebel Safra. *Owenites koeneni* fauna, Smithian.

All natural size unless otherwise indicated.

Plate 9

1a

1b

1c

2a

2b

2c

3

4a

4b

5a

5b

5c

6a

6b

7a

7b

PLATE 10

Fig. 1a-c: *Dieneroceras* cf. *dieneri* HYATT & SMITH 1905. PIMUZ 27353. Loc. HB912, Jebel Safra. *Owenites koeneni* fauna, Smithian.

Fig. 2a-c: *Dieneroceras* cf. *dieneri* HYATT & SMITH 1905. PIMUZ 27354. Loc. Baid-B. *Owenites koeneni* fauna, Smithian.

Fig. 3a-d: *Dieneroceras* sp. indet. PIMUZ 27355. Loc. JS8, Jebel Safra. *Owenites koeneni* fauna, Smithian.

Fig. 4a-b: *Baidites hermanni* n. gen. et sp. PIMUZ 27356. Loc. HB911, Baid. *Baidites hermanni* fauna, Smithian.

Fig. 5: *Baidites hermanni* n. gen. et sp. PIMUZ 27357. Loc. HB911, Baid. *Baidites hermanni* fauna, Smithian. ×0.75

All natural size unless otherwise indicated.

Plate 10


1a


1b


1c


3a


3b


2a


2b


2c


3c


3d


5


4a


4b

PLATE 11

Fig. 1a-e: *Baidites hermanni* n. gen. et sp. PIMUZ 27358, holotype. Loc. HB911, Baid. *Baidites hermanni* fauna, Smithian. 1e ×1.5.

Fig. 2a-d: *Baidites hermanni* n. gen. et sp. PIMUZ 27359. Loc. HB911, Baid. *Baidites hermanni* fauna, Smithian.

Fig. 3: *Baidites hermanni* n. gen. et sp. PIMUZ 27500. Loc. HB911, Baid. *Baidites hermanni* fauna, Smithian. Cross section showing ontogenetic change in whorl section.

Fig. 4a-c: *Baidites hermanni* n. gen. et sp. PIMUZ 27360. Loc. HB911, Baid. *Baidites hermanni* fauna, Smithian. 3a ×1.5.

All natural size unless otherwise indicated.

Plate 11


1a


1b


2a


2b


2c


2d

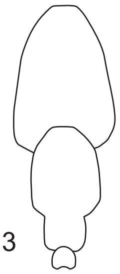
3


1e


4a


1c


1d


4b


4c

PLATE 12

Fig. 1a-c: *Flemingites rursiradiatus* CHAO 1959. PIMUZ 27361. Loc. Baid-A. *Flemingites rursiradiatus* fauna, Smithian. ×0.75.

Fig. 2: *Flemingites rursiradiatus* CHAO 1959. PIMUZ 27362. Loc. Baid-A. *Flemingites rursiradiatus* fauna, Smithian. ×0.75.

Fig. 3a-c: *Flemingites rursiradiatus* CHAO 1959. PIMUZ 27363. Loc. Baid-A. *Flemingites rursiradiatus* fauna, Smithian. ×0.75.

Fig. 4a-b: *Flemingites rursiradiatus* CHAO 1959. PIMUZ 27364. Loc. Baid-A. *Flemingites rursiradiatus* fauna, Smithian. ×0.75.

Fig. 5: *Flemingites rursiradiatus* CHAO 1959. PIMUZ 27365. Loc. Baid-A. *Flemingites rursiradiatus* fauna, Smithian.

Fig. 6a-c: *Flemingites* sp. indet. PIMUZ 27366. Loc. SA3, Jebel Safra. *Rohillites omanensis* fauna, Smithian.

All natural size unless otherwise indicated.

Plate 12

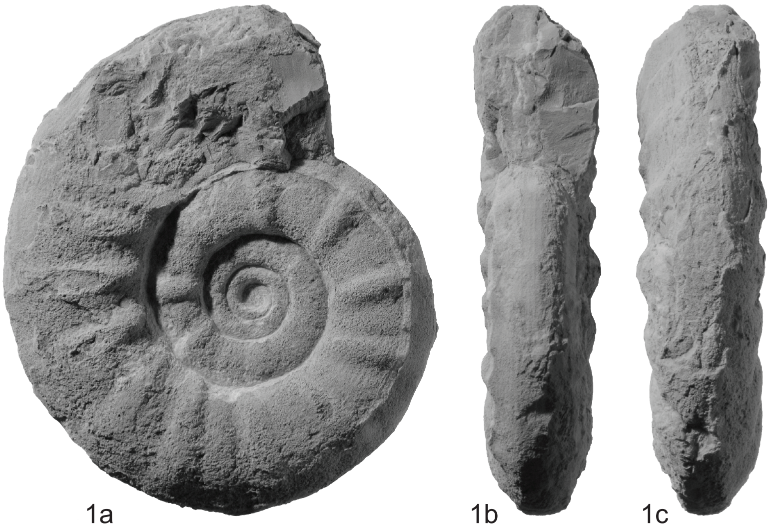

1a 1b 1c

2

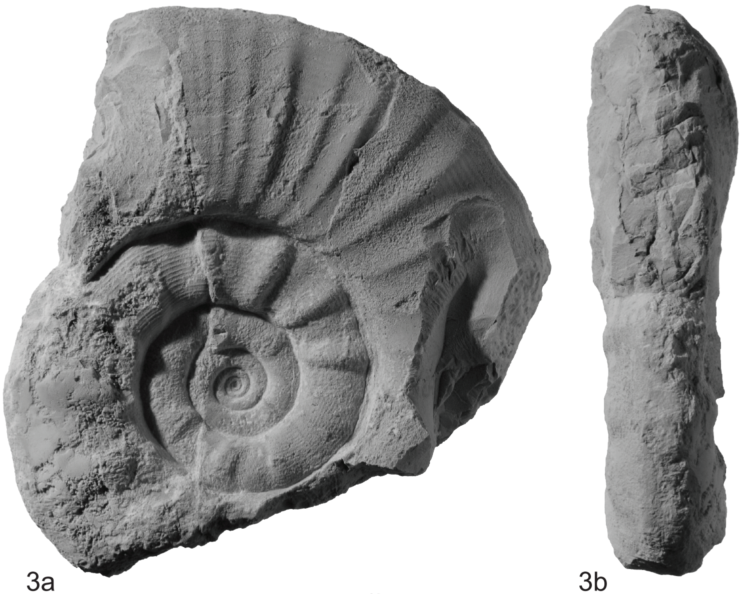

3a 3b

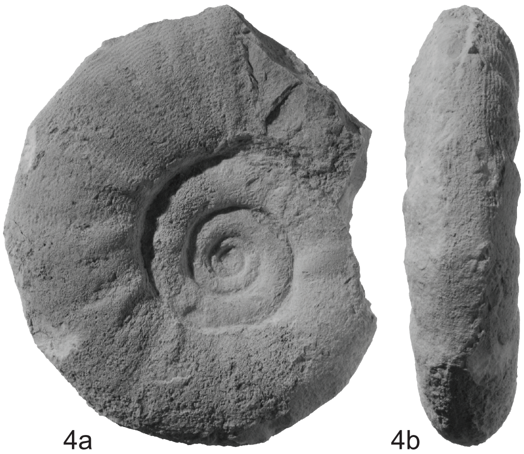

4a 4b

5

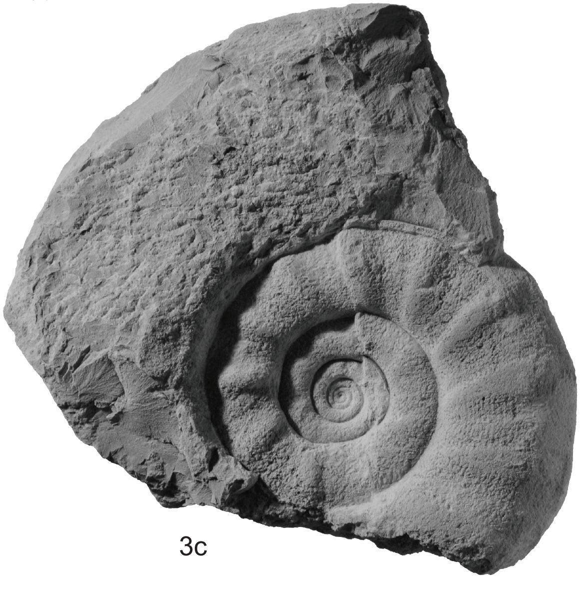

3c

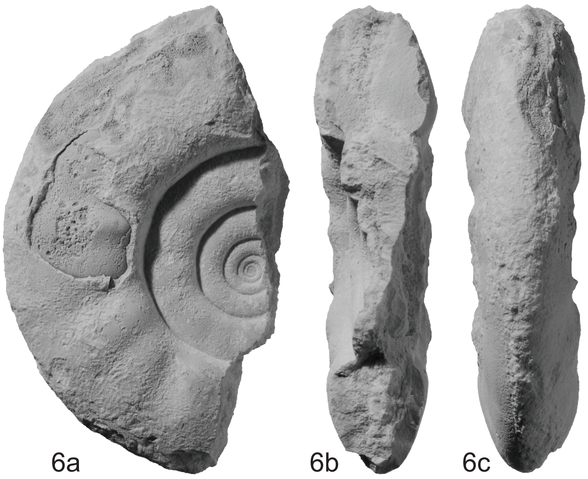

6a 6b 6c

PLATE 13

Fig. 1a-c: *Subflemingites involutus* (WELTER 1922). PIMUZ 27367. Loc. JS13, Jebel Safra. *Nammalites pilatoides* fauna, Smithian.

Fig. 2a-c: *Subflemingites involutus* (WELTER 1922). PIMUZ 27368. Loc. JS13, Jebel Safra. *Nammalites pilatoides* fauna, Smithian.

Fig. 3: *Subflemingites involutus* (WELTER 1922). PIMUZ 27369. Loc. JS13, Jebel Safra. *Nammalites pilatoides* fauna, Smithian.

Fig. 4a-b: *Rohillites omanensis* n. sp. PIMUZ 27370. Loc. JS11, Jebel Safra. *Rohillites omanensis* fauna, Smithian.

Fig. 5a-c: *Rohillites omanensis* n. sp. PIMUZ 27371, holotype. Loc. SA3, Jebel Safra. *Rohillites omanensis* fauna, Smithian.

Fig. 6: *Rohillites omanensis* n. sp. PIMUZ 27372. Loc. SA3, Jebel Safra. *Rohillites omanensis* fauna, Smithian.

Fig. 7a-c: *Rohillites omanensis* n. sp. PIMUZ 27373. Loc. JS11, Jebel Safra. *Rohillites omanensis* fauna, Smithian.

Fig. 8a-b: *Rohillites omanensis* n. sp. PIMUZ 27374. Loc. SA3, Jebel Safra. *Rohillites omanensis* fauna, Smithian.

Fig. 9a-c: *Anaxenaspis* cf. *lidacensis* (WELTER 1922). PIMUZ 27375. Loc. WM8, Wadi Musjah. *Owenites koeneni* fauna, Smithian. 9a ×2.

Fig. 10a-d: *Anaxenaspis* cf. *lidacensis* (WELTER 1922). PIMUZ 27376. Loc. HB904, Wadi Musjah. *Owenites koeneni* fauna, Smithian.

Fig. 11: *Anaxenaspis* cf. *lidacensis* (WELTER 1922). PIMUZ 27377. Loc. Baid-B. *Owenites koeneni* fauna, Smithian.

All natural size unless otherwise indicated.

Plate 13

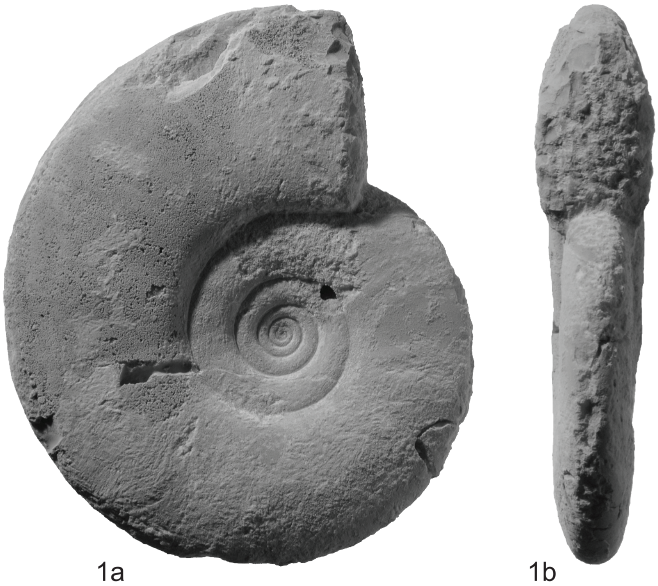
1a 1b 1c

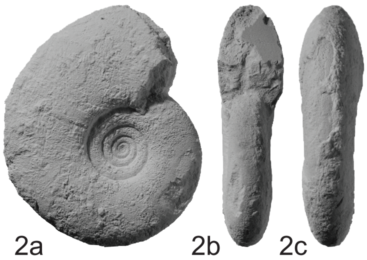
2a 2b 2c

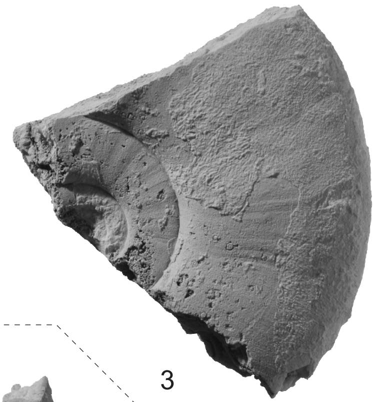
3


4a 4b

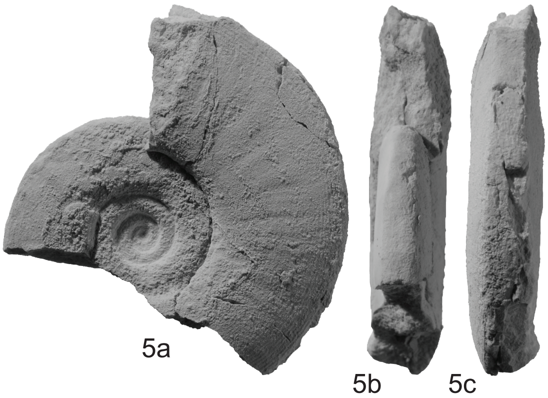
5a 5b 5c


6

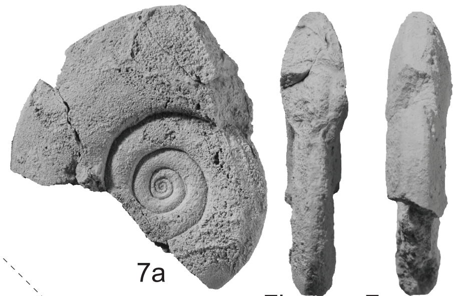
7a 7b 7c


8a 8b


9a

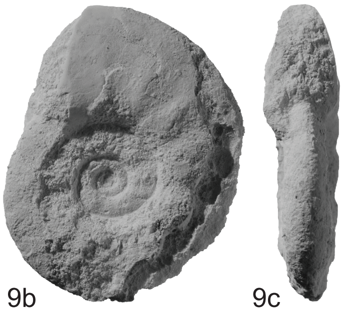
9b 9c

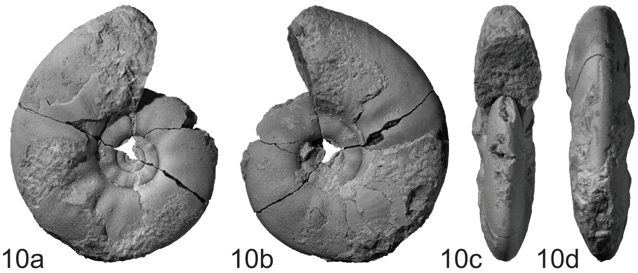
10a 10b 10c 10d


11

PLATE 14

Fig. 1a-c: *Anaxenaspis* cf. *lidacensis* (WELTER 1922). PIMUZ 27378. Loc. Baid-B. *Owenites koeneni* fauna, Smithian. ×0.5.

Fig. 2a-b: *Anaxenaspis* cf. *lidacensis* (WELTER 1922). PIMUZ 27379. Loc. Baid-B. *Owenites koeneni* fauna, Smithian.

Fig. 3a-d: *Anaxenaspis* cf. *lidacensis* (WELTER 1922). PIMUZ 27380. Loc. Baid-B. *Owenites koeneni* fauna, Smithian.

Fig. 4: *Pseudoflemingites goudemandi* BRAYARD & BUCHER 2008. PIMUZ 27381. Loc. JS12, Jebel Safra. *Owenites koeneni* fauna, Smithian.

Fig. 5a-c: *Pseudoflemingites goudemandi* BRAYARD & BUCHER 2008. PIMUZ 27382. Loc. JS12, Jebel Safra. *Owenites koeneni* fauna, Smithian.

Fig. 6a-b: *Galfettites omani* n. sp., PIMUZ 27384. Loc. JS13, Jebel Safra. *Nammalites pilatoides* fauna, Smithian.

Fig. 7a-b: *Galfettites omani* n. sp. PIMUZ 27383, holotype. Loc. JS13, Jebel Safra. *Nammalites pilatoides* fauna, Smithian.

Fig. 8a-c: *Galfettites omani* n. sp. PIMUZ 27385. Loc. JS13, Jebel Safra. *Nammalites pilatoides* fauna, Smithian.

All natural size unless otherwise indicated.

Plate 14

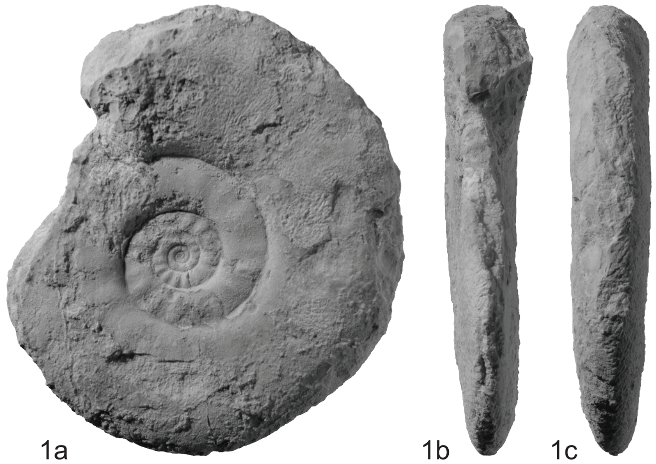
1a 1b 1c

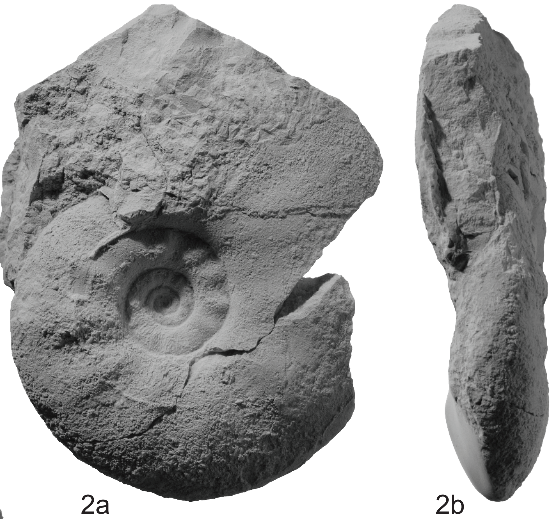
2a 2b


3a 3b 3c


3d


4

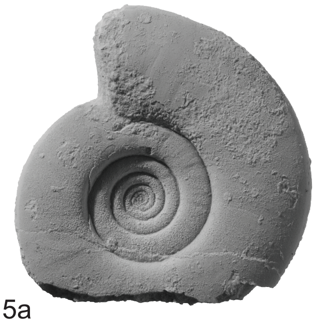
5a

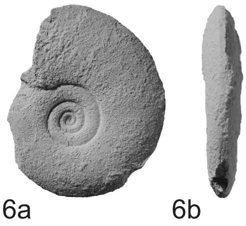
6a 6b

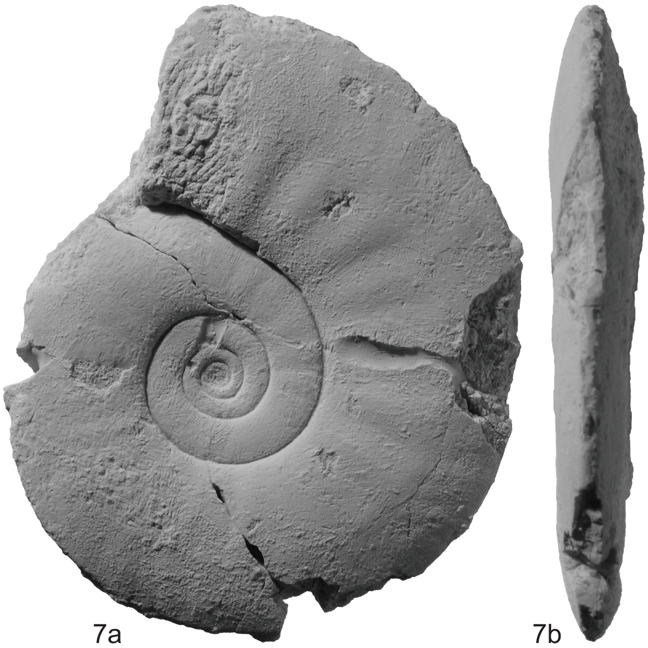
7a 7b


8a

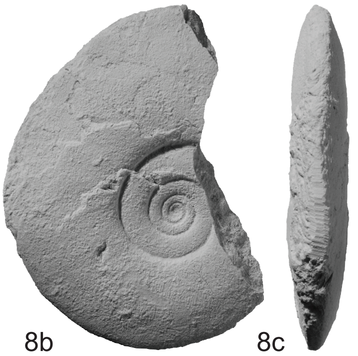
8b 8c


5b 5c

PLATE 15

Fig. 1a-c: *Galfettites simplicitatis* BRAYARD & BUCHER 2008. PIMUZ 27386. Loc. HB912, Jebel Safra. *Owenites koeneni* fauna, Smithian.

Fig. 2a-d: *Galfettites simplicitatis* BRAYARD & BUCHER 2008. PIMUZ 27387. Loc. Baid-B. *Owenites koeneni* fauna, Smithian. 2d ×2.

Fig. 3a-b: *Galfettites simplicitatis* BRAYARD & BUCHER 2008. PIMUZ 2790. Loc. HB912, Jebel Safra. *Owenites koeneni* fauna, Smithian.

Fig. 4a-c: *Galfettites simplicitatis* BRAYARD & BUCHER 2008. PIMUZ 2788. Loc. HB912, Jebel Safra. *Owenites koeneni* fauna, Smithian.

All natural size unless otherwise indicated.

Plate 15


1a


1b


1c


2a


2b


2c


2d


3a


3b


4a


4b


4c

PLATE 16

Fig. 1a-d: *Galfettites simplicitatis* BRAYARD & BUCHER 2008.PIMUZ 27389. Loc. HB912, Jebel Safra. *Owenites koeneni* fauna, Smithian.

Fig. 2a-d: ?*Galfettites* sp. indet. PIMUZ 27394. Loc. HB912, Jebel Safra. *Owenites koeneni* fauna, Smithian. 2d ×1.5.

Fig. 3a-c: *Galfettites kyrae* n. sp. PIMUZ 27393. Loc. Baid-B. *Owenites koeneni* fauna, Smithian.

Fig. 4a-d: *Galfettites kyrae* n. sp. PIMUZ 27392. Loc. HB902, Wadi Musjah, *Owenites koeneni* fauna, Smithian. 4d ×2.

Fig. 5a-d: *Galfettites kyrae* n. sp. PIMUZ 27391, holotype. Loc. HB900, Wadi Musjah. *Owenites koeneni* fauna, Smithian.

All natural size unless otherwise indicated.

Plate 16

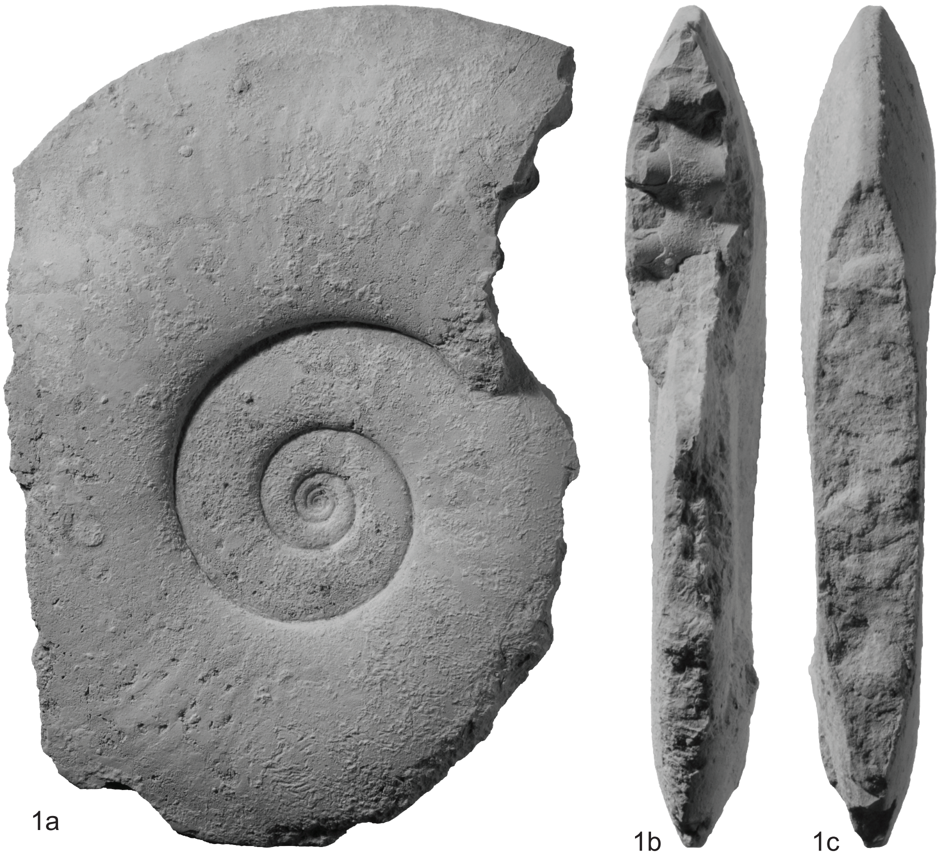

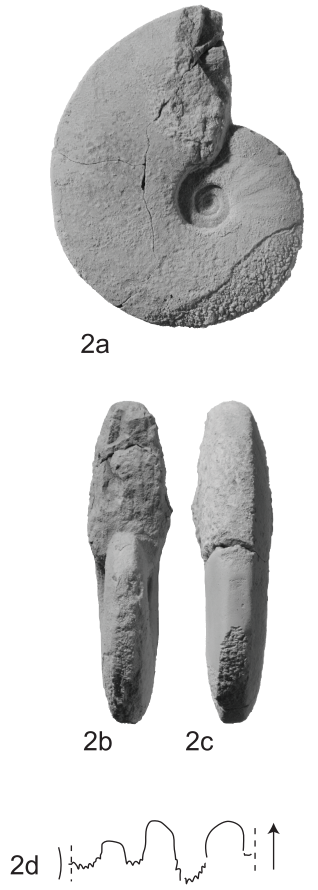

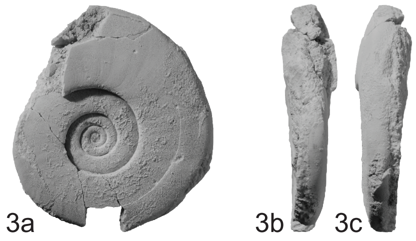

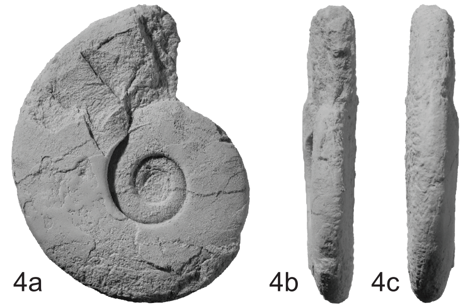

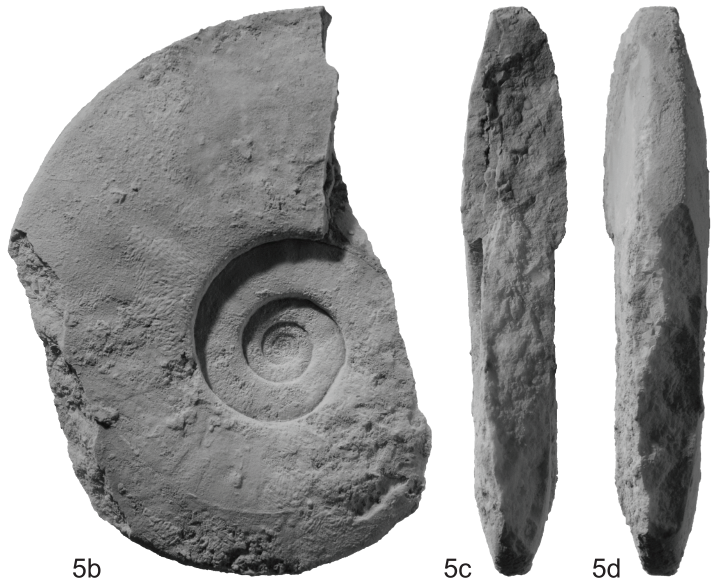

PLATE 17

Fig. 1a-c: *Submeekoceras mushbachanum* (WHITE 1879). PIMUZ 27402. Loc. JS12, Jebel Safra. *Owenites koeneni* fauna, Smithian.

Fig. 2a-d: *Submeekoceras mushbachanum* (WHITE 1879). PIMUZ 27401. Loc. JS4, Jebel Safra. *Owenites koeneni* fauna, Smithian. 1a-c ×0.4.

Fig. 3a-c: *Submeekoceras mushbachanum* (WHITE 1879). PIMUZ 27403. Loc. Baid-A. *Flemingites rursiradiatus* fauna, Smithian. 3b-c ×0.6.

Fig. 4: *Pseudaspidites planus* n. sp. PIMUZ 27793. Loc. Loc. JS12, Jebel Safra. *Owenites koeneni* fauna.

Fig. 5a-b: *Pseudaspidites planus* n. sp. PIMUZ 27404. Loc. Loc. JS12, Jebel Safra. *Owenites koeneni* fauna, Smithian. ×0.6.

All natural size unless otherwise indicated.

Plate 17


1a


1b


1c

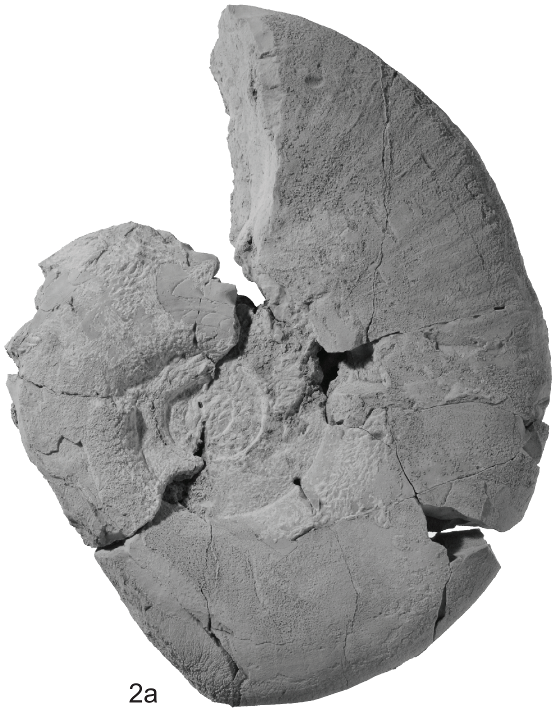
2a


2b


2c

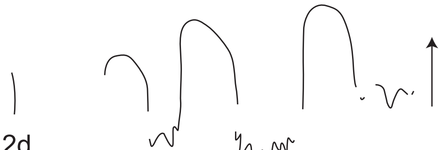
2d

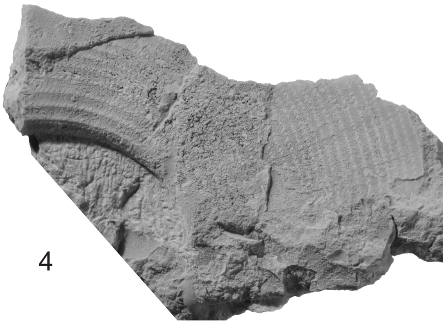
4


3a


3b


3c

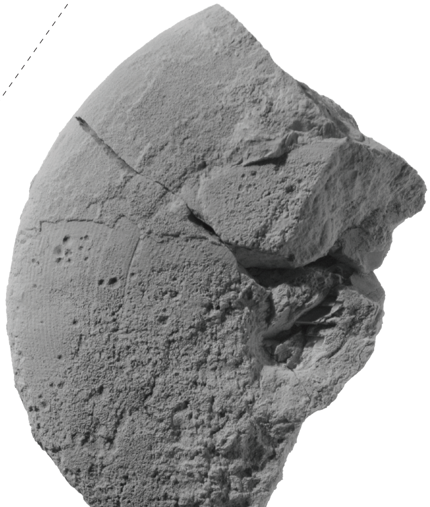
5a


5b

PLATE 18

Fig. 1a-d: *Nammalites pilatoides* (Guex 1978). PIMUZ 27405. Loc. JS13, Jebel Safra. *Nammalites pilatoides* fauna, Smithian.

Fig. 2: *Nammalites pilatoides* (Guex 1978). PIMUZ 27406. Loc. JS13, Jebel Safra. *Nammalites pilatoides* fauna, Smithian.

Fig. 3a-c: *Nammalites pilatoides* (Guex 1978). PIMUZ 27407. Loc. JS13, Jebel Safra. *Nammalites pilatoides* fauna, Smithian.

Fig. 4: *Nammalites pilatoides* (Guex 1978). PIMUZ 27408. Loc. JS13, Jebel Safra. *Nammalites pilatoides* fauna, Smithian.

Fig. 5a-c: *Nammalites pilatoides* (Guex 1978). PIMUZ 27409. Loc. JS13, Jebel Safra. *Nammalites pilatoides* fauna, Smithian.

Fig. 6a-b: *Nammalites pilatoides* (Guex 1978). PIMUZ 27410. Loc. JS13, Jebel Safra. *Nammalites pilatoides* fauna, Smithian.

Fig. 7a-c: *Nammalites pilatoides* (Guex 1978). PIMUZ 27411. Loc. JS13, Jebel Safra. *Nammalites pilatoides* fauna, Smithian.

Fig. 8: *Parussuria compressa* (Hyatt & Smith 1905). PIMUZ 27412. Loc. JS13, Jebel Safra. *Nammalites pilatoides* fauna, Smithian.

Fig. 9: *Parussuria compressa* (Hyatt & Smith 1905). PIMUZ 27413. Loc. HB903, Wadi Musjah. *Owenites koeneni* fauna, Smithian.

Fig. 10a-b: *Parussuria compressa* (Hyatt & Smith 1905). PIMUZ 27414. Loc. JS13, Jebel Safra. *Nammalites pilatoides* fauna, Smithian.

Fig. 11a-c: *Parussuria compressa* (Hyatt & Smith 1905). PIMUZ 27415. Loc. Baid-B. *Owenites koeneni* fauna, Smithian.

Fig. 12: *Parussuria compressa* (Hyatt & Smith 1905). PIMUZ 27416. Loc. HB912, Jebel Safra. *Owenites koeneni* fauna, Smithian. Specimen with fine strigation.

Fig. 13a-c: *Parussuria compressa* (Hyatt & Smith 1905). PIMUZ 27417. Loc. JS13, Jebel Safra. *Nammalites pilatoides* fauna, Smithian.

Fig. 14a-c: *Parussuria compressa* (Hyatt & Smith 1905). PIMUZ 27418. Loc. JS13, Jebel Safra. *Nammalites pilatoides* fauna, Smithian.

All natural size unless otherwise indicated.

Plate 18

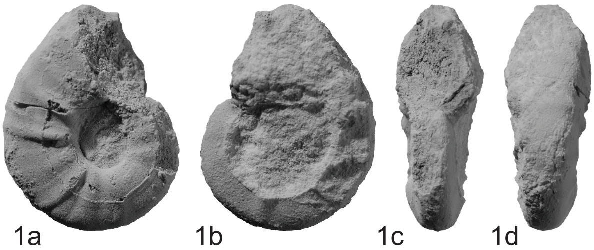
1a 1b 1c 1d


2


3a 3b 3c


4


5a 5b 5c


6a 6b

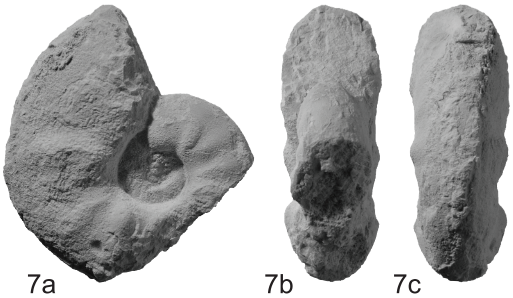
7a 7b 7c


11a


8


9


10a 10b


11b


11c


12


13a 13b 13c


14a 14b 14c

PLATE 19

Fig. 1a-d: *Anasibirites multiformis* WELTER 1922. PIMUZ 27419. Loc. HB901, Wadi Musjah. *Anasibirites multiformis* fauna, Smithian.

Fig. 2: *Anasibirites multiformis* WELTER 1922. PIMUZ 27420. Loc. HB901, Wadi Musjah. *Anasibirites multiformis* fauna, Smithian.

Fig. 3: *Anasibirites multiformis* WELTER 1922. PIMUZ 27797. Loc. HB901, Wadi Musjah. *Anasibirites multiformis* fauna, Smithian.

Fig. 4: *Anasibirites multiformis* WELTER 1922. PIMUZ 27421. Loc. HB901, Wadi Musjah. *Anasibirites multiformis* fauna, Smithian.

Fig. 5a-d: *Anasibirites multiformis* WELTER 1922. PIMUZ 27422. Loc. HB901, Wadi Musjah. *Anasibirites multiformis* fauna, Smithian.

Fig. 6a-b: *Anasibirites multiformis* WELTER 1922. PIMUZ 27423. Loc. HB901, Wadi Musjah. *Anasibirites multiformis* fauna, Smithian.

Fig. 7a-c: *Procolumbites safraensis* n. sp. PIMUZ 27424, holotype. Loc. SA4, Jebel Safra, Spathian.

Fig. 8: *Procolumbites safraensis* n. sp. PIMUZ 27425. Loc. SA4, Jebel Safra, Spathian. ×2.

Fig. 9a-d: *Hemiprionites* cf. *butleri* (MATHEWS 1929). PIMUZ 27426. Loc. HB902, Wadi Musjah. *Owenites koeneni* fauna, Smithian.

Fig. 10a-e: *Hemiprionites* cf. *butleri* (MATHEWS 1929). PIMUZ 27427. Loc. HB901, Wadi Musjah. *Anasibirites multiformis* fauna, Smithian. 10a ×2.

All natural size unless otherwise indicated.

Plate 19


1a


1b


1c


1d


2


3


4

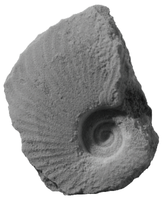
5a

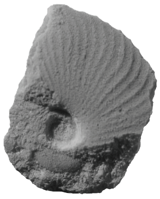
5b


5c


5d


6a


6b


7a


7b


7c


8

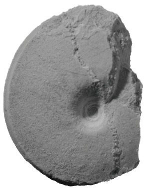
9a


9b


9c


9d

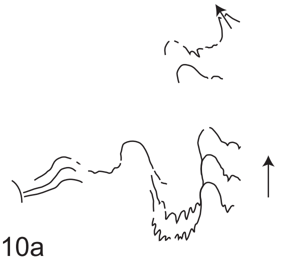
10a


10b


10c


10d


10e

PLATE 20

Fig. 1a-d: *Prionites* sp. indet. PIMUZ 27428. Loc. HB912, Jebel Safra. *Owenites koeneni* fauna, Smithian. 1d ×0.75.

Fig. 2a-d: ?Arctoceratidae gen. indet. PIMUZ 27429. Loc. SA1, Jebel Safra. ?*Nammalites pilatoides* fauna, Smithian. 2d ×2.

Fig. 3a-d: Prionitidae gen. indet. A. PIMUZ 27430. Loc. HB901, Wadi Musjah. *Anasibirites multiformis* fauna, Smithian.

Fig. 4a-d: *Lanceolites compactus* HYATT & SMITH 1905. PIMUZ 27431. Loc. JS4, Jebel Safra. *Owenites koeneni* fauna, Smithian. 4d ×2.

Fig. 5a-b: *Lanceolites compactus* HYATT & SMITH 1905. PIMUZ 27432. Loc. HB900, Wadi Musjah. *Owenites koeneni* fauna, Smithian.

Fig. 6a-d: *Lanceolites compactus* HYATT & SMITH 1905. PIMUZ 27334. Loc. JS12, Jebel Safra. *Owenites koeneni* fauna, Smithian. 7d ×2.

Fig. 7a-d: *Lanceolites bicarinatus* SMITH 1932. PIMUZ 27433. Loc. HB900, Wadi Musjah. *Owenites koeneni* fauna, Smithian. 6d ×2.

All natural size unless otherwise indicated.

Plate 20

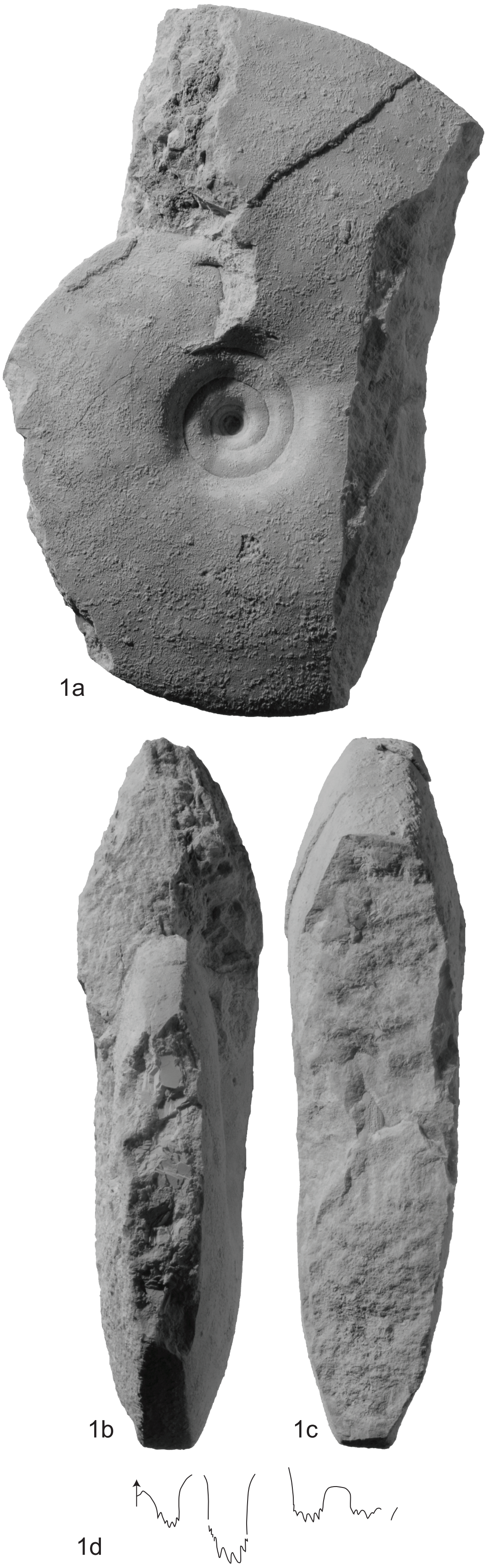

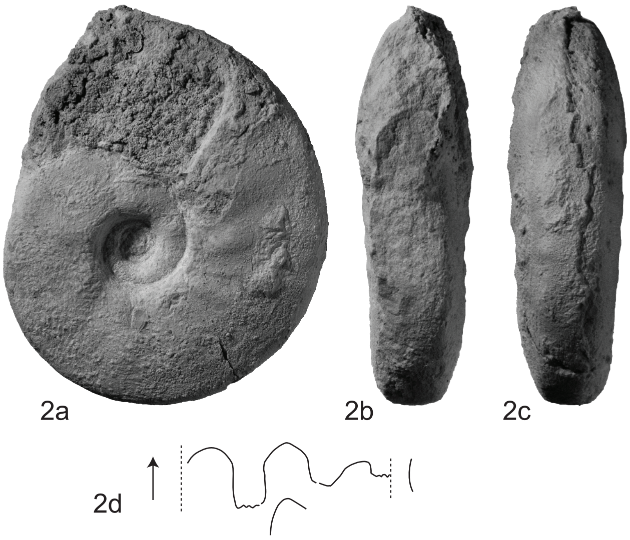

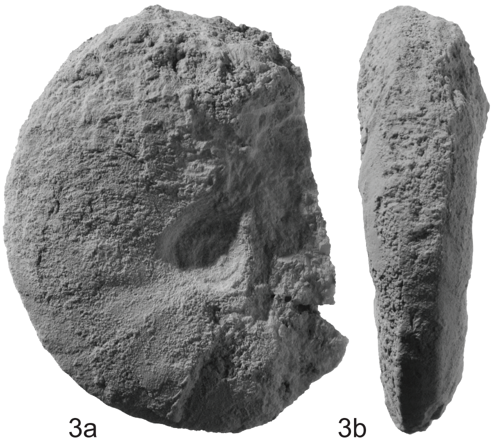

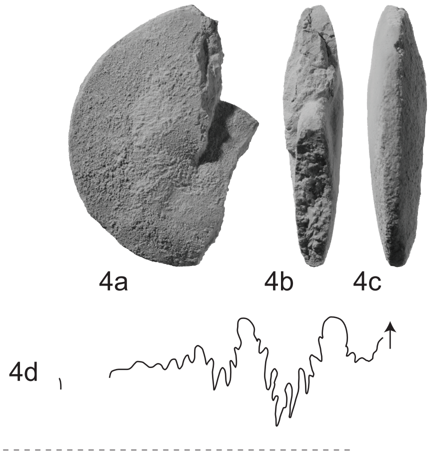

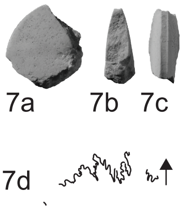

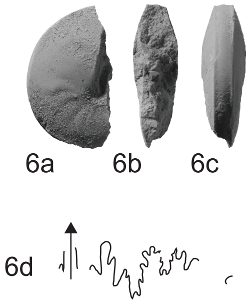

PLATE 21

Fig. 1a-b: *Inyoites oweni* HYATT & SMITH 1905. PIMUZ 27438. Loc. HB900, Wadi Musjah. *Owenites koeneni* fauna, Smithian.

Fig. 2: *Inyoites oweni* HYATT & SMITH 1905. PIMUZ 27439. Loc. HB908, Wadi Musjah. *Owenites koeneni* fauna, Smithian.

Fig. 3a-d: *Inyoites oweni* HYATT & SMITH 1905. PIMUZ 27440. Loc. HB900, Wadi Musjah. *Owenites koeneni* fauna, Smithian. 6d ×2.

Fig. 4: *Inyoites oweni* P HYATT & SMITH 1905. PIMUZ 27442. Loc. HB900, Wadi Musjah. *Owenites koeneni* fauna, Smithian. ×2.

Fig. 5: *Inyoites oweni* HYATT & SMITH 1905. PIMUZ 27441. Loc. HB900, Wadi Musjah. *Owenites koeneni* fauna, Smithian. ×2.

Fig. 6a-d: *Inyoites oweni* HYATT & SMITH 1905. PIMUZ 27436. Loc. HB900, Wadi Musjah. *Owenites koeneni* fauna, Smithian.

Fig. 7a-b: *Inyoites krystyni* BRAYARD & BUCHER 2008. PIMUZ 27435. Loc. JS12, Jebel Safra. *Owenites koeneni* fauna, Smithian.

Fig. 8a-c: *Inyoites* sp. indet. PIMUZ 27437. Loc. HB902, Wadi Musjah. *Owenites koeneni* fauna, Smithian.

Fig. 9a-b: *Subvishnuites welteri* SPATH 1930. PIMUZ 27445. Loc. HB904, Wadi Musjah. *Owenites koeneni* fauna, Smithian.

Fig. 10a-c: *Subvishnuites welteri* SPATH 1930. PIMUZ 27447. Loc. HB904, Wadi Musjah. *Owenites koeneni* fauna, Smithian.

Fig. 11a-b: *Subvishnuites welteri* SPATH 1930. PIMUZ 27444. Loc. HB904, Wadi Musjah. *Owenites koeneni* fauna, Smithian.

Fig. 12a-d: *Subvishnuites welteri* SPATH 1930. PIMUZ 27446. Loc. HB904, Wadi Musjah. *Owenites koeneni* fauna, Smithian.

Fig. 13a-d: *Subvishnuites welteri* SPATH 1930. PIMUZ 27443. Loc. HB904, Wadi Musjah. *Owenites koeneni* fauna, Smithian.

Fig. 14a-c: *Subvishnuites* sp. indet. PIMUZ 27448. Loc. HB901, Wadi Musjah. *Anasibirites multiformis* fauna, Smithian.

All natural size unless otherwise indicated.

Plate 21

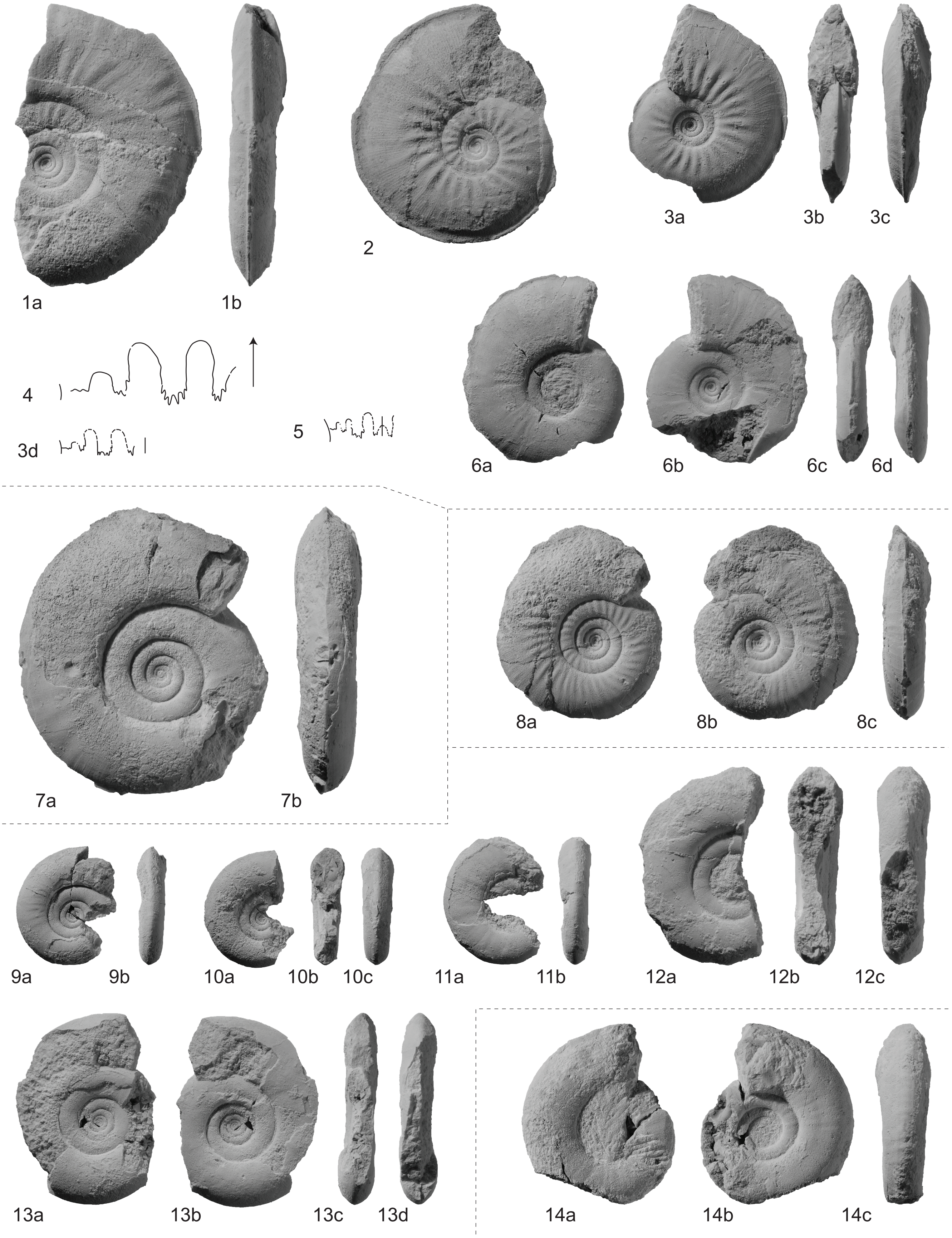
1a
1b
2
3a
3b
3c
3d
4
5
6a
6b
6c
6d
7a
7b
8a
8b
8c
9a
9b
10a
10b
10c
11a
11b
12a
12b
12c
13a
13b
13c
13d
14a
14b
14c

PLATE 22

Fig. 1a-d: *Juvenites* cf. *thermarum* (SMITH 1927). PIMUZ 27449. Loc. WM7, Wadi Musjah. *Owenites koeneni* fauna, Smithian. 1d ×2.

Fig. 2a-c: *Juvenites* cf. *thermarum* (SMITH 1927). PIMUZ 27453. Loc. WM7, Wadi Musjah. *Owenites koeneni* fauna, Smithian.

Fig. 3a-d: *Juvenites* cf. *thermarum* (SMITH 1927). PIMUZ 27452. Loc. HB900, Wadi Musjah. *Owenites koeneni* fauna, Smithian.

Fig. 4a-d: *Juvenites* cf. *thermarum* (SMITH 1927). PIMUZ 27454. Loc. HB900. *Owenites koeneni* fauna, Smithian.

Fig. 5a-d: *Juvenites* cf. *thermarum* (SMITH 1927). PIMUZ 26262. Loc. HB900. *Owenites koeneni* fauna, Smithian.

Fig. 6a-d: *Juvenites* cf. *thermarum* (SMITH 1927). PIMUZ 27455. Loc. HB900. *Owenites koeneni* fauna, Smithian.

Fig. 7: *Juvenites* cf. *thermarum* (SMITH 1927). PIMUZ 27451. Loc. HB902. *Owenites koeneni* fauna, Smithian. ×2.

Fig. 8a-c: *Juvenites* cf. *thermarum* (SMITH 1927). PIMUZ 26263. Loc. HB900. *Owenites koeneni* fauna, Smithian.

Fig. 9a-c: *Juvenites* cf. *thermarum* (SMITH 1927). PIMUZ 27450. Loc. HB900. *Owenites koeneni* fauna, Smithian.

Fig. 10a-c: *Juvenites procurvus* BRAYARD & BUCHER 2008. PIMUZ 27477. Loc. JS12, Jebel Safra. *Owenites koeneni* fauna, Smithian

Fig. 11a-d: *Juvenites procurvus* BRAYARD & BUCHER 2008. PIMUZ 27478. Loc. JS2, Jebel Safra. *Owenites koeneni* fauna, Smithian

Fig. 12a-d: *Juvenites spathi* (FREBOLD 1930). PIMUZ 27456. Loc. JS13, Jebel Safra. *Nammalites pilatoides* fauna, Smithian. 10d ×2.

Fig. 13a-c: *Juvenites spathi* (FREBOLD 1930). PIMUZ 27457. Loc. JS13, Jebel Safra. *Nammalites pilatoides* fauna, Smithian.

Fig. 14a-c: *Juvenites spathi* (FREBOLD 1930). PIMUZ 27458. Loc. JS13, Jebel Safra. *Nammalites pilatoides* fauna, Smithian.

Fig. 15a-c: *Juvenites spathi* (FREBOLD 1930). PIMUZ 27459. Loc. SA1. ?*Nammalites pilatoides* fauna, Smithian.

Fig. 16: *Juvenites spathi* (FREBOLD 1930). PIMUZ 27460. Loc. JS13, Jebel Safra. *Nammalites pilatoides* fauna, Smithian.

Fig. 17a-c: *Juvenites spathi* (FREBOLD 1930). PIMUZ 27461. Loc. JS13, Jebel Safra. *Nammalites pilatoides* fauna, Smithian

All natural size unless otherwise indicated.

Plate 22

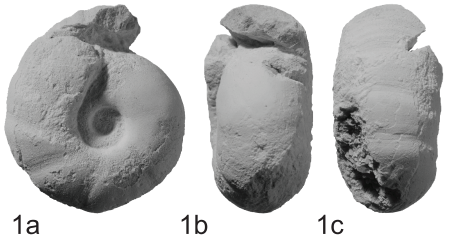

1a 1b 1c

1d

2a 2b 2c

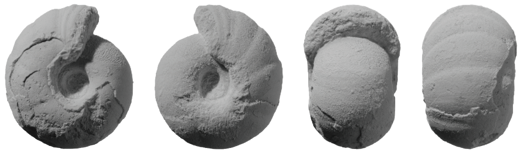

3a 3b 3c 3d

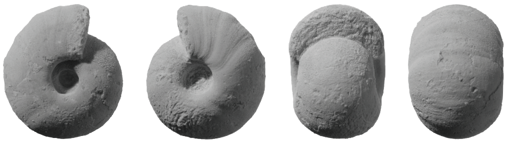

4a 4b 4c 4d

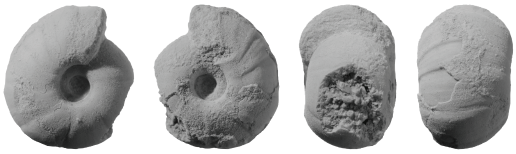

5a 5b 5c 5d

6a 6b 6c 6d

7

8a 8b 8c

9a 9b 9c

10a 10b 10c

11a 11b 11c 11d

12a 12b 12c

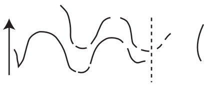

12d

13a 13b 13c

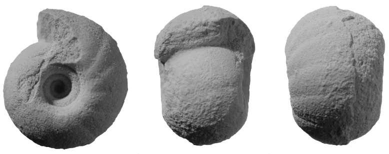

14a 14b 14c

15a 15b 15c

16

17a 17b 17c

PLATE 23

Fig. 1a-c: *Paranannites baudi* n. sp. PIMUZ 27462, holotype. Loc. SA3, Jebel Safra. *Rohillites omanensis* fauna, Smithian.

Fig. 2a-b: *Paranannites baudi* n. sp. PIMUZ 27463. Loc. JS11, Jebel Safra. *Rohillites omanensis* fauna, Smithian.

Fig. 3a-b: *Paranannites baudi* n. sp. PIMUZ 274646. Loc. SA3, Jebel Safra. *Rohillites omanensis* fauna, Smithian.

Fig. 4a-c: *Paranannites baudi* n. sp. PIMUZ 27465. Loc. JS11, Jebel Safra. *Rohillites omanensis* fauna, Smithian.

Fig. 5a-c: *Paranannites baudi* n. sp. PIMUZ 27466. Loc. JS11, Jebel Safra. *Rohillites omanensis* fauna, Smithian.

Fig. 6a-c: *Paranannites baudi* n. sp. PIMUZ 27467. Loc. JS11, Jebel Safra. *Rohillites omanensis* fauna, Smithian.

Fig. 7a-b: *Paranannites baudi* n. sp. PIMUZ 27468. Loc. JS11, Jebel Safra. *Rohillites omanensis* fauna, Smithian.

Fig. 8a-c: *Paranannites baudi* n. sp. PIMUZ 27469. Loc. JS11, Jebel Safra. *Rohillites omanensis* fauna, Smithian.

Fig. 9a-c: *Paranannites baudi* n. sp. PIMUZ 27470. Loc. JS11, Jebel Safra. *Rohillites omanensis* fauna, Smithian.

Fig. 10a-b: *Paranannites baudi* n. sp. PIMUZ 27471. Loc. JS11, Jebel Safra. *Rohillites omanensis* fauna, Smithian.

Fig. 11a-d: *Omanites musjahensis* n. gen. et sp. PIMUZ 27472. Loc. HB910, Wadi Musjah. *Owenites koeneni* fauna, Smithian.

All natural size unless otherwise indicated.

Plate 23

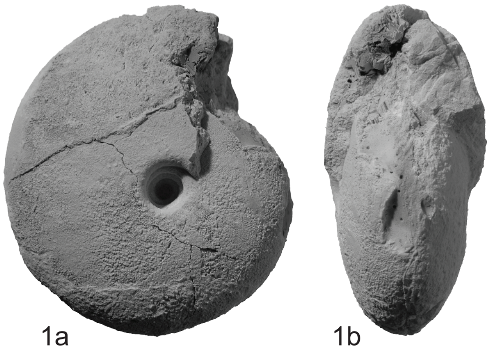
1a 1b 1c

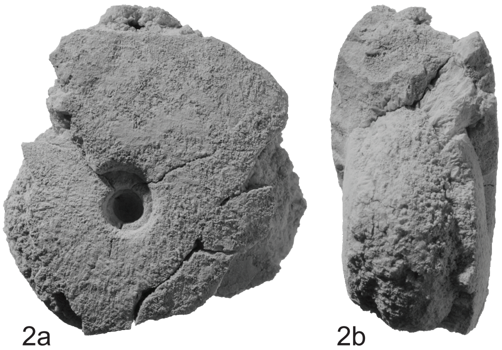
2a 2b


3a 3b

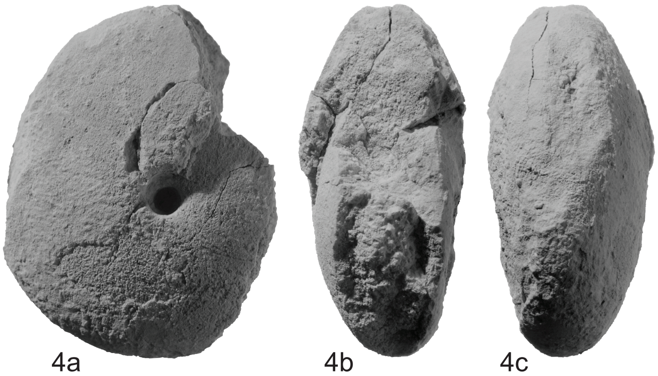
4a 4b 4c


5a 5b 5c


6a 6b 6c

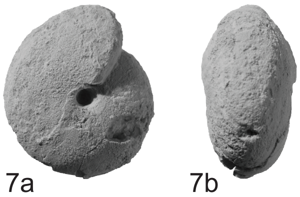
7a 7b


8a 8b 8c


9a 9b 9c


10a 10b

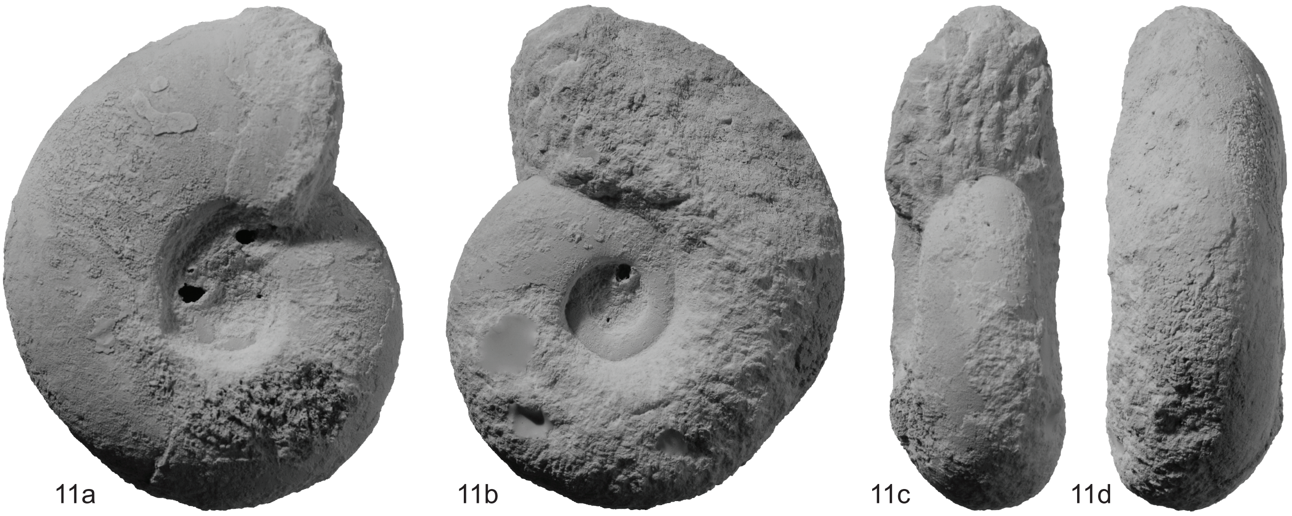
11a 11b 11c 11d

PLATE 24

Fig. 1a-d: *Omanites musjahensis* n. gen. et sp. PIMUZ 27473. Loc. HB910, Wadi Musjah. *Owenites koeneni* fauna, Smithian.

Fig. 2a-c: *Omanites musjahensis* n. gen. et sp. PIMUZ 27474. Loc. HB910, Wadi Musjah. *Owenites koeneni* fauna, Smithian. 2c ×2.

Fig. 3a-d: *Omanites musjahensis* n. gen. et sp. PIMUZ 27475, holotype. Loc. HB910, Wadi Musjah. *Owenites koeneni* fauna, Smithian.

Fig. 4a-c: *Omanites musjahensis* n. gen. et sp. PIMUZ 27476. Loc. HB910, Wadi Musjah. *Owenites koeneni* fauna, Smithian.

Fig. 5a-d: *Owenites* cf. *simplex* WELTER 1922. PIMUZ 27479. Loc. JS13, Jebel Safra. *Nammalites pilatoides* fauna, Smithian.

Fig. 6a-d: *Owenites* cf. *simplex* WELTER 1922. PIMUZ 27480. Loc. JS13, Jebel Safra. *Nammalites pilatoides* fauna, Smithian. 6d ×2.

Fig. 7a-c: *Owenites* cf. *simplex* WELTER 1922. PIMUZ 27481. Loc. JS13, Jebel Safra. *Nammalites pilatoides* fauna, Smithian.

Fig. 8a-b: *Owenites* cf. *simplex* WELTER 1922. PIMUZ 27482. Loc. JS13, Jebel Safra. *Nammalites pilatoides* fauna, Smithian.

Fig. 9a-c: *Owenites* cf. *simplex* WELTER 1922. PIMUZ 27483. Loc. JS13, Jebel Safra. *Nammalites pilatoides* fauna, Smithian.

Fig. 10a-b: *Owenites simplex* WELTER 1922. PIMUZ 27484. Loc. JS13, Jebel Safra. *Nammalites pilatoides* fauna, Smithian.

Fig. 11a-b: *Owenites simplex* WELTER 1922. PIMUZ 27485. Loc. JS13, Jebel Safra. *Nammalites pilatoides* fauna, Smithian.

Fig. 12: *Owenites simplex* WELTER 1922. PIMUZ 27486. Loc. JS13, Jebel Safra. *Nammalites pilatoides* fauna, Smithian.

Fig. 13a-b: *Owenites simplex* WELTER 1922. PIMUZ 27487. Loc. JS13, Jebel Safra. *Nammalites pilatoides* fauna, Smithian.

Fig. 14a-c: *Owenites simplex* WELTER 1922. PIMUZ 27488. Loc. JS13, Jebel Safra. *Nammalites pilatoides* fauna, Smithian.

All natural size unless otherwise indicated.

Plate 24

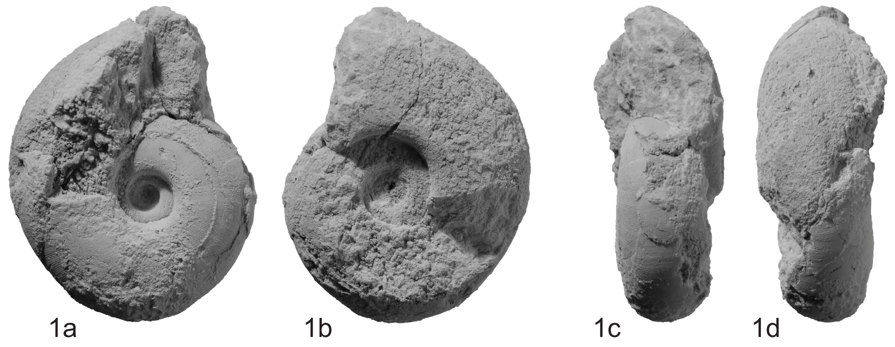
1a 1b 1c 1d

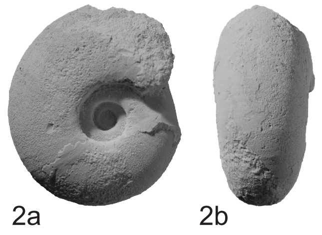
2a 2b


3a 3b 3c 3d


4a 4b 4c


2c

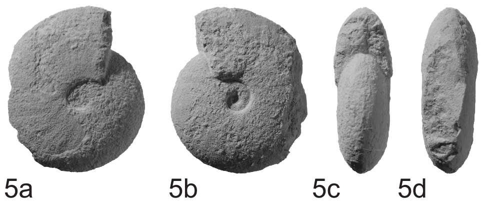
5a 5b 5c 5d


6a 6b 6c


7a 7b 7c


8a 8b


9a 9b 9c


6d

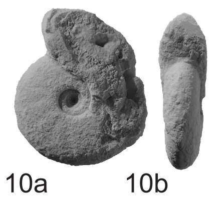
10a 10b


11a 11b


12

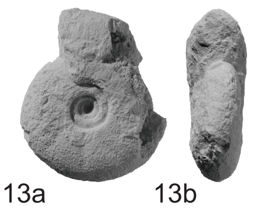
13a 13b


14a 14b 14c

PLATE 25

Fig. 1a-c: *Owenites koeneni* HYATT & SMITH 1905. PIMUZ 27489. Loc. HB912, Jebel Safra. *Owenites koeneni* fauna, Smithian.

Fig. 2a-c: *Owenites koeneni* HYATT & SMITH 1905. PIMUZ 27490. Loc. HB912, Jebel Safra. *Owenites koeneni* fauna, Smithian.

Fig. 3a-d: *Owenites koeneni* HYATT & SMITH 1905. PIMUZ 27491. Loc. Baid-B. *Owenites koeneni* fauna, Smithian.

Fig. 4a-c: *Owenites koeneni* HYATT & SMITH 1905. PIMUZ 27492. Loc. Baid-B. *Owenites koeneni* fauna, Smithian.

Fig. 5a-c: *Owenites koeneni* HYATT & SMITH 1905. PIMUZ 27493. Loc. Baid-B. *Owenites koeneni* fauna, Smithian.

Fig. 6a-b: *Owenites koeneni* HYATT & SMITH 1905. PIMUZ 27494. Loc. HB912, Jebel Safra. *Owenites koeneni* fauna, Smithian.

Fig. 7a-c: *Owenites carpenteri* SMITH 1932. PIMUZ 27798. Loc. HB904, Wadi Musjah. *Owenites koeneni* fauna, Smithian.

Fig. 8a-d: *Owenites carpenteri* SMITH 1932. PIMUZ 27799. Loc. HB904, Wadi Musjah. *Owenites koeneni* fauna, Smithian.

All natural size unless otherwise indicated.

Plate 25

PLATE 26

Fig. 1a-c: *Aspenites acutus* HYATT & SMITH 1905. PIMUZ 27495. Loc. JS13, Jebel Safra. *Nammalites pilatoides* fauna, Smithian.

Fig. 2a-c: *Aspenites acutus* HYATT & SMITH 1905. PIMUZ 27496. Loc. HB908, Wadi Musjah. *Owenites koeneni* fauna, Smithian.

Fig. 3a-b: *Pseudaspenites layeriformis* (WELTER 1922). PIMUZ 27497. Loc. SA1. ?*Nammalites pilatoides* fauna, Smithian.

Fig. 4a-d: *Pseudosageceras multilobatum* NOETLING 1905. PIMUZ 27498. Loc. Baid-B. *Owenites koeneni* fauna, Smithian.

Fig. 5a-c: *Goudemandites sinensis* n. gen. et sp. PIMUZ 27499. Loc. HB904, Wadi Musjah. *Owenites koeneni* fauna, Smithian.

All natural size unless otherwise indicated.

Plate 26


1a


1b


1c


2a


2b


2c


3a


3b


4a


4b


4c


4d


5a


5b


5c

CHAPTER 9:

High-resolution biochronology and diversity dynamics of the Early Triassic ammonoid recovery: the Smithian faunas of the Northern Indian Margin

High-resolution biochronology and diversity dynamics of the Early Triassic ammonoid recovery: the Smithian faunas of the Northern Indian Margin

Thomas Brühwiler[a,*], Hugo Bucher[a*], Arnaud Brayard[b] and Nicolas Goudemand[a]

[a]Paläontologische Institut und Museum, Universität Zürich, Karl Schmid-Strasse 4, 8006 Zürich, Switzerland.
[b]UMR CNRS 5561 Biogéosciences, Université de Bourgogne, 6 Bd. Gabriel, 21000 Dijon, France.

Submitted to *Palaeogeography, Palaeoclimatology, Palaeoecology.*

Abstract: Based on new collections of abundant and well preserved material from the Salt Range (Pakistan), Spiti (Northern India) and Tulong (South Tibet), several recent studies focussed on the taxonomic revision and detailed biostratigraphy of Smithian ammonoids. In this work, biochronological data for these three well-documented basins are analysed by means of the Unitary Associations Method, resulting in a biochronological scheme of unprecedented high resolution for the Smithian of the Northern Indian Margin (NIM). Data for each basin are first processed separately, thus yielding three local biochronological zonations. Then, the three sequences are processed together as a regional three-sections data set for the construction of the inter-basin sequence, i.e. of the NIM. The latter comprises 16 Unitary Associations grouped into 13 zones for the entire Smithian. Analysis of ammonoid diversity dynamics based on this new highly resolved time frame highlights (i) a marked diversification during the early Smithian, (ii) a severe extinction during the late Smithian, and (iii) an overall very high turnover throughout the Smithian. At a global spatial scale and stage resolution, the diversity of Smithian ammonoid genera appears surprisingly high, as highlighted by a previous study. We show that at a smaller geographic scale and with the most highly resolved time frame, Smithian ammonoids of the NIM reached their explosive diversity peak essentially through extremely high turnover rates rather than through a classic diversification process of high origination rates coupled with low extinction rates. Based on recently published U/Pb ages, regional apparent total rates of origination and extinction of more than 100 species per My can be inferred for the Smithian ammonoids of the NIM.

Keywords: Early Triassic recovery; Smithian; ammonoids, Northern Indian Margin; biochronology; diversity.

1. Introduction

In the aftermath of the end-Permian mass extinction, ammonoids were among the fastest clades to recover. The recent analysis of a global diversity data set of ammonoid genera from the Late Carboniferous to the Late Triassic shows that Triassic ammonoid genera actually reached levels of diversity higher than in the Permian less than 2 million years after the Permian-Triassic Boundary (PTB) (Brayard et al., 2009). The evolution of Early Triassic ammonoids was neither a smooth, nor a gradual process. It is characterized by the following main features: (i) a very low diversity in the Griesbachian (early Induan), (ii) a moderate diversity increase in the Dienerian (late Induan), (iii) an explosive radiation in the early Smithian (early Olenekian), (iv) a late Smithian extinction event followed by (v) a second explosive radiation during the early Spathian (late Olenekian, Brayard et al., 2006), and (vi) another significant diversity drop around the Spathian/Anisian boundary (Bucher, 1989; Brayard et al., 2009).

Several localities on the Northern Indian Margin (NIM) such as the Salt Range (Pakistan), Kashmir, Spiti (Northern India) and Tulong (South Tibet) have long been known for their abundant Early Triassic ammonoid faunas (Mojsisovics et al., 1895; Waagen, 1895; Diener, 1897; Frech, 1905; Krafft and Diener, 1909; Diener, 1913; Spath, 1934; Schindewolf, 1953; Kummel, 1966; Kummel, 1970; Wang and He, 1976; Guex, 1978; Bando, 1981). Among these, the Salt Range and Spiti have played central roles in the development of the Early Triassic time scale. However, the majority of Smithian ammonoids from the NIM areas were hitherto insufficiently known due to small numbers of individuals and/or poor preservation, all of which influences the definition of taxa and as a consequence, their biostratigraphic distributions. Moreover, the exact stratigraphic occurrences of many taxa remained either approximate or unknown. Based on new collections of abundant and well preserved material, a number of recent studies focussed on the taxonomic revision and detailed biostratigraphy of Smithian ammonoids from the Salt Range (Brühwiler et al., submitted [c]), from Spiti (Krystyn et al., 2007a, b; Brühwiler et al., submitted [b, d]) and from Tulong (Brühwiler et al., accepted) (Fig. 1). These studies have resulted in the most complete and detailed Smithian ammonoid records presently known world-wide (compare e.g. to the well documented records from Canada [Tozer, 1994] or South China [Brayard and Bucher, 2008]). Diverse and well preserved Smithian ammonoid faunas have also recently been reported also from exotic blocks of Hallstatt facies from Oman (Brühwiler et al., submitted [a]). However, the poor superpositional control inherent to this type of occurrence precludes using the Oman data in the construction of biochronologic correlations.

In this work, we present a synthetic biochronological analysis of the Salt Range, Spiti and Tulong basins, which yields a high-resolution zonation for the Smithian of the NIM. This new zonation provides a firm basis for further palaeogeographical extension of Early Triassic biochronological correlations (e.g. with Nevada, California, South China, etc.) in order to achieve global correlations and improve our knowledge of global recovery patterns in time and space. Based on this new zonation, we then analyze the dynamics of ammonoid diversity throughout the Smithian of the NIM with an unprecedented resolution.

2. Biochronology

2.1. Unitary Associations Method

The taxonomically revised and homogenized data set at the species-level is analysed by means of the Unitary Associations (UA) Method (Guex, 1991). This quantitative and deterministic biochronological method is based on both real and virtual (i.e. in time but not in space) coexistences of taxa. UAs represent unique and mutually exclusive assemblages of taxa and are the finest possible subdivisions based on the association principle. They are isolated from each others by intervals of separation, and their discrete (non-continuous) character is in agreement with the discontinuous nature of the fossil record. For an exhaustive methodological description of the UA method, the reader is referred to Guex (1991) and Monnet and Bucher (2002). The method has been automated by the BioGraph computer program (Savary and Guex, 1991, 1999) and implemented in the palaeontological data analysis software PAST (Hammer et al., 2001), used for this study. Recently, Galster et al. (2010) have highlighted that the UA Method is unique in that it provides a complete analysis of the internal complexity of any biochronological problem, and thus differs from other quantitative biochronological methods that ignore the significance of biostratigraphic contradictions and may either destroy real, documented associations or create new but fake associations. Last but not least, the UA method has been demonstrated to provide reliable values of species richness, whatever the (unknown) duration of each UA-Zone (Escarguel & Bucher, 2004). Hence, species counts based on UA-Zones avoid the pitfall of constructing artificial, contiguous time bins of equal duration by utilizing inappropriate interpolated intervals between the few available radio-isotopically calibrated biochronozones (see Ovtcharova et al., 2006; Galfetti et al., 2007b).

The flow chart of the procedure applied here is given in Fig. 2. Ammonoids were collected from three sections in the Salt Range, Pakistan (Chiddru, Nammal and Zaluch) (Brühwiler et al., submitted [c]), four sections in the Spiti region, Northern India (Mud, Guling, Lalung and Losar) (Krystyn et al., 2007a, b; Brühwiler et al., submitted [b, d]) and several sections in the area of Tulong, South Tibet (Brühwiler et al., accepted). For the Tulong area, we were able to construct a single composite section based on bed-by-bed correlation. The basic step consisted in the thorough taxonomic revision and standardization of the ammonoid faunas. Special attention was devoted to intraspecific variation (i.e. Buckmann Law of Covariation, see Hammer and Bucher 2005; Urdy et al. 2009) so that the resulting figures of taxonomic richness are certainly conservative in comparison with the traditional usage of ammonoid taxonomy. For the subsequent biochronological analysis, long-ranging species, taxa left in open nomenclature, occurrences based on poorly preserved material and occurrences found in float blocks have been omitted from the data set (Fig. 2). Local UAs for the Salt Range and for Spiti were then processed with UA-Graph, and the data from the Tulong region were directly reduced to residual maximal horizons. The resulting local zonations were then converted into "sections" that were in turn processed for the construction of UAs at the paleogeographical scale of the NIM. Taxa that had previously been removed from the data set were then dated and re-introduced into the data set. The final step consisted in merging poorly laterally reproducible UAs and in constructing UA-zones for the NIM.

2.2. Results and discussion

The procedure described above yields 12 local UAs for the Salt Range (SR1-12), without any conflicting stratigraphic relationships (Fig. 3). These local UAs correspond to the 12 successive Smithian ammonoid faunas that have been detected empirically by Brühwiler et al. (submitted [c]). For the Spiti region, 14 local UAs were detected (SP1-14), again without any conflicting stratigraphic relationships. The oldest three UAs from Spiti (SP-1-3) comprise the earliest Smithian *Flemingites bhargavai* beds, the Kashmiritidae gen. nov. beds and the *Vercherites* cf. *pulchrum* beds of Brühwiler et al. (submitted [d]). The three subsequent UAs (SP4-6) are included within the *Flemingites* beds of Krystyn et al. (2007a, b). SP-4 corresponds to the *Rohillites rohilla* zone of these authors. Note that the ammonoid faunas from the *Flemingites* beds are still the subject of ongoing work (Krystyn et al., work in progress). The remaining eight UAs from Spiti (SP7-14) correspond to the eight ammonoid faunas of middle to latest Smithian age recognized empirically by Brühwiler et al. (submitted [b]). The six residual maximal horizon from Tulong (TU1-6) correspond to the six middle-latest Smithian ammonoid assemblages described previously (Brühwiler et al., accepted). The subsequent analysis at the pooled level of the three basins based on the three local zonations yields 16 UAs for the NIM (NIM1-16; Fig. 3). Again, no conflicting stratigraphic relationships were detected. A synthetic range chart showing the biochronological distribution of Smithian ammonoid species of the NIM is given in Fig. 4. Six of the UAs of the NIM have been found in one of the three studied regions only. In general, such poorly laterally reproducible UAs should be merged in order to enhance lateral reproducibility (Guex, 1991). A short discussion on the UAs in question is provided hereafter.

- NIM-3. This UA has been recognized in the Salt Range only, where it occurs in two sections (*Xenodiscoides perplicatus* beds; Chiddru and Nammal). It has no species in common with the under- or overlying UAs (except for the long-ranging *Pseudosageceras multilobatum*). Therefore, merging it with either the one or the other would be arbitrary. Moreover, this association possibly occurs in Spiti, but ammonoids are very poorly preserved in the corresponding horizon (Bed 11 of Krystyn et al., 2007a, b; Brühwiler et al., submitted [d]). Thus, NIM-3 is here preferably treated as a distinct zone.

- NIM-5. This UA has been recognized in a single section in the Salt Range only (*Radioceras evolvens* beds; Chiddru). It is distinguished from the underlying UA by only one species. Therefore, it is merged with NIM-4.

- NIM-6 has been recognized in Spiti only. As shown by Krystyn et al. (2007a, b, ongoing work) this assemblage represents a distinct fauna (i.e. the *Rohillites rohilla* Zone), which can probably be correlated with part of the *Kashmirites kapila* beds from South China (Brayard and Bucher, 2008). This correlation is also corroborated by conodonts (Goudemand, unpublished). Thus, NIM-6 is here retained as a distinct zone.

- NIM-8 has been recognized in Spiti only. Based on the similarity of its faunal content, it is grouped with NIM-7.

- NIM-10 has been identified in Spiti only (*Escarguelites* horizon). Within this region, NIM-10 shows a good lateral continuity, from Mud to Losar. It shares parts of its faunal content with the overlying NIM-11, but it also contains a distinct and unique fauna consisting of three species. Therefore, it is here preserved as a distinct zone.

- NIM-15. This UAs has been identified only in one section in the Spiti area (*Subvishnuites posterus* beds; Mud). It is distinguished from the overlying UA by only one species. Based on the close affinity of its faunal content, it is merged with NIM-16.

This procedure results in 13 successive UA-zones for the Smithian of the NIM (SM1-SM13; Fig. 3). Three of these zones represent groupings of two preliminary UAs. In the following diversity analysis, these 13 UA-zones are used for all counts at the pooled level of the three studied basin, i.e. the NIM. For counts at the basin levels, the local and preliminary UAs are used.

Generally, conflicting relationships between taxa can be generated by the discontinuous nature of the fossil record (i.e. sedimentary gaps, inappropriate facies, selective preservation, ecological exclusion but also insufficient sampling) (Monnet and Bucher, 2002). The fact that no such contradictions were found during the biochronological analysis highlights the excellent quality of our primary data. Therefore, the zonation presented here closely matches the empirical succession of faunal associations that have been established previously (Brühwiler et al., 2007, accepted, submitted [b, c, d]).

Recently published high-precision U-Pb ages from South China and their calibration with ammonoid faunas yielded an age of 251.22±0.20 Ma for the early Smithian *Kashmirites kapila* beds, and an age of 250.55±0.40 Ma for the early Spathian *Tirolites*/*Columbites* beds (Ovtcharova et al., 2006; Galfetti et al., 2007b). Thus, a duration of 0.67±0.6 My is inferred for the bracketed time interval. As mentioned above, the *Kashmirites kapila* beds from South China correlate with the UA-zone SM-5. The *Tirolites*/*Columbites* beds represent the second ammonoid zone of the early Spathian (Bucher, unpublished). For the NIM, we now have 10 UA-zones within this interval, which leads to an estimated average maximal duration of 67±60 Ky per zone (inclusive of the intervals of separation intercalated between the zones). Simulations have shown that the total amount of elapsed time captured by UAs is of about 30%, whereas the rest lies within the intervals of separation (Escarguel and Bucher, 2004). This figure is only valid for simple maximal associations and not for UA-zones corresponding to reunions of preliminary UA-zones (inclusive of their separation intervals). Considering the 12 UAs (NIM-5 to NIM-16) of the concerned time interval, this leads to an estimated average duration of 17.5±15 Ky for the UAs of the NIM.

Based on the U/Pb single zircon ages obtained by Ovtcharova et al. (2006) and Galfetti et al. (2007b), the following average zone durations (inclusive of the intervals of separation) can be estimated for the Griesbachian-Anisian interval of North America:

- Griesbachian-earliest Smithian: 1.38±0.4 Ma divided by 6 zones (Tozer, 1994) = 230±67 Ky per zone.
- Smithian: 0.67±0.6 My divided by 3 zones (Tozer, 1994) = 223±20 Ky per zone.
- Spathian: 2.43±0.68 My divided by 7 zones (Guex et al., 2005a, b and Bucher et al., ongoing work) = 347±97 Ky per zone.
- Anisian: 6.92+1.2/-1.0 My divided by 31 zones (Monnet and Bucher, 2005, 2006)= 223+39/-32 Ky per zone.

Hence, these estimations highlight that the average duration of ammonoid UA-zones of the Smithian of the NIM is likely to be the shortest of all Early Triassic and Anisian stages or substages.

3. Diversity dynamics

3.1. Methods

Following Monnet et al. (2003), species richness is defined as the total number of species occurring within a given UA zone. Originations and extinctions correspond to the number of species appearing and disappearing between two successive UA-zones. The percentage of origination is defined as the number of originations divided by the total number of species occurring in the overlying UA zone; the percentage of extinction is defined as the number of extinctions divided by the total number of species occurring in the underlying zone. The turnover is defined as the sum of originations and extinctions between two zones. The percentage of turnover is the turnover divided by the total number of species occurring in the two bracketing UA zones. Species richness, originations/extinctions and turnover are counted separately within the Salt Range, Spiti and the Tulong basins, and at the pooled level of the NIM. In order to evaluate the effect of sample size on species counts, we performed a rarefaction analysis using PAST (Hammer et al., 2001). We also counted the generic richness, as well as the originations/extinctions and the turnover at the genus level at the pooled level of all three basins (i.e. the NIM). Further insights are provided by poly-cohort analysis (Raup, 1978, 1986; Foote, 1988; Hartenberger, 1988). A poly-cohort is a set of species existing during a given time bin. A poly-cohort survivorship curve is a time plot of the percentage of species still existing after a timespan δt, showing the forward decay of the target assemblage by extinction of its constituent species; conversely, a poly-cohort prenascence curve is a time plot of the percentage of species already existing before a timespan δt. Survivorship and prenascence curves are visualized in a poly-cohort matrix (Escarguel and Legendre, 2006; Escarguel et al., 2008; Brayard et al., 2009). Finally, absolute and relative species richness of each ammonoid family was plotted against the twelve UA-zones of the NIM. This plot provides useful insights into the dynamics of the different clades of Smithian ammonoids.

3.2. Results

Fig. 5 shows the curves of species richness within each studied basin and at the pooled level of all three basins, i.e. the NIM. During this time span, the total species richness of the Salt Range, Spiti and Tulong areas is 52, 59 and 27 taxa, respectively. The comparatively low sum of ammonoid species from Tulong is explained by the absence of early Smithian faunas due to a preservation bias in this area (i.e. absence of carbonate rocks; Brühwiler et al., 2009; Brühwiler et al., accepted). In the Salt Range, species richness fluctuates only slightly between values of 3 to 8 species per UA. A first high is reached in SR-3. Low values are recorded in the remaining part of the early Smithian and the lower part of the middle Smithian (SR5-7). Higher values are subsequently recorded in the remaining part of the middle Smithian (SR-8-10) and the lower part of the late Smithian (SR-11), whereas diversity is very low again in the latest Smithian (SR-12). In Spiti, species richness shows larger fluctuations, with values ranging from 1 to 13 species per UA. Moderate values are recorded in the first two UAs SP-1 and 2, followed by a brief decrease in SP-3. Note that ammonoids are poorly preserved and rare in this level, leading to a preservation bias (Krystyn et al., 2007a, b). With SP-4, species richness increases abruptly, and then reaches its peak value in SP-7. Throughout the middle Smithian, it shows an overall decline, with two brief drops and rebounds. Species richness declines abruptly between the middle and late Smithian, reaching its lowest value in the latest Smithian. In Tulong, values of species richness range from 2 to 8. Moderately high values are recorded in the middle Smithian, with a brief drop in TU-3. The transition to the late Smithian is marked by an abrupt diversity decline.

At the pooled level of the NIM, species richness ranges from values of 6 to 16 species per UA zone. A low value is recorded in the first zone (SM-1), and is followed by slightly higher and constant values in the next three zones (SM-2 to SM-4). Subsequently, an increase occurs during the late early Smithian (SM-5 and SM-6), reaching its highest value in the beginning of the middle Smithian (SM-7). This maximum is followed by a brief but severe drop (SM-8), a subsequent rebound (SM-9), another severe drop (SM-10) and an additional weaker rebound (SM-11). Low diversity values are recorded in the late Smithian (SM-12 and SM-13).

The results of the rarefaction analyses are shown in Fig. 6. They show that the comparative lower diversity in the Salt Range in the middle part of the record represents a genuine signal and is not biased by either preservation or sampling. In their relative fluctuations, all rarefied diversity curves for the three basins closely match the species counts (Fig. 5), revealing no important bias in our data. The only exception hereof is the case of the middle Smithian of Spiti, where the species counts (Fig. 5) indicate a diversity increase from SP-8 (=SM-8) to SP-9 (=SM-9). The rarefied diversity curve reveals that this apparent change is caused by the larger sample size of SP-9. The rarefied diversity curve at the NIM level closely matches the species counts, revealing no important bias in our data.

Absolute values (bars) and percentages (shaded areas) of originations and extinctions are plotted in Fig. 7. The entire Smithian is characterized by relatively high values of originations and extinctions. Within the lower part of the early Smithian, values of originations and extinctions are balanced, whereas in the upper part of the early Smithian, originations exceed extinctions. Highest origination values occur at the early-middle Smithian transition and within the middle Smithian. Highest extinction values clearly occur at the early-middle Smithian transition, within the middle Smithian and at the middle-late Smithian transition. Within the late Smithian, values of extinctions exceed those of originations. Thus, the early Smithian appears as a time of predominating origination. The middle Smithian appears as a time of both high originations and extinctions, whereas the late Smithian is a time of prevailing extinctions. Percentages of originations and extinctions are very high (usually more than 50%, sometimes up to 100%) throughout the Smithian. Taking into account the recently published U/Pb ages from South China (Ovtcharova et al., 2006; Galfetti et al., 2007b; see above), impressive regional apparent total rates of origination and extinction of more than 100 species per My can be inferred for the Smithian of the NIM.

Absolute turnover values (bars) and percentages of turnover (shaded areas) are plotted in Fig. 8. Absolute values of turnover are high throughout the Smithian, with peak values within the middle Smithian and at the middle-late Smithian transition. Percentages of turnover are very high throughout the Smithian. Generic richness and counts of origination, extinction and turnover at the genus level are shown in Fig. 9. They closely match the counts at the species level, except that curves appear slightly smoothed out.

Fig. 10a shows Brayard et al.'s (2009) contour graph of the ammonoid poly-cohort matrix (PCM) for the global data set at the genus level spanning the Late Carboniferous - Late Triassic time interval. The Early Triassic is a time of extremely contracted contour lines of the PCM, which is diagnostic of high evolutionary rates. Our regional data set at the species level is given in Fig. 10b, which zooms into a part of the Early Triassic. It also shows extremely contracted and mirroring survivorship and prenascence contour lines, which reflects the very high turnover throughout the Smithian, i.e. the fact that most species are confined to a single zone. Phases where the contour lines depart to some extent from the diagonal are generated by the few species which have a slightly longer range and occur in more than a single zone (compare range chart in Fig. 4). The long-ranging species

Pseudosageceras multilobatum is present in all zones, explaining why the percentages for survivorship and prenascence curves never drop to zero.

Fig. 11 shows the species richness of each Smithian ammonoid family plotted against the 13 UA-zones of the NIM (absolute and relative values). The early Smithian is characterized by a small number of families. These include the youngest representatives of the Gyronitidae which range up from the Dienerian, the long-ranging Proptychitidae and Hedenstroemiidae as well as the first typical Smithian families Flemingitidae, Kashmiritidae and Galfettitidae., The last representatives of the Gyronitidae disappear during the earliest Smithian. The course of the early and middle Smithian shows the successive appearance of a large number of new families (i.e. Dieneroceratidae, Aspenitidae, Melagathiceratidae, Arctoceratidae, Paranannitidae, Ussuriidae, Prionitidae and Inyoitidae). Many of these families disappear during the middle Smithian, and the middle-late Smithian transition is crossed only by Hedenstroemiidae, Inyoitidae and Prionitidae. The following UA-zone SM-12 is largely dominated by Prionitidae. Finally, this family also disappears before the latest Smithian UA-zone SM-13, which is characterized by Xenoceltitidae, Hedenstroemiidae and rare Inyoitidae and early representatives of Palaeophyllitidae.

3.3. Discussion

The comparison of diversity curves reveals significant differences between the Salt Range on one hand and Spiti and Tulong on the other. The Salt Range clearly departs from the general trends of the NIM since the middle Smithian diversity peak is not observed in the Salt Range. Instead, the faunas from the corresponding levels are of noticeably low diversity. These observed differences may be explained by the different sedimentary environment of the Salt Range, which is characterized by a much higher clastic input (Brühwiler et al., accepted, submitted [b, c]). The evidently smaller clastic load of the water column in Spiti and Tulong may have been a more hospitable environment for many ammonoid species. In Oman, Smithian ammonoids bearing exotic blocks consist exclusively of reddish limestone (Hallstadt facies) and blocks of mid-Smithian age also yield the highest values of species richness (Brühwiler et al. submitted [a]). A climatic cause (i.e. temperature) for the observed diversity differences is unlikely due to the close palaeogeographical position of the three basins (e.g. Smith et al., 1994). In the "Niveaux Intermédiares" of the Salt Range, where the terrigenous influx is regionally at its highest, the fauna of Spathian age also differs in its composition from coeval faunas from Tulong and Spiti. The clastic load of the water thus appears to be one of the primary factors that regulate the local composition of faunas.

Our data, focusing on the Smithian from the NIM, highlight the following three main features for the diversity dynamics of Smithian ammonoids: (i) a radiation during the early Smithian, (ii) a severe extinction in the late Smithian, (iii) an overall very high turnover throughout the Smithian.

These findings essentially support the known patterns of the Early Triassic ammonoid recover at the genus-level. It has well been established that the early Smithian radiation and the late Smithian extinction represent global events (Tozer, 1981; Brayard et al., 2006, and references therein). For instance, this pattern has well been documented from Guangxi, South China (Brayard and Bucher, 2008), and is also recognizable in the ammonoid faunas from exotic blocks from Oman (Brühwiler et al., submitted [a]). Moreover, the very high evolutionary tempo of Early Triassic ammonoids in comparison with pre-Triassic and post-Early Triassic has recently been recognized by Brayard et al. (2009) (Fig. 10) at a much coarser time resolution (i.e. stage level). Owing to an exceptional high temporal resolution, our study provides a very detailed picture of the diversity dynamics of Smithian ammonoids from the NIM. Ammonoid diversity dynamics throughout the Smithian is mainly characterized by high values of turnover between all UA-zones, indicating unabated intensity of restructuration of communities rather than accumulation of newly originated taxa. They achieved their explosive diversity peak essentially through extremely high turnover rates rather than through a standard diversification process of high origination rates coupled with low extinction rates. The high evolutionary rates are also reflected by the high number of Smithian ammonoid zones, and their very short average durations (e.g. in comparison with the Spathian or Anisian, see above).

Beyond the complementary hierachical time and space resolutions at which the recovery is looked upon, the fundamental question that persists is that of the factors which control the high evolutionary tempo of Smithian ammonoids. One possible explanation simply involves high intrinsic evolutionary rates of the Early Triassic Ceratitidae, which could lead to the observed high values of originations and extinctions (Brayard et al. 2009). From another point of view, external factors such as repeated environmental stresses could be considered as causes for the observed high level of turnover throughout the Smithian. The Early Triassic is well-known for several large and short-lived fluctuations of the carbon cycle, before it stabilizes in the Middle Triassic (Baud et al., 1996; Atudorei and Baud, 1997; Atudorei, 1999; Payne et al., 2004; Richoz, 2004; Corsetti et al., 2005; Galfetti et al., 2007a-c; Horacek et al., 2007a, b; Brühwiler et al., 2009). Environmental instabilities account well for the late Smithian ammonoid extinction event, including a global positive $\delta^{13}C$ excursion at the Smithian-Spathian boundary (e.g. Payne et al., 2004; Galfetti et al., 2007a; Richoz et al., 2007), deposition of organic-rich sediments, changes in palynological assemblages indicating major climatic change, and possibly acidification of surface waters (Brayard et al., 2006; Galfetti et al., 2007a, c). Other possible explanations for the observed high turnover of Smithian ammonoids include (i) the dependence of ammonoids on available primary producers and consumers, or (ii) possible faunal immigration from other provinces which could destabilise the regional communities. This second hypothesis is probably less significant because of the pronounced latitudinal differentiation that characterizes the global distribution of Smithian ammonoid genera (Brayard et al. 2006). Before a complete understanding of the cause (or combination of causes) responsible for the high evolutionary turnover of Smithian ammonoids can be achieved, it is important to compare our high-resolution ammonoid record from the NIM with ammonoid records of comparable resolution from other areas, and to get a better understanding of the origin and fluctuations of the primary production in the Early Triassic ocean.

4. Conclusions

This study represents a synthesis of several recent works focussing on the taxonomic revision and detailed biostratigraphy of Smithian (Early Triassic) ammonoids from the Salt Range (Brühwiler et al., [c]), from Spiti (Krystyn et al., 2007a, b; Brühwiler et al., submitted [b, d]) and from Tulong (Brühwiler et al., accepted). Biochronological analysis of the taxonomically revised and homogenized data set at the species-level by means of the Unitary Associations Method (Guex, 1991) yields a biochronological scheme of unprecedented high resolution for the Smithian of the Northern Indian Margin. During the analysis, no conflicting relationships between taxa were found, which highlights the excellent quality of our primary data. Comparison with recently published U/Pb ages from South China (Ovtcharova et al., 2006; Galfetti et al., 2007b) leads to a very short estimated *average* zone duration of 70±60 Ky per Smithian ammonoid zone (inclusive of the separation intervals).

Analysis of ammonoid diversity dynamics based on this new zonation highlights the following three main features for the Smithian ammonoids of the NIM: i) a radiation during the early Smithian, (ii) a severe extinction in the late Smithian, (iii) an overall very high turnover throughout the entire Smithian. Results of this work focusing only on the Smithian substage thus confirm the very high evolutionary tempo of Early Triassic ammonoids, as previously shown in a larger scale analysis (Brayard et al. 2009). At the much smaller scale of the UA-zones, the very high evolutionary turnover rate of ammonoids during the Smithian opens a new and complementary level in the hierarchical structure of their Early Triassic recovery process.

Acknowledgements

Claude Monnet (Zürich) kindly provided his statistical analysis software. David Ware (Zürich) is thanked for field assistance and numerous discussions. This work is a contribution to the Swiss National Foundation (project n° 200020-127716 to H.B.) and to the team “Forme, Evolution, Diversité” of the UMR-CNRS 5561 Biogéosciences (A.B).

References

Atudorei, N.-V. 1999: Constraints on the upper Permian to upper Triassic marine carbon isotope curve. Case studies from the Tethys. PhD Thesis, Lausanne, 155 pp.

Atudorei, N.-V., Baud, A., 1997. Carbon isotope events during the Triassic. Albertiana 20, 45-49.

Bando, Y., 1981. Lower Triassic ammonoids from Guryul Ravine and the spur three kilometers north of Barus. Palaeontologia Indica n. ser. 46, 135-178.

Baud, A., Atudorei, V., Sharp, Z., 1996. Late Permian and Early Triassic evolution of the Northern Indian margin: Carbon isotope and sequence stratigraphy. Geodinamica Acta 9, 57-77.

Brayard, A., Bucher, H., 2008. Smithian (Early Triassic) ammonoid faunas from northwestern Guangxi (South China): taxonomy and biochronology. Fossils and Strata 55, 1-179.

Brayard, A., Bucher, H., Escarguel, G., Fluteau, F., Bourquin, S., Galfetti, T., 2006. The Early Triassic ammonoid recovery: Paleoclimatic significance of diversity gradients. Palaeogeography, Palaeoclimatology, Palaeoecology 239, 374-395.

Brayard, A., Escarguel, G., Bucher, H., Monnet, C., Brühwiler, T., Goudemand, N., Galfetti, T., Guex, J., 2009. Good Genes and Good Luck: Ammonoid Diversity and the End-Permian Mass Extinction. Science 325, 1118-1121.

Brühwiler, T., Bucher, H., Goudemand, N., accepted. Smithian (Early Triassic) ammonoids from Tulong, South Tibet. Geobios.

Brühwiler, T., Bucher, H., Goudemand, N., Brayard, A., 2007. Smithian (Early Triassic) ammonoid faunas of the Tethys: new preliminary results from Tibet, India, Pakistan and Oman. New Mexico Museum of Natural History and Science Bulletin 41, 25-26.

Brühwiler, T., Bucher, H., Goudemand, N., Galfetti, T., submitted [a]. Smithian (Early Triassic) ammonoid faunas from Exotic Blocks from Oman: taxonomy and biochronology. Palaeontographica.

Brühwiler, T., Bucher, H., Krystyn, L., submitted [b]. Middle and late Smithian (Early Triassic) ammonoids from Spiti (India). Palaeontology.

Brühwiler, T., Bucher, H., Ware, D., Roohi, G., Rehman, K., Yaseen, A., submitted [c]. Smithian (Early Triassic) ammonoids from the Salt Range, Pakistan. Special Papers in Palaeontology.

Brühwiler, T., Goudemand, N., Galfetti, T., Bucher, H., Baud, A., Ware, D., Hermann, E., Hochuli, P.A., Martini, R., 2009. The Lower Triassic sedimentary and carbon isotope records from Tulong (South Tibet) and their significance for Tethyan palaeoceanography. Sedimentary Geology 222, 314-332.

Brühwiler, T., Ware, D., Bucher, H., Krystyn, L., Goudemand, N., submitted [d]. New Early Triassic ammonoid faunas from the Dienerian/Smithian boundary beds at the Induan/Olenekian GSSP candidate at Mud (Spiti, Northern India). Journal of Asian Earth Sciences.

Bucher, H., 1989. Lower Anisian ammonoids from the northern Humboldt Range (northwestern Nevada, USA) and their bearing upon the Lower-Middle Triassic boundary. Eclogae Geologicae Helvetiae 82, 943-1002.

Corsetti, F.A., Baud, A., Marenco, P.J., Richoz, S., 2005. Summary of Early Triassic carbon isotope records. Comptes Rendus Palevol 4, 473-486.

Diener, C., 1897. The Cephalopoda of the Lower Trias. Palaeontologia Indica, ser. 15, Himalayan Fossils 2, 1-181.

Diener, C., 1913. Triassic faunae of Kashmir. Palaeontologia Indica, n. ser. 5, 1-133.

Escarguel, G., Bucher, H., 2004. Counting taxonomic richness from discrete biochronozones of unknown duration: a simulation. Palaeogeography, Palaeoclimatology, Palaeoecology 202, 181-208.

Escarguel, G., Legendre, S., 2006. New methods for analyzing deep-time meta-community dynamics and their application to the Paleogene mammals from the Quercy and Limagne area (Massif Central, France). Strata 13 245-273.

Escarguel, G., Legendre, S., Sige, B., 2008. Unearthing deep-time biodiversity changes: The Palaeogene mammalian metacommunity of the Quercy and Limagne area (Massif Central, France). Comptes Rendus Geoscience 340, 602-614.

Foote, M., 1988. Survivorship Analysis of Cambrian and Ordovician Trilobites. Paleobiology 14, 258-271.

Frech, F. 1905: Lethaea geognostica. Das Mesozoicum. I, Trias, Stuttgart, 623 pp.

Galfetti, T., Bucher, H., Brayard, A., Hochuli, P.A., Weissert, H., Guodun, K., Atudorei, V., Guex, J., 2007a. Late Early Triassic climate change: Insights from carbonate carbon isotopes, sedimentary evolution and ammonoid paleobiogeography. Palaeogeography, Palaeoclimatology, Palaeoecology 243, 394-411.

Galfetti, T., Bucher, H., Ovtcharova, M., Schaltegger, U., Brayard, A., Brühwiler, T., Goudemand, N., Weissert, H., Hochuli, P.A., Cordey, F., Guodun, K.A., 2007b. Timing of the Early Triassic carbon cycle perturbations inferred from new U-Pb ages and ammonoid biochronozones. Earth and Planetary Science Letters 258, 593-604.

Galfetti, T., Hochuli, P.A., Brayard, A., Bucher, H., Weissert, H., Vigran, J.O., 2007c. Smithian-Spathian boundary event: Evidence for global climatic change in the wake of the end-Permian biotic crisis. Geology 35, 291-294.

Galster, F., Guex, J., Hammer, O., 2010. Neogene biochronology of Antarctic diatoms: A comparison between two quantitative approaches, CONOP and UAgraph. Palaeogeography, Palaeoclimatology, Palaeoecology 285, 237-247.

Guex, J., 1978. Le Trias inférieur des Salt Ranges, Pakistan: problèmes biochronologiques. Eclogae Geologicae Helvetiae 71, 105-141.

Guex, J. 1991: Biochronological correlations. Springer-Verlag.

Guex, J., Hungerbühler, A., Jenks, J., Taylor, C., Bucher, H., 2005a. Dix-huit nouveaux genres d'ammonites du Spathien (Trias inférieur) de l'Ouest américan (Idaho, Nevada, Californie): Note préliminaire. Bulletin de Géologie Lausanne, 362, 1-32.

Guex, J., Hungerbühler, A., Jenks, J., Taylor, D., Bucher, H., 2005b. Dix-neuf nouvelles espèces d'ammonites du Spathien (Trias inférieur) de l'Ouest américan (Idaho, Nevada, Californie): Note préliminaire. Bulletin de Géologie Lausanne 363, 1-25.

Hammer, Ø., Bucher, H. 2005. Buckman's law of covariation - a case of proportionality. Lethaia 38, 67-72.

Hammer, Ø., Harper, D.A.T., Ryan, P.D., 2001. PAST: Paleontological Statistics Software Package for Education and Data Analysis. Palaeontologia Electronica 4, 9pp. http://palaeo-electronica.org/2001_1/past/issue1_01.htm.

Hartenberger, J.L., 1988. Taxonomic Survivorship in Fossil Mammals During the Paleogene in Europe. Comptes Rendus De L Academie Des Sciences Serie Ii 306, 1197-1204.

Horacek, M., Brandner, R., Abart, R., 2007a. Carbon isotope record of the P/T boundary and the Lower Triassic in the Southern Alps: Evidence for rapid changes in storage of organic carbon. Palaeogeography, Palaeoclimatology, Palaeoecology 252, 347-354.

Horacek, M., Richoz, S., Brandner, R., Krystyn, L., Spötl, C., 2007b. Evidence for recurrent changes in Lower Triassic oceanic circulation of the Tethys: The [delta]13C record from marine sections in Iran. Palaeogeography, Palaeoclimatology, Palaeoecology 252, 355-369.

Krafft, A.v., Diener, C., 1909. Lower Triassic cephalopoda from Spiti, Malla Johar, and Byans. Palaeontologia Indica, ser. 15, 6, 1-186.

Krystyn, L., Bhargava, O.N., Richoz, S., 2007a. A candidate GSSP for the base of the Olenekian Stage: Mud at Pin Valley; district Lahul & Spiti, Himachal Pradesh (Western Himalaya), India. Albertiana 35, 5-29.

Krystyn, L., Richoz, S., Bhargava, O.N., 2007b. The Induan-Olenekian Boundary (IOB) in Mud – an update of the candidate GSSP section M04. Albertiana 36, 33-45.

Kummel, B., 1966. The Lower Triassic formations of the Salt Range and Trans-Indus Ranges, West Pakistan. Bulletin of the Museum of Comparative Zoology, Harvard University 134, 361-429.

Kummel, B., 1970. Ammonoids from the Kathwai Member, Mianwali Formation, Salt Range, West Pakistan. In: B. Kummel and C. Teichert (Editors), Stratigraphic Boundary Problems: Permian and Triassic of West Pakistan. Department of Geology, University of Kansas, Special Publication pp. 177-192.

Mojsisovics, E., Waagen, W., Diener, C., 1895. Entwurf einer Gliederung der pelagischen Sedimente des Trias-Systems. Sitzungsberichte der Akademie der Wissenschaften in Wien (I) 104, 1271-1302.

Monnet, C., Bucher, H., 2002. Cenomanian (early Late Cretaceous) ammonoid faunas of Western Europe - Part 1: Biochronology (Unitary Associations) and diachronism of datums. Eclogae Geologicae Helvetiae 95, 57-73.

Monnet, C., Bucher, H., 2005. New Middle and Late Anisian (Middle Triassic) ammonoid faunas from northwestern Nevada (USA): taxonomy and biochronology. Fossils and Strata 52, 1-121.

Monnet, C., Bucher, H., 2006. Anisian (Middle Triassic) ammonoids from North America: quantitative biochronology and biodiversity. Stratigraphy 2, 281-296.

Monnet, C., Bucher, H., Escarguel, G., Guex, J., 2003. Cenomanian (early Late Cretaceous) ammonoid faunas of Western Europe - Part II: Diversity patterns and the end-Cenomanian anoxic event. Eclogae Geologicae Helvetiae 96, 381-398.

Ovtcharova, M., Bucher, H., Schaltegger, U., Galfetti, T., Brayard, A., Guex, J., 2006. New Early to Middle Triassic U-Pb ages from South China: Calibration with ammonoid biochronozones and implications for the timing of the Triassic biotic recovery. Earth and Planetary Science Letters 243, 463-475.

Payne, J.L., Lehrmann, D.J., Wei, J.Y., Orchard, M.J., Schrag, D.P., Knoll, A.H., 2004. Large perturbations of the carbon cycle during recovery from the end-Permian extinction. Science 305, 506-509.

Raup, D.M., 1978. Cohort Analysis of Generic Survivorship. Paleobiology 4, 1-15.

Raup, D.M., 1986. Biological Extinction in Earth History. Science 231, 1528-1533.

Richoz, S., 2004. Stratigraphie et variations isotopiques du carbone dans le Permian supérieur et le Trias inférieur de la Néotéthys (Turquie, Oman et Iran). PhD., University of Lausanne, Switzerland. 281p.

Richoz, S., Krystyn, L., Horacek, M., Spötl, C., 2007. Carbon isotope record of the Induan-Olenekian candidate GSSP Mud and comparison with other sections. Albertiana 35, 35-40.

Savary, J., Guex, J., 1991. BioGraph: un nouveau programme de construction des corrélations biochronologiques basées sur les association unitaires. Bulletin de la Société vaudoise de Sciences naturelles 80, 317-340.

Savary, J., Guex, J., 1999. Discrete biochronological scales and unitary associations: description of the BioGraph computer program. Mémoires de Géologie (Lausanne) 34, 1-281.

Schindewolf, O., 1953. über die Faunenwende vom Paläozoikum zum Mesozoikum. Zeitschrift der Deutschen Geologischen Gesellschaft 105, 153-182.

Smith, A.G., Smith, D.G., Funnell, B.M. 1994: Atlas of Mesozoic and Cenozoic Coastlines. Cambridge University Press, Cambridge.

Spath, L.F. 1934: Part 4: The ammonoidea of the Trias, Catalogue of the fossil cephalopoda in the British Museum (Natural History). The Trustees of the British Museum, London, 521 pp.

Tozer, E.T., 1981. Triassic Ammonoidea; classification, evolution and relationship with Permian and Jurassic forms. In: M.R. House and J.R. Senior (Editors), The Ammonoidea; the evolution, classification, mode of life and geological usefulness of a major fossil group. Systematics Association Special Volume. Academic Press [for the] Systematics Association, London-New York, International, pp. 65-100.

Tozer, E.T. 1994: Canadian Triassic ammonoid faunas. Bulletin - Geological Survey of Canada. Geological Survey of Canada, Ottawa, ON, Canada, 663 pp.

Urdy, S., Goudemand, N., Bucher, H., Chirat, R. 2010. Growth dependent phenotypic variation of molluscan shell shape: a theoretical and empirical comparison using gastropods. Journal of Experimental Zoology 314B: DOI: 10.1002/jez.b.21338.

Waagen, W., 1895. Salt-Range fossils. Vol 2: Fossils from the Ceratite Formation. Palaeontologia Indica 13, 1-323.

Walker, T.D., Valentine, J.W., 1984. Equilibrium-Models of Evolutionary Species-Diversity and the Number of Empty Niches. American Naturalist 124, 887-899.

Wang, Y.G., He, G.X., 1976. Triassic ammonoids from the Mount Jolmo Lungma region, A report of scientific expedition in the Mount Jolmo Lungma region (1966-1968).

Figure captions

Fig. 1: Simplified Early Triassic palaeogeography (modified after Brayard et al., 2006) with the positions of the Salt Range, Spiti and South Tibet.

Fig. 2: Flow chart illustrating the successive steps of the process for the UA biochronological analysis.

Fig. 3: UAs of each basin, inter-basin UAs and inter-basin UA-zonation. Grey-scale for inter-basin UAs: dark grey, UA present in all three basins; light grey, UA present in two basins; white, UA present in only one basin. Designation of local UAs according to the empirical succession of faunal associations that have been established previously (Krystyn et al., 2007a, b; Brühwiler et al., accepted; Brühwiler et al., submitted [b-d]). Note that we herein use the appearance of the first typical Smithian ammonoids (i.e. Flemingitidae and Kashmiritidae) for defining the base of the Smithian, as we have proposed previously (Brühwiler et al., submitted [d]).

Fig. 4: Synthetic range chart for the Northern Indian Margin showing the distribution of Smithian ammonoid species. White squares indicate virtual occurrences. Species marked by an asterisk (*) are those that were omitted in the data set for the construction of the UAs (see text). They are dated and reincorporated into the range chart at the end of the processing. The note "group" means that this taxon is a grouping of closely related species.

Fig. 5: Plots of ammonoid species richness for the Salt Range, Spiti, Tulong and synthesis for the NIM.

Fig. 6: Rarefied species richness curves including 95% confidence intervals. The curves for the Salt Range, Spiti and Tulong have been rarefied to a sample size of n=15; that of the NIM to a sample size of n=48. Asterisks (*) mark samples of very small size that have not been included in the rarefaction analysis (SP-3: 6 specimens; TU-5: 4 specimens). Note that virtually present species (compare Fig. 4) are not included within this data set.

Fig. 7: Values (bars) and percentages (shaded areas) of origination and extinction of all ammonoids throughout the Smithian.

Fig. 8: Values (bars) and percentages (shaded areas) of turnover of all ammonoids throughout the Smithian.

Fig. 9: Generic richness, origination, extinction and turnover at the genus level throughout the Smithian of the Northern Indian Margin.

Fig. 10: (A) Brayard et al.'s (2009, modified) contour graph of the ammonoid poly-cohort matrix (PCM) for the global data set at the genus level spanning the Late Carboniferous - Late Triassic time interval. Each column of the PCM records the prenascence (upper triangle) and survivorship (lower triangle) percentages of a target assemblage located on the diagonal "100% cell". Abbreviations: PTB, Permian-Triassic boundary; 1, Kasimovian; 2, Gzhelian; 3, Asselian; 4, Sakmarian; 5, Artinskian; 6, Kungurian; 7, Roadian; 8, Wordian; 9, Capitanian; 10, Wuchiapingian; unlabeled successive intervals, Changhsingian, Griesbachian, Dienerian, Smithian; 15, Spathian; 16, Early Anisian; 17, Middle Anisian; 18, Late Anisian; 19, Ladinian; 20, Early Carnian; 21, Late Carnian; 22, Early Norian; 23, Middle Norian; 24, Late Norian; 25, Rhaetian. (B) Contour graph of the ammonoid PCM for the regional data set at the species level for the Smithian of the Northern Indian Margin.

Fig. 11: Absolute and relative species richness for each Smithian ammonoid family plotted against the 13 UA-zones of the Northern Indian Margin.

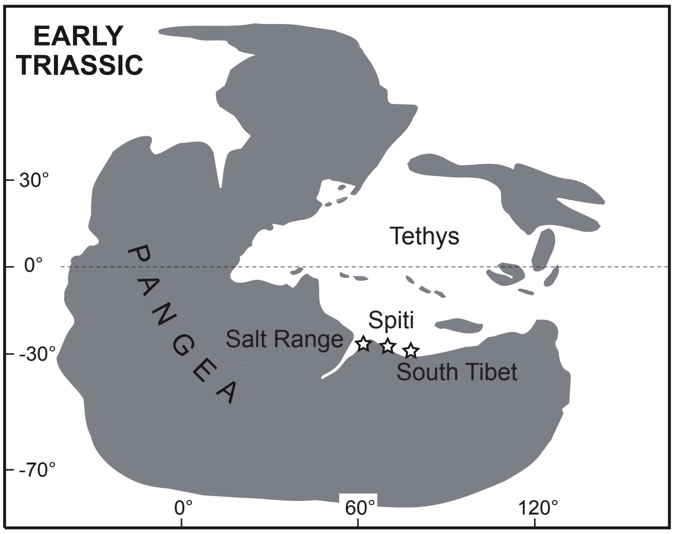
EARLY TRIASSIC
30°
0°
-30°
-70°
0°
60°
120°
PANGEA
Tethys
Salt Range
Spiti
South Tibet

Fig. 1

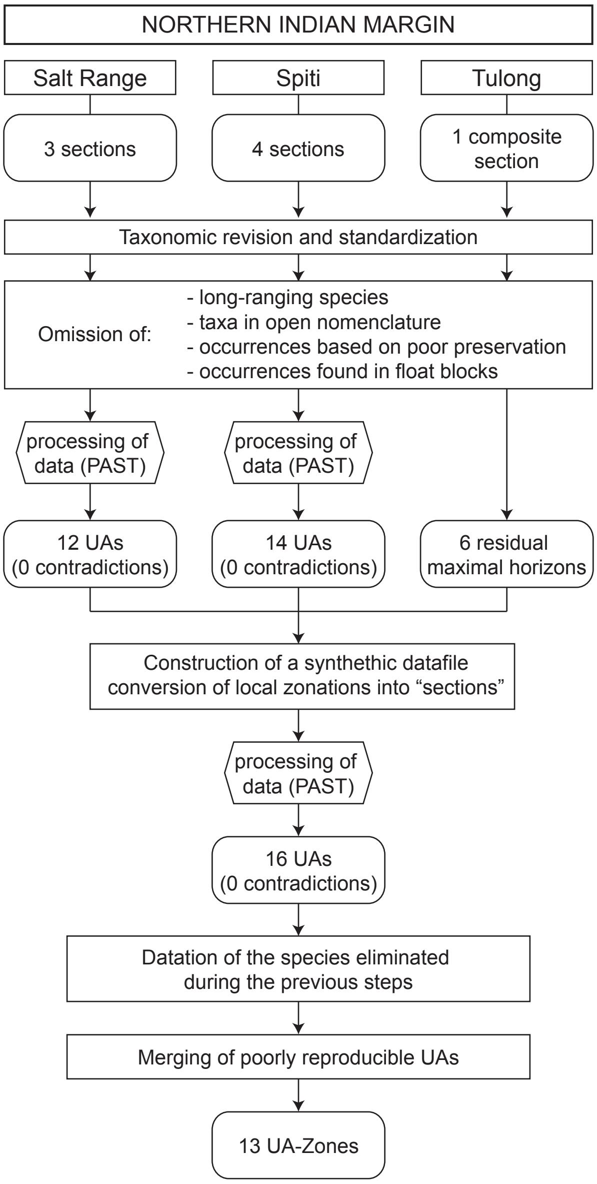
NORTHERN INDIAN MARGIN
Salt Range
Spiti
Tulong
3 sections
4 sections
1 composite section
Taxonomic revision and standardization
Omission of:
- long-ranging species
- taxa in open nomenclature
- occurrences based on poor preservation
- occurrences found in float blocks
processing of data (PAST)
processing of data (PAST)
12 UAs (0 contradictions)
14 UAs (0 contradictions)
6 residual maximal horizons
Construction of a synthethic datafile conversion of local zonations into "sections"
processing of data (PAST)
16 UAs (0 contradictions)
Datation of the species eliminated during the previous steps
Merging of poorly reproducible UAs
13 UA-Zones

Fig. 2

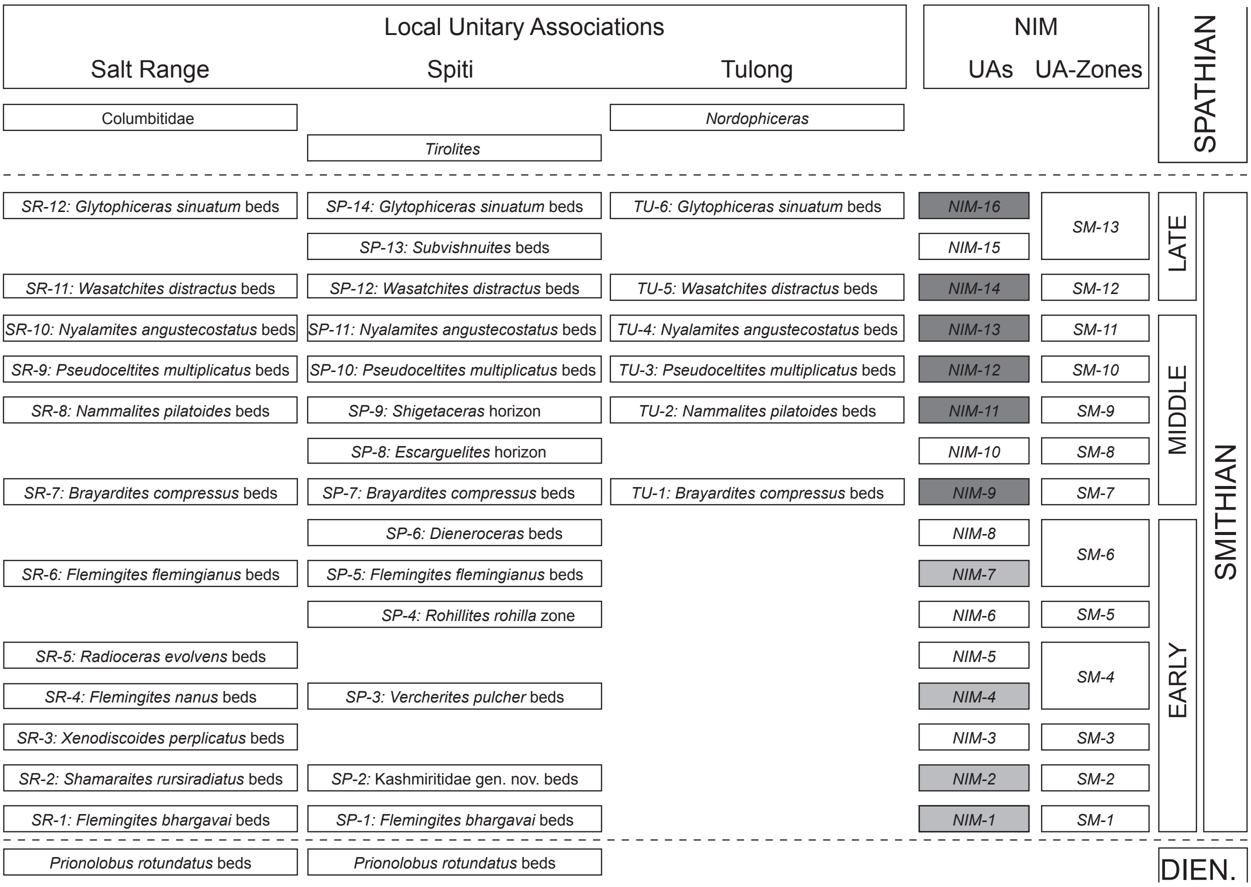

Local Unitary Associations			NIM			
Salt Range	Spiti	Tulong	UAs	UA-Zones		
Columbitidae		*Nordophiceras*				SPATHIAN
	Tirolites					
SR-12: Glytophiceras sinuatum beds	*SP-14: Glytophiceras sinuatum* beds	*TU-6: Glytophiceras sinuatum* beds	*NIM-16*	*SM-13*	LATE	SMITHIAN
	SP-13: Subvishnuites beds		*NIM-15*			
SR-11: Wasatchites distractus beds	*SP-12: Wasatchites distractus* beds	*TU-5: Wasatchites distractus* beds	*NIM-14*	*SM-12*		
SR-10: Nyalamites angustecostatus beds	*SP-11: Nyalamites angustecostatus* beds	*TU-4: Nyalamites angustecostatus* beds	*NIM-13*	*SM-11*	MIDDLE	
SR-9: Pseudoceltites multiplicatus beds	*SP-10: Pseudoceltites multiplicatus* beds	*TU-3: Pseudoceltites multiplicatus* beds	*NIM-12*	*SM-10*		
SR-8: Nammalites pilatoides beds	*SP-9: Shigetaceras* horizon	*TU-2: Nammalites pilatoides* beds	*NIM-11*	*SM-9*		
	SP-8: Escarguelites horizon		*NIM-10*	*SM-8*		
SR-7: Brayardites compressus beds	*SP-7: Brayardites compressus* beds	*TU-1: Brayardites compressus* beds	*NIM-9*	*SM-7*		
	SP-6: Dieneroceras beds		*NIM-8*	*SM-6*	EARLY	
SR-6: Flemingites flemingianus beds	*SP-5: Flemingites flemingianus* beds		*NIM-7*			
	SP-4: Rohillites rohilla zone		*NIM-6*	*SM-5*		
SR-5: Radioceras evolvens beds			*NIM-5*	*SM-4*		
SR-4: Flemingites nanus beds	*SP-3: Vercherites pulcher* beds		*NIM-4*			
SR-3: Xenodiscoides perplicatus beds			*NIM-3*	*SM-3*		
SR-2: Shamaraites rursiradiatus beds	*SP-2:* Kashmiritidae gen. nov. beds		*NIM-2*	*SM-2*		
SR-1: Flemingites bhargavai beds	*SP-1: Flemingites bhargavai* beds		*NIM-1*	*SM-1*		
Prionolobus rotundatus beds	*Prionolobus rotundatus* beds					DIEN.

Fig. 3

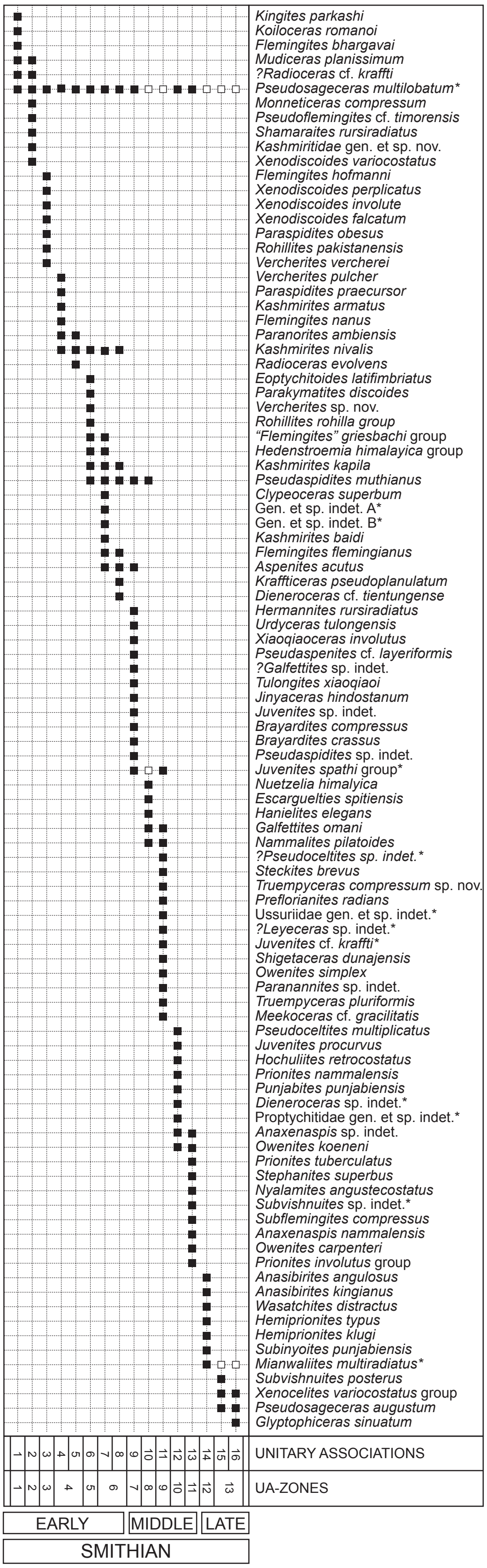
Kingites parkashi
Koiloceras romanoi
Flemingites bhargavai
Mudiceras planissimum
?Radioceras cf. kraffti
Pseudosageceras multilobatum*
Monneticeras compressum
Pseudoflemingites cf. timorensis
Shamaraites rursiradiatus
Kashmiritidae gen. et sp. nov.
Xenodiscoides variocostatus
Flemingites hofmanni
Xenodiscoides perplicatus
Xenodiscoides involute
Xenodiscoides falcatum
Paraspidites obesus
Rohillites pakistanensis
Vercherites vercherei
Vercherites pulcher
Paraspidites praecursor
Kashmirites armatus
Flemingites nanus
Paranorites ambiensis
Kashmirites nivalis
Radioceras evolvens
Eoptychitoides latifimbriatus
Parakymatites discoides
Vercherites sp. nov.
Rohillites rohilla group
"Flemingites" griesbachi group
Hedenstroemia himalayica group
Kashmirites kapila
Pseudaspidites muthianus
Clypeoceras superbum
Gen. et sp. indet. A*
Gen. et sp. indet. B*
Kashmirites baidi
Flemingites flemingianus
Aspenites acutus
Kraffticeras pseudoplanulatum
Dieneroceras cf. tientungense
Hermannites rursiradiatus
Urdyceras tulongensis
Xiaoqiaoceras involutus
Pseudaspenites cf. layeriformis
?Galfettites sp. indet.
Tulongites xiaoqiaoi
Jinyaceras hindostanum
Juvenites sp. indet.
Brayardites compressus
Brayardites crassus
Pseudaspidites sp. indet.
Juvenites spathi group*
Nuetzelia himalyica
Escarguelties spitiensis
Hanielites elegans
Galfettites omani
Nammalites pilatoides
?Pseudoceltites sp. indet.*
Steckites brevus
Truempyceras compressum sp. nov.
Preflorianites radians
Ussuriidae gen. et sp. indet.*
?Leyeceras sp. indet.*
Juvenites cf. kraffti*
Shigetaceras dunajensis
Owenites simplex
Paranannites sp. indet.
Truempyceras pluriformis
Meekoceras cf. gracilitatis
Pseudoceltites multiplicatus
Juvenites procurvus
Hochuliites retrocostatus
Prionites nammalensis
Punjabites punjabiensis
Dieneroceras sp. indet.*
Proptychitidae gen. et sp. indet.*
Anaxenaspis sp. indet.
Owenites koeneni
Prionites tuberculatus
Stephanites superbus
Nyalamites angustecostatus
Subvishnuites sp. indet.*
Subflemingites compressus
Anaxenaspis nammalensis
Owenites carpenteri
Prionites involutus group
Anasibirites angulosus
Anasibirites kingianus
Wasatchites distractus
Hemiprionites typus
Hemiprionites klugi
Subinyoites punjabiensis
Mianwaliites multiradiatus*
Subvishnuites posterus
Xenocelites variocostatus group
Pseudosageceras augustum
Glyptophiceras sinuatum
1 2 3 4 5 6 7 8 9 10 11 12 13 14 15 16
UNITARY ASSOCIATIONS
1 2 3 4 5 6 7 8 9 10 11 12 13
UA-ZONES
EARLY
MIDDLE
LATE
SMITHIAN

Fig. 4

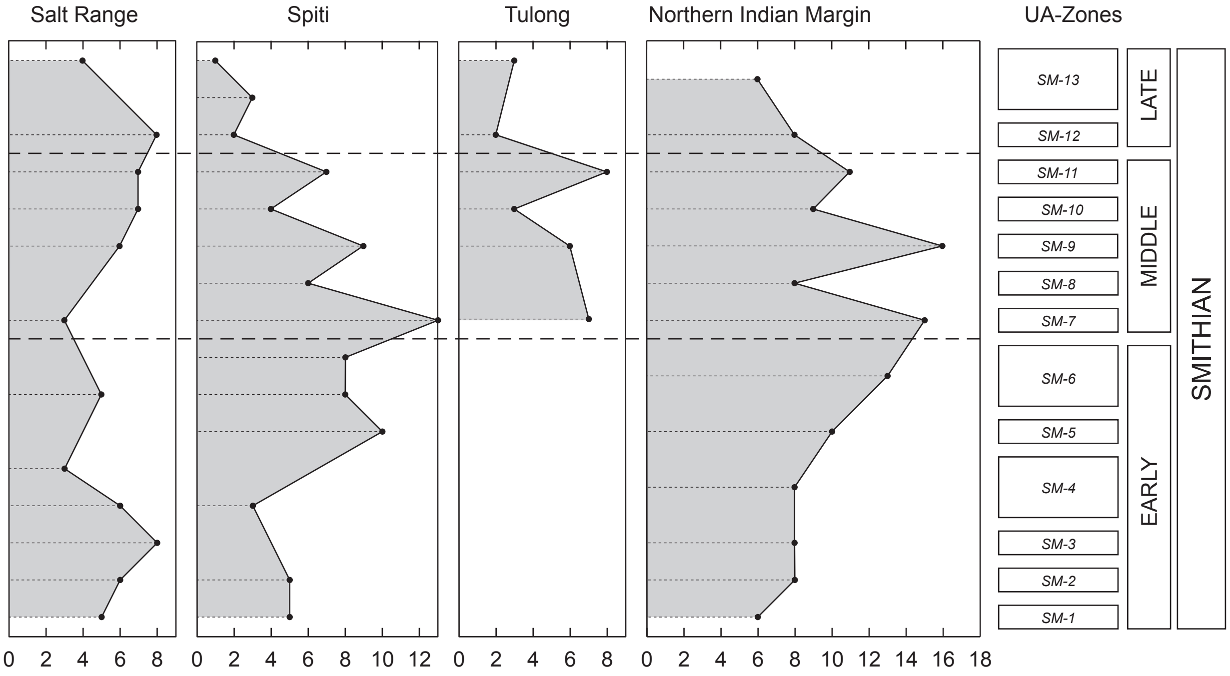
Salt Range
Spiti
Tulong
Northern Indian Margin
UA-Zones
SM-13
SM-12
SM-11
SM-10
SM-9
SM-8
SM-7
SM-6
SM-5
SM-4
SM-3
SM-2
SM-1
LATE
MIDDLE
EARLY
SMITHIAN
0 2 4 6 8
0 2 4 6 8 10 12
0 2 4 6 8
0 2 4 6 8 10 12 14 16 18

Fig. 5

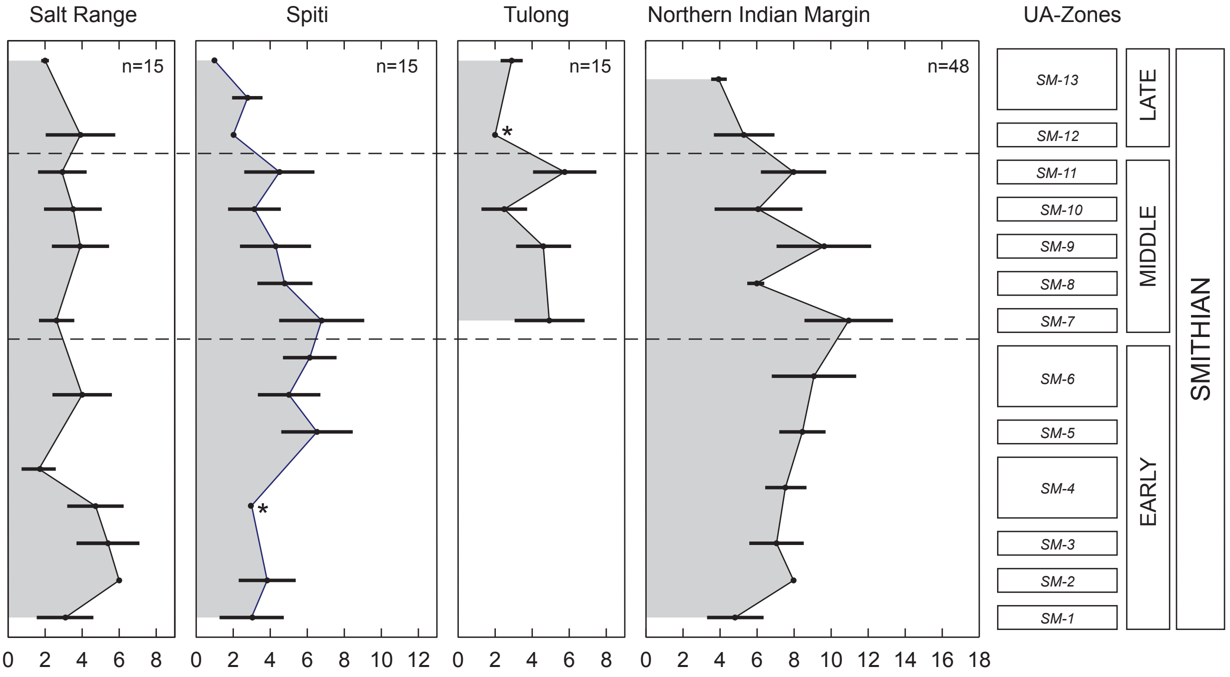
Salt Range
Spiti
Tulong
Northern Indian Margin
UA-Zones
n=15
n=15
n=15
n=48
*
*
SM-13
SM-12
SM-11
SM-10
SM-9
SM-8
SM-7
SM-6
SM-5
SM-4
SM-3
SM-2
SM-1
LATE
MIDDLE
EARLY
SMITHIAN
0 2 4 6 8
0 2 4 6 8 10 12
0 2 4 6 8
0 2 4 6 8 10 12 14 16 18

Fig. 6

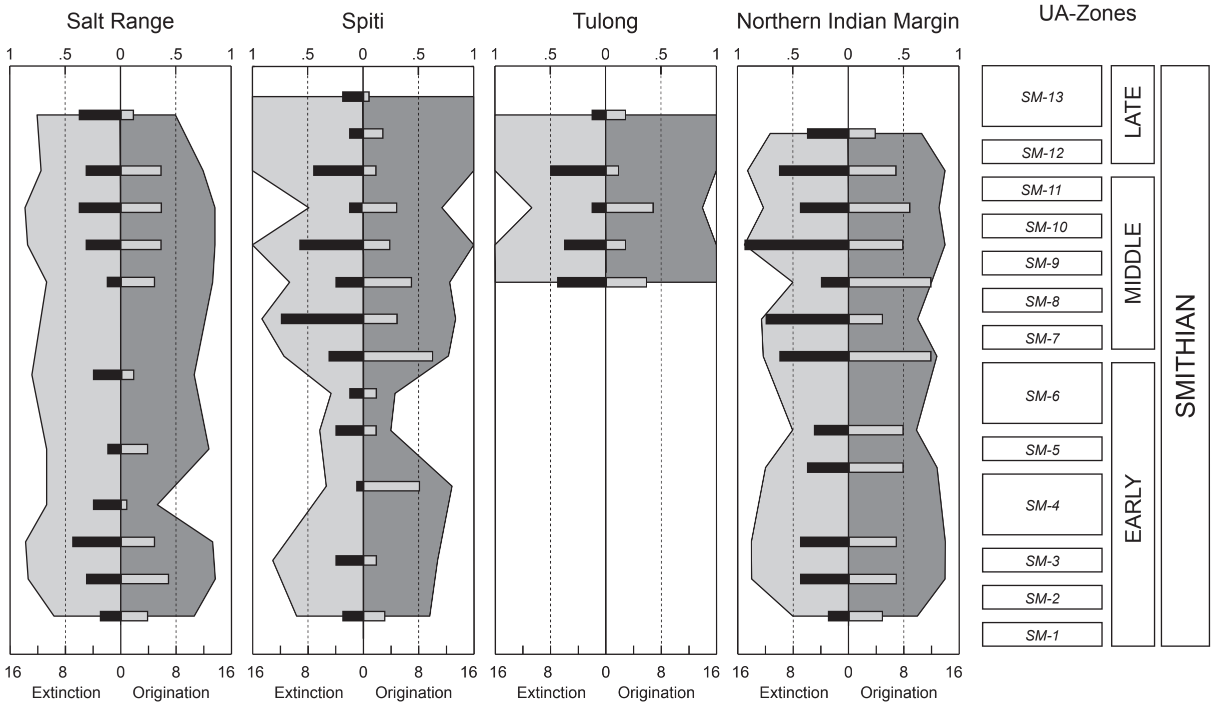
Salt Range
Spiti
Tulong
Northern Indian Margin
UA-Zones
1 .5 0 .5 1
16 8 0 8 16
Extinction
Origination
SM-13
SM-12
SM-11
SM-10
SM-9
SM-8
SM-7
SM-6
SM-5
SM-4
SM-3
SM-2
SM-1
LATE
MIDDLE
EARLY
SMITHIAN

Fig. 7

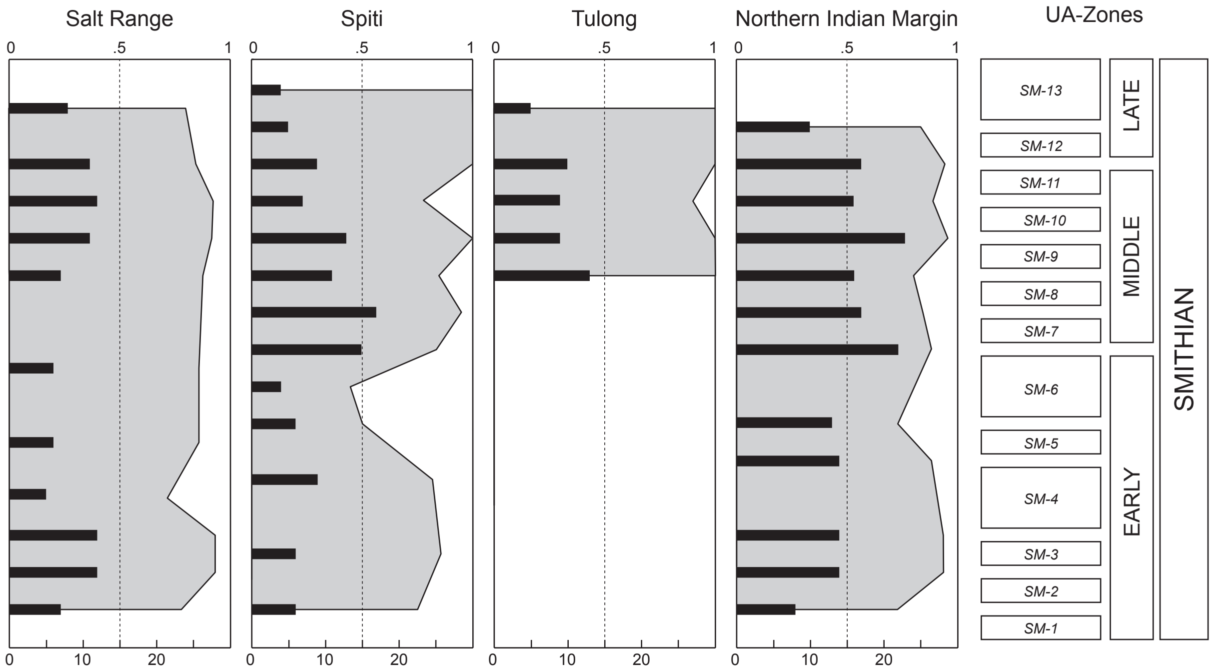
Salt Range
Spiti
Tulong
Northern Indian Margin
UA-Zones
0 .5 1
0 10 20
SM-13
SM-12
SM-11
SM-10
SM-9
SM-8
SM-7
SM-6
SM-5
SM-4
SM-3
SM-2
SM-1
LATE
MIDDLE
EARLY
SMITHIAN

Fig. 8

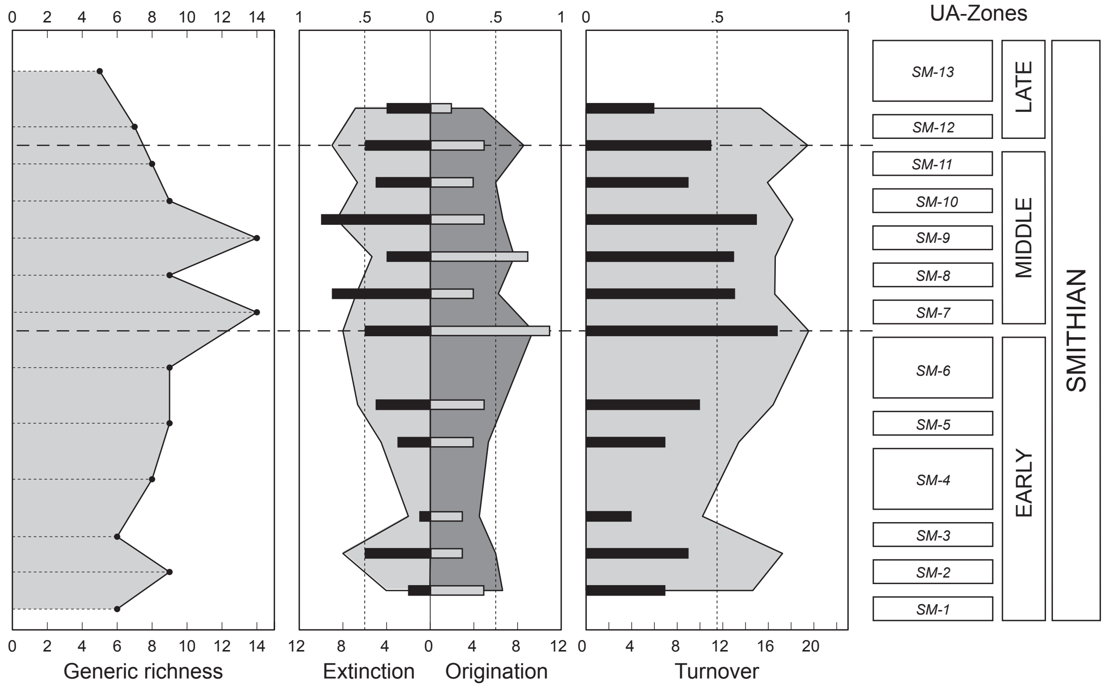
0 2 4 6 8 10 12 14
Generic richness
1 .5 0 .5 1
12 8 4 0 4 8 12
Extinction
Origination
0 .5 1
0 4 8 12 16 20
Turnover
UA-Zones
SM-13
SM-12
SM-11
SM-10
SM-9
SM-8
SM-7
SM-6
SM-5
SM-4
SM-3
SM-2
SM-1
LATE
MIDDLE
EARLY
SMITHIAN

Fig. 9

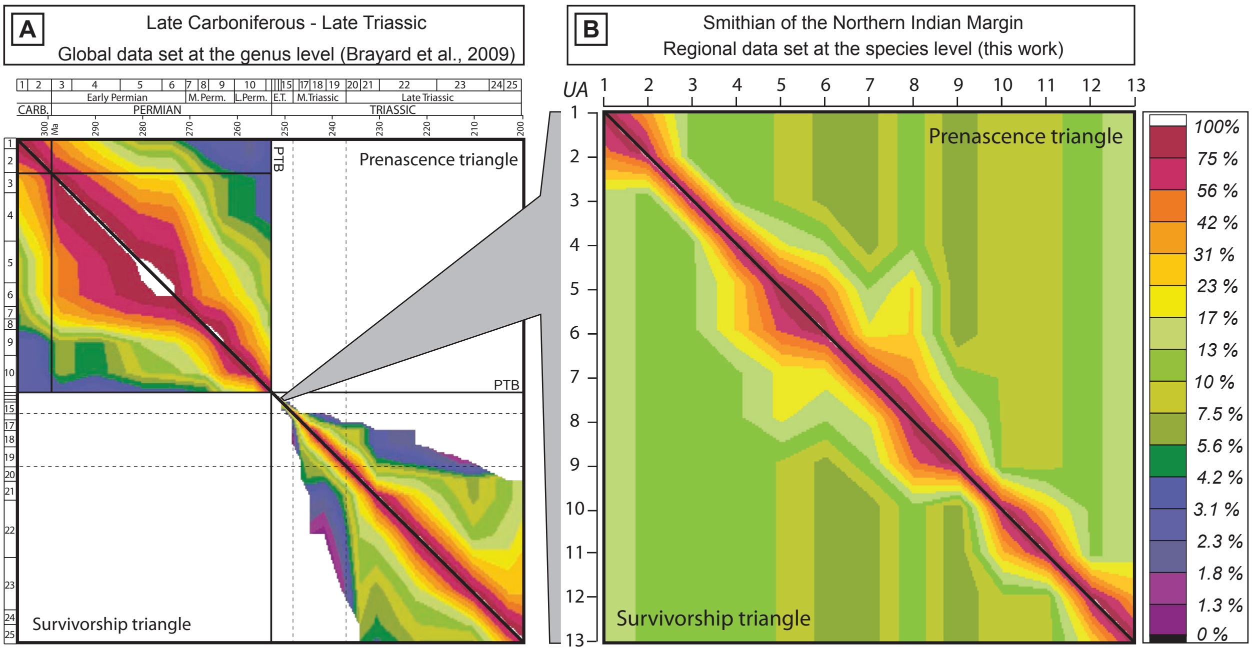
A
Late Carboniferous - Late Triassic
Global data set at the genus level (Brayard et al., 2009)
Early Permian
M.Perm.
L.Perm.
E.T.
M.Triassic
Late Triassic
CARB.
PERMIAN
TRIASSIC
300 Ma
290
280
270
260
250
240
230
220
210
200
PTB
Prenascence triangle
Survivorship triangle
B
Smithian of the Northern Indian Margin
Regional data set at the species level (this work)
UA
1 2 3 4 5 6 7 8 9 10 11 12 13
Prenascence triangle
Survivorship triangle
100%
75 %
56 %
42 %
31 %
23 %
17 %
13 %
10 %
7.5 %
5.6 %
4.2 %
3.1 %
2.3 %
1.8 %
1.3 %
0 %

Fig. 10

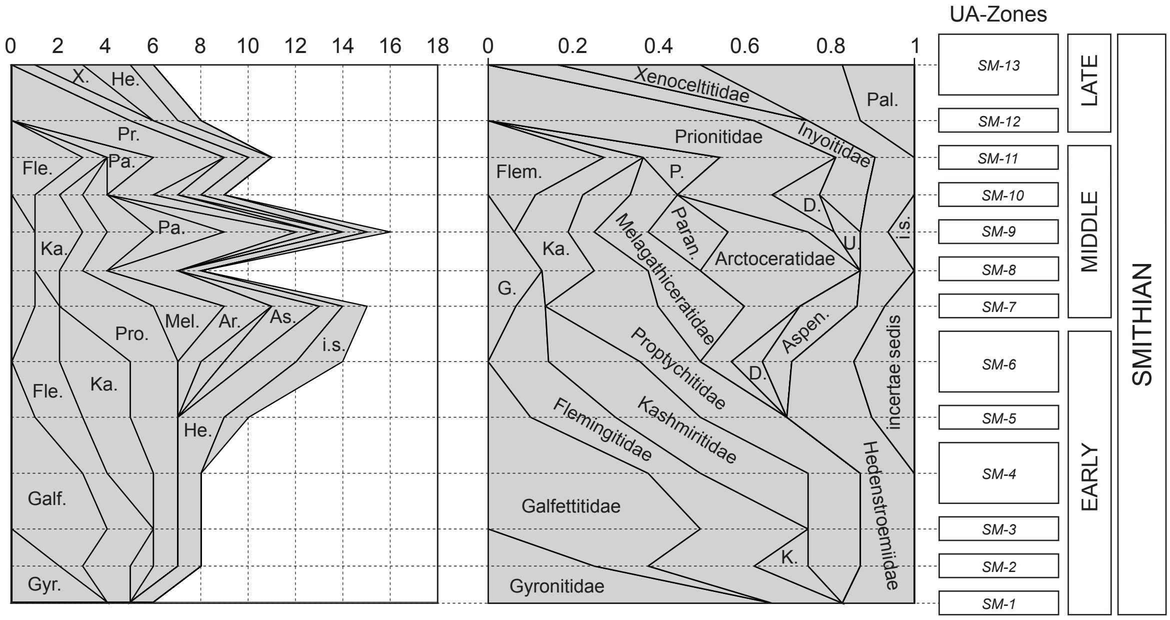
UA-Zones
0
2
4
6
8
10
12
14
16
18
0
0.2
0.4
0.6
0.8
1
X.
He.
Pr.
Fle.
Pa.
Ka.
Pa.
Pro.
Mel.
Ar.
As.
i.s.
Fle.
Ka.
He.
Galf.
Gyr.
Xenoceltitidae
Pal.
Prionitidae
Inyoitidae
Flem.
P.
D.
Paran.
i.s.
Ka.
Melagathiceratidae
U.
Arctoceratidae
G.
Proptychitidae
Aspen.
incertae sedis
D.
Kashmiritidae
Flemingitidae
Hedenstroemiidae
Galfettitidae
K.
Gyronitidae
SM-13
SM-12
SM-11
SM-10
SM-9
SM-8
SM-7
SM-6
SM-5
SM-4
SM-3
SM-2
SM-1
LATE
MIDDLE
EARLY
SMITHIAN

Fig. 11

APPENDIX:

Co-authored publications linked to this dissertation

Co-authored publications linked to this dissertation (abstracts only):

- Klug, C., Brühwiler, T., Korn, D., Schweiger, G., Brayard, A. and Tisley, J. 2007: Ammonoid shell structures of primary organic composition. Palaeontology, 50 (6), 1-16.

- Brayard, A., Bucher, H., Brühwiler, T., Galfetti, T., Goudemand, N., Jenks, J., Escarguel, G. and Guodun, K. 2007: *Proharpoceras* Chao: a new ammonoid lineage surviving the end Permian mass extinction. Lethaia, 40, 175-181.

- Galfetti T., Bucher H., Ovtcharova, M., Schaltegger U., Brayard A., Brühwiler T., Goudemand N., Weissert H., Hochuli P. A., Cordey F. and Guodun K. 2007: Timing of the Early Triassic carbon cycle perturbations inferred from new U-Pb ages and ammonoid biochronozones. Earth and Planetary Science Letters, 258, 593-604.

- Galfetti T., Bucher H., Martini R., Hochuli P. A., Weissert H., Crasquin-Soleau S., Brayard A., Goudemand N., Brühwiler T. and Guodun K. 2008: Evolution of Early Triassic outer platform paleoenvironments in the Nanpanjiang Basin (South China) and their significance for the biotic recovery. Sedimentary Geology, 204, 36-60.

- Brayard, A., Escarguel, G., Bucher, H. and Brühwiler, T. (2009): Smithian and Spathian (Early Triassic) ammonoid assemblages from terranes: Paleoceanographic and paleogeographic implications. Journal of Asian Earth Sciences, 36, 420-433.

- Brayard, A., Brühwiler, T., Bucher, H. and Jenks, J. 2009. *Guodunites*, a low-palaeolatitude and trans-panthalassic Smithian (Early Triassic) ammonoid genus. Palaeontology 52, 471-481

- Brayard, A., Escarguel, G., Bucher, H., Monnet, C., Brühwiler, T., Goudemand, Galfetti, T. and Guex, J. (2009). Good Genes and Good Luck: Ammonoid Diversity and the End-Permian Mass Extinction. Science, 325, 1118-1121.

- Kaim, A., Nützel, A. Bucher, H., Brühwiler, T. and Goudemand, N. accepted. Early Triassic (Late Griesbachian) gastropods from South China (Shanggan, Guangxi). Swiss Journal of Geoscience.

- Forel, M.B., Crasquin, S., Brühwiler, T., Goudemand, N., Bucher, H., Baud, A., Randon, C., submitted. Ostracod recovery after Permian-Triassic boundary mass-extinction in South Tibet. Palaeogeography, Palaeoclimatology, Palaeoecology.

- Elke Hermann, Peter Hochuli, Sabine Méhay, Hugo Bucher, Thomas Brühwiler, Ghazala Roohi, Michael Hautmann and David Ware (in prep.). Organic matter and palaeoenvironmental signals in the Early Triassic of the Salt Range and Surghar Range, Pakistan. Palaeogeography, Palaeoclimatology, Palaeoecology.

Ammonoid shell structures of primary organic composition

Christian Klug[a], Thomas Brühwiler[a], Dieter Korn[b], Günter Schweigert[c], Arnaud Brayard[d] and John Tisley[e]

[a]Paläontologisches Institut und Museum der Universität Zürich, Karl Schmid-Str. 4, CH-8006 Zürich, Switzerland.
[b]Museum für Naturkunde der Humboldt-Universität zu Berlin, Invalidenstr. 43, D-10115 Berlin, Germany.
[c]Staatliches Museum für Naturkunde, Rosenstein 1, D-70191 Stuttgart, Germany.
[d]UMR 5561 CNRS Biogéosciences, Université de Bourgogne, 6 boulevard Gabriel, F-21000, Dijon, France.
[e]Ansell Road, Sheffield S11 7PE, UK.

Abstract

Palaeozoic and Mesozoic cephalopod conchs occasionally reveal dark organic coatings at the aperture. A number of these coatings, including still unrecorded examples, are described, figured and interpreted herein. On the basis of elemental analysis, actualistic comparison and a comparison with Triassic bivalves, some of these coatings are shown to consist of apatite and primarily probably of conchiolin (and also probably melanin). In several Mesozoic ammonoid genera such as *Paranannites*, *Psiloceras*, *Lytoceras*, *Phylloceras*, *Harpoceras* and *Chondroceras*, some of these coatings (recorded herein for most of these taxa for the first time) are interpreted as a structure similar to the black band, which was previously known only from Recent *Allonautilus* and *Nautilus*. In contrast to these nautilid genera, however, the organic material of some Mesozoic ammonoids was not deposited on the inside of the shell but externally, albeit positioned at the terminal aperture as in Recent nautilids. Some ammonoids of Carboniferous and Triassic age show several such bands at more or less regular angular distances on the ultimate whorls and at the aperture, e.g. *Nomismoceras*, *Gatherites*, *Owenites*, *Paranannites*, *Juvenites* and *Melagathiceratidae* gen. et sp. nov. Triassic material from Oman shows that the black coating was probably secreted from the inside, because the position of this organic deposit changes from interior to exterior in an anterior direction (i.e. adaperturally). This structure has previously been referred to as a 'false colour pattern' and is here interpreted as having been formed at an interim aperture or megastria ('alter Mundrand'). All structures discussed in the paper are considered to have been secreted by a single organ and to have been initiated by some form of stress or adverse conditions. Thus, certain environmental parameters and growth anomalies appear to have influenced their formation.

Keywords: Ammonoidea; mature modifications; body chamber; growth; taphonomy.

PALAEONTOLOGY **50** (6), 2007, 1463–1478.

Proharpoceras Chao: a new ammonoid lineage surviving the end-Permian mass extinction

Arnaud Brayard[a], Hugo Bucher[b], Thomas Brühwiler[b], Thomas Galfetti[b], Nicolas Goudemand[b], Kuang Guodun[c], Gilles Escarguel[a] and Jim Jenks[d]

[a]UMR 5125 PEPS CNRS, 69622 Villeurbanne Cedex, France; Université Lyon 1, Campus de la Doua, Bât. Géode, 69622 Villeurbanne Cedex, France.
[b]Paläontologisches Institut und Museum der Universität Zürich, Karl-Schmid Strasse 4, CH-8006 Zürich, Switzerland.
[c]Guangxi Bureau of Geology and Mineral Resources, Jiangzheng Road 1, Nanning, Guangxi 530023, China.
[d]134 Johnson Ridge Lane, West Jordan, Utah 84084, USA.

Abstract

Based on new, bed-rock controlled material from northwestern Guangxi and Oman, the Early Triassic genus Proharpoceras Chao is shown to be a representative of Otocerataceae. Character analysis excludes a direct link with the Griesbachian Otoceratidae and favours a derivation of Proharpoceras from the late Permian Anderssonoceratidae. The biostratigraphic range of Proharpoceras is restricted to the Smithian and its biogeographic distribution comprises Oman, South China, and Primorye, thus indicating an essentially low palaeolatitudinal distribution. Proharpoceras has no apparent relatives among other Early and Middle Triassic Ceratitida and is thus considered to be the last representative of Otocerataceae. This offshoot of the late Permian Anderssonoceratidae implies that an additional ammonoid lineage survived the end Permian extinction and that it dwindled away for some 2 Myr before going extinct.

Keywords: Ammonoids; Oman; Otocerataceae; Primorye; Smithian (Early Triassic); South China

LETHAIA **40**, 2007, 175-181.

Timing of the Early Triassic carbon cycle perturbations inferred from new U–Pb ages and ammonoid biochronozones

Thomas Galfetti[a], Hugo Bucher[a], Maria Ovtcharova[b], Urs Schaltegger[b], Arnaud Brayard[c], Thomas Brühwiler[a], Nicolas Goudemand[a], Helmut Weissert[d], Peter A. Hochuli[a], Fabrice Cordey[e], Kuang Guodun[f]

[a]Paläontologisches Institut der Universität Zürich, Karl Schmid-Strasse 4, 8006 Zürich, Switzerland.
[b]Department of Mineralogy, University of Geneva, rue des Maraîchers 13, CH-1205 Geneva, Switzerland.
[c]UMR 5561 CNRS Biogéosciences, Université de Bourgogne, 6 boulevard Gabriel, F-21000, Dijon, France.
[d]Department of Earth Science, ETH, Sonneggstrasse 5, 8006 Zürich, Switzerland.
[e]UMR 5125 PEPS CNRS, Université Lyon I, Campus de la Doua, 69622 Villeurbanne Cedex, France.
[f]Guangxi Bureau of Geology and Mineral Resources, Jiangzheng Road 1, 530023 Nanning, China.

Abstract

Based on analyses of single, thermally annealed and chemically abraded zircons, a new high-precision U–Pb age of 251.22±0.20 Ma is established for a volcanic ash layer within the "*Kashmirites densistriatus* beds" of early Smithian age (Early Triassic) from the Luolou Formation (northwestern Guangxi, South China). This new date, together with recalculated uncertainties of previous U– Pb ages from the same section [M. Ovtcharova, H. Bucher, U. Schaltegger, T. Galfetti, A. Brayard, J. Guex. New Early to Middle Triassic U–Pb ages from South China: calibration with ammonoid biochronozones and implications for the timing of the Triassic biotic recovery. Earth Planet. Sci. Lett. 243 (2006) 463–475.] allows constraining the time framework of the Early Triassic and leads to an estimated duration of (i) ca. 0.7±0.6 My for the Smithian and (ii) a maximal duration of ca. 1.4±0.4 My for the Griesbachian– Dienerian time interval. The new U–Pb age considerably reduces the absolute age gap comprised between the Permian–Triassic boundary and the Spathian (late Early Triassic). The new age framework provides the basis for the calibration of a new carbonate carbon isotope and ammonoid records of the Early Triassic Luolou Fm., which in turn are of high significance for global correlations and for carbon cycle modeling. This calibration indicates that the most significant and fastest Early Triassic carbon isotope perturbations occur between the earliest Smithian and the early Spathian, thus spanning a time interval of about 1 My. Whatever caused these carbon cycle shifts of high intensity and short duration, there is evidence for connections between these fluctuations, the pulsate recovery of ammonoids and conodonts as well as climate changes.

Keywords: carbon isotope; U–Pb age; time scale; ammonoid; Early Triassic; South China

EARTH AND PLANETARY SCIENCE LETTERS **258**, 2007, 593–604.

Evolution of Early Triassic outer platform paleoenvironments in the Nanpanjiang Basin (South China) and their significance for the biotic recovery

Thomas Galfetti[a], Hugo Bucher[a], Rossana Martini[b] Peter A. Hochuli[a], Helmut Weissert[c], Sylvie Crasquin-Soleau[d], Arnaud Brayard[e], Nicolas Goudemand[a], Thomas Brühwiler[a], Kuang Guodun[f]

[a]Paläontologisches Institut der Universität Zürich, Karl Schmid-Strasse 4, 8006 Zürich, Switzerland.
[b]Department of Geology, University of Geneva, Rue des Maraîchers 13, 1205 Geneva, Switzerland.
[c]Department of Earth Science, ETH, Universitätstrasse 16, 8092 Zürich, Switzerland.
[d]UMR 5143 CNRS, Université Pierre et Marie Curie, 75252 Paris Cedex 05, France.
[e]UMR 5561 CNRS Biogéosciences, Université de Bourgogne, 6 boulevard Gabriel, F-21000, Dijon, France.
[f]Guangxi Bureau of Geology and Mineral Resources, Jiangzheng Road 1, 530023 Nanning, China.

Abstract

Detailed microfacies and paleoenvironmental analyses were conducted through the Early Triassic interval of the outer platform ammonoid-rich series of the Nanpanjiang Basin (Luolou Formation, Guangxi Province, South China). Extensive investigations on outcrops and on thin sections reveal that the widely reported well-diversified latest Permian fauna, dominated by abundant corals, calcareous algae, calcareous sponges, crinoids, brachiopods, gastropods, ostracods and foraminifera, is abruptly replaced by decimated Early Triassic communities essentially composed of low-diversity bivalves, microgastropods, ostracods, and rare foraminifera. Along with this drastic change in faunal assemblages, the recolonization of devastated habitats by calcimicrobial frameworks is observed in the aftermath of the end Permian mass extinction. Calcimicrobialites of Griesbachian age are followed by mixed, ammonoid- and conodont-rich carbonate-siliciclastic series consisting of dark, suboxic, laminated mudstones intercalated with organic-rich shales of Dienerian to late Smithian age. The carbonate-siliciclastic series are interrupted by a brief carbonate episode during the early middle Smithian. Massive carbonate production resumes only from the early Spathian onward and persists throughout the Spathian. The initial deposition of both carbonate episodes is coeval with (i) re-establishment of welloxygenated conditions, (ii) a marked (early Smithian) to extreme (early Spathian) ammonoid/conodont diversification, (iii) a significant increase in the skeletal grain diversity and abundance and, (iv) peak carbon isotope values. A short interval of black, organic-rich shales precedes the onset of these two distinct carbonate events, which are both marked by a positive carbonate carbon isotope excursion known from other Tethyan marine localities. The comparison between the Early Triassic stratigraphic evolution of Tethyan outer platform paleoenvironments and platform/basin margin settings of the Nanpanjiang Basin suggests a causal connection between large fluctuations of the global carbon cycle, climate shifts, sealevel changes, oxygen availability in the oceans and the biological rediversification in the wake of the end-Permian biotic crisis.

Keywords: Early Triassic; Paleoenvironments; Microfacies; Luolou Fm; Nanpanjiang Basin; South China.

SEDIMENTARY GEOLOGY **204**, 2008, 36–60.

Smithian and Spathian (Early Triassic) ammonoid assemblages from terranes: paleoceanographic and paleogeographic implications

Arnaud Brayard[a], Gilles Escarguel[b], Hugo Bucher[c], Thomas Brühwiler[c]

[a]UMR 5561 CNRS Biogéosciences, Université de Bourgogne, 6 boulevard Gabriel, F-21000, Dijon, France.
[b]UMR 5125 PEPS CNRS, France; Université Lyon 1, Campus de la Doua, Bât. Géode, F-69622 Villeurbanne Cedex, France.
[c] Paläontologisches Institut und Museum, Universität Zürich, Karl-Schmid Strasse 4, CH-8006 Zürich, Switzerland.

Abstract

Early Triassic paleobiogeography is characterised by the stable supercontinental assembly of Pangea. However, at that time, several terranes such as the South Kitakami Massif (SK), South Primorye (SP) and Chulitna (respectively, and presently located in Japan, eastern Russia and Alaska) straddled the vast oceans surrounding Pangea. By means of quantitative biogeographical methods including Cluster Analysis, Non-metric Multidimensional Scaling and Bootstrapped Spanning Network applied to Smithian and Spathian (Early Triassic) ammonoid assemblages; we analyze similarity relationships between faunas and suggest paleopositions for the above-cited terranes. Taxonomic similarities between faunas indicate that primary drivers of the ammonoid distribution were Sea Surface Temperature and currents. Possible connections due to current-controlled faunal exchanges between both sides of the Panthalassa are shown and terranes such as SK, SP and Chulitna played an important role as stepping stones in the dispersal of ammonoids. SK and SP terranes show strong subequatorial affinities during the Smithian, thus suggesting a location close to South China. At the same time, the Chulitna terrane shows strong affinities with equatorial faunas of the eastern Panthalassa. This paleoceanographic pattern was markedly altered during the Spathian, possibly indicating significant modifications of oceanic circulation at that time, as illustrated by the development of a marked intertropical faunal belt across Tethys and Panthalassa.

Keywords: Early Triassic; Ammonoids; Biotic recovery; Terranes; Chulitna; South Primorye; South Kitakami; Biogeography; Paleoceanography.

JOURNAL OF ASIAN EARTH SCIENCES **36**, 2009, 420–433.

Guodunites, a low-palaeolatitude and trans-panthalassic Smithian (Early Triassic) ammonoid genus

Arnaud Brayard[a], Thomas Brühwiler[b], Hugo Bucher[b] and Jim Jenks[c]

[a]UMR 5561 CNRS Biogéosciences, Université de Bourgogne, 6 boulevard Gabriel, F-21000, Dijon, France.
[b]Paläontologisches Institut und Museum, Universität Zürich, Karl Schmid-Strasse 4, CH-8006 Zürich, Switzerland.
[c]1134 Johnson Ridge Lane, West Jordan, UT 84084, USA.

Abstract

Based on new, bed-rock controlled material from Oman and Utah, USA, the Early Triassic genus *Guodunites*, which was recently erected on the basis of scarce specimens from northwestern Guangxi, South China, is now shown to be a representative of Proptychitidae. This solves the question of the previously unknown phylogenetic affinity of this genus. The genus is restricted to the late middle Smithian, and to date, its biogeographical distribution comprises Oman, South China and Utah, thus indicating an essentially low palaeolatitudinal distribution during the Early Triassic. Its palaeobiogeographical distribution further strengthens the existence of significant equatorial faunal exchanges between both sides of the Panthalassa at that time. It also suggests that, in addition to the potential stepping stones represented by Panthalassic terranes, vigorous equatorial oceanic currents must have contributed largely to the dispersal of ammonoids during such time intervals.

Keywords: Ceratitida; oceanic currents; Oman; Proptychitidae; Smithian (Early Triassic); South China; Utah.

PALAEONTOLOGY **52** (2), 2009, 471–481.

Good Genes and Good Luck: Ammonoid Diversity and the End-Permian Mass Extinction

Arnaud Brayard[a], Gilles Escarguel[b], Hugo Bucher[c], Claude Monnet[c], Thomas Brühwiler[c], Nicolas Goudemand[c], Thomas Galfetti[c], Jean Guex[d]

[a]UMR 5561 CNRS Biogéosciences, Université de Bourgogne, 6 boulevard Gabriel, F-21000, Dijon, France.
[b]UMR-CNRS 5125 PEPS, Université Lyon 1, Campus de la Doua, Bât. Géode, 2 Rue Dubois, F-69622 Villeurbanne Cedex, France.
[c]Paläontologisches Institut und Museum, Universität Zürich, Karl-Schmid Strasse 4, CH-8006 Zürich, Switzerland.
[d]Department of Geology and Paleontology, University of Lausanne, l'Anthropole, Lausanne, Switzerland.

Abstract

The end-Permian mass extinction removed more than 80% of marine genera. Ammonoid cephalopods were among the organisms most affected by this crisis. The analysis of a global diversity data set of ammonoid genera covering about 106 million years centered on the Permian-Triassic boundary (PTB) shows that Triassic ammonoids actually reached levels of diversity higher than in the Permian less than 2 million years after the PTB. The data favor a hierarchical rather than logistic model of diversification coupled with a niche incumbency hypothesis. This explosive and nondelayed diversification contrasts with the slow and delayed character of the Triassic biotic recovery as currently illustrated for other, mainly benthic groups such as bivalves and gastropods.

SCIENCE **28**, August 2009, Vol. 325, no. 5944, 1118 - 1121.

Early Triassic (Late Griesbachian) gastropods from South China (Shanggan, Guangxi)

Andrzej Kaim[a,b], Alexander Nützel[a,] Hugo Bucher[c], Thomas Brühwiler[c] and Nicolas Goudemand[c]

[a]Bayerische Staatssammlung für Paläontologie und Geologie; Ludwig-Maximilians-University Munich, Department für Geo- und Umweltwissenschaften, Sektion für Paläontologie, 80333 München, Germany.
[b]Instytut Paleobiologii PAN, ul. Twarda 51/55, 00-818 Warszawa, Poland.
[c]Paläontologisches Institut und Museum, Universität Zürich, Karl Schmid-Strasse 4, CH-8006 Zürich, Switzerland.

Abstract

An Early Triassic (Griesbachian) gastropod fauna is reported from South China (Shanggan, Guangxi) and consists of four species: *Bellerophon abrekensis*, *Wannerispira shangganensis* Kaim & Nützel sp. nov., *Naticopsis* sp., and *Palaeonarica guangxinensis* Kaim & Nützel sp. nov. The taxon *Wannerispira* Kaim & Nützel nom. nov. replaces *Pagodina* Wanner non Van Beneden. This is the first report of *Bellerophon abrekensis* from China. Previously, it was only known from its type locality in Far East Russia. *Wannerispira shangganensis* sp. is the first certain Triassic report of the Permian subfamily Neilsoniinae and represents a holdover taxon. The neritimorph *Palaeonarica* is reported for the first time from the Early Triassic and this is the oldest occurrence of this genus. Compared with other Griesbachian gastropods, the present material is relatively well preserved so that the taxonomy rests on rather firm ground. Very few nominal taxa have been reported from the Griesbachian and therefore the present report presents substantial additional information about gastropods from the aftermath of the end-Permian mass extinction event. The gastropod association from Shanggan shares one species with Primorye, Far East Russia (*B. abrekensis*). Two species, *W. shangganensis* and *P. guangxinensis*, closely resemble specimens reported from the Griesbachian of Oman. This could suggest that Griesbachian gastropod faunas of the Tethys were rather homogenous although the data are still scarce.

Keywords: Gastropoda; China; Early Triassic; extinction; recovery; taxonomy.

Accepted for publication in the SWISS JOURNAL OF GEOSCIENCES.

Ostracod recovery after Permian-Triassic boundary mass-extinction in South Tibet

Marie-Béatrice Forel[a], Sylvie Crasquin[a], Thomas Brühwiler[b], Nicolas Goudemand[b], Hugo Bucher[b], Aymon Baud[c], Carine Randon[a]

[a]CNRS, UPMC Univ. Paris 06, UMR 7207 CR2P, Laboratoire de Micropaléontologie, T.46-56, E.5, case 104, 75252 Paris cedex 05, France.
[b]Paläontologisches Institut und Museum der Universität Zürich, Karl Schmid-Strasse 4, 8006 Zürich, Switzerland.
[c]BGC, Parc de la Rouveraie 28, 1018 Lausanne, Switzerland.

Abstract

Early to Middle Triassic ostracods from the Tulong section, south Tibet, are described here for the first time. The first two stages of the Early Triassic (Griesbachian and Dienerian) are barren for ostracods; the following stage (Smithian) revealed some ostracod faunas, but diversification in taxa began at the base of the fourth stage (Spathian) and developed into the first stage of the Middle Triassic (Anisian). Furthermore, exploration of ecological niches is developed in the Spathian and Anisian, with notable occurrence of burrowing taxa. Important numbers of burrowing and filter-feeding specimens in Spathian and early Anisian units reveal epi- and endobenthic restriction, probably oxygen depletion. This benthic compartment restriction allowed thriving of typical Mesozoic affinities ostracod fauna, challenging the statement that oxygen depletion hindered recovery. Affinities with other Tethyan areas, mainly Northern part of Tethys, bring to the idea of a 2 connected gyres circulation, one in Palaeo-Tethys (North) and the other bathing Neo-Tethys (South), during Smithian to Anisian.

Keywords: Ostracods; Early Triassic; Middle Triassic; South Tibet; Tulong.

Submitted to PALAEOGEOGRAPHY, PALAEOCLIMATOLOGY, PALAEOECOLOGY.

Organic matter and palaeoenvironmental signals in the Early Triassic of the Salt Range and Surghar Range, Pakistan

Elke Hermann[a], Peter Hochuli[a], Sabine Méhay[b], Hugo Bucher[a], Thomas Brühwiler[a], Michael Hautmann[a], David Ware[a], Ghazala Roohi[c]

[a]Institute and Museum of Palaeontology, University of Zurich, Karl Schmid-Str. 4, 8006 Zurich, Switzerland
[b]MIT EAPS, 44 Carleton Street, E25-625 Cambridge, MA 02139, USA
[c]Pakistan Museum of Natural History, Garden Avenue, Islamabad 44000, Pakistan

Abstract

Early Triassic mixed siliciclastic-carbonate shelf deposits of the northern Gondwana margin have been studied in three main sections (Chitta-Landu, Nammal and Chhidru) and a smaller stratigraphic interval (Narmia) in the Salt Range and Surghar Range, Pakistan. The stratigraphic range encompasses Upper Permian to the Middle Triassic. Sedimentological and palynofacies patterns combined with a high resolution ammonoid based age control have been used to detect environmental changes such as sea-level change, oxygenation conditions and proximity of the individual sections to the shore in the aftermath of the end Permian mass extinction.

The base and the top of the Early Triassic are marked by sequence boundaries. Within the Early Triassic two further sequence boundaries near the Dienerian-Smithian and near the Smithian-Spathian boundary could be delineated by means of palynofacies analysis and sedimentology. Further lower order sequences and parasequences are reflected in the sedimentological record of Nammal.

The observed changes in the composition of the particulate organic matter (POM) indicate a general shallowing upward trend, which is modulated by smaller transgressive-regressive cycles supporting the sedimentologically defined sequence boundaries or representing further sequences or parasequences. The POM is mostly dominated by terrestrial phytoclasts and sporomorphs. The strongest marine influence is reflected by increased amorphous organic matter (AOM) in the lower part of the Ceratite Marls at Nammal (late Dienerian) and Chhidru (earliest Smithian) and the Lower Ceratite Limestone at Chitta-Landu (late Dienerian) indicating reduced oxygen contents in these intervals. The following transgressive events are reflected by increased numbers of acritarchs, reaching up to 50% of the POM. Well oxygenated conditions and low total organic carbon (TOC) contents continue up to the top of the Early Triassic Mianwali Formation. The most pronounced terrestrial influx is displayed in the Middle Triassic.

Biomarker studies on the saturated hydrocarbon fraction of three samples from the Nammal section indicate an enhanced bacterial productivity, especially after the Dienerian, reflected in extremely high hopanes relative abundance. Redox sensitive biomarkers, AOM abundance and increased TOC values indicate dysoxic conditions in the Dienerian. The new POM and TOC data and stratigraphical results demonstrate that environmental conditions in the Early Triassic were well-oxygenated with the exception of late Dienerian to earliest Smithian strata, which might have suppressed the recovery of benthic organism but has no affect on the recovery of nektonic organisms. There is no evidence for a shallow water anoxic event in the late Griesbachian in these sections.

In preparation for submission to PALAEOGEOGRAPHY, PALAEOCLIMATOLOGY, PALAEOECOLOGY.

ACKNOWLEDGEMENTS

This dissertation is the result of several years of research performed at the Palaeontological Institute and Museum of the Universtity of Zurich (PIMUZ) under the supervision of Prof. Dr. Hugo Bucher. I want to thank Hugo for his constant support, his scientific advice, his experience and his enthusiasm for Early Triassic ammonoids.

I also gratefully acknowledge:

- Dr. Nicolas Goudemand (PIMUZ) for numerous discussions on the Early Triassic, for his help during field work in South China and for initiating and organizing our field trips to South Tibet.
- Dr. Arnaud Brayard (Dijon, formerly PIMUZ) for many discussions on Smithian ammonoids, and for agreeing to evaluate this thesis.
- David Ware (PIMUZ) for many discussions on Early Triassic (especially Dienerian) ammonoids and for his help in the field in Pakistan and India.
- Elke Hermann (PIMUZ) for discussions and for the collaboration during field work in Pakistan.
- Prof. Dr. Peter Hochuli (PIMUZ) for scienfic assistance and friendly support.
- Dr. Claude Monnet (PIMUZ) for providing his statistical analysis software.
- Dr. Thomas Galfetti (Zürich, formerly PIMUZ) for collaboration and discussions on Early Triassic carbon isotopes and for his help during field work in the Indian Himalayas.
- Markus Hebeisen (PIMUZ) for his masterly preparation of the most delicate ammonoid specimens, and for his continuous friendly support and advice for my own preparation activity.
- Julia Huber and Leonie Pauli (PIMUZ) for preparing a large part of my ammonoid collection.
- Rosie Roth (PIMUZ) for taking all ammonoid photographs and preparing part of my material.
- Prof. Dr. Leopold Krystyn (Vienna) for our fruitful collaboration on the Smithian of Spiti, for numerous discussions on ammonoid taxonomy and for accepting to evaluate this thesis.
- Prof. Dr. Om Bhargava (Haryana) for his friendly guidance in the Spiti area.
- Ghazala Roohi (Islamabad) for her huge bureaucratic and logistic effort for enabling our field work in the Salt Range.
- Khalil Rehman and Aamir Yaseen (Islamabad) for their guidance during field work in the Salt Range.
- Dr. Li Guobiao (Lhasa) for enabling our first field trip to South Tibet.
- Dr. Kuang Guodun (Nanning) for his guidance and help in the field in South China.

- Prof. Dr. Wan Xiaoqiao (Beijing) for his logistic support during field work in China.
- Dr. Aymon Baud (Lausanne) for the fruitful collaboration on the Lower Triassic of South Tibet.
- Jim Jenks (Salt Lake City) for improving the English text of large parts of this work.
- Prof. Dr. Jean Guex (Lausanne) and Prof. Dr. Marcelo Sanchez (PIMUZ) for accepting to evaluate this thesis.

CURRICULUM VITAE

BRÜHWILER Thomas

Geburtsdatum: 29.08.1979

Heimatort: Fischingen TG

Ausbildung:

1994-1999	Kantonsschule Im Lee, Winterthur, Eidgenössische Matura Typus D
1999-2004	Studium von Geologie und Paläontologie, Universität Zürich
2004	Diplomarbeit: Biostratigraphie der Reiflinger Schichten Liechtensteins und Vorarlbergs. Paläontologisches Institut und Museum der Universität Zürich.
2005-2010	Doktorand am Paläontologischen Institut der Universität Zürich

Publikationen während des Promotionsstudiums:

Artikel

- Klug, C., Brühwiler, T., Korn, D., Schweiger, G., Brayard, A. and Tisley, J. 2007: Ammonoid shell structures of primary organic composition. *Palaeontology*, 50 (6), 1-16.

- Brayard, A., Bucher, H., Brühwiler, T., Galfetti, T., Goudemand, N., Jenks, J., Escarguel, G. and Guodun, K. 2007: *Proharpoceras* Chao: a new ammonoid lineage surviving the end Permian mass extinction. *Lethaia*, 40, 175-181.

- Galfetti T., Bucher H., Ovtcharova, M., Schaltegger U., Brayard A., Brühwiler T., Goudemand N., Weissert H., Hochuli P. A., Cordey F. and Guodun K. 2007: Timing of the Early Triassic carbon cycle perturbations inferred from new U-Pb ages and ammonoid biochronozones. *Earth and Planetary Science Letters*, 258, 593-604.

- Galfetti T., Bucher H., Martini R., Hochuli P. A., Weissert H., Crasquin-Soleau S., Brayard A., Goudemand N., Brühwiler T. and Guodun K. 2008: Evolution of Early Triassic outer platform paleoenvironments in the Nanpanjiang Basin (South China) and their significance for the biotic recovery. *Sedimentary Geology*, 204, 36-60.

- Brühwiler, T., Brayard, A., Bucher, H. and Guodun, K. (2008): Griesbachian and Dienerian (Early Triassic) ammonoid faunas from northwestern Guangxi and southern Guizhou (South China). *Palaeontology*, 51, 1151-1180.

- Brayard, A., Escarguel, G., Bucher, H. and Brühwiler, T. (2009): Smithian and Spathian (Early Triassic) ammonoid assemblages from terranes: Paleoceanographic and paleogeographic implications. *Journal of Asian Earth Sciences*, 36, 420-433.

- Brayard, A., Brühwiler, T., Bucher, H. and Jenks, J. 2009. *Guodunites*, a low-palaeolatitude and trans-panthalassic Smithian (Early Triassic) ammonoid genus. *Palaeontology* 52:471-481.

- Brayard, A., Escarguel, G., Bucher, H., Monnet, C., Brühwiler, T., Goudemand, Galfetti, T. and Guex, J. (2009). Good Genes and Good Luck: Ammonoid Diversity and the End-Permian Mass Extinction. *Science*, 325, 1118-1121.

- Brühwiler, T., Goudemand, N., Galfetti, T., Bucher, H., Baud, A. Ware, D., Hermann, E., Hochuli, P.A. and Martini, R. (2009). The Lower Triassic sedimentary and carbon isotope records from Tulong (South Tibet) and their significance for Tethyan palaeoceanography. *Sedimentary Geology*, 222, 314-332.

- Brühwiler, T., Bucher, H. and Goudemand, N. (2010). Smithian (Early Triassic) ammonoids from Tulong, South Tibet. *Geobios*, in press.

- Brühwiler, T., Bucher, H., Goudemand, N. and Galfetti, T. (submitted). Smithian (Early Triassic) ammonoid faunas from Exotic Blocks from Oman: taxonomy and biochronology. *Palaeontographica*.

- Brühwiler, T., Ware, D., Bucher, H., Krystyn, L. and Goudemand, N. (submitted). New Early Triassic ammonoid faunas from the Dienerian-Smithian boundary beds at the Induan-Olenekian GSSP candidate at Mud (Spiti, India). *Journal of Asian Earth Sciences*.

- Brühwiler, T. and Bucher, H. (submitted): Smithian ammonoids from the Salt Range, Pakistan. *Special Papers in Palaeontology*.

- Brühwiler, T. Bucher, H. and Krystyn, L. (submitted): Middle and late Smithian ammonoids from Spiti, Northern India. *Palaeontology*.

- Brühwiler, T., Bucher, H., Brayard, A. and Goudemand, N. (submitted): High-resolution biochronology and diversity dynamics of the Early Triassic ammonoid recovery: the Smithian faunas of the Northern Indian Margin. *Palaeogeography, Palaeoclimatology, Palaeoecology.*

- Kaim, A., Nützel, A. Bucher, H., Brühwiler, T. and Goudemand, N. accepted. Early Triassic (Late Griesbachian) gastropods from South China (Shanggan, Guangxi). Swiss Journal of Geoscience.

- Forel, M.B., Crasquin, S., Brühwiler, T., Goudemand, N., Bucher, H., Baud, A., Randon, C., submitted. Ostracod recovery after Permian-Triassic boundary mass-extinction in South Tibet. Palaeogeography, Palaeoclimatology, Palaeoecology.

Abstracts für Vorträge an Fachtagungen

- Brühwiler, T., Bucher, H., Goudemand, N. and Brayard, A. (2007): Smithian (Early Triassic) ammonoid faunas of the Tethys: new preliminary results from Tibet, India, Pakistan and Oman. The global Triassic, Albuquerque, USA. New Mexico Museum of Natural History and Science Bulletin, 41, 25-26.

- Brühwiler T., Goudemand N., Galfetti T. and Bucher H. (2007): Early Triassic ammonoid biostratigraphy and a new high-resolution carbon isotope record from Tulong area, South Tibet. 5th Swiss Geoscience Meeting, Geneva.

- Brühwiler, T., Bucher, H., Brayard, A., Goudemand, N., Galfetti, T., Hermann, E. and Hochuli, P.A. (2008): Smithian ammonoids: the first diversity peak in ammonoid recovery following the Permian-Triassic mass extinction. GSA 2008 Joint Annual Meeting, Houston, USA, Paper No. 318-2.

- Brühwiler T., Bucher H., , Goudemand N., Ware D., and Hermann E. (2009): Smithian ammonoids (Early Triassic): explosive evolutionary radiation following the Permian/Triassic mass extinction. 7th Swiss Geoscience Meeting, Neuchâtel.